Metal Transport in the Aberjona River System: Monitoring, Modeling, and Mechanisms

by

Helena Solo-Gabriele

B.S. and M.S., Civil Engineering
University of Miami, 1987 and 1988

Submitted to the Department of
Civil and Environmental Engineering
in Partial Fulfillment of the Requirements
for the Degree of

DOCTOR OF PHILOSOPHY
in Civil and Environmental Engineering
at the

Massachusetts Institute of Technology

February 1995

Signature of Author_____
Department of Civil and Environmental Engineering
November 18, 1994

Certified by_____
Frank E. Perkins
Dean of the Graduate School & Professor of Civil and Environmental Engineering
Thesis Advisor

Accepted by_____
Joseph M. Sussman
Departmental Committee on Graduate Studies

Metal Transport in the Aberjona River System: Monitoring, Modeling, and Mechanisms

by

Helena Solo-Gabriele

Submitted to the Department of Civil and Environmental Engineering on November 18, 1994
in partial fulfillment of the requirements for the Degree of
Doctor of Philosophy in Civil and Environmental Engineering

ABSTRACT

The primary objective of this research is to increase the general understanding of contaminant transport processes in river systems. For the current study, our approach is based on investigating the transport of four metals (Fe, Cr, Cu, and metalloid As) within one particular watershed, the Aberjona River watershed.

In this study we found that both streamflow and sediment transport are important factors in controlling the transport of metals through the Aberjona River system where the effects of each of these factors were significantly different between the Aberjona River and its largest tributary, the Horn Pond Creek tributary.

One of the most noticeable features of the streamflow hydrographs observed along the Aberjona River is their consistent pattern in response to storm events. Our interpretation of these patterns is that streamflow is composed of three components: quick storm flow, slow storm flow, and longterm baseflow. Sediment input mechanisms were postulated in association with each of these streamflow components. Quick-sediment inputs are assumed to be governed by a build-up and wash-off mechanism. With this conceptualization, the initial burst of suspended sediments observed at the beginning of each storm event could be reproduced. Slow and longterm-baseflow sediment inputs are assumed to be governed by a potential concentration mechanism which supply relatively low but constant suspended sediment concentrations to the river. Once the sediments enter the channel, channel deposition and erosion may affect transport.

Along the Horn Pond Creek tributary, streamflow did not respond with distinct quick, slow, and longterm baseflows. Furthermore, suspended sediment transport was characterized by two different types of sediments: an organic phase and an inorganic phase. The organic phase exhibited significant seasonal fluctuations and was apparently controlled by the growth of biological material within a drainage pond during the summer months. The inorganic phase was inversely related to water hydraulic residence times and was presumably controlled by the settling of inorganic particulates.

Along the river, metal concentrations varied significantly between low flow and storm conditions, whereas between storm events fluctuations were not as pronounced. A large amount of the variability could be explained by postulating that each streamflow and sediment component had a different metal concentration.

To quantify these effects, a series of box models is developed which characterizes the watershed's geometry and each of the streamflow and sediment inputs. Variations of metal concentrations and fluxes (dissolved and particulate) are modeled by combining each flow or suspended sediment component. Results indicate that most of the sediment is transported in "bursts" at the beginning of each storm event. As a result, the number and magnitude of large storm events during a given model period will significantly affect the predicted sediment transport. For As and Fe, dissolved and particulate transport are each responsible for roughly one half of the transport. Most of the Cr is carried in the particulate phase, whereas most of the Cu is carried in the dissolved phase. For all metals, dissolved-metal transport is carried primarily by the longterm-baseflow component. For arsenic and iron, particulate transport is primarily associated with longterm-baseflow sediments, whereas for chromium and copper, particulate transport is primarily associated with quick sediments.

Thesis Advisor: Professor Frank E. Perkins
Title: Dean of the Graduate School and Professor of Civil and Environmental Engineering

ACKNOWLEDGMENTS

In completing this project I have interacted with many people from Parson's Lab, M.I.T., and outside agencies. I consider myself very fortunate in that just about everyone with whom I have had contact has been friendly and has always tried, to the best of their ability, to assist me. Below I mention just a small fraction of those from whom I have received assistance. But to those not mentioned by name, I thank you too.

First, I would like to thank my advisor, Professor Frank Perkins, who believed in me from the very beginning. It was his encouragement, during our first meeting, that helped me overcome my own apprehension about pursuing a doctoral degree. Since this meeting, Professor Perkins' support has been immeasurable. His guidance has served as a "constructive filter of ideas" in which my (sometimes vague) ideas along with his suggestions, produced a much more coherent understanding of the data. This resulted in a more directed path for which I would follow in the development of my research. Furthermore, through his exceptional communication skills, Professor Perkins has helped me immensely in the ability to organize my technical work in such a way that others can understand. I feel extremely fortunate to have had him as my advisor.

I would also like to thank Professor Harry Hemond for his support. I greatly appreciate the opportunity to work on the Aberjona project and to participate in his research group meetings. The added interaction by being a part of "a group" has enhanced my research and my educational experience.

I also greatly appreciate the participation of the rest of my thesis committee who have also provided me with suggestions and constructive advice concerning my research.

As for my field work, I could never have obtained the much needed field data without the help of others. I would like to first thank John D. for introducing me to the watershed and for teaching me the maintenance details of the streamgaging stations. I would also like to especially thank two UROP students, Claudia and Jock, each of whom assisted me in the field on a weekly basis for over a year. It was their consistent energy and enthusiasm that made the long field trips, especially those during inclement weather, much more endurable. I would also like to thank the occasional field help that I received from others including: Sara, Andrew, Eric, Peter, Jamie P., Jim, Becky, Kim, and David. A special thanks goes to Heekyung who helped me on a full day of sampling on a miserable winter day of slushy rain.

I also would like to thank the personnel from the U.S.G.S. Specifically, I thank: Russell Gadoury for granting permission to install and access equipment within the U.S.G.S. gage house; Joe Zanca and Domenic Murino who taught me their streamflow calibration techniques and who informed me of the periodic maintenance work in the gage house; and, Dave McCarthy and Tom Shepard for their orderly response to innumerable information requests. I also thank Robert Lautzenheizer of the N.C.D.C. for the tour of his gaging station and for the prompt supply of several requests for precipitation and temperature data.

I also would like to thank personnel from the Woburn Public Works Department including Bill Nieman for access to the Horn Pond monitoring station and Bob Andrews who installed the vault at the Horn Pond gage to help deter vandalism. Also a special thanks goes to Don Grossman and Chris Newman of Coastal Leasing who on many occasions repaired the streamgages free of charge. I also appreciate Mike E.'s help with electronics, machining, and photography.

In the laboratory, I also received a large amount of assistance. I greatly appreciate Henry's help in repairing and in teaching me the use of the ICP and the arsenic hydride generation system. I also thank: Trine for teaching me how to use the T.O.C. analyzer; Dianne for showing me how to use her PID hydride generation system; Rob for showing me how to use the AA; Barry Grant for assistance with the ICP-MS; and Dr. Ilhon Olmez for performing the Neutron Activation Analysis of several samples.

I am especially thankful to my family for their love, support, and encouragement throughout my research endeavors. I want to especially thank my husband, Frank, for his companionship and emotional support at home.

I dedicate this work to my daughter, Christina Elena, born October 5, 1994.

TABLE OF CONTENTS

VOLUME I

VOLUME II

LIST OF FIGURES

VOLUME I

LIST OF FIGURES

VOLUME II

LIST OF TABLES

VOLUME I

LIST OF TABLES

VOLUME II

LIST OF EQUATIONS

VOLUME I

VOLUME II

I. MOTIVATION, OBJECTIVES, & LITERATURE REVIEW

I.1 MOTIVATION

Rivers are dynamic systems which serve to transport and/or store contaminants which are carried to them from outside sources. The negative impacts of contaminants carried by rivers include, for instance, the disruption of ecosystems due to the toxicity to aquatic organisms and possible human exposure which may result in chronic and acute ailments. If contaminants are readily transported, the river provides a means by which contaminants can migrate and adversely impact downstream areas. If stored, the accumulated contaminants may result in localized unfavorable conditions and may also present a potential contaminant reservoir which can be released at a later time. Due to this potential threat, it is important to understand the processes (or mechanisms) which control the transport of contaminants in rivers.

One specific advantage of understanding river transport is that it enables the identification of drainage areas from which contaminants are originating and accumulating. Knowledge of source areas, for example, helps to identify entities responsible for downstream contamination whereas knowledge of accumulation areas helps to identify "hot spots" where contaminant discharges may have resulted in considerable damage.

The understanding of transport mechanisms also provides the basis for a model which can be used to quantitatively describe transport. One benefit of a quantitative model is that it can be used to determine the extent to which either natural or man-made control measures affect the transport of contaminants downstream. For example, one may be able to estimate hydrologic conditions required to flush a contaminant reservoir (e.g. river sediment) and thus determine whether natural processes will efficiently flush the system or whether human intervention is necessary. Another benefit of a quantitative model is that it can be used to establish policies concerning river effluent discharges, land use changes, and construction procedures. For instance, if an additional contaminated sediment source were discharged into the system, (e.g., due to earth-moving activities near the river), the model can potentially be used to estimate the time distribution of the sediment load to downstream areas and therefore help to determine whether or not such a discharge is permissible.

Furthermore, the understanding of transport mechanisms may also help in implementing control measures. For example, assume that the transport of contaminants to downstream areas must be reduced. If transport is associated with particulate matter which is moved primarily during high streamflow, then a reduction of storm peaks by increasing the hydraulic detention times will inhibit the transport of the contaminant. If a corrective action is required, the design of a flow-through detention area which is

periodically flushed may provide a means of removing a large fraction of the contaminant in a controlled manner. If, on the other hand, transport is associated with low flows, a treatment plant designed to treat the bulk of the river water at low flows may be used to also remove a significant portion of the contaminant from the river. For each of the remediation schemes, the amount of the contaminant transported to downstream areas after the treatment process is implemented can be estimated if a quantitative model is also developed.

Thus, the understanding of contaminant transport processes provides the basis for assessing problems associated with contaminant discharges. A qualitative assessment may be obtained by simply having an understanding of these mechanisms whereas a quantitative assessment will require the development of a model which incorporates these mechanisms.

I.2 OBJECTIVES

The primary objective of the current research is to increase the general understanding of contaminant transport processes in river systems. For the current study, our approach is based on investigating the transport of four metals (Fe, Cr, Cu, and metalloid As[1]) within one particular watershed, the Aberjona River watershed in eastern Massachusetts. The Aberjona River watershed was chosen because of the availability of extensive hydrologic data and the feasibility of monitoring the area for metal transport. Although an exhaustive understanding of contaminant transport processes is beyond the scope of this research, it is hoped that this study will contribute to the identification of universal mechanisms which control transport for polluted watersheds.

The secondary objective is the development of a model which can be used to quantify transport. The model is developed from the analysis of field data from the Aberjona River watershed and is, therefore, intended to be watershed specific. The primary purpose of the model is to provide quantitative feedback concerning the adequacy of postulated mechanisms. Through such feedback, a cycle of model formulation and modification is established which enhances our understanding of transport mechanisms.

[1]For discussion purposes, arsenic will be referred to as a metal throughout the rest of the present study.

I.3 LITERATURE REVIEW: MECHANISMS OF METAL TRANSPORT

In describing the mechanisms which control the composition of freshwaters, two contradictory theories were discussed in the early literature. The first of these theories is an extension of the generally accepted "constant composition" notion of ocean waters, where the ratio of major ions in the water is assumed constant regardless of the total ion concentration. In its application to freshwater systems authors have applied the theory to describe the ionic composition of freshwaters (Rodhe, 1949) or to describe the partitioning of contaminants in the particulate phase. (Gibbs, 1973) The simplifying aspect of the "constant composition" theory is that a mechanism describing the variability of a particular chemical constituent would not be necessary.

The second theory, which has received much wider acceptance in more recent times, is that freshwater composition is not constant, but rather controlled by various factors which lead to differences in composition. (Livingstone, 1963) In the application of this theory, "controlling factors" are used to explain non-homogeneities in the composition of different waters.

In developing our understanding of the mechanisms of metal transport, the "controlling factor" concept is adopted. A controlling factor is defined, in the context of this study, as a variable which significantly influences the transport of metals within a river system. In clarifying terms, assume, for instance, that metals within a watershed are derived from the solution of rocks by rainfall. Once in solution these metals infiltrate into the groundwater and are eventually incorporated into the river as baseflow. Such a process description exemplifies a mechanism of transport whereas controlling factors for this mechanism include rainfall properties, rock composition, soil infiltration rates, and groundwater flow rates. Thus controlling factors may also be viewed as variables used in describing a mechanism or as input parameters for a transport model. These factors can be broadly categorized as:

a. *Hydrologic Processes*: Many investigations have focused on river streamflow as a primary hydrologic influence. (Livingstone, 1963; Salomons & Eysink, 1981; Bradley, 1984; Leenaers, 1989; Yeats & Bewers, 1982; Meybeck, 1976; Gibbs, 1972) Additionally, studies which monitor transport specifically within the particulate phase, also identify the importance of river sediment, especially suspended sediment, in governing transport. (Gibbs, 1977; Salomons & Eysink, 1981; Ongley, 1982; Yeats & Bewers, 1981; Trefry & Presley, 1976; Bradley, 1984; Delfino & Otto, 1986) Other controlling factors may include antecedent river conditions (Bird,

1987; Morrison, et. al., 1984), and relative importance of surface versus subsurface runoff. (Livingstone, 1963; Bird, 1987) For rivers which receive discharges of industrial effluent, or highly contaminated flows from tributary rivers, the river's available dilution with respect to the inflows may be of importance. (Bird, 1987)

b. *Watershed Characteristics*: Watershed characteristics which may affect transport include adjacent land-use (Wilber & Hunter, 1977; Morrison, et. al., 1984), topographic relief (Gibbs, 1967; Meybeck, 1976; Martin & Meybeck, 1979; Stallard & Edmond, 1983), lithography (Gibbs, 1967; Meybeck, 1976; Stallard & Edmond, 1983), weathering rates (Gibbs, 1967; Martin and Meybeck, 1979; Subramanian, 1979; Ming-hui, et.al., 1982; Stallard & Edmond, 1983), watershed size (Meybeck, 1976), availability of the metals (Morrison, et. al., 1984), climatic conditions (Gibbs, 1967; Ongley, 1982; Meybeck, 1976; Martin & Meybeck, 1979, Delfino & Otto, 1986), and seasonal effects (Livingstone, 1963; Gibbs, 1972; Ongley, 1982, Delfino & Otto, 1986; Cossa, et. al., 1990). Other morphoclimatic parameters affecting total transport include altitude, precipitation, temperature and protective vegetation cover. (Meybeck, 1976; Gibbs, 1967) Additionally, affects of reservoirs, such as dams (Meybeck, 1976; Martin & Meybeck, 1979; Delfino & Otto, 1986) or lakes (Yeats and Bewers, 1981) on transport have been noted.

c. *Chemical and Biological Properties*: Chemical properties such as river water pH (Sholkovitz & Copland, 1981; Bird, 1987), Eh (Delfino & Otto 1986), chemical constituents (Tessier, et.al., 1980; Waslenchuk, 1979; Sholkovitz & Copland, 1981; Tipping, 1981; Delfino & Otto, 1986), and photo-chemical processes (McKnight, et. al., 1988; Waite & Morel, 1984) may be of importance due to their effects upon the partitioning of metals which in turn affects metal mobility. Biological processes of importance may include: uptake of soil ions by vegetation which makes those ions unavailable for weathering action (Stallard & Edmond, 1983), degradation of plant material resulting in the leaching of ions to nearby surface waters (Foster, et. al, 1983), and microbiological uptake of contaminants (Heikkenen, 1990).

Many controlling factors have been listed above. These factors have been identified for a wide variety of watersheds, including watersheds of varying size, degrees of contamination, and climatic conditions. However, when one focuses upon a particular "class" of watershed, the list of controlling factors may be reduced.

I.3.1 Comprehensive Studies for Large Unpolluted Watersheds

Comprehensive studies performed on major rivers of the world have identified factors which govern transport. These comprehensive studies focused on watersheds of very large size (area > 400,000 km^2) and of relatively little degree of anthropogenic contamination. It should be noted that most of these studies, especially the earlier ones, investigated total elemental transport rather than metal transport in particular. Nevertheless, these studies do provide credible theories for overall river transport and provide considerable groundwork for understanding processes controlling the transport of metals.

Major factors which control surface water chemistry of large relatively uncontaminated watersheds have been identified as (Gibbs, 1970): 1) atmospheric precipitation, which controls the composition of tropical rivers in chemically leached soils of low relief, 2) rock-dominance, which controls the composition of waters which are in partial equilibrium with the materials within their basins, and 3) evaporation and crystallization processes, which are characteristic of hot, arid regions, where evaporation serves to increase the salinity of the waters whereas chemical precipitation changes the relative proportions of major ions in river waters.

Variations of these controlling factors are described by: 1) Meybeck, 1976, who in his comprehensive study of the world's major rivers, identified topographic relief and climate as the most important parameters in the control of total dissolved elemental transport in river systems, and 2) Martin and Meybeck, 1979, in research concerning weathering and elemental fluxes on a global scale, observed that the composition of river waters is dependent upon climatic features of the river basins. They identified two different types of rivers according to the intensity of the weathering action and general elemental components of the river waters. Their two category classification defined general characteristics of tropical rivers and temperate/arctic rivers.

By interpreting the literature one may conclude that primary controlling factors for large uncontaminated basins are:

a. *Climate*: Basins of similar climate tend to have river waters with similar elemental compositions. The similarity is controlled, in part, by the soil types associated with various climates. For example, highly leached soils are characteristic of tropical regions. Since few elements are available for leaching, the composition of resulting river waters in tropical environments is similar to the composition of the basin's precipitation. (as noted by Gibbs, 1970). Additionally, climate influences the predominance of certain processes. For example, evaporation and crystallization, as described by Gibbs, 1970, is dominant in hot-arid regions which are conducive to intense evaporation and over-saturation of certain elements.

b. *Composition of a watershed's rocks/soils and their weathering rates.* In addition to atmospheric input, the watershed's rocks/soils represent the source of elements to river water. The amount released is related to the intensity of the weathering action, which is influenced by topographic relief and climate. One example emphasizing the importance of topographic relief on weathering action was presented by Stallard & Edmond, 1983, who suggest that dissolution of watershed soils in flat terrains is transport limited, whereas in steep terrains it is limited by weathering rates.

I.3.2 Watershed Based Studies of Anthropogenically Contaminated Systems

Comprehensive studies, as discussed above, have identified fundamental morphoclimatic factors which affect the availability and transport of chemical constituents in rivers. However, in reviewing the literature concerning anthropogenically contaminated watersheds, the general perception obtained is that each watershed has its own characteristic behavior. The *apparent* non-homogeneity for this type of watershed is primarily due to the difficulty in characterizing the important factors which affect transport. At the current state of research, the general approach indicated by the literature is to study an individual watershed through an intensive monitoring program from which governing transport processes are identified for that particular watershed. It is hoped, however, that review of this research, will elucidate universal mechanisms which control transport for anthropogenically contaminated watersheds. From the literature, some of the observed trends and processes are discussed below.

I.3.2.1 The Flushing Effect

Streamflow vs Total Metal Transport

Wilber and Hunter, 1977, reported, for the Saddle River in New Jersey, that in general metal concentrations during the rising limb of the hydrograph were typically higher than those during the descending limb, while peak concentrations of metals were generally observed shortly after the initiation of runoff. These findings indicated that a "flushing-effect" may have been occurring. In other words, contaminants which accumulated in the channel or in contributing areas prior to the storm were quickly removed from the system upon increasing flow conditions. Thus transport was "contaminant-limited" in that the amount of transport was a function of the amount accumulated between events. Similar trends have been reported in other studies. (Bradley & Lewin, 1982; Trefry & Presley, 1976; Grimshaw, et. al., 1976)

Variations of the first-flush concept have been used to interpret contaminant peaks not associated with the initiation of runoff. Morrison, et. al, 1984, discussed "late flushes" or peaks after the discharge or suspended sediment peak has occurred, as resulting from a variable areas concept. The author postulated that metals were flushed from different sub-areas contributing to the observation point. The contribution of metals from each of the sub-areas may have not coincided, either due to different rates of mobilization or because of longer travel times. Because of timing variations, the metals mobilized from a highly contaminated area may have reached the observation point after the flow and suspended sediment contributions from the rest of the sub-areas have been observed.

1.3.2.2 The Dilution Effect

Streamflow vs Dissolved Metal Transport

For the dissolved phase, streamflow may or may not have a significant effect upon metal transport. Numerous studies, corresponding to rivers of varying size and industrial influences, have reported that metal concentrations for the dissolved phase exhibited a degree of long-term stability and were not significantly affected by variations in streamflow. (Yeats & Bewers, 1982; Leenaers, 1989; Treyfry & Presley, 1976; Williams, et al., 1973) In contrast, other studies have reported significant variations in dissolved metal transport. Salomons and Eysink, 1981, for the Rhine and Meuse Rivers in the Netherlands, observed that dissolved metals concentrations decrease with increasing streamflow. This variation, as reported by the researchers, was due to the dilution of the streamflow by the contribution of relatively uncontaminated runoff during high flow events. Similar results were observed by Grimshaw, et. al., 1976 for dissolved zinc transport in the River Ystwyth, who attributed the dilution effect to evapo-transpiration losses of water during low flow conditions. Because of enhanced evapo-transpiration, the chemical constituents in the river water during low flow conditions were more concentrated relative to the concentration during high flow conditions. Bird, 1987, for the River Tawe in South Wales, attributed the dilution effect of dissolved nickel and copper to variations in dilution ratios of river flow to effluent and to the relative residence time of subsurface water in contact with waste sites. The author postulated that during low flow, the residence time of subsurface water increased allowing more effective solution of metals from waste sites and thus resulting in more highly contaminated subsurface flow.

Streamflow vs Particulate Metal Transport

Several studies reported an overall decrease in sediment metal concentration (mass of metal/mass of sediment) with increasing streamflow. (Bradley & Lewin, 1982; Bradley, 1984; Salomons & Eysink, 1981; Schneider & Angino, 1980) All researchers attributed this trend, at least in part, to a "dilution effect," where contaminated suspended sediment was diluted by the relatively clean sediment sources which were activated during high flow conditions. Some of these sediment sources were identified as either sediments from the upper levels of channel banks or floodplains (Bradley, 1984), leached soils from adjacent land areas (Schneider & Angino, 1980) and relatively cleaner coarse particles that were suspended during high flow conditions (Delfino & Otto, 1986). Additionally, some authors have also postulated that sorption processes between the particulate and dissolved phases may have contributed to these trends. Salomons and Eysink, 1981, suggested that sorption of metals from the river water was restricted during high flows since, the residence time of the suspended sediment in river was reduced because of the increased flow velocity. Thus, because of differences in particle residence time, clean sediment sorbed less metals under high flows than during low flows. On the other hand, Schneider & Angino, 1980, postulated that metals desorbed during flood flows. These authors suggested that during a flood event a concentration gradient may have been established between: 1) trace elements loosely adsorbed onto suspended sediments and 2) highly dilute river water. Thus, the movement of trace elements from the sediment surface to the water was preferred under these flow conditions. It may be noted, that although both studies refer to sorption processes in explaining trends, sorption of metals from contaminated waters, as suggested by Salomons and Eysink, 1981, will tend to offset the dilution effect, whereas desorption of metals from particles during high flow events, as suggested by Schneider & Angino, 1980, will tend to enhance this effect.

Although the "dilution effect" has been well illustrated in many river studies, not all rivers exemplify the general trend. As a contrast to the "dilution effect," the concentration of particulate associated metals has been observed to increase with increasing streamflow. (Williams, et. al., 1973) This peculiar trend, as discussed by the authors, was due to the resuspension of highly contaminated bottom sediments mostly in the form of ooze that accumulated during periods of low or negligible streamflow.

Mixed trends were observed by Leenaers, 1989, for the Geul River in the Netherlands. For a particular flood event, sediment and metal concentrations of Zn and Cd were observed to peak at or immediately after the first discharge peak. At the second rising stage, which occurred 30 hours later, suspended sediment concentrations increased again but metals levels remained low. The author suggested that: 1) the tendency of metal concentrations to increase with discharge was due to the activation of contaminated sources and 2) the tendency of metal concentrations to decrease with increasing discharge as observed during the second peak was due to a "dilution effect" from the activation of relatively clean

sediment sources. From the observations, the author concluded that metal loads were governed to only a limited extent by river discharge and suspended sediment concentration. During flood peaks the role of river discharge was dominant, but at the intermediate stages between peaks the quantity and quality of transported sediment depended on the variable activity of sediment sources upstream.

Seasonal Trends vs Particulate Metal Transport

For the Elbe River in Germany, Kaiser, et. al., 1989, found that seasonal variations of metal concentrations in suspended matter were also associated with a dilution effect. Most of the metals observed at their sampling station were transported from upstream areas by highly contaminated suspended material. During one summer within a lower reach of the river, a phytoplankton bloom which produced relatively cleaner phytoplankton particulates resulted in a "dilution" of the contaminated sediments from upstream areas. After the break-down of the phytoplankton bloom the metal concentration in the suspended sediments at the sampling station increased again.

1.3.2.3 The Significance of Bedload

In addition to suspended sediment, particulate associated metals may be transported within river systems as bedload. In general, many studies concerned with metal transport in rivers claimed that contaminant transport by this phase was insignificant. (Trefry & Presley, 1976; Meybeck, 1976; Martin and Meybeck, 1979; Gibbs, 1967) For example, Trefry and Presley, 1976 for the Mississippi River mentioned that bed loads have been estimated to be only 10 - 20% of the suspended load and because they have a much lower trace metal content would probably contribute less than 10% to the total load.

I.3.2.4 Summary of Controlling Factors: Anthropogenically Contaminated Watersheds

Although many controlling factors and their effects on transport have been described above, a summary of what we believe to be the most important factors may be summarized as:

a. *Streamflow*. Total streamflow is a determining factor in the transport capability of a river. The amount transported in the dissolved and particulate phases is in direct proportion to the volumetric streamflow and to the metal concentration. The concentration of metals within each of the phases is also influenced by streamflow through its relationship to 1) metal sources, 2) residence times, and 3) to the sediment transport capability of the stream.

With respect to source, streamflow affects metal concentrations through its components, i.e. surface and subsurface runoff. The relative metal concentration of each of these components and their mixing ratios will greatly influence the overall metal transport in a river.

Additionally, streamflow influences metal transport through residence time variations. During high flows the residence time of matter carried by the rivers is less than the residence time during low flow conditions. This variation affects the partitioning of metals within the river by altering the time available for chemical reactions to occur.

The sediment transport capability is also greatly influenced by streamflow. Streamflow is related to sediment transport through its effect on streambed shear and turbulence which moves the river's available sediment. The sediment transport will define the amount of matter moved in the particulate phase, which has a direct relationship to particulate metal concentrations.

b. *Suspended Sediment*. Suspended sediment can potentially carry a large fraction of the metal burden of a river. The flux of metals carried by this phase is proportional to both the amount of sediment carried by the river, and to the particulate metal concentration.

The amount of suspended sediment carried by rivers is a function of: 1) the carrying capacity of the river, which is partly governed by river geometry and streamflow, and 2) the availability of the sediments, which is influenced by antecedent river conditions and by soil erodibility.

The metal concentration of the suspended sediment is affected by its source and by its residence time within the river. With respect to source, the proportion of sediment which comes from contaminated versus uncontaminated sources will affect the overall suspended sediment

concentration. The relative residence time of the suspended sediment will determine the extent to which the sediment will incorporate or lose metals upon entering the river.

c. *Contaminant Availability*. The availability of metals to a river is a function of the degree of contamination within the watershed, the distribution of contaminants, and the relative mobility of the metals from their sources. These factors vary greatly from watershed to watershed and are probably the most difficult to quantify.

Thus, in summary for a watershed with a given contaminant availability, the hydrological parameters of streamflow and suspended sediment concentration will most likely be the primary controlling factors which influence the mobility of metals through a river system. Bedload may be influential in the control of metal mobility, but probably not to the extent of streamflow and suspended sediment concentration. Chemical/biological interactions and variations of the metal source may be used to explain observed trends not associated with the primary controlling factors.

I.3.3 Concluding Remarks

The controlling factors identified for each class of watershed are influenced by the watershed size, study objective, and degree of contamination. It may be noted that most studies in anthropogencially contaminated areas have been performed on relatively small watersheds (notable exceptions are the Mississippi and the St. Lawrence Rivers), whereas the comprehensive studies investigating "natural" controls have been performed on very large watersheds.

For large watersheds the variables of streamflow and suspended sediments have not been listed as controlling factors. The reason these variables are not included is due to a large watershed's ability to "filter-out" short-term fluctuations of these variables. As a result, typical time scales of significant streamflow and suspended sediment fluctuations for large watersheds are on the order of months. Since these variables are relatively stable on a seasonal basis, variations of elemental transport due to these factors, are generally lumped into the watershed's climate/seasonal variability and are therefore not included as primary controlling factors. However, for smaller watersheds these variables are of importance due to their large variability on short time scales, and are generally the predominant controlling factors for this type of watershed.

The focus of the study is also of importance in the identification of controlling factors. Comprehensive studies attempt to identify specific watershed characteristics which control elemental transport whereas single-watershed studies attempt to identify specific hydrologic processes. Not only is the difference due to the difference in watershed size between each type of study, but it is also due to the different study objectives. In general, watershed-based studies investigate trends in which watershed characteristics such as climate and composition/weathering of soils are a considered "given." The variable factors which control observed trends for this type of study would therefore be primarily hydrologic parameters. Comprehensive studies, on the other hand, generally attempt to compare transport trends for many different watersheds. By comparing many watersheds, these studies may derive general relationships which describe river chemistry, average streamflow, and suspended sediment concentrations from watershed climate, topography, and size. Thus, comprehensive studies use watershed characteristics to describe hydrologic parameters. Theoretically, perhaps, watershed characteristics can also be used to describe transport trends for anthropogenically contaminated watersheds, once a comprehensive understanding of these types of watersheds has been obtained.

In order to obtain a comprehensive understanding of anthropogenically contaminated watersheds, a measure of the degree of contaminant availability would be needed. Although such a measurement is beyond the scope of this research, it would provide a useful tool in beginning to understand the behavior of watersheds as a whole. Such a factor would incorporate watershed rocks and soil composition/weathering as listed for the large "natural" watersheds, in addition to local contamination.

II. WATERSHED SPECIFIC BACKGROUND INFORMATION & PRELIMINARY ANALYSIS

II.1 WATERSHED SPECIFIC BACKGROUND INFORMATION

This chapter presents: 1) background information specific to the watershed, and 2) the results from preliminary sampling within the watershed. This information provides insight in determining dominant transport processes and provides the basis for various assumptions which strongly influence the direction of the monitoring program.

II.1.1 Watershed Description

Detailed hydrologic characteristics of the Aberjona watershed are provided in Chapter IV.

II.1.1.1 Location

The Aberjona River watershed is located 10 to 12 miles northwest of Boston. (figure II.1-1) The watershed area includes parts of 7 municipalities: City of Woburn and the Towns of Winchester, Stoneham, Reading, Wilmington, Burlington, and Lexington. The City of Woburn is located in the central portion of the watershed and occupies the bulk of the watershed area. A significant fraction of the watershed is also occupied by the Town of Winchester which is located on the southern end. The remaining 5 towns lie along the periphery of the watershed and occupy smaller fractions of the watershed area.

II.1.1.2 Land-Use

The basin is highly urbanized. Urbanization is primarily due to residential communities with isolated commercial and industrial areas. Commercial areas are concentrated in town centers, along Route 38, and at major street intersections, while a lightly industrialized area is located near the northern border.

The land-use distribution in the watershed as measured from maps dated in 1979 and as projected for 1995 are: (Camp Dresser & McKee Inc., 1981)

Land Use	Fraction of Surface Area	
	1979	1995(projected)
Open Space	27%	14%
Residential	59%	65%
Industrial/Commercial	13%	20%
Water Bodies	1%	1%

Of the watershed area, approximately 53% was storm sewered and 25% was impervious during 1979. 61% storm sewered and 29% impervious were projected for 1995. (Camp Dresser & McKee, 1981)

A sanitary sewer system (which is separate from the storm sewer system) serves between 95 to 100% of the population within the watershed. (Metropolitan Area Planning Council, 1977) Sanitary wastewater is discharged to the MSD-Deer Island treatment facility located outside of the watershed.

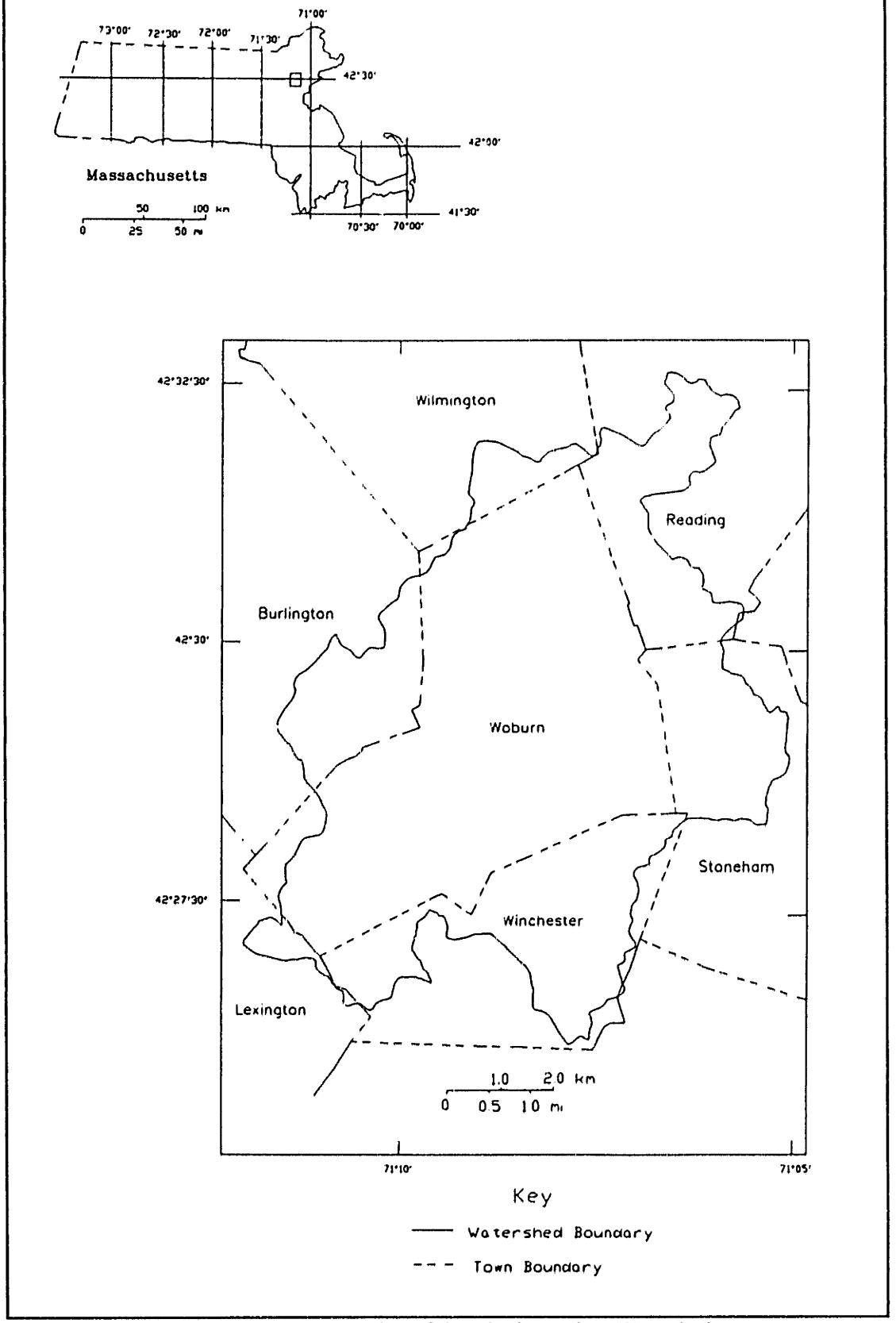

Figure II.1-1: Location of the Aberjona River Watershed

II.1.1.3 River Geometrical and Travel Time Characteristics

The drainage area of the basin is approximately 25 square miles (65 km^2). The Aberjona River (which is the primary river in the system) originates at an elevation of 120 ft. NGVD in a wetland area located in the northeastern portion of the watershed. (figure II.1-2) The river flows for approximately 9 miles in a southward direction and discharges at an elevation of 3 ft. NGVD into the Mystic Lakes. The Mystic Lakes are drained by the Mystic River which eventually discharges into Boston Harbor.

The overall slope of the Aberjona River is 0.002 ft/ft. Localized channel relief is characterized by steeper slopes on the upstream reaches and shallower slopes with localized flat swampy areas along the downstream end. The channel slope on the upstream end of the river within the Town of Reading corporate limits is roughly 0.004 ft/ft. Within the City of Woburn and Town of Winchester, the average channel slope is roughly 0.0015 ft/ft. The longest swampy reach of the river, the Wells G & H wetlands area, generally has a slope of 0.0003 ft/ft.

The width and depth of the river are quite variable and depend largely upon channel topography and climatic conditions. Generally, the size of the river increases in the downstream direction. During low flow conditions, at the confluence of the Aberjona River with Halls Brook the width and depth of the channel are roughly 20 and 2 feet, respectively, whereas downstream, at the river's outlet to the Mystic Lakes, the river is roughly 40 feet wide and 3 feet deep.

Travel times of the river water are dependent upon flow conditions. For the 10 and 500 year storms, travel times from the confluence of the Aberjona River with Halls Brook to the outlet at the Mystic Lakes have been approximated as 6.4 and 5.9 hours, respectively. (F.E.M.A., 1980; F.E.M.A., 1979) During low flow conditions, travel times are longer. A flow time-of-travel study conducted by the Unites States Geological survey, found that at low flows (3 cfs as measured near the outlet of the Aberjona) it took over 135 hours for water to travel from the confluence with Halls Brook to the confluence with the Mystic Lakes and that at medium flows (45 cfs) it took only 20 hours to travel the same distance. (Fratoni, et.al., 1982)

The main tributary to the Aberjona River is the Horn Pond Creek tributary which drains roughly 40% of the watershed area. The area-normalized streamflow from this tributary is significantly less than the area-normalized streamflow from other areas within the watershed. The small streamflow contribution (given the large drainage area) is due to large groundwater withdrawals in the vicinity of Horn Pond.

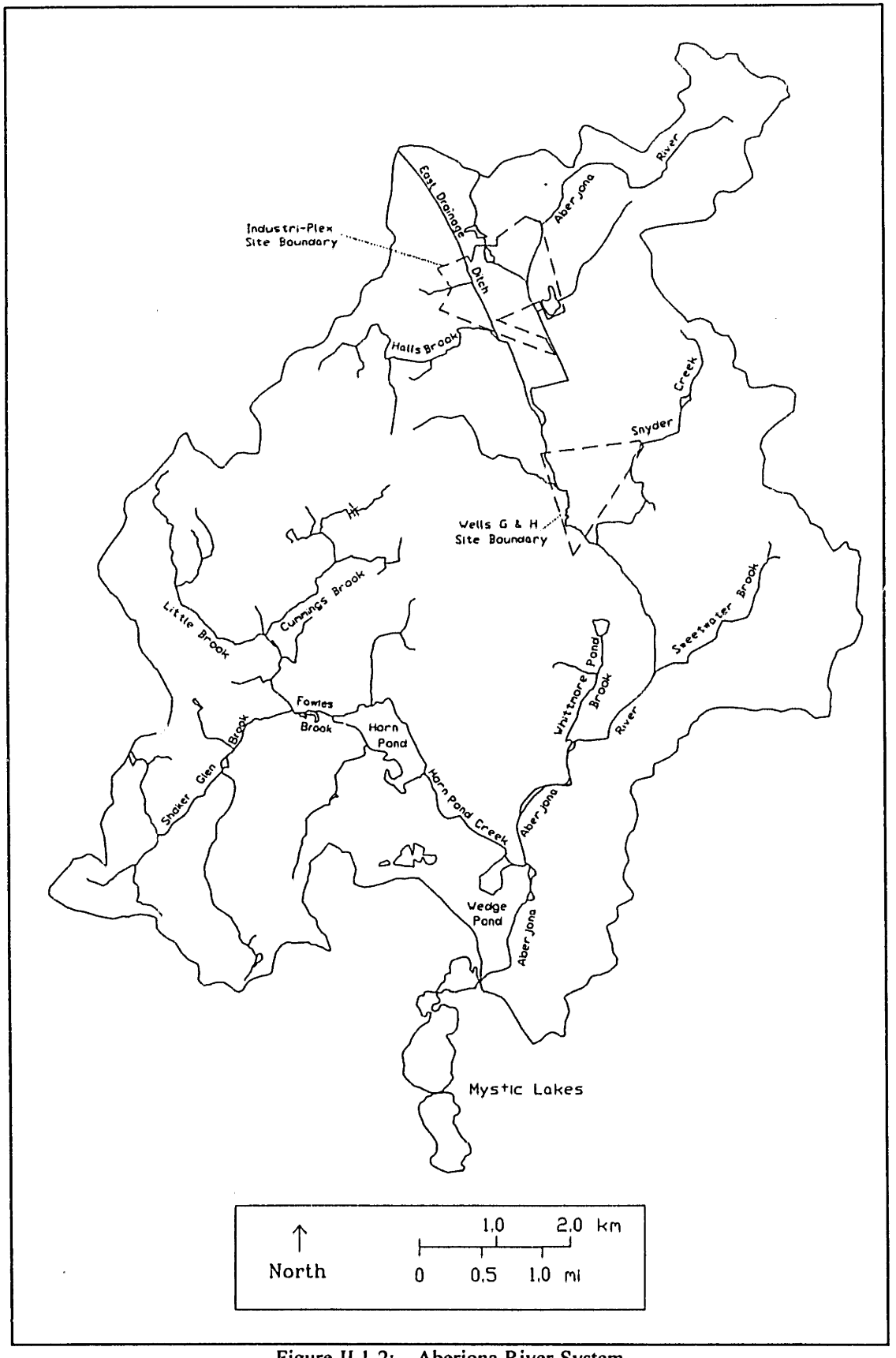

Figure II.1-2: Aberjona River System

The average channel slope of the Horn Pond Creek tributary is 0.003 ft/ft which is steeper than the main trunk of the Aberjona River. The Creek basically acts as a conduit by which water is rapidly transported between Horn Pond and Wedge Pond, each located on opposite ends of the Creek. Travel time along the tributary is on the order of a fraction of an hour for both the 10 and 500 year storms. (F.E.M.A., 1980; F.E.M.A., 1979). Travel times through each of the ponds are significantly larger (up to several days) and depend highly upon flow conditions and antecedent reservoir volumes.

Due to the long hydraulic detention times, the reservoirs tend to attenuate storm flow peaks from the Horn Pond Creek tributary. During large storm events, Wedge Pond may even receive backwater from the Aberjona River, aiding the attenuation of the peak flow along the Aberjona River. (F.E.M.A., 1979)

Other tributaries to the Aberjona River include: Halls Brook, Snyder Creek, Sweetwater Brook, and Whittemore Pond Brook. Tributaries to Horn Pond Creek include: Fowles Brook, Shaker Glen Brook, Cummings Brook, and Little Brook.

For more details concerning river geometrical characteristics, please refer to the F.E.M.A. studies listed in the reference section.

II.1.1.4 Water Sources

The source of surface water within the watershed is primarily precipitation which drains to the river through man-made drainage facilities or through the ground. Although the relief of the watershed is generally flat, a quick storm flow response can be expected from the urban areas, due to the drainage facilities. The water supply to the river between storm events would primarily come from the groundwater system.

Groundwater circulation within the watershed is characterized by recharge areas in the upland areas near the groundwater divide (near the watershed boundary) and discharge areas of the Aberjona River. (Reynolds, 1993) Upon reaching the stream, the groundwater flow will, under most conditions, converge upward and discharge toward the river. During times when the river stage increases rapidly, however, the groundwater contribution can be significantly reduced (Brainard, 1990; Reynolds, 1993) or may even reverse (Reynolds, 1993) resulting in a loss of river water to the groundwater system.

II.1.1.5 Anthropogenic Contamination

The Aberjona River watershed has been subject to contamination via industrial effluent and land disposal of toxic chemicals. Primary sources of metals include numerous former leather tannery operations (Durant, et. al, 1990), chemical plants (Aurilio, 1992) and automobile emissions. At present, there are two federally-designated, and over 20 state-identified hazardous waste sites in the Aberjona, some of which contain large quantities of toxic metals, including chromium, arsenic, and lead. (Aurilio, 1992) The federally-designated sites (figure II.1-2) are known as: 1) Industriplex Superfund site, located in the northern part of the watershed, north of the confluence of Hall's Brook with the Aberjona River and east of Halls Brook, and 2) the Wells G & H Superfund site, located in the wetland area on the Aberjona River between Route 128 and Montvale Avenue.

Records indicate that the predominant time period of metal contamination from the leather tannery was from the early 1900's to the 1930's. (Durant, et. al., 1990) During this time, the tannery industry was very productive and leather finishing wastes were discharged into surface water bodies and into sludge lagoons and dumps. The primary method of tanning during this period was chrome-tanning which subsequently resulted in the discharge of considerable quantities of chromium used for processing the hides and in discharges of cadmium, chromium, iron, lead, arsenic, and copper associated with the use of dyes, hide preservatives, and depilatories. (Durant, personal conversation) By the mid-1930's most of the tannery and leather finishing companies within the watershed were connected to sewerage systems. (Durant, et. al., 1990)

Significant arsenic contamination within the watershed is associated with sulfuric acid and arsenical pesticide manufacturing, and to a lesser degree, the tanning industry. (Aurilio, 1992) The arsenic associated with sulfuric acid manufacturing is derived from the burning of pyrites which contained many impurities including arsenic, zinc, copper, lead, and magnesium. As much as 200 to over 700 metric tons of arsenic are estimated to have been released at one site in the watershed. The predominant time frame for sulfuric acid and arsenical pesticide manufacture is from the late 1800's to the early 1930's.

II.1.1.6 Metals Reconnaissance

Bottom Sediments

A metal reconnaissance of river and lake bottom sediments (Knox, 1991; Spliethoff & Hemond, 1994; Zeeb, 1994) has revealed a widespread distribution of metal contamination along the Aberjona River. Within the bottom sediments of the Aberjona River, the highest metal concentrations were generally observed in the sediment deposits of the Wells G & H wetlands area. Maximum concentrations of surficial sediments within the wetlands for arsenic, chromium, copper, lead, zinc, iron, and manganese were measured as 1000 mg/kg, 3400 mg/kg, 800 mg/kg, 1000 mg/kg, 3500 mg/kg, 12 %, and 1%, respectively. Higher concentrations have been detected at depth in cores taken within the peatland deposits of Wells G & H and within the lake bottom sediments of the Upper Mystic Lakes.

In general, bottom sediment concentrations in the Horn Pond Creek drainage area tend to be lower than trace metal concentrations in the Aberjona River. With the exception of lead, many of the river bottom samples within the Horn Pond area are not orders of magnitudes above estimated background concentration values. (Knox 1991; Spliethoff & Hemond, 1994)

Surface Waters

As part of an urban runoff study in the watershed (Fratoni, et. al., 1982) metal concentrations were measured in the surface waters of the Aberjona River during 1981. Samples were collected during both wet weather and dry weather conditions. A total of 5 to 20 samples were analyzed for each metal. For these samples the concentrations ranged from:

	Wet Weather	Dry Weather
Location: Confluence of Halls Brook & Aberjona River		
Arsenic	4 - 45 µg/l	7 - 40 µg/l
Cadmium	< 10 - 10 µg/l	< 10 - 10 µg/l
Chromium	< 20 µg/l	< 20 µg/l
Iron	2.3 - 3.2 mg/l	1.4 - 2.6 mg/l
Copper	250 - 300 µg/l	< 10 to 10 µg/l
Lead	3 - 100 µg/l	< 30 to 30 µg/l
Zinc	90 - 210 µg/l	20 - 130 µg/l
Location: 2600 ft Upstream of the Mystic Lakes		
Arsenic	4 - 18 µg/l	2 - 20 µg/l
Cadmium	< 10 - 10 µg/l	< 10 - 10 µg/l
Chromium	< 20 µg/l	< 20 µg/l
Iron	0.62 - 2.4 mg/l	0.05 - 1.3 mg/l
Copper	10 - 410 µg/l	< 10 - 20 µg/l
Lead	30 - 180 µg/l	< 30 - 40 µg/l
Zinc	30 - 140 µg/l	10 - 60 µg/l

Results of Fratoni, et. al., 1982 also indicate that metal concentrations (except for lead) decrease in the downstream direction. This trend was attributed to both dilution by downstream waters and to the settling of particulate metals within the river channel. Furthermore, Frantoni, et. al., 1982 noted that wet weather concentrations for copper, iron, lead, and zinc were generally higher than dry weather implicating runoff as an important source.

An investigation analyzing arsenic concentrations in three lakes of the Aberjona River found considerable differences in arsenic concentrations. (Aurilio, 1992) The most contaminated lake investigated was the Halls Brook Storage Area. The Halls Brook Storage Area is an artificial 9 hectare impoundment, located just outside the boundaries of the Industri-Plex Superfund site. It drains the northwestern part of the watershed and discharges into the Aberjona River just north of Route 128. For the Halls Brook Storage Area concentrations of arsenic were observed to decrease in the downstream direction. The highest concentration detected was observed on the upstream end and was measured as 83 μg/l. This value is contrasted with the maximum concentration observed at the downstream end which was measured as 10 μg/l. A mass balance for arsenic within the storage area indicates that most of the arsenic that flows into the storage area (98 grams/day) is deposited in the lake bottom prior to discharging into the Aberjona River. As a result of the arsenic deposition in the Halls Brook Storage Area there is a potential for resuspension of the arsenic, especially during storm conditions.

Arsenic concentrations at the other two lakes, the Upper and Lower Mystic lakes, were much lower. The Upper Mystic Lake drains the Aberjona River at its downstream end. The Lower Mystic Lake is immediately downstream of the Upper Mystic Lake. Concentrations of the epilimnetic waters of each of the lakes were measured at roughly 1 and 0.5 μg/l, respectively. A mass balance of the Upper Mystic Lake also indicates that roughly one half of the arsenic that flows into the lake is deposited to the lake bottom.

II.2 A PRELIMINARY ANALYSIS

II.2.1 Metal Concentrations

II.2.1.1 Reference Table for Background Concentrations

A reference table for background concentrations is included in this section. (table II.2-1) Concentrations included in this table provide a rough estimate (order-of-magnitude) of background concentrations for dissolved and particulate material in the surface waters of the watershed. Concentrations were compiled from three sources: 1) concentrations at the inlet to Horn Pond, 2) comprehensive river water studies, and 3) mean crustal concentrations. The justification for using each of these sources of information is as follows:

1) Since concentrations on the Horn Pond side of the watershed tend to be the lowest within the watershed (except for lead), it is assumed that this area of the watershed has been impacted to a lesser degree by anthropogenic contamination than other areas. If it is assumed that natural conditions at Horn Pond are representative of natural conditions for the entire watershed, then measured concentrations in the vicinity of Horn Pond can be assumed to represent an upper-bound for natural background metal concentrations.

2) Comprehensive studies which measure elemental concentrations in unpolluted river waters can be used to estimate natural background concentrations of individual rivers, if it is assumed that natural conditions of individual rivers do not deviate significantly from the world average. In some cases, however, when a particular element is geochemically enriched, strong deviations may be expected.

   One of the most comprehensive studies of world river waters which investigated concentrations in both the dissolved and particulate phases was compiled by Martin and Meybeck, 1979. In their compilation, highly polluted rivers were discarded and therefore the composition reported should closely represent the *natural* composition of world river waters.

3) The chemical abundance of elements in continental crust may provide an indication of whether or not metal concentrations of river suspended sediments are strongly elevated. Taylor, 1964, provided a comprehensive list of average concentrations for

69 elements. Taylor's list can be used to estimate background concentrations for elements not included in comprehensive river studies.

From table II.2-1, mean river suspended sediment concentrations were within an order of magnitude of mean crustal averages for all elements listed except, Sb, Pb, and U. The exceptions may be indicative that either: 1) river suspended sediments on average are generally enriched in Sb, Pb, and U, or 2) the river suspended sediment samples used in the comprehensive river studies were contaminated.

Suspended sediment concentrations at Horn Pond were generally lower than either average river suspended sediment concentrations or mean crustal concentrations. Exceptions include: 1) Mn, Fe, Mo, Sb which were at similar or slightly higher concentrations, and 2) Zn, As, Se, Br, and Au which were significantly higher. The high concentrations for Zn, As, Se, Br, and Au indicate that these metals are either naturally or anthropogenically enriched at Horn Pond.

For the dissolved phase, Horn Pond metal concentrations were lower or at similar values as the concentrations given for mean river waters. The exceptions include: Fe, Ni, and Au which are at levels significantly higher than mean river water.

Element	River Water Dissolved Phase, µg/l		River Water Particulate Phase, mg/kg		
	Horn Pond[1]	World Average[2]	Horn Pond[3]	World Average[2]	Crustal Ave[4]
Na		5,100	2,238	7,100	23,600
Mg		3,800		11,800	23,300
Al		50	8,393	94,000	82,300
Si		5,420		285,000	281,500
Cl					130
K		1,350	4,667	20,000	20,900
Sc		0.004	3.4	18	22
Ti		10	1,464	5,600	5,700
V	1.95	1.0	81	170	135
Cr	< 0.2 [7]	1	48	100	100
Mn	7.33	8.2	1140	1,050	950
Fe	210 [7]	40	66,334	48,000	56,300
Co		0.2	16.3	20	25
Ni	12.5	2.2		90	75
Cu	2.7 [7]	10		100	55
Zn	2.9	30	563	350	70
Ga		0.09	1.38	25	15
As	0.3 [7]	1.7	31	5	1.8
Se			6.7		0.05
Br		20	45	5	2.5
Rb		1.5	15	100	90
Sr	11.8	60		150	375
Mo	0.08	0.5	4.05	3	1.5
Cd	0.68 [7]	0.1 [6]		1	0.2
Sb	0.01	1.0	2.1	2.5	0.2
I	4.9				0.5
Cs		0.035	1.33	6	3
Ba		60	218	600	425
La	0.02	0.05	19	45	30
Ce	0.02	0.08	31	95	60
Nd		0.04	17	35	28
Sm		0.008	2.8	7	6.0
Eu		0.001	0.4	1.5	1.2
Gd		0.008	2.5	5	5.4
Tb		0.001	0.4	1.0	0.9
Yb		0.004	0.9	3.5	3.0
Lu		0.001	0.2	0.5	0.50
Hf			0.6	6	3
Ta			0.8	1.25	2
W			1.2		1.5
Au	0.04	0.002	0.024		0.004
Tl	0.01	0.01-1 [6]			0.45
Pb	0.65	1.0		150	12.5
Th		0.1	3.4	14	9.6
U		0.04	0.95	30	2.7

[1]Sample Collected Oct.12,'92 & Analyzed by ICP-MS
[2]Martin & Meybeck, 1979
[3]Sample Collected March 29 1992 & Analyzed by NAA
[4]Taylor, 1964
[5]Sample Collected Nov.1,'92& Analyzed by GFAA
[6]Merian, 1991
[7]Mean of 12 Samples Collected 2/92 - 1/93, Fe Analyzed by ICP-AES, Cu & Cr Analyzed by GFAA, As Analyzed by HGAA

Table II.2-1: Reference Table for River Water Background Concentrations

II.2.1.2 Inventory of Metals in River Water Column

An inventory of elemental concentrations in the river water (dissolved and suspended) was developed: 1) to determine which elements are present in elevated concentrations within the surface water system, and 2) to aid in the selection of a few metals which will be included as part of a more in-depth sampling program in the present study.

Metals (and elements) chosen for analysis were those metals which were easily analyzed given the instrumentation and resources available. Analytical techniques included: 1) Atomic Absorption Spectroscopy with Graphite Furnace Atomization, 2) Inductively Coupled Plasma - Atomic Emission Spectroscopy, 3) Inductively Coupled Plasma - Mass Spectroscopy, and 4) Neutron Activation Analysis. Discussion concerning each of the techniques are included in section III.4.3 and in appendices III.E and III.F. Results of analysis are summarized in figure II.2-1 for the dissolved phase and in figure II.2-2 for the particulate phase[2]. Numerical values of the analytical results are given in appendices III.E and III.F.

For the dissolved phase, Ti, Cr, Mn, Ni, Cu, Zn, As, and Pb were detected at levels higher than mean river concentrations by at least a factor of 2. Fe, Co, and Au were detected at concentrations higher than mean river water by at least an order of magnitude.

For the particulate phase, Cr, Mn, Fe, Mo, Sm, W, Pb, and U were elevated above mean crustal averages (Taylor, 1964) by at least a factor of 2. Cl, Co, Cu, Zn, As, Se, Br, Cd, Sb, and Au were detected at levels at least one order of magnitude higher than mean crustal concentrations. Causes of elevated concentrations may be due to a natural enrichment or may be due to an anthropogenic influence.

[2]In separating samples between the operationally defined "dissolved" versus "particulate" phase, different filter sizes and media were used for different analytical methods. Please refer to chapter III and appendices III.E and III.F for details.

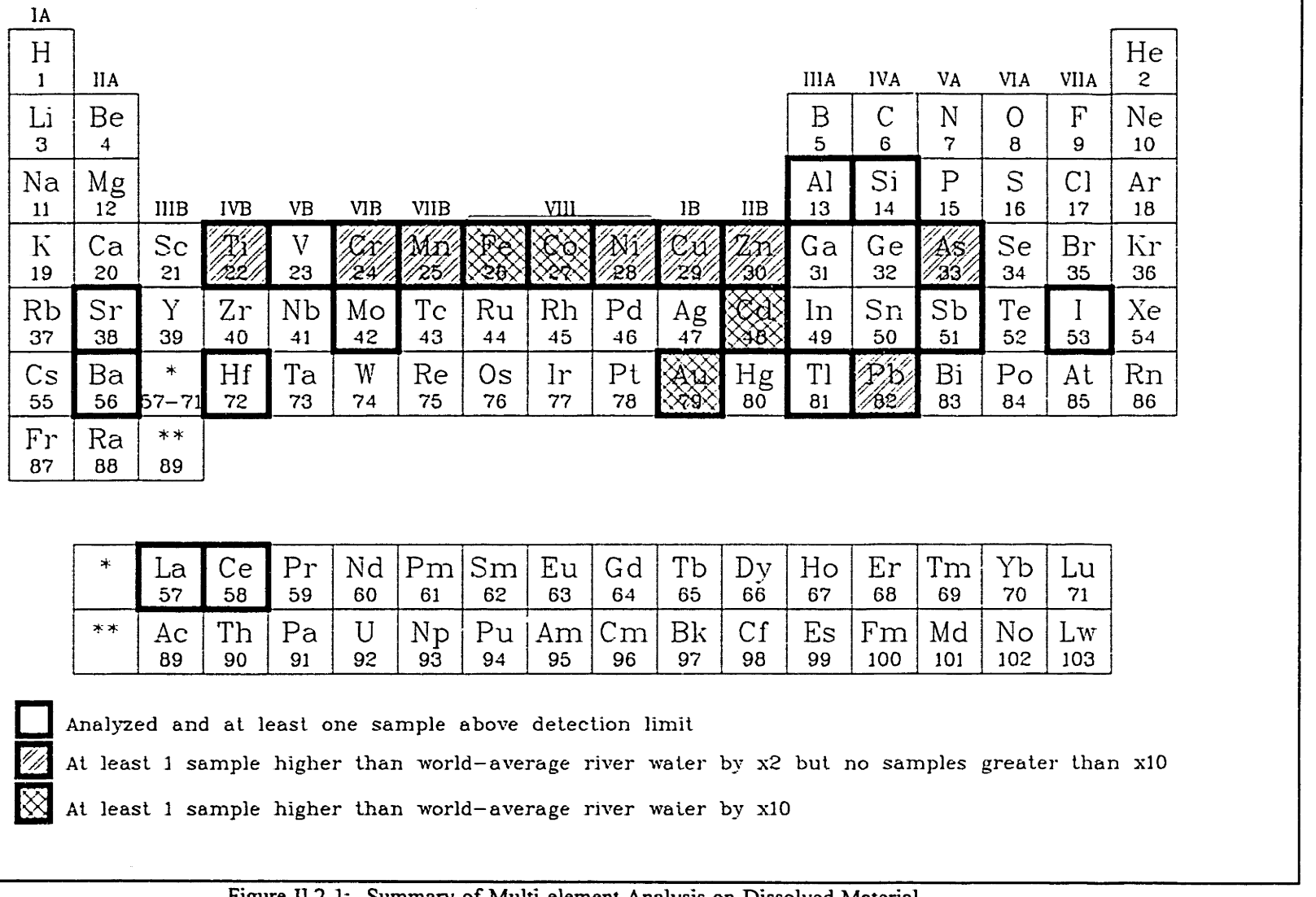

Figure II.2-1: Summary of Multi-element Analysis on Dissolved Material

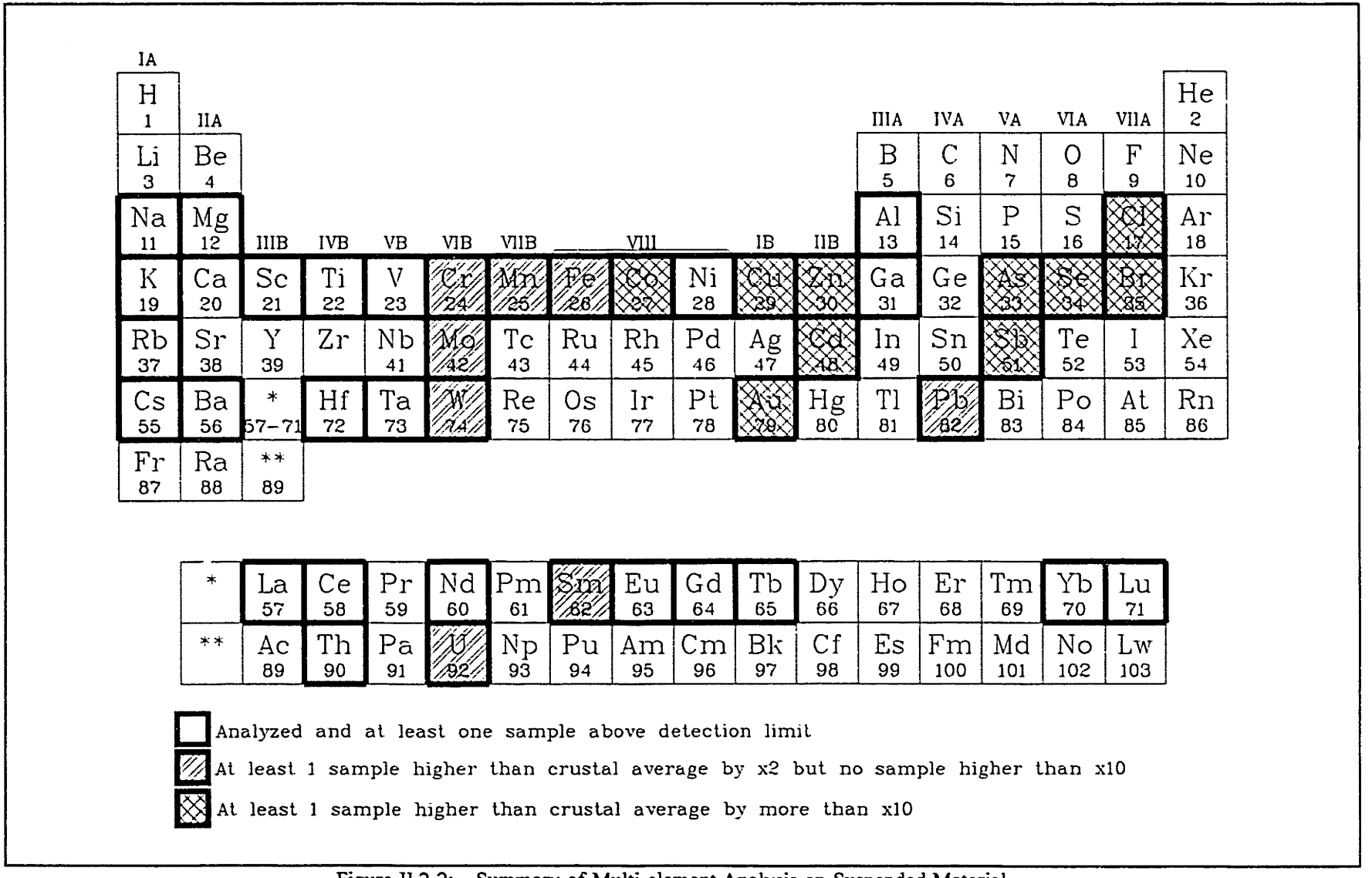

Figure II.2-2: Summary of Multi-element Analysis on Suspended Material

II.2.1.3 Metals Chosen for More In-depth Research

The metals, **arsenic, chromium, copper,** and **iron,** were chosen for the current research to enhance our understanding of metal transport processes.

All four metals were detected at concentrations significantly above background concentrations. Arsenic and chromium are of interest because of their association with the long history of industrial contamination within the watershed.

Copper was chosen because its transport may be dominated by a mechanism that is different than that for arsenic and chromium. This notion is supported by the observations of Fratoni, et. al., 1982, who found that the highest concentrations of copper were transported during wet weather flows whereas for arsenic and chromium there was no strong difference between wet weather and dry weather concentrations. Such a result suggests that surface runoff is a strong source of copper but not necessarily a strong source of arsenic and chromium.

Iron was chosen for study because of its potential to scavenge metals from the water column (Dzombak & Morel, 1990) and therefore alter the transport of other metals.

II.2.2 Bedload

For the Aberjona River, a preliminary investigation indicated that transport of metals in association with bedload sediments is negligible. This finding is supported by: 1) attempts to sample the bedload (using a Healy-Smith bedload sampler) which resulted in a negligible quantity of bedload sediment mass transport compared to suspended sediment, and 2) visual observation of the channel bottom during low and high flows which showed no evidence of significant bedload transport. Furthermore, metal analysis of different size fractions of the river bed sediments indicated that metal concentrations strongly increase as particle size decrease. (See appendix III.G) Therefore, the bulk of the metal transport would be associated with the sediment fines, which would quickly become entrained as suspended sediment upon increasing flow conditions.

II.2.3 Chemical Factors

Our interpretation of the data collected in this study is that physical processes (e.g. conservative mixing of different waters) rather than chemical factors are the primary cause of the large shifts in the partitioning of metals between the dissolved and particulate phases observed during storm conditions. Implied in this interpretation is that the phase association of a metal (whether associated with the dissolved or particulate phase) will not change significantly *through chemical interactions*. Such an assumption does not rule out that equilibrium (low flow) partitioning may be controlled by chemical factors; it merely states that when the partitioning changes, chemical factors are not the likely cause.

To support this interpretation, the data indicate that during storm conditions, when the partitioning of metals between the dissolved and particulate phase changes the most, the chemical status of the water appears to be constant as given by relatively constant values of river water pH, total organic carbon, and water temperature. (See appendix III.F) River water conductivity, on the other hand, was observed to vary. However, the shift in the partitioning was the opposite of what would be expected from the conductivity change. One may consider, for example, that as the salt content of a river water increases, its conductivity should also increase. Because of the coagulative properties of salt solutions (Sholkovitz & Copland, 1981) one would therefore expect colloidal metals within the "dissolved"[3] phase to coagulate into larger filterable "particulates." The net result should be a shift in metal concentration toward the particulate phase as the conductivity increases. However, the measured data (appendix III.F) illustrate the opposite trend: a strong decrease in conductivity during peak flows when metals are most strongly partitioned toward the particulate phase.

The assumption of limited phase exchange may be further substantiated if one recognizes that metals may not always be readily available or exchangeable into a form which quickly undergoes chemical reactions. With regard to availability, the distribution of metals within a water system can be broadly subdivided into the following three categories: 1) in solution or within the ion-exchangeable fraction of solids, where they are readily available, 2) in organic materials or metallic hydroxides, where chemical changes are required before they are released, so they are less available, and 3) in the crystal structures of suspended material, where they are nearly unavailable in nature. (Gibbs, 1973) Thus the most efficient exchange mechanism (between dissolved and particulate phases) would be associated with the ion-exchangeable fraction of the particulate load. Preliminary results from a sequential extraction of river bottom fines suggest that a very small fraction of the metal load is ion-exchangeable, whereas

---

[3]Colloidal metals are very likely incorporated within our operationally defined "dissolved" phase (filterable using 0.5 μm pore size filter).

the bulk of the metals are associated with organic matter or metallic coatings. (See appendix III.G) These results indicate that relatively complex chemical reactions are required before metals are released from the particulate phase. These reactions would include oxidation for the release of organically bound metals and reduction for the release of metals associated with metallic coatings. Furthermore, considering the relatively short travel time of the river water along the Aberjona during storm conditions (≈6 hours), even if the oxidation/reduction potential of the river water and its metal sources differ along the river's length, the amount of metal converted from one phase to the other could very possibly be limited by the kinetics of the reaction.

Without further investigation, the assumption of limited phase exchange will be considered valid. In other words, during storm conditions, once a metal enters the river in the dissolved phase it will be assumed to remain dissolved and once a metal enters the river in the particulate phase it will be assumed to remain particulate.

Therefore, the monitoring program will not focus on the chemistry of the river system but rather on the physical process which govern transport. For modeling purposes, partitioning will be assumed to be a property of the waters supplying the river during low flow conditions. The mixing of different water sources, each with different dissolved to particulate metal ratios, will be used to model transport during storm conditions.

III. MONITORING PROGRAM

III.1 INTRODUCTION

The monitoring program was initiated with the specific purposes of:

1) Identifying controlling factors responsible for the transport of metals in the watershed,
2) Developing relationships between these controlling factors and metal mobility,

In determining which parameters to measure, it is useful to separate the total metals flux, F_t into two[4] components as:

$$F_t = F_d + F_p$$

where: F_d = Dissolved Metal Flux, (mass dissolved metal/time)
F_p = Particulate Metal Flux, (mass suspended metal/time)

One can then subdivide F_d and F_p into components:

$$F_d = [M_d]Q \quad \text{and} \quad F_p = [M_p][SS]Q$$

or

$$F_t = [M_d]Q + [M_p][SS]Q$$

where: $[M_d]$ = Metal Concentration in the Dissolved Phase (mass dissolved metal/volume river water)
$[M_p]$ = Metal Concentration in the Particulate Phase (mass particulate metal/mass sediment)
[SS] = Suspended Sediment Concentration (mass suspended sediment/volume river water)
Q = Streamflow (volume river water/time)

As written the expression for F_t above appears to be relatively simple with $[M_d]$, $[M_p]$, [SS], and Q as controlling factors for metal transport. However, the difficulty in obtaining metal fluxes from these components occurs when F_t must be estimated over long (yearly) time scales. Early observations showed that the fluxes varied significantly during time scales of the order of hours, and that neither baseflow

[4]Metal transport associated with bedload sediments is assumed to be negligible, (See section II,3,2)

nor stormflow dominated metal transport. In addition, results indicated that metal fluxes varied significantly from location to location within the watershed and that relative changes in F_i for a given location were due: 1) primarily to changes in Q, 2) secondarily to changes in [SS], and 3) thirdly due to changes in $[M_d]$ and $[M_p]$.

With these observations, the monitoring program was designed to focus on measurements of $[M_d]$, $[M_p]$, [SS], and Q at various locations with the intent of developing relationships that could model fluxes using an hourly time step during both low and storm flows. These primary efforts included:

1) Continuous monitoring of Q on an hourly time scale at the 5 monitoring stations.
2) Continuous monitoring of [SS] on an hourly time scale at gage 5.
3) Collection of instantaneous samples on monthly time intervals at the 5 monitoring stations. These samples were then analyzed for $[M_d]$, $[M_p]$, and [SS].
4) Collection of sample sets on an hourly time scale during low and high flow conditions at gage 5. These samples were then analyzed for $[M_d]$, $[M_p]$, and [SS].

Additional data collection was performed such that the factors controlling the time variation of $[M_d]$, $[M_p]$, [SS], and Q could be better understood. These additional efforts, either routine or occasional, included:

1) The compilation of precipitation data.
2) Measurements of suspended sediment physical parameters, including volatile solids, particle size, and microscopy analysis.
3) Measurement of additional water parameters, including pH, temperature, conductivity, and dissolved organic carbon.
4) Analysis of river bottom sediments, including particle size analysis, specific gravity analysis, volatile solids analysis, x-ray diffraction analysis, and a series of sequential extractions for metals.

For purposes of organization the description of the monitoring program is ordered in a "cause & effect" sequence. A primary hydrologic input into the watershed is precipitation (section III.2). Precipitation strongly affects streamflow (section III.3) which then influences the transport of suspended sediment and metals. (section III.4)

III.2 PRECIPITATION

The data discussed in this section have been obtained by either government agencies or private consulting firms. Precipitation monitoring by these sources includes point precipitation gaging stations located within or near the watershed, and a temperature gaging station located within the watershed. Although temperature is not a measurement of precipitation, it is included with the precipitation data because it helps to determine whether precipitation occurred as rain or snow.

The locations of each rain gaging station and the temperature gaging station are illustrated in figure III.2-1. A more detailed description of each station follows.

III.2.1 Point Precipitation Gaging Stations

- *Reading Station (NCDC)*: This station is located in the northern area of the watershed at latitude 42-31 and longitude 71-8W. The data are collected using two gages. The first is a standard rain gage (installed in 1957) used to collect daily values, while the second is a weighing bucket rain gage (installed in 1981) used to collect hourly values. Approximately 35 years of daily precipitation and 11 years of hourly precipitation are available at the site.

  This station is funded by the National Climatic Data Center (NCDC) and data collection is conscientiously performed by Mr. R.E. Lautzenheizer, climatologist. Data are available through either the NCDC or by writing to Mr. Lautzenheizer at 35 Arcadia Ave., Reading, MA 01867.

  Period-of-record data up to September 30, 1993 are available in digital format in appendix IV.C. Additionally, some of the data are discussed in section IV.1 and are plotted in appendices IV.A and IV.B.

- *Reading Station (100 acre Pumping Station)*: Daily rainfall is monitored at the water supply pumping station for the Town of Reading. This station is located within one mile of the northern part of the watershed. Daily rainfall data dating back to 1899 are available at this location and are available in the *Town of Reading, Annual Reports*. Average monthly values from 1899 to 1957 are included in appendix IV.A.

- *Winchester Station*: The Winchester gaging station has been in operation since 1875. The station has been located at 15 Lake Street in Winchester, Massachusetts, from September 1977 to the present. Prior to 1977 the station was located at the Water Department Shop.

  Daily precipitation values are monitored at this station. Monthly values for the entire period of record are given in appendix IV.A and discussed in section IV.1. Daily precipitation records from January 1964 are available through the Massachusetts Commonwealth Office, Department of Environmental Management, Division of Water Resources, Boston.

- *Burlington Station*: Hourly data were recorded from August 1988 to August 1990 by consultants from Camp, Dresser, and McKee. These data were needed for a runoff study conducted by the firm. The station was located within the watershed at 3 Rolling Lane in Burlington, Massachusetts.

III.2.2 Temperature Gaging Station

- *Reading Station (NCDC)*: The location of this station is described above. Daily maximum, minimum, and continuous air temperature measurements have been monitored at the NCDC Reading station since 1957. Continuous temperature data are measured using a thermograph. Maximum and minimum temperatures are measured using max/min thermometers. The mean daily temperature reported for this station is the average of the maximum and minimum daily temperatures.

  Continuous temperature data are available exclusively through Mr. R.E. Lautzenheizer and daily maximum-minimum data are available through the NCDC or from Mr. Lautzenheizer. Hourly temperature data for the 1991, 1992, and 1993 winter months are included in appendix V.B.

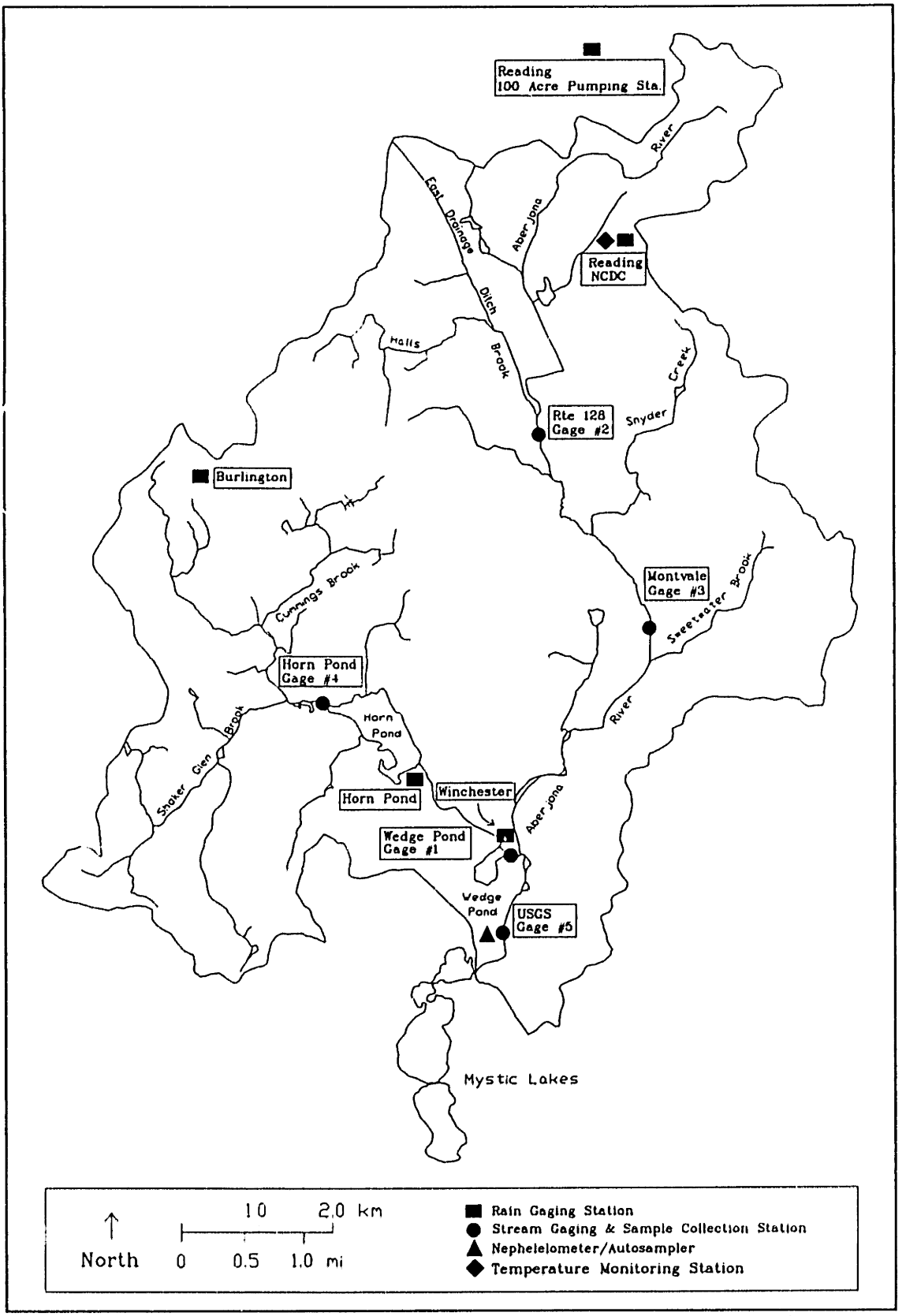

Figure III.2-1: Locations of In-Field Monitoring and Sample Collection Stations (Basemap from Durant, 1991)

III.3 STREAMFLOW MONITORING

III.3.1 Introduction

Streamflow has been monitored at 5 gaging stations within the watershed. Four of the gaging stations (gages 1 to 4) are maintained through M.I.T. research, whereas the remaining station (gage 5) is maintained by the United States Geological Survey (USGS gage 01102500).

The M.I.T. stations were installed between January and May 1989 through a prior study (Durant, 1991). During this study, flows were monitored, between January 1989 to December 1990, with the purpose of understanding the spatial and temporal variability of surface runoff within the watershed. Average daily streamflow values corresponding to the 1989 to 1990 period are summarized in the referenced material.

The time period of streamflow data collection for the present study is from January 1991 to January 1993. The purpose of continuing the streamflow monitoring program was to augment the previously established understanding of watershed hydrology and, by the addition of suspended sediment and metals sampling programs, to increase our understanding of metal transport within the watershed. Due to 1) initiation of the suspended sediment and metals sampling programs after January 1991, 2) a shorter time scale for monitoring flows (15 minute intervals rather than hourly), and 3) different data analysis methods, all the streamflow data discussed in the present study correspond to the time period after January 1991.

III.3.2 Streamgage Locations

Location of the stream-gaging stations is given in figure III.2-1. Criteria used in selecting M.I.T. gaging sites included proximity to industrial/hazardous waste sites, spatial distribution and accessibility.(Durant, 1991) Three of the five gages, (#2,3, and 5) are located on the Aberjona River, whereas the remaining two gages, (#1 and 4) are located on the Horn Pond Creek tributary, the main tributary to the Aberjona. The specific gage locations are given as follows:

- *Gage 1 (Wedge Pond Gage)*: Located in Winchester, Massachusetts on the downstream side (east) of the Main Street bridge over Wedge Pond. Located approximately 600 feet upstream of the confluence with the Aberjona River.

- *Gage 2 (Rte 128 Gage)*: Located in Woburn, Massachusetts on the upstream (north) side of the Rte 128 culvert over the Aberjona River. This gaging station is located approximately 600 feet downstream of the confluence of Halls Brook and the Aberjona & approximately 0.5 mile upstream of Wells G & H.
- *Gage 3 (Montvale Gage)*: Located in Woburn, Massachusetts on the upstream side (north) of the Montvale bridge over the Aberjona River. This station is located approximately 1.25 miles downstream of Wells G & H and 0.2 and 2.1 miles upstream of the confluence of Sweetwater Brook and Horn Pond Creek, respectively.
- *Gage 4 (Horn Pond Gage)*: Located in Woburn, Massachusetts on the upstream side (west) of a wooden bridge at the outlet of Fowles Brook into Horn Pond. This station is located approximately 120 feet upstream of the upper forebay of Horn Pond.
- *Gage 5 (USGS Gage)*: Located in Winchester, Massachusetts on the Aberjona River at the intersection of Mystic Avenue (projected) and the Mystic Valley Parkway. Located approximately 2600 feet upstream of the inlet to the Mystic Lakes. Due to the close proximity of the USGS Station (gage 5) to the inlet of the Mystic Lakes, flow measured at this station is considered to be representative of flow from the entire Aberjona watershed.

III.3.3 USGS Streamgaging Station

Method of Streamflow Measurement

Streamflow measurement at the USGS station was effected using two water stage recorders (primary recorder and a back-up) located upstream of a control structure. The stage recorders are housed in a concrete gage house equipped with two stilling wells. Friez FA-3 chart recorders were used to record stage data from 1939 to 1980. After 1980, measurements were made using a Fischer and Porter digital recorder set on a 15 minute punch cycle.

Low-water control is provided by a reinforced-concrete Trenton-type weir, 44 feet long, with a shallow v-crest. The weir has flat sloping abutments flush with the banks. The lower water control submerges at about a 13 foot stage, above which the channel serves as the control. (McDonough, 1983)

The river stage is converted to streamflow through use of a rating curve. Rating curves are obtained from current-meter calibration measurements below 400 cfs and extended above by logarithmic plotting. (McDonough, 1983) A total of 27 different rating tables have been developed for this station.

Calibration is performed once a month by USGS personnel. An area-velocity method is used for the determination of calibration discharge. Velocity and depth determinations are recorded at approximately 30 verticals. Price current meters are used for the velocity measurement. (Zanca, J. 1991, personal communication)

III.3.4 MIT Streamgaging Stations

III.3.4.1 Pre-existing Equipment: An Evaluation

Equipment and installation for stations 1 to 4 were established through a prior MIT study. (Durant, 1991) These gages monitored streamflow through the measurement of depth and velocity at one point within the flow cross-section. The equipment manufacturer recommends using the depth measurement to estimate the cross-sectional area of flow and using both the depth and the point velocity measurement to estimate the average cross-sectional velocity. Specific mathematical relationships referred to as Point Velocity Discharge Measurement (PVDM) equations are recommended by the equipment manufacturers (Marsh McBirney, 1987) for the conversion of depth and point velocity to overall average velocity. The product of the area and average velocity is then used to compute the value of streamflow.

Upon commencement of the current study, the ability to use the existing equipment to measure streamflow was re-evaluated. The depth measurement was found to be a reasonably good means by which flow cross-sectional area could be estimated. Additionally, for two of the stations, depth was also found to be a good indicator of flow. The point velocity measurement, on the other hand, was not a very good indicator of average cross-sectional velocity. Evaluation of velocity distributions in the field indicated that the theory behind the PVDM equations for conversion of point velocity to average velocity was not adequate for the monitoring sections. For further discussion concerning PVDM equations refer to Appendix III.D.

Recognizing the limitations of the PVDM method and being influenced by time and monetary constraints, flow monitoring was continued using the pre-existing equipment. However, the rationale for measuring depth and point velocity are much different in this study than recommended by the equipment manufacturers.

III.3.4.2 Rationale for Measuring Depth and Point Velocity

To determine which parameters to measure for the estimation of discharge, one approach is to recognize that:

$$Q = AV$$

where: Q = Flow

A = Cross-sectional Area of Flow

V = Average velocity in the cross-section

For measurement purposes, the channel geometry may be assumed fixed in which case, A is a function of water depth, d_{gage}, at a fixed point in the flow cross-section and:

$$Q = f(d_{gage}, V)$$

The water depth can be measured directly by the equipment employed. However, measurement of V must be performed by making one of three assumptions.

Possible Assumption #1:

The first assumption is that a unique relationship exists between the velocity at one point in the cross-section, v_p, and the overall average cross-section velocity, or:

$$V = f(v_p) \text{ and}$$
$$Q = f(d_{gage}, v_p)$$

However, prior to making field measurements, 1) there is no proof that a unique function between a point velocity and average velocity exists, 2) the relationship between point velocity and average velocity is unknown, and 3) the best location for the point velocity measurement is also unknown.

Possible Assumption #2:

The second assumption for fitting the equipment parameters to the computation of discharge involves the use of Manning's equation which in functional form is expressed as: (modified from Herschy, 1985)

$$V = f(n,A,P,S) \text{ or}$$
$$Q=f(n,A,P,S)$$

where: n = Empirical Roughness Coefficient

A = Cross-sectional Area of Flow

P = Wetted Perimeter of Section

S = Energy Gradient

If the channel geometry is assumed fixed, A and P are uniquely related to water depth, d_{gage}, and:

$$Q = f(n, d_{gage}, S)$$

Changes in "n" may be associated with: a) seasonal changes in vegetation growth within the channel, and b) with changes in sediment sizes that dominate the channel surface before and after storm events. Nevertheless, for further simplification, changes in friction coefficients will be assumed to be of secondary importance and will be assumed to be constant. For a constant n value, the functional flow relationship can be further simplified to:

$$Q = f(d_{gage}, S)$$

One must then assume that the energy gradient, S is a function of a point velocity measurement, v_p, such that:

$$Q = f(d_{gage}, v_p)$$

Possible Assumption #3:

The third assumption, is a modification of assumption number 2 where:

$$Q = f(d_{gage}, S)$$

In the simplest of cases, one may assume that the energy gradient, S, is constant. Such an assumption implies no variable backwater effects relating to conditions downstream. (Herschy, 1985) For this assumption there is a unique stage-discharge relation given in functional form as:

$$Q = f(d_{gage})$$

Discussion of Assumptions

In the case of a section characterizedby a stable stage-discharge relationship, the third assumption would be most appropriate. However, if the flow is a function of factors other than depth, then either assumption #1 or #2 must be applied. For this situation, the weakest functional relationships most likely involve $V=f(v_p)$ or $S=f(v_p)$, respectively.

The important consideration of the above analysis is that a restricting mathematical relationship between discharge and the measured parameters is not postulated prior to performing calibration measurements. Rather a mathematical relationship for converting the measured parameters (z and v_p) to flow is obtained after calibration measurements are completed.

III.3.4.3 Equipment Description

Point depth, d_{gage}, and point velocity, v_p, measurements were obtained using Marsh-McBirney Model 265 streamgages equipped with Coastal Leasing Scarecrow retrofit packages. (figures III.3-1 and III.3-2) The resolution of the depth and velocity measurement was 1 inch and 0.04 ft/s, respectively. The Marsh-McBirney part of the gage consists of a stainless-steel canister which houses an air compressor, pressure transducer, and voltage signal processing electronics. The depth measurements were obtained through use of the compressor and transducer which are connected to an air line with an outlet set at the base of an underwater probe. The compressor forces air through the air line while the transducer measures the line's back pressure. This back pressure reading is then assumed to be proportional to the submersion depth of the tube. Point velocity measurements were made through use of the voltage signal processing electronics which are connected to an electromagnet and electrodes housed in the underwater probe. The electromagnet generates a magnetic field while the electrodes sense the voltage generated by the stream water as it passes through the field. Voltage measurements are converted into point velocity readings through use of Faraday's Law of Induction, which states that the velocity of a conductor is directly proportional to the voltage generated by the conductor as it passes through an electromagnetic field.

The Scarecrow part of the equipment is a microcomputer which stores data in solid-state memory, controls sampling intervals, and provides an interface for initializing the instrument. The solid-state memory eliminates the need for a chart recorder on the original Marsh-McBirney 265 and allows for a much more efficient means of data retrieval. Field data retrieval was performed using Coastal Leasing's Wizard software installed on a Toshiba T1000 portable computer. The collected data were then processed in the lab for conversion to discharge.

All the MIT gages were powered by 12 volt DC deep cycle marine batteries. The only exception occurred during early stages of the monitoring program when gages 1 and 4 were powered from 12 Volt DC power supplies operated from 110 volt AC power. Due to repeated vandalism of power supply lines and occasional fluctuations and surges in AC power, these stations were converted to battery power.

The underwater probe was mounted on a plastic strip which was either tied to the top of a cinder block (Gage 1) or secured to the channel bottom by placing cinder blocks (Gages 2 and 3) or large rocks (Gage 4) on top of the mounting strip. Cinder blocks or rocks placed on top of the mounting strip were located at least 1 foot from the probe to help minimize interferences with probe measurements. Equipment maintenance is described in appendix III.A.

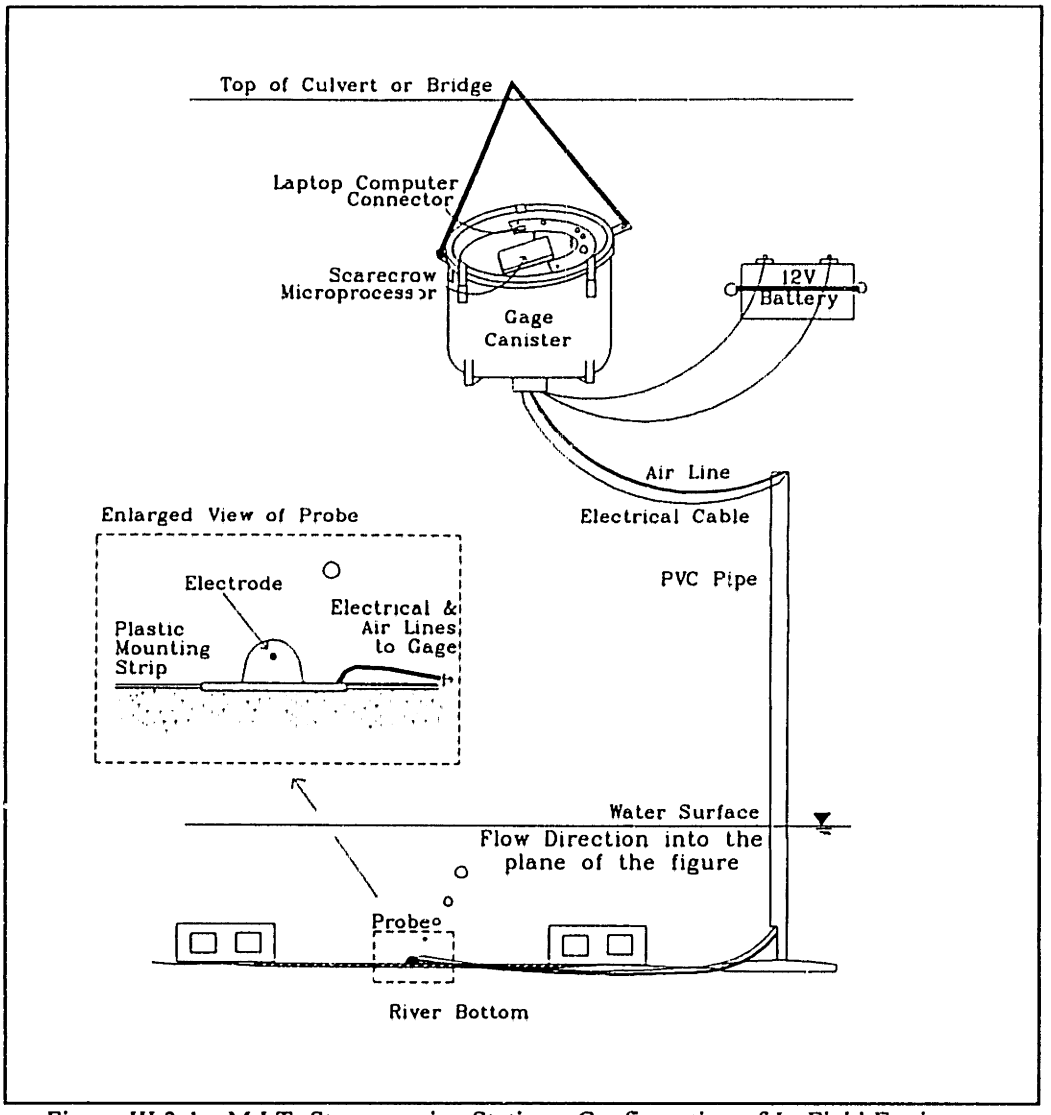

Figure III.3-1: M.I.T. Streamgaging Station: Configuration of In-Field Equipment

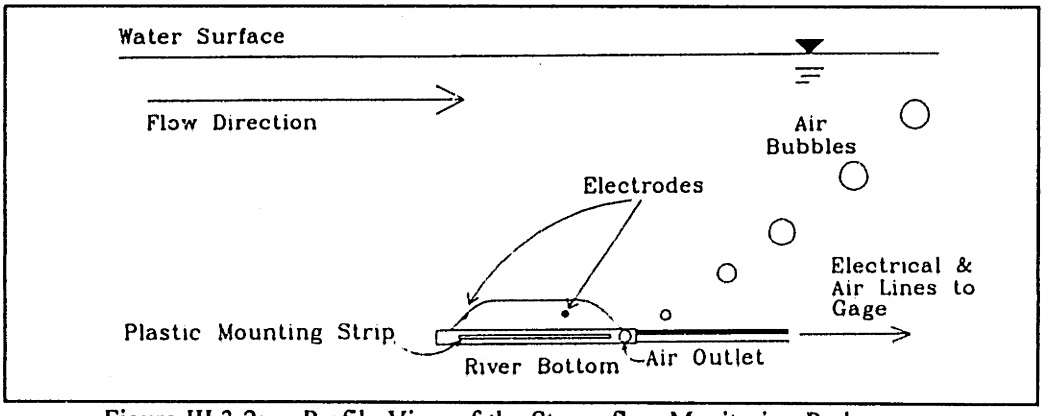

Figure III.3-2: Profile View of the Streamflow Monitoring Probe

III.3.4.4 Calibration

Field Procedure

Determination of the relationship between actual streamflow (also referred to as "manual" streamflow) and measured values of d_{gage} and v_p involved a calibration process which was performed as follows. First, depth and velocity readings were taken at pre-determined verticals across the river cross-section. Location of verticals for each section is indicated in figures III.3-3 to III.3-6 and were identified in the field by hanging a measuring tape across the cross-section. Depth measurements were made using a yardstick, while velocity measurements were made using a Marsh-McBirney 201 electromagnetic current meter mounted on a wading rod. Either one, two, or three velocity readings were taken at each vertical. The number of velocity measurements taken at each vertical depended on water depth, the deeper the water the more velocity measurements taken. Depth of point velocity readings and the vertical averaging procedure were consistent with the 0.6 depth and the 0.2, 0.8 depth methods (Herschy, 1985; Petersen, 1986) The mean-section method (Herschy, 1985) was then used to compute total cross-section streamflow from the depth and vertically averaged velocity measurements.

The only exception to the calibration method described above was for the August 20, 1991 calibration at Gage 3. Due to the deep water and strong current the calibration was performed by attaching the current meter to a high flow sampler. (Figure III.3-7) This sampler was lowered from the bridge at Gage 3 and enabled depth and velocity readings at several verticals across the section.

In order to compare measurements from different calibrations and to determine elevations of the water surface and channel bottom, each calibration cross-section had a vertical, horizontal, and longitudinal control. Definition and locations of control points are described in appendix III.B. The vertical and horizontal control points for each station are also illustrated in figures III.3-3 to III.3-6.

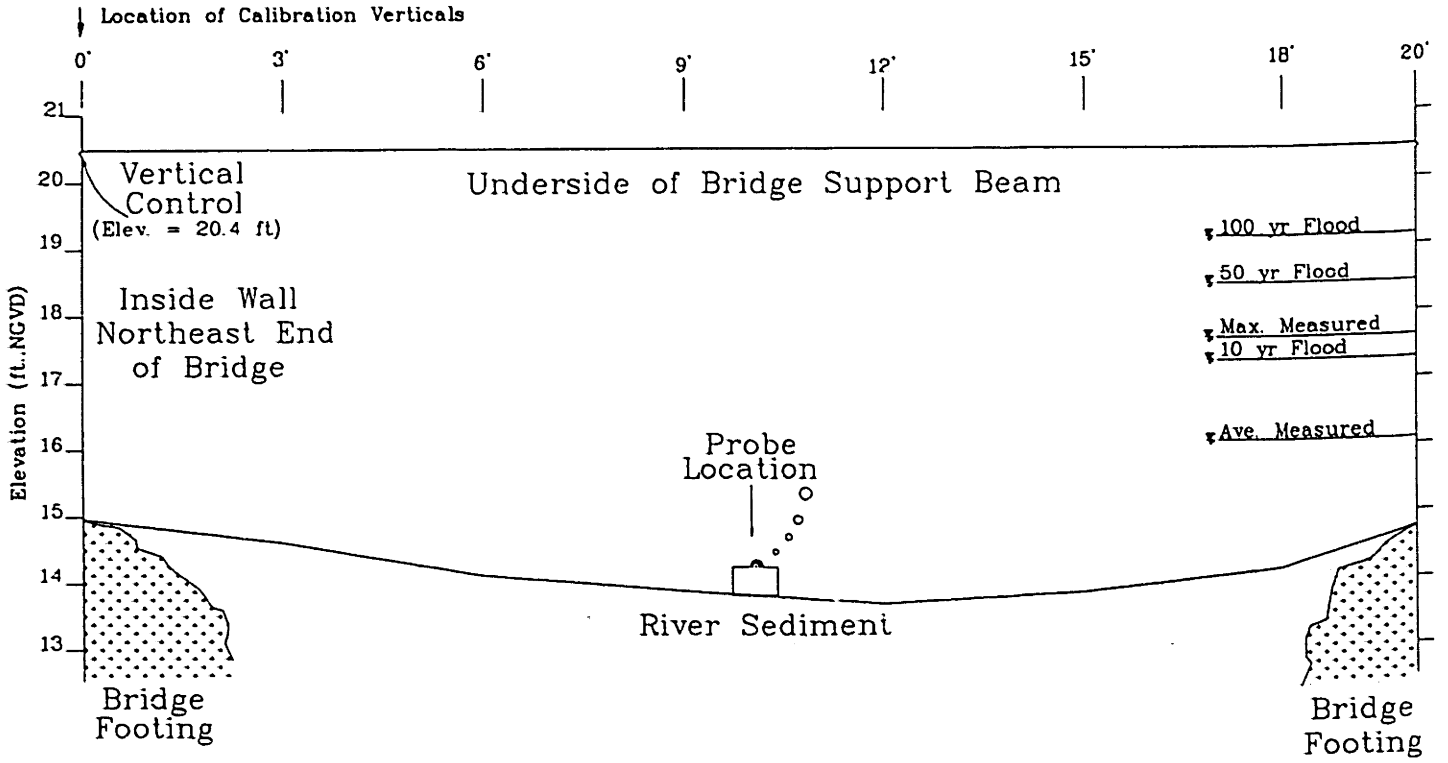

Figure III.3-3: Streamflow Monitoring Cross-section: Gage #1, Wedge Pond

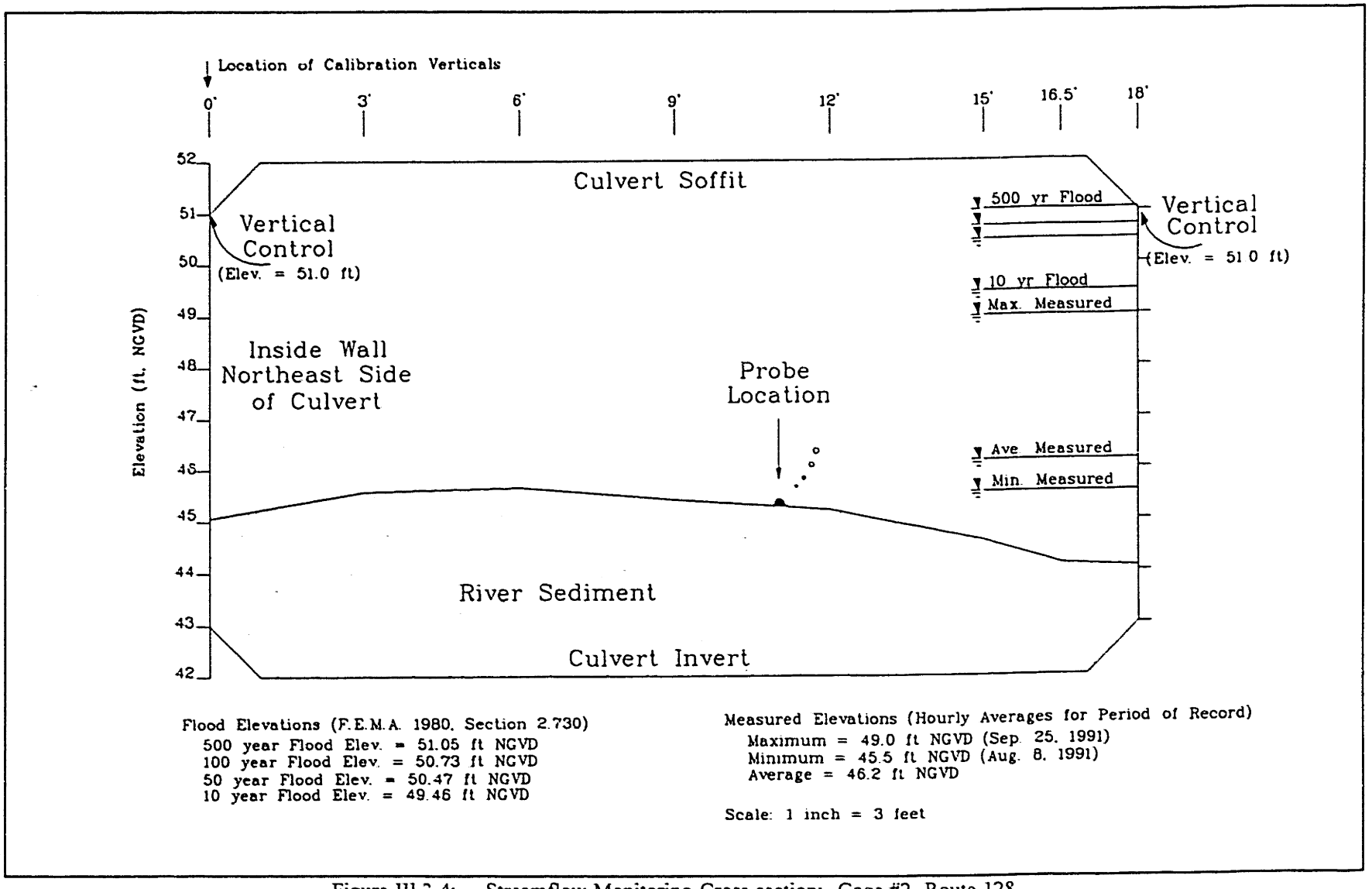

Figure III.3-4: Streamflow Monitoring Cross-section: Gage #2, Route 128

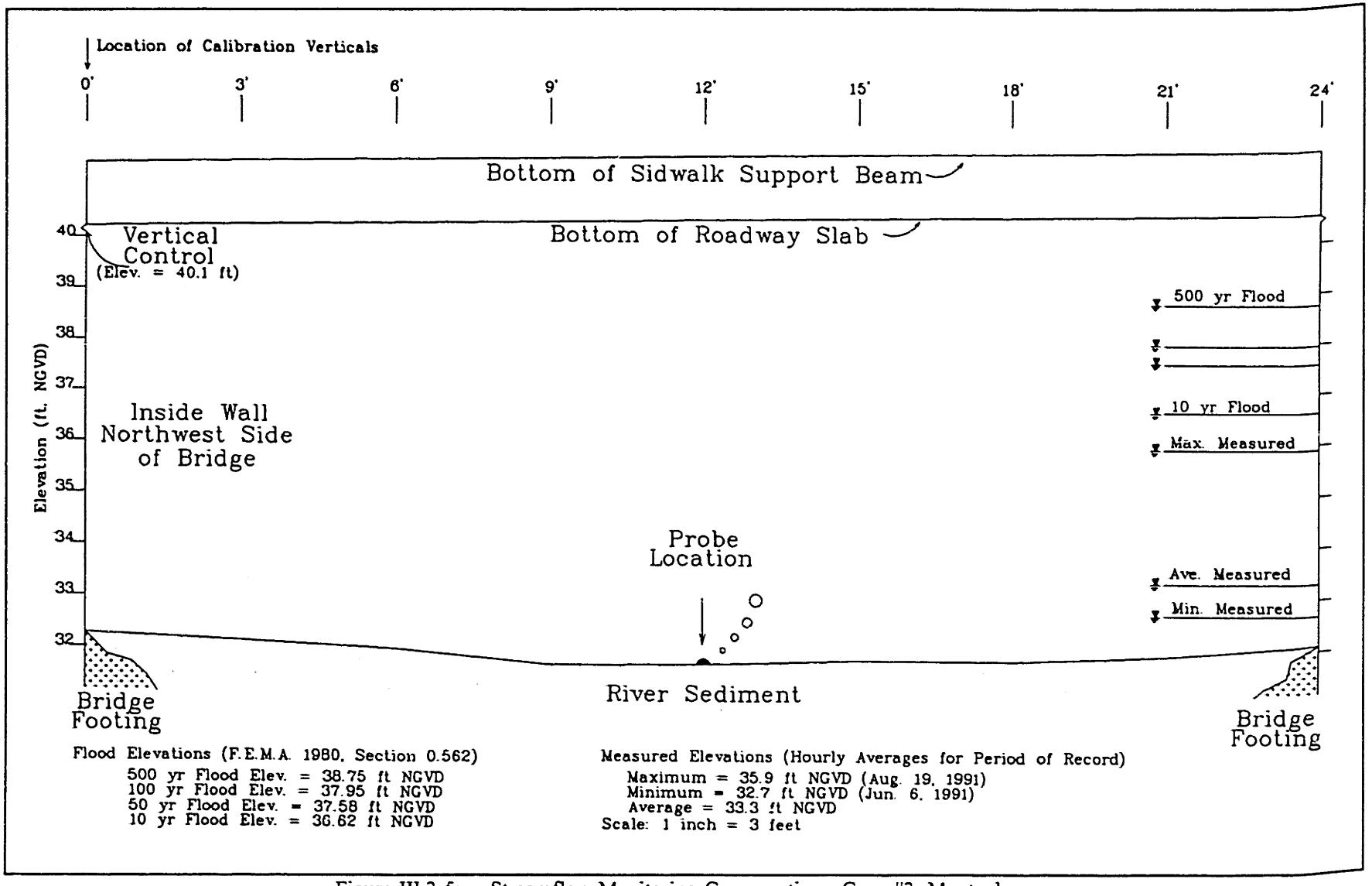

Figure III.3-5: Streamflow Monitoring Cross-section: Gage #3, Montvale

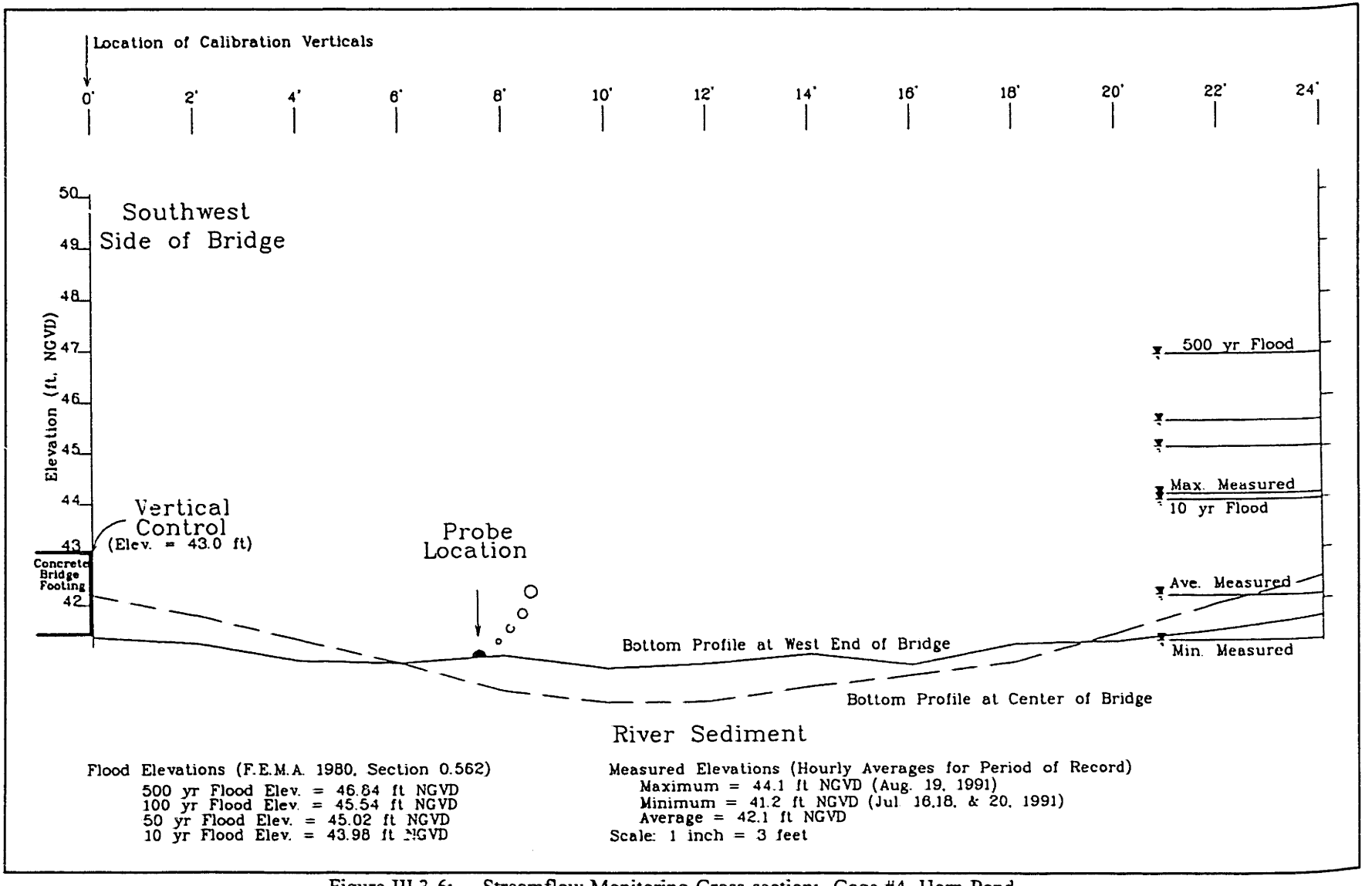

Figure III.3-6: Streamflow Monitoring Cross-section: Gage #4, Horn Pond

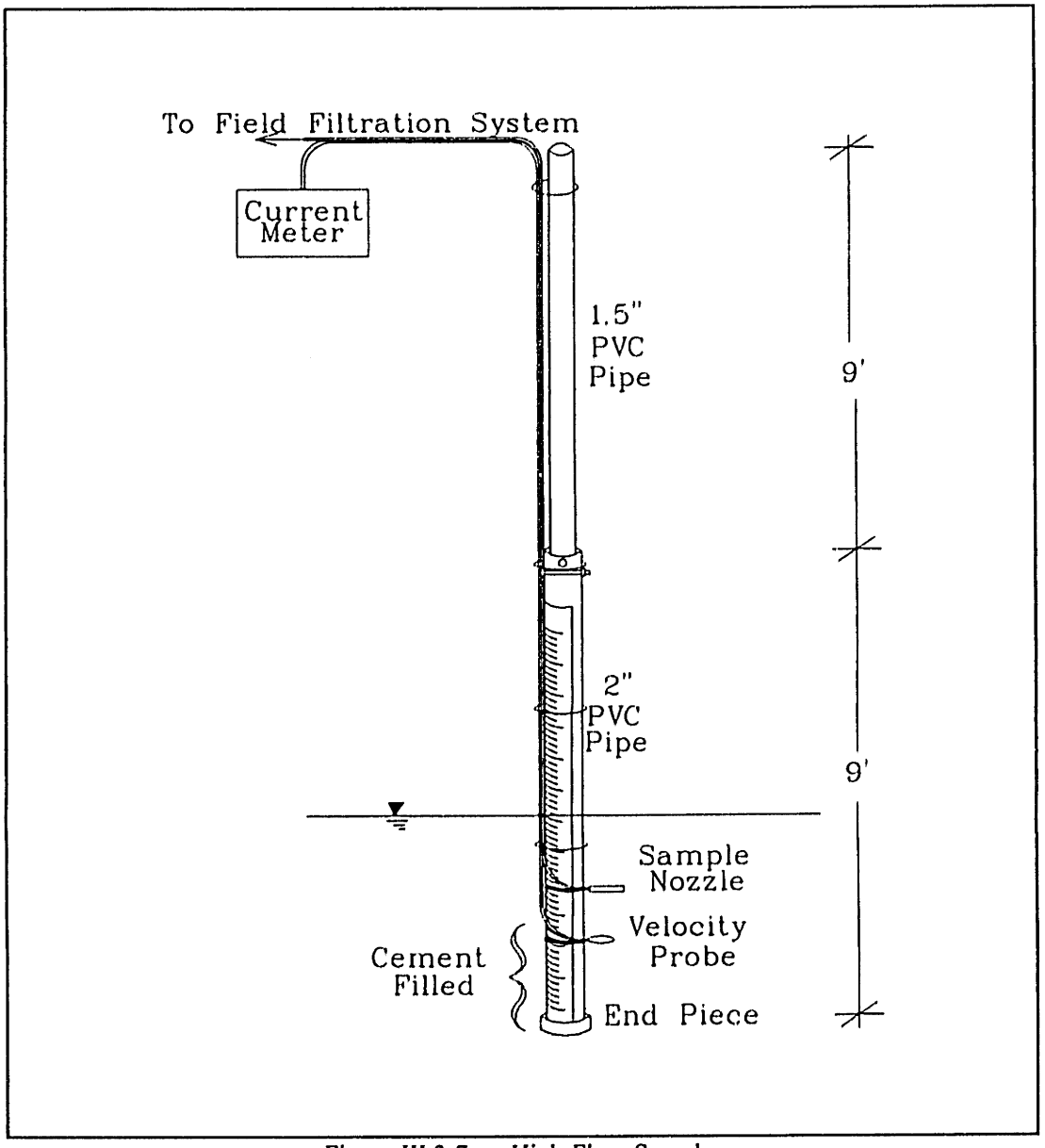

Figure III.3-7: High-Flow Sampler

Preliminary Data Processing

Prior to analyzing the calibration results, preliminary processing of the data was required. Preliminary processing included converting the gage depth reading, d_{gage}, to a depth reading relative to the channel bottom, D. (figure III.3-8) The purpose of this adjustment was to provide a consistent means of comparing water depths due to changes in the probe offset, p_o, (distance between the channel bottom and probe). The velocity measurement, v_p, was assumed to be insignificantly affected by small changes in p_o. The relationships between d_{gage} and D, in feet, are as follows:

$$D = d_{gage} + p_o$$

Gage 1: p_o = 0.125 ft (before May 28, 1991)
0.0 ft (between May 28 and June 7, 1991)
0.72 ft (after June 6, 1991)

Gage 2: p_o = 0.052 ft

Gage 3: p_o = 0.110 ft

Gage 4: p_o = 0.128 ft (before May 28, 1991 or after June 7, 1991)
p_o = 0.0 ft (between May 28, 1991 and June 7, 1991)

Knowing the elevation of the vertical control and noting the vertical distance between the vertical control and the channel bottom at the probe, gage depth readings can be converted to water surface elevations, E. The relationships for conversion of D (in feet) to E (ft. NGVD) are as follows:

Gage 1: E = 13.79 + D

Gage 2: E = 45.28 + D

Gage 3: E = 31.70 + D

Gage 4: E = 40.97 + D

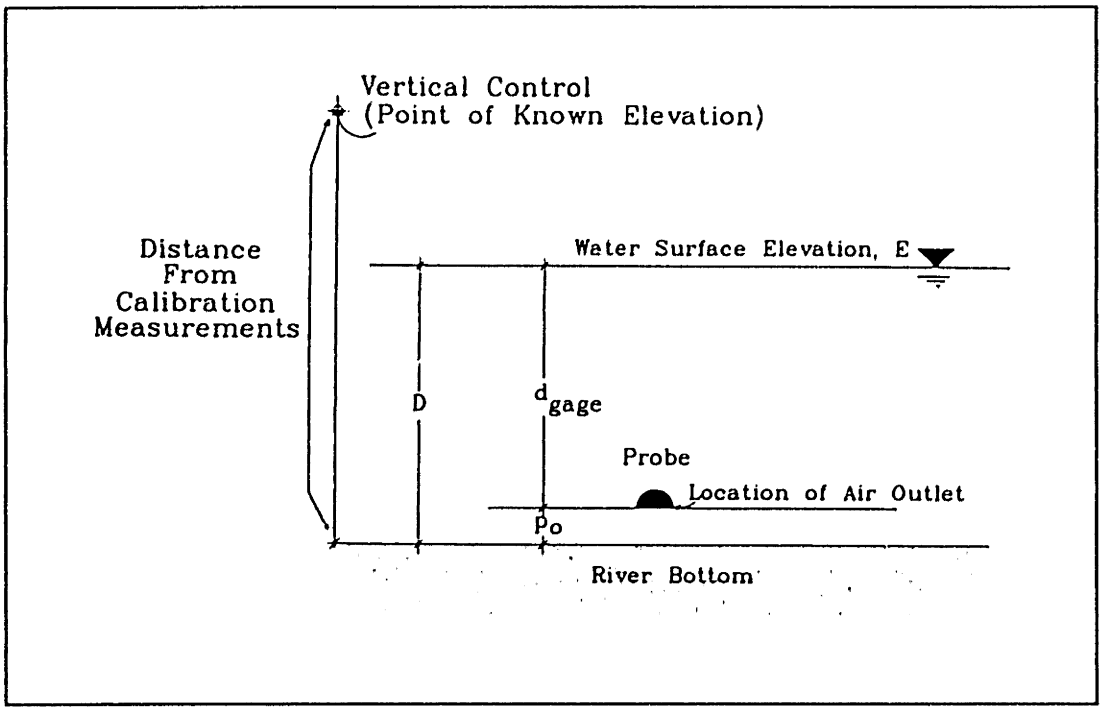

Figure III.3-8: Definition Sketch of Depth & Elevation Parameters

Flow, Area, and Velocity Relationships

Flow

Relationships between the gage parameters, D and v_p, and streamflow, cross-sectional area, and average cross-sectional velocity were finalized after field calibrations were performed. The optimal relationship for flow was obtained by regression analysis of the manually measured flow (flow from calibration measurements) versus different functional combinations of the gage parameters at each gaging station. The regression with the highest coefficient of determination (R^2 value) was the one used for conversion of the gage parameters to the streamgage flow. Expressions tested include relationships between manually measured flow and 1) depth only, 2) point velocity only, and 3) both depth and point velocity together. Functional relationships tested included combinations of linear, logarithmic, and power law relationships. For D, in feet, v_p, in ft/s, and Q, in cfs, the optimized relationships for flow for each station were obtained as: (Data points in figures III.3-9 through III.3-12 provide the range covered in the calibrations)

Gage 1:	$Q = 2.88\ D^{2.032} v_p^{0.225} + 1.529,$	$R^2 = 0.874$
Gage 2:	$Q = 9.29\ D^{1.60},$	$R^2 = 0.944$
Gage 3:	$Q = 3.48\ D^{3.13},$	$R^2 = 0.891$
Gage 4:	$Q = 17.15\ D^{1.75} v_p^{0.72} - 0.604,$ (If $Q < 0$, then $Q = 0$)	$R^2 = 0.880$

A comparison of flow values for each calibration is illustrated in figures III.3-9 to III.3-12. (Numerical values are provided in tables III.C-1 to III.C-4 in appendix III.C)

Of the above relationships, expressions for gages 2 and 3, (interestingly the two stations on the Aberjona River), depend only upon the gage depth readings. The power law relationships between flow and water depth, as observed for these two stations, is typical of channels whose flow is regulated by a control, i.e. a channel feature that stabilizes flow and eliminates variable backwater effects from downstream areas. (Herschy, 1985) Because of its geometry (232 feet long, 18 feet wide) and constriction of flow associated with the inlet/outlet, the culvert in which gage 2 is located may act as the control for flow at this station. For gage 3, possible controls include the bridge where the gage is located (83 feet long, 24 feet wide) or a natural channel control downstream.

The flow relationships for gages 1 and 4 are a function of both gage depth and velocity. The need for the point velocity reading for gage 1 is due to the small variability of the water depth at this station. The water depth at this location is controlled by both the Wedge Pond and the Winchester Falls control structures. Note that the minimum flow that can be computed for gage 1 is 1.53 cfs. The flow regime at gage 4 is largely dependent upon the water level of the Horn Pond reservoir. Depending upon the elevation of the reservoir, flow at gage 4 may vary from shallow swift flows to deep slow moving flows. Unlike the other stations, the depth of the water has no clear relationship with how fast the water is moving. For this reason the point velocity measurement, in addition to the depth measurement, provides an improvement in flow estimation. Although the flow equation for gage 4 allows for slightly negative flows, adjustments have been made in processing the raw data such that no flows less than zero are computed.

Area

Cross-sectional area relationships for each station were obtained through geometrical relationships between the channel bottom geometry and the water depth at a given point. These relationships are valid if: 1) the bottom geometry of the channel is unchanging and, 2) the angle of the water surface (cross-sectional view) with the horizontal remains constant. The bottom geometry used was the overall average geometry obtained from the calibrations. The overall average bottom geometry for each station is illustrated in figures III.3-3 to III.3-6. (Numerical values of the average bottom elevations and the bottom elevations for each calibration are provided in tables III.C-6 to III.C-9 in appendix III.C) The expressions for cross-sectional area, A, in square feet using the average bottom geometries are given below. The gage 4 expressions correspond to the section at the west end of the bridge.

Gage 1: For 1.17 <= D $R^2 = 0.663$

$$A = 20\ D - 7.015$$

Gage 2: For 0.37 <= D $R^2 = 0.954$

$$A = 18\ D + 2.27$$

For 0.13 <= D < 0.37

$$A = 6.25\ D^2 + 7.375\ D + 4.223$$

Gage 3: For 0.57 <= D $R^2 = 0.954$

$$A = 24\ D - 4.575$$

Gage 4: For 0.81 <= D

$$A = 24\ D - 4.815$$

For 0.58 <= D < 0.81

$$A = 4.41\ D^2 + 16.85\ D - 1.921$$

For 0.47 <= D < 0.58

$$A = 9.25\ D^2 + 11.25\ D - 0.292$$

For 0.27 <= D < 0.47

$$A = 11.98\ D^2 + 8.67\ D + 0.311$$

Gage areas were obtained from the gage depth reading and the equations above whereas manual cross-sectional areas were obtained from calibration measurements. A comparison of these areas for gages 1,2, and 3 is provided figures III.3-9 to III.3-11. (Numerical values of these areas are provided in tables III.C-1 to III.C-3 in appendix III.C) Area relationships were not plotted for gage 4 since most of the calibrations were done at "the middle of bridge" section whose areas do not correspond to the relationship above. Area relationships at the middle of the bridge were not estimated due to the large standard deviations in the bottom elevation measurements. (Table III.C-9)

For gages 2 and 3 the cross-sectional area relationships were characterized by R^2 values near one, indicating a good fit. Such a result indicates that the channel bottom geometry is reasonably stable for the flows measured. Nevertheless, upon close inspection of table III.C-2 one may note that the bottom elevations on the eastern side of the gage 2 cross-section (BE0 and BE3) have gradually increased since the time when the first calibration measurements were made. Additionally, a comparison of the bottom geometry of the gage 2 section during low and high flows, indicates that the geometry at the central portion of the section varies during different flow conditions. For the high flow (figure III.D-5d) the channel appears to have been eroded as evidenced by a slight valley in the central portion of the section, which is not present during the lower flows. (figure III.D-5a & III.D-5b) The poorer R^2 value for gage 1 is due to errors in gage and manually measured readings which were significant compared to observed changes in cross-sectional area.

Velocity

Average cross-sectional velocity was calculated for each station using the following relationship:

$$V = Q/A$$

Manual velocities correspond to the calibration measurements whereas gage velocities are obtained from the gage parameters and the equations for Q,A, and V above. A comparison of manual versus gage values of average velocity for gages 1,2, and 3, are provided in figures III.3-9 to III.3-11. (Numerical values are provided in tables III.C-1 to III.C-4 in appendix III.C)

For gages 2 and 3, the V relationship was a poorer fit than the Q and A relationships. The especially poor fit for the last two calibration measurements (12/17/91 and 1/25/93) at gage 3, indicate perhaps, a change in the Q and V relationships.

The V relationship for gage #1 is characterized by a larger R^2. This larger R^2, however, may be misleading due to the clustering of many points near zero and a few points which are significantly greater than zero which "influence" (Hamilton, 1990) the regression. The "influence" suggests that the R^2 for the velocity relationship is strongly affected by the few points significantly different from zero and not strongly affected by the cluster of points near zero.

Limitations

Due to the possibility of significant changes in bottom geometry and flow characteristics over time, the relationships above may not be satisfactory for time periods after January 1993. After January 1993, the cross-sections should be recalibrated to 1) assure that the above relationships are still valid, or 2) derive new relationships for the gages.

Additionally, one should keep in mind the range of flows for which calibration measurements were performed. Generally, calibrations were made during low to average flows. Only a very few calibrations were performed during high flows. Thus there is more certainty in applying the relationships for low flows than for high flows. For future calibrations, more emphasis should be placed on making calibrations during high flow conditions.

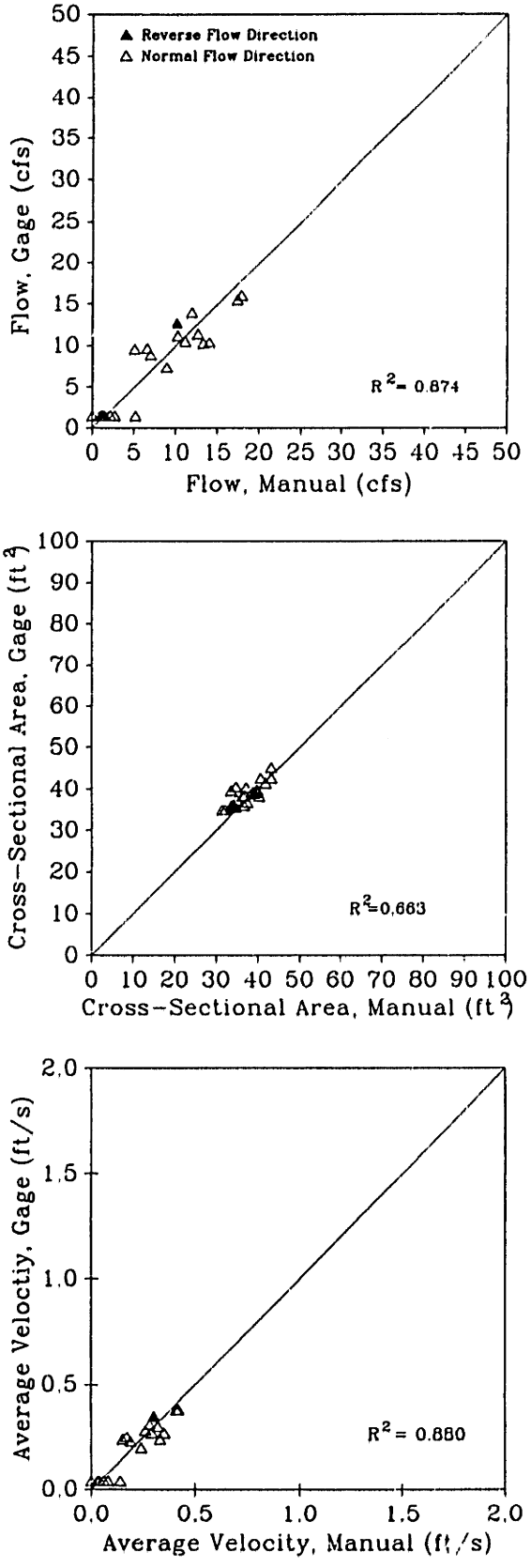

Figure III.3-9: Flow, Area, and Velocity Calibration for Gage 1, Wedge Pond

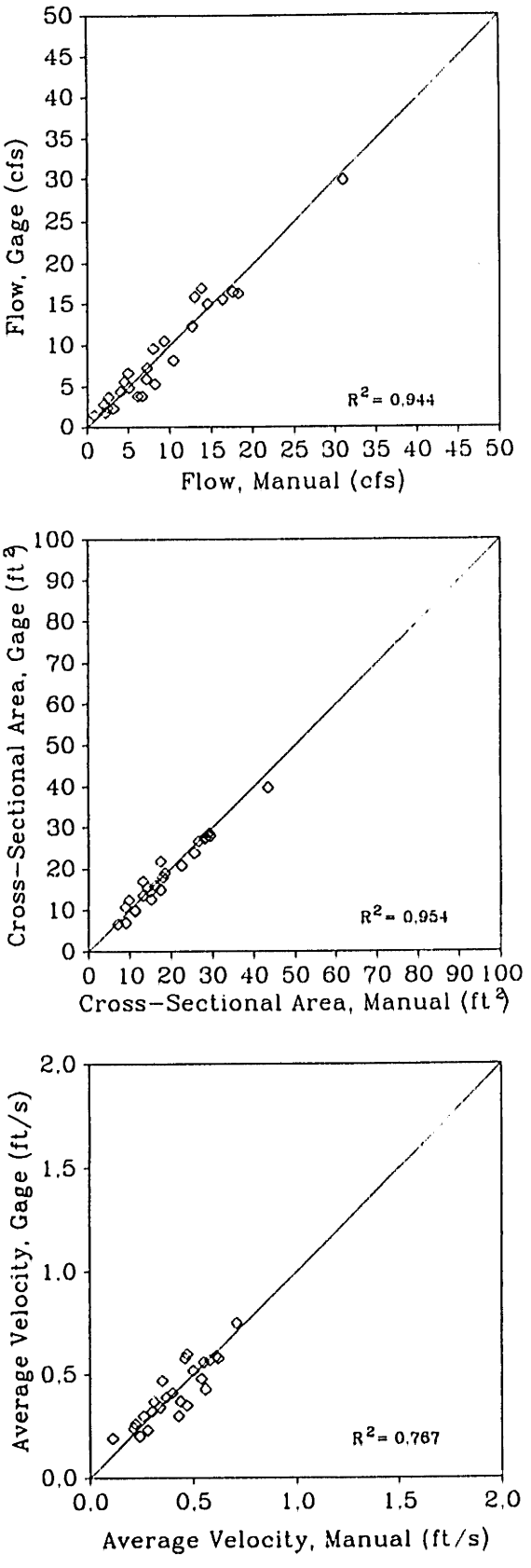

Figure III.3-10: Flow, Area, and Velocity Calibration for Gage 2, Route 128

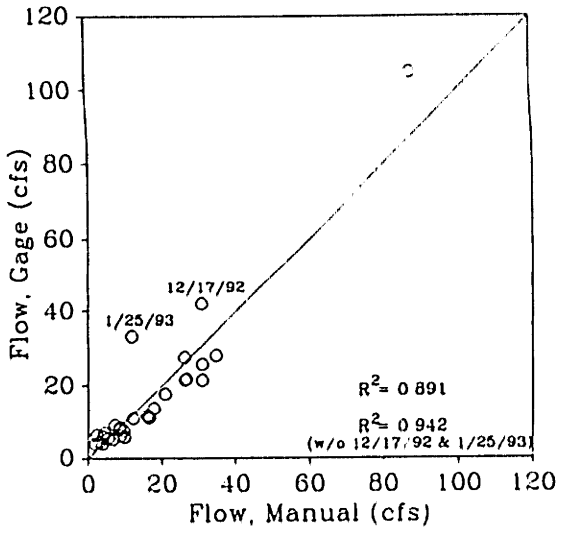

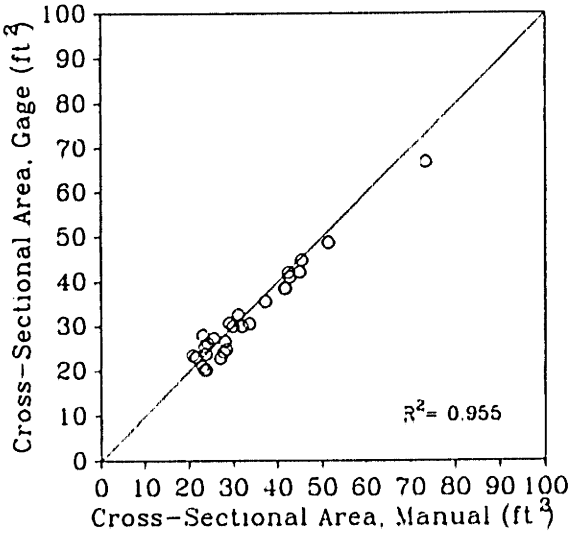

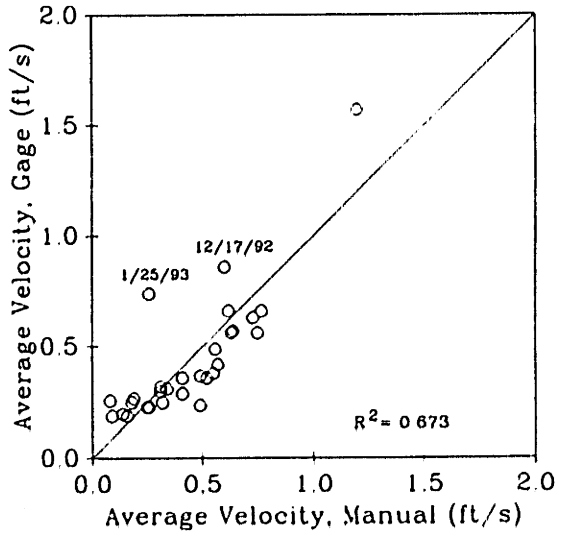

Figure III.3-11: Flow, Area, and Velocity Calibration for Gage 3, Montvale

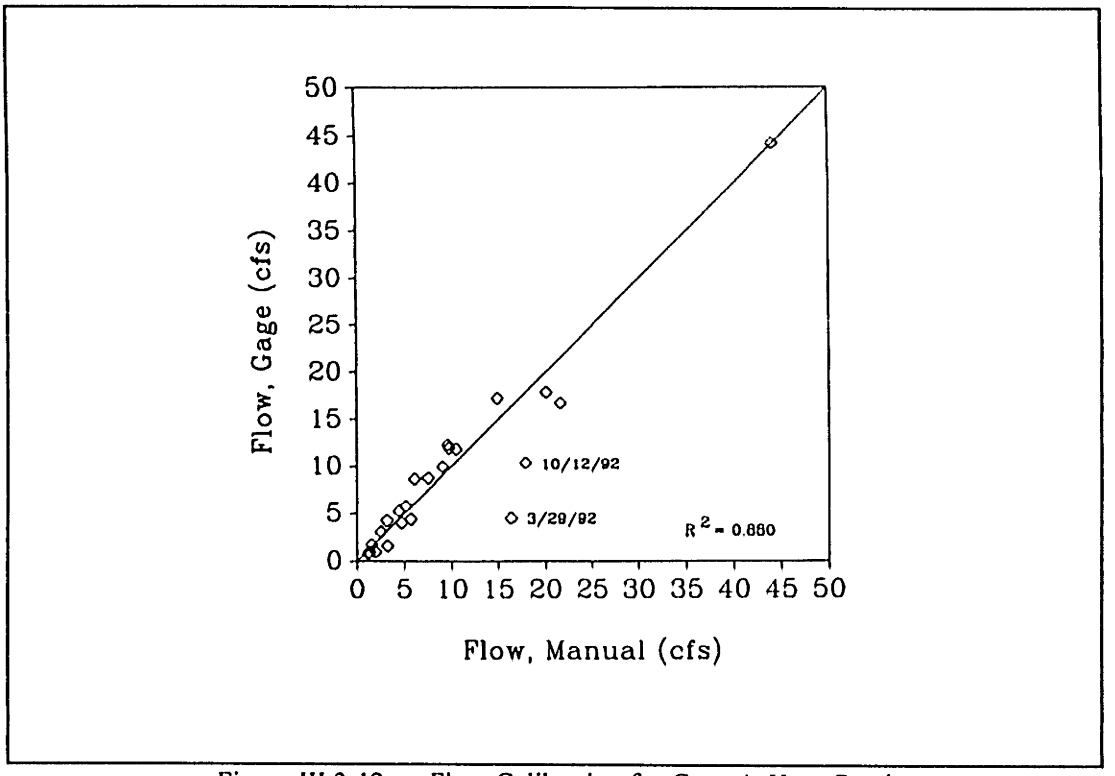

Figure III.3-12: Flow Calibration for Gage 4, Horn Pond

III.3.5 Recommendations for Improvement of Streamflow Monitoring Program

The equipment used provided estimates of volumetric flow rates which, given the relatively small investment and simplicity of installation, can be considered reasonable. However, the current monitoring system does have some drawbacks which compromise the accuracy and reliability of the measurements. These drawbacks include: 1) freezing of water in the air lines during the winter months, which causes erroneously high depth readings, 2) poor housing for the gage electronics which results in occasional gage malfunction especially during freezing and wet weather, 3) location of the probe in the center of the channel where it was susceptible to dislodging by river debris, and 4) lack of vandal proofing.

To improve upon the existing flow monitoring system, the use of pre-existing control structures is recommended. Such structures include the Horn Pond Dam, a horse-shoe shaped weir (in disrepair) at Wedge Pond, Winchester Falls Dam, 2 small flashboard dams at Davidson Park, and possibly the 7 foot diameter culverts under the playfields at Winchester High School. The primary advantages of control structures are:

1) Only one parameter, water depth, needs to be measured. The depth measurement has the added advantage that it is a relatively easy quantity to measure accurately. Additionally, since depth can be measured using several different techniques, one can chose the depth measuring system which is most reliable for the watershed's climate and flow conditions.
2) They tend to stabilize a stage-discharge relationship providing long-term reliability.
3) When properly calibrated, they can provide accurate flow measurements.

For the depth measurement, the use of acoustic depth measuring devices or float type recorders is recommended. Precautions should be taken to assure that the devices are not hit by river debris. Use of a stilling well with safeguards to minimize vandalism and freezing-related problems would be ideal.

At locations where channel controls are non-existent, the use of the relationship, Q=VA, may provide an alternative. A depth measurement can be used to estimate A whereas ultrasonic velocity techniques can possibly be used to obtain a better estimate of V. Ultrasonic devices have an advantage over point electromagnetic devices in that the average velocity over the entire width of the cross-section at one level in the vertical is measured rather than measuring a single point velocity. Configurations for use of ultrasonic devices for velocity measurements in rivers have been conceptualized (Lynnworth, 1989; Lynnworth, 1991, personal communication) and could possibly provide a more accurate means by which flow velocity can be estimated.

III.4 SAMPLE COLLECTION AND ANALYSIS: Suspended Sediments and Metals

River water samples were collected for routine analysis of suspended sediment and metal concentrations. These sample collection efforts are described below.

III.4.1 Suspended Sediment Sample Collection

Suspended sediments were monitored on both monthly intervals and on a continuous basis. Instantaneous samples were collected in monthly intervals at each of the five streamflow gaging stations whereas the continuous monitoring of suspended sediment was performed only at gage 5.

Monthly Sample Collection Method: Refer to section III.4.2 for details.

Continuous Monitoring: Suspended sediment concentrations were monitored continuously at the USGS station, using two separate systems (figure III.4-1) housed in the USGS gage house. River water samples were drawn into the monitoring systems by pumping water from the river through a set of sample lines. Sample inlet nozzles (figure III.4-2) were located in the river channel approximately 15 feet upstream of the control structure. These monitoring systems are described as follows:

1. *Nephelometer System*: This system provided an estimate of suspended sediment concentrations on a continuous basis through the measurement of the intensity of light (in nephelometric turbidity units, ntu's) scattered by particles in the water.

   The nephelometer system (figure III.4-1) provided for the recirculation of river water through a nephelometer (Turner Designs Model 40 fitted with a 40-070 Continuous Flow Attachment). The system included: 1) a peristaltic pump (Cole Parmer Masterflex® L/S Standard Driver), 2) a set of gages for controlling recirculation water parameters, e.g. pressure and flow gages, 3) an in-line injection of NaOCl (laundry bleach) to retard algal growth, and 4) a data recording device (Campbell Scientific CR-10).

   A calibration curve of NTU vs Suspended Sediment Concentration is provided in figure III.C-1 and table III.C-5 in appendix III.C.

2. *Autosampler*: The autosampler (ISCO 3700 Series) system permitted the gathering of 24, 1 liter samples (usually programmed in 1 hour intervals) which were analyzed for suspended sediment concentrations and metals content. Samples were collected during both low flow and high flow conditions. The sampler was actuated by a liquid level sensor (ISCO 1640 Actuator) which initiated the autosampler's peristaltic pump when the river water surface had risen to a specified elevation. Samples collected were refrigerated within 36 hours of retrieval and vacuum filtered in the laboratory within 60 hours. A list of samples collected using the autosampler is provided in table III.A-7 in appendix III.A.

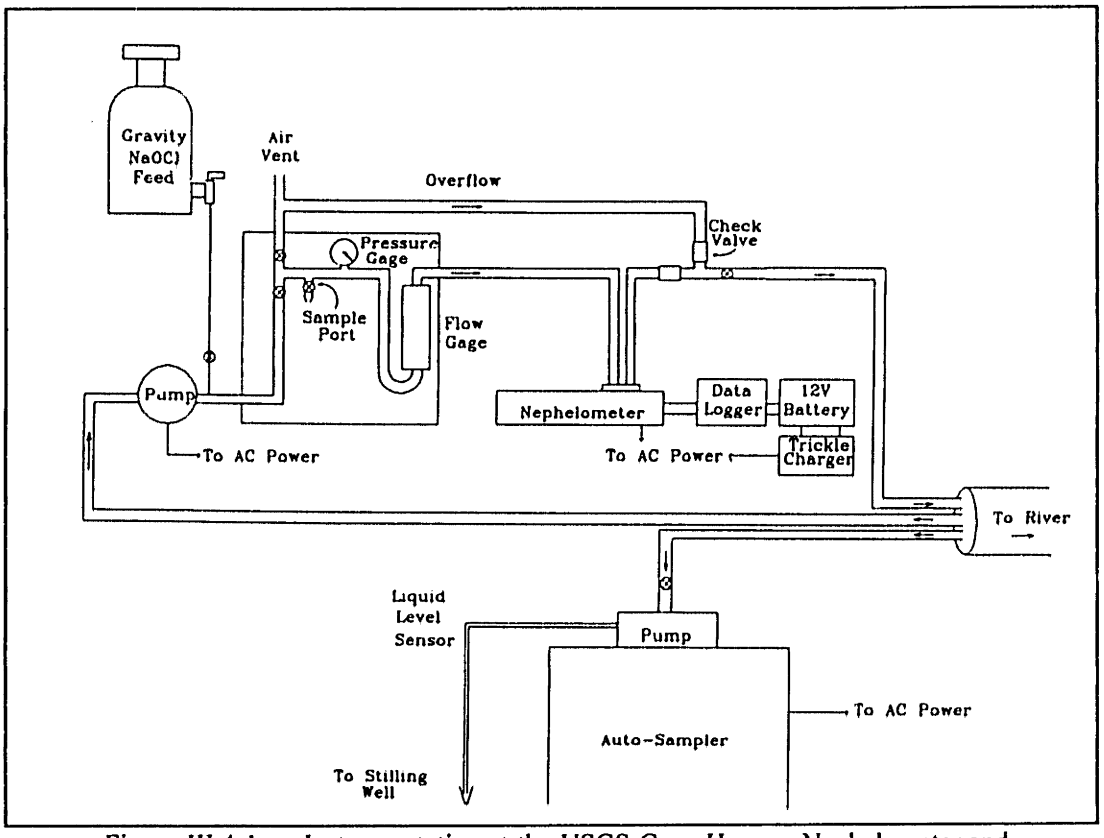

Figure III.4-1: Instrumentation at the USGS Gage House: Nephelometer and Autosampler Systems

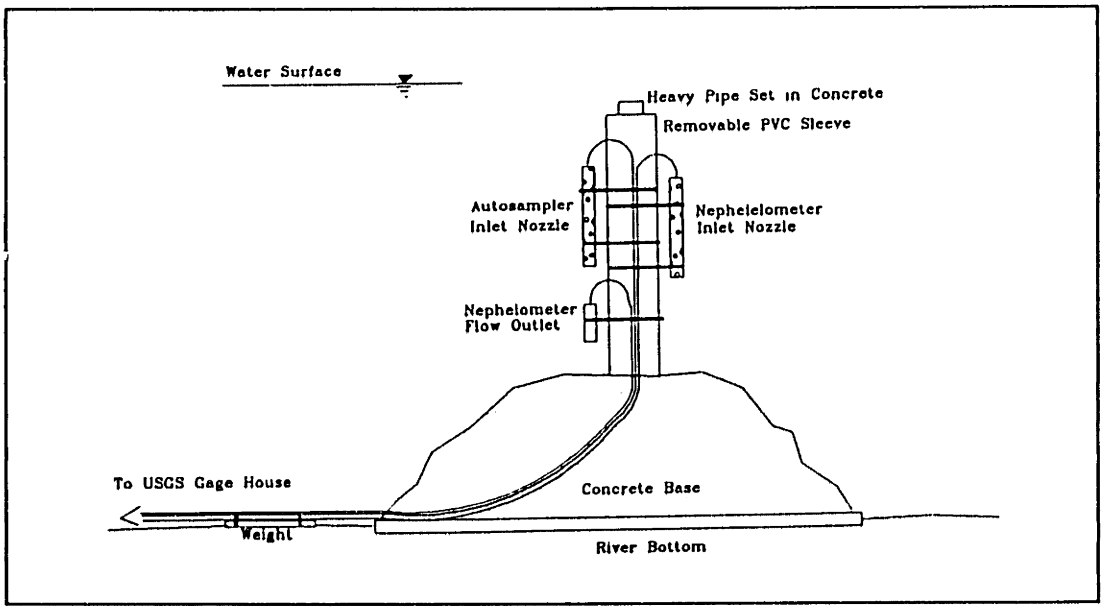

Figure III.4-2: Inlet Nozzle Holder for Instrumentation at the USGS Gage

III.4.2 Metals Sample Collection

River water samples for metals analysis were collected using one of two procedures: 1) during monthly field trips, or 2) by use of an autosampler.

1. *Monthly Sample Collection Methods*: Instantaneous samples were collected for metals and suspended sediment analysis in approximately monthly intervals from May 1991 to January 1993. During most field trips, all five stations were sampled on the same day, where the time between first and last sample collected was about 7 hours. In order to determine metal and sediment fluxes corresponding to each sample, the streamflows at gages 1, 2, 3, and 4 were also measured "manually" using the calibration procedure described in section III.3.4. Streamflow a gage 5 was obtained by noting the stage reading at gage 5 during sample collection and converting the reading to streamflow using a rating curve.

   Generally, samples were collected in the field by pumping water through pre-weighed 0.5 μm pore size, 9 cm diameter in-line filters (Gelman Metrigard Glass Fiber) At each station, river water was pumped through three filters and one filtrate sample was collected. Additionally, unfiltered samples were collected for subsequent lab vacuum filtration through 1.5 μm pore size, 9 cm diameter filters. (Whatman Glass Microfiber 934-AH) The only exceptions occurred when either the pump was inoperative or if below freezing conditions existed. During these situations grab samples (submerging the sample bottle in the river and capping) were collected, with all subsequent filtration performed in the lab.

   The system used for controlling field filtration is illustrated in figure III.4-3. The components include a battery powered peristaltic pump (Cole Parmer Masterflex® L/S 12 VDC Drive), an acrylic flow meter (Key Instruments FR4000), 9 cm diameter stainless steel filter holder (Microfiltration Pressure Holder), a pressure gage, and a series of PVC valves and polypropylene fittings. In-field filtration was performed until 40 psi back-pressure on the filters was obtained. The volume of water filtered through each filter varied from 1 to 10 liters, whereas the mass of suspended sediment collected per filter varied from 8 to 30 mg.

   Prior to sample collection, the field filtration system was flushed with several liters of river water. All *bottles and filters* used for sample collection were pre-acid washed in 1N HNO_3. Filtrate samples were immediately acidified to approximately 0.5% acid with concentrated HNO_3. Immediately after collection, unfiltered samples were kept in a cooler with ice and/or refrigerated. All lab filtration was performed within 48 hours of sample collection. At the end

of a field trip, the system was flushed with several liters of de-ionized distilled water and field-blank filters and filtrate samples were collected.

To assure that representative samples were obtained, attempts were made to maintain sample intake and ambient water velocities as nearly equal as possible. Estimates of ambient water velocity were obtained from measurements with an electromagnetic flow meter. Intake velocity was estimated by measuring the flow rate through the pump system (figure III.4-3) and noting the cross-sectional area of flow at the intake. The intake velocity was controlled by use of various intake nozzle sizes. Configuration of the inlet nozzles (which consists of three simultaneously active sample ports) is illustrated in figure III.4-4.

Rijn, 1980 investigated suspended sediment sampling systems and the effects of differing ambient and intake velocities on retrieving representative samples. In his study, Rijn established relationships between particle size, ratios of ambient to intake velocities, and ratios of sampled to actual suspended sediment concentrations. From these relationships, Rijn found that the smaller the suspended sediment particles, the smaller the sampling errors associated with a given ratio of ambient to intake velocity. For the suspended sediment particle sizes ($\approx$ 10 μm average diameter) observed in the Aberjona River, differences between in-take velocity and local stream velocity were inconsequential. (A summary of ambient and intake velocities during various field sampling trips are provided in tables III.A-8 through table III.A-12 for reference)

A summary of sample collection dates and methodology used to collect the samples is given in tables III.A-8 to III.A-11 in appendix III.A.

2. *Autosampler*: Description of the autosampler method is given in section III.4.1. For metal analysis purposes, all sample bottles put into the autosampler were pre-acid washed with 1N HNO_3.

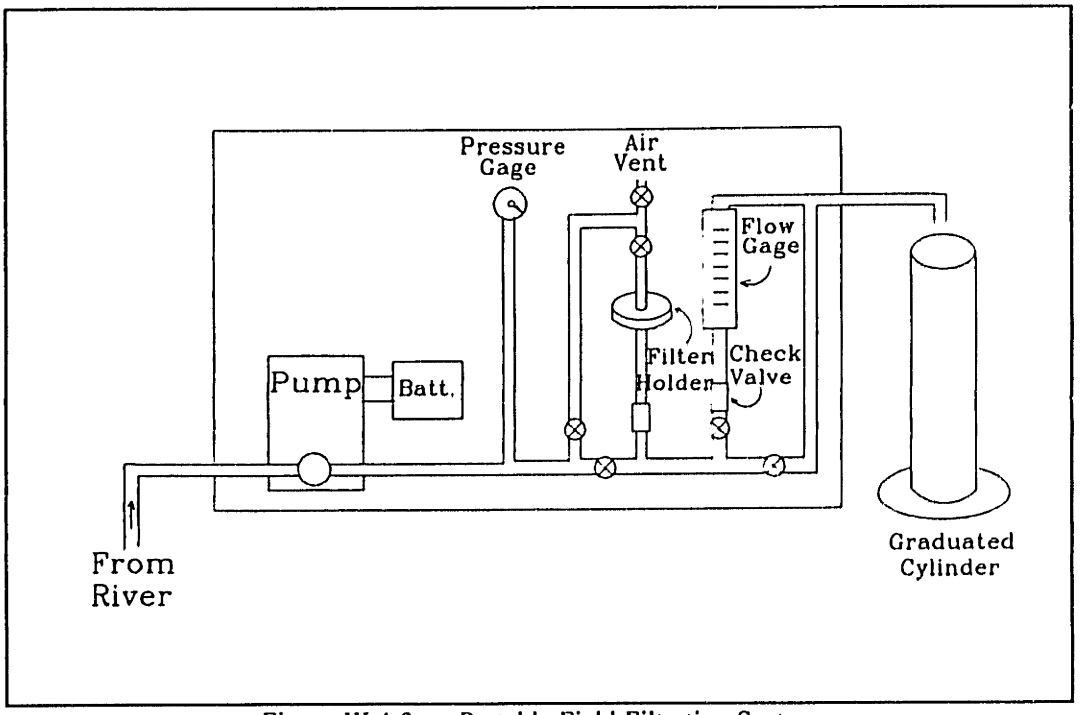

Figure III.4-3: Portable Field Filtration System

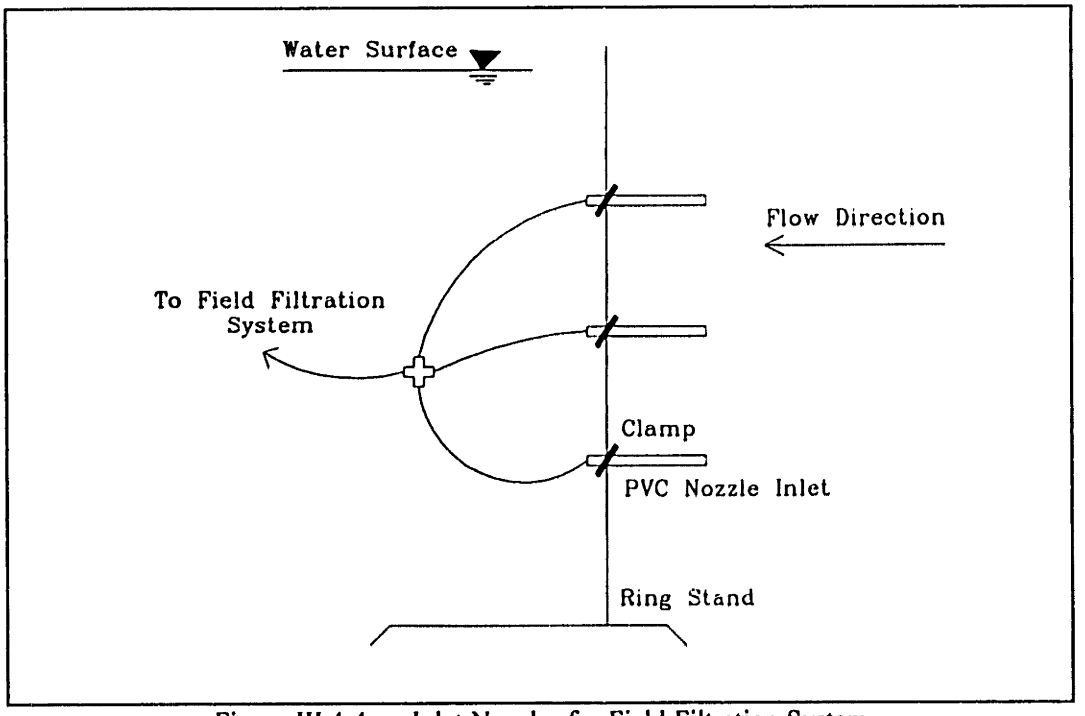

Figure III.4-4: Inlet Nozzles for Field Filtration System

III.4.3 Laboratory Analytical Procedures

Standards & Reagents

Metal concentration standards were prepared from concentrated shelf liquid standards. (Plasma-Pure Standards from Leeman Labs MA or Atomic Absorption Standards from EM Science NJ) Dilutions were generally made in 10:1 ratios in the concentration ranges that bridged sample concentrations. For low sample concentrations near detection limits, 5:1 standard dilutions were generally used. All standards were diluted with de-ionized water and acidified to either 1% or 5% HNO_3.

All de-ionized water was purified through a Milli-Q® system. All acids used were Mallinckrodt Analytical Reagent unless otherwise specified.

Sample Preparation: Dissolved Phase

Filtrate (dissolved phase) samples were immediately acidified upon sample filtration to approximately 0.5% acid with concentrated HNO_3.

Sample Preparation: Particulate Phase

Particulate phase sample analysis and preparation consisted of several steps. These steps included:

1) *Suspended Sediment Analysis*: Suspended sediment analysis followed the method 2540 D outlined in Clesceri, et. al., 1989. A known volume of water was filtered through a pre-weighed acid-washed filter. Filter media used was either: 1) 9 cm diameter, 0.5 μm pore size (Gelman Metrigard) or 2) 9 cm diameter, 1.5 μm pore size (Whatman 934-AH). The filter was then dried for 1 hour at 103-105 °C and placed in a desiccator for at least 1 hour. The filters were then re-weighed. Calculations included determining: 1) the sediment mass collected on the filter (equal to the difference in filter mass before and after filtration), and 2) the suspended sediment concentration. (equal to the mass of sediment on the filter divided by the volume of filtered river water)

   Blank filters were carried through each analysis set to assure that the weight of the filter media before and after drying had not changed significantly. Generally, changes in filter mass represented less than 5% of the collected suspended sediment mass. A correction was included to account for the minor loss in the weight of the filter media. Replicate sample analysis generally resulted in standard deviations from 0.2 to 0.4 mg/l.

2) *Volatile Solids Analysis*: Volatile solids analysis was performed using the method 2540 E in Clesceri, et. al., 1989. The mass of volatile solids in a sample is a rough estimate of the amount of organic matter present in the sample. For this analysis, a known volume of water was filtered through 1.5 μm pore size, 9 cm diameter glass fiber filters (Whatman 934-AH). The filters were then oven dried, weighed, and combusted in a muffle furnace (Thermolyne Type 1400 Furnace) at a temperature of 550 °C for 15 minutes. After cooling, the filters were kept in a desiccator until they were re-weighed. The loss of mass after combustion is the measure of volatile solids.

For each set of samples analyzed, three blank filters were carried through the procedure to assure that the weight of the filter media before and after combustion had not changed significantly. Mean weight loss of the filter media was 0.6 mg which represented generally less than 10% of the volatile solid mass. The results were corrected for this loss.

3) *Filter Digestion*: The purpose of the digestion step was to dissolve the metals from the sediment particles into a liquid. The digestion procedure was a modification of Method 3050 in EPA, 1986. The method used included the following steps:

a) 5 ml of de-ionized water were added to each filter (cut-up) in acid-washed Phillips Beakers covered with watch glasses. Water is added to wet the filters.

b) 5 ml of concentrated HNO_3 were added to each sample. The samples were then heated for 30 minutes on a hot plate such that the temperature was kept just below boiling. After 30 minutes samples were removed from the hot plate and allowed to cool. 5 more ml of concentrated HNO_3 were added and samples were re-heated for 30 minutes. Cooling, heating and 5 ml HNO_3 additions were repeated until 20 ml of HNO_3 had been added to each sample.

c) Samples were cooled. 2 ml of H_2O_2 (30% Fischer Scientific) were added and samples were re-heated until the effervescence subsided. Samples were again cooled and 2 more ml of H_2O_2 were added. Heating, cooling and 2 ml H_2O_2 additions were continued until 10 ml of H_2O_2 had been added to each sample.

d) Samples were then cooled. 5 ml of concentrated HCl (37%) were added and the samples were re-heated for 2 hours.

e) After allowing the samples to cool, the digestate was poured through a paper filter (8-12 μm nominal pore size, Schliecher & Schuell #595) into a graduated cylinder. Beakers and filtered material were rinsed with de-ionized water to assure that all the digestate had been poured. The final volume of the digestate was noted.

f) Samples were then stored in acid-washed polypropylene bottles until analysis.

In addition to samples, filter blanks and reagent blanks were carried through each set of samples that were digested.

Analytical Techniques: Metals

Routine analysis for As, Cr, Cu, and Fe was performed using a combination of analytical techniques. These techniques included: a) Inductively Coupled Plasma - Atomic Emission Spectroscopy (ICP-AES), b) Atomic Absorption Spectroscopy with Graphite Furnace Atomization (GFAA) and, 3) Hydride Generation followed by Atomic Absorption Spectroscopy (HGAA). Analysis methods for each metal are summarized in table III.4-1 below:

METAL	PHASE	Analytical Method
Arsenic	Dissolved	HGAA
	Particulate	HGAA
Chromium	Dissolved	GFAA
	Particulate	ICP-AES
Copper	Dissolved	GFAA
	Particulate	ICP-AES
Iron	Dissolved	ICP-AES
	Particluate	ICP-AES

Table III.4-1: Analytical Method for Metal Determination

ICP-AES: ICP-AES analysis is based on the measurement of element-emitted light by optical spectrometry. The emission source is an inductively coupled argon plasma (i.e. a highly ionized gas) which is produced by flowing argon gas past a radio frequency electromagnetic field. Liquid samples are introduced into the plasma as an aerosol. In the plasma, the aerosol is desolvated, atomized, and the elements are excited. Upon excitation, the atoms that comprised the sample emit light at their characteristic wavelengths which can then be monitored by an optical system.

A Thermo Jarell Ash Atomscan® 25 was used for all ICP-AES analysis. The system consisted of a power unit, a plasma emission source, an optical system, and a host computer for equipment control, analysis and data collection. Sample introduction was through use of a peristaltic pump and nebulizer

system and the optical system consisted of a slew scanning monochromator. Operation and data acquisition were performed through the Thermospec® software supplied by the equipment manufacturer.

The instrument was calibrated using low and high concentration standards. Intermediate standards in the vicinity of sample concentrations were interdispersed throughout a sample run to check for proper calibration. Error estimates from replicate analysis of standards are given in Table III.4-2. The table indicates that the coefficient of variation of standards in the Fe, Cu, and Cr concentration range typical of gage 2 and 3 digestates was within 5%, whereas the coefficient of variation for standards in the concentration range typical of gage 1 and 4 digestates was within 20%.

Metal Concentration Range	Coefficient of Variation	Samples Corresponding to Metal Concentration Range
0.4 mg/l < [Fe] < 200 mg/l	4%	Particulate Digestates for Gages 1 to 5 Most Dissolved Samples for Gages 2 & 3
0.1 mg/l < [Fe] < 0.4 mg/l	10%	Dissolved Samples for Gages 1,4 & 5 Few Dissolved Samples for Gages 2 & 3
0.25 mg/l < [Cu] < 1.0 mg/l	5%	Particulate Digestates for Gages 2 & 3 and Some of Gage 5
0.04 mg/l < [Cu] < 0.25 mg/l	20%	Particulate Digestates for Gages 1 & 4 and Some of Gage 5
0.2 mg/l < [Cr] < 0.25 mg/l	4%	Particulate Digestates for Gages 2 & 3 and Most of Gage 5
0.1 mg/l < [Cr] < 0.2 mg/l	20%	Particulate Digestates for Gages 1 & 4 and a Few of Gage 5

Table III.4-2: Summary of Replicate Analysis using Metal Standards

Spike analysis on particulate phase samples indicated that:

1) Recovery of Fe was on average within 2% of the Fe mass spiked. Standard deviation of the recovery relative to the spike mass was 5.4%.

2) Recovery of Cu was on average within 2% (3.6% standard deviation) of the Cu mass spiked for concentrations typical of particulate samples at gages 2,3, and 5. 82% of the spike mass was recovered for concentrations typical of particulate digestates at gages 1 and 4 . (8.5% standard deviation)

3) 70% of the Cr spike mass was recovered for concentrations typical of gage 2,3,and 5. (4.5% standard deviation) Poor recovery was obtained for Cr in concentration rages typical of gage 1 and 4.

GFAA: Atomic Absorption Spectroscopy is based on the measurement of absorbed light due to the atomic transition of electrons from a ground state to an excited state. The measurement technique consists of a hollow-cathode lamp which emits a beam of radiation in the characteristic wavelength for the element to be measured. Atomization of the sample is performed such that the atoms formed absorb radiation from the lamp, reducing the intensity of the incident beam. The reduction of beam intensity (i.e. absorbance) can be used to determine the amount of the element present in the sample. For GFAA, the sample is atomized through electrical heating using a graphite furnace.

All GFAA analysis was performed using a Perkin Elmer 372 Atomic Absorption Spectrophotometer with a Perkin Elmer HGA 400 graphite furnace. Sample introduction into the furnace was through an autosampler (Perkin Elmer AS-40) and data output was through peak height analysis using a printer sequencer. (Perkin Elmer PRS-10) Furnace programs included drying, charring, atomization, clean-out, and cool-down steps.

All analyses were performed in triplicate. Average standard deviations of the dissolved Cu and Cr analysis were 0.4 µg/l and 0.07 µg/l respectively. The coefficient of variation for both Cu and Cr analysis was generally within 10%. For comparison, some particulate digestate samples were analyzed by both GFAA and ICP-AES. Results showed that sample concentrations analyzed using both GFAA and ICP-AES were within 10% of one another for Cu. For Cr, ICP-AES analyzed sample concentrations were typically lower than GFAA analyzed sample concentrations by 60 to 70%. All particulate Cr concentrations reported correspond to ICP-AES analysis, whereas dissolved Cr concentrations correspond to GFAA analysis.

HGAA: HGAA analysis was performed for total dissolved and total particulate arsenic analysis. The experimental set-up was built through the work of Aurilio, 1992 and Spliethoff, 1994 which followed the analytical procedures of Andreae 1977 and Massacheleyn, 1991. The basis of the technique is that arsenic forms a gaseous phase, arsine, under strong reducing and acidic conditions. This gaseous phase can then be concentrated permitting a very sensitive analytical method for arsenic. The analytical method included the addition of sodium borohydride as the reductant, and the addition of 6N HCl to

lower the pH. After the addition of these reagents, the arsines were stripped by bubbling an inert gas, helium, through the solution. The purged arsine was then collected on gas chromatographic packing using a cold trap. Upon completion of the purge/trap step, the chromatographic packing was heated allowing for the elution of arsine which was then carried into a burner which combusted the arsine in a hydrogen-air flame. The burner was mounted onto the beam of an atomic absorption spectrophotometer (Perkin Elmer 403) which monitored the absorption signals from the atomization of the arsine in the flame. Signals were recorded by use of an integrator. (Hewlett Packard HP 3396 Series II).

25 ml reaction vessels (silanized glass) were used. Dissolved Samples were analyzed without dilution while particulate phase samples were diluted between 2.5:1 to 10:1. Standards were analyzed after every 4 to 6 samples. Coefficient of variation for repeated analysis was generally between 0.03 to 0.10.

IV. DISCUSSION OF MONITORING DATA

The purpose of the first four sections of this chapter is to provide descriptions of: 1) hydrologic and contaminant transport characteristics of the watershed, 2) data which influenced the formulation of the computer model, 3) data which would help to explain differences between modeled and measured data, and 4) data which would be helpful in developing a transport history. Discussions of the data which were of secondary importance are included within the appendices.

A conceptual model which summarizes my interpretation of the data is presented in section IV.5.

IV.1 PRECIPITATION

This section includes: 1) a description of the Reading data, 2) a discussion of the spatial variability of the data, and 3) a discussion of air temperature data. The purpose of describing the Reading data is to provide general hydrologic information for the watershed, to summarize data which were needed to run the computer model, and to describe aspects of the data which affected the interpretation of the model results. In describing the Reading data, a discussion of the hourly data from 1991 to 1993 is included because the hourly data are used as an input to the model. A summary of monthly precipitation values is also included because the values are needed for the computation of the longterm baseflow component by the streamflow model. Changes in the statistics of the Reading data have implications in the development of a transport history.

A discussion of the spatial variability of precipitation is included because spatially variable precipitation could be a source of model input errors. The model uses precipitation data from only one station, the Reading station. If precipitation is spatially variable then data collected from one station may not be representative of precipitation over the entire watershed.

A discussion of temperature data is included because of the importance of temperature in the development of a snowmelt model and in determining the times when precipitation occurred as rainfall or snowfall within the watershed.

IV.1.1 Reading Data

Yearly

Average yearly precipitation at the Reading station was 43.1 inches. The minimum yearly precipitation was 27.1" measured in 1965 and the maximum was 63.5" measured in 1983. The yearly distribution of precipitation (figure IV.1-1 and table IV.A-1) was characterized by significant changes in rainfall depths from year to year. Close inspection of the data also indicates that the statistics of the precipitation have changed between pre- and post- 1957. From 1899 to 1957 the mean precipitation depth was 41.0", while from 1958 to 1992 the precipitation depth was 46.5". Between these two time periods the mean precipitation depth increased by 13% (or by roughly one standard deviation). This change, however, may be due, in part, to the fact that the Reading rainfall recording station was moved from the 100 acre Pumping station location to the NCDC station in 1957. (Refer to section III.2 for locations)

The effect of relocating the Reading station is partly supported by comparing the pre- and post- 1957 precipitation depths for the Winchester station. (table IV.A-2) For the 1899 to 1957 time period the mean precipitation depth at Winchester was 41.9" and for the 1958 to 1992 time period the precipitation depth was 43.5". The corresponding increase in precipitation between these two time periods was approximately 4% which was less than the 13% observed for Reading. Assuming that the overall average fluctuations in precipitation depths were the same for each station, the extra increase observed at Reading can possibly be associated with the gage relocation.

Monthly

The distribution of average monthly precipitation (figure IV.1-2 and table IV.1-1) indicates that average precipitation depths did not vary significantly from month to month. However, inspection of daily and hourly data indicate that the form of the precipitation and the time distribution of the precipitation did change significantly throughout the year. During the winter, a fraction of the precipitation occurred as snow whereas during other seasons all of the precipitation occurred as rainfall. The time distribution of rainfall in the summer was characterizedby short intense storms whereas during other seasons storms were generally of lower intensity and of longer duration.

Daily

Daily precipitation values for the 1957 to 1993 period of record are included in ASCII format in appendix IV.C. A histogram of these data is plotted in figure IV.1-3. The frequency distribution of daily precipitation appears to follow an exponential decrease. For the period of record, 64% of the days had no rain, 78% had less than 0.1 inch, and 97% had less than 1 inch.

A summary of the 8 largest 24 hour precipitation events is included in table IV.1-2. Comparing the 24 hour precipitation values with the return periods for eastern Massachusetts (Soil Conservation Service, 1975, table IV.A-3), one 100 year storm, one 10 year storm, one 5 year, and thirteen 2 year storms were observed during the 36 year record.

Hourly

Hourly precipitation data from 1981 to 1993 are included in ASCII format in appendix IV.B. Data from January 1991 to September 1993 are plotted in appendix IV.B. A qualitative evaluation of these data indicates that the distribution of hourly rainfall differed between winter (December, January, and February) and summer (June, July, August). Large precipitation events during the winter were generally of lower intensity (peak intensity generally < 0.25 in/hour) and of longer duration (greater than 10 hours). During the summer, on the other hand, large storms were generally of higher intensity (peak intensity > 0.25 in/hr) and were of shorter duration (less than 15 hours).

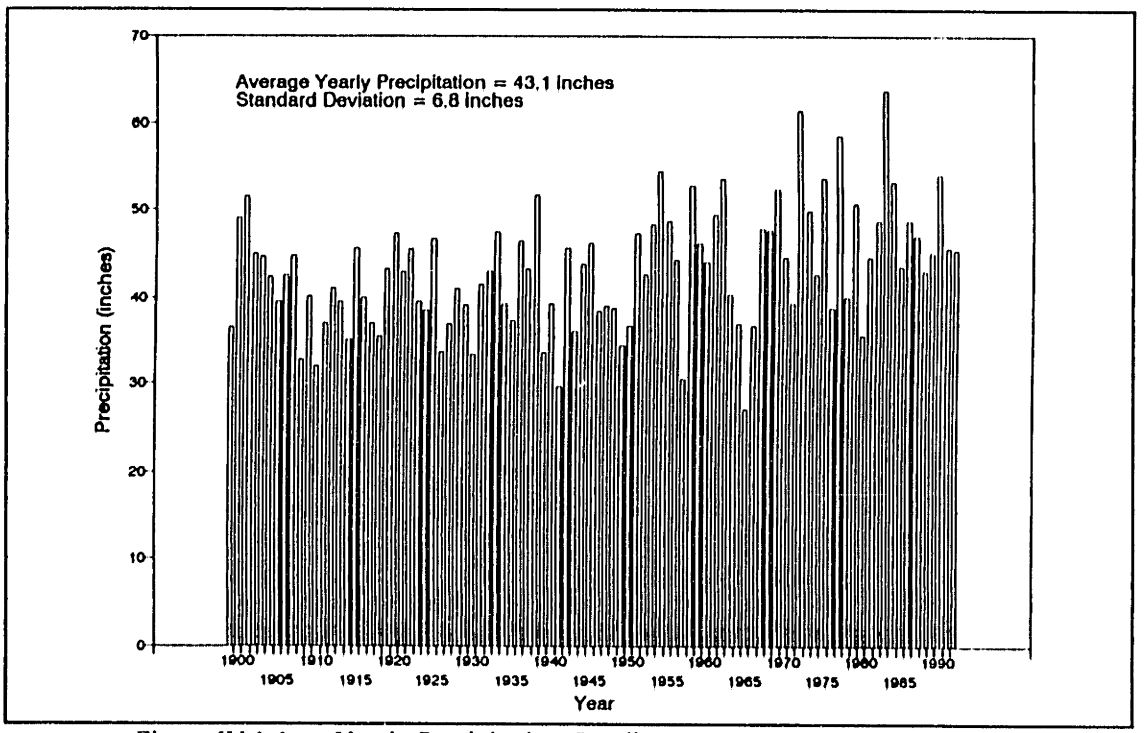

Figure IV.1-1: Yearly Precipitation, Reading NCDC Station, 1899 to 1992

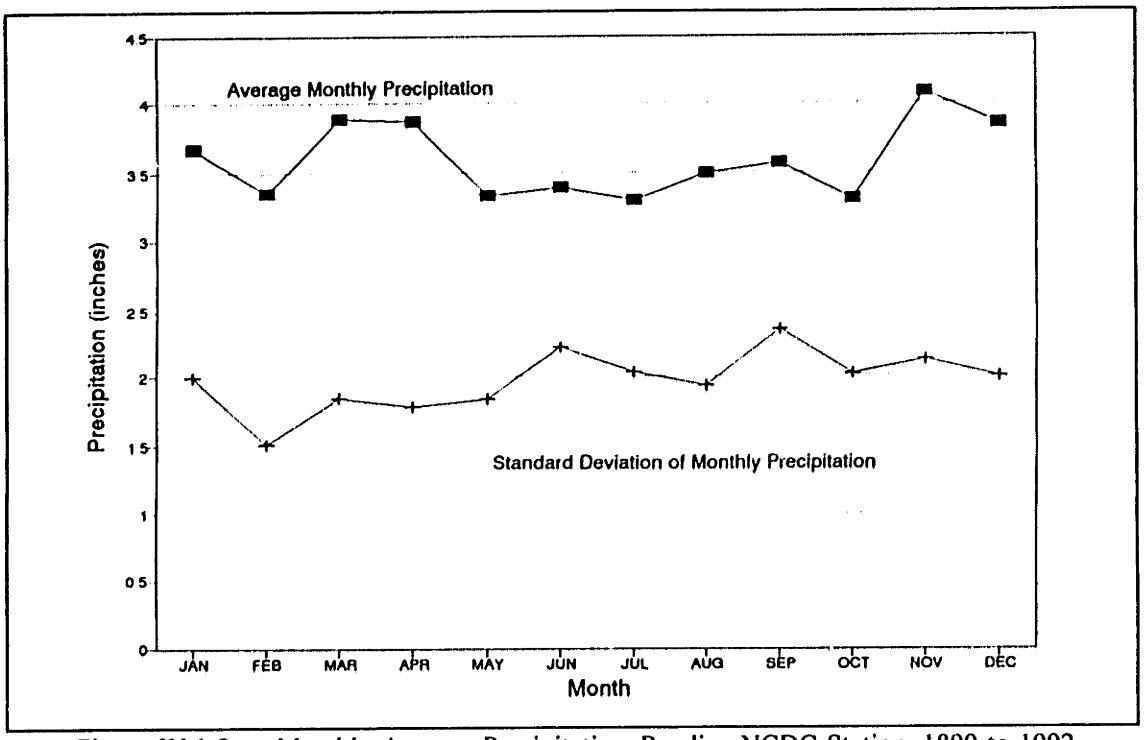

Figure IV.1-2: Monthly Average Precipitation, Reading NCDC Station, 1899 to 1992

Month	Average Precipitation (in)	Maximum Precipitation (in)	Minimum Precipitation (in)
January	3.90	13.00	0.60
February	3.65	7.68	0.33
March	4.07	10.80	0.82
April	3.99	10.09	1.50
May	3.49	9.70	0.85
June	3.44	11.77	0.36
July	3.30	8.80	0.47
August	3.47	8.13	0.91
September	3.60	8.45	0.57
October	3.83	12.85	1.14
November	4.78	11.02	0.81
December	4.47	10.55	1.13

Table IV.1-1: Monthly Precipitation, Reading Station, 1957-1992

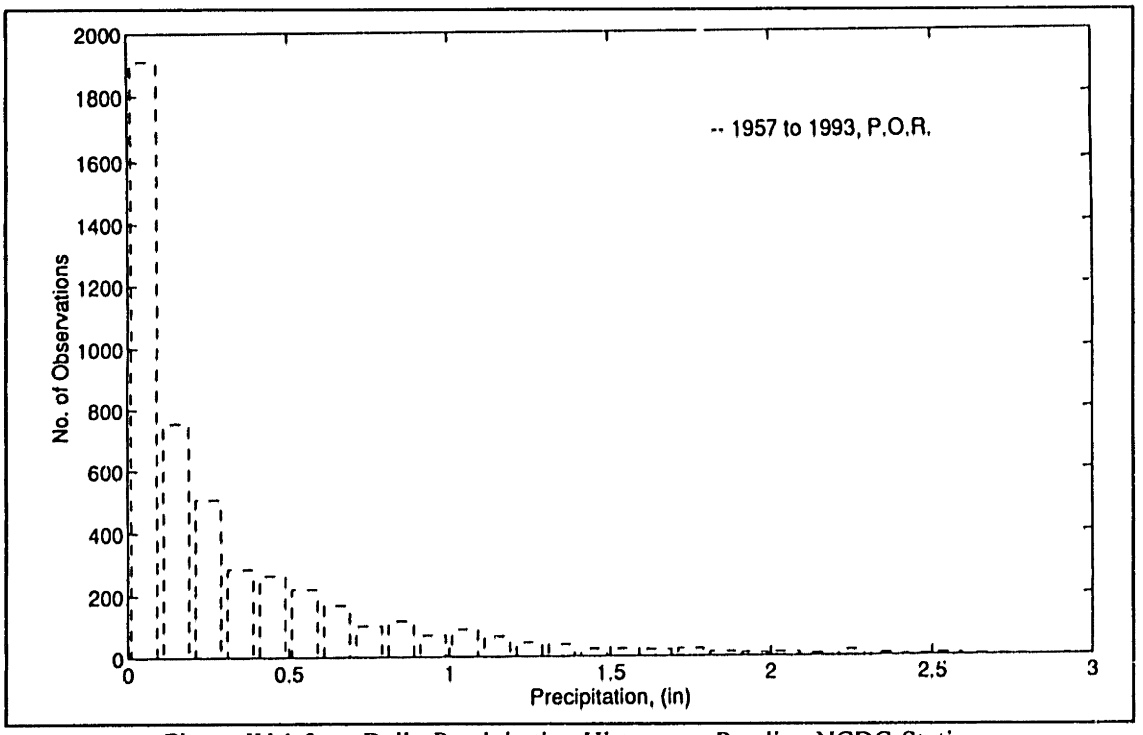

Figure IV.1-3: Daily Precipitation Histogram, Reading NCDC Station

24 hour Rain Depth (in)	Approx. Return Period*	Date YR-MO-DA
6.96	100 yr	621006
4.50	10 yr	620921
4.26	5 yr	600911
3.90	2 yr	790125
3.83	2 yr	900811
3.72	2 yr	900725
3.65	2 yr	901013
3.51	2 yr	840531

* Soil Conservation Service, 1975

Table IV.1-2: Summary of the 8 Largest 24 hour Precipitation Events Reading Station, 1957-1993

IV.1.2 Spatial Variability of Precipitation

Significant spatial variations of precipitation were observed within the watershed. A comparison of yearly (figure IV.A-1 and tables IV.A-1 and IV.A-2) and monthly precipitation totals (tables IV.A-1 and IV.A-2) for the Reading and Winchester stations indicates that 10 to 15% differences in the precipitation depths were common.

Variability of daily data was even more extreme. As an example, consider the daily precipitation depths for July 1990 for the Reading, Burlington, and Winchester stations. (table IV.A-4) For some of the days with light rainfall (<0.5") precipitation was observed at one station and not at the others. For the large event, July 25, differences as high as 60% (4.72" at Burlington versus 1.95" at Winchester) were observed. Part of these differences may have been associated with inconsistencies in the times at which the daily rainfall measurements were made. For example, assume that the rainfall distribution was spatially uniform and assume that the storm started during the late afternoon, at 3:00 pm, and ended the next day at 1:00 am. If the daily precipitation measurement was recorded at 5:00 pm at one station and at 12:00 am at another station, each station would have reported different daily totals even though the rainfall was spatially uniform. If the Winchester station measurement was recorded earlier than at Reading and Burlington, one may assume that the July 25th storm at Winchester was actually the sum of the precipitation occurring on the 25th and 26th. For such an assumption the difference in precipitation depths is reduced to a 25% difference (3.72" at Reading versus 4.70" at Burlington). Nevertheless, such a difference is still significant and indicates that the spatial distribution of precipitation did affect the quantities of water supplied to different parts of the watershed.

A comparison of the hourly distributions for the Reading and Burlington stations during the July 24, 1990 event is provided in table IV.A-5. Again, from the hourly record, the spatial distribution of precipitation is evident. Not only were the total storm depths significantly different but the timing of the hourly rainfall intensities was also significantly different. For example, the most intense part of the storm observed at Reading occurred at 3:00 am July 25, whereas the most intense part of the storm observed at Burlington occurred 10 hours later at 1:00 pm.

IV.1.3 Temperature

A discussion of air temperature is included within the precipitation section, since air temperature affects whether or not precipitation occurs as rain or snow. This data is used to determine months during which: 1) precipitation may occur as snow and, 2) streamflow could likely be affected by snowmelt.

The overall average temperature measured at the Reading NCDC Station for the 1961 to 1990 period of record was 48.0 °F. The mean temperature was computed by taking the average of the maximum and minimum daily temperature for a given month. A summary of mean monthly temperatures for the same period of record are given in table IV.1-3.

Month	Mean Temperature (°F)
January	24.5
February	26.7
March	35.8
April	45.7
May	56.2
June	65.4
July	71.0
August	69.3
September	61.1
October	50.5
November	40.8
December	29.4

Table IV.1-3: Mean Monthly Temperature at the Reading NCDC Station, 1961-1990

Below freezing temperatures were generally observed during December, January, and February. During these months, therefore, a large fraction of the precipitation probably occurred as snow. The data also suggest that, snowfall and snowmelt are possible during March, April, and November. During the other months, snowfall is unlikely.

IV.2 STREAMFLOW

This section includes: 1) a summary of average streamflows at each of the 5 gaging stations during the 1991 to 1993 period of record, 2) a description of watershed sub-basins, groundwater withdrawals and runoff fractions, 3) a discussion of hourly flow data, and 4) a discussion of the USGS historical streamflow record. The primary purpose of presenting a summary of average streamflow for each station and to discuss the longer record at the USGS station, is to provide general hydrologic information for the watershed. Knowledge of the watershed sub-basins, groundwater withdrawals, and characteristics of the hourly flow was needed for the formulation of the computer model. Runoff fractions were helpful in developing a general understanding of the watershed hydrology. Within the section discussing the historical streamflow record at the USGS station, a longterm baseflow analysis is presented along with a description of urbanization effects within the watershed. Results of the longterm baseflow analysis are used as an input to the computer model for the computation of the longterm baseflow component of streamflow. Conclusions concerning urbanization effects have implications in the development of a transport history.

IV.2.1 Summary

Average flows (for the January 1991 to February 1993 period of record) at each gaging station are given in table IV.2-1 below. The location of each gaging station is illustrated in figure III.2-1. More detailed data (including instantaneous maximum and minimum flows and water elevation data) are provided in appendix IV.A.

Station	Ave Flow 1/91-2/93 (cfs)	Drainage Area (mi^2)	Normalized Flow (cfs/mi^2)
Wedge Pond, Station #1	7.3	10.5	0.70
Route 128, Station #2	8.8	6.2	1.42
Montvale, Station #3	18.6	8.7	2.14
Horn Pond, Station #4	9.7	7.1	1.37
USGS, Station #5	28.9	25.0	1.16

Table IV.2-1: Average Streamflow for 1/91 to 2/93 Period of Record

The small value of the normalized flow at the Wedge Pond station was due to significant groundwater

withdrawals occurring within upstream drainage areas. The highest value of the normalized flow corresponds to the Montvale station. Implications associated with this high value are discussed in section IV.2.2.

Along the Aberjona River, average streamflows (from gage 2 to 3 to 5) increased in the downstream direction, whereas on the Horn Pond Creek tributary average streamflows decreased. The increase in streamflow along the Aberjona was due to the accumulation of inflows along the river's length. The decrease in flow on Horn Pond Creek was due to significant groundwater withdrawals occurring in the drainage area between the Horn Pond and the Wedge Pond stations.

The seasonal variations of mean monthly flows for all stations (except Montvale, gage 3) were similar, with low flows observed during the summer-early fall months and high flows observed during the winter and spring seasons (figure IV.2-1). From June to December the bulk of the flow observed at the USGS station (gage 5) can be accounted for by streamflow at Montvale. However, from February to May, the bulk of the streamflow at the USGS station is accounted for by streamflow at both Montvale and Wedge Pond (gage 1).

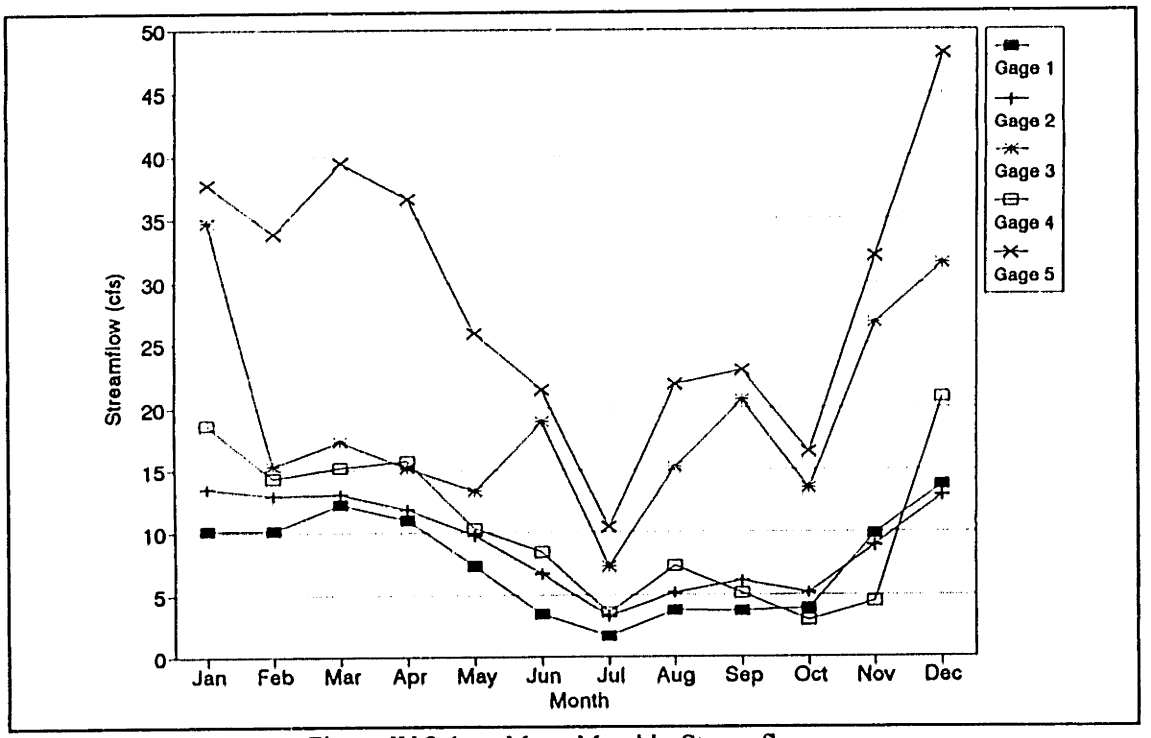

Figure IV.2-1: Mean Monthly Streamflow
All Stations, Jan 1991 to Feb 1993

IV.2.2 Watershed Sub-basins, Groundwater Withdrawals and Runoff Fractions

Sub-basins

Given the locations of the gaging stations and the surface topography, the watershed can be sub-divided into drainage sub-basins (figure IV.2-2). Three of the sub-basins are located on the Aberjona River. These basins include: 1) the Woburn North sub-basin (drained by the Route 128 gage), 2) the Woburn Central sub-basin (drainage area between the Route 128 and Montvale gages), and 3) the Winchester sub-basin (drainage area between the USGS and the Montvale gages, excluding the area drained by the Wedge Pond gage). The other two sub-basins are drained by Horn Pond Creek, the main tributary to the Aberjona. These sub-basins include: 1) the Burlington sub-basin (area drained by the Horn Pond gage) and, 2) the Horn Pond sub-basin (the drainage area between the Horn Pond and Wedge Pond gages). The location and area of each of the sub-basins are defined in figure IV.2-2.

Groundwater Withdrawals

Three areas of significant groundwater withdrawals have been identified within the watershed. (figure IV.2-3) These withdrawals include:

	Withdrawal, mgd
Woburn Water Supply	4.5
Burlington Water Supply	0.1
Atlantic Gelatin	1.8
Total =	6.4

The Woburn Water Supply consists of several wells in the vicinity of the Horn Pond reservoir. The average withdrawal rate over a 5 year period of record was 4.5 mgd[5]. (Commonwealth of Massachusetts, 1990a) For that period, the withdrawal rate was highest from May through October, enhancing low flow conditions which persisted throughout the summer and early fall.

Only one of the wells from the Burlington water supply cluster (P.S. #8) is located within the watershed. The average withdrawal rate over a two year period of record was 0.13 mgd. (Commonwealth of Massachusetts, 1990b)

[5]The average was determined from the amounts withdrawn in 1981 (4.8 mgd), 1986 (4.2 mgd), 1987 (4.4 mgd), 1988 (4.4 mgd), and 1989 (4.8 mgd). The withdrawal rates were obtained from permits which were on file at the Commonwealth of Massachusetts office during a visit in 1990.

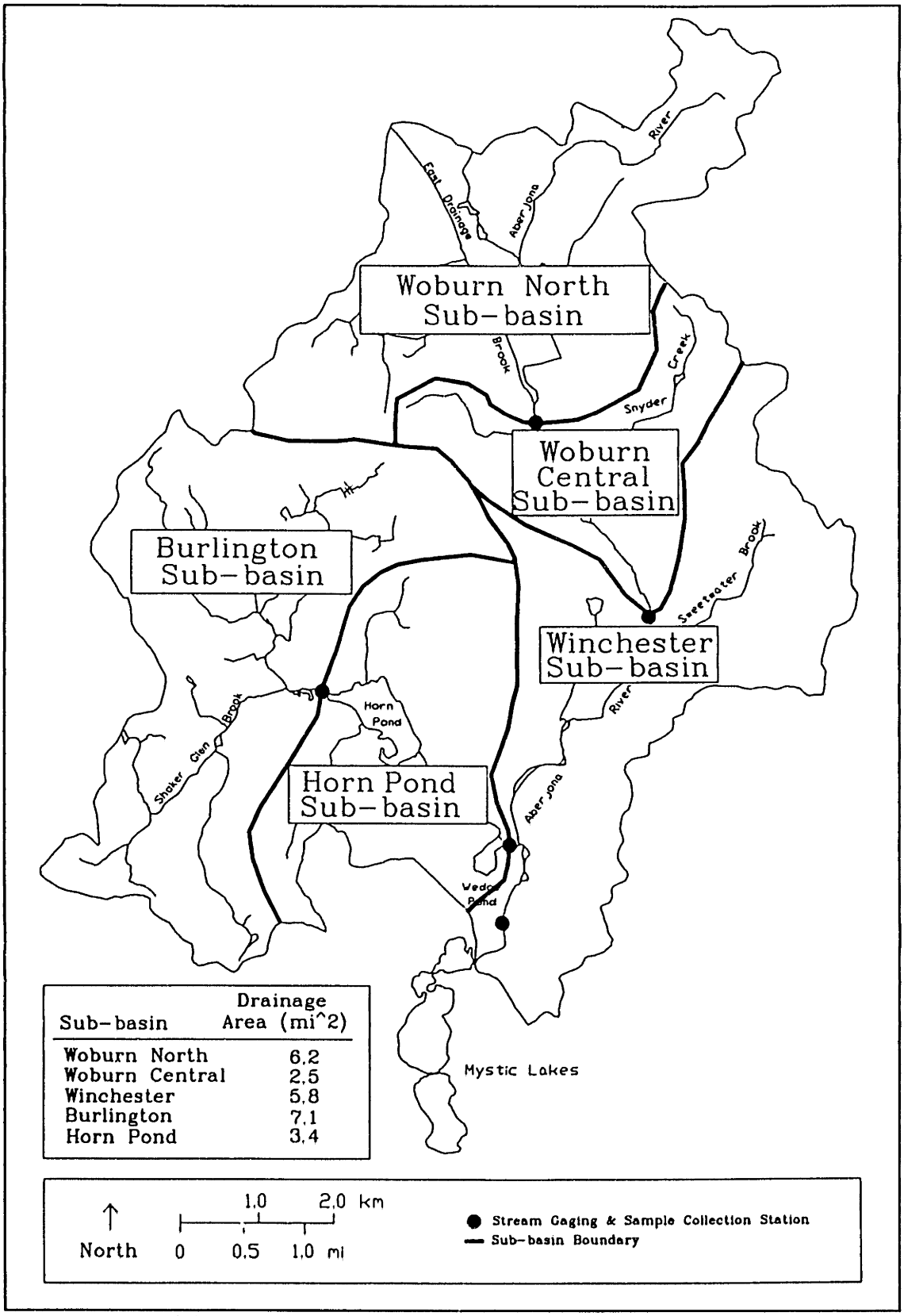

Figure IV.2-2: Sub-basins of the Aberjona River Watershed
(Basemap from Durant, 1991)

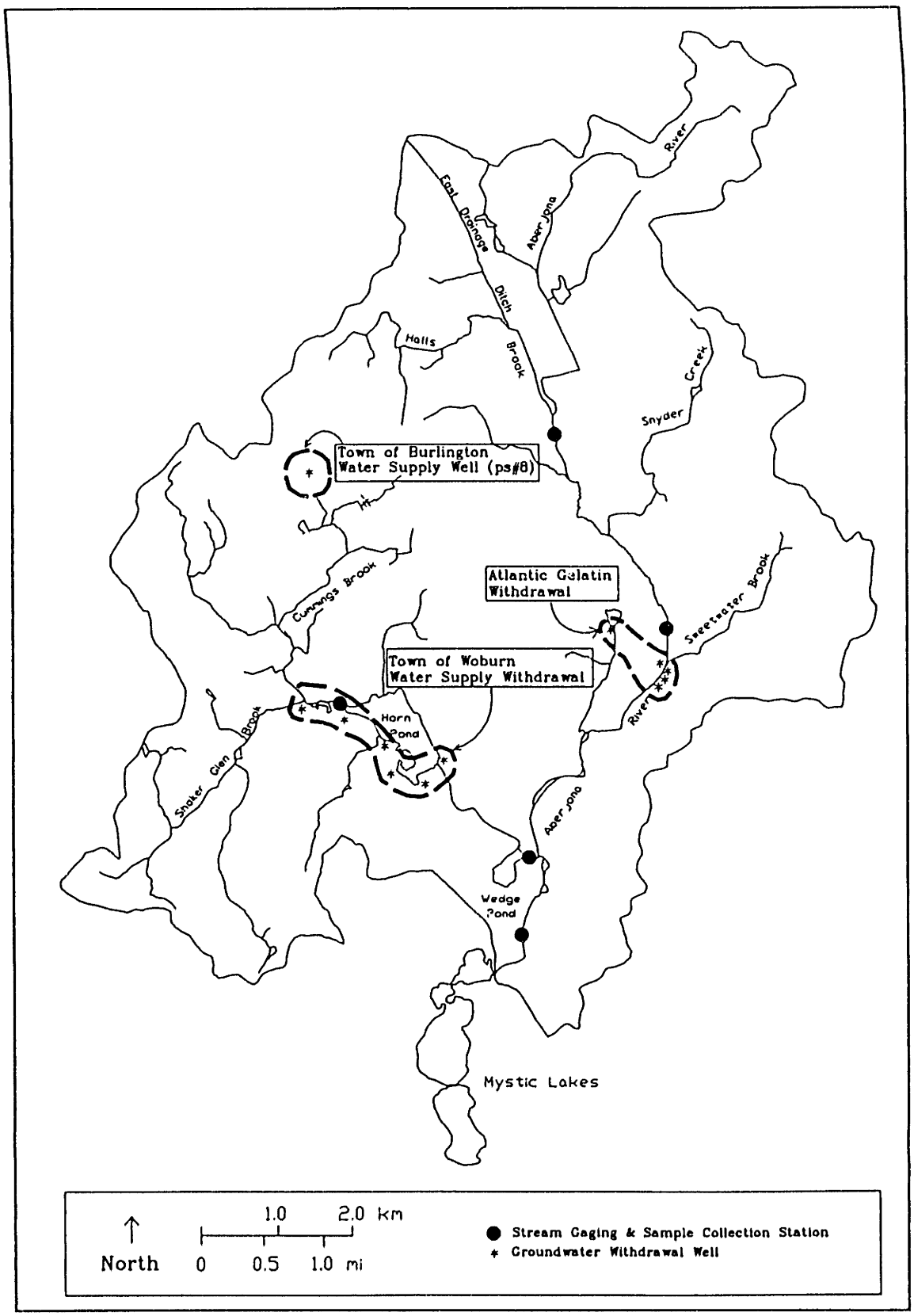

Figure IV.2-3: Locations of Major Groundwater Withdrawal Wells
(Basemap from Durant, 1991)

The Atlantic Gelatin withdrawal consists of a set of 5 groundwater withdrawal wells. Four of these wells are located immediately downstream of the Montvale gage and the remaining well is located south of Whittemore Pond which discharges into the Aberjona River downstream of the Montvale gage, (figure IV.2-3) Over a two year period of record, the average rate of withdrawal from these wells was 1.8 mgd (2.8 cfs). (Commonwealth of Massachusetts, 1988a) The month to month variability in the withdrawal rate showed no distinct seasonal trend. The standard deviation of the monthly withdrawals was 0.3 mgd. Once withdrawn, the water is discharged into the sanitary sewer system and therefore represents a loss of water from the watershed.

Other withdrawals include the McCord-Winn Textron (0.2 mgd), and other minor withdrawals for agricultural purposes. (Commonwealth of Massachusetts, 1988b, 1989a, and 1989b) McCord-Winn Textron discharges the withdrawn water (used for cooling purposes) into the Aberjona River. Agricultural withdrawals are assumed to be used for irrigation purposes which will tend to recharge the groundwater aquifer. For either, the McCord-Winn Textron or the agricultural withdrawals, it is assumed that these water removals do not significantly affect the overall water balance over the course of a year.

Sub-basin Runoff and "Accountable Water" Fractions

Runoff and "accountable water" fractions are useful for determining the fraction of incident precipitation that is converted to streamflow or to "accountable water." These fractions are defined as;

$$\text{Runoff Fraction} = \frac{\text{Streamflow Volume}}{\text{Precipitation Volume}}$$

$$\text{Accountable Water Fraction} = \frac{\text{Accountable Water Volume}}{\text{Precipitation Volume}}$$

The precipitation volume is the product of the precipitation depth for the time period of interest and the surface area of the sub-basin considered.

The streamflow volume corresponds to the net streamflow coming from a particular sub-basin. It is equal to the streamflow volume at the downstream end of the sub-basin minus the streamflow volume entering at the upstream end of the sub-basin.

The "accountable water" is the sum of the net streamflow contribution plus the amount of water withdrawn in association with controlled groundwater withdrawals. Within a given sub-basin, the volume of accountable water is equal to the streamflow volume plus the volume of water removed using groundwater withdrawal wells.

The precipitation depth used for computation purposes was 45.3 inches, the average yearly rainfall at the Reading station for 1991 and 1992. The runoff values at each station correspond to the average streamflows measured at each station during the January 1991 to January 1993 period of record. The results of the computation are provided in figure IV.2-4. For the entire watershed, the runoff fraction was 35% whereas the "accountable water" fraction was 47%. The fraction of the precipitation that was not associated with the "accountable water," was most likely associated with evapo-transpiration or deep groundwater (bedrock) losses.

The "accountable water" fraction for each sub-basin (except the Woburn Central sub-basin) was relatively consistent, with values in the range from 31 to 43%. The fraction observed for the Woburn Central sub-basin was 118%. Oddly, the 118% observed for the Woburn Central sub-basin indicates that an excess of water is produced over that which can be accounted for by direct precipitation within the sub-basin.

The large fraction observed for the Woburn Central sub-basin may be partly due to errors. Possible sources of error include: 1) errors in the precipitation measurements, 2) errors in the streamflow measurements, and 3) errors in the sub-basin area determination. The combination of these errors, however, is not likely to be large enough to affect the computed fraction for the Woburn Central sub-basin by a large amount.

Assuming that the computed fractions are correct, the very high fraction computed for the Woburn Central sub-basin may perhaps be due to the inflow of waters from areas outside the sub-basin boundaries. One possibility, although speculative, includes the occurrence of a highly permeable underground connection between the Woburn Central sub-basin and a water source with a larger hydraulic head. The Woburn North sub-basin could be one possible source of water since groundwater elevations within this sub-basin are generally higher than the groundwater elevations in the Woburn Central sub-basin. Other possible sources include waters from other sub-basins and/or other waters from outside the watershed boundary. However, it is emphasized that these explanations are purely speculative and in the absence of further investigation, no definitive conclusions should be drawn from the results.

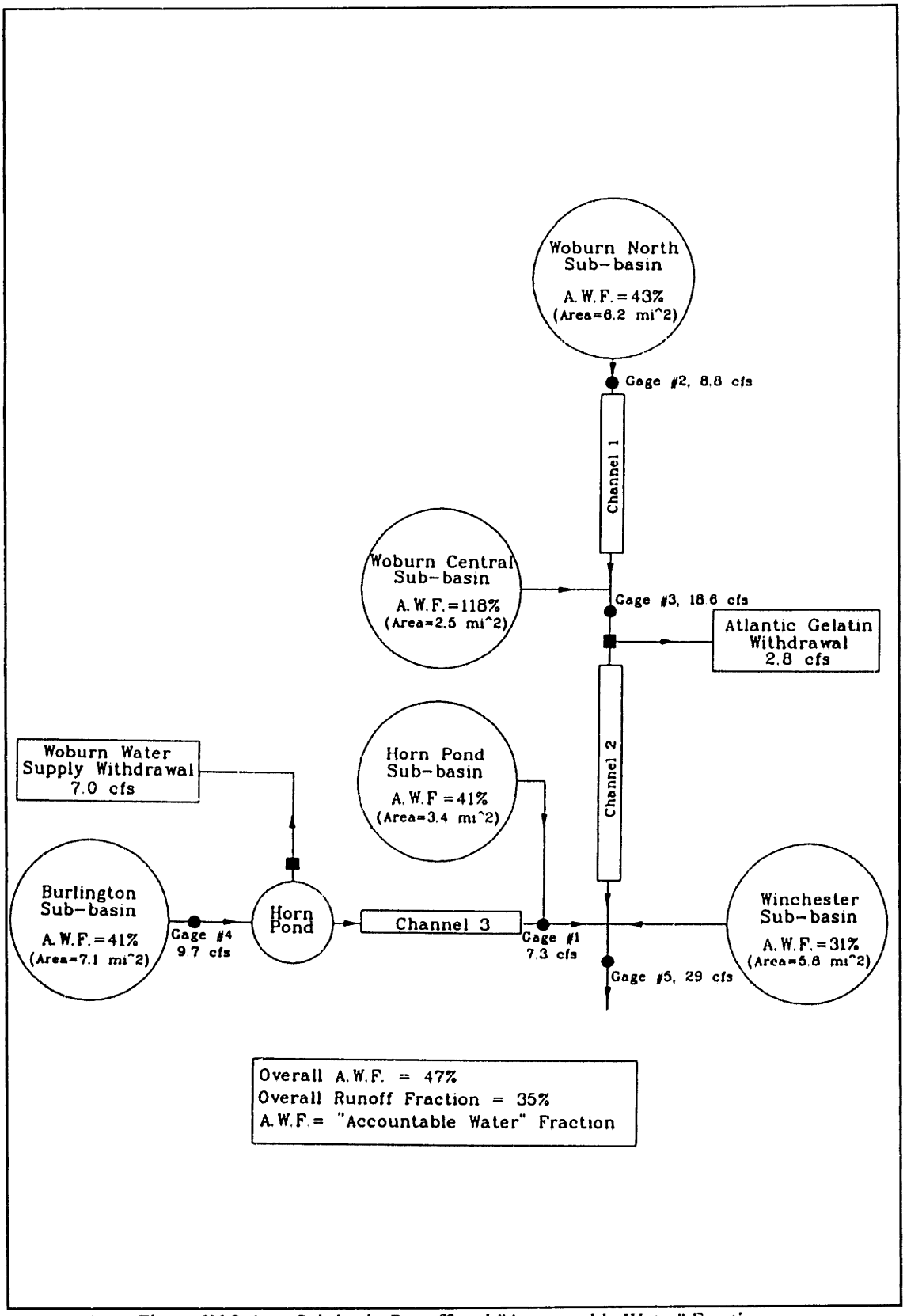

Figure IV.2-4: Sub-basin Runoff and "Accountable Water" Fractions

IV.2.3 Discussion of Hourly Flow Data

Hourly flow plots from January 1991 through September 1993 are included in appendix IV.B. The data are also provided in ASCII format in appendix IV.C. The river's characteristic response to precipitation events is described below. Anomalous fluctuations in the record are discussed in appendix IV.B.

Storm Response

One of the most noticeable features of the streamflow hydrographs observed along the Aberjona River is their consistent pattern in response to storm events. This pattern is exemplified by the set of three hydrographs (July 6, 9, and 11, 1992) plotted in figure IV.2-5. Prior to each of these events, streamflow on the Aberjona was constant or slowly decreasing in time. Upon the occurrence of a storm, streamflow responded very quickly (within approximately 2 hours) with a rapid increase in streamflow followed by a rapid decline in streamflow. This initial response resulted in a very sharp peak in each of the hydrographs. After the quick decline, one of two responses was observed. The first response is exemplified by the USGS and Route 128 hydrographs where after the rapid decline in flow, the rate of decrease "slowed-down" for a few hours and was then followed by a more rapid decline down to typical values observed during low flows. The second type of response is exemplified by the Montvale hydrographs, where after the initial rapid decline in flow, streamflow then increased again followed by a second peak. In this case the second peak was more rounded. After the second peak, the flow decreased at a quick rate to typical values observed during low flow conditions.

A possible interpretation of these patterns is that streamflow is composed of various components of flow. For example, I have chosen to separate the hydrographs (figure IV.2-6) into three distinct components: 1) a quick storm response, 2) a slow storm response, and 3) longterm baseflow. "Quick" water corresponds to the first peak which is characterized by the rapid increase and subsequent rapid decrease in flow. These waters are associated with mechanisms that are able to transmit water quickly to the river. The quick water systems may include: 1) sewer flows, 2) direct precipitation into the channel, 3) direct runoff close to the channel and, 4) impervious area runoff. "Slow" water is associated with the slower rate of decline (USGS and Route 128 station) or with the second peak (Montvale station). These waters tend to respond more slowly to a storm event. Sources of these waters probably travel through the ground before entering the channel. Sources may include: 1) interflow, which is that portion of groundwater flow (induced by infiltration) which reaches the river prior to reaching the groundwater table and, 2) groundwater sources associated with the steepening of the water table due to storm water infiltration. Additionally, for the Montvale and USGS hydrographs, the slow component may also incorporate flows from upstream source areas (a combination of quick and slow flows) whose response was attenuated due to routing effects of the river channel. Longterm baseflow is a component that

responds to changes in precipitation and climate over long (seasonal) time scales. Longterm baseflow may be characterizedas a groundwater inflow which is not strongly affected by short term storm events.

Flows at the Horn Pond and Wedge Pond stations also responded to storm events. However, for these stations, flow responses were characterized by a single peak with no apparent occurrence of separate "quick" and "slow" flows.

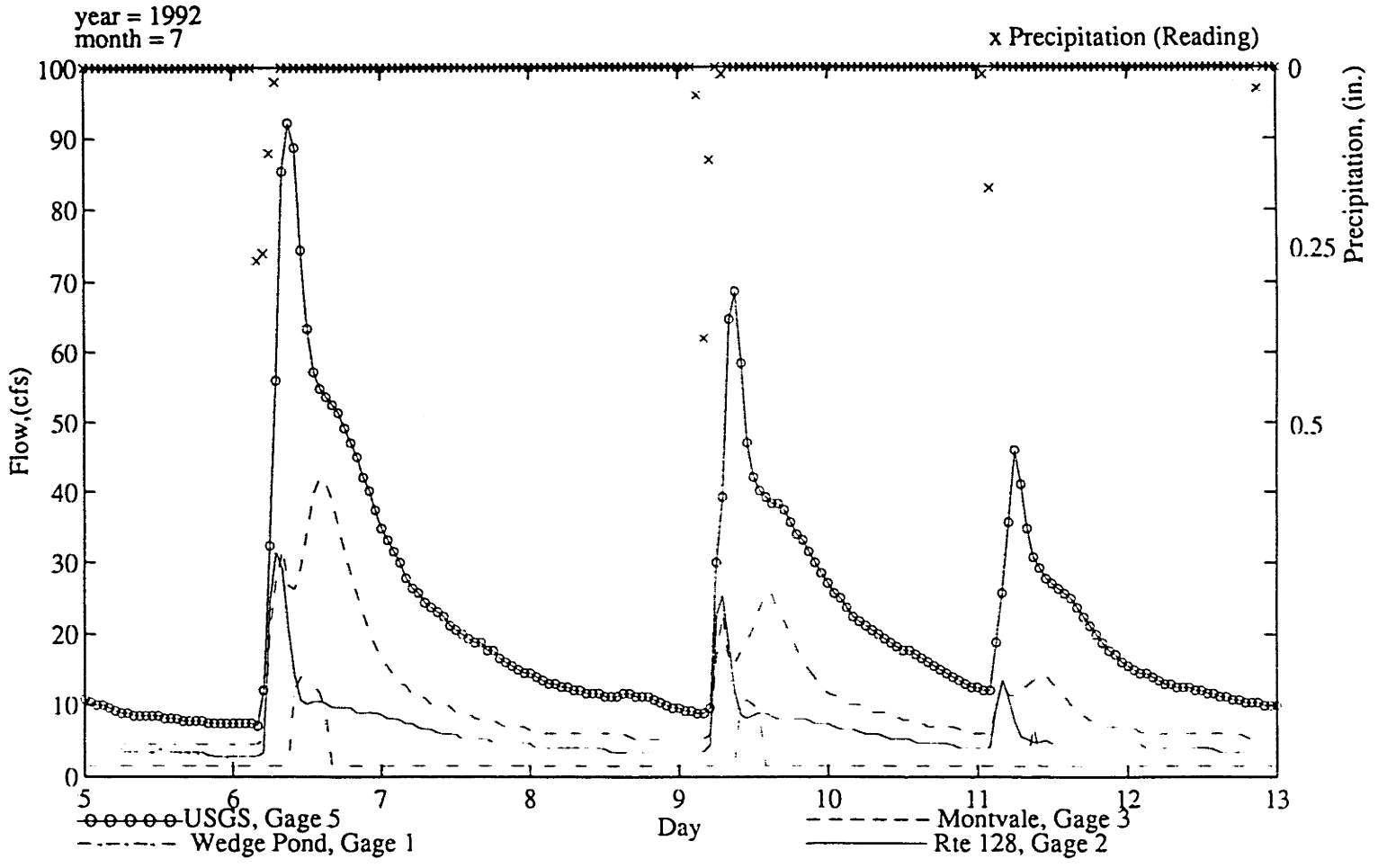

Figure IV.2-5: Streamflow Versus Time, July 5-13, 1992

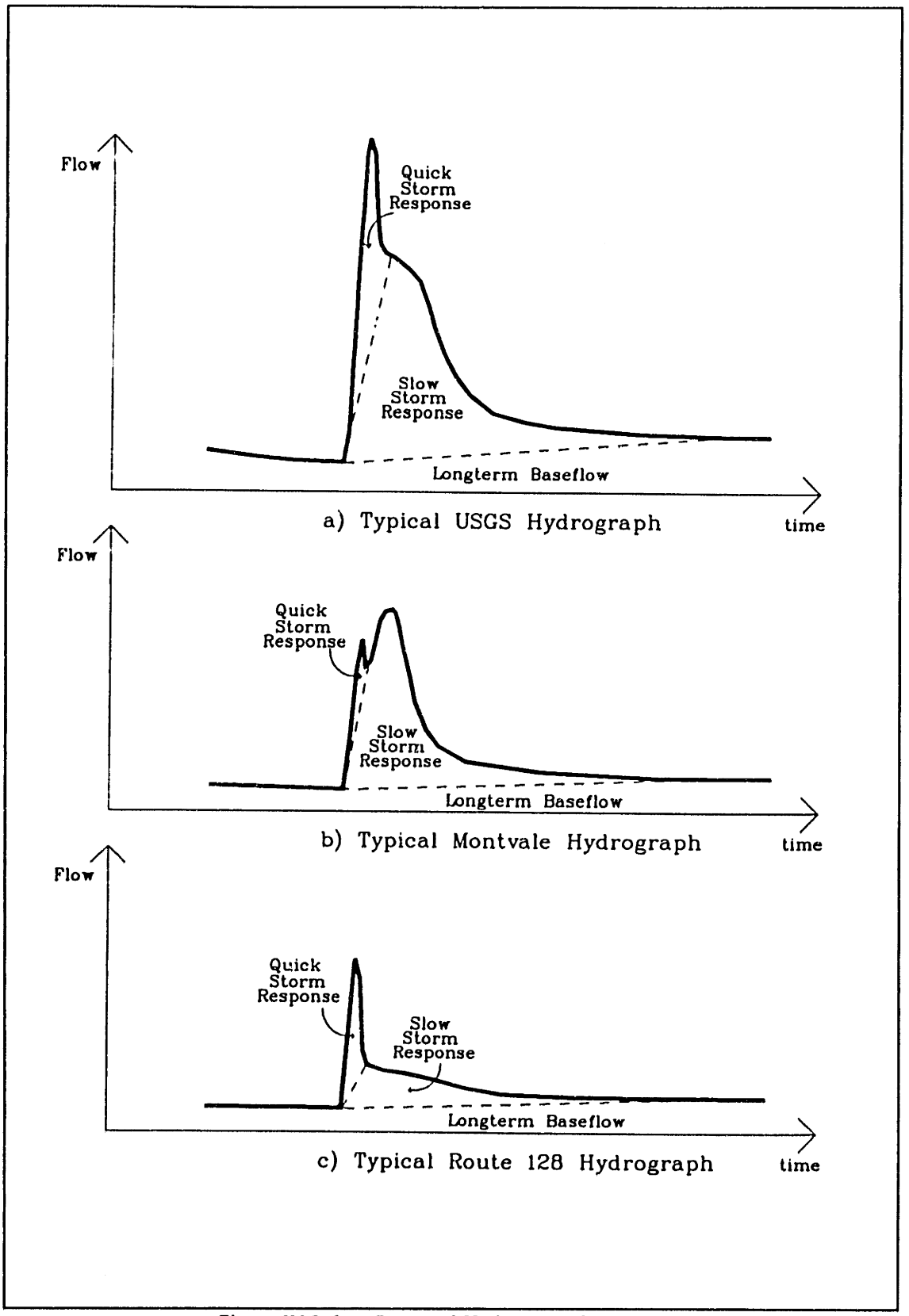

Figure IV.2-6: Proposed Hydrograph Components

IV.2.4 USGS Data

Monthly and Yearly Flows

The overall average streamflow at gage 5 for the USGS period of record (May 1939 to September 1993) was 29.0 cfs. The minimum observed daily flow was near zero (less than 1 cfs) and the maximum observed daily flow was 951 cfs. The instantaneous maximum flow was 1330 cfs observed on January 25, 1979. The frequency distribution of daily average flows (figure IV.2-7) indicates that flows tend to be at values less than 10 cfs during 38% of the time and at values of less than 20 cfs during 55% of the time. The overall distribution of flow frequencies appears to decrease exponentially as flows increase.

The monthly distribution of streamflow was characterizedby higher flows during the spring months and lower flows during the summer. (figure IV.2-8) The maximum average monthly flow was observed in March (64.5 cfs) while the minimum average monthly flow was observed in September (9.4 cfs). The seasonal distribution of monthly flows can be contrasted with a more uniform distribution of precipitation depth throughout the year (figure IV.1-2).

The distribution of monthly streamflow was partly due to the accumulation of precipitation, occurring as snow, during the winter months. During the spring, as temperatures increase, the accumulated snow melted resulting in additional contribution of water to the river. During the summer as temperatures increased and vegetation growth increased, evapo-transpiration was high, resulting in a more efficient loss of water during this time of year. The combined effects of both processes, snow melt in the spring and increased evapo-transpiration during the summer is the primary cause of the observed pattern of monthly streamflows.

The yearly distribution of average streamflow is characterized by a maximum yearly flow of 51.6 cfs which occurred in 1983 and a minimum yearly flow of 9.12 cfs which occurred in 1966. (figure IV.2-9, table IV.A-11) The standard deviation of the yearly streamflow is 9.5 cfs. A large portion of the yearly variability in streamflow can be associated with yearly changes in precipitation depths. (figure IV.2-10) In general, years with high streamflows occur during years with large precipitation depths.

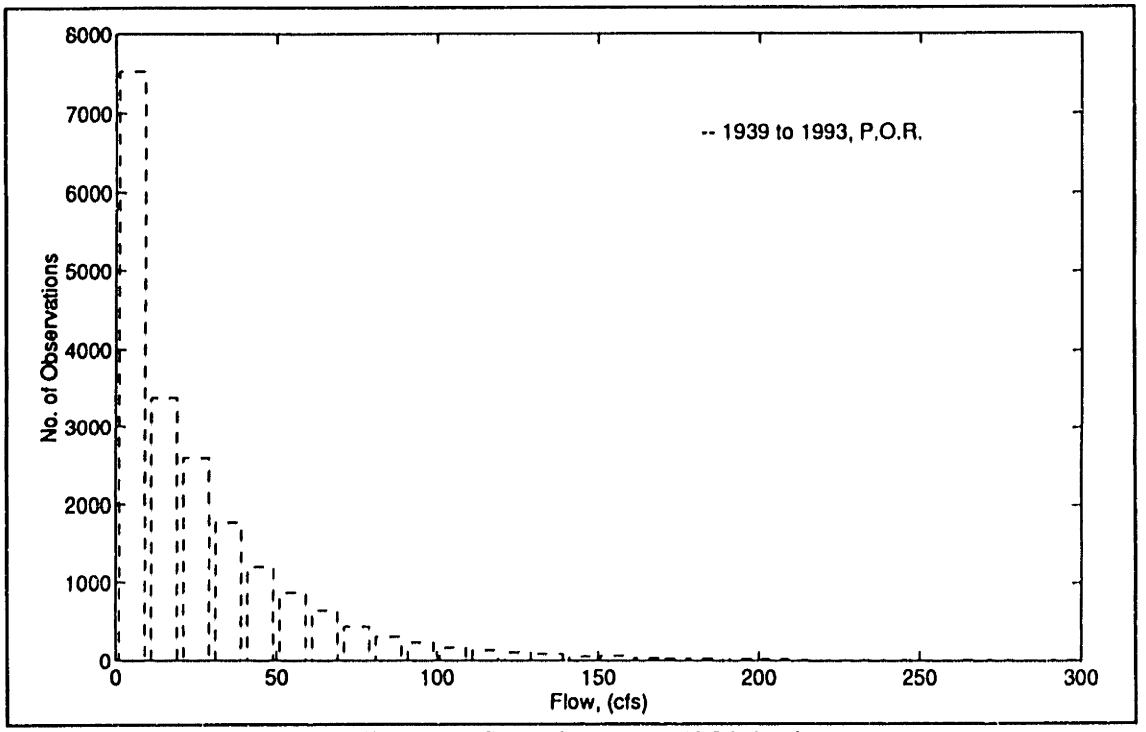

Figure IV.2-7: Daily Streamflow Histogram, USGS Station
Max Flow = 951 cfs, Histogram up to 300 cfs for Clarity

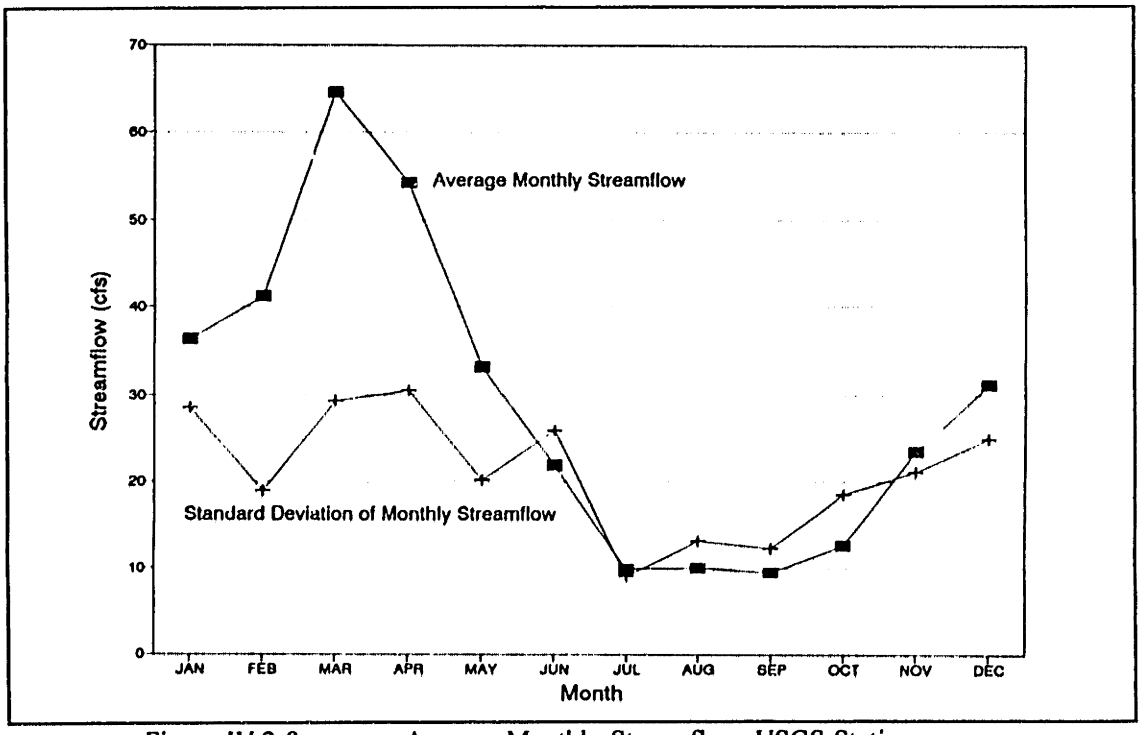

Figure IV.2-8: Average Monthly Streamflow, USGS Station
May 1939 to Sept 1993

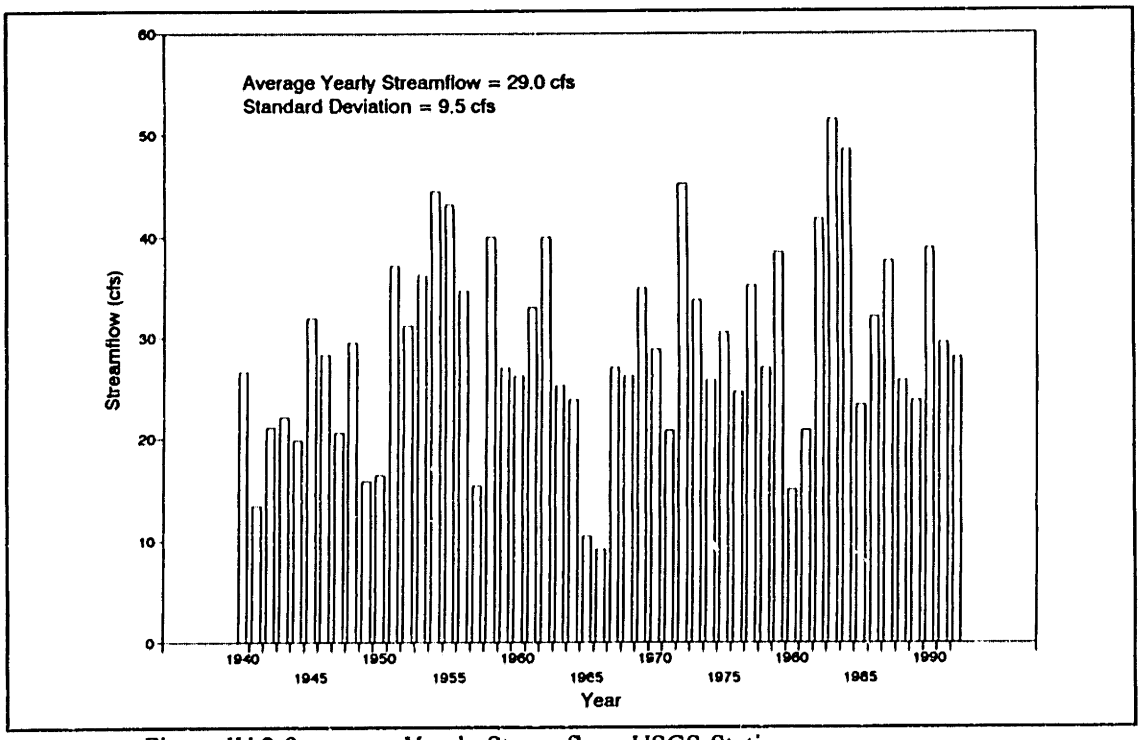

Figure IV.2-9: Yearly Streamflow, USGS Station 1940 to 1992

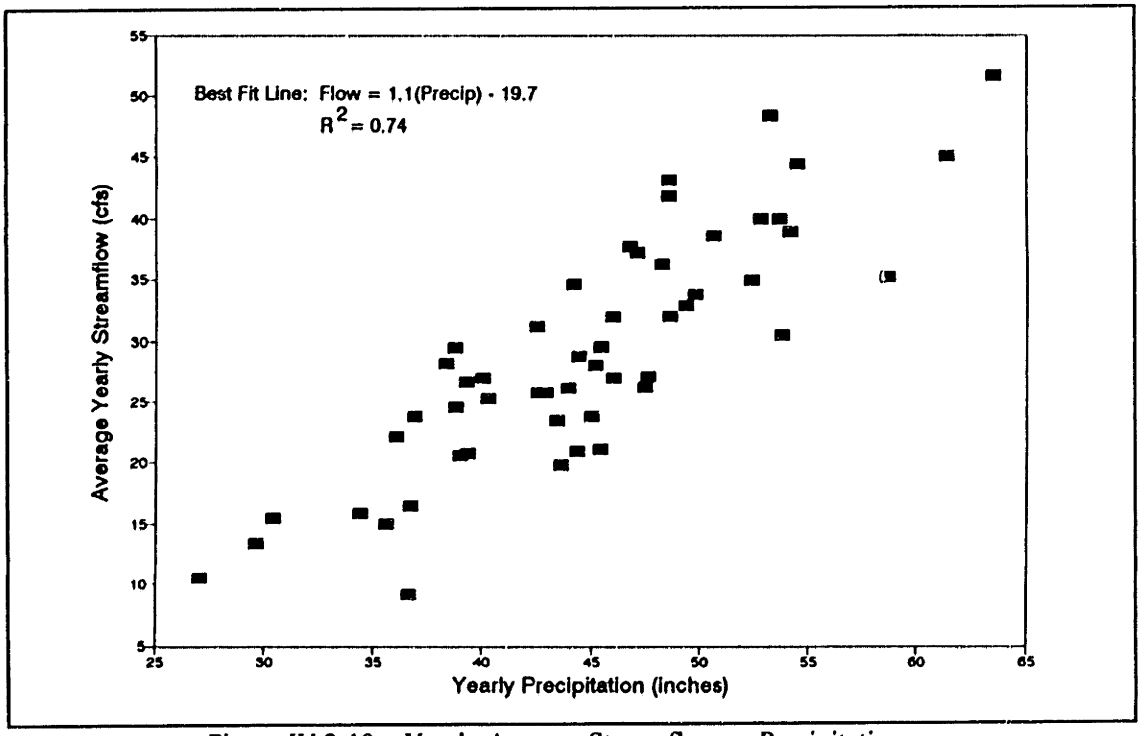

Figure IV.2-10: Yearly Average Streamflow vs Precipitation USGS Station, 1940-1992

Urbanization Effects

A preliminary analysis of the data indicates that recent urbanization did not significantly affect the overall volume of water carried by the river. Rather the volume of streamflow carried by the river was more strongly associated with changes in longterm (yearly) precipitation depths. However, recent urbanization appears to have had a strong effect on the time distribution of streamflow in response to a storm event.

River Water Volume

To analyze longterm water volume changes the daily flow record was separated into 5 groups of 10 successive years. As the groups progress from the 40's to the 80's, the degree of urbanization is assumed to increase. Rainfall and runoff water volumes for each 10 year group are provided in table IV.2-2.

Time Period	Ave. Daily Flow (cfs)	Ave. Yearly Runoff Depth (in)	Mean Yearly Precipitation (in.)	Precip. Converted to Runoff (%)
1940-1949	22.9	12.4	39.0	31.8
1950-1959	32.5	17.7	45.1	39.2
1960-1969	25.6	13.9	45.5	30.5
1970-1979	31.0	16.8	47.9	35.1
1980-1989	31.0	16.8	47.2	35.7

Table IV.2-2: Water Volume Statistics for successive 10 year time periods

From the data above, the fraction of precipitation converted to runoff varied from 30 to 40%. There was no significant trend associated with more urbanized time periods. Therefore, no strong conclusion can be made concerning urbanization and the overall volume of water transported by the river.

The only generalized trend that may be observed is that during drier years a smaller fraction of rainfall was converted to streamflow. The 1940-1949 time period was characterized by low precipitation volumes and low runoff fractions. Within the 1960-1969 period there were two years with extremely low precipitation depths which shifted the runoff fraction for this time period to lower values. During these two years (1965 and 1966) the runoff fractions were 21.1% and 13.5%.

Timing of Streamflow Response

Increased urbanization may result in a change in the shape of the streamflow hydrographs (Bras and Perkins, 1975). One typical characteristic of urbanization is an increase in man-made storm drainage systems. These systems tend to transport runoff to a discharge point (i.e. river) very quickly. Because of this effect, one would expect larger peak streamflows occurring during earlier times of the hydrograph.

Review of the 1939 to 1993 daily streamflow data indicate that the hydrographs have become more "flashy" (or characterized by quicker response times and larger peaks) in more recent years. One possible cause of this trend is an increase in urbanization. Examples of the differences (1945 versus 1983) are provided in figures IV.2-11 and IV.2-12. The most notable change between the two years is the number, size, and time base of notable peaks. For more recent years, the frequency and size of notable peaks have increased while the time base of the peaks has decreased.

To further investigate the effects of urbanization on the peak flows, the days with the average daily streamflows greater than 400 cfs were identified and ranked. Characteristics of flows for these dates are given in table IV.2-3.

Results in table IV.2-3 indicate that peak streamflows have increased in more recent times. Of the 10 highest daily flows, only 2 peaks occurred prior to 1979, whereas of the highest 28 flows, only 9 peaks occurred prior to 1978. None of the largest 28 peaks occurred during the first 22 years of record (1939-1953). Some of the occurrences of large peaks may be correlated with the occurrences of large precipitation events (e.g. 621007) whereas peaks that occur in the winter-spring months may be associated with large snowmelt events. However, assuming that the distribution of large storms/melt events is uniform throughout the record, the inferred trend is that streamflow hydrographs are becoming "peakier" as time progresses. A probable cause of this trend is an increase in urbanization.

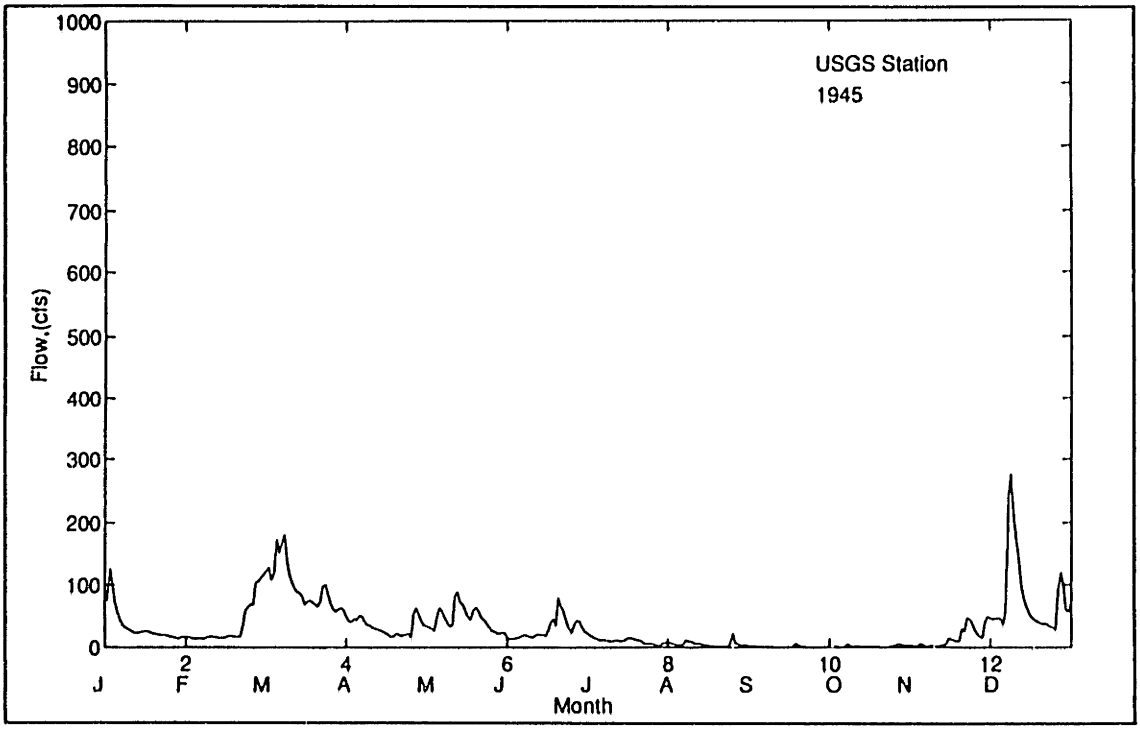

Figure IV.2-11: Daily Flow versus Time, USGS Station, 1945

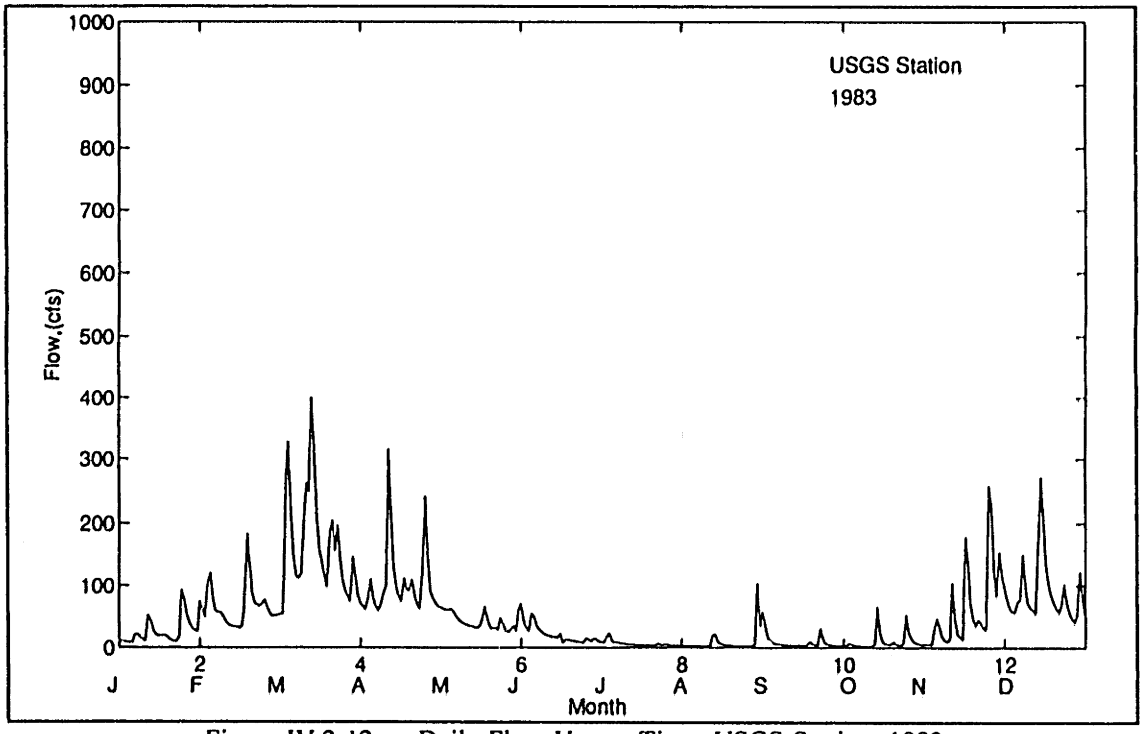

Figure IV.2-12: Daily Flow Versus Time, USGS Station, 1983

Rank	Daily Flow,(cfs)	Date (YR-MO-DA)	Precipitation Characteristics	Antecedent Precipitation
1	951	790126	4.1" in 3 days 3.9" in one of the days	4 days earlier, 1 day with 3.1"
2	830	790125	4.1" over 3 days 3.9" in one of the days	3 days earlier, 1 day with 3.1"
3	780	870407	6.1" in 5 days	4 days earlier, 2.9" in 2 days
4	732	621007	11.1" over 3 days	6 days earlier, 3.0" in 4 days
5	690	820606	4.6" in 3 days	4 days earlier, 3.3" in 1 day
6	686	870406	6.1" in 4 days	4 days earlier, 2.9" in 2 days
7	668	820607	5.4" in 4 days	5 days earlier, 3.3" in 1 day
8	613	840601	6.6" in 5 days	no large prior storm
9	612	550820		
10	603	790122	3.1" in 1 day	no large prior storm
11	580	691227	5.0" in 2 days	5 days earlier, 1.1" in 1 day
12	543	840602	8.1" in 6 days	no large prior storm
13	541	680319	4.1" in 3 days	no large prior storm
14	513	870405	3.8" in 2 days	5 days earlier, 2.9"
15	494	550819		
16	462	621006	9.1" in 2 days	5 days earlier, 3.0" in 4 days
17	462	621008	11.1" in 2 days	7 days earlier, 3.0" in 4 days
18	457	840603	8.1" in 6 days	no large prior storm
19	456	540912		
20	452	840531	5.9" in 4 days	no large prior storm
21	446	930330	1.6" in 3 days	no large prior storm
22	442	870408	6.1" in 5 days	8 days earlier, 2.91"
23	441	780126	2.5" in 2 days	9 days earlier, 3.0" in 6 days
24	439	680318	3.9" in 2 days	no large prior storm
25	431	820608	4.6" in 3 days	4 days earlier, 3.3" in 1 day
26	414	901014	6.0" in 7 days	no large prior storm
27	408	861219	3.6" in 3 days	no large prior storm
28	401	830312	4.6" in 6 days	10 days earlier, 2.3" in 1 day

Table IV.2-3: Largest Daily Peak Streamflows at the USGS Station

Long-term Baseflow Analysis

One model for estimating groundwater discharge to an adjacent stream is a linear reservoir model where:

$$\frac{dS}{dt} = I - Q$$

$$S = kQ$$

where:
- S = Volume of storage in the groundwater system
- I = Inflow into the Groundwater System
- Q = Outflow from the Groundwater System (= River Flow During Long-term Baseflow Conditions)
- t = Time
- k = Proportionality Constant (Recession Constant)

For a situation where I = 0 (no recharge), Q is given as:

$$Q = Q_o e^{-k(t-t_o)}$$

where:
- Q_o = Streamflow at the Onset of Pure Longterm Baseflow,
- t_o = Time at the Onset of Pure Longterm Baseflow,

One common method of determining values of the recession constant, k, is by plotting the logarithm of flow versus time. (Linsley et. al., 1982; Fetter, 1988; Singh, 1988) The first point on the receding limb where a straight line can be fit through the data, is considered to be Q_o. The slope of this line is defined as k. The value of k for the Aberjona watershed was determined using the hourly streamflow data at the USGS for the 1987 to 1993 period of record. For the analysis, the slopes of the linear portions of the log(flow) graph were identified. The overall average of these slopes, k, was 0.054/day = 0.0022/hour. The inverse of k, the time constant of the long-term baseflow system, is 19 days.

The 19 day time constant compares favorably with the values determined by Brainard, 1990 who in his study obtained time constants of: 1) 14.7 days, and 2) 16.2 days. The 14.7 day time constant was determined using the methodology described above except that daily flows and a one year time period were analyzed. The 16.2 day time constant was determined using the analytical solution of a 1

dimensional groundwater flow equation with a fully penetrating river with no recharge. From that solution, the 16.2 day time constant was computed using estimated values of aquifer storativity, transmissivity, and length.

To determine the seasonal variability of long-term baseflow over the course of a year, daily streamflow data at the USGS station from 1957 to 1992 were analyzed. To expedite the analysis, a computer program was written to identify days during which streamflow was likely dominated by longterm baseflow. Criteria used to identify these days was based upon the slope of the recession curve and upon antecedent precipitation. The primary assumption is that days characterized by a relatively flat receding limb and by small antecedent rainfalls are considered to be days which could be dominated by longterm baseflow. Specifically, the criteria used were:

a) $0 <= \text{slope} < k$, where $\text{slope} = \log_{10}(\text{flow}(i-1)) - \log_{10}(\text{flow}(i))$. Flow(i) is the daily average streamflow for a given day, i, and flow(i-1) is the daily average streamflow for the previous day. k, the recession constant, was set to 0.054/day.
b) rain(i-1) < 0.04", where rain(i-1) is the rain depth (at the Reading station) for the previous day.

The days identified were then super-imposed on the streamflow hydrographs and points were eliminated which were not considered long-term baseflow. Points eliminated included days occurring along the peak of the hydrograph and plateau points not associated with baseflow. After the elimination of erroneous data points, the average, maximum, and minimum bi-monthly long-term baseflows were then computed.

Results (table IV.2-4 and figure IV.2-13) indicate that longterm baseflows vary over the course of a year. The maximum longterm baseflows occur primarily during the spring and the minimum longterm baseflows occur during the summer. The variability of the longterm baseflow is also larger during the spring than during the summer.

Time	Average Long-term Baseflow (cfs)	Maximum Long-term Baseflow (cfs)	Minimum Long-term Baseflow (cfs)
Jan 1-14	16.4	44.0	2.4
Jan 15-31	16.0	49.0	1.5
Feb 1-14	15.3	32.0	1.7
Feb 15-28(29)	21.8	42.0	3.2
Mar 1-14	22.7	44.0	3.3
Mar 15-31	29.1	67.0	9.9
Apr 1-14	30.3	66.0	9.6
Apr 15-30	26.5	76.0	7.7
May 1-14	17.8	34.0	9.5
May 15-31	11.7	27.0	5.6
Jun 1-14	9.85	22.0	0.90
Jun 15-30	6.14	22.0	0.85
Jul 1-14	3.09	6.7	0.70
Jul 15-31	2.73	7.8	0.77
Aug 1-14	3.59	14.0	0.50
Aug 15-31	2.51	6.1	0.45
Sep 1-14	2.51	6.8	0.35
Sep 15-30	2.41	5.6	0.40
Oct 1-14	2.41	7.7	0.35
Oct 15-31	4.51	14.0	0.45
Nov 1-14	3.47	19.0	0.55
Nov 15-30	10.6	38.0	0.50
Dec 1-14	15.8	45.0	0.94
Dec 15-31	15.6	50.0	0.76

Table IV.2-4: Long-term Baseflow at USGS gage, 1957 to 1992

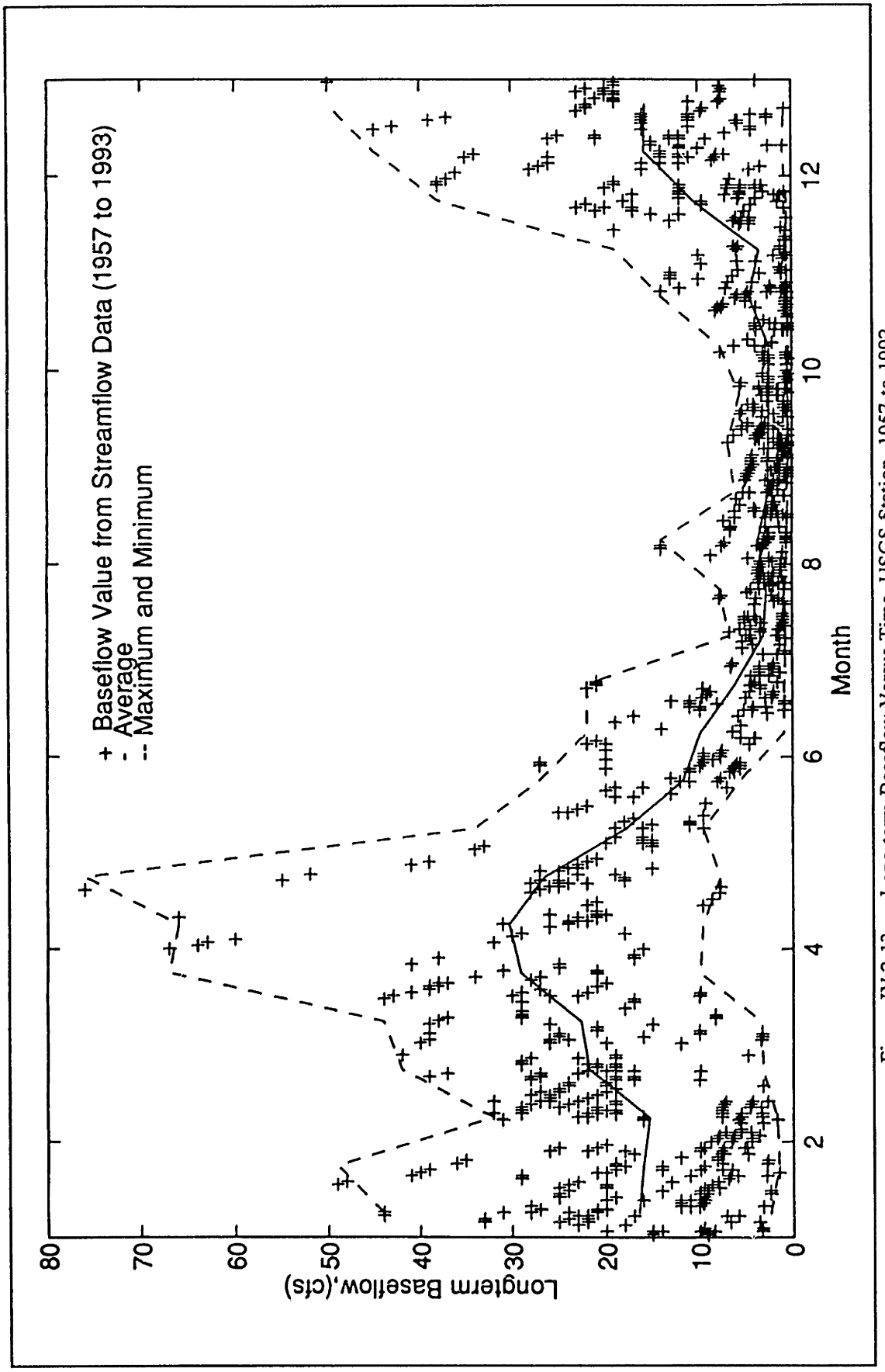

Figure IV.2-13: Long-term Baseflow Versus Time, USGS Station, 1957 to 1992

IV.3 SUSPENDED SEDIMENTS

This section describes suspended sediment data with the purposes of: 1) providing average concentrations and fluxes, 2) describing the general behavior of sediment transport, 3) postulating models for sediment transport, and 4) providing quantitative relationships which will be useful for modeling sediment transport.

IV.3.1 Summary

Suspended sediment concentrations in the Aberjona River were generally low (relative to its potential transport capacity; see section IV.3.7), with a maximum observed concentration of 86 mg/L. Concentrations during low flows for the three stations along the Aberjona were relatively constant with values typically between 2 and 15 mg/l. During storm flow conditions more variable and higher concentrations were observed.

Suspended sediment concentrations on the Horn Pond Creek tributary were also low with concentrations generally between 1 and 10 mg/l. On this tributary, however, changes in suspended sediment concentrations were generally associated with seasonally varying factors rather than storm events. Typically the highest concentrations were observed during the summer and early-fall months.

IV.3.2 Brief Comparison of Data from All 5 Gaging Stations

Comparisons of suspended sediment concentrations and fluxes for samples collected on one occasion each month between February 1992 and January 1993 are provided in figures IV.3-1 and IV.3-2. All concentrations correspond to filtration using a 0.5 μm pore size filter. Tables summarizing these suspended sediment results are provided in appendix IV.D. All but one sample was collected during the receding limb of the streamflow hydrograph. The one exception is the sample for December 17 which was collected during the rising limb. Additionally, (other than the December 17 samples) all samples were collected during predominantly longterm baseflow conditions except March, April, and September samples which were collected during times dominated by slow flow and the October samples which were collected during times dominated by quick flow.

Figure IV.3-1 indicates that the concentrations of suspended sediments were predominantly between 1 and 12 mg/l at all stations. Changes in suspended sediment concentrations between one station and

another (for the receding limb of the hydrograph) appear to be primarily uncorrelated, with maximum concentrations for Route 128, Wedge Pond, Horn Pond and Montvale occurring on different low flow sampling dates. The strongest correlation occurred between Montvale and USGS samples where changes in concentration between each successive sample followed a similar pattern from May 1992 to January 1993. For the rising limb condition (December 17), the samples collected at Route 128, Montvale, and USGS exhibited large increases in concentrations over typical values observed during low flows. This similarity indicates that perhaps these three stations have a similar sediment transport response to storm events.

Suspended sediment fluxes for the same sampling dates are illustrated in figure IV.3-2. The data indicate that during low flow conditions suspended sediment fluxes at all stations generally varied between a 1 to 20 kg/hr. The higher fluxes observed at the USGS station for samples collected March 29 and April 18 were associated with higher streamflows, not high suspended sediment concentrations. Such a result indicates that, for samples dominated by longterm baseflow or slow storm water, suspended sediment fluxes were proportional to the streamflow. During a storm event (December 17) or immediately after a storm event (October 12) large increases in sediment fluxes were observed at the stations on the Aberjona River, especially for the USGS and Montvale stations. Unlike the March 29 and April 18 samples, these increases in sediment flux were associated with both an increase in streamflow and suspended sediment concentration. This observation indicates that the sediment transport during quick dominated flows was different from sediment transport during conditions dominated by longterm baseflow or slow flow. During quick- dominated flows, increased sediment fluxes are due to an increase in both suspended sediment concentration and streamflows whereas during longterm baseflow or slow dominated flow conditions changes in sediment fluxes are due primarily to changes in streamflow.

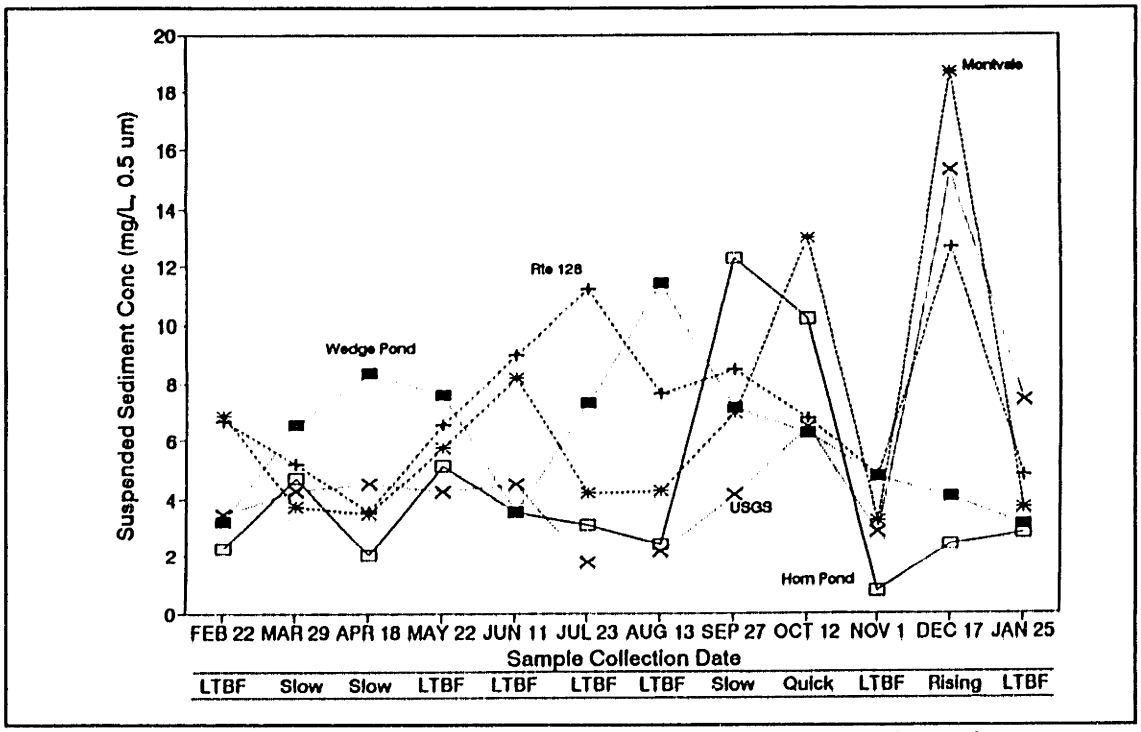

Figure IV.3-1: Suspended Sediment Concentration, Manual Samples
All Stations, Feb 1992 to Jan 1993

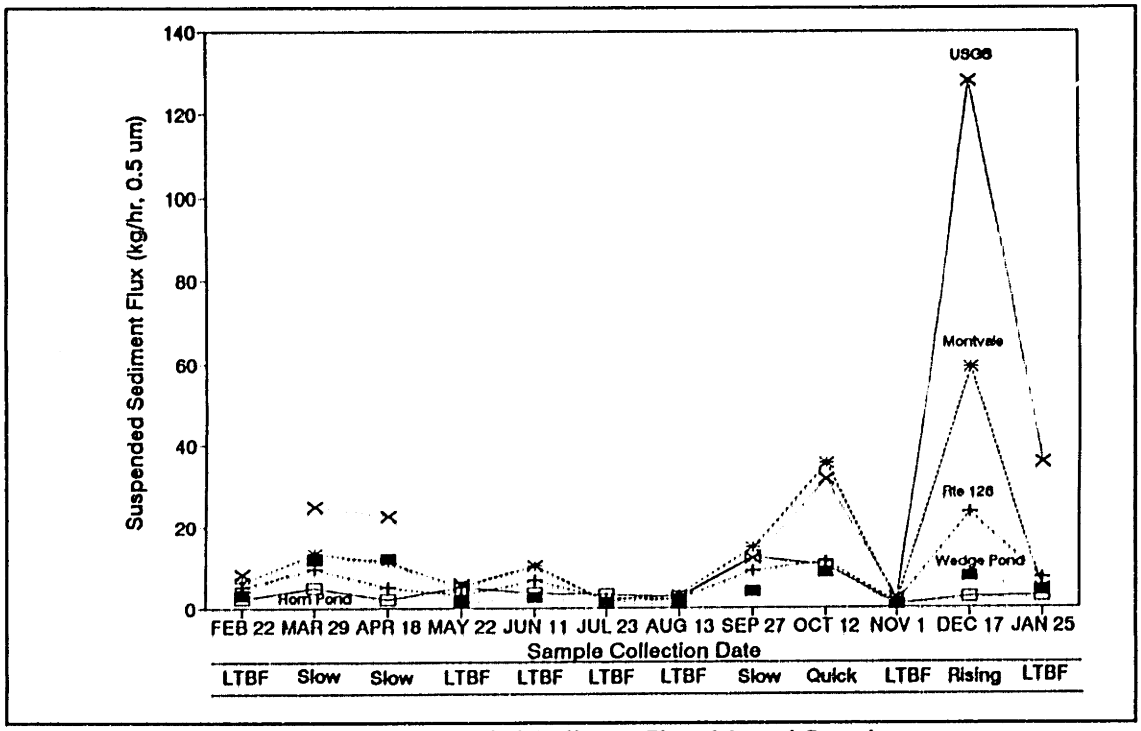

Figure IV.3-2: Suspended Sediment Flux, Manual Samples
All Stations, Feb 1992 to Jan 1993

IV.3.3 Observations for Wedge Pond, Gaging Station 1

Suspended sediment properties and concentrations at Wedge Pond appear to be dependent upon seasonal factors. These factors include: 1) water temperature, and 2) flow rate.

Total Suspended Sediment Concentrations: Seasonal Trends

Measured suspended sediment concentrations at Wedge Pond (figure IV.3-3) were between 2 and 15 mg/L. Within this range of concentrations the data exhibited seasonally distinct trends. During the winter months suspended sediment concentrations were generally at their lowest with values between 3 and 6 mg/L. These low concentrations were accompanied by streamflows which were average to high for this station. During the fall and early spring months concentrations were slightly higher, between 5 and 8 mg/L, while the flow rates were at similar values observed during the winter months. The highest variability in suspended sediment concentration was observed during the late spring - early summer, even though streamflows were generally low. Suspended sediment concentrations during these months varied from 2 to 16 mg/L.

Visual Characteristics: Effects of Season and Antecedent Flow Conditions

Visual characteristics of the suspended material at Wedge Pond were also observed to vary from season to season. During the 1991 and 1992 summer months suspended sediments collected on the filters were characteristically green in color. The green color was due to the predominance of algae in the filtered material. The likely source of this algal material is the Wedge Pond reservoir which is immediately upstream of this station. The water in this reservoir during the summer months was characterized by increased growth of floating aquatic plants and by periodic algal blooms. These blooms would, on occasion, migrate from the reservoir downstream past the sampling station, in essence "verifying" that the reservoir was the source of the greenish suspended material.

During the colder seasons, however, the aquatic plants were much less predominant and algal blooms were no longer observed. Apparently due to the lack of algal material, suspended materials collected during the colder months were brown in color. This color may have been due to sediments of mineralogical origin or to decaying organic matter.

Electron-micrographs of sediment material (figure III.E-6 and III.E-7, Appendix III.E) collected in July 1991 after a prolonged period of low flow, support the finding that algae predominated the Wedge Pond suspended sediments. In these figures the predominance of diatomaceous (i.e. algal) material in the suspended sediments is well illustrated.

For another sample collected in August 1991 shortly after a large storm event (figure III.E-8, Appendix III.E) the proportion of the sample dominated by diatoms was significantly reduced. This observation indicates that the diatoms which dominated suspended material in the July sample were either: a) flushed-out of the system (Wedge Pond) after the storm event, or b) diluted by an increase in non-diatomaceous sediments. For either situation, these results indicate that antecedent flow conditions are of importance in determining the characteristics of suspended sediments at the Wedge Pond station.

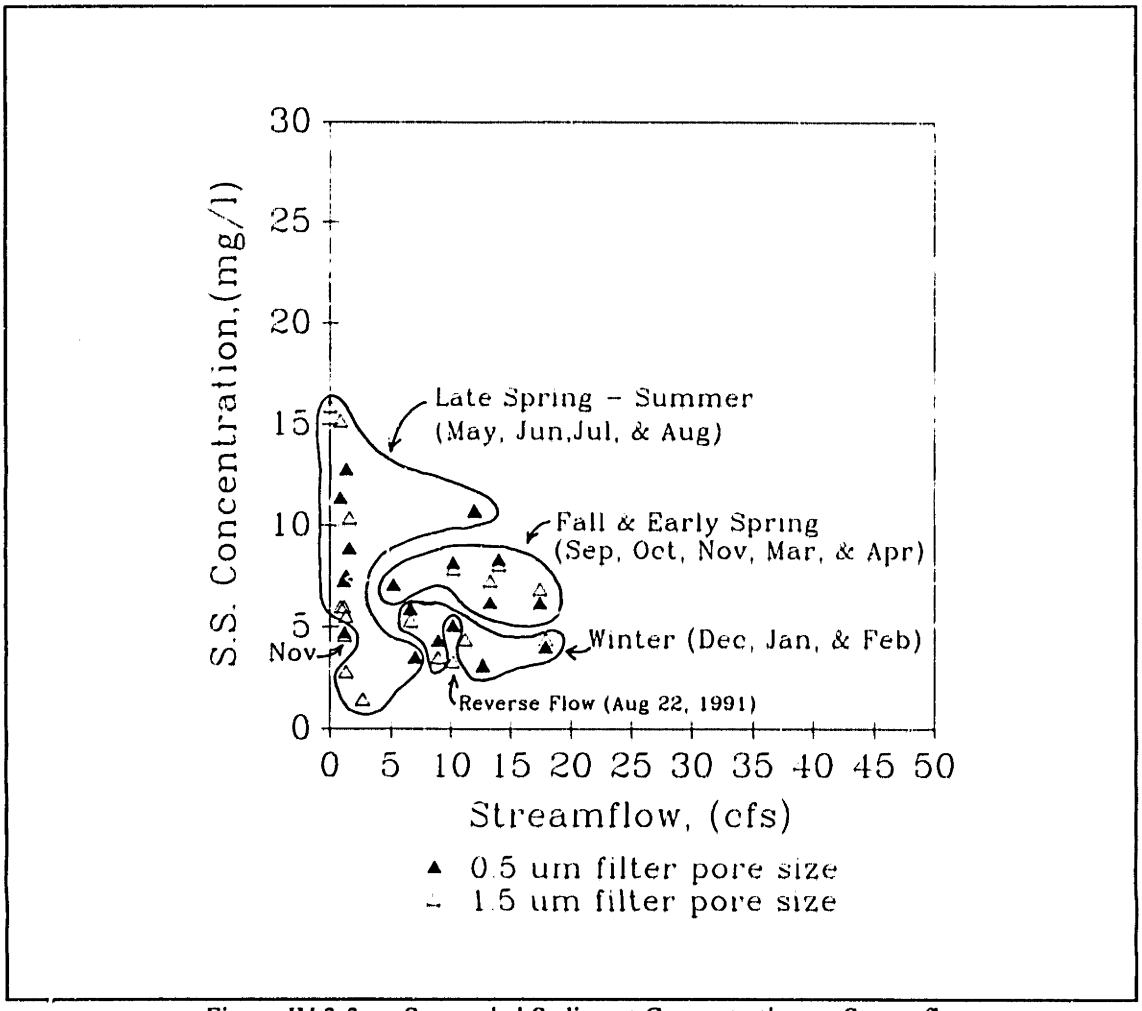

Figure IV.3-3: Suspended Sediment Concentration vs Streamflow, Wedge Pond Station, Gage #1

Suspended Sediment Components: Seasonal Trends and Settling Basin Assumption

Volatile (i.e. organic) suspended sediments also varied with seasons. (figure IV.3-4, Table IV.D-1) The highest concentrations were observed during the mid-summer to early-fall months. These high concentrations were likely associated with warmer temperatures which promote the growth of algae in the Wedge Pond reservoir. During other seasons, organic suspended sediment concentrations were typically lower and probably consisted of lower algal concentrations and decaying organic material.

Non-volatile (i.e. inorganic) suspended sediment concentrations exhibited a somewhat different seasonal pattern. Significantly higher non-volatile suspended sediment concentrations were observed during March and April when flows are typically highest. A comparison of non-volatile concentration with average monthly flow (figure IV.3-5), indicates that each variable exhibited a similar pattern of fluctuation[6]. This similarity is especially apparent if one lags the average monthly flow by one month. (figure IV.3-6) One interpretation of this similarity is that non-volatile suspended sediment concentrations entering Wedge Pond were constant over the course of a year. Once within Wedge Pond, these non-volatile sediments were subject to settling due to the more quiescent conditions in the lake. The longer the residence time of the water - the more particles removed. Since residence time is inversely proportional to the flow rate (for a constant reservoir volume at steady state), one would expect low non-volatile suspended sediment concentrations after long periods of low flow conditions (due to efficient removal via settling) and high non-volatile suspended sediment concentrations after long periods of high flow conditions. The one month lag in the pattern of non-volatile concentration and average monthly flow may have been associated with the residence time of the particles in the pond which attenuated the suspended sediment response to changes in flow.

[6]A comparison between an instantaneous value (non-volatile concentration) to a monthly average value (flow) may appear to be inconsistent. However, the settling basin assumption offsets the difference in time scales of each of the parameters being compared. Because of this assumption, non-volatile suspended sediment concentrations may be considered to be an average over the residence time of the water in Wedge Pond, which is typically on the order of 15 days.

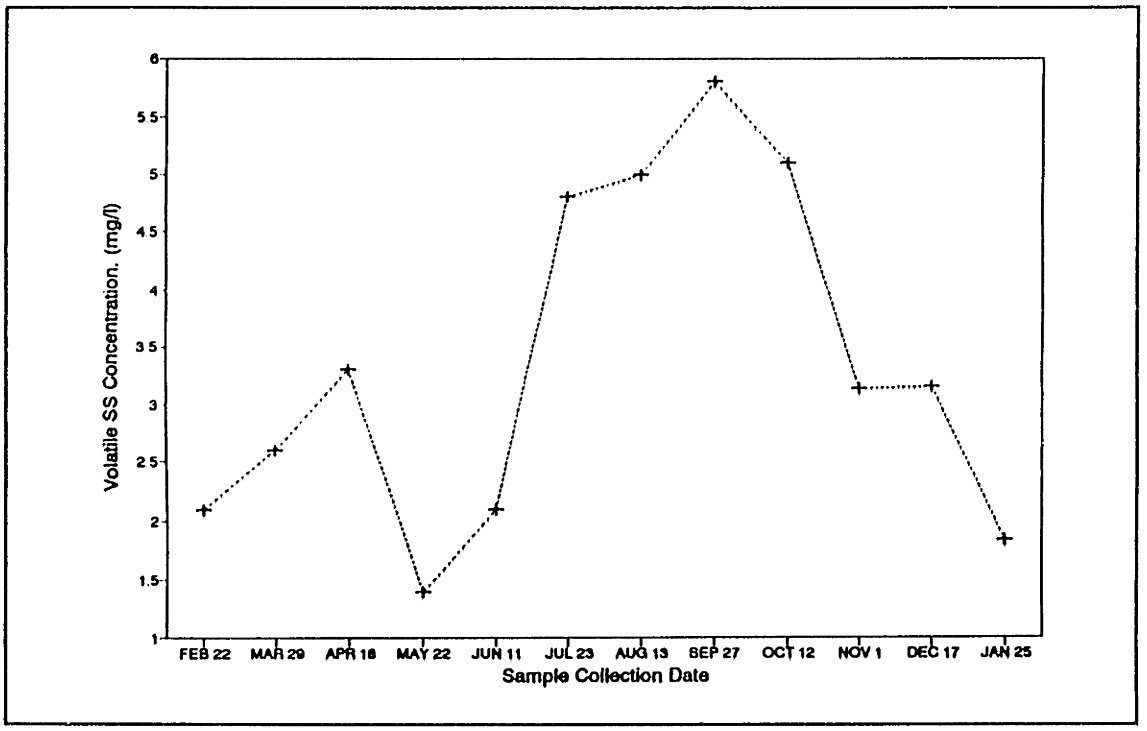

Figure IV.3-4: Organic SS Concentration vs Sampling Date
Wedge Pond, Feb 1992 to Jan 1993

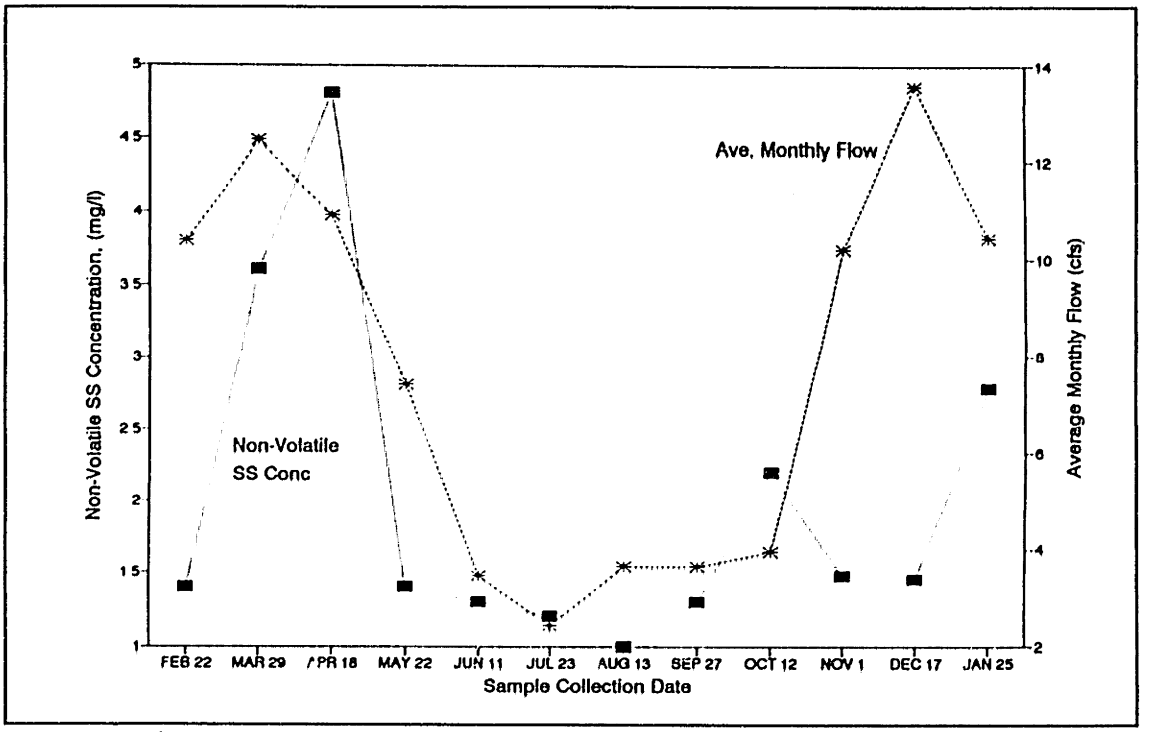

Figure IV.3-5: Inorganic SS Concentration & Ave. Monthly Flow vs Date
Wedge Pond Station, Feb 1992 to Jan 1993

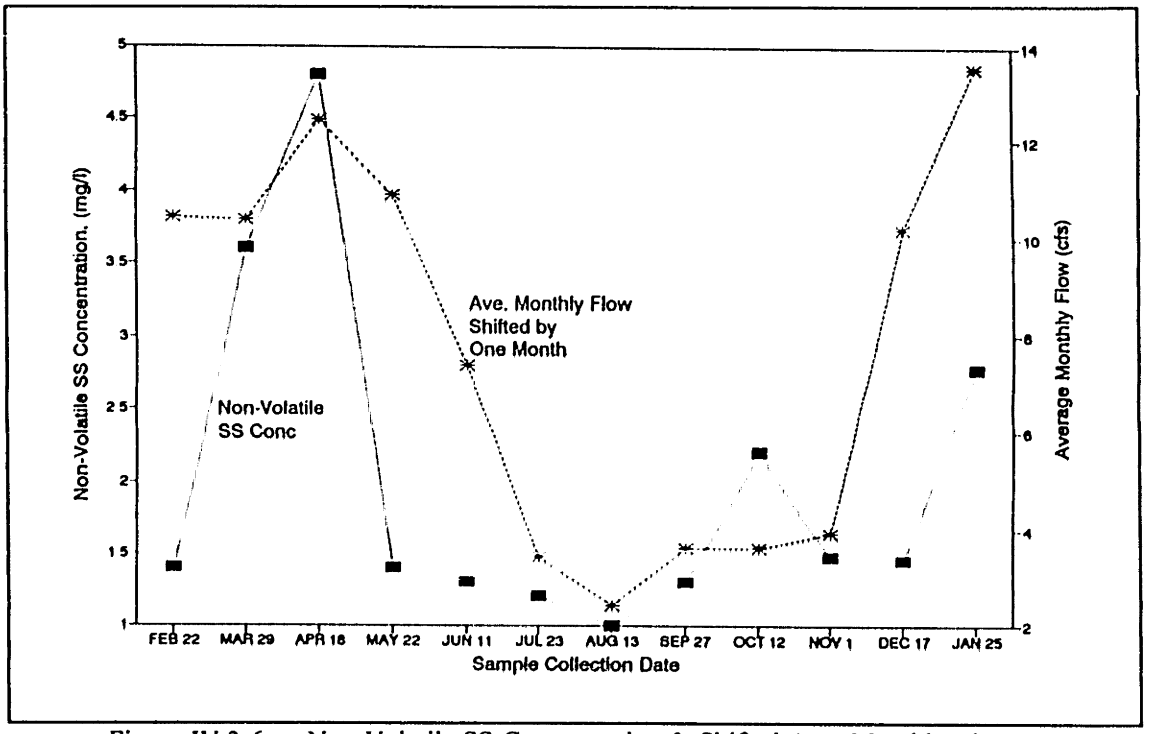

Figure IV.3-6: Non-Volatile SS Concentration & Shifted Ave. Monthly Flow vs Date
Wedge Pond Station, Feb 1992 to Jan 1993

Implications

The preceding results indicate that sediment transport at the Wedge Pond station was characterized by two distinct types of sediments - volatile suspended sediments and non-volatile suspended sediments. The volatile suspended sediments appear to be strongly correlated with water temperature and flow whereas non-volatile suspended sediments appear to be strongly correlated with antecedent flows.

Volatile Sediments

In describing the fluctuation of volatile (organic) suspended sediments, one can model Wedge Pond as a continuous flow stirred tank reactor (CFSTR). A CFSTR can be used to describe the changes in volatile solids (i.e. algal) concentrations throughout the year (figure IV.3-4). Variables required for the CFSTR are:

1) The Water Temperature: Rate constants for the growth of biological material are affected by water temperature (Metcalf and Eddy, 1972). Rapid growth rates would be expected during warmer weather whereas slow growth rates would occur during the colder months. Therefore, for a constant flow rate and a constant reservoir volume, the highest volatile suspended sediment concentrations would be expected during the warmer months (because of faster growth rates). Similarly lower concentrations would be expected during the colder months.

2) Flow Conditions: Flow conditions at the outlet can be used to estimate the residence time of water within the Wedge Pond reservoir. Assuming a constant volume for Wedge Pond and steady state conditions, the residence time of the water would be inversely proportional to the flow rate. After prolonged periods of low flows, a higher algal concentration in the pond would be expected. For large antecedent flows lower organic concentrations would be expected.

Non-Volatile Sediments

Non-volatile (inorganic) suspended sediment concentrations were dependent upon prior flow conditions. In an attempt to capture the observed trend (figure IV.3-5), Wedge Pond may be considered as a large settling basin for non-volatile sediments where concentrations entering the pond are constant in time. Upon entering the reservoir, these influent particles will begin to settle to the lake bottom. The amount settled would be dependent upon water residence time which is a function of prior flow conditions. During low flow conditions non-volatile material in the inflow has more time to settle due to longer hydraulic residence times. As a result, lower concentrations would be expected at the pond outlet. After a period of high flow conditions, on the other hand, high non-volatile suspended sediments would be

expected in the water column due to reduced residence times of the water. Therefore, computing hydraulic residency times will be necessary for modeling the concentrations of non-volatile sediments at the outlet of Wedge Pond.

It is also conceivable that volatile suspended sediments can settle out of solution, especially if most of the volatile material were not viable. However, conceptually, the volatile suspended sediments in the reservoir will be assumed to be composed primarily of live micro-organisms which are capable of maintaining themselves suspended in the water column.

IV.3.4 Observations for Route 128, Gaging Station 2

Suspended sediment concentrations at Route 128 (figure IV.3-7) were between 3 and 13 mg/L for all samples collected. The highest concentration observed at this station, 12.6 mg/L, corresponded to the only sample collected on the rising limb of the streamflow hydrograph. Such a result is indicative of the possibility that significantly higher concentrations may be observed during storm conditions. This inference is consistent with the observed increases in concentrations at the USGS during storm events. (See section IV.3.7)

For all the samples collected during falling limb conditions, suspended sediment concentrations were, for the most part, constant. One interpretation of this observation is that suspended sediment concentrations during low flow/falling limb conditions are associated with a source (i.e. groudwater) which is characterized by a constant suspended sediment concentration.

As will be demonstrated later, the low flow behavior at Route 128 is clearly different from the behavior observed for the other stations on the Aberjona (i.e. Montvale and USGS). At extremely low flows, suspended sediment concentrations at Montvale and the USGS tend to decrease with decreasing streamflow, whereas at the Route 128 concentrations remain relatively constant. One interpretation of this observation is that suspended sediments at this station have not yet been subjected to quiescent flow conditions which are conducive for settling. As sediments travel from Route 128 to Montvale and ultimately to the USGS station, they may experience localized areas of low flow velocities which promote particle settling. Logical settling locations include 1) the Well's G and H wetland located between Route 128 and Montvale, and 2) the quiescent waters behind several dams between Montvale and the USGS. These dams, which control flow along the Aberjona, include the Winchester Falls and Davidson Park dams.

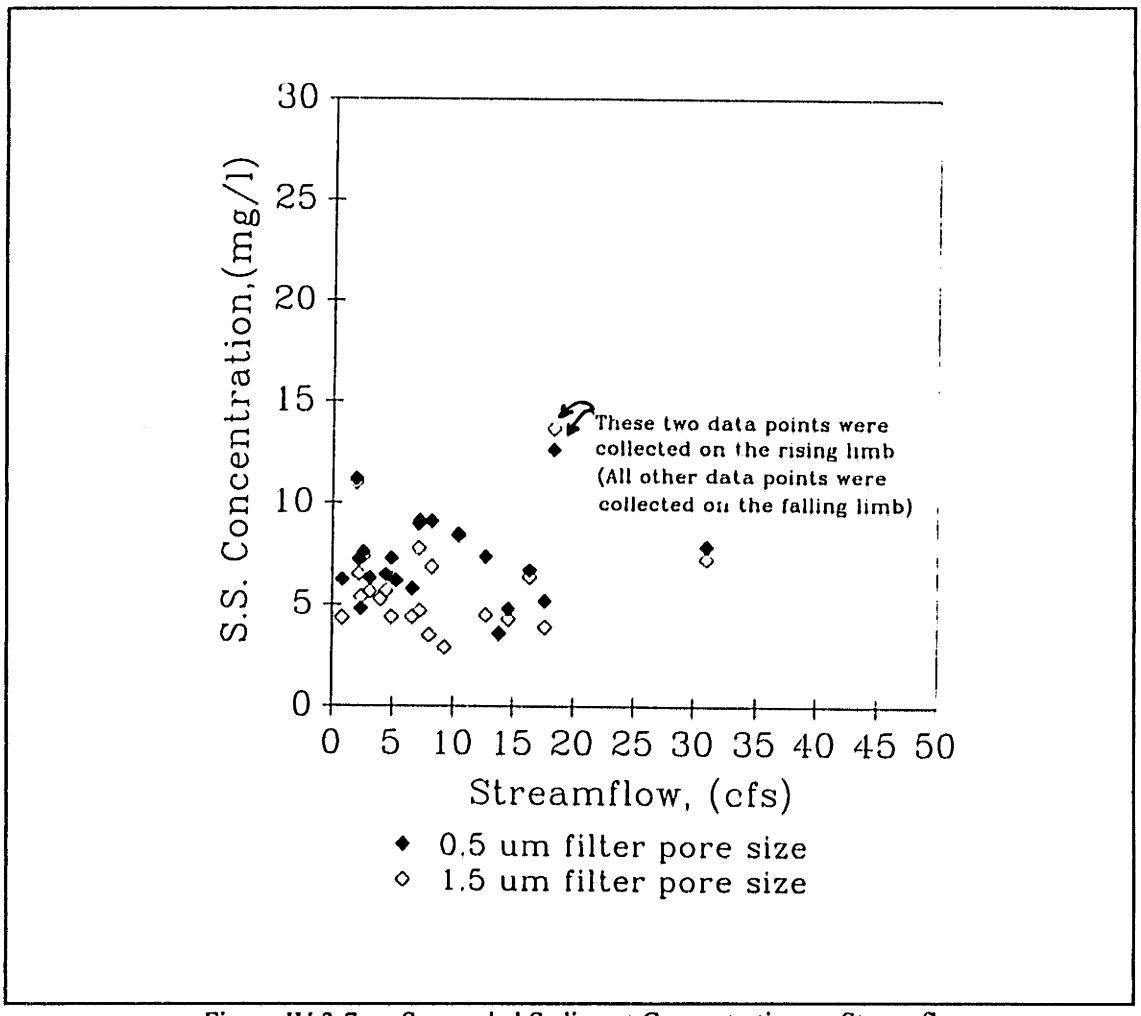

Figure IV.3-7: Suspended Sediment Concentration vs Streamflow, Route 128 Station, Gage #2

IV.3.5 Observations for Montvale, Gaging Station 3

Suspended sediment concentrations at the Montvale station (figure IV.3-8) generally varied between 1 and 10 mg/L during low flow conditions. The maximum measured concentration was 18.7 mg/L which corresponded to the only sample collected on the rising limb of the streamflow hydrograph. The second highest concentration, 13 mg/L, was collected just after the peak flow of a small storm which occurred on October 12, 1992. Such results indicate that during storm conditions significantly higher concentrations are likely to occur. This inference is also consistent with the storm event observations at the USGS station downstream.

Furthermore, the data show that at extremely low flows suspended sediment concentrations generally decreased with decreasing streamflows. For comparative purposes, the best fit line for the low flow data at the USGS station is super-imposed onto the Montvale graph (figure IV.3-8). This line corresponds to a) suspended sediment concentrations determined using a 0.5 μm filter pore size, and 2) drainage area normalized flows (See section V.2.3.1, Channel Suspended Sediments, for normalization assumptions). For flows less than 10 cfs, the rate of decrease in suspended sediment concentration with decreasing streamflow is consistent for both stations. This trend is interpreted as particle settling due to limited river transport capacity.

At higher flows (>10 cfs, Montvale; >16 cfs, USGS, figure IV.3-10) during the receding limb, suspended sediment concentrations at both stations level-off, with concentrations consistently between 2 and 15 mg/L. This leveling-off may be associated with a source limitation. Assuming that during receding limb conditions the source of water to the river comes from primarily the groundwater system, the source of sediment associated with the groundwater system can be such that a constant concentration of suspended sediment is produced in the channel. Although transport of "large" (> 0.5 μm) particles through the groundwater system is unlikely, the groundwater can be assumed to have a potential for forming suspended sediments once it reaches the river. (Refer to section IV.3.7.1)

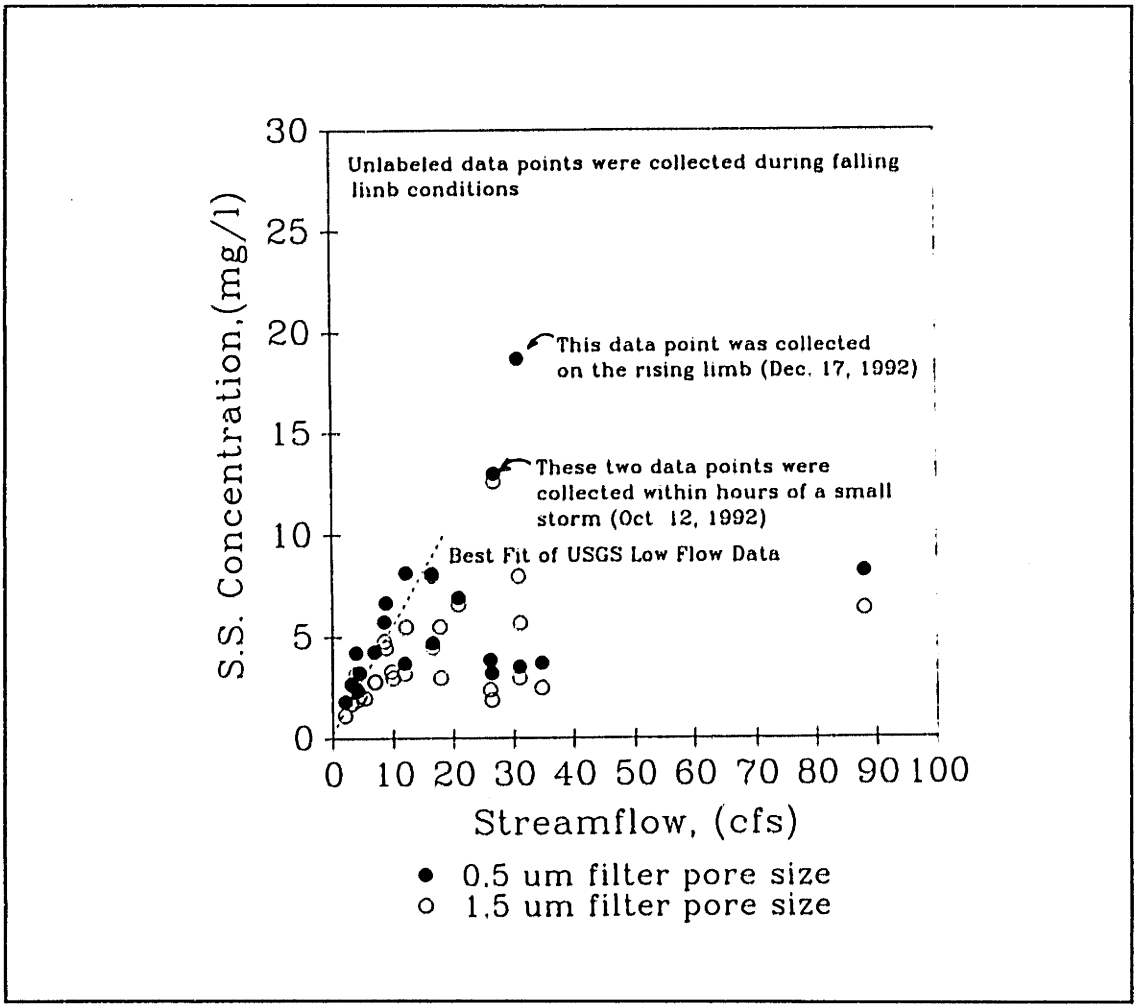

Figure IV.3-8: Suspended Sediment Concentration vs Streamflow, Montvale Station, Gage #3

IV.3.6 Observations for Horn Pond, Gaging Station 4

Horn Pond suspended sediment concentrations (figure IV.3-9) varied from a fraction of a mg/L to 20 mg/L. As observed for Wedge Pond, the Horn Pond data exhibited a seasonal trend. The largest fluctuation in concentration (from 1 to 20 mg/L) occurred from late spring to early fall where higher suspended sediment concentrations were observed with higher streamflows. From late fall to early spring, suspended sediment concentrations were significantly lower with concentrations typically between 1 and 5 mg/L. Such data indicate that storm events could possibly supply relatively high suspended sediment concentrations to the Horn Pond reservoir during the late spring to early fall months, whereas during other seasons lower concentrations would be expected. Therefore, suspended sediment transport at this station appears to be affected by a seasonally-dependent availability of sediments.

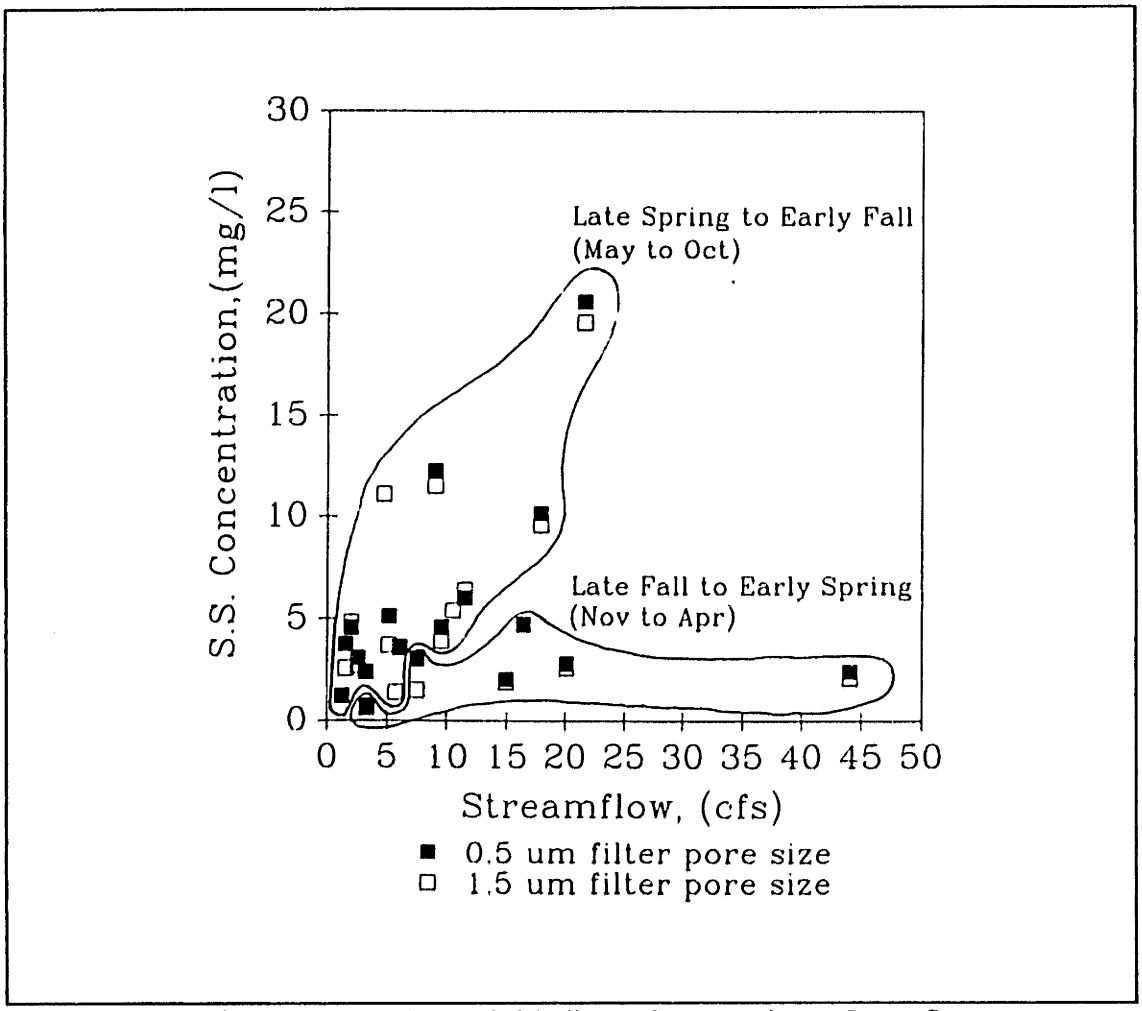

Figure IV.3-9: Suspended Sediment Concentration vs Streamflow, Horn Pond Station, Gage #4

IV.3.7 Observations for USGS, Gaging Station 5

IV.3.7.1 Suspended Sediment Measurements

Suspended sediment concentrations at the USGS station were highly dependent upon flow conditions. During extremely low flows (less than 16 cfs and on the falling limb of the hydrograph) suspended sediment concentrations varied between 2 and 5 mg/l with lower concentrations generally occurring with lower flows. For receding limb flows greater than 16 cfs, suspended sediment concentrations were relatively constant, between 5 and 10 mg/L, and exhibited no strong correlation with streamflow. Concentrations during storm flows, however, were subject to hysteretic effects and were much more variable, with concentrations ranging from 5 to 85 mg/L. For all storm flows, the amount of sediment carried by the river was less than the computed transport capacity. Therefore, transport during storm flows was limited by sediment availability.

Extremely Low Flow (<16cfs, falling limb)

At extremely low flows (figure IV.3-10) concentrations of suspended sediments decreased with decreasing streamflow. The best fit line through the data (corresponding to 0.5 μm filter pore size) is:

$$ss = flow^{0.316} + 0.286 \qquad \text{eqn. IV.3-1}$$

where: ss = Suspended Sediment Concentration (mg/L)

flow = Streamflow (cfs) (Corresponding to the Falling Limb of the Hydrograph)

Equation IV.3-1 is interpreted as representing the sediment transport capacity of the river during falling limb conditions. If sediments are supplied to the river such that the concentration is higher than that given by the equation, channel deposition of the excess sediment would be expected. Implied in equation IV.3-1 is also an assumption that the relationship observed during extremely low flows can be extrapolated linearly to higher flow conditions. The only basis for this assumption is that the relationship was linear for low flows and does not violate any of the falling limb concentrations observed at higher flows.

Receding Flows (>16cfs, falling limb)

Falling limb concentrations during receding flows greater than 16 cfs (figure IV.3-10) indicate that concentrations (0.5 μm pore size) varied between 4 and 10 mg/L. These data exhibit a slight increase in concentration with increasing flow. However, this trend is not consistent for all data points.

One interpretation of these observations is that: 1) receding flows (>16 cfs) supply a relatively constant concentration of suspended sediments, at roughly 5 mg/L, and 2) the receding flow sediment supply plus the erosion of previously deposited sediments from the channel are responsible for concentrations higher than 5 mg/L.

The interpretation of a constant suspended sediment concentration during receding flows (>16 cfs) is that the water supplying the river during these conditions was primarily groundwater. This groundwater may be assumed to have a constant potential concentration (≈ 5 mg/L) for forming particulates upon entering the channel. This interpretation does not imply that large (>0.5 μm) particulates were transported through the groundwater system. Rather, the assumption is that groundwater, due to dissolved nutrients or reduced forms of dissolved metals, was capable of forming large particles once within the river channel. Dissolved nutrients could have been transformed into particulate organic material through biological activity. Reduced forms of metals may have been capable of precipitating out of solution to form large particulate material due to changes in oxidation potential between the groundwater and river systems.

For streamflows dominated by groundwater inputs, the groundwater sediment supply plus the erosion of previously deposited sediments from the channel is a possible explanation for suspended sediment concentrations greater than 5 mg/L. (figure V.3-10) According to equation IV.3-1, the river is capable of carrying a 5 mg/L suspended sediment concentration at a flow rate greater than 16 cfs. Due to the excess transport capacity at a flow rates greater than 16 cfs, sediments that were deposited previously within the channel can possibly be eroded. If channel sediments are eroded, suspended sediment concentrations in excess of the groundwater input concentration (5 mg/L) would, therefore, be expected.

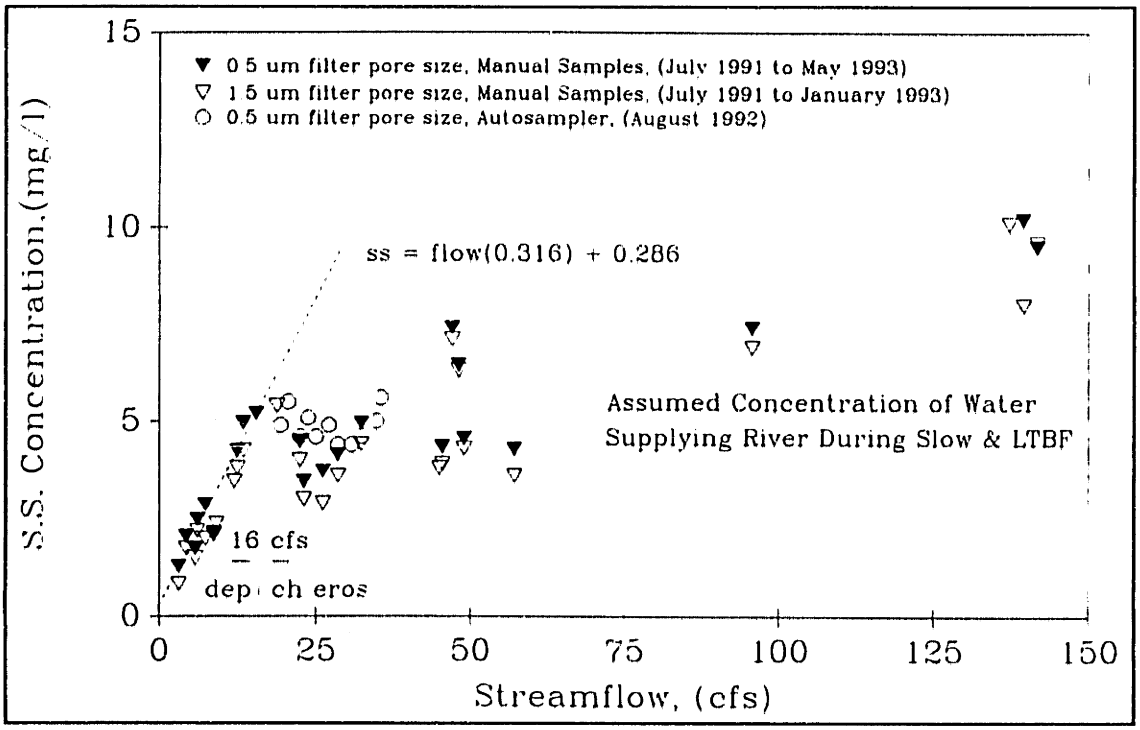

Figure IV.3-10: Suspended Sediment Concentration vs Streamflow, USGS Station, Gage #5 (All data correspond to the falling limb of the streamflow hydrograph)

Storm Flows

Time histories of suspended sediment concentrations versus streamflow during various storm events are illustrated in figure IV.3-11. Increasing time is in the direction of the arrows. Solid lines between successive points correspond to a 1 hour sampling interval. Dashed lines indicate that more than one hour elapsed between each successive sample. (For clarity each event is plotted separately in figures IV.D-1 to IV.D-3 in appendix IV.D)

Each of these storm event histories exhibits a significant hysteresis loop behavior. For each storm event, suspended sediment concentrations on the rising limb of the hydrograph were much higher than concentrations on the falling limb. For the August 18, 1992, the peak suspended sediment concentration coincided with the peak flow, whereas for the December and March storms suspended sediment concentrations peaked prior to the streamflow peak. If all sediments were supplied by the channel, a peak suspended sediment concentration prior to the peak streamflow would indicate that the channel had been flushed of sediment prior to the occurrence of the peak flow rate. Similarly, channel sediments may not have been entirely flushed from the channel, in those cases where the peak flow and suspended sediment concentrations coincided. For the latter situation, however, an inconsistency occurs (figure IV.3-11) since the same concentrations would be expected on both the rising and falling limbs of the streamflow hydrographs.

The data in figure IV.3-11 consistently demonstrate that once the peak flow had occurred, suspended sediment concentration for all events decreased quickly (within hours) to typical values observed during low flow conditions. Whether the peak occurred at 200 cfs (August and December storms) or at 500 cfs (March storm) the response after the peak was a similar rapid return of concentrations to low values. The concentration to which the suspended sediments kept declining is interpreted as the potential suspended sediment concentration associated with groundwater inflows.

Plotting the storm data on time series plots (figures IV.3-12 to IV.3-14), indicates that for all storms suspended sediment concentrations were highest when quick flow dominated the streamflow hydrograph. For example, the times dominated by quick flow for the August storm were 2:00 to 8:00 hours which also corresponded to times when suspended sediments were higher than 25 mg/L. Also note that the domination of quick flow was strongest on the rising limb of the hydrograph. After the peak flow, slow storm water became a significant contributor to the total flow. Once slow storm water began to dominate the hydrograph, suspended sediment concentrations decreased to typical values observed during groundwater dominated flow conditions (between 2 and 15 mg/L). Such results indicate that for all storms, quick flow resulted in a "burst" of sediments to the river water column. These bursts may have been due to the quick water: 1) activating and transporting an outside source of sediment to the river

channel, 2) increasing the flushing of channel sediment due to increases in streamflow, or 3) more efficiently eroding sediment from the river channel.

The hypothesis that quick flow was more efficient at eroding sediment from the channel is unlikely. This effect (although probably minor) may have been associated with how "quick" waters are incorporated into the river flow. If one assumes that quick water is associated with sewer inflow to the river (which is typically characterized by concentrated inflows at right angles to the river), an increase in turbulence at the outlet of the quick water discharge point would be expected. This configuration would cause localized areas of increased turbulence and more efficient removal of sediments. However, this effect is very localized at sewer discharge points and probably does not strongly affect the overall erosive capabilities of the river flow.

Additionally, measurements of the river water's physical properties between low and high flow conditions provided no evidence that the quick water (which typically dominates at high flows) was capable of eroding sediments more efficiently. For example the pH of the water (appendix III.F) remained relatively constant throughout a storm (whether or not the flow was dominated by slow or quick waters). If pH had changed significantly one could consider the possibility of changes in the cohesive properties of particles which would then affect their erodibility. Additionally, there was no evidence of large temperature changes between low and high flows which could have affected water viscosity and its eroding capabilities. Other than increased water turbidity, no other visual changes in the characteristics of the samples were apparent.

The hypothesis that high streamflows (enhanced by quick flow) may flush large quantities of previously deposited channel sediments can, in part, explain the large increase in suspended sediment fluxes during storm events. In order to quantify such an effect the amount of sediments accumulated in the channel must be estimated. However, from the low flow data and the assumptions concerning the sediment supply of the groundwater, it is not likely that sufficient sediment will be deposited to account for the total increase in sediment flux during a storm event. According to the low flow data interpretation, channel deposition will occur (at the USGS station) only during flows less than 16 cfs. Given that the concentration of the water supplying the river during these low flows is 5 mg/L and that the transport capacity is given by equation IV.3-1, it will take over 200 consecutive days of 8 cfs flows to account for the excess sediment transported during the August 18, 1992 storm ($\approx$ 8700 kg). Since 200 days of low antecedent flows did not occur prior to this storm (actually a small storm occurred immediately before the August event) the channel could not have supplied all of the sediment transported during the storm. Therefore, an additional source of suspended sediments appears to be active during a storm event.

The hypothesis that quick water activates an outside source of sediment is the most likely explanation for the observed bursts of sediment at the initiation of a storm event. For example, one can consider a situation where quick water enters the channel by a system which is physically separate from the slow or longterm baseflow water (e.g. storm sewers versus groundwater flow). One can further consider that the quick water conveyance system (e.g. storm sewers) or areas drained by the conveyance system (e.g. impervious areas) have much more sediment available for erosion than do the slow, longterm baseflow, and channel systems. For such a situation, increasing quick water flows will result in a removal of relatively large amounts of sediment from "quick areas" causing large increases (or "bursts") in suspended sediment concentrations in the river.

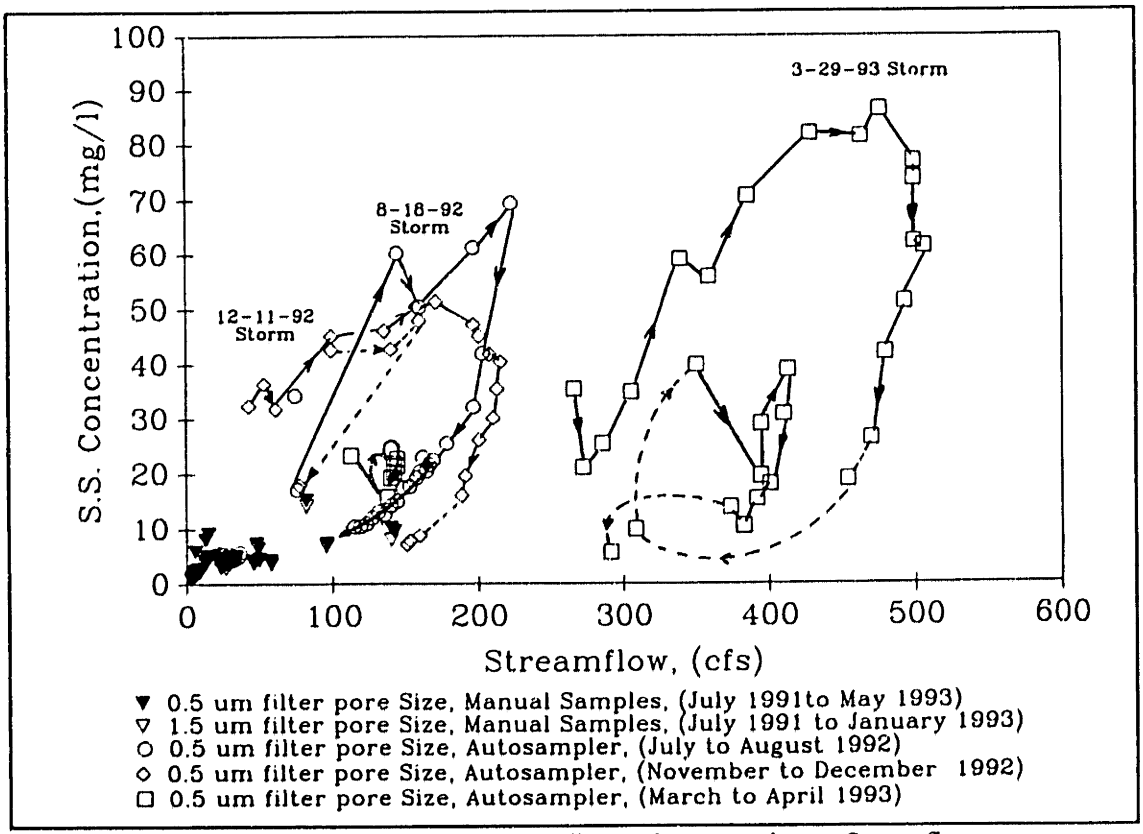

Figure IV.3-11: Suspended Sediment Concentration vs Streamflow
USGS Station, Gage #5

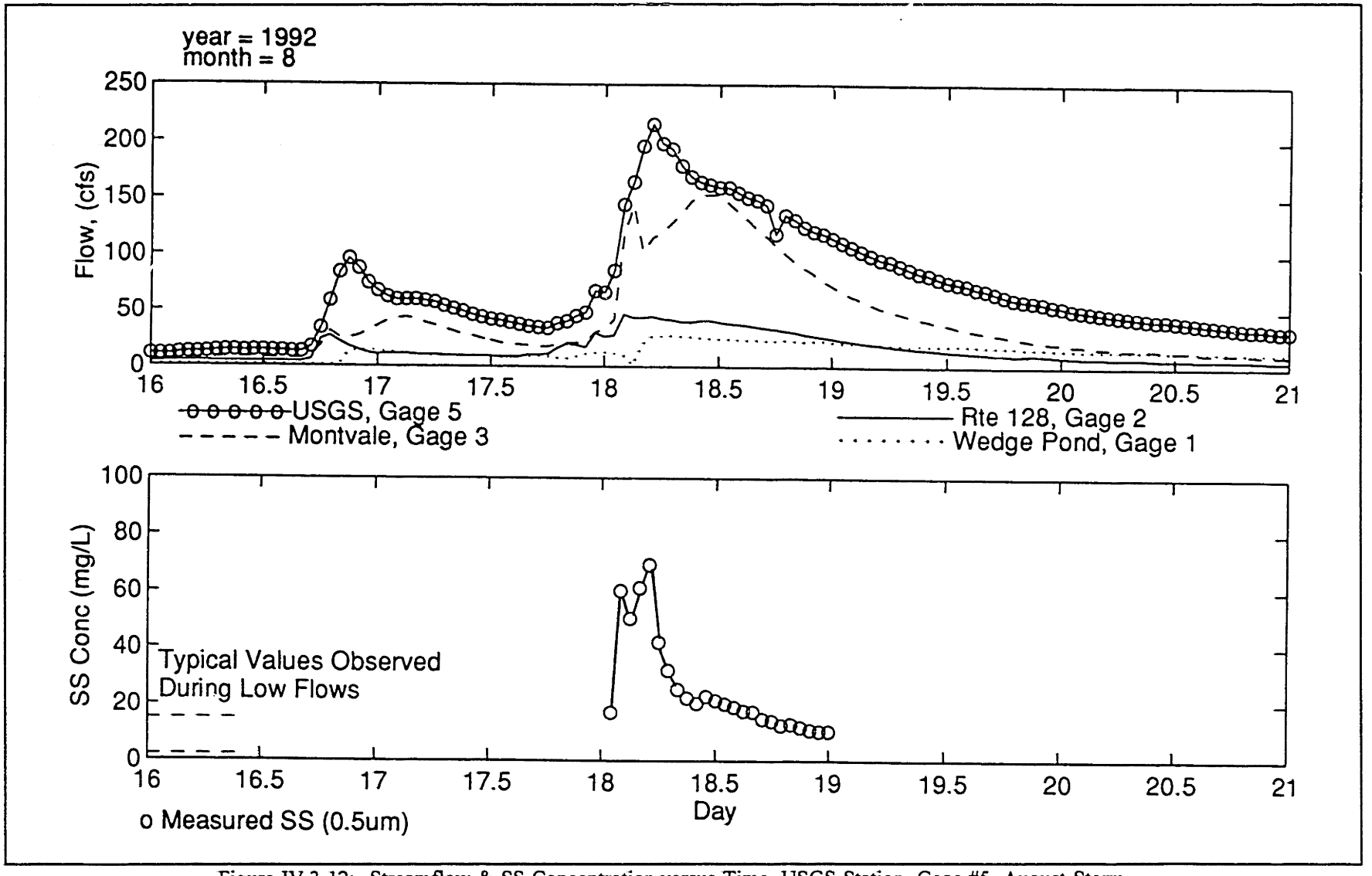

Figure IV.3-12: Streamflow & SS Concentration versus Time, USGS Station, Gage #5, August Storm

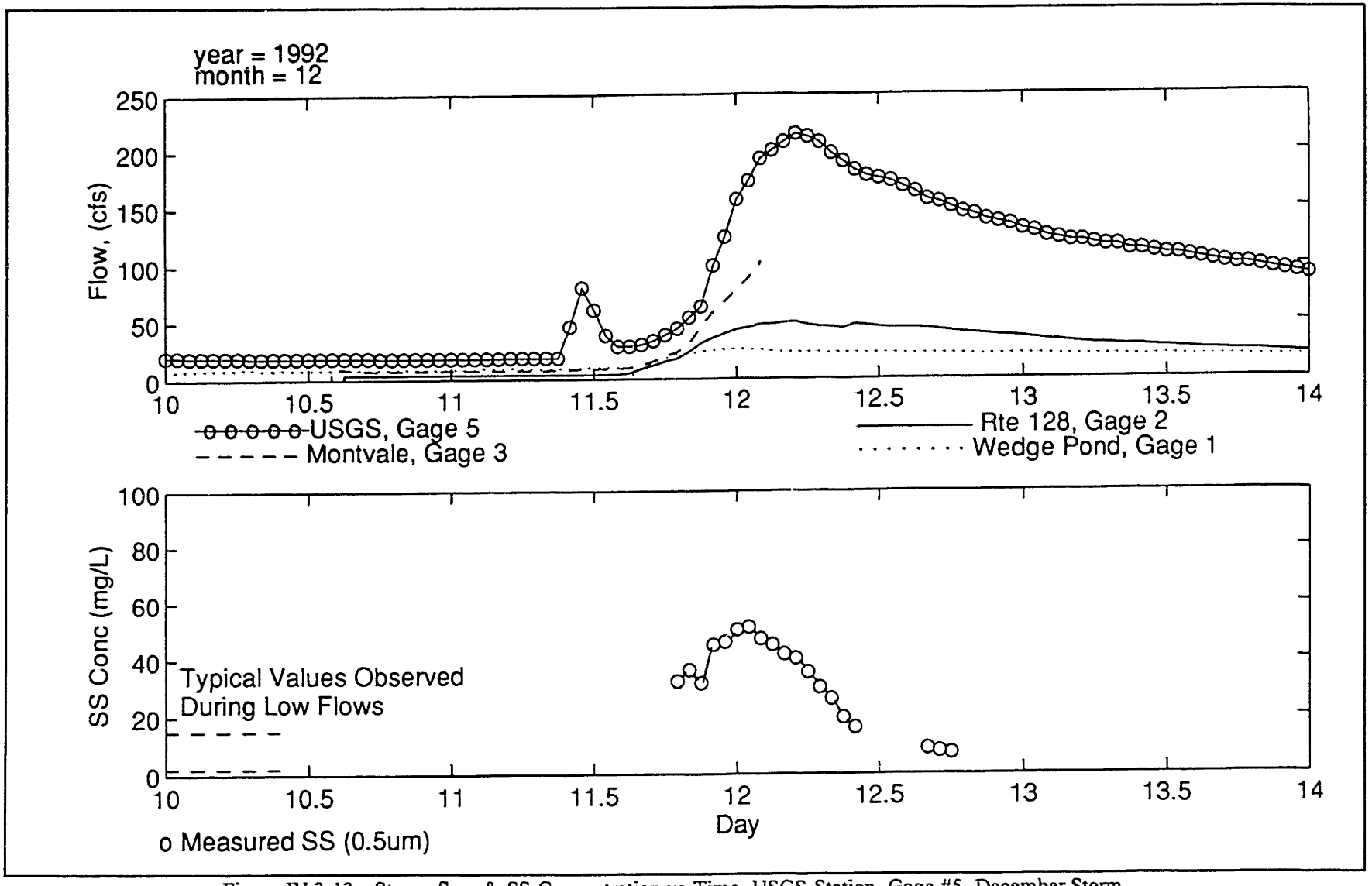

Figure IV.3-13: Streamflow & SS Concentration vs Time, USGS Station, Gage #5, December Storm

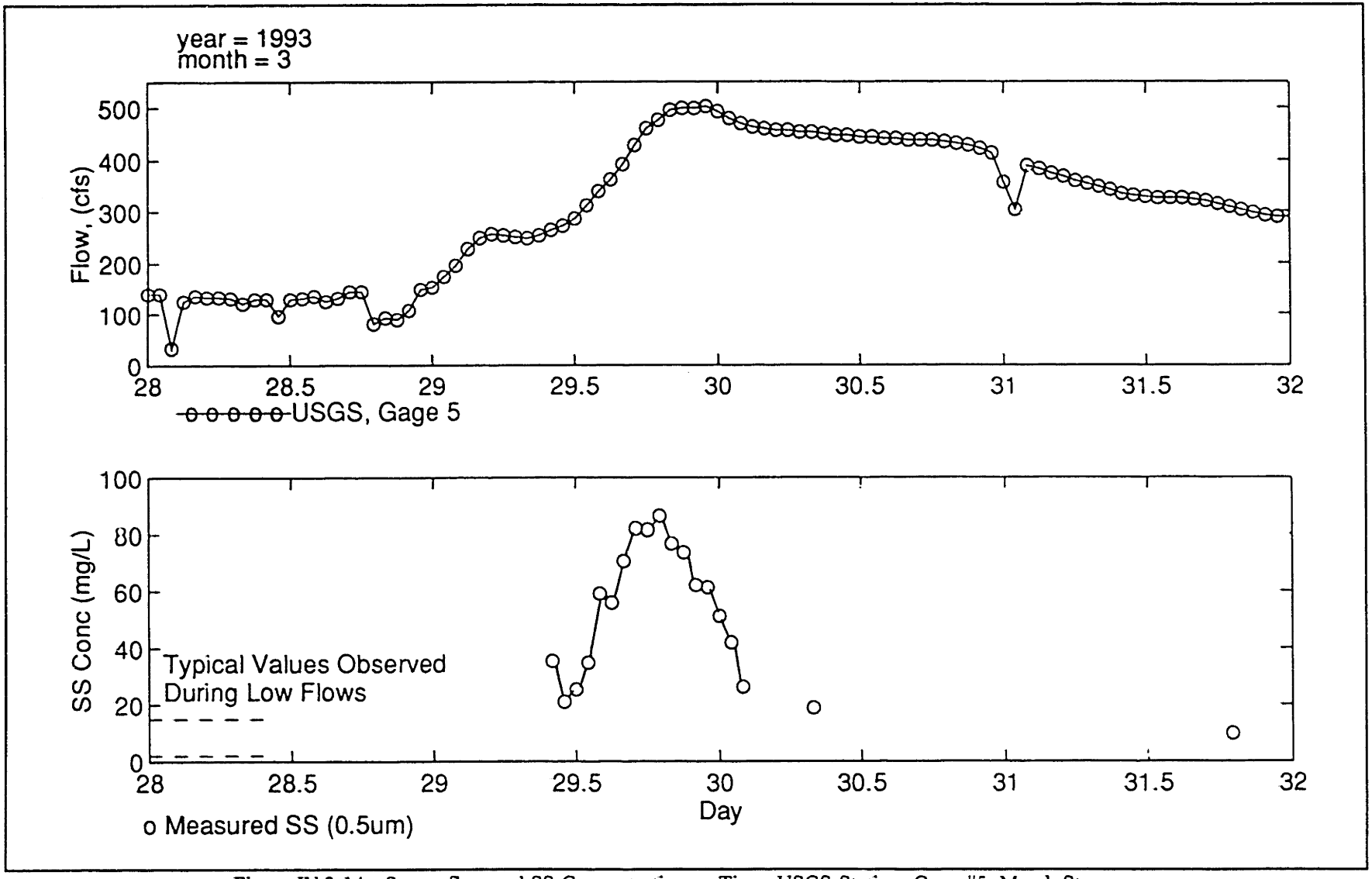

Figure IV.3-14: Streamflow and SS Concentration vs Time, USGS Station, Gage #5, March Storm

Transport Capacity

A computed transport capacity curve for a particular particle size distribution is super-imposed on the rating curve in figure IV.3-15. (See appendix IV.D for computation details) The capacity curve indicates that the amount of sediment carried by the river during storm events is significantly less than the transport capacity. In other words, sediment transport for the river is limited by the amount of sediment that is available, such that the key to modeling sediment transport for the Aberjona River will be to model the inputs into the river.

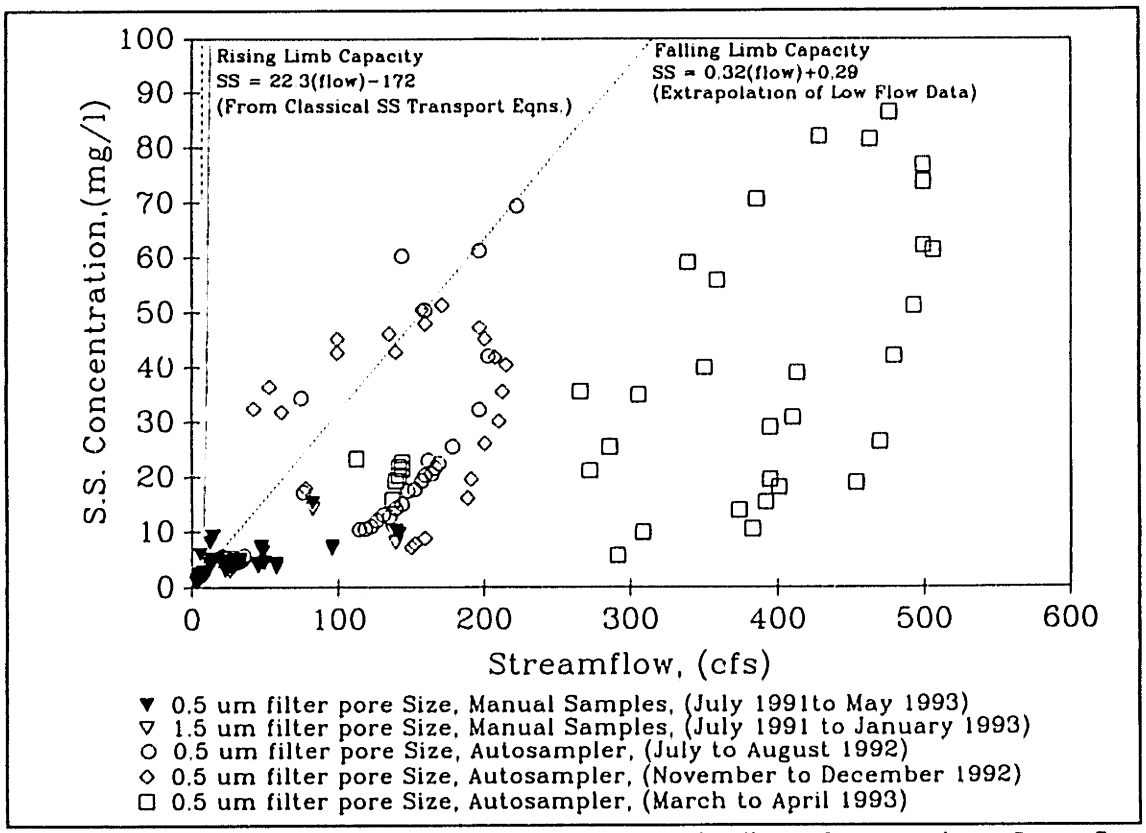

Figure IV.3-15: Measured and Computed Suspended Sediment Concentration vs Streamflow USGS Station, Gage #5

Implications

In light of these observations one may conclude that the key for modeling sediment transport for the sub-basins on the Aberjona River will be to model the availability of sediment to the river, where availability is different for the various components of flow. From the data, the quick flow system appears to have large amounts of sediment available for erosion such that it supplies water with very high suspended sediment concentrations, whereas slow and longterm baseflow systems supply relatively constant suspended sediment concentrations in the vicinity of 5 mg/L. At extremely low flows, the sediment transport capacity is reached, such that some of the suspended sediment supplied by the slow and long term baseflow waters is deposited in the channel. This deposited sediment may be eroded at later times during increased flow conditions.

IV.3.7.2 Turbidity Measurements

Selected turbidity measurements from the USGS station are included in figures IV.3-16 to IV.3-20. Additional plots are included in appendix IV.D. On these figures the nephelometric turbidity units (NTUs) were multiplied by 10 for proper vertical scaling. Streamflows for all five gaging stations and precipitation at the Reading station are included on the plots for reference. Symbols for turbidity, streamflow, and precipitation are spaced at one hour time intervals. Please note changes in the scale of the vertical axis from one plot to another.

Figures IV.3-16 to IV.3-19 are sequenced in the order of increasing storm flows. Figure IV.3-16 corresponds to a very small storm event which occurred on November 17, 1992. Before the precipitation event, both the turbidity and streamflow were relatively constant. Shortly after the event, streamflow rose slightly to approximately 20 cfs while the turbidity also increased to a peak of approximately 5 ntu. After the peaks, both the streamflow and turbidity returned to levels that were observed prior to the storm. For this small event, the lag time between the streamflow peak and the turbidity peak was approximately 22 hours.

Figure IV.3-17 corresponds to a slightly larger storm event which occurred October 24, 1992. As in figure IV.3-16, prior to and shortly after the storm, both turbidity and streamflow were relatively constant. As a result of the storm, however, streamflow and turbidity increased, where the turbidity peak lagged the streamflow peak by approximately 15 hours. Also illustrated in this figure is a "quick" turbidity peak (at 24.8 days) which coincided with the increase in streamflow and with the occurrence of precipitation.

Figure IV.3-18 corresponds to a streamflow peak of approximately 40 cfs which occurred November 13, 1992. For this event, again as depicted for the smaller storms, both streamflow and turbidity records were relatively constant before and after the storm event. As a result of the storm, both streamflow and turbidity increased. Interestingly, the turbidity record for this event was characterized by three individual peaks. The first peak coincided with both the increase in streamflow and the occurrence of precipitation. The second peak occurred one hour after the streamflow peak while the third and largest turbidity peak occurred approximately 10 hours after the streamflow peak.

The event depicted in figure IV.3-19 corresponded to a streamflow peak of approximately 90 cfs, and two turbidity peaks. The first peak, in this case, occurred *prior to* the increase in streamflow and coincided only with the occurrence of rainfall. The second turbidity peak coincided with the peak streamflow. For this larger flow condition, there was no turbidity peak that lagged behind the

streamflow peak.

Comparing these first four figures, a few conclusions can be made. The first is that river water turbidity was relatively constant during non-storm conditions. During storm events, the turbidity became more variable with at least one distinct peak. The second conclusion is that turbidity peaks lagged behind streamflow peaks for small storm events. The smaller the storm the larger the lag time. This trend may be associated with routing effects of flows and sediments along the Aberjona River where, as the flood wave passed through the channels, it "dragged" suspended sediments. This observation is supported theoretically through the work of Singh and Prasad, 1982. In their study, Singh and Prasad derived explicit solutions to the kinematic equation for erosion on an infiltrating bed. In their derivation they coupled equations describing continuity of water, suspended sediments, and momentum (kinematic wave assumption). Solutions were presented for transport on a sloping plane. These solutions explicitly solved for the timing of streamflow and suspended sediment concentrations at the outlet of the plane. Their results indicated that suspended sediment peaks should lag behind streamflow peaks and that the magnitude of the lag is a function of streamflow, where large flows would result in smaller time lags and smaller flows would result in larger time lags. Using Singh and Prasad's solution, flows of 20 and 400 cfs would result in lag times of approximately 20 and 1 hour, respectively, assuming: 1) that Manning's equation is valid, 2) 5 mile travel length for both water and sediment, and 3) 160 ft^2 cross-sectional area of flow. The computed lag time for a flow of 20 cfs compares favorably with observed streamflows and corresponding lag times. From the observed data, however, a one hour lag time would be expected at flows less than 400 cfs.

Finally, the data also indicate that the turbidity peaks which occur prior to the streamflow peak are likely associated with increasing flow conditions and/or rainfall. Peaks associated with increasing flow conditions may be associated with the flushing of channel sediments as flows begin to rise. Rainfall may also affect sediment transport by dislodging sediments (due to raindrop impact) immediately adjacent to the channel[7].

Figure IV.3-20 illustrates two storm events in succession. During the first event (October 10, 1992) two increases in turbidity were observed. The first increase occurred prior to the increase in flow and coincided with the occurrence of precipitation. As mentioned above, this small peak may have been associated with the dislodgement of sediments by rainfall immediately adjacent to the channel. The second increase in turbidity was characterized by a double peak which was very similar to the double

[7]Rainfall also indirectly affects turbidity through the production of "quick" flow which also carries sediment. However, "quick" flow is considered a separate sediment transport mechanism.

peak observed for the streamflow. This similarity in pattern is indicative that the magnitude of streamflow may have directly influenced sediment transport. After this second increase the turbidity then decreased back to its typical low flow value. For the second event which was observed two days later on October 12, 1992, the turbidity was not characterized by a distinct increase. Rather, during this second event, the turbidity record was characterized by variable turbidity values which then became more constant after the flows began to decline. The large increase in turbidity during the first event followed by the lack of a turbidity increase in the second indicates that sediments were perhaps flushed out of the system. In other words, by the time the second event had occurred, sediments were no longer available for transport. Such a result is evidence that modeling sediment availability is an important factor in determining sediment transport for the river.

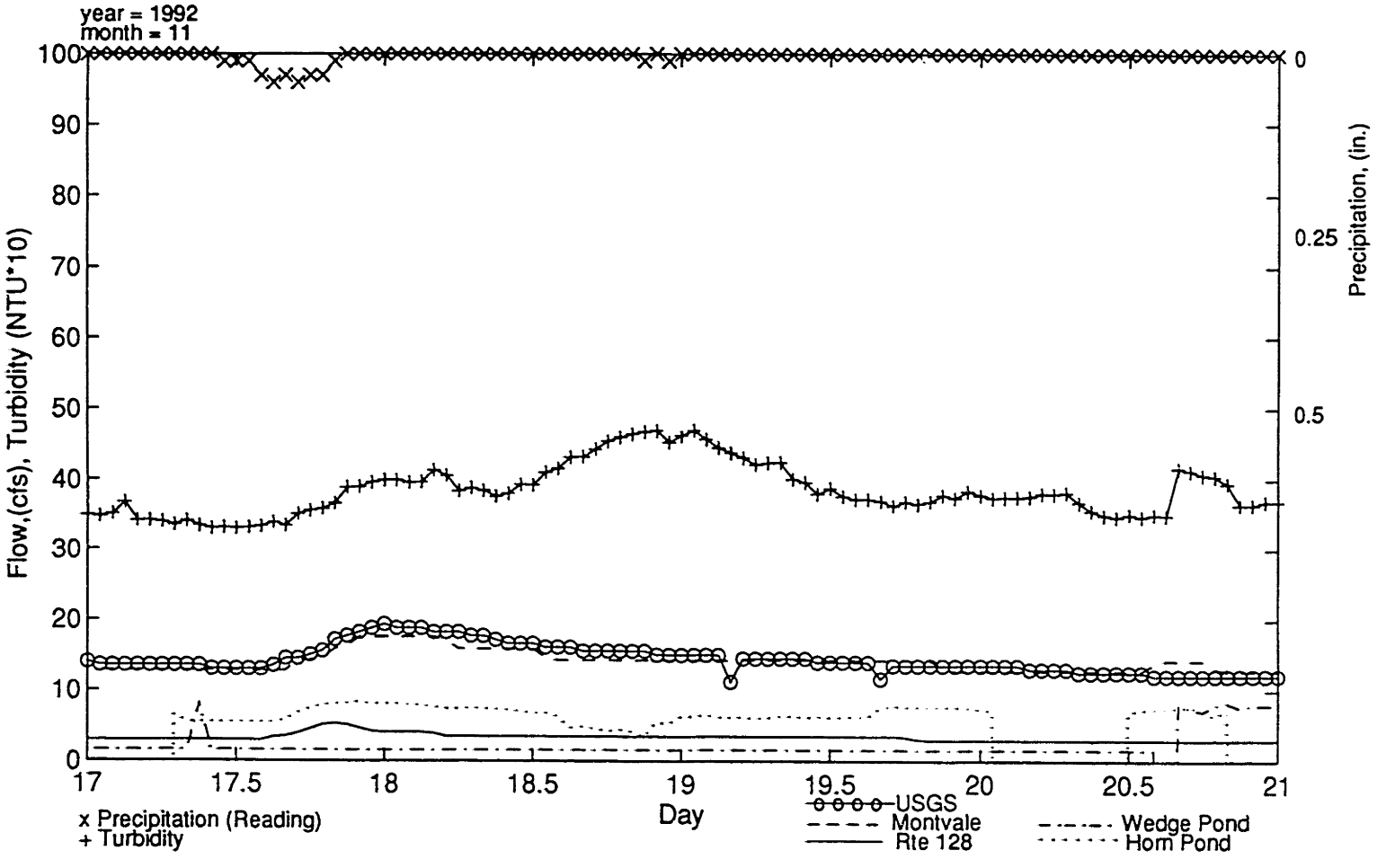

Figure IV.3-16: Streamflow & Turbidity versus Time, USGS Station, Gage #5, November 17 to 20, 1992

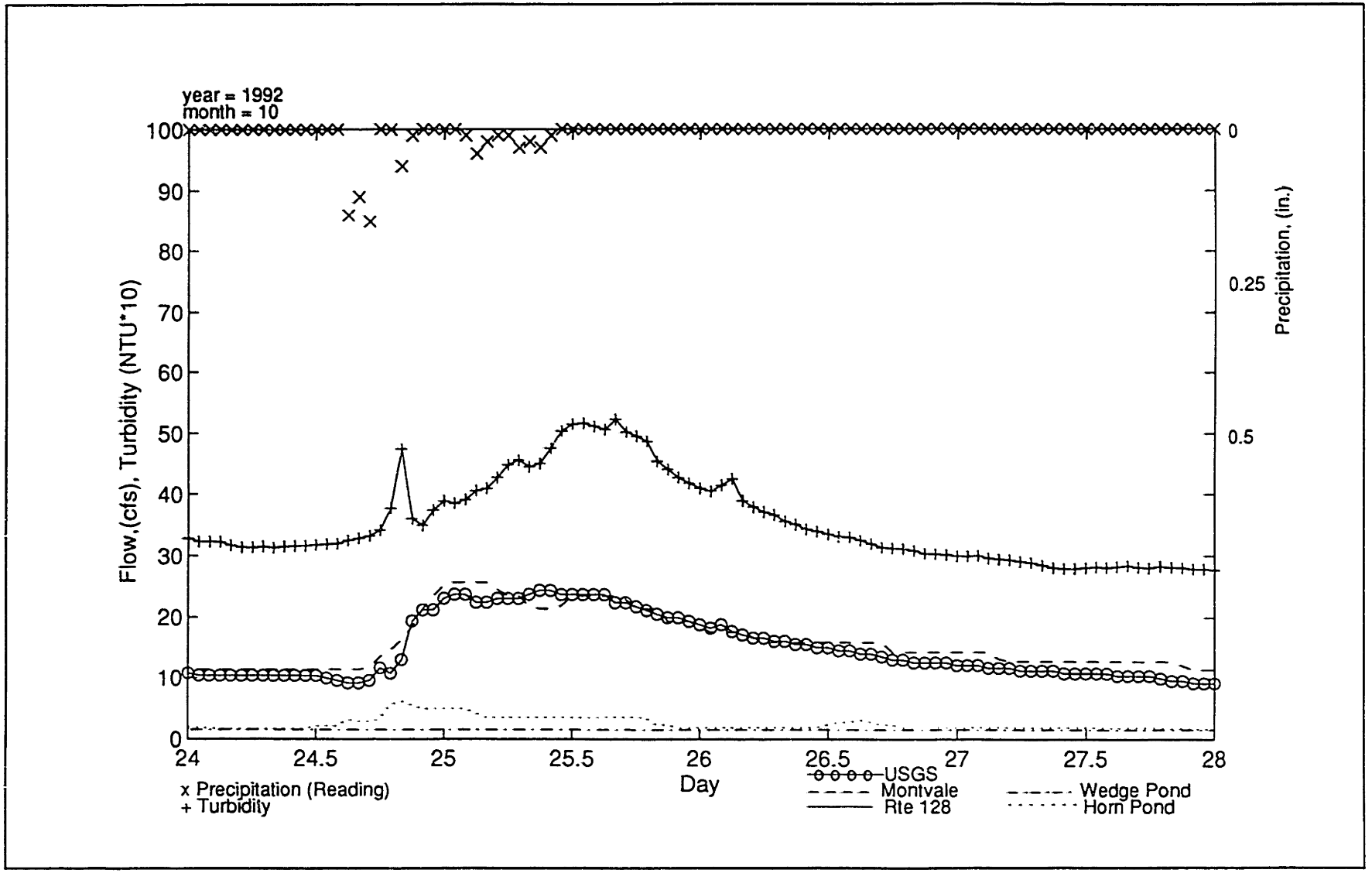

Figure IV.3-17: Streamflow & Turbidity versus Time, USGS Station, Gage #5, October 24 to 28, 1992

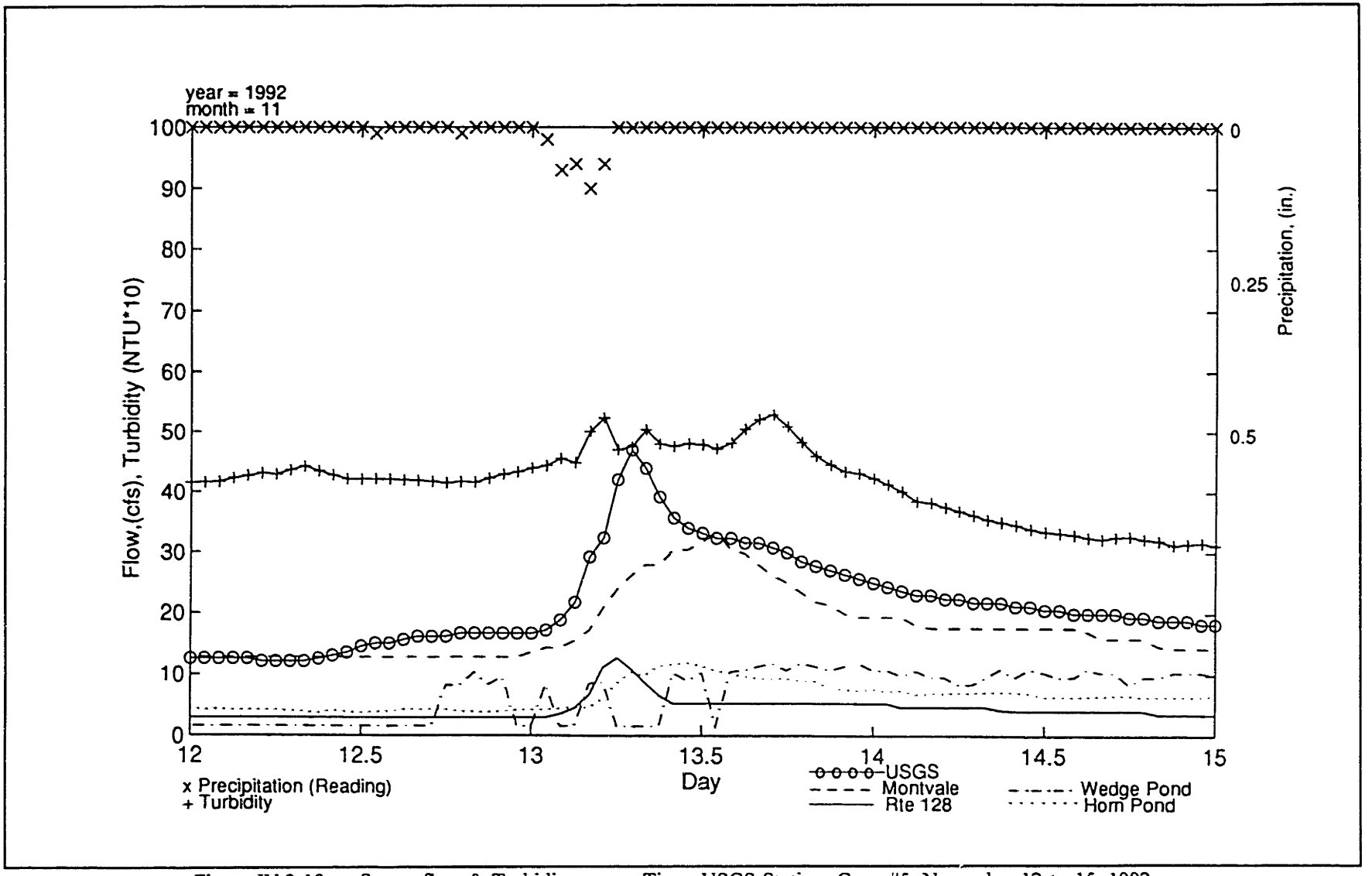

Figure IV.3-18: Streamflow & Turbidity versus Time, USGS Station, Gage #5, November 12 to 15, 1992

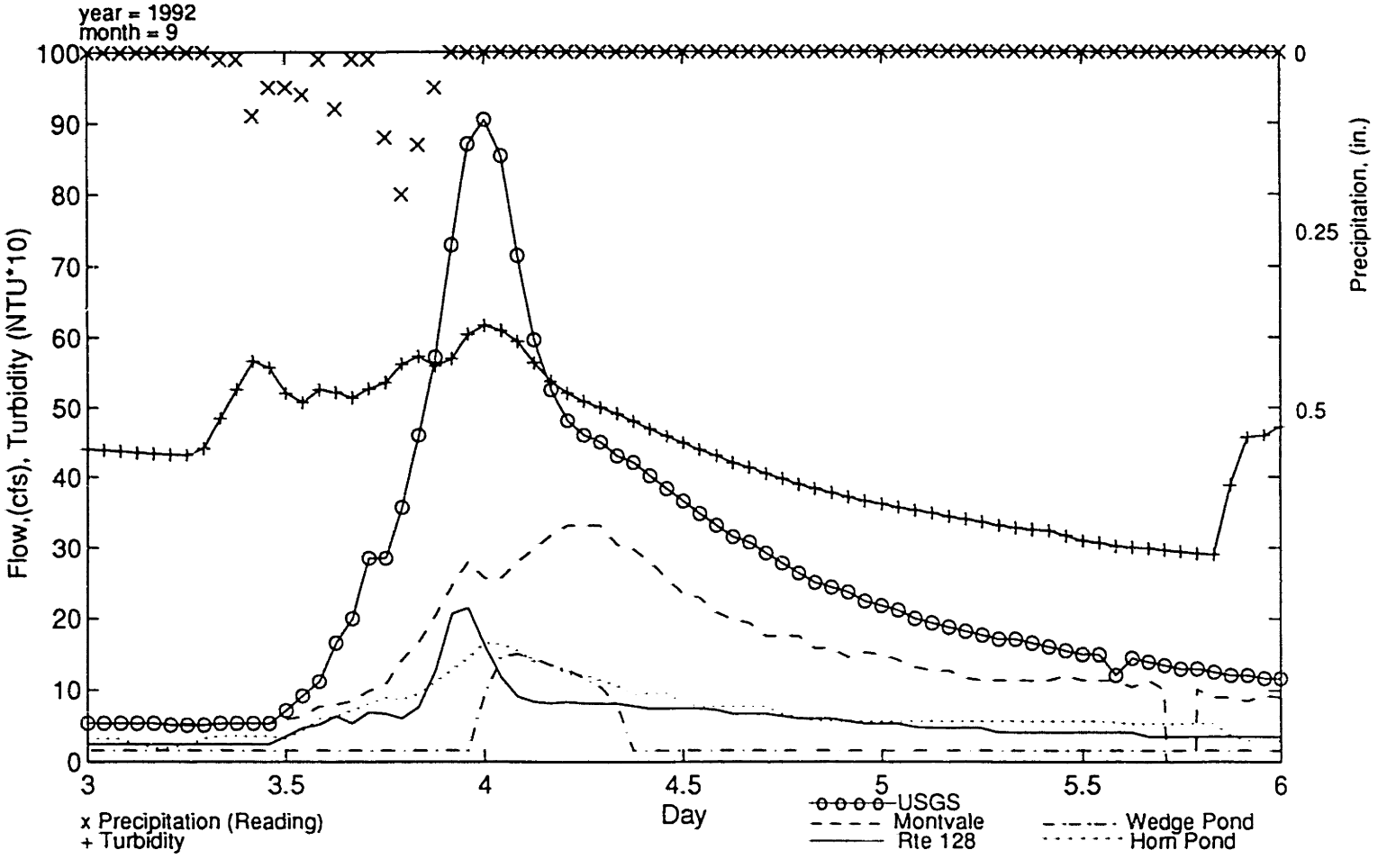

Figure IV.3-19: Streamflow & Turbidity versus Time, USGS Station, Gage #5, September 3 to 6, 1992

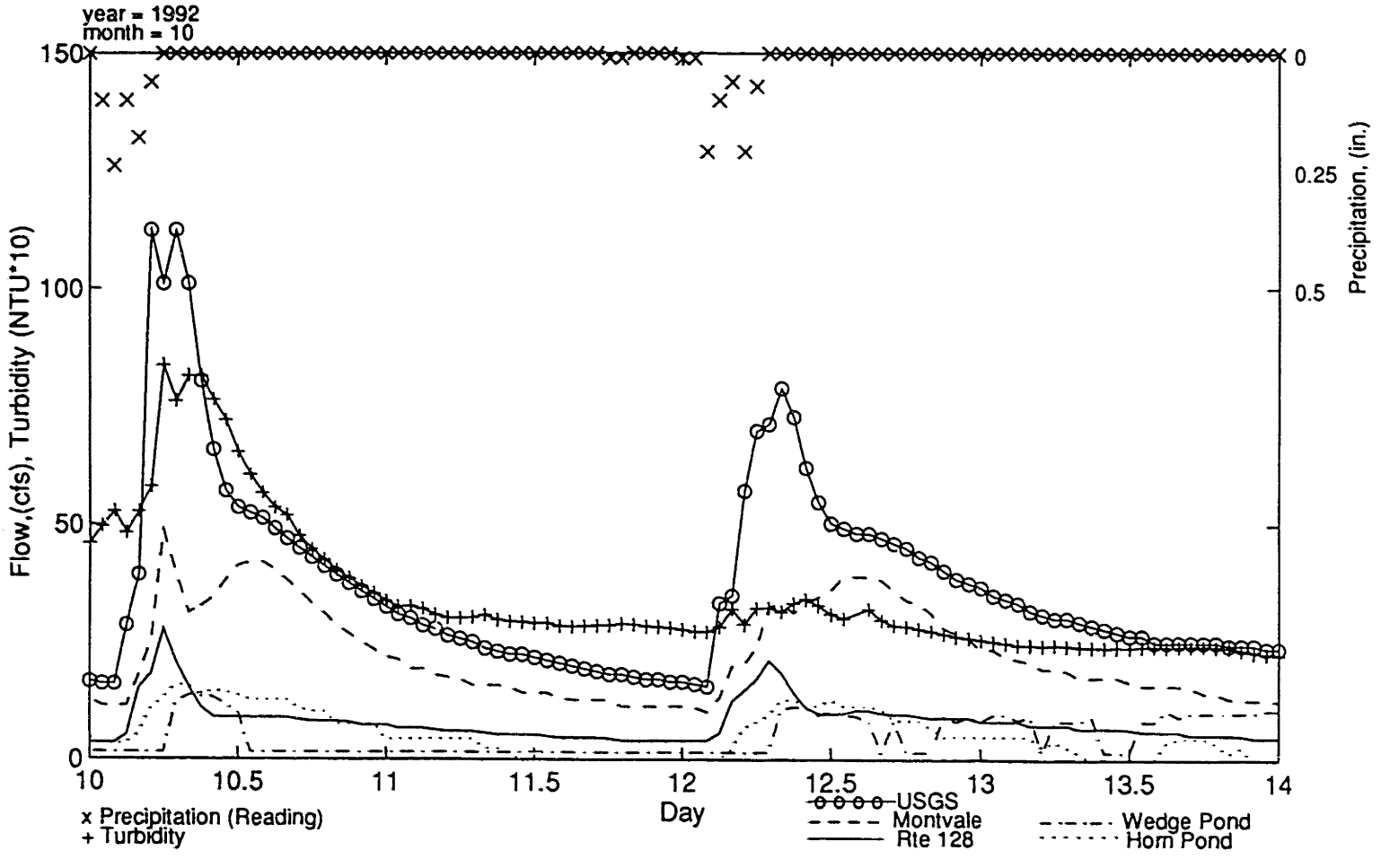

Figure IV.3-20: Streamflow & Turbidity versus Time, USGS Station, Gage #5, October 10 to 14, 1992

IV.4 METALS

This section describes metals data with the purposes of: 1) providing average concentrations and fluxes, 2) providing data concerning the partitioning of metals between the filterable (dissolved) and unfilterable (particulate) phases, 3) describing the general behavior of metal transport, and 4) postulating approaches for modeling metal transport.

For reference, metal concentrations and fluxes of each sample are provided in tables IV.E-1 to IV.E-20 in appendix IV.E. All concentrations and fluxes plotted in this section correspond to a 0.5 μm pore size filter.

IV.4.1 Low Flow Data, Gages 1,2,3,4, & 5

Summary

Average metal concentrations of samples collected "manually" are given in table IV.4-1 below. These samples are the same samples that were analyzed for suspended sediment concentrations. (figures IV.3-1 and IV.3-2) All but one sample was collected during receding flow conditions. Most of the samples collected during receding flows were also collected during low flow conditions. Flow conditions corresponding to each sample are discussed in more detail in section IV.3.2.

Strong differences in concentrations were observed within different parts of the watershed. Metal concentrations were highest on the upper reaches of the Aberjona River and lowest along the Horn Pond Creek tributary. Concentrations at the USGS, (located after the confluence with the Aberjona River and Horn Pond Creek) were generally at intermediate concentrations.

The primary sources of metals during receding flow conditions were the Woburn North and Woburn Central sub-basins. Samples collected shortly before or shortly after storm peaks indicate that the Woburn Central and the Winchester sub-basins may have served as significant sources of metals during storm conditions.

Particulate arsenic and iron concentrations exhibited a strong correlation with streamflow, where higher concentrations were observed during lower flows. (figures IV.4-6 and IV.4-19) The interpretation of this trend is that the different suspended sediment components had characteristically different particulate metal concentrations. For example, longterm baseflow sediments, which predominated during low flows, had high metal concentrations, whereas quick suspended sediments, which predominated at high flows, had low metal concentrations. Particulate chromium and copper behaved differently in that concentrations were not strongly correlated with streamflow. Similarly, for all metals, the dissolved phase did not exhibit a strong correlation with streamflow.

During low flow conditions and for a given monitoring station, the partitioning of metals between the dissolved and particulate phases was relatively constant. Samples collected immediately before or after storm peaks, however, indicate that storm flows had a tendency of shifting the partitioning toward the particulate phase. Copper was the metal most strongly partitioned toward the dissolved phase. For all stations, the dissolved phase generally represented approximately 70% of the copper. Chromium was the metal which was the least strongly partitioned toward the dissolved phase. Generally only 30 to 35% of the chromium was present within the dissolved phase for all stations. Partitioning of arsenic and iron was intermediate between chromium and copper.

Station	Diss Fe mg/l	Part Fe %	Total Fe mg/l	Diss Cu µg/l	Part Cu mg/kg	Total Cu µg/l	Diss Cr µg/l	Part Cr mg/kg	Total Cr µg/l	Diss As µg/l	Part As mg/kg	Total As µg/l
Wedge Pond	0.17	2.6	0.32	2.7	86	3.2	<0.2	<80	--	1.21	22	1.35
Rte 128	0.77	12.8	1.67	8.7	424	11.8	1.39	383	4.06	7.06	852	13.2
Montvale	0.53	11.0	1.21	9.0	360	11.6	1.59	553	5.65	4.21	801	9.10
Horn Pond	0.21	4.3	0.38	2.7	71	3.0	<0.2	<80	--	0.30	14.6	0.39
USGS	0.38	8.2	0.73	6.0	238	7.3	0.37	257	1.71	2.96	350	4.27

Table IV.4-1: Mean Concentrations of Manually Collected Samples, (Feb'92 to Jan'93)

IV.4.1.1 Arsenic

Contaminant Source Evaluation

Arsenic concentrations were highest on the Aberjona River side of the watershed. The highest total concentration of 24.1 µg/l was measured at Route 128 on July 23, 1992. For this sample, 8.8 µg/l were associated with the dissolved phase and 15.3 µg/l were associated with the particulate phase. The corresponding particle concentration (on a per mass of suspended sediment basis) was 1370 mg/kg. The lowest arsenic concentrations were generally measured on the Horn Pond Creek tributary. All concentrations measured on this tributary were less than 2.5 µg/l.

Along the Aberjona River total arsenic concentrations generally decreased in the downstream direction. This trend was especially evident for the dissolved phase (figure IV.4-1), where for most sampling dates, dissolved arsenic concentrations decreased from Route 128, to Montvale, and to the USGS. One interpretation of this trend is that a source of contaminated water is located upstream of the Route 128 station. As the contaminated water continued to travel downstream, relatively cleaner waters were added to the overall flow. As a result, a dilution effect was observed, where arsenic concentrations decreased in the downstream direction.

Observation of the dissolved arsenic fluxes (figure IV.4-2) support the notion that a large fraction of the dissolved arsenic originated from upstream sources. All of the samples (except the December 17 samples) were collected during the falling limb of the streamflow hydrograph. For these "falling-limb" samples, a large fraction of the dissolved flux observed along the Aberjona can be associated with the flux observed at Route 128. The primary exception to the trend is the December sample which indicates that different processes may have dominated during "rising-limb" conditions.

An enhancement of the dilution effect was observed for the USGS station which not only received groundwater inflows during low flow conditions but also received inflows from the Horn Pond Creek tributary. Arsenic concentrations from this tributary were generally at lower levels than concentrations along the Aberjona upstream of this tributary (figure IV.4-1). As a result the Horn Pond Creek waters diluted the arsenic concentration of the Aberjona River after the confluence. Therefore, at the USGS, a dilution effect was probably associated with two processes: 1) inflows of cleaner groundwaters, and 2) mixing of cleaner tributary inflows.

For the particulate phase the dilution effect was not evident between the Route 128 and Montvale gages. (figure IV.4-3) For these stations particulate metal concentrations (per suspended sediment basis) were at similar values for most sampling dates. Additionally, for sampling dates dominated by longterm

baseflow and slow waters, the overall fluxes of particulate arsenic (figure IV.4-4) were usually slightly larger at Montvale than at Route 128. One interpretation of this trend is that the Woburn Central sub-basin did not serve as a major source of "transportable" particulate arsenic during low flow conditions. Perhaps, during low flows, significant quantities of particulate arsenic did in fact enter the river channel from the sub-basin. These significant quantities, if they occurred, however, did not get transported downstream and were most likely deposited/stored in the Wells G & H wetland area.

Support of the deposition notion for the Wells G & H site is provided by the two samples which were collected during either quick dominated flow (October 12) or during rising limb conditions (December 17). For these samples, particulate arsenic fluxes increased significantly from the Route 128 to the Montvale gage indicating that the Woburn Central sub-basin served as a significant source of particulate arsenic. In justifying this trend one may postulate that during storm conditions: 1) particulate arsenic previously deposited during low flows within the Woburn Central sub-basin was eroded from the channels during increasing flows, or 2) an outside sediment source supplied arsenic laden sediments to the channel.

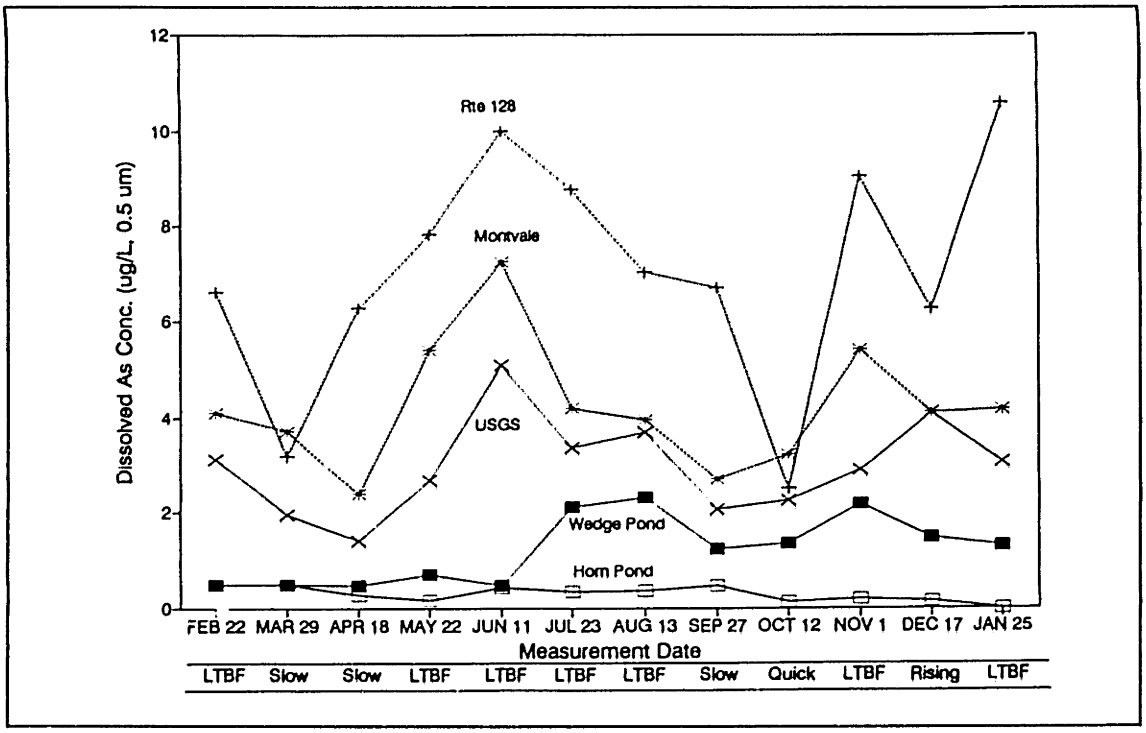

Figure IV.4-1: Dissolved As Concentration versus Measurement Date
All Stations, February 1992 to January 1993

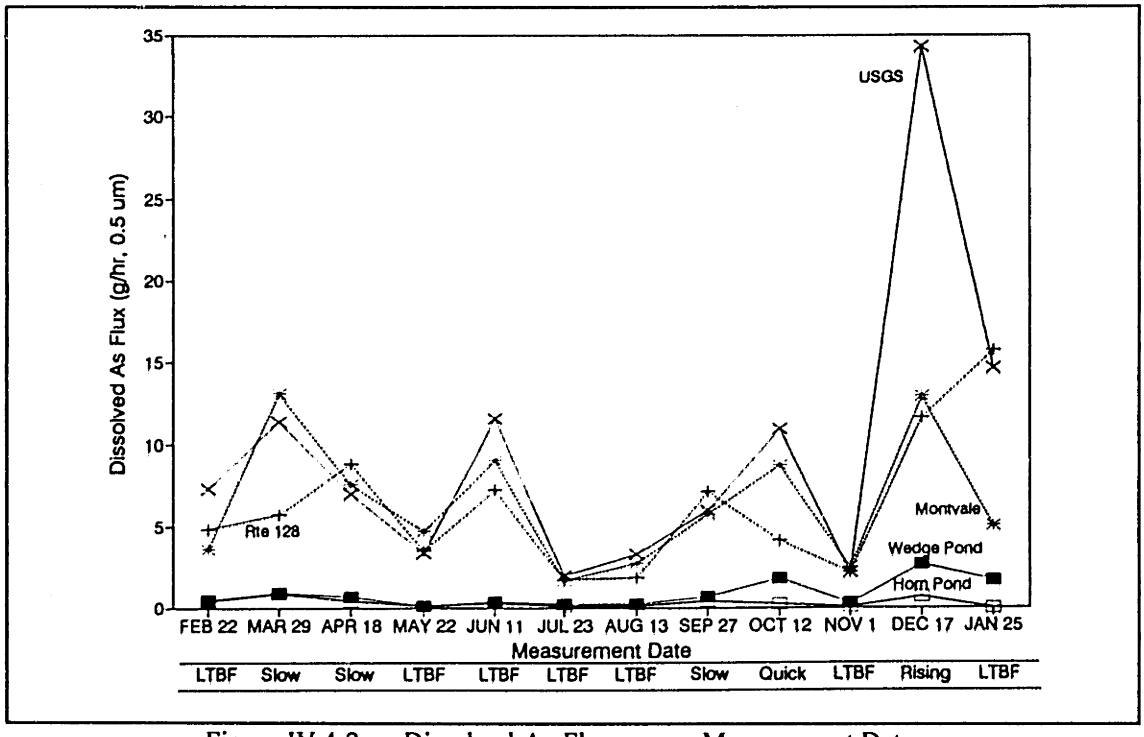

Figure IV.4-2: Dissolved As Flux versus Measurement Date
All Stations, February 1992 to January 1993

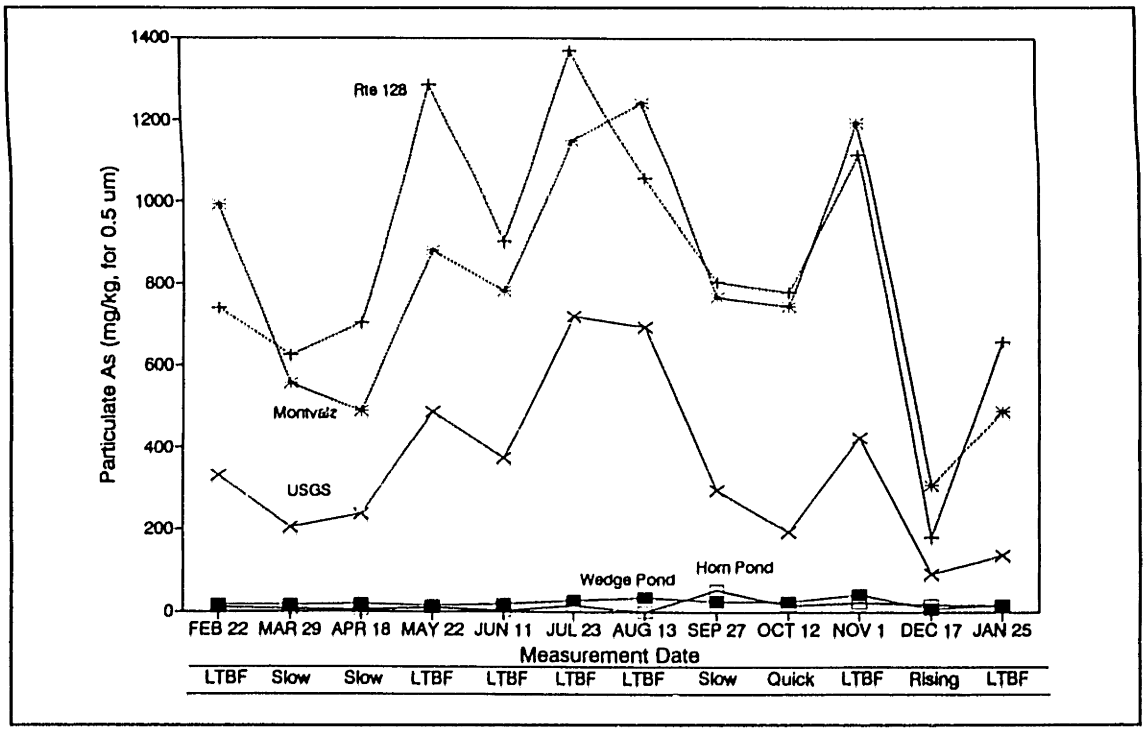

Figure IV.4-3: Particulate As Concentration versus Measurement Date
All Stations, February 1992 to January 1993

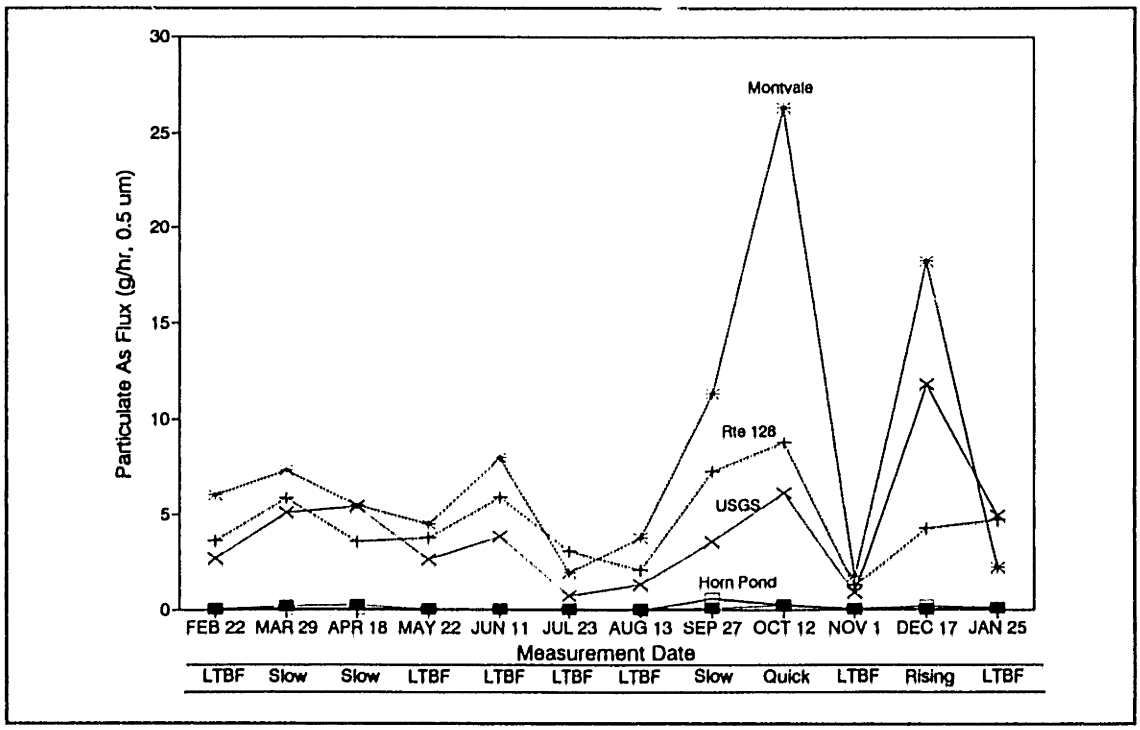

Figure IV.4-4: Particulate As Flux versus Measurement Date
All Stations, February 1992 to January 1993

Effects of Streamflow

For a given sampling station, particulate phase arsenic (figure IV.4-6) appeared to have been affected by changes in streamflow whereas dissolved phase arsenic (figure IV.4.5) showed no strong correlation with streamflow. The only trend observed for the dissolved phase was that each sampling station generally had different average arsenic concentrations.

The primary trend for the particulate phase is a decrease in arsenic concentrations with increasing flows. One possible *but unlikely* interpretation of such a trend is associated with channel sediments where, fine channel sediments which predominated during low flows were diluted by relatively cleaner coarse channel sediments which were transported in association with higher flows. Such an explanation seems logical especially if one considers trends in transport capacity. Assume that the river bottom sediments are characterized by a non-uniform grain size distribution. During low flow conditions, the shear velocities at the river bed are generally lower resulting in lower sediment transport capacities. Therefore, during low flows, only the finer particles will be transported. During high flows (or higher shear velocities), larger particles will be transported. At these higher flows, a mixture of both fine and coarse sediments would be expected. Data indicate that metal concentrations of sediments increase with decreasing particle size (appendix III.E and appendix III.G). During low flows, because of the predominance of fine particles, higher particulate metal concentrations would be expected. During higher flows, coarser (but cleaner) particles would dilute the more contaminated fines that predominate during low flow conditions.

However, transport capacity calculations (appendix IV.D) indicate that suspended sediment transport in the river was not governed by carrying capacity but rather by the availability of sediments. In other words, for a given low flow condition, the particle size and metal concentration that were being transported by the river was governed by the supply. Furthermore, evidence exists that the suspended sediment particle size remained relatively constant regardless of flow condition. (appendix III.E) Therefore, the particle dilution effect associated with different size channel particles is not a satisfying interpretation of the data.

An alternative interpretation of the observed data is that there are different sources of suspended sediments each with characteristically different particulate arsenic concentrations. During very low flows, longterm baseflows are generally the dominant source of sediments. Because of the high particulate arsenic concentration observed during low flows, these sediments may be assumed to have high particulate metal concentrations associated with them. During higher flows, a mixture of longterm baseflow and slow storm waters are assumed to be transported where, the higher the flow, the larger the fraction of flow dominated by slow waters. Because of the lower particulate arsenic concentration

observed during higher flows, one may further postulate that slow waters have a low concentration of particulate arsenic. The observed trend, decreasing particulate arsenic concentrations with increasing streamflow, may therefore be associated with the mixing of these waters in different proportions. During low flows, longterm baseflow dominates resulting in high arsenic concentrations whereas during higher flows, slow storm water dominates resulting in lower arsenic concentrations.

Partitioning of Arsenic Between Dissolved and Particulate Phases

Arsenic concentrations for samples collected at Route 128 and Montvale stations were almost equally distributed between the dissolved and particulate phases. (figures IV.4-7 & IV.4-8) This partitioning is contrasted by the samples collected at Horn Pond and Wedge Pond where over 80% of the arsenic was generally in the dissolved phase. (figures IV.4-10 and IV.4-11) Samples collected at the USGS station were intermediate between the two sets of samples, with generally about 70% of the arsenic in the dissolved phase. (figure IV.4-9)

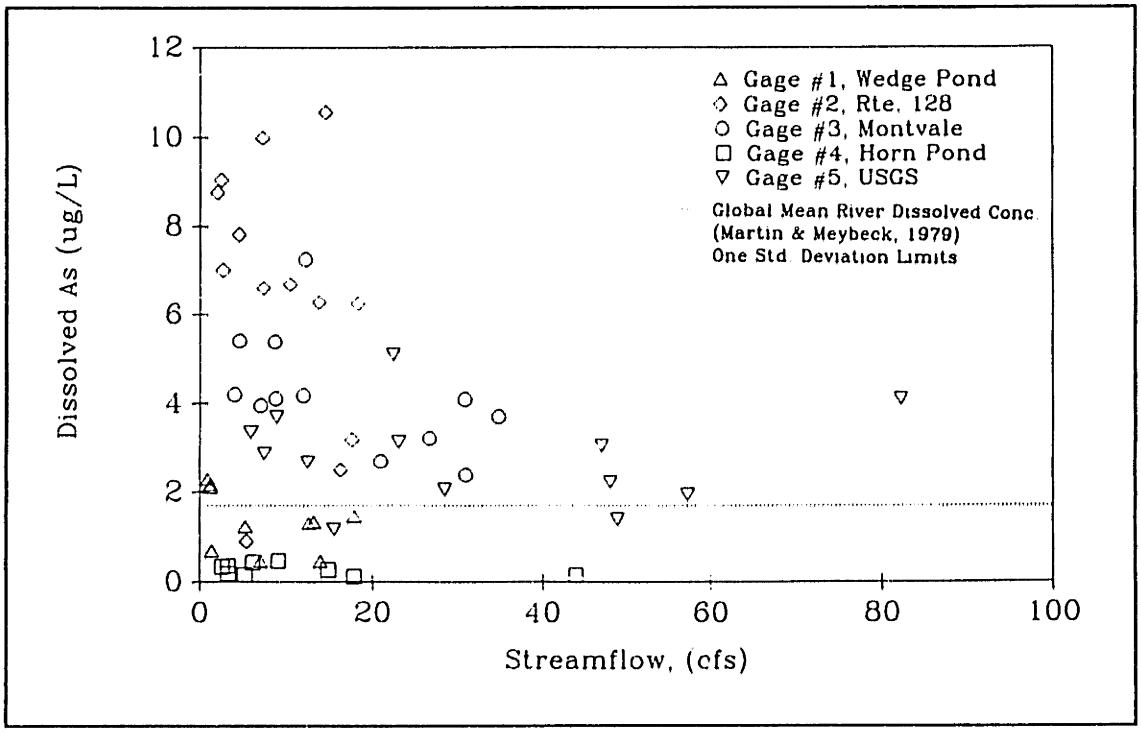

Figure IV.4-5: Dissolved As Concentration versus Flow
All Stations, Manual Samples, February 1992 to May 1993

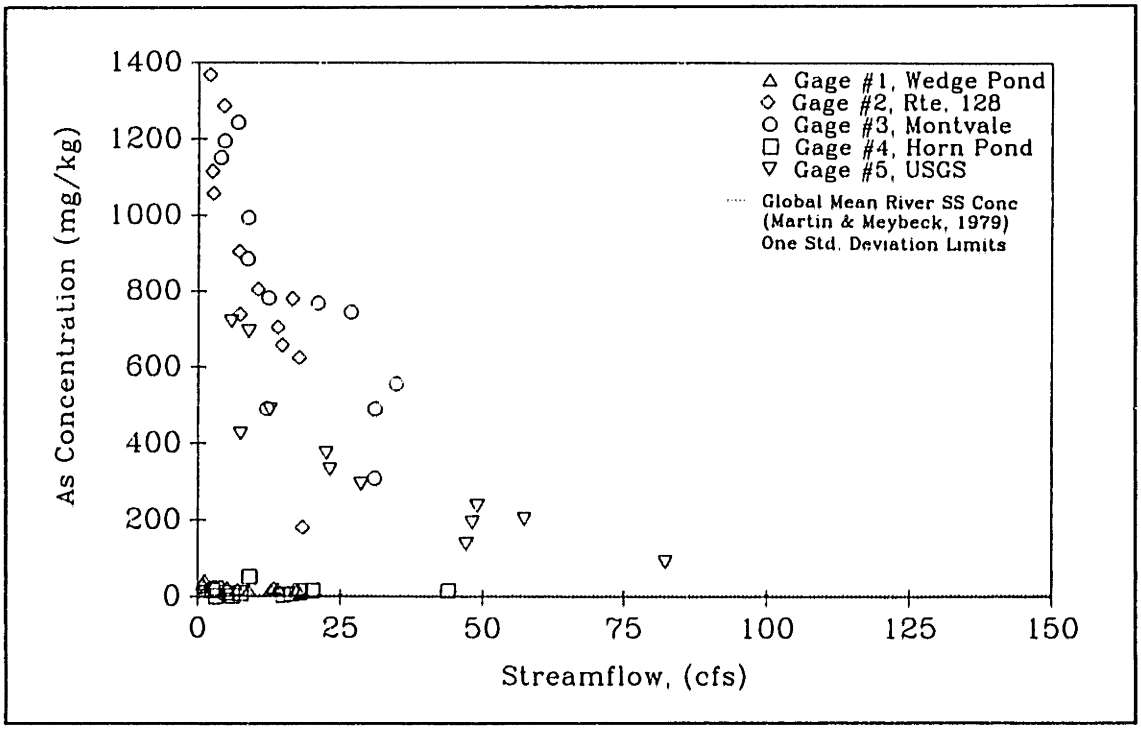

Figure IV.4-6: Particulate As Concentration versus Flow
All Stations, Manual Samples, February 1992 to January 1993

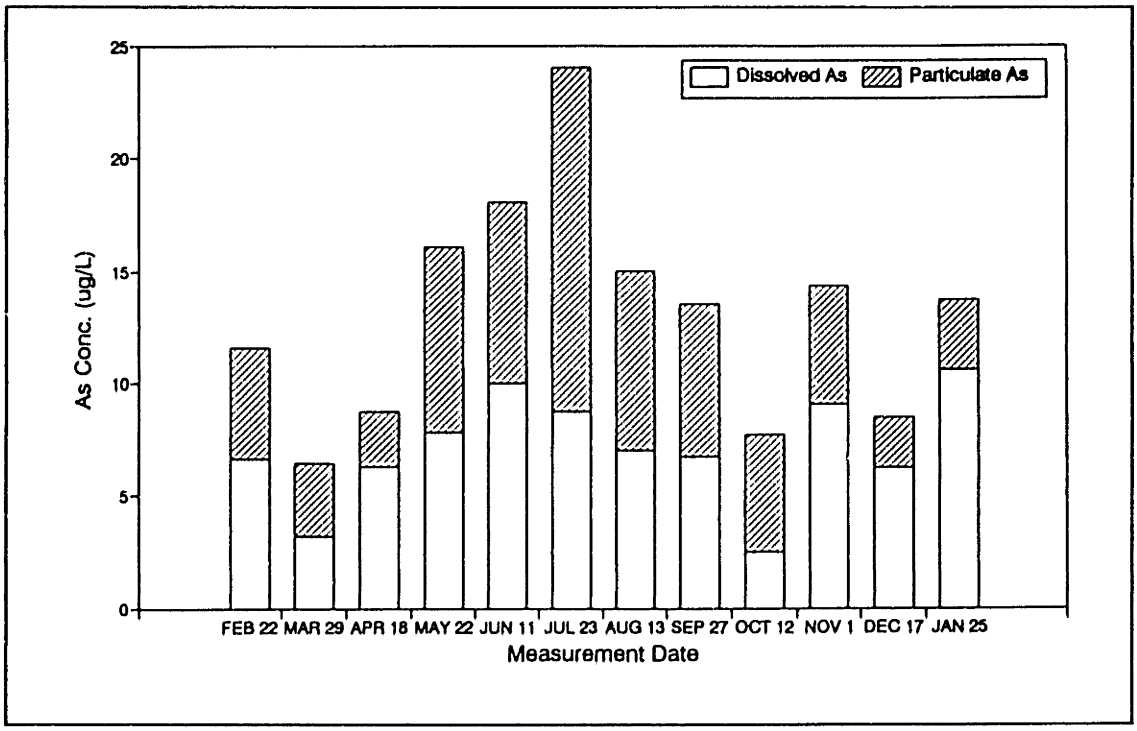

Figure IV.4-7: As Concentration versus Measurement Date, Gage #2, Route 128 Manual Samples, February 1992 to January 1993

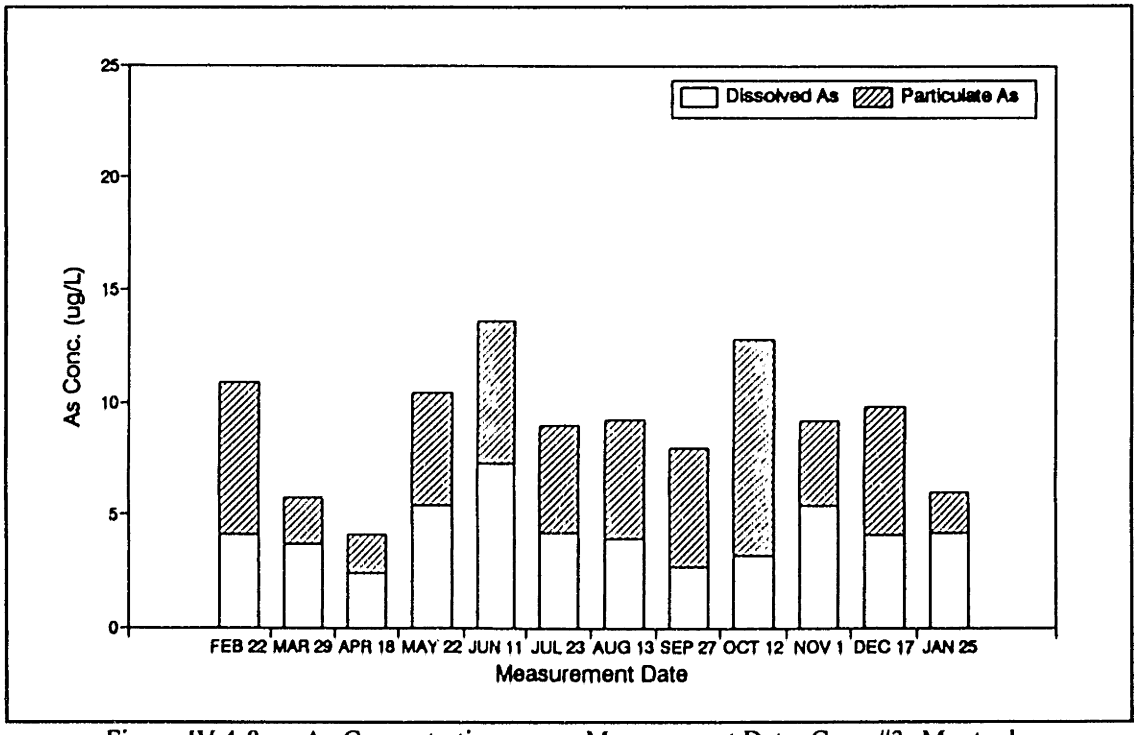

Figure IV.4-8: As Concentration versus Measurement Date, Gage #3, Montvale Manual Samples, February 1992 to January 1993

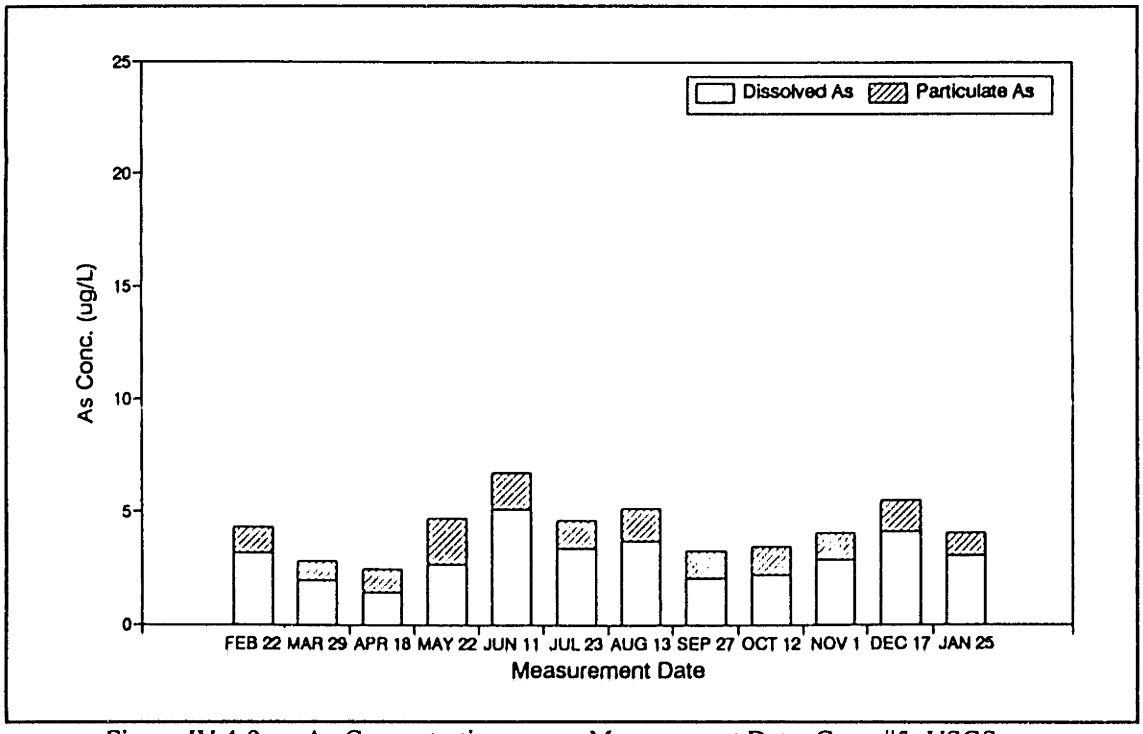

Figure IV.4-9: As Concentration versus Measurement Date, Gage #5, USGS Manual Samples, February 1992 to January 1993

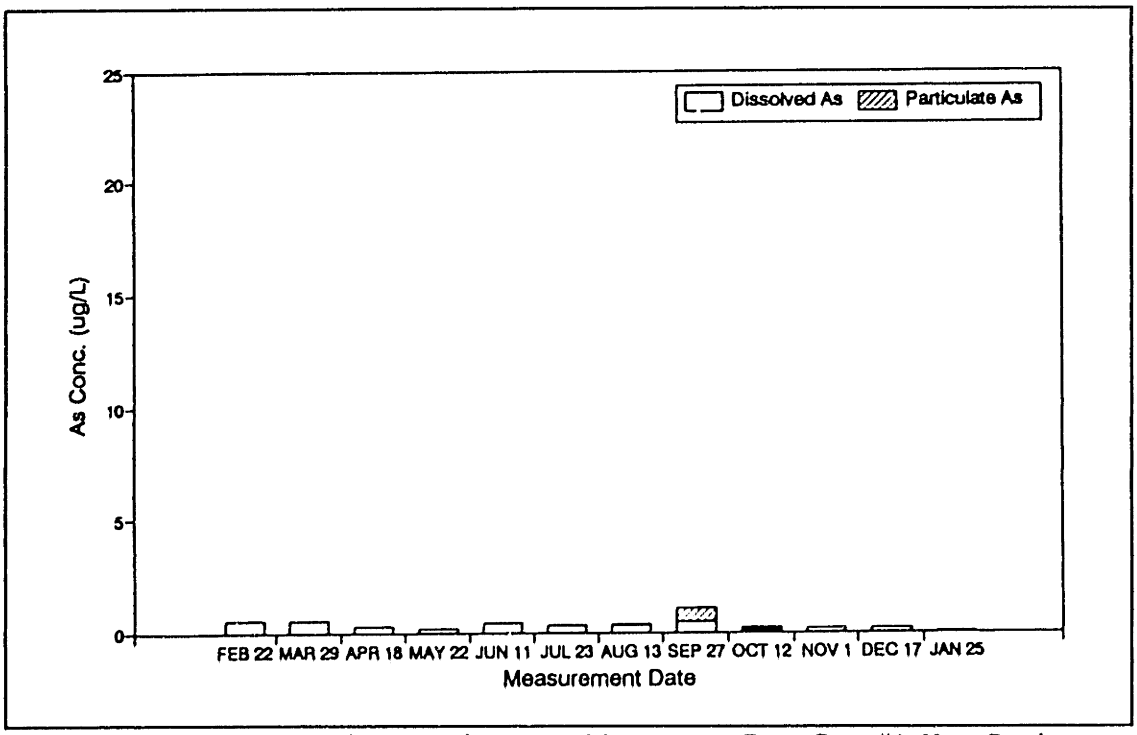

Figure IV.4-10: As Concentration versus Measurement Date, Gage #4, Horn Pond Manual Samples, February 1992 to January 1993

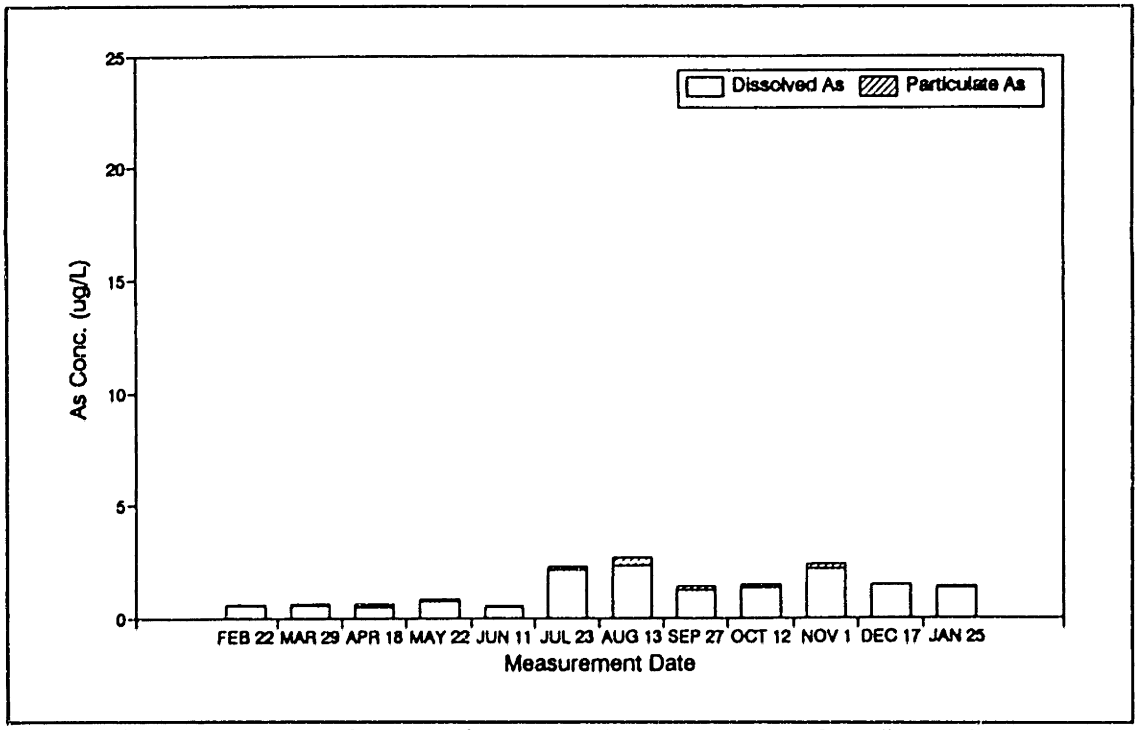

Figure IV.4-11: As Concentration versus Measurement Date, Gage #1, Wedge Pond Manual Samples, February 1992 to January 1993

General Comments Concerning the Partitioning of Metals Between the Dissolved and Particulate Phases

For a given sampling station, the partitioning of metals between the dissolved ($[M_d]$ = mass dissolved metal per volume of river water) and particulate phases ($[M_{pss}] = [M_p][SS]$ = mass particulate metal per volume of river water) was surprisingly constant, regardless of total metal concentration, pH, and other parameters. (for example, figures IV.4-7 and IV.4-20) This consistency was especially evident for samples collected when flows were dominated by slow and longterm baseflow waters. The consistency of this partitioning may be explained through the work of Morel and Gschwend, 1987, who attributed constant partitioning to the presence of colloids within the operationally defined "dissolved" phase.

From a purely theoretical perspective (if colloids were successfully removed from the dissolved phase), one would expect that the ratio of $[M_p]$ (mass metal per mass of suspended sediment) and $[M_d]$ to be constant, not the ratio of $[M_{pss}]$ to $[M_d]$. The ratio of $[M_p]$ to $[M_d]$ is referred to as a partition coefficient. A constant partition coefficient implies that the attractiveness of the suspended material for the metal remains constant for all levels of $[M_p]$ of interest. (Schwarzenbach, et. al., 1992)

However, for the case where colloids are entrained within the "dissolved" phase, the operationally defined dissolved metal concentration is no longer a quantification of the "true" dissolved phase needed for the determination of partition coefficients. For such a case, the assumption of a constant partition coefficient is no longer valid.

Morel and Gschwend, 1987, derived an "observed partition coefficient" which explicitly accounted for the entrainment of colloids within the dissolved phase. In their derivation they assumed that most of the metals were associated with the solid (colloidal or suspended) material. No matter what the size of the solid, it contained a constant metal to particulate mass ratio and changes in overall solid concentration resulted in a uniform increase in the concentrations of all particle sizes. For such a situation, Morel and Gschwend, 1987, presented that the ratio of $[M_{pss}]$ to $[M_d]$ was a constant. Such assumptions may be valid for a river system if the particulates transported equilibrate to a consistent size distribution and composition.

However, not all samples exhibited a consistent ratio of $[M_{pss}]$ to $[M_d]$. Rather, for some samples (especially the rising limb and quick flow dominated samples), the partitioning shifted toward the particulate phase ($[M_{pss}]$). This shift may be associated with the mobilization of excess particulate metals during quick flow conditions. Because of the rapidly changing conditions and activation of different particulate sources, the assumptions postulated by Gschwend and Morel, 1987, may not be valid during quick flows.

IV.4.1.2 Iron

Contaminant Source Evaluation

As for the other metals, higher concentrations of iron were observed on the Aberjona River side of the watershed than on the Horn Pond Creek side of the watershed. The highest concentration of 2.7 mg/l was observed at Route 128 on July 23, 1992. For this sample 0.9 mg/l were associated with the dissolved phase whereas 1.8 mg/l were associated with the particulate phase. The corresponding concentration of iron on a per suspended sediment mass basis was 16 %. Concentrations on the Horn Pond Creek tributary were generally less than 0.5 mg/l.

As observed for arsenic, iron concentrations also decreased along the Aberjona River in the downstream direction. This dilution effect was most apparent for the dissolved phase (figure IV.4-12). The interpretation of this dilution effect is that the sub-basin upstream of Route 128 supplied contaminated waters. These waters, as they traveled downstream, were diluted by relatively cleaner inflows causing the decrease in dissolved iron concentration in the downstream direction. The only exception to the trend was the October 12 sample in which the dissolved iron concentration was lower at Route 128 than at Montvale. This exception may have been associated with the fact that the October samples were collected when quick flow dominated the streamflow hydrograph. The quick flows from the Woburn North sub-basin may have been cleaner than from the Woburn Central sub-basin. With this assumption one would expect lower iron concentrations at Route 128 during quick-flow dominated flows. Also quick flows tend to change significantly on the order of hours. Since each station was sampled at a different time on any given sampling date, the contribution of quick flow at each of the stations may have been significantly different, and may therefore have resulted in an inconsistent comparison.

The particulate phase also exhibited a dilution effect for most of the sampling dates (figure IV.4-14). The primary exceptions occurred on May 22, June 11, and July 23 where the iron concentrations at the USGS were almost equal to the concentrations at Montvale.

A large fraction of both the particulate and dissolved phase iron flux can be accounted for by the flux observed at Route 128. (figures IV.4-13 and IV.4.15) Therefore, the sub-basin upstream of Route 128 may be considered as one of the primary sources of iron within the watershed. The primary exceptions occurred October 12 and December 17 for both the dissolved and particulate phases. The large increases at Montvale and the USGS stations were most likely associated with the fact that they were collected during or immediately after a storm. During a storm, the iron fluxes were most likely affected by: 1) quick flows which carry dissolved and particulate iron to the river, and 2) erosion of iron laden particulates which were deposited during earlier times in the channel.

Comparison of arsenic and iron in both the dissolved and particulate phases (figures IV.4-16 and IV.4.-17) shows similarities between the transport of each component. The similarity is especially evident for the particulate phase, where from one measurement date to another, increases in iron concentrations were generally accompanied by increases in arsenic concentrations. This similarity indicates that perhaps iron and arsenic were: 1) either mobilized from a similar source, or 2) were transported in association with one another.

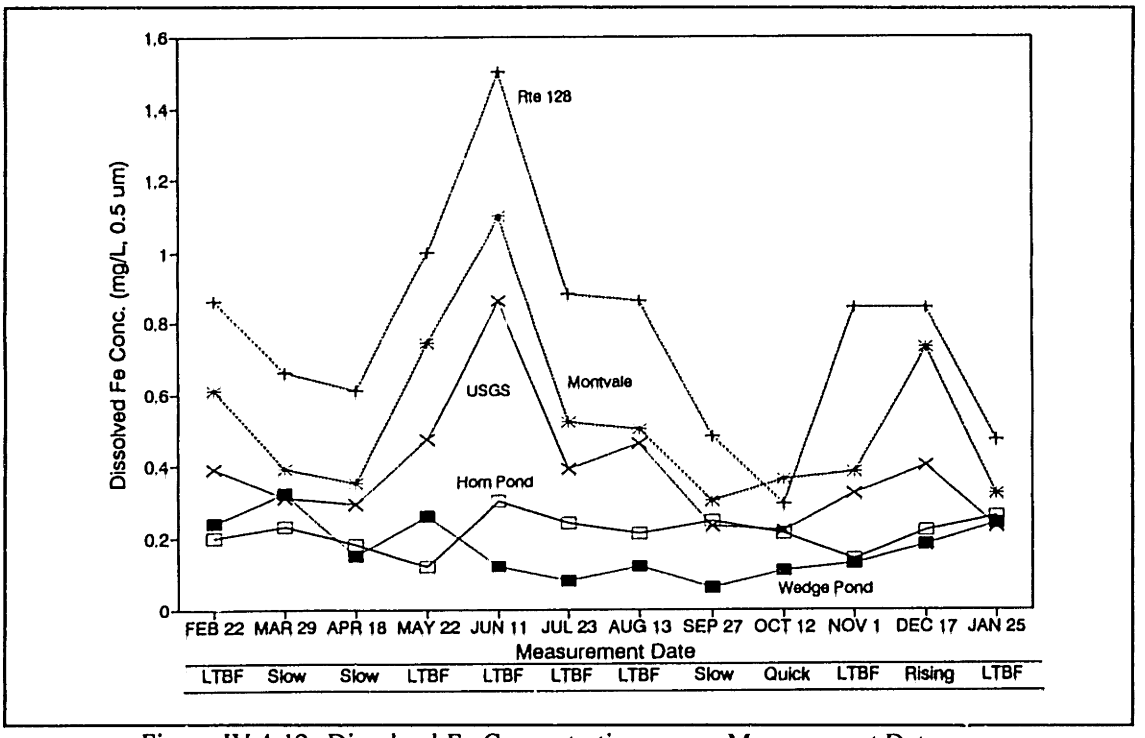

Figure IV.4-12: Dissolved Fe Concentration versus Measurement Date
All Stations, February 1992 to January 1993

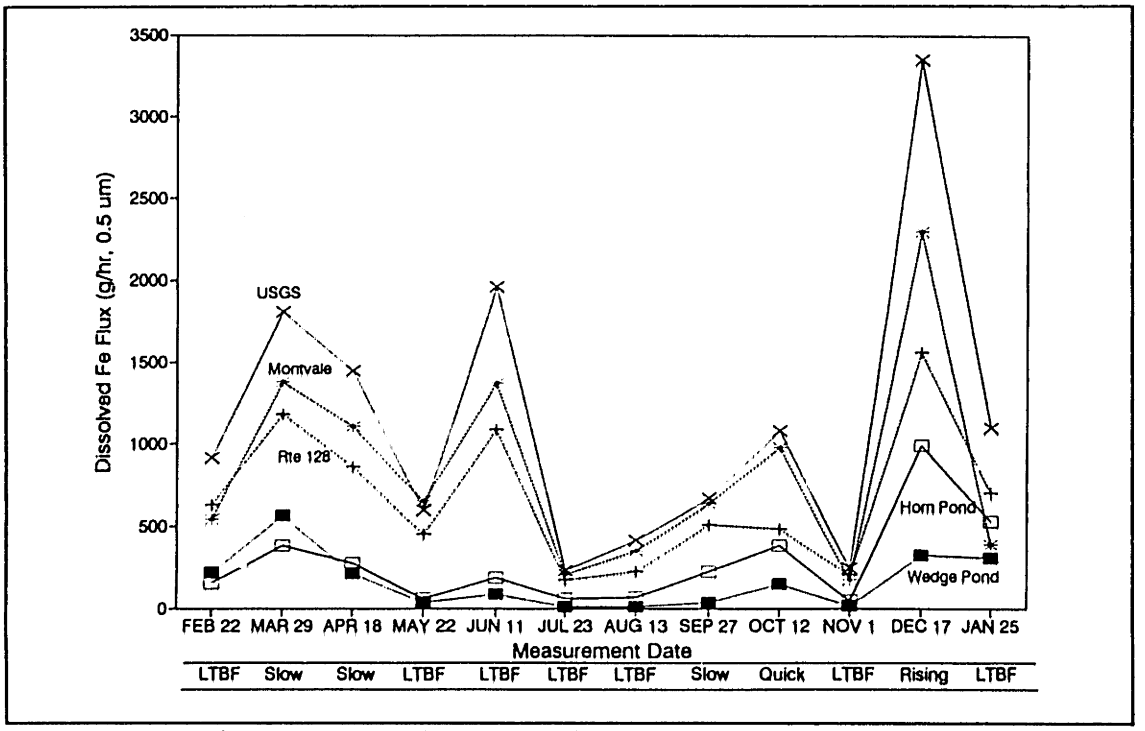

Figure IV.4-13: Dissolved Fe Flux versus Measurement Date
All Stations, February 1992 to January 1993

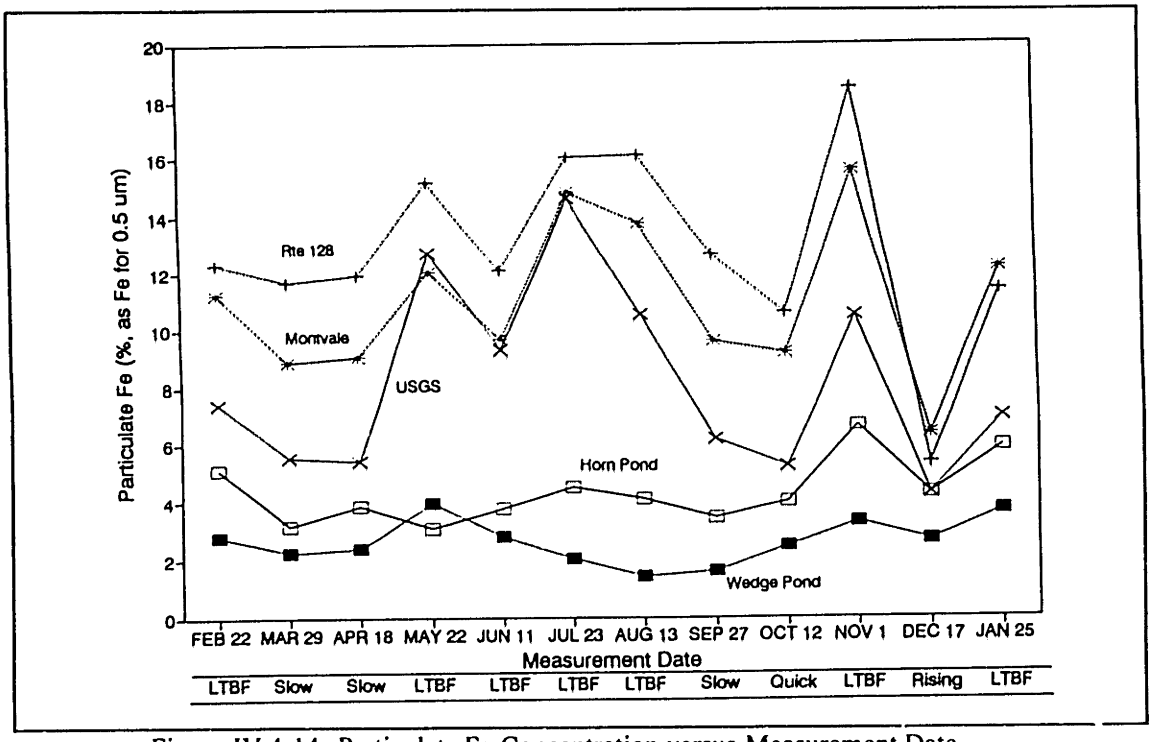

Figure IV.4-14: Particulate Fe Concentration versus Measurement Date
All Stations, February 1992 to January 1993

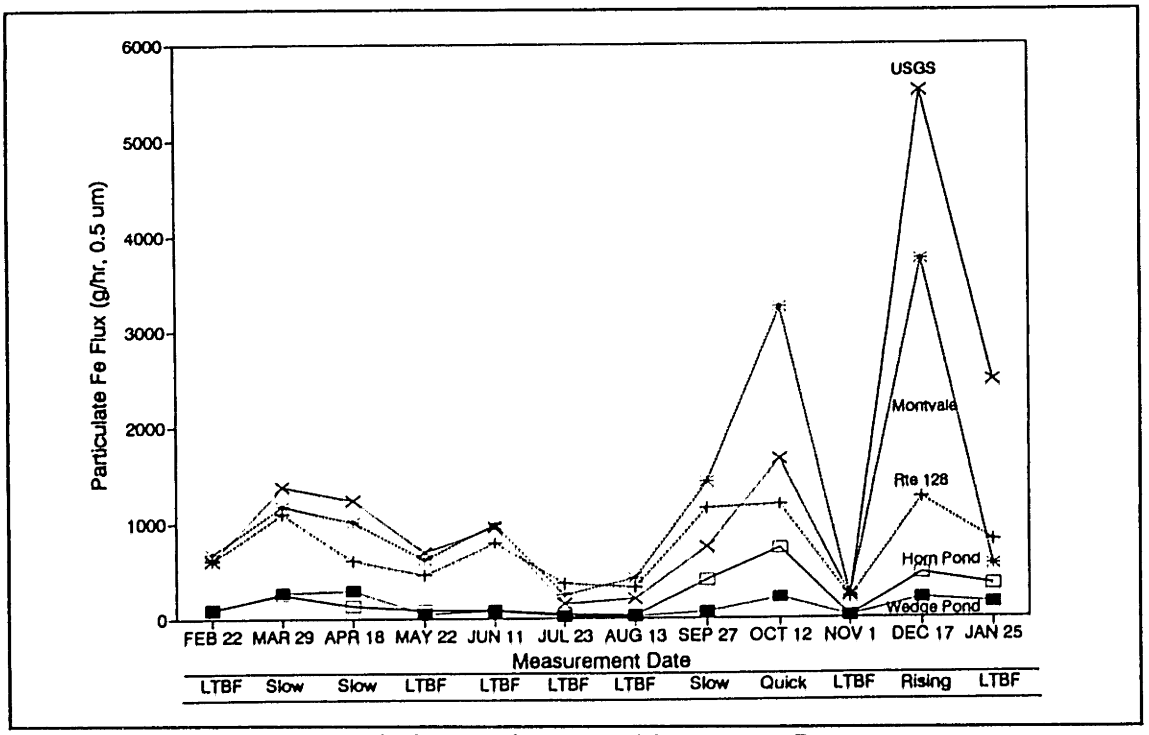

Figure IV.4-15: Particulate Fe Flux versus Measurement Date
All Stations, February 1992 to January 1993

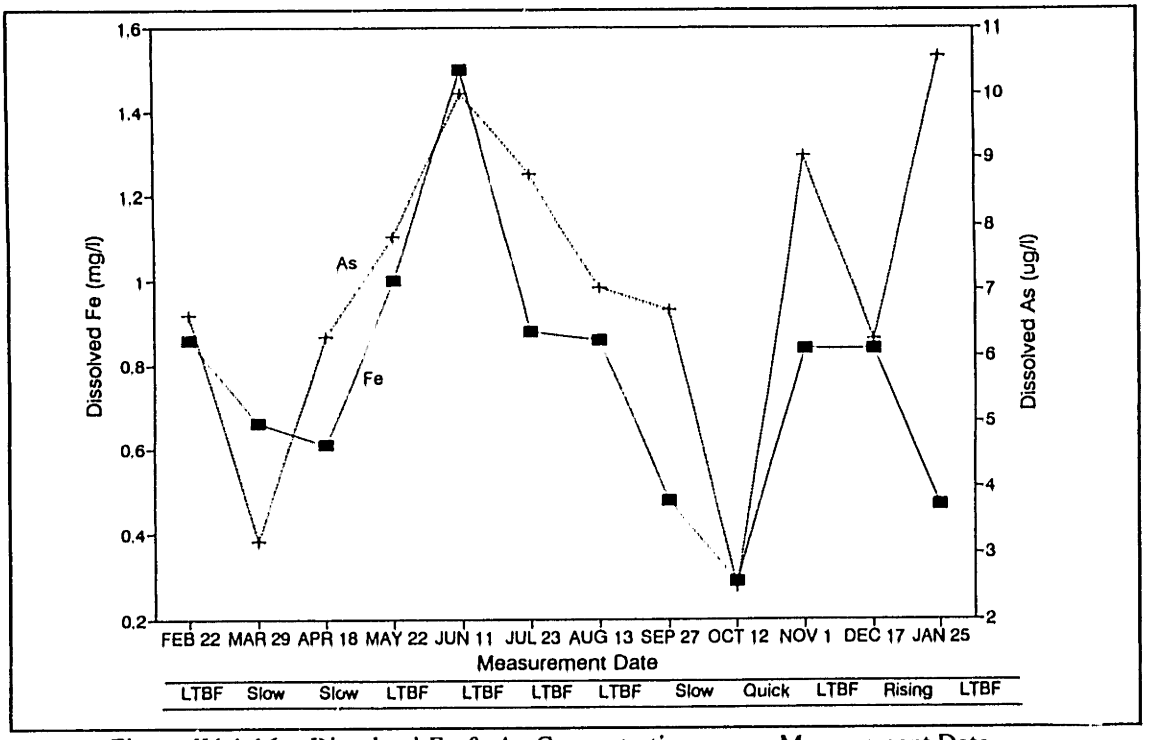

Figure IV.4-16: Dissolved Fe & As Concentration versus Measurement Date
Route 128 Station, February 1992 to January 1993

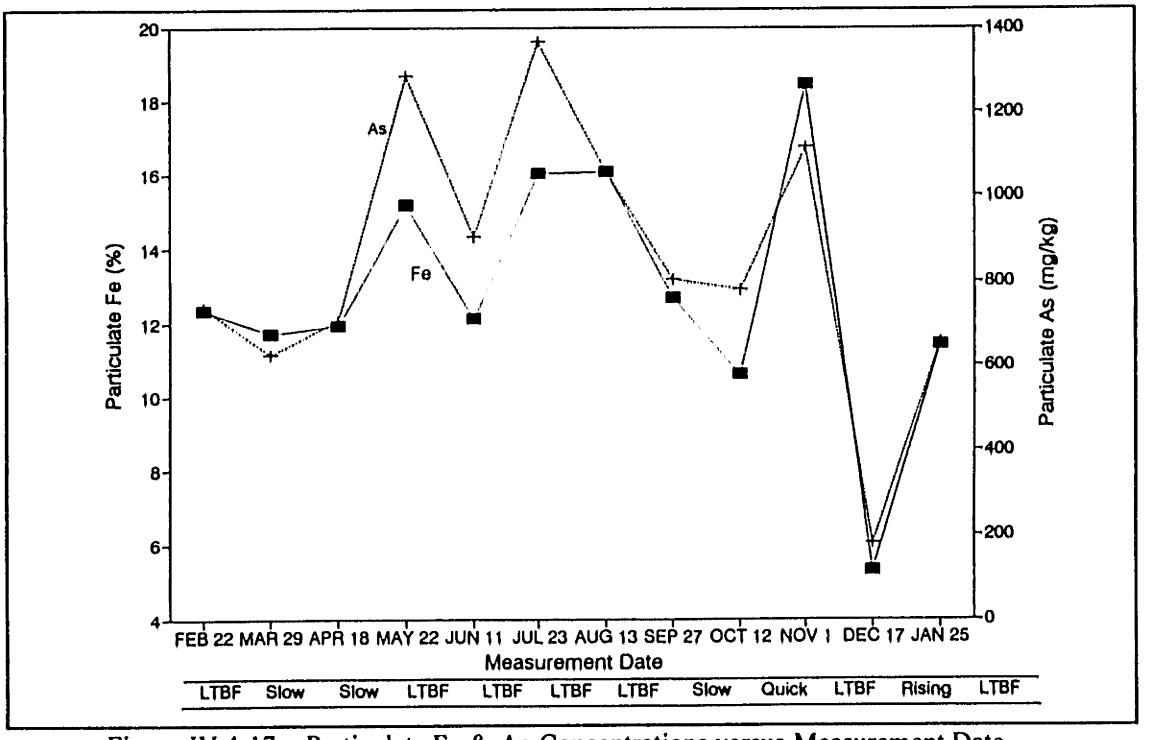

Figure IV.4-17: Particulate Fe & As Concentrations versus Measurement Date
Route 128 Station, February 1992 to January 1993

Effects of Streamflow

For a given sampling station, dissolved iron concentrations (figure IV.4-18) were not strongly correlated with streamflow, whereas particulate concentrations (figure IV.4-19) decreased with decreasing streamflow. The interpretation for the particulate phase is similar to that made for arsenic. At very low flows, the source of particulate iron is from contaminated longterm baseflow sediments, whereas at higher flows, cleaner sediments associated with slow flows contribute significantly to the overall suspended sediment flux.

The primary exceptions to the particulate iron trend occurred for samples collected from August 20 to 22, 1991. (figure IV.4-19) These samples correspond to the receding limb of a hurricane event (Hurricane Bob) that occurred on August 19, 1991. As far as precipitation quantities, this hurricane was not much greater than other large storms for which samples were collected. However, the hurricane did appear to cause a short-term change in contaminant transport which was not observed for other large storm events. Perhaps, speculatively, the high winds speeds associated with the hurricane affected metal transport. For example, the high winds could have possibly caused; 1) an enhanced re-suspension of contaminated channel bottom sediments, 2) the "washing" of new surface sources by wind-blown rain, and/or 3) caused an excess of wind-blown debris to enter the river. This debris could have possibly been a source of excess metals.

Additionally, a flow reversal was observed at the Wedge Pond station shortly after the hurricane (August 22, 1991). (figure IV.4-19) A sample collected at the Wedge Pond station during the reverse flow exhibited an increased concentration of particulate iron above the typical observed concentrations. This increase was due to the contribution of more contaminated waters from the Aberjona River.

Partitioning of Iron Between Dissolved and Particulate Phases

On average, the dissolved phase represented approximately 60% of the iron at Horn Pond. (figure IV.4-23) For the remaining stations, the dissolved phase generally represented from 40 to 50% of the sample. (figures IV.4-20, IV.4-21, IV.4-22, IV.4-24) The partitioning between the dissolved and particulate phases was relatively constant for each of the sampling stations.

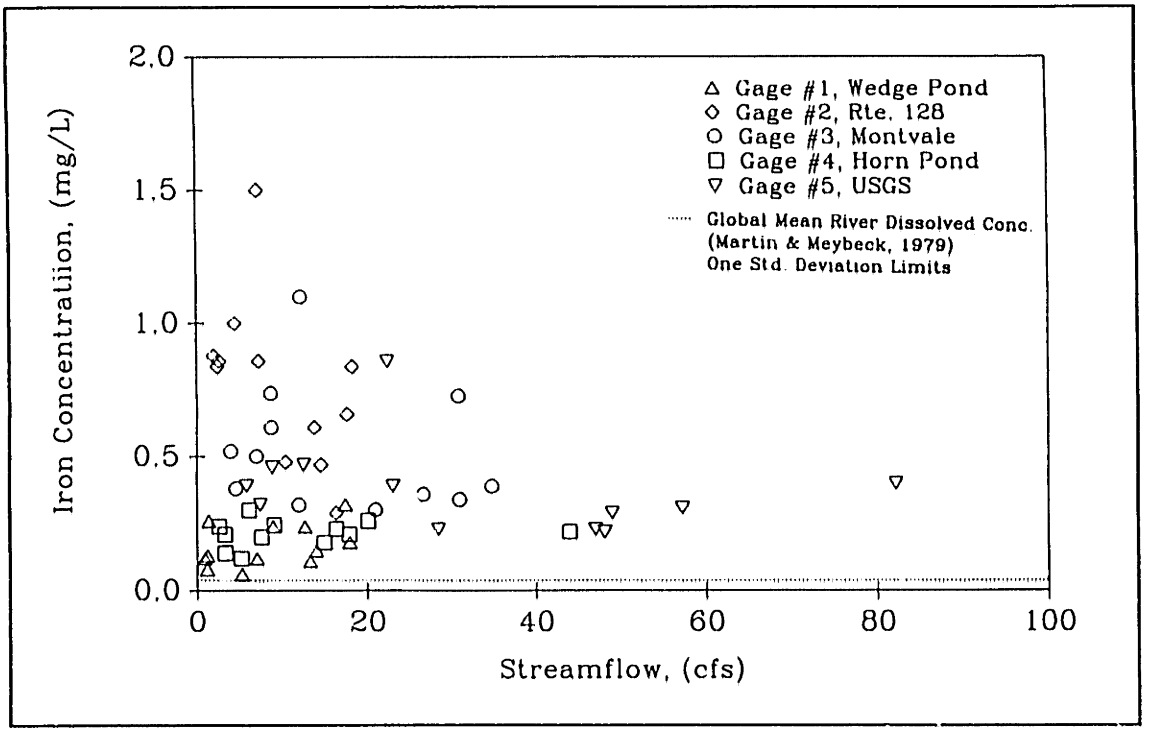

Figure IV.4-18: Dissolved Fe Concentration versus Flow
All Stations, Manual Samples, February 1992 to May 1993

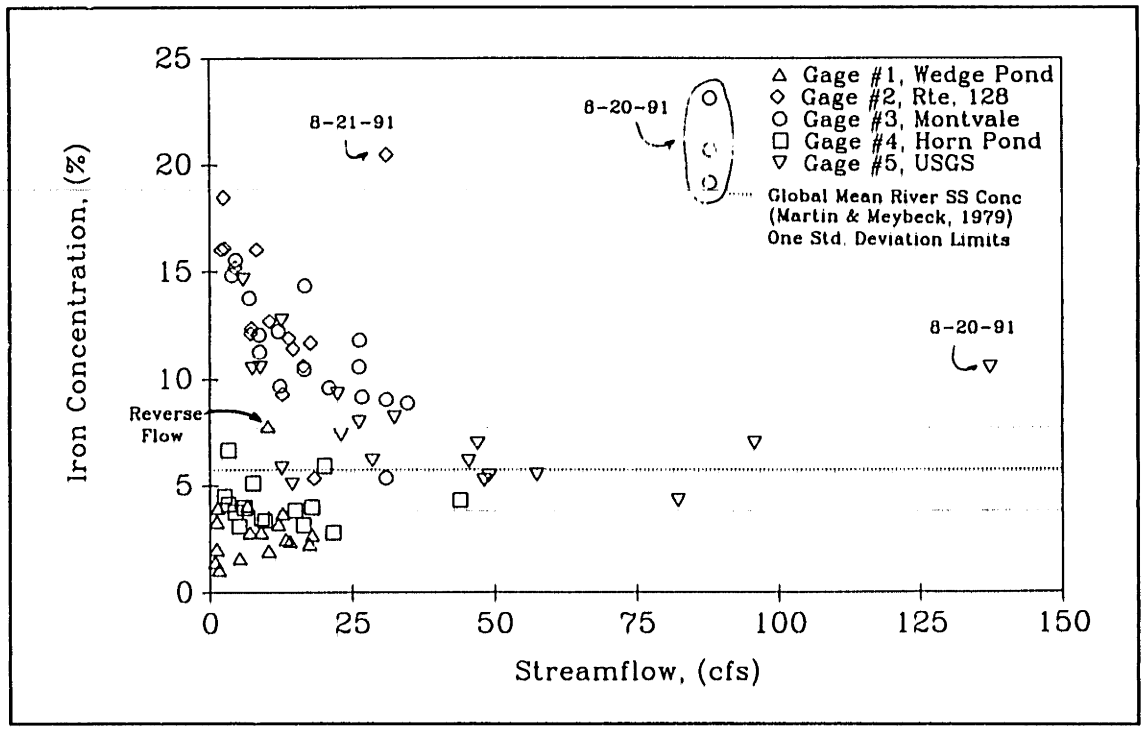

Figure IV.4-19: Particulate Fe Concentration versus Flow
All Stations, Manual Samples, August 1991 to January 1993

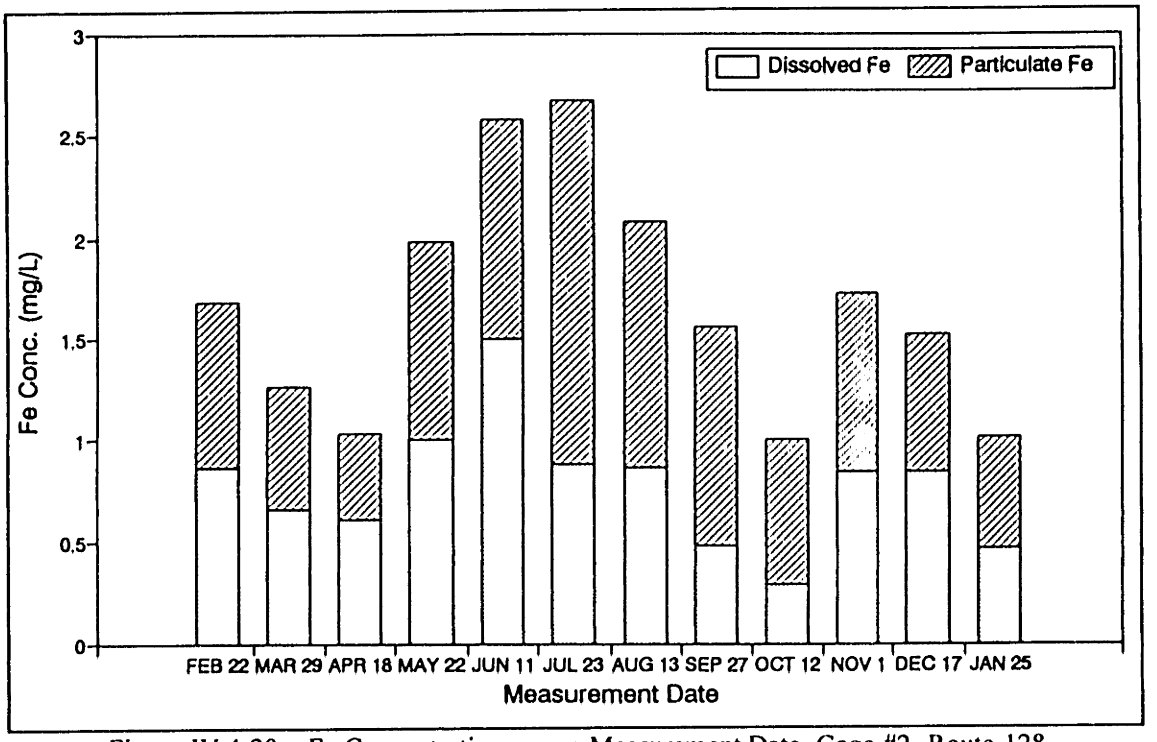

Figure IV.4-20: Fe Concentration versus Measurement Date, Gage #2, Route 128 Manual Samples, February 1992 to January 1993

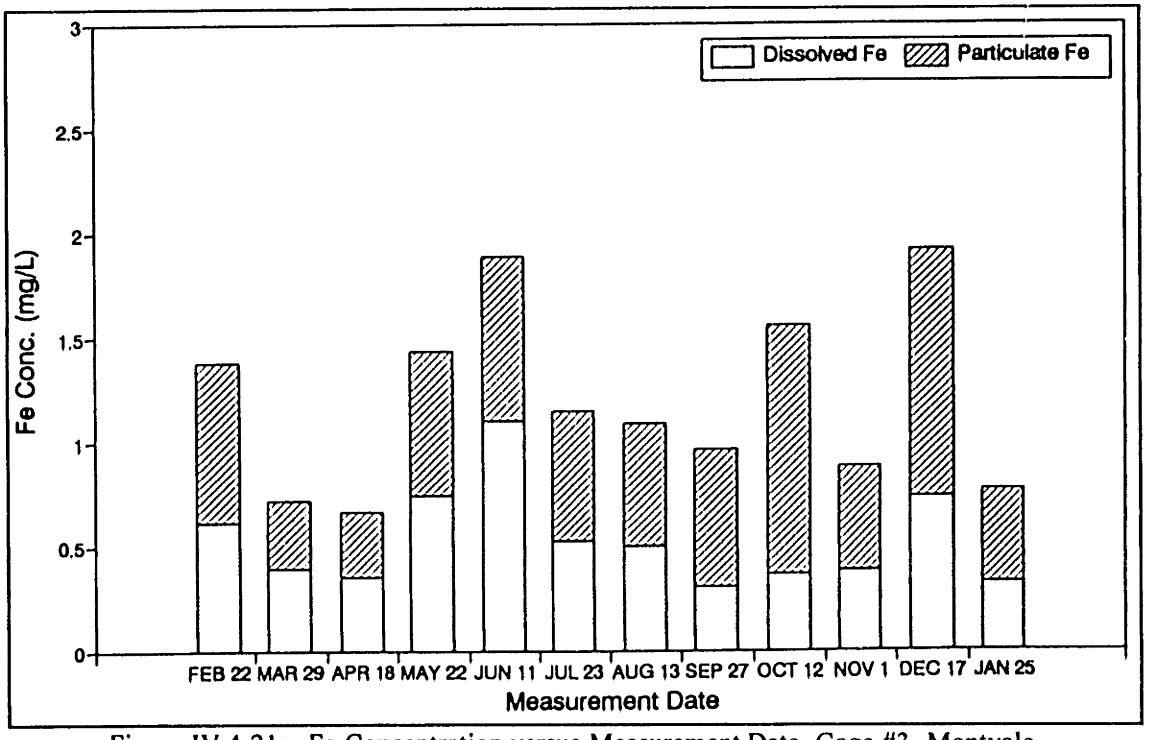

Figure IV.4-21: Fe Concentration versus Measurement Date, Gage #3, Montvale Manual Samples, February 1992 to January 1993

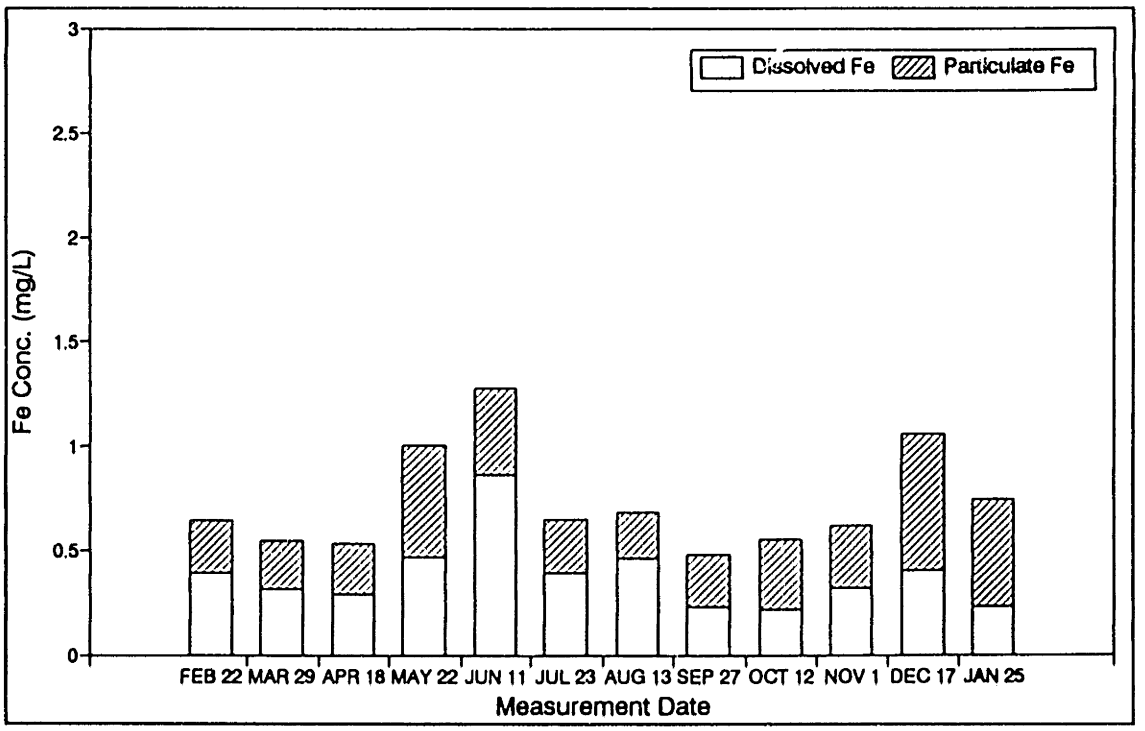

Figure IV.4-22: Fe Concentration versus Measurement Date, Gage #5, USGS Manual Samples, February 1992 to January 1993

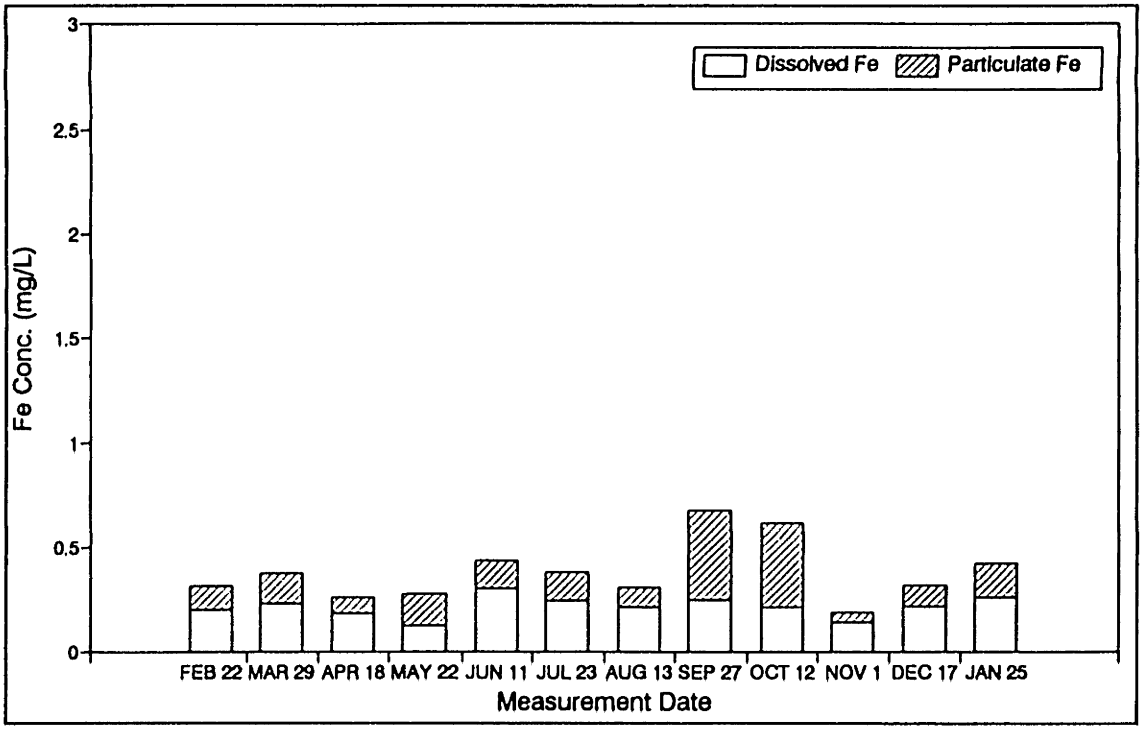

Figure IV.4-23: Fe Concentration versus Measurement Date, Gage #4, Horn Pond Manual Samples, February 1992 to January 1993

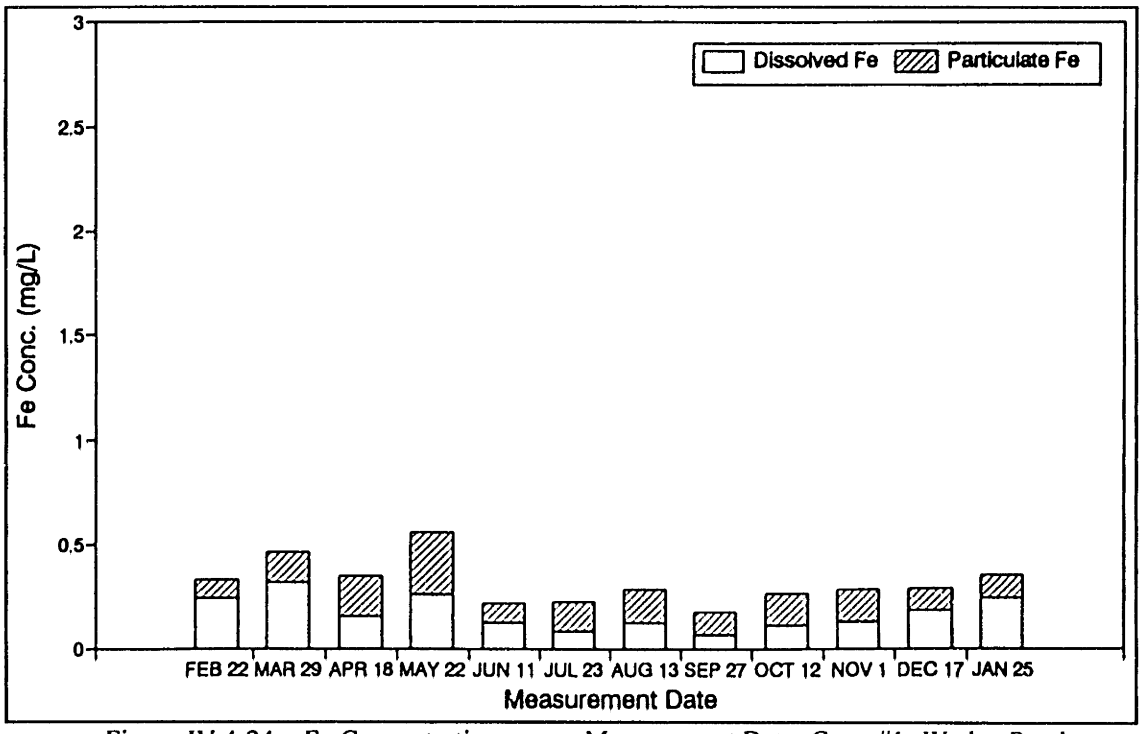

Figure IV.4-24: Fe Concentration versus Measurement Date, Gage #1, Wedge Pond Manual Samples, February 1992 to January 1993

IV.4.1.3 Chromium

Contaminant Source Evaluation

Chromium concentrations on the Aberjona River were generally higher than concentrations on the Horn Pond Creek tributary. The highest observed concentration of 12.5 µg/l was observed October 12, 1992 at Montvale. For this sample, 1.2 µg/l were in the dissolved phase and 11.3 µg/l were in the particulate phase. The corresponding particulate concentration on a per suspended sediment mass basis was 870 mg/kg. The total chromium concentrations along the Horn Pond Creek tributary were generally less than 0.8 µg/l.

Unlike iron and arsenic, chromium did not exhibit a strong dilution effect along the Aberjona. Rather, from Route 128 to Montvale, chromium concentrations generally increased for both the dissolved and particulate phases. (figures IV.4-25 and IV.4-27) Additionally, the flux of dissolved chromium increased significantly for most sampling dates (figure IV.4-26) and the flux of particulate chromium increased significantly for the October and December samples. (figure IV.4-28) The interpretation of this trend is that the sub-basins draining both the Route 128 and Montvale gages (Woburn North and Woburn Central) represented significant source areas of chromium. The Woburn Central sub-basin was an especially significant source of particulate chromium during rising limb and quick flow conditions. The increase in particulate transport during quick and rising limb flows may be associated with: 1) large inputs of particulate chromium from quick storm waters supplying the Woburn Central sub-basin, and/or 2) erosion of particulate chromium which was deposited in the channel during prior low flow conditions. However, a decrease in the fluxes is generally observed from Montvale to the USGS, indicating that the Winchester sub-basin may act as a sink for particulate chromium.

Effects of Streamflow

For a given sub-basin, the concentration of chromium in both the dissolved and particulate phases (figure IV.4-29 and IV.4-30) was not correlated with streamflow. This observation indicates that there may not have been a strong chromium concentration difference between different components of flow or suspended sediments.

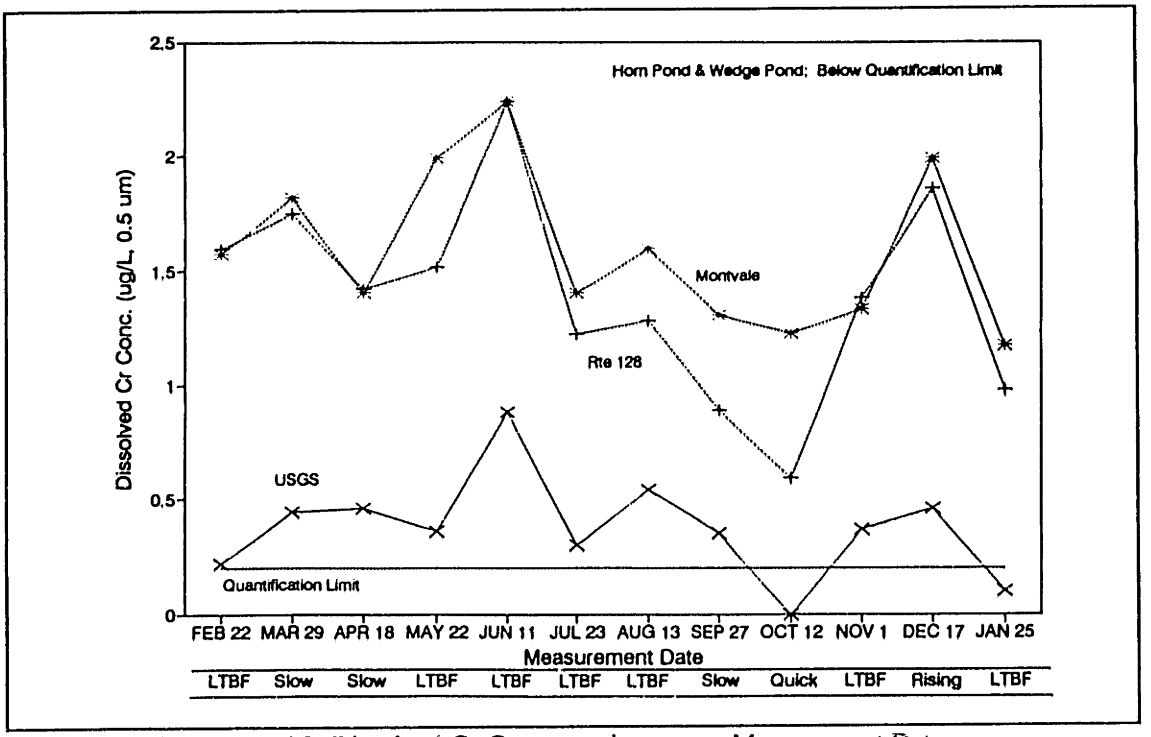

Figure IV.4-25: Dissolved Cr Concentration versus Measurement Date
All Stations, February 1992 to January 1993

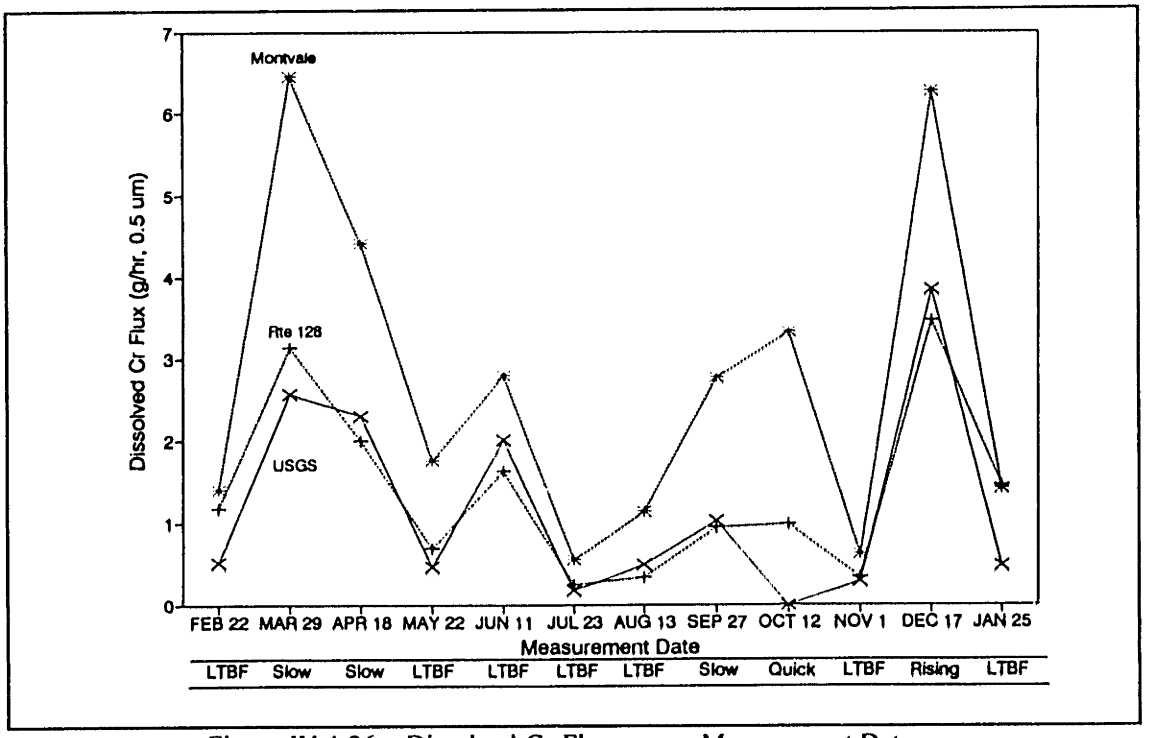

Figure IV.4-26: Dissolved Cr Flux versus Measurement Date
All Stations, February 1992 to January 1993

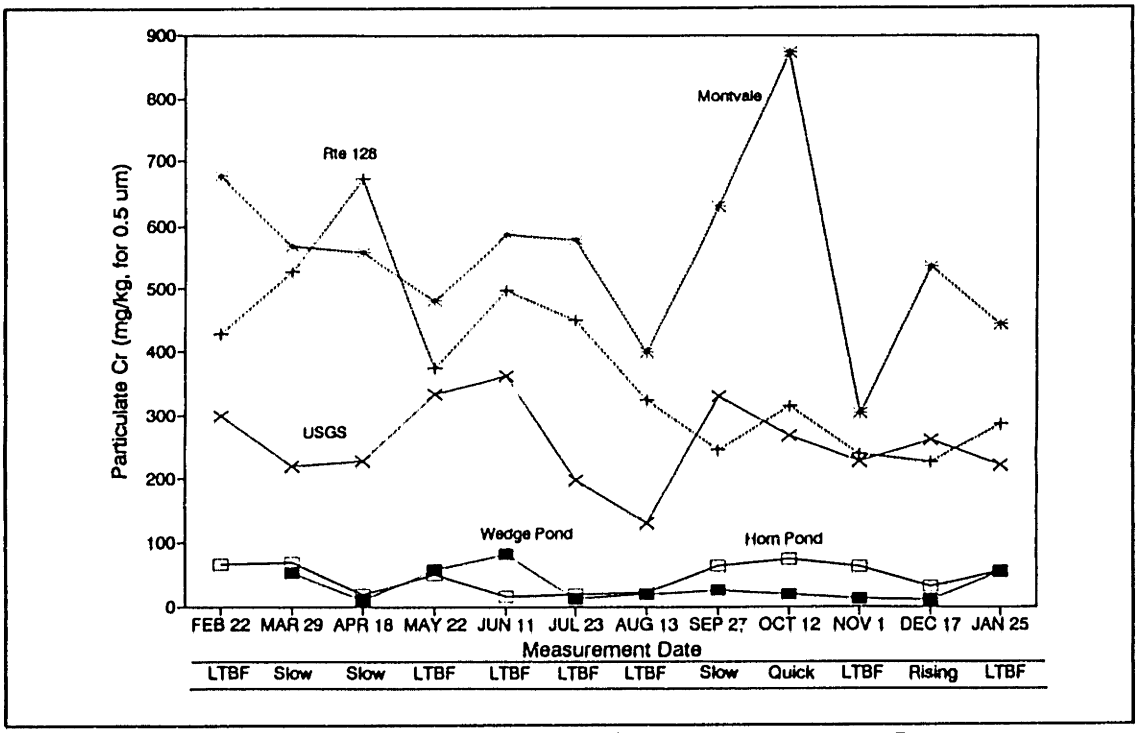

Figure IV.4-27: Particulate Cr Concentration versus Measurement Date
All Stations, February 1992 to January 1993

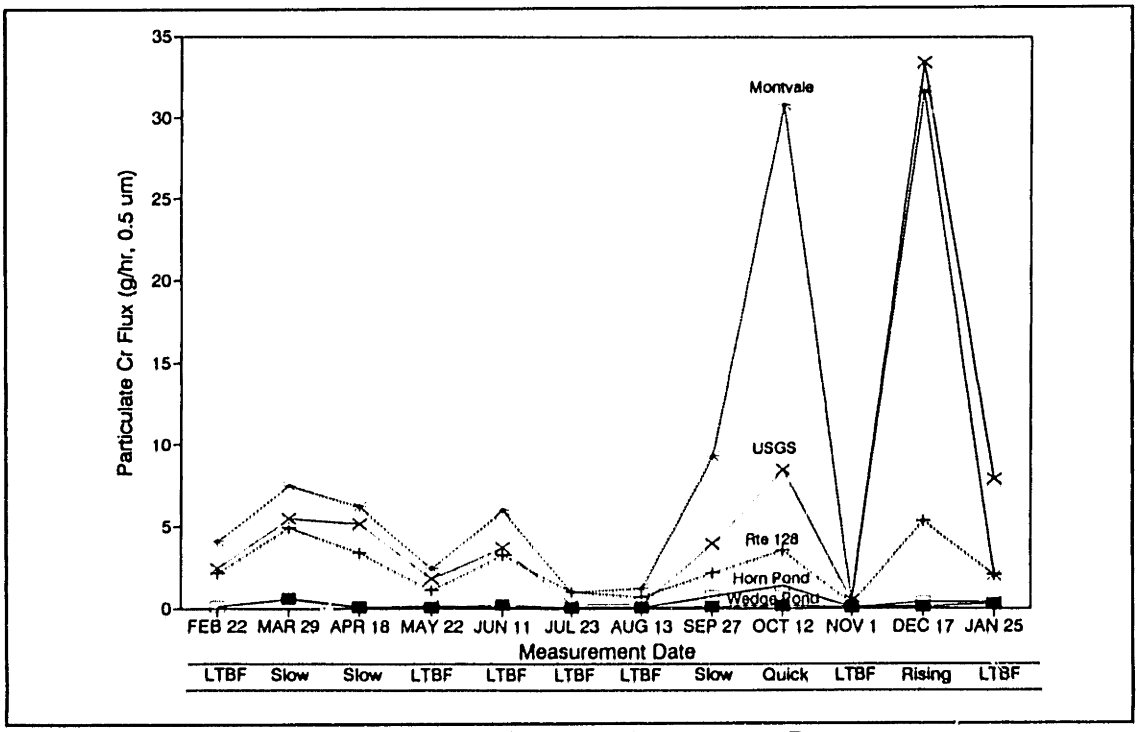

Figure IV.4-28: Particulate Cr Flux versus Measurement Date
All Stations, February 1992 to January 1993

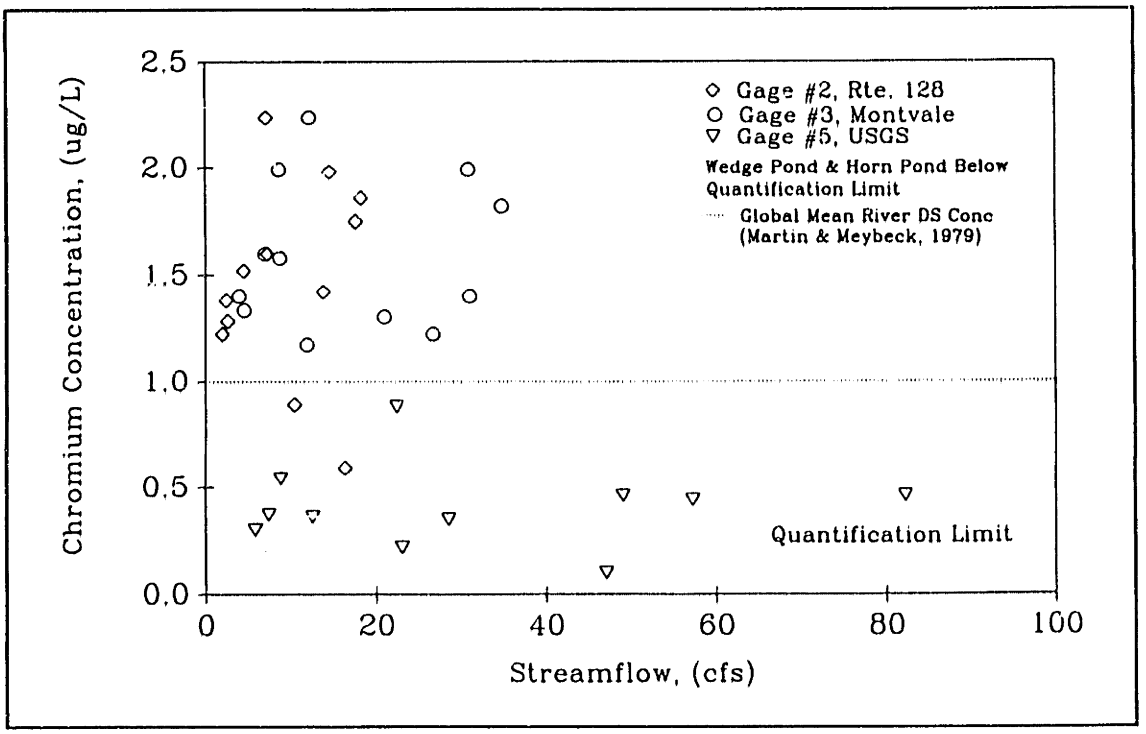

Figure IV.4-29: Dissolved Cr Concentration versus Flow
All Stations, Manual Samples, February 1992 to May 1993

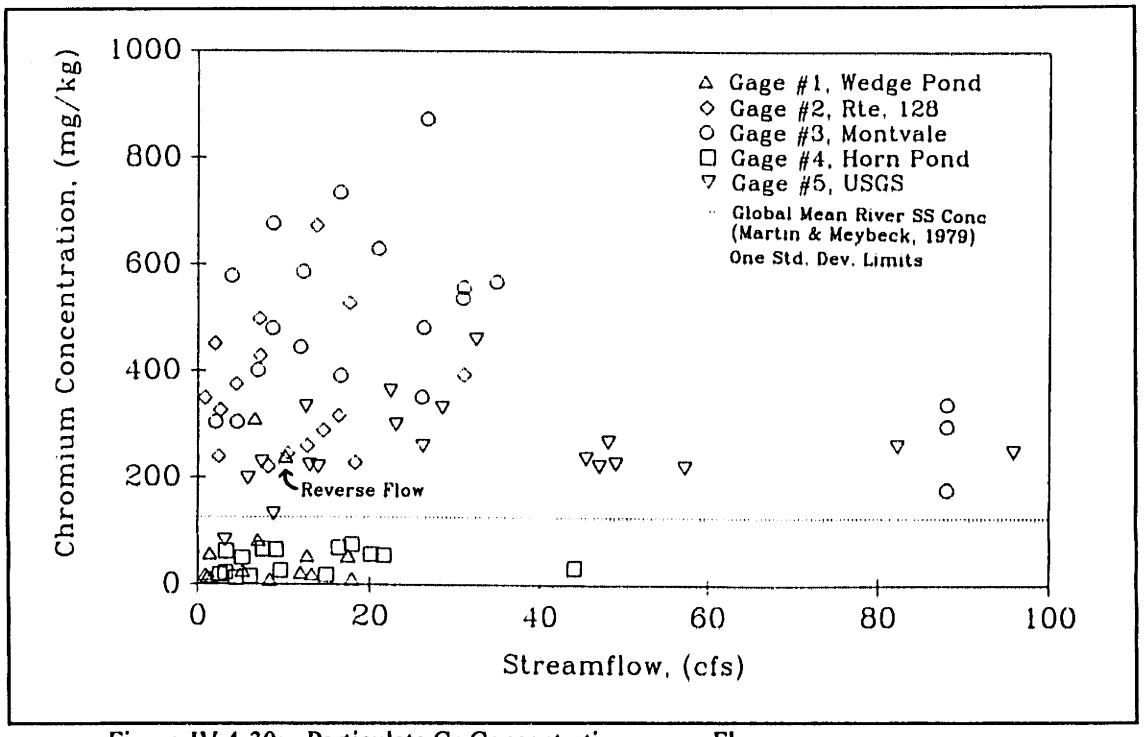

Figure IV.4-30: Particulate Cr Concentration versus Flow
All Stations, Manual Samples, August 1991 to January 1993

Partitioning of Chromium Between the Dissolved and Particulate Phases

Chromium was the metal most strongly partitioned toward the particulate phase. On average for both Route 128 and Montvale, the dissolved phase represented approximately 35% of the chromium. (figures IV.4-31 and IV.4-32) The range, however, was quite large with individual samples varying from 10% to 60% at these stations. At the USGS station, on average 30% of the chromium was in the dissolved phase. (figure IV.4-33) The range of the partitioning for this station was between 0% to 66%.

Part of the large variability in the partitioning may be associated with the mobilization of particulates during storm events. This hypothesis is supported by the October and December samples at Montvale where during rising limb conditions and quick-dominated flow, the particulate concentration increased significantly, causing the partitioning of chromium to shift strongly toward the particulate phase. For samples with dissolved concentrations near the detection limit partitioning may also be affected by errors in the chemical analysis procedure.

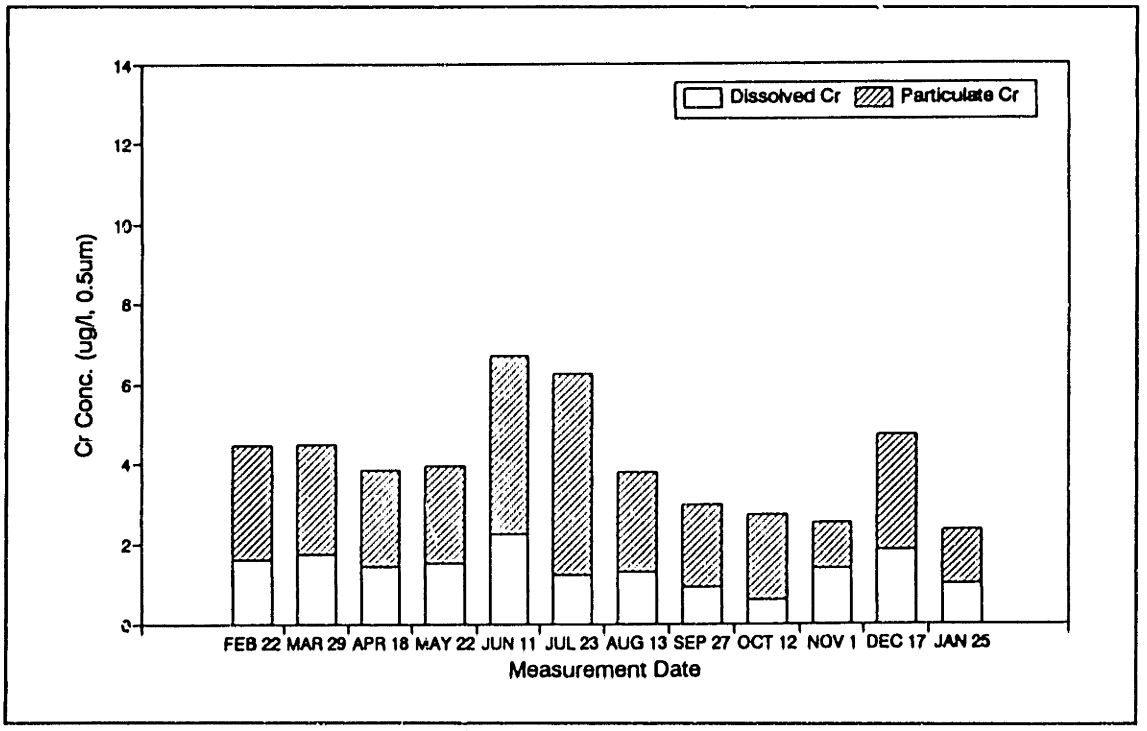

Figure IV.4-31: Cr Concentration versus Measurement Date, Gage #2, Route 128 Manual Samples, February 1992 to January 1993

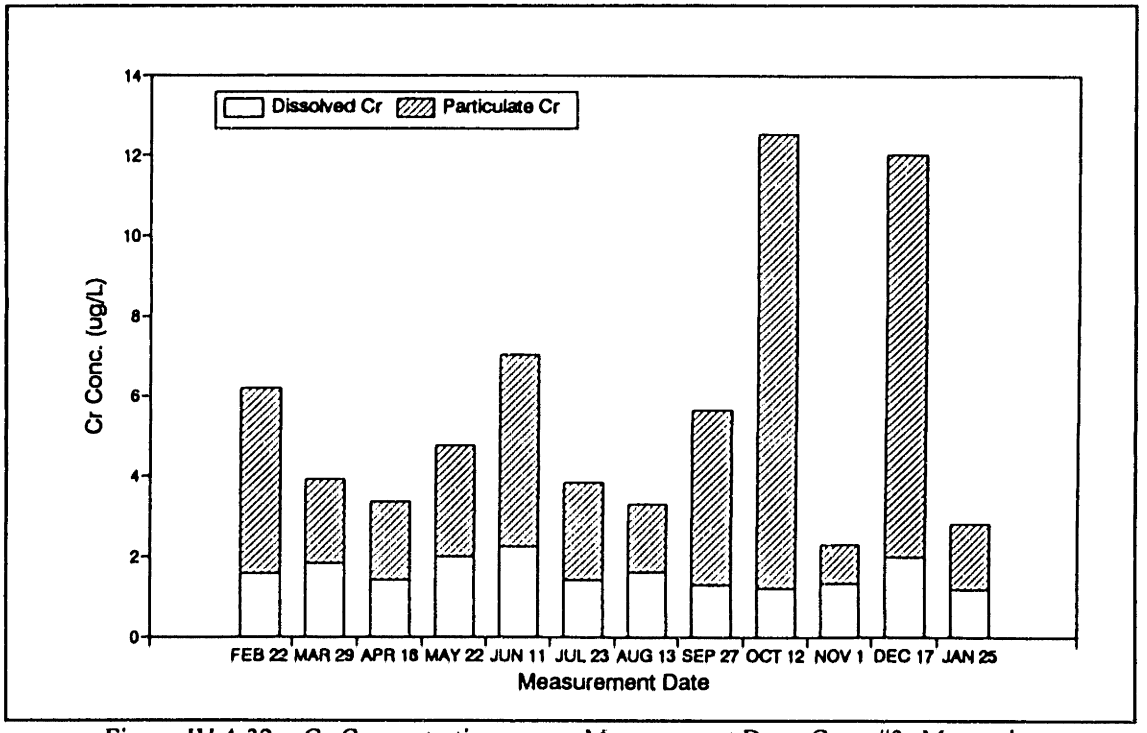

Figure IV.4-32: Cr Concentration versus Measurement Date, Gage #3, Montvale Manual Samples, February 1992 to January 1993

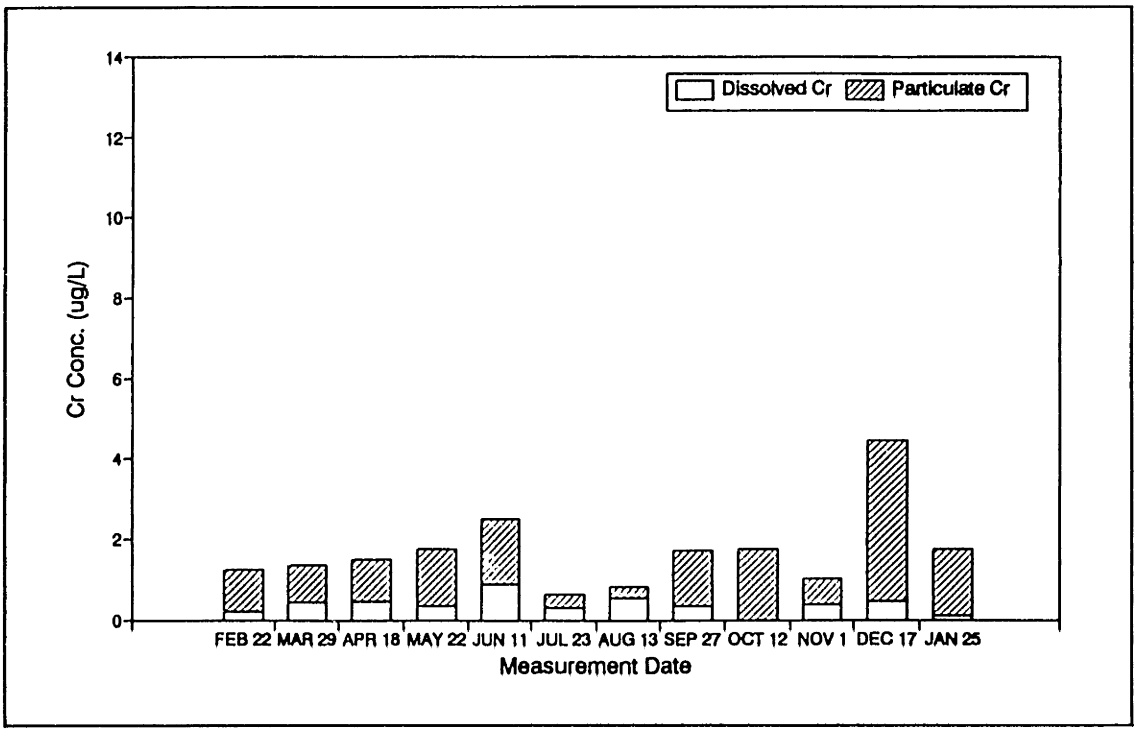

Figure IV.4-33: Cr Concentration versus Measurement Date, Gage #5, USGS Manual Samples, February 1992 to January 1993

IV.4.1.4 Copper

Contaminant Source Evaluation

Copper concentrations along the Aberjona River were generally higher than concentrations along Horn Pond Creek. The highest concentration of 24.0 µg/l was observed May 22, 1992 at Montvale. For this sample, 22.3 µg/l was associated with the dissolved phase whereas 1.7 µg/l was associated with the particulate phase. The corresponding particulate concentration on a per mass of suspended sediment basis was 300 mg/kg. Copper concentrations in the Horn Pond Creek tributary were generally less than 5 µg/l.

As with chromium, dissolved and particulate copper concentrations did not exhibit a strong dilution effect along the Aberjona. (figure IV.4-34 and IV.4-36) Except for the May 22 sample, dissolved copper concentration at Route 128 and Montvale were at similar values. The reason for the large increase in the concentration at Montvale on May 22 is unknown. Concentrations of particulate copper were either at similar values at both Montvale and Route 128 or concentrations at Route 128 were slightly higher. The concentration of both dissolved and particulate copper at the USGS was generally between the concentrations observed in the upper reaches of the Aberjona and the Horn Pond Creek tributary. The only dilution effect observed is associated with the Horn Pond Creek surface water inflows which dilute the more contaminated waters from the upstream areas of the Aberjona.

Areas draining both Route 128 and Montvale contributed significantly to the overall flux of copper along the Aberjona. (figures IV.4-35 and IV.4-37) During the rising limb and quick-flow-dominated samples, the contribution of copper from the Woburn Central and Winchester sub-basins was especially evident.

Effects of Streamflow

For each sub-basin, there was not a strong correlation between copper concentrations and streamflow (figures IV.4-38 and IV.4.39) indicating that the concentration of different components of water/sediments did not differ significantly from one another.

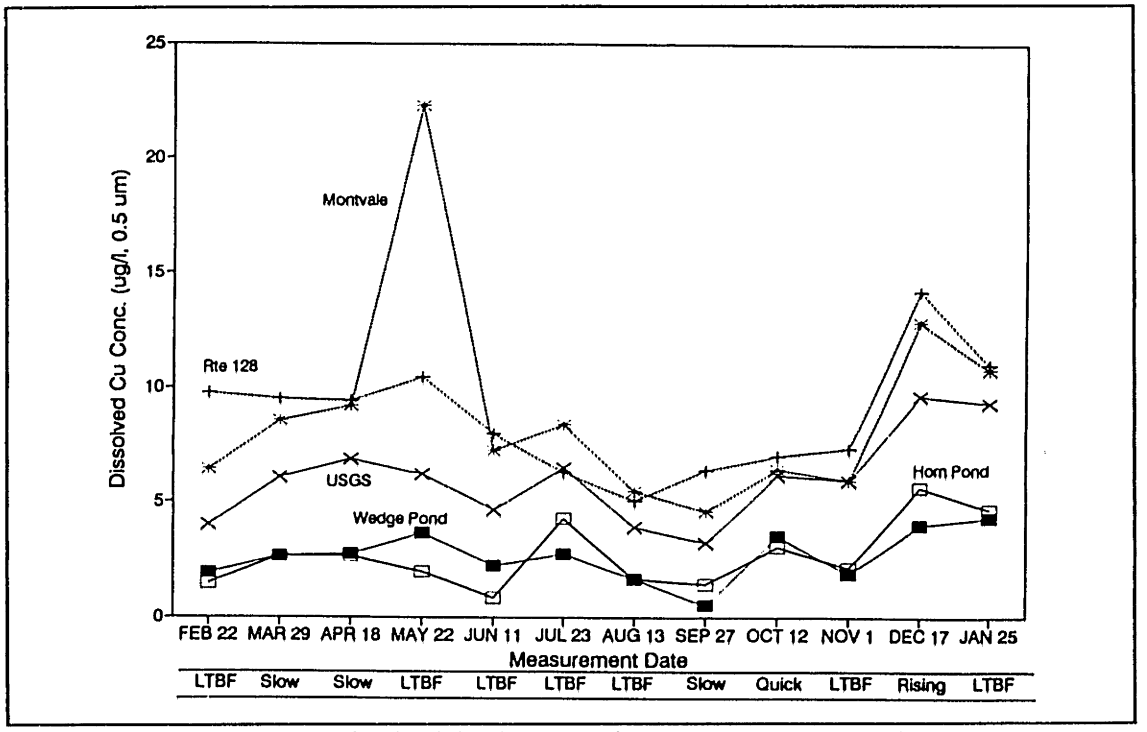

Figure IV.4-34: Dissolved Cu Concentration versus Measurement Date
All Stations, February 1992 to January 1993

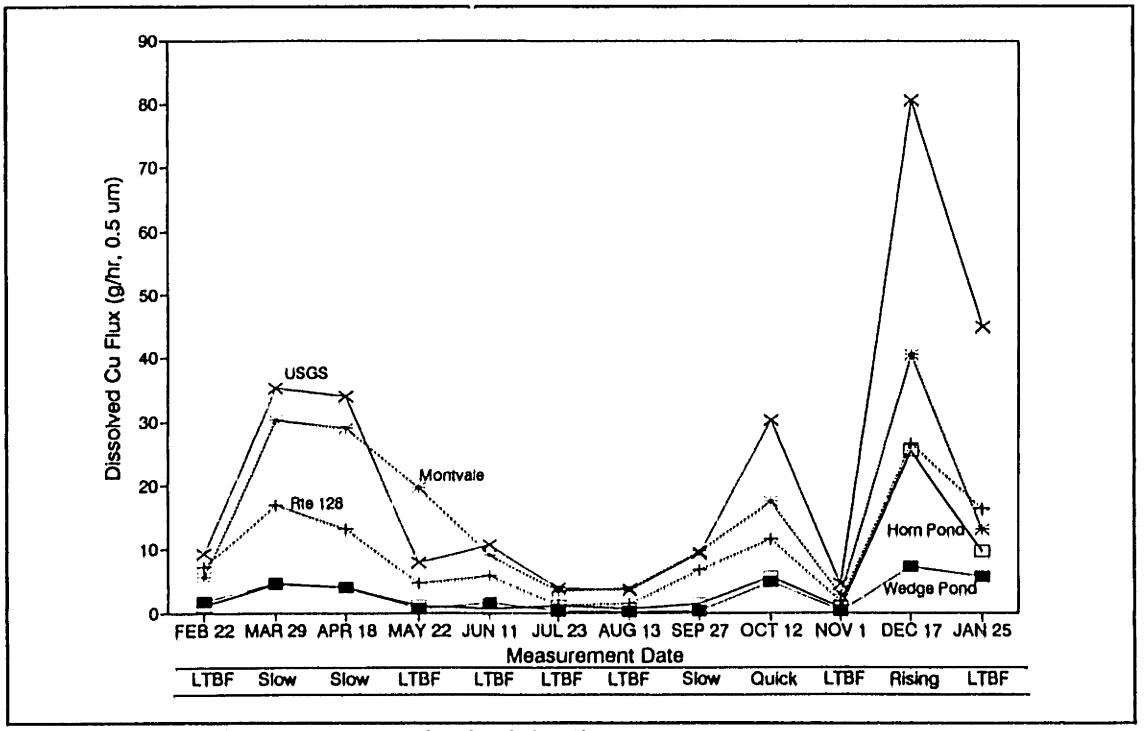

Figure IV.4-35: Dissolved Cu Flux versus Measurement Date
All Stations, February 1992 to January 1993

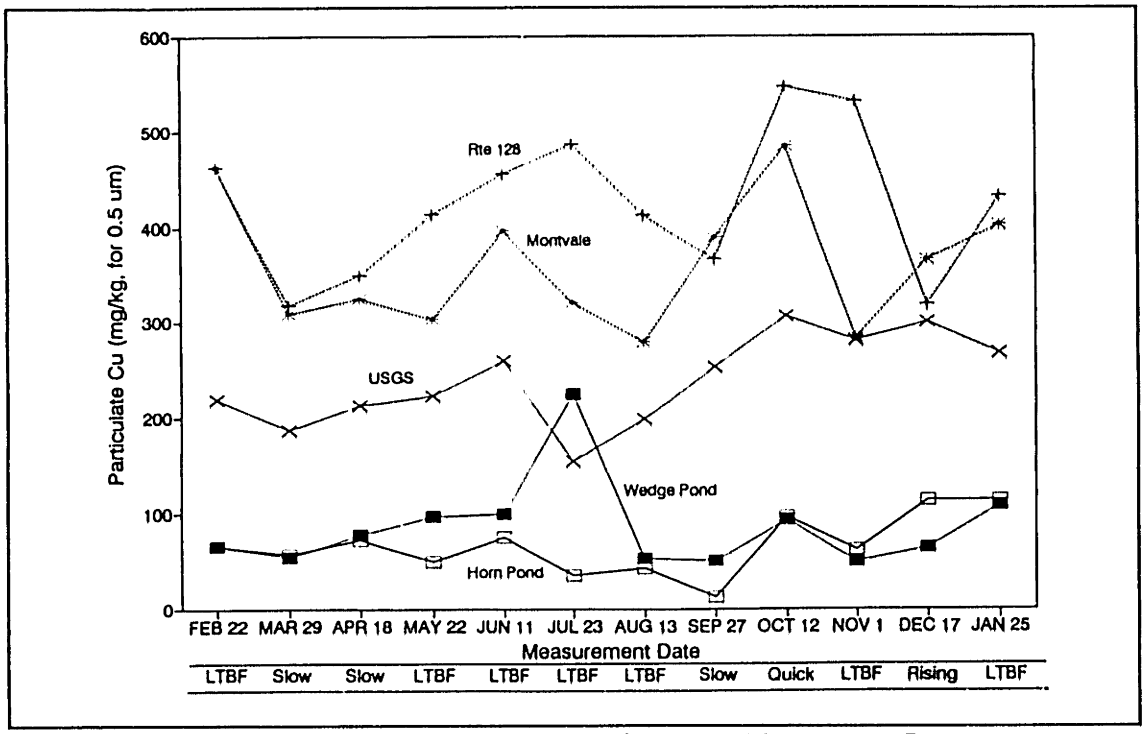

Figure IV.4-36: Particulate Cu Concentration versus Measurement Date
All Stations, February 1992 to January 1993

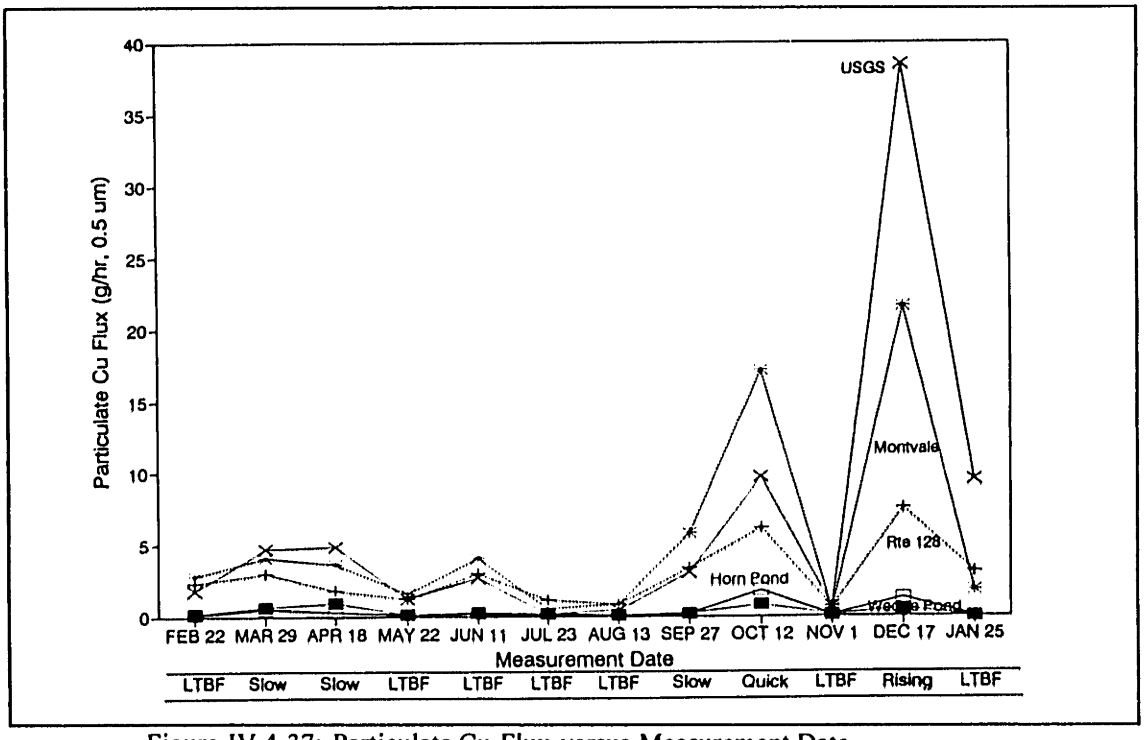

Figure IV.4-37: Particulate Cu Flux versus Measurement Date
All Stations, February 1992 to January 1993

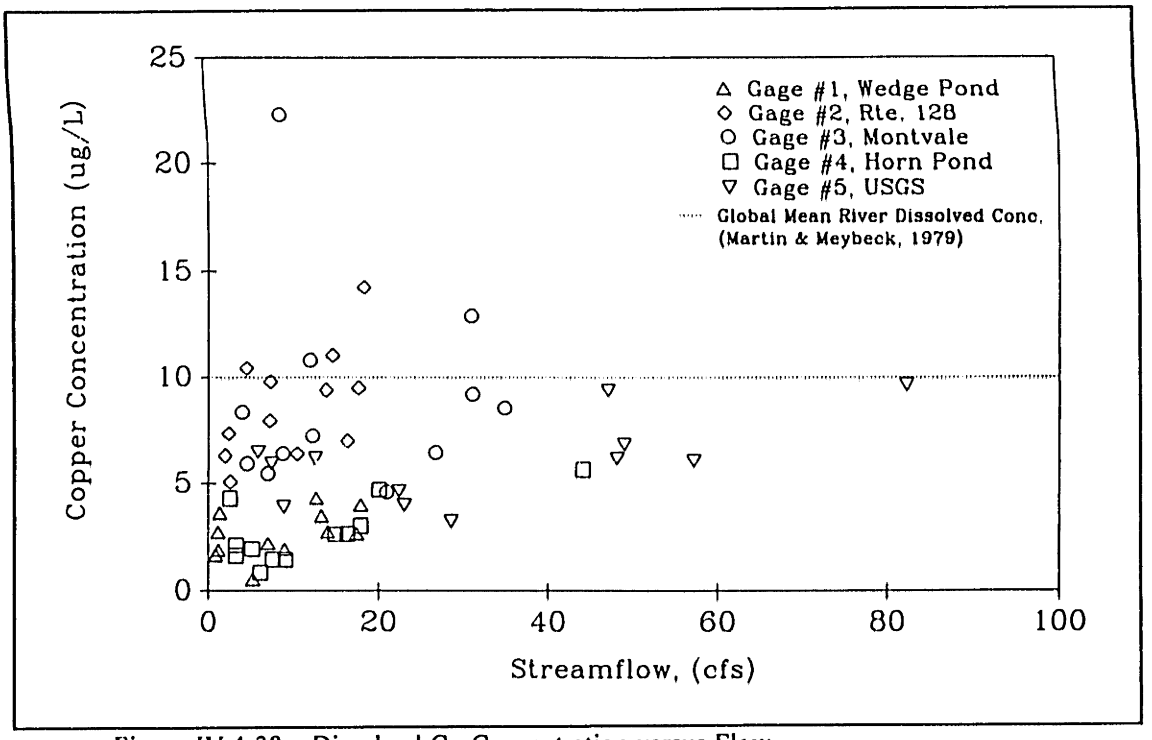

Figure IV.4-38: Dissolved Cu Concentration versus Flow
All Stations, Manual Samples, February 1992 to May 1993

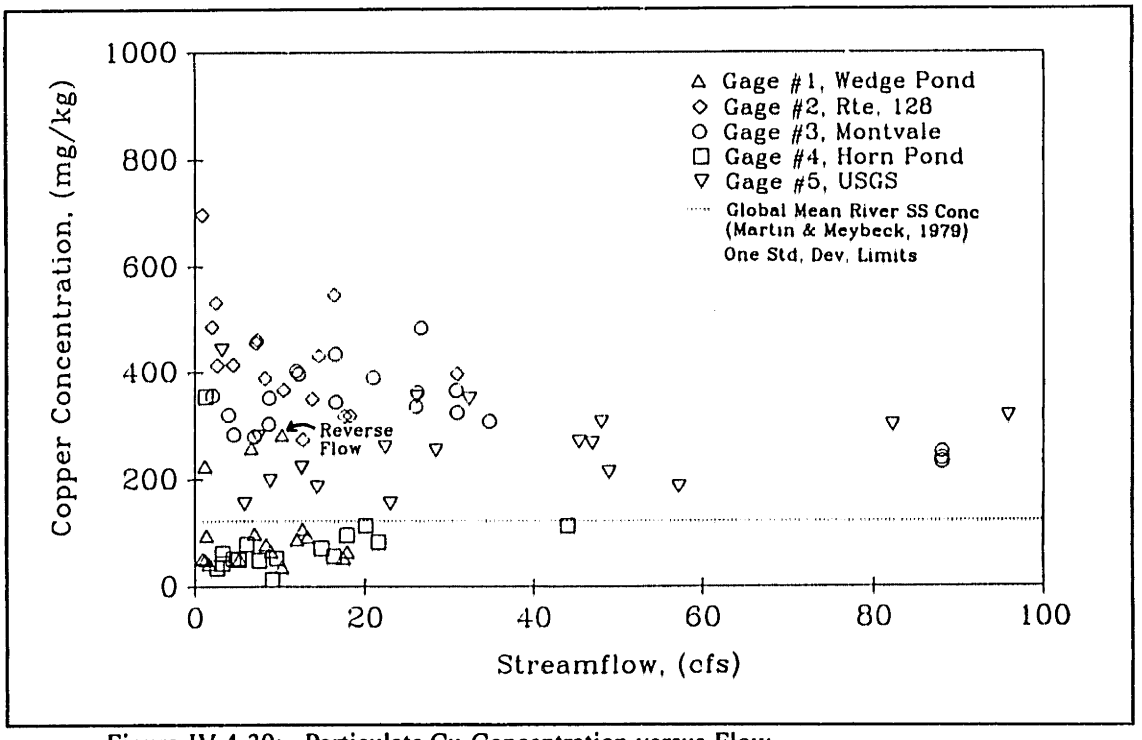

Figure IV.4-39: Particulate Cu Concentration versus Flow
All Stations, Manual Samples, August 1991 to January 1993

Partitioning of Copper Between the Dissolved and Particulate Phases

Of all the metals studied, copper was most strongly partitioned toward the dissolved phase. On average, the dissolved phase represented over 70% of the copper transport. Partitioning at Horn Pond was the strongest (figure IV.4-43), where on average the dissolved phase represented over 90% of the copper. For the other stations, on average, the dissolved phase represented between 73 to 84 % of the copper. (figures IV.4-40, IV.4-41, IV.4-42, and IV.4-44) For Montvale, the partitioning shifted more strongly toward the particulate phase for the October and December samples. This shift in the partitioning was accompanied by a significant increase in the copper transport (figure IV.4-37). This observation indicates that perhaps during rising limb and quick dominated flows, an excess particulate flux is mobilized.

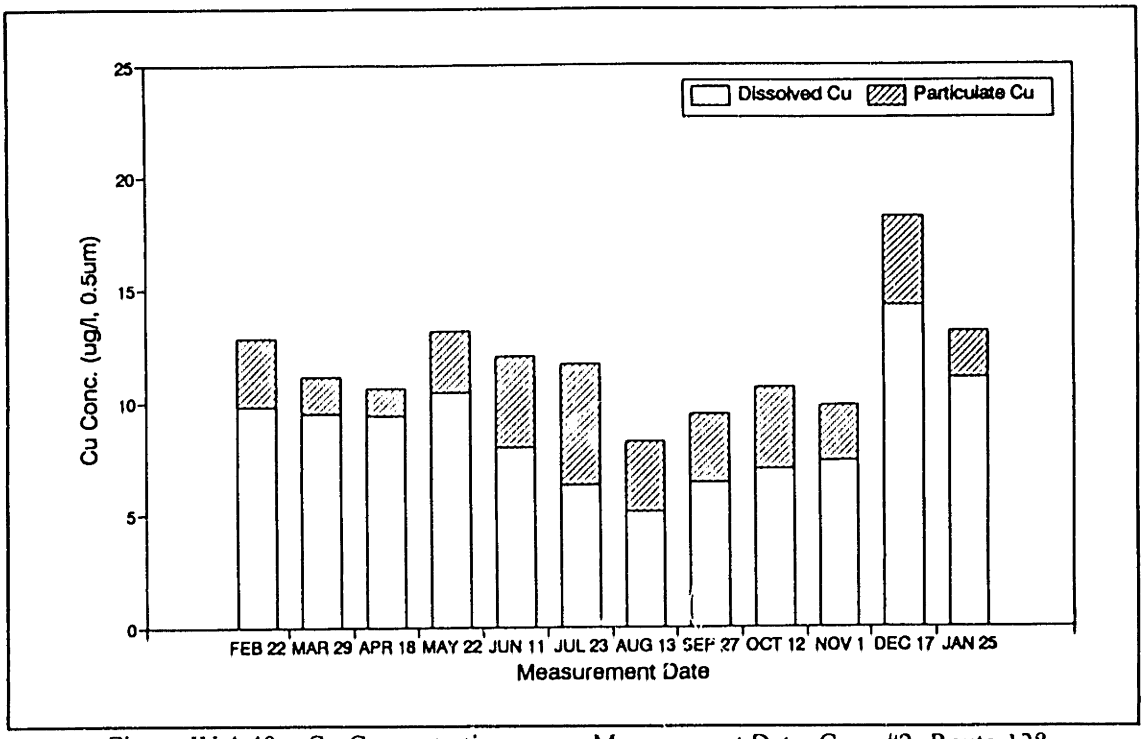

Figure IV.4-40: Cu Concentration versus Measurement Date, Gage #2, Route 128 Manual Samples, February 1992 to January 1993

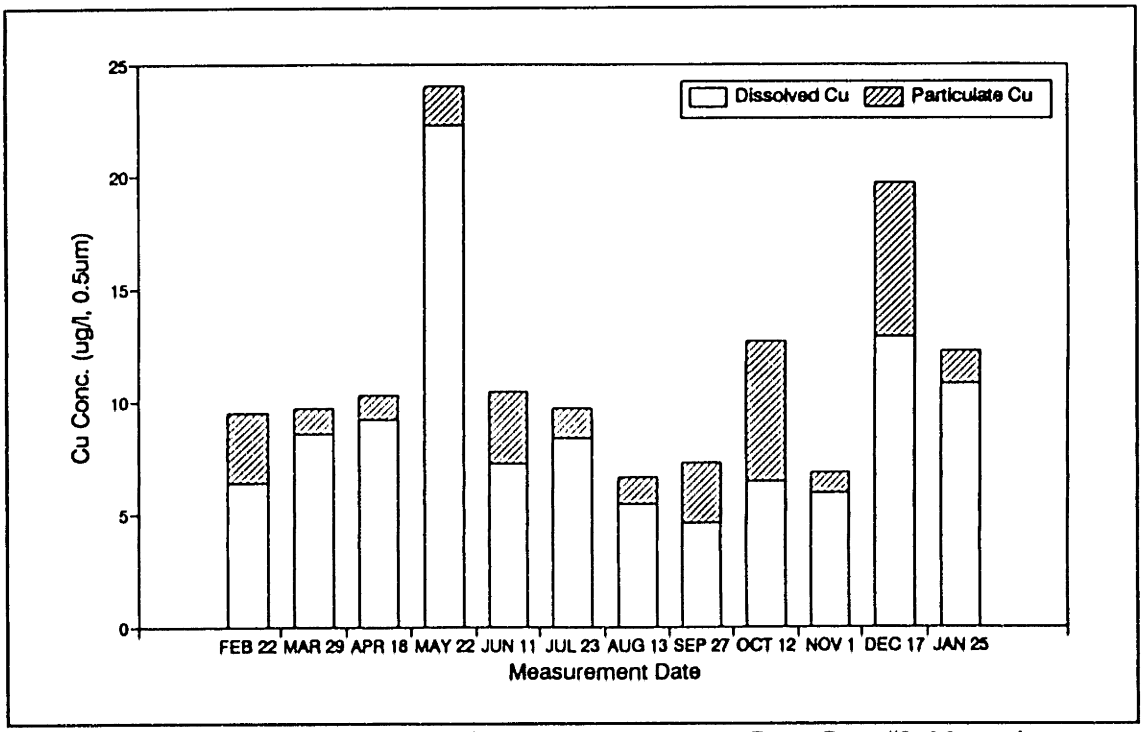

Figure IV.4-41: Cu Concentration versus Measurement Date, Gage #3, Montvale Manual Samples, February 1992 to January 1993

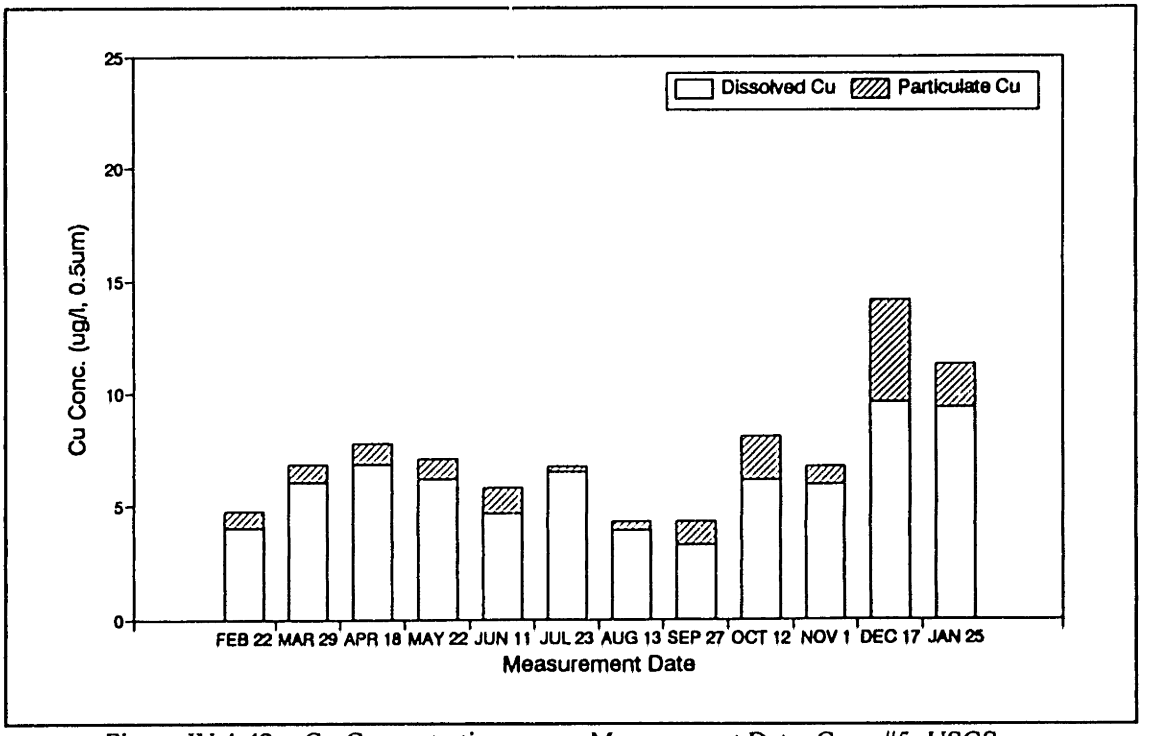

Figure IV.4-42: Cu Concentration versus Measurement Date, Gage #5, USGS Manual Samples, February 1992 to January 1993

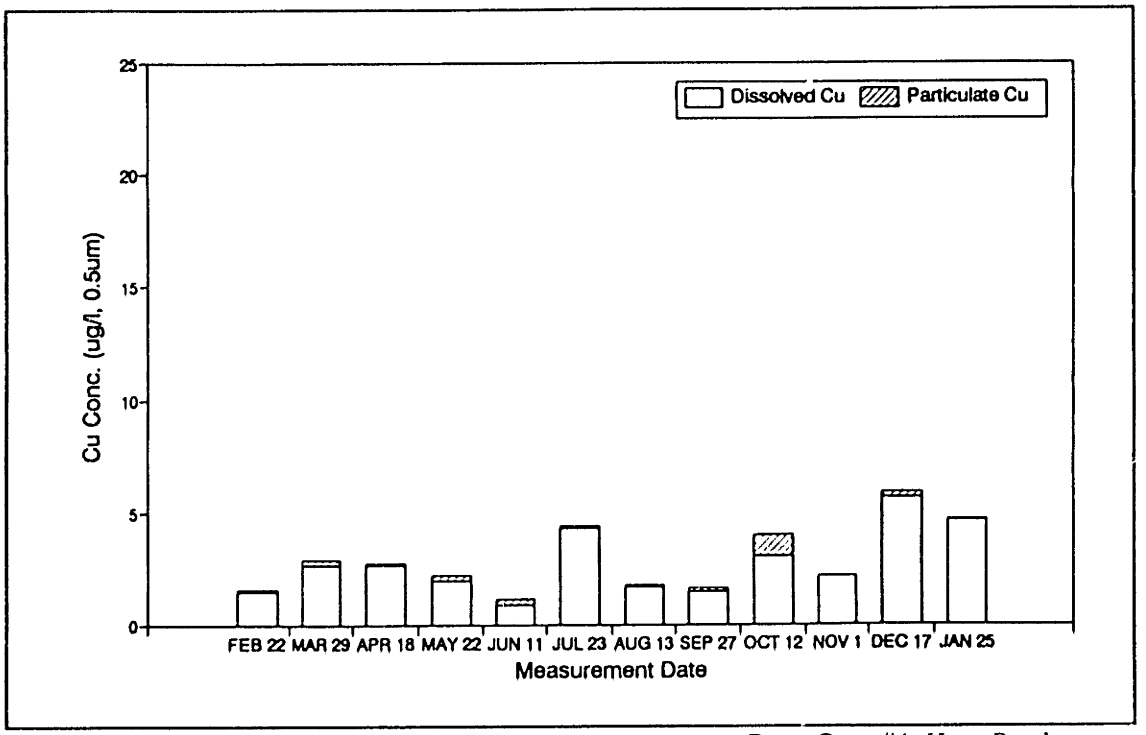

Figure IV.4-43: Cu Concentration versus Measurement Date, Gage #4, Horn Pond Manual Samples, February 1992 to January 1993

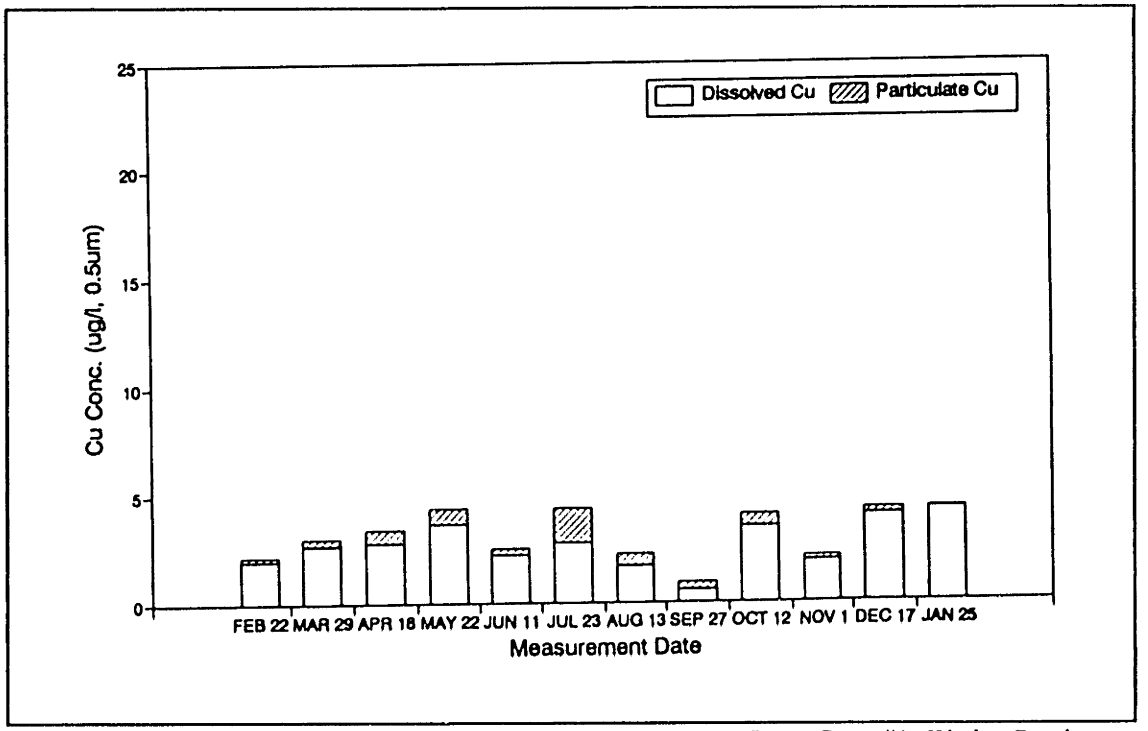

Figure IV.4-44: Cu Concentration versus Measurement Date, Gage #1, Wedge Pond Manual Samples, February 1992 to January 1993

IV.4.2 Storm Events, Gage 5

Sets of at least 18 samples were collected during three major flow events. These events included the August 18, 1992 storm, the December 11, 1992 storm, and the March/April 1993 storms. This section begins with a summary of the characteristics of metal transport as observed from each of these events. Following this summary a general discussion concerning the relations between streamflow and metals concentration is presented. The section closes with a description of metal transport associated with each flow event. For exemplification purposes, the figures corresponding to the August 18, 1992 storm are included within the main body of the thesis. Figures corresponding to the December and March/April events are included in appendix IV.E. Additionally, for reference, descriptions of streamflow and suspended sediment characteristics of each event are also included in appendix IV.E.

IV.4.2.1 Brief Summary

Concentrations of arsenic and iron (dissolved: per river water volume basis, and particulate: per suspended sediment mass basis) were lower during storm events than during low flow conditions, supporting the notion of a dilution effect during storm conditions. Chromium and copper concentrations, on average, were either similar or slightly higher than concentrations observed during low flow conditions. Such an observation indicates that for chromium and copper strong concentration differences did not exist between each component of flow and each component of suspended sediment.

Metal fluxes were strongly influenced by the size of the streamflow event. In general, the larger the event the larger the dissolved and particulate metal fluxes observed. The increase observed for the particulate phase was always higher than the increase observed for the dissolved phase. The result of this disproportionate increase was a strong shift in the partitioning of the metals toward the particulate phase during storm conditions.

For all storms, metal fluxes increased more for chromium and copper than for arsenic and iron. This trend was due to the stronger dilution effect associated with arsenic and iron, which diminished the amount of the increase.

IV.4.2.2 Effects of Streamflow

Particulate arsenic and iron concentrations had a strong tendency to decrease with increasing streamflow, (figures IV.4-46 and IV.4-48) The most dramatic change occurred in the flow range of 5 cfs to 50 cfs, during which arsenic concentrations decreased from 700 mg/kg to 150 mg/kg and iron concentrations decreased from 15% to 5%.

A mixing of different sediment components may explain some of the variability. Assuming that suspended sediments are the sum of quick, slow, and longterm baseflow sediments, then from mass balance considerations:

$$[M_p]_{river}[SS]_{river}Q_{river} = [M_p]_{quick}[SS]_{quick}Q_{quick} + [M_p]_{slow}[SS]_{slow}Q_{slow} + [M_p]_{ltbf}[SS]_{ltbf}Q_{ltbf}$$

where: $[M_p]$ = Particulate Metal Concentration, subscripts quick, slow, ltbf, and river imply concentrations in quick, slow, longterm baseflow, and river waters, respectively

Q = Streamflow

If it is further assumed that: 1) flow conditions are such that the quick sediment contribution is negligible (i.e. during non-storm conditions) and 2) slow and longterm baseflow waters have equal suspended sediment concentrations, then:

$$[M_p]_{river} = \frac{[M_p]_{slow}Q_{slow} + [M_p]_{ltbf}Q_{ltbf}}{Q_{river}}$$

The characteristics of streamflow are such that streamflow is generally dominated by longterm baseflow, Q_{ltbf}, during very low flows (e.g. 5 cfs) and dominated by slow storm water, Q_{slow}, at intermediate flows (e.g. 50 cfs). Noting the expression above, then at extremely low flows the value of $[M_p]_{river}$ would approach the value of $[M_p]_{ltbf}$ and at intermediate flows the value of $[M_p]_{river}$ would approach the value of $[M_p]_{slow}$. Therefore, if $[M_p]_{ltbf}$ is assumed to have a value of 700 mg/kg and if $[M_p]_{slow}$ is assumed to have a value of 150 mg/kg, then as streamflow varies from extremely low flows to intermediate flows, the concentration of particulate arsenic in the river, $[As_p]_{river}$, would be expected to gradualy decrease from 700 mg/kg to 150 mg/kg as illustrated in figure IV.4-46.

The example described above, however, greatly simplifies the behavior in the field. In actuality, at a given streamflow, 1) suspended sediment concentrations from each sediment source are variable and not necessarily equal to one another, 2) the relative proportions of each of the flow components (i.e. Q_{slow} to Q_{ltbf} ratio) are not constant, 3) the quick component of flow could also be a significant source of sediments, and 4) the relative contribution of flow and sediments from each sub-basin may vary. Given this situation, a metal transport model should be developed which quantifies different streamflow and sediment components from each sub-basin such that the metal contribution from each component can be better estimated.

The variation of dissolved arsenic and iron was not as systematic as the variation of the particulate phases. (figures IV.4-45 and IV.4-47) The trends observed are that: 1) the dissolved phase exhibited a larger variability during lower flows than during higher flows, and 2) the minimum dissolved concentrations observed during lower flows were in the same vicinity as the concentrations observed during higher flows. These trends may have been due to: 1) mixing of different components in a non-systematic fashion at lower flows, 2) more variable dissolved concentrations for components that dominate at lower flows, or 3) storm based variabilities since, samples obtained at lower flows were obtained after many different events, and samples obtained at higher flows were associated with only one of three independent events.

Chromium and copper concentrations (in either the dissolved or particulate phases), on the other hand, showed no apparent trend with changes in flow. (figures IV.4-49, IV.4-50, IV.4-51, and IV.4-52) The interpretation of this observation is that: 1) concentrations of each of the flow components were more variable, and 2) no strong concentration difference existed between quick, slow, and longterm baseflow waters.

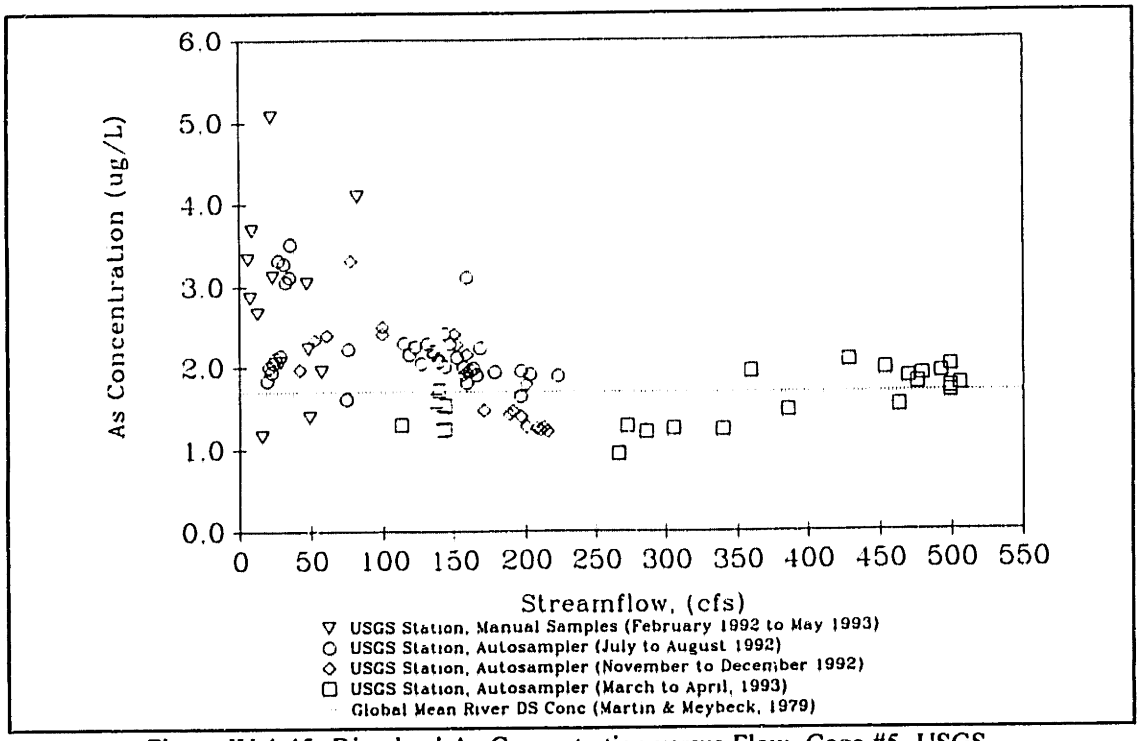

Figure IV.4-45: Dissolved As Concentration versus Flow, Gage #5, USGS February 1992 to April 1993

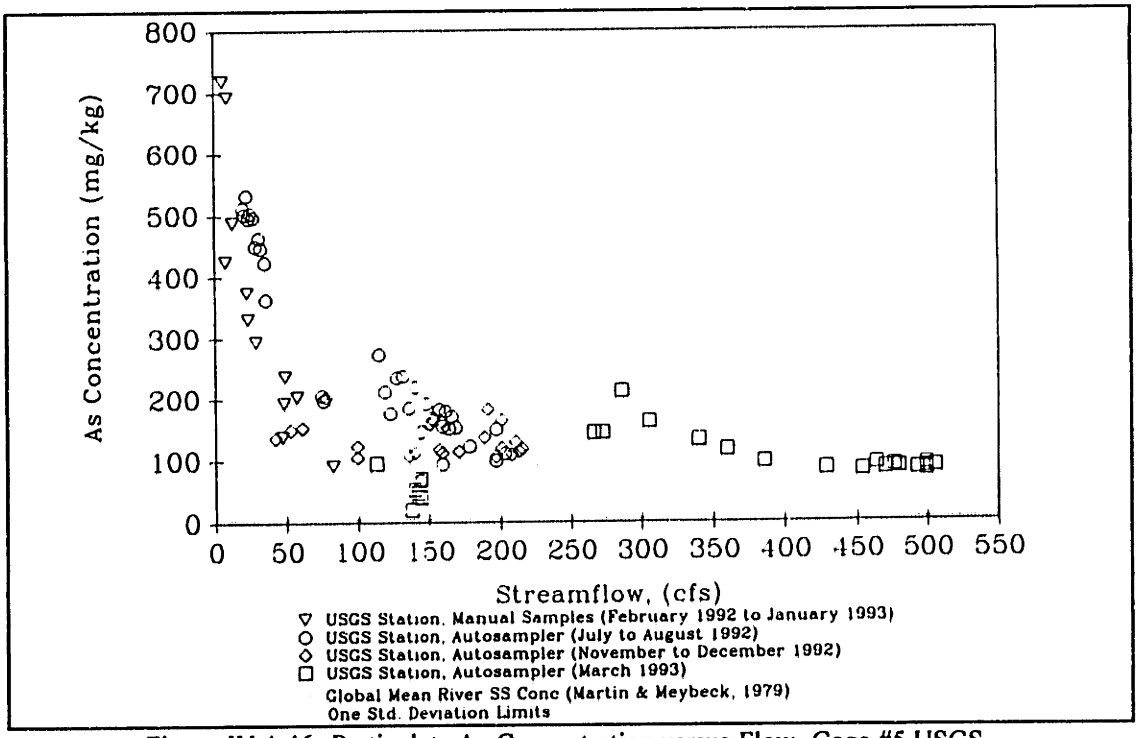

Figure IV.4-46: Particulate As Concentration versus Flow, Gage #5,USGS February 1992 to March 1993

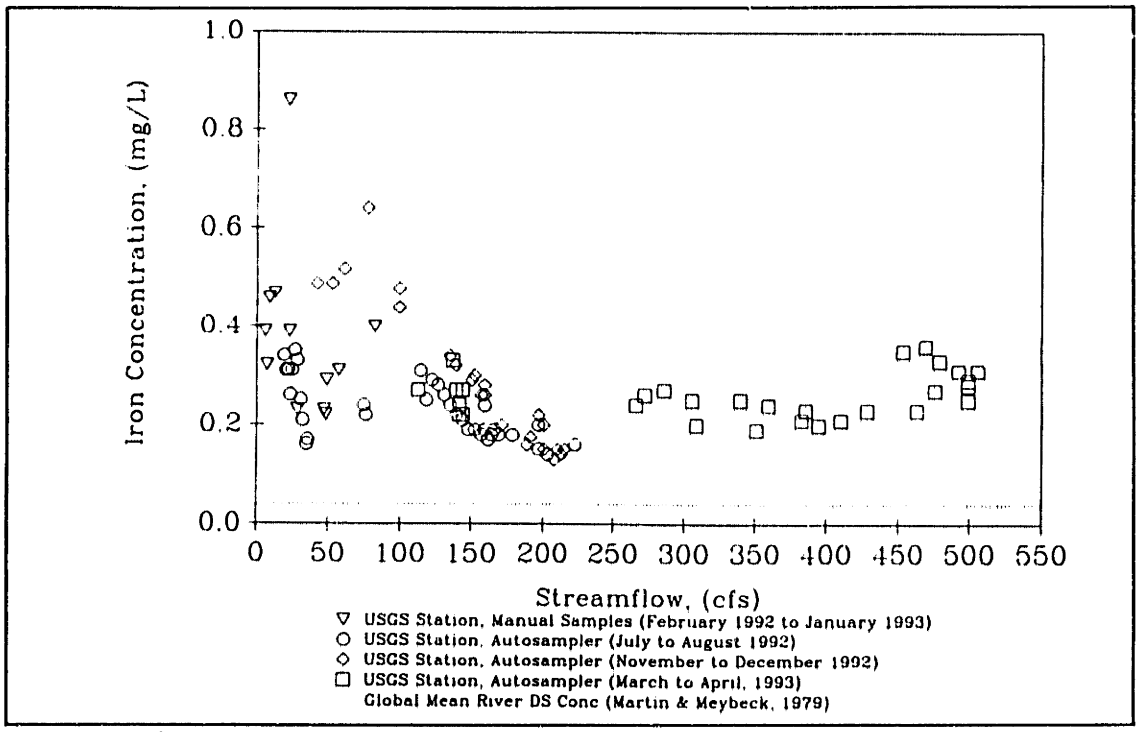

Figure IV.4-47: Dissolved Fe Concentration versus Flow, Gage #5, USGS February 1992 to April 1993

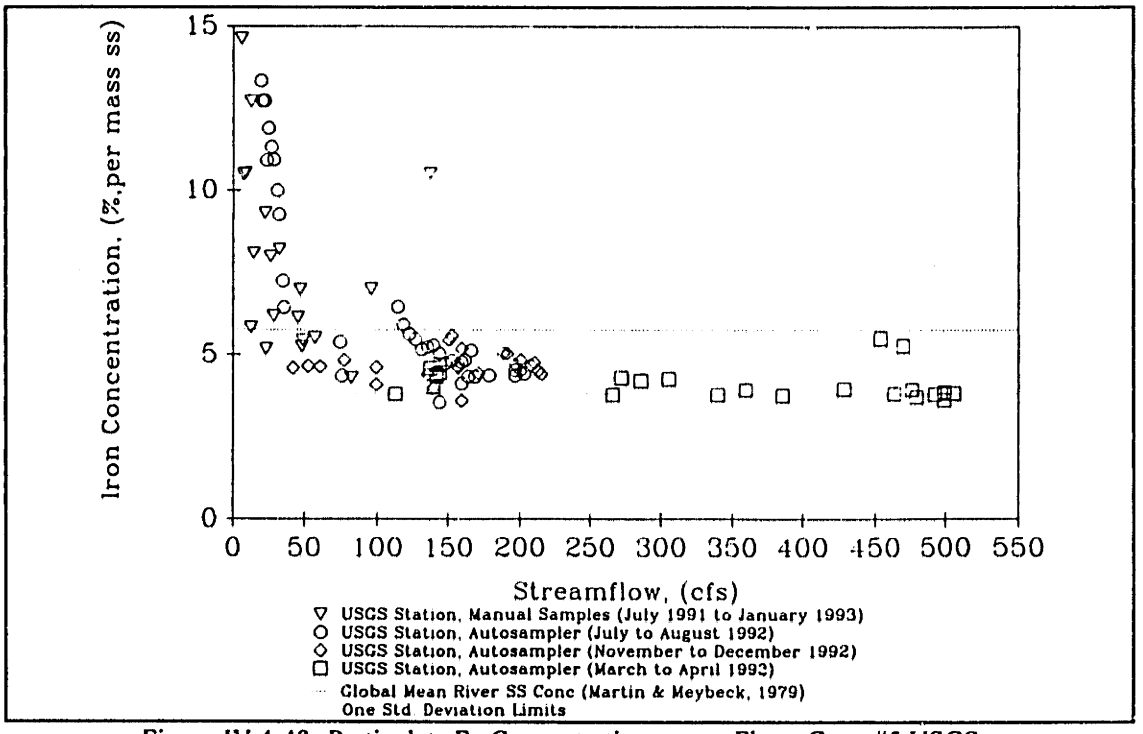

Figure IV.4-48: Particulate Fe Concentration versus Flow, Gage #5,USGS August 1991 to March 1993

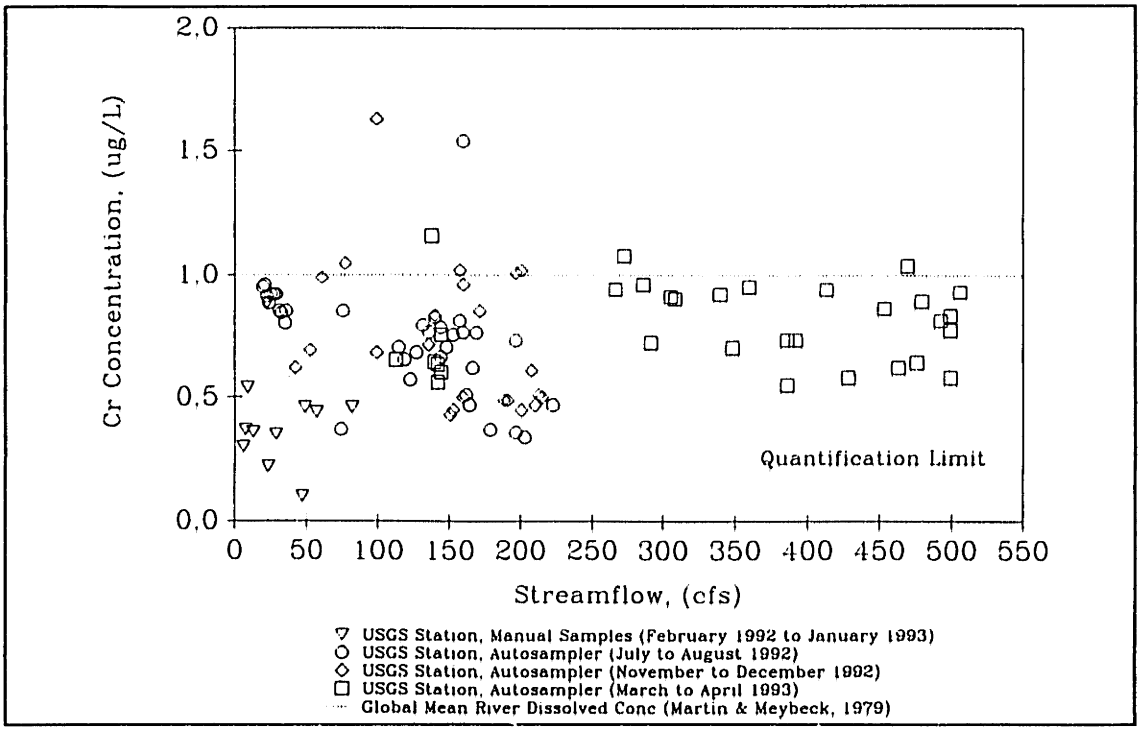

Figure IV.4-49: Dissolved Cr Concentration versus Flow, Gage #5, USGS February 1992 to April 1993

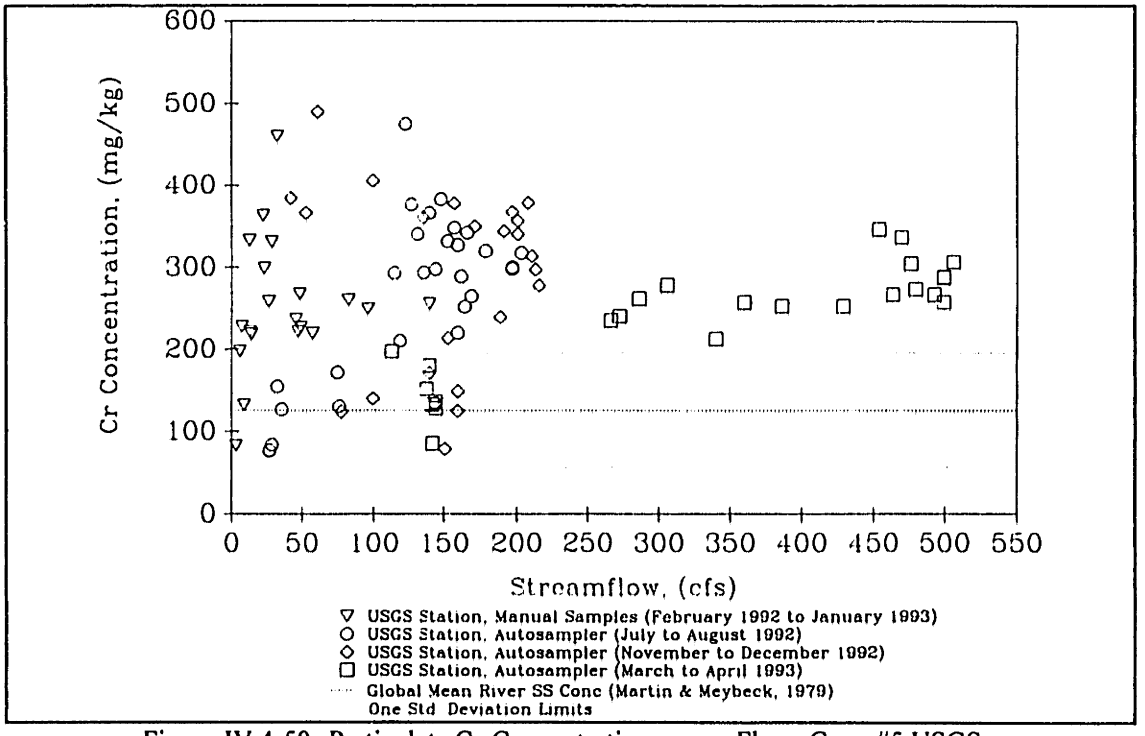

Figure IV.4-50: Particulate Cr Concentration versus Flow, Gage #5,USGS February 1992 to March 1993

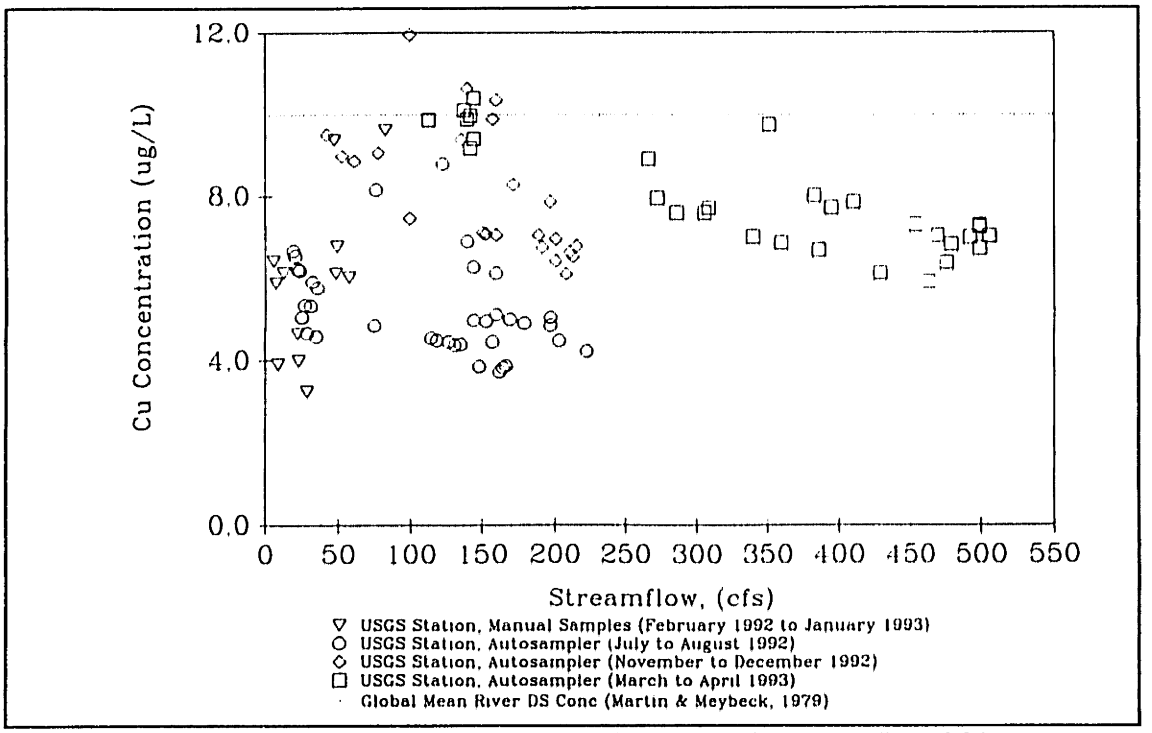

Figure IV.4-51: Dissolved Cu Concentration versus Flow, Gage #5, USGS February 1992 to April 1993

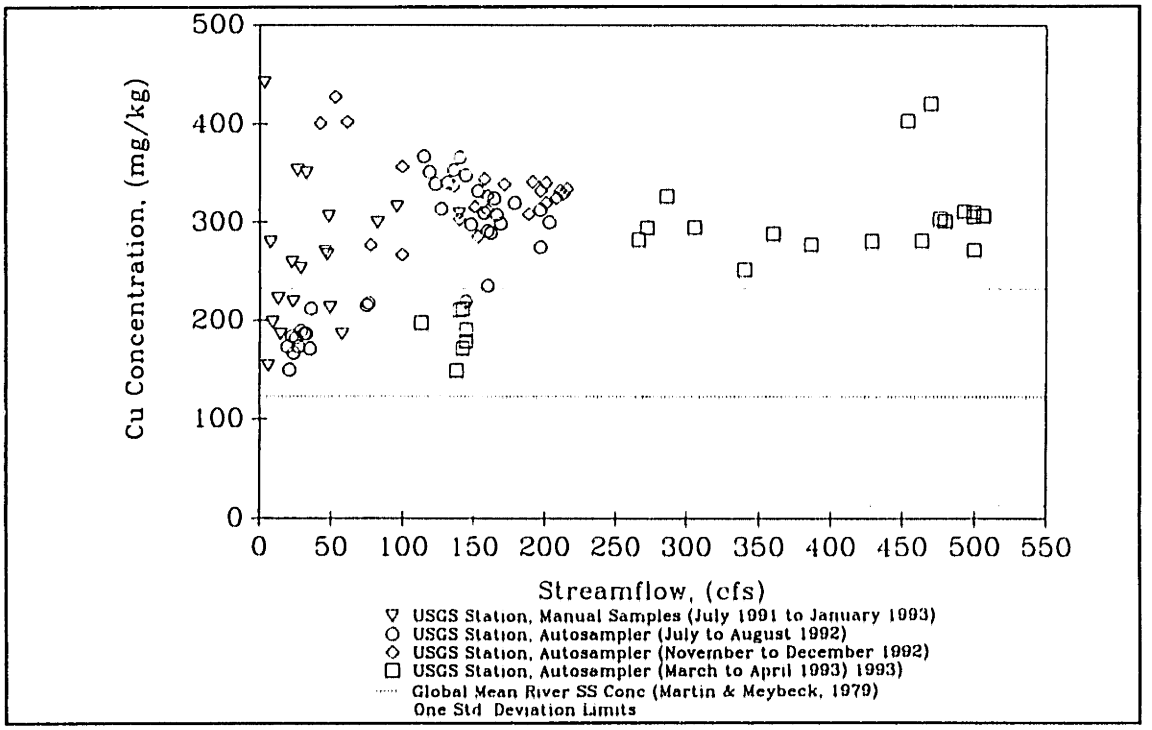

Figure IV.4-52: Particulate Cu Concentration versus Flow, Gage #5,USGS July 1991 to March 1993

IV.4.2.3 Dissolved Metals: Fluxes and Concentrations

Fluxes

Dissolved metal fluxes were higher during storm events than during low flow conditions. (figures IV.4-55, IV.4-57, IV.4-59, and IV.4-61, also see appendix IV.E) The larger the storm event, the larger the flux. The March 29 event, which had the largest peak flow (502 cfs), had hourly metal fluxes which were at least an order of magnitude higher than those observed during low flows. Typical dissolved metal fluxes for this event were 75, 12000, 35, and 300 g/hr for arsenic, iron, chromium, and copper, respectively. For the smaller flow events, August (peak flow = 223 cfs) and December (peak flow = 215 cfs) storms, the metal fluxes were similar to one another but lower than observed for the March 29th storm. For the August and December events, fluxes were elevated above typical low flow values: 1) by a factor of 3 to 4 for dissolved arsenic and iron, and 2) by a factor of 4 to 6 for dissolved chromium and copper. The similarities in the fluxes observed during each event were due to the similarity in the magnitude of streamflows. Apparently seasonal factors did not strongly affect the flux of metals, since the two storms occurred during a different season but still responded with similar dissolved metal fluxes. The March 26 event, which had the smallest streamflows (peak flow = 144 cfs), was characterized by fluxes slightly smaller than observed for the August and December events.

Furthermore, dissolved fluxes increased more for chromium and copper than for arsenic and iron. For all events, fluxes increased above typical low flow values by a factor of: 1) 4 to 20 for chromium and copper, and 2) 2 to 10 for arsenic and iron. Such a result is due to: 1) the more efficient mobilization of dissolved chromium and copper, and 2) a dilution of dissolved arsenic and iron during storm conditions.

Within a given storm event, changes in the dissolved metal flux ($[M_d]Q$) were strongly affected by: 1) changes in streamflow, Q, in the vicinity of the streamflow peak, and 2) by changes in concentration, $[M_d]$, for times after the peak. (figures IV.4-54 to IV.4-61) This behavior was due to the large variation of streamflow in the vicinity of the peak while metal concentrations, on the other hand, were not quite as variable. However, metal concentration changes did affect the dissolved metal flux, once the streamflow was no longer changing significantly.

For example, iron concentrations exhibited a dilution effect during the peak streamflow. (Between 2:00 and 8:00 in figure IV.4-56) However, during the streamflow peak, the volumetric flow rate of water increased much more than the concentration decreased. The result was for a net increase in the dissolved flux at 4:00 and 5:00. (figure IV.4-57). Flows became more constant after the peak streamflow (after 8:00). At this time, fluctuations in the flux were more strongly affected by

fluctuations in the dissolved metals concentrations. For example, the peak dissolved flux at 13:00 was due to the peak in the concentration.

Concentrations

Dissolved arsenic and dissolved iron concentrations were generally lower during storm events than during low flow conditions. This observation supports the notion of a dilution effect in which cleaner waters entering the river during stormflows, dilute more concentrated waters which predominate during low flow conditions. Assuming that flow can be separated into components of quick, slow, and longterm baseflow, the dilution effect can then be explained by recognizing that each of the components can be present in different proportions throughout a storm. For example, assume that: 1) longterm baseflow dominated during low flows, 2) quick and slow storm waters dominated during storm flows, and 3) longterm baseflows had higher dissolved metals concentrations than quick and slow waters. Then a decrease in concentration during a storm event could have been due to the predominance of quick and slow storm waters which were relatively cleaner. After the storm, concentrations should gradually increase to values typical of longterm baseflow waters due to the increasing predominance of the longterm baseflow component.

Within a storm event, the dilution effect was also exhibited by arsenic and iron. For example, during the August storm a dip in the concentrations was observed in the vicinity of the peak streamflow. (figure IV.4-54 and IV.4-56) The dip in concentration can be explained in a similar fashion as described above if one considers that during the storm: 1) quick flow dominated in the vicinity of the peak, 2) slow flows dominated after the peak, and 3) slow flows had higher dissolved metal concentrations than quick flows. As a result, lower dissolved metals concentrations in the vicinity of the peak would be expected because of the predominance of quick flow. After the peak, a gradual increase in concentrations up to values which are characteristic of slow storm waters would be expected.

Near peak flows, dissolved chromium and dissolved copper, on the other hand, were either at similar values or slightly higher than concentrations observed during low flow conditions. Such an observation indicates that waters associated with storm events (quick and slow storm waters) tend to be of similar or slightly higher concentrations than longterm baseflow waters for these metals. Within each event, however, chromium and copper exhibited a dilution effect, in which concentrations before and after the peak were generally higher than during the peak streamflow. This effect may be associated with the mixing of quick and slow storm waters, where quick waters which dominated at the peak flow were cleaner and slow waters which dominate before and after the peak were more contaminated.

An interesting fluctuation in the August storm is observed at 13:00, (figure IV.4-53) At this time, all dissolved metals exhibited a peak, which is an indication that a more contaminated water predominated the flow at this time. Speculatively, it may have been associated with flows from the upstream reaches of the Aberjona River.

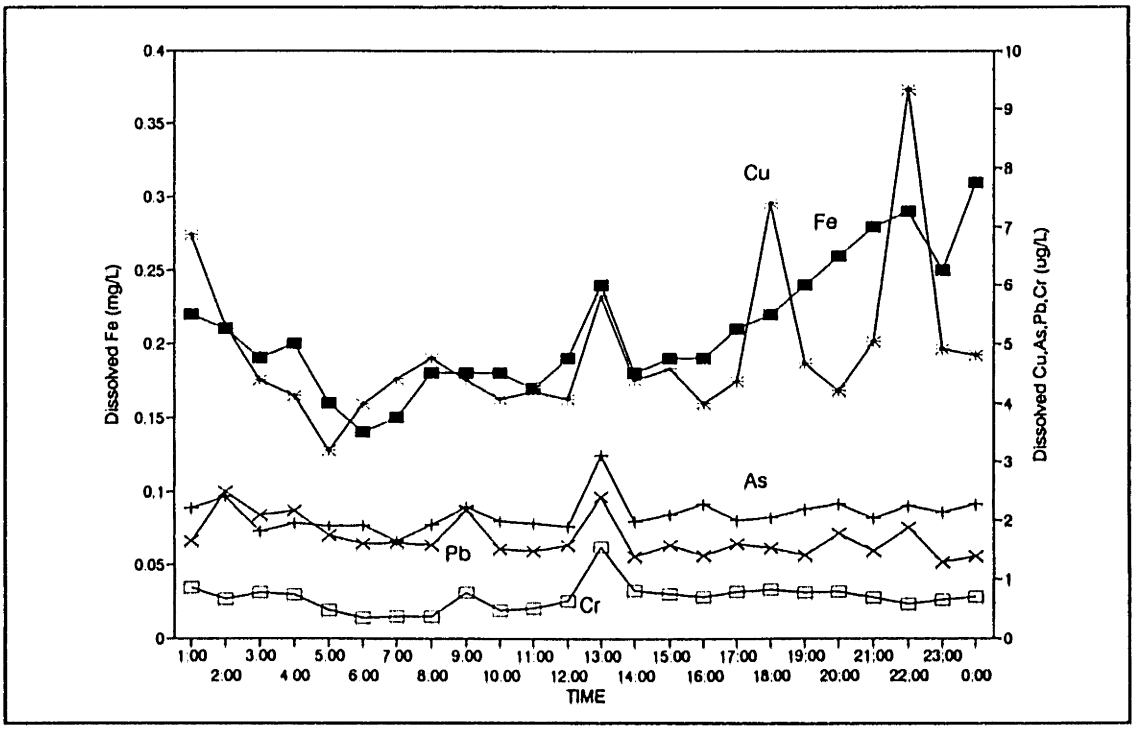

Figure IV.4-53: Dissolved Metal Concentration versus Time, Gage #5,USGS
August 18, 1992 Storm

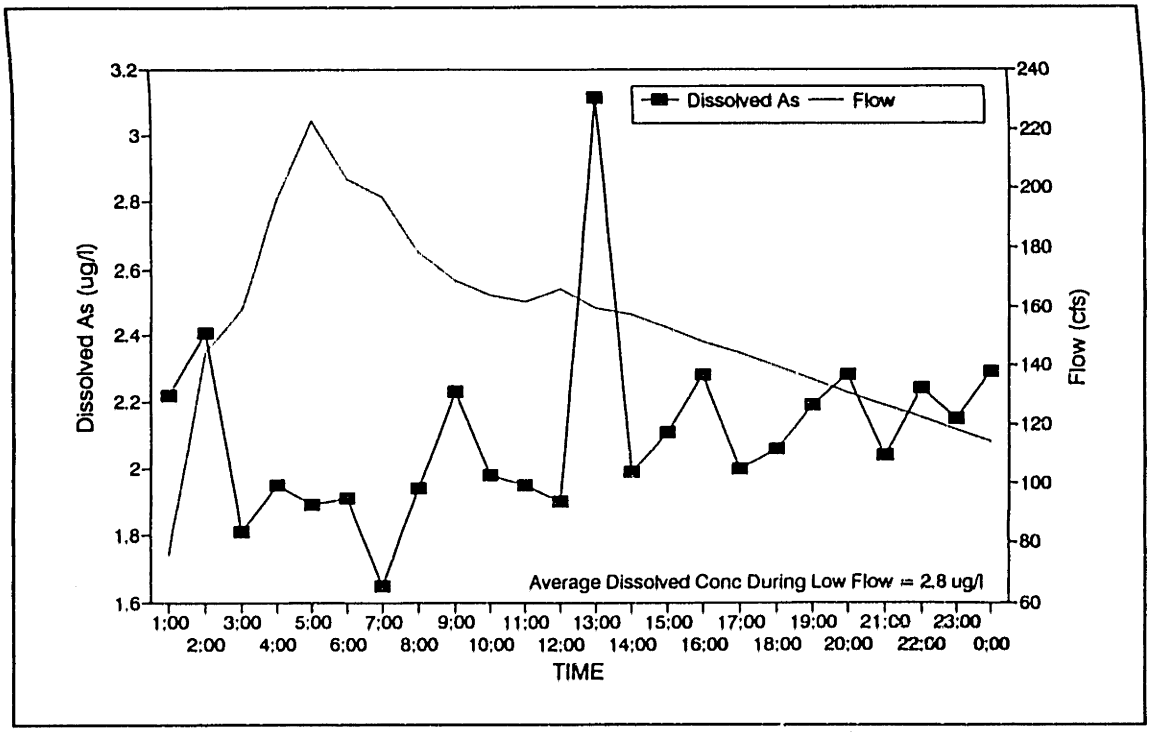

Figure IV.4-54: Dissolved As Concentration and Flow versus Time, Gage #5, USGS August 18, 1992 Storm

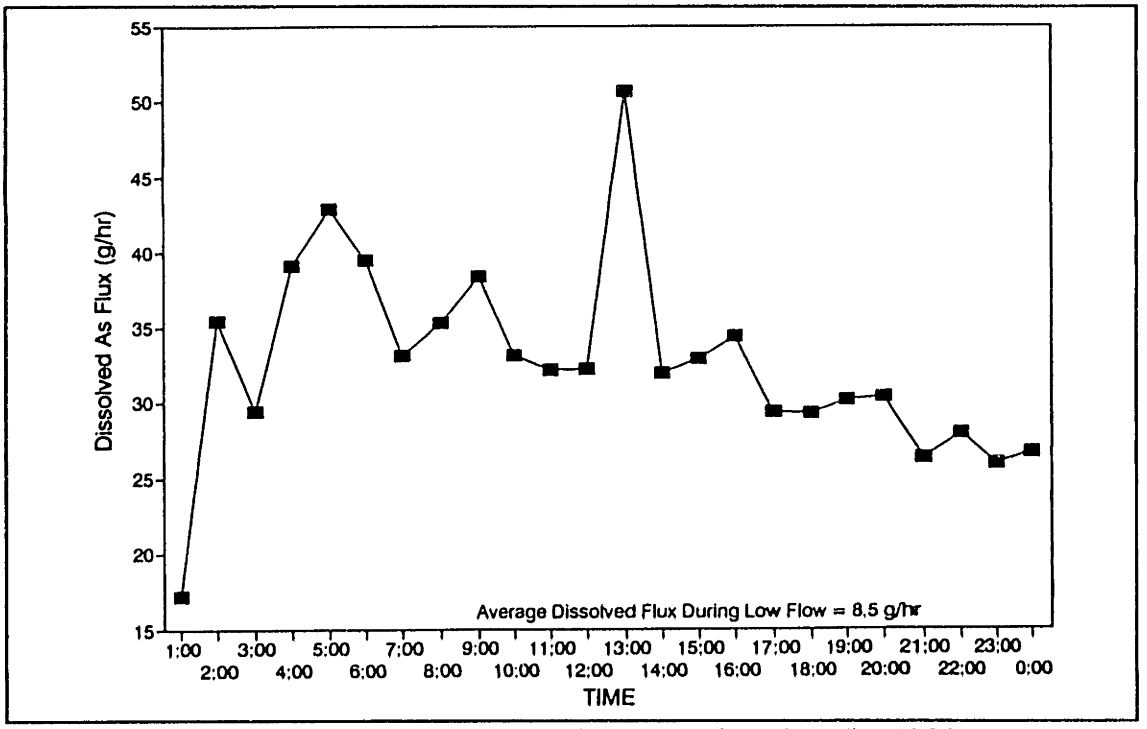

Figure IV.4-55: Dissolved As Flux versus Time, Gage #5, USGS August 18, 1992 Storm

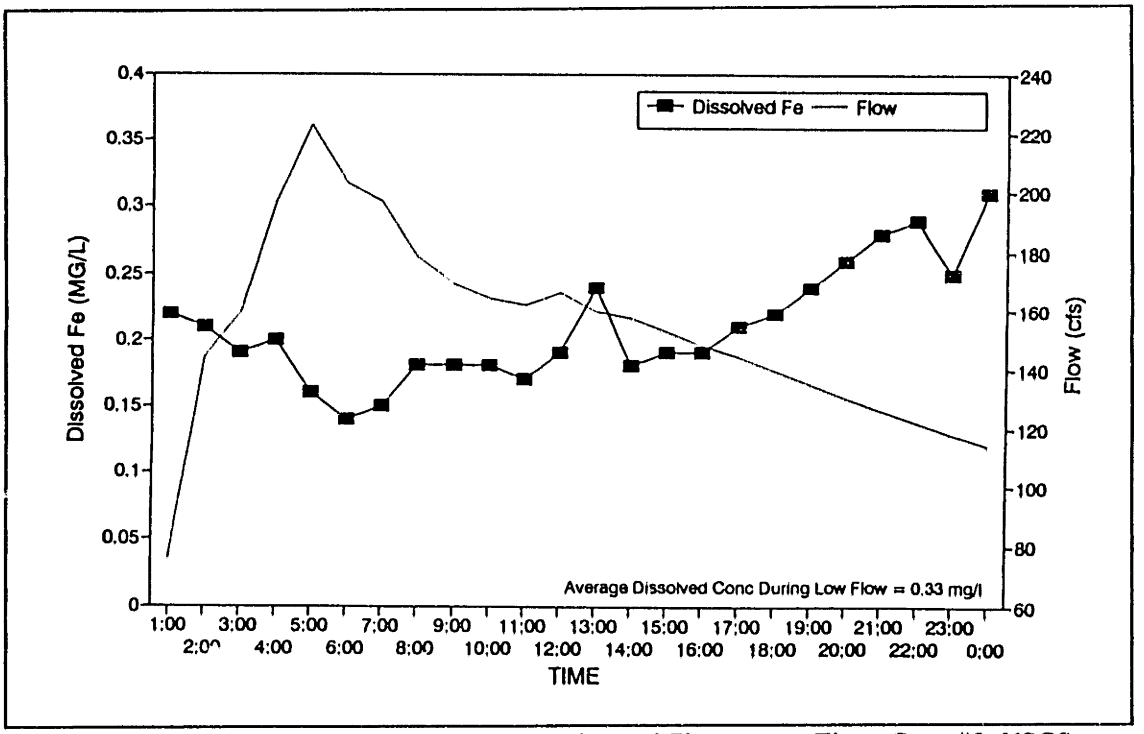

Figure IV.4-56: Dissolved Fe Concentration and Flow versus Time, Gage #5, USGS August 18, 1992 Storm

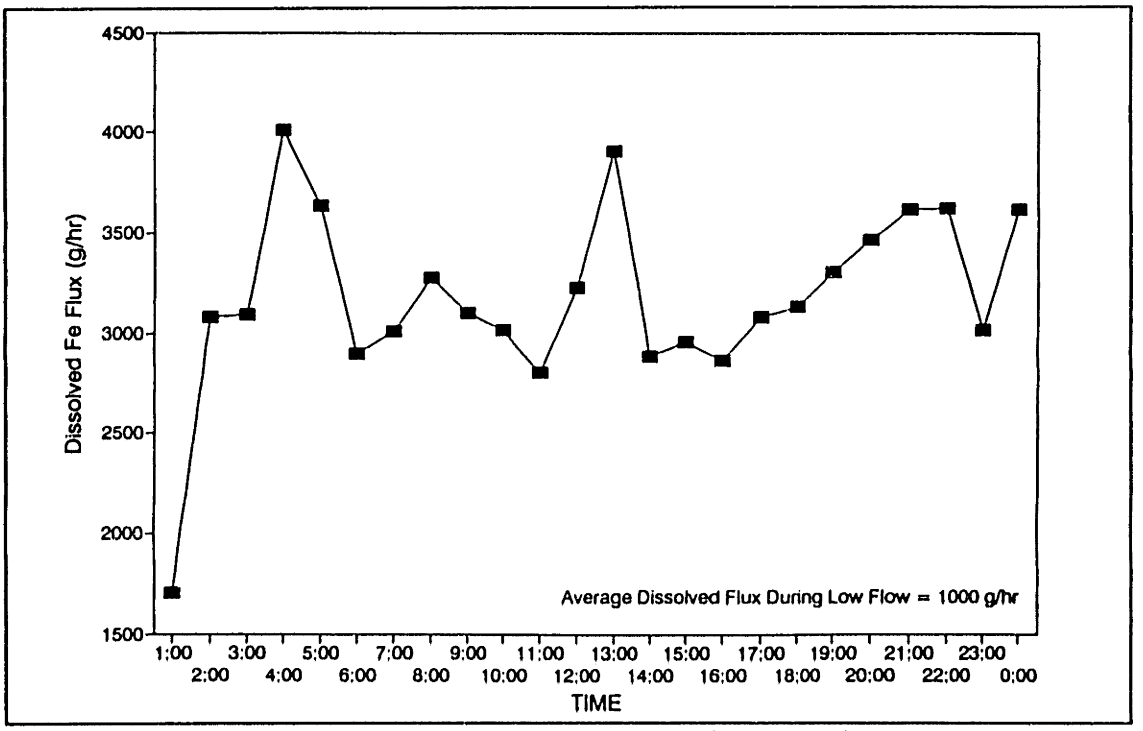

Figure IV.4-57: Dissolved Fe Flux versus Time, Gage #5, USGS August 18, 1992 Storm

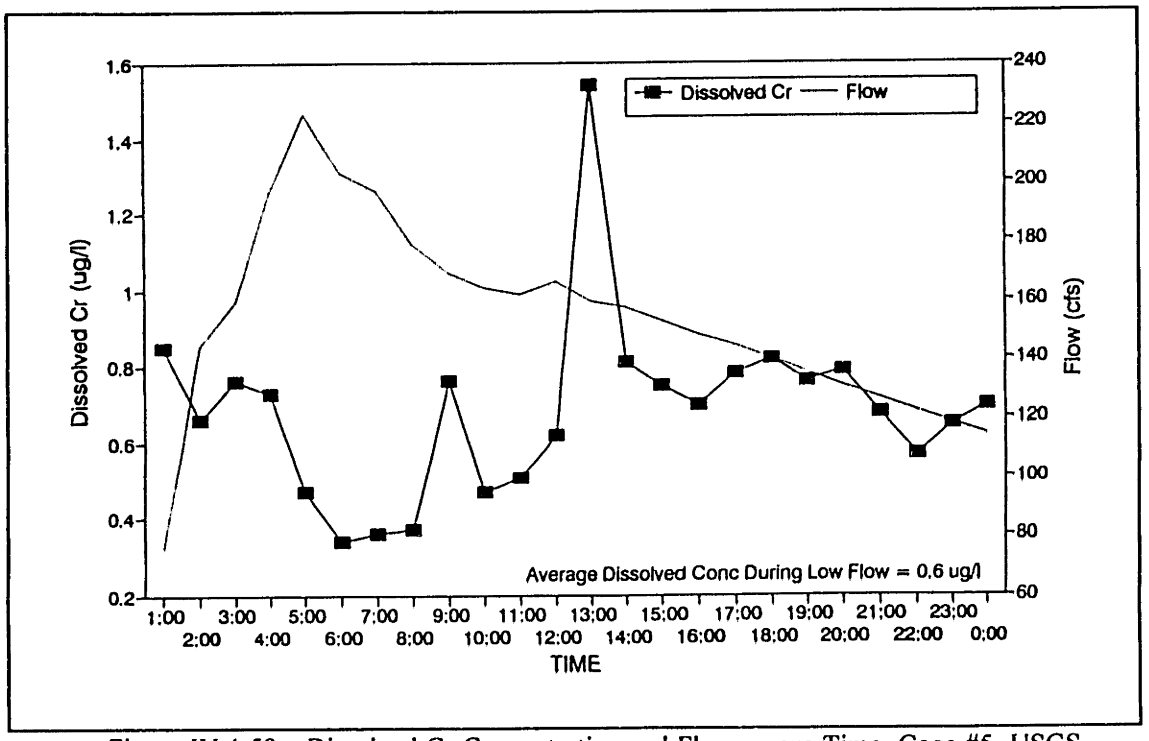

Figure IV.4-58: Dissolved Cr Concentration and Flow versus Time, Gage #5, USGS August 18, 1992 Storm

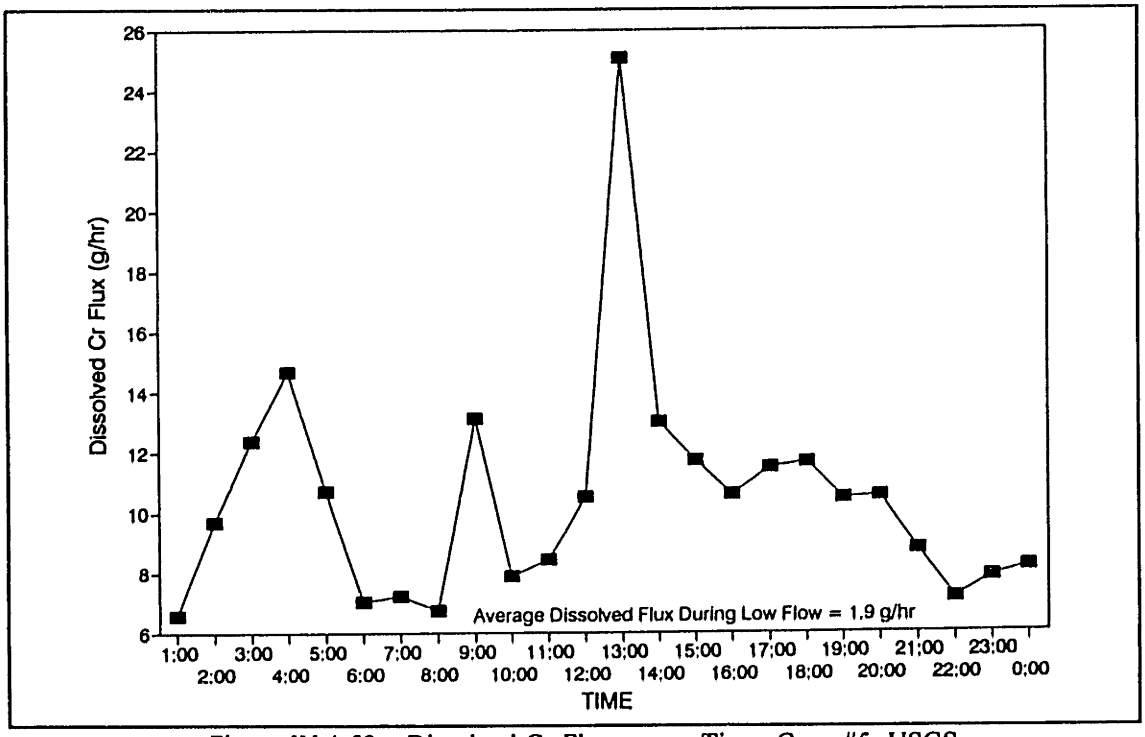

Figure IV.4-59: Dissolved Cr Flux versus Time, Gage #5, USGS August 18, 1992 Storm

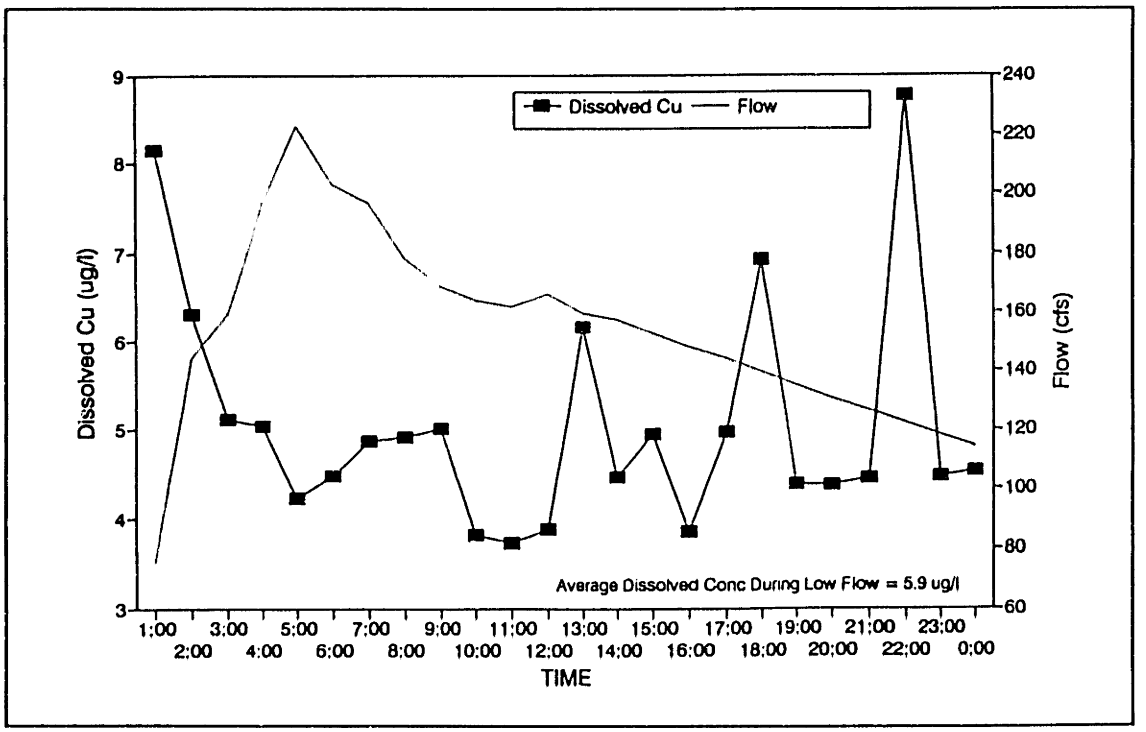

Figure IV.4-60: Dissolved Cu Concentration and Flow versus Time, Gage #5, USGS August 18, 1992 Storm

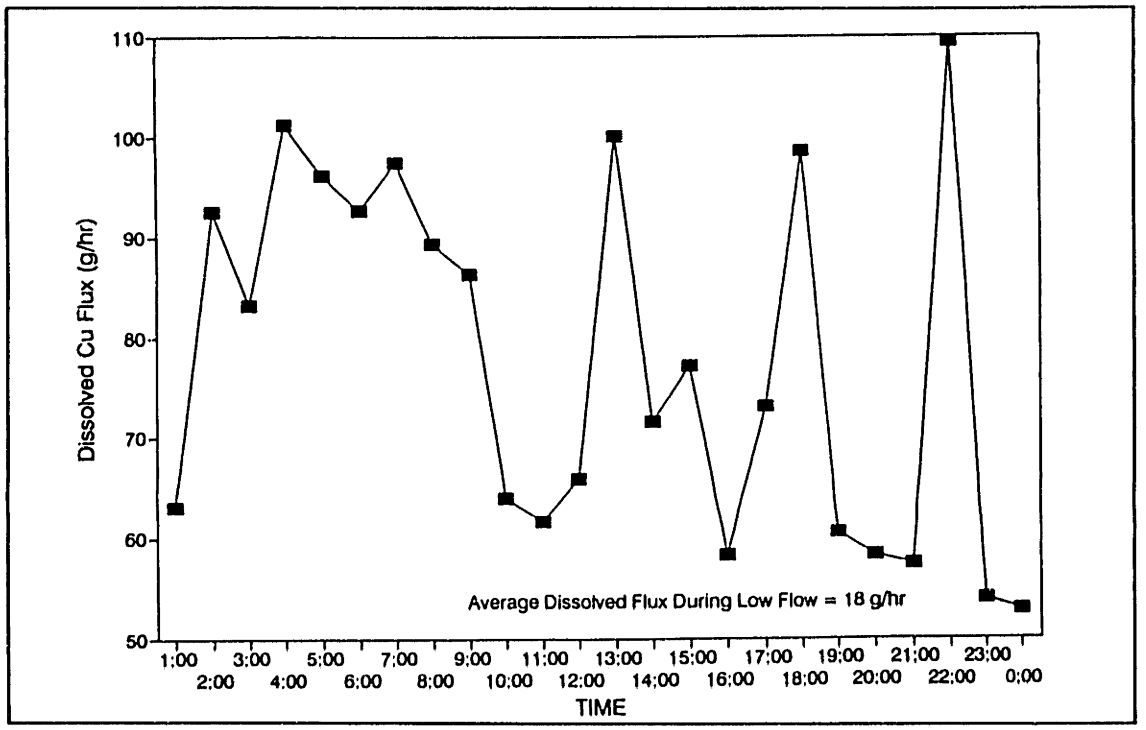

Figure IV.4-61: Dissolved Cu Flux versus Time, Gage #5, USGS August 18, 1992 Storm

IV.4.2.4 Particulate Metals: Fluxes and Concentrations

Fluxes

Particulate metal fluxes were also higher during stormflows than during low flow conditions. (figures IV.4-64, IV.4-66, IV.4-68, and IV.4-70, also see appendix IV.E) The larger the flow event the larger the metal flux carried by the river. For the March 29 event, the largest event sampled (peak flow = 502 cfs), the metal flux was generally two orders of magnitude higher than observed during low flows. For this event, particulate As, Fe, Cr, and Cu fluxes were in the vicinity of 250, 120000, 800, and 900 g/hr. These fluxes are much larger than the corresponding fluxes in the dissolved phase. Thus during storm flows, most of the metal flux is carried by the particulate phase. For the two smaller events, the August (peak flow = 223 cfs) and December (peak flow = 215 cfs) storms, metal fluxes were at similar values and less than that observed for the March 29 event. The particulate flux for these events was elevated above typical low flow values by: 1) slightly larger than an order of magnitude for arsenic and iron, and 2) between 1.5 to 2 orders of magnitude for chromium and copper. As for the dissolved phase, the similarity in particulate fluxes between the August and December events was primarily due to the similarities in streamflows and suspended sediment concentrations. Furthermore, since the two events occurred during different seasons, seasonal factors did not appear to strongly affect the particulate metals flux. A slightly smaller event observed March 26, 1993 (peak flow = 144 cfs) exhibited smaller dissolved fluxes than the August and December events.

Within a storm event, changes in the particulate metal flux (= $[M_p][SS]Q = [M_p]$*SS flux) were strongly affected by the suspended sediment flux, since the variability of the suspended sediment flux was much larger than the variability of the particulate metal concentration. (figures IV.4-63 to IV.4-70) For all metals, the peak metal flux occurred when the suspended sediment flux peaked. Furthermore, after the peak, the metal flux decreased as did the suspended sediment flux, regardless of the fluctuations of the particulate metal concentrations. The net result was for bursts of particulate metal transport at the initiation of storm flow conditions.

Concentrations

For all events, particulate arsenic and particulate iron concentrations (per suspended sediment mass basis) were lower during storm events than during low flow conditions. Such an observation indicates that suspended sediments which were active during storm conditions (quick, slow, and channel sediments) were relatively cleaner than suspended sediments which dominated during low flows (longterm baseflow sediments). Particulate chromium and particulate copper, on the other hand, had concentrations during the storms which were, on average, slightly higher than concentrations typical of low flow conditions. This observation indicates the converse of what was observed for arsenic and iron. For chromium and

copper, suspended sediments which were active during storm conditions were on average more contaminated than suspended sediments which predominated during low flow conditions.

Within the storm events, particulate arsenic concentrations exhibited a dilution effect during each storm, in which concentrations before and after the suspended flux peak were higher than concentrations during the peak. (figure IV.4-63) Such an observation may be due to the dilution of more contaminated slow suspended sediments by relatively cleaner quick suspended sediments.

For the other metals, no consistent trend was observed. During the August and December storms, particulate iron concentrations gradually increased throughout the events. During the March 29 storm a dilution effect was observed. Chromium and copper concentrations generally increased as the August and March 29 storms progressed. However, during the December storms, a gradual decrease in concentration was observed during the storm.

For the August event, the behavior of all metals was consistent in that particulate metal concentrations generally increased for all metals after the first suspended sediment peak had occurred (after 2:00). (figure IV.4-62) However, for other storms this consistency between metals was not necessarily observed. For example, for the December event, particulate iron and arsenic generally increased after the suspended sediment peak whereas chromium and copper generally decreased.

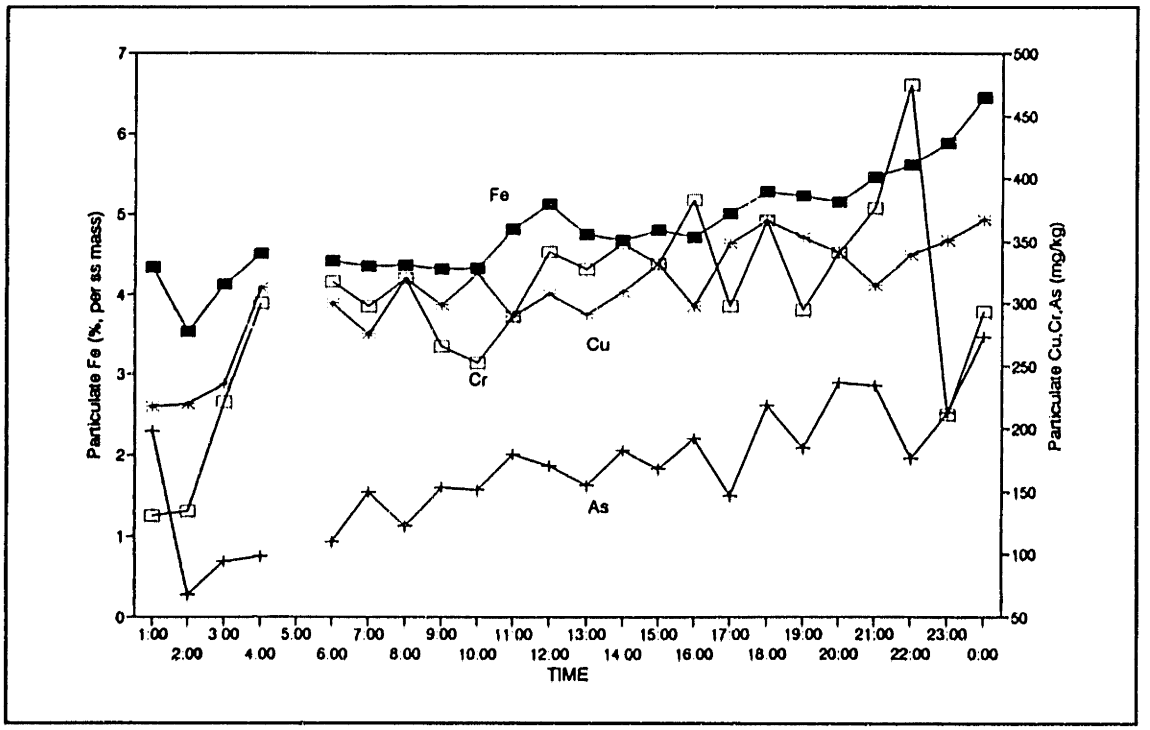

Figure IV.4-62: Particulate Metal Concentration versus Time, Gage #5,USGS August 18, 1992 Storm

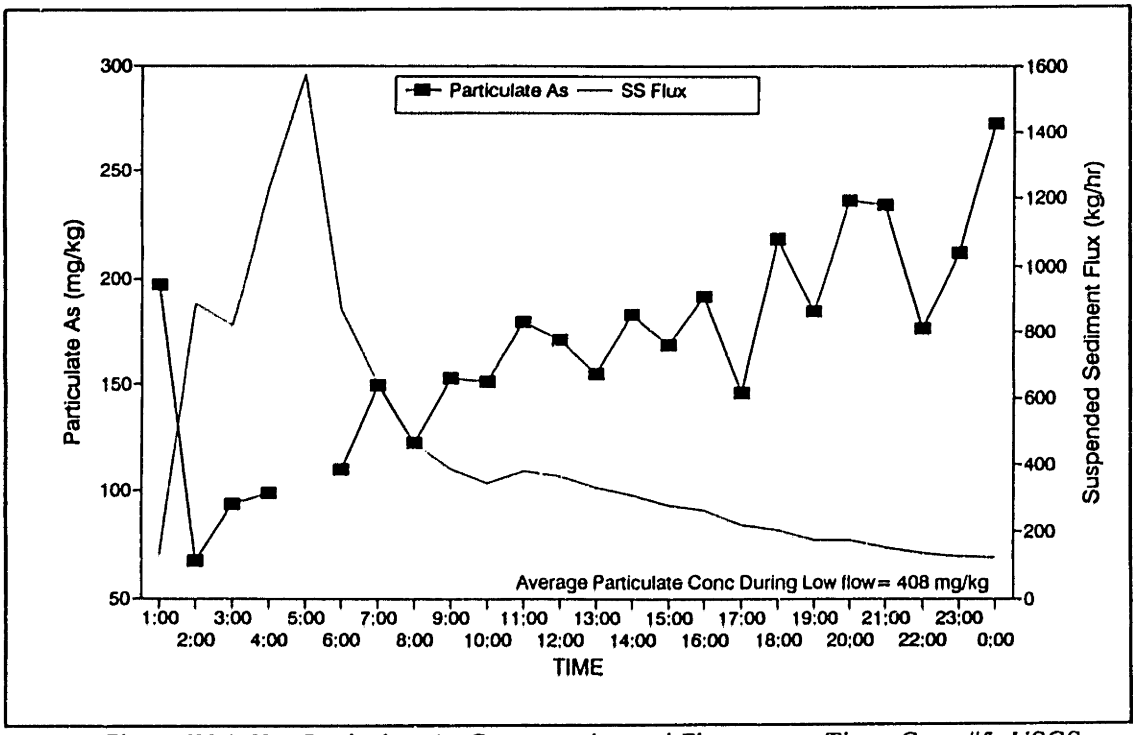

Figure IV.4-63: Particulate As Concentration and Flow versus Time, Gage #5, USGS August 18, 1992 Storm

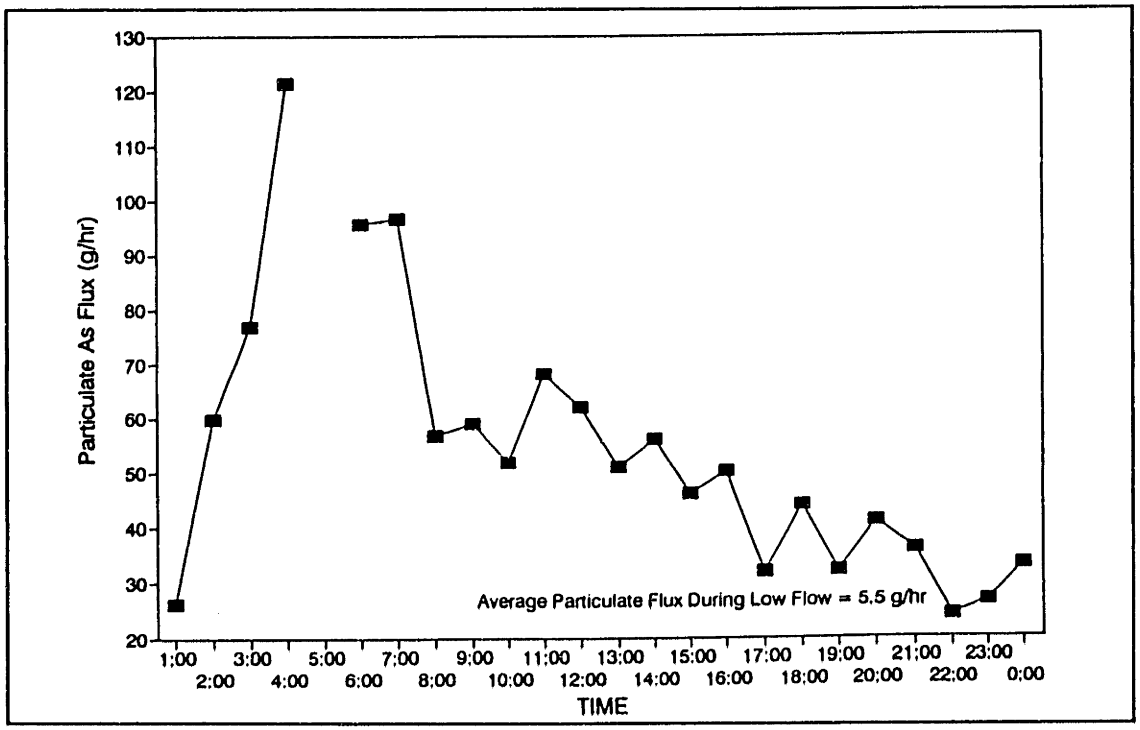

Figure IV.4-64: Particulate As Flux versus Time, Gage #5, USGS August 18, 1992 Storm

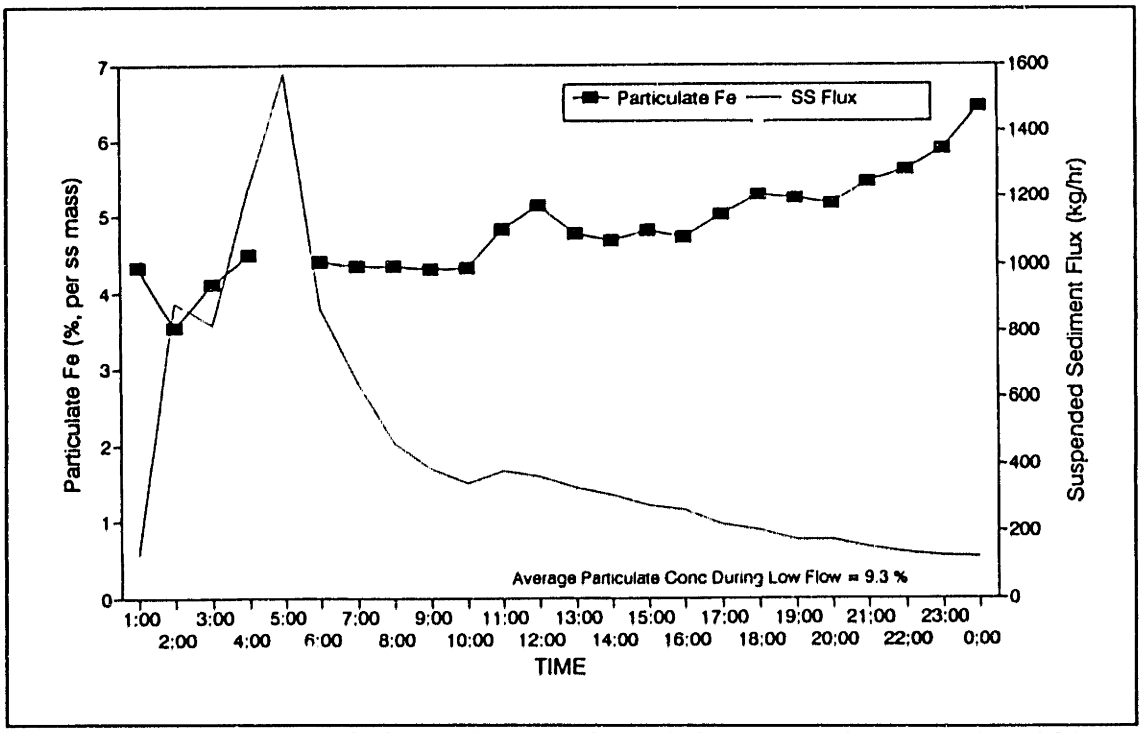

Figure IV.4-65: Particulate Fe Concentration and Flow versus Time, Gage #5, USGS August 18, 1992 Storm

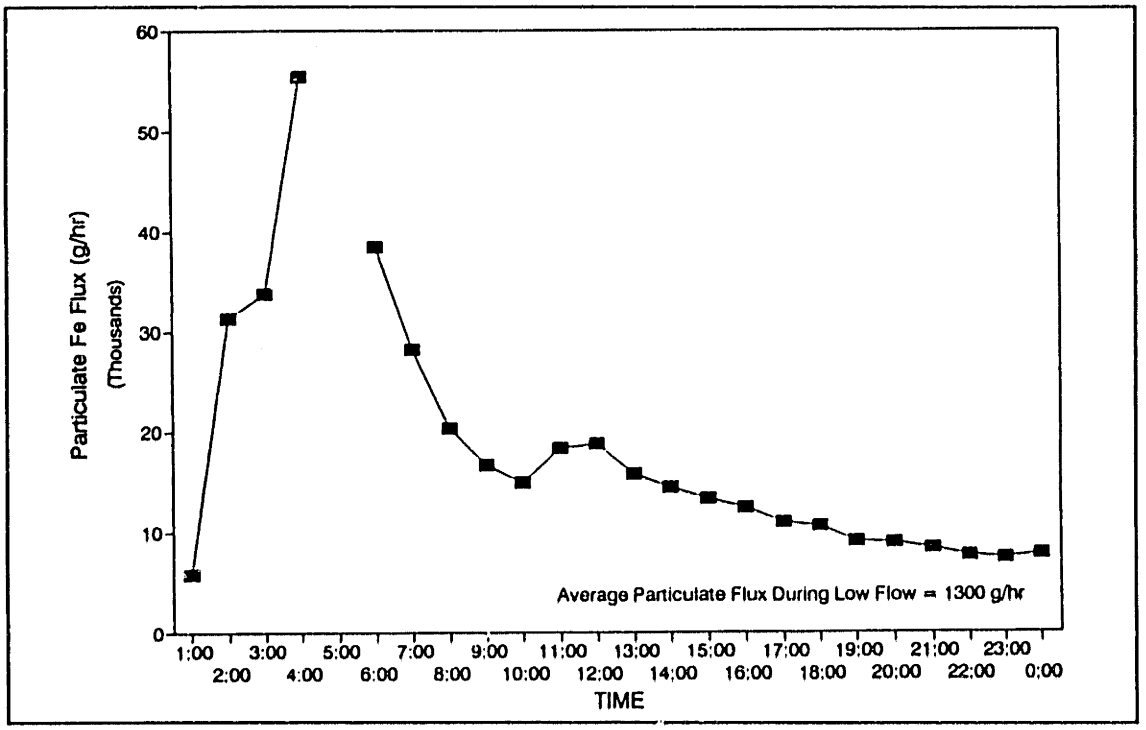

Figure IV.4-66: Particulate Fe Flux versus Time, Gage #5, USGS August 18, 1992 Storm

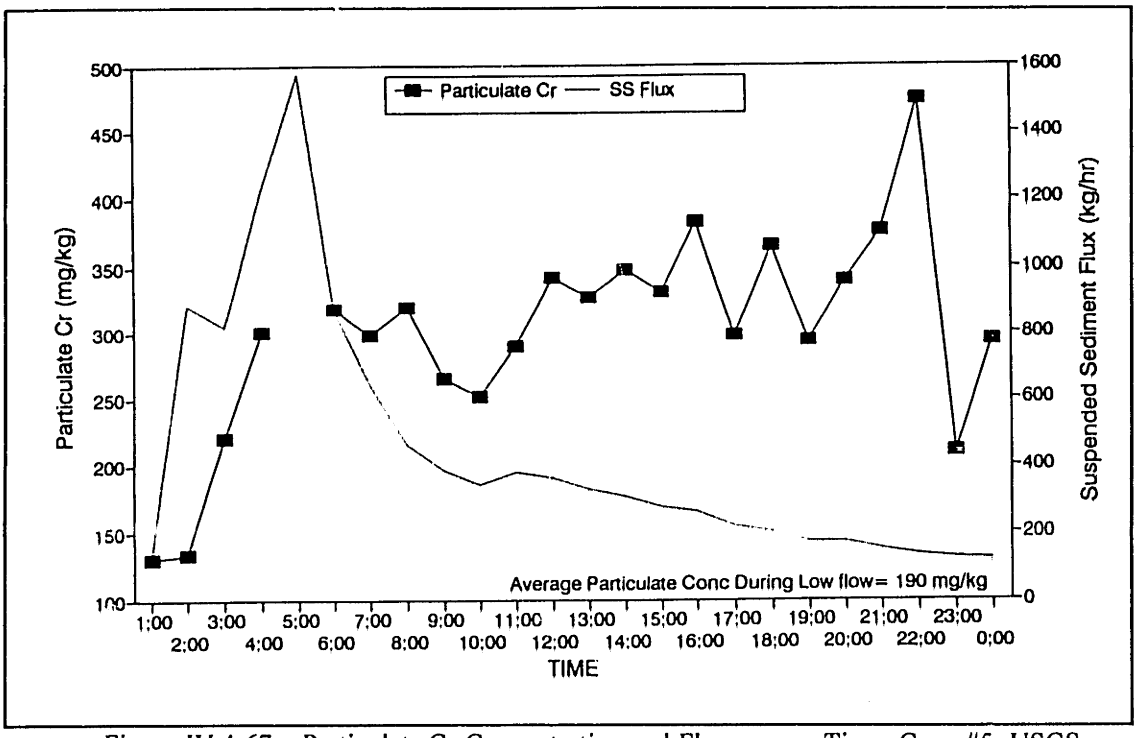

Figure IV.4-67: Particulate Cr Concentration and Flow versus Time, Gage #5, USGS August 18, 1992 Storm

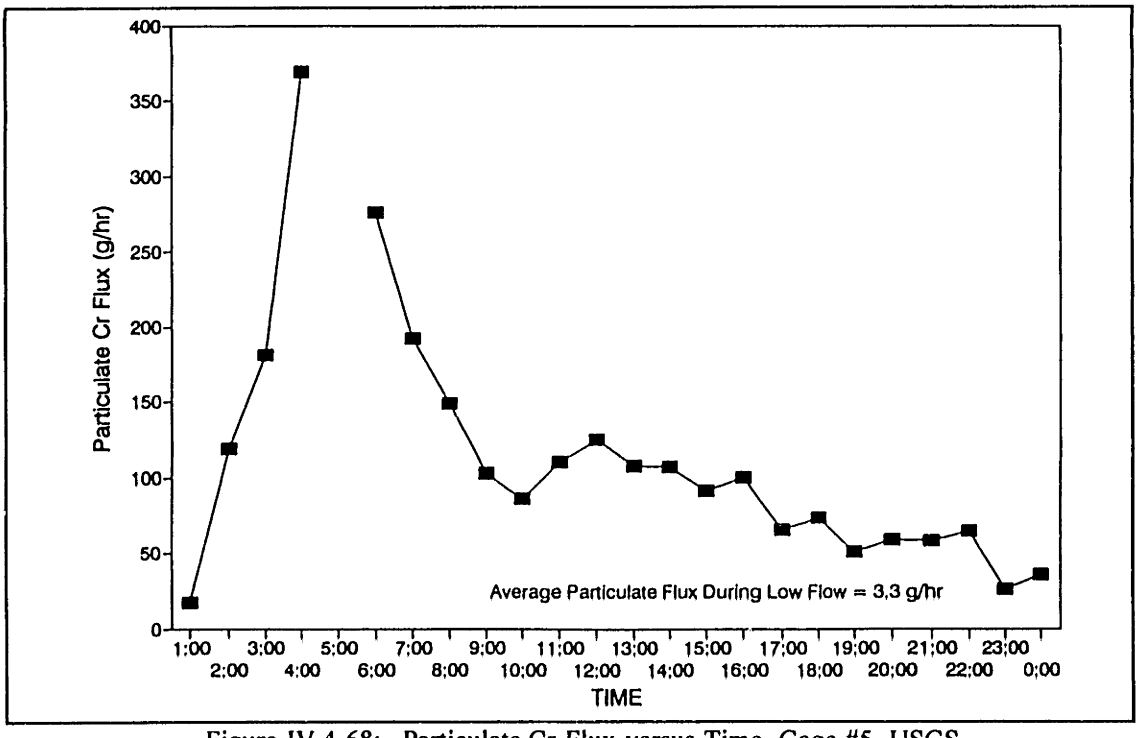

Figure IV.4-68: Particulate Cr Flux versus Time, Gage #5, USGS August 18, 1992 Storm

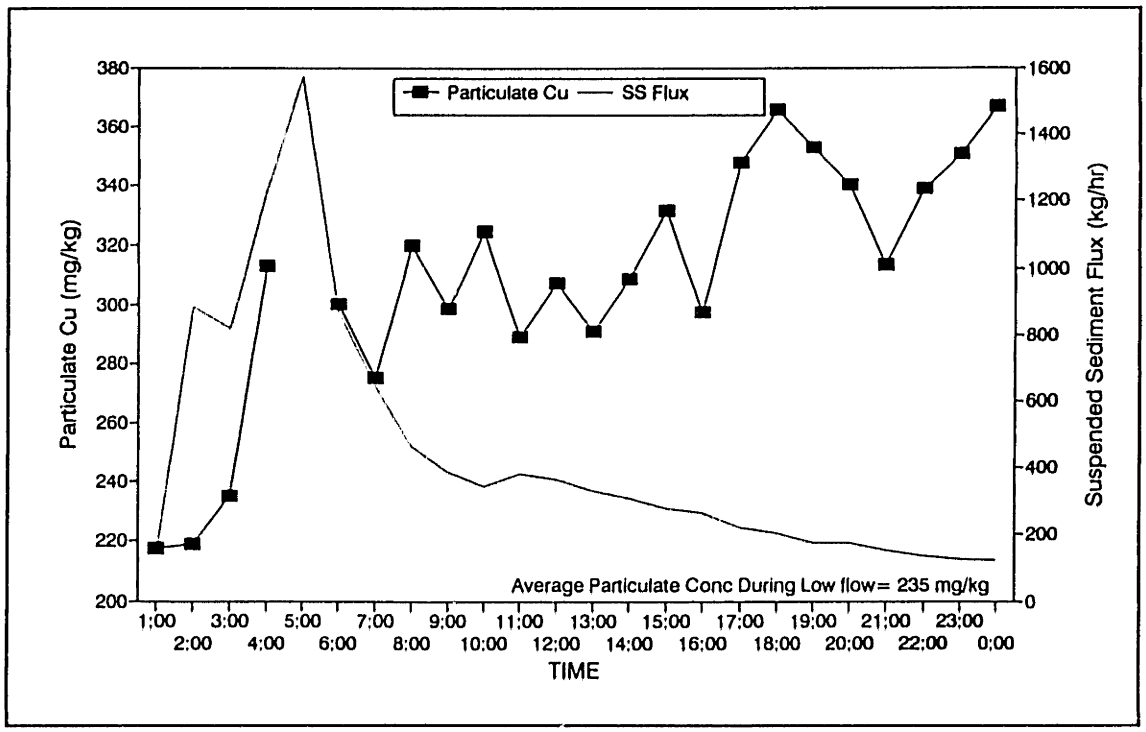

Figure IV.4-69: Particulate Cu Concentration and Flow versus Time, Gage #5, USGS August 18, 1992 Storm

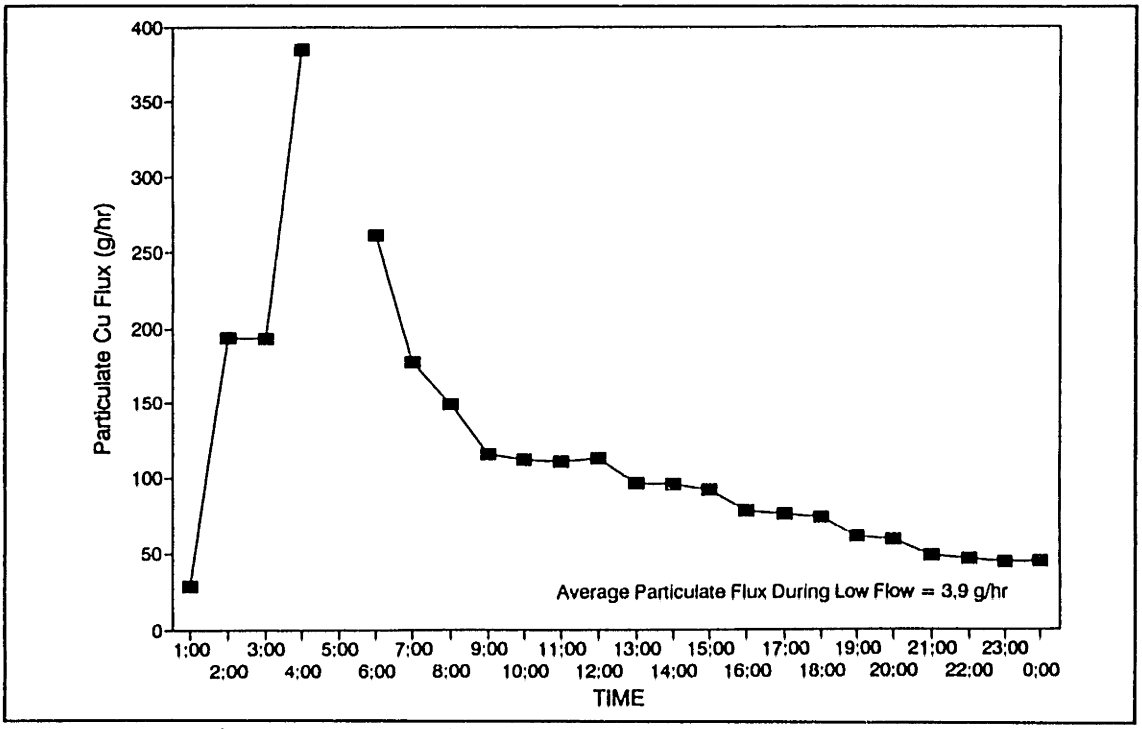

Figure IV.4-70: Particulate Cu Flux versus Time, Gage #5, USGS August 18, 1992 Storm

IV.4.2.5 Partitioning of Metals Between the Dissolved and Particulate Phases

Total metal concentrations (per river water volume basis) were higher during storm conditions than during low flow conditions. (figures IV.4-71 to IV.4-74) During storm events, particulate metal concentrations (per river water volume) increased significantly above typical concentrations observed during low flows. The dissolved concentrations also fluctuated; however, these fluctuations were not as large as the fluctuations observed for the particulate phase. The overall result was a strong shift in the partitioning of the metals toward the particulate phase. By the end of each storm: 1) total metal concentrations, and 2) partitioning of the metal between the dissolved and particulate phases, were near values typically observed during low flows.

The observed shift in the partitioning between low flow and storm conditions is interpreted as being primarily due to the physical processes, including: 1) dilution effects for the dissolved phase (for some metals), and 2) activation of particulate metal sources during storm conditions. Implied in this explanation is that the phase association of a metal (whether associated with dissolved or particulate phase) will not change significantly through chemical interactions as it is being transported. (See section II.3.3 for further discussion)

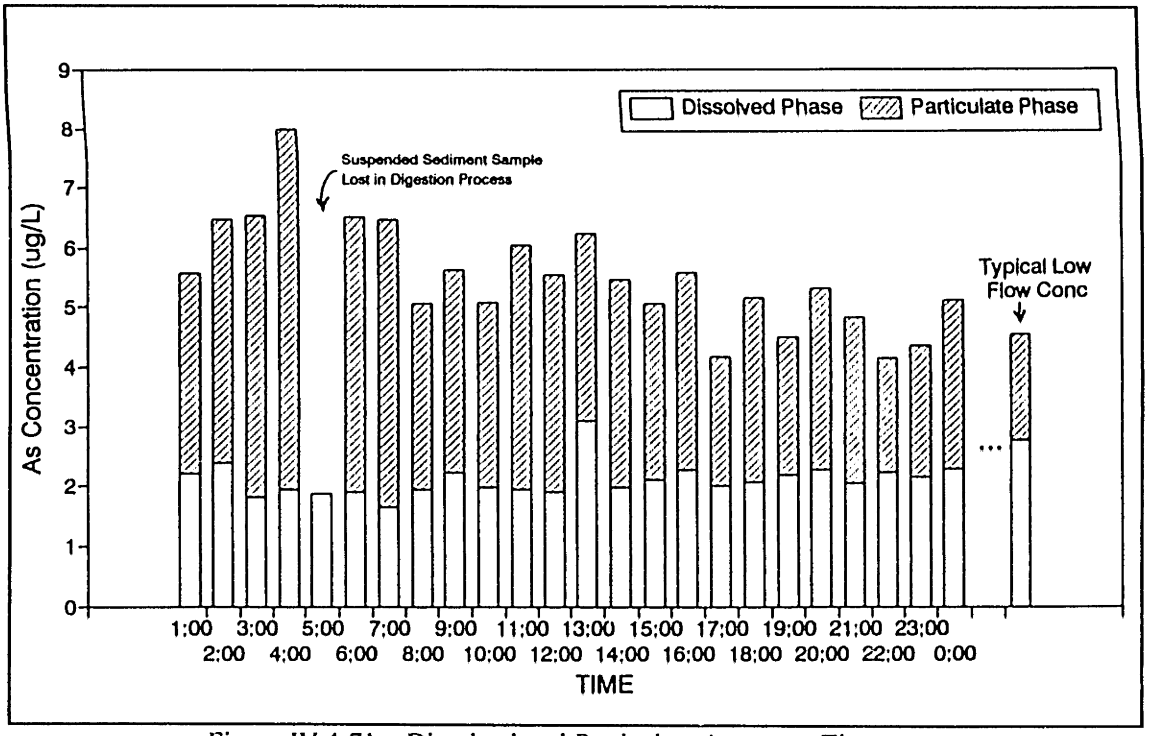

Figure IV.4-71: Dissolved and Particulate As versus Time
Gage #5, USGS, August 18, 1992 Storm

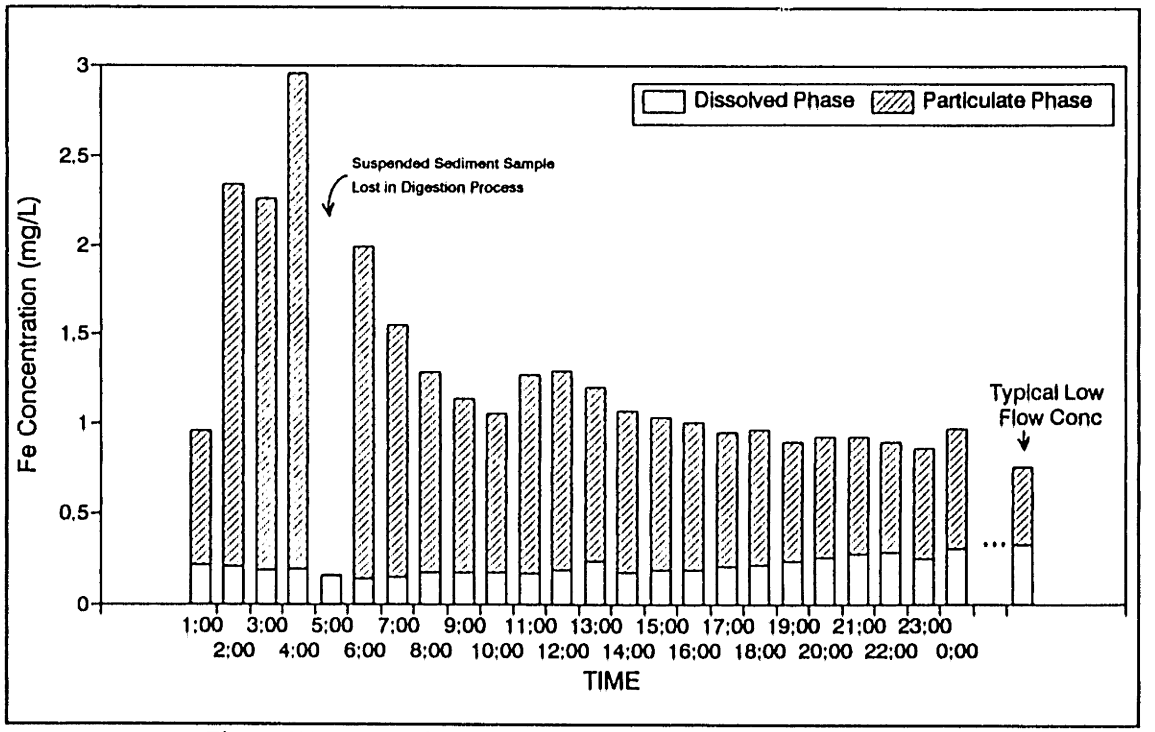

Figure IV.4-72: Dissolved and Particulate Fe versus Time
Gage #5, USGS, August 18, 1992 Storm

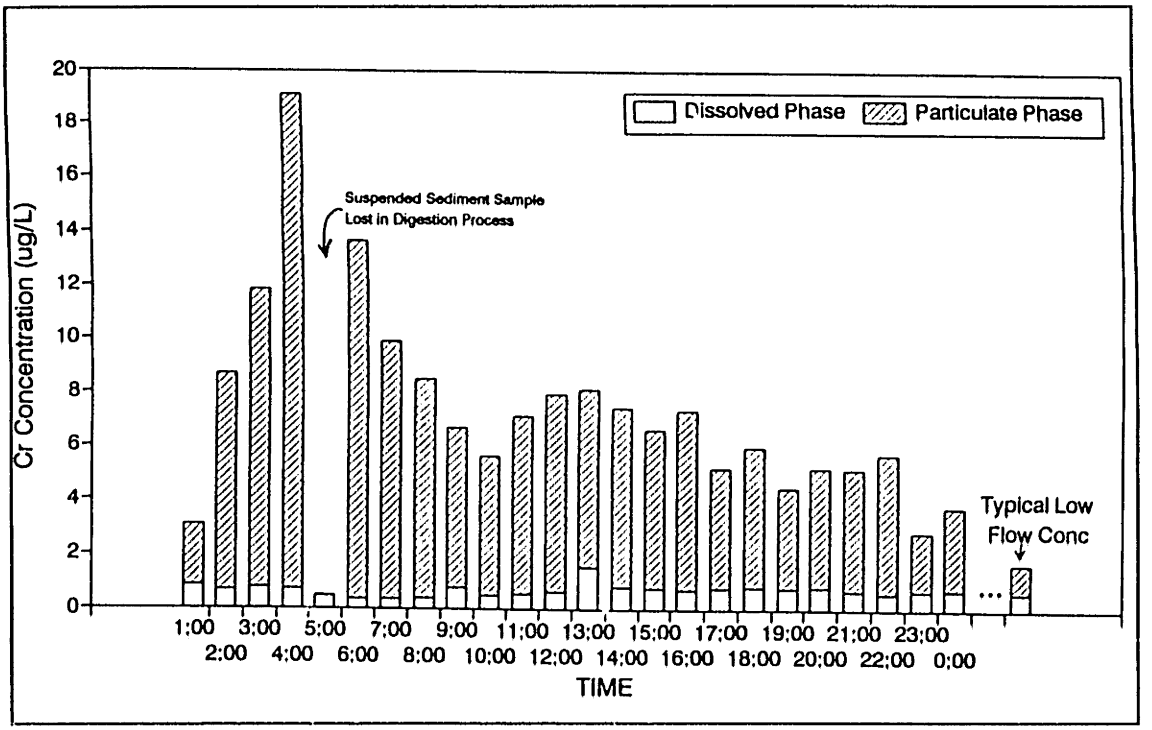

Figure IV.4-73: Dissolved and Particulate Cr versus Time
Gage #5, USGS, August 18, 1992 Storm

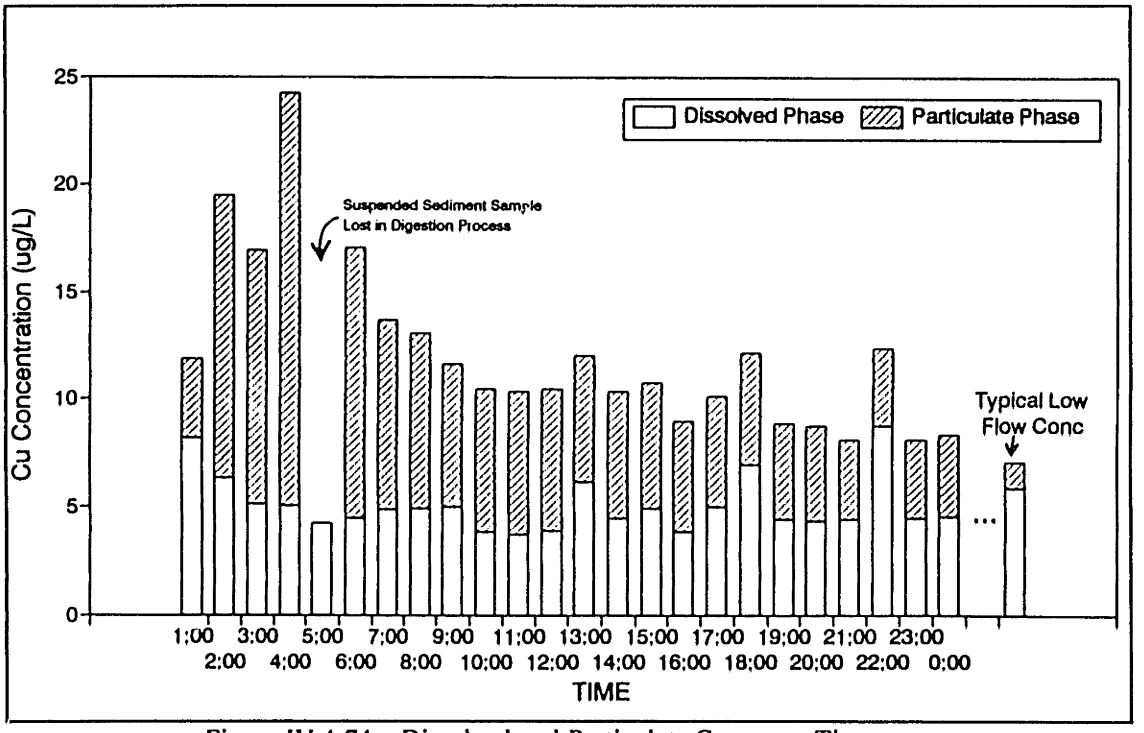

Figure IV.4-74: Dissolved and Particulate Cu versus Time
Gage #5, USGS, August 18, 1992 Storm

IV.5 CONCEPTUAL MODEL

The conceptual model represents my interpretation of the data presented in the preceding sections of this chapter, and is a summary of the underlying concepts which were incorporated into the computer model (Section V.1). In the presentation of the conceptual model, some equations are presented for discussion purposes. For details of the model formulation, please refer to the following chapter.

In developing a conceptual model for the Aberjona River, an attempt was made to incorporate only those mechanisms that most strongly dominated the transport of metals. The need to address only the most dominant mechanisms comes from the practical desire to develop the simplest model that can be used to estimate the overall flux of metals being transported from the watershed, and to remain within the boundaries imposed by the available data set. It is recognized that the model does not capture all of the mechanisms that may be represented in that data set and that some of the less dominant transport mechanisms may also be of interest from a scientific point of view. Analysis of such mechanisms is left for future investigations.

IV.5.1 Watershed Geometry

Watershed geometry was schematically represented by sub-dividing the watershed into sub-basins. The purpose of this sub-division was to capture the area-wide distribution of contaminant sources. For example, concentrations of metals were much higher on the upper reaches of Aberjona River than along Horn Pond Creek. After the confluence of Horn Pond Creek with the Aberjona, metal concentrations generally decreased due to a surface water dilution effect. Furthermore, for some metals a dilution effect was observed along the Aberjona River, with some concentrations decreasing in the downstream direction. The interpretation of this trend was that a source of contaminated waters exists on the upstream end of the Aberjona. As this water travels downstream, relatively cleaner inflows dilute the river water. The net result is a decrease in concentration in the downstream direction.

Given such observations, the watershed was sub-divided into four sub-basins. (figure IV.5-1) Three of the sub-basins were located along the Aberjona River. These sub-basins included: 1) the Woburn North sub-basin, "WN", 2) the Woburn Central sub-basin "WC", and 3) the Winchester sub-basin, "WI". The delineation of these sub-basins was based upon surface topography and location of the sampling stations. The fourth sub-basin, the Woburn West sub-basin, "WW", represented the area draining the Horn Pond Creek tributary.

Since two sampling stations were located along Horn Pond Creek, the Woburn West sub-basin could have been separated into two smaller sub-basins. This complication was rejected because: 1) of the relatively small contribution of Horn Pond Creek to the streamflow, suspended sediment, and metal flux of the Aberjona River, and 2) this separation would have significantly complicated the model since different hydrologic processes apparently control streamflow within the Woburn West sub-basin. (These hydrologic processes include the storage of water and contaminants in the Horn Pond and Wedge Pond reservoirs, and large groundwater withdrawals in the vicinity of Horn Pond.) The western part of the watershed was, therefore, lumped into one sub-basin, thus simplifying the treatment of this less contaminated area and permitting a greater focus on the Aberjona side of the watershed.

In an attempt to capture the timing effects associated with waters coming from different areas within the watershed, two channel components were added. The first channel represented the Aberjona River between Route 128 and Montvale, while the second channel represented the Aberjona River between Montvale and the USGS station. These channels served as routing units for streamflow, suspended sediment, and metal fluxes.

Additionally, a component that modeled the effects of the Atlantic Gelatin groundwater withdrawal was also included. This component modified the river streamflow, suspended sediments and metal transport due to a significant removal of streamflow from the area.

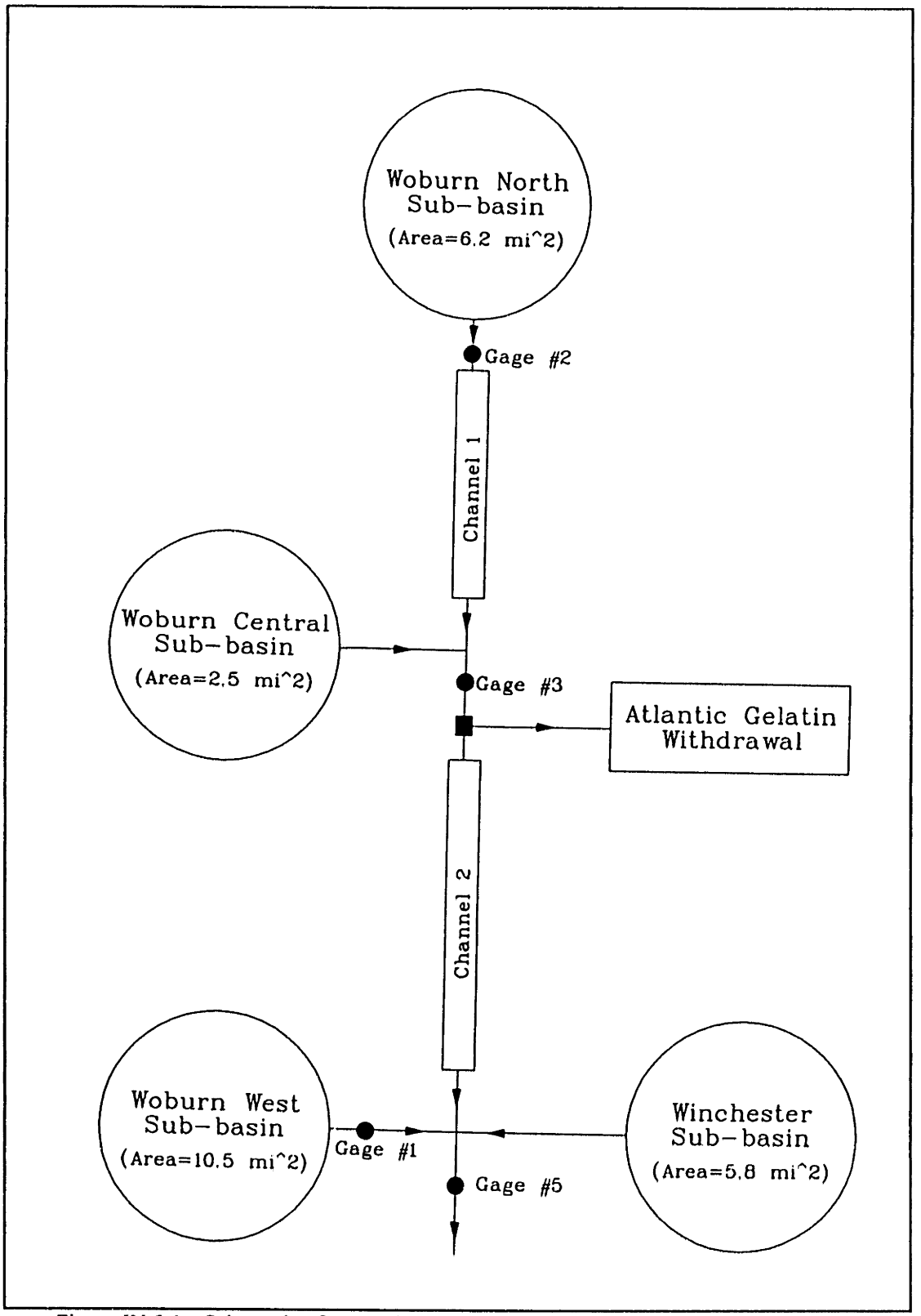

Figure IV.5-1: Schematic of Watershed Geometry and Major Hydrologic Components

IV.5.2 Streamflow Components

Data presented in earlier sections indicate that streamflow responded in a well-defined manner to precipitation. A major characteristic of the response is that streamflow, "Q_j", from each sub-basin along the Aberjona River (WN, WC, WI) is apparently composed of different components. (figure IV.5-2) These components include: 1) a quick storm response, "flowq", 2) a slow storm response, "flows", and 3) longterm baseflow, "ltbf", or:

$$Q_j = flowq_j + flows_j + ltbf_j$$

where subscript "j" refers to a particular Aberjona sub-basin

Since the contribution of each component changes between storm flow and low flow conditions, a computer model which captures the variability of each of the components over time is developed in the following chapter.

For the Woburn West sub-basin, "WW", streamflow was not characterized by distinct quick, slow, and longterm baseflow components. Furthermore, during storm events, the magnitude of the streamflow at Wedge Pond was much smaller than flow along the Aberjona River. Given the small flow during storm events, only one component of streamflow, "flowt", was considered for the Woburn West sub-basin, or: (figure IV.5-2)

$$Q_{WW} = flowt$$

Streamflow from the Woburn West sub-basin is used as an input into the computer model.

Upon entering the main channels, (Channel 1 and Channel 2) the streamflow inputs from a given sub-basin are subject to channel routing effects. For example, to model the flow at gage #3, the streamflow from the Woburn North sub-basin, "Q_{WN}", is routed through Channel 1. The routed flow from Woburn North is then added to the streamflow input from the Woburn Central sub-basin, "Q_{WC}"; the sum of which is the modeled flow at gage #3.

The Atlantic Gelatin site is a location where streamflow is removed from the river. Therefore, immediately after gage #3, streamflow is adjusted according to the Atlantic Gelatin withdrawal rate. The adjusted flow from gage #3 is then routed through Channel 2 and added to the streamflow inputs from the Woburn West, "Q_{WW}", and Winchester, "Q_{WI}", sub-basins. The sum of these flows represents the modeled flow at gage #5.

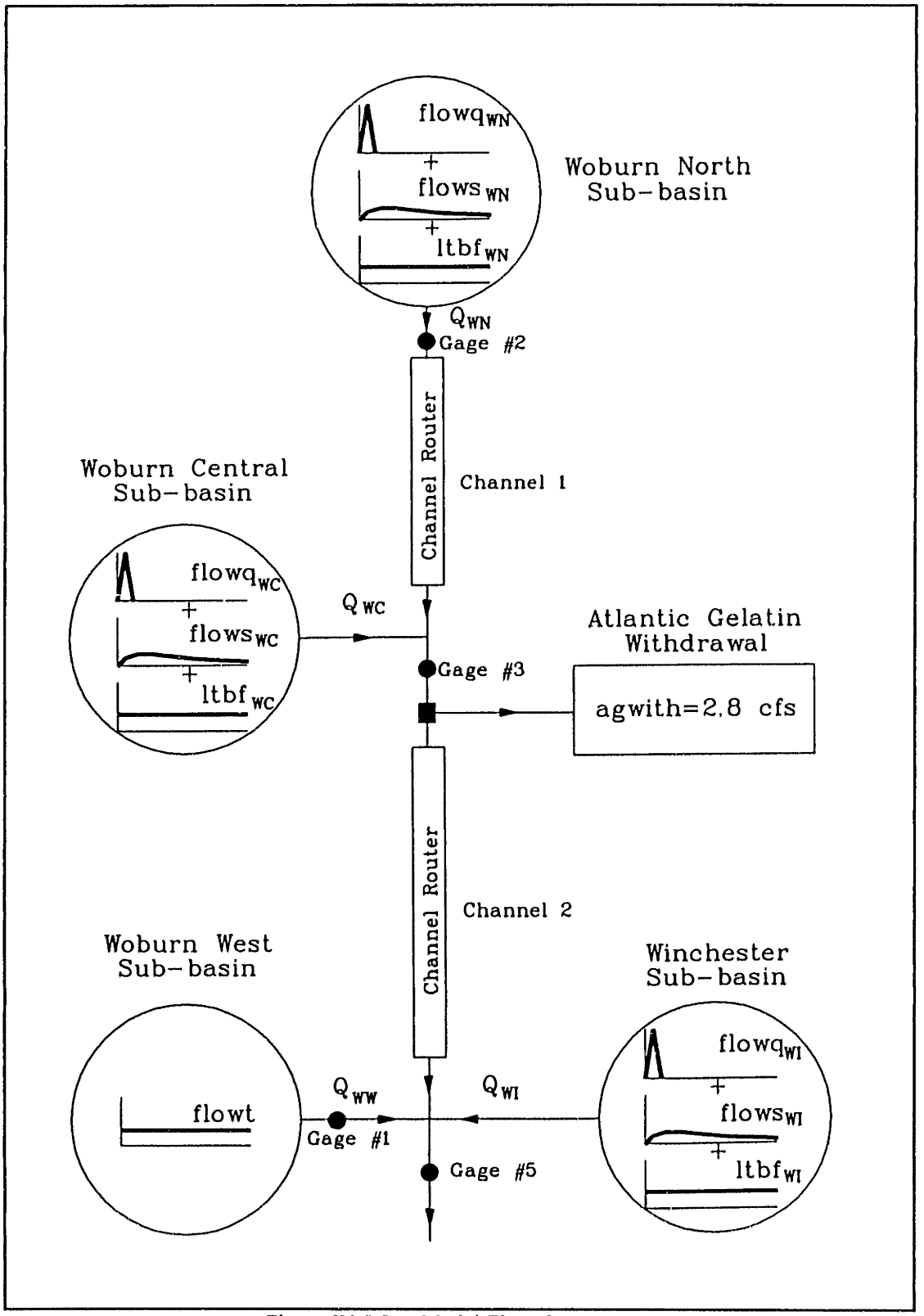

Figure IV.5-2: Model Flow Components

IV.5.3 Dissolved Metals

My interpretation of the data is that dissolved metals transported *from each sub-basin on the Aberjona River* can be sub-divided into components, where:

$$F_t = [M_d]_{net}Q = F_{quick} + F_{slow} + F_{ltbf}$$
$$= [M_d]_{quick}flowq + [M_d]_{slow}flows + [M_d]_{ltbf}ltbf$$

where: F_t = Total Dissolved Flux

$[M_d]_{net}$ = Net Dissolved Metal Concentration of Water Coming From a Particular Sub-basin

Q = Total Streamflow from a Particular Sub-basin

F_{quick} = Dissolved Flux Associated with Quick Streamflow

F_{slow} = Dissolved Flux Associated with Slow Streamflow

F_{ltbf} = Dissolved Flux Associated with Longterm Baseflow

$[M_d]_i$ = Dissolved Metal Concentration Associated with Streamflow Component i

By sub-dividing the total metal flux into components as given above, the observed changes in the dissolved metal concentrations can be explained by changes in the relative contributions of each of the dissolved metal components. For example, a dilution effect associated with storm flows can be explained by postulating that quick storm waters and slow storm waters are relatively cleaner than longterm baseflow (i.e. $[M_d]_{quick} < [M_d]_{ltbf}$, $[M_d]_{slow} < [M_d]_{ltbf}$). Assume for instance that prior to and immediately after a storm event, longterm baseflow is the dominant component of water in the river (i.e. ltbf >> flowq, ltbf >> flows) Then during these conditions, the river water concentrations would approach the dissolved metal concentration of the longterm baseflow component, or:

$$[M_d]_{net} = \frac{[M_d]_{quick}flowq + [M_d]_{slow}flows + [M_d]_{ltbf}ltbf}{flowq + flows + ltbf}$$

$$= \frac{\approx 0 + \approx 0 + [M_d]_{ltbf}ltbf}{\approx 0 + \approx 0 + ltbf}$$

$$\approx [M_d]_{ltbf}$$

During a large storm event, on the other hand, the longterm baseflow component of flow is generally much smaller than the quick and slow components of streamflow. (i.e. ltbf << flowq, ltbf << flows) Assuming that the dissolved metal concentrations are not orders-of-magnitude different from one another, then:

$$[M_d]_{net} = \frac{[M_d]_{quick}flowq + [M_d]_{slow}flows + [M_d]_{ltbf}ltbf}{flowq + flows + ltbf}$$

$$\approx \frac{[M_d]_{quick}flowq + [M_d]_{slow}flows}{flowq + flows}$$

Since $[M_d]_{quick}$ and $[M_d]_{slow}$ were assumed to be cleaner than $[M_d]_{ltbf}$, then the dissolved metal concentration of the river would be lower during storm conditions than during low flows.

For simplification purposes, the dissolved metal concentrations of each of the components ($[M_d]_{quick}$, $[M_d]_{slow}$, $[M_d]_{ltbf}$) from each of the sub-basins will be assumed constant in time; however, the time-constant-values can still be different from one another. (See section VI.3.4.1 for discussion concerning assumption) Furthermore, it is re-emphasized that although the individual components are assumed constant in time, the net dissolved metal concentration coming from a particular sub-basin can vary in time due to changes in the relative contributions of each of the flow components (as presented in the example above).

For the Woburn West sub-basin, there is only one dissolved metal component since only one streamflow component is considered, or:

$$F_t = [M_d]flowt$$

Once the dissolved metal inputs from each sub-basin enter the main channels, the dissolved metal fluxes are then routed and combined in a sequence that is identical to the sequence used for streamflow. At the Atlantic Gelatin site, dissolved metals are assumed to be removed from the river along with the streamflow withdrawal.

IV.5.4 Suspended Sediment Components

The data indicate that along the Aberjona River different streamflow components have different sediment input characteristics. Given this observation, sediment inputs for the Woburn North, Woburn Central, and Winchester sub-basins were separated into (figure IV.5-3): 1) quick suspended sediments, "$smqs_{input}$", 2) slow suspended sediments, "$smss_{input}$", and 3) longterm baseflow suspended sediments, "$smbf_{input}$".

A build-up/wash-off mechanism (Hedges, et. al., 1986) apparently dominates the quick sediment source which contributes sediment to the river when either quick flow or rainfall are active. For example, for two storms in succession (figure IV.3-20), the turbidity record indicates that a large quantity of sediment was transported by the river during the first storm. During the second event, which followed after 2 days, suspended sediment concentrations did not increase to the same level as observed in the antecedent event. Apparently, prior to the first event the quick sediment supply had been "built-up", such that once the quick streamflow and rainfall were active, a burst of sediment was supplied to the river. During the second event, however, quick sediments were no longer available because they were "washed-off" by the antecedent event.

Slow and longterm baseflow sediments are characterized by low and relatively constant suspended sediment concentrations. Conceptually, these sediments are considered to be associated with groundwater inflows which have *a potential for forming particles* upon entering the river.

The data also indicate that during some conditions channel deposition and erosion may affect the amount of sediment transported from a given sub-basin. For example, during extremely low flows, suspended sediment concentrations were observed to decrease linearly with streamflow (see section IV.3). The interpretation of this trend was that during these extremely low flow conditions, the transport capacity of the river had been reached and the excess sediment was being deposited within the channel.

Since data indicate that channel deposition and erosion can occur, the sediment transport model for the Aberjona sub-basins also includes relationships by which sediment erosion, "$smch_{eros}$", deposition, "$smch_{depos}$", and transportable channel sediment, "$smch_{tr}$" *within each sub-basin*[8] can be quantified. (figure IV.5-3) For the model, if the sum of the sediment inputs, smtot, ($smqs_{input}$ + $smss_{input}$ + $smbf_{input}$ + $smch_{eros}$) exceeds the transport capacity, then the excess is deposited within the sub-basin channel. The

[8]In addition to the main channels (Channel 1 and Channel 2) each sub-basin is also assumed to have a channel component in which sediment deposition and erosion can occur. Routing of quick and slow effective rainfalls from each sub-basin is performed using unit hydrographs. Channel routing of sediments *within a sub-basin* is not considered.

amount deposited from each input is weighted on the mass contribution of that input. (See section V.1.2.1 for details) The difference between the input and the excess removed is the amount transported from each sub-basin. If the sum of the sediment inputs do not exceed the transport capacity, then the amount transported from the sub-basin is equal to the input (i.e. $smqs_{tr}=smqs_{input}$, $smss_{tr}=smss_{input}$, $smbf_{tr}=smbf_{input}$, $smch_{tr}=smch_{eros}$). The source of channel sediments (within each sub-basin) is assumed to only come from quick, slow, or longterm baseflow sediments which were deposited in the sub-basin channel during earlier times.

As discussed in section IV.3.3, sediment transport from the Woburn West sub-basin differs from transport along the Aberjona River. For this basin, sediment transport is characterized by two distinct types of sediment: organic and inorganic sediments. For the organic phase, the longer the hydraulic residence time and the higher the water temperature, the larger the organic suspended sediment concentration. In capturing this effect, the Wedge Pond reservoir is modeled as a continuous-flow stirred-tank reactor for the growth of organic particles.

The inorganic phase was correlated with Wedge Pond hydraulic residence times; the longer the residence time the lower the inorganic suspended sediment concentration. The interpretation of this trend is that increased residence times within the reservoir permit more efficient settling of inorganic particulates.

Therefore, the sediment transport model for the Woburn West sub-basin, consists of two parts. One part is a continuous-flow stirred tank-reactor model which computes the organic suspended sediment concentration. The other part, estimates the inorganic concentration by relating it to hydraulic residence times.

Once the sediment contributions from each sub-basin are determined, the contributions are then routed and combined in a sequence which is dictated by watershed geometry. (figure IV.5-4) The sequence is very similar to the sequence used for streamflow. The main differences are that: 1) at the end of each main channel unit (Channel 1 and Channel 2) a sediment deposition and erosion check is also included, and 2) at the Atlantic Gelatin site sediments are *not* removed along with the streamflow.

A sediment deposition and erosion check is needed at the end of each main channel unit (Channel 1 and Channel 2) because the routing scheme redistributes the time history of the water and sediment fluxes. In other words, because of the redistribution of flow relative to sediment fluxes, there is a possibility that on the downstream end of each main channel unit the sediment transport capacity may be exceeded. Furthermore, if the capacity is not exceeded, there is the possibility of eroding channel sediments that

were deposited during earlier times. The only source of sediments in the main channels is from routed sediments that were deposited when the transport capacity was exceeded.

At the Atlantic Gelatin site, suspended sediments associated with the withdrawal are assumed to remain within the channel. Once the water is removed (without the sediment), then relationships quantifying channel deposition and erosion are applied. The relationships used are similar to those used for each Aberjona sub-basin and for each main channel unit.

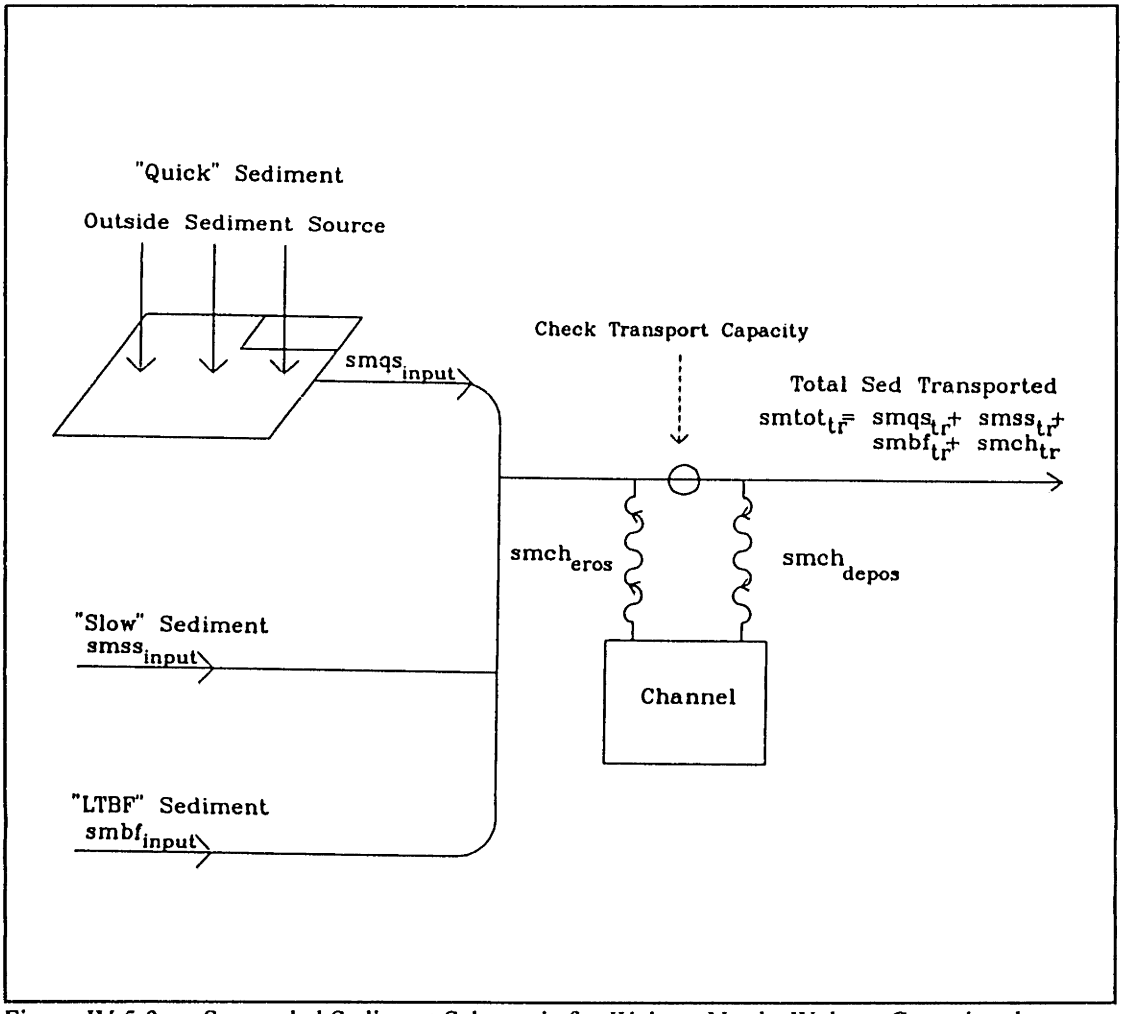

Figure IV.5-3: Suspended Sediment Schematic for Woburn North, Woburn Central and Winchester Sub-basins (Subscript "tr" implies a transported quantity)

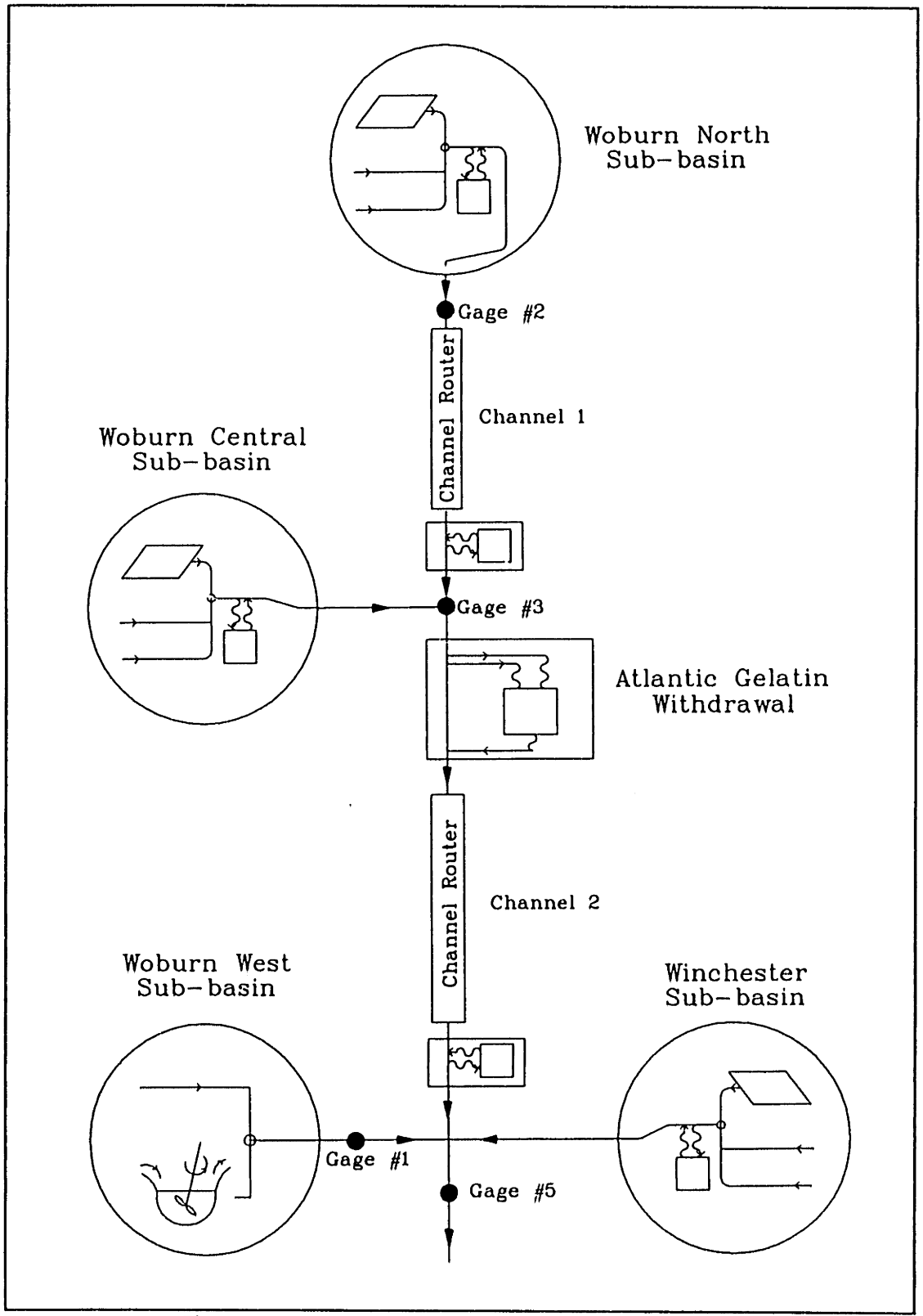

Figure IV.5-4: Model of Suspended Sediment Components

IV.5.5 Particulate Metals

My interpretation of particulate metal transport is very similar to my interpretation for dissolved metal transport in that particulate metals transported *from each sub-basin on the Aberjona River* can be sub-divided into components, where:

$$F_t = [M_p]_{net} \frac{dsmtot_{tr}}{dt} = F_{quick} + F_{slow} + F_{ltbf} + F_{ch}$$

$$= [M_p]_{quick} \frac{dsmqs_{tr}}{dt} + [M_p]_{slow} \frac{dsmss_{tr}}{dt} + [M_p]_{ltbf} \frac{dsmbf_{tr}}{dt}$$

$$+ \{frq[M_p]_{quick} + frs[M_p]_{slow} + (1\text{-}frq\text{-}frs)[M_p]_{ltbf}\} \frac{dsmch_{tr}}{dt}$$

where: F_t = Total Particulate Metal Flux

$[M_p]_{net}$ = Net Particulate Metal Concentration of Suspended Sediments Coming From an Aberjona Sub-basin (mass metal/mass ss)

$smtot_{tr}$ = Total Sediment Mass Transported from an Aberjona Sub-basin $= smqs_{tr} + smss_{tr} + smbf_{tr} + smch_{tr}$

t = time

F_{quick} = Particulate Metal Flux Associated with Quick Sediments

F_{slow} = Particulate Metal Flux Associated with Slow Sediments

F_{ltbf} = Particulate Metal Flux Associated with Longterm Baseflow Sediments

F_{ch} = Particulate Metal Flux Associated with Channel Sediments

$[M_p]_i$ = Particulate Metal Concentration Associated with Suspended Sediment Component i, (mass metal/mass ss)

frq = Fraction of Channel Sediment From Quick Suspended Sediments

frs = Fraction of Channel Sediment From Slow Suspended Sediments

By sub-dividing the total metal flux into components as given above, the observed changes in the river particulate metal concentrations, can be explained by changes in the relative contributions of each of the particulate metal components. Arguments similar to those presented in section IV.5.3 for the dissolved phase can be used to explain changes in "$[M_p]_{net}$" for the particulate phase.

As for the dissolved phase, the particulate metal concentrations of each of the components ($[M_p]_{quick}$, $[M_p]_{slow}$, $[M_p]_{ltbf}$) from each of the sub-basins will be assumed constant in time. However, the time-constant-values can still be different from one another. (Refer to section VI.3.4.1 for discussion concerning this assumption)

For the Woburn West sub-basin, only one component of the particulate metal flux is considered:

$$F_t = [M_p] \frac{d\text{smtot}}{dt}$$

where: smtot = Sum of the Organic and Inorganic Suspended Sediments, mass

Once the particulate metal inputs from each sub-basin enter the main channels, the particulate metal fluxes are then routed and combined in a sequence that is identical to the sequence used for suspended sediments. At the Atlantic Gelatin site, particulate metals are assumed to deposit and erode in association with the suspended sediments.

V. METAL TRANSPORT MODEL

V.1 FORMULATION OF THE COMPUTER MODEL

Purpose of the Computer Model

The purposes of the computer model are to: 1) organize individual aspects of the conceptual model into a coherent model for the entire watershed, 2) improve our understanding of metal transport processes, and 3) provide a time-efficient means by which metal fluxes can be computed over long (yearly) time scales.

Individual aspects of the conceptual model presented in section IV.5 are straight forward and simple to apply. However, the model becomes much more complicated when combining all components to estimate transport for the entire watershed. A computer model is an ideal tool for such a situation since it is an efficient means by which a coherent model can be developed from individual model units.

By organizing our ideas, the computer model provides us with feedback concerning our understanding of the mechanisms of transport. If the fit between the computer results and observed data are poor, the original formulation may then be considered inadequate and should then be modified. Upon modification, the computer model can be re-run and the results can then be re-evaluated. The cycle of model formulation with subsequent modification improves our understanding of transport mechanisms by permitting us to converge on a set of mechanisms which provide a plausible explanation for the observed trends in transport.

The model was written as a continuous model (models both low flows and storm flows) using an hourly time step. This type of model was needed because the data indicate that: 1) both storm flows and low flow conditions are of significance, and 2) during storm events metal fluxes vary significantly from hour to hour. Because of the short time step and long (yearly) simulation time, the only time-efficient means of performing the computations was by using a computer model.

Need for a New Computer Model

Rather than using commercially available models, a new computer model was developed. The model developed is considered to be watershed specific rather than general purpose.

Development of a new computer model for the Aberjona River was necessary for two reasons: organization and flexibility. By developing a new model, computational aspects of several different models can be organized into one model, which greatly simplifies running the program. For example, HEC-1 (U.S. Army Corps of Engineers, 1987) could have been used to estimate quick and slow flows

using a unit hydrograph technique, whereas a separate program could have been written to model the yearly fluctuation of the longterm baseflow component. The output of each of these models would then have to be coupled with adequate sediment and contaminant transport models. By developing a new model, the complication of using several different commercially available models is averted.

Developing a new model provides much needed flexibility when developing equations for modeling transport processes. For example, the build-up and wash-off relationships used in the SWMM model (Overton, 1976) have been modified significantly within the present study. These modifications were possible only by developing our own source code.

Type of Model Developed

Types of computer models range from physically-based models to regression models. Physically-based models quantify processes through fundamental physical relationships. For example, in modeling sediment transport a physically-based model may use equations for conservation of sediment mass, conservation of flow, and the full momentum equations. For physically-based models, the equations and parameters can be determined from the characteristics of the system being modeled and therefore a *true* physically-based model does not require field data prior to its application. In hydrologic applications, however, field data is usually needed since the characteristics of hydrologic systems are not entirely known and because many of the "theoretical" relationships used in practice represent a simplified version of the physics.

Regression type models, on the other hand, are not based upon fundamental physical relationships. Rather, the equations used in these models are best-fit relationships between one measurable parameter and another. The equations and parameters used in a regression model are determined after an adequate set of field data is collected.

The model developed in this study is considered to be semi-physically based. It is like a physically-based model in that within each model unit there is a physical interpretation of the processes being modeled. However, the model is like a regression model in that the equations were not derived directly from theory. Furthermore, for the model developed in this study, some of the calibration parameters do have a direct physical interpretation, whereas, others may represent a combination of several physically-based parameters lumped into one parameter.

The reason a semi-physically based model was chosen is because: 1) of its computational simplicity, and 2) it enables us to establish some of the physical processes governing transport. Computationally simple models are desirable because they reduce the time needed for model development and for model runs.

Establishment of physical processes enables us to: 1) better predict transport for a situation for which there are no observations, and 2) predict the trends for watersheds whose transport is governed by similar physical processes.

V.1.1 Basic Model Units: Model Flow Diagrams

Flow diagrams for the computer model are given in figures V.1-1 to V.1-4. These diagrams correspond to the four major units of the model: 1) sub-basin model for the Woburn North, Woburn Central, and Winchester sub-basins (section V.1.1.1), 2) sub-basin model for the Woburn West sub-basin (section V.1.1.2), 3) model for the Atlantic Gelatin area (V.1.1.3), and 4) a model for channels (section V.1.1.4). Section V.1.1.5 describes the computation sequence of model units in the main program. The model source code is included in appendix V.A and V.B.

For details concerning the formulation of each of the model units, please refer to section V.1.2.

V.1.1.1 Sub-basin Model for Woburn North, Woburn Central, and Winchester Sub-basins: Outline

The inputs into the Woburn North, Woburn Central, and Winchester sub-basin model include hourly precipitation, and hourly temperature. (figure V.1-1) If the temperature is greater than 32 °F then the precipitation occurs as rain; if not, precipitation occurs as snow. From the hourly time sequence of rainfall, the effective rainfall (that portion of the rainfall that contributes directly to streamflow) is then calculated for the quick and slow systems. Effective rainfall computation for the quick system involves the separation of the hourly sequence of rainfall into individual storms using storm separation criteria specific to the quick system. For each storm, the total rainfall is then reduced to an effective rainfall by applying a quick-system abstraction parameter and a quick-system runoff coefficient. The slow effective rainfall is computed in a similar fashion as for the quick system except that slow-system parameters are used. The result is the computation of two different effective rainfalls: a quick-system effective rainfall and a slow-system effective rainfall.

A unit hydrograph technique is then used to route the effective rainfall to streamflow. Quick flow is computed using the quick effective rainfall and a quick unit hydrograph while slow flow is computed using the slow effective rainfall and a slow unit hydrograph.

Snow will accumulate as long as the temperature remains at or below 32 °F. Once the temperature rises above 32 °F, criteria are invoked by which the snowmelt process is initiated. Once the snow begins to melt, a degree-hour method is used to quantify the amount of snowmelt. Effective snowmelt is computed in a similar fashion as for effective rainfall described above, except that melt-system parameters are used. A melt-flow unit hydrograph is then used to route the effective snowmelt. A fraction of the melt flow is then applied to the quick system while the remaining fraction is applied to the slow system.

Parameters which are used to estimate the longterm baseflow are also included as part of the input. These parameters include: 1) maximum, average, and minimum bi-monthly longterm baseflows as obtained from the gage 5 (USGS) record and, 2) maximum, average, and minimum monthly precipitation as obtained from the Reading station record. To estimate the longterm baseflow at gage 5 for a model simulation step, the antecedent precipitation for the model period is compared to the historical precipitation and historical longterm-baseflow records. The maximum longterm baseflow is then computed for a given sub-basin. For a sub-basin, the maximum longterm-baseflow component is based upon: 1) the simulation-step longterm-baseflow value determined at gage 5, 2) a multiplicative factor to estimate the maximum, 3) mass balance considerations, and 4) the areas of each of the individual sub-basins. The longterm baseflow computed in this manner is then adjusted by assuming a linear increase in time during storm conditions and an exponential decrease in time after a storm event.

The total flow from a sub-basin is computed by summing the adjusted quick, adjusted slow, and longterm baseflows. Once each flow component has been determined, the dissolved-metal model is invoked, and assigns dissolved-metal concentrations to each component.

After computation of the flow components, suspended sediment fluxes are then determined. Suspended sediment transport is separated into fluxes associated with quick, slow, longterm baseflow, and channel suspended sediments. Quick suspended sediments are modeled by assuming that there is an area physically separated from the river where sediments can accumulate. When either quick flow or rainfall is active, sediments can be flushed from this area to provide a supply of sediments to the river. Slow and longterm-baseflow sediments are modeled with low and constant suspended sediment concentrations. Channel sediments are a mixture of quick, slow, or longterm-baseflow sediments which have been deposited during prior time steps. Deposition and erosion of the channel sediments is based on a balance between sediment input and river transport capacities.

Once each component of suspended sediment has been determined, the particulate-metal flux is then modeled by assigning to each sub-basin and to each component, a particulate-metal concentration (per mass of suspended sediment basis).

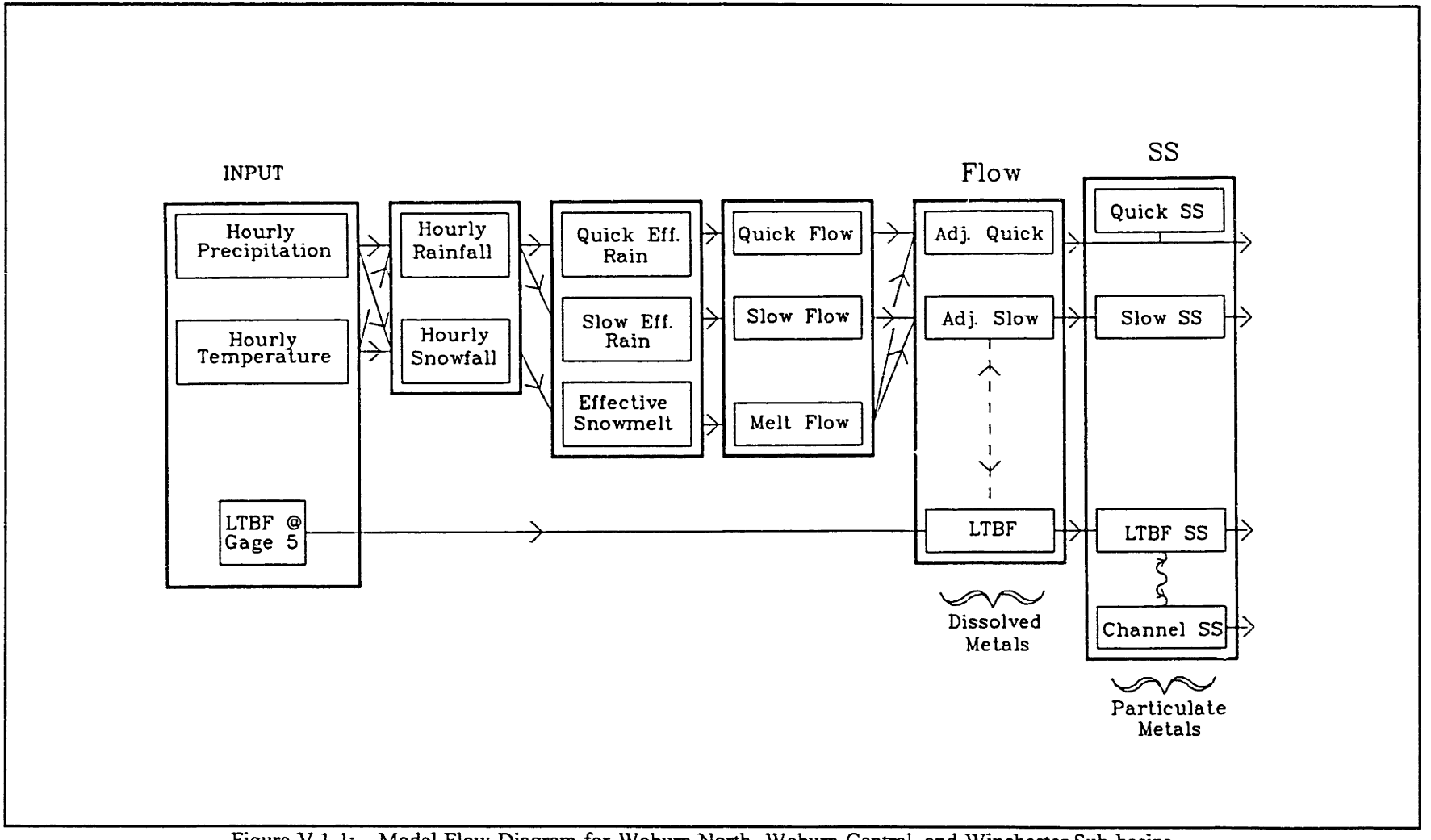

Figure V.1-1: Model Flow Diagram for Woburn North, Woburn Central, and Winchester Sub-basins

V.1.1.2 Sub-basin Model for the Woburn West Sub-basin: Outline

Inputs into the Woburn West sub-basin model (figure V.1-2) include: 1) streamflow, 2) water temperature, and 3) organic suspended sediment concentration in the inflow.

For this sub-basin, streamflow is assumed to consist of one component: the total streamflow. The input of the total hourly streamflow consists of an interpolation of monthly streamflows as observed at Gage #1 during the period of record. The reason for this simplification is that during storm events: 1) consistently distinct components of flow were not apparent, and 2) the contribution of the Woburn West sub-basin to streamflow along the Aberjona River was relatively small.

The data indicate that suspended sediments from this sub-basin can be separated into two distinct types: organic and inorganic sediments. Observations show that organic suspended sediments are strongly correlated with water temperature and with visual observations of high algal growth in the Wedge Pond reservoir. In capturing this effect, the Wedge Pond reservoir is modeled as a continuous-flow stirred-tank reactor for the growth of organic particulates. The organic suspended sediment concentration in the inflow to reservoir is assumed to be a constant in time. Within the reservoir, the concentration of organic suspended sediments is a function of the growth rate of organic particles and the hydraulic residence time of the water. The growth rate is assumed to be a function of water temperature. The hydraulic residence time is a function of streamflow and reservoir volume.

The inorganic suspended sediments are correlated with the hydraulic residence time of the Wedge Pond reservoir. The longer the residence time the lower the inorganic suspended sediment concentration. The interpretation of this trend is that the reservoir essentially acts as a settling basin for inorganic particles. For this model, the inorganic concentration in the outflow is assumed to be inversely proportional to the residence time of the water.

For the dissolved phase, a dissolved-metal concentration is assigned to the total flow. Similarly, for the particulate phase, a constant particulate-metal concentration is assigned to the sum of the organic and inorganic suspended sediment fluxes. These concentrations are representative of the overall average dissolved and particulate concentrations observed at Gage #1. The need for a more elaborate model for metals is not warranted since the flux of metals from this sub-basin represents a relatively small contribution to the total metal flux on the Aberjona River.

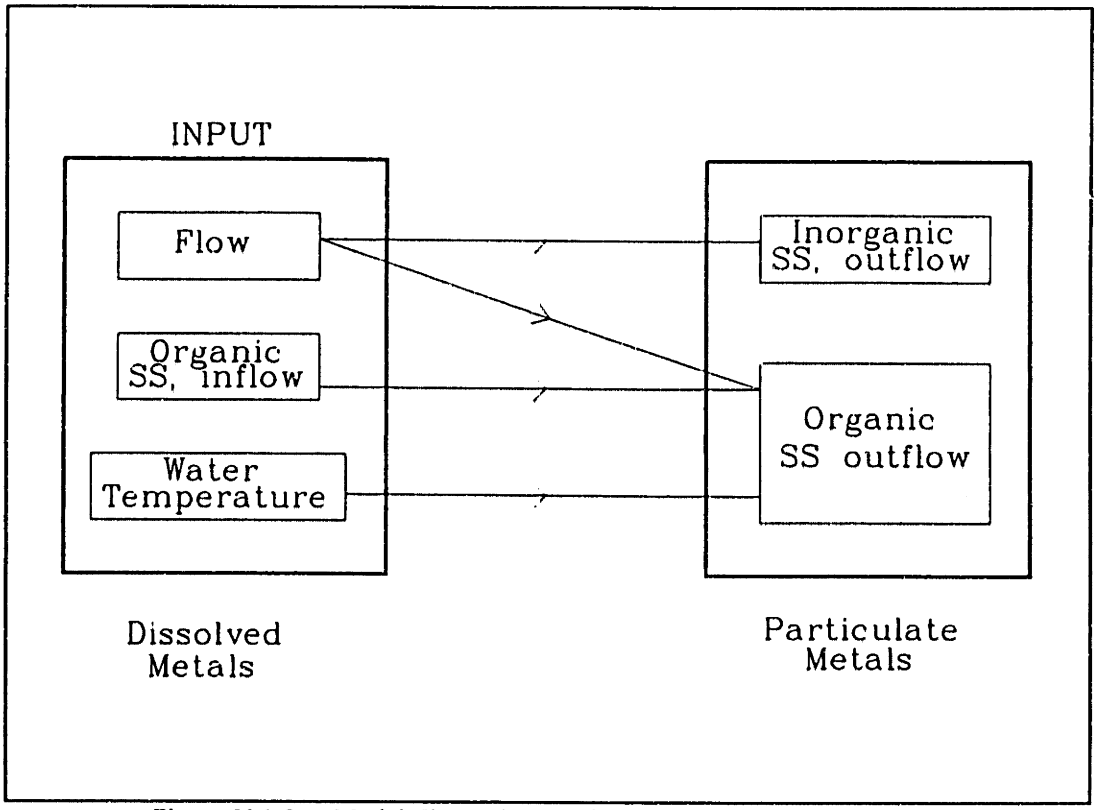

Figure V.1-2: Model Flow Diagram for the Woburn West Sub-basin

V.1.1.3 Model for the Atlantic Gelatin Area: Outline

The Atlantic Gelatin area is modeled using mass conservation. (figure V.1-3) The groundwater removed from the Atlantic Gelatin site is assumed to be removed directly from the river. All the suspended sediments associated with the withdrawal are assumed to remain within the channel. (See section VI.3.4.1 for discussion of these assumptions) If the transport capacity of the river is exceeded, then the suspended sediments will deposit and accumulate; if not, previously deposited sediments can then be eroded from the channel bed. Dissolved metals are assumed to be removed along with the groundwater withdrawal, whereas the particulate metals are assumed to remain within the channel.

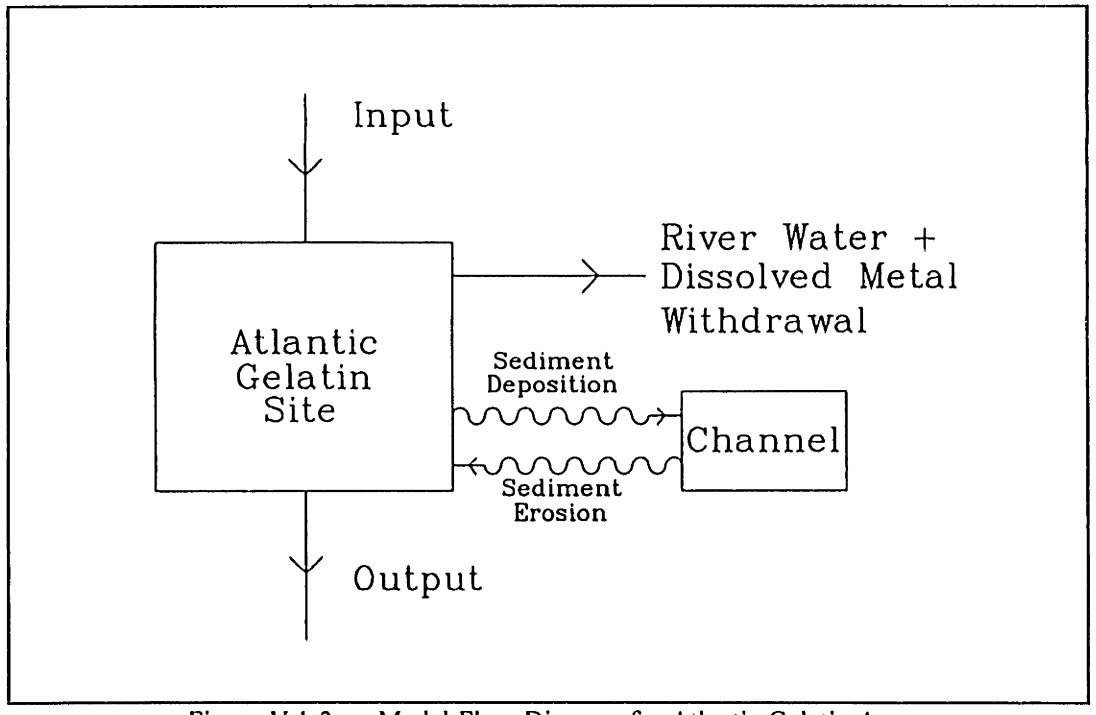

Figure V.1-3: Model Flow Diagram for Atlantic Gelatin Area

V.1.1.4 Model for Main Channels: Outline

The purpose of the channels is to route the water, sediment, and metals from sub-basin to sub-basin, (figure V.1-4) In this way, the timing effects of waters and sediments coming from different areas of the watershed can be captured.

The routing procedure used for streamflow is the Muskingum method. (McCarthy, 1940) This procedure was modified (Section V.1.2.4) such that the same method could be used to route sediment and metal fluxes. The inputs into the channel, are the combined flows, suspended sediment, and metal fluxes at the upstream end of each channel. The Muskingum router functions to attenuate the peaks and translate the centroid of the input in time. In doing so, the router redistributes the time history of streamflow relative to suspended sediment fluxes.

Due to the redistribution of streamflow and suspended sediment, a sediment deposition and erosion check is included at the end of each channel. If the suspended sediment flux at the end of the channel exceeds the transport capacity, then the excess is deposited. If the flux is lower than the capacity, then suspended sediment can be eroded. (Refer to section V.1.1.5; *Channel Suspended Sediments* and section V.1.2.4 for details)

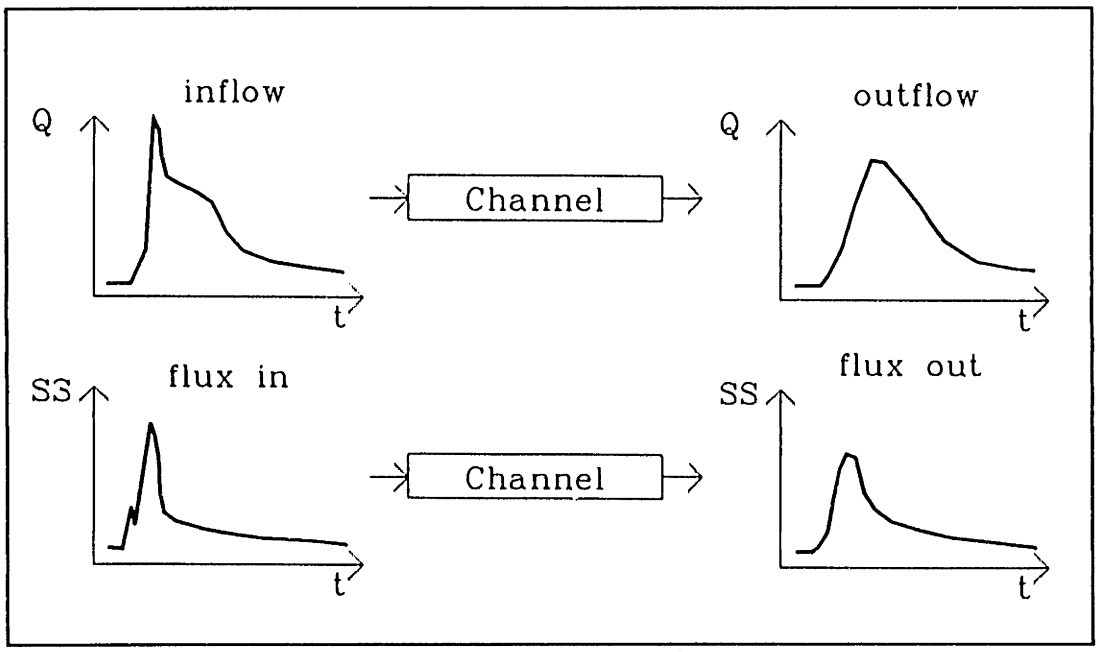

Figure V.1-4: Model Schematic for Channels

V.1.1.5 Computation Sequence of Model Units in the Main Program

The program begins by initiating variables that are needed for subsequent computations. These initial steps include: 1) setting the number of hours to be modeled, 2) the identification of the start date and time, 3) reading the rainfall and temperature data input, 4) setting the Atlantic Gelatin withdrawal rate, 5) reading baseflow parameters, and 6) reading the flow input for the Woburn West sub-basin.

Sequence of Major Computation Steps

After initiating the variables, computations for major units of the program proceed in a downstream direction. (figure IV.5-1) In other words, all flow, suspended sediment, and metal transport computations are performed first for the Woburn North sub-basin. The next unit modeled is channel 1 which routes streamflow, sediment, and metal fluxes from gage #2 to gage #3. Variables are then computed for the Woburn Central sub-basin and the results are then combined with the routed variables from channel 1. The net result provides the modeled variables at gage 3.

After gage 3, the water, sediment, and metal fluxes are adjusted due to the Atlantic Gelatin withdrawal. After the adjustment, the water, sediment, and metal fluxes are routed through channel 2. Variables are then computed for the Woburn West and the Winchester sub-basins. The sub-basin fluxes are then combined with the routed fluxes from channel 2. The net result provides the modeled variables at gage 5.

As the various steps are performed, various input and output files are accessed. A summary of the program input and output files is provided in appendix V.A.

Computation Sequence for the Aberjona Sub-basin Model

Computations for the Aberjona sub-basins begin by computing each streamflow component. The computation begins with reading sub-basin parameters and unit hydrograph ordinates for the quick, slow, and melt flow systems. After reading the parameters, quick flows, slow flows, melt flows, and longterm baseflows are computed in that order. Quick flow is determined by computing the effective rainfall for the quick system and then routing the effective rainfall using the quick unit hydrograph. The slow flow is then computed using a method that is identical to the quick flow except that the parameters corresponding the slow system are used. Computations for the melt system begin by first quantifying the amount of snow that melts at each time step. Parameters corresponding to the melt system are then used to quantify the effective snowmelt and the melt flow. Once the melt flow is determined, a fraction of the melt flow is added to the quick system while the remaining fraction is added to the slow system, such that the adjusted quick and adjusted slow flows are computed. Longterm-baseflow computations

begin by determining the antecedent precipitation at each time step. This antecedent precipitation is compared with the historical record of precipitation and the historical record of longterm baseflow to estimate the longterm baseflow during each time step for the model year.

After the streamflow computations, the model then proceeds to compute the suspended sediment from each of the Aberjona sub-basins. In the computation, the rising limb and the falling limb of the streamflow hydrograph are determined and the suspended sediment parameters are read by the program. Next, sediment inputs associated with quick, slow, and longterm baseflows and the erosion of channel sediments are computed. The sum of the sediment inputs is then compared to the transport capacity. If the inputs exceed the capacity, then the excess sediment is deposited; if not, all inputs are transported from the sub-basin. If excess sediments are deposited in the sub-basin channel, the program will update the fraction of the channel sediments that are associated with quick and slow sediment sources.

After completing the suspended sediment computations, metal transport from each of the Aberjona sub-basins is then computed. The metal transport computation begins by reading the dissolved and particulate metal concentrations associated with each component from the given sub-basin. Dissolved iron, arsenic, chromium, and copper fluxes are then computed for each streamflow component. Particulate iron, arsenic, chromium, and copper fluxes are similarly computed for each suspended sediment component.

Computation Sequence for the Woburn West Sub-basin Model

Streamflow for the Woburn West sub-basin is an input into the model and is read at the very beginning of the main program. Suspended sediment and metal computations are performed after the channel 2 routing step. The suspended sediment computation begins by initializing various sediment transport and metal concentration parameters. At each time step, the inorganic suspended sediment concentration, the organic concentration, the dissolved-metal fluxes (for iron, arsenic, chromium, and copper) and the particulate-metal fluxes are computed.

Computation Sequence for the Atlantic Gelatin Site

At the Atlantic Gelatin site, streamflow from the upstream combination point (at gage #3) is reduced according to the assigned withdrawal rate. Sediment and metal fluxes are then adjusted due to the withdrawal. The suspended sediment adjustment begins with the determination of the rising and the falling limb of the streamflow hydrograph and reading suspended sediment parameters. Within a given time step, 1) the deposition of sediments due to the water withdrawal is computed, 2) the amount of channel sediment that can be potentially eroded is calculated, and 3) the actual amount of suspended sediment that is transported is computed from transport capacity considerations. The dissolved-metal

flux through the Atlantic Gelatin site is reduced in accordance with the amount of water withdrawn whereas the particulate-metal flux is adjusted in accordance with sediment deposition and erosion.

Computation Sequence for Main Channel Components

Channel computations begin by setting channel routing parameters. Computations proceed by routing streamflow, suspended sediments, and metals through the channel. After the routing procedure, a deposition and erosion check is performed. The deposition/erosion check begins by determining the rising and the falling limbs of the streamflow hydrograph and by reading suspended sediment parameters. At each computation step: 1) the amount of channel sediment that can be eroded is computed, and 2) the actual amount of suspended sediment that is transported is computed from transport capacity considerations. If the transport capacity is exceeded, the excess sediment is assumed to deposit within the channel. Particulate-metal fluxes are adjusted in accordance with channel deposition and erosion.

V.1.2 Computation Details of Basic Model Units

V.1.2.1 Sub-basin Model for Woburn North, Woburn Central, and Winchester Sub-basins: Details

Inputs

The inputs to the model include hourly precipitation and hourly temperature. Input files for 1991, 1992, and 1993 are included in ASCII format in appendix V.B. Precipitation is needed for every time step throughout the model run. Temperatures are needed only if running the model for November, December, January, February, March, and/or April.

Input parameters are also included for the purpose of modeling longterm baseflows for each sub-basin. These parameters include: 1) bimonthly maximum, average, and minimum longterm baseflows as obtained from the gage 5 (USGS) record and, 2) maximum, average, and minimum monthly precipitation as obtained from the Reading station record. The corresponding input file is labeled "bf.ave" and is included in appendices V.A and V.B. These data are also plotted in figure V.1-5. On this figure, individual "x" and "+" correspond to values obtained from the data. The solid line corresponds to the average (monthly for precipitation or bi-monthly for longterm baseflow) values and the dashed lines correspond to the maximum and minimum values. Both the precipitation and longterm-baseflow data correspond to the 1957 to 1993 period of record. Identification of longterm-baseflow values from this record is described in section IV.2.4.

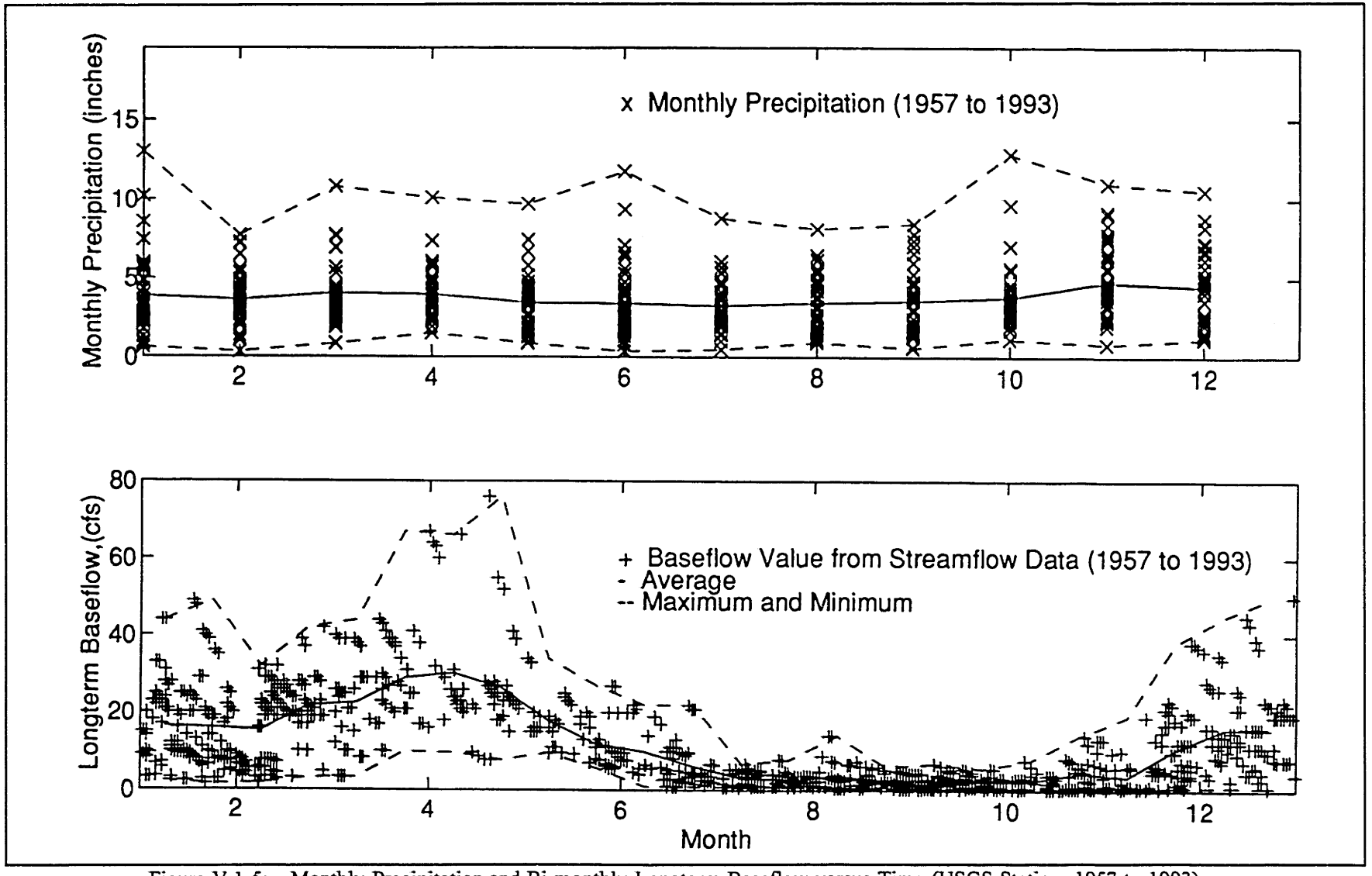

Figure V.1-5: Monthly Precipitation and Bi-monthly Longterm Baseflow versus Time (USGS Station, 1957 to 1993)

For the months of May through October (inclusive) precipitation is assumed to occur as rainfall. (figure V.1-6) From November to April, precipitation is assumed to occur either as rainfall or as snowfall. If the temperature is less than 32 °F the precipitation is assumed to occur as snow; if not, the precipitation is assumed to occur as rain.

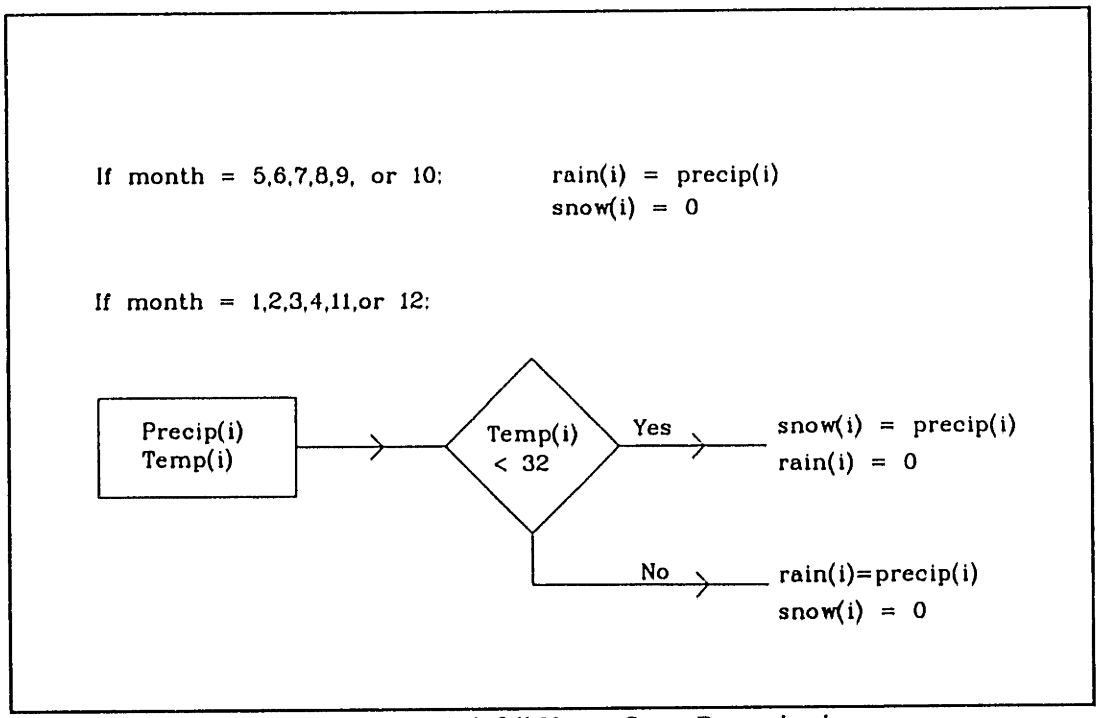

Figure V.1-6: Rainfall Versus Snow Determination

Quick and Slow Effective Rainfall

The hourly time sequence of rainfall is separated into individual storm events, using a "water response time" criterion. A water response time, WRT, can be considered as the time needed to empty most of the system of water after rainfall has ceased. The underlying assumption in the use of a water response time is that once the system is empty (or almost empty), an additional amount of water (i.e. an initial abstraction, IA) is needed before the system can start supplying water to the river. This initial abstraction is only applied when the WRT has elapsed. (figure V.1-7)

Once a storm event begins, an initial abstraction of rainfall is assumed "lost" from the system. If the total storm depth is less than the initial abstraction, no water is converted to effective rainfall. If the storm depth is greater than the initial abstraction, then a fraction, K, of the remaining rainfall is assumed to contribute to the effective rainfall. The computations are illustrated in figure V.1-7.

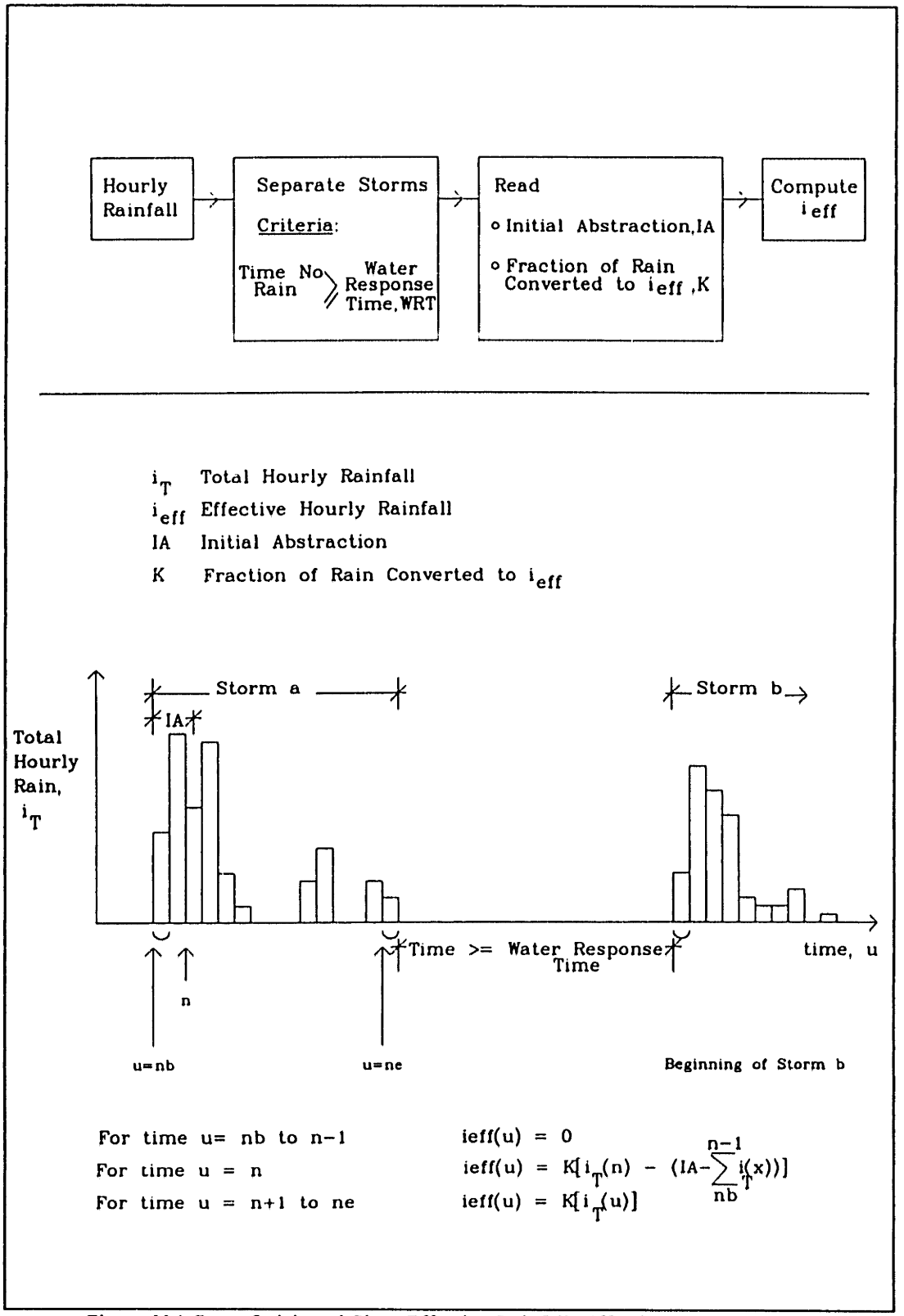

Figure V.1-7: Quick and Slow Effective Rainfall; Effective Snowmelt

Quick and Slow Flow

A unit hydrograph technique is used to convert the effective rainfall to streamflow. (Chow et. al., 1988) Initial estimates of the unit hydrographs were obtained by determining the quick and slow streamflows associated with the August 18, 1992 storm. The time distribution of the quick and slow flows was then assumed to be a result of a unit pulse of rainfall. (1 inch in one hour) In other words, the quick and slow unit hydrographs were initially estimated by normalizing the area under each hydrograph to one inch. As part of the initial analysis, unit graphs were derived for each sub-basin. The Woburn North unit graph was based upon the observed hydrograph at gage 2. The Woburn Central unit graph was based upon the difference between the hydrographs observed at gage 3 and gage 2. The Winchester unit graph was based upon the gage 5 hydrograph, minus the hydrographs from gage 1 and 3, plus a constant contribution from the Atlantic Gelatin withdrawal. Quick unit hydrographs and slow unit hydrographs were not significantly different from sub-basin to sub-basin. Therefore, one hydrograph was estimated for the quick system and one hydrograph was estimated for the slow system. The same quick and slow unit hydrographs were applied to all three sub-basins along the Aberjona River.

While calibrating the model against the 1992 data, the initial estimates of the unit hydrographs were adjusted. Numerical values of the unit hydrograph ordinates (non-normalized) are provided in input files "ui.wn", "ui.wc", and "ui.wi" in appendices V.A and V.B. Non-normalized hydrographs as inputs were satisfactory since the program was written to normalize the input graphs to 1 inch.

An outline of the computation procedure and plots of the unit hydrographs are provided in figure V.1-8. The quick and slow unit hydrographs are plotted in greater detail in figures V.1-9, and V.1-10. The quick unit graph is characterized by a sharp peak which occurs over a relatively short time scale. The slow unit graph is characterized by a smoother peak with a long tail. The time base and centroid of the quick hydrograph are 9 and 5 hours, respectively. For the slow unit graph, the time base and centroid are 74 and 20 hours, respectively.

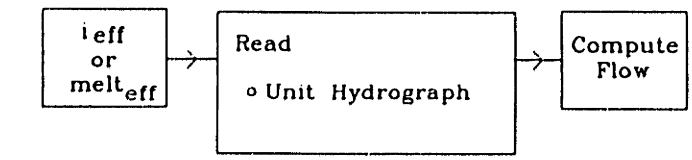

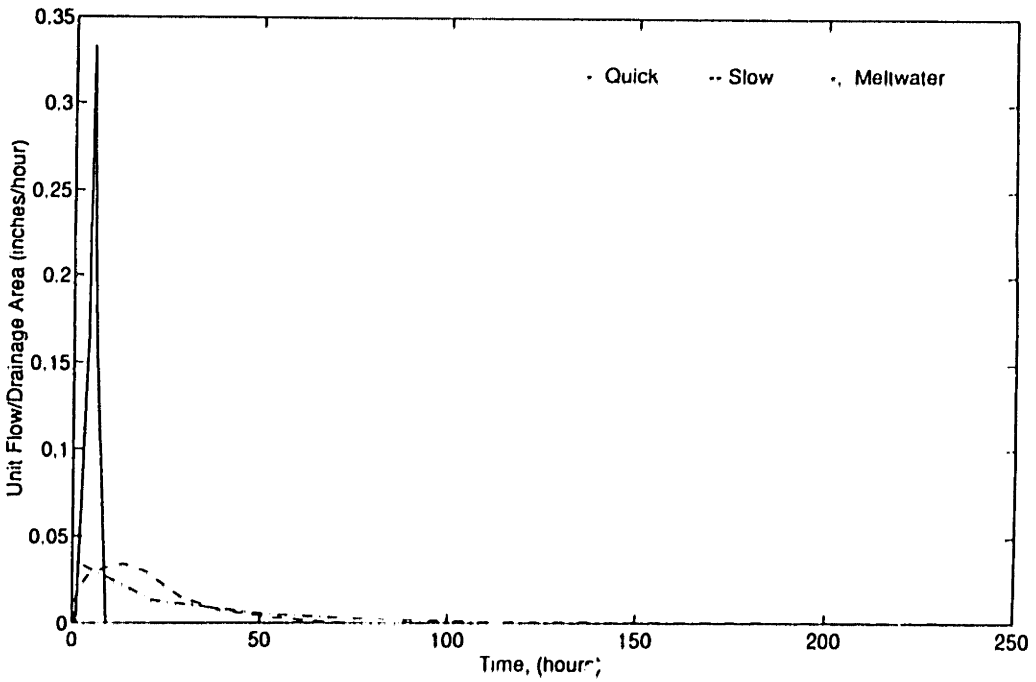

$$\text{Flow}\ (i) = \sum_{j=k}^{i} i_{eff}\,(j) \cdot U(i-j-1)$$

U = Unit Hydrograph Ordinate

i_{eff} = Effective Rainfall

Figure V.1-8: Quick, Slow, and Meltwater Flows

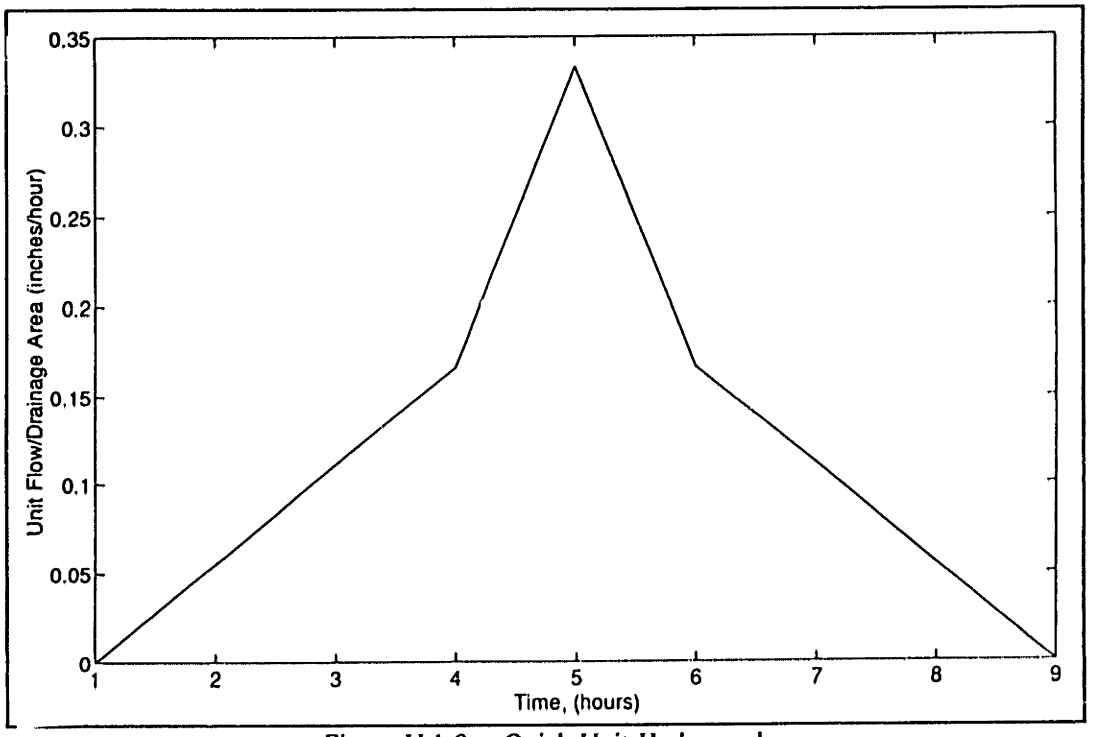

Figure V.1-9: Quick Unit Hydrograph

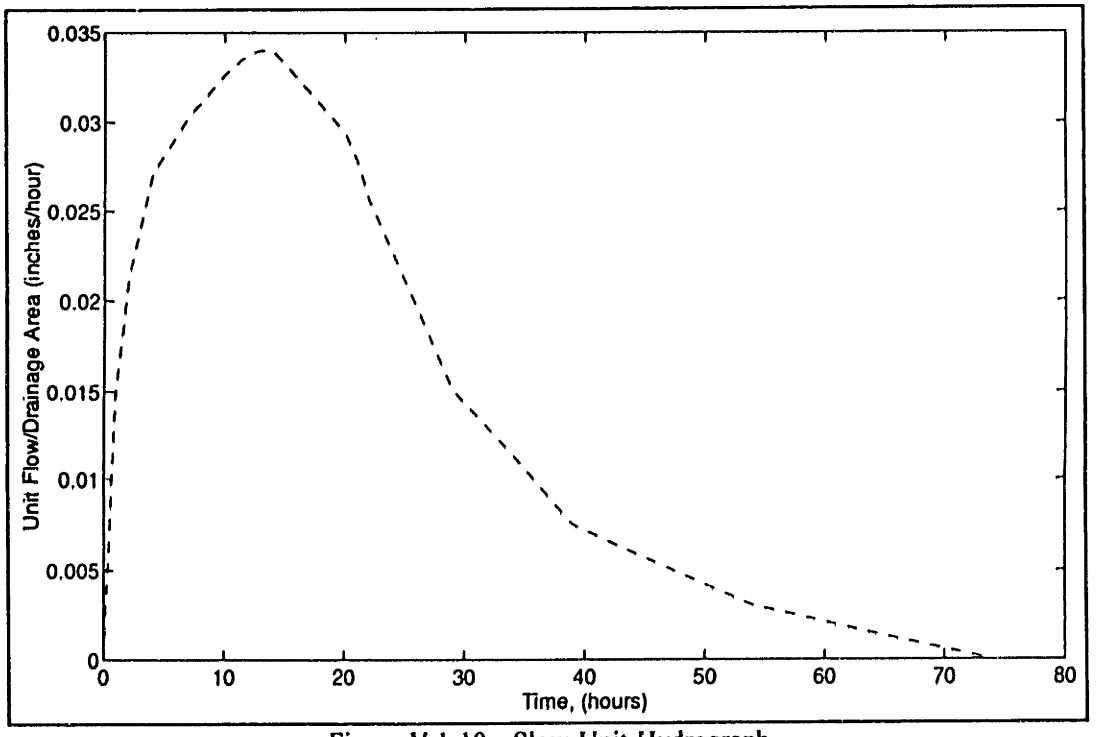

Figure V.1-10: Slow Unit Hydrograph

Effective Snowmelt

Once the temperature rises above 32 °F, snowmelt has the possibility of being initiated. (figure V.1-11) The initiation of snowmelt is based upon a degree-hour criterion, lagdh. The lagdh is the sum of the degree-hours in the current and previous six time steps, inclusive. If there is no rain in the current time step, then a lagdh greater than 80 degree-hours is needed to initiate snowmelt. If it is raining in the current time step, then a lagdh greater than 18 degree-hours is needed to initiate snowmelt. The values of lagdh for snowmelt initiation were determined by calibrating the model against the 1993 streamflow data at gage 5.

The basis for use of a lagdh parameter is that snow does not immediately melt once the temperature increases above 32 °F. Rather, a certain amount of heat must be applied to the snow to: 1) raise the temperature of the snow to 32 °F and 2) to overcome the latent heat of fusion of the snow. To permit for the heat transfer, above-freezing temperatures applied over specified time are required to initiate the melting process.

The lagdh required to initiate the snowmelt process is smaller for times when it is raining. The basis for this assumption is that when it rains there is a heat transfer to the snow from two sources: from the rain water and from the air. When it is not raining, there is a heat transfer from the air only. To further make the snow melt process occur faster during a rainfall event, one may also note that: 1) the heat transfer capacity of water (i.e. thermal conductivity) is more than an order of magnitude higher than the transfer capacity of air (Lide, 1991) and 2) rain can penetrate considerable depths into the snow resulting in a mass transport of heat which is distributed more uniformly throughout the snow pack. (Gray & Male, 1981) Therefore, for a given temperature rise, snowmelt would be initiated at an earlier time if rainfall also were occurring.

Once the snowmelt process is initiated, the potential meltwater, meltp, in inches of equivalent rainfall, is computed. One of two relationships may be applied. One corresponds to a time step without rainfall and the other corresponds to a time step with rainfall. The relationships used are:

$$\text{if rain(i)} = 0\text{: meltp(i)} = \text{snowf1(temp(i)-32)}^{a} \qquad \text{eqn. V.1-1}$$

$$\text{if rain(i)} > 0\text{: meltp(i)} = \text{snowf2(temp(i)-32)}^{a}\text{(rain(i)}\cdot 100)^{a} \qquad \text{eqn. V.1-2}$$

where: rain(i) = Rainfall in Current Time Step,i (inches)
temp(i) = Temperature in Current Time Step (°F)
snowf1 = Snow Factor 1, Constant
snowf2 = Snow Factor 2, Constant
a = Exponent, Constant

The potential meltwater is then compared to the amount of snow remaining in storage, snaccum, in inches of equivalent rainfall. If snaccum is greater than meltp, then the amount of snowmelt, melt, is equal to meltp; if not, snowmelt is equal to snaccum. The snowmelt cycle ends once the temperature reaches 32 °F.

Snowmelt is then converted to effective snowmelt using the same procedure used to convert rainfall to quick effective rainfall and slow effective rainfall. (figure V.1-7) The hourly time sequence of snowmelt is separated into individual melt events using a water response time, WRT_m, parameter. Once a melt event begins, an initial abstraction of snowmelt, IA_m, is assumed "lost" from the system. The effective snowmelt is then equal to a fraction, K_m, of the remaining snowmelt.

A summary of the computation procedure is given in figure V.1-11.

Equations V.1-1 an V.1-2 listed above represent modifications of the degree-day method. The degree-day method is one of the traditional methodologies used when data are limited to primarily air temperature measurements. The equation is a simple empirical relationship which relates snowmelt to the net temperature above freezing, or:

meltp = snowf(temp(i)-32)

where: snowf = snowmelt factor
temp(i) = Air temperature (°F) at Time Step, i

The degree-day equation above can also be used to quantify snowmelt using degree-hours by simply using an appropriate snowf and an hourly time step. However, when using a degree-hour equation, precautions must be taken to account for effects of the snowmelt process which occur during short (hourly) time scales. For example, the lag between the time when air temperatures rise above freezing and the initiation of the melt process may not be of concern when using a daily time scale if the melt process is initiated within several hours after a given temperature rise. However, the lag time will be

of significance in modeling the timing of the snowmelt process when using hourly time scales.

The formulation of the degree-day (or degree-hour) relationship is simply empirical. There is no strong evidence to suggest that snowmelt should be directly proportional to the net temperature above freezing, (temp(i)-32). Rather from more theoretically-based considerations evidence exists that snowmelt is due to many different factors including (temp(i)-32). Furthermore, theory also suggests that the snowmelt dependence upon the (temp(i)-32) factor is also non-linear. For example, Gray & Male, 1981 in their discussion of the physics of snowmelt, described snowmelt as;

$$meltp = \frac{Q_m}{\rho h_f B}$$

where: ρ = Density of Water, Constant

h_f = Latent Heat of Fusion, Constant

B = Fraction of Ice in a Unit Mass of Wet Snow

Q_m = Energy Flux Available for Melt
$= Q_{sn} + Q_{ln} + Q_h + Q_e + Q_g + Q_p - dU/dt$

and: Q_{sn} = Net Short Wave Radiation Flux Absorbed by Snow
$= f$(short wave radiation to and from the snow)

Q_{ln} = Net Long Wave Radiation Flux
$= f$(Temp of Air^4, Temp of Snow^4, Vapor Pressure)

Q_h = Convective Flux from the Air
$= f$(Wind Speed, Air Temperature-Snow Temperature)

Q_e = Flux of the Latent Heat
$= f$(Wind Speed, vapor pressure)

Q_g = Conductive Flux from Snow-Ground Interface
$= f$(Temperature Gradient along the Soil Depth)

Q_p = Flux of Heat from Rain
$= f$(Rain Temp - Snow Temp, Rainfall Intensity)

dU/dt = Rate of Change of Stored Energy in Snow
$= f$(Rate of Change of Temperature in Time)

For the relationship above, if: 1) all the variables other than temperature and rainfall intensity, R, are assumed constant (air temperature and rainfall intensity are the only data available for the Aberjona), 2) temperature of the snow is assumed to equal 32 °F, and 3) temperature of the rain is assumed to equal the air temperature, temp) then:

$$meltp = C1\ [\ C2 + C3 \cdot temp^4 + C4 \cdot temp + C5 \cdot (temp-32)R\ ] \qquad \text{eqn. V.1-3}$$

where: C1,C2,C3,C4, and C5 = Constants

Even with all its simplifications, equation V.1-3 indicates that snowmelt is not a linear function of (temp-32) and is therefore inconsistent with the degree-day method. As a compromise between: 1) equation V.1-3 which was derived by assuming many variables constant and which requires 5 calibration parameters, C1, C2, C3, C4, and C5, and 2) degree-day method which is entirely empirical and requires only one calibration constant, snowmelt in the model was assumed to be related to two power functions of (temp-32): one power function applied for times when there is no rain (equation V.1-1), the other function applied for times with rain (equation V.1-2). For both equation V.1-1 and equation V.1-2, three parameters must be calibrated.

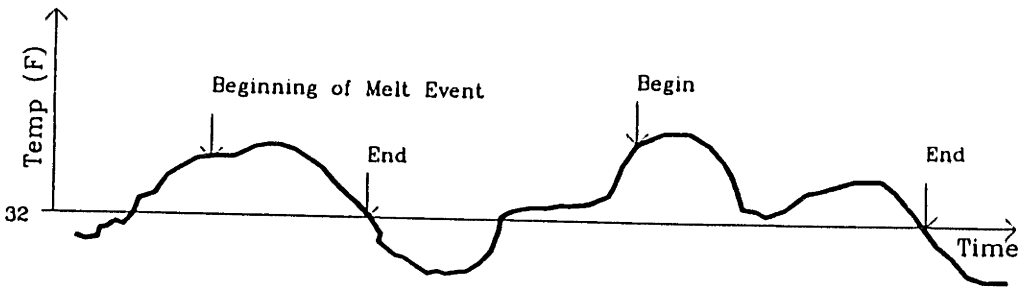

Initiate Melt Event

- lagdh = $\sum_{i-6}^{i-0}$ degree hours

if temp>32
  degree hour = temp(i)−32

If temp<= 32
  degree hour = 0

- Begin Melt Event

  If lagdh > 80 & rain(i)=0
  If lagdh > 18 & rain(i)>0

Compute Potential Snowmelt

- if rain(i) = 0: meltp(i) = snowf1(temp(i)−32)^a
- if rain(i) > 0: meltp(i) = snowf2(temp(i)−32)^a (rain(i)*100)^a

Compute Actual Snowmelt

if meltp < snaccum
  melt(i) = meltp
else
  melt(i) = snaccum

Compute Effective Snowmelt (Same procedure as for quick and slow Effective Rainfall)

Update snaccum

Figure V.1-11: Effective Snowmelt

Melt Flow

The effective snowmelt is routed to the river as melt flow using a unit hydrograph technique. The melt-flow unit hydrograph was determined through a trial and error process using 1993 streamflow data.

Numerical values of the melt-flow unit hydrograph ordinates (non-normalized) are provided in input files "ui.wn", "ui.wc", and "ui.wi" in appendices V.A and V.B. Non-normalized hydrographs as inputs were satisfactory since the program was written to normalize the input graphs to 1 inch.

An outline of the computation procedure and a plot of the unit hydrograph are provided in figure V.1-8. The melt-flow unit hydrograph is plotted separately in figure V.1-12. The melt-flow unit graph is characterized by a long tail which decreases almost exponentially in time. The time base and centroid of the melt-flow hydrograph are 245 and 33 hours respectively.

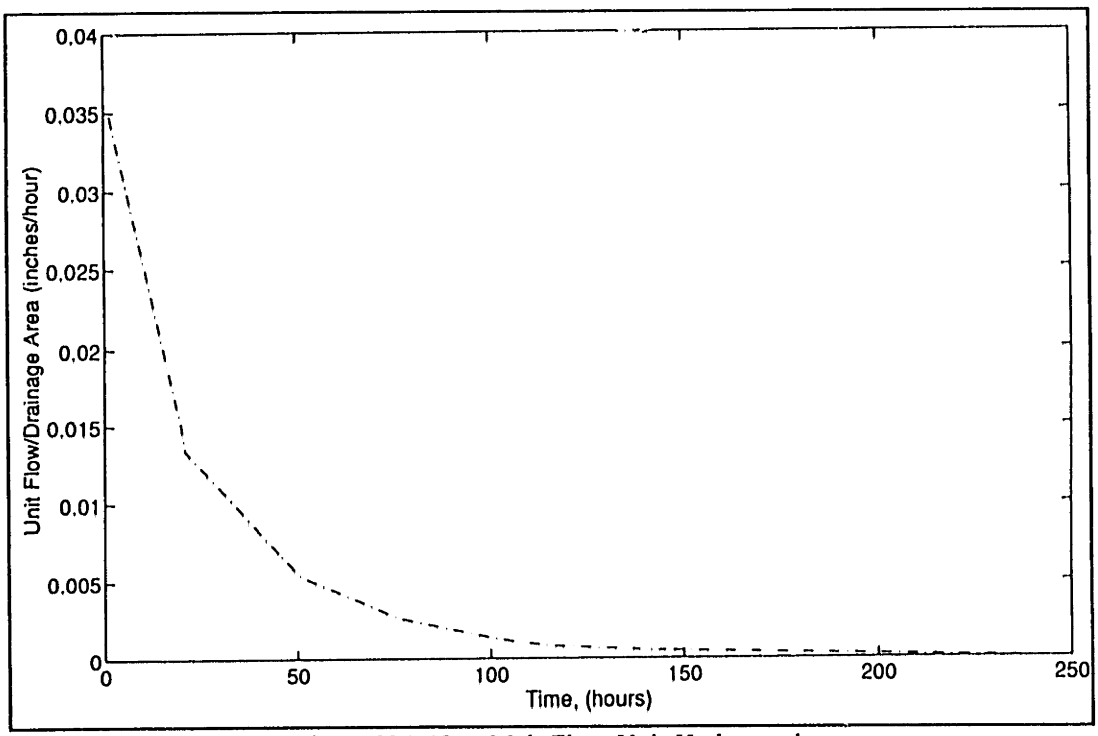

Figure V.1-12: Melt Flow Unit Hydrograph

Adjusted Quick and Slow Flow

Once the melt flow is computed, a fraction of the melt flow is applied to the quick system while the remaining fraction is applied to the slow system. The melt flow is applied to the quick and slow systems prior to the computation of water quality parameters thereby eliminating the need to separately assign suspended sediment and metal parameters to the melt flow waters.

The justification for this adjustment is based upon the physical interpretation of quick and slow systems. The quick system is considered to include any process which can quickly transmit water to the river system. These processes include, for example, storm sewer flows and direct surface runoff in the vicinity of the channel. The slow system includes processes with slower response times which would include, for example, groundwater inflows that are associated with storm events.

The primary assumption is that melt flow can enter the river through either the quick or the slow systems and can therefore pick-up water quality characteristics that are typical of those systems. For example, the melt flow applied to the quick system could be assumed to travel through the storm sewer system while the melt flow applied to the slow system could then be assumed to travel through the ground prior to discharging into the river. The relationships used for modeling purposes are:

$$\text{Adjusted flowq} = \text{flowq} + (x)\text{flowm}$$

$$\text{Adjusted flows} = \text{flows} + (1-x)\text{flowm}$$

where: flowq = Quick Flow
flows = Slow Flow
flowm = Melt Flow
x = Fraction of flowm Applied to Quick System

Longterm Baseflow

The computation of the longterm baseflow for a given sub-basin begins by first determining the longterm baseflow at gage 5, (figure V.1-13) To determine the longterm baseflow at gage 5 for a given time step, the sum of the precipitation over the prior 19 days is computed. The 19 days correspond to the response time of the longterm-baseflow system as determined in section IV.2.4. The basic assumption is that the precipitation occurring over the 19 days immediately preceding the current time step will affect the longterm baseflow at that current time step. Once the 19-day antecedent precipitation has been determined, the value is compared with the historical precipitation and longterm-baseflow (gage 5) records. An interpolation scheme is then used to estimate the longterm baseflow at gage 5 for the given model time step.

The longterm baseflow for a given sub-basin is then computed through mass balance considerations. The equation used is:

$$ltbf_{ij} = [LTBF5_i + agwith - bfww_i] \frac{A_j}{(A_{wn}+A_{wc}+A_{wi})}$$

where: $ltbf_{ij}$ = Longterm Baseflow for Sub-basin j at Time Step i

$LTBF5_i$ = Longterm Baseflow at Gage 5 at Time Step i

agwith = Atlantic Gelatin Withdrawal, Constant

$bfww_i$ = Longterm Baseflow for Woburn West Sub-basin at Time Step i

A_j = Area of Sub-basin j

Subscripts wn, wc, and wi Correspond to Woburn North, Woburn Central, and Winchester Sub-basins, Respectively

The Woburn West baseflow is assumed constant and equal to 1.53 cfs. On the best-fit line of gage versus calibrated streamflow, the 1.53 cfs corresponds to the minimum gage streamflow, (section III.3.4) The Atlantic Gelatin withdrawal is set at a constant 2.8 cfs. (See section IV.2.2)

The maximum longterm baseflow for a given sub-basin is then computed by using a multiplicative factor, mult. The multiplicative factor is used because the values determined from the historical record are representative of the average values rather than peak values. The longterm-baseflow data from the historical record include values near the maximum and also include values corresponding to times

significantly after storm events in which longterm baseflows have had time to recede from their maximum value. A value of mult = 1.2 was determined through the calibration of 1992 streamflow data.

During a storm, the longterm baseflow is permitted to increase by 0.25 cfs during each time increment until the maximum longterm baseflow is reached. Upon reaching the maximum, the longterm baseflow will remain at the maximum until after the storm. The 0.25 cfs increase was determined through the calibration process.

The end of a storm corresponds to the time when the sum of the quick and slow flow components has dropped to values less than 0.05 cfs. At this time, the longterm baseflow is permitted to decrease exponentially according to the following relationship:

$$ltbf(i) = 10^{\log(ltbf(i-1)) - R}$$

where: R = Time Constant for the Longterm Baseflow System = 0.0022/hr

Note that the inverse of the value of R is equal to 19 days which corresponds to the response time of the longterm-baseflow system (See section IV.2.4).

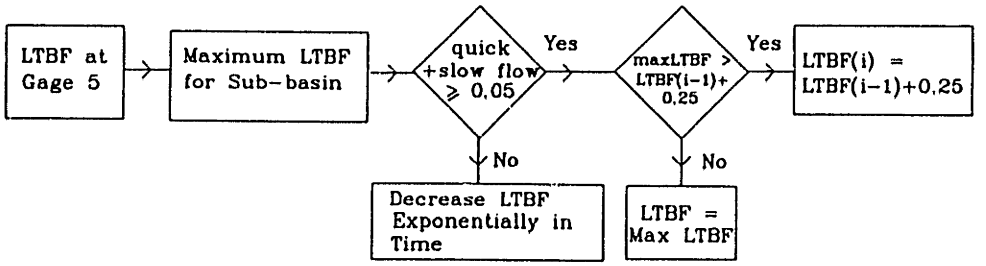

LTBF @ Gage 5

- Calculate sum precip for prior 19 days
- Compare this sum with the Historical Precipitation and LTBF Records

Max LTBF for Sub-basin

$$= \text{mult}\left[\begin{array}{c}\text{LTBF @}\\ \text{Gage 5}\end{array} + \begin{array}{c}\text{Atl Gel}\\ \text{Withdrawal}\end{array} - \begin{array}{c}\text{Woburn}\\ \text{West Flow}\end{array}\right] \frac{\text{Sub-basin Area}}{A_{wn}+A_{wc}+A_{wi}}$$

During Storm

- Increase LTBF by 0.25 cfs during each time increment until max LTBF

After Storm

- Exponentially Decreasing LTBF

  LTBF(i) = 10^[log (LTBF(i-1) - R)]
  R = 0.0022/hour

Figure V.1-13: Computation of Longterm Baseflow

Quick Suspended Sediments

The quick suspended sediment representation was chosen to model the observed "bursts" of sediment transport at the initiation of storm events. In capturing this observed behavior, a "build-up" (input) and a "wash-off" (output) of sediment in an area physically separated from the river are modeled. (figures V.1-14 and V.1-15) In this area, quick sediments, accumq, are stored. The overall rate of change of accumq over time is equal to the difference of: 1) the input rate of change and, 2) the output rate of change.

$$\left(\frac{d\text{accumq}}{dt}\right) = \left(\frac{d\text{accumq}}{dt}\right)_{\text{input}} - \left(\frac{d\text{accumq}}{dt}\right)_{\text{output}}$$

The methodology used for modeling sediment build-up (or input) is similar to the method described in Overton, 1976 and the Stormwater Management Model (SWMM). Applying Overton's conceptualization, the build-up of sediment in "quick" areas (figure V.1-14) is a function of: 1) a constant deposition rate, and 2) a deposition loss which is proportional to the amount of sediment that has accumulated in the "quick" areas. Deposition in quick areas may be associated with dustfall, tree leaves, litter, and tire and exhaust residue from automobiles. The deposition loss may be considered to be associated with air currents (e.g. natural or due to automobile traffic) which remove particles from quick areas. (Overton, 1976) Mathematically, the build-up of sediment in the "quick" area is modeled as:

$$\left(\frac{d\text{accumq}}{dt}\right)_{\text{input}} = \underbrace{\text{Constant Deposition Rate}} - \underbrace{\text{Deposition Loss}}$$

$$= \text{maxlq}\cdot A - k\cdot \text{accumq}$$

where: accumq = Accumulated Sediment in Quick Areas, mass

maxlq = Constant Input Deposition Rate of Sediment per Unit Area, mass/(time·length^2)

A = Sub-basin Drainage Area (length^2)

k = Deposition Loss Rate Coefficient (/time)

With no sediment output from quick areas, the amount of quick sediment is permitted to accumulate over time until a maximum value of maxlq·A/k is reached.

The wash-off (or output) of sediments from the quick system represents an input of sediment into the river. The equation used to model wash-off is a modification of the equation presented by Overton, 1976. Overton, 1976 assumed that the rate of pollutant removal is proportional to the amount of pollutant remaining or:

$$\left(\frac{d\text{accumq}}{dt}\right)_{\text{output}} = V \cdot \text{accumq} \qquad \text{eqn. V.1-4}$$

where: V = Velocity of Pollutant Removal by Stormwater = C·Q/IMA

Q = Runoff Rate, cfs

IMA = Impervious Area of Watershed, acres

C = Constant[9] = 4.6, per inch

Application of Overton's expression to the current modeling effort included two conceptual modifications to the interpretation of variable, V, the variable that accounts for hydrologic effects on erosion. The first of these modifications is that wash-off of sediment from quick areas occurs in association with two erosive processes: quick flow and rainfall. Erosion due to quick flow may be considered erosion due to the tractive forces of flow through the quick system, whereas erosion due to rainfall may be considered erosion due to the impact of rainfall on soils in exposed areas.[10] Since quick flows can travel through areas not exposed to direct rainfall (e.g. sewer pipes) and through areas affected by rainfall impact, quick flow is assumed to affect the entire mass of accumq. Rainfall impact, on the other hand, is assumed to affect only a fraction of accumq, frac, that is exposed to direct rainfall. (figure V.1-15) This modification, therefore, implies that:

$$V = V_{\text{quick flow}} + \text{frac} \cdot V_{\text{rainfall}} \qquad \text{eqn. V.1-5}$$

The second modification is that transport for each erosive process is governed by a power function of the difference between the erosive component and a threshold value, as opposed to being governed by

---

[9]The value of C comes from the assumption that a uniform rainfall of $^1/_2$ in/hr washes away 90% of the sediments in 1 hour. Solving equation V.1-4:

$$C = -\frac{\ln(\text{accumq}_{t=t}/\text{accumq}_{t=0})}{(Q/A)\,t} = -\frac{-2.3}{(0.5)\cdot 1} = 4.6$$

[10]Separation of erosion into a component which addresses tractive forces of flow and a component which addresses rainfall impact erosion has been presented by Singh & Prasad, 1981 and by Svensson 1987.

a linear function of a velocity term (i.e. Q/IMA) as suggested by Overton, 1976.

For the quick-flow erosive process, the rationale for the second modification is obtained from classical sediment transport theory. For example, in the classical formulation of Meyer-Peter & Muller for *non-cohesive* bedload sediment transport combined with the formulation of Einstein for suspended sediments[11], the suspended sediment flux may be considered to be a function of:

$$(\tau_b - \tau_c)^{3/2}$$

where: τ_b = Bottom Shear Stress

τ_c = Critical Shear Stress

Recognizing that the shear stress is proportional to the square of the shear velocity, u*, then the flux may be considered to be a function of:

$$(u_*^2 - u_{*c}^2)^{3/2}$$

Using the values of flowq/A and thresq/A as surrogates for u* and u_{*c}, respectively, then:

$$((^{flowq}/_{A})^2 - (^{thresq}/_{A})^2)^{3/2}$$

If it is further assumed that thresq is small relative to flowq, then:

$$(^{flowq}/_{A})^3$$

For these assumptions, the values of the exponent would be 3. In Overton's formulation, the value of the exponent is fixed at a value of 1.

Furthermore, more recent work in *cohesive* sediment transport indicates that the values of the exponent can be even larger than 3. Using assumptions similar to those above, and substituting model parameters (flowq, thresq, and A) for shear velocities, exponent values of 4 (Lick 1989) and 6 (Galiani, 1991; Ziegler & Nisbet, 1993; Cardenas, 1993) have been estimated for modeling cohesive sediment transport in rivers.

---

[11]In estimating the suspended sediment flux, the classical equations presented by Einstein represent the suspended sediment flux as being proportional to the bedload sediment flux. The proportionality factor for the Einstein equations are a function of the Einstein integrals (See appendix IV.D) which are complicated functions of water depth, particle size and shear velocity. For simplification purposes, the proportionality factor is assumed constant relative to the bedload flux term.

Given these observations, then:

$$V_{quick\ flow} = C_q \cdot ((flowq - thresq)/A)^n \qquad \text{eqn. V.1-6}$$

where: C_q = Quick Erosion Coefficient, ($time^{n-1}/length^n$) (Calibration Parameter)
flowq = Quick Flow, (volume/time)
thresq = Threshold Value for Quick Flow Erosion, (volume/time)
A = Drainage Area, $length^2$
n = Exponent, (Calibration Parameter)

Sediment flux due to rainfall impact has been estimated by Singh & Prasad, 1981, as a power function of the rainfall intensity:

$$C_r \cdot rain^n$$

where: C_r = Rainfall Erosion Coefficient, ($time^{n-1}/depth^n$)
rain = Rainfall Intensity, depth/time
n = Exponent

To include the concept that a critical rainfall intensity is required to initiate erosion due to rainfall, the "rain" variable has been replaced by "rain-thresr", where thresr represents the critical rainfall intensity. Furthermore, to minimize the number of calibration parameters in the model the exponent n value for rainfall impact is assumed to equal the exponent used for erosion associated with quick flow. There is no strong justification for using the same exponent for each expression except for: 1) purposes of minimizing the number of parameters, and 2) lack of good calibration data, since data for calibrating rainfall-associated sediment transport were not of ideal quality for the Aberjona. For these changes:

$$V_{rainfall} = C_r \cdot (rain\text{-}thresr)^n \qquad \text{eqn. V.1-7}$$

Combining equations V.1-4 through V.1-7, the final expression used for modeling purposes is thus:

$$\left(\frac{d\,accumq}{dt}\right)_{output} = C_q\ accumq\ [(flowq\text{-}thresq)/A]^n + C_r\ \ frac\ accumq\ [(rain - thresr)]^n \qquad \text{eqn. V.1-8}$$

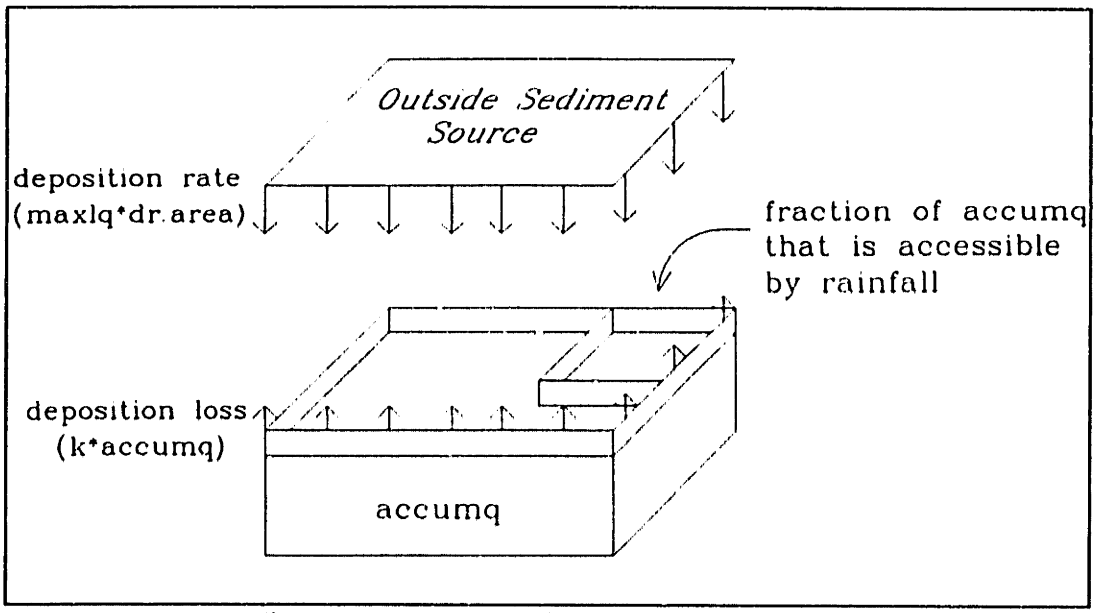

Figure V.1-14: Input of Sediment to Quick Areas

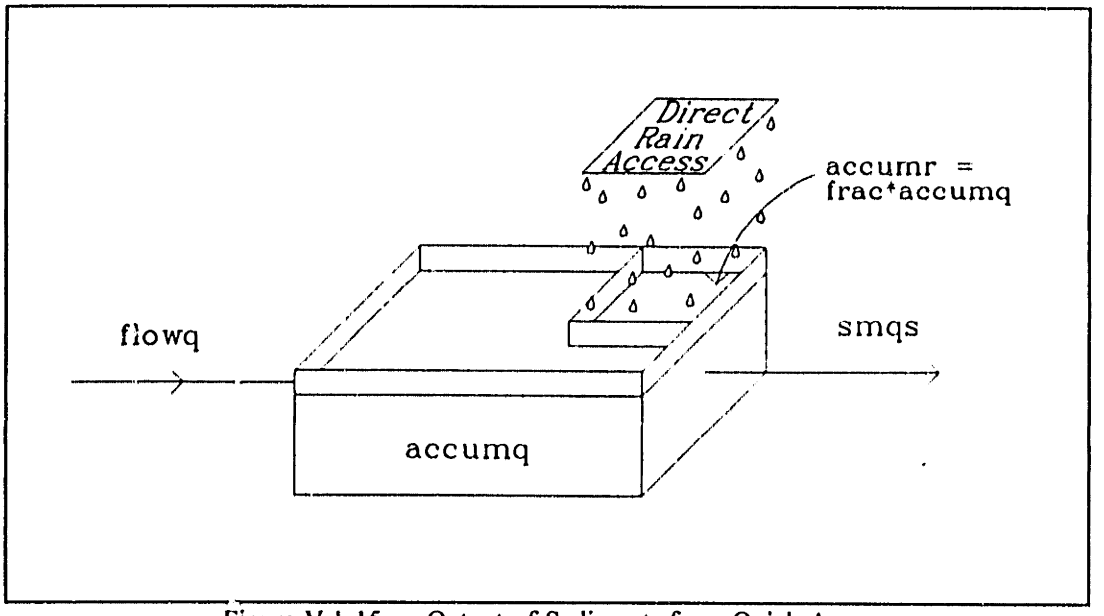

Figure V.1-15: Output of Sediments from Quick Areas

Slow and Longterm Baseflow Suspended Sediments

The data show that when slow and longterm-baseflow waters dominate the streamflow hydrograph, suspended sediment concentrations are low and at relatively constant values. The interpretation of this trend is that the sediment source associated with these waters is governed by low and constant suspended sediment concentrations. Deviations from the constant concentration are assumed to be due to the deposition and resuspension of channel sediments.

Conceptually, slow and longterm-baseflow waters are assumed to be groundwaters which have a constant potential for forming suspended sediments upon reaching the river. Groundwaters are not assumed to carry these sediments through the aquifer. Rather the assumption is that upon reaching the river, some of the dissolved material carried by the groundwater is converted to particulates instantaneously. (See section IV.3.7.1 for discussion) Mathematically, these sediment inputs are modeled as follows:

$$\left(\frac{d\text{smss}}{dt} \right)_{\text{input}} = \text{bfpot} \cdot \text{flows}$$

$$\left(\frac{d\text{smbf}}{dt} \right)_{\text{input}} = \text{bfpot} \cdot \text{ltbf}$$

where:

smss = Sediment Mass Associated with Slow Storm Water, (mass)

smbf = Sediment Mass Associated with Longterm Baseflow, (mass)

bfpot = Potential Suspended Sediment Concentration, (mass/volume)

flows = Slow Flow, (volume/time)

ltbf = Longterm Baseflow, (volume/time)

Channel Suspended Sediments

A river's transport capacity represents the maximum amount of sediment that can be transported for a given set of hydrologic conditions. The actual amount of sediment transported is always less than or equal to the river's transport capacity. Therefore, in the model, when suspended sediment inputs from a sub-basin exceed the river's transport capacity, the excess sediments are assumed to deposit within the sub-basin channel. The excess sediments will accumulate until the sediment input to the river is equal to or less than the transport capacity. Once the sediment input falls below the transport capacity then all of the sediment input from a sub-basin is transported from the sub-basin.

In estimating the transport capacity of the river, two relationships are used: one for the rising limb of the streamflow hydrograph and one for the falling limb. The need for two separate relationships is due to the observation that the river's transport capacity was consistently lower on the falling limb of the streamflow hydrograph than on the rising limb. This behavior is most evident in figure V.1-16 where three samples collected during extremely low flows and during rising-limb conditions, had higher suspended sediment concentrations than samples collected also during extremely low flows but during falling-limb conditions. At these low flows, the linear decrease in suspended sediment concentration with decreasing streamflow for the falling-limb data is interpreted as representing the transport capacity during low flow and falling-limb conditions. The rising-limb suspended sediment concentrations, which were at higher values than the falling-limb data, indicate that a different transport capacity relationship is valid for rising-limb conditions.

The relationship used to define the transport capacity on the falling limb is a best-fit regression line through the low-flow, falling-limb data points. The area-normalized form of this relationship is given as:

$$ss_{fl} = flowt \cdot 0.316 \frac{(A_{wn}+A_{wc}+A_{wi})}{cuma} + 0.286$$

where: ss_{fl} = Concentration of Suspended Sediment at Transport Capacity, mg/l
Subscript "fl" Implies Falling Limb

flowt = Total Flow in the Channel at the Location of Interest, cfs

cuma = Cumulative Drainage Area at the Location of Interest, Not Including the Woburn West Sub-basin

A = Sub-basin Area, Subscripts "wn", "wc", and "wi" Correspond to the Woburn North, Woburn Central and Winchester Sub-basins, Respectively.

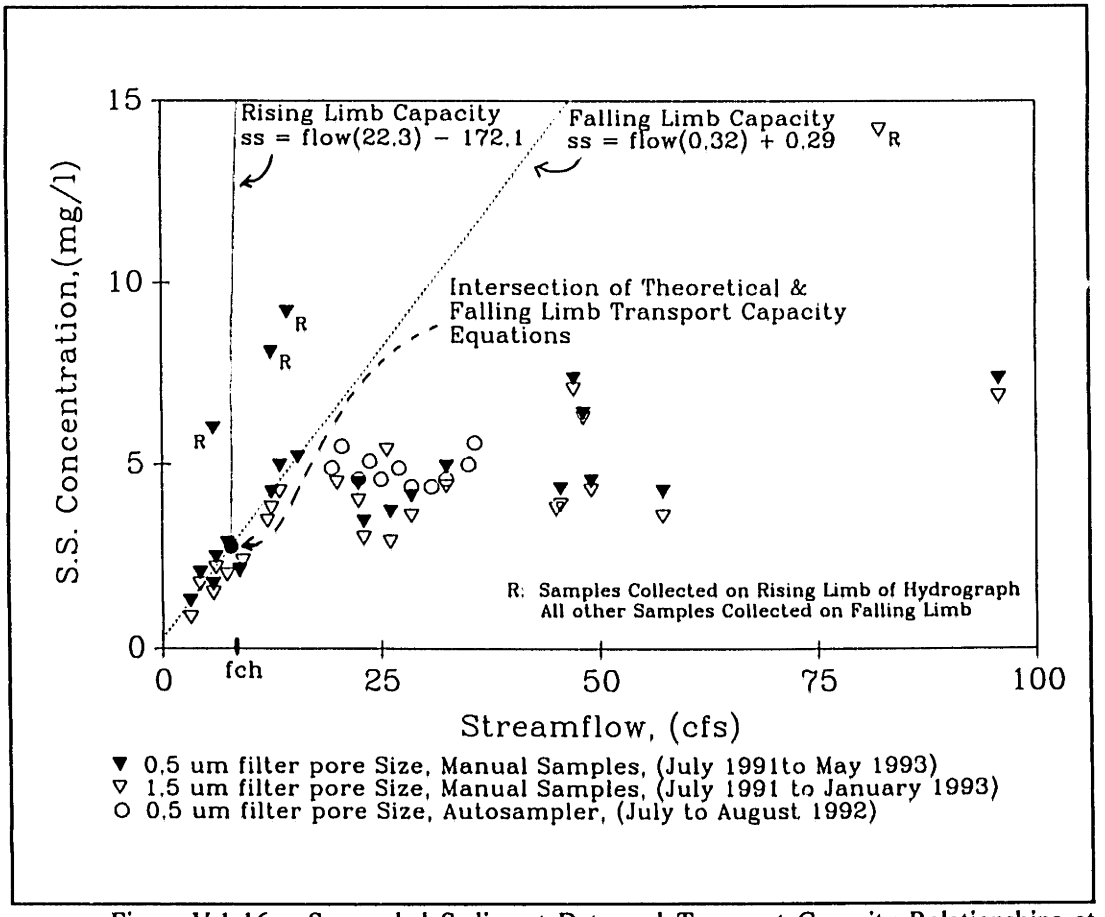

Figure V.1-16: Suspended Sediment Data and Transport Capacity Relationships at Gage 5 (flow < 100 cfs)

The normalization of this relationship is based upon the assumptions that; 1) the Woburn West sub-basin does not affect the overall suspended sediment concentrations significantly, and 2) the suspended sediment concentration at a given location is a function of the "Aberjona area" normalized flow.

The relationship above implies that during falling-limb conditions the transport capacity can be linearly extrapolated to flows beyond those for which the linear increase in suspended sediment concentration with streamflow was observed. The only basis for this extrapolation is that the relationship was observed to be linear for low flows and did not violate any of the falling-limb concentrations observed at higher flows. (figure IV.3-15)

The relationship for rising-limb conditions is based on; 1) the theoretical transport capacity as determined from the classical sediment transport equations of Meyer-Peter & Muller and Einstein (Please refer to appendix IV.D for details), and 2) the relationship used for falling-limb conditions. At very low flows, the theoretical transport equation intersects the falling-limb capacity relationship, (figure V.1-16) Above the intersection, the rising-limb transport capacity is assumed to equal the theoretical capacity. Below the intersection, the sediment transport capacity for the rising limb is assumed to then follow the falling-limb relationship. The flow rate at which the break occurs, fch, in cfs, is defined as;

$$fch = 7.85 \cdot \frac{cuma}{(A_{wn}+A_{wc}+A_{wi})}$$

The relationships used for the rising-limb transport capacity are therefore;

For flowt >= fch

$$ss_{rl} = flowt \cdot 22.3 \frac{(A_{wn}+A_{wc}+A_{wi})}{cuma} - 172.1$$

For flowt < fch

$$ss_{rl} = flowt \cdot 0.316 \frac{(A_{wn}+A_{wc}+A_{wi})}{cuma} + 0.286$$

where: ss_{rl} = Concentration of Suspended Sediment at Transport Capacity, mg/l

Subscript "rl" implies rising limb, All flows are in cfs

To compute the actual amount of sediment that is transported from a sub-basin, the transport capacity

is compared with sediment inputs. In addition to sediment inputs associated with quick sediments, $smqs_{input}$, slow sediments, $smss_{input}$, and longterm-baseflow sediments, $smbf_{input}$, as discussed earlier, there is a possibility for an additional channel input, $smch_{eros}$, which associated with the erosion of channel sediments.

The erosion of channel sediments is represented in a manner similar to that used for the erosion of quick suspended sediments. The relationship is:

$$\left(\frac{d\text{smch}}{dt}\right)_{eros} = C_s \text{ accum } [(\text{flowt-thres})/\text{cuma}]^n$$

where:

smch = Channel Sediment Mass

C_s = Channel Erosion Coefficient, $time^{n-1}/length^n$

thres = Threshold Value for Channel Erosion, (volume/time)

n = Exponent

accum = Accumulated Sediment in the Channel, (mass)

The value of thres was set to maxf, cfs. "maxf" corresponds to the flow rate at which the slow and longterm-baseflow sediment concentration equals bfpot. maxf is defined as:

$$\text{maxf} = \frac{(\text{bfpot} - 0.286)}{0.316} \cdot \frac{\text{cuma}}{(A_{wn}+A_{wc}+A_{wi})}$$

When the total sediment input into the river, smtot (= $smqs_{input}+smss_{input}+smbf_{input}+smch_{eros}$), is less than or equal to the transport capacity, smmax, all the sediment inputs are transported from the sub-basin such that:

For smtot <= smmax

$$\left(\frac{d\text{smqs}}{dt}\right)_{transported} = \left(\frac{d\text{smqs}}{dt}\right)_{input}$$

$$\left(\frac{d\text{smss}}{dt}\right)_{\text{transported}} = \left(\frac{d\text{smss}}{dt}\right)_{\text{input}}$$

$$\left(\frac{d\text{smbf}}{dt}\right)_{\text{transported}} = \left(\frac{d\text{smbf}}{dt}\right)_{\text{input}}$$

$$\left(\frac{d\text{smch}}{dt}\right)_{\text{transported}} = \left(\frac{d\text{smch}}{dt}\right)_{\text{eros}}$$

and

$$\left(\frac{d\text{accum}}{dt}\right) = - \left(\frac{d\text{smch}}{dt}\right)_{\text{eros}}$$

where: accum = The Mass of Sediment Accumulated within the Channel

When the transport capacity of the river is exceeded, the amount of sediment that is transported is weighted by its input.

For smtot > smmax

$$\left(\frac{d\text{smqs}}{dt}\right)_{\text{transported}} = \left(\frac{\text{smmax}}{\text{smtot}}\right) \cdot \left(\frac{d\text{smqs}}{dt}\right)_{\text{input}}$$

$$\left(\frac{d\text{smss}}{dt}\right)_{\text{transported}} = \left(\frac{\text{smmax}}{\text{smtot}}\right) \cdot \left(\frac{d\text{smss}}{dt}\right)_{\text{input}}$$

$$\left(\frac{d\text{smbf}}{dt}\right)_{\text{transported}} = \left(\frac{\text{smmax}}{\text{smtot}}\right) \cdot \left(\frac{d\text{smbf}}{dt}\right)_{\text{input}}$$

$$\left(\frac{d\text{smch}}{dt}\right)_{\text{transported}} = \left(\frac{\text{smmax}}{\text{smtot}}\right) \cdot \left(\frac{d\text{smch}}{dt}\right)_{\text{eros}}$$

and:

$$\left(\frac{d\text{accum}}{dt}\right) = \left(\frac{d\text{smqs}}{dt}\right)_{\text{deposited}} + \left(\frac{d\text{smss}}{dt}\right)_{\text{deposited}} + \left(\frac{d\text{smbf}}{dt}\right)_{\text{deposited}} + \left(\frac{d\text{smch}}{dt}\right)_{\text{deposited}}$$

where:

$$\left(\frac{d\text{smqs}}{dt}\right)_{\text{deposited}} = \left(1 - \frac{\text{smmax}}{\text{smtot}}\right) \cdot \left(\frac{d\text{smqs}}{dt}\right)_{\text{input}}$$

$$\left(\frac{d\text{smss}}{dt}\right)_{\text{deposited}} = \left(1 - \frac{\text{smmax}}{\text{smtot}}\right) \cdot \left(\frac{d\text{smss}}{dt}\right)_{\text{input}}$$

$$\left(\frac{d\text{smbf}}{dt}\right)_{\text{deposited}} = \left(1 - \frac{\text{smmax}}{\text{smtot}}\right) \cdot \left(\frac{d\text{smbf}}{dt}\right)_{\text{input}}$$

$$\left(\frac{d\text{smch}}{dt}\right)_{\text{deposited}} = - \left(\frac{\text{smmax}}{\text{smtot}}\right) \cdot \left(\frac{d\text{smch}}{dt}\right)_{\text{eros}}$$

Note that in the model, sub-basin channel sediments are composed of quick, slow, or longterm-baseflow sediments that have been deposited earlier. There are no other sources of channel sediments.

For metal accounting purposes, the deposited sediment associated with quick, slow, and longterm baseflow must be quantified at each time step. It is assumed that channel sediments have particulate-metal concentrations corresponding to the mixture of quick, slow, and longterm-baseflow sediment components. Such an assumption implies physical mixing only and does not account for any chemical reactions that may occur.

To keep track of channel sediment quality, the program computes, during each time step, the fraction of channel sediment that is associated with each of the components. These fractions include:

frq = Fraction of Channel Sediment from Quick Sediment Sources
frs = Fraction of Channel Sediment from Slow Sediment Sources
1-frq-frs = Fraction of Channel Sediment from Longterm-Baseflow Sources

The computation of each of these fractions may be explained by considering time step, i, for which frq(i-1), frs(i-1), and accum(i-1) are known. During this time step, the model computes each of the sediment inputs ($smqs_{input}(i)$, $smss_{input}(i)$, $smbf_{input}(i)$, and $smch_{eros}(i)$) If smtot is greater than smmax, then sediment deposition occurs. For this situation, the program computes frq and frs based upon mass balance considerations (figure V.1-17). The relationships used are as follows:

For smtot > smmax

$$frq(i) = \frac{frq(i-1)\cdot accum(i-1) + (smqs_{input}(i)-smqs_{tr}(i)) + frq(i-1)(smch_{eros}(i)-smch_{tr}(i))}{accum(i)}$$

$$frs(i) = \frac{frs(i-1)\cdot accum(i-1) + (smss_{input}(i)-smss_{tr}(i)) + frs(i-1)(smch_{eros}(i)-smch_{tr}(i))}{accum(i)}$$

where: subscript "tr" implies the transported quantity

For the situation where smtot is less than smmax, only the total mass of channel sediment is affected and not the relative distribution of one component versus the other. In other words,

For smtot <= smmax

$$frq(i) = frq(i-1)$$
$$frs(i) = frs(i-1)$$

Given these fractions the particulate metal concentration of channel sediments, $[M_p]_{channel}$, is represented as:

$$[M_p]_{channel} = \{frq[M_p]_{quick} + frs[M_p]_{slow} + (1-frq-frs)[M_p]_{ltbf}\}$$

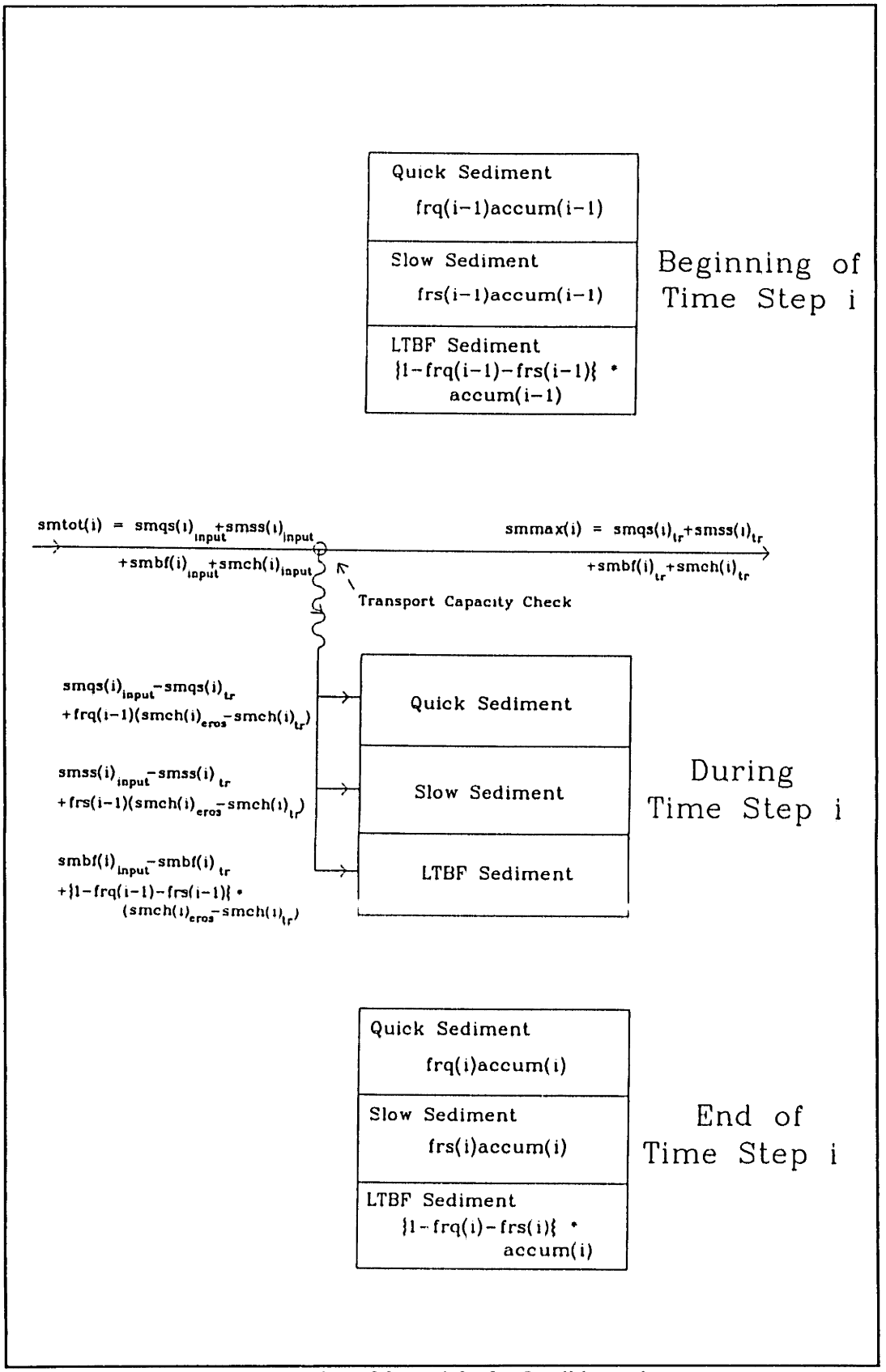

Figure V.1-17: Computation of frq and frs for Conditions when smtot > smmax

Dissolved Metals

Dissolved-metal fluxes and concentrations from each sub-basin along the Aberjona River are computed by assuming that each flow component has a dissolved-metal concentration which is a constant in time. (See section VI.3.4.1 for discussion concerning this assumption) (figure V.1-18) Mathematically, the dissolved-metal flux from a sub-basin is represented as:

$$\left(\frac{d\text{Mass}_d}{dt} \right) = [M_d]_{quick}\ \text{flowq} + [M_d]_{slow}\ \text{flows} + [M_d]_{ltbf}\ \text{ltbf}$$

where:

Mass_d = Mass of Dissolved Metal, (mass)

t = Time

$[M_d]_{quick}$ = Dissolved-Metal Concentration Corresponding to Quick Flow (mass/volume of river water)

$[M_d]_{slow}$ = Dissolved-Metal Concentration Corresponding to Slow Flow (mass/volume of river water)

$[M_d]_{ltbf}$ = Dissolved-Metal Concentration Corresponding to Longterm Baseflow, (mass/volume of river water)

flowq = Quick Flow, (volume/time)

flows = Slow Flow, (volume/time)

ltbf = Longterm Baseflow, (volume/time)

The dissolved-metal concentration from a given sub-basin is represented as:

$$[M_d]_{net} = \frac{[M_d]_{quick}\text{flowq} + [M_d]_{slow}\text{flows} + [M_d]_{ltbf}\text{ltbf}}{(\text{flowq} + \text{flows} + \text{ltbf})}$$

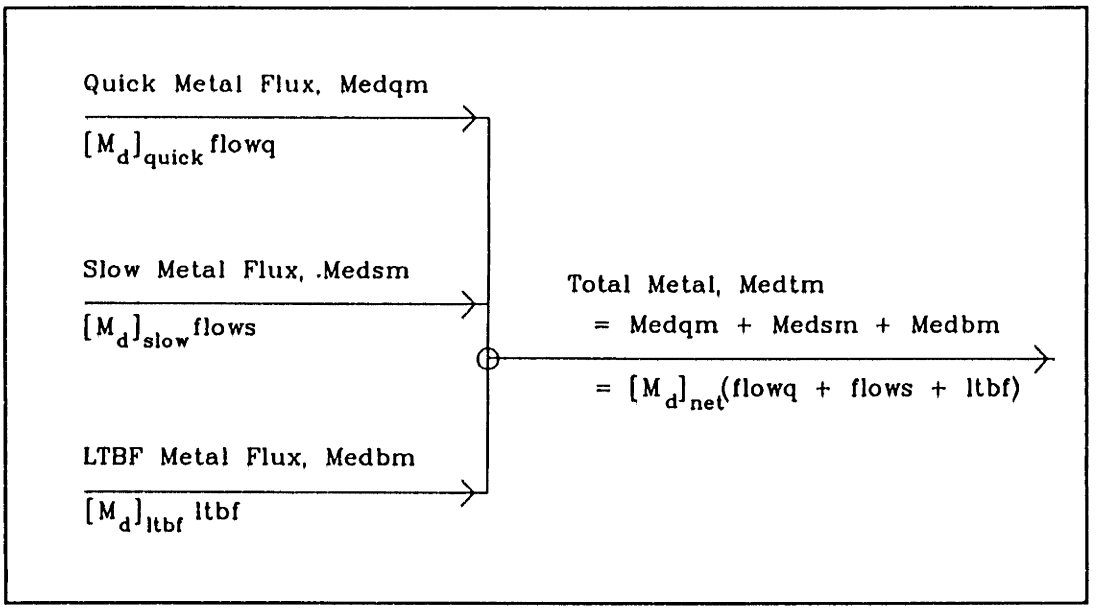

Figure V.1-18: Schematic of Dissolved Metal Model

Particulate Metals

Sub-basin particulate-metal fluxes and concentrations are computed by assuming that a particulate-metal concentration can be assigned to each sediment component from each sub-basin, (figure V.1-19) (See section VI.3.4.1 for discussion concering the constant concentration terms.) Mathematically, the total particulate-metal flux transported from a sub-basin along the Aberjona River is represented as:

$$\left(\frac{dMass_p}{dt} \right)_{transported} = [M_p]_{quick} \frac{dsmqs_{tr}}{dt} + [M_p]_{slow} \frac{dsmss_{tr}}{dt} + [M_p]_{ltbf} \frac{dsmbf_{tr}}{dt} + [M_p]_{channel} \frac{dsmch_{tr}}{dt}$$

where:

$Mass_p$ = Mass of Particulate Metal, (mass)

t = Time

$[M_p]_{quick}$ = Particulate-Metal Concentration Corresponding to Quick Suspended Sediments, (mass metal/mass ss)

$[M_p]_{slow}$ = Particulate-Metal Concentration Corresponding to Slow Suspended Sediments, (mass metal/mass ss)

$[M_p]_{ltbf}$ = Particulate-Metal Concentration Corresponding to Longterm Baseflow Suspended Sediments,(mass metal/mass ss)

$[M_p]_{channel} = \{frq[M_p]_{quick} + frs[M_p]_{slow} + (1\text{-}frq\text{-}frs)\{M_p]_{ltbf}\}$

= Particulate-Metal Concentration of the Channel Sediments, (mass metal/mass ss)

frq = Fraction of Channel Sediments from Quick Suspended Sediments

frs = Fraction of Channel Sediments from Slow Suspended Sediments

$smqs_{tr}$ = Quick Suspended Sediment Mass Transported from Sub-basin

$smss_{tr}$ = Slow Suspended Sediment Mass Transported from Sub-basin

$smbf_{tr}$ = Longterm-Baseflow Sediment Mass Transported from Sub-basin

$smch_{tr}$ = Channel Sediment Mass Transported from Sub-basin

The particulate-metal concentration transported from a given sub-basin is represented as:

$$[M_p]_{net} = \frac{[M_p]_{quick}smqs_{tr}+[M_p]_{slow}smss_{tr}+[M_p]_{ltbf}smbf_{tr}+[M_p]_{channel}smch_{tr}}{(smqs_{tr} + smss_{tr} + smbf_{tr} + smch_{tr})}$$

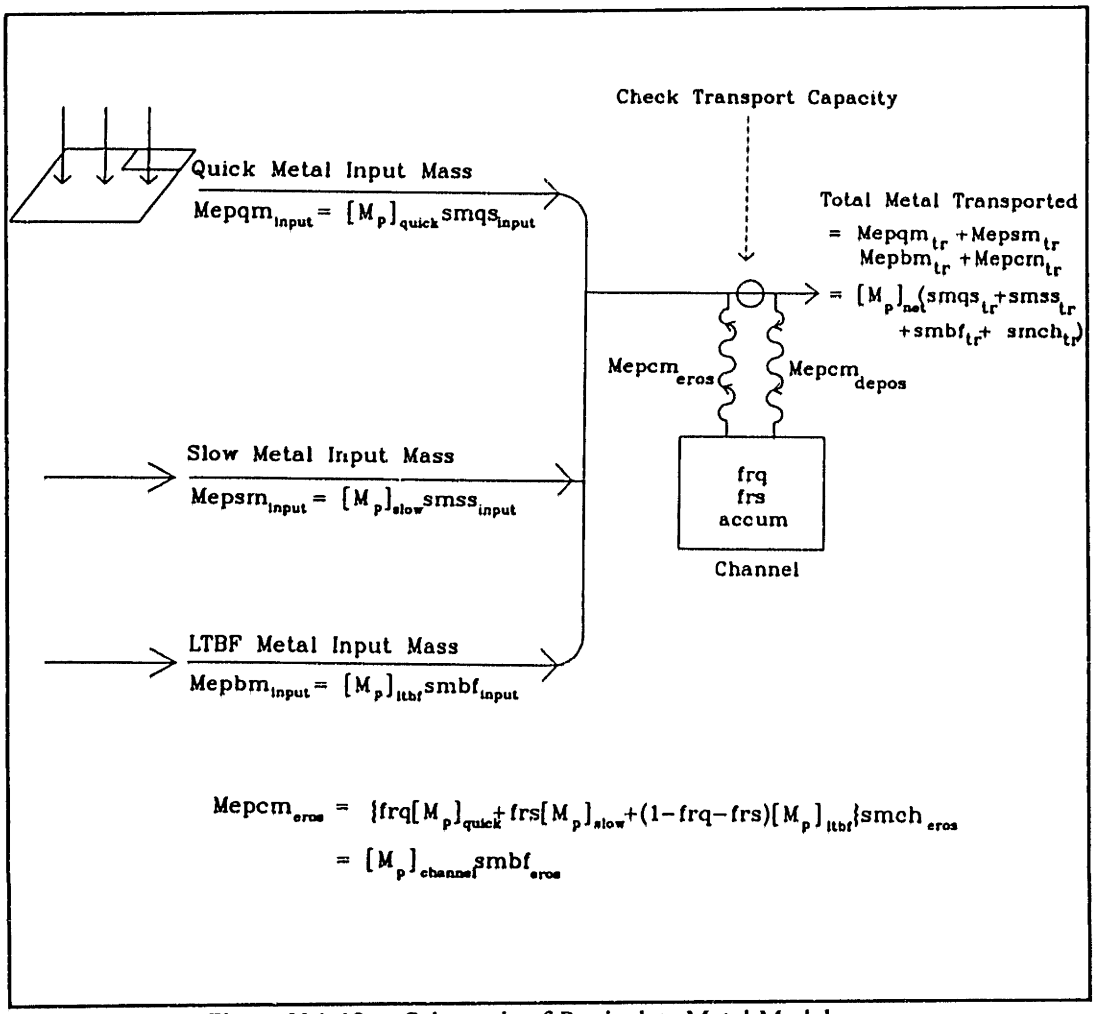

Figure V.1-19: Schematic of Particulate Metal Model
(Subscript "tr" Implies Transported)

V.1.2.2 Sub-basin Model for the Woburn West Sub-basin: Details

Inputs

Inputs into the Woburn West sub-basin model include: 1) streamflow, 2) water temperature, and 3) organic suspended sediment concentration in the inflow.

For this sub-basin, streamflow is assumed to consist of one component; the total streamflow. The input of the total hourly streamflow consists of an interpolation of monthly streamflows as observed at Gage #1 during the period of record. Average monthly flows for this station are provided in table IV.A-10 in appendix IV.A. The reason for this simplification is that during storm events: 1) consistently distinct components of flow were not apparent, and 2) the contribution of the Woburn West sub-basin to streamflow along the Aberjona River was relatively small.

The water temperature is a sinusoidal fit to the observed water temperature at Wedge Pond. (figure V.1-20) The relationship used for modeling purposes is:

$$T = 12 \sin((\pi/6)t - (4.7\pi/6)) + 14$$

where: T = Water Temperature, (°C)
t = month(i) + (day(i)/days in month(i))
month(i) and day(i) are month and day corresponding to time step i

The organic suspended sediment concentration in the inflow to the Wedge Pond reservoir is assumed constant and represents the minimum possible concentration in the outflow. The value used was 1.8 mg/l.

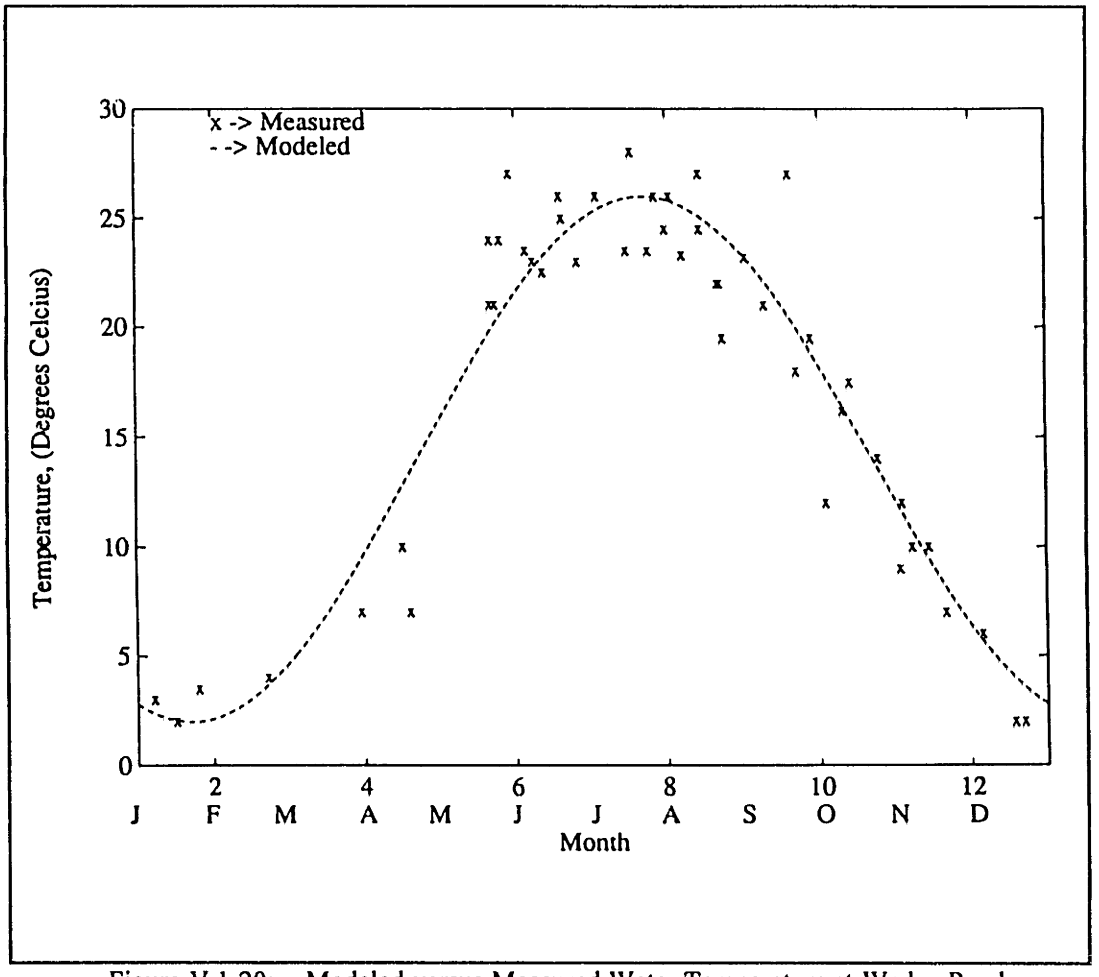

Figure V.1-20: Modeled versus Measured Water Temperature at Wedge Pond, Gage #1

Organic and Inorganic Suspended Sediments

The total suspended sediment delivered by the Woburn West sub-basin is the sum of the organic suspended sediments and the inorganic suspended sediments.

$$[SS]_{total} = [SS]_{org} + [SS]_{inorg}$$

where: $[SS]_{total}$ = Total Suspended Sediment Concentration
$[SS]_{org}$ = Organic Suspended Sediment Concentration
$[SS]_{inorg}$ = Inorganic Suspended Sediment Concentration

The organic suspended sediment concentration is quantified by assuming that the Wedge Pond reservoir acts as a continuous-flow stirred-tank reactor (refer to section IV.3.3 and to section VI.3.4.1) and that the growth of organic material is governed by a first order reaction. (figure V.1-21) Mathematically, organic suspended sediments within the pond are represented as:

$$V \frac{d[SS]_{org}}{dt} = Q\,[SS]_{org,input} - Q\,[SS]_{org} + k_T\,[SS]_{org}\,V$$

where: V = Volume of the Wedge Pond Reservoir
t = Time
Q = Streamflow, (volume/time)
$[SS]_{org,\ input}$ = Organic Suspended Sediment Concentration in the Inflow, (mass/volume)
k_T = Organic Sediment Growth Rate Constant, (1/time)

The volume of Wedge Pond is approximately 9.9×10^6 ft^3 (Durant, 1993). Streamflow is assumed at steady state such that the inflow equals the outflow. The value of Q is therefore set to the interpolated monthly values as measured at the Wedge Pond station. The value of $[SS]_{org,\ input}$ is assumed constant and set at 1.8 mg/l. A constant value for $[SS]_{org,input}$ may be justified by noting that the water within Wedge Pond is much more eutrophic than the waters feeding the pond. The growth rate constant is assumed to be a function of water temperature only. The temperature dependence is based on an approximation to the van't Hoff-Arrhenius relationship (Metcalf and Eddy, Inc., 1979), where:

$$k_T = k_{20}\theta^{(T-20)}$$

where: k_{20} = Growth Rate at 20 °C, Constant

θ = Temperature-Activity Coefficient

T = Water Temperature, °C

The values of k_{20} and θ were assumed to be calibration parameters.

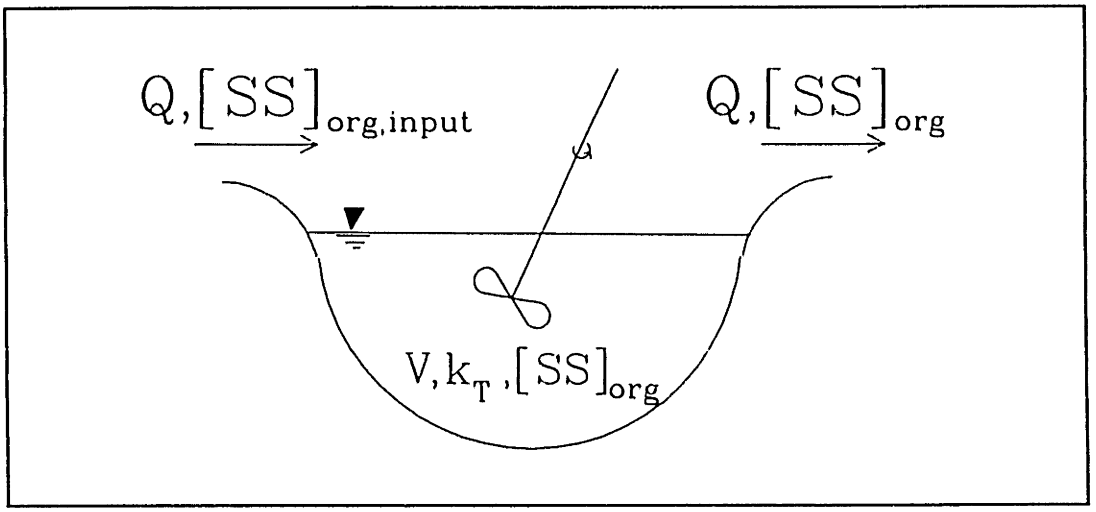

Figure V.1-21: Continuous Flow Stirred Tank Reactor Parameters for Wedge Pond Organic Suspended Sediments

The inorganic phase was observed to be correlated with Wedge Pond hydraulic residence times. The longer the residence time the lower the inorganic suspended sediment concentration. One possible explanation for this trend is that larger residence times within the reservoir allow for more efficient settling of inorganic particulates.

For this model the inorganic concentration in the outflow is assumed to be inversely proportional to the residence time of the water. The residence time is computed for each time step. The computation involves: 1) summing the volume of water at gage 1 over the prior time steps, vres, and 2) keeping track of the number of time steps in the summation process. The residence time corresponds to the time it takes for "vres" to become greater than the volume of the Wedge Pond reservoir, V. The inorganic suspended sediment concentration, in mg/l, is then assumed to be inversely proportional to the residence

time, (refer to section IV.3.3) where:

$$[SS]_{inorg} = \frac{K_r}{restim}$$

where: K_r = Proportionality Constant, hour·(mg/liter)

restim = Hydraulic Residence Time, hours

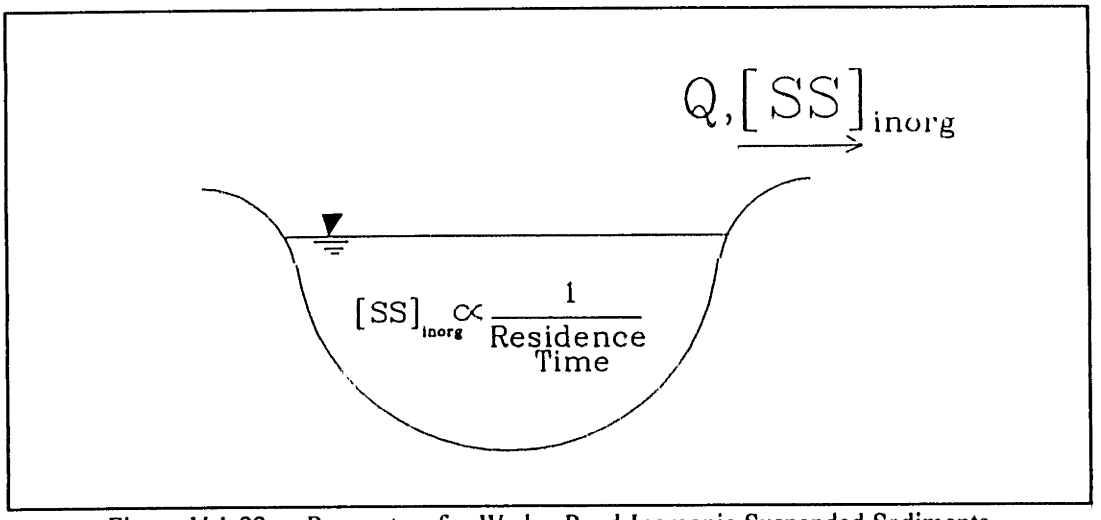

Figure V.1-22: Parameters for Wedge Pond Inorganic Suspended Sediments

Dissolved Metals

The dissolved-metal concentrations for the Woburn West sub-basin are assumed a constant in time regardless of the total flow rate. The concentrations are set at the average values of the 1992 data. The values used were:

Sub-basin	$[As]_d$ µg/l	$[Fe]_d$ mg/l	$[Cr]_d$ µg/l	$[Cu]_d$ µg/l
Woburn West	1.20	0.16	0.10	2.5

Table V.1-1: Dissolved Metal Concentrations for the Woburn West Sub-basin

With a few exceptions, these concentrations are lower than the concentrations of all the components modeled for the sub-basins along the Aberjona River. (See table V.2-4)

Given a constant metal concentration, the flux of metals from the Wedge Pond sub-basin is given as:

$$\frac{d\text{Mass}_d}{dt} = [M_d]\ \text{flowt}$$

where: Mass_d = Mass of Dissolved Metal

t = Time

$[M_d]$ = Dissolved-Metal Concentration, (mass/volume)

flowt = Total Streamflow, (volume/time)

A more elaborate model for dissolved metals was not warranted since the flux of metals from this sub-basin was small relative to the total metal flux of the Aberjona River.

Particulate Metals

Particulate-metal concentrations from the Woburn West sub-basin are assumed constant with respect to time regardless of the suspended sediment flux. The concentrations are set at the average values for the 1992 data. The values used were:

Sub-basin	$[As]_p$ mg/kg	$[Fe]_p$ %	$[Cr]_p$ mg/kg	$[Cu]_p$ mg/kg
Woburn West	22	2.5	30	80

Table V.1-2: Particulate Metal Concentrations for the Woburn West Sub-basin

The Woburn West particulate-metal concentrations are comparable to the concentrations assigned to the "slow" suspended sediment fluxes for sub-basins along the Aberjona River. (See table V.2-6) For the Aberjona sub-basins, the slow component was generally cleaner than the quick or longterm-baseflow components.

Given a constant metal concentration, the flux of metals from the Wedge Pond sub-basin is given as:

$$\frac{d\text{Mass}_p}{dt} = [M_p]\,[SS]_{total}\,\text{flowt} = [M_p] \cdot \text{SS Flux}$$

where: Mass_p = Mass of Particulate Metal

t = Time

$[M_p]$ = Particulate-Metal Concentration, (mass metal/mass of ss)

$[SS]_{total}$ = Total Suspended Sediment Concentration, (mass/volume of river water)

flowt = Total Streamflow, (volume/time)

SS Flux = Suspended Sediment Flux, (mass of suspended sediment/time)

A more elaborate model for particulate metals was not warranted since the flux of metals from this sub-basin was relatively small compared to the total metal flux of the Aberjona River.

V.1.2.3 Model for the Atlantic Gelatin Area: Details

Inputs

The inputs into the Atlantic Gelatin area model include the modeled streamflow, suspended sediment flux, and metal fluxes after the combination point at gage 3.

Flow

Streamflow through the Atlantic Gelatin area is modeled by assuming that all the groundwater removed from the Atlantic Gelatin site is removed directly from the river. (Refer to section VI.3.4.1 for discussion concerning this assumption) The withdrawal rate, agwith, at this site is modeled as 2.8 cfs. (See section IV.2.2) If the combined flow after gage 3 is greater than agwith, then the total agwith flow rate is subtracted from the inflow; if not, the amount subtracted is equal to the inflow. In other words,

$$\text{If } flow_{in} > agwith \qquad flow_{out} = flow_{in} - agwith$$

$$\text{If } flow_{in} <= agwith \qquad flow_{out} = 0$$

Suspended Sediments

Suspended sediments are modeled at the Atlantic Gelatin area by assuming that all the suspended sediments associated with the withdrawal remain within the channel. (figure V.1-23) (Refer to section VI.3.4.1 for discussion concerning this assumption) Within a given computation step, these sediments are assumed to first deposit within the channel. The amount deposited is proportional to the amount of water removed, or:

$$\text{If } flow_{in} > agwith \qquad depos1 = (agwith/flow_{in}) \cdot smto3c$$

$$\text{If } flow_{in} <= agwith \qquad depos1 = smto3c$$

where: depos1 = Sediment Deposition Rate Associated with the Water Withdrawal, (mass/time)

smto3c = Suspended Sediment Flux in the Input, (mass/time)

Then, the amount of sediment that can be eroded is computed. The erosion relationship is the same one used for channel erosion from the Aberjona sub-basins, where:

$$\left(\frac{d\text{accumg}}{dt}\right)_{\text{output}} = C_s \text{ accumg } [(\text{flow}_{out}\text{-thres})/\text{cuma}]^n$$

$$= \text{eros}$$

where:

accumg = Accumulated Sediment at the Atlantic Gelatin Site, (mass)

C_s = Channel Erosion Coefficient, $\text{time}^{n-1}/\text{length}^n$

thres = Threshold Value for Channel erosion, (volume/time)

n = Exponent

eros = Sediment Eroded from the Atlantic Gelatin Site, (mass/time)

flow_{out} = Total Flow in the Channel at the Atlantic Gelatin Site

cuma = Cumulative Drainage Area at the Atlantic Gelatin Site

The transport capacity of the river is then computed. If the capacity is exceeded, then deposition of the excess particles, depos2, occurs. The transport capacity relationships are described in section V.1.2.1. The net input of sediment into the channel is thus,

$$\left(\frac{d\text{accumg}}{dt}\right)_{\text{input}} = \text{depos1} + \text{depos2}$$

The net accumulation of sediment at the Atlantic Gelatin site is therefore:

$$\left(\frac{d\text{accumg}}{dt}\right) = \text{depos1} + \text{depos2} - \text{eros}$$

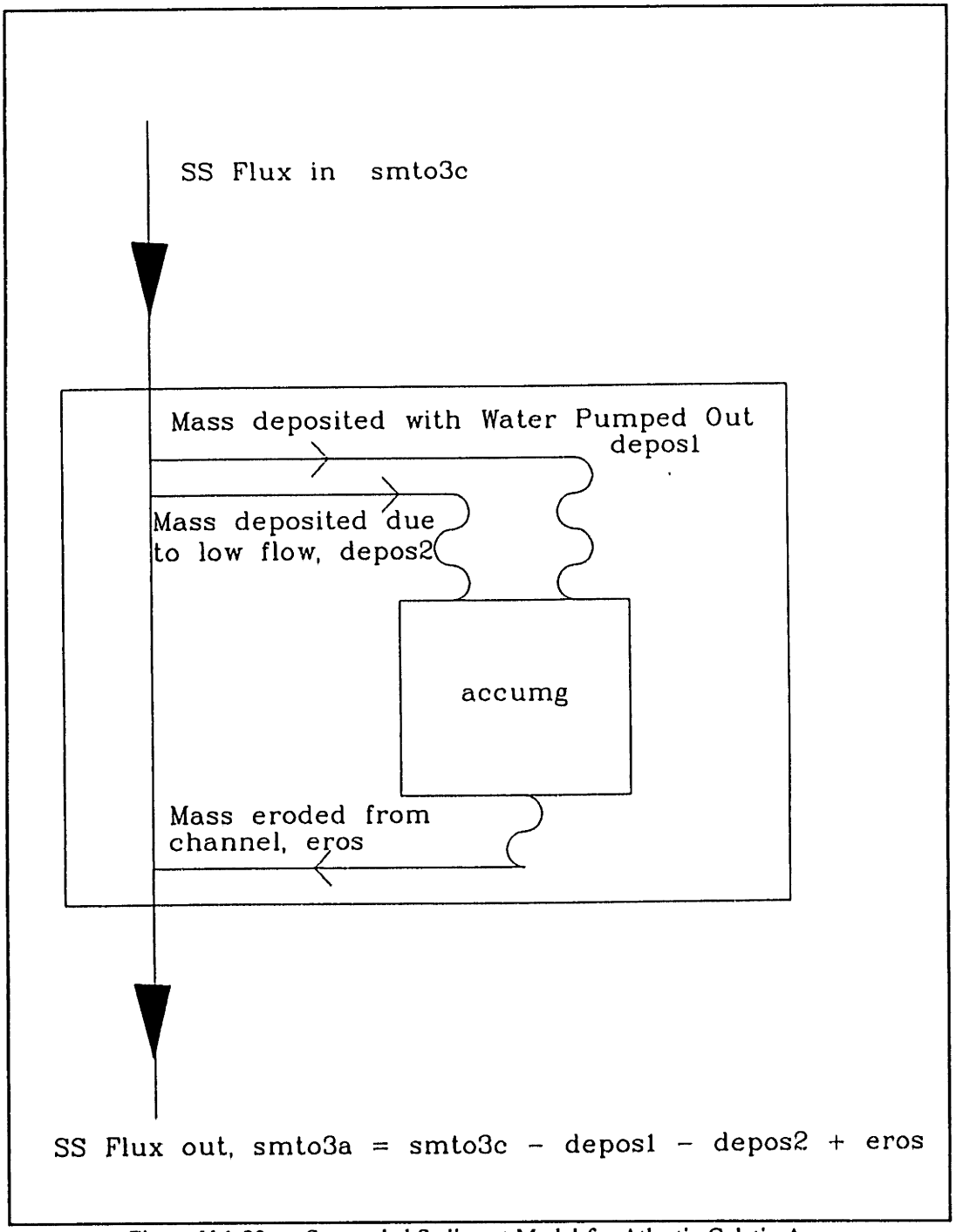

Figure V.1-23: Suspended Sediment Model for Atlantic Gelatin Area

Dissolved Metals

The concentration of dissolved metals does not change through the Atlantic Gelatin site. However, since water is removed from the site, the overall flux of dissolved metals is decreased. The amount of dissolved-metal mass removed is:

$$\left(\frac{d\text{Mass}_d}{dt}\right)_{\text{removed}} = [M_d]\,(\text{flow}_{in} - \text{flow}_{out})$$

where: Mass_d = Mass of Dissolved Metal

t = Time

$[M_d]$ = Dissolved-Metal Concentration, (mass dissolved metal/vol. of river water)

flow_{in} = Streamflow Flowing Into the Atlantic Gelatin Site, (volume/time)

flow_{out} = Streamflow Flowing Out of the Atlantic Gelatin Site, (volume/time)

The flux after the Atlantic Gelatin site is represented as:

$$\left(\frac{d\text{Mass}_d}{dt}\right)_{\text{out}} = [M_d]\,(\text{flow}_{out})$$

Particulate Metals

Particulate metals are deposited and eroded from the Atlantic Gelatin site in the same manner as the suspended sediments. When suspended sediments are deposited, the particulate metals associated with those sediments are also deposited. The particulate-metal deposition associated with the water withdrawal is described as:

If $flow_{in}$ > agwith depos1M = (agwith/$flow_{in}$) · Mmtp3c

If $flow_{in}$ <= agwith depos1M = Mmtp3c

where: depos1M = Particulate-Metal Deposition Rate Associated with the Water Withdrawal, (mass/time)

Mmto3c = Particulate-Metal Flux in the Input, (mass/time)

When a sediment input in excess of the sediment transport capacity enters the river, the amount of particulate metal deposited is proportional to the fraction of the suspended sediment deposited, or:

$$depos2M = Mmtp3a \cdot (depos2/smto3a)$$

where: depos2M = Deposition Rate of Particulate Metals Due to Transport Capacity Considerations, (particulate metal mass/time)

Mmtp3a = Particulate-Metals Transport Prior to the Transport Capacity Check, (particulate metal mass/time)

depos2 = Deposition Rate of Suspended Sediments Due to Transport Capacity Considerations, (ss mass/time)

smto3a = Suspended Sediment Transport Prior to the Transport Capacity Check, (ss mass/time)

The amount of particulate metal that is eroded with the suspended sediments is proportional to the amount of suspended sediment particles eroded.

$$erosM = eros \cdot (accumM/accumg)$$

where: erosM = Particulate Metals Eroded from the Channel, (particulate metal mass/time)

eros = Suspended Sediments Eroded from the Channel, (ss mass/time)

accumM = Particulate-Metal Mass Stored Within the Channel, (mass metal)

accumg = Suspended Sediment Mass Stored Within the Channel, (mass ss)

The net accumulation of particulate metals at the Atlantic Gelatin site is therefore:

$$\left(\frac{d\text{accumM}}{dt} \right) = \text{depos1M} + \text{depos2M} - \text{erosM}$$

V.1.2.4 Channels

Muskingum Router

The routing procedure used for streamflow is the Muskingum method. (McCarthy, 1940) For this study, the conceptualization of this procedure was expanded, such that the same method could also be used to route sediment and metal fluxes.

The Muskingum method is a two-parameter, lumped, linear model. (Singh, 1988) The method consists of a spatially lumped form of the continuity equation,

$$\frac{dS}{dt} = I - Q \qquad \text{eqn. V.1-9}$$

where: S = Channel Storage, (volume)
t = Time
I = Channel Inflow, (volume/time)
Q = Channel Outflow, (volume/time)

and a linear relationship between storage and inflow/outflow:

$$S = KxI + K(1-x)Q \qquad \text{eqn. V.1-10}$$

where: K = Routing Parameter, (time)
x = Routing Parameter

K may be physically interpreted as the time between the centroids of the inflow and outflow hydrographs. x is a coefficient used to weight the relative effects of inflow and outflow.

Expressing equation V.1-9 in finite-difference form and combining with equation V.1-10:

$$Q_{i+1} = C_1 I_{i+1} + C_2 I_i + C_3 Q_i$$

where: Q_{i+1} = Outflow at Time Step i+1
I_{i+1} = Inflow at Time Step i+1
I_i = Inflow at Time Step i
Q_i = Outflow at Time Step i

and: $C_1 = (1 - (2Kx))/(2K(1-x) + 1)$

$C_2 = (1 + (2Kx))/(2K(1-x) + 1)$

$C_3 = (2K(1-x) - 1)/(2K(1-x) + 1)$

One interpretation of the Muskingum method is to assume that storage is actually the sum of two compartments: one compartment, S_I, a function of I only, the second compartment S_Q, a function of Q only. (figure V.1-24)

$$S = S_I + S_Q$$

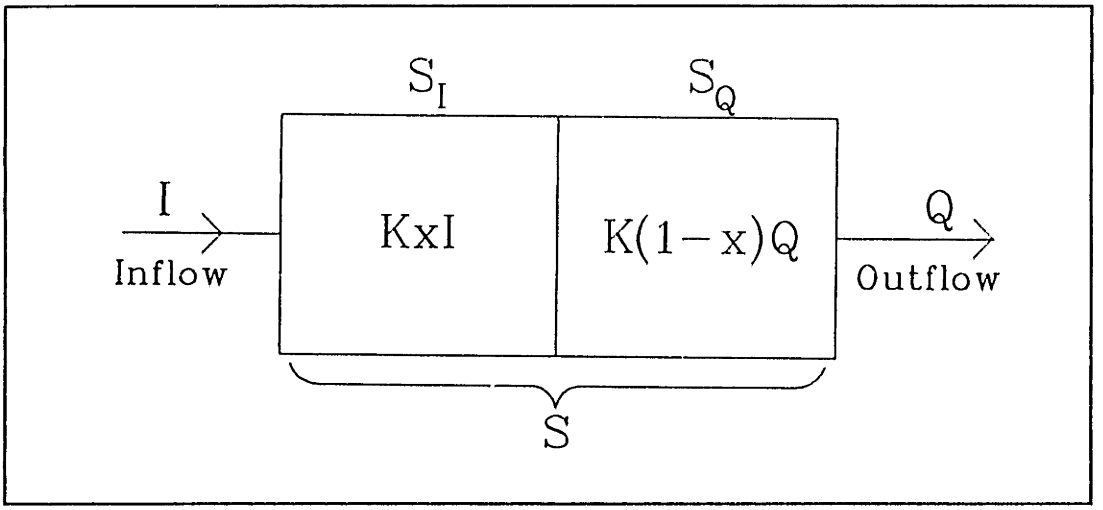

Figure V.1-24: Conceptualization of Muskingum Router: Streamflow

Note that in the above figure, only the inflow variable, I, affects the S_I compartment, whereas only the output variable, Q, affects the S_Q compartment.

Now consider a pollutant, M, being carried with I and Q where:

C_I = Concentration of M in the Inflow, (mass/volume)

C_Q = Concentration of M in the Outflow, (mass/volume)

M_S = Total Mass of M in Storage

M_{SI} = Mass of M in S_I Compartment

M_{SQ} = Mass of M in S_Q Compartment

F_I = Flux of M with the Inflow, (mass/time) = $I \cdot C_I$

F_Q = Flux of M with the Outflow, (mass/time) = $Q \cdot C_Q$

Thus, by analogy with the flow system: (figure V.1-25)

$$M_S = M_{SI} + M_{SQ}$$

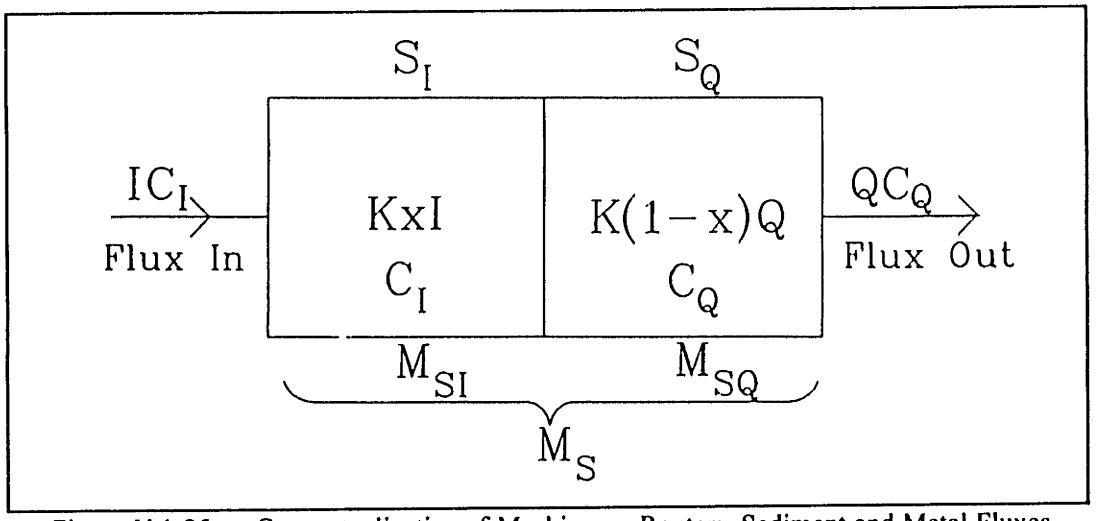

Figure V.1-25: Conceptualization of Muskingum Router: Sediment and Metal Fluxes

Note that in the above figure, only the input variables, I and C_I affect the S_I compartment, whereas only the output variables, Q and C_Q affect the S_Q compartment.

From continuity:

$$\frac{dM_S}{dt} = I \cdot C_I - Q \cdot C_Q \qquad \text{eqn. V.1-11}$$

and by analogy with the flow system:

$$M_S = KxI \cdot C_I - K(1-x)Q \cdot C_Q \qquad \text{eqn. V.1-12}$$

and combining equations V.1-11 and V.1-12:

$$(Q \cdot C_Q)_{i+1} = C_1(I \cdot C_I)_{i+1} + C_2(I \cdot C_I)_i + C_3(Q \cdot C_Q)_i$$

The equation above is almost identical to the streamflow result. The only difference is that contaminant fluxes, rather than streamflows, are routed. The physical implication of such a result is that the contaminants are entirely entrained in the streamflow and are carried downstream along with the flow.

Deposition and Erosion Check

A sediment deposition and erosion check is included at the end of each main channel (Channel 1 and Channel 2). If the suspended sediment flux exceeds the transport capacity, then the excess is deposited. If the flux is lower than the capacity, then: 1) all the input into the channel is transported out of the channel, and 2) additional suspended sediment can be eroded from the channel. The computational procedure is almost identical to the procedure used for the Aberjona sub-basins. The only difference is that the input of sediment comes from routed channel sediments. Particulate metals are assumed to deposit and erode in association with the suspended sediments. The method used to account for particulate metals is similar to the procedure used for the Atlantic Gelatin area.

V.2 MODEL CALIBRATION

Calibration of the model was subjective (McCuen, 1989) in the sense that no analytical or numerical optimization procedure was used. Rather, changes to the calibration parameters were made in response to the observed behavior of several different criteria. For the streamflow model, the criteria included: 1) mass balance considerations, 2) standard deviations, 3) R^2 values, and 4) a visual comparison of time series plots. (See section V.3) For suspended sediment and metals, the comparison was based upon: 1) R^2 values, and 2) a visual comparison of time series plots.

V.2.1 Streamflow Model

V.2.1.1 Calibration and Verification Procedure

Calibration of the streamflow model was performed using 1992 and 1993 data. The 1991 streamflow data were used to verify the model. The model run periods for each year correspond to an hourly time step within the following dates:

Year	Run Period
1991	January 15, 1991 to December 31, 1991
1992	January 1, 1992 to December 31, 1992
1993	January 1, 1993 to September 30, 1993

The 1992 data were used to calibrate parameters for the quick flow, slow flow, and longterm-baseflow systems for the Woburn North, Woburn Central, and Winchester sub-basins and were also used to calibrate the channel parameters. Parameters for the Woburn North sub-basin were calibrated by comparing the sum of the quick, slow and longterm baseflows with the observed streamflow at gage number 2. Parameters adjusted included: 1) the effective rainfall parameters for the Woburn North quick and slow systems (WRT_q, WRT_s, IA_q, IA_s, K_q, K_s), 2) the unit hydrograph ordinates for the quick and slow systems, and 3) the longterm-baseflow parameter (mult).

Parameters for the Woburn Central sub-basin were calibrated next. Calibration was performed by comparing the sum of the routed flow from gage 2 and the streamflow from the Woburn Central sub-basin, with the measured streamflow at gage number 3. Parameters adjusted during this phase included: 1) the effective rainfall parameters for the Woburn Central quick and slow systems (WRT_q, WRT_s, IA_q, IA_s, K_q, K_s), 2) the re-adjustment of unit hydrograph ordinates for the quick and slow systems, 3) the re-adjustment of the longterm-baseflow parameter (mult), and 3) the routing parameters for channel 1 (K and x).

Calibration of the Winchester sub-basin parameters was performed by comparing modeled and measured streamflows at gage number 5. At gage 5, the modeled streamflow consisted of: 1) the routed flow from gage number 3, (Prior to routing, these flows were reduced by the Atlantic Gelatin withdrawal rate, agwith), 2) streamflow from the Woburn West sub-basin. (The Woburn West sub-basin flows were input directly into the model and did not require calibration) and, 3) the sum of the flow components from the Winchester sub-basin. During this phase of calibration: 1) the effective rainfall parameters for the Winchester quick and slow systems (WRT_q, WRT_s, IA_q, IA_s, K_q, K_s) were adjusted, 2) the unit

hydrograph ordinates for the quick and slow systems were re-adjusted, 3) the longterm-baseflow parameter (mult) was re-adjusted, and 3) the routing parameters for channel 2 (K and x) were calibrated.

Once the parameters were calibrated against the 1992 flow data, the melt-system parameters were calibrated using 1993 data. During 1993, streamflow data were only available at gage 5. Since streamflow data for 1993 were not available for gage numbers 2 and 3, the melt-flow parameters for the Woburn North, Woburn Central, and Winchester sub-basins could not be calibrated individually. Rather, calibration of melt parameters for these sub-basins was performed indirectly by comparing the sum of the contributions from all the sub-basins with the measured flows at gage 5. Parameters adjusted using the 1993 data set included: 1) parameters used to initiate the snowmelt process (lagdh), 2) parameters used to quantify snowmelt (snowf1, snowf2, a) 3) parameters used to compute the effective snowmelt (WRT_m, IA_m, K_m for the Woburn North, Woburn Central, and Winchester sub-basins) and, 4) the unit hydrograph ordinates for melt flow.

The calibration process was re-iterated until overall model performance was satisfactory. The need for the re-iteration procedure was due to the re-adjustment of the same parameters during different steps of the calibration process. For example, the re-adjustment of the unit hydrograph ordinates and the longterm-baseflow parameters affected the modeled flow for all the sub-basins. Additionally, attempts were also made to keep the WRT_q's, WRT_s's, and WRT_m's for each of the sub-basins the same.

Streamflow for the Woburn West sub-basin is an input into the model and therefore required no calibration.

V.2.1.2 Evaluation of Effective Rainfall Parameters for the Quick and Slow Systems: WRT, IA, and K

Values of WRT, IA, and K used for model runs are provided in table V.2-1. Initial values of K and IA were determined by performing mass balances for storms in the 1992 period of record. For each storm event analyzed, the volume of the quick and slow response was determined. The data were plotted on a graph of runoff volume versus total precipitation depth. From a best fit line, an initial value of the K and IA were determined for both the quick and slow systems. Calibration continued by adjusting the initial values through a subjective comparison of modeled and measured streamflows.

WRT

In table V.2.1 it is noted that the quick-system WRT is smaller than the slow-system WRT. This is consistent with the conceptualization that the quick system responds faster than the slow system. The value of WRT_q (8 hours) is equal to the time base of the quick unit graph. Therefore after the WRT_q time has elapsed the quick system is no longer contributing to streamflow. This observation is consistent with the definition of WRT as being the time needed to empty the system of water after rainfall has ceased.

The value of WRT for the slow system, WRT_s, is equal to 24 hours. The first 24 hours of the slow unit hydrograph represents 70% of the unit graph volume. Therefore, the calibrated value of WRT_s implies that at least 70% of the water must be removed from the slow system before an initial abstraction is applied to the next storm event.

IA

The use of a constant initial abstraction, IA, implies that the amount of water initially lost from a system is independent of antecedent conditions. IA is set to a time-constant value to simplify the model formulation. However, such a formulation is only a rough approximation since in reality, the true IA is dependent upon antecedent hydrologic conditions.

The values of IA determined for the quick system range from 0.06 to 0.15 inches. The IA_q may be associated with depression storage in impervious areas and initial storage of water in storm sewer catch basins. These values are consistent with the constant 0.1 inch value recommended for small urban watersheds. (McCuen, 1989)

The IA values for the slow system (0.2 to 0.3 inches) were larger than the IA estimated for the quick system. The larger IA_s value is consistent if it is considered that the slow system requires a larger initial storage prior to runoff generation. This initial storage for the slow system may include: 1) interception

of precipitation by vegetation, and 2) storage of water in the soil unsaturated zone due to a soil moisture deficit.

K

The fraction of the rainfall (over and above the initial abstraction) which contributes to the effective rainfall, K, is represented as the product of two factors:

$$K_j = (SA_j)\cdot(f_j) \qquad \text{eqn. V.2-1}$$

where: SA_j = Fraction of Surface Area Covered by System j

f_j = Fraction of Water Reaching System j that is Converted to Effective Rainfall

The SA_j factor is included to account for the fraction of the watershed that is accessible to each system. Assume, for example, for a particular watershed that the quick system covers 10% of the watershed's surface area, A, and the slow system covers the remaining 90%. Then for a 1 inch storm an equivalent volume of 0.1 inches of precipitation over area A will flow through the quick system and an equivalent volume of 0.9 inches over area A will flow through the slow system.

SA_q and f_q

To estimate the fraction of the surface area covered by the quick system, SA_q, equation V.2-1 can be used given estimates of f_q and K_q. K_q values calibrated for each sub-basin are provided in table V.2-1. A value of $f_q = 1$ would be expected assuming that losses (after the initial abstraction) are negligible from the quick system. Given the values of K_q and f_q, values of SA_q for the Woburn North, Woburn Central, and Winchester sub-basins are estimated as 0.03, 0.08, and 0.14, respectively. Therefore, for all sub-basins, the surface area accessible by quick water represents less than 15% of the sub-basin surface area, where the fraction of the surface area accessible by quick water increases for sub-basins in the downstream direction.

The increase in SA_q is consistent with the increase in sub-basin urbanization in the downstream direction, where urbanized areas for the Woburn North, Woburn Central, and Winchester sub-basins represent 63%, 83%, 95%, of the total area for each sub-basin, respectively. (Kristine McCaffrey, personal communication, 1994)

The values of SA_q are significantly less than the areas of each sub-basin which has been urbanized.

Possible reasons why the SA_q's are much smaller than the fraction of urbanized areas is that: 1) within the urbanized areas a large fraction of the area can drain into a slow system directly (e.g. lawns which drain into the groundwater system) and 2) a large fraction of the impervious areas within urbanized areas do not drain into the quick system. Examples of impervious areas which do not drain into the quick system include: 1) building roof tops which drain into grassy areas, and 2) parking lots and paved roadways which drain into adjacent grassy swales, ponds, and ditches which are not directly connected to the river.

SA_s

Assuming that the remaining surface areas are accessible to the slow system, then the SA_s's for the Woburn North, Woburn Central, and Winchester sub-basins are estimated as 0.97 (1-0.03), 0.92 (1-.08), and 0.86 (1-.14), respectively. Such results indicate that the bulk of the precipitation drains through the slow system.

f_s

To compute the f_s's for the slow system, losses of water to evapo-transpiration, and to the longterm baseflow system should be considered. Computationally, f_s may be expressed as:

$$f_s = (1 - EV)\frac{V_s}{V_s + V_{ltbf}}$$

where: EV = Fraction of Precipitation Lost to Evapo-transpiration (Excludes Initial Abstraction Losses)

V_s = Volume of Water Associated with Slow Flow

V_{ltbf} = Volume of Water Associated with Longterm Baseflow

Within the watershed, total evapo-transpiration represents approximately 36% of the precipitation. (Brainard, 1990) Total evapo-transpiration is assumed to account for evapo-transpiration losses associated with initial abstractions and with evapo-transpiration losses after initial abstractions. Assuming that initial abstractions account for roughly 6% of the precipitation losses, the evapo-transpiration loss after initial abstractions may be approximated as 30%.

Of the slow plus the longterm-baseflow water, a mass balance of the streamflow hydrographs indicates that roughly 20%, 60%, and 30% of the water is observed as slow storm water ($V_s/(V_s+V_{ltbf})$) for the Woburn North, Woburn Central, and Winchester sub-basin, respectively.

Therefore, one would expect that the values of f_s for the Woburn North, Woburn Central, and Winchester sub-basins would equal 0.14 ((1-0.3)*0.2), 0.42 ((1-0.3)*0.6), and 0.21 ((1-0.3)*0.3),

respectively.

K_s

Noting the values of f_s and SA_s estimated above, the values of K_s are computed (equation V.2-1) as 0.14, 0.39, and 0.18 for the Woburn North, Woburn Central, and Winchester sub-basins, respectively. The computed values compare very favorably with the calibrated values of K_s (table V.2-1) for both the Woburn North and Winchester sub-basins. The computed K_s value for the Woburn Central sub-basin under-estimated the calibrated value by a factor of two.

Sub-basin	Water Response Time (hr)		Initial Abstraction (in)		Fraction of Rain Converted to Effective Rainfall	
	WRT_q	WRT_s	IA_q	IA_s	K_q	K_s
Woburn North	8	24	0.06	0.30	0.03	0.10
Woburn Central	8	24	0.06	0.20	0.08	0.75
Winchester	8	24	0.15	0.25	0.14	0.20

Subscripts "q" and "s" imply quick and slow systems respectively

Table V.2-1: Model Parameters Used for Computation of Effective Rainfall

V.2.1.3 Evaluation of Snowmelt Parameters: snowf1, snowf2, and a

Using the 1993 streamflow data, the values of snowf1, snowf2, and "a" were calibrated to values of 0.00038 inches/°F^a, 0.00014 inches^{1-a}(hr/°F)^a, and 1.5.

The value of a = 1.5 is close to the value of 1 which is characteristic to the degree-day method. The 1.5 value is also within the range from 1 to 4 which would be expected from equation V.1-3. For an exponent of a = 1, snowmelt factors typically range from 0.0021 to 0.0042 inches/(hr/°F) (Linsley, et. al., 1982). These snowmelt factors are approximately an order of magnitude larger than the factors determined for the present study, which were determined for an exponent of 1.5.

V.2.1.4 Evaluation of Effective Snowmelt Parameters for the Melt System: WRT_m, IA_m, and K_m

The effective snowmelt parameters were determined through calibrations using 1993 streamflow data. The values of these parameters were calibrated as:

Sub-basin	Water Response Time (hr)	Initial Abstraction (in)	Fraction of Rain Converted to Effective Rainfall
	WRT_m	IA_m	K_m
Woburn North	24	0.20	0.75
Woburn Central	24	0.20	0.75
Winchester	24	0.20	0.85

Subscript "m" implies melt water parameter

Table V.2-2: Model Parameters Used for Computation of Effective Snowmelt

The WRT for the melt system can be considered to represent the time it takes for meltwater to drain through the snow pack. The value of WRT (24 hours) used for the melt system is comparable to the WRT (24 hours) value used for the slow system. Approximately 57% of the unit hydrograph volume is represented in the first 24 hours of the snowmelt unit graph. Therefore, at least 57% of the water must be removed from the melt system prior to applying an initial abstraction to the next storm.

The value of IA used for the melt system (IA=0.20 inch) is comparable to the value used for the slow system. The IA_m represents the volume of snow melt that is needed to get the snow melt to begin contributing flow to the river. It represents water which fills voids in the snow pack, evapo-transpiration losses, and storage of water in the quick system and slow systems.

The values of K_m used for modeling purposes ranged from 0.75 to 0.85. This result indicates that of the snow that melts, roughly 75% to 85% of the water (after initial abstractions) shows up in the river as streamflow. The snowmelt that does not show up in the river is assumed "lost" from the system. Losses may include, depression storage and evaporation losses and losses to longterm baseflow.

V.2.1.5 Evaluation of the Melt-Flow Distribution Parameter: x

In the model, x was set at 0.6. This value was determined by calibrating the model against 1993 suspended sediment data.

The value of x represents the fraction of snowmelt which drains through the quick system. There are two methods for evaluating this parameter. The first method is to assume that it is equal to the fraction of the Woburn North, Woburn Central, and Winchester sub-basins covered by urbanized areas. The justification for this method is that during the winter the entire urbanized area will likely drain toward the storm sewer system because: 1) storm drains are cleared periodically allowing for drainage, and 2) the ground is frozen thus limiting the drainage through the ground. Therefore, areas that would normally drain into the soil during warm weather will instead flow through the quick system during snowmelt because of reduced drainage through the frozen ground. The net result is that during snowmelt, the quick area is effectively larger. The fraction of the Aberjona River drainage areas that are urbanized is 79% which is slightly larger than the 60% value determined for x.

The second method for evaluating x is by adjusting equation V.2-1 to account for a flow through both the quick and slow systems, or:

$$K_m = xf_q + (1-x)f_s$$

Using the values of: 1) $f_q = 1$ for the quick system (i.e. no losses), 2) f_s (0.14,0.42,0.21) estimated earlier, and 3) noting the values of K_m (0.75,0.75,0.85) from the calibration, the values of x estimated for the Woburn North, Woburn Central, and Winchester sub-basins are computed as 0.71, 0.57, and 0.81, respectively. These values for x are comparable with the value of 0.6 determined from the model calibration.

V.2.1.6 Evaluation of Main Channel Parameters: K and x

From the calibrations using 1992 data, the parameters for the Muskingum router have been estimated as follows:

	K (hrs)	x
Channel 1	7	0.0
Channel 2	8	0.0

Table V.2-3: Parameters for Channel Routing Components

A zero value for x implies that the channel basically behaves as a linear reservoir ($S=KQ$, $M_s=K[QC_Q]$) In other words, storage in the channel is only a function of channel outflow and not a function of river inflow.

The drawback associated with the Muskingum method is that travel time through a given reach is a constant and therefore independent of flow conditions. In actuality, travel times can be significantly different between low and high flows. For: 1) the values of K determined for Channel 1 (7 hours) and 2 (8 hours) and 2) lengths of Channel 1 (2.2 miles) and 2 (3.0 miles), the average travel velocity through both channels would be approximately 2 ft/s. Measured streamflow velocities for the Aberjona River indicate that a 2 ft/s figure corresponds to primarily high flow conditions. During low flow conditions slower velocities are expected.

V.2.2 Dissolved-Metals Model

V.2.2.1 Calibration and Verification Procedure

The dissolved-metal parameters were calibrated after the streamflow model was calibrated. Dissolved-metal parameters included the assignment of dissolved-metal concentrations to each component of flow ($[M_d]_{quick}$, $[M_d]_{slow}$, and $[M_d]_{ltbf}$) from each sub-basin. Initial estimates of $[M_d]_{quick}$, $[M_d]_{slow}$, and $[M_d]_{ltbf}$ were obtained from plots of dissolved-metal concentrations versus streamflow at each of the gaging stations. Metal concentrations were assumed to be dominated by: 1) longterm baseflows during low streamflows, 2) slow storm waters during intermediate streamflows, and 3) quick storm waters during higher streamflows. For example, initial estimates of dissolved arsenic concentrations at gage 5 can be obtained from figure IV.4-45. From this figure dissolved arsenic concentrations associated with each flow condition ($[As_d]_{quick}$, $[As_d]_{slow}$, and $[As_d]_{ltbf}$) may be assigned values of 1.5, 2.0, and 4.0, respectively, for the Winchester sub-basin. These initial estimates can also be adjusted for slightly higher arsenic concentrations coming in from upstream sub-basins and the lower concentration coming from the Woburn West sub-basin. The initial estimates of dissolved-metal concentration were then re-adjusted during the calibration process.

Calibrations were performed using 1992 dissolved-metals data. The 1992 data correspond to instantaneous samples collected at monthly intervals at each of the gaging stations plus instantaneous samples collected using the autosampler at gage 5. For gaging stations 1, 2, and 3, eleven measurements were available at each station. Seventy measurements were available at gaging station 5. (See tables IV.E-1 through IV.E-20 for sample times and dates)

Calibrations proceeded in the downstream direction. Parameters for the Woburn North sub-basin ($[M_d]_{quick}$, $[M_d]_{slow}$, and $[M_d]_{ltbf}$) were calibrated against gage 2 dissolved-metal data. $[M_d]_{quick}$, $[M_d]_{slow}$, and $[M_d]_{ltbf}$ for the Woburn Central sub-basin were calibrated next. The calibration was based upon the sum of: 1) the routed dissolved metals from the Woburn North sub-basin, with 2) the dissolved metals from the Woburn Central sub-basin. This sum was compared with the dissolved-metal fluxes measured at gage 3 and values of $[M_d]_{quick}$, $[M_d]_{slow}$, and $[M_d]_{ltbf}$ for the Woburn Central sub-basin were then adjusted depending upon the fit of the data.

$[M_d]_{quick}$, $[M_d]_{slow}$, and $[M_d]_{ltbf}$ values for the Winchester sub-basin were calibrated against the measured fluxes and concentrations as observed at gage 5. The measured data at gage 5 were compared with the sum of: 1) the routed dissolved metals from gage 3. (These fluxes were adjusted for the Atlantic Gelatin withdrawal prior to the routing step), 2) the dissolved metal-flux from the Woburn West sub-

basin. (Woburn West concentrations were set at the average concentrations for 1992), and 3) the dissolved metals from the Winchester sub-basin.

Verification of the dissolved-metal model was performed using 1993 dissolved-metals data which consisted primarily of 32 instantaneous samples collected at gage 5.

The verification was run after the value of x (the fraction of melt flow applied to the quick system) had been determined from the suspended sediment calibration. The x parameter affects the dissolved-metal flux since it distributes the amount of melt flow between waters of potentially different quality. (i.e. quick waters versus slow waters) This parameter was especially important for the 1993 runs, since streamflows during this year were strongly affected by snowmelt which, through the x parameter, affected the modeled net water quality.

V.2.2.2 Evaluation of Dissolved Metal Parameters: $[M_d]$'s

From calibrations using 1992 data, the concentration of dissolved metals associated with each flow component is provided in table V.2-4.

Sub-basin	Arsenic			Iron			Chromium			Copper		
	$[As_d]_{quick}$ µg/l	$[As_d]_{slow}$ µg/l	$[As_d]_{ltbf}$ µg/l	$[Fe_d]_{quick}$ mg/l	$[Fe_d]_{slow}$ mg/l	$[Fe_d]_{ltbf}$ mg/l	$[Cr_d]_{quick}$ µg/l	$[Cr_d]_{slow}$ µg/l	$[Cr_d]_{ltbf}$ µg/l	$[Cu_d]_{quick}$ µg/l	$[Cu_d]_{slow}$ µg/l	$[Cu_d]_{ltbf}$ µg/l
Woburn North	0.90	2.50	8.50	0.06	0.30	0.95	0.20	1.00	1.50	6.10	7.00	7.90
Woburn Central	1.50	1.70	0.50	0.20	0.20	0.35	0.50	0.70	4.10	3.10	2.80	14.00
Winchester	1.50	1.50	3.00	0.05	0.20	0.80	0.90	0.00	0.50	11.00	1.40	8.00

Table V.2-4: Dissolved-Metal Concentrations Associated with Each Streamflow Component

For a given metal, the quick, slow, and ltbf dissolved-metal concentrations from a given sub-basin were generally within an order of magnitude of one another. The primary exception was observed for iron at the Woburn North and Winchester sub-basins, where the concentrations were within 2 orders of magnitude of one another.

For arsenic and iron, the value of $[M_d]_{ltbf}$ was generally larger than $[M_d]_{quick}$. The values of $[M_d]_{slow}$ were generally between the values of $[M_d]_{ltbf}$ and $[M_d]_{quick}$. The primary exceptions were the arsenic concentrations in the Woburn Central sub-basin, where the concentration of the quick component was larger than the concentration of the longterm-baseflow component. These results suggest that if dissolved iron and arsenic transport are to be reduced from the Aberjona River, the most efficient remediation scheme would include treatment of the longterm-baseflow component from the Woburn North and Winchester sub-basins.

For chromium and copper, the dissolved-metal concentration was generally higher for the longterm-baseflow component than for the quick-flow components. The primary exception was at the Winchester sub-basin where the opposite relation was observed. For all of the sub-basins, the slow component never had the highest dissolved-metal concentration.

The highest chromium and copper concentrations were estimated for the longterm-baseflow component from the Woburn Central sub-basin. Therefore, if transport of these metals is to be reduced, the most efficient method would involve a clean-up of the longterm-baseflow component from the Woburn Central sub-basin.

V.2.3 Suspended Sediment Model

V.2.3.1 Calibration and Verification Procedure

Gages 2,3, and 5

Consistent suspended sediment parameters were maintained throughout the model. For example, the same channel erosion coefficient was used for channel erosion from all sub-basins, main channels, and from the Atlantic Gelatin area. Similarly, the suspended sediment parameters for all the quick areas had the same values regardless of the sub-basin in which they were applied. Therefore, the calibration of the suspended sediment model was performed by adjusting each parameter until the best fit to the gage 5, 3, and 2 data could be obtained.

Calibration of suspended sediment parameters was based upon data collected in 1992. Strong emphasis was placed upon calibrations against suspended sediment concentrations determined through filtration analysis, since suspended sediment concentrations using this technique were assumed to be the most accurate. For gaging stations 2 and 3, a) eleven measurements for samples filtered through 0.5 μm filters, and b) twelve measurements for samples filtered through 1.5 μm filters, were available at each station. Seventy measurements (0.5 μm) and twelve (1.5 μm) were available at gaging station 5. Times and dates of sample collection are given in tables IV.E-1 through IV.E-20.

Suspended sediment data from turbidity measurements were also used for calibration purposes; however, because of the less accurate suspended sediment data obtained from these measurements, turbidity-derived suspended sediment information was used only to approximate general increases and decreases in suspended sediment data. In other words, the turbidity data were not used to fit suspended sediment concentrations on a one-to-one basis.

The only exception to the calibration process was the "x" parameter (the fraction of melt flow applied to the quick system), which was calibrated using 1993 data rather than 1992 data. This parameter is of importance in sediment transport modeling because it affects the distribution of water between different suspended sediment sources. The reason this parameter was calibrated using 1993 data was because 1993 (and not 1992) was strongly affected by melt flow. Because of the need to calibrate this one parameter during 1993, the run using 1993 data is considered a "pseudo-verification".

The pseudo-verification data set consisted of 38 instantaneous suspended sediment samples (0.5 μm) collected at gage 5 during 1993.

For calibration purposes, a minimum value of maxlq·A/k, a quick-system parameter, was obtained by estimating the mass of quick sediments transported by the largest storm sampled (the March 29 storm). For this storm the mass of quick sediments transported was approximately 50,000 kg and therefore during the calibration process values of maxlq·A/k were set at values larger than 50,000 kg.

The value of k, the quick-sediment deposition-loss coefficient, controls how quickly the maximum value of the quick accumulation can be reached. The smaller the value of k the quicker the rate of increase. The k parameter was calibrated subjectively by analyzing storms for which the necessary suspended sediment data were available.

Quick-system transport parameters, C_q, thresq, C_r, thresr, and frac, and the channel parameter, C_s, were calibrated against data collected at the initiation of storm events. The values of C_r, thresr, and frac, (rainfall-impact sediment transport parameters) were modified such that the initial blips in the suspended sediment concentrations observed immediately prior to a quick-flow response could be reproduced.

The slow and longterm-baseflow parameters, bfpot, were adjusted within the 2 to 15 mg/l range which corresponds to the low suspended sediment concentrations observed shortly after storm events. Adjustments to bfpot were made against suspended sediment data collected during primarily low flows.

Gage 1

Calibration runs for gage 1 were performed against observed values of non-volatile (inorganic) and volatile (organic) suspended sediment concentrations for samples collected in 1992. The 1992 data set consists of instantaneous samples collected at roughly monthly intervals. Twelve volatile and twelve non-volatile measurements (using 1.5 μm pore size filters) were available for calibration purposes.

The values adjusted for the calibration of the organic phase included: 1) the growth rate constant, k_{20}, 2) the temperature activity coefficient, θ, and 3) the organic suspended sediment concentration in the input, $[SS]_{org,input}$. For the inorganic phase, the proportionality constant, K_r, was adjusted.

V.2.3.2 Evaluation of Quick System Parameters: maxlq, k, C_q, thresq, n, C_r, frac, and thresr

The calibrated values of the build-up and wash-off coefficients are given in table V.2-5. These values were calibrated using 1992 data.

Coefficient	Calibrated Value
maxlq	200000 g/(hr·mile^2)
k	0.01 /hr
C_q	1.3 x 10^{-7} (1/hr)·(mile^2/cfs)^n
thresq	0 cfs
n	4
C_r	3 (1/hr)·(hr/inch)^n
frac	0.2
thresr	0 cfs

Table V.2-5: Calibrated Values of Quick System Suspended Sediment Parameters

Sartor & Boyd, 1972 provided a list of solids loads and accumulation rates for various land-uses. For solids loads (maxlq/k) they listed values of 1200, 2800, and 290 $^{lb}/_{curb\ mile}$ for residential, industrial, and commercial land-uses, respectively. For urbanized lands within the Aberjona Watershed there are approximately 42 curb miles per square mile.[12] Applying the various conversion factors, the model value of maxlq/k is computed as:

$$\frac{maxlq}{k} = \frac{200{,}000\ ^{g}/_{hr\cdot mi^2}}{0.01\ /_{hr}}$$

$$= 20{,}000{,}000\ ^{g}/_{mi^2}$$

$$= 1050\ ^{lb}/_{curb\ mile}$$

[12]To convert curb mile to mi^2 the average size of a city block was estimated from a topographic map of the Aberjona Watershed. Several city blocks were randomly chosen from the map and their average area was determined as 260,000 ft^2. Noting that each square mile is equal to 28 x 10^6 ft^2, approximately 110 (28 x 10^6/260000) city blocks are incorporated within a square mile. Assuming that the curb miles per mi^2 can be estimated by assuming that these city blocks are arranged as 10 vertical streets and 11 horizontal streets, then a total of 21 (10+11) miles of road are associated with a square mile. Noting that for each mile of road there are 2 miles of curb, then there should be approximately 42 curb miles associated with each square mile.

The model value of 1050 $^{lb}/_{curb\ mile}$ compares well with the residential value listed by Sartor & Boyd, 1972.

In Overton & Meadows, 1976, the rates of solids accumulation, maxlq, are listed as 590, 1400, and 180 $^{lb}/_{curb\ mile \cdot day}$ for residential, industrial, and commercial land uses, respectively. The model value of maxlq was determined as:

$$\begin{aligned} \text{maxlq} &= 200{,}000\ ^{g}/_{hr \cdot mile^2} \\ &= 250\ ^{lb}/_{day \cdot curb\ mile} \end{aligned}$$

This value of maxlq corresponds to a value somewhere between the commercial and residential values listed by Overton & Meadows, 1976.

The values of thresq = 0 and thresr = 0 indicate that the critical velocities required to initiate motion are small compared to the values of "flowq" and "rain". The value of frac equal to 0.2 indicates that approximately 20% of the quick area is exposed to direct rainfall impact. The value of n = 4 corresponds to the low-end of the value that would be expected for cohesive sediment transport (Lick 1989; Galiani, 1991; Ziegler & Nisbet, 1993; Cardenas, 1993) and is higher than the value of n = 3 derived from classical sediment transport theory.

Converting the value of $C_q = 1.3 \times 10^{-7}$ (1/hr)·(mile^2/cfs)^n to units consistent with C_r results in a C_q value that is equal to 22,500 (1/hr)·(hr/in)^n. This value of C_q is much larger than the C_r of 3 (1/hr)·(hr/inch)^n. The two values differ by roughly 4 orders of magnitude. However, considering that roughly 10% of the rainfall is converted to quick flow, there is actually a 3 order of magnitude difference in the erosive capacities of the quick flow and rainfall impact. Such a result indicates that quick flow is a much more efficient eroder of sediment than rainfall.

V.2.3.3 Evaluation of the Slow and Longterm Baseflow System Parameter: bfpot

The value of bfpot was set at 5.0 mg/l. This value was determined from calibrations using 1992 data and is consistent with the observed concentrations during low flow conditions.

The bulk of the waters from both the slow and longterm-baseflow systems may be assumed to travel through the ground prior to discharge into the river. Since the same value of bfpot was satisfactory for each system, apparently the aquifer is capable of imparting a potential suspended sediment concentration on each of these waters. For the Aberjona River the potential concentration imparted by the aquifer was: 1) constant regardless of the response time of a given system (i.e. bfpot for the slow system equals the bfpot for the longterm baseflow system) and 2) was constant in time for a particular system.

V.2.3.4 Evaluation of Channel Parameters: C_s and n

From calibrations using 1992 data, the values $C_s = 8 \times 10^{-5}$ (1/hour)·(mile^2/cfs)^n and $n = 4$ were determined. The value of $n = 4$ has been discussed in detail in the section V.1.2.1 and in section V.2.3.2.

The value of $C_s = 8 \times 10^{-5}$ (1/hour)·(mile^2/cfs)^n is almost three orders of magnitude larger than the value of C_q. Because of the larger value of C_s, sediments in the channel are more efficiently eroded than sediments in quick areas. The net result is for a periodic but complete flushing of sediments from the channel, whereas only a fraction of the sediment from quick areas is periodically flushed. On the other hand, considering that: 1) sediment transport is also a function of the amount of sediment in each system and, 2) the quick area generally stores much more sediment (approximately 3 orders of magnitude greater) than the channel, the rate of sediment output from the quick system is comparable to the *potential*[13] rate of sediment output from the channel. In the event that an excess of sediments is supplied to the river channel, the channel will be very efficient at mobilizing those sediments to downstream areas.

[13] Potential rate of transport is emphasized since the sediment supply may be exhausted from the channel.

V.2.3.5 Evaluation of Woburn West Sub-basin Parameters: θ, k_{20}, and K_r

From calibrations using 1992 data, the values of k_{20}, θ, and K_r were determined as 1.05 x 10^{-7}/hr, 1.30, and 1000 hour·(mg/liter) respectively.

The value of θ = 1.3 from calibration runs is slightly larger than the values reported for biological treatment processes. Typical values of θ for biological treatment processes range from 1.0 to 1.14. (Metcalf & Eddy, 1979) From the van't Hoff-Arrhenius equation, the larger θ indicates that the activation energy of chemical reactions required for growth of organic particles in Wedge Pond is larger than the activation energy associated with wastewater treatment processes.

The value of k_{20} = 1.05 x 10^{-7} /hr is orders of magnitude smaller than the values typical of activated sludge processes. (Typical growth rate constants for activated sludge processes are generally in the vicinity of 0.2 /hr; Metcalf & Eddy, 1979) A value which is orders of magnitude lower is as expected since in the natural environment growth tends to be much more limited in nutrients. (Brock & Madigan, 1991)

The value of K_r defines the suspended sediment concentration associated with a particular hydraulic residence time. For example, for K_r = 1000 hour·(mg/liter), a suspended sediment concentration of 0.4 mg/l and 4.0 mg/l would be expected for average flow through rates of 1 and 10 cfs, respectively.

V.2.4 Particulate-Metals Model

V.2.4.1 Calibration and Verification Procedure

The particulate-metal parameters were calibrated after the streamflow and suspended sediment models were calibrated. The procedure used for the particulate-metal calibration was similar to the procedure used for dissolved metals. Calibration included the adjustment of particulate-metal concentrations corresponding to each sediment component ($[M_p]_{quick}$, $[M_p]_{slow}$, $[M_p]_{ltbf}$). Initial estimates of $[M_p]_{quick}$, $[M_p]_{slow}$, and $[M_p]_{ltbf}$ were obtained from plots of particulate-metal concentrations versus streamflow at each of the gaging stations. The initial estimates were then adjusted during the calibration process.

The sequence of the calibration was again similar to the sequence used for the calibration of the dissolved metals. (See section V.2.2.1 for more details) Calibration was performed using 1992 particulate-metals data. "Pseudo-verification" (See section V.2.3.1) was performed using 1993 particulate-metals data. Calibration data corresponded to: 1) eleven instantaneous samples (0.5 μm) collected at approximately monthly intervals at gaging stations 1, 2, and 3, and 2) seventy samples (0.5 μm) collected at monthly intervals and during storm events at gage 5. Pseudo-verification data correspond to 26 samples collected at gage 5.

V.2.4.2 Evaluation of Particulate Metal Parameters: $[M_p]$'s

From calibrations using 1992 data, the concentration of particulate metals associated with each suspended sediment input is provided in table V.2-6.

Sub-basin	Arsenic			Iron			Chromium			Copper		
	$[As_p]_{quick}$ mg/kg	$[As_p]_{slow}$ mg/kg	$[As_p]_{ltbf}$ mg/kg	$[Fe_p]_{quick}$ %	$[Fe_p]_{slow}$ %	$[Fe_p]_{ltbf}$ %	$[Cr_p]_{quick}$ mg/kg	$[Cr_p]_{slow}$ mg/kg	$[Cr_p]_{ltbf}$ mg/kg	$[Cu_p]_{quick}$ mg/kg	$[Cu_p]_{slow}$ mg/kg	$[Cu_p]_{ltbf}$ mg/kg
Woburn North	40	20	1100	2.5	3.5	20.0	120	120	600	400	150	450
Woburn Central	40	20	600	2.0	2.0	12.0	450	120	950	300	20	400
Winchester	100	20	500	5.0	1.0	15.0	350	20	300	350	0	200

Table V.2-6: Particulate Metal Concentrations Associated with Each Suspended Sediment Input

For all metals, $[M_p]_{slow}$ was generally cleaner than $[M_p]_{quick}$ and $[M_p]_{ltbf}$. The only exception was the $[M_p]_{slow}$ for iron from the Woburn North sub-basin. For arsenic and iron, $[M_p]_{quick}$ was much smaller than $[M_p]_{ltbf}$. For chromium and copper, the values of $[M_p]_{quick}$ were comparable to the values of $[M_p]_{ltbf}$. From a remediation point of view, it would be most desirable to treat the longterm-baseflow components for all metals and the quick components for chromium and copper.

It is interesting to note that $[M_p]_{ltbf}$ was calibrated to be consistently larger than $[M_p]_{slow}$. Conceptually, waters from both slow and longterm-baseflow systems may be considered to come from a groundwater source. The primary difference between each of these systems that could result in a different particulate-metal concentration is the residence time of the water. One may recall that the time constant for the slow system, the Water Response Time (WRT_s), was calibrated as 24 hours (section V.2.1.2) whereas the time constant of the longterm-baseflow system was estimated as 19 days (section IV.2.4). Because of the longer time constant, waters from the longterm-baseflow system have more time to "pick-up" metals from the groundwater aquifer and consequently have higher $[M_p]$ values. Waters from the quick system, on the other hand, are assumed to travel through an entirely different system than slow and longterm-baseflow waters and will therefore attain a metal concentration that is typical of that system.

V.3 MODEL PERFORMANCE

V.3.1 General Comments Concerning Model Evaluations

Model Errors

Model errors may be subdivided into three categories: 1) input errors, 2) errors in data measurements, and 3) model errors. (Hromadka, et. al., 1990) A model can be perfectly formulated, but if the inputs or data measurements are incorrect large discrepancies between modeled and measured data may occur. Therefore, criteria used to evaluate overall model performance should be viewed, not simply as the evaluation of the model formulation, but rather as an evaluation of the sum of errors associated with model inputs, data measurements, and model formulation.

Criteria Used for Model Evaluation

For the present study, criteria used to evaluate streamflow model performance include: 1) the goodness of fit R^2 parameter, 2) mass balances, 3) comparison of standard deviations, 4) time series plots, and 5) comparison of flow histograms. For the water quality part of the model, criteria include: 1) the R^2 parameter, and 2) time series plots. By using more than one criterion, different aspects of model performance can be evaluated.

V.3.1.1 Evaluation of Streamflow Models

Goodness of Fit, R^2

The R^2 parameter is a measure of the goodness of fit between modeled and measured values. It is the fraction of the measured variance that can be explained by the model. Computationally, it is equivalent to the square of the correlation coefficient[14]:

$$R^2 = \frac{\sum_i (\text{modeled value}_i - \text{measured mean})^2}{\sum_i (\text{measured value}_i - \text{measured mean})^2}$$

[14]Since values of streamflow are not independent over short time scales, the statistical assumptions that underlie the correlation coefficient are not valid. Therefore, the R^2 value cannot be used as a statistical quantity in standard tests of significance in evaluating the performance of streamflow models, although the parameter does provide a good index of fit. (McCuen, 1989)

The R^2 parameter tends to weigh heavily upon the extreme values of the modeled versus measured flows. (Hamilton, 1990) For the Aberjona River extreme values are represented by a few high flows as observed from the streamflow histogram (figure IV.2-7). For the Aberjona River, the R^2 value would depend heavily upon the ability of the model to estimate peak streamflows.

One drawback of the R^2 parameter is that it is based upon a one-to-one comparison of measured and modeled values at the same point in time. Because of this attribute, this criteria tends to penalize strongly for a time shift error between modeled and measured flows. For example, assume that: 1) streamflow is modeled perfectly, except that there is a 4 hour time shift between the modeled and measured values, and 2) assume that the streamflow hydrograph is characterized by a streamflow response with a rapid increase and decrease in streamflow occurring within 3 hours. For this example, the magnitude of the peak was estimated perfectly by the model. However, because of the time shift, the modeled peak occurred during a measured low flow value. The result would be an extremely poor R^2 value, indicating poor model performance. In this situation, the measure of the R^2 value would provide no indication that the model was capable of capturing the magnitude of the peak.

R^2 values for several models on various watersheds are summarized from a series of papers. (Table V.3-1) From the table, R^2 values varied from 0.90 down to values less than zero. A value of 1 represents a perfect fit, whereas a value less than zero indicates that the model performed worse than simply using the average streamflow. From the range of values provided in the table, high R^2 values may be considered to lie within the following range:

$$\text{High } R^2 \text{ Values: } 0.7 < R^2 < 1.0$$

A discussion of some of these papers is included in appendix V.C.

Paper	Basin Description	Model Characteristics	R^2 Calibration	R^2 Verification
Franchini & Pacciani, 1991	Sieve Basin, Italy 320 mi^2, 10% imperv 4 Rain Gages	Watershed Specific Continuous, Hourly	0.88 (1 month)	0.85 (3 months)
Thomas, 1990	Urban Watershed, NM 0.12 mi^2, 1 Rain Gage	DR3M Model Event, 5 min	0.77 (38 storms) peaks	0.90 (46 storms) peaks
Marivort & Vandeweile, 1980	River Dijle, Belgium Non-Urban Hirnant Basin Non-Urban	Watershed Specific Continuous, Hourly Watershed Specific Continuous, 30 min.	0.79 (79 storms) 0.80 (9 storms)	
Prakash & Dearth, 1990	Upper Santa Rosa Crk N. Calif., 12.6 mi^2 Urbanized	NWSRFS Model Continuous, Daily	0.59 (11 years)	
Warwick & Wilson, 1990	Bachman Branch, TX 10 mi^2, Urban/Resid	STORM Model Event, Hourly	(1 storm) peaks	0.58 (10 strm) peaks
Tucci & Clarke, 1980	Rio Capivari, Brazil 312 mi^2, 1 rain gage	Watershed Specific Continuous, Daily	(6 months)	0.56 (2 months)
Nikolaidis,et. al. 1993	Experimental Watershed VT, 3.2 mi^2 Grassland-Forest	Watershed Specific + Energy Balance Continuous, Daily	0.21 (5 years)	0.24 (3 years)
Loague & Freeze, 1985	Prairie Grassland, OK 0.04 mi^2 Pasture & Cult. Fields, PN, 2.8 mi^2	Regression, UH Kin. Wave, Event Regression, UH Kin. Wave, Event		0.1 to 0.4 (36 peaks) -.1 to 0.1 (72 peaks)

Table V.3-1: Summary of R^2 Values from Selected Papers in the Literature

Mass Balances Between Modeled and Measured Flows

For the papers summarized in table V.3-1, the magnitude of the errors in the mass balance between overall modeled and measured streamflow varied from 3 to 100%. (Loague & Freeze, 1985 (30 to 100% and -12 to -100%); Nikolaidis, et. al., 1993 (-3% & 4.5%); Prakash & Dearth, 1990 (-6%); Thomas, 1990 (-11%)) This error is defined as:

$$\text{mass balance \% error} = \frac{\text{measured mean flow - modeled mean flow}}{\text{measured mean flow}} \cdot 100\%$$

The closer the % error is to 0% the better the model performance. Considering the range of the errors in the papers reviewed, a mass balance in the following range will be considered acceptable for this study:

$$\text{Acceptable Mass Balance:} \qquad -10\% < \%\ \text{error} < +10\%$$

Better mass balances between modeled and measured flows did not necessarily correspond with higher R^2 values. For example, in the study presented by Nikolaidis et. al. 1993, the calibration R^2 valuc was 0.21 whereas the mass balance was within 3%. In the Thomas, 1990 study, the overall calibration R^2 was 0.77 while the mass balance was 11%. Such a result indicates that the model presented by Thomas was good at matching streamflow extremes but was not as good at representing the overall average streamflow. The model presented by Nikolaidis et. al. 1993, on the other hand, did not capture the extremes as well but performed very well in representing the overall water balance.

Standard Deviation Between Modeled and Measured Flow

A comparison of the standard deviations, σ, of modeled and measured flows provide another means by which a model may be evaluated. The difference between the modeled and measured standard deviations is represented as a % error:

$$\sigma\ \%\ \text{error} = \frac{\sigma_{measured} - \sigma_{modeled}}{\sigma_{measured}} \cdot 100\%$$

$$= 1 - \left(\frac{\sum_i (\text{modeled value}_i - \text{modeled mean})}{\sum_i (\text{measured value}_i - \text{measured mean})} \right) \cdot 100\%$$

The σ % error is very similar to the definition of $1 - \sqrt{R^2}$. The primary difference is that the modeled mean rather than the measured mean is used to evaluate the numerator. If the measured and modeled

means are similar to one another, one would expect that the lower the σ % error the higher the R^2 value.

Values of σ were not cited in the papers reviewed nor were ranges of acceptibility identified. Therefore, we adopted the same range as for the mass balance % errors:

$$\text{Acceptable } \sigma \text{ \% error:} \quad -10\% < \sigma \text{ \% error} < +10\%$$

Time Series Plots

Time series plots are plots of modeled and measured streamflows versus time. These plots are extremely useful since they can be used to evaluate many different aspects of model performance. These aspects include: 1) the magnitude of peaks, 2) the timing of peaks, 3) the characteristics of the receding limbs, 4) the characteristics of low flows, and 5) the overall patterns between modeled and measured flows. Pattern recognition is one aspect of time series plots which is not available through other criteria and is also the aspect which makes time series plots especially useful when formulating and calibrating a model. For example, assume that modeled values increase when the measured data increase and vice versa; however, the rate of increase and decrease are different. Such a result indicates that the model is capable of capturing the general streamflow response to the input. However, the way in which the model represents the overall increase and decrease must be adjusted. For example, if unit graphs are used to model flow, the user may adjust the shape of the unit graphs such that the rates of increase and decrease of the streamflow are better represented.

The main drawback associated with time series plots is their qualitative nature. When using time series plots to evaluate model performance, there is no quantitative measure by which models can be ranked with respect to one another. Rather, the user is required to make a subjective judgment.

Histograms

Histograms are plots of streamflow versus the number of occurrences. These plots enable the user to quickly pin-point the range of streamflows in which the model does not perform properly. For example, from a histogram plot, one can quickly determine whether too few peaks or whether too few low flows are modeled. These plots do not penalize for time shifts between modeled and measured flows.

One of the drawbacks of this evaluation criteria is that it is qualitative in nature. Therefore, as with time series plots, the user must make a subjective judgment when comparing the performance of one model versus another.

V.3.1.2 Evaluation of Water Quality Models

From review of the literature, water quality models can be subdivided into two broad categories: storm load models and pollutograph models. Storm load models provide only the total pollutant load for a given storm event. These models do not provide any information concerning how the pollutant load is distributed in time during a storm event. Pollutograph models, on the other hand, do describe how the pollutant load is distributed during a storm event. The model developed within this thesis is a pollutograph model.

Within the literature, pollutograph models were generally characterized by a lack of data. In some instances these models were applied with no data for either calibration or verification. In other cases, where some data were available, the data were inadequate. For example, a model may predict a large increase in a pollutant load during a storm event followed by a long receding limb. However, the only data available for model calibration would be a few data points on the far end of the receding limb with no data to verify that a large increase in pollutant load occurred during the storm event. For the few studies which appear to have sufficient data measurements (Overton & Meadows, 1976; Svensson, 1987) the authors, in general, did not rigorously evaluate the pollutograph model using quantitative criteria. Rather, the authors presented time series plots of modeled versus measured values. For these studies, model performance was generally characterized by a lack of one-to-one correspondence between modeled and measured data. For example, Overton and Meadows, 1976, applied the USEPA STORM Model to model streamflow, suspended sediment, and BOD in a river. Their data generally showed an increasing trend prior to a storm and a decreasing trend after the storm. The model also showed the same general trend; however, the rate of increase and decrease and the magnitude of the peaks were significantly different between modeled and measured data.

Our general conclusion concerning the evaluation of pollutograph models is that at the current state of research, pollutograph-type water quality models have not performed particularly well. For this reason, acceptable ranges of quantitative measures of performance will not be suggested in the current study.

V.3.2 Streamflow Model

R^2, Mass Balances, and Standard Deviations

Statistics of modeled versus measured flows for the 1991, 1992, and 1993 run periods are provided in tables V.3-2 to V.3-5. A summary of the dates corresponding to each run period are given in section V.2.1.1.

Due to occasional gage malfunction, there are some gaps in the measured data. (See tables IV.A-6 through IV.A-9 in Appendix IV.A for the fraction of time that measured data is available.) R^2, mean streamflows, and standard deviations were computed only for the time steps when both measured and modeled flows were available. For each calibration and verification year, plots of modeled versus measured flows are also provided in figures V.C-1 to V.C-9 in appendix V.C.

The R^2 values at gages 2,3, and 5 are considered to be within the high range, indicating that the model performed well in estimating the extreme streamflows on a one-to-one basis in time. The only exception was for the 1991 verification year at gage 2 where the R^2 value was 0.64. This lower R^2 value was due, in large part, to the model over-estimating the amount of snowmelt during December 10 to 15, 1991. The over-estimation of snowmelt, may have been associated with improperly identifying precipitation as snowfall during earlier time steps.

The R^2 values at gage 1 were significantly lower than at gages 2,3, and 5. The reason for the poorer performance was due to the manner in which the streamflow data for gage 1 were input into the model. For gage 1, the streamflow input consisted of an interpolation of mean monthly streamflows. The model, therefore, had no way of capturing streamflow peaks in response to precipitation events at this gage. Because of the inability to capture the streamflow peaks, the R^2 at gage 1 tended to be low.

The mass balances between modeled and measured flows were well within the acceptable range for gages 5 and 1. For gages 2 and 3, the mass balances were just outside the acceptable range, but within +-20%. The only exception was the 1991 verification run at gage 3 which had a mass balance error of 21.4%.

The standard deviations between the modeled and measured flows at gage 2 and at gage 3 for the 1992 calibration year were within acceptable ranges. For gage 5, the standard deviations were just outside the acceptable range, within +-15%. Gage 1 had the largest errors, with errors between 33 and 39%. These large errors were due to the manner in which these data were input into the program. The

streamflows at gage 1 were input as interpolated values of the overall mean monthly flow. These interpolated values had a standard deviation on the order of the monthly flow fluctuations, whereas the measured data had a standard deviation resulting from streamflow fluctuations occurring on shorter time scales. These shorter time scales correspond to the time scales of individual storm events.

Larger errors generally occurred during storms which were affected by snowmelt and/or snowfall. During these times, the input error tended to be larger because both the precipitation and temperature inputs were used by the model to estimate streamflow; during times without snowmelt and/or snowfall, only the precipitation input was used by the model. Therefore, during winter storms, errors in either of the inputs will tend to give erroneous results, which would, in turn, increase the likelihood of large discrepancies between modeled and measured flows.

Model Year	Mean Streamflow			Standard Deviation			R^2
	Meas cfs	Mod cfs	Diff %	Meas cfs	Mod cfs	Diff %	
1992 Calibration	28.3	29.2	-3.2	25.5	28.6	-12.2	0.80
1993 Calibration	37.9	37.2	1.8	56.9	57.3	-0.7	0.88
1991 Verification	29.3	29.1	0.7	29.6	33.9	-14.5	0.78

Table V.3-2: Statistics of Modeled and Measured Streamflows, Gage 5

Model Year	Mean Streamflow			Standard Deviation			R^2
	Meas cfs	Mod cfs	Diff %	Meas cfs	Mod cfs	Diff %	
1992 Calibration	17.5	14.9	14.9	18.8	17.0	9.6	0.70
1991 Verification	19.2	15.1	21.4	28.0	21.8	22.1	0.75

Table V.3-3: Statistics of Modeled and Measured Streamflows, Gage 3

Model Year	Mean Streamflow			Standard Deviation			R^2
	Meas cfs	Mod cfs	Diff %	Meas cfs	Mod cfs	Diff %	
1992 Calibration	7.9	7.1	10.1	7.5	7.2	4.0	0.83
1991 Verification	9.1	7.4	18.7	8.1	7.7	4.9	0.64

Table V.3-4: Statistics of Modeled and Measured Streamflows, Gage 2

Model Year	Mean Streamflow			Standard Deviation			R^2
	Meas cfs	Mod cfs	Diff %	Meas cfs	Mod cfs	Diff %	
1992	7.0	6.5	7.1	6.0	3.7	38.3	0.54
1991	7.4	6.8	8.1	5.6	3.7	33.9	0.35

Table V.3-5: Statistics of Modeled and Measured Streamflows, Gage 1

Time Series Plots

For exemplification purposes two time series plots for gage 5 are included within the main body of this thesis. One plot corresponds to a summer storm event; the other corresponds to a large snowmelt event. Additional plots and more thorough discussions are included in appendix V.C.

On each time series plot, snow and rainfall are plotted on the inverted scales. Modeled flow corresponds to the solid line and the measured flow corresponds to the dotted line. Other lines correspond to modeled components which were added together to obtain the total modeled flow. The "+" signs on these plots correspond to times when water samples were taken. Additionally, for the snowmelt event, temperatures (> 32°F) are plotted on the lower axis.

For the summer storm event (figure V.3-1) the model was capable of reproducing the peak streamflows and a large portion of the receding flows. For the August 18th event, the streamflow model performed very well. For the August 10th event, the model over-estimated the measured peak flow and the measured streamflow during times when samples were collected. As observed from the dashed line (Winchester sub-basin contribution), the peaks observed at the initiation of the storm events are primarily composed of waters which come from the Winchester sub-basin. Of the Winchester water, most of the initial peak is due to a quick storm response. A large portion of the waters that are observed immediately after the initial peak are associated with the routed storm flows (i.e. quick and slow storm responses) from the Woburn North and Woburn Central sub-basins. After most of the storm flow has traveled through gage 5, then the streamflow is dominated by longterm-baseflow waters from all sub-basins on the Aberjona River and by streamflow from the Woburn West sub-basin. The sum of each of these responses results in the observed streamflow behavior at gage 5 which is characterized by: 1) an initial quick response from the quick system of the Winchester sub-basin, resulting in the initial streamflow peak, 2) a slower rate of decline (slow response) of the receding limb after the storm events, resulting from the routed storm flows from the Woburn North and Woburn Central sub-basins, and 3) more constant flows after the storm event, which are primarily due to longterm-baseflow contributions from the Aberjona River sub-basins and flows from the Woburn West sub-basin.

For the March 1993 time period which was strongly affected by snowmelt, (figure V.3-2) flows from March 17 to March 24 were slightly under-estimated. On the 24th, the model predicted a streamflow response to a precipitation event. The measured data, however, showed no evidence of a streamflow response. This error was most likely due to an input error. The input error could have been due to either: 1) an incorrect temperature measurement (i.e. temperature was actually < 32 °F rather than >

32 °F such that precipitation as snow rather than rain actually occurred) or, 2) an incorrect precipitation measurement (i.e. precipitation measured at Reading over-represented the precipitation on the entire watershed).

The following two peaks, on March 26 and March 27, were snowmelt responses due to temperature spikes. The model, also predicted a snowmelt response; however, the rate of the increase and decrease in streamflow were not precisely modeled.

Furthermore, from the 17 to the 28th, the measured data showed abrupt and somewhat random fluctuations in streamflow which the model was not able to capture. These fluctuations are believed to be associated with short-term freezing and thawing of the water entering the river. (See appendix IV.B for discussion) Since the model does not halt the routing of snowmelt once the temperatures fall below freezing, the model is unable to capture abrupt changes in streamflow associated with freezing and thawing effects.

During the March 29 event, the model was capable of properly estimating the peak flow. However, flows on the rising limb were slightly over-estimated by the model, whereas flows on the falling limb were slightly under-estimated.

During the March 29th event, the baseflow (Woburn West plus the longterm-baseflow contribution from Winchester) was characterized by relatively constant and elevated levels with: 1) Winchester quick and slow storm responses, and 2) flows routed from upstream areas, super-imposed on the elevated baseflow values. For the March 29th event, the initial storm peak is primarily associated with the quick response from the Winchester sub-basin. The slower rate of decline of the receding limb of the hydrograph is primarily associated with the routed storm flows (quick and slow) from the Woburn North and Woburn Central sub-basins.

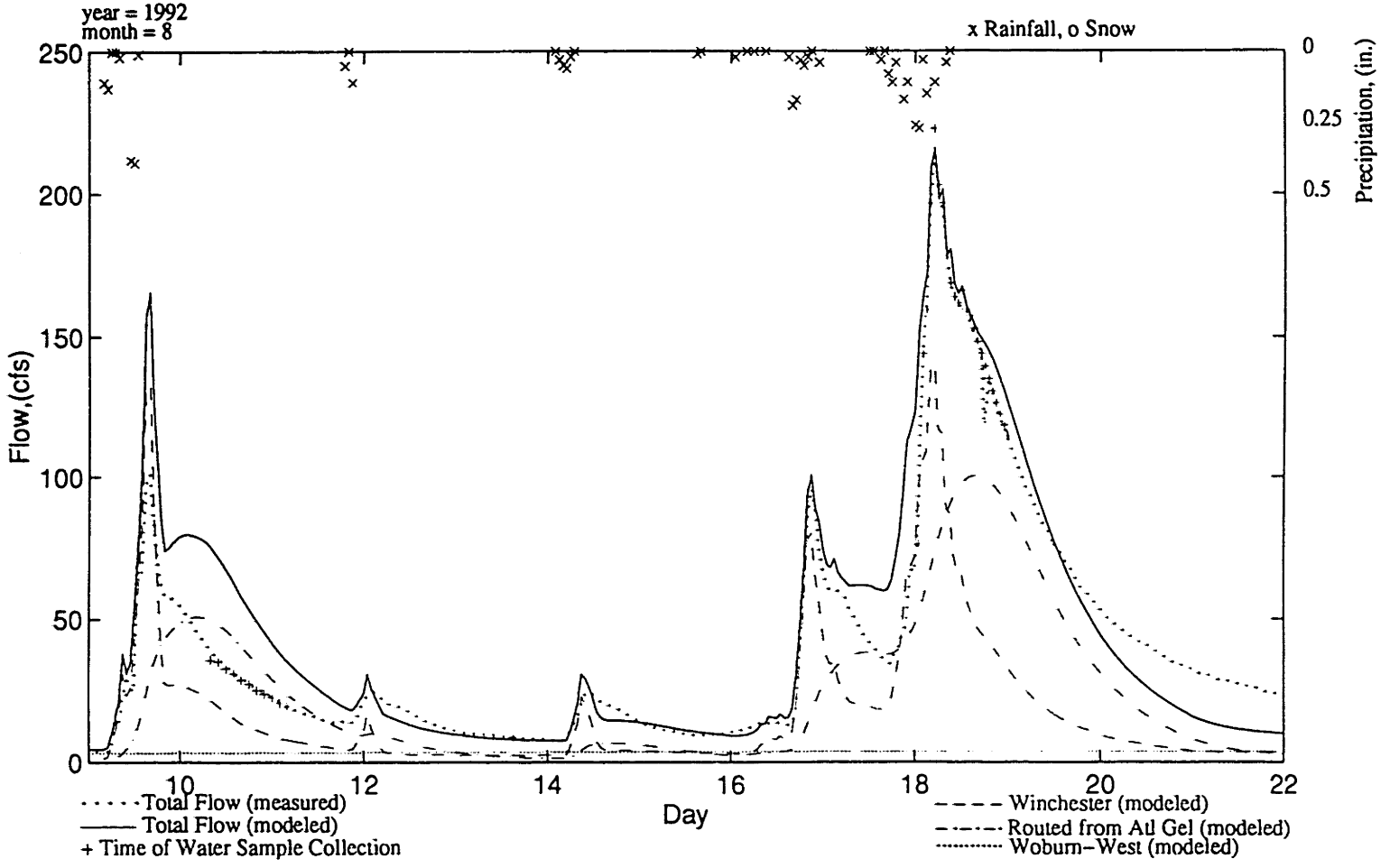

Figure V.3-1: Modeled versus Measured Streamflow, Time Series Plot, August 1992, USGS (Gage 5)

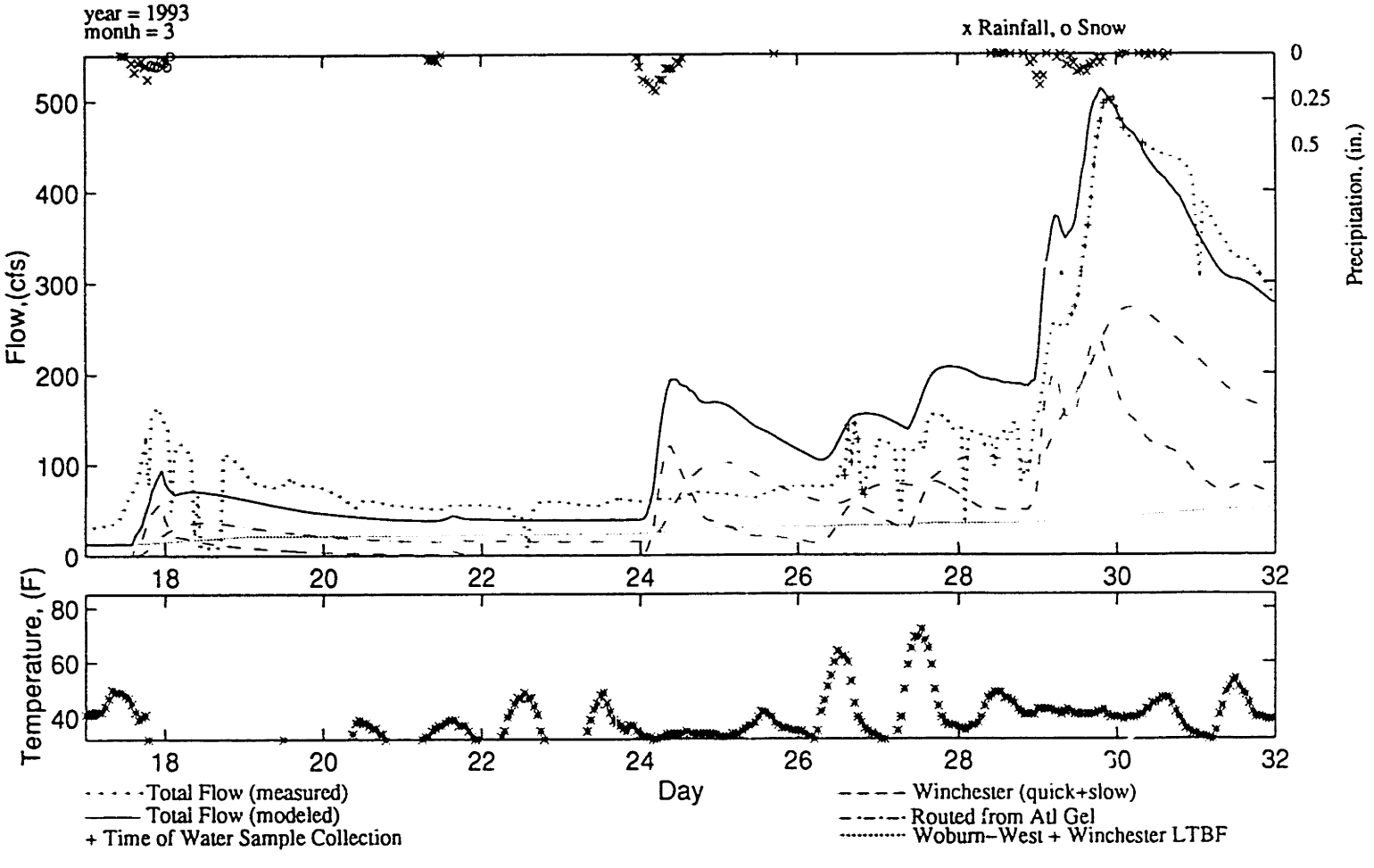

Figure V.3-2: Modeled versus Measured Streamflow, Time Series Plot, March 1993, USGS (Gage 5)

Histogram Plots

Histograms of modeled and measured streamflows are provided in figures V.3-3 to V.3-5. In general, the fit between the modeled and measured frequency plots is reasonable. For 1992 (figure V.3-3), the measured data indicate that the largest number of hourly streamflow values corresponds to the 10 to 20 cfs range. The modeled data have two peak occurrences: one within the 0 to 10 cfs range and the other within the 20 to 30 cfs range. For flows larger than 30 cfs, both the modeled and measured data for 1992 show exponential decreases.

For 1993 (figure V.3-4), both the modeled and measured data had: 1) the largest number of hourly streamflow values within the 0 to 10 cfs range, and 2) an exponential decrease in the number occurrences with increasing streamflows. Notable differences in the 1993 histograms correspond to the model over-estimating the number of occurrences in the 10 to 40 cfs range and under-estimating the number occurrences in the 40 to 110 cfs range.

During 1991 (figure V.3-5), both the modeled and measured data had two peaks in the number of hourly streamflow values: the first peak corresponded to the 0 to 10 cfs range and the second peak corresponded to the 20 to 30 cfs range. After 30 cfs, both the modeled and measured number of occurrences generally decreased with increasing streamflow. From 10 to 40 cfs the model generally under-estimated the number of occurrences, whereas from 0 to 10 cfs the model generally over-estimated the number of occurrences.

Model Evaluation: Streamflow

The model performed well in that it was capable of reproducing the general variations in streamflow. The R^2 values for both calibration and verification years were within the high range for the gaging stations along the Aberjona River. Mass balance and standard deviation errors, although a little high for some stations, were reasonable.

A large part of the error between the modeled and measured data may have been associated with input errors. As discussed in section IV.1, spatial variability of precipitation is a factor in describing overall precipitation for the watershed. Since only one hourly precipitation gaging station was available, the model could not be formulated to capture local differences in precipitation characteristics within the watershed. The errors in the precipitation inputs were compounded by errors in the temperature data, during the winter and spring months. As a result, the model did not perform as well during the winter/spring months as it did during the summer/fall months.

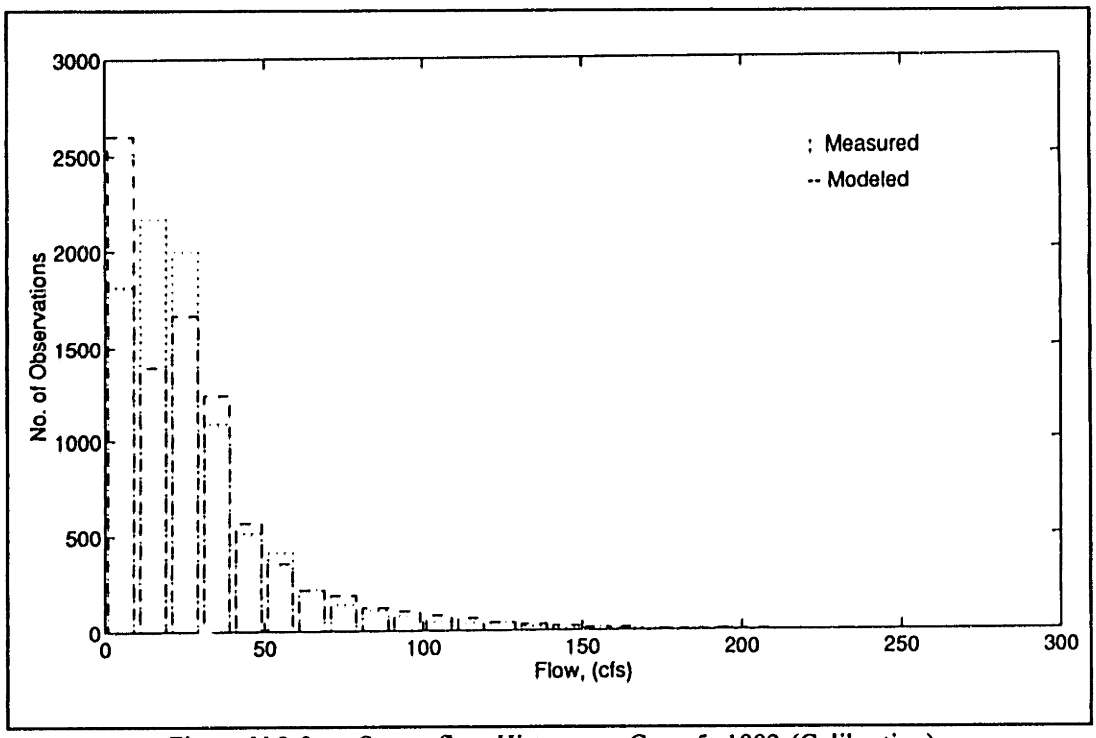

Figure V.3-3: Streamflow Histogram, Gage 5, 1992 (Calibration)

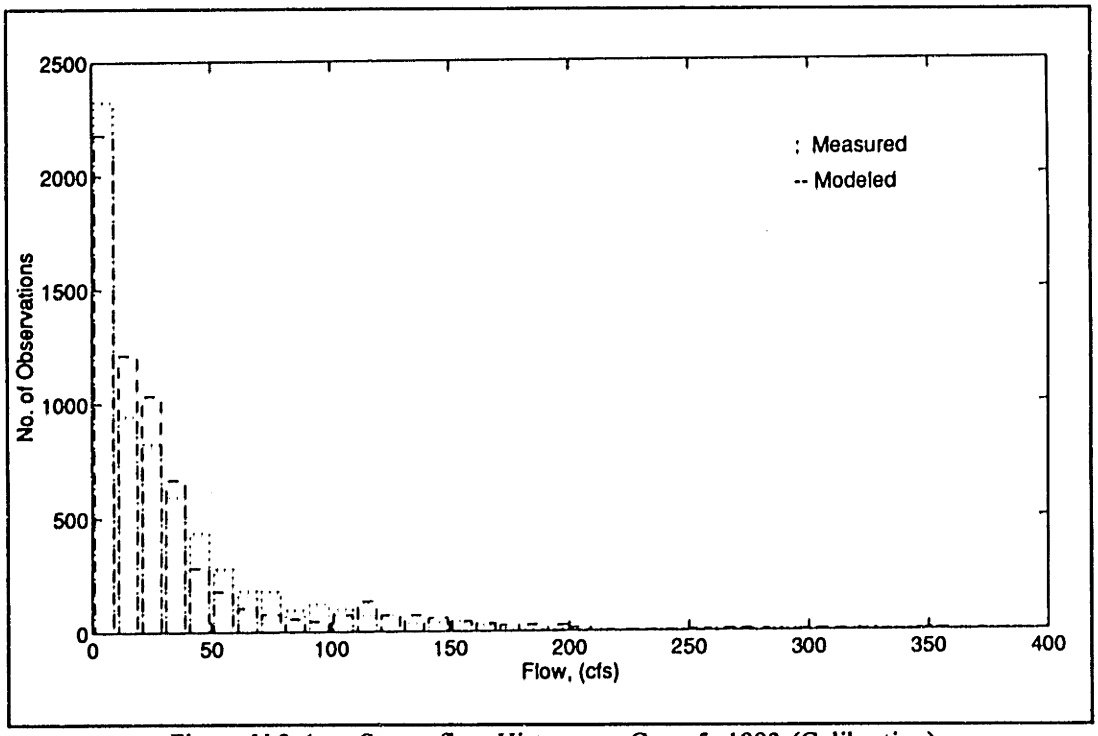

Figure V.3-4: Streamflow Histogram, Gage 5, 1993 (Calibration)

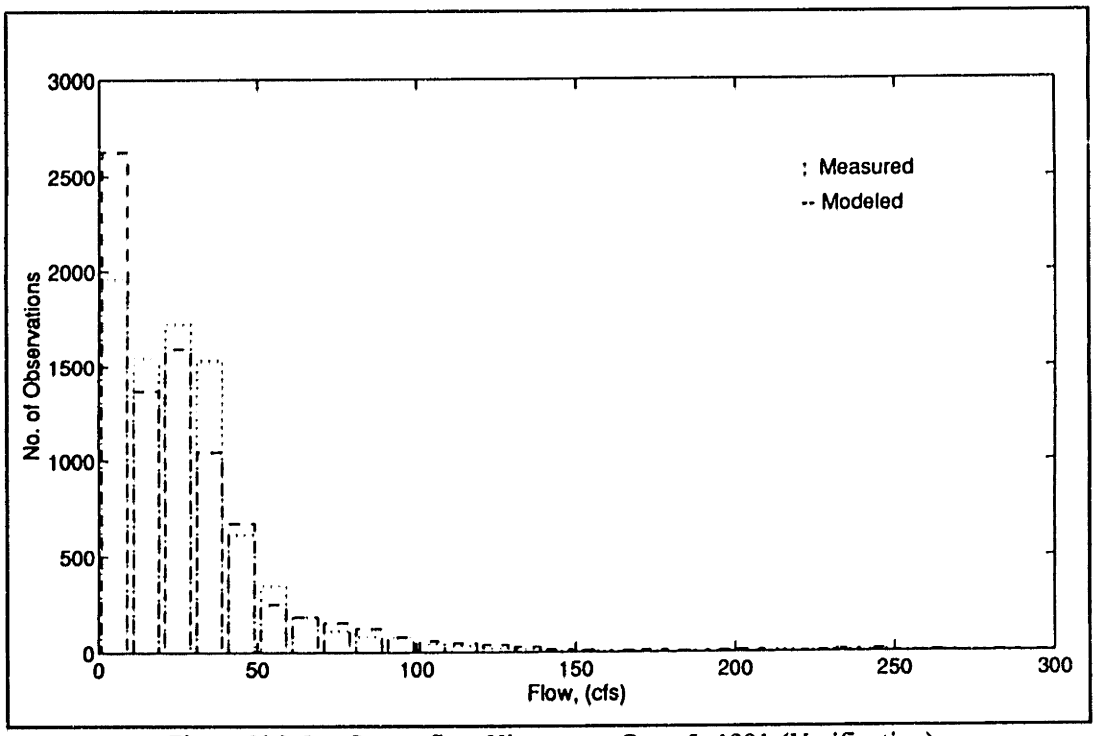

Figure V.3-5: Streamflow Histogram, Gage 5, 1991 (Verification)

V.3.3 Dissolved Metals

Goodness of Fit, R^2

R^2 values for modeled metal fluxes at gage 5 are reported in table V.3-6. The 1992 and 1993 statistics correspond to roughly 70 samples collected in 1992 and 32 samples collected in 1993, respectively. Plots of modeled versus measured fluxes and time series plots for dissolved arsenic are provided in figures V.3-6 to V.3-10. For figures V.3-6 and V.3-9, the number next to each data point corresponds to the month during which each sample was collected.

The method used to model the dissolved fluxes for each metal was identical for each metal except for the concentration values assigned to the quick ($[M_d]_{quick}$), slow ($[M_d]_{slow}$), and longterm-baseflow ($[M_d]_{ltbf}$) components. Because of the similarity in modeling each metal, results for only one metal, arsenic, are included within the main body of the thesis. Details of model performance for the other metals, including plots of modeled versus measured fluxes and time series plots for chromium, iron and copper, are provided in appendix V.C.

Model Year	Dissolved Metal Flux, R^2			
	As	Fe	Cr	Cu
1992 Calibration	0.71	0.44	0.60	0.77
1993 Verification	0.41	0.62	0.73	0.69

Table V.3-6: Statistics of Modeled and Measured Dissolved Metal Fluxes, Gage 5

Details of Model Performance: Dissolved Arsenic

For 1992 and 1993, the R^2 values at gage 5 were determined as 0.71 and 0.41, respectively. For 1992, a large portion of the measured dissolved arsenic flux was relatively well estimated by the model. (figure V.3-6) Two notable outliers include, however, the August 18 13:00 sample and the December 17 sample. The August 18 13:00 sample appears as an isolated point of higher concentration and flux. (figure V.3-7) The abrupt concentration increase indicated that more contaminated waters had reached gage 5 at this time (Section IV.4.2.3). However, the model was not capable of reproducing this abrupt increase. The error associated with the December 17th sample (figure V.3-8) was due to the model: 1) strongly under-estimating the streamflow, Q, (figure V.C-19) and 2) under-estimating the dissolved arsenic concentration, $[M_d]$ (figure V.3-8); therefore, the flux ($[M_d]Q$) was also under-estimated.

The R^2 value for the 1993 verification year was not as good as determined for 1992. The primary reason, for this observation was that on the rising limb of the dissolved arsenic graph (figure V.3-10): 1) the streamflow was over-estimated (figure V.3-2), and 2) dissolved arsenic concentrations were slightly over-estimated (figure V.3-10); therefore, the flux was also over-estimated.

Model Evaluation: Dissolved Metals

The model performed reasonably well. Concentrations and fluxes were all modeled within an order of magnitude of the measured values. Furthermore, the model was capable of capturing the general trends in metal fluxes, where large fluxes of dissolved metals occurred during storm events, and the smaller fluxes of dissolved metals occurred during low flows. The primary errors in the dissolved metals model were associated with: 1) errors in modeling the overall streamflow, and 2) the inability of the model to capture abrupt changes in metal concentrations. These abrupt changes, however, may have been due, in part, to laboratory analytical errors associated with measuring metal concentrations.

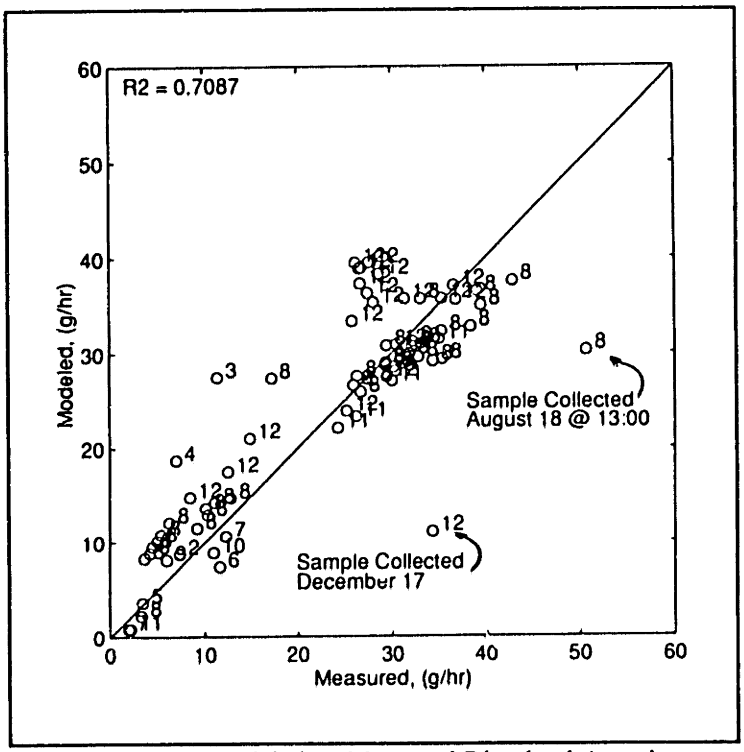

Figure V.3-6: Modeled vs Measured Dissolved Arsenic Flux, Gage 5, 1992 (Calibration)

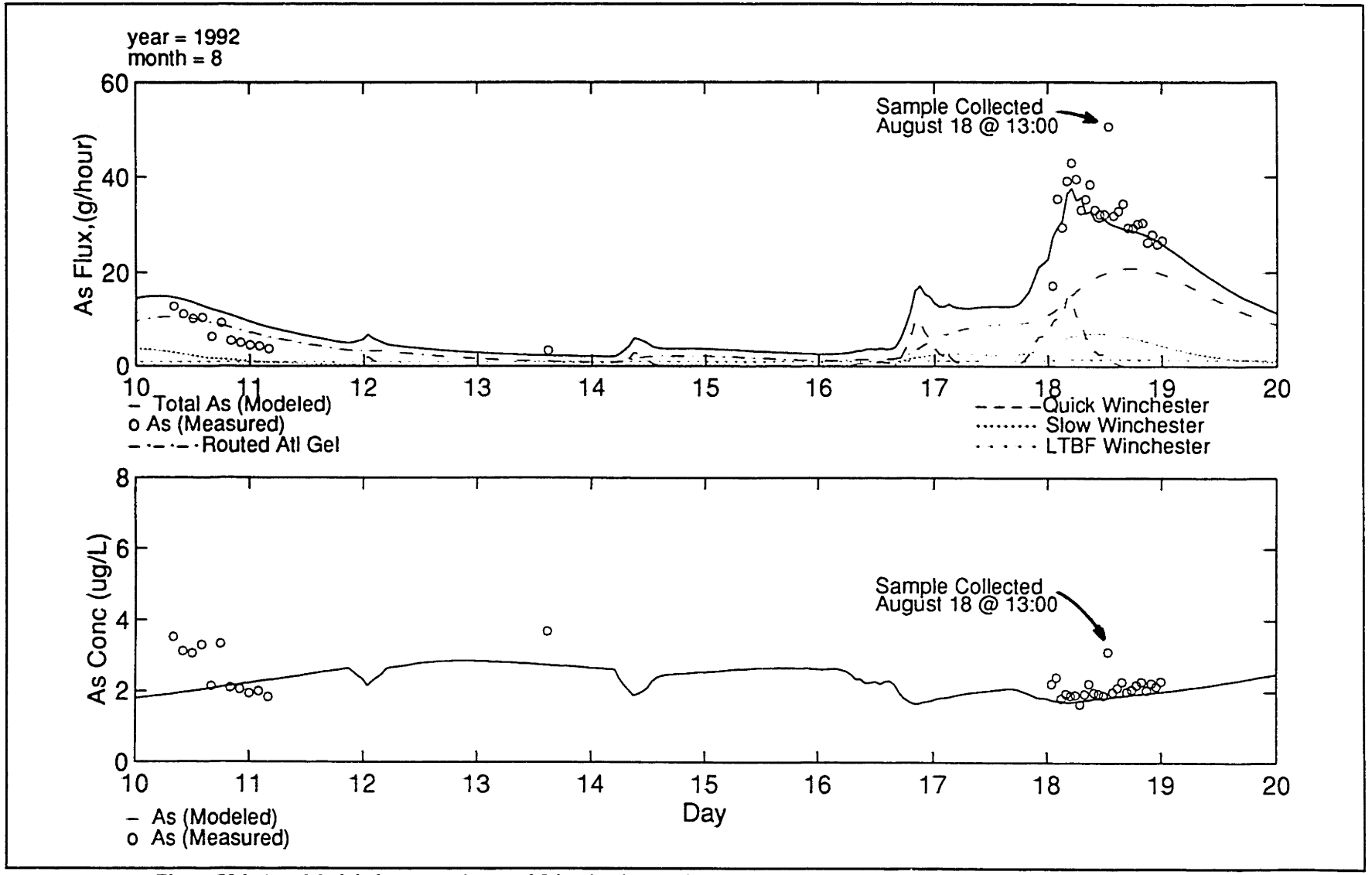

Figure V.3-7: Modeled versus Measured Dissolved Arsenic, Time Series Plot, August 10-19 1992, USGS (Gage 5)

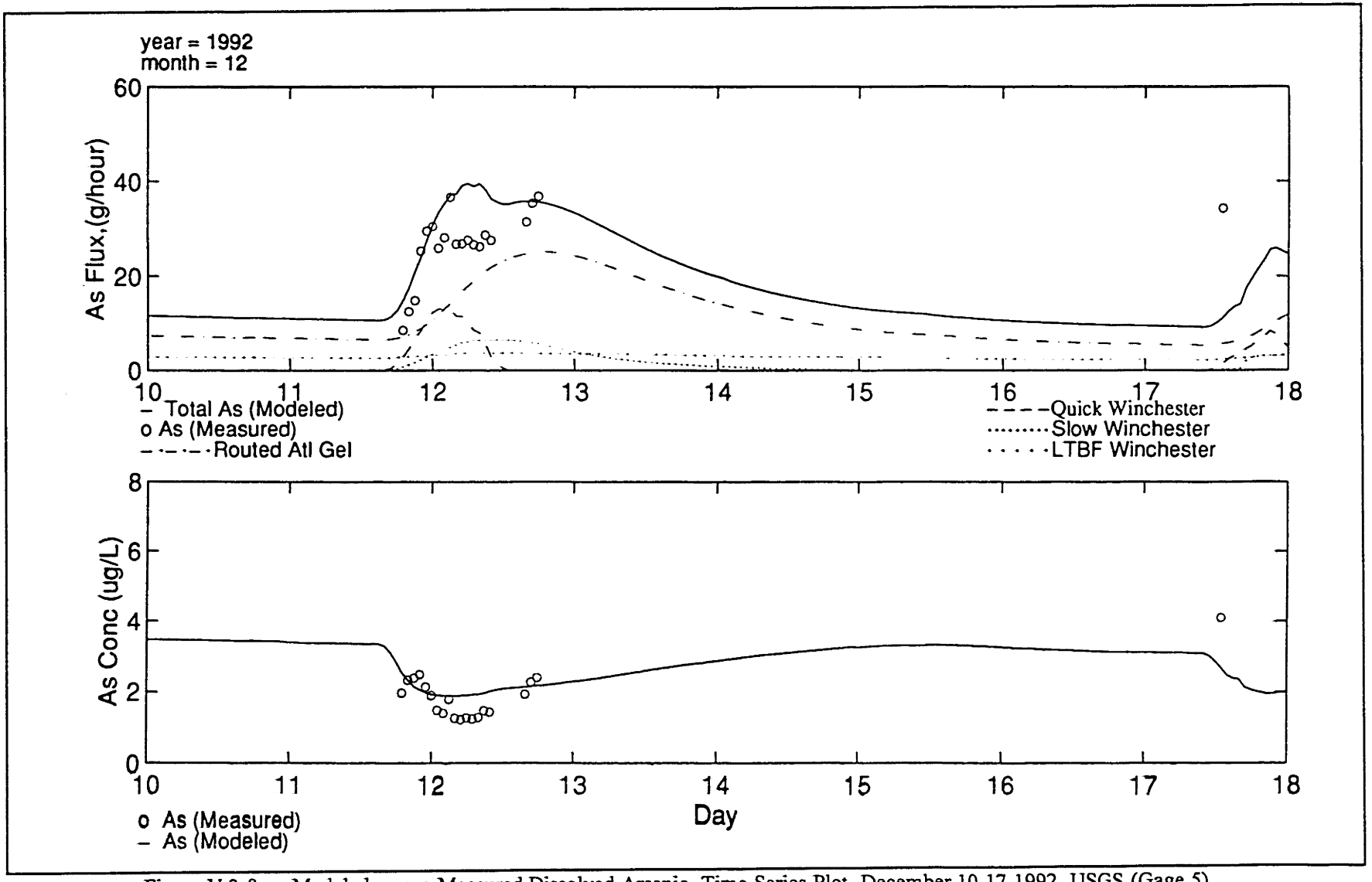

Figure V.3-8: Modeled versus Measured Dissolved Arsenic, Time Series Plot, December 10-17 1992, USGS (Gage 5)

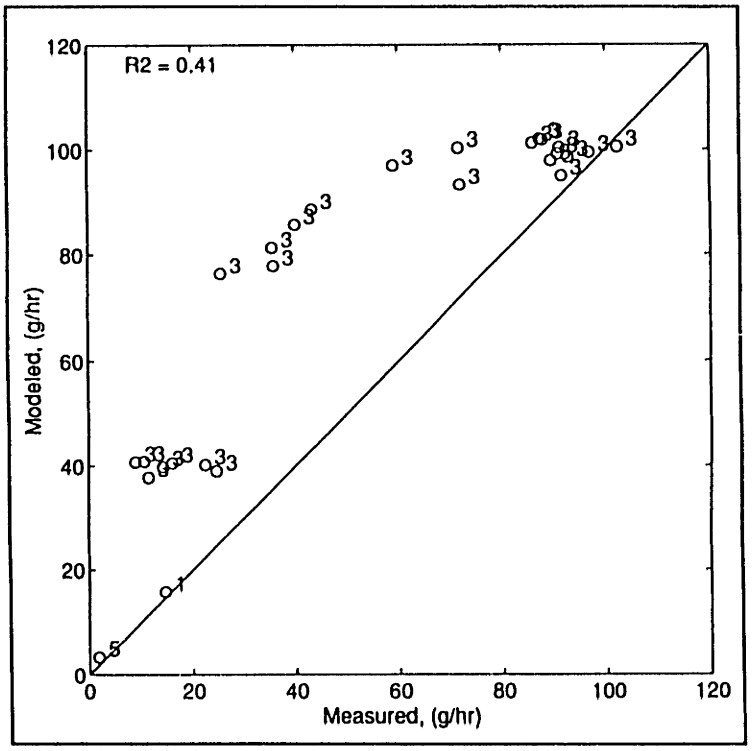

Figure V.3-9: Modeled vs Measured Dissolved Arsenic Flux, Gage 5, 1993 (Verification)

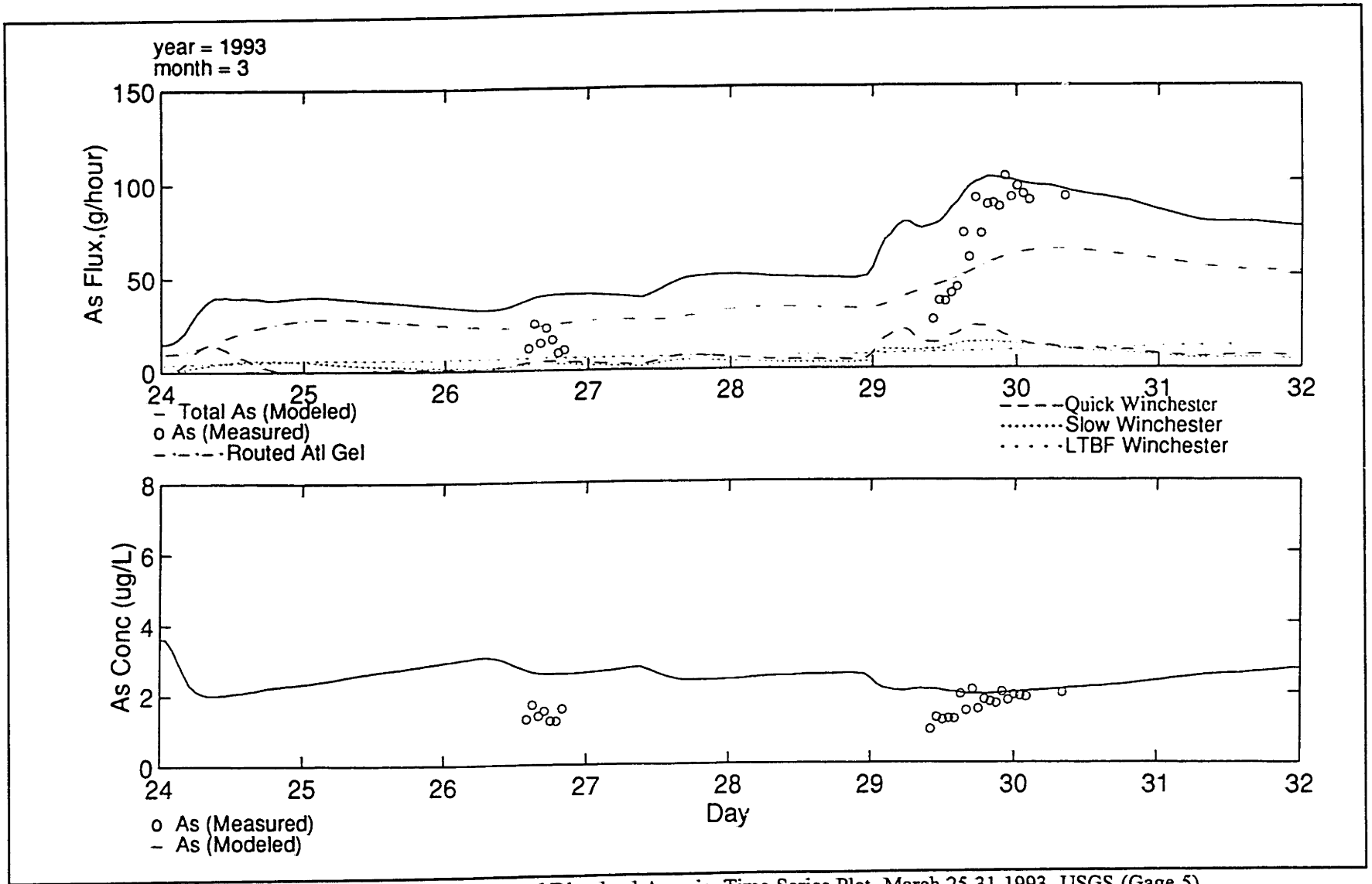

Figure V.3-10: Modeled versus Measured Dissolved Arsenic, Time Series Plot, March 25-31 1993, USGS (Gage 5)

V.3.4 Suspended Sediments

Goodness of Fit, R^2

R^2 values for suspended sediment fluxes at gage 5 for samples collected in 1992 and 1993 are given in table V.3-7. All statistics were computed from suspended sediment data which were collected using 0.5 μm pore size filters. The 1992 and 1993 statistics correspond to 70 samples collected in 1992 and 38 samples collected in 1993, respectively. Plots of modeled versus measured fluxes are provided in figures V.3-11 and V.3-15. In these figures, the number next to the data point corresponds to the month during which the samples were collected. Time series plots are provided in figures V.3-12, V.3-13, V.3-14 and V.3-16. The time series plots include: 1) plots of suspended sediment flux, 2) suspended sediment concentration, and 3) accumulation of sediments in both channel and quick areas.

Model Year	Suspended Sediment Flux R^2
1992 Calibration	0.54 (0.80)
1993 Pseudo-Verification	0.65

Table V.3-7: Statistics of Modeled and Measured Suspended Sediment Fluxes, Gage 5
The value in parenthesis was computed without the November 1992 data points

Details of Model Performance: Suspended Sediments

For 1992 the R^2 value was 0.54. This value was strongly affected by three samples collected during the November 23, 1992 storm (figures V.3-11 and V.3-13). For this particular event (which was unaffected by snowfall or snowmelt), the quick flow component in the vicinity of the peak was over-estimated. (figure V.C-16) Since the quick flow was over-estimated, the suspended sediment transported from the quick areas was strongly over-estimated because quick sediment transport is a function of quick flow raised to the power of n = 4 (Section V.2.3.2). The apparently large error in the suspended sediment flux thus resulted primarily from a relatively small error in the streamflow model.

The other notable outlier is associated with the first sample collected during the August 18th storm. (figure V.3-12) At the initiation of the August 18th storm event, the data were characterized by a

double suspended sediment peak. The modeled data also exhibited a double peak. However, the timing of the first peak was characterized by a time shift error. The result was for the first modeled point to be strongly over-estimated. Other than for this first sample, however, the model performed very well in estimating the suspended sediment flux for the samples collected in August.

For the December 10th event (figure V.3-14), the suspended sediment flux was well estimated. At the beginning of this particular event, the turbidity data agreed reasonably well with the measured suspended sediment concentrations. (using filtration analysis) Between December 13 and 14th, the turbidity data were characterized by significant fluctuations which were not captured by the model. These fluctuations may have truly occurred, or may have been associated with occasional power failures which occurred after the December 10th storm event.

Positive qualities of the model that were observed for all calibration events, include the capability of the model to capture: 1) the initial burst of suspended sediment that occurred at the very beginning of the storm event, primarily associated with quick flows, and 2) the slower rate of decline after the initial peak, which was associated with primarily slow storm waters. Furthermore, the model was capable of capturing the extremely low sediment fluxes during very low flows (August 13th), when streamflow was dominated by longterm baseflow.

For the 1993 pseudo-verification year, the R^2 value was 0.65. A large portion of the error associated with this event was due to a time shift error. (figure V.3-16) For the March 29th event, the model was capable of capturing the rate of increase and decrease in the suspended sediment flux, and the magnitude of the peak. In modeling the timing of this occurrence the model was off by two hours. If the modeled results were shifted by 2 hours, a much higher "shifted" R^2 value of 0.81 would have been computed.

Note that for all the time series plots (refer to bottom graph on each figure), the mass of sediment accumulated in quick areas tends to be at least 2 orders of magnitude higher than the sediment accumulated in the channel. Because of this large difference, a large portion of the initial burst of sediment transported at the initiation of a storm is associated with sediments from quick areas; channel sediments play a much smaller role during storm events.

The fit between the total modeled and measured suspended sediment concentration at gage 1 was reasonable. (figure V.3-17) The fit was especially good during the summer months, where both the measured and model data showed an increase in the suspended sediment concentration during the early summer followed by a decrease during the fall. During the spring months the data show a second

maximum which was not predicted well by the model.

The model predicted the highest organic suspended sediment concentrations during the summer months with a maximum value predicted shortly after the water temperature maximum. The inorganic suspended sediment fluctuations followed the pattern of modeled streamflow fluctuations on an attenuated scale.

Model Evaluation: Suspended Sediments

The suspended sediment model performed reasonably well. The model was capable of capturing: 1) the initial burst of suspended sediments observed at the initiation of a storm, associated with quick suspended sediments, 2) the slower rate of suspended sediment decline immediately following the peak, and 3) the extremely low sediment fluxes which were observed during very low flow conditions.

Errors in the estimation of suspended sediment fluxes were primarily associated with errors in the streamflow model. An error in the streamflow estimate is "magnified" in the suspended sediment model because of the fourth power dependence of the quick suspended sediment concentration on streamflow. Errors were also associated with time shift errors. The effect of a time shift error was evident in the March 29th event in which a 2 hour time shift of the modeled values resulted in an improved R^2 value.

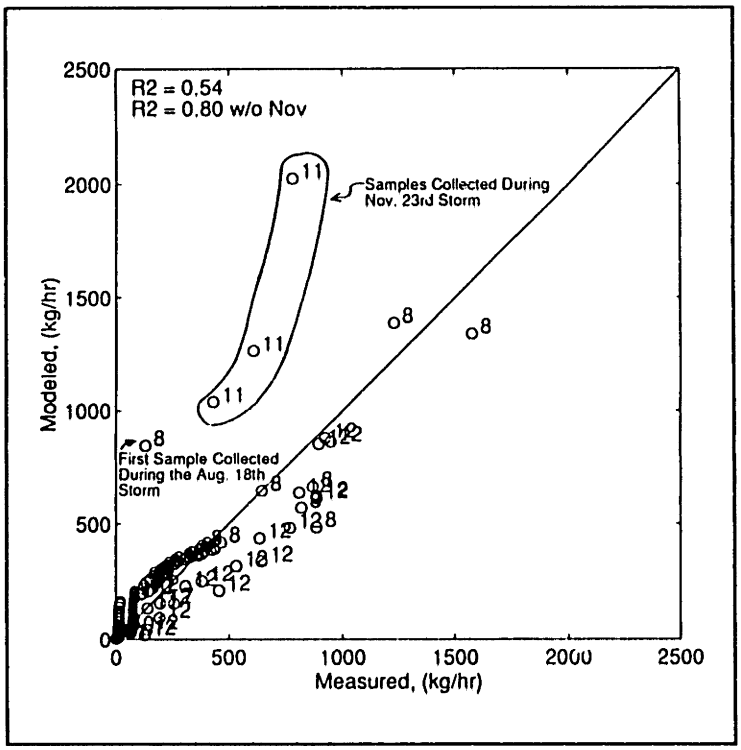

Figure V.3-11: Modeled vs Measured Suspended Sediment Flux, Gage 5, 1992 (Calibration)

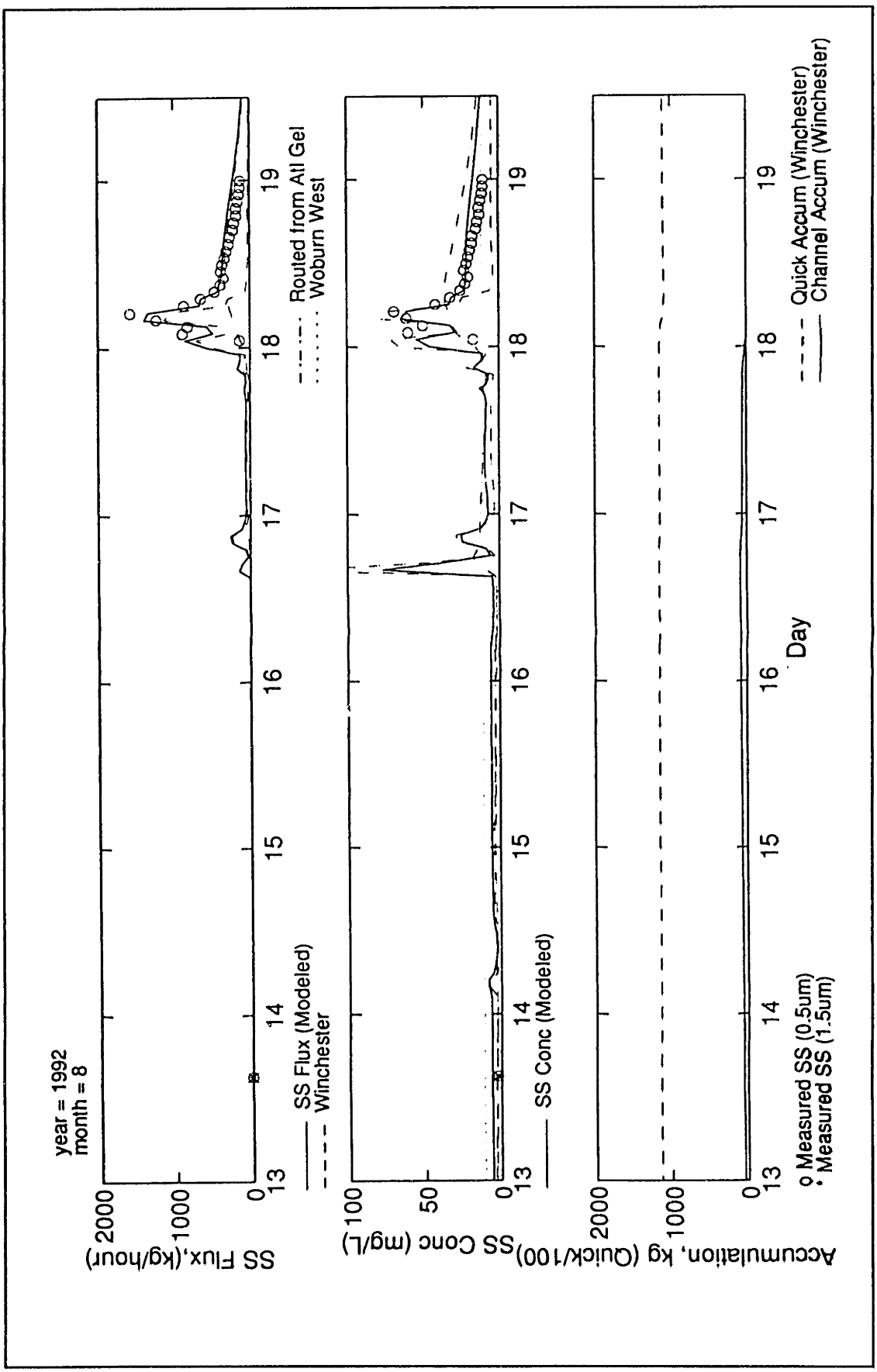

Figure V.3-12: Modeled versus Measured Suspended Sediment, Time Series Plot, August 10-19 1992, USGS (Gage 5)

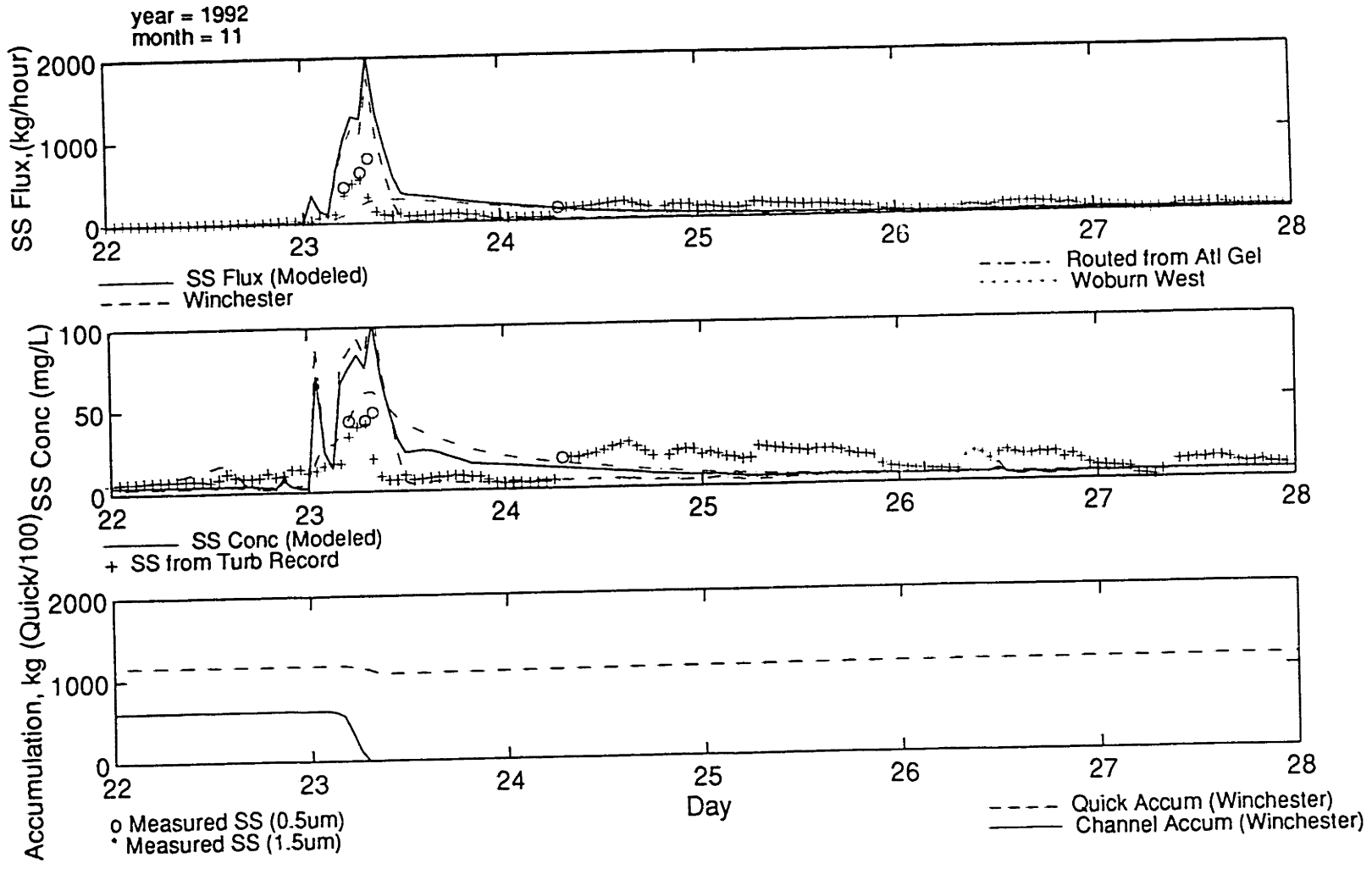

Figure V.3-13: Modeled versus Measured Suspended Sediment, Time Series Plot, November 20-28 1992, USGS (Gage 5)

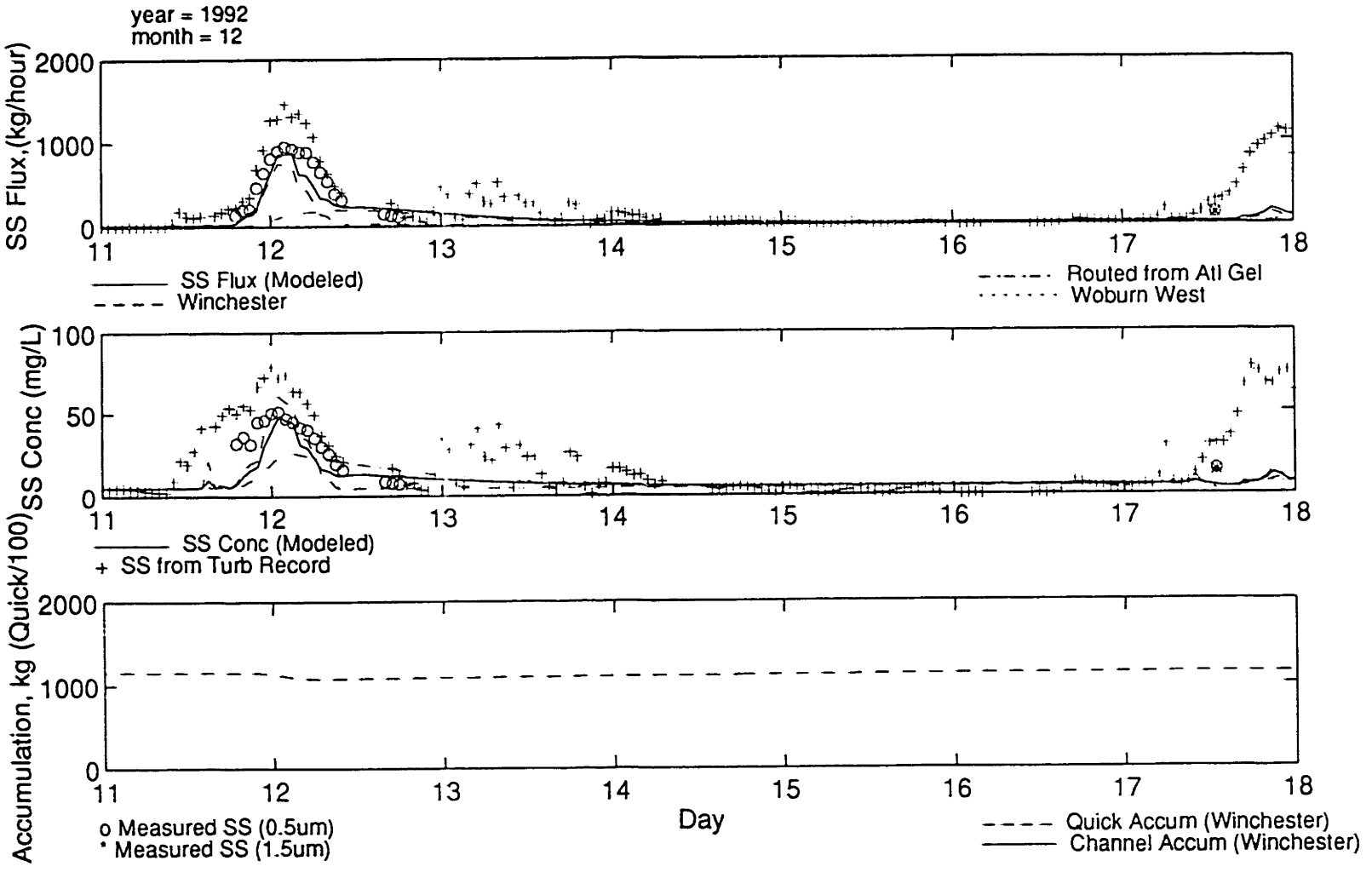

Figure V.3-14: Modeled versus Measured Suspended Sediment, Time Series Plot, December 10-17 1992, USGS (Gage 5)

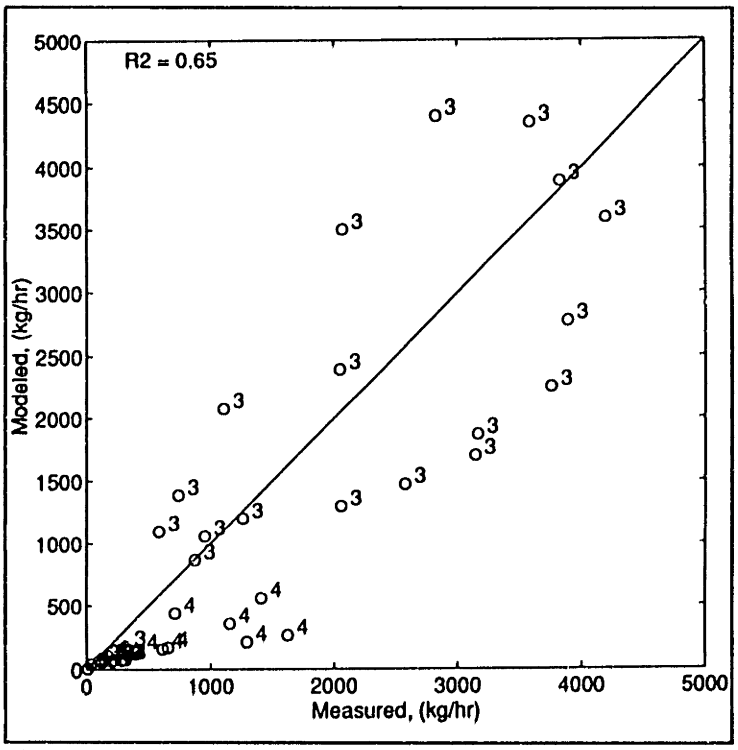

Figure V.3-15: Modeled vs Measured Suspended Sediment Flux, Gage 5, 1993 (Pseudo-verification)

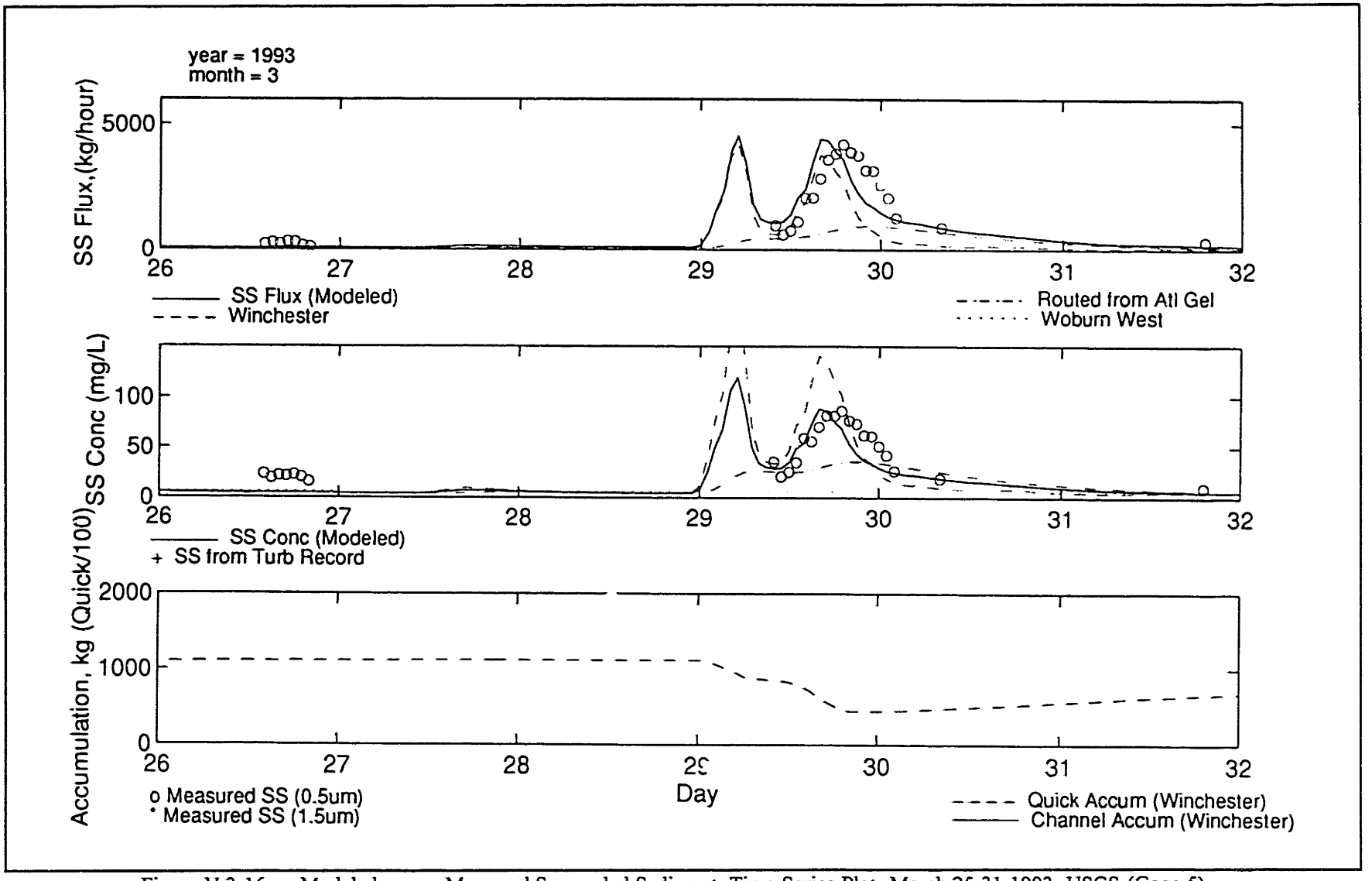

Figure V.3-16: Modeled versus Measured Suspended Sediment, Time Series Plot, March 25-31 1993, USGS (Gage 5)

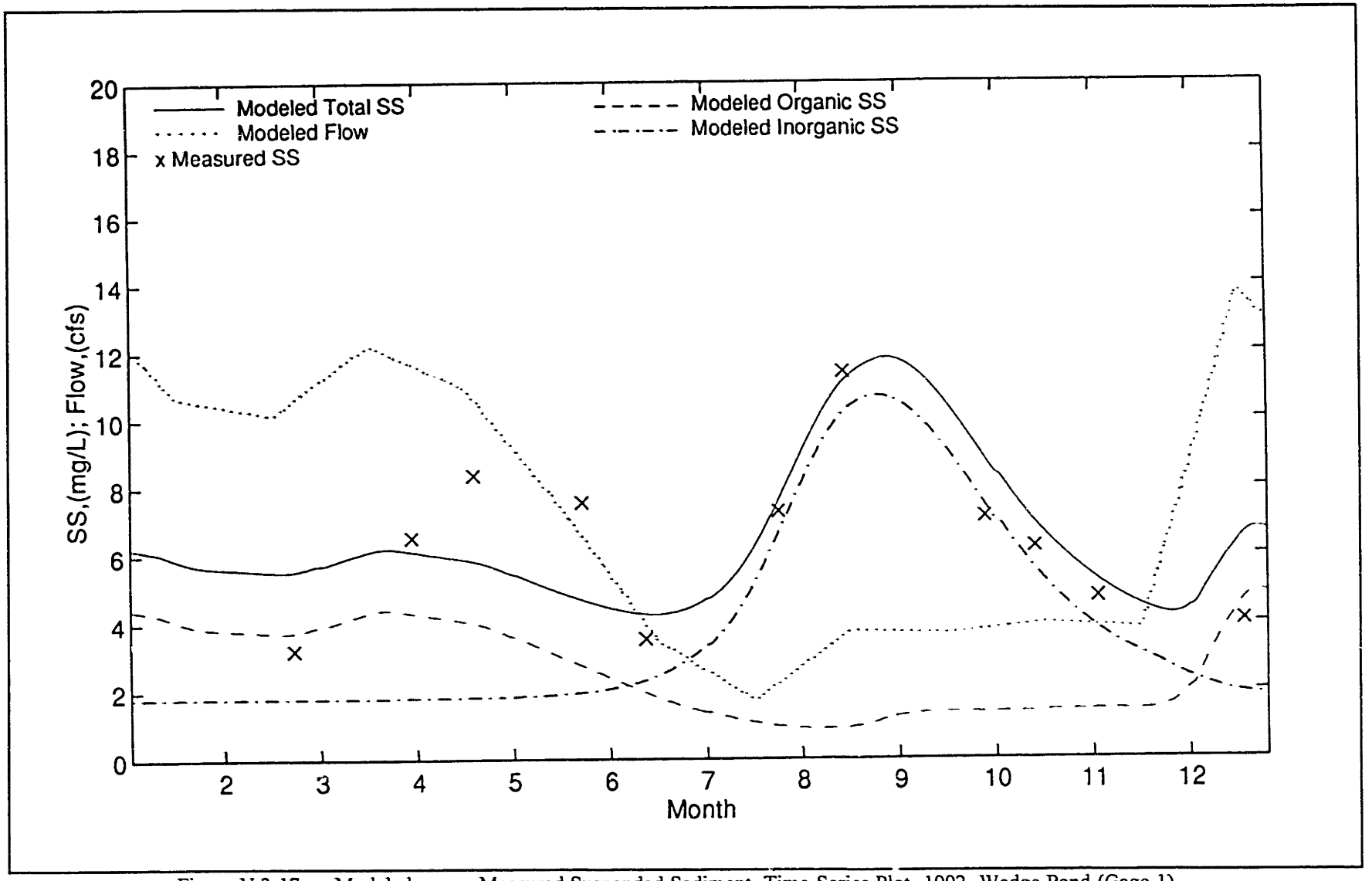

Figure V.3-17: Modeled versus Measured Suspended Sediment, Time Series Plot, 1992, Wedge Pond (Gage 1)

V.3.5 Particulate Metals

Goodness of Fit, R^2

R^2 values for modeled metal fluxes at gage 5 are reported in table V.3-8. The 1992 and 1993 statistics correspond to roughly 70 samples collected in 1992 and 26 samples collected in 1993, respectively. Plots of modeled versus measured fluxes and time series plots for particulate arsenic are provided in figures V.3-18 to V.3-23. For figures V.3-18 and V.3-22, the number next to each data point corresponds to the month during which each sample was collected.

The method used to model particulate fluxes for each metal was identical except for the concentration values assigned to the quick ($[M_p]_{quick}$), slow ($[M_p]_{slow}$), and longterm baseflow ($[M_p]_{ltbf}$) components. Because of the similarity in modeling each metal, results for only one metal, arsenic, are included within the main body of the thesis. Details of the model performance for the other metals, including plots of modeled versus measured fluxes and time series plots for chromium, iron and copper, are provided in appendix V.C.

Model Year	Metal Flux, R^2			
	As	Fe	Cr	Cu
1992 Calibration	0.13 (0.75)	0.04 (0.80)	-.06 (0.71)	0.37 (0.77)
1993 Pseudo-Verification	0.69	0.47	0.44	0.54

Table V.3-8: Statistics of Modeled and Measured Particulate Metal Fluxes, Gage 5
Values in parenthesis were computed without the November 1992 data points.

Details of Model Performance: Particulate Arsenic

The R^2 value for arsenic fluxes at gage 5 during the 1992 calibration year was 0.13. Although the R^2 value appears to be low, most of the modeled fluxes did correspond reasonably well with the measured data. The primary outliers which significantly reduced the R^2 values were collected during November. For the November data the model over-estimated the measured data by a factor of two to three. Without the November data points the overall R^2 value was significantly improved to a value of 0.75.

For the August 1992 samples, the model performed reasonably well, (figure V.3-19) During the August 18th sampling period, the model was capable of capturing the initial burst of particulate arsenic flux at

the very beginning the storm event and the slower decline in the flux which occurred just after the initial burst. For this sampling period, the model also closely estimated the streamflow (figure V.3-1) and arsenic concentration (figure V.3-19). The suspended sediment concentration was also well modeled except for the timing of the very first suspended sediment peak (figure V.3-12). This error in the timing of the suspended sediment concentration is reflected in the particulate arsenic flux plot (V.3-19), where the model over-estimated the particulate flux for the first data point in a similar fashion as the suspended sediment concentration for this point was also over-estimated. The model, as evidenced by the August 13th sample, was also capable of capturing the extremely low arsenic fluxes that occurred during very low flow conditions. For the August 10th samples, errors between the streamflow and particulate arsenic concentrations partially canceled out. The model, during this time; 1) over-estimated the streamflow, 2) over-estimated the suspended sediment concentration, [SS], and 2) under-estimated the particulate arsenic concentration, $[As_p]$. The net result was for a reasonable fit of the flux data.

For the November 1992 samples (figure V.3-20), the primary source of the modeling error was associated with the estimation of the suspended sediment flux (figure V.3-13). For these samples, the model was capable or reproducing the particulate arsenic concentrations. However, since the suspended sediment flux was over-estimated, the particulate arsenic flux was also over-estimated. Although the values of the modeled and measured fluxes do not coincide, there is a positive result in the pattern between the modeled and measured data. When the measured data shows an increase in the flux with time the model also shows an increase with time and vice versa.

For the December 1992 samples (figure V.3-21), the model performed reasonably well. When the measured data showed an increase in the particulate arsenic flux in time, the modeled data also showed an increase with time. A similar statement can be made for decreasing data. Additionally, both the model and measured data peak at the same time, and for most of the data points there is a close one to one correspondence between the modeled and measured fluxes. The primary exceptions occur for the later part of the receding limb of the particulate flux plot. During this time, the lack of one to one correspondence is due to the over-estimation of the particulate arsenic concentration.

The R^2 value for particulate arsenic flux for the 1993 pseudo-verification data was 0.69. During the March 29 1993 event (figure V.3-23), the model was capable of capturing: 1) the rate of increase and decrease of the flux, and 2) the magnitude of the arsenic peak. The primary error in the estimate was associated with a time shift error between the model and measured data.

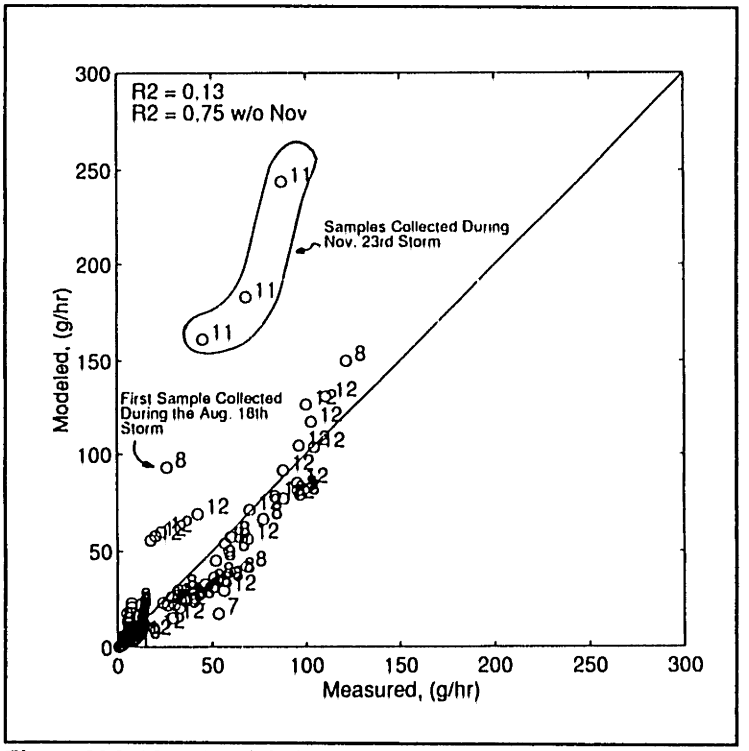

Figure V.3-18: Modeled vs Measured Particulate Arsenic Flux, Gage 5, 1992 (Calibration)

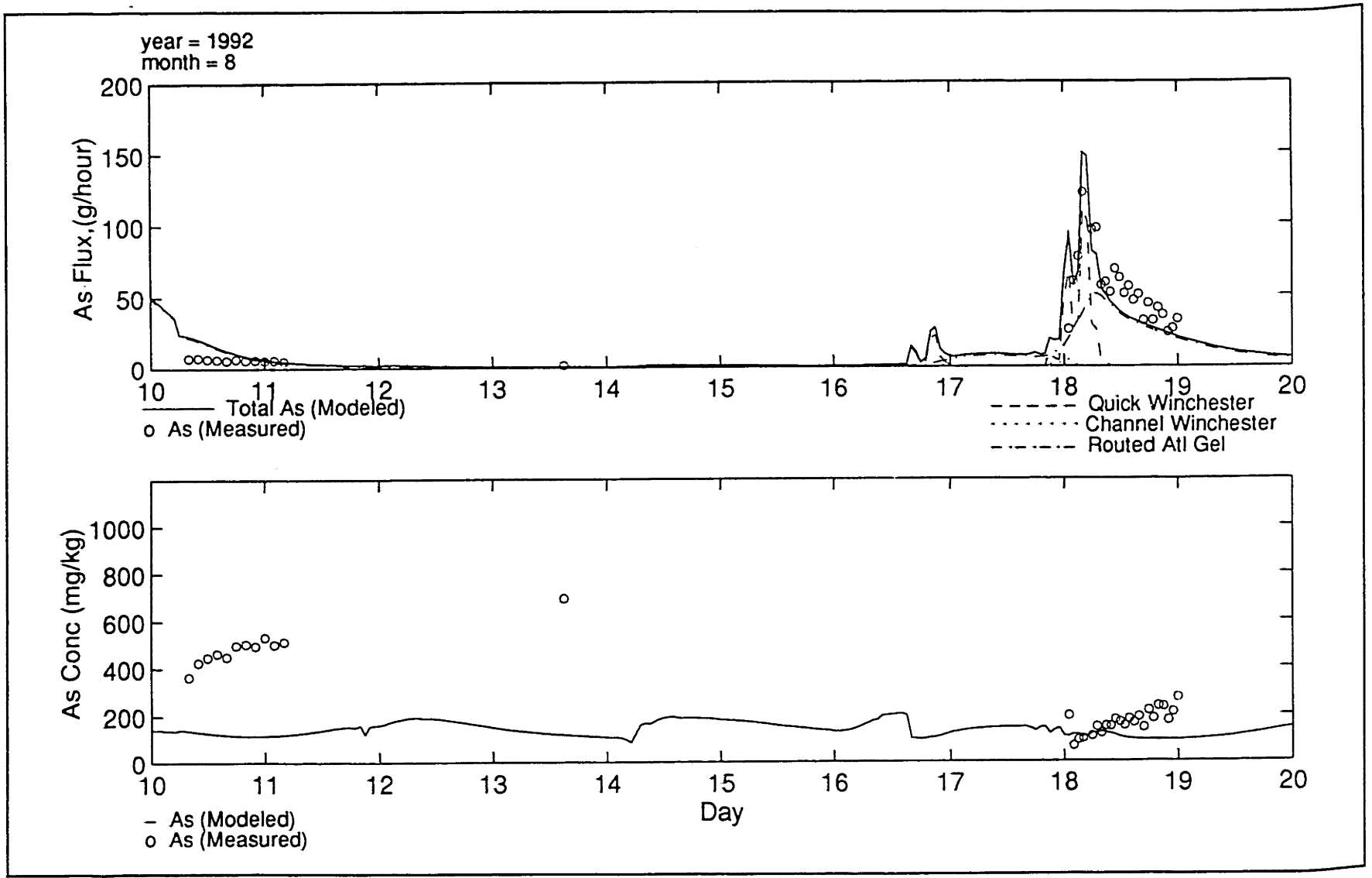

Figure V.3-19: Modeled versus Measured Particulate Arsenic, Time Series Plot, August 10-19 1992, USGS (Gage 5)

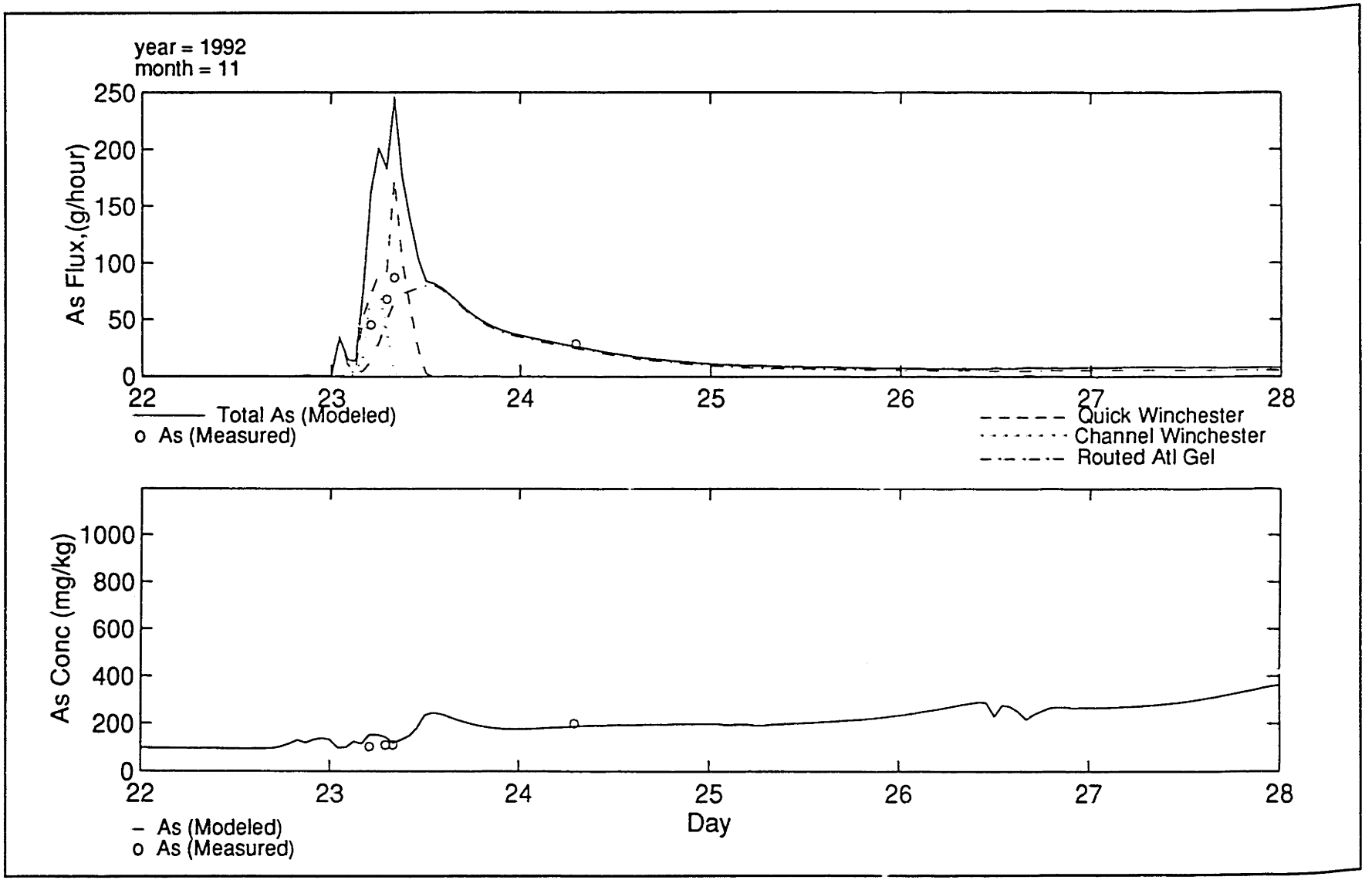

Figure V.3-20: Modeled versus Measured Particulate Arsenic, Time Series Plot, November 20-28 1992, USGS (Gage 5)

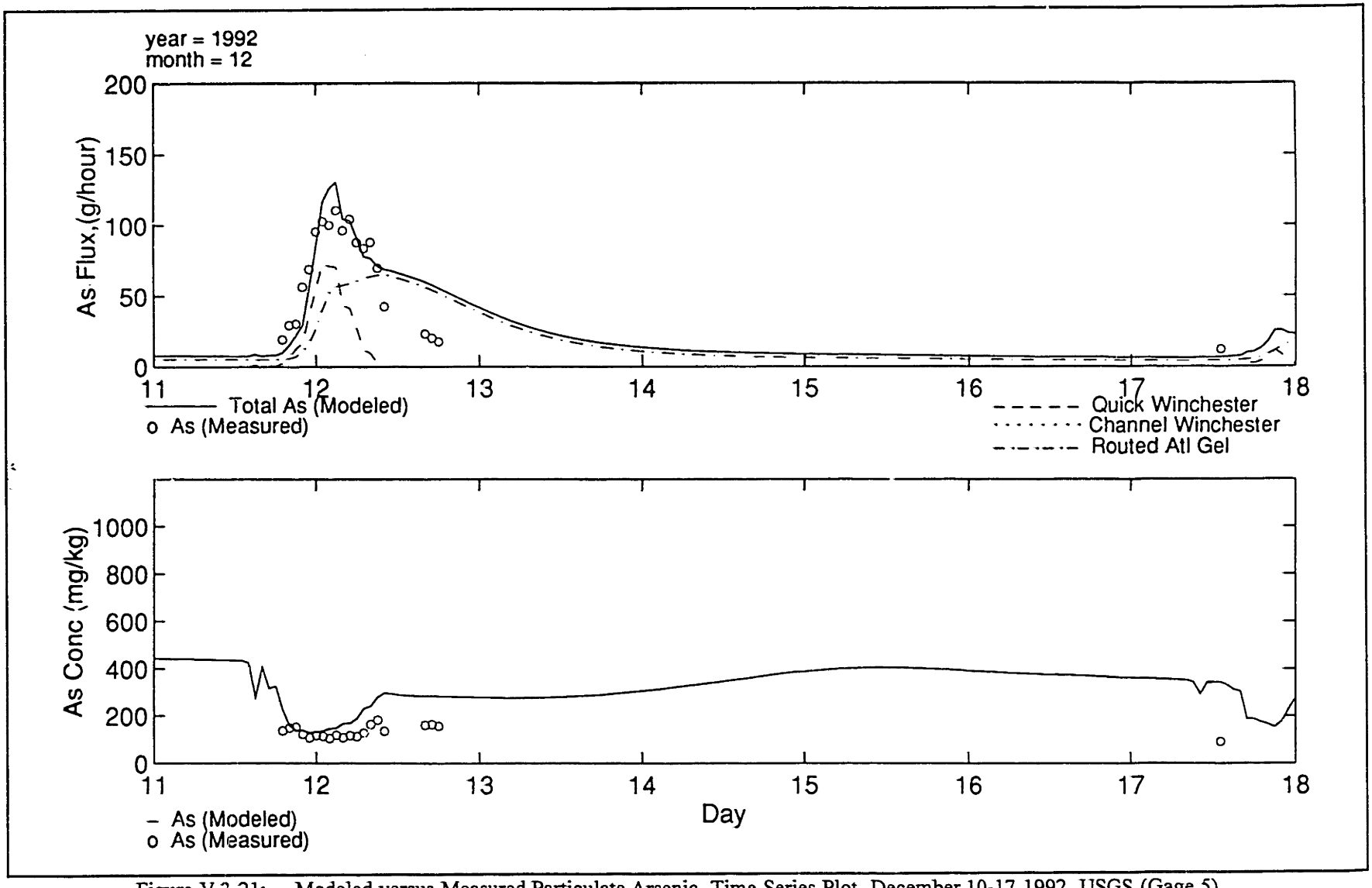

Figure V.3-21: Modeled versus Measured Particulate Arsenic, Time Series Plot, December 10-17 1992, USGS (Gage 5)

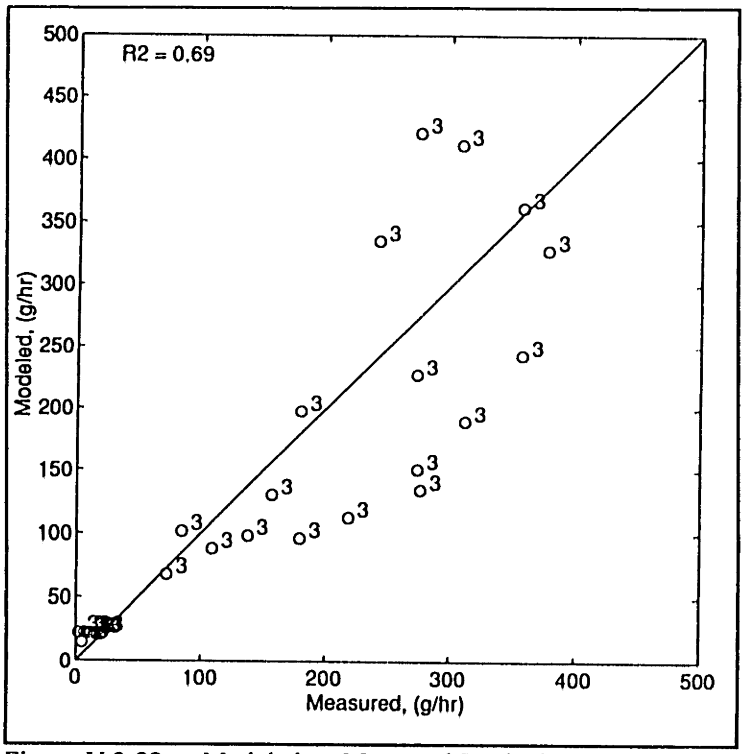

Figure V.3-22: Modeled vs Measured Particulate Arsenic Flux, Gage 5, 1993 (Pseudo-verification)

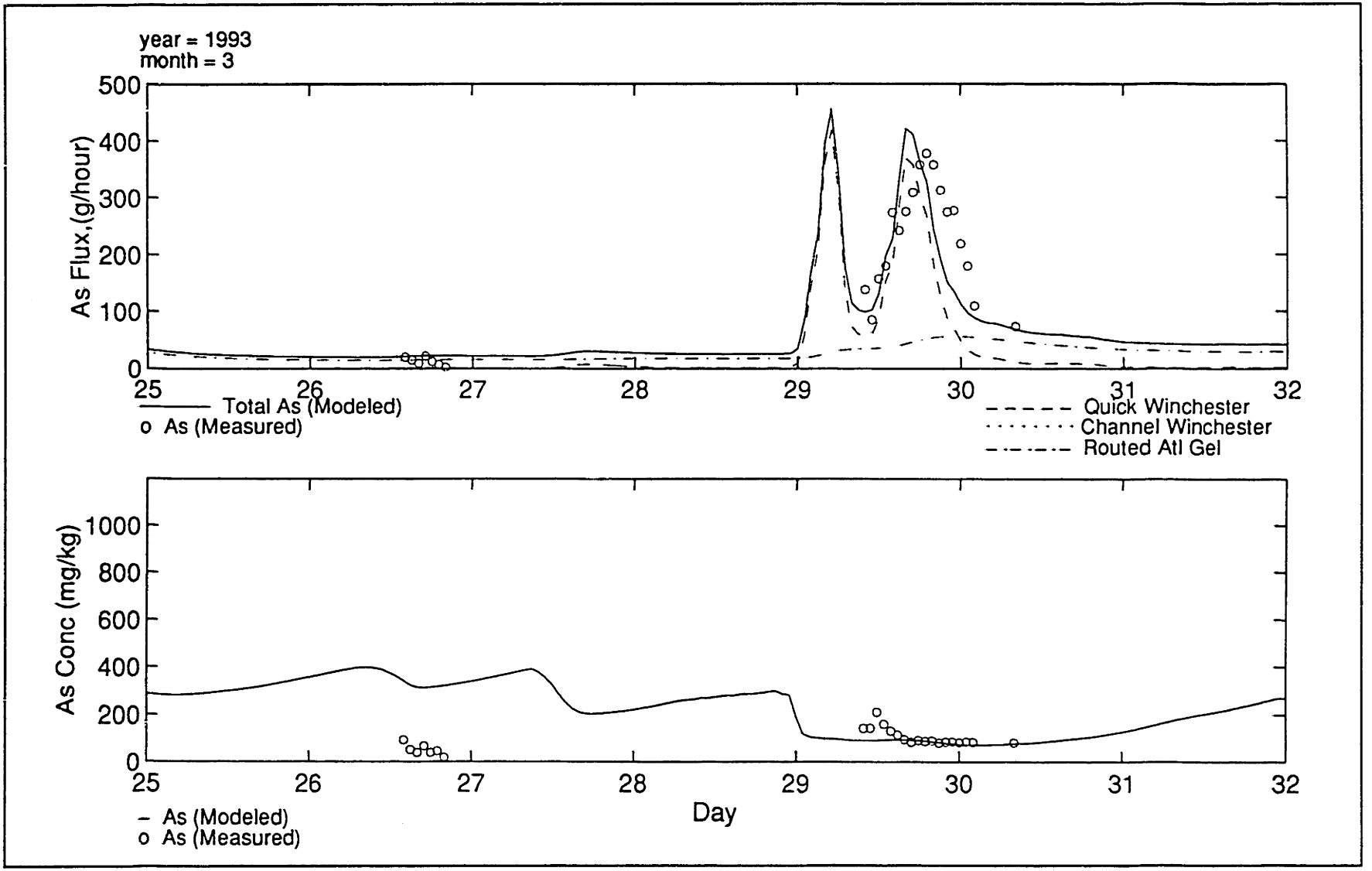

Figure V.3-23: Modeled versus Measured Particulate Arsenic, Time Series Plot, March 25-31 1993, USGS (Gage 5)

Model Evaluation: Particulate Metals

The performance of the model in reproducing observed particulate metal fluxes depended highly upon the model's capability to reproduce the suspended sediment flux. The estimation of the particulate metal concentration was of secondary importance. This result is associated with the observed behavior of the system, where during storm events, the suspended sediment fluxes changed significantly during the course of the storm while the particulate metal concentrations remained relatively constant.

Additionally, the model was capable of reproducing: 1) the initial burst of particulate metal fluxes associated with quick sediments, that were observed at the beginning of each event, 2) the slower rate of decline of the metal flux associated with slow sediments immediately after the storm peak, and 3) the extremely low metal fluxes observed during very low flows, when longterm baseflow sediments dominated.

For all metals, the November data exhibited large errors. These errors were primarily associated with the over-estimation of suspended sediment fluxes. Without the November data, the R^2 values were relatively high for all metals.

V.4 MODEL RESULTS

V.4.1 Introduction

The data set compiled through this study consists of: 1) a semi-continuous hourly record of streamflow at 5 gaging stations, 2) instantaneous monthly samples for suspended sediment and metals at five gaging stations, and 3) storm-event samples for suspended sediment and metals at the USGS station. Although the amount of data compiled through this study is generally larger than the amount used in other studies, the availability of more data would significantly improve our understanding of metal transport processes for the Aberjona River system.

To augment our data set, synthetic records of streamflow, suspended sediment, and metal transport for the 1991, 1992, and 1993 run periods (See section V.2.1.1 for dates) were generated using the model developed in this study. From the model-generated results the following trends were analyzed (Section V.4.2): year to year variations, importance of different flow and sediment components, and the relative contributions from each of the different sub-basins. Furthermore, a brief overview of the monthly variation of metal fluxes is also included in Section V.4.3.

V.4.2 Water, Suspended Sediment, and Metal Balances for the 1991, 1992, and 1993 Run Periods

The 1991 and 1992 model periods were hydrologically very similar. The 1991 and 1992 model periods had total precipitation depths of 41.2 and 41.9 inches, respectively. Of the total precipitation, approximately 2 inches (equivalent rain depth) fell as snow during 1991 and approximately 3 inches fell as snow during 1992. The **measured** average streamflows at gage 5 during 1991 and 1992 model periods were 29 and 28 cfs, respectively.

The 1993 model period was significantly different than 1991 and 1992. During the 1993 model run period a large fraction of the precipitation occurred as snowfall; of the 24 inches of precipitation that were observed, approximately 6 inches fell as snow. The snowfall depth was much larger for 1993 than for the 1991 and 1992 run periods, especially considering that only part of the winter season was

modeled for 1993. As a result of the large snowfall depth, streamflow during the 1993 model period was significantly affected by snowmelt. The average **measured** streamflow during the 1993 model period was 38 cfs.

A summary of the results is provided in tables V.4-1 to V.4-11. The "fraction" column on tables V.4-2, V.4-5, V.4-8, and V.4-11 is equal to the ratio of the contribution from either Woburn North (WN), Woburn Central (WC), Winchester (WI), Woburn West (WW), or Atlantic Gelatin (AG) to the totai of those contributions. Positive values correspond to a contribution to the river whereas negative values correspond to a removal from the river.

Streamflow Water Balance

Modeled values of the mean flow rates at the watershed outlet for the 1991, 1992, and 1993 model periods are given in table V.4-1. The hydrologic similarity between 1991 and 1992 is reflected in the model by the similar flow rates predicted for each year; the 1993 model run period had a higher mean streamflow due to a large snowmelt event.

For each of the model periods, 14 to 20% of the streamflow volume was due to quick flow, 25 to 35% was due to slow flow, and 50 to 60% was due to longterm baseflow. For the 1991 and 1992 model years the distribution of flow between the different components was almost identical. The 1993 model year was characterized by a slightly larger quick and longterm baseflow contributions.

Each sub-basin contributes between 20 and 35% of the total flow (table V.4-2) Comparisons of drainage-area-normalized flows for each sub-basin were highly variable. The Woburn West sub-basin had the lowest drainage area normalized flow (0.67 cfs/mi^2) whereas the Woburn Central sub-basin had the highest (2.97 cfs/mi^2). The large groundwater withdrawals in the vicinity of Horn Pond is the primary reason for the small streamflow per unit area from the Woburn West sub-basin. The large area-normalized flow from the Woburn Central sub-basin is consistent with the runoff fractions computed from the observed data in section IV.2. Possible reasons for the large runoff fraction from this sub-basin are also discussed in section IV.2.

Run Period	Mean Streamflow at Watershed Outlet (cfs)	Quick Fraction	Slow Fraction	Longterm Baseflow Fraction
1991	29	0.14	0.35	0.51
1992	29	0.14	0.32	0.54
1993	37	0.19	0.25	0.56

Table V.4-1: Mean Flow Rates at Watershed Outlet for 1991, 1992, & 1993 Model Periods (Modeled Values)

Model Unit	Streamflow Fraction	Drainage Area Normalized Flow (cfs/mi^2)
Woburn North Sub-basin	0.28	1.44
Woburn Central Sub-basin	0.23	2.97
Winchester Sub-basin	0.35	1.91
Woburn West Sub-basin	0.22	0.67
Atlantic Gelatin Withdrawal	-0.12	--

Table V.4-2: Average Streamflow Fractions and Area Normalized Flows for Model Units (1991, 1992, & 1993 Model Years)

Dissolved Metals

Average fluxes of dissolved metals for each model period are provided in table V.4-3. The fluxes were similar for 1991 and 1992; for 1993, the fluxes were higher by roughly 40%. The larger flux is due to: 1) the larger flow rate during 1993 (1993 flows were larger than 1991 and 1992 flows by 28%), and 2) higher dissolved-metals concentrations. The higher dissolved-metal concentrations were due to the larger contribution of longterm-baseflow waters to the overall streamflow. Note that the concentration of longterm-baseflow waters is generally higher than the concentrations of the other components. (See table V.2-4)

For each run period 70% or more of the dissolved-metal flux was transported with the longterm-baseflow component. In general, the quick component of flow carried the smallest proportion (<10%) of the total metal flux. (table V.4-4) The only exception was dissolved copper, where the quick component represented 18% of the flux and the slow component represented 14% of the flux.

It is not surprising that the quick component carried the smallest proportion of dissolved metals[15] because: 1) the quick component corresponded to the smallest streamflow volume (between 14 and 20% of the total streamflow), and 2) the quick component *generally* had the smallest dissolved concentration, $[M_d]$, assigned to it. Exceptions include the dissolved concentrations assigned to copper. For each of the sub-basins, dissolved copper concentrations assigned to the quick components were either the highest or comparable to the concentrations assigned to the slow and longterm-baseflow components. (See table V.2-4)

Most of the dissolved metal within the watershed came from sub-basins draining into gage 3 station. (The Woburn North and Woburn Central sub-basins, table V.4-5) For iron and copper, the Winchester sub-basin also contributed a significant fraction. The Woburn West sub-basin contributed less than 10% of the total dissolved-metal fluxes. Of the total flux of metal coming off the various sub-basins, the Atlantic Gelatin area was responsible for removal of 10 to 20% of the metal from the river system.

The highest area-normalized dissolved-metal fluxes originated from either the Woburn North sub-basin or the Woburn Central sub-basin. The Woburn Central sub-basin had the highest values for chromium and copper. Part of the reason for these large values for the Woburn Central sub-basin is due to the large area-normalized flow for this sub-basin relative to other sub-basins. The Woburn North sub-basin had the highest values for arsenic and iron. The high arsenic and iron fluxes from the Woburn North

---

[15]A similar but converse argument can be made for the large fractions of dissolved metal flux carried by the longterm baseflow component.

basin were due to large dissolved concentrations, [M_d], assigned to the longterm-baseflow component. The area-normalized flux of iron from the Winchester sub-basin was also relatively large. The lowest area-normalized fluxes were modeled for the Woburn West sub-basin. The values for the Woburn West sub-basin were low due to a combination of: 1) small area-normalized flows, and 2) relatively low dissolved-metal concentrations.

Run Period	Mean Dissolved Metal Flux at Watershed Outlet, (g/hr)			
	As	Cr	Fe	Cu
1991	7.7	2.3	1,160	17
1992	8.1	2.4	1,220	17
1993	11.0	3.3	1,650	24

Table V.4-3: Mean Dissolved Metal Flux for 1991, 1992, & 1993 Model Periods (Modeled Values)

Dissolved Metal Component	Fraction of Total Dissolved Flux			
	As	Cr	Fe	Cu
Quick	0.06	0.08	0.02	0.18
Slow	0.16	0.15	0.14	0.14
Longterm Baseflow	0.78	0.76	0.84	0.68

Table V.4-4: Average Dissolved Metal Fractions for Quick, Slow, and Longterm Baseflow Components (1991, 1992, & 1993 Model Years)

Model Unit	Fraction of Total Dissolved Flux				Drainage Area Normalized Flux g/(hr·mi^2)			
	As	Cr	Fe	Cu	As	Cr	Fe	Cu
Woburn North Sub-basin	0.66	0.43	0.49	0.35	0.95	0.18	106	1.1
Woburn Central Sub-basin	0.11	0.54	0.14	0.26	0.38	0.56	76	2.04
Winchester Sub-basin	0.29	0.20	0.41	0.41	0.45	0.09	95	1.37
Woburn West Sub-basin	0.10	0.03	0.09	0.09	0.08	0.01	11	0.17
Atlantic Gelatin Withdrawal	-0.16	-0.20	-0.13	-0.11	---	---	---	---

Table V.4-5: Average Dissolved Metal Fractions and Area Normalized Fluxes for Model Units (1991, 1992, & 1993 Model Years)

Suspended Sediments

For each of the run periods, quick sediment was the component that was responsible for most of the sediment transport in the Aberjona River, representing 57% of the total sediment flux, whereas slow, longterm baseflow, and channel sediments each represented between 10 and 20% of the total flux, (table V.4-7) Since channel sediments are generally transported during increasing flow conditions which occur when quick flows are active, a large fraction (≈70%) of the sediment flux is transported in "bursts" at the beginning of each storm event. These bursts are relatively short-lived (on the order of the storm duration) and occur relatively infrequently (on time scales of inter-storm duration periods). As a result, the number and magnitude of large storm events during a given model period will significantly affect the predicted sediment transport. Since a fraction of the melt flow contributes to the quick system, melt-flow events also affect the predicted sediment transport, but to a lesser extent than rainfall events.

The effects of different storm characteristics is reflected in table V.4-6 where sediment fluxes and concentrations were different for each run period. During 1992 there were 5 storms with rainfall depths (as defined for the quick system) greater than 1.5 inches. Of the 5 storms, the largest storm depth was 1.99 inches. During 1991 there were also 5 storms with a precipitation depths greater than 1.5 inches. Of the 5 storms for 1991, however, two were very large with precipitation depths of 4.36" (Sept. 24) and 3.43" (Aug. 18). The transport associated with the 5 large (>1.5") storms in 1992 was 81,700 kg as opposed to 294,000 kg for the 1991 storms. During 1991, the two largest storms were responsible for roughly 263,000 kg or almost 50% of the 1991 total for the entire run period. Therefore, the larger sediment transport for 1991 was due to the large quantity of sediment mobilized during the two very large storm events. The importance of large storm events is a result of the model formulation where sediment transport is a function of quick flow raised to a power n, where n = 4.

For the 1993 run period, the magnitude of the sediment flux fell between the 1991 and 1992 fluxes. The reason the flux was larger for 1993 than 1992 is due to a large snow melt event in 1993 which was responsible for elevated suspended sediment concentrations (and streamflow) for a few weeks in the 1993 period. Because of the elevated streamflow (which dilutes the sediment flux being transported), however, the mean suspended sediment concentration for 1993 is much closer to the value for 1992. As opposed to 1991, the 1993 flux was not strongly affected by very large precipitation events, and for this reason the 1993 sediment flux did not exceed the 1991 value. The maximum precipitation event observed during the 1993 was 1.71 inches.

For each of the model periods, the average concentration of the quick waters was back calculated. The range of the quick-water concentration was from 64 mg/l for 1993 to 170 mg/l for 1991. These

concentrations are contrasted with the 5.0 mg/l concentrations which were associated with slow and longterm-baseflow sediment inputs. These results indicate that if sediment transport in the river must be reduced, the most efficient treatment option would include a system which controls sediment transport of the quick-streamflow component.

The Winchester sub-basin contributes the largest fraction of suspended sediments to the river system. (48%, table V.4-8). The large suspended sediment contribution from Winchester is due to the relatively large quick-streamflow component of the Winchester sub-basin relative to the other sub-basins.

The sub-basin which contributed the smallest amount of sediment was the Woburn West sub-basin. The small contribution from Woburn West is due to the sub-basin's model formulation which does not incorporate a quick-sediment component. For this sub-basin, the suspended sediment model estimates relatively low and constant concentrations regardless of storm conditions.

Run Period	Mean Suspended Sediment Flux at Watershed Outlet (kg/hr)	Mean Suspended Concentration at Watershed Outlet (mg/l)
1991	66	22
1992	32	11
1993	44	12

Table V.4-6: Mean Suspended Sediment Flux and Concentration at Watershed Outlet for 1991, 1992, & 1993 Model Periods (Modeled Values)

Suspended Sediment Component	Fraction of Total Flux
Quick	0.57
Slow	0.11
Longterm Baseflow	0.18
Channel	0.15

Table V.4-7: Average Suspended Sediment Fractions for Quick, Slow, Longterm Baseflow and Channel Components (1991, 1992, & 1993 Model Years)

Model Unit	Fraction of Total Flux	Drainage Area Normalized Flux kg/(hr*mi^2)
Woburn North Sub-basin	0.27	2.04
Woburn Central Sub-basin	0.16	2.96
Winchester Sub-basin	0.48	3.96
Woburn West Sub-basin	0.10	0.42

Table V.4-8: Average Suspended Sediment Fractions and Area Normalized Fluxes for Model Units (1991, 1992, & 1993 Model Years)

Particulate Metals

A comparison of particulate-metal transport (table V.4-9) with dissolved-metal transport (V.4-3) indicates that each were responsible for roughly 50% of the transport for arsenic and iron. Most of the chromium was carried by the particulate phase, whereas most of the copper was carried by the dissolved phase.

Particulate metals were primarily transported by quick or longterm-baseflow sediments. (table V.4-10) For arsenic and iron, transport was primarily associated with longterm-baseflow sediments, whereas for chromium and copper transport was primarily associated with quick sediments. Whether quick or longterm-baseflow sediments dominate the transport of a metal depends highly upon the relative concentration values assigned to the quick and longterm-baseflow components. (See table V.2-6) If particulate-metal concentrations, $[M_p]$, for each component were equal to one another, one would expect that quick sediments would be the dominant metal transport mechanism, since quick sediments represent the bulk of the sediment transport in the river. However, the values of $[M_p]$ assigned to each component are not equal. In general, the $[M_p]$ concentration assigned to the longterm-baseflow component were either close to or much larger than the concentration assigned to the quick components. For the metals where $[M_p]_{ltbf}$ is much larger than $[M_p]_{quick}$ the longterm-baseflow component is responsible for the bulk of the transport (e.g. As and Fe). For the metals where the value of $[M_p]_{ltbf}$ is close to the value of $[M_p]_{quick}$, the quick component is responsible for the bulk of the transport (e.g. Cr and Cu).

Slow sediments carried the smallest proportion of particulate metals (< 3%). The reason for this small contribution is due to a combination of: 1) small sediment fluxes associated with this component (≈11%), and 2) generally low $[M_p]$ values assigned to this component (table V.2-6)

The effect of different $[M_p]$ values assigned to different sediment components is also reflected in the year to year variation of the particulate-metal flux. (table V.4-9) For 1993, the particulate-metal flux for arsenic and iron was almost equal or slightly larger than the 1991 flux, despite the much larger total sediment flux carried during 1991. This result is due to the large longterm-baseflow sediment component in 1993. Since the longterm-baseflow component has higher $[As_p]$ and $[Fe_p]$ values, the large amount of more-contaminated longterm-baseflow sediments transported in 1993 approximately balance the very large amount of less-contaminated quick sediments transported in 1991. For chromium and copper, on the other hand, the 1993 metal fluxes were lower than the 1991 metal fluxes. This trend is a result of comparable $[Cr_p]$ and $[Cu_p]$ values determined for both the quick and longterm-baseflow components. The relatively small particulate-metal fluxes modeled for 1992 (table V.4-9) are due to the lower suspended sediment fluxes which were composed primarily of quick sediments.

For arsenic, iron, and copper both the Woburn North and Winchester sub-basins were responsible for a large fraction of the total metal flux. (table V.4-11) The Woburn North contribution was large because of the high [M_p] value assigned to the longterm-baseflow sediment component. The large contribution from the Winchester sub-basin was large because of the relatively large amount of sediment that is transported from the sub-basin.

For chromium, the largest contributors were the Woburn Central and Winchester sub-basins. The primary reason for the large contribution from the Woburn Central sub-basin is due to the large [M_p] values assigned to the quick and longterm-baseflow components. Again, as for the other metals, the reason for the large chromium contribution from the Winchester sub-basin is due to the large sediment flux from the sub-basin.

Run Period	Mean Particulate Metal Flux at Watershed Outlet, (g/hr)			
	As	Cr	Fe	Cu
1991	8.4	15.9	2,840	16.5
1992	6.9	8.8	1,960	8.0
1993	9.1	12.3	2,610	11.0

Table V.4-9: Mean Particulate Metal Flux for 1991, 1992, & 1993 Model Periods (Modeled Values)

Particulate Metal Component	Fraction of Total Particulate Flux			
	As	Cr	Fe	Cu
Quick	0.19	0.49	0.33	0.58
Slow	0.01	0.03	0.03	0.02
Longterm Baseflow	0.66	0.32	0.49	0.23
Channel	0.14	0.15	0.14	0.18

Table V.4-10: Average Particulate Metal Fractions for Quick, Slow, and Longterm Baseflow Components (1991, 1992, & 1993 Model Years)

Model Unit	Fraction of Total Particulate Flux				Drainage Area Normalized Flux g/(hr*mi^2)			
	As	Cr	Fe	Cu	As	Cr	Fe	Cu
Woburn North Sub-basin	0.47	0.23	0.33	0.32	0.61	0.44	132	0.61
Woburn Central Sub-basin	0.13	0.25	0.11	0.13	0.40	1.21	109	0.63
Winchester Sub-basin	0.39	0.51	0.51	0.51	0.55	1.11	219	1.05
Woburn West Sub-basin	0.01	0.01	0.05	0.03	0.01	0.01	11	0.03

Table V.4-11: Average Particulate Metal Fractions and Area Normalized Fluxes for Model Units (1991, 1992, & 1993 Model Years)

V.4.3 Monthly Metal Fluxes

The monthly distribution of the total metal flux is characterizedby months with high metal fluxes versus months with low metal fluxes. Examples of the monthly distribution for arsenic and chromium for the 1992 model period are provided in figures V.4-1 and V.4-2. In general, months with high metal fluxes correlate with months with high streamflows (figure V.4-3).

During the summer months, the correlation with high streamflows is more pronounced for chromium than for arsenic. This effect is due to the particulate phase which plays a much stronger role in the transport of chromium than in the transport of arsenic. For example, during months of low flow conditions (May and July, figure V.4-3), a large fraction of the chromium supplied to the river accumulates within the channel due to deposition of the particulate phase. If a low flow month is followed by a month with higher flows (June and August, figure V.4-3), then a large portion of the chromium accumulated in the channel will be flushed from the river bottom during the later month, resulting in significantly large increases in chromium transport during the high flow month.

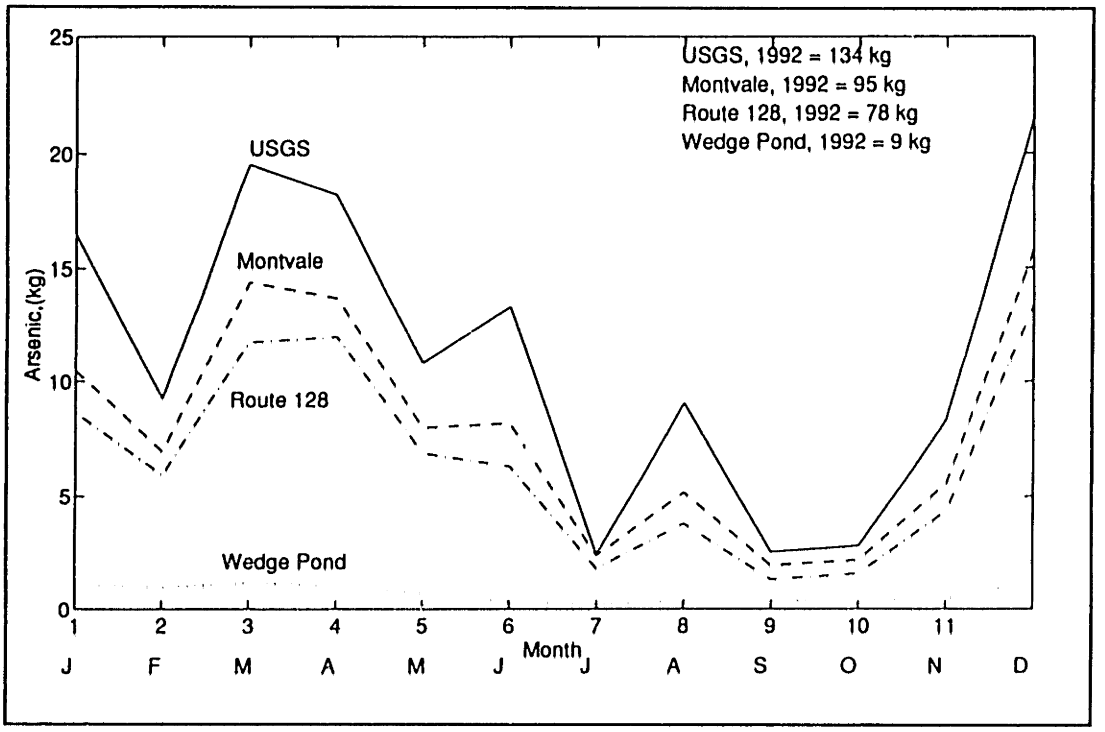

Figure V.4-1: Arsenic Flux, kg/month vs Time, USGS, 1992

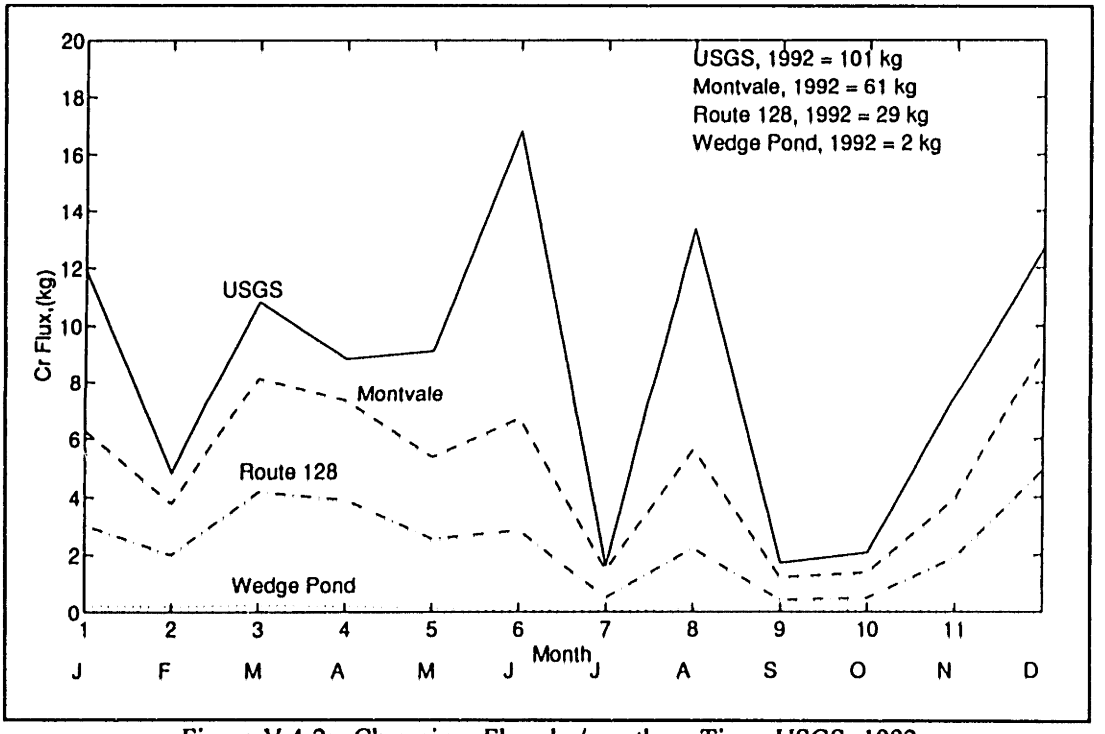

Figure V.4-2: Chromium Flux, kg/month vs Time, USGS, 1992

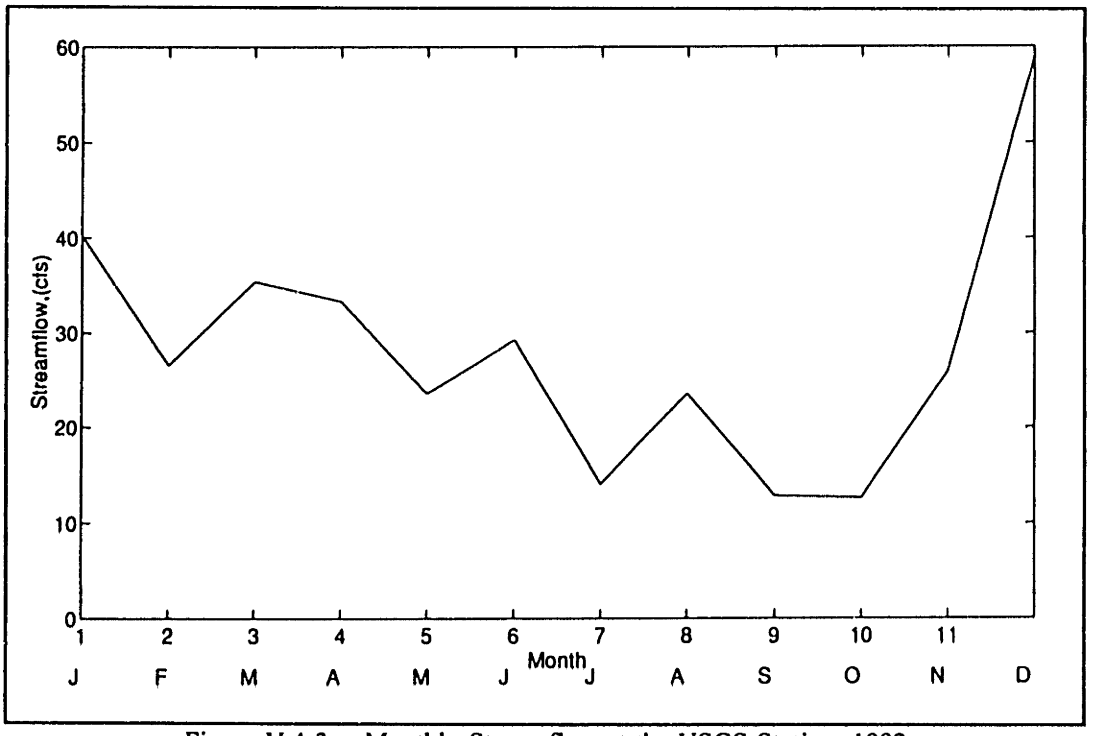

Figure V.4-3: Monthly Streamflow at the USGS Station, 1992

VI. SUMMARY, CONCLUSION, & DISCUSSION

VI.1 SUMMARY

The primary objective of the current research is to increase the general understanding of contaminant transport processes in river systems. For the current study, our approach is based on investigating the transport of four metals (Fe, Cr, Cu, and metalloid As) within one particular watershed, the Aberjona River watershed.

To investigate metal transport for the Aberjona River system, we initiated a monitoring program. The primary units of the monitoring program included: 1) continuous measurements of streamflow and instantaneous monthly sampling for suspended sediment and metals at five gaging stations, and 3) semi-continuous monitoring of turbidity and storm-event sampling for suspended sediment and metals at the outlet of the watershed.

From the data collected, we postulated transport processes. To further test our understanding of the mechanisms of metal transport, these processes were quantified and incorporated into a computer model. From our analysis, we found that in the Aberjona River system, streamflow, suspended sediment, and metal transport responded in a reproducible fashion to changes in hydrologic conditions. One of the most noticeable features of the streamflow hydrographs observed along the Aberjona River is the consistent pattern in streamflows associated with storm events. Our interpretation of these patterns is that streamflow is composed of three components: quick storm flow, slow storm flow, and longterm baseflow. Each of these components are defined from the timing of the river response.

Sediment input mechanisms were postulated in association with each of these streamflow components. Quick sediment inputs were assumed to be governed by a build-up and wash-off mechanism. With this formulation, the initial burst of suspended sediments observed at the beginning of each storm event could be reproduced. Slow and longterm-baseflow sediments were assumed to be governed by a "potential concentration" mechanism which supplies relatively low but constant suspended sediment concentrations to the river. Once the sediments enter the channel, channel deposition and erosion may affect transport.

The separation of streamflow and suspended sediment into components facilitated our understanding of metal transport within the Aberjona River watershed. It was observed that metal concentrations varied significantly between low flow and storm conditions, whereas between storm events fluctuations were not as pronounced. A large amount of the variability could be explained by postulating that each streamflow and sediment component had a different metal concentration.

The data also indicate that metal transport was also affected by watershed-wide variations of metal contamination between sub-basins. For some metals, the bulk of the flux could be traced to upstream sub-basins, where downstream inflows diluted more contaminated waters originating upstream. Differences between sub-basins were modeled by postulating that the concentration of metals associated with streamflow and suspended sediment components from each sub-basin were different.

Incorporating these mechanisms into a computer model, we found that for the model periods, roughly 70% of the sediment was transported in "bursts" at the beginning of each storm event. As a result, the number and magnitude of large storm events during a given model period significantly affects the predicted sediment transport. For As, Cr, Fe, and Cu, the yearly average dissolved-metal flux was 8-11, 2-3, 1200-1700, and 17-24 g/hr, respectively. The yearly average particulate-metal flux for As, Cr, Fe, and Cu was 7-9, 9-16, 2000-2800, and 8-16 g/hr, respectively. Dissolved and particulate transport were each responsible for roughly one half of the transport for As and Fe. Most of the Cr was carried in the particulate phase, whereas most of the Cu was carried in the dissolved phase. For all metals, dissolved-metal transport was carried primarily by the longterm-baseflow component. For arsenic and iron, particulate transport was primarily associated with longterm-baseflow sediments, whereas for chromium and copper, particulate transport was primarily associated with quick sediments.

VI.2 CONCLUSION: DESCRIPTION OF MAJOR TRANSPORT MECHANISMS FOR THE ABERJONA RIVER SYSTEM

In this study we found that both streamflow and sediment transport are important factors in controlling the transport of metals through the Aberjona River system. By observing the timing of these factors in response to storm events, we were able to infer mechanisms of transport for the main trunk of the Aberjona River. These mechanisms are associated with quick storm waters, slow storm waters, and longterm-baseflow waters.

We found that at the beginning of each event the river's response was characterized by rapid increases and decreases in streamflow, suspended sediment fluxes, and metal fluxes. Our interpretation of this response is that upon the initiation of a storm, transport is dominated by quick-system waters. The quick system is assumed to be any system that can quickly transport water to the river. The quick system may include, for example,: 1) storm sewer discharges, 2) direct channel precipitation, and 3) direct runoff from areas adjacent to the channel. Once within this system, waters are assumed to "pick-up" dissolved metals, such that when the quick system is active dissolved metals are supplied to the river.

Sediment generation for the quick system consists of a build-up/wash-off mechanism, in which sediments accumulate (build-up) in the system between storm events, and are removed from the system (wash-off) when the quick system is active. Mechanisms of sediment removal from this system are most likely associated with tractive forces associated with the quick component of streamflow and with the erosive capacity of rainfall impact in quick areas exposed to direct precipitation. It is assumed that the sediments within the quick system are contaminated with metals such that when the quick system supplies sediment to the river, particulate metals are also supplied.

Immediately after the quick response, streamflow is dominated by slow storm waters. This slow response is characterized by a slower rate of decrease after the initial quick burst or by even a second peak which occurs after the quick peak. Our interpretation of this observation is that shortly after the activation of the quick system, the slow system will begin to dominate transport in the river. The slow system consists of any system that supplies water more slowly to the river. Examples include: 1) groundwater inflows in response to a storm event, 2) interflow, and 3) water from upstream areas whose contribution was delayed because of routing effects. It is also assumed that waters flowing through the slow system are capable of "picking-up" dissolved contaminants, such that when flow through this system is active, dissolved metals are supplied to the river.

During prolonged periods between storm events, streamflow was dominated by longterm-baseflow waters. These waters are assumed to be primarily groundwaters that do not respond strongly to short-term storm events. Similarly as for the quick and slow systems, these waters are also assumed to "pick-up" dissolved metals such that they too are a source of the dissolved-metal flux to the river.

When slow or longterm-baseflow waters dominate streamflow, it was also observed that suspended sediment concentrations in the river were low and relatively constant. The interpretation of this observation is that these waters have a potential for forming particles upon reaching the river. In other words, as slow or longterm-baseflow waters traverse through their corresponding systems, they pick-up dissolved material that is capable of precipitating out of solution upon reaching the river. For the Aberjona River system, the potential concentration associated with the slow and longterm-baseflow system is low and relatively a constant in time. These particles that are formed may also be contaminated with metals such that they also transport metals to the river system.

Upon reaching the channel, the various inputs associated with each system are assumed to be mixed together. Since each of these inputs can potentially have different metal concentrations, the net concentration of dissolved and particulate metals is a result of the mixing of each of these waters. An example of the effects of mixing is the observed "dilution effect" of particulate arsenic and iron. The observed dilution effect can be described by assuming that more contaminated sediments that dominated during low flow conditions (sediments from the longterm-baseflow system) are mixed with relatively clean sediments activated during a storm (sediments from quick and slow systems).

Furthermore, upon reaching the channel, sediments and their associated particulate metals are capable of depositing or eroding within the channel. Deposition is believed to occur primarily during extremely low flow conditions. Erosion is believed to occur primarily at the onset of a storm event. This erosion along with the activation of quick-sediment sources gives rise to the observed "flushing effect" of particulates at the beginning of each storm. The magnitude of transport associated with channel erosion at the onset of a storm is believed to be small compared to the transport associated with quick sources.

Transport mechanisms along the Horn Pond Creek tributary were apparently different than transport along the Aberjona River. Along this tributary, streamflow did not respond with distinct quick, slow, and longterm baseflows. Furthermore, metal concentrations were significantly lower on the tributary than along the Aberjona River. In general transport from this tributary was characterized by relatively low and relatively constant metal transport. Furthermore, suspended sediment concentrations transported from Wedge Pond were characterized by two distinct types of sediments: an organic phase and an inorganic phase. The organic phase exhibited significant seasonal fluctuations and was apparently

controlled by the growth of biological material in Wedge Pond during the summer months. The inorganic phase was inversely related to water hydraulic residence times. Apparently this phase was controlled by settling of inorganic particulates entering the pond in the inflow.

Localized areas of contamination also apparently affect variations in metal concentrations throughout the watershed. For example, along the Aberjona River, the observed decrease in metal concentration in the downstream direction can be explained by assuming that the primary source of metals comes from the upstream reaches. As contaminated waters from the upstream source travel downstream, they are diluted by relatively cleaner inflows, resulting in the observed concentration decrease.

VI.3 DISCUSSION

VI.3.1 Possible Application to Other Watersheds

Some of concepts presented in this study may be applicable to other watersheds. For example, a logical extension of the concept of quick versus slow storm flows would be to model streamflows and water quality parameters in urbanized watersheds. The characteristic of urbanized watersheds that makes this application feasible is that within urbanized watersheds water can potentially enter a river system through many different systems. Some of these systems, such as storm sewer systems, are capable of transporting storm water quickly to the river, whereas other systems, such as a groundwater system, will transport storm water more slowly to the river. Therefore, one would expect that for a watershed with separate systems for the conveyance of water, separation of streamflow into the components of quick and slow storm flow would be useful. Furthermore, since each of these systems (quick and slow systems) can have a different effect on water quality, the separation of streamflow into components is a logical starting point for the development of water quality models for other watersheds.

VI.3.2 Model Formulation: Contribution

Some of the relationships used in the model are routine relationships which are commonly used in the engineering field to model hydrologic processes. Routine relationships incorporated within the model include: 1) use of a unit hydrograph technique for routing effective rainfall to streamflow, 2) use of a degree-hour method to quantify snow-melt, 3) routing of streamflow using the Muskingum method, 4) use of a continuous-flow stirred-tank reactor model to estimate the growth of material within a reservoir, 5) use of a build-up and wash-off mechanism for estimating the input and transport of sediments from sewers, and 6) use of transport capacity concepts in the quantification of sediment transport in channels.

Although many routine concepts are incorporated into the computer model, the model still has many innovative features. These features can be categorized into two groups: 1) unconventional applications of established concepts, and 2) innovative approaches for modeling hydrologic processes.

Unconventional Applications of Established Concepts

An example of an unconventional application is the determination of storm flow from one sub-basin using more than one unit hydrograph. In this study, for each sub-basin on the Aberjona River, effective

rainfall is routed to the river using two different unit hydrographs: a quick unit hydrograph and a slow unit hydrograph. Although quantification of quick and slow flows involved the familiar notion of a unit hydrograph, it was the separation of storm flow into these components that revealed apparently consistent relationships by which water quality parameters responded to changes in hydrologic conditions.

The degree-hour method for snowmelt quantification was also applied in a new manner. The distinctive parts of the snow-melt model include the use of: 1) a lag parameter which postpones the snowmelt process until a certain number of degree-hours have been observed, 2) use of separate relationships to quantify the lag parameter: one for above freezing temperatures during times with no rainfall and one for above freezing temperatures during times with rainfall and, 3) permitting the potential meltwater relationships to be a function of degree-hours raised to a variable exponent, "a". Usually, the exponent in the degree-hour formulation is set to a value of one. (Gray & Male, 1981; Linsley, 1982; Bras, 1990)

In quantifying the effective rainfall, the application of *two* "Water Response Times", WRT, (one for the quick system and one for the slow system) provides a slightly different twist on a routine method of separating hourly precipitation into individual storm events. The WRT is considered to be the time needed to empty or almost empty an individual system of water. (Computationally, the WRT is the time which must elapse with no precipitation such that an hourly time sequence can be identified as a storm event.) Since water is removed from the quick system more quickly than from the slow system, one value of WRT was used for the quick system and another value was used for the slow system. It is the use of two different separation times (one for each system) which enabled the proper estimation of streamflow.

The Muskingum method is a classical technique which is widely used for routing streamflow through river channels. In this study, a new interpretation of the Muskingum method is included such that a similar methodology can also be used to route sediment and metal fluxes. Routing of sediment and metal fluxes using the Muskingum method has not (to our knowledge) been documented in the literature.

The peculiar aspect of the Wedge Pond model is that the suspended sediment fluxes were separated into inorganic and organic components. Quantification of each of these components, however, generally followed classical relationships in which the organic phase was estimated by use of a continuous-flow stirred-tank reactor model and the inorganic phase was correlated with pond hydraulic residence times. It is the separation of the sediment into these two components that simplified the modeling of suspended sediment from the pond.

Use of a build-up and wash-off mechanism has been incorporated into other computer models for estimation of sediment transport in storm sewer systems. (Overton, 1976) The unusual application for the model presented in the current study is that a component of flow, the quick component, was used to estimate the wash-off potential. The application of only part of the streamflow to the "build-up and wash-off" system was the part of the formulation which enabled the model to reproduce the observed bursts of sediment which were transported in the river at the beginning of each storm event. Furthermore, the formulation and relationships described by Overton, 1976 for sediment "build-up and wash-off" have been modified significantly within the present study. These modifications include: 1) that wash-off of sediment from quick areas occurs in association with two erosive processes: quick flow and rainfall, and 2) transport for each erosive process is governed by a power function of the difference between the erosive component and a threshold value.

The concept of sediment transport capacity is routinely used in engineering practice for the quantification of sediment transport. An interesting twist to this concept, (however, generally over-looked in text-books) is the field observation that sediment transport tends to be different between the rising and falling limbs of the streamflow hydrograph. (Walling, 1977) The computer model developed for the present study takes note of that field observation and uses different transport capacity relationships: one for the rising limb and one for the falling limb. The rising-limb relationship is based upon classical sediment transport theory. The falling-limb relationship is based upon observed field data.

Innovative Approaches for Modeling Hydrologic Processes

Innovative concepts are also incorporated within the model. These concepts include: 1) the application of different streamflow components to modeling suspended sediment and metal transport, 2) the interpretation of the different streamflow components, and 3) application of melt flow to the quick and slow systems.

By handling streamflow components individually, each streamflow component can produce separate water quality components. The mechanisms used to describe water quality generation can, as a consequence of the separation, also be different from one another. For example, two different mechanisms for modeling sediment inputs are proposed for the current study. One mechanism is a build-up and wash-off mechanism for the quick system. The other formulation is a potential concentration mechanism for the slow and longterm-baseflow system. It is the use of different water quality generation characteristics along with the streamflow separation that presents a different method of modeling contaminant transport in rivers.

In the literature a common analysis of a streamflow hydrograph includes its separation into components.

Usually, only two components, direct runoff and baseflow, are identified. (Gray, 1973; Fetter, 1988; McCuen, 1989) The separation of a streamflow hydrograph into direct runoff and baseflow implies that there are specific mechanisms by which the streamflow enters the river. Direct runoff implies surface runoff whereas baseflow implies groundwater runoff. (Davis & DeWiest, 1966; Gray, 1973; Fetter, 1988; McCuen, 1989) In this study, the streamflow hydrograph was separated into three components: quick, slow, and longterm baseflow. The interpretation of these flow components comes from the timing of the river response, rather than from specific physical mechanisms of runoff generation as implied in more traditional separation techniques.

To emphasize the differences between the direct runoff versus quick/slow flow interpretations, consider the following situation. Assume that the area of interest consists of one home which is adjacent to a street. The roof of the home drains into a grassy area between the home and the street. Water from the roof can discharge into the river by either: 1) infiltrating into the lawn and traveling to the groundwater table which eventually discharges to a river, or 2) flowing over the lawn and into the street which then discharges into the river through a storm sewer system. For a small storm event, which is preceded by dry antecedent conditions, most of the water which drains the roof of the home will infiltrate into the lawn. As a result, the water falling on the roof will take a considerable amount of time before it travels through the groundwater and eventually to the river. Because of the slow response-time of the water, the roof of the home is considered to be a part of the slow system for the small event. For a larger storm preceded by antecedent wet conditions, however, a large fraction of water drained by the roof may flow over the lawn (because of limiting infiltration capacity) into the street and eventually into the storm sewer system. Since for this scenario the water is transported much faster to the river, the roof, for this case, is considered to be part of the quick-flow system. Since for the more traditional streamflow separation methods, impervious areas are considered to contribute to direct runoff, the roof of the home is considered to be a direct runoff component for both the small and large storms. For the quick/slow system the roof is considered to contribute to the slow system for a small storm and contribute to the quick system for a large storm.

Application of melt flow to the quick and slow systems is an extension of the streamflow separation method used for the current study. This application is based upon the assumption that melt flow can enter the river through either quick or slow systems and can therefore pick-up water quality characteristics that are typical to those systems. In other words, precipitation as snow is assumed to affect the time distribution of the streamflow response. However, the systems by which melt flow is conveyed to the river are not different than the systems which convey routed rainfall, and therefore melt flows will have water quality characteristics that are analogous to the systems (i.e. quick and slow systems) that convey rainfall.

VI.3.3 Engineering Application

The results of this study have several engineering applications. Specifically results can be used: 1) in the design of remediation programs, 2) to determine the impacts of a potential change to the system, and 3) for human health studies.

Design of Remediation Programs

Knowing how and when metals are transported within the river system can assist in the establishment of remediation plans. For instance, if most of the metal is carried by the longterm baseflow system, a channel-based facility which treats the bulk of the low flows is one alternative by which metals can be removed from the river. To numerically quantify contaminant removal using such an option, consider, for example, that the amount of arsenic impacting the Mystic Lakes must be reduced. The data indicate that the bulk of the arsenic transported within the river system is generated primarily from the Woburn North sub-basin and, for this sub-basin, most of the transport is carried with the longterm-baseflow component. Therefore a treatment facility located at the outlet of this sub-basin should be designed to treat roughly 5.7 cfs (yearly average streamflow of the longterm-baseflow component from the Woburn North sub-basin in 1992) or 23% of the total amount of water coming off of the Aberjona watershed. Assuming that the treatment facility can remove 90% of both the dissolved and particulate arsenic from the water, then roughly 62 kg of the 131 kg of arsenic transported to the Mystic Lakes (or 47% of the total) would be removed. Such a removal is a significant considering the relatively small amount of flow that must be treated.

Furthermore, knowing whether a metal is transported primarily in the dissolved versus particulate phase is also important from a remediation perspective. For example, such knowledge can be used to determine what type of treatment process should be used. For instance, a sedimentation treatment process could be used to remove particulate metals, whereas a process that is capable of binding dissolved metals is needed if the dissolved phase must be treated.

Knowledge of the processes governing transport may also assist in a remediation plan by identifying possible source areas. For example, if it is known that most of the metal is carried by the longterm-baseflow component, then a likely source of the metal is the groundwater system and a treatment system designed to clean-up or reduce the groundwater discharge can be designed. If it is known that the bulk of the metals are associated with particulates, then possible depositional areas (ponds, wetlands, and river reaches upstream of dams) could be likely dredging candidates if the contaminants must be removed quickly. If contaminated sediments are to remain, then care must be taken in dredging or in installing any system that may cause a remobilization of the deposited metals.

Evaluate Impacts of a Potential Change to the System

With the understanding transport processes, an engineer can better predict the effect of potential changes on the transport of contaminants. For example, for the Aberjona River, sediment and particulate-metal transport are limited by the availability of sediments. Therefore if more sediments are added to the river, for example in association with earth-moving near the river, the river will be capable of transporting the sediments downstream. Such a scenario may cause turbidity problems and, if the sediment has a high metal concentraiton, may also cause contamination problems downstream.

The data also show that increasing urbanization is resulting in a flashier streamflow response. Prior to increasing development within the watershed, precautions should be taken to assure that the larger peak flows do not cause or aggravate flooding.

Human Health Studies

Knowledge of metal transport processes may also be of use in human health studies. Knowing where most of the metals come from may assist in identifying populations which are at risk of being exposed to the contamination. Furthermore, transport processes may provide clues as to when exposures may have been highest. For example, arsenic and iron concentrations are highest during low flow conditions. Therefore, exposure would generally be highest during dry summer months which is usually the time when people are most likely to use the river and ponds for recreational purposes.

VI.3.4 Future Work

VI.3.4.1 General Areas of Study

General areas of future work include: 1) upgrading the current monitoring program, 2) improving the computer model, 3) applications of the computer model, and 4) new studies.

Upgrading the Current Monitoring Program

Upgrading the monitoring program would help to more firmly support (or reject) the inferences obtained from the data in the present study. Recommended upgrades include: 1) the addition of precipitation gaging stations, 2) improved methods of streamflow monitoring, 3) measurement of the flow reversals at Wedge Pond, and 4) the collection and analysis of more samples.

The addition of precipitation gaging stations would increase the accuracy of precipitation measurements throughout the watershed. Better precipitation measurements would improve water balance estimates and would reduce model errors associated with the spatial distribution of precipitation. Currently there is one station located in the north-eastern part of the watershed. As a minimum, one located at the southern end of the watershed (perhaps at the USGS gaging station) and one located in the west-central part of the watershed should be considered.

An improved method of streamflow monitoring (See section III.3.5) would improve estimates of surface water volumes coming from each area of the watershed. The gages which should be given the highest priority are the ones located at Route 128 and Montvale. Improved flow monitoring at these stations would help to verify whether or not the Woburn Central sub-basin does have a very high runoff fraction. If future monitoring of these areas does indeed indicate that this sub-basin produces an uncharacteristically large amount of water, then the source of these waters should be investigated in more detail.

Measurement of the flow reversal at Wedge Pond would help to quantify the amount of water which backflows from the Aberjona River. Because the water from the Aberjona tends to have higher concentrations of metals, the flow reversal could impact the pond by temporarily elevating metal concentrations. This impact from the Aberjona River may be of special importance during the summer months when a public beach at Wedge Pond is open for swimming.

Collection and analysis of more samples (either with the current system or with an upgraded system) would be extremely useful in verifying the observed trends in sediment and metal transport.

Recommended upgrades to the sample collection system would include the addition of auto-samplers for storm event monitoring at both Route 128 and Montvale. Such an upgrade would help to identify processes which control the transport of metals from the Woburn North and Woburn Central sub-basins during storm conditions.

Improving the Computer Model

Improvements to the computer model developed in the present study would include: 1) incorporating a true water balance, 2) an improved snowmelt model, and 3) time-varying metal concentrations.

A true water balance would make the streamflow part of the model more coherent. With a true water balance, all precipitation "lost" from the system would be explicitly accounted for through either evapo-transpiration losses or groundwater losses. There would be no need to define a constant initial abstraction (which is physically inconsistent), since in a full water balance initial abstractions would be computed directly from antecedent conditions. Furthermore, a water balance model which sub-divides the groundwater aquifer into different zones, (e.g. Stanford Watershed Model) would also be a more physically-based way to account for different sources of groundwater (i.e. slow storm water versus longterm baseflows).

An improved snowmelt model will provide more accurate estimates of streamflow during the winter months. For the current model adjustments may include, for example, allowing the snowmelt factors to vary as a function of antecedent temperature. Ideally, however, improvements should proceed toward a snowmelt model that is more physically-based.

In the current model, metal concentrations associated with each component are assumed to be constant in time. Allowing these concentrations to vary in time would improve the concentration estimates. For example, after a storm, data indicate that concentrations of particulate arsenic and iron during longterm baseflows increased as the time since the previous storm increased. In capturing this trend, metal concentrations can be modeled: 1) as a function of antecedent conditions, or 2) from a more physically-based chemical reaction algorithm.

Application of the Computer Model

A direct application of the computer model would include the development of a transport history which provides information concerning the long-term chemical fluxes within the watershed. Once developed, the transport history can be compared with the depositional history of metals as reflected in the lake core sediments of the watershed's downstream reservoir: the Upper Mystic Lake. (Spliethoff & Hemond,

1994) Such a comparison can be used to estimate the extent to which the factors of streamflow and sediment transport affect the distribution of metals within the lake cores.

In order to develop the transport history, the historical record of daily precipitation (which dates back to the 1900's) must be disaggregated into hourly precipitation. A method for performing this disaggregation is presented in appendix VI.A.

New Studies

New studies would include: 1) investigating the mechanisms of streamflow generation in more detail, 2) investigating the sources of sediments and metals, 3) development of a new and more physically-based model, 4) additional laboratory investigations, 5) a water circulation study for Wedge Pond, and 6) investigating the effect of the Atlantic Gelatin pumping wells on transport within the river.

Investigating the mechanisms of streamflow generation would help to support (or reject) the notion of separate quick, slow, and longterm-baseflow water sources. Such a study could be performed by isolating a river reach and carefully monitoring all water inputs and outputs. Especially interesting results could potentially include the river reach within the Woburn Central sub-basin. The data collected in the current study indicate that the Woburn Central sub-basin produces an uncharacteristically large amount of water. It would be very interesting to verify that a large amount of water is indeed flowing from the sub-basin and to determine where this water is coming from. Perhaps tracer studies in this area would be useful in identifying the water sources of interest.

Investigating the sources of sediments and metals would help to more accurately pinpoint the physical mechanisms by which different components of suspended sediments and metals are generated. Examples of source-based studies could include:

1) Monitoring major storm sewer/impervious area discharges into the river. In such a study, a) the accumulation and removal rates of suspended sediments and metals can be estimated and compared with the build-up and wash-off parameters used for the quick-system model, and b) the time variation of metals can be compared with the time-constant representation used in the current study.

2) Investigating suspended sediment and metal inputs associated with groundwater sources. Such a study may help to: a) determine if a constant particle forming potential associated with slow and longterm-baseflow waters is a reasonable assumption, b) determine if groundwater sources can physically be sub-divided into two types, (slow storm water versus longterm baseflow), and c) determine if a time-constant metal concentration is reasonable.

3) Investigating of the importance of raindrop impact and overland flow as a source of metals to the river. Such a study would help to better quantify the sediment and metal contributions from these sources.

4) Analyzing for different metal species within the dissolved and particulate phases. Such an analysis may provide information concerning the chemical processes governing transport within the river. For example, speciation studies can be used to determine the extent to which redox reactions control the distribution of metals between the dissolved and particulate phases.

With an improved understanding of streamflow, sediment, and metal sources a more physically-based model for metal inputs can then be developed. One may even couple a more physically-based input algorithm with a more physically-based routing algorithm (e.g. the 2, or even better 3, dimensional equations of fluid and sediment motion). The equations of motion would serve as a substitute for the Muskingum router used in the current study. An interesting river reach to apply such a model would be the reach within the Woburn Central sub-basin, between Route 128 and Montvale. This reach is especially interesting from both a metal transport and from a public opinion point-of-view because: 1) the data indicate that during storms this reach may serve as a metal source, and 2) it incorporates the controversial Wells G & H Superfund site.

Laboratory-based efforts would also be of value. For example, data indicate that arsenic and iron tend to be transported in a similar fashion. It would be interesting to determine whether this association is due to arsenic binding with iron or whether arsenic just happens to be mobilized in a similar fashion as iron. Other laboratory work may include research investigating the extent to which partitioning is controlled by the metal source versus chemical factors.

A water circulation study for Wedge Pond will help to determine the adequacy of the continuous-flow stirred-tank reactor (CFSTR) representation. A CFSTR implies no backflow of water (which was observed on one occasion) and implies that the pond is completely mixed. However, the "completely mixed" assumption may be an over-simplification if: 1) stratification inhibits mixing, and 2) the orientation of the inflow and outflow from the pond (since they are adjacent to one another) permits short-circuiting of the water.

It would also be interesting to investigate the adequacy of the Atlantic Gelatin component of the model. It is likely that the amount of water removed by the wells from the river is not a constant (as assumed in the model) but a function of flow, groundwater elevations, and climatic conditions. Furthermore, there is the possibility that the wells can cause the extraction of particulates from the river - perhaps

through the transport of colloidal particles from the river into the river bed and groundwater aquifer. Complex chemical reaction can also occur at the sediment-water interface in the river which could negate the assumptions made concerning metals transport.

VI.3.4.2 Proposed Project

If I had the opportunity to continue investigating the mechanisms of metal transport in the Aberjona River system, my efforts would combine several of the recommendations for future work mentioned above. The project I envision would be focused within the Wells G & H river reach (Aberjona river between Route 128 and Montvale Avenue). The primary goal of the study would be to estimate water, sediment, and metal inputs to (or outputs from) the river system from the groundwater aquifer in the Wells G & H area.

In order to under-take such a project, I would consider the development of a physically-based, three-dimensional, sediment and metal transport model of the river system. The model should be formulated to capture the transient effects of water, sediment, and metal storage within the reach. In applying such a model, groundwater inputs to the river can be estimated through a calibration procedure.

To develop the model, a monitoring program should be initiated to collect the following information: 1) deposition and erosion properties of the type of sediment found within the Wells G & H area, 2) changes in river-bottom geometry and river-bottom metal characteristics over time, and 3) monitoring water, sediment, and metal transport at upstream and downstream ends of the reach.

Deposition and erosion properties of the sediment would be incorporated within the model formulation. Water, sediment, and metal transport at the upstream end of the reach would be used as an input into the model. River-bottom characteristics and transport at the downstream end of the reach would be used to calibrate and verify the model.

Depending upon the initial results, the monitoring program can be expanded such that: 1) the mechanisms of streamflow generation can be better understood (e.g. through a tracer study), and 2) the effects of chemical processes on transport can be better quantified (e.g. by analyzing for different metal species) Results of such studies can be used to modify and improve the model.

REFERENCES

REFERENCES

Adario, J.A., 1993. Personal Communication. Mr. Adario works for the Massachusetts Institute of Technology, Center for Materials Science and Engineering, X-Ray Diffraction Facility, Cambridge, MA.

Amber Science, Inc., 1989. Instruction Manual, Digital Conductivity Meter, Model 604. 277 Blair Blvd. Eugene, Oregon.

Andreae, L.C.D., 1977. Determination of Arsenic Species in Natural Waters. Analytical Chemistry, 49(6): 820-823.

Arnseth, R.W., and Turner, R.S., 1988. Sequential Extraction of Iron, Manganese, Aluminum, and Silicon in Soils from Two Contrasting Watersheds. Soil Sci. Soc. Am. J., 52: 1801-1807.

Aurilio, A.C., 1992. Arsenic in the Aberjona Watershed. Master of Science Thesis, Massachusetts Institute of Technology.

Bird, S.C., 1987. The Effect of Hydrological Factors on Trace Metal Contamination in the River Tawe, South Wales. Environmental Pollution, 45: 87-124.

Bradley, S.B., 1984. Flood Effects on the Transport of Heavy Metals. International Journal of Environmental Studies, 22: 225-230.

Bradley, S.B. and J. Lewin, 1982. Transport of Heavy Metals on Suspended Sediments Under High Flow Conditions in a Mineralized Region of Wales. Environmental Pollution (Series B) 4: 257-267.

Brainard, E.C., 1990. Groundwater Modeling of the Aberjona Basin. Master of Science Thesis, Massachusetts Institute of Technology.

Bras, R.L., and Perkins, F.E., 1975. Effects of Urbanization on Catchment Response. Journal of Hydraulic Engineering, Division of the American Society of Civil Engineers, 101(HY3): 451-466.

Bras, R.L., 1990. Hydrology, An Introduction to Hydrologic Science. Addison-Wesley Publishing Company, New York.

Brock, T.D., and Madigan, M.T., 1991. Biology of Microorganisms, Sixth Edition. Prentice Hall, New Jersey.

Camp Dresser & McKee, Inc., 1981. Mystic River Comprehensive Hydrology Study, Final Report. Printed by: Camp Dresser & McKee, Inc., Waltham, MA. Submitted to: The Commonwealth of Massachusetts, Metropolitan District Commission, Boston, MA.

Capone, J., 1993. Personal Communication. Mr. Capone is the Winchester Town Engineer.

Cardenas, M.P., 1993. The Transport and Fate of Fine-grained Sediments in the Lower Saginaw River. Master of Science Thesis in Mechanical and Environmental Engineering, University of California, Santa Barbara.

Carpenter, R.H., Pope, T.A., and Smith, R.L., 1975. Fe-Mn Oxide Coatings in Stream Sediment Geochemical Surveys. Journal of Geochemical Exploration, 4: 349-363.

Chao, T.T., and Theobald Jr., P.K., 1976. The Significance of Secondary Iron and Manganese Oxides in Geochemical Exploration. Economic Geology,71: 1560-1569.

Chao, T.T. and Zhou, L., 1983. Extraction Techniques for Selective Dissolution of Amorphous Iron Oxides from Soils and Sediments. Soil Sci. Soc. Am. J., 47: 225-232.

Chao, T.T., 1984. Use of Partial Dissolution Techniques in Geochemical Exploration. Journal of Geochemical Exploration, 20: 101-135.

Chester, R. and Hughes, M.J., 1967. A Chemical Technique for the Separation of Ferro-Manganese Minerals, Carbonate Minerals and Adsorbed Trace Elements from Pelagic Sediments. Chemical Geology, 2: 249-262.

Chow, V.T., 1959. Open-Channel Hydraulics. McGraw-Hill Book Company, Inc., New York.

Chow, V.T., Maidment, D.R., and Mays, L.W., 1988. Applied Hydrology. McGraw-Hill Publishing Company, New York.

Clesceri, L.S., Greenberg, A.E., Trussell, R.R. and Franson, M.A, (eds.), 1989. Standard Methods for the Examination of Water and Wastewater, 17th edition. American Public Health Association, American Water Works Association, and Water Pollution Control Federation. Washington, DC.

Coastal Leasing, Inc., 1988. Scarecrow User's Manual. 179 Sidney Street, Cambridge, Massachusetts 02139.

Commonwealth of Massachusetts, 1988a. Registration Statement for Estimated Water Withdrawal. Atlantic Gelatin, Registrant.

Commonwealth of Massachusetts, 1988b. Registration Statement for Estimated Water Withdrawal. Wilson Farm, Registrant.

Commonwealth of Massachusetts, 1989a. Registration Statement for Estimated Water Withdrawal. Wm Spence & Son, Inc., Registrant.

Commonwealth of Massachusetts, 1989b. Registration Statement for Estimated Water Withdrawal. McCord-Winn Textron, Registrant.

Commonwealth of Massachusetts, 1990a. Division of Water Supply, Community Public Water Supply Statistics for Horn Pond. 1981, 1986, 1987, 1988, 1989 on file.

Commonwealth of Massachusetts, 1990b. Division of Water Supply, Community Public Water Supply Statistics for Town of Burlington Water Supply. 1988, 1989 on file.

Cossa, D., Tremblay, G.H., and Gobeil, C., 1990. Seasonality in Iron and Manganese Concentrations of the St. Lawrence River. The Science of the Total Environment, 97/98: 185-190.

Coulter Electronics Inc., 1984. Coulter Counter® Model ZM Product Reference Manual. Hialeah, FL.

Coulter Electronics Inc., 1984. Operator's Handbook for the Coulter Channelizer® 256. Hialeah, FL.

Coulter Electronics Inc., 1984. Reference Manual for the Coulter Channelizer® 256. Hialeah, FL.

Coulter Electronics Inc., 1989. Reference Manual for Coulter® Multisizer, Software Level 4.1. Hialeah, FL.

Das, B.M., 1985. Principles of Geotechnical Engineering. PWS Publishers, Boston, MA.

Davis, S.N., and DeWiest, R.J.M., 1966. Hydrogeology. John Wiley & Sons, Inc., New York.

Debnam, O., Commonwealth of Massachusetts, Department of Public Works, Personal Communication. Fax sent July 14, 1993 describing benchmark data for the Town of Woburn.

Delfino, J.J., and Otto, R.G., 1986. Trace Metal Transport in Two Tributaries of the Upper Chesapeake Bay: The Susquehanna and Bush Rivers. Marine Chemistry, 20: 29-44.

Durant, J.L., Zemach, J.J., and Hemond, H.G., 1990. The History of the Leather Industry Waste Contamination in the Aberjona River Watershed: A Mass Balance Approach. Civil Engineering Practice, Journal of the Boston Society of Civil Engineers Section/ASCE, 5(2): 41-66.

Durant, J.L., 1991. Industrial History, Mutagenicity, and Hydrologic Transport of Pollutants in the Aberjona Watershed. Master of Science and Civil Engineer Thesis. Massachusetts Institute of Technology.

Durant, J.L., 1993. Detection and Identification of Human Cell Mutagens in Sediments and Surface Waters of the Aberjona Watershed. Ph.d Thesis, Massachusetts Institute of Technology.

Dzombak, D.A., and Morel, F.M.M., 1990. Surface Complexation Modeling. John Wiley & Sons, New York.

Edwards and Kelcey, Engineers and Consultants, 1958. The Commonwealth of Massachusetts, Proposed Bridge Woburn, Montvale Avenue Relocation Over Aberjona River Relocation. A copy is available at the Commonwealth of Massachusetts, Department of Public Works.

Einstein, H.A., 1950. The Bed-Load Function for Sediment Transportation in Open Channel Flows. USDA Technical Bulletin No. 1026. Washington D.C.

Entekhabi, D. and Hawk, K., 1992. Computer programs (not included in this list are supportfiles, i.e. input files, imsl files etc.. which were also copied and used for the generation of some of the data in this paper): 1) bart.for (used for the simulation of hourly precipitation), 2) hour_tally.f (used for the computation of hourly and daily statistics), 3) zmin.f (optimization program to determine input parameters for bart.for)

Environmental Protection Agency, 1986. Test Methods for Evaluating Solid Waste. EPA/530/SW-846.

Federal Emergency Management Agency, 1979. Flood Insurance Study, Town of Winchester, Massachusetts, Middlesex County. Community Number 250228.

Federal Emergency Management Agency, 1980. Flood Insurance Study, City of Woburn, Massachusetts, Middlesex County. Community Number 250229.

Federal Emergency Management Agency, 1981. Flood Insurance Study, Town of Reading, Massachusetts, Middlesex County. Community Number 250211.

Federal Emergency Management Agency, 1984. Flood Insurance Study, Town of Burlington, Massachusetts, Middlesex County. Community Number 250185.

Fetter, C.W., 1988. Applied Hydrogeology, Second Edition. Macmillan Publishing Company, New York.

Filipek, L.H. and Owen, R.M., 1979. Geochemical Associations and Grain-Size Partitioning of Heavy Metals in Lacustrine Sediments. Chemical Geology, 26(1/2): 105-117.

Foster, I.D.L., Carter, A.D., and Grieve, I.C., 1983. Biogeochemical Controls on River Water Quality in a Forested Drainage Basin, Warwickshire, UK. In Dissolved Load of Rivers and Surface Water Quantity/Quality Relationships, Proceedings of the Hamburg Symposium, IAHS Publication No. 141.

Forstner, U. and Wittmann, G.T.W., 1979. Metal Pollution in the Aquatic Environment. Springer-Verlag, New York.

Franchini, M., and Pacciani, M., 1991. Comparative Analysis of Several Conceptual Rainfall-Runoff Models. Journal of Hydrology, 122: 161-219.

Fratoni, N.A., Cranker, N., and Kaufman, S., 1982. Upper Mystic Lake Watershed Urban Runoff Project, Main Report. Massachusetts Department of Environmental Quality Engineering, Office of Planning and Program Management.

Gailani, J., Ziegler, K, and Lick, W., 1991. Transport of Suspended Solids in the Lower Fox River. Journal of Great Lakes Research, 17(4): 479-494.

Gatehouse, S., Russell, D.W., and Van Moort, J.C., 1977. Sequential Soil Analysis in Exploration Geochemistry. Journal of Geochemical Exploration, 8: 483-494.

Gibbs, R.J., 1967. The Geochemistry of the Amazon River System: Part I. The Factors that Control the Salinity and the Composition and Concentration of the Suspended Solids. Geological Society of America Bulletin, 78: 1203-1232.

Gibbs, R.J., 1970. Mechanisms Controlling World Water Chemistry. Science, 170: p. 1088-1090.

Gibbs, R.J., 1972. Water Chemistry of the Amazon River. Geochimica et Cosmochimica Acta, 36: 1061-1066.

Gibbs, R.J., 1973. Mechanisms of Trace Metal Transport in Rivers. Science, 180: 71-73.

Gibbs, R.J., 1977. Transport Phases of Transition Metals in the Amazon and Yukon Rivers. Geological Society of America Bulletin, 88(6): 829-843.

Goldstein, J.I., Newbury, D.E., Echlin, P., Joy, D.C., Fiori, C., Lifshin, E., 1981. Scanning Electron Microscopy and X-Ray Microanalysis. Plenum Press, New York.

Graf, W.H. 1971. Hydraulics of Sediment Transport. McGraw-Hill Book Company, New York.

Gray, D.M.,(ed.) 1973. Handbook on the Principles of Hydrology. Water Information Center, Inc., Port Washington, NY.

Gray, D.M., and Male, D.H., 1981. Handbook of Snow. Pergamon Press, New York.

Green International Affiliates Inc., Consulting Engineers, 1987. Town of Winchester, Bridge Deck Replacement, Main Street over Wedge Pond. Copy available at Winchester Town Hall, Engineering and Planning. (Note elevations on this plan correspond to the Winchester Datum and not to standard National Geodetic Vertical Datum)

Grimshaw, D.L., Lewin, J., and Fuge, R., 1976. Seasonal and Short-term Variations in the Concentration and Supply of Dissolved Zinc to Polluted Aquatic Environments. Environmental Pollution, 11(1): 1-7.

Hamilton, L.C., 1990. Modern Data Analysis: A First Course in Applied Statistics. Brook/Cole Publishing Company. Pacific Grove, California.

Hartley, D.M., Sheng, T.C., and Stein, O.R., 1986. Evaluation of a Simplified Process Model for Water and Sediment Yield Prediction. Proceedings of the International Conference on Water Quality Modelling in the Inland Natural Environment, Bournemouth, England. BHRA, the Fluid Engineering Centre. p. 121-130.

Hedges, P.D., Wren, J.H., and Chidley, T.R.E., 1986. A Conceptual Model for Investigating the Pathways Utilised by Heavy Metal Pollutants in Urban Stormwater Runoff. Proceedings of the International Conference on Water Quality Modelling in the Inland Natural Environment, Bournemouth, England. BHRA, the Fluid Engineering Centre. p. 559-578

Heikkinen, K., 1990. Seasonal Changes in Iron Transport and Nature of Dissolved Organic Matter in a Humic River in Northern Finland. Earth Surface Processes and Landforms, 15: 583-596.

Hendersen, F.M., 1966. Open Channel Flow. The Macmillan Company, New York.

Herschy, R.W., 1985. Streamflow Measurement. Elsevier Applied Science Publishers, New York.

Holmgren, G.G.S, 1967. A Rapid Citrate-Dithionate Extractable Iron Procedure. Soil Sci. Soc. Amer. Proc. 31: 210-211.

Horiba Instruments Inc., 1987. Instruction Manual for Horiba Model PIR-2000, General Purpose Analyzer. Irvine, California.

Hromadka, T.V., and McCuen, R.H., and Whitley, R.J., 1990. Uncertainty Estimates For Rainfall-Runoff Model. Hydraulic Engineering, Volume 1, Proceedings of the 1990 National Conference. American Society of Civil Engineers, New York. p. 323 -329.

H.W. Moore Associates, Inc., 1977. Proposed Construction Drawings for the Bridge at Mishawum Road over the Aberjona River. A copy is available at the Commonwealth of Massachusetts, Department of Public Works.

Ionics, Inc., 1989. Model 555 Total Organic Carbon Analyzer, Instruction Manual. Watertown, MA.

Jeffery, J.W., 1971. Methods of X-Ray Crystallography. Academic Press, New York.

Jenne, E.A., 1968. Controls on Mn, Fe, Co, Ni, Cu, and Zn Concentrations in Soils and Water: the Significant Role of Hydrous Mn and Fe Oxides. In Trace Organics in Water, Advances in Chemistry Series, no. 73. R. F. Gould (ed.). American Chemical Society, Washington D.C.

Jennings, M.E., and Tasker, G.D., 1988. Estimation of Urban Stormwater Quality. Hydraulic Engineering, Proceedings of the 1988 National Conference Sponsored by the Hydraulics Division of the American Society of Civil Engineers. American Society of Civil Engineers, New York. p. 78-83.

Kaiser, M., Irmer, U., and Weller, K., 1989. Monitoring of Water Quality: Seasonal Variations of Heavy Metals in Sediment, Suspended Particulate Matter and Tubificids of the Elbe River. Environmental Technology Letters, 10: 845-854.

Knox, M.L., 1991. The Distribution and Depositional History of Metals in Surface Sediments of the Aberjona River Watershed. Master of Science Thesis, Massachusetts Institute of Technology.

Leenaers, H., 1989. The Transport of Heavy Metals During Flood Events in the Polluted River Geul (The Netherlands). Hydrological Processes, 3:325-338.

Lick, W., 1989. The Flocculation, Deposition, and Resuspension of Fine-Grained Sediments. Unpublished paper. Department of Mechanical and Environmental Engineering, University of California, Santa Barbara, CA 93106.

Lide, D.R., (ed.), 1991. CRC Handbook of Chemistry and Physics. CRC Press. Boston.

Linsley, R.K. Jr., Kohler, M.A., and Paulhus, J.L.H., 1982. Hydrology for Engineers, 3rd Edition. McGraw-Hill Book Company, New York.

Lion, L.W., Altmann, R.S., and Leckie, J.O., 1982. Trace-Metal Adsorption Characteristics of Estuarine Particulate Matter: Evaluation of Contributions of Fe/Mn Oxide and Organic Surface Coatings. Environ. Sci. Technol, 16: 660-666.

Livingstone, D.A., 1963. Data of Geochemistry, Sixth Edition, Chapter G. Chemical Composition of Rivers and Lakes. Geological Survey Professional Paper 440-G. United States Government Printing Office, Washington.

Loague, K.M. and Freeze, R.A., 1985. A Comparison of Rainfall-Runoff Modeling Techniques on Small Upland Catchments. Water Resources Research, 21(2): 229-248.

Lynnworth, L.C., 1989. Ultrasonic Measurements for Process Control. Academic Press, London, 694pp.

Madsen, O.S., 1975. Lecture Notes on Mechanics of Sediment Transport in Steady Flow, 1.67 Sediment Transport and Coastal Processes. Massachusetts Institute of Technology, Department of Civil Engineering.

Madsen, O.S., 1991. From Course Problem Set, 1.67: Sediment Transport. Massachusetts Institute of Technology. The problem consisted of fitting a best-fit line through a plot of ψ_c versus Reynolds Number for fine grains and flakes. The data is provided in: a) Raudkivi, A.J., 1990. Loose Boundary Hydraulics, 3rd Edition. Pergamon Press, New York, p. 33, and b) Mantz, P.A., 1973. Cohesionless, fine-grained, flaked sediment transport by water. Nature, Physical Science Vol. 246, p 14-16.

Marivoet, J.L., and Vandewiele, G.L., 1980. A Real Time Rainfall-Runoff Model. Hydrological Forecasting, Proceedings of the Oxford Symposium. IAHS-AISH Publication No. 129. p. 409-418.

Marsh-McBirney, Inc., 1987. Open Channel Flow Calculations. Technical Note #9. Gaithersburg, MD.

Marsh-McBirney, Inc., Undated. Instruction Manual Model 201 Portable Water Current Meter. Marsh-McBirney Inc., Gaithersburg, Maryland. 15 pp.

Marsh-McBirney, Inc., Undated. Technical Manual, Model 265 Portable Flowmeter. Marsh-McBirney Inc., Gaithersburg, Maryland.

Martin, J. and Meybeck, M., 1979. Elemental Mass-Balance of Material Carried by Major World Rivers. Marine Chemistry 7(3): 173-206.

Massacheleyn, P.H., Delaune, R.D., and Partick Jr., W.H., 1991. A Hydride Generation Atomic Absorption Technique for Arsenic Speciation. Journal of Environmental Quality, 20: 96-100.

McCarthy, G.T., 1940. Engineering Construction: Flood Control. The Engineer School, Ft. Belvoir, VA. p. 147-156. (See also, McCarthy, G.T., The Unit Hydrograph an Flood Routing. Presented at Conf. North Atl. Div., U.S. Corps Engineers, June 1938.)

McCuen, R.H., 1989. Hydrologic Analysis and Design. Prentice Hall, New Jersey.

McDonough, W.J., 1983. U.S. Geological Survey Description of Gaging Station, 01102500 Aberjona River at Winchester, MA. United States Geological Survey, Marlborough, MA.

McKnight, D.M., Kimball, B.A., and Bencala, K.E., 1988. Iron Photoreduction and Oxidation in an Acidic Mountain Stream. Science, 240: 577-692.

Merian, E., (ed.), 1991. Metals and Their Compounds in the Environment, Occurrence, Analysis, and Biological Relevance. VCH, New York.

Metcalf and Eddy, Inc., 1972. Wastewater Engineering, Treatment/Disposal/Reuse. McGraw-Hill Inc., New York.

Metropolitan Area Planning Council, 1977. Mystic River Basin, Preliminary Report. Water Quality Project, 11 Beacon Street, Boston, MA 02108.

Meybeck, M., 1976. Total Mineral Dissolved Transport by World Major Rivers. Hydrological Sciences Bulletin, 21(2): 265-284.

Ming-hui, H., Stallard, R.F., and Edmond, J.M., 1982. Major Ion Chemistry of Some Large Chinese Rivers. Nature, 298(5874): 550-553.

Moore, J.W., and S. Ramamoorthy, 1984. Heavy Metals in Natural Waters. Springer-Verlag, New York.

Morel, F.M.M., and Gschwend, P.M., 1987. The Role of Colloids in the Partitioning of Solutes in Natural Waters. In Aquatic Surface Chemistry, Chemical Processes at the Particle-Water Interface. W. Stumm (ed.). p. 405-422.

Morrison, G.M.P., Revitt, D.M., Ellis, J.B., Svensson, G., and Balmer, P., 1984. Variations of Dissolved and Suspended Solid Heavy Metals Through an Urban Hydrograph. Science and Technology Letters, 7: 313-318.

Nikolaidis, N.P., Hu, H., Ecsedy, C., and Lin, J.D., 1993. Hydrologic Response of Freshwater Watersheds to Climatic Variability: Model Development. Water Resources Research, 29(10): 3317-3328.

Ongley, E.D., 1982. Influence of Season, Source and Distance on Physical and Chemical Properties of Suspended Sediment. In: Recent Developments in the Explanation and Prediction of Erosion and Sediment, D.E. Walling (editor). International Association of Hydrological Sciences Publication no. 137.

Overton, D.E., and Meadows, M.E., 1976. Stormwater Modeling. Academic Press, New York.

Parr, A. D., Judkins, J.F., and Jones, T.E., 1981. Point-Velocity Discharge Measurement Method for Sewers. Journal of the Water Pollution Control Federation 53(1): 113-118.

Perkin Elmer Corp., 1977. Analytical Methods for Atomic Absorption Spectroscopy using the Graphite Furnace. Norwalk, CT.

Perkin Elmer Corp., 1977. Model 372 and 373 Atomic Absorption Spectrophotometers. Norwalk, CT.

Perkin Elmer Corp., 1979. Instructions, PRS-10 Printer Sequencer. Norwalk, CT.

Perkin Elmer Corp., 1980. Analytical Methods for Furnace Atomic Absorption Spectroscopy. Norwalk, CT.

Perkin Elmer Corp., undated. AS-40 Auto Sampler Standard Version Operators Manual. Norwalk, CT.

Perkin Elmer Corp., undated. HGA-400 Graphite Furnace Operators Manual. Norwalk, CT.

Petersen, M.S., 1986. River Engineering. Prentice-Hall, New Jersey.

Prakash, A., and Dearth, G., 1990. Streamflow Simulation Using Deterministic Model. Journal of Irrigation and Drainage Engineering, American Society of Civil Engineers, 116(4): 566-580.

Press, W.H., Flannery, B.P., Teulolsky, S.A., and Vetterling, W.T., 1989. Numerical Recipes, [Fortran Version]. Cambridge University Press, New York.

Reynolds, J.E., 1993. Three-dimensional, Transient Groundwater Modeling of the Aberjona Watershed. Master of Science Thesis, Massachusetts Institute of Technology.

Rijn, L.C. van, 1980. Methods of In-situ Separation of Water and Sediment. Research Report S 404-part II. Delft Hydraulics Laboratory.

Robbins, J.M., Lyle, M. and Heath, R.G., 1984(?). A Sequential Extraction Procedure for Partitioning Elements Among Co-existing Phases in Marine Sediments. College of Oceanography, Oregon State University, Reference 84-3.

Robinson, G.D., 1981. Adsorption of Cu, Zn, and Pb Near Sulfide Deposits by Hydrous Manganese-Iron Oxide Coatings on Stream Alluvium. Chemical Geology, 33: 65-79.

Rodhe, W., 1949. The Ionic Composition of Lake Waters. International Association of Theoretical and Applied Limnology Proc., 10: 377-386.

Rodriguez-Iturbe, I., Cox, D.R. and Isham, V., 1987. Some Models for Rainfall Based on Stochastic Point Processes. Proc. R. Soc. Lond. (A410): 269-288.

Rodriguez-Iturbe, I., Cox, D.R., and Isham, V., 1988. A Point Process Model for Rainfall: Further Developments. Proc. R. Soc. Lond. (A417): 283-298.

Rodriguez-Iturbe, I., Febres de Power, B., and Valdes, J.B., 1987. Rectangular Pulses Point Process Models for Rainfall: Analysis of Empirical Data. Journal of Geophysical Research (92/D8): 9645-9656.

Ross, G.J., Wang, C., and Schuppli, P.A., 1985. Hydroxylamine and Ammonium Oxalate Solutions as Extractants for Iron and Aluminum From Soils. Soil Sci. Soc. Am. J., 49: 783-785.

Ryan, J.N., and Gschwend, P.M., 1991. Extraction of Iron Oxides from Sediments Using Reductive Dissolution by Titanium(III). Clays and Clay Minerals, 39(5): 509-518.

Salomons, W. and W.D. Eysink, 1981. Pathways of Mud and Particulate Trace Metals from Rivers to the Southern North Sea. In Halocene Marine Sedimentation in the North Sea Basin. Blackwell Scientific Publications, Boston, Mass.

Salomons, W. and U. Forstner, 1984. Metals in the Hydrocycle. Springer-Verlag, New York.

Sartor, J.D., and Boyd, G.B., 1972. Water Pollution Aspects of Street Surface Contaminants. Office of Research and Monitoring, U.S. Environmental Protection Agency, Washington D.C. 20462. (EPA-R2-72-081)

Schlichting, H., 1968. Boundary-Layer Theory, 7th edition. McGraw-Hill Book Company, New York.

Schneider, H.I. and Angino, E.E., 1980. Trace Element, Mineral, and Size Analysis of Suspended Flood Materials from Selected Eastern Kansas Rivers. Journal of Sedimentary Petrology 50(4): 1271-1278.

Schuppli, P.A., Ross, G.J., and McKeague, J.A., 1983. The Effective Removal of Suspended Materials from Pyrophosphate Extracts of Soils from Tropical and Temperate Regions. Soil Sci. Soc. Am. J., 47: 1026-1032.

Schwarzenbach, R.P., Gschwend, P.M., and Imboden, D.M., 1993. Environmental Organic Chemistry. John Wiley and Sons, New York.

Sholkovitz, E.R., and Copland, D., 1981. The Coagulation, Solubility and Adsoprtion Properties of Fe, Mn, Cu, Ni, Cd, Co, and Humic Acids in a River Water. Geochimica et Cosmochimica Acta, 45: 181-189.

Singh, V.P., and Prasad, S.N., 1982. Explicit Solutions to Kinematic Equations for Erosion on an Infiltrating Plane. In Modeling Components of the Hydrologic Cycle, p. 515-538. (V.P. Singh, ed.) Water Resources Publications, Littleton, Colorado.

Singh, V.P., 1988. Hydrologic Systems, Volume I, Rainall-Runoff Modeling. Prentice Hall, New Jersey.

Soil Conservation Service, 1975. Guidelines for Soil and Water Conservation in Urbanizing Areas of Massachusetts. United States Department of Agriculture.

Spliethoff, H.M., and Hemond, H.F., 1994. History of Toxic Metal Discharge to Surface Waters of the Aberjona Watershed. Environmental Science & Technology (in submission).

Spliethoff, H., 1994. Master's thesis in preparation. Massachusetts Institute of Technology.

Stallard, R.F., and Edmond, J.M., 1983. Geochemistry of the Amazon 2. The Influence of Geology and Weathering Environment on the Dissolved Load. Journal of Geophysical Research, 88(C14): 9671-9688.

Subramanian, V., 1979. Chemical and Suspended-Sediment Characteristics of Rivers of India. Journal of Hydrology, 44: 37-55.

Svensson, G., 1987. Modelling of Solids and Metal Transport from Small Urban Watersheds. Thesis. Chalmers University of Technology, Department of Sanitary Engineering. Goteburg, Sweden. Dissertation No. 7, ISSN 0280-4581.

Taylor, D., 1964. Neutron Irradiation and Activation Analysis. George Newnes Limited, London.

Taylor, S.R., 1964. Abundance of Chemical Elements in the Continental Crust: A New Table. Geochimica et Cosmochimica Acta, 28: 1273-1285.

Tefry, J.H. and Presley, B.J., 1976. Heavy Metal Transport from the Mississippi River to the Gulf of Mexico. In: Marine Pollutant Transfer, Windom, H.L. and Duce, R.A. (editors). Skidaway Institute of Oceanography, U.S.A.

Tessier, A., Campbell, P.G.C., and Bisson, M., 1980. Trace Metal Speciation in the Yamaska and St. Francois Rivers (Quebec). Canadian Journal of Earth Science, (17): 90-105.

Tessier, A., Campbell, P.G.C., and Bisson, M., 1979. Sequential Extraction Procedure for the Speciation of Particulate Trace Metals. Analytical Chemistry, 51(7): 844-850.

Tessier, A., Campbell, P.G.C., and Bisson, M., 1982. Particulate Trace Metal Speciation in Stream Sediments and Relationships with Grain Size: Implications for Geochemical Exploration. Journal of Geochemical Exploration, 16: 77-104.

Thermo-Jarrel Ash Corp., 1989. Atomscan® 25 Spectrometer, Operator's Manual. Franklin, MD 1989.

Thermo-Jarrel Ash Corp., 1989. Atomscan® 25 Spectrometer, Service's Manual. Franklin, MD 1989.

Thomas, R.P., 1990. Application of the DR3M Watershed Model on a Small Urban Basin. Water Resources Bulletin, 26(5): 757-766.

Thompson, M., and Walsh, J.N., 1989. Handbook of Inductively Coupled Plasma Spectrometry. Blackie and Son Ltd, New York.

Tipping, E., 1981. The Adsorption of Aquatic Humic Substances by Iron Oxides. Geochimica et Cosmochimica Acta, 45: 191-199.

Town of Reading, Annual Reports. 1899 to 1993. Copies of these reports are located in the Reading Town Library.

Tucci, C.E.M., and Clarke, R.T., 1980. Adaptive Forecasting with a Conceptual Rainfall-Runoff Model. Hydrological Forecasting, Proceedings of the Oxford Symposium. IAHS-AISH Publication No. 129, p. 445-454.

U.S. Army Corps of Engineers, 1987. HEC-1 Flood Hydrograph Package Users Manual. The Hydrologic Engineering Center, Davis, CA.

Utility Engineers Inc., 1960. Proposed Construction Drawings for the Widening of Route 128 over the Aberjona River. A copy is available at the Commonwealth of Massachusetts, Department of Public Works.

Van Loon, J.C., 1980. Analytical Atomic Absorption Spectroscopy. Academic Press, New York.

VG Elemental, 1988. VG PlasmaQuad System Manual, Version 2b, June 1988. Danvers, MA.

VG Elemental, 1990. VG PlasmaQuad Software Manual, Issue 3.2.1. Danvers, MA.

Waite, T.D., and Morel, F.M.M., 1984. Photoreductive Dissolution of Colloidal Iron Oxides in Natural Waters. Environmental Science and Technology, 18(11): 860-868.

Walling, D.E., 1977. Limitations of the Rating Curve Technique for Estimating Suspended Sediment Loads, with Particular Reference to British Rivers. IAHS - International Association of Hydrological Sciences.

Warwick, J.J., and Wilson, J.S., 1990. Estimating Uncertainty of Stormwater Runoff Computations. Journal of Water Resources Planning and Management, 116(2): 187-204.

Waslenchuk, D.G., 1979. The Geochemical Controls on Arsenic Concentrations in Southeastern United States Rivers. Chemical Geology, (24): 315-325.

Welton, J.E., 1984. SEM Petrology Atlas. The American Association of Petroleum Geologists, Tulsa, Oklahoma.

Westrich, B., 1986. Hydromechanic Aspects of Contaminated Sediment Transport in Fluvial Systems. In: Sediment and Water Interactions, P.G. Sly (editor). Springer-Verlag, New York. pp. 63-68.

Whitney, P.R., 1975. Relationship of Manganese-Iron Oxides and Associated Heavy Metals to Grain Size in Stream Sediments. Journal of Geochemical Exploration, 4: 251-263.

Wilber, W.G. and J.V. Hunter, 1977. Aquatic Transport of Heavy Metals in the Urban Environment. Water Resources Bulletin, 13(4): 721-734.

Williams, L.G., J.C. Joyce, and J.T. Monk Jr., 1973. Stream-Velocity Effect on the Heavy-Metal Concentrations. Journal, American Water Works Association, 65(4): 275-279.

Yeats, P.A. and Bewers, J.M., 1981. Discharge of Metals from the St. Lawrence River. Canadian Journal of Earth Sciences, 19(5): 982-992.

Yoon, K.S., Yoo, K.H., Soileau, J.M., and Touchton, J.T., 1992. Simulation of Sediment and Plant Nutrient Losses by the Creams Water Quality Model. Water Resources Bulletin, 28(6): 1013-1021.

Zeeb, P., 1994. Personal Communication concerning metal concentration levels in sediment cores retrieved from the Wells G & H site.

Zevenbergen, L.W., and Peterson, M.R., 1988. Evaluation and Testing of Storm-Event Hydrologic Models. Hydraulic Engineering, Proceedings of the 1988 National Conference Sponsored by the Hydraulics Division of the American Society of Civil Engineers. American Society of Civil Engineers, New York. p. 467-472.

Ziegler, C.K., and Nisbet, B., 1993. Fine-Grained Sediment Transport in the Pawtuxet River. In press. To be submitted to ASCE, Journal of Hydraulic Engineering. Primary author may be contacted at HydroQual Inc., 1 Lethbridge Plaza, Mahwah, New Jersey 07430.

APPENDICES

APPENDIX III.A

Equipment Maintenance and Sample Collection Logs

Streamgage Maintenance

During the stream monitoring program routine field trips were planned every 7 to 10 days for gage maintenance and check-up. Additional trips were made to: 1) check gage operation after large storms, 2) to replace or re-attempt a repair on equipment that was unrepairable during a previous visit, and 3) for gage calibration purposes. Specific description of the calibration procedure is provided in section III.3.4.

Routine maintenance included checking the gage for proper operation, changing batteries, and downloading data. Gage operation was checked by wading to the probe location and measuring the depth (using a yardstick) at the probe and comparing it to the gage reading. If the depth reading was off by more than 1 inch attempts were made to find and correct the problem. Gage velocity was also recorded and qualitatively checked by noting the swiftness of the river. Additionally, the probe alignment was checked and debris caught in the probe vicinity or on the probe lines was removed.

Batteries were changed when their voltage fell to less than 11.5 V. In the lab, the uncharged batteries were then recharged using a 10 amp battery charger, battery water level was checked, and the terminals were cleaned to ensure good contact. Additionally, battery contacts on the gage were sanded in the field prior to a battery change.

More specific details of the maintenance program are given in the maintenance logs for each gage. (Tables III.A-1 to III.A-4) These tables provide: 1) the date and time of each maintenance trip, 2) the gage depth and velocity readings, 3) the measured depth at the probe and to the channel bottom at the probe, 4) the power voltage, and 5) extra notes describing specific maintenance procedures performed at each field trip. The index to the "notes" column is given in Table III.A-5. Adequacy of the depth measurements can be checked by comparing the gage depth with the measured depth at the probe. The offset of the probe from the channel bottom, p_o, is obtained by taking the difference between the measured depth at the probe and the measured depth to the bottom. The power voltage given is either the voltage of the battery upon arrival to the gaging station or the voltage of the new battery if the battery was changed.

Nephelometer Maintenance

A detailed summary of nephelometer maintenance is given in table III.A-6. This table includes: 1) the date and time of each maintenance trip, 2) the nephelometer calibration values, and 3) maintenance notes. Nephelometer calibration was performed using a 20 ntu standard. 2 and 5 ntu standards were used to check the precision of the calibration. Table III.A-6 indicates that the values of the 2 and 5 ntu

standards (although inaccurate) were reproducible. Since relative ntu values were of concern, the reproducibility of the low standard calibration (not the accuracy) was the determining factor of a good calibration.

During the maintenance of the nephelometer system, the system was periodically "checked." Checking the system implies assuring that the system was operational and adding NaOCl to the chlorination system as needed. "Routine maintenance" included, 1) changing the peristaltic pump tubing, 2) cleaning the nephelometer flow through cell and check valves, and 3) re-calibrating the nephelometer.

Autosampler Maintenance

Maintenance of the autosampler system included: 1) changing the peristaltic pump tubing, 2) checking the autosampler for sample retrieval, and 3) changing sample bottles. A summary of autosampler maintenance and sample retrieval is given in table III.A-7.

Sample Collection

Sample collection logs for field trips to monitoring stations 1 through 5 are given in tables III.A-8 to III.A-12. Each table provides: 1) the date and time of sample collection, 2) a summary of which samples were collected (filters vs filtrate) and how they were collected, 3) a listing of nozzle inlet versus ambient river water velocities, and 4) extra notes concerning field conditions and non-routine sample analysis. Filter pore sizes used for sample filtration are indicated in parenthesis. Additional samples were collected at gage 5 using an autosampler. A listing of the samples collected using the autosampler is provided in the autosampler maintenance log (table III.A-7).

fn: 1mlog

Date MO/DA/YR	Time	Gage Depth (ft)	Gage Velocity (ft)	Meas.Depth @ Probe (ft)	Meas.Depth to Bottom (ft)	Power Voltage (V)	Notes
01-29-91	12:30 pm	2.16		2.17			1,3
02-22-91	3:30 pm						3,22
03-03-91	1:00 pm	2.22	0.06	2.25			3
03-20-91	3:05 pm	2.27	0.12	2.25			18
04-12-91	3:00 pm	2.22		2.17			3,4
04-15-91	3:55 pm	2.22	0.02	2.21			2
04-22-91	3:25 pm						23
04-28-91	12:25 pm	2.38		2.29			2,3
05-08-91	3:00 pm	2.46		2.33	2.46		
05-20-91	3:00 am	1.49	0.00	1.33	2.06		2,24
05-24-91	1:20 pm	1.47	0.00	1.38	2.04		2,3,9,10
05-28-91	1:30 pm	2.22	0.00	1.46	2.13		2,25(8.5")
06-07-91	1:25 pm	1.41	0.00	1.35	2.02		2,3,33
06-20-91		1.46	0.00	1.38	2.04		
07-10-91	1:40 pm	1.41	0.00	1.35	2.08		3
07-16-91	1:00 pm	1.41	0.00	1.33	2.08		2
07-26-91	2:30 pm	1.41	0.00	1.33	2.02		
08-01-91	3:05 pm	1.41	0.00	1.33	2.00	11.6	
08-13-91	3:00 am	1.41	0.00	1.38	2.02	12.0	1
08-20-91	10:40 am	1.95	0.12	1.92	2.52	12.1	2
08-22-91	9:30 am	1.46	0.41	1.33	2.02	12.1	2,3,26,27
08-28-91	10:30 am	1.35	0.00	1.33	2.08	11.9	3,27
09-10-91	2:15 pm	1.35	0.00	1.27	2.00	11.5	22
09-21-91	9:35 am	1.51	0.00	1.42	2.08	11.5	2
09-27-91	2:15 pm	2.16	0.47	2.13	2.79	11.5	3
10-04-91	2:45 pm	1.19	0.06	1.17	1.81	11.5	
10-11-91	2:30 pm	1.41	0.00	1.35	2.05	11.5	
10-25-91	2:20 pm	1.41	0.00	1.35	2.05		3
11-02-91	9:50 am	1.62	0.12	1.58	2.27	11.5	2
11-08-91	2:05 pm	1.51	0.08	1.44	2.16	11.6	3,4
11-22-91	4:05 pm	1.79	0.08	1.71	2.38	12.4	1,3
11-29-91	12:40 pm	1.68	0.18	1.58	2.26	12.2	
12-06-91	4:00 pm	1.68	0.10	1.63	2.31	11.5	22
12-21-91	9:55 am	1.57	0.04	1.52	2.22		2,3
01-15-92	11:45 am	7.25	0.08	1.63	2.33	11.4	2,3,7
01-31-92	2:20 pm	1.51				11.3	3
02-22-92	2:00 pm	1.48	0.04	1.44	2.15	11.4	2
03-07-92	12:45 pm	1.62	0.20	1.54	2.21	11.4	3
03-20-92	3:35 pm	1.51	0.22	1.48	2.19	11.4	3,28
03-29-92	3:20 pm	1.73	0.35	1.67	2.35	11.4	2
04-08-92	2:40 pm	1.54	0.08	1.50	2.15	12.3	3,29
04-18-92	1:35 pm	1.62	0.08	1.58	2.29	11.9	2
05-01-92	3:50 pm	1.51	0.04	1.46	2.17	11.4	3
05-05-92	2:20 pm	1.62	0.20	1.58	2.25	12.3	1
05-20-92	12:45 pm	1.46	0.00	1.42	2.10	11.4	
05-22-92	9:25 am	1.46	0.00	1.35	2.06	12.1	1,2
06-04-92	12:45 pm	1.57	0.00	1.42	2.13	11.5	3
06-04-92	2:10 pm					12.6	1
06-11-92	3:20 pm	1.60	0.02	1.44	2.13	12.4	1,2
06-19-92	1:00 pm	1.46	0.00	1.35	2.02	12.1	
06-25-92	12:40 pm	1.57	0.00	1.48	2.13	12.0	2
07-02-92	3:25 pm	1.46	0.00	1.38	2.00	12.6	3
07-14-92	11:25 am	1.46	0.00	1.33	2.02	12.1	
07-23-92	3:40 pm	1.43	0.00	1.33	2.01	12.3	1,2
07-30-92	10:25 am	1.51	0.00	1.44	2.10	12.0	3

Table III.A-1: Streamgage Maintenance Log, Wedge Pond Station (Gage #1)

Date MO/DA/YR	Time	Gage Depth (ft)	Gage Velocity (ft)	Meas.Depth @ Probe (ft)	Meas.Depth to Bottom (ft)	Power Voltage (V)	Notes
08-06-92	10:15 am	1.46	0.00	1.38	2.01	12.3	1
08-13-92	1:30 pm	1.46	0.00	1.38	2.05	12.0	2
08-21-92	12:30 pm	1.62	0.16	1.50	2.16	12.4	1
08-31-92	10:50 pm	1.46	0.00	1.35	2.02	12.3	1,3
09-08-92	3:30 pm	1.51	0.00	1.42	2.17	12.1	
09-18-92	3:30 pm	1.46	0.00	1.33	2.04	12.5	1
09-27-92	1:50 pm	1.62	0.00	1.50	2.19	12.1	2
10-02-92	3:05 pm	1.57	0.00	1.40	2.07	12.2	1,3
10-09-92	3:05 pm	1.51	0.00	1.38	2.05	12.4	1
10-12-92	1:25 pm	1.79	0.04	1.69	2.35	12.1	2
10-23-92	4:00 pm	1.62	0.00	1.42	2.10	12.1	1
10-30-92	12:00 pm	1.57	0.00	1.46	2.13	11.7	3
11-01-92	1:45 pm	1.53	0.00	1.42	2.10	12.2	1,2
11-06-92	2:50 pm	1.79	0.16	1.67	2.33	12.1	
11-13-92	2:55 pm	1.79	0.04	1.65	2.31	12.1	1
11-20-92	3:15 pm	1.35	0.04	1.29	2.00	12.8	1,3,9,10
12-02-92	12:05 pm	1.51	0.20	1.40	2.10	12.3	3
12-04-92	3:25 pm	1.62	0.23	1.50	2.22	12.5	1
12-16-92	3:50 pm	1.62	0.55	1.54	2.23	12.1	
12-17-92	2:30 pm	1.79	0.31	1.71	2.40	12.1	2
12-23-92	1:00 pm	1.79	0.51	1.71	2.43	12.3	1
01-06-93	1:25 pm			1.77	2.51		8
01-08-93	11:15 am	1.68	0.47			12.7	1,3
01-15-93	1:45 pm	1.79	0.27	1.46	2.15	12.2	7
01-24-93	1:45 pm	1.57	0.20	1.46	2.19	11.9	3
01-25-93	11:15 am	1.57	0.16	1.50	2.21	12.6	1,2
02-05-93	3:30 pm	1.41	0.08	1.35	2.06	12.3	
07-02-93	3:25 pm						16

Table III.A-1: (continued)

fn: 2mlog

Date MO/DA/YR	Time	Gage Depth (ft)	Gage Velocity (ft)	Meas.Depth @ Probe (ft)	Meas.Depth to Bottom (ft)	Battery Voltage (V)	Notes
01-29-91	3:30 pm	0.81	0.55	0.84			1,3,11
02-22-91	2:15 pm			1.00			2,6
03-03-91	3:00 pm	1.14	0.43	1.17			1,5
03-20-91	4:55 pm	1.03	0.25	1.00			6
03-29-91	11:15 am	1.03	0.51	1.00			2,6
04-06-91	2:00 pm	0.92	0.55	0.92			1,6
04-15-91	12:15 pm	0.76	0.48	0.75			2,6
04-22-91	4:15 pm						12
04-28-91	2:00 pm	1.08	0.12	1.04			3,13
05-08-91	4:00 pm	1.17	0.51	1.08	1.08		
05-24-91	11:30 am						9,10,11
05-30-91	12:45 pm	0.65	0.04	0.67	0.71		2
06-07-91	9:30 am	0.49	0.23	0.50			2
06-20-91	10:10 am	0.51	0.67	0.54	0.63		1,2,3,11
07-10-91	3:30 pm	0.32	0.10	0.29	0.27		3,11
07-16-91	9:45 am	0.32	0.31	0.33	0.38		2,11
07-26-91	10:00 am	0.27	0.16	0.25	0.29		1,2
08-01-91	11:15 am	0.27	0.23	0.25	0.29	12.0	
08-13-91	10:15 am	0.32	0.29	0.25	0.33	11.7	2,3
08-21-91	9:30 am	2.06	0.63	2.13	2.17	12.7	1,2,3,9,10
08-28-91	12:00 pm	0.49	0.00	0.50	0.58	12.3	3
09-10-91	4:00 pm	0.43	0.00	0.46	0.50	11.9	
09-21-91	2:25 pm	0.65	0.00	0.71	0.75	11.6	2
09-27-91	4:15 pm	1.73	0.39	1.75	1.92	12.4	14,19
10-04-91	5:00 pm	0.65	0.18	0.63	0.79	12.3	
10-11-91	3:45 pm	0.60	0.00	0.60	0.75	12.1	
10-25-91	4:00 pm	0.60	0.00	0.58	0.71	11.8	
11-02-91	1:05 pm	1.14	0.55	1.19	1.29	11.5	2
11-08-91	5:00 pm	0.65	0.66	0.71	0.79	12.0	1,3,4,6
11-22-91	2:35 pm	1.73	0.66	1.79	1.88	11.9	3,6,19
11-29-91	9:50 am	0.97	0.55	1.04		11.5	3,9,10
12-06-91	2:35 pm	1.14	0.50	1.29	1.21	12.6	1
12-17-91	10:35 am	0.97	0.43	1.00	1.08		2,7
12-21-91	2:15 pm	1.03	0.39	1.10	1.19	12.1	3
01-15-92	8:30 am	1.35	0.47	1.38	1.42	12.1	1,2,3
01-31-92	12:00 pm	0.81	0.43	0.81	0.85	13.2	1,3
02-07-92	2:45 pm	0.65	0.43	0.71	0.71	12.9	1
02-22-92	9:00 am	0.81	0.35	0.85	0.88	12.0	2
03-07-92	10:00 am	0.81	0.43	0.79	0.79	12.5	1,35
03-20-92	2:00 pm	0.92	0.35	0.96	0.96	12.2	1,3,19
03-29-92	3:00 pm	1.41	0.45	1.42	1.46	12.0	1,2,3
04-08-92	12:20 pm	0.87	0.35	0.92	0.92	12.2	1,3,4
04-18-92	8:30 am	1.41	0.47	1.44	1.48	11.9	2
05-05-92	1:00 pm	1.03	0.47	1.04	1.08	11.9	3,5,14
05-20-92	3:00 pm	0.70	0.63	0.67	0.67	11.7	3,6
05-22-92	3:00 pm	0.70	0.55	0.67	0.67	11.7	2,3
06-04-92	11:00 am	0.70	0.74	0.71	0.75	12.2	1,3,5
06-11-92	10:00 am	0.70	0.98	0.71	0.79	11.7	2
06-19-92	3:00 pm	0.49	0.63	0.48	0.56	12.2	1
06-25-92	9:30 am	0.92	0.59	0.92	1.00	12.0	
07-02-92	10:00 am	0.43	0.31	0.42	0.50	11.3	3
07-14-92	9:45 am	0.49	0.16	0.42	0.44	12.4	1,15
07-23-92	9:00 am	0.43	0.02	0.40	0.42	12.0	2
07-30-92	2:35 pm	0.49	0.35	0.50	0.54	12.4	1,3,16

Table III.A-2: Streamgage Maintenance Log, Route 128 Station (Gage #2)

Date MO/DA/YR	Time	Gage Depth (ft)	Gage Velocity (ft)	Meas.Depth @ Probe (ft)	Meas.Depth to Bottom (ft)	Battery Voltage (V)	Notes
08-06-92	1:15 pm	0.40	0.04	0.38	0.46	12.1	
08-13-92	9:00 am	0.49	0.46	0.46	0.50	12.1	1,2
08-21-92	10:00 am	0.65	0.78	0.63	0.67	13.4	1,5
08-31-92	1:35 pm	0.38	0.16	0.42	0.46	12.1	1,3
09-08-92	10:00 am	0.43	0.2	0.44	0.50	12.3	1
09-18-92	1:45 pm	0.38	0.04	0.46	0.40	11.9	
09-22-92	12:45 pm						1
09-27-92	9:10 am	0.87	0.70	0.92	0.96	12.1	2
10-02-92	1:50 pm	0.38	0.12	0.42	0.46	12.0	3
10-09-92	1:45 pm	0.32	0.04	0.40	0.44	12.3	5
10-12-92	8:45 am	1.35	0.43	1.44	1.50	12.2	2,6
10-23-92	1:45 pm	0.43	0.08	0.46	0.50		1,3,9
10-30-92	10:30 am	0.43	0.35	0.50	0.52	12.3	4,10
11-01-92	8:45 am	0.38	0.31	0.46	0.50	12.2	2
11-06-92	1:45 pm	0.70	0.74	0.77	0.79	12.0	
11-13-92	1:50 pm	0.65	0.66	0.71	0.77	12.3	1
11-20-92	1:35 pm	0.43	0.04	0.50	0.54	12.1	
12-02-92	10:45 am	0.65	0.74	0.69	0.73	12.5	1,3,19
12-04-92	1:35 pm	0.92	0.70	0.96	1.04	12.3	
12-16-92	2:00 pm	1.14	0.47	1.19	1.29	12.0	19
12-17-92	9:30 am	1.35	0.55	1.42	1.50		2
12-23-92	10:30 am	1.14	0.59	1.21	1.25	12.4	3
01-06-93	10:30 am	1.57	0.58	1.67	1.75	12.1	
01-15-93	2:30 pm	2.49	0.51	0.90	0.98	12.3	1,7
01-24-93	11:45 am	1.14	0.47	1.21	1.25	12.6	1,3
01-25-93	9:00 am	1.30	0.45	1.33	1.42	12.5	2
02-05-93	1:45 pm	0.65	0.55	0.67	0.79	12.1	

Table III.A-2: (continued)

fn: 3mlog

Date MO/DA/YR	Time	Gage Depth (ft)	Gage Velocity (ft)	Meas.Depth @ Probe (ft)	Meas.Depth to Bottom (ft)	Battery Voltage (V)	Notes
01-29-91	11:30 am	0.92	0.55	0.92			1,10
02-22-91	12:45 pm						2,14,17,19
03-03-91	12:30 pm	1.41	0.70	1.38			9,10
03-20-91	2:30 pm	1.41	0.47	1.42			11,14,18,19
03-28-91	1:55 pm	1.47	0.43	1.46			19
03-29-91	2:20 pm	1.36	0.43	1.38			2
04-06-91	12:35 pm	1.20	0.23	1.23			1,3,19
04-15-91	10:20 am	1.09	0.27	1.10			2,4,19
04-22-91	3:15 pm						12
04-28-91	10:25 am	1.44	0.39	1.42			1,2,9,10
05-08-91	3:30 pm	1.49	0.35	1.50	1.60		
05-20-91	11:00 am	1.17	0.23	1.15			2
05-24-91	10:20 am	1.06	0.18	1.08	1.15		2
05-28-91	11:15 am	1.44	0.33	1.46	1.54		1,2
05-30-91	9:45 pm	1.14	0.16	1.13	1.21		2,3,33(from 0.5")
06-07-91	2:35 pm	0.87	0.09	1.04	1.13		2
06-20-91	12:30 pm						9
07-10-91	12:30 pm	0.92	0.04	0.92	0.96		10
07-16-91	4:00 pm	1.03	0.08	1.00	1.04		2
07-26-91	4:15 pm	0.92	0.00	0.88	0.96	12.2	2
08-01-91	10:00 am	0.97	0.06	0.94	1.00	12.0	
08-13-91	4:00 pm	0.97	0.04	0.92	1.00	11.7	2
08-20-91	3:30 pm	2.92	0.82				2
08-21-91							3,8
08-22-91	2:45 pm	1.84	0.63	1.83	2.00	12.8	1,2
09-10-91	3:30 pm	1.08	0.00	1.04	1.04	12.3	
09-21-91	12:55 pm	1.35	0.45	1.38	1.46	12.0	2
09-27-91	3:40 pm	2.27	1.02	2.33	2.46	11.9	6
10-04-91	4:45 pm	1.19	0.37	1.17	1.21	11.8	
10-11-91	3:15 pm	1.14	0.27	1.11	1.17	12.8	1
10-25-91	3:45 pm	1.14	0.31	1.13	1.17	12.4	
11-02-91	11:45 am	1.68	0.94	1.75	1.83	12.2	2
11-08-91	4:05 pm	1.14	0.39	1.17	1.25	12.0	
11-22-91	3:05 pm	2.32	0.84	2.25	2.33	11.7	
11-29-91	11:20 am	1.41	0.20	1.44	1.54	12.8	1,3
12-06-91	3:05 pm	1.51	0.65	1.56	1.71	12.3	
12-21-91	12:45 pm	1.30	0.56	1.33	1.58	12.8	1,2
01-15-92	9:30 am	1.68	0.35	1.75	1.83	12.6	1,2,3
01-31-92	1:15 pm	1.24	0.43	1.29		13.0	3
02-07-92	3:25 pm	1.08	0.43	1.13	1.21	12.8	1
02-22-92	10:30 am	1.19	0.31	1.27	1.38	12.4	2,5
03-07-92	11:00 am	1.35	0.43	1.42	1.54	13.0	1,3
03-20-92	2:40 pm	1.30	0.35	1.42	1.35	12.7	1,3
03-29-92	9:10 am	1.84	0.59	1.92	2.00	12.4	2
04-08-92	1:20 pm	1.30	0.43	1.33	1.42	12.6	3,4
04-18-92	10:20 am	1.79	0.70	1.88	1.98	12.3	2
05-05-92	1:35 pm	1.51	0.42	1.54	1.58	12.6	1,3
05-20-92	2:30 pm	1.24	0.23	1.17	1.25	11.6	
05-22-92	1:35 pm	1.19	0.23	1.15	1.21	12.5	1,15
06-04-92	1:25 pm	1.35	0.31	1.29	1.44	12.2	3
06-11-92	11:30 am	1.35	0.43	1.29	1.42	12.1	2,6
06-19-92	2:30 pm	1.14	0.23	1.08	1.23	12.4	1
06-25-92	10:05 am	1.62	0.70	1.60	1.77	12.1	
07-02-92	10:55 am	0.92	0.23	0.96	1.19	13.4	1,3,5,15

Table III.A-3: Streamgage Maintenance Log, Montvale Station (Gage #3)

Date MO/DA/YR	Time	Gage Depth (ft)	Gage Velocity (ft)	Meas.Depth @ Probe (ft)	Meas.Depth to Bottom (ft)	Battery Voltage (V)	Notes
07-14-92	10:25 am	0.92	0.23	0.98	1.17	12.3	
07-23-92	10:45 am	0.92	0.20	0.96	1.13	12.0	2
07-30-92	1:15 pm	1.14	0.27	1.13	1.33	12.4	1,3,16
08-06-92	11:50 am	0.92	0.16	0.96	1.13	12.0	16
08-13-92	10:20 am	1.03	0.25	1.04	1.17	12.6	1,2
08-21-92	11:00 am	1.19	0.31	1.21	1.33	12.9	1,15
08-31-92	1:00 pm	0.97	0.2	0.96	1.13	12.3	3
09-08-92	10:45 am	1.08	0.27	1.04	1.21	12.4	1
09-18-92	2:10 pm	0.97	0.12	0.96	1.10	12.1	
09-27-92	10:30 am	1.57	0.59	1.67	1.83	12.8	1,2
10-02-92	2:10 pm	0.97	0.16	1.02	1.19	12.6	3
10-09-92	2:20 pm	0.92	0.12	0.96	1.15	12.4	14
10-12-92	10:05 am	1.68	0.7	1.77	1.96	12.3	2
10-23-92	3:00 pm	1.19	0.08	1.17	1.25	12.7	1,14,20
10-30-92	11:00 am	1.24	0.1	1.21	1.33	12.4	3
11-01-92	9:55 am	1.14	0.10	1.17	1.25	12.3	2
11-06-92	2:10 pm	1.46	0.39	1.46	1.54	12.3	
11-13-92	2:15 pm	1.68	0.47	1.67	1.75	12.2	
11-20-92	2:00 pm	1.19	0.12	1.21	1.25	12.9	1
12-02-92	11:15 am	1.30	0.27	1.31	1.42	12.1	3,6
12-04-92	2:30 pm	1.68	0.27	1.71	1.83	12.5	1,14,21
12-16-92	2:45 pm	1.84	0.59	1.92	2.04	12.2	14
12-17-92	10:50 am	2.11	0.55	2.17	2.33	12.2	2
12-23-92	11:15 am	1.84	0.66	1.96	2.04	12	3
01-06-93	11:45 am	2.22	1.00	2.38	2.46	12.9	1
01-15-93	2:10 pm	2.33	0.47	1.63	1.71	12.5	7
01-24-93	12:35 pm	1.84	0.55	1.92	2.00	12.3	3
01-25-93	9:45 am	1.95	0.59	2.00	2.13	12.2	2
02-05-93	2:15 pm	4.00	0.35	1.40	1.50	12	7
07-02-93	12:30 pm						16

Table III.A-3: (continued)

fn: 4mlog

Date MO/DA/YR	Time	Gage Depth (ft)	Gage Velocity (ft/s)	Meas.Depth @ Probe (ft)	Meas.Depth to Bottom (ft)	Power Voltage (V)	Notes
01-29-91	1:30 pm	0.70	0.82	0.69			3,6
03-03-91	2:30 pm	0.81	0.70	0.77			3,6
03-20-91	4:20 pm	0.76	0.78	0.75			30
03-29-91	4:00 pm	0.70	0.90	0.75			3,20,30
04-03-91							20,31
05-20-91	2:00 pm						32,30
05-24-91	4:10 pm	0.92	0.16	0.96	1.21		2,3,10,29
05-28-91	2:15 pm	1.44	0.23	1.17,1.42	1.46		2,25(3")
06-07-91	11:30 pm	0.87	0.16	0.88	1.13		2,3,33
06-20-91							23
07-10-91	2:05 pm	0.22	0.43	0.19	0.35		1
07-16-91	11:20 pm	0.16	0.59	0.17	0.46		2,14
07-26-91	1:00 pm	0.16	0.59	0.17	0.42		1,2
08-01-91	2:25 pm	0.22	0.39	0.25	0.42	11.9	3
08-13-91	12:35 pm	0.22	0.55	0.25	0.42	12.3	1,2,3
08-20-91	1:00 pm	0.70	1.62	0.79	0.96	11.7	2
08-22-91	11:00 am	0.92	0.63	0.83	1.08	11.8	2,6
08-28-91	11:15 am	0.54	0.20	0.56	0.83	12.7	1,3
09-10-91	3:00 pm	0.38	0.59	0.38	0.58	12.1	20,14,30
09-21-91	11:00 am	0.43	0.94	0.46	0.67	11.9	2
09-27-91	2:55 pm	1.95	0.43	1.96	2.08	11.7	6,34
10-04-91	3:45 pm	1.03	0.16	1.00	1.19	12.4	1
10-11-91	2:50 pm	0.81	0.27	0.81	0.92	12.1	
10-25-91	3:00 pm						3,31
11-08-91	3:15 pm	0.49	0.70	0.54	0.79	12.4	1,10
11-22-91	3:35 pm	0.70	1.66	0.79	0.96	12.1	3,6
11-29-91	11:30 pm						31
01-31-92	1:55 pm	0.60	3.64	0.63	0.83	12.3	10
02-07-92	3:50 pm	0.43	3.56	0.48	0.625	12.2	
02-22-92	12:30 pm	0.54	1.09	0.63	0.75	12.2	1,2
03-07-92	12:20 pm	0.70	1.60	0.75	0.88		1,3
03-20-92	3:15 pm	0.65	1.09	0.69	0.79	12.4	1,3
03-29-92	1:40 pm	1.03	0.16	1.02	1.10	12.3	2
04-08-92	1:45 pm	0.70	1.02	0.69	0.79	12.4	1,3
04-18-92	11:35 am	1.41	0.39	1.35	1.44	12.1	2
05-01-92	3:30 pm	1.30	0.31	1.27	1.38	12.2	1,3
05-20-92	1:45 pm	0.97	0.23	0.92	1.04	12.3	1
05-22-92	11:05 am	0.97	0.20	0.96	1.04	12.2	2
06-04-92	12:05 pm	1.68	0.08	1.60	1.73	12.0	3
06-11-92	1:45 pm	1.68	0.08	1.63	1.75	11.8	2
06-19-92	1:25 pm	1.24	0.08	1.23	1.35	11.7	
06-25-92	10:35 am	1.30	0.27	1.25	1.33	12.4	1,2
07-02-92	2:55 pm	1.08	0.08	1.08	1.17	11.9	3
07-14-92	10:55 am	1.35	0.04	1.29	1.35	12.1	1
07-23-92	1:00 pm	1.19	0.04	1.17	1.25	12.2	1,2
07-30-92	11:05 am	1.19	0.16	1.13	1.23	12.1	3,16
08-06-92	10:50 am	1.08	0.08	1.04	1.15	12.6	1
08-13-92	11:45 am	1.24	0.08	1.17	1.27	12.3	2
08-21-92	12:00 pm	1.79	0.08	1.73	1.83	12.0	
08-31-92	11:55 am	1.24	0.08	1.21	1.29	12.2	1,3
09-08-92	11:40 am	1.35	0.12	1.27	1.38	12.0	
09-18-92	2:40 pm	1.08	0.08	1.08	1.17	12.3	1
09-27-92	12:05 pm	1.57	0.16	1.52	1.63	11.9	2
10-02-92	2:45 pm	1.46	0.04	1.44	1.54	12.4	1,3
10-09-92	2:45 pm	1.41	0.00	1.33	1.42	12.2	

Table III.A-4: Streamgage Maintenance Log, Horn Pond Station (Gage #4)

Date MO/DA/YR	Time	Gage Depth (ft)	Gage Velocity (ft/s)	Meas.Depth @ Probe (ft)	Meas.Depth to Bottom (ft)	Power Voltage (V)	Notes
10-12-92	11:30 am	1.79	0.12	1.75	1.83	12.1	2
10-23-92	3:30 pm	1.08	0.04	1.04	1.15	11.9	
10-30-92	11:30 am	1.08	0.04	0.98	1.08	12.6	1,3
11-01-92	11:40 am	1.03	0.04	0.94	1.04	12.3	2
11-06-92	2:30 pm	1.14	0.08	1.08	1.19	12.2	
11-13-92	2:30 pm	0.70	0.66	0.67	0.79	12.2	1
11-20-92	2:20 pm	0.43	1.52	0.38	0.48	12.0	
12-02-92	11:40 am	0.70	0.66	0.67	0.77	12.1	1,3
12-04-92	3:05 pm	0.87	0.35	0.88	0.96	11.8	6
12-09-92	1:40 pm					12.7	1,23
12-16-92	3:15 pm	1.19	0.35	1.13	1.21	12.2	
12-18-92	12:00 pm	1.68	0.90	1.63	1.71	12.1	2
12-23-92	12:00 pm	1.30	0.43	1.25	1.33	12.4	1,3
01-06-93	12:45 pm	1.14	0.60	1.08	1.17	12.3	1
01-24-93	1:15 pm	0.65	1.41	0.63	0.75	12.1	1,3
01-25-93	10:45 am	0.76	1.49	0.75	0.83	11.9	2
02-05-93	2:55 pm	0.49	1.96	0.42	0.50	12.2	1
02-18-93	3:45 pm	3.46	0.55	0.98	1.08	12.1	7
02-26-93	2:40 pm	2.65	1.52	0.5	0.625	11.9	1,7
03-19-93	4:05 pm	3.52	0.55	1.0625	1.125	12.6	1,7

Table III.A-4: (continued)

Notes Index:

1 - Changed Battery (Battery Voltage Shown is New Battery Voltage)
2 - Calibrated Gage
3 - Downloaded Data
4 - Reset Time (due to hour time change)
5 - Removed Sediment which Plugged Probe Air Line
6 - Removed Debris Which Accumulated in Front of Probe
7 - Erroneously High Gage Depth Readings Due to Water Frozen in Air Line
8 - Battery Dead, Could Not Change
9 - Removed Gage Due to Malfunction
10 - Redeployed Gage
11 - Unburied Probe from Sediment
12 - Could not access gage, Water Too Deep
13 - Removed Tree Which Fell in Front of Culvert
14 - Repositioned Probe
15 - Changed Battery Band
16 - Surveyed Vertical Control
17 - Gage Malfunctioning
18 - Cleaned Probe
19 - Removed Debris from Gage Lines
20 - Gage Vandalized
21 - Changed Air Tubing
22 - Reconnected Power Supply
23 - Could not Communicate with Gage
24 - Put Probe on Cinder Block
25 - Probe Height Set to Non-Zero Value
26 - Reverse Flow Direction
27 - Oriented Probe in Flow Direction
28 - Power Line Disconnected, Reconnected Power
29 - Power Supply not Working, Installed Battery
30 - Power Supply line vandalized
31 - Removed gage due to aggressive vandalism
32 - Vault installed
33 - Probe Height Set to zero
34 - Mapped-out River Bottom
35 - Corrected Gage Date due to Leap Year

Table III.A-5: Streamgage Maintenance Logs, Notes Index for Tables A.1 through A.4

fn: s5log

Date MO/DA/YR	Time	Nephelometer Calibration 2 ntu	Nephelometer Calibration 5 ntu	Maintenance Notes
10-25-91	2:15 pm			Measured Gage House Dimensions & Vicinity to River
11-02-91	8:30 am			Measured Weir Dimensions
11-22-91	5:00 pm			Measured Gage House Dimensions & Vicinity to River
01-15-92	1:00 pm			Installed Preliminary Equipment, Max/Min Thermometer
01-30-92	9:35 am			Installed Heater, and Other Preliminary Equipment
02-07-92				Checked Heater Operation, Max/Min Thermometer
02-22-92	3:15 pm			Checked Heater Operation, Max/Min Thermometer
03-17-92				Installed Continuous SS Equipment
03-20-92				Primed Diaphragm Pump & Started System
03-26-92	10:00 am			Diaphragm Pump Lost Prime, Re-primed
03-29-92	11:30 am			Downloaded Data
04-08-92	3:00 pm			Checked SS System,Algae growing inside Flow Through Cell
04-17-92	2:30 pm			Downloaded Data, Installed Shelf for Chlorine System
04-18-92	2:35 pm			Downloaded Data, Pump Lost Prime, Re-primed
04-30-92				Pump Broken, Took System back to Lab
05-20-92	12:15 pm			Maintained Data Logger & Battery
06-04-92	12:40 pm			Dropped-off Old Pump at Gage House
06-18-92		1		Re-installed SS System
06-19-92	10:00 am			Connected Chlorination System
06-19-92	4:00 pm			Checked System
06-22-92	12:00 pm			Routine Maintenance, Downloaded Data
06-25-92	1:45 pm			Routine Maintenance, Downloaded Data
06-29-92	5:30 pm			Checked System
07-02-92	3:45 pm			Routine Maintenance, Downloaded Data
07-14-92	12:30 pm			Routine Maintenance
07-16-92	7:15 am			Routine Maintenance
07-20-92	7:00 am			Pump Broken
07-21-92	4:00 pm			Repaired Pump, Routine Maintenance
07-22-92	7:10 pm			Pump Broken, Repaired in Field
07-23-92	2:30 pm			Downloaded Data
07-26-92	11:45 am			Checked System
07-28-92	1:00 pm			Pump System not Working, Could not Finish Repair
07-28-92	5:45 pm	0.9		Could not finish pump Repair
07-30-92	9:55 am			Installed Battery Operated Peristaltic Pump
07-30-92	4:15 pm			Battery-Powered Peristaltic Pump Inoperative
08-06-92	9:45 am			Pump Broken
08-22-92	6:45 pm			Installed New AC Powered Peristaltic Pump
08-23-92	1:25 pm			Nephelometer not Operating Properly, Took it back to Lab
08-28-92	7:15 am			Re-installed Nephelometer
08-28-92	6:45 pm	1.8		Re-initiated System
08-29-92	4:30 pm			Checked System,Downloaded Data
08-30-92	1:45 pm			Checked System
08-31-92	9:45 am	1.3	4.6	Routine Maintenance, Downloaded Data
09-03-92				Checked System
09-08-92	1:00 pm	1.9	4.5	Routine Maintenance, Downloaded Data
09-11-92	8:15 am			Checked System
09-15-92	7:00 am	0.30	4.20	Routine Maintenance, Downloaded Data
09-18-92	3:50 pm			Checked System
09-22-92	9:30 am	1.2	4.2	Routine Maintenance, Downloaded Data
09-27-92	3:00 pm			Checked System, Downloaded Data
10-01-92	7:00 am	1.3	3.3	Routine Maintenance, Downloaded Data
10-02-92	3:35 pm			Checked System
10-09-92	3:30 pm	0.5	1.8	Routine Maintenance, Downloaded data
10-12-92	2:30 pm			Checked System
10-15-92	12:25 pm	0.7	2	Routine Maintenance, Downloaded Data
10-22-92	5:20 pm	0.6	1.5	Routine Maintenance, Downloaded Data
10-23-92	4:15 pm			Checked System
10-30-92	12:30 pm	0.5	1.5	Routine Maintenance, Downloaded Data, Change Time due to Time Change

Table III.A-6: Nephelometer System Maintenance Log

Date MO/DA/YR	Time	Nephelometer Calibration 2 ntu	5 ntu	Maintenance Notes
11-01-92	3:05 pm			Checked System
11-03-92	8:15 am			Checked System
11-06-92	3:05 pm			Checked System
11-07-92	10:40 am	0.5	1.5	Routine Maintenance, Downloaded Data
11-13-92	3:15 pm			Checked System
11-15-92	9:55 am	0.4	1.3	Routine Maintenance, Downloaded Data
11-20-92	3:45 pm			Checked System
11-23-92	6:30 am			Downloaded Data
11-24-92	6:30 am			Downloaded Data
11-27-92	8:15 am	0.5	1	Routine Maintenance, Downloaded Data
12-02-92	12:30 pm	0.5	1.9	Routine Maintenance, Downloaded Data
12-04-92	3:40 pm			Checked System
12-09-92	12:00 pm	0.6	1.9	Routine Maintenance, Downloaded Data
12-11-92	7:00 pm			Checked System
12-14-92	11:30 am			Downloaded Data
12-16-92	4:00 pm	0.6	1.8	Routine Maintenance
12-17-92	12:30 pm			Checked System
12-23-92	1:30 pm	0.9	2	Routine Maintenance, Downloaded Data
01-05-92	2:45 pm	0.7	3.1	Routine Maintenance, Downloaded Data
				Condensation noted on equipment
01-06-93	1:30 pm	0.6	2.5	Inlet Line Plugged, Unplugged by back-flushing
				Routine Maintenance
01-08-93	1:00 pm			Checked System
01-15-93	1:15 pm	0.6	2.4	Routine Maintenance, Downloaded Data
01-25-93				Checked System
01-24-93	2:00 pm	0.9	2.4	Routine Maintenance, Downloaded Data
02-04-93	1:15 pm	0.6	2.3	Routine Maintenance, Downloaded Data
				Lines Plugged (Frozen?), could not unplug
02-15-93	4:30 pm	0.5	2.2	Routine Maintenance, Downloaded Data
				Lines Plugged (Frozen?), could not unplug
03-02-93	6:30 am	0.5	2.1	Routine Maintenance, Downloaded Data
				Lines Plugged (Frozen?), could not unplug
03-07-93	11:15 am			Downloaded Data
03-20-93	10:00 am	0.4	3.7	Lines Plugged (Frozen?), could not unplug
				Downloaded Data
03-21-93				Could not unplug lines, Line Blockage Suspect
03-28-93				Could Not Retrieve Inlet Nozzle Holder from River Channel
				Current too Strong
05-04-93	9:15 am	0.4	1.6	Unplugged inlet, Routine Maintenance
05-07-93	6:40 pm			Checked System
				Reset Time due to Time Change
05-15-93	11:30 am	0.3	1	Routine Maintenance, Downloaded Data
05-25-93	8:00 am	0.6	1.5	Routine Maintenance, Downloaded Data
06-07-93	6:05 pm	0.6		Routine Maintenance, Downloaded Data
				Inlet Line Plugged Upon Arrival, Unplugged Line
06-15-93	6:00 pm	0.6	1.4	Routine Maintenance, Downloaded Data
06-24-93	6:15 pm	0.6	1.4	Routine Maintenance, Downloaded Data
06-30-93	6:30 pm	0.6	1.1	Routine Maintenance, Downloaded Data
07-02-93				Checked System
07-11-93	6:30 pm	0.8	1.3	Routine Maintenance
				Note: Power Failure 19:12 July 8 to 5:06 July 9
				00:14 July 10 to 03:55 July 10
07-13-93	8:00 pm			Routine Maintenance, Downloaded Data
07-18-93	6:15 pm	0.8	1.6	Routine Maintenance
07-27-93	6:30 am			Routine Maintenance, Downloaded Data
08-03-93	6:45 pm	0.8	1.3	Water not Circulating upon Arrival,Routine Maintenance
08-04-93	6:00 pm			Checked System
08-13-93	7:45 pm	0.5	1.4	Routine Maintenance, Downloaded Data

Table III.A-6: (continued)

Date MO/DA/YR	Time	Nephelometer Calibration		Maintenance Notes
		2 ntu	5 ntu	
08-20-93	7:30 am	0.8	1.3	Nephelometer Bulb Burnt-out, Re-installed Spare
				Routine Maintenance
08-21-93	9:50 am			Downloaded Data
08-25-93	12:30 pm	0.6	1.7	Routine Maintenance, Downloaded Data
09-08-93	6:25 am	0.5	1.7	Water not Circulating upon Arrival,Left Lines Backflushing
09-09-93	6:40 am	0.6	1.8	Started Water Circulation, Routine Maintenance
09-15-93	6:40 am	0.7	1.6	Routine Maintenance, Downloaded Data
09-21-93	6:30 am	0.4	1.9	Water not Circulating upon Arrival, Routine Maintenance
09-24-93	6:45 pm	0.6	1.9	Routine Maintenance, Downloaded Data
09-29-93	3:15 pm	0.4	1.9	Routine Maintenance, Downloaded Data
10-06-93	9:15 am			Water not Circulating upon Arrival,Downloaded Data
				Removed Equipment from Gage House
				Removed Sample Lines in River
				Left Buried lines from Gage House to River's Edge
				Left Nozzle Holder in River

Table III.A-6: (continued)

fn: s5log

Date MO/DA/YR	Time	Notes
06-18-92		Installed Autosampler in Gage House
06-19-92	10:00 am	Connected Liquid Level Sensor to Autosampler
06-25-92	1:45 pm	Checked Sampler: No Samples Taken
06-29-92	5:30 pm	Checked Sampler: No Samples Taken
07-14-92	12:30 pm	Checked Sampler: No Samples Taken
07-16-92	7:15 am	Checked Sampler: No Samples Taken
07-20-92	7:00 am	Checked Sampler: No Samples Taken
07-21-92	4:00 pm	Checked Sampler: No Samples Taken
07-22-92	7:10 pm	Checked Sampler: No Samples Taken
07-23-92	2:30 pm	Checked Sampler: No Samples Taken
07-26-92	11:45 am	Checked Sampler: No Samples Taken
07-28-92	1:00 pm	Checked Sampler: No Samples Taken
07-30-92	9:55 am	Samples Taken: Bottle #1, 21:57 July 29
		Bottle #2, 22:57 July 29
08-02-92	8:30 am	Checked Sampler: No Samples Taken
08-06-92	9:45 am	Checked Sampler: No Samples Taken
08-10-92	7:10 am	Checked Sampler: No Samples Taken
		Set Sampler to Begin Taking Hourly Samples
08-12-92	7:00 am	Samples Taken: Bottle #3, 8:00 August 10
		Bottle #4, 9:00 August 10
		Bottle #5, 10:00 August 10
		Bottle #6, 11:00 August 10
		Bottle #7, 12:00 August 10
		Bottle #8, 13:00 August 10
		Bottle #9, 14:00 August 10
		Bottle #10, 15:00 August 10
		Bottle #11, 16:00 August 10
		Bottle #12, 17:00 August 10
		Bottle #13, 18:00 August 10
		Bottle #14, 19:00 August 10
		Bottle #15, 20:00 August 10
		Bottle #16, 21:00 August 10
		Bottle #17, 22:00 August 10
		Bottle #18, 23:00 August 10
		Bottle #19, 0:00 August 10
		Bottle #20, 1:00 August 10
		Bottle #21, 2:00 August 10
		Bottle #22, 3:00 August 10
		Bottle #23, 4:00 August 10
		Bottle #24, 5:00 August 10
08-13-92	2:30 pm	Installed Bottles #1a to# 24a
08-17-92	7:30 am	Checked Sampler: No Samples Taken
08-19-92	7:30 am	Samples Taken: Bottle #1a, 1:08 August 18
		Bottle #2a, 2:08 August 18
		Bottle #3a, 3:08 August 18
		Bottle #4a, 4:08 August 18
		Bottle #5a, 5:08 August 18
		Bottle #6a, 6:08 August 18
		Bottle #7a, 7:08 August 18
		Bottle #8a, 8:08 August 18
		Bottle #9a, 9:08 August 18
		Bottle #10a, 10:08 August 18
		Bottle #11a, 11:08 August 18
		Bottle #12a, 12:08 August 18
		Bottle #13a, 13:08 August 18
		Bottle #14a, 14:08 August 18
		Bottle #15a, 15:08 August 18

Table III.A-7: Autosampler Maintenance Log

Date MO/DA/YR	Time	Notes
08-19-92 (con'd)		Bottle #16a, 16:08 August 18 Bottle #17a, 17:08 August 18 Bottle #18a, 18:08 August 18 Bottle #19a, 19:08 August 18 Bottle #20a, 20:08 August 18 Bottle #21a, 21:08 August 18 Bottle #22a, 22:08 August 18 Bottle #23a, 23:08 August 18 Bottle #24a, 0:08 August 19
08-28-92	7:15 am	Installed Bottles #1 to #24 Changed Pump Tubing & Recalibrated Sample Volume
08-29-92	4:30 pm	Checked Sampler; No Samples Taken
08-31-92	9:45 am	Checked Sampler; No Samples Taken
09-03-92		Checked Sampler; No Samples Taken
09-08-92	1:00 pm	Checked Sampler; No Samples Taken
09-11-92	8:15 am	Checked Sampler; No Samples Taken
09-15-92	7:00 am	Checked Sampler; No Samples Taken
09-18-92	3:50 pm	Checked Sampler; No Samples Taken
09-22-92	9:30 am	Checked Sampler; No Samples Taken
09-27-92	3:00 pm	Checked Sampler; No Samples Taken
10-01-92	7:00 am	Checked Sampler; No Samples Taken
10-02-92	3:35 pm	Checked Sampler; No Samples Taken
10-09-92	3:30 pm	Sample Taken: Bottle #22, due to well maintenance by USGS Sample Disregarded
10-12-92	2:30 pm	Checked Sampler; Re-initialized Sampling Program Sampler reported attempts to take samples, but no samples taken
10-15-92	12:25 pm	Checked Sampler; No Samples Taken
10-22-92	5:20 pm	Checked Sampler; No Samples Taken Installed Bottle #22
10-30-92	12:30 pm	Checked Sampler; No Samples Taken Reset clock due to time change
11-01-92	3:05 pm	Checked Sampler; No Samples Taken
11-03-92	8:15 am	Checked Sampler; No Samples Taken Lowered Liquid Level Sensor, to Initiate Sampler
11-04-92	6:45 am	Samples Taken: Bottles #1 to #22 at hourly intervals starting at 8:36 November 3 These Samples were later disregarded
11-07-92	10:40 am	Installed Bottles 1a to 24a
11-13-92	3:15 pm	Checked Sampler; No Samples Taken
11-15-92	9:55 am	Checked Sampler; No Samples Taken
11-20-93	3:45 pm	Checked Sampler; No Samples Taken
11-23-92	6:30 am	Samples Taken: Bottle #1a, 4:47 November 23 Bottle #2a Missed due to Power Failure Re-initiated Program to start @ 6:47 Bottle #3a, 6:47 November 23
11-24-93	6:30 am	Samples Taken: Bottle #4a, 7:47 November 23 Bottles #5a to #24a missed, Program error Sample (Bottle #5a)Manual Mode,6:38 Nov 24
11-25-92	6:40am	Checked Sampler; No Samples Taken Hooked-up Sampler to a Surge Supressor
11-27-92	8:15 am	Checked Sampler; No Samples Taken
12-02-92	12:30 pm	Checked Sampler; No Samples Taken
12-04-92	3:40 pm	Checked Sampler; No Samples Taken
12-09-92	12:00 pm	Checked Sampler; No Samples Taken
12-11-92	7:00 pm	Checked Sampler; No Samples Taken Lowered Liquid Level Sensor to Initiate Sampler
12-12-92	8:00 am	Could not make it to gage house, Too much snow

Table III.A-7: (continued)

Date MO/DA/YR	Time	Notes
12-14-92	11:30 am	Samples Taken: Bottle #1, 18:48 December 11
		Bottle #2, 19:48 December 11
		Bottle #3, 20:48 December 11
		Bottle #4, 21:48 December 11
		Bottle #5, 22:48 December 11
		Bottle #6, 23:48 December 11
		Bottle #7, 0:48 December 12
		Bottle #8, 1:48 December 12
		Bottle #9, 2:48 December 12
		Bottle #10, 3:48 December 12
		Bottle #11, 4:48 December 12
		Bottle #12, 5:48 December 12
		Bottle #13, 6:48 December 12
		Bottle #14, 7:48 December 12
		Bottle #15, 8:48 December 12
		Bottle #16, 9:48 December 12
		Bottle #17, Missed, Power Failure
		Bottle #18, Missed, Power Failure
		Bottle #19, Missed, Power Failure
		Bottle #20, Missed, Power Failure
		Bottle #21, Missed, Power Failure
		Bottle #22, 15:52 December 12
		Bottle #23, 16:48 December 12
		Bottle #24, 17:48 December 12
12-16-92	4:00 pm	Changed Pump Tubing
		Turned-off Autosampler due to below Freezing Conditions
03-20-93	10:00 am	Put Bottles #1 to #24 in Autosampler
03-21-93		Turned Sampler on, Flushed lines
		Calibrated Sample Volume, Liquid Level Sensor Inoperative
03-23-93	12:15 P	Installed New Liquid Level Sensor
		Old Sensor Repaired at Lab
03-26-93	6:15 am	Checked Sampler: No Samples Taken
03-28-93		Samples Taken: Bottle #1, 14:23 March 26
		Bottle #2, 15:23 March 26
		Bottle #3, 16:23 March 26
		Bottle #4, 17:23 March 26
		Bottle #5, 18:23 March 26
		Bottle #6, 19:23 March 26
		Bottle #7, 20:23 March 26
		Increased Liquid Level Sensor Elevation
03-30-93	7:45 am	Samples Taken: Bottle #8, 9:41 March 29
		Bottle #9, 10:41 March 29
		Bottle #10, 11:41 March 29
		Bottle #11, 12:41 March 29
		Bottle #12, 13:41 March 29
		Bottle #13, 14:41 March 29
		Bottle #14, 15:41 March 29
		Bottle #15, 16:41 March 29
		Bottle #16, 17:41 March 29
		Bottle #17, 18:41 March 29
		Bottle #18, 19:41 March 29
		Bottle #19, 20:41 March 29
		Bottle #20, 21:41 March 29
		Bottle #21, 22:41 March 29
		Bottle #22, 23:41 March 29
		Bottle #23, 0:41 March 30
		Bottle #24, 1:41 March 30
		Took Sample, Manual Mode, Bottle #2a, 8:00 March 30
		Reloaded Autosampler with bottles, #1a & #3a to #24a
		(Bottle #1a in position 2)
		Set Sampler Start Time for 0:00 April 1

Table III.A-7: (continued)

Date MO/DA/YR	Time	Notes
03-31-93	6:50 pm	Took Sample #4B in Manual Mode, 18:45 March 31
04-02-93	6:15 pm	Samples Taken: Bottle #1a, 16:16 April 1
		Bottle #3a, 17:15 April 1
		Bottle #4a, 18:15 April 1
		Bottle #5a, 19:15 April 1
		Bottle #6a, 20:15 April 1
		Bottle #7a, 21:15 April 1
		Bottle #8a, 22:15 April 1
		Bottle #9a, 23:15 April 1
		Bottle #10a, 0:15 April 2
		Took Sample, Manual Mode, Bottle #2N, 18:15 April 2
		Turned-off Autosampler
05-04-93	9:15 am	Turned-on Autosampler
		Put in Bottles #1a to #10a, Calibrated Sample Volume
05-25-93	8:00 am	Checked Sampler: No Samples Taken
06-07-93	6:05 pm	Checked Sampler: No Samples Taken
06-15-93	6:00 pm	Checked Sampler: No Samples Taken
06-24-93	6:15 pm	Checked Sampler: No Samples Taken
06-30-93	6:30 pm	Checked Sampler: No Samples Taken
07-11-93	6:30 pm	Checked Sampler: No Samples Taken
		Re-initiated Sampler Program due to Power Failure
10-06-93	9:15 am	Removed Auto Sampler From Gage House

Table III.A-7: (continued)

fn: s1log

Date	Time	Field Filtration		Lab Filtration		Water Velocity (cm/s)		Notes
MO/DA/YR		Filter Samples	Dissolved Samples	Grab Samples	Pumped Samples	Nozzle Inlet	River Water	
04-15-91	3:55pm	X(0.5)						Sample Disregarded
05-20-91	3:00pm			X(1.5)	X(1.5)			
05-24-91	1:20pm			X(1.5)				
05-28-91	1:30pm				X(1.5)			
06-07-91	1:25pm			X(1.5)				
07-16-91	1:00 pm	X(0.5)			X(1.5)			
08-20-91	10:40am	X(0.5)			X(1.5)	4.7	9.5	
08-22-91	9:30 am	X(0.5)			X(1.5)	16.6	16	Reverse Flow
09-21-91	9:35am	X(0.5)			X(1.5)		1	
11-02-91	10:20am	X(0.5)			X(1.5)	5.5	7.5	
12-21-91	11:00am	X(0.5)			X(1.5)		5	
01-15-92	11:45am			X(1.5)				Below Freezing
02-22-92	2:00pm	X(0.5)	X(0.5)		X(1.5)	4.7	4	
03-29-92	3:20pm	X(0.5)	X(0.5)		X(1.5,0.2)	15.5	8	
04-18-92	1:35pm	X(0.5)	X(0.5)		X(1.5)	5.0	9.5	
05-22-92	9:25am	X(0.5)	X(0.5)		X(1.5)	3.3	0.3	
06-11-92	3:20pm	X(0.5)	X(0.5)		X(1.5,0.2)		6	
07-23-92	3:40pm	X(0.5)	X(0.5)		X(1.5)		1.2	
08-13-92	1:30pm	X(0.5)	X(0.5)		X(1.5)	4.7	1	
09-27-92	1:50pm	X(0.5)	X(0.5)		X(1.5,0.2)	4.7	3	0.2 filter analyzed by neutron activation
10-12-92	1:25pm	X(0.5)	X(0.5)		X(1.5)	4.4	7	
11-01-92	1:45pm	X(0.5)	X(0.5)		X(1.5)	4.7	0.5	
12-17-92	2:30pm	X(0.5)	X(0.5)		X(1.5)		12	
01-25-93	11:15am			X(0.5,1.5)				Below Freezing Dissolved (0.5) in lab

Table III.A-8: Sample Retrieval Log, Wedge Pond Station (Gage #1)

fn: s2log

Date	Time	Field Filtration		Lab Filtration		Water Velocity (cm/s)		Notes
MO/DA/YR		Filter Samples	Dissolved Samples	Grab Samples	Pumped Samples	Nozzle Inlet	River Water	
02-21-91	12:45 pm				X(1.5)			Samples Disregarded
03-29-91	11:15 am				X(1.5)			Samples Disregarded
04-15-91	12:15 pm	X(0.5)			X(1.5)			Samples Disregarded
05-30-91	12:45 pm				X(1.5)			Bottom Sediment Sampled
06-07-91	9:30 am			X(1.5)				
06-20-91	10:10 am	X(0.5)			X(1.5)			
07-16-91	9:45 am	X(0.5)			X(1.5)			
07-26-91	10:00 am	X(0.5)			X(1.5)			
08-13-91	10:15 am	X(0.5)			X(1.5)	4.4	5	
08-21-91	9:30 am	X(0.5)			X(1.5)	21.0	23	
09-21-91	2:25 pm	X(0.5)			X(1.5)	18.8	10	
11-02-91	1:05 pm	X(0.5)			X(1.5)	24.4	25	
12-17-91	10:35 am			X(1.5)			20	Below Freezing
01-15-92	8:30 am			X(1.5)			25	Below Freezing
01-31-92								Bottom Sediment Sampled
02-22-92	9:00 am	X(0.5)	X(0.5)	X(0.5)	X(1.5)	5.0	20	
03-29-92	3:05 pm	X(0.5)	X(0.5)		X(1.5,0.2)		25	0.2 filter analyzed by neutron activation
04-18-92	8:30 am	X(0.5)	X(0.5)		X(1.5)	22.1	23	
05-22-92	3:00 pm	X(0.5)	X(0.5)		X(1.5)	5.5	15	
06-11-92	10:00 am	X(0.5)	X(0.5)		X(1.5,0.2)	5.5	30	
07-23-92	9:00 am	X(0.5)	X(0.5)		X(1.5)	5.5	9	
08-13-92	9:00 am	X(0.5)	X(0.5)		X(1.5)	5.5	15	
09-27-92	9:10 am	X(0.5)	X(0.5)		X(1.5,0.2)	23.2	30	
10-12-92	8:45 am	X(0.5)	X(0.5)		X(1.5)	22.1	25	
11-01-92	8:45 am	X(0.5)	X(0.5)		X(1.5)	5.3	10	
12-17-92	9:30 am	X(0.5)	X(0.5)		X(1.5)		25	
01-25-93	9:00 am			X(0.5,1.5)				Below Freezing Dissolved (0.5) in lab
05-25-93	9:15 am			X(0.5)				Dissolved (0.5) in lab

Table III.A-9: Sample Retrieval Log, Route 128 Station (Gage #2)

fn: s3log

Date	Time	Field Filtration		Lab Filtration		Water Velocity (cm/s)		Notes
MO/DA/YR		Filter Samples	Dissolved Samples	Grab Samples	Pumped Samples	Nozzle Inlet	River Water	
02-21-91	12:45 pm				X(1.5)			Samples Disregarded
03-29-91	2:20 pm				X(1.5)			Samples Disregarded
04-06-91	12:35 pm			X(1.5)				Samples Disregarded
04-15-91	10:20 am	X(0.5)			X(1.5)			Samples Disregarded
05-20-91	11:00 am			X(1.5)				
05-24-91	10:20 am			X(1.5)				
05-28-91	11:15 am				X(1.5)			
05-30-91	9:45 am				X(1.5)			Bottom Sediement Sampled
06-07-91	2:35 pm			X(1.5)				
07-16-91	4:00 pm	X(0.5)			X(1.5)			
07-26-91	4:15 pm	X(0.5)			X(1.5)			
08-13-91	4:00 pm	X(0.5)			X(1.5)	4.7	6	
08-20-91	3:30 pm	X(0.5)			X(1.5)	18.8	60	
08-22-91	2:45 pm	X(0.5)			X(1.5)	16.6	24	
09-21-91	12:55 pm	X(0.5)			X(1.5)	12.2	22	
11-02-91	12:25 pm	X(0.5)		X,(0.5)	X(1.5)	21.0	21	
12-21-91	1:20 pm	X(0.5)			X(1.5)		19	
01-15-92	9:30 am			X(1.5)				Below Freezing
01-31-92								Bottom Sediment Sampled
02-22-92	10:30 am	X(0.5)	X(0.5)		X(1.5)	4.4	2	
03-29-92	9:10 am	X(0.5)	X(0.5)		X(1.5,0.2)	14.4	30	0.2 filter analyzed by neutron activation
04-18-92	10:20 am	X(0.5)	X(0.5)		X(1.5)	21.0	22	
05-22-92	1:35 pm	X(0.5)	X(0.5)		X(1.5)	4.4	14	
06-11-92	11:30 am	X(0.5)	X(0.5)		X(1.5,0.2)	5.0	1	
07-23-92	10:45 am	X(0.5)	X(0.5)		X(1.5)	4.7	5	
08-13-92	10:20 am	X(0.5)	X(0.5)		X(1.5)	4.4	9	
09-27-92	10:30 am	X(0.5)	X(0.5)		X(1.5,0.2)	16.6	30	
10-12-92	10:05 am	X(0.5)	X(0.5)		X(1.5)	18.8	40	
11-01-92	9:55 am	X(0.5)	X(0.5)		X(1.5)	4.2	12	
12-17-92	10:50 am	X(0.5)	X(0.5)		X(1.5)		40	
01-25-93	9:45 am			X(0.5,1.5)				Below Freezing Dissolved (0.5) in Lab

Table III.A-10: Sample Retrieval Log, Montvale Station (Gage #3)

fn: s4log

Date	Time	Field Filtration		Lab Filtration		Water Velocity (cm/s)		Notes
MO/DA/YR		Filter Samples	Dissolved Samples	Grab Samples	Pumped Samples	Nozzle Inlet	River Water	
05-24-91	4:10pm			X(1.5)				
05-28-91	2:15pm				X(1.5)			
06-07-91	11:30am			X(1.5)				
07-16-91	11:20am	X(0.5)			X(1.5)			
07-26-91	1:00pm	X(0.5)			X(1.5)			
08-13-91	12:35pm	X(0.5)			X(1.5)	3.3	3	
08-20-91	1:00pm			X(0.5,1.5)				
08-22-91	11:00am	X(0.5)			X(1.5)	14.4	26	
09-21-91	11:00am	X(0.5)		X(0.5)	X(1.5)	3.9	14	
02-22-92	12:30pm	X(0.5)	X(0.5)		X(1.5)		15	
03-29-92	1:40pm	X(0.5)	X(0.5)		X(1.5,0.2)		28	0.2 filter analyzed by neutron activation
04-18-92	11:35am	X(0.5)	X(0.5)		X(1.5)	19.9	19	
05-22-92	11:05am	X(0.5)	X(0.5)		X(1.5)	4.4	9	
06-11-92	1:45pm	X(0.5)	X(0.5)		X(1.5,0.2)	4.7	6	
07-23-92	1:00pm	X(0.5)	X(0.5)		X(1.5)	4.4	4	
08-13-92	11:45am	X(0.5)	X(0.5)		X(1.5)	4.7	6	
09-27-92	12:05pm	X(0.5)	X(0.5)		X(1.5,0.2)	4.4	11	
10-12-92	11:30am	X(0.5)	X(0.5)		X(1.5)	4.7	19	
11-01-92	11:40am	X(0.5)	X(0.5)		X(1.5)		5	
12-18-92	12:00pm	X(0.5)	X(0.5)		X(1.5)		53	
01-25-93	10:45am			X(0.5,1.5)				Below Freezing Dissolved (0.5) in lab

Table III.A-11: Sample Retrieval Log, Horn Pond Station (Gage #4)

fn: s5log

Date	Time	Field Filtration		Lab Filtration		Water Velocity (cm/s)		Notes
MO/DA/YR		Filter Samples	Dissolved Samples	Grab Samples	Pumped Samples	Nozzle Inlet	River Water	
05-24-91	3:15pm			X(1.5)				Extra Sample Taken at Footbridge (20 yds downstream of weir)
05-28-91	12:00pm				X(1.5)			
06-07-91	2:10pm			X(1.5)				
06-20-91		X(0.5)			X(1.5)			
07-16-91	2:45pm	X(0.5)			X(1.5)			
07-26-91	3:15pm	X(0.5)			X(1.5)			
08-13-91	2:10pm	X(0.5)			X(1.5)	3.0	9.4	
08-20-91	8:50am	X(0.5)			X(1.5)	22.1	36.5	
08-21-91	1:30pm	X(0.5)			X(1.5)	17.7	27.7	
08-22-91	8:55am	X(0.5)				4.4	10.8	
09-21-91	8:35am	X(0.5)			X(1.5)	4.4	13.8	
11-02-91	8:45am	X(0.5)			X(1.5)	18.8	17.7	
12-21-91	8:45am	X(0.5)			X(1.5)			
01-15-92	1:00am			X(1.5)				Below Freezing
02-22-92	3:15pm	X(0.5)	X(0.5)		X(1.5)	4.7	13.2	
03-29-92	11:30pm	X(0.5)	X(0.5)		X(1.5,0.2)	16.6	20.0	0.2 filter analyzed by neutron activation
04-18-92	2:35pm	X(0.5)	X(0.5)		X(1.5)			
05-22-92	8:15am	X(0.5)	X(0.5)		X(1.5)	2.8	11.1	
06-11-92	5:00pm	X(0.5)	X(0.5)		X(1.5,0.2)			
07-23-92	2:30pm	X(0.5)	X(0.5)		X(1.5)	4.4	9.7	
08-13-92	2:30pm	X(0.5)	X(0.5)		X(1.5)			
09-27-92	3:00pm	X(0.5)	X(0.5)		X(1.5,0.2)	4.7	14.3	
10-12-92	2:30pm	X(0.5)	X(0.5)		X(1.5)			
11-01-92	3:05pm	X(0.5)	X(0.5)		X(1.5)	4.7	10.1	
12-17-92	12:30pm	X(0.5)	X(0.5)		X(1.5)	4.7	25.0	
01-25-93	12:35pm			X(0.5,1.5)				Below Freezing Dissolved (0.5) in lab
05-25-93	8:00am			X(0.5)				Dissolved (0.5) in lab

Table III.A-12: Sample Retrieval Log, USGS Station (Gage #5)
(Additional samples were collected using the autosampler, See Table III.A-7)

APPENDIX III.B

Controls Used in Calibration Measurements

CONTROLS

Vertical, longitudinal, and horizontal controls are needed such that: 1) measurements from different calibrations can be compared, and 2) elevations of the water surface and channel bottom can be determined. Each calibration cross-section had a vertical, horizontal and longitudinal control. (The only exception was gage 4 "in the middle of the bridge" section which lacked a horizontal control) A vertical control is a point of known elevation and is the point from which water surface and section bottom elevations are referenced. During each calibration the distance from the water surface to the vertical control was measured. Assuming a horizontal water surface, channel bottom elevations could then be computed by noting the distance from the water surface to the channel bottom. A horizontal control is a point from which distances along the width of the river (perpendicular to the flow direction) are referenced. The purpose of the horizontal control point was to assure that vertical locations for each calibration were in approximately the same place, allowing for comparisons of channel bottom geometry from different calibrations. The longitudinal control is a reference point which aligns the calibration section along the river's length. For all stations the longitudinal control corresponded to a set distance from the end of a culvert or bridge. Details concerning controls for each station are given below.

WEDGE POND, GAGE 1

Vertical Control

Description: Bottom of seam on the inside wall, 2 feet west from the end of the northeast side of bridge over the Aberjona River at Main Street, Winchester. (See figure III.3-3)

Elevation: 20.40 ft NGVD = 25.87 ft Winchester Datum

Determination of Vertical Control Elevation: Elevation of this vertical control was estimated using the following procedure.

1) The elevation reference is the northwest bonnet nut (elevation 31.33 ft Winchester Datum = 25.86 ft NGVD) of the hydrant located approximately 125 feet south of the bridge on the sidewalk on the east side of Main Street. This elevation was the reference benchmark used for bridge construction as noted on the Winchester Town Hall copy of the proposed construction drawings: Bridge Deck Replacement, Main Street over Wedge Pond (Green International Affiliates, Inc., 1987) Please note that elevations on this plan correspond to a Winchester Datum (Boston Harbor Mean-Low Water) which is 5.47 feet lower than NGVD Datum. (Capone, 1993) Level measurements were made from this reference to the vertical control for an elevation = 20.40 ft NGVD.

An independent measure of the vertical control elevation was used to double check the elevation of the first measurement. The procedure used for this second measurement was as follows:

2) The elevation (20.83 ft, NGVD) of the underside of the support beam at the northeast end of bridge as given by the proposed construction plans (Green International Affiliates, Inc., 1987) was noted. The width of the seam was then subtracted from this elevation for an approximate vertical control elevation of 20.75 ft NGVD.

The difference in the elevation from each method was 0.35 feet. This difference, although large, was not a significant factor in determining streamflow measurements at this station and for determining changes in river bottom contours; for these determinations, only a consistent control point (irregardless of elevation) was required. However, the vertical control point should be re-surveyed prior to using the elevation data presented in this thesis, if the elevation data is to be used for other purposes where errors of several inches are unacceptable.

Longitudinal Control: Two feet west from the northeast side of bridge over the Aberjona River at Main Street.

Horizontal Control: Inside wall, northeast side of bridge over the Aberjona River at Main Street.

ROUTE 128, GAGE 2:

Vertical Control

Two locations were used as the vertical control. The control on the northeast side of the culvert was used when streamflow was flowing over the entire width of the culvert whereas the control on the northwest side of the culvert was used during very low flow conditions when streamflow moved through only the west side of culvert.

Description, (northeast or northwest side): Bottom of the top corner notch on the inside wall, 2 feet south from the end of the northeast (or northwest) side of the Route 128 culvert over the Aberjona River. (See figure III.3-4)

Elevation of Vertical Controls: 51.0 ft NGVD

Determination of Vertical Control Elevation: The elevation of these vertical control points was determined using two methods. The first method was assumed to be the most accurate whereas the second method was used to check the first. The difference in the vertical control elevation computed from each method was 0.03 feet and is assumed to be indicative of the accuracy of this determination.

1) The elevation of the culvert soffit was noted from the proposed construction drawings for widening Route 128 over the Aberjona River. (Utility Engineers, Inc. 1960) The height of the notch (1 foot) in the top corners of the culvert cross-section was subtracted from this elevation to obtain the vertical control elevation of 51.0 ft NGVD.

2) The elevation of the top of the southeast tip of the culvert wingwall was noted (elevation 47.50 ft) from the proposed construction drawings for the culvert at Mishawum Road over the Aberjona River. (H.W. Moore Associates, Inc. 1977) Level measurements were made from this reference to the vertical control points. Elevation from this method was 51.03 ft NGVD.

Longitudinal Control: Two feet south from the end of the north side of the Route 128 culvert over the Aberjona River.

Horizontal Control: Inside Wall on the east side of the Route 128 culvert over the Aberjona River.

MONTVALE, GAGE 3:

Vertical Control

Description: Bottom of seam on the inside wall, 2 feet south from the northwest side of bridge at Montvale Avenue over the Aberjona River, Woburn. (See figure III.3-5)

Elevation of Vertical Control: 40.07 ft NGVD

Determination of Vertical Control Elevation: The elevation of this control point was determined by making level measurements from benchmark: TBM Aberjona River #8. (Debnam, 1993) The description of this benchmark is as follows:

> TBM Aberjona #8: In the southeasterly part of Woburn 1.7 miles southeast of City Hall on the south side of the B&M R.R. (Stoneham Branch). A chiseled square over the Aberjona River.

Comparing the leveled point elevation with the construction drawings: Proposed Montvale Avenue Over the Aberjona River Relocation (Edwards and Kelcey Engineers and Consultants, 1958) The vertical control elevation corresponds to the elevation of the top of the westerly wingwall abutment of the bridge.

Longitudinal Control: 2 feet south from the north end of bridge at Montvale Avenue over the Aberjona River.

Horizontal Control: Inside wall of the west side of the bridge at Montvale Avenue over the Aberjona River.

HORN POND, GAGE 4:

Vertical Control

Description: Top edge on the north side of the southwest cylindrical concrete support foundation for the wooden bridge over the outlet of Fowles Brook into Horn Pond, Woburn. (See figure III.3-6) The bridge is located on a dirt road 0.2 miles west of Woburn Parkway.

Elevation: 43.04 ft NGVD

Determination of Vertical Control Elevation: The elevation of this control point was determined by making level measurements from benchmark: TBM Aberjona River #38. (Debnam, 1993) The description of this benchmark is as follows:

> TBM Aberjona River #38: In the southwestern part of Woburn, on the northwest side of Horn Pond. A chiseled square, on south end of concrete curb of west parapet wall of Woburn Parkway bridge over mouth of Fowles Brook. (Elevation 42.69 ft NGVD).

Longitudinal Control

Two sections were used at this station for calibration purposes. These sections are identified as: 1) "the front of bridge" section, and 2) "the middle of bridge" section. The longitudinal control for "the front of bridge section" was: Zero feet from the wooden support column set in the southwest cylindrical concrete support foundation for the bridge over the outlet of Fowles Brook into Horn Pond. The longitudinal control for "the middle of bridge" section was: Midway between the two cylindrical concrete support foundations on the south side of the bridge over the outlet of Fowles Brook into Horn Pond.

Horizontal Control

Of the two sections used for calibration, only "the front of bridge" section had a horizontal control. The description of the horizontal control for this section is: Outside edge on the north side of the southwest cylindrical concrete support foundation for the bridge over the outlet of Fowles Brook into Horn Pond.

APPENDIX III.C

Streamgage Calibration, Nephelometer Calibration, and Bottom Profile Tables

Streamgage Calibration Tables

Streamgage calibration tables (tables III.C-1 to III.C-4) provide a listing of: 1) date and time of each calibration trip, 2) values of the manually measured (from calibrations) flow, area, and cross-sectional average velocities, 3) gage depth and gage point velocity readings, and 4) the computed flow, area, and cross-sectional average velocities using the gage raw data. Equations used for conversion of gage raw data to gage values of flow, area, and average cross-sectional velocities are given in section III.3.4.

Gage depth and point velocity measurements were read from the streamgage before and after calibration. During most calibrations, readings taken before calibration were not significantly different than readings taken after. In a few situations where the readings were different, the gage values reported were the average of the two measurements.

The calibration measurements for each gage were performed at the same cross-section. The only exception was gage 4 whose calibration measurements were done at one of two sections. The sections for gage 4 calibratations are identified as the sections: 1) in "front of bridge" and, 2) in "the middle of bridge." The section in the "front of bridge" corresponded to the probe location and was used for most of the earlier calibrations. However, due to 1) the difficulty in estimating the bottom configuration at this section due to a rocky bottom, and 2) exposure of rocks above the water surface during low flows, the calibration section was moved to the "middle of bridge" section. In the "middle of bridge" section, calibration measurements were more reliable since the bottom varied in smoother transitions and tended to be submerged along its width during low flows.

Nephelometer Calibration

Calibration measurements comparing nephelometric turbidity units (NTU) and suspended sediment concentrations are provided in table III.C-5 and are plotted in figure III.C-1. NTU measurements were obtained using one of two methods. The first was to note the ntu measurement from the data logger corresponding to the time when a sample was obtained. The second method was to measure the ntu's of a sample aliquot (prior to filtration). All suspended sediment concentrations correspond to samples which were filtered and analyzed for suspended sediment.

Due to the scatter in the data suspended sediment concentration computed from the nephelometer measurements are assumed to be rough estimates. The strength of the nephelometer measurements is in observing relative changes in concentrations over short time scales (days), not in determining the precise value of suspended sediment concentrations.

Bottom Profile Tables

River bottom elevations for each calibration cross-section are given in tables III.C-6 to III.C-9. Each table provides: 1) the date of the elevation determination, and b) elevations of the river bottom at specified locations in the section. Each location is referenced from the horizontal control point, where BE0 corresponds to the elevation 0 feet from the control, BE3 corresponds to the elevation 3 feet from the control etc.. Locations of BE0, BE3, etc.. and average bottom profiles are illustrated in figures III.3-3 to III.3-6.

The large standard deviations of the bottom elevation measurements for gage 4 (table III.C-9) are primarily due to a lack of horizontal control. Without a horizontal control, the horizontal alignment of measurements cannot be assured. Thus, the horizontal locations of measured bottom elevations for gage 4 "middle of the bridge" calibrations, are a rough estimate.

FN: Calib1b

Date mo-da-yr	Time	Manually Measured			Gage Raw Data		Computed from Gage Raw Data		
		Flow (cfs)	Area (ft^2)	Average Velocity (ft/s)	Depth (ft)	Velocity (ft/s)	Flow (cfs)	Area (ft^2)	Average Velocity (ft/s)
04-15-91	3:55 pm	5.0	34.6	0.15	2.25	0.04	9.6	40.4	0.24
05-20-91	3:00 pm	1.3	33.5	0.04	2.20	0.00	1.5	39.5	0.04
05-24-91	1:20 pm	0.0	33.5	0.00	1.46	0.00	1.5	35.8	0.04
05-28-91	1:30 pm	2.7	34.1	0.08	1.44	0.00	1.5	35.5	0.04
06-07-91	1:25 pm	0.9	32.2	0.03	1.41	0.00	1.5	34.9	0.04
07-16-91	1:30 pm	1.3	31.4	0.04	1.41	0.00	1.5	34.9	0.04
08-20-91	10:40 am	12.0	43.1	0.28	1.92	0.12	14.0	45.1	0.31
08-22-91**	10:00 am	10.2	33.6	0.30	1.46	0.41	12.7	35.9	0.35
09-21-91	9:35 am	1.6	36.7	0.04	1.46	0.00	1.5	35.9	0.04
11-02-91	9:50 am	10.2	39.7	0.26	1.65	0.10	11.2	39.7	0.28
12-21-91	9:55 am	6.6	39.1	0.17	1.60	0.06	9.7	38.7	0.25
01-15-92	11:45 am	11.2	38.8	0.29	1.63 *	0.08	10.5	39.3	0.27
02-22-92	2:00 pm	8.9	37.4	0.24	1.50	0.02	7.4	36.7	0.20
03-29-92	3:20 pm	17.4	41.8	0.42	1.73	0.39	15.5	41.3	0.38
04-18-92	1:30 pm	14.0	39.8	0.35	1.62	0.08	10.4	39.1	0.27
05-22-92	9:25 am	1.4	34.0	0.04	1.46	0.00	1.5	35.9	0.04
06-11-92	3:20 pm	7.0	36.8	0.19	1.58	0.04	8.9	38.3	0.23
06-25-92	12:40 pm	2.2	36.3	0.06	1.57	0.00	1.5	38.1	0.04
07-23-92	3:40 pm	1.2	34.5	0.03	1.44	0.00	1.5	35.5	0.04
08-13-92	1:30 pm	0.9	34.4	0.03	1.46	0.00	1.5	35.9	0.04
09-27-92	1:50 pm	5.2	37.1	0.14	1.68	0.00	1.5	40.3	0.04
10-12-92	1:25 pm	13.3	40.5	0.33	1.79	0.04	10.3	42.5	0.24
11-01-92	1:45 pm	1.2	34.9	0.03	1.53	0.00	1.5	37.3	0.04
12-17-92	2:30 pm	17.9	43.2	0.41	1.79	0.37	16.0	42.5	0.38
01-25-93	11:15 am	12.7	40.2	0.32	1.57	0.15	11.4	38.1	0.30

* Gage Depth Reading erroneous, Reported value is the Measured Depth

** Reverse Flow Direction

Table III.C-1: Streamgage Calibration, Wedge Pond Station (Gage #1)

FN: Calib2b

Date mo-da-yr	Time	Manually Measured			Gage Raw Data		Computed from Gage Raw Data		
		Flow (cfs)	Area (ft^2)	Average Velocity (ft/s)	Depth (ft)	Velocity (ft/s)	Flow (cfs)	Area (ft^2)	Average Velocity (ft/s)
03-29-91	11:15 am	9.30	17.4	0.54	1.03	0.51	10.5	21.7	0.48
04-15-91	12:15 pm	4.92	13.2	0.37	0.76	0.48	6.7	16.9	0.39
05-30-91	12:45 pm	5.03	14.9	0.34	0.62	0.51	4.9	14.4	0.34
06-07-91	9:30 am	4.02	13.2	0.30	0.57	0.25	4.4	13.5	0.32
06-20-91	10:10 am	6.58	15.2	0.43	0.52	0.67	3.8	12.6	0.30
06-20-91	10:40 am	6.09	14.1	0.43	0.52	0.67	3.8	12.6	0.30
07-16-91	9:45 am	3.12	11.3	0.28	0.36	0.35	2.3	9.7	0.23
07-26-91*	10:00 am	0.81	7.1	0.11	0.27	0.18	1.5	8.1	0.19
08-13-91*	10:15 am	2.20	9.1	0.24	0.30	0.30	1.8	8.6	0.20
08-21-91	9:30 am	31.02	43.4	0.71	2.03	0.56	29.9	39.7	0.75
09-21-91	2:25 pm	8.17	17.5	0.47	0.65	0.04	5.3	14.9	0.35
11-02-91	1:05 pm	12.72	25.6	0.50	1.14	0.55	12.3	23.7	0.52
12-17-91	10:35 am	8.00	22.6	0.35	0.97	0.45	9.6	20.7	0.47
01-15-92	8:30 am	13.0	28.3	0.46	1.35	0.45	15.9	27.5	0.58
02-22-92	9:00 am	7.2	18.0	0.40	0.81	0.45	7.3	17.8	0.41
03-29-92	3:00 pm	17.6	28.7	0.61	1.38	0.44	16.5	28.0	0.59
04-18-92	9:00 am	13.8	29.2	0.47	1.41	0.45	17.0	28.6	0.60
05-22-92	3:00 pm	4.4	14.3	0.31	0.68	0.55	5.6	15.4	0.37
06-11-92	10:00 am	7.1	16.2	0.44	0.70	0.94	5.9	15.8	0.37
07-23-92*	9:00 am	2.0	8.8	0.22	0.42	0.03	2.8	10.8	0.26
08-13-92*	9:00 am	2.6	9.8	0.26	0.51	0.47	3.7	12.4	0.30
09-27-92	9:10 am	10.4	18.4	0.56	0.87	0.71	8.2	18.9	0.43
10-12-92	8:45 am	16.4	28.1	0.58	1.33	0.49	15.6	27.1	0.57
11-01-92*	8:45 am	2.4	11.2	0.21	0.38	0.29	2.4	10.0	0.24
12-17-92	9:30 am	18.3	29.4	0.62	1.37	0.55	16.3	27.9	0.58
01-25-93	9:00 am	14.6	26.6	0.55	1.30	0.44	15.0	26.6	0.56

* Bottom Exposed

Table III.C-2: Streamgage Calibration, Route 128 Station (Gage #2)

FN: Calib3

Date mo-da-yr	Time	Manually Measured Flow (cfs)	Area (ft^2)	Average Velocity (ft/s)	Gage Raw Data Depth (ft)	Velocity (ft/s)	Computed from Gage Raw Data Flow (cfs)	Area (ft^2)	Average Velocity (ft/s)
03-29-91	2:20 pm	16.1	29.1	0.55	1.36	0.43	11.60	30.7	0.38
04-15-91	10:20 am	8.9	27.8	0.32	1.09	0.27	6.15	24.2	0.25
05-20-91	11:00 am	9.8	24.2	0.41	1.17	0.23	7.52	26.1	0.29
05-24-91	10:20 am	10.0	20.7	0.49	1.06	0.18	5.68	23.5	0.24
05-28-91	11:15 am	17.8	31.1	0.57	1.44	0.33	13.68	32.6	0.42
05-30-91	9:45 am	7.2	23.1	0.31	1.25	0.16	9.09	28.1	0.32
06-07-91	2:35 pm	5.4	21.6	0.25	1.04 *	0.09	5.38	23.0	0.23
07-16-91	3:30 pm	4.2	23.8	0.18	1.07	0.08	5.83	23.7	0.25
07-26-91	4:15 pm	2.1	23.4	0.09	0.92	0.02	3.81	20.1	0.19
07-26-91	6:35 pm	2.3	28.4	0.08	1.11	0.04	6.47	24.7	0.26
08-13-91	4:00 pm	3.1	22.9	0.14	0.95	0.04	4.17	20.9	0.20
08-20-91	3:30 pm	88.0	73.4	1.20	2.87	0.81	105.02	66.8	1.57
08-22-91	2:45 pm	26.1	42.4	0.62	1.83	0.62	27.60	42.0	0.66
09-21-91	12:55 pm	16.6	33.7	0.49	1.35	0.44	11.35	30.5	0.37
11-02-91	11:46 pm	26.3	41.8	0.63	1.68	0.92	21.46	38.4	0.56
12-21-91	12:45 pm	16.5	32.0	0.52	1.33	0.60	10.87	30.0	0.36
01-15-92	9:20 am	31.1	41.6	0.75	1.68	0.27	21.46	38.4	0.56
02-22-92	10:30 am	8.7	28.1	0.31	1.19	0.33	7.90	26.6	0.30
03-29-92	9:10 am	34.8	44.9	0.77	1.84	0.61	28.05	42.2	0.66
04-18-92	10:20 am	31.0	42.6	0.73	1.79	0.68	25.86	41.0	0.63
05-22-92	1:35 pm	8.6	25.5	0.34	1.22	0.22	8.48	27.3	0.31
06-11-92	11:30 am	12.3	29.9	0.41	1.33	0.41	10.87	30.0	0.36
07-23-92	10:45 am	3.9	23.9	0.16	0.92	0.20	3.81	20.1	0.19
08-13-92	10:20 am	6.9	27.0	0.26	1.03	0.26	5.24	22.8	0.23
09-27-92	10:30 am	20.9	37.2	0.56	1.57	0.59	17.60	35.7	0.49
10-12-92	10:05 am	26.7	41.6	0.64	1.69	0.74	21.84	38.6	0.57
11-01-92	9:55 am	4.5	23.5	0.19	1.14	0.09	6.99	25.4	0.27
12-17-92	10:50 am	30.9	51.4	0.60	2.11	0.57	42.06	48.7	0.86
01-25-93	9:45 am	12.0	45.3	0.26	1.95	0.59	33.29	44.9	0.74

* Gage Depth Reading erroneous, Reported value is the Measured Depth

Table III.C-3: Stream gage Calibration, Montvale Station (Gage #3)

FN: Calib4

Date mo-da-yr	Time	Manually Measure Flow (cfs)	Gage Raw Data Depth (ft)	Gage Raw Data Velocity (ft/s)	Computed from Gage Raw D Flow (cfs)
05-24-91	4:10 pm	5.7	0.92	0.16	4.40
05-28-91	2:15 pm	10.5	1.42	0.22	11.84
06-07-91	11:30 am	4.7	0.87	0.16	3.99
07-16-91	11:20 am	1.3	0.18	0.53	0.95
07-16-91	11:20 pm	2.0	0.18	0.63	0.96
07-26-91	1:00 pm	1.2	0.16	0.63	0.78
08-13-91	12:35 pm	1.6	0.25	0.71	1.77
08-20-91	1:00 pm	21.6	0.70	1.62	16.80
08-22-91	11:30 am	9.6	0.90	0.63	12.31
09-21-91	11:00 am	4.5	0.43	0.94	5.30
02-22-92	12:30 pm	7.5	0.56	1.09	8.75
03-29-92	1:40 pm	16.4	1.03	0.13	4.53
04-18-92	11:35 am	15.0	1.41	0.37	17.25
05-22-92	11:05 am	5.1	0.97	0.20	5.77
06-11-92	1:45 pm	6.1	1.68	0.10	8.67
06-25-92	10:35 am	9.7	1.30	0.27	11.91
07-23-92	1:00 pm	2.6	1.19	0.06	3.10
08-13-92	11:45 am	3.2	1.24	0.08	4.25
09-27-92	12:05 pm	9.1	1.57	0.14	9.98
10-12-92	11:30 am	17.9	1.79	0.11	10.41
11-01-92	11:40 am	3.3	1.03	0.04	1.60
12-18-92	12:00 pm	44.1	1.68	0.90	44.21
01-25-93	10:45 am	20.1	0.76	1.49	17.93

Table III.C-4: Streamgage Calibration, Horn Pond Station (Gage #4)

fn: neph

Date MO-DA-YR	Time	SS Concentration 0.5 um (mg/l)	SS Concentration 1.5 um (mg/l)	Nephelometer Reading (NTU)	NOTES
032992	11:40am	4.3	3.6	5.3	Field Filtration
072392	2:45pm	1.75	1.5	3.88	"
092792	3:15pm	4.14	3.6	2.9	"
101292	4:45pm	6.43	6.3	3	"
110192	3:15pm	2.86	2	3.8	"
112392	4:47	42.7		7.34	Autosampler
"	6:47	42.8		9.06	"
"	7:47	48		8.86	"
112492	6:38	17.9		4.01	"
032693	14:00	23.3		7.35	Autosampler
"	15:00	19.2		7.4	"
"	16:00	21.8		8.4	"
"	17:00	21.3		9.65	"
"	18:00	22.6		11.15	"
"	19:00	20.2		10.75	"
"	20:00	15.8		10.1	"
032993	10:00	35.5		7.17	Autosampler
"	11:00	21.1		6.83	"
"	12:00	25.4		6.67	"
"	13:00	34.9		8.1	"
"	14:00	59.1		11.5	"
"	15:00	55.9		11.63	"
"	16:00	70.7		14.07	"
"	17:00	82		14.9	"
"	18:00	81.5		14.6	"
"	19:00	86.4		12.67	"
"	20:00	76.9		12.5	"
"	21:00	73.8		13.17	"
"	22:00	62.2		9.87	"
"	23:00	61.4		11.33	"
033093	0:00	51.3		9.57	"
"	1:00	42.1		8	"
"	2:00	26.4		8.5	"
033093	8:00	18.9		6.2	"
033193	19:00	9.9		2.6	"
040193	16:00	39.9		6.6	"
"	17:00	19.5		8.35	"
"	18:00	29		7.05	"
"	19:00	39		10.45	"
"	20:00	30.8		9.4	"
"	21:00	18.1		6.6	"
"	22:00	15.4		4.65	"
"	23:00	10.5		4.15	"
040293	0:00	13.9		4.15	"
040293	17:00	5.7		2.5	"
052593	9:00	5.2		3.7	Grab Sample

Table III.C-5: Nephelometer Calibration

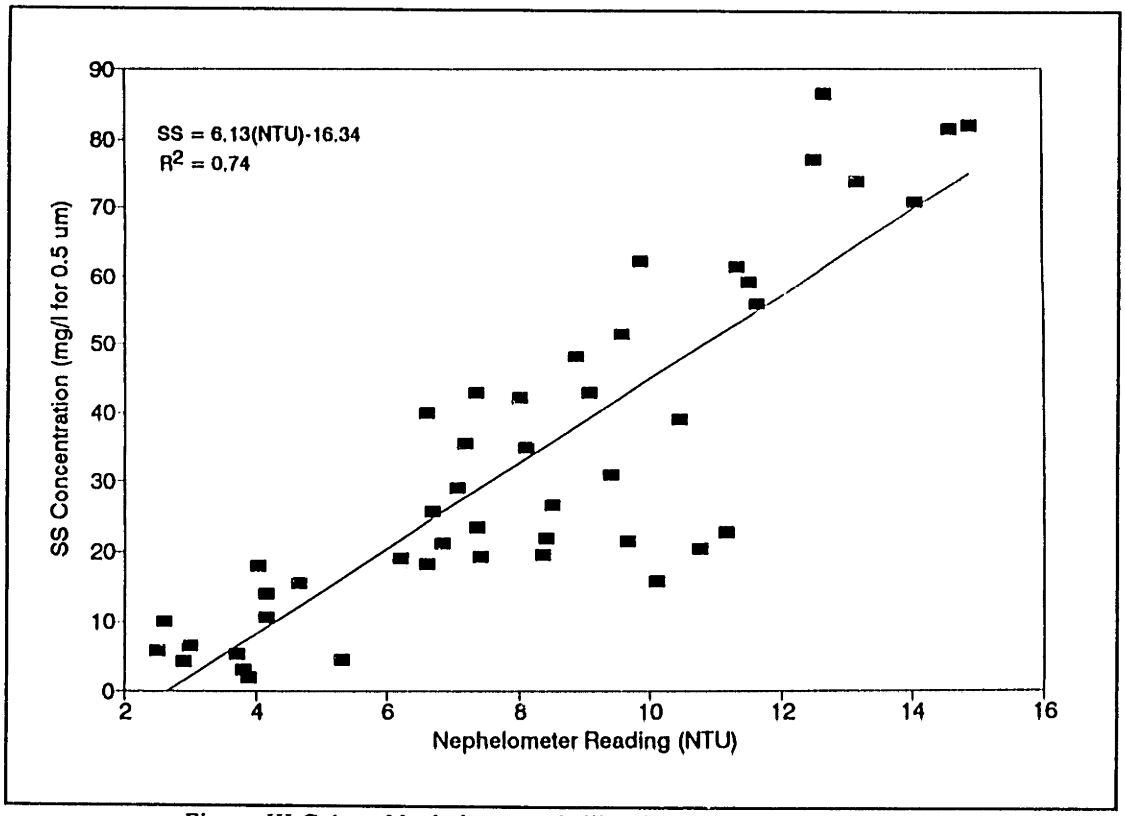

Figure III.C-1: Nephelometer Calibration Curve: USGS Station

Elev. of Vertical Control: 25.87 ft NGVD FN:1btmelv

Date	BE0*	BE3	BE6	BE9	BE12	BE15	BE18	BE20
05-20-91	20.70	20.12	19.62	19.33	19.29	19.41	19.70	20.29
05-24-91	20.66	20.16	19.66	19.37	19.16	19.29	19.54	20.29
05-28-91	20.70	20.29	19.72	19.47	19.33	19.39	19.72	20.37
06-07-91	20.70	20.29	19.70	19.41	19.25	19.33	19.62	20.33
07-16-91	20.66	20.25	19.75	19.54	19.29	19.37	19.70	20.33
08-20-91	20.45	20.33	19.75	19.45	19.20	19.33	19.62	20.37
08-22-91	20.37	20.04	19.41	19.25	19.08	19.16	19.58	20.16
09-21-91	20.20	19.95	19.50	19.37	19.08	19.29	19.50	20.12
11-02-91	20.54	20.08	19.58	19.33	19.12	19.37	19.66	20.29
12-21-91	20.45	20.00	19.54	19.20	19.12	19.29	19.75	20.20
01-15-91	20.29	20.12	19.54	19.25	19.08	19.25	19.45	20.12
02-22-92	20.29	20.00	19.50	19.25	19.04	19.25	19.66	20.16
03-29-92	20.37	20.04	19.58	19.37	19.04	19.37	19.70	20.29
04-18-92	20.33	20.00	19.41	19.20	19.00	19.25	19.58	20.12
05-22-92	20.62	20.29	19.66	19.50	19.25	19.41	19.79	20.37
06-11-92	20.41	20.08	19.50	19.29	18.95	19.29	19.66	20.33
06-25-92	20.62	20.31	19.83	19.58	19.33	19.45	19.66	20.45
07-23-92	20.37	19.91	19.45	19.37	19.04	19.29	19.75	20.16
08-13-92	20.29	19.95	19.50	19.25	19.08	19.33	19.70	20.20
09-27-92	20.29	20.00	19.45	19.20	19.04	19.25	19.58	20.12
10-12-92	20.37	19.87	19.50	19.20	19.12	19.29	19.75	20.20
11-01-92	20.20	19.87	19.37	19.12	19.04	19.20	19.58	20.12
12-17-92	20.29	20.00	19.50	19.25	19.12	19.25	19.62	20.12
01-25-93	20.20	20.04	19.58	19.29	19.04	19.16	19.45	20.29
Average	20.43	20.08	19.57	19.33	19.13	19.30	19.64	20.24
Std Dev	0.17	0.14	0.12	0.12	0.11	0.08	0.09	0.10

* BE0 = Bottom Elevation 0 feet from Horizontal Control Point

Table III.C-6: Bottom Profile, Wedge Pond Station (Gage #1)
All Values are in ft. NGVD

Elev. of Vertical Control: 51.0 ft NGVD FN:2btmelv

Date	BE0*	BE3	BE6	BE9	BE12	BE15	BE16.5	BE18
05-30-91	44.83	45.33	45.67	45.58	45.21	44.46	44.02	43.92
06-07-91	44.83	45.25	45.75	45.54	45.21	44.58	43.96	44.08
06-20-91	44.88	45.50	45.71	45.54	45.21	44.38	43.96	44.00
06-20-91	44.88	45.58	45.75	45.63	45.38	44.67	44.04	44.08
07-16-91	44.83	45.50	45.71	45.46	45.29	44.50	44.00	44.00
07-26-91				45.75	45.50	44.71	44.21	44.04
08-13-91				45.38	45.38	44.38	44.17	44.04
08-21-91	45.00	45.42	45.63	45.33	45.21	44.54	44.08	44.00
09-21-91	44.92	45.38	45.50	45.25	45.25	44.42	44.04	44.04
11-02-91	45.00	45.54	45.63	45.38	45.25	44.67	44.25	44.17
12-17-91	45.00	45.50	45.58	45.29	44.98	44.42	44.13	44.00
01-15-91	45.17	45.63	45.67	45.46	45.25	44.71	44.29	44.17
02-22-92	45.13	45.58	45.63	45.38	45.25	44.63	44.25	44.08
03-29-92	45.04	45.58	45.63	45.33	45.13	44.46	44.29	44.04
04-18-92	45.08	45.58	45.58	45.33	45.25	44.46	44.25	44.08
05-22-92	45.08	45.65	45.65	45.40	45.31	44.56	44.15	44.23
06-11-92	45.04	45.75	45.58	45.42	45.25	44.58	44.17	44.19
07-23-92			45.69	45.40	45.15	44.90	44.19	44.13
08-13-92			45.67	45.38	45.21	44.83	44.17	44.08
09-27-92	45.33	45.83	45.75	45.46	45.08	44.88	44.25	44.13
10-12-92	45.29	45.79	45.71	45.38	45.17	44.71	44.25	44.21
11-01-92			45.38	45.25	45.00	44.54	44.17	44.08
12-17-92	45.42	45.75	45.71	45.29	45.08	44.79	44.08	44.13
01-25-93	45.33	45.67	45.67	45.33	45.08	44.79	44.21	44.08
Average	45.06	45.57	45.65	45.41	45.21	44.61	44.15	44.08
Std Dev	0.18	0.15	0.09	0.12	0.12	0.16	0.10	0.07

*BEO = Bottom Elevation at 0 Feet from Horizontal Control Point

Table III.C-7: Bottom Profile, Route 128 Station (Gage #2)
All Values are in ft. NGVD

Elev. of Vertical Control: 40.1 ft NGVD FN:3btmelv

Date	BE0*	BE3	BE6	BE9	BE12	BE15	BE18	BE21	BE24
04-15-91	30.74	30.53	30.49	30.24	30.45	30.24	30.15	30.49	30.70
04-28-91	30.65	30.55	30.53	30.47	30.28	30.24	30.65	30.78	30.99
05-20-91	31.99	31.82	31.61	31.20	31.20	31.36	31.53	31.53	31.86
05-24-91	31.99	31.78	31.63	31.32	31.22	31.28	31.45	31.45	31.78

Elev. of Vertical Control: 40.1 ft NGVD

Date	BE0*	BE3	BE6	BE9	BE12	BE15	BE18	BE21	BE24
05-28-91	32.57	32.36	32.15	31.70	31.82	31.95	32.03	32.11	32.28
05-30-91	32.49	32.32	32.03	31.65	31.74	31.78	31.90	32.11	32.20
06-07-91	32.49	32.20	32.20	31.82	31.70	31.78	31.78	31.90	32.20
07-16-91	32.40	32.07	31.99	31.74	31.86	31.74	31.82	31.82	32.11
07-26-91	32.32	32.20	32.11	31.82	31.78	31.82	31.65	31.78	32.20
08-13-91	32.32	32.28	32.11	31.82	31.95	31.90	31.74	31.86	32.20
08-22-91	32.20	32.05	32.05	31.74	31.65	31.82	31.74	31.90	32.07
09-21-91	32.28	32.11	31.99	31.61	31.65	31.86	31.70	31.90	32.07
11-02-91	32.28	32.11	32.03	31.70	31.57	31.65	31.78	31.86	32.20
12-21-91	32.28	32.20	32.03	31.74	31.78	31.74	32.15	32.07	32.11
01-15-91	32.20	32.07	32.03	31.61	31.78	31.70	31.82	31.86	32.11
02-22-92	32.24	32.11	31.99	31.78	31.84	31.82	31.86	31.99	32.07
03-29-92	32.24	32.15	31.95	31.61	31.65	31.99	31.8[illegible]	31.86	32.11
04-18-92	32.28	32.20	32.07	31.95	31.65	31.86	31.95	32.11	32.20
05-22-92	32.26	32.20	31.95	31.72	31.84	31.88	31.84	31.92	32.17
06-11-92	31.65	31.57	31.36	31.20	31.11	31.20	31.07	31.15	31.53
07-23-92	32.20	32.07	31.90	31.78	31.65	31.65	31.70	31.70	32.07
08-13-92	32.24	32.07	31.95	31.61	31.61	31.70	31.70	31.78	32.07
09-27-92	32.24	32.28	31.95	31.57	31.74	32.20	31.78	31.86	32.03
10-12-92	32.28	32.24	32.03	31.82	31.70	31.82	31.90	31.99	32.15
11-01-92	32.24	32.07	31.90	31.82	31.90	31.74	31.90	31.90	32.07
12-17-92	32.24	31.99	31.86	31.40	31.53	31.65	31.61	31.90	32.03
01-25-93	32.24	32.20	31.86	31.78	31.70	31.70	31.78	31.95	32.11
Average	32.27	32.13	31.98	31.69	31.70	31.78	31.78	31.88	32.10
Std Dev	0.16	0.15	0.16	0.15	0.16	0.18	0.19	0.19	0.14

BE0 = Bottom Elevation 0 feet from Horizontal Control Point

Table III.C-8: Bottom Profile, Montvale Station (Gage #3)
All Values are in ft. NGVD

Elev. of Vertical Control: 43.0 ft NGVD

Section Upstream of Bridge FN:4btmelv

Date	BE0*	BE3	BE6	BE9	BE12	BE15	BE18	BE21	BE24
05-24-91	41.37	41.00	40.87	40.79	40.71	40.71	40.96	41.29	41.71
05-28-91	41.39	40.98	40.94	40.77	40.69	40.75	40.98	41.35	41.73
06-07-91	41.37	41.21	40.79	40.58	40.79	40.71	41.00	41.37	41.71
07-16-91	41.37	41.17	40.96	40.96	40.87	40.87	41.37	41.37	41.37
08-22-91	41.54	41.17	40.96	40.71	40.87	40.87	41.12	41.12	41.67
Average	41.41	41.10	40.90	40.76	40.79	40.78	41.09	41.30	41.64
Std Dev	0.07	0.10	0.06	0.12	0.08	0.08	0.16	0.09	0.13

Section Upstream of Bridge

Date	BE0*	BE2	BE4	BE6	BE8	BE10	BE12	BE14	BE16	BE18	BE20	BE22	BE24
06-25-92	41.37	41.25	40.92	40.87	41.00	40.75	40.83	41.00	40.79	41.17	41.21	41.42	41.67

Section in Middle of Bridge

Date	BE0*	BE2	BE4	BE6	BE8	BE10	BE12	BE14	BE16	BE18	BE20	BE22	BE24
07-16-91				41.01	40.09	39.67	39.84	40.01	40.38	40.72			
07-26-91					40.20	39.99	39.90	40.15	40.49	40.65			
08-13-91					40.24	39.99	39.99	40.24	40.57	40.74			
08-20-91		41.28	40.74	40.44	40.19	39.94	39.78	40.11	40.69	41.19			
09-21-91				40.88	40.26	39.92	39.92	39.92	40.34	40.61	40.97		
02-22-92				40.97	40.38	39.97	39.97	40.17	40.55	40.55	40.92		
03-29-92			41.48	41.07	40.36	40.27	40.15	40.27	40.61	40.69	41.11		
04-18-92		41.82	41.28	40.90	40.07	39.82	40.03	40.57	40.57	40.95	41.24	42.15	
05-22-92			41.38	40.80	40.76	40.13	40.30	40.46	40.67	40.96	41.55		
06-11-92		41.76	41.26	40.72	40.17	40.26	40.17	40.47	40.76	40.92	41.67		
06-25-92		41.79	41.29	40.79	40.21	40.09	40.25	40.71	40.67	40.92	41.79		
07-23-92		41.77	41.18	40.81	40.18	40.18	40.23	40.39	40.68	40.98	41.48		
08-13-92		41.73	41.19	40.78	40.23	40.23	40.32	40.57	40.73	40.94	41.65		
09-27-92		42.06	41.23	41.06	40.56	40.23	40.23	40.40	40.65	40.73	41.19	41.90	
10-12-92		41.95	41.70	41.08	40.62	40.28	40.12	41.08	40.62	40.70	41.20	41.91	
11-01-92		41.82	41.23	40.82	40.32	40.27	40.27	40.52	40.65	41.02	41.77		
12-18-92		42.05	41.82	41.17	40.55	40.22	40.17	40.30	40.38	40.67	41.01	41.84	
01-25-93				40.59	40.38	40.17	40.17	40.42	40.59	40.92	41.59		
Average		41.80	41.32	40.87	40.32	40.09	40.10	40.38	40.59	40.83	41.37	41.95	
Std Dev		0.21	0.26	0.19	0.18	0.17	0.16	0.26	0.12	0.17	0.30	0.12	

* BE0 = Bottom Elevation 0 feet from Horizontal Control Point

Table III.C-9: Bottom Profile, Horn Pond Station (Gage #4)
All Values are in ft. NGVD

APPENDIX III.D

Discussion Concerning PVDM Methods

- Derivation of PVDM expression for Flow
- Inadequacy of PVDM expressions

DISCUSSION CONCERNING PVDM METHODS

The use of the point velocity discharge measurement (PVDM) technique has been recommended by equipment manufacturers (Marsh-McBirney, 1987; Coastal Leasing, 1988) and by other researchers (Parr et. al., 1981) The PVDM method includes: 1) the measurement of water depth and a point velocity and 2) a mathematical relationship between the measured parameters and streamflow. Calibration results done for the current study indicated that the PVDM mathematical relationship between streamflow and depth/point velocity was *not* the optimum relationship for the monitoring stations. A derivation of the PVDM expressions and a discussion of why they do not adequately describe flow is given below.

DERIVATION OF PVDM EXPRESSIONS FOR FLOW

The PVDM expressions are a set of mathematical relationships which express discharge as a function of depth and point velocity. In the derivation discharge is expressed as:

$$Q = AV \qquad \text{eqn. III.D-1}$$

where:
Q = Discharge
A = Cross-sectional Area of Flow
V = Average cross-section velocity

Given the bottom geometry of the cross-section, A can be computed from the point depth measurement. In order to compute V, the first relationship invoked is Manning's equation. In English units this equation is expressed as:

$$V = \frac{1.49}{n} R^{2/3} S^{1/2} \qquad \text{eqn. III.D-2}$$

where:
R = Hydraulic Radius of Flow, (A/P)
S = Slope of the Energy Grade Line
n = Manning's Roughness Coefficient

R can be computed from the depth measurement given that the cross-sectional geometry is known. The Manning's roughness coefficient, n, can be roughly estimated prior to measurements by noting channel vegetation growth, construction, etc. (Chow, 1959) The PVDM procedure recommends fine-tuning n to obtain a better fit of calibrated versus gage flows.

Given that R can be computed from the depth measurement and n can be estimated and later fine-tuned,

the only parameter left in equation III.D-2 that must be estimated is S. In uniform flow, S is equal to the bottom slope of the channel. However, in non-uniform flow, which is typical of most river systems, S, must be estimated through other means.

The PVDM expression for S (in non-uniform flow) is derived as follows. The first relationship referenced is obtained from a balance of forces. In steady flow, the gravity force (the weight component of water in the channel direction) balances the shear force, (the friction resistance to flow primarily developed along the channel wall). This force balance is given mathematically as:

$$\tau = \rho g R S \qquad \text{eqn. III.D-3}$$

where: τ = Shear Stress = ρu_*^2

u_* = Shear Velocity

ρ = Density of Water

g = Gravitational Acceleration

Solving the above expression for $S^{1/2}$:

$$S^{1/2} = \frac{u_*}{(\rho g R)^{1/2}} \qquad \text{eqn. III.D-4}$$

The second expression invoked is the Prandtl - von Karman Universal Velocity Distribution Law which states that the velocity of flow is a logarithmic function of distance from the bottom boundary. Mathematically this relationship is given as:

$$u_y = \frac{u_*}{K} \ln \frac{y}{y_o} \qquad \text{eqn. III.D-5}$$

where: u_y = Velocity of Flow a Distance y from the Bottom Boundary

K = Empirical (von Karman) Constant

y_o = Integration Constant

The above equation is applicable for flow that is two dimensional with the principal direction of flow in the longitudinal direction. (Schlichting, 1968) From Nikuradse's experiments using circular pipes, an expression for y_o can be obtained which for fully rough turbulent flow can be expressed as:

$$y_o = \frac{k_s}{M} \qquad \text{eqn. III.D-6}$$

where: k_s = Nikuradse's Equivalent Sand Grain Roughness

M = Empirical Constant (30 for circular pipes)

Additionally, comparing the work of Nikuradse with Manning's equation, Hendersen 1966, derived the following expression:

$$k_s = (n/0.031)^6 \qquad \text{eqn. III.D-7}$$

Combining equations III.D-4, III.D-5, III.D-6 and III.D-7 one obtains:

$$S^{1/2} = \frac{u_y K}{(\rho g R)^{1/2} \ln(yM(0.031/n)^6)} \qquad \text{eqn. III.D-8}$$

Substituting equation III.D-8 into III.D-2 one then obtains:

$$V = \frac{1.49 R^{1/6} u_y K}{n \ln(yM(0.031/n)^6)} \qquad \text{eqn. III.D-9}$$

Values for K and M for the PVDM expressions are assumed to be empirically derived fitting parameters for which values must be assumed prior to making calibration measurements. (Parr, 1981; Marsh-McBirney,1987) Recommended values for rectangular channels are given as: (Marsh-McBirney, 1987):

$$K = 1/1.3 = 0.77$$

$$M = 3300$$

Approximating a river channel as a rectangle, the PVDM expression for V is given as:

$$V = \frac{1.49 R^{1/6} u_y (0.77)}{n \ln(y3300(0.031/n)^6)} \qquad \text{eqn. III.D-10}$$

INADEQUACY OF PVDM EXPRESSIONS

The primary drawbacks of the PVDM expressions are associated with whether or not the combination of theoretical expressions (expressions used in the PVDM derivation) are applicable for flow in natural river channels. Specific concerns involve the assumptions: 1) that K and M are known for a natural river section, 2) of logarithmic velocity distribution, and 3) of two-dimensional flow.

Assigning Values to K and M

The von Karman constant, K, is considered a universal constant of turbulent flow which is: 1) independent of boundary roughness and 2) dependent on cross-sectional shape. (Schlichting, 1968) Generally, in the literature there appears to be a consensus for the value of the proportionality constant, K, for circular pipes (K = 0.4, for clear waters) (Schlichting, 1968; Hendersen, 1966; Madsen, 1975) However, in determining the value of K for other section shapes, significantly fewer studies and sometimes contradictory results have been reported. (Schlichting, 1968; Madsen, 1975; Parr, 1981; Marsh-McBirney, 1987)

Similar concerns are associated with the value of M, which can also be considered to vary with cross-section shape. Again, in the literature there appears to be a consensus for the value of M for fully rough turbulent flow in a circular pipes, M=30. (Schlichting, 1968; Madsen, 1975) However, when it comes to other shapes, a range of values have been reported in the literature. (Schlichting, 1968; Madsen, 1975; Parr, 1981; Marsh-McBirney, 1990)

Due to the range of reported values for different cross-section shapes and the difficulty in extrapolating these values to a more complex natural river section, assigning values to K and M for a natural river channel prior to making measurements is over-ambitious at the current state of research. Thus, having to determine K and M values for the section of interest is a significant drawback to the application of the PVDM method to natural river channels.

Logarithmic Velocity Distribution

To investigate the adequacy of the logarithmic velocity distribution for the sections of interest, velocity profiles were measured on two occasions at both Montvale and Route 128 gages. A comparison of the measured distribution with the PVDM distribution (from the gage point velocity reading during the measurement and assuming K=0.77, M=3300, and n=0.027) is given in figures III.D.1 to III.D.4. For profiles at Route 128, the mean value of the PVDM velocity and the measured velocities in the vertical section are within 30% of one another. However, both of the measured profiles are clearly not logarithmic, violating the assumptions used in deriving the PVDM expressions. The peculiar pattern of the measured vertical profiles is due, in part, to upstream obstructions and non two-dimensional flow

conditions. For the Montvale profiles, the correspondence between the mean PVDM velocity and the mean measured velocity in the vertical section are especially poor, where the values differ by a factor of three. In the Montvale case, if one smooths consecutive measured velocity readings, a logarithmic distribution can be fit reasonably well to the data; however, this fit does not correspond to the PVDM predicted distribution. These results clearly indicated that the assumption of a logarithmic velocity distribution defined through predetermined values of K and M was inadequate for the vertical velocity profiles at the sections of interest.

Two Dimensional Flow Assumption

To investigate the assumption of two dimensional flow, cross-sectional velocity distributions at Montvale and Route 128 gages on 4 occasions are illustrated in figures III.D-5 and III.D-6. From these measurements, one clearly can see that flow is: 1) not two-dimensional and, 2) does not necessarily vary in a systematic fashion.

The non-systematic behavior of the velocity distribution can be noted by observing the shift in the location of peak velocity between 9 and 12 feet at the gage 3 station, (figure III.D-6) with no apparent preference to either location for either low or high flow conditions. Another indicator of the non-systematic behavior of the velocity distribution are the changes in the fraction of cross-sectional area dominated by less than 5 cm/s velocities. One would expect that the fraction of area dominated by low flows would systematically decrease as flows get larger. However, this is not the case for Montvale where, as the flow increases, there is no systematic decrease (or increase) in the area dominated by velocities less than 5 cm/s.

The changes in the cross-sectional velocity distribution at gage 2 are especially dramatic (figure III.D-5). At extremely low flows only part of the river bottom is exposed resulting in a concentration of flow in the west side of the culvert. Upon increasing flow, when the entire width of the culvert is contributing to flow, streamflow is concentrated in two areas of the cross-section: in the center and on the west side. At high flows, the velocity tends to be concentrated entirely in the central portion of the channel.

The changes in the velocity distribution at both stations illustrate the complexity of estimating velocity distributions in a natural channel. Such observations clearly indicate that the assumptions of the PVDM analysis method have been violated and illustrate the difficulty in estimating an overall average velocity from a single point velocity measurement.

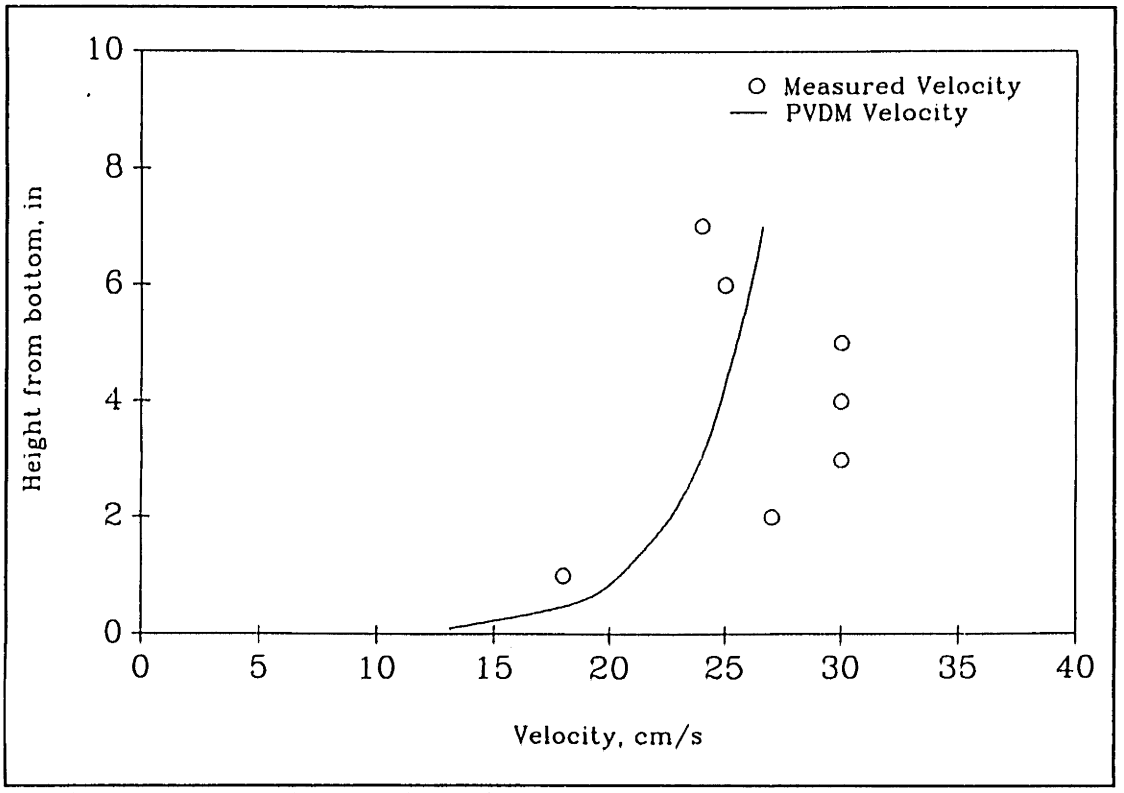

Figure III.D-1: Vertical Velocity Profile at the Probe, Route 128, 7-20-91, Flow=6.6 cfs

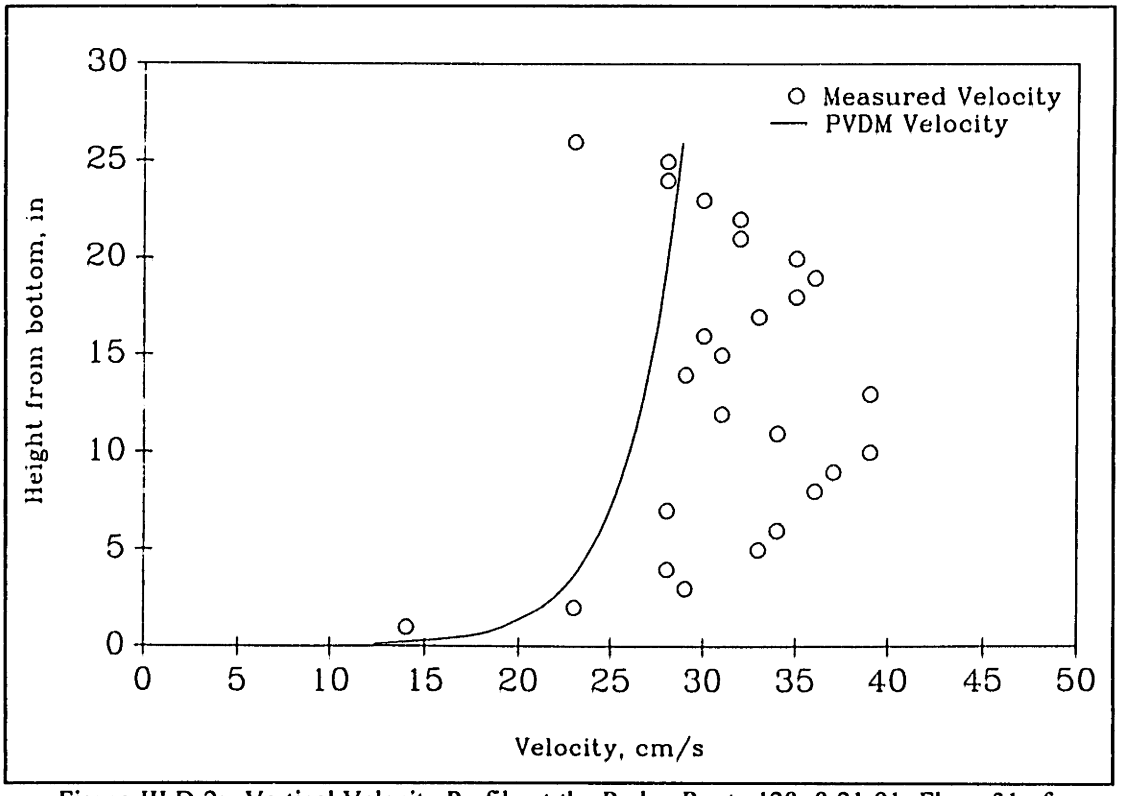

Figure III.D-2: Vertical Velocity Profile at the Probe, Route 128, 8-21-91, Flow=31 cfs

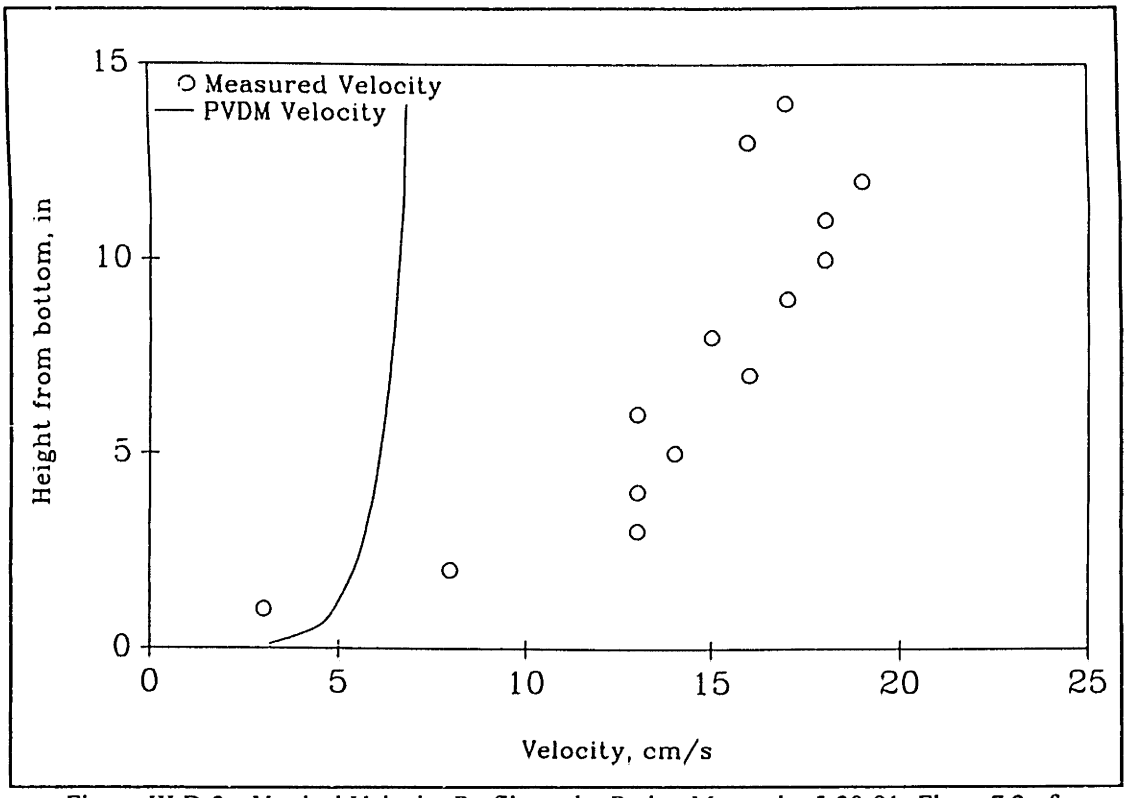

Figure III.D-3: Vertical Velocity Profile at the Probe, Montvale, 5-30-91, Flow=7.2 cfs

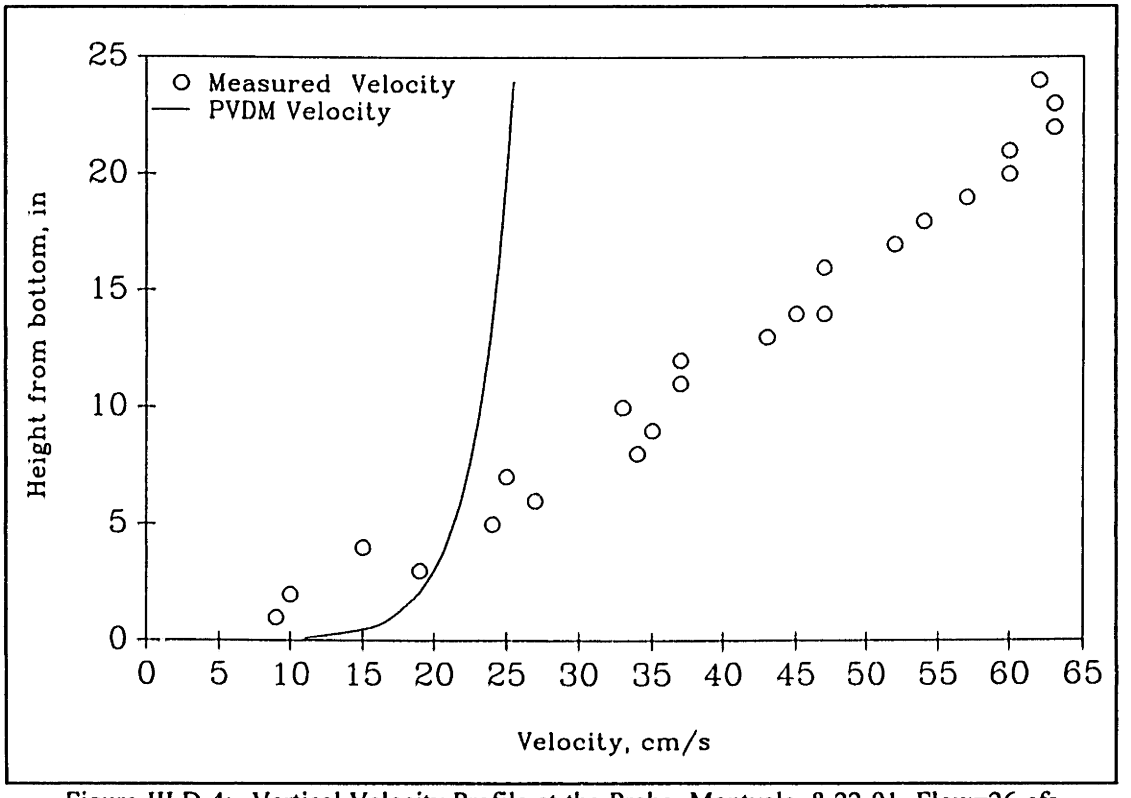

Figure III.D-4: Vertical Velocity Profile at the Probe, Montvale, 8-22-91, Flow=26 cfs

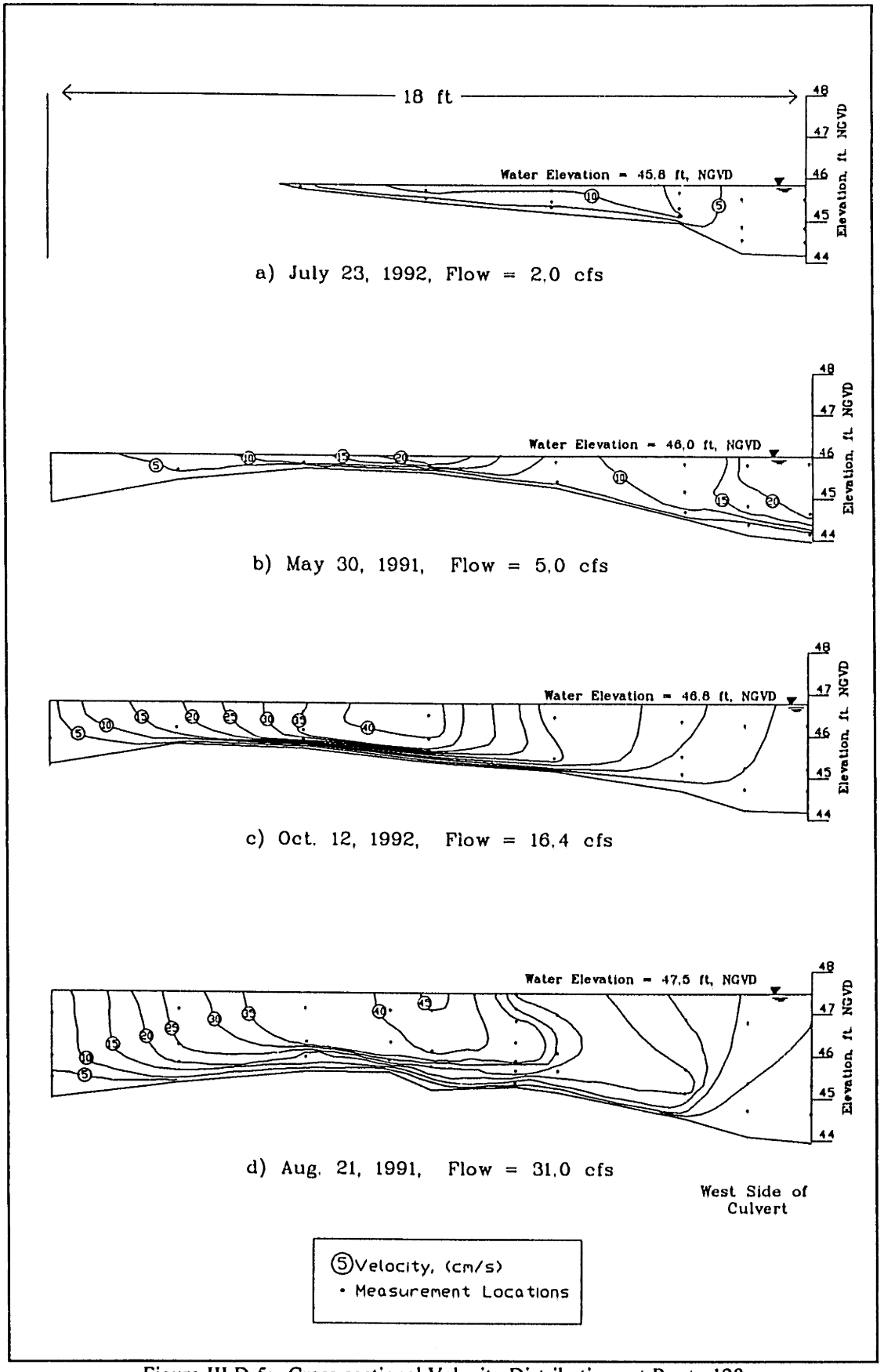

Figure III.D-5: Cross-sectional Velocity Distributions at Route 128

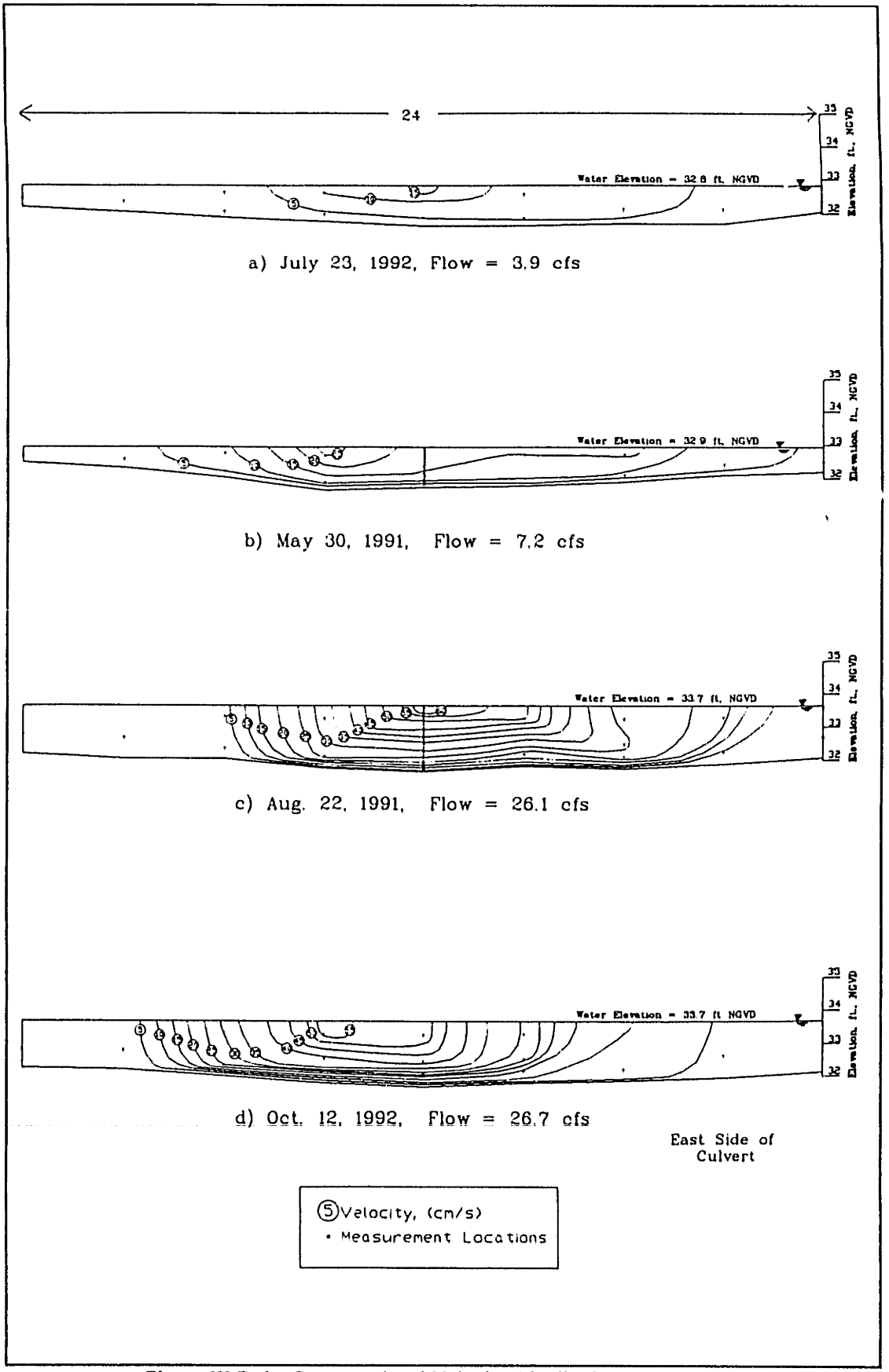

a) July 23, 1992, Flow = 3.9 cfs

b) May 30, 1991, Flow = 7.2 cfs

c) Aug. 22, 1991, Flow = 26.1 cfs

d) Oct. 12, 1992, Flow = 26.7 cfs

Figure III.D-6: Cross-sectional Velocity Distributions at Montvale

APPENDIX III.E

Other Analyses: Suspended Sediments

- X-ray Diffraction Analysis
- SEM-EDS
- Coulter Counter Analysis
- Metals versus Filter Pore Size
- TOC Analysis
- Neutron Activation Analysis
- ICP-AES (Non-Routine Metals)
- GFAA (Non-Routine Metals)

X-RAY DIFFRACTION ANALYSIS: This technique was used to determine the primary mineral components of sediment samples through the analysis of their crystal structure. The basis for x-ray diffraction analysis is that crystal lattices can be used as a three-dimensional diffraction grating, since the wave-length of x-rays is in the same size range as interatomic distances. Measurements include detection of the intensity and angle of constructive interferences, from which the arrangement of molecules within a crystal can be calculated.

All x-ray diffraction analysis was performed by M.I.T.'s x-ray diffraction facility at the Center for Materials Science and Engineering under the supervision of Mr. Joseph Adario. Analysis was performed using a Rigaku RU300 Rotating Anode X-ray Generator with a Copper Anode fitted with a fully automated diffractometer and graphite diffracted beam monochromator. The control of the diffractometer and the data processing was done on a DEC VAX Station II Computer. (Adario, 1993)

One suspended sediment and three river bottom sediments were analyzed. The river bottom sediments were separated into different size ranges by wet sieving and drying. Once dried the sediments were crushed using an agate mortar. River bottom sediment size ranges analyzed included: 1) fines <53 μm, all particles passing the 270 sieve, 2) 53 to 149 μm (Particles retained between the 270 and 100 sieve), and 3) 420 to 710 μm (Particles retained between 40 and 25 sieve). The river bottom sediment sample was collected at gage 2 on January 31, 1992 while the suspended sediment sample corresponded to filter 5c collected March 29, 1992 at gage 5. Filter interference was not considered a problem due to the amorphous filter material structure. (Adario, 1993)

The mineralogical composition of the suspended sediment is one indicator of its metal carrying capacity. For all four analysis the primary crystalline structure identified was quartz, (SiO_2). Pure quartz typically does not have a large amount of metals entrained within its crystal structure nor is it particularly effective at sorbing metals. (Dzombak & Morel, 1990) Detailed result for each sample, including intensity versus diffraction angle plots and peak file listings, are available from the author.

SCANNING ELECTRON MICROSCOPE ANALYSIS (SEM) WITH ENERGY DISPERSIVE X-RAY SPECTROSCOPY (EDS): Scanning electron microscopes provide a magnified image of microscopic objects (nanometer resolution) by scanning the object with electrons. Impingement of these electrons on the object produce signals, (e.g. backscattered electrons, secondary electrons, absorbed electrons and x-rays) By measuring the magnitude of these signals the determination of sample properties (e.g. topography, composition, etc.) can be made. The SEM image formation is produced by mapping the information obtained from the signals to a visual display.

Energy Dispersive X-ray Spectroscopy permits elemental analysis of a sample through the measurement of x-rays emitted at characteristic wavelengths by the element of interest. These x-rays are emitted from the sample when it is scanned by electrons. From the relative intensity of the x-ray emissions estimates of elemental concentrations (on the order of a few %) can be made.

The strength of combining the two analytical techniques is that elemental analysis can be performed on a sample as it is viewed through the SEM.

All SEM-EDS analysis was performed at M.I.T.'s electron microscope facility at the Center for Materials Science and Engineering. Analysis was performed on an Environmental SEM built by Electroscan Corporation.

Selected electron micrographs and EDS results are given in figures III.E-1 to III.E-8. All elemental concentrations were normalized with respect to the total number of atoms detected. Only elements with atomic numbers higher than 8 were included in the analysis. Therefore, elements with low atomic numbers, including C, H, and O, were not included in the normalization. Additionally, note that the "stringy" background material is from the filter media (see figure III.E-1) and not from the suspended sediment samples.

Visual characterization of the suspended materials for all sampling stations is that they are composed of heterogeneous materials. However, for each sampling station, these heterogeneous materials have discernable bulk characteristics. Gage 2 samples tend to be dominated by clusters of small particles. (figure III.E-2) In the magnified image of one of these clusters (figure III.E-3), the smallest discernable particle tends to be platelet shaped, approximately 4 μm long and 1 μm thick. The larger particles tend to be composed of (or covered with) an amorphous (fluffy looking) material. From the geometry of the particles one may postulate that the platelet material may be a clay and, judging from the high iron concentrations detected in the samples (20 to 40%), the amorphous material can be identified as an amorphous iron oxide. The link between amorphousity and the iron oxide is supported by observing

that the gage 4 suspended sediment (figure III.E-4) which is characterized by relatively low iron concentrations (2 to 3%), lacks the "fluffy-look" on magnified particles (figure III.E-5).

Additionally noting that x-ray diffraction identified quartz as the primary mineral of the suspended sediment particles, one may further postulate that the "fluffy looking" materials are quartz particles with a surface coating of amorphous iron oxide.

As a contrast, samples for gage 1 collected during a low flow (summer month) tend to dominated by biological material. (figure III.E-6 and III.E-7) For the material illustrated in these figures, most of the circular/elliptical suspended sediments can be identified as diatoms. For the gage 1 sample collected shortly after a storm event (figure III.E-8) the proportion of the sample dominated by diatoms tends to be significantly reduced. This observation indicates that the diatoms which dominated suspended material during very low flow conditions were flushed-out of the system (Wedge Pond) after a large storm event.

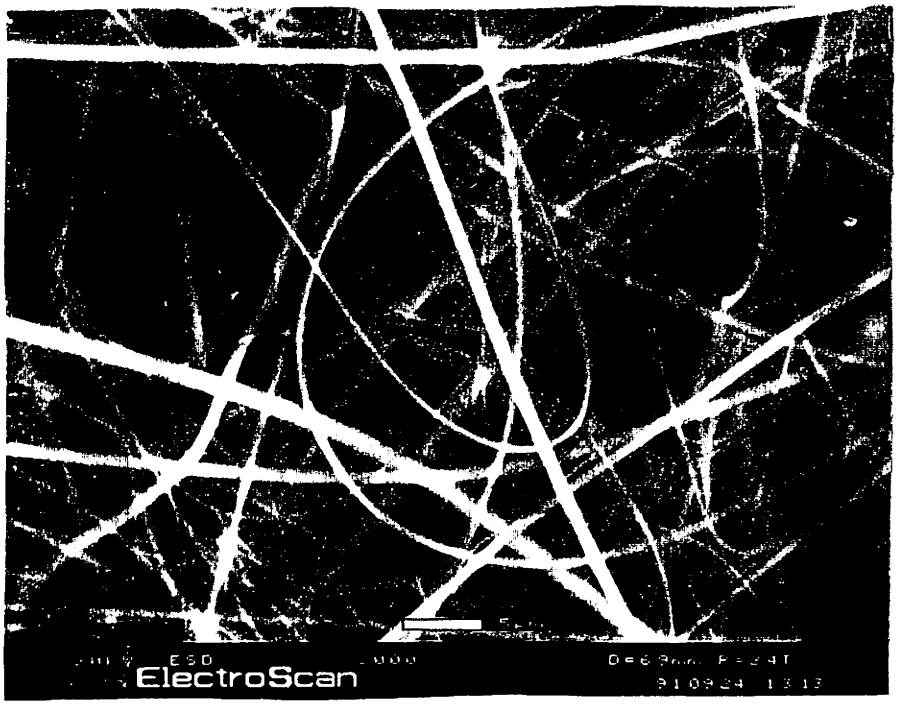

Element	%
Na	34.2
Mg	1.7
Al	5.9
Si	49.1
K	3.0
Ca	1.5
Zn	2.7
Ba	1.7

Figure III.E-1: Blank Filter Media, 0.5 μm Pore Size, Gelman Brand

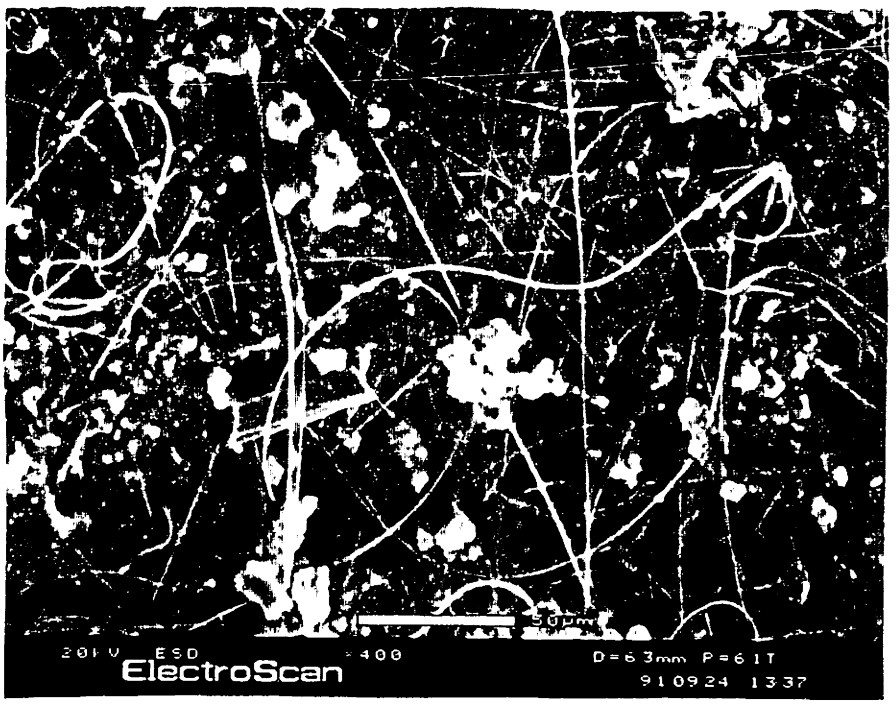

Element	%
Na	29.3
Mg	2.3
Al	6.4
Si	40.7
S	0.8
Cl	0.9
K	2.1
Ca	1.9
Fe	12.4
Zn	1.7
Ba	1.3

Figure III E-2 Filter Sample Collected at Route 128, July 26, 1991

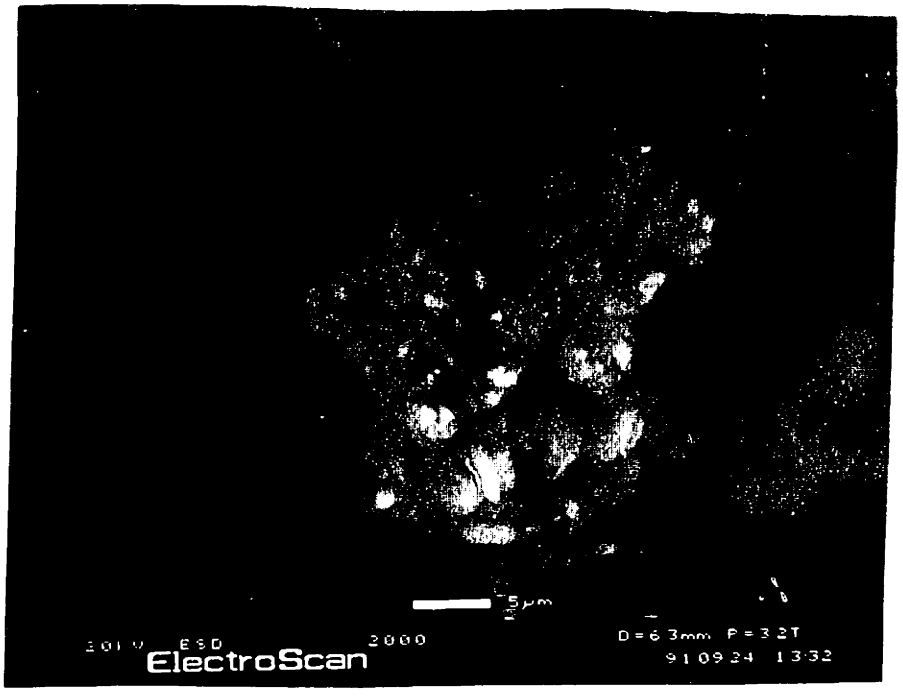

Figure III E-3 Higher Magnification of Cluster in Figure III E-2

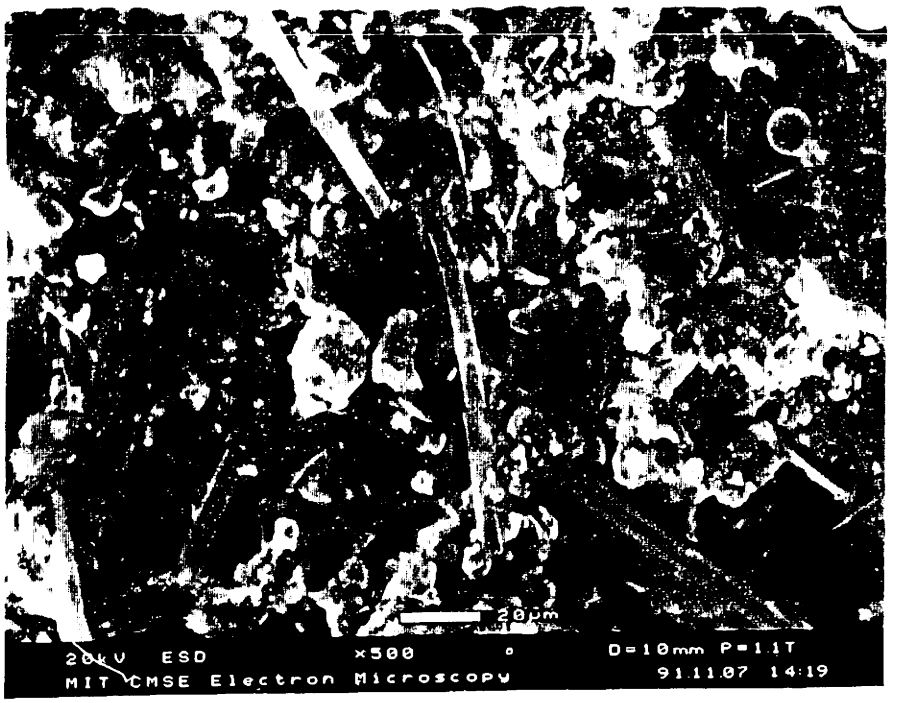

Element	%
Na	15.2
Mg	3.2
Al	13.5
Si	17.6
S	1.0
Cl	0.9
K	3.2
Ca	2.8
Fe	6.4
Ba	1.0
P	2.3
Mn	1.1
Zn	1.9

Figure III E-4: Filter Sample Collected at Horn Pond, August 20, 1991

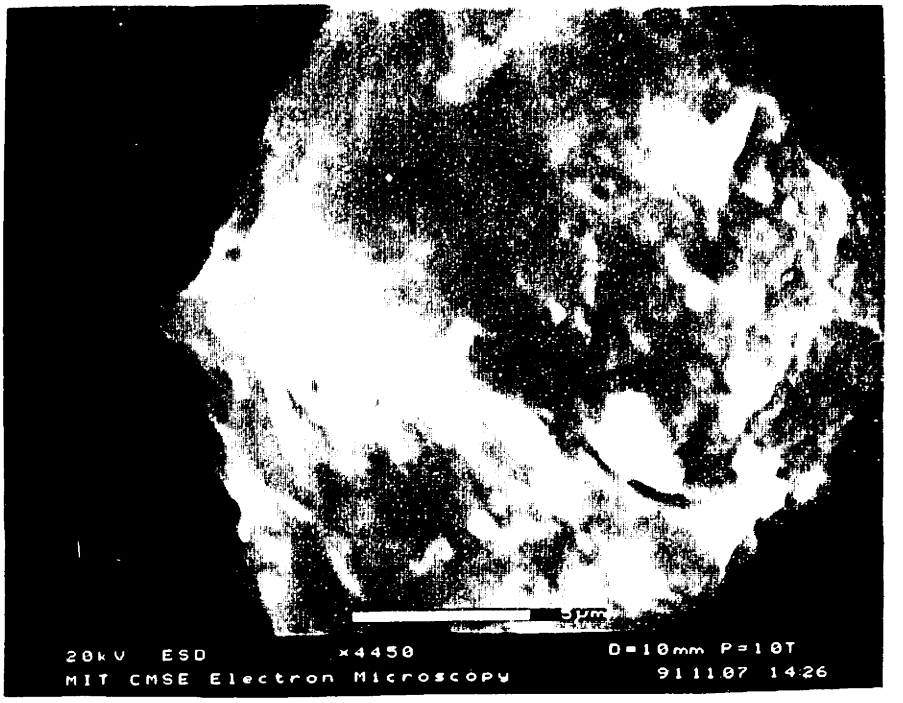

Element	%
Na	8.9
Mg	1.8
Al	23.4
Si	30.8
S	0.3
Cl	0.3
K	0.9
Ca	10.3
Fe	6.8
Ba	1.2
Ti	10.7
P	3.2
Mn	0.4
Zn	0.7

Figure III E-5: Higher Magnification of Particle in Figure III E-4

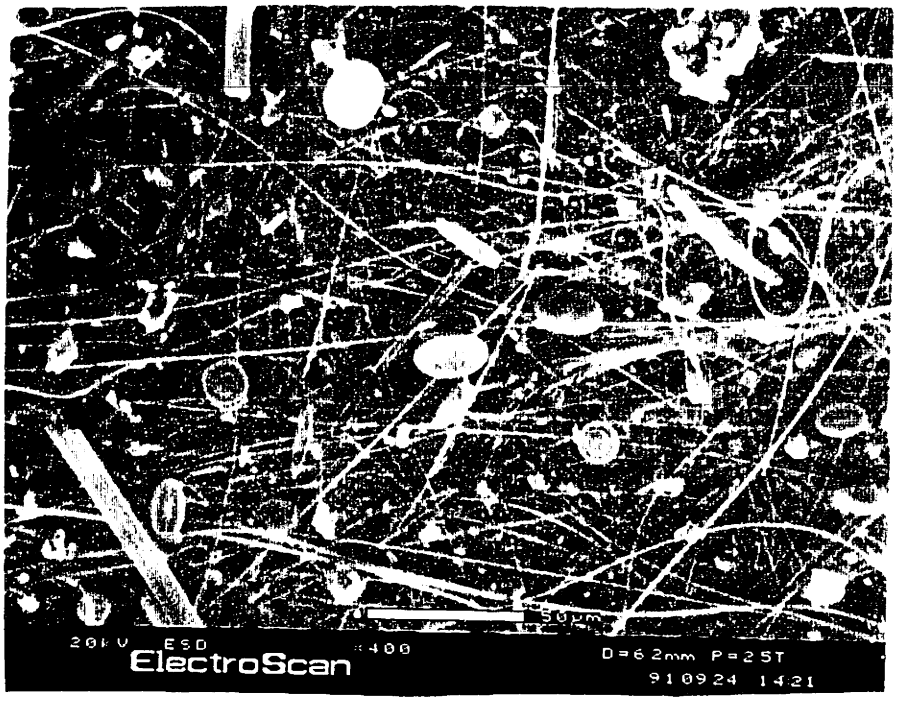

Element	%*
Na	27.3
Mg	1.8
Al	6.3
Si	48.2
S	0.7
Cl	0.6
K	2.5
Ca	1.8
Mn	0.2
Fe	7.9
Zn	1.6
Ba	1.1

Figure III.E-6: Filter Sample Collected at Wedge Pond, July 26, 1992 (Low Flows)

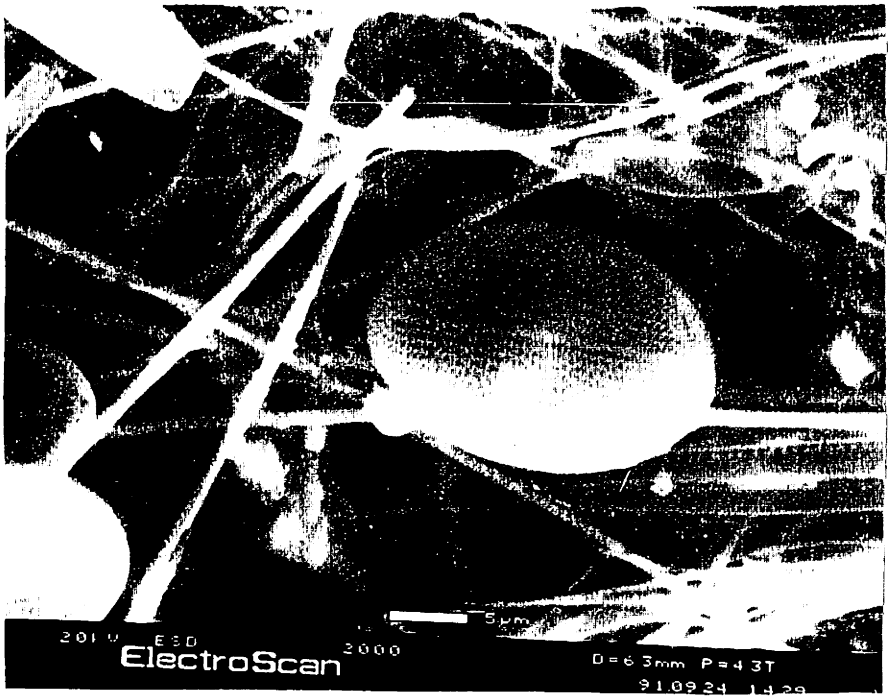

Figure III.E-7: Higher Magnification of Diatom in Figure III.E-6

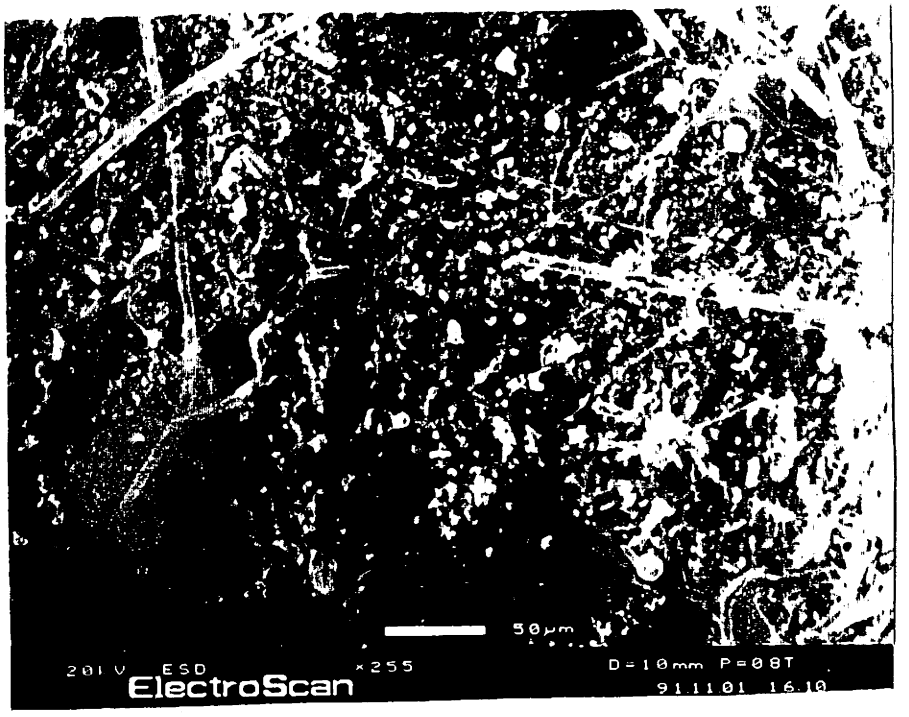

Element	%
Na	18,8
Mg	3,2
Al	13,7
Si	49,0
S	1,6
Cl	0,5
K	2,7
Ca	1,3
Fe	3,8
Ba	1,1
P	1,7
Mn	0,5
Zn	1,9

Figure III.E-8: Filter Sample Collected at Wedge Pond After a Storm Event, August 20, 1991

COULTER COUNTER® ANALYSIS: A coulter counter measures the number and size of particles by measuring the impedance of particles as they pass through a small aperture. Changes in impedance is measured as an electrical pulse through a set of electrodes placed on opposite sides of the aperture. The magnitude of the electrical pulse is proportional to the particle volume.

All particle size measurements using this technique were performed on a Coulter Counter® Model ZM with a Coulter 256 Channelizer® accessory (C256). The ZM included a sampling stand, a vacuum control unit, and an analyzer. The analyzer is the microprocessor of the system and houses the switches used to define operating conditions. The C256 is an accessory analyzer which presented the particle-size distribution in graphical form and served as an interface to an IBM XT which was used for data storage. Measurements were performed using a 100 μm aperture and filtered river water (using 0.5 μm pore size filter) as the analyte. Before each analysis set, the coulter counter was calibrated with 10.5 and 20.3 μm microsphere standards. (Coulter Counter Standards) Accuracies within 1 to 3 μm were obtained.

A summary of mean particle sizes for suspended sediment samples analyzed is given in table III.E-1. The mean particle size for all the samples analyzed varied from 7 to 12 μm. This small variation in particle size is surprising considering the different flow conditions during which the samples were obtained.

Most of the samples had very similar particle size distributions. These "characteristic" size distributions are exemplified by the distributions of samples 93032617, 93032911, and 93040120 plotted in figure III.E-9. The slope of these log-log plots is -4. The only samples which deviated slightly from the norm were 93032921, 93052508, and 93052509 (at gage 2). Sample distributions for 93032921 and 93052508 are also plotted in figure III.E-9. 93052509 had a very similar distribution to 93052508. The slope of the log-log plot for sample 93052508 is -5. Additionally, an inconsistency in the data is apparent in these plots in that the total volume of particles (sum of the products of total particle number times the particle volume) for the 93052508 sample (low suspended sediment concentration) was larger than the total for the other samples which had higher suspended sediment concentrations. This discrepancy may be due to either: 1) experimental error, or 2) different operational settings on the coulter counter during each analysis.

fn: coulter

Sample Date/Time YR-MO-DA-HR	Flow (cfs)	SS Concentration (mg/L)	Mean Particle Size (microns)
USGS Gage			
93032614	87.1	23.3	11.5
93032615	141.7	19.2	11.2
93032616	101.1	21.8	10.9
93032617	144.0	21.3	10.6
93032618	126.5	22.6	11.2
93032619	71.5	20.2	10.2
93032620	66.0	15.8	10.0
93032910	264.2	35.5	9.4
93032911	272.2	21.1	9.9
93032912	285.8	25.4	10.3
93032913	311.3	34.9	10.7
93032914	339.5	59.1	9.9
93032915	362.2	55.9	9.2
93032916	391.7	70.7	10.7
93032917	428.3	82.0	9.7
93032918	459.8	81.5	10.8
93032919	476.0	86.4	10.4
93032920	495.7	76.9	11.7
93032921	499.1	73.8	9.6
93032922	499.1	62.2	11.4
93032923	502.4	61.4	10.6
93033000	492.4	51.3	10.5
93033001	479.2	42.1	11.1
93033002	469.5	26.4	8.7
93033008	453.4	18.9	10.7
93033119	308.4	9.9	9.2
93040116	348.0	39.9	9.5
93040117	359.4	19.5	8.7
93040118	391.7	29.0	10.0
93040119	410.0	39.0	10.3
93040120	413.0	30.8	10.0
93040121	356.5	18.1	9.5
93040122	391.7	15.4	9.5
93040123	385.7	10.5	9.1
93040200	376.8	13.9	8.3
93040217	291.4	5.7	9.5
93052508	15.6	5.20	7.7
Route 128 Gage			
93052509	5.3	6.20	7.95

Table III.E-1: Suspended Sediment Mean Particle Size

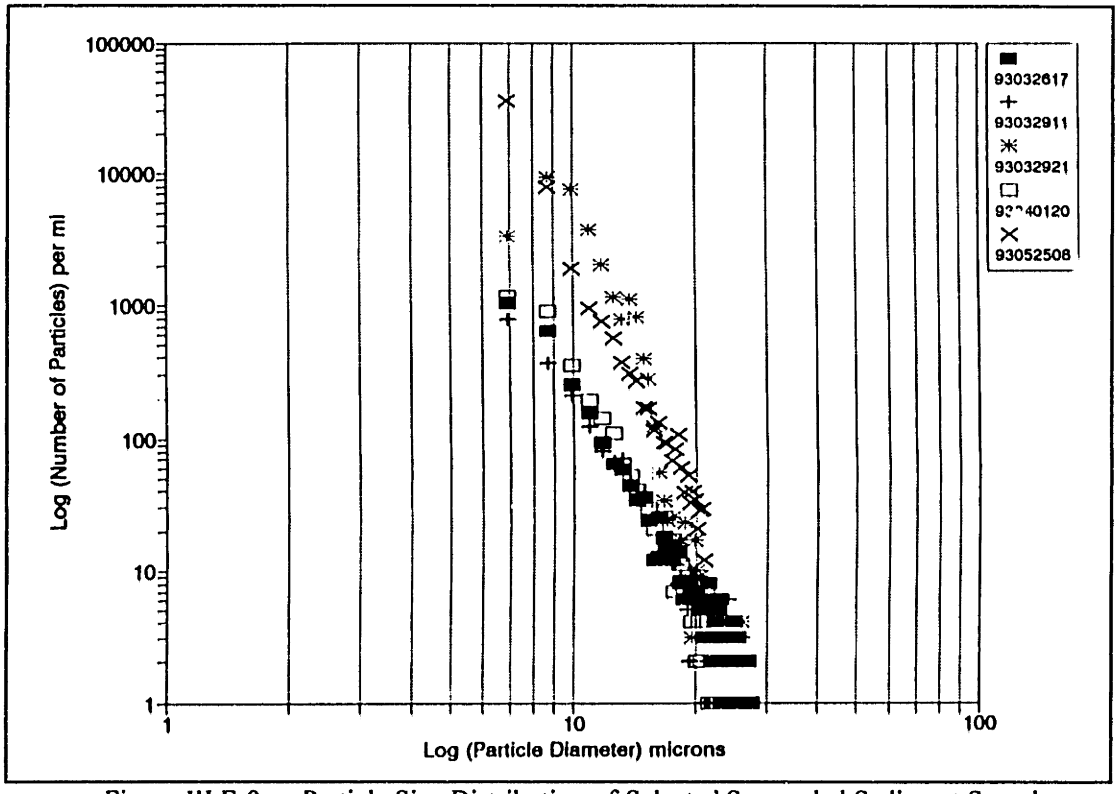

Figure III.E-9: Particle Size Distribution of Selected Suspended Sediment Samples USGS Station

METALS ANALYSIS USING FILTERS OF DIFFERENT PORE SIZES: Metal concentration versus suspended sediment particle size was investigated by filtering samples through filters of different pore sizes. Filter pore sizes and types included 0.2 μm Nucleopore, 0.5 μm Gelman Metrigard, and 1.5 μm Whatman filters. Filtration through each filter was performed using whole (bulk) samples. Suspended sediment and metal concentration data corresponding to a specific size range were obtained by difference.

Results of suspended sediment, Fe, and Cr analysis for samples collected at Montvale and Route 128 are provided in tables III.E-2 and III.E-3 and figures III.E-10 to III.E-21. Volatile concentrations are included in figures III.E-15 and III.E-17 for reference. Results for Fe indicate that a large fraction of the sediment mass in the 0.2 to 0.5 μm size range is composed of Fe. For both Montvale and Route 128, iron in this size range represented over 60% of the bulk suspended sediment. Converting the Fe into an equivalent amount of Fe_2O_3 would imply that over 85% of the suspended sediment in the 0.2 μm to 0.5 μm size range was in the form of Fe_2O_3. (Note that if Fe as $Fe(OH)_3$ is considered, a mass balance problem is detected where over 120% of the sediment must be composed of $Fe(OH)_3$.) Such a result indicates that the suspended sediment fines (< 0.2 μm) are composed primarily of an iron oxide. Because iron oxides have high sorption capacities for other metals, these fines may also be responsible for the bulk of metal transport. For the larger sizes, the Fe concentrations are significantly lower representing less than 15% of the suspended sediment mass, where the bulk of the sediment mass for the >1.5 μm size range is composed of volatile (organic) material. If metals are associated with the organic phase, then the larger suspended sediments (> 1.5 μm) will be responsible for a large proportion of their transport. Results for Chromium, on the other hand, indicate that Cr represents only a very small fraction of the bulk sediment mass (less than 0.1%). Additionally, except for the 200 mg/kg concentration detected for the Route 128 sample in the 0.5 to 1.5 μm size range, Cr concentrations were generally between 550 to 700 mg/kg. Apparently, Cr is not strongly correlated with different suspended sediment particle sizes.

FN: size

Pore Size	Differential Size	Bulk SS (mg/l)	Differential SS (mg/l)	Bulk Fe %	Differential Fe %	Bulk Cr mg/kg	Differential Cr mg/kg
0.2 um	0.2-0.5 um	6.2	1.01	20.3	64.5	542.0	616.0
0.5 um	0.5-1.5 um	5.19	1.29	11.7	3.2	527.6	201.1
1.5 um	>1.5 um	3.9	3.9	14.5	14.5	635.6	635.6

Table III.E-2: Suspended Sediment, Fe, and Cr Concentrations Versus Filter Pore Size, Montvale Station, March 29, 1992

Pore Size	Differential Size	Bulk SS (mg/l)	Differential SS (mg/l)	Bulk Fe %	Differential Fe %	Bulk Cr mg/kg	Differential Cr mg/kg
0.2 um	0.2-0.5 um	4.3	0.59	16.1	61.6	583	678.0
0.5 um	0.5-1.5 um	3.71	1.21	8.87	7.0	567.9	630.5
1.5 um	>1.5 um	2.5	2.5	9.78	9.8	537.6	537.6

Table III.E-3: Suspended Sediment, Fe and Cr Concentration Versus Filter Pore Size, Route 128 Station, March 29, 1992

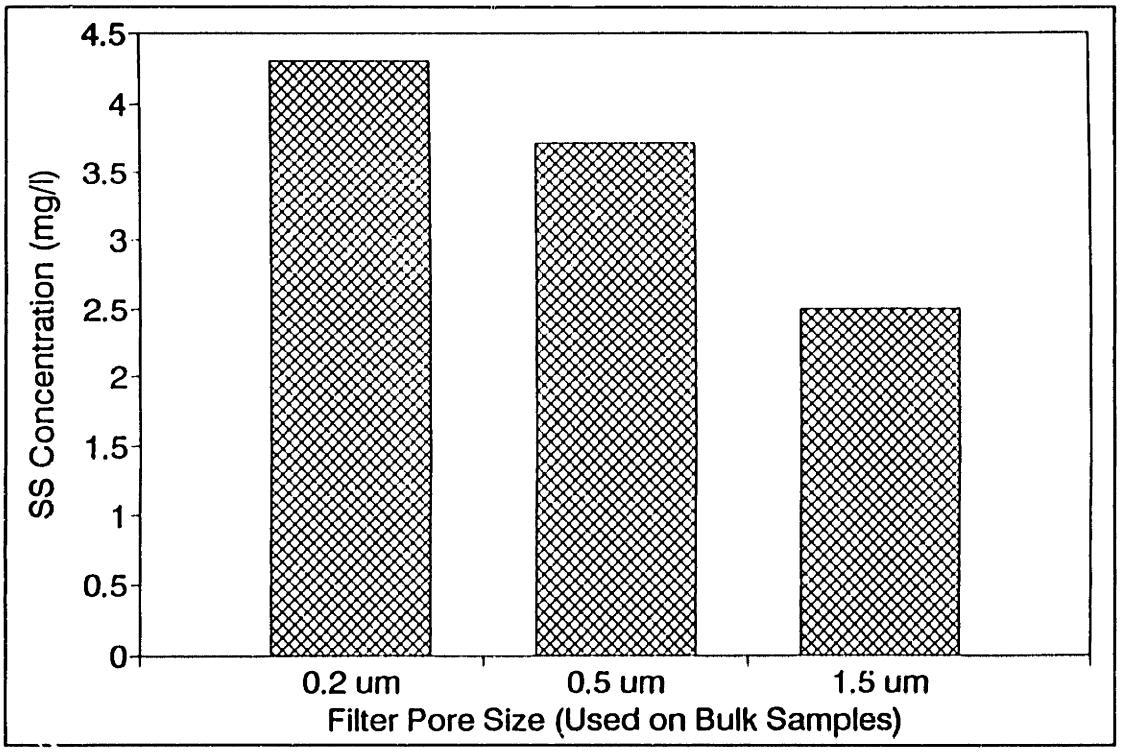

Figure III.E-10: Bulk Suspended Sediment Concentration versus Filter Pore Size, Montvale Station, March 29, 1992

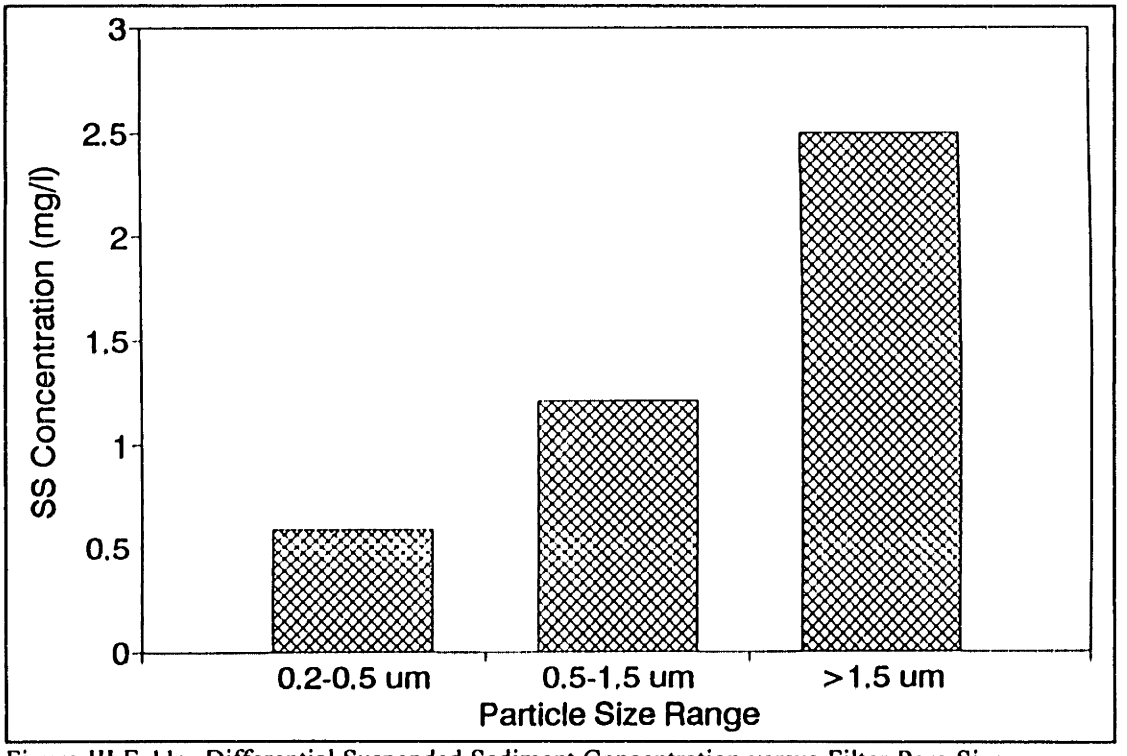

Figure III.E-11: Differential Suspended Sediment Concentration versus Filter Pore Size, Montvale Station, March 29, 1992

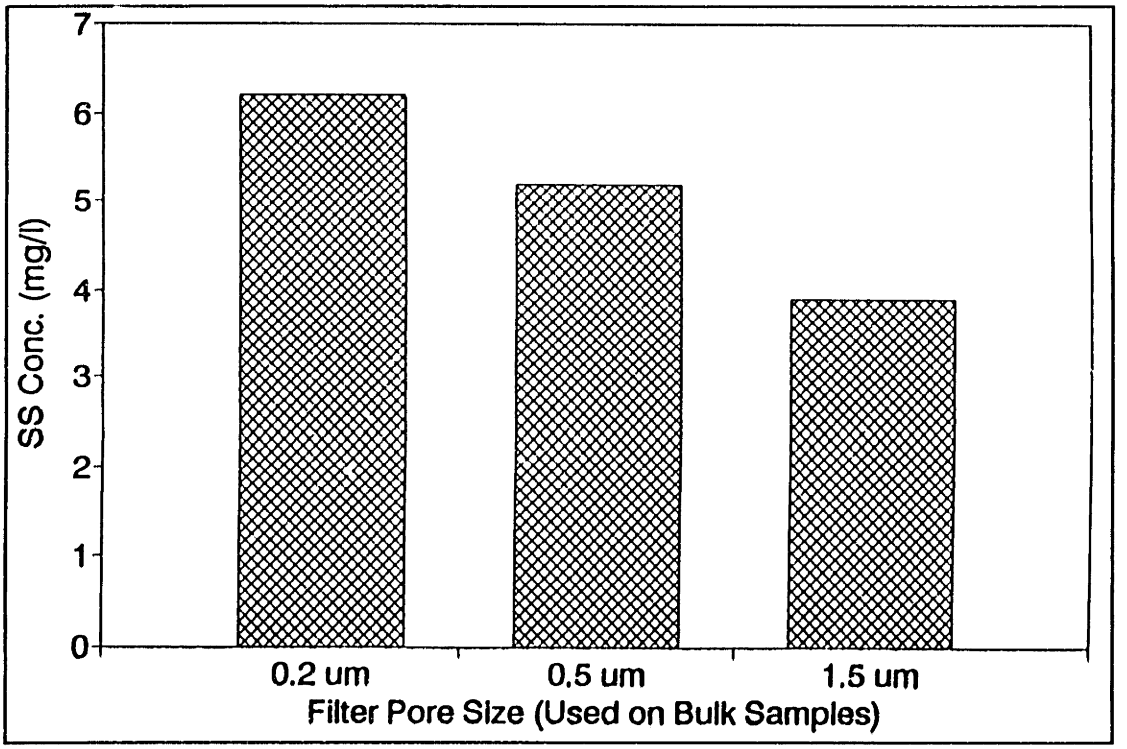

Figure III.E-12: Bulk Suspended Sediment Concentration versus Filter Pore Size, Route 128, March 29, 1992

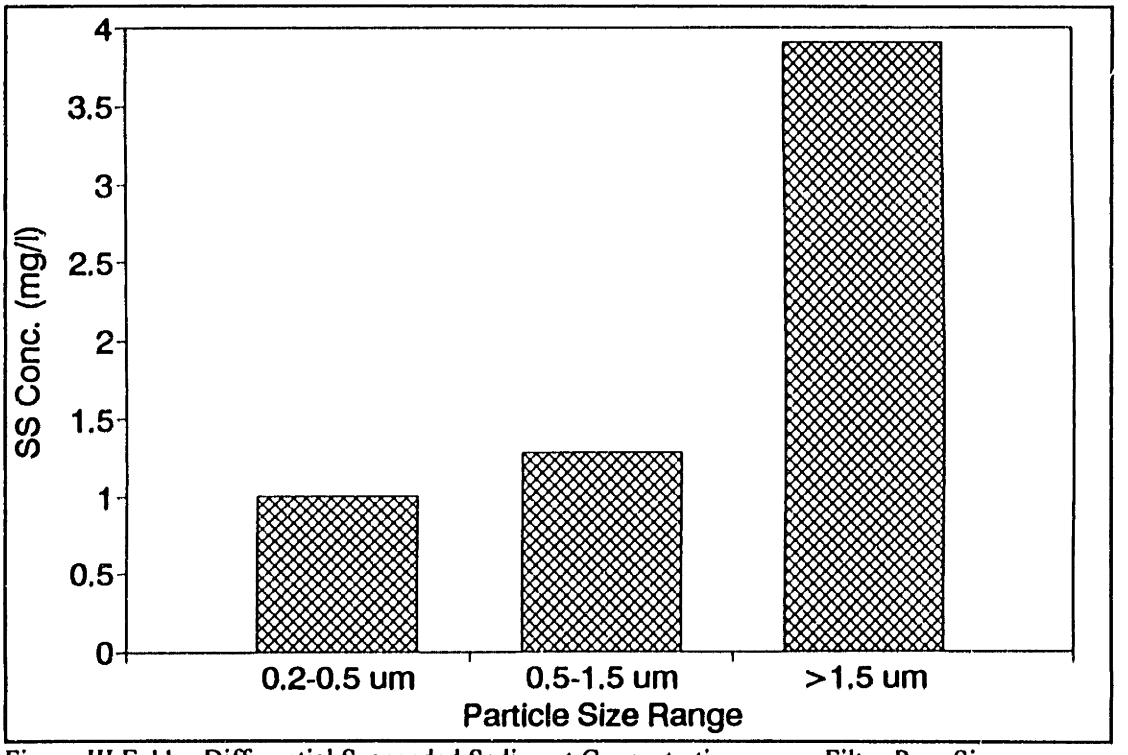

Figure III.E-11: Differential Suspended Sediment Concentration versus Filter Pore Size, Route 128, March 29, 1992

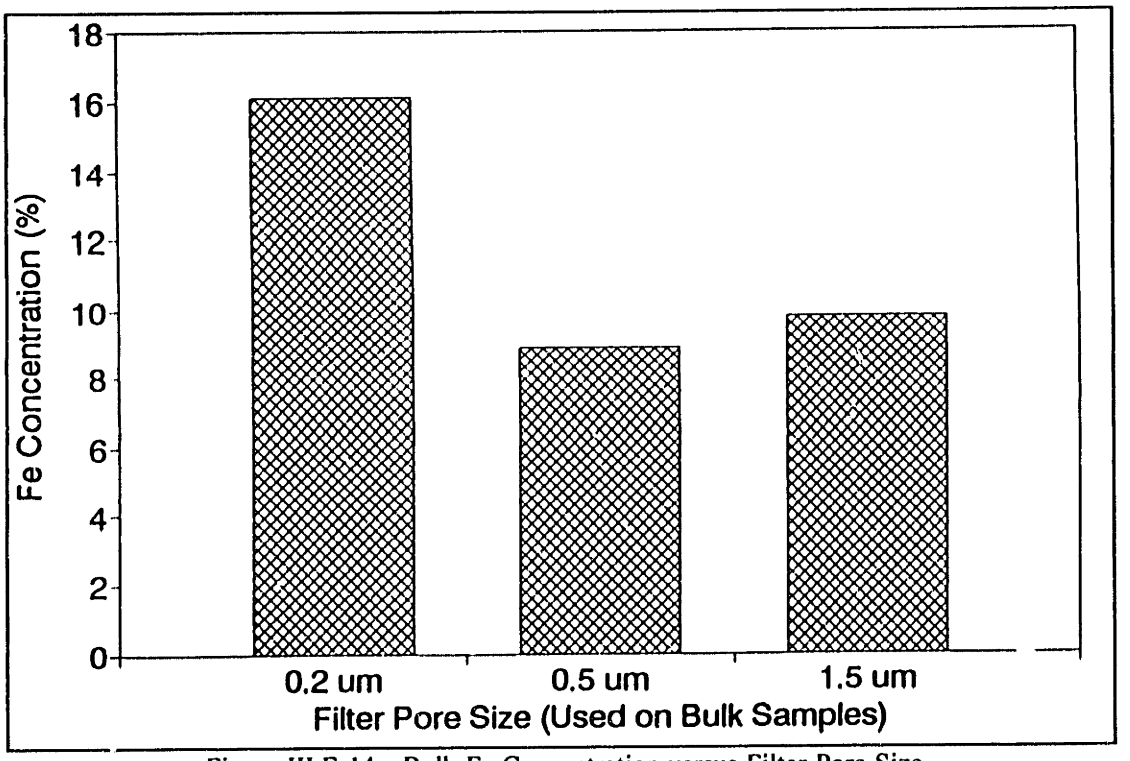

Figure III.E-14: Bulk Fe Concentration versus Filter Pore Size, Montvale Station, March 29, 1992

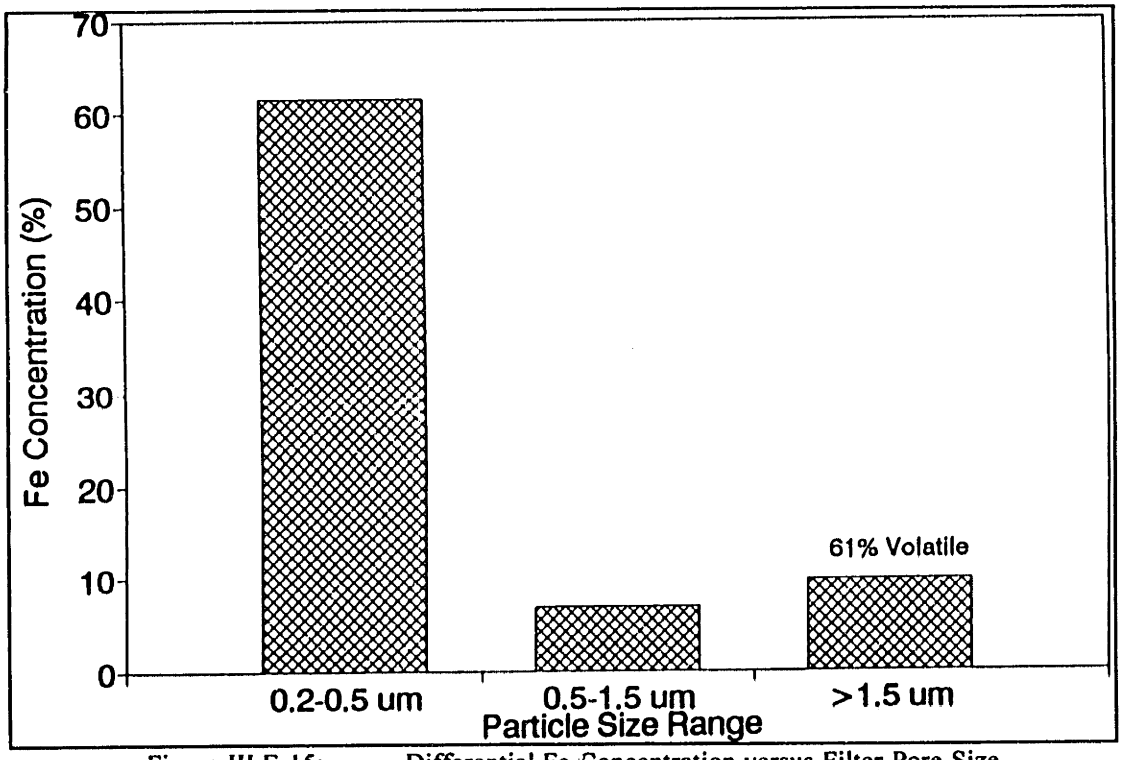

Figure III.E-15: Differential Fe Concentration versus Filter Pore Size, Montvale Station, March 29, 1992

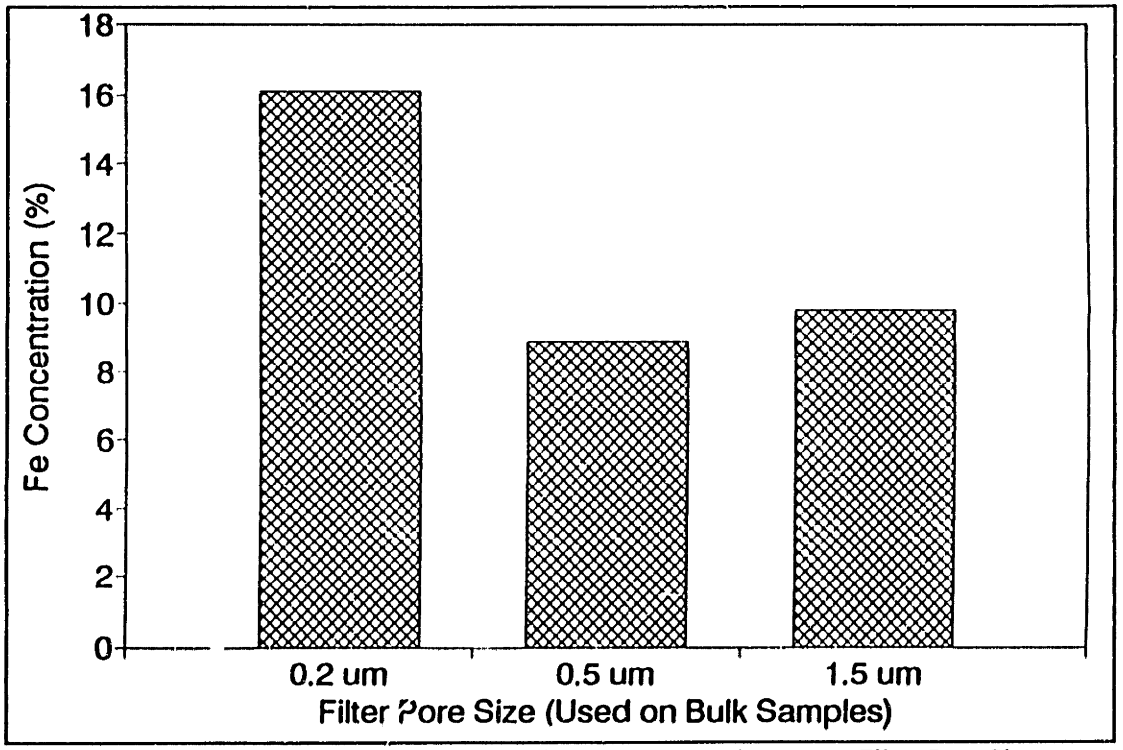

Figure III.E-16: Bulk Fe Sediment Concentration versus Filter Pore Size, Route 128, March 29, 1992

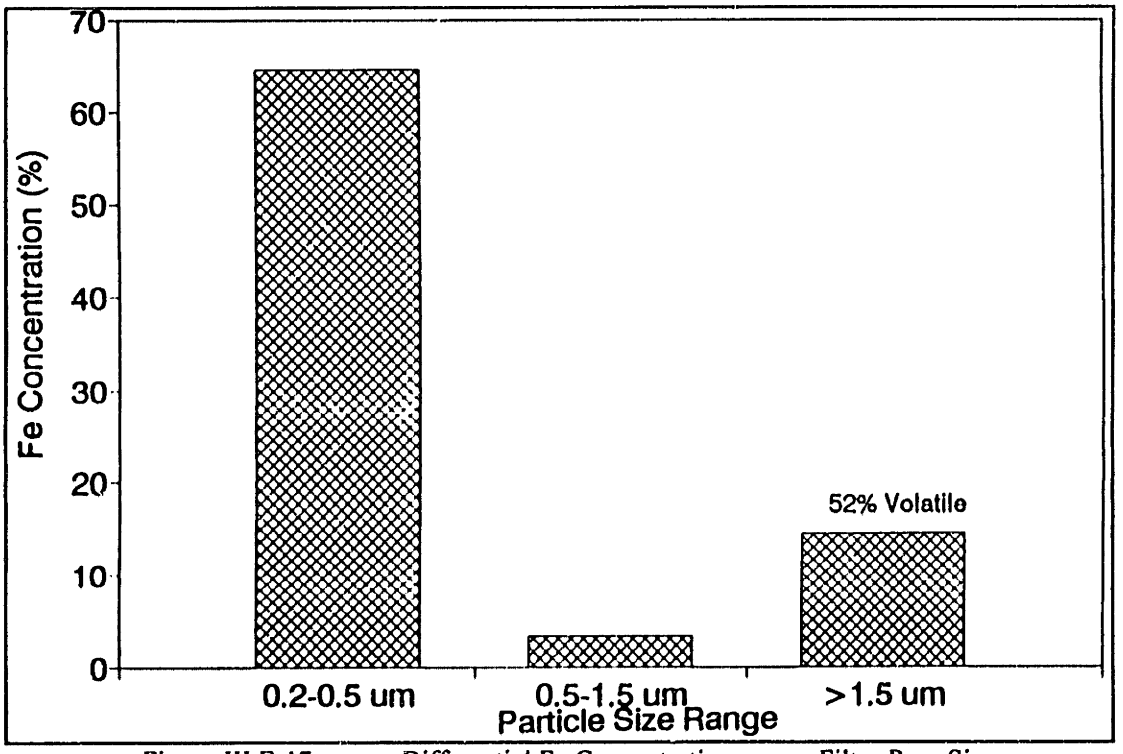

Figure III.E-17: Differential Fe Concentration versus Filter Pore Size, Route 128, March 29, 1992

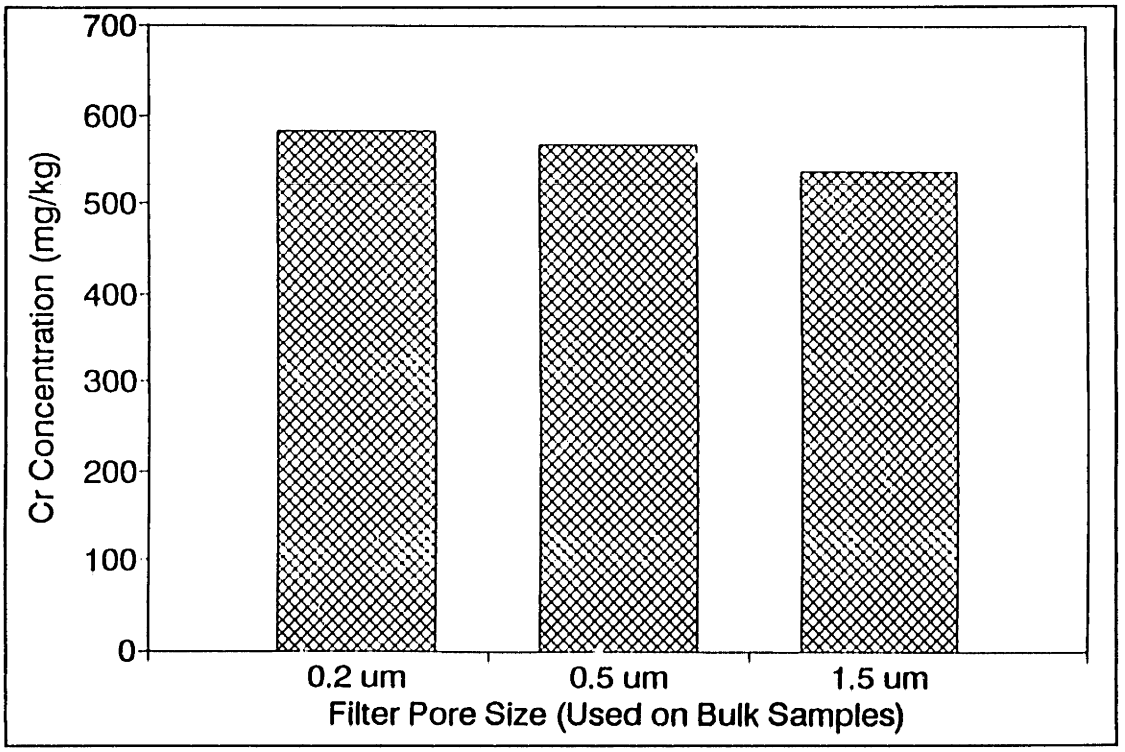

Figure III.E-18: Bulk Cr Concentration versus Filter Pore Size, Montvale Station, March 29, 1992

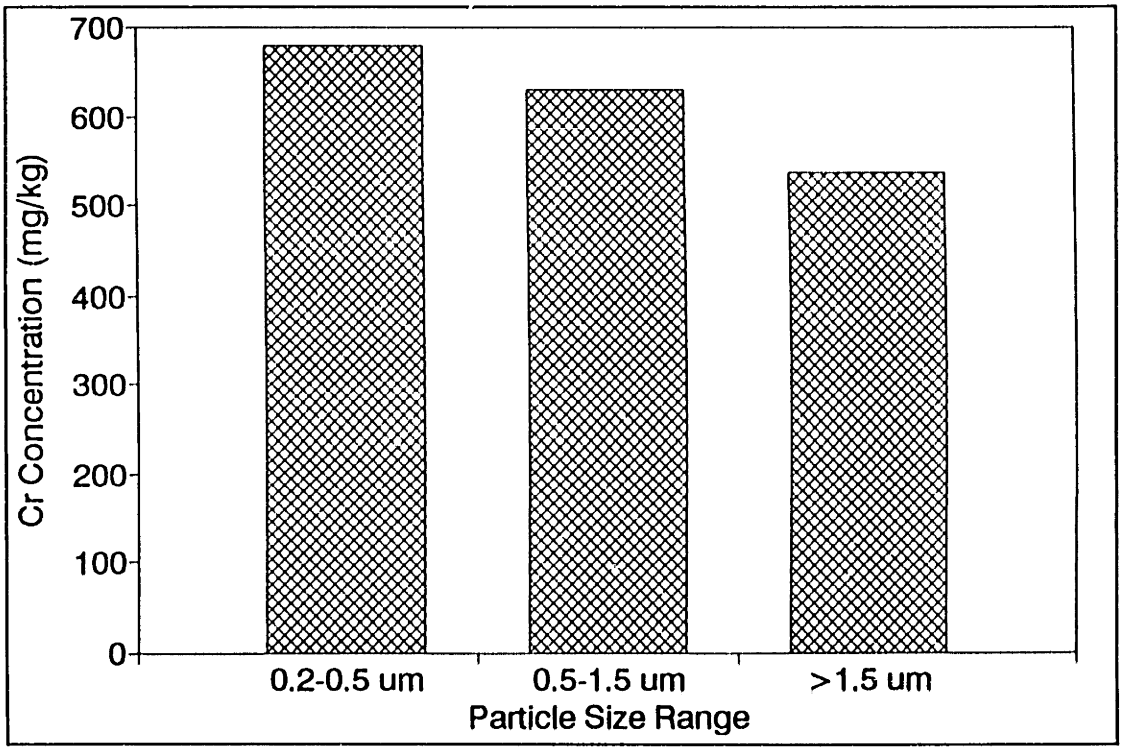

Figure III.E-19: Differential Cr Concentration versus Filter Pore Size, Montvale, March 29, 1992

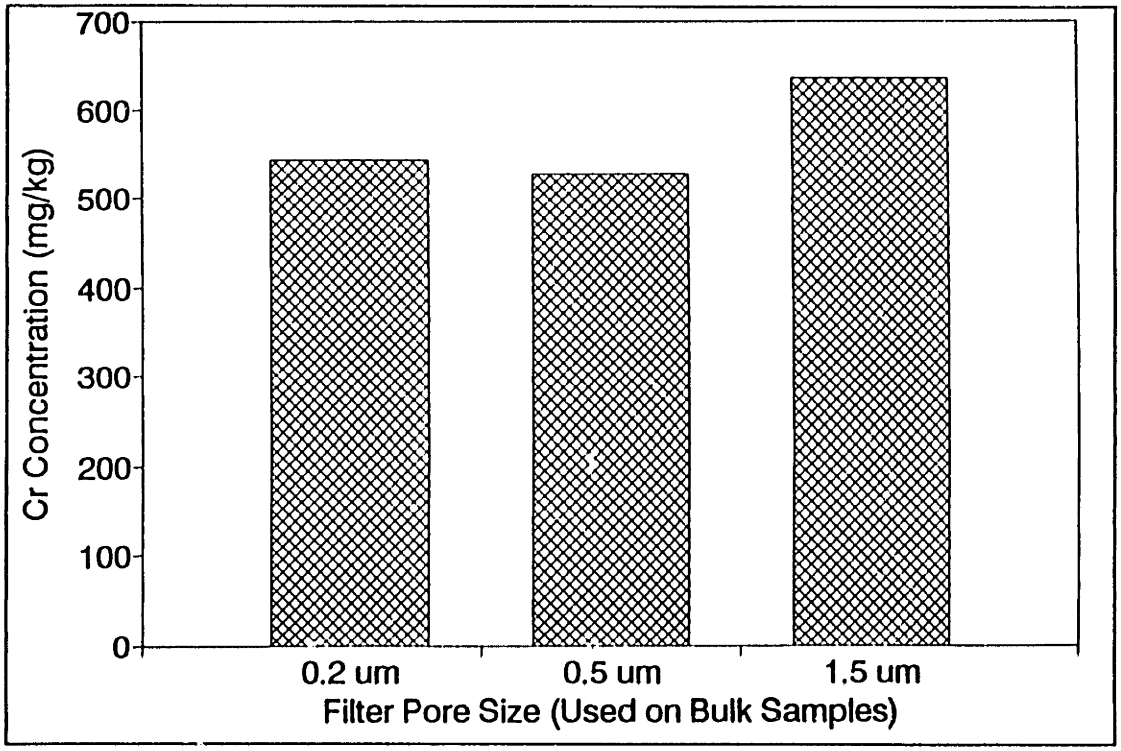

Figure III.E-20: Bulk Cr Concentration versus Filter Pore Size, Route 128, March 29, 1992

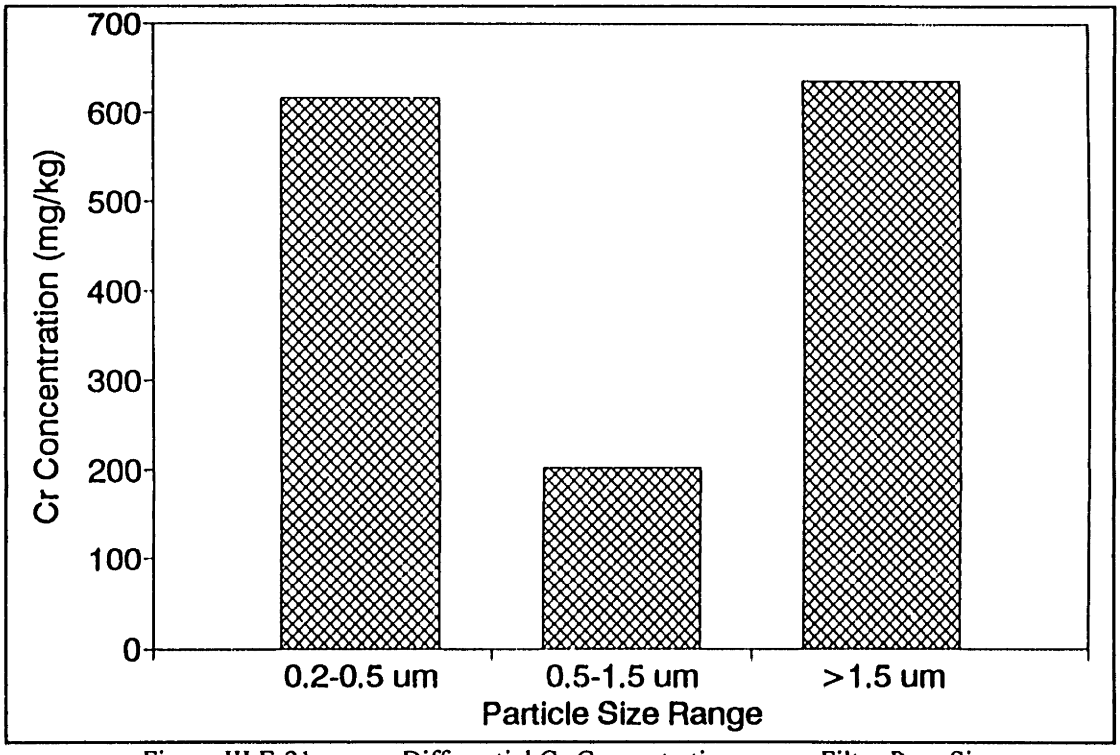

Figure III.E-21: Differential Cr Concentration versus Filter Pore Size, Route 128, March 29, 1992

TOTAL ORGANIC CARBON, (TOC): Filtered and unfiltered river water samples were analyzed for TOC. The difference between filtered and unfiltered samples is equivalent to the particulate TOC. Refer to appendix III.F for details and results of TOC analysis.

NEUTRON ACTIVATION ANALYSIS: Neutron activation analysis is a method of elemental analysis by irradiating a sample with neutrons and observing the radioactivity induced. (Taylor, 1964) The magnitude of the radiation response, at an energy level characteristic of a particular element, is a direct measure of the amount of that element present in the sample.

One advantage of this technique is that many different elements can be analyzed using the same sample by detecting radiation at different energy levels. The technique is also extremely sensitive and permits the confirmation of elemental identification. The sensitivity is due to the fact that very minute quantities of radioactivity can be detected. Confirmation is through the measurement of different types of radiation. These types of radiation include: 1) prompt radiation which is emitted promptly after a neutron is added to a nucleus, and 2) alpha and beta radiation which decays at a characteristic half-life from the radioactive nucleus formed from the neutron addition.

All neutron activation analysis was performed by the nuclear reactor facility at M.I.T. under the supervision of Dr. Ilhon Olmez. Sample preparation consisted of filtering river water through acid-washed 0.2 μm Nucleopore filters (0.45 cm diameter) and noting the weight of sediment collected. Samples analyzed included suspended sediment samples collected: 1) March 29, 1992 at gages 2,3,4, and 5, and 2) June 11, 1992 at gage 1.

Results of neutron activation analysis are given in tables III.E-4 and III.E-5. Na, Mg, Al, Cl, K, Sc, Ti, V, Cr, Mn, Fe, Co, Zn, Ga, As, Se, Br, Rb, Mo, Sb, Cs, Ba, La, Ce, Nd, Sm, Eu, Gd, Tb, Yb, Lu, Hf, Ta, W, Au, Th, and U were all detected above blank values. Cr, Mo, W, Mn, Fe, U, and Sm were detected at levels at that were higher than mean crustal average concentrations (Taylor, 1964) by a factor of 2. Co, Zn, Au, As, Se, Br, Cl, and Sb were detected at levels that were higher than mean crustal average by a factor of 10. Most of the enrichment corresponded to samples collected on the Aberjona side of the watershed. The only exception, was Se which was enriched at the Horn Pond station and Au which appears to be enriched at all stations except Wedge Pond.

		Wgt(mg)	1.7	Wgt(mg)	1.9	Wgt(mg)	0.9	Wgt(mg)	2.1	Wgt(mg)	0.8	FN:n0329
Element	Filter Blank	1N Wedge Pond		2N Rte 128		3N Montvale		4N Horn Pond		5N USGS		Crustal* Average
	ng/flt	raw ng/flt	correct mg/kg	raw ng/flt	correct mg/kg	raw ng/flt	correct mg/kg	raw ng/flt	correct mg/kg	raw ng/flt	correct mg/kg	mg/kg
Na	2200	5400	3176	5700	1842	5000	3111	6900	2238	4700	3125	23600
Mg	230					12000	13078			3340	3888	23300
Al	275	19700	11588	17900	9276	12500	13583	17900	8393	12100	14781	82300
Cl	1700	2200	1294	2600		3200	1667	1540		1650		130
K	1400			6900	2895	6000	5111	11200	4667	1400	0.00	20900
Sc	0.03			5.8	3.0	4.3	5	7.2	3.4	3	3.7	22.0
Ti	26	1350	794	1500	776	1200	1304	3100	1464	9.5		5700
V	0.2	66	39	129	68	75	83	170	81	140	175	135
Cr	470			1500	542	995	583	570	48	540	88	100
Mn	5.4	3600	2118	1680	881	2900	3216	2400	1140	870	1081	950
Fe	698			387000	203317	146000	161447	140000	66334	41200	50628	56300
Co	6.7			34	14.4	121	127	41	16.3	22	19.1	25.0
Zn	58			5800	3022	3200	3491	1240	563	664	758	70
Ga						9.8	11	2.9	1.38			15
As	1.2			1500	789	543	602	67	31	106	131	1.8
Se	0.9							15	6.7	4.1	4.0	0.05
Br	49			174	66	100	57	144	45	63	18	2.5
Rb	5.7					27	24	38	15	30	30	90
Mo				24	12.6	11	12	8.5	4.05	2.8	3.5	1.5
Sb	0.3			20	10.4	12	13	4.7	2.10	5.2	6.1	0.2
Cs	0.6			1.1	0.26			3.4	1.33	2.4	2.25	3.00
Ba				585	308	579	643	457	218			425
La				65	34.2	33	37	40	19	15	19	30
Ce	3.6			145	74.4	77	82	69	31	33	37	60
Nd	6			42	18.9	30	27	42	17	8.8	3.5	28.0
Sm				8.8	4.6	40	44	5.8	2.76	2.2	2.8	6.0
Eu	0.2			1.4	0.63	0.9	0.78	1.1	0.43			1.2
Gd				7.2	3.79	3.6	4.0	5.3	2.52	1.9	2.37	5.40
Tb	0.07					0.2	0.14	1	0.44	0.9	1.04	0.90
Yb	0.06			2.9	1.49	1.6	1.71	2	0.92	1	1.18	3.00
Lu	0.009			0.6	0.31	0.3	0.32	0.4	0.19	0.2	0.24	0.50
Hf				1.1	0.58	1.2	1.33	1.2	0.57	2.1	2.63	3.00
Ta								1.6	0.76			2.00
W				3.4	1.79	3.1	3.4	2.6	1.24	2.3	2.87	1.50
Au	0.021			0.097	0.040	0.055	0.038	0.072	0.024	0.052	0.039	0.004
Th				6	3.16	5	5.6	7.1	3.38	3.9	4.88	9.60
U				13	6.84	6.2	6.9	2	0.95	1.2	1.50	2.70

* Reference: Taylor, 1964

Table III.E-4: Results of Neutron Activation Analysis for Samples Collected at Gages 1 to 5 on March 29, 1992

Wgt(mg) 0.87 FN: N061192

Element	Filter Blank	1N Wedge Pond		Crustal* Average
		raw	correct	
	ng/flt	ng/flt	mg/kg	mg/kg
Na				23600
Mg				23300
Al				82300
Cl				130
K				20900
Sc	0.055	2.6315	2.96	22.0
Ti				5700
V				135
Cr	239.56	312.57	83.9	100
Mn				950
Fe	308.13	35649.5	40622	56300
Co	3.9	10.825	7.96	25.0
Zn	31.973	237.65	236	70
Ga				15
As	0.174	30.274	<35	1.8
Se	0.3155	0.491	0.202	0.05
Br	33.767	101.004	77.3	2.5
Rb	6.99	10.749	4.32	90
Mo	0.15	3.871	4.28	1.5
Sb	0.131	1.441	1.51	0.2
Cs	0.574	1.223	0.75	3.00
Ba	33.16	277.042	280.3	425
La	0.047	11.43	13.1	30
Ce	2.525	17.024	16.7	60
Nd	7.165	8.362	1.38	28.0
Sm	0.002	1.361	1.56	6.0
Eu	0.173	0.264	0.10	1.2
Gd	0.11	0.702	0.68	5.40
Tb	0.035	0.146	0.13	0.90
Yb	<0.097	0.633	<0.62	3.00
Lu	0.011	0.149	0.159	0.50
Hf	0.263	0.364	0.116	3.00
Ta	0.235	1.112	1.008	2.00
W				1.50
Au	8.27	8.072		0.004
Th	0.144	2.676	<2.91	9.60
U	0.106	1.316	1.39	2.70

*Reference: Taylor, 1964

Table III.E-5: Results of Neutron Activation Analysis for a Sample Collected at Gage 1 on June 11, 1992

INDUCTIVELY COUPLED PLASMA - ATOMIC EMISSION SPECTROSCOPY ANALYSIS (ICP-AES): ICP-AES analysis is discussed in section III.4.3. Non-routine ICP-AES analysis was performed for Zn, Ba, Ti, Co, and Ni determinations. Results are presented in table III.E-6. Results indicated that Zn and Co were elevated significantly above mean crustal average concentrations. The highest concentrations of both elements were measured on the upper reaches of the Aberjona River.

ATOMIC ABSORPTION ANALYSIS WITH GRAPHITE FURNACE ATOMIZATION (GFAA): GFAA analysis is discussed in section III.4.3. Non-routine GFAA analysis was performed for Cd and Pb determinations. Results (table III.E-7) indicate that both particulate Cd and Pb were elevated significantly above mean crustal concentrations. The highest concentrations of Cd were measured from samples collected on the Aberjona. The highest Pb concentrations were measured at the USGS and Montvale stations.

fn: icpaes

Location & Date	Zn (mg/kg)	Ba (mg/kg)	Ti (mg/kg)	Co (mg/kg)	Ni (mg/kg)
Wedge					
12-21-91(W)			1570		
12-21-91(1C)			980	800	
12-21-91(1B)			1400		
02-22-92(G)			485	813	
02-22-92(W)	467				
03-29-92(N)			794		
03-29-92(G)			704		
03-29-92(W)	422				
04-18-92(G)			482		
04-18-92(W)	304				
Rte 128					
12-17-91(W)	1920				
02-22-92(G)			338		
02-22-92(W)	2576				
03-29-92(G)			510		
03-29-92(W)	2712				
04-18-92(G)			377		
04-18-92(W)	1742				
Montvale					
07-26-91(G2)					
08-20-91(L)			3300	2700	
12-21-91(3c)			1100	870	82
12-21-91(W)			523		
02-22-92(G)			407		
02-22-92(W)	2360				
03-29-92(G)			686		
03-29-92(W)	1667				
04-18-92(G)			594		
04-18-92(W)	1523				
Horn					
08-20-91(G)			1000		
02-22-92(G)			609		
02-22-92(W)	484				
03-29-92(G)			966		
03-29-92(W)	359				
04-18-92(G)			559		
USGS					
12-21-91(5C)			950		
12-21-91(W)	1393		850		
02-22-92(G)			461		
02-22-92(W)	1797				
03-29-92(G)			847		
03-29-92(W)	497				
04-18-92(G)			666		
04-18-92(W)	1237				
Mean Crustal Concentration*	70	425	5700	25	75

* Reference: Taylor, 1964

Table III.E-6: Results of ICP-AES Analysis for Zn, Ba, Ti, Co and Ni, Samples Collected at Gages 1 to 5

fn: gf

Location & Date	Cd (mg/kg)	Pb (mg/kg)
Wedge		
02-22-92(W)	<1.00	200
03-29-92(W)	<1.69	152
04-18-92(W)	2.58	359
05-22-92(G)	2.29	<236
05-22-92(W)	34.7	<401
06-11-92(N)	1.28	
06-11-92(G)	<0.83	293
06-11-92(W)		376
07-23-92(G)	<1.48	232
07-23-92(W)		174
08-13-92(G)	<2.68	150
09-27-92(G)	<1.27	<135
10-12-92(G)	2.07	191
11-01-92(G)	<0.11	142
Rte 128		
02-22-92(W)	14.4	191
03-29-92(N)	1.20	
03-29-92(W)	11.3	172
04-18-92(W)	14.1	165
05-22-92(G)	4.58	<132
05-22-92(W)	12.3	187
06-11-92(G)	5.24	329
07-23-92(G)	9.44	284
08-13-92(G)	7.52	268
09-27-92(G)	1.75	184
10-12-92(G)	9.12	247
11-01-92(G)	5.90	223
Montvale		
07-26-91(G2)	18.1	
02-22-92(G)	22.0	
02-22-92(W)	14.2	279
03-29-92(N)	2.40	
03-29-92(W)	7.47	215
04-18-92(W)	8.95	251
05-22-92(G)	3.39	<151
05-22-92(W)	18.4	198
06-11-92(G)	<2.51	300
06-11-92(W)		526
07-23-92(G)	4.46	324
07-23-92(W)		419
08-13-92(G)	<1.27	289
09-27-92(G)	1.20	349
10-12-92(G)	6.97	462
11-01-92(G)	2.41	207

Table III.E-7: Results of GFAA Analysis for Cd and Pb, Samples Collected at Gages 1 to 5

Location & Date	Cd (mg/kg)	Pb (mg/kg)
Horn		
02-22-92(W)	<0.16	212
03-29-92(N)	2.20	
03-29-92(G)		
03-29-92(W)	13.5	148
04-18-92(G)		
04-18-92(W)	2.99	159
05-22-92(G)	1.71	<158
05-22-92(W)	<0.04	295
06-11-92(G)	<0.76	197
06-11-92(W)		205
07-23-92(G)	<0.88	<142
07-23-92(W)		256
08-13-92(G)	<1.08	<87
09-27-92(G)	<0.65	240
10-12-92(G)	3.13	332
11-01-92(G)	<1.3	319
USGS		
02-22-92(W)	3.44	295
03-29-92(W)	4.04	238
04-18-92(W)	10.3	226
05-22-92(G)	3.78	<355
05-22-92(W)	2.83	839
06-11-92(G)	5.42	277
06-11-92(W)		346
07-23-92(G)	<1.34	355
07-23-92(W)		405
08-13-92(G)	<0.16	297
09-27-92(G)	<1.95	463
10-12-92(G)	5.19	550
11-01-92(G)	2.43	402
Mean Crustal Average*	0.2	12.5

* Reference: Taylor, 1964

Table III.E-7:(con'd)

APPENDIX III.F

Other Analysis: River Water

- pH
- Temperature
- Conductivity
- TOC Analysis
- ICP-MS
- ICP-AES (Non-Routine Metals)
- GFAA (Non-Routine Metals)

pH: River water pH was measured using a specific ion meter (Orion Research Model 407A) fitted with a 0 to 14 pH electrode (VWR Scientific). Prior to each measurement, pH was calibrated with 4.0 and 10.0 standards and checked with a 7.0 standard. Calibration with 4 and 10 standards was performed until the pH of the 7.0 standard fell within 6.9 to 7.1.

River water pH measurements from February 1991 to January 1993 are illustrated in figure III.F-1 and are presented in table III.F-1. Generally river water pH's tend to be in the near-neutral range between 6.5 to 7.5. The primary exception is gage 1 during the summer months where a pH as high as 9.0 was observed. Possible explanations for the high pH at gage 1 may include: 1) pH fluctuations associated with algal blooms, and 2) discharge of a caustic material to the pond - perhaps lime from residential lawn treatments.

River water pH's during the March/April 1993 high flow events are provided in table III.F-2. The average pH's of the samples collected on March 26, 1993, March 29, 1993, and April 1, 1993 are 7.2, 6.7, and 6.8, respectively. *Within* each event there was a pH range of 0.1 to 0.3 units whereas *between* events a maximum shift of 0.5 pH units was observed. Such a trend, although speculative with the limited amount of data, is indicative that pH varies gradually from event to event with relatively constant values from hour to hour. The lack of variability during a storm event indicates that pH changes are not likely to control the distribution of metals between the dissolved and particulate phases during high flow conditions.

FN:pH

Date	Station				
	USGS Gage #5	Montvale Gage #3	Rte 128 Gage #2	Wedge Pond Gage #1	Horn Pond Gage #4
02-22-91		7.2	7.1		
08-20-91	6.85	6.9		7.2	
08-21-91	6.6		6.95		
08-22-91	6.6	6.7		7.1	7.15
09-21-91	6.9	6.8	6.9	7.1	7.0
11-02-91	6.85	6.85	6.8	7.2	
12-17-91			6.9		
12-21-91	7.0	6.7		7.0	
01-15-92	7.1	7.0	7.1	7.1	
02-22-92	7.4	7.0	7.0	7.65	7.2
03-29-92	7.3	7.0	7.15	7.8	7.3
05-05-92		6.9	6.9	8.3	
05-20-92	7.2	7.25	7.0	8.4	7.4
05-22-92	7.1	7.5	7.1		7.2
06-04-92	7.0	7.0	6.85	7.6	7.0
06-11-92	6.9	7.0	6.8	7.6	7.25
06-18-92	7.0			8.0	
06-19-92	7.0	7.1	7.0	7.7	7.3
06-22-92	6.8				
06-25-92	7.2	6.7	6.5	7.45	7.15
07-02-92		6.7	6.55		
07-14-92	6.9	6.9	6.9	7.5	7.15
07-23-92	6.9	7.0	6.9	7.9	7.2
07-30-92	6.7	6.8	6.9	8.2	6.9
08-06-92	6.8	6.95	7.0	8.6	7.1
08-13-92	6.9	7.0	6.8	9.0	7.2
08-21-92		6.9	6.8	8.1	7.1
08-31-92	7.1	7.2	7.1	8.5	7.3
09-08-92		6.9	6.5		6.9
09-18-92	6.9	6.9	7.0	8.8	7.2
10-02-92	7.25	7.15	6.9	6.9	7.2
10-09-92	6.9	7.1	7.15	7.2	7.4
10-12-92	7.0	6.7	6.6	7.3	6.85
10-23-92	7.0	7.1	7.0	7.2	7.2
11-01-92	7.0	6.9	6.8	7.0	6.85
11-06-92	6.9	6.7	6.8	7.2	6.8
11-13-92	7.0	6.65	6.8	7.0	6.8
11-20-92	6.9	6.9	6.7	6.9	6.8
12-04-92	6.8	6.5	6.4	6.9	6.4
01-06-93	6.3	6.5	6.3	6.35	6.2
01-24-93	6.7	6.65	6.6	6.7	6.6

Table III.F-1: River Water pH

fn:pHs

Date YR-MO-DA-HR	pH
93032614	7.2
93032615	7.2
93032616	7.0
93032617	7.2
93032618	7.1
93032619	7.3
93032620	7.2
93032910	6.7
93032911	6.7
93032912	6.8
93032913	6.8
93032914	6.8
93032915	6.7
93032916	6.8
93032917	6.8
93032918	6.7
93032919	6.7
93032920	6.7
93032921	6.7
93032922	6.7
93032923	6.7
93033000	6.7
93033001	6.7
93033002	6.7
93033008	6.7
93033119	6.8
93040116	6.8
93040117	6.8
93040118	6.8
93040119	6.8
93040120	6.8
93040121	6.8
93040122	6.9
93040123	6.8
93040200	6.9
93040217	6.9

Table III.F-2: pH at Gage 5 During March/April 1993 High Flows

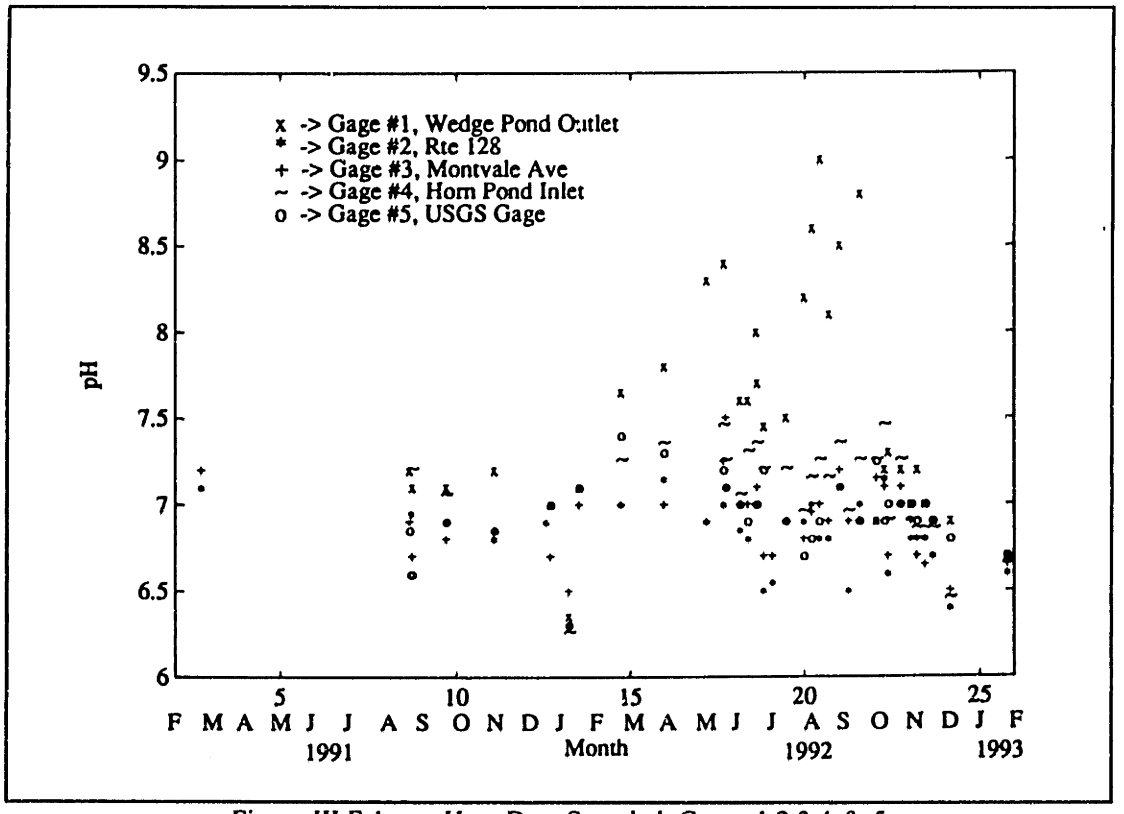

Figure III.F-1: pH vs Date Sampled, Gages 1,2,3,4 & 5

TEMPERATURE: Temperature of the river water was measured by using a mercury thermometer (-20 to 110 °C). Measurements were made by submerging the bulb of the thermometer a few inches below the water surface and allowing the mercury to rise to an equilibrium level.

River water temperatures were measured from February 1991 to January 1993. Results for each of the five monitoring stations are illustrated in figure III.F-2 and are presented in table III.F-3. From figure III.F-2 a clear seasonal trend in water temperature was observed, where temperatures varied from 20 to 30 °C during summer months to near freezing temperatures during winter months. Super-imposed on the seasonal trend, one may also observe a day to day fluctuation of water temperatures on the order of several °C. During the summer months, gage 1 generally had the highest temperatures while gage 2 and gage 4 generally had the lowest. One possible explanation for this observation is that during the summer months water coming into the channel tends to be heated by the warmer air and through solar radiation. The longer the residence time of the water, the longer the time for the water to be heated and thus the higher the water temperatures. Gage 2 and gage 4 stations are on the upper reaches of the Aberjona River and Horn Pond Creek, respectively. As a consequence, the waters reaching these two stations will have a shorter channel residence time (i.e. lower temperatures) than the waters at monitoring stations downstream (gage 1,3, and 5). Waters monitored at gage 1 have very high residence times due to the effect of two reservoirs, Horn Pond and Wedge Pond. Other possible explanations for water temperature differences between stations may be associated with: 1) differences in groundwater temperatures from various areas in the watershed, 2) differences in water temperatures coming from non-groundwater sources, and 3) heating of water associated with frictional resistance of flowing water over the channel bed.

Temperature of the river water is of importance in theoretical/empirical computations of sediment transport capacities, due to its effect on the viscosity of the water. Additionally, water temperature is helpful in determining the "growth" of particles of biological origin.

FN:tempera

Date	Station				
	USGS Gage #5	Montvale Gage #3	Rte 128 Gage #2	Wedge Pond Gage #1	Horn Pond Gage #4
02-22-91		7	6.6		
03-29-91		9	10		
04-15-91		9	10	10	
05-20-91		17.5		24	
05-24-91	20			24	19.5
05-28-91	20.5	21		27	20
05-30-91		21	26		
06-07-91	19	22	16	23	17.5
06-20-91	22	23.5	25		
07-16-91	24	26	22	28	20.5
07-26-91	23		22	26	21
08-01-91		20	22	26	22
08-13-91	23	24		27	21
08-20-91	21	20		22	20
08-21-91	18.5		18.5		
08-22-91	19	22		19.5	20
09-21-91	13.5	14.5	16	18	13
11-02-91	11	10.5	12	12	
12-17-91			3		
12-21-91	2	2		2	
01-15-92	2	0.5	2	2	
02-22-92	3.5	2.5	3	4	3.5
03-29-92	5	4.5	9	7	8
04-18-92	6	5	6	7	6
05-05-92					
05-20-92	17	21	20	21	16
05-22-92	19	24	23	21	18
06-04-92	20	22	18	23.5	17
06-11-92	21	19	17.5	22.5	17
06-18-92	22			26	
06-19-92	21	23	23.3	25	20
06-22-92	21.8				
06-25-92	19	16.5	18.5	23	17
07-02-92	23	21	18	26	19.3
07-14-92	22	19.5	19.3	23.5	18
07-23-92	21	19.2	19.2	23.5	17.5
07-30-92	22	22	25	24.5	20.5
08-06-92	20.5	20	23	23.3	18
08-13-92	22.2	19.3	19.3	24.5	18
08-21-92		17	17.5	22	16
08-31-92	21	21	23	23.2	19
09-08-92	19	18.5	19	21	17
09-18-92	22	22.3	22.5	27	20
09-27-92	17.5	16.5	16.2	19.5	16
10-02-92	17	11.5	13.4	12	10
10-09-92	13	13	14.5	16.2	13
10-12-92	16	15	15	17.5	14.8
10-23-92	11.5	11	13	14	10.5
11-01-92	8.5	6	8	9	6.8
11-06-92	9.5	9	10	10	9
11-13-92	11	12	12.5	10	11
11-20-92	5	4	6	7	3
12-04-92	5	5	6.3	6	5
12-17-92	3	4	4.5	2	4
12-23-92			4		
01-06-93	4.3	4	4.3	3	4
01-24-93	4	3	4.5	3.5	4.5

Table III.F-3: River Water Temperature (°C)

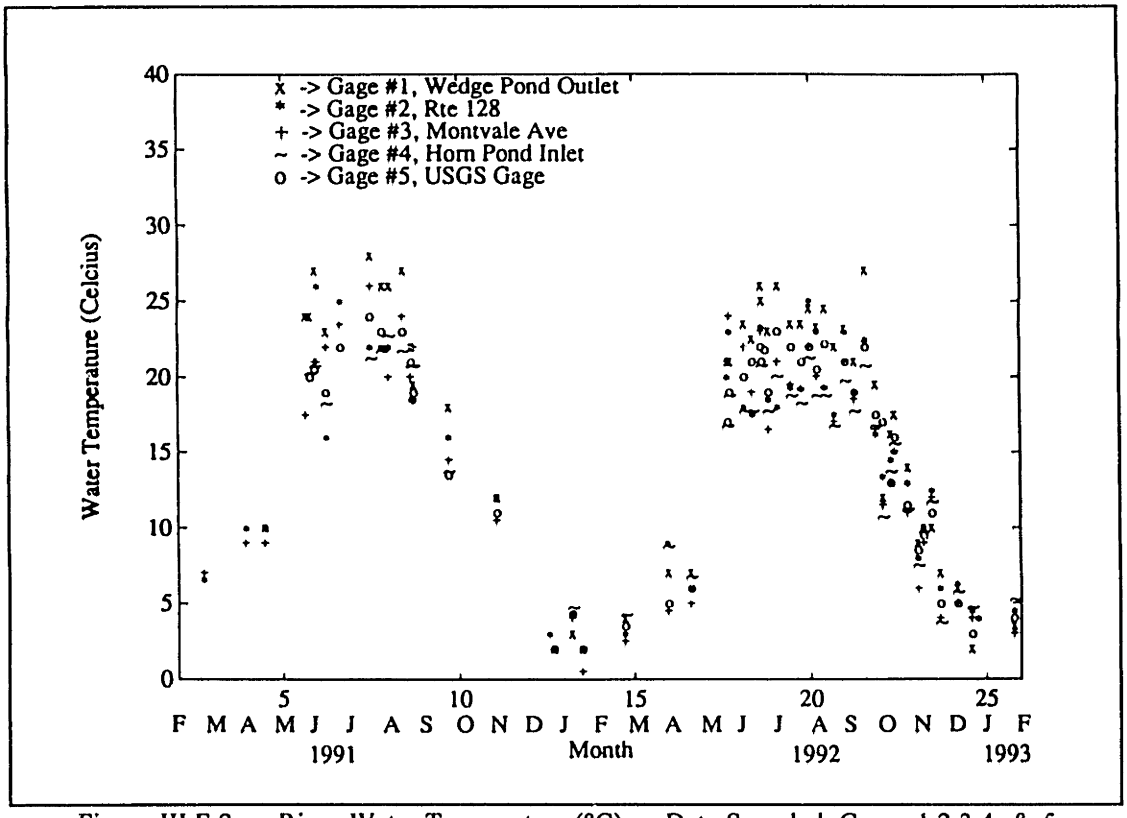

Figure III.F-2: River Water Temperature (°C) vs Date Sampled, Gages 1,2,3,4, & 5

CONDUCTIVITY: Conductivity measurements are usually performed by immersing two metallic plates in an aqueous sample. A current is transmitted from one plate to the other, and the resistance of the solution between the plates is measured. The reciprocal of the resistance is equal to the conductance, which is given in units of Siemens and symbolized as mho.

Conductivity is an indirect measure of dissolved ions in water. Larger conductance implies a higher concentration of dissolved ions in the sample solution.

Conductivity was measured using a Cole Parmer Amber Science Model 604 Conductivity Meter. The meter was checked for linearity using 0.01N KCl and 0.035N NaCl standards. All sample measurements were performed in triplicate. The average standard deviation of the analysis was 8 μmho.

River water conductivity was measured during the March 29 through April 2, 1993 high flow events. Results are provided in table III.F-4 and in figure III.F-3. From figure III.F-3 a strong inverse relationship between conductivity and flow is observed. This relationship is indicative of a dissolved ion dilution effect where water associated with high flows dilute more concentrated waters associated with lower flows.

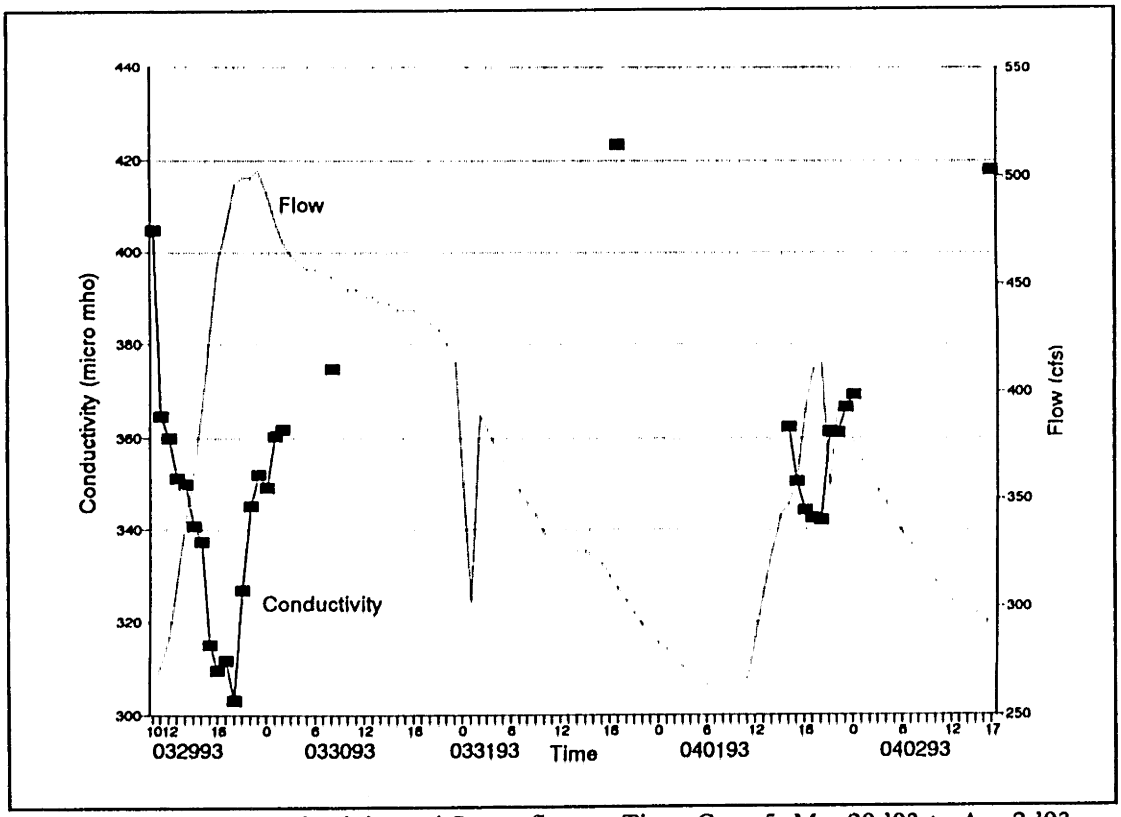

Figure III.F-3: Conductivity and Streamflow vs Time, Gage 5, Mar 29,'93 to Apr 2,'93

fn:cond

Date YR-MO-DA-HR	Conductivity (micro mho)
93032910	405
93032911	365
93032912	360
93032913	351
93032914	350
93032915	341
93032916	337
93032917	315
93032918	309
93032919	312
93032920	303
93032921	327
93032922	345
93032923	352
93033000	349
93033001	360
93033002	362
93033008	375
93033119	423
93040116	362
93040117	350
93040118	344
93040119	342
93040120	342
93040121	361
93040122	361
93040123	367
93040200	369
93040217	418

Table III.F-4: River Water Conductivity at Gage 5 During March/April 1993 High Flows

TOTAL ORGANIC CARBON: Total Organic Carbon (TOC) analysis is based upon the principle that molecules absorb infrared radiation at a characteristic wavelength. In a TOC analyzer, samples are injected into a reaction chamber which is maintained at elevated temperatures (850 to 900 °C) and which is packed with a catalyst. Upon introduction into the chamber, the sample is converted into a gaseous phase and oxidized. During this process all of the carbon originally present in the sample is converted to carbon dioxide; the concentration of carbon dioxide generated is directly proportional to the concentration of carbon in the sample. The absorption of carbon dioxide is measured using an infrared radiation detector, set at a wavelength unique to carbon dioxide absorption. The greater the absorption the higher the concentration of carbon dioxide.

All analysis was performed using an Ionics Model 555 Carbon Analyzer. Oxygen was the carrier gas. Peak height analysis was used for the determination of concentrations. Peaks were obtained from the analyzer's digital display. The time distribution of the signal was qualitatively checked through use of a chart recorder.

The instrument was calibrated with potassium acid phthalate standards at 2:1 dilutions in concentration ranges which bridged the sample concentrations. To assure that only organic carbon was measured, inorganic carbon was stripped from the samples. This step of sample preparation included adding 4 drops of 10% H_3PO_4 and purging the sample with N_2 gas for 4 minutes. 50 µl samples were injected into the analyzer.

Results of TOC analysis, for filtered and unfiltered samples, are provided in figure III.F-4 and in table III.F-5. TOC concentrations for the March to April 1993 sample set generally ranged between 2 and 12 mg/l. The primary exception is a TOC between 15 to 18 mg/l observed for sample 93030711, which corresponded to a low flow condition. For most samples the difference between filtered and unfiltered concentrations (equal to the particulate concentration) was generally on the order of a few mg/l. This difference was consistent with suspended sediment volatile analysis which also resulted in volatile ss concentrations on the order of a few mg/l.

The constancy of the particulate TOC concentration can be contrasted with the large changes in total suspended sediment concentration during the March - April 1993 storms. Such a result indicates that the flux of metals associated with the organic phase would increase in direct proportion to increases in streamflow, whereas the flux of metals associated with the non-organic phase of the suspended sediment would increase in proportion with the increases in streamflow and increases in the non-organic suspended sediments.

Sample Date/Time YR-MO-DA-HR	Flow (cfs)	Unfiltered TOC (mg/l)	Filtered TOC (mg/l)
93030711	33.21	17.46	15.82
93032614	87.12	6.21	6.44
93032615	141.70	7.00	5.13
93032616	101.10	7.19	4.85
93032617	144.00	5.18	6.49
93032618	126.50	6.44	4.11
93032619	71.46	6.56	3.69
93032620	65.99	5.69	5.93
93032910	264.20	12.79	5.93
93032911	272.20	6.58	4.43
93032912	285.80	7.19	4.76
93032913	311.30	7.61	3.83
93032914	339.50	8.17	4.06
93032915	362.20	7.84	4.39
93032916	391.70	8.82	4.11
93032917	428.30	10.55	3.83
93032918	459.80	6.67	3.69
93032919	476.00	11.57	4.25
93032920	495.70	8.03	4.20
93032921	499.10	7.70	4.43
93032922	499.10	9.24	4.81
93032923	502.40	7.65	4.39
93033000	492.40	9.71	4.53
93033001	479.20	8.87	4.71
93033002	469.50	5.97	4.90
93033008	453.40	7.00	4.39
93033119	308.40	6.72	6.06
93040116	348.00	6.61	5.05
93040117	359.40	8.44	2.71
93040118	391.70	8.13	4.95
93040119	410.00	8.18	2.67
93040120	413.00	7.07	7.37
93040121	356.50	5.76	2.58
93040122	391.70	5.50	1.87
93040123	385.70	6.06	4.48
93040217	291.40	6.46	4.34

Table III.F-5: TOC Analysis for Samples Collected at Gage 5 During March to April 1993

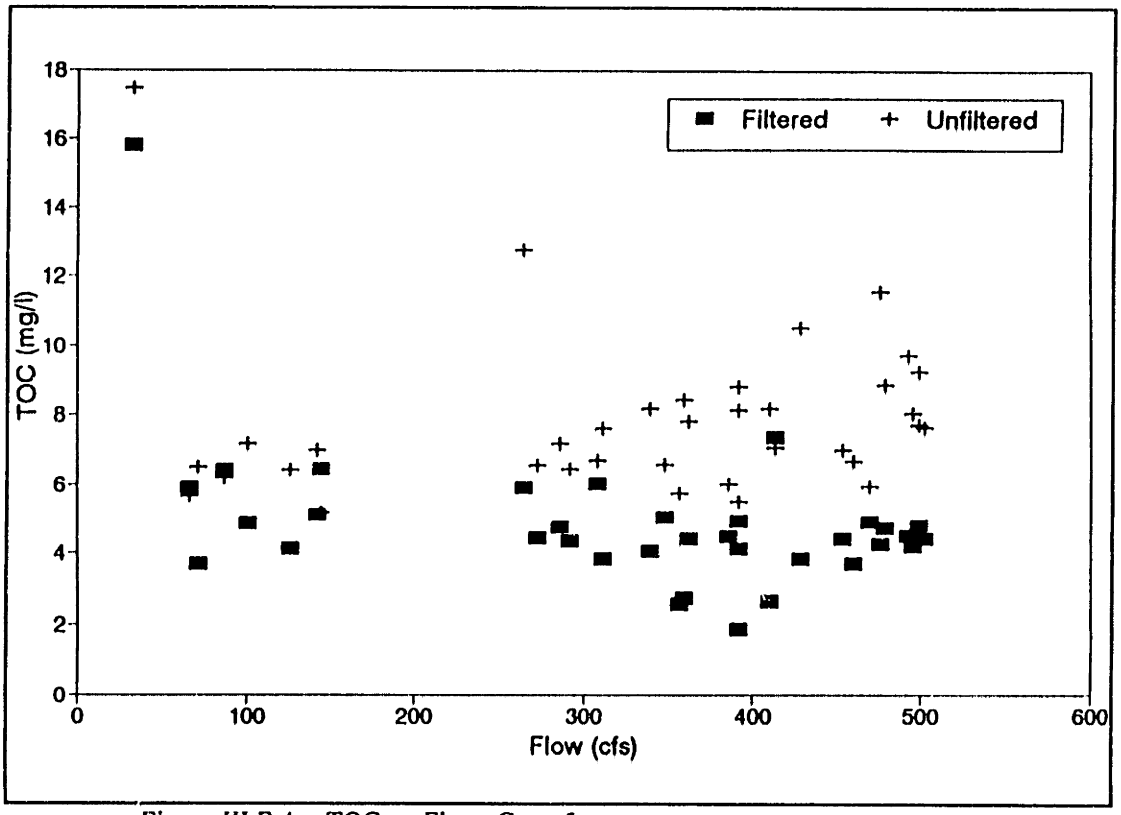

Figure III.F-4: TOC vs Flow, Gage 5
Samples Collected March 29, 1993 to April 2, 1993

NON-ROUTINE METAL'S ANALYSIS

Non-routine metal's analyses (metal's analysis other than As,Cr,Cu and Fe) were performed using a variety of analytical techniques including: ICP-AES, GFAA, and ICP-MS. ICP-AES and GFAA instrumentation and methodologies are discussed in section III.4. This appendix includes: 1) a discussion of ICP-MS instrumentation and methodology, and 2) a discussion of dissolved metals data for metals *other than* As,Cr,Cu, and Fe.

ICP-MS: Inductively Coupled Plasma Mass Spectroscopy (ICP-MS) is similar to ICP-AES (discussed in Section III.4) only in the manner in which the sample is initially treated. Like ICP-AES, liquid samples are nebulized and introduced into an inductively coupled argon plasma. However, after this point ICP-AES and ICP-MS are very different. Unlike ICP-AES where the objective is to produce excited atoms which emit light, the primary purpose of the plasma for ICP-MS analysis is for the production of ions. For ICP-MS, a section of the plasma core containing positive sample ions is introduced into a quadrupole mass filter through a set of small orifices and electrostatic lenses. The quadrupole then transmits ions of a selected mass to charge ratio to an ion detector. Each naturally occurring element has a unique set of integer mass to charge ratios corresponding to its stable isotopes, allowing for identification of the element being detected. The ion detector quantifies the number of ions in the sample and therefore provides a means of determining the concentration of the element in the sample.

All ICP-MS analysis was performed using a VG PlasmaQuad under the supervision of Mr. Barry Grant. The system consisted of a horizontally mounted ICP, a quadrupole mass filter, ion detector, a set of vacuum pumps, and data processing/system monitoring software supplied by VG. The interface between the plasma and the quadrupole consisted of two cones and a series of cylindrical electrodes designed to extract and focus the ions from the interface into the quadrupole.

The ICP-MS was run both in survey scan analysis and in quantitative analysis modes. Survey scan analysis is a *semi*quantitative method which scans a sample for most of the elemental mass range. Quantitative analysis mode is a data acquisition methodology for fully quantitative work and is well suited for analysis of only a few elements per sample. Peak jumping option was used for all quantitative analysis.

Prior to all analysis, the PlasmaQuad was initially tuned using a 10 µg/l Indium (mass 115) standard. Blanks and standards were included in each sample set. Results are reported only for those elements which were significantly above detection limits. (Detectable is defined as: a sample concentration higher

than the average blank value plus 3 standard deviations of the blank.) All samples and standards were prepared in 1% HNO_3.

Survey Scan Analysis

Survey scan analysis was performed on 3 blanks samples and on 3 river water samples. The samples analyzed were collected October 12, 1992 at Route 128, USGS, and Horn Pond Stations. Results for these samples are provided in table III.F-6. Results indicate that V, Mn, Ni, Zn, Sr, Mo, Sb, I, La, Ce, Hf, Au, Tl, and Pb were measured at detectable levels. Of these elements Mn concentration was elevated by at least a factor of two above average river water (Martin and Meybeck, 1979), while Ni and Au were elevated by over a factor of ten. The highest enrichment of Mn occurred for the Route 128 sample whereas the highest enrichment of Au occurred in the Horn Pond sample.

Quantitative Analysis

Quantitative lead (Pb) analysis was performed for most of the dissolved phase samples collected. Analysis included detection of two lead isotopes (206 & 208). Generally, concentrations from lead 208 detection were 7% higher (standard deviation of the difference was equal to 3%) than concentrations from the lead 206 detection. The average of the concentrations obtained from lead 208 and lead 206 is the reported concentration for the analysis. Standards were generally characterized by: 1) a mean coefficient of variations equal to 3% and, 2) a standard deviation of the coefficient of variation equal to 4%. Results of the analysis are given in table III.F-7 and are plotted in figures III.F-5 and III.F-6. In figure III.F-6, the direction of the arrows is in the direction of increasing time. Solid lines between successive data points indicates that one hour elapsed between the collection of each sample. A dashed line indicates that more than one hour elapsed.

Generally, the concentration of dissolved lead for the river system was between 0.2 μg/l and 6.0 μg/l. There appears to be no strong difference in concentrations between gaging stations (figure III.F-5), indicating a watershed wide distribution of dissolved lead contamination. Additionally, both figure III.F-5 and III.F-6 indicate that there was no strong relationship between lead concentrations and flow. The only trend observed is that the lowest lead concentrations were observed during low flows whereas the highest concentrations were observed during the December and March high flow events, indicating that perhaps during winter/spring storms an additional source of lead is mobilized. However, at this point it is emphasized that prior to gathering more data, an interpretation of this weak trend is purely speculative.

ICP-AES: ICP-AES analysis was used to measure Zn, Al, Ba, Si, Ti, Co concentrations. Results (table III.F-8) indicate that for some samples Zn and Ti were elevated above mean river water (Martin & Meybeck, 1979) by a factor of two and Co was elevated by over a factor of ten.

GFAA: GFAA analysis was used to measure a few dissolved samples for cadmium. Results are given in table III.F-7. Concentrations ranged from 0.7 µg/l to 2.2 µg/l. The highest concentrations corresponded to samples collected on the Aberjona River. Results indicate that cadmium concentrations within the river are significantly elevated above the mean river water concentration, which was estimated at a value of 0.1 µg/l by Merian, 1991.

fn: icpmsd

Element	Mass	Dissolved Blanks ID			Blank Statistics			Dissolved Sample Concentration			Ave
		030792 DB	030792 DB	101292 DB	Ave	Std	Ave+3Std	101292D2 Rte 128	101292D5 USGS	101292D4 Horn Pond	River Water*
V	46	0.895	0.89	2.231	1.3387	0.631	3.23	1.41	1.67	1.95	1
Mn	55	1.288	1.242	1.765	1.4317	0.236	2.14	32.08	16.98	7.33	8.2
Ni	60	49.783	53.138	59.84	54.254	4.181	66.80	15.52	11.49	12.46	2.2
Zn	66	1.252	1.322	2.673	1.749	0.654	3.71	37.76	10.59	3.35	30
Zn	68	3.007	3.236	8.649	4.964	2.607	12.79	39.02	10.10	2.47	30
Sr	88	0.794	0.688	0.455	0.6457	0.142	1.070	11.00	12.02	11.82	60
Mo	98	0.478	0.534	0.682	0.5647	0.086	0.823	0.45	0.05	0.08	0.5
Sb	121	0.052	0.055	0.062	0.056	0.004	0.069	0.06	0.04	0.01	1
I	127	0.537	0.514	0.894	0.648	0.174	1.170	6.25	2.54	4.94	
La	139	0.015	0.025	0.032	0.024	0.007	0.045	0.01	0.02	0.02	0.05
Ce	140	0.026	0.029	0.023	0.026	0.002	0.033	0.04		0.02	0.08
Hf	178	0.061	0.052	0.049	0.054	0.005	0.069		0.02		
Au	197	0.079	0.055	0.067	0.067	0.01	0.096	0.03	0.01	0.04	0.002
Tl	205	0.016	0.01	0.017	0.014	0.003	0.024	0.02	0.00	0.01	
Pb	208	0.053	0.128	0.128	0.103	0.035	0.209	0.82	1.61	0.65	1

* Martin and Meybeck, 1979

Table III.F-6: Results of ICP-MS Elemental Scans for Dissolved Phase Samples Collected at Gage 2,4, and 5 on October 12, 1992

fn:gfd

Date/Time YR-MO-DA-HR	DS Cd (ug/l) (0.5um)	DS Pb (ug/l) (0.5um)
Wedge Pond		
92022214		2.18
92032915		3.02
92041814		1.36
92052209		2.25
92061115		0.74
92072316		0.28
92081314		0.81
92092714		0.65
92101213		1.20
92110114	0.75	1.30
92121715		1.64
93012511		1.67
Rte 128		
92022209		1.95
92032915		1.30
92041809		1.40
92052215		1.26
92061110		2.47
92072309		0.61
92081309		0.74
92092709		1.28
92101209		1.27
92110109	1.36	1.17
92121710		2.99
93012509		1.07
93052509		0.31
Montvale		
92022211		1.71
92032909		1.88
92041810		1.04
92052214		1.37
92061112		1.98
92072311		0.52
92081310		0.55
92092711		1.23
92101210		2.27
92110110	2.21	0.85
92121711		3.01
93012510		1.14
Horn Pond		
92022213		0.78
92032914		1.28
92041812		0.78
92052211		0.38
92061114		0.78
92072313		0.53
92081312		0.51
92092712		1.52
92101212		1.07
92110112	0.68	0.50
92121712		1.40
93012511		1.42

Table III.F-7: Results of Cd and Pb Analsis for Dissolved Phase Samples
Cd analyzed by GFAA, Pb analyzed by ICP-MS

Date/Time YR-MO-DA-HR	DS Cd (ug/l) (0.5um)	DS Pb (ug/l) (0.5um)
USGS		
92022215		1.32
92032912		1.71
92041815		1.80
92052208		1.76
92061117		2.18
92072315		0.82
92072922		1.42
92081008		1.04
92081010		0.75
92081012		1.00
92081014		1.07
92081016		1.12
92081018		1.17
92081020		0.96
92081022		0.82
92081100		0.94
92081102		1.02
92081104		1.06
92081315		1.23
92081801		1.65
92081802		2.49
92081803		2.09
92081804		2.16
92081805		1.73
92081806		1.59
92081807		1.62
92081808		1.58
92081809		2.17
92081810		1.51
92081811		1.48
92081812		1.57
92081813		2.40
92081814		1.39
92081815		1.57
92081816		1.40
92081817		1.60
92081818		1.53
92081819		1.41
92081820		1.77
92081821		1.48
92081822		1.87
92081823		1.27
92081900		1.39
92092715		2.55
92101215		2.48
92110115	2.16	1.50
92112305		4.42
92112307		3.32
92112308		3.46
92112407		2.13

Table III.F-7: (con'd)

Date/Time YR-MO-DA-HR	DS Cd (ug/l) (0.5um)	DS Pb (ug/l) (0.5um)
USGS (con'd)		
92121119		4.25
92121120		4.69
92121121		4.78
92121122		3.71
92121123		3.86
92121200		3.85
92121201		2.51
92121202		2.96
92121203		2.98
92121204		1.99
92121204		1.87
92121206		1.87
92121207		1.96
92121208		1.80
92121209		1.97
92121210		1.67
92121216		1.82
92121217		1.92
92121218		1.87
92121713		3.55
93012513		1.79
93032614		2.85
93032615		2.88
93032616		2.92
93032617		3.34
93032618		2.91
93032619		2.73
93032620		4.94
93032910		1.42
93032911		1.89
93032912		1.75
93032913		1.89
93032914		2.22
93032915		2.12
93032916		1.88
93032917		2.12
93032918		2.17
93032919		2.26
93032920		2.43
93032921		2.29
93032922		2.20
93032923		2.53
93033000		2.17
93033001		2.05
93033002		2.40
93033008		1.98
93033119		2.93
93040116		4.44
93040118		5.02
93040120		5.63
93040123		3.55
93040217		3.08
93052509		1.14

Table III.F-7: (con'd)

fn:icpaesd

Location & Date	Filter Type	Zn (mg/L)	Al (mg/L)	Ba (mg/L)	Si (mg/L)	Ti (mg/L)	Co (mg/L)
Wedge							
02-22-92	G		0.02	0.02	2.80		
03-29-92	G		0.09	0.02	2.60		
04-18-92	G				1.40		
05-22-92	G			0.01	0.06		
06-11-92	G						
07-23-92	G						
08-13-92	G						
09-27-92							
Rte 128							
02-22-92	G	0.20	0.04	0.04	4.70		
03-29-92	G	0.14	0.06	0.02	4.00		
04-18-92	G	0.13	0.05		3.40		
05-22-92	G			0.03	3.20		
06-11-92	G						
07-23-92	G						
08-13-92	G						
09-27-92							
Montvale							
02-22-92	G	0.11	0.03	0.03			
03-29-92	G	0.13	0.04	0.03	3.60		
04-18-92	G	0.07	0.03	0.02	3.30	0.01	0.01
05-22-92	G			0.03	3.20		
06-11-92	G						
07-23-92	G						
08-13-92	G						
09-27-92							
Horn							
02-22-92	G			0.02	4.70		
03-29-92	G		0.03	0.02	3.70	0.03	
04-18-92	G		0.04	0.02	3.60	0.01	
05-22-92	G			0.03	2.60		
06-11-92	G						
07-23-92	G						
08-13-92	G						
09-27-92							
USGS							
02-22-92	G		0.02	0.03	4.20		
03-29-92	G			0.02	2.90		
04-18-92	G			0.02	2.80		
05-22-92	G			0.03	3.10	0.01	
06-11-92	G						
07-23-92	G						
08-13-92	G						
09-27-92							
Ave River Water*		0.03	0.05	0.06	5.42	0.01	0.0002

* Reference: Martin & Meybeck, 1979

Table III.F-8: Results of ICP-AES Analysis for Zn, Al, Ba, Si, Ti & Co Dissolved Phase Samples at Gages 1,2,3,4 & 5

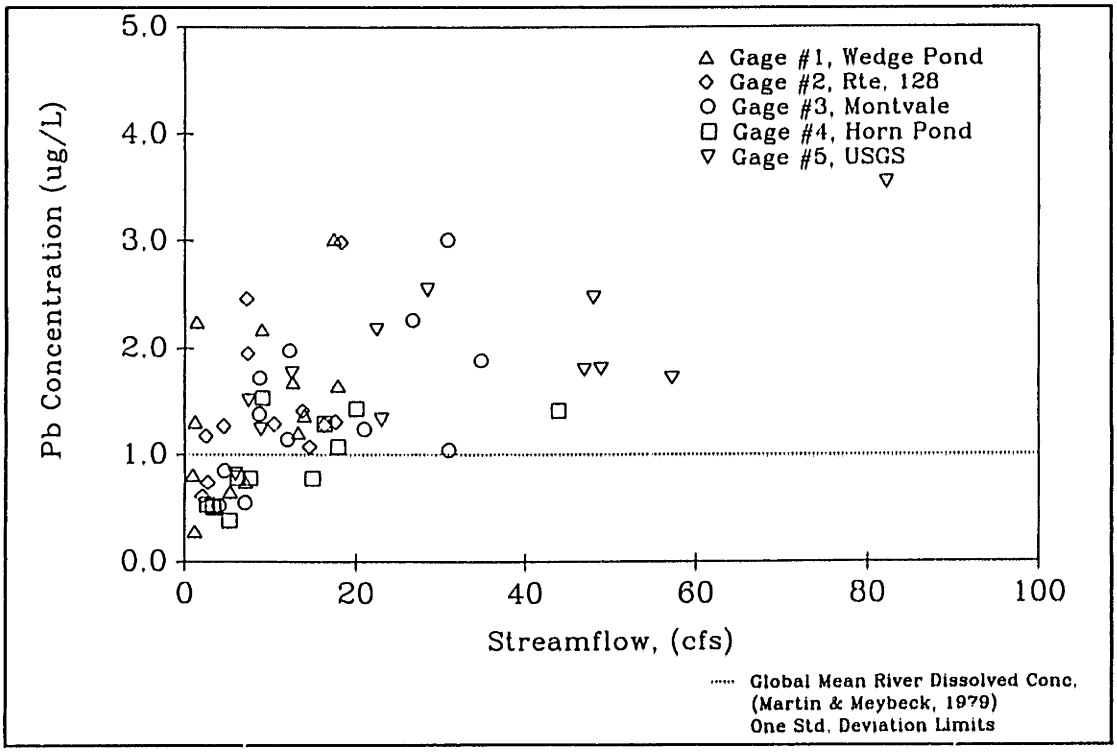

Figure III.F-5: Streamflow vs Dissolved Phase Pb Concentration, Gages 1,2,3,4, & 5
(Sample filtered through a 0.5 μm pore size filter)

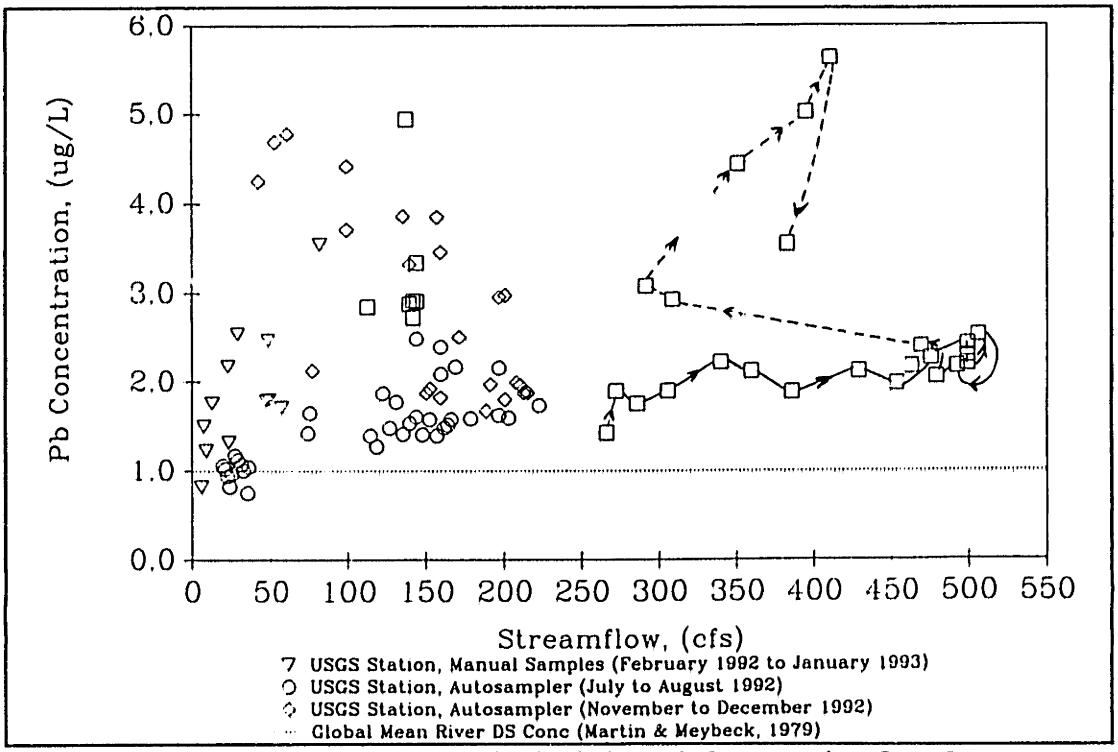

Figure III.F-6: Streamflow vs Dissolved Phase Pb Concentration, Gage 5
(Samples filtered through a 0.5 μm pore size filter)

APPENDIX III.G

River Bottom Sediment Analysis

- Specific Gravity Analysis
- X-Ray Diffraction Analysis
- Grain Size Distributions
- Volatile Solids Analysis versus Particle Size
- Metal Concentrations versus Particle Size
- Sequential Extractions

SPECIFIC GRAVITY ANALYSIS: Specific Gravity analysis was performed using a pycnometer test following ASTM Standard D854-58. Results are given in table III.G-1. The overall average specific gravity of all the samples was 2.64 which is a typical value for quartz. (Das, 1985)

Knowledge of the specific gravity of the bottom sediments was necessary for computing sediment transport capacities from theoretical/empirical relationships.

Sample Description	Specific Gravity
Rte 128 05-31-91 East Bank	2.65
Rte 128 05-31-91 Center	2.68
Montvale 05-31-91 Center	2.68
Montvale 05-31-91 West Bank	2.55

Table III.G-1: Results of Specific Gravity Analysis

X-RAY DIFFRACTION ANALYSIS: The primary mineral identified for the bottom sediment samples analyzed was quartz. Refer to Appendix III.E for details.

The mineralogical composition of the sediment is one indicator of its metal carrying capacity. Pure quartz typically does not have a large amount of metals entrained within its crystal structure nor is it particularly effective at sorbing metals. (Dzombak & Morel, 1990)

GRAIN SIZE DISTRIBUTIONS: Grain size distribution analysis was performed by wet sieving using standard ASTM sieves. Water and fines were collected in an evaporating dish. Sediments collected in the sieves and evaporating dish were dried in an oven over a three day period. Once dried, the sieves were placed on a shaker for 30 minutes after which they were weighed. The mass of the dry sediments collected on each sieve was then computed.

Results of the analysis are given in tables III.G-2 and III.G-3 and figures III.G-1, III.G-2, and III.G-3. The data indicate that the grain size distribution of the river bottom sediments is fairly uniform in the sand size range. Typical d_{50} (diameter corresponding to 50% finer) for the samples measured varied from 0.25 to 0.55 mm, where slightly finer sands were generally measured along the channel banks and slightly coarser sands were measured in the center of the channel.

Knowledge of the grain size distribution analysis was necessary for computing sediment transport capacities from theoretical/empirical relationships.

FN: gsize

Sieve Number	Sieve Opening (mm)	Percent Finer				
		Rte 128 05-30-91 East Bank	Rte 128 05-30-91 Center	Montvale 05-30-91 East Bank	Montvale 05-30-91 Center	Montvale 05-30-91 West Bank
10	2	99.5	97.6	99.8	97	98.3
25	0.71	94.6	62.9	94	68.9	95
40	0.42	74.6	25.8	88	31.5	85.8
50	0.3	54.1	11.4	73.7	10.2	60
100	0.149	21.4	2.4	29.7	1.7	26.7
200	0.074	4.8	0	8.3	0.8	7.5
d50 (mm)		0.25	0.55	0.25	0.55	0.25

Table III.G-2: Bottom Sediment Size Distributions for Samples Collected May 30, 1991

Sieve Number	Sieve Opening (mm)	Percent Finer	
		Rte 128 01-31-92 East Bank	Rte 128 01-31-92 Center
12	1.68	99	84.1
25	0.71	80.2	60
40	0.42	35.4	36.8
60	0.25	10.4	13.3
80	0.177	4.8	5.4
100	0.149	2.8	3
270	0.053	0.4	0.4
d50 (mm)		0.4	0.5

Table III.G-3: Bottom Sediment Size Distributions for Samples Collected January 31, 1992

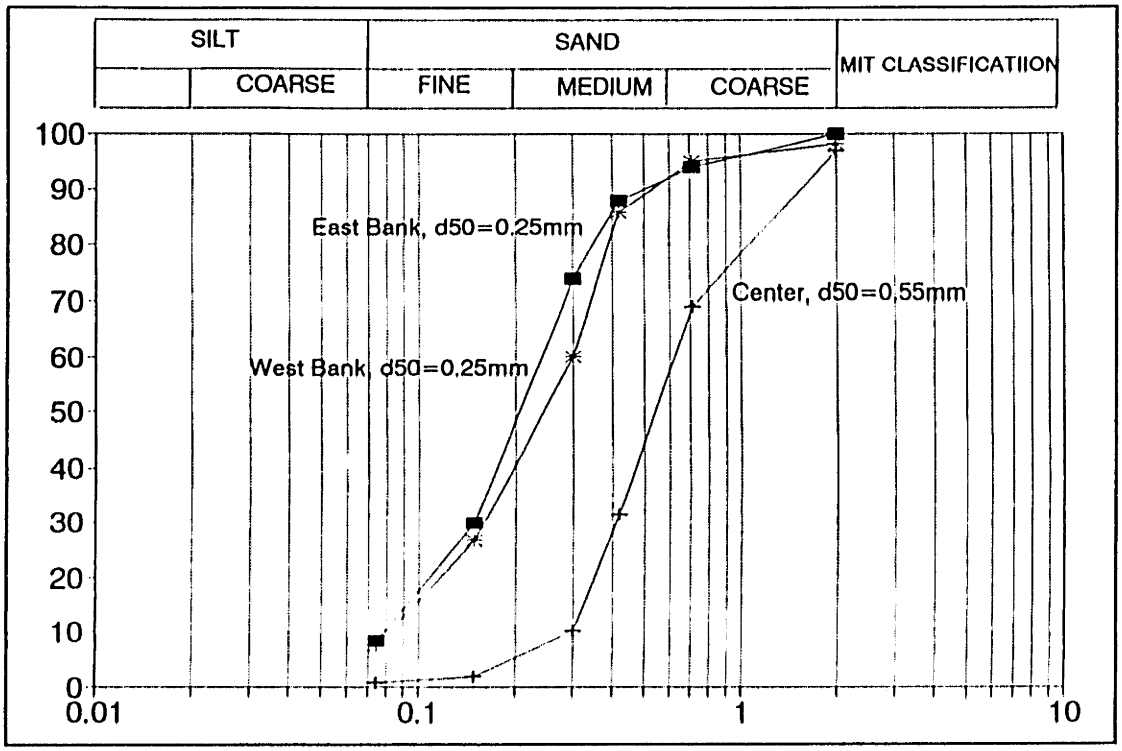

Figure III.G-1: Bottom Sediment Size Distribution for Samples Collected at Montvale, May 30, 1991

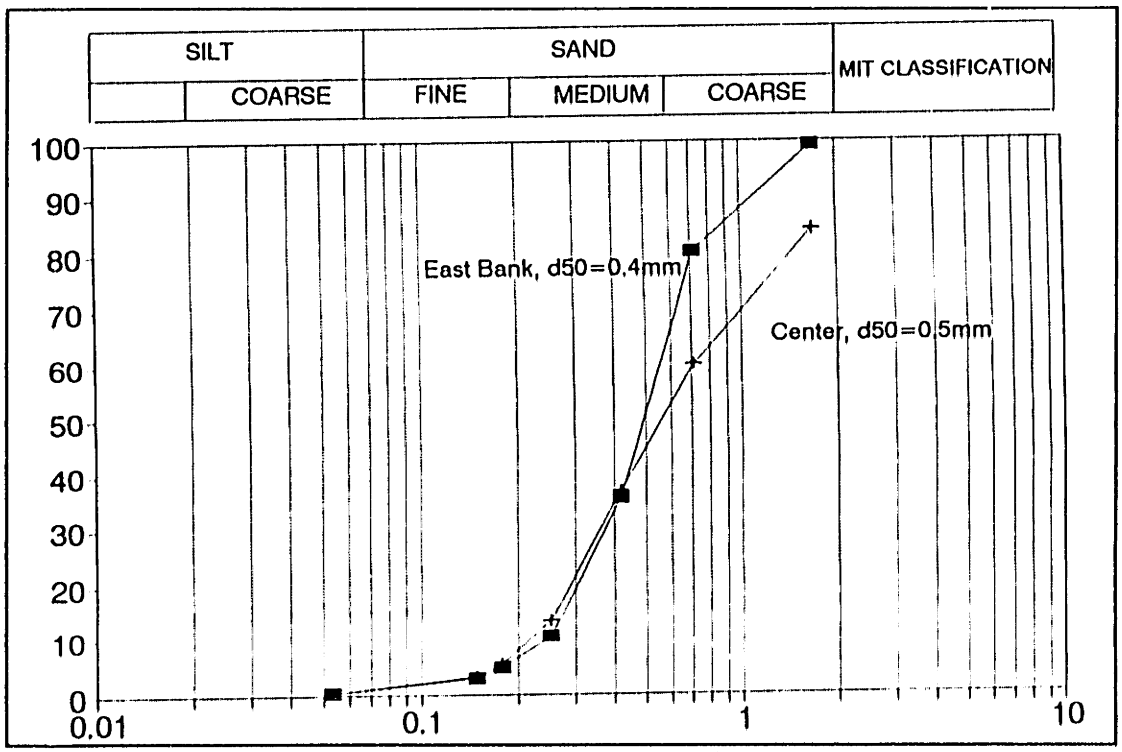

Figure III.G-2: Bottom Sediment Size Distribution for Samples Collected at Route 128, May 30, 1991

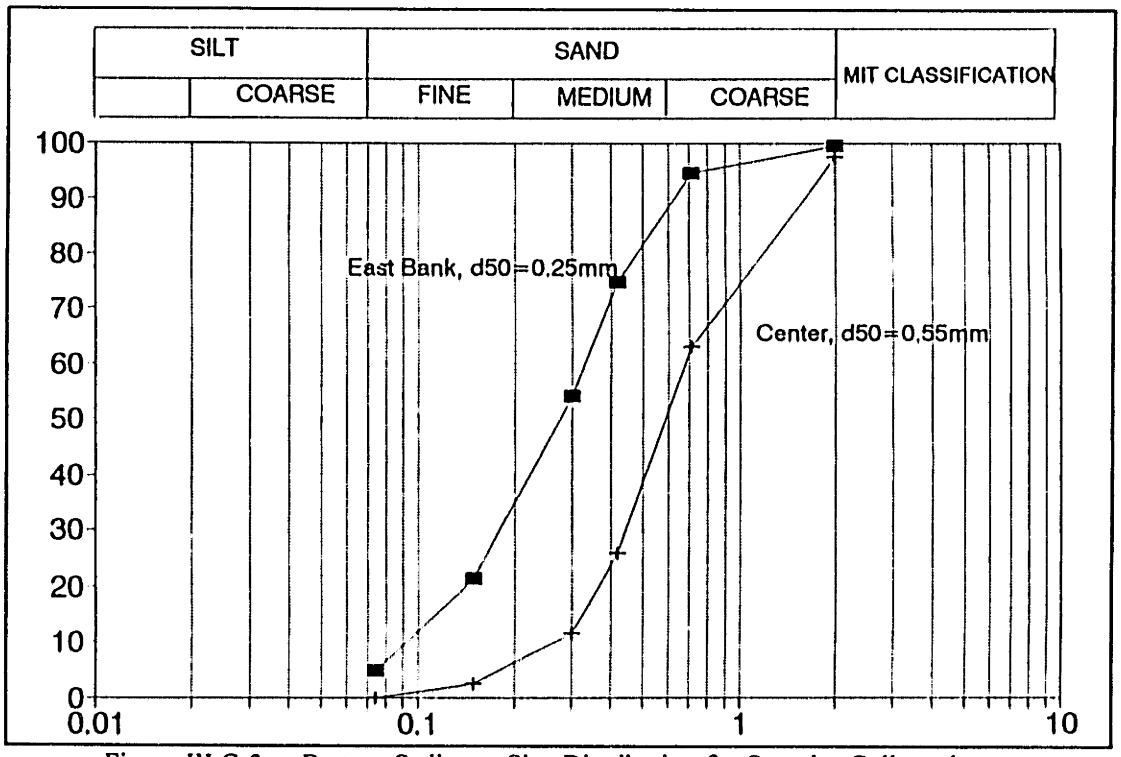

Figure III.G-3: Bottom Sediment Size Distribution for Samples Collected at Route 128, January 31, 1992

VOLATILE SOLIDS ANALYSIS VERSUS PARTICLE SIZE: The volatile solid mass provided a rough estimate of the organic material present in the sample. For this analysis, a bottom sediment sample was placed in a pre-weighed drying tin and was dried overnight at 90 °C. The sample was then: 1) cooled in a desiccator, 2) reweighed, and 3) combusted in a muffle furnace (Thermolyne Type 1400 Furnace) for 5 hours as 450 °C. Once combusted, the sample was then cooled in a desiccator and again reweighed. The difference in sample mass before and after combustion was the mass of the volatile sediments.

Two river bottom sediments were collected for volatile analysis. These samples were both collected on January 31, 1992 at Route 128. One sample was collected at the center of the channel while the other was collected at the east bank of the channel. Each of these samples were sieved and dried. For each of the bottom sediment samples, volatile analysis was performed on: 1) one unsieved aliquot (a composite sample), and 2) sample aliquots retained on each of the sieves. Results of the analysis are provided in table III.G-4 and in figures III.G-4 and III.G-5. The number next to each data point on figures III.G-4 and III.G-5 is the weight fraction of the sample retained on the corresponding sieve. The "composite check" is the concentration of volatile sediments by adding-up the contribution from each of the sieved aliquots. The closer the composite sample concentration is to the "composite check," the better the data quality.

Figure III.G-4 and III.G-5 indicate that volatile solids concentrations increase with decreasing particle size. Since organic matter can potentially sorb metals, fines may serve as an efficient means by which metals are transported in association with the particulate phase.

fn: organic

Sieve Number	Sieve Opening (mm)	Center		East Bank	
		Fraction Retained	% Volatile	Fraction Retained	% Volatile
12	1.680	0.159	0.7	0.010	1.67
25	0.725	0.241	1.1	0.188	0.40
40	0.425	0.232	0.7	0.448	0.38
60	0.250	0.235	0.7	0.250	0.51
80	0.180	0.079	0.6	0.056	0.72
100	0.150	0.024	0.8	0.020	0.83
270	0.053	0.026	1.6	0.024	2.19
Evap Dish	0.000	0.004	4.8	0.004	13.00
Composite Check			0.83		0.60
Composite Sample			0.91		0.55

Table III.G-4: Volatile Solids Analysis for River Bottom Sediments Collected at at Route 128, January 31, 1992

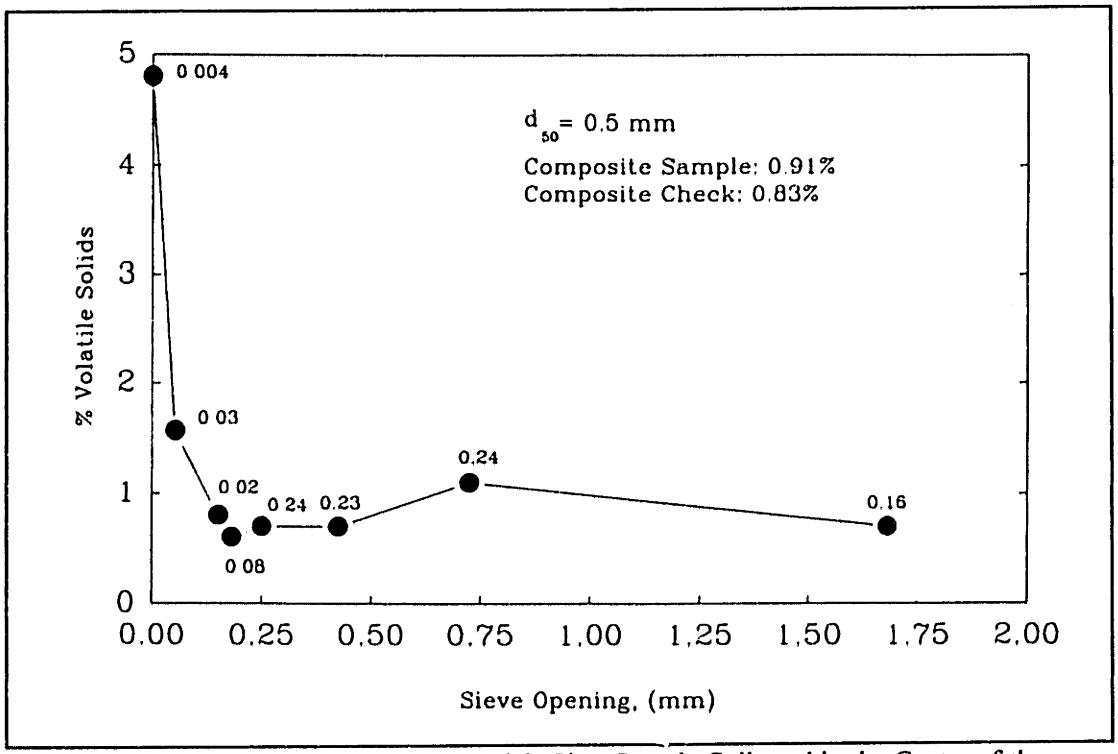

Figure III.G-4: Volatile Solids versus Particle Size, Sample Collected in the Center of the Channel at Route 128, January 31, 1992

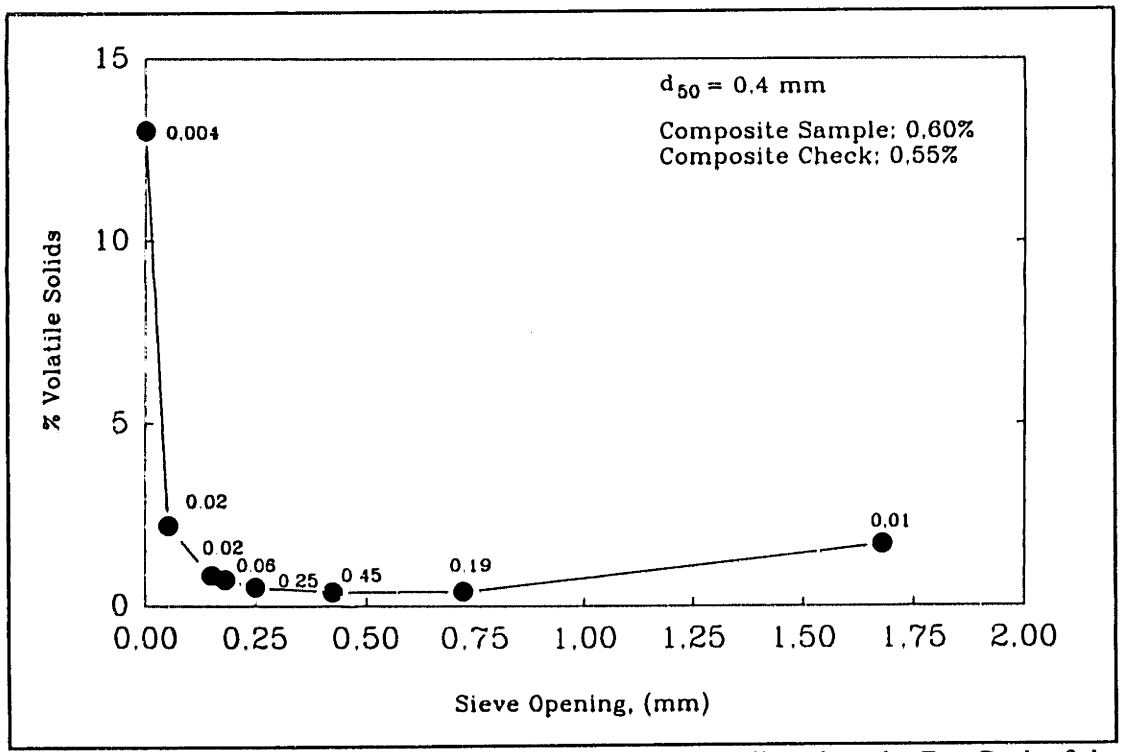

Figure III.G-5: Volatile Solids versus Particle Size, Sample Collected on the East Bank of the Channel at Route 128, January 31, 1992

METAL CONCENTRATIONS VERSUS PARTICLE SIZE: Determination of metal concentrations versus particle size was performed by sieving the sediment into separate size fractions, digesting a known mass of sediment, and analyzing the digestate for metals. Separation of the sediment into size fractions followed the procedure described in the "grain size distribution" section in this appendix. The mass of sediment digested ranged from 0.8 to 10 grams. Digestion procedure followed the HNO_3-H_2O_2-HCl procedure described in section III.4.3. Metals analysis of the digestates was performed using the ICP-AES technique described in section III.4.3.

For quality control purposes, the sediment sample was split prior to sieving. One split was sieved and later digested while the second split (composite sample) was digested without size separation. In this manner the sum of the metals concentrations associated with each size fraction could be compared with the composite sediment concentration. The closer each of the values, the better the analytical quality. The "composite check" is the sum of the concentrations from each of the size fractions.

Samples were collected at Route 128 on January 31, 1992. Two samples were analyzed. The first corresponded to a sample collected at the center of the channel; the second corresponded to a sample collected on the east bank. Results indicate (tables III.G-5 and III.G-6 and figures III.G-6, III.G-7, and III.G-8) that metal concentrations increase significantly with decreasing particle size. One may speculate from such a result that the river fines are the primary size fraction responsible for the transport of metals within the river system, especially if one considers that they are also the most mobile.

FN: p013192

Sample ID	% Size fraction	% Organic	Amt (g)	Vol (ml)	Cr mg/kg	Cd mg/kg	As mg/kg	Al mg/kg	Si mg/kg	Ti mg/kg	Fe mg/kg	Co mg/k	Ni mg/k	Ba mg/kg
Sieve 12	15.94	0.7	8.05	50	11.2	0.3	8.0	2607	35.5	161.5	6832	2.1	5.8	14.9
Sieve 25	24.1	1.1	5.61	50	13.4	0.5	15.0	2582	66.1	151.5	6416	1.2	4.7	8.6
Sieve 40	23.2	0.7	5.48	50	18.2	0.6	18.1	2278	100.5	136.9	6842	0.7	4.1	8.5
Sieve 60	23.5	0.7	5.37	50	14.0	0.7	17.5	2139	58.8	84.7	5958	0.6	3.7	7.0
Sieve 80	7.9	0.6	4.83	50	25.9	0.8	23.6	2688	114.1	186.3	7038	1.1	4.3	11.4
Sieve 100	2.4	0.8	4.84	50	32.0	1.0	26.7	2579	103.5	175.6	7230	1.7	5.2	14.5
Sieve 270	2.6	1.57	3.81	50	45.9	1.4	37.8	3539	144.6	315.0	11416	2.8	9.8	18.4
Bott.Pan	0.43	4.8	0.84	50	422.6	29.8	832.1	1826	209.5	952.4	77376	24.4	53.6	214.3
Composite	---	0.91	6.56	51	20.2	0.7	19.3	2485	85.7	124.4	6763	1.1	4.1	7.8
					1.8	0.0	1.3	415.5	5.7	25.7	1089	0.3	0.9	2.4
					3.2	0.1	3.6	622.2	15.9	36.5	1546	0.3	1.1	2.1
					4.2	0.1	4.2	528.5	23.3	31.8	1587	0.2	1.0	2.0
					3.3	0.2	4.1	502.6	13.8	19.9	1400	0.1	0.9	1.6
					2.0	0.1	1.9	212.4	9.0	14.7	556	0.1	0.3	0.9
					0.8	0.0	0.6	61.9	2.5	4.2	174	0.0	0.1	0.3
					1.2	0.0	1.0	92.0	3.8	8.2	297	0.1	0.3	0.5
					1.8	0.1	3.6	7.9	0.9	4.1	333	0.1	0.2	0.9
Check Composite					18.3 Sum	0.7 Sum	20.2 Sum	2443 Sum	74.9 Sum	145.1 Sum	6982 Sum	1.2 Sum	4.8 Sum	10.7 Sum

Table III.G-5: Metal Concentration versus Particle Size for a River Bottom Sediment Sample Collected in the Center of the Channel at Route 128, January 31, 1992

FN: ps013192

Sample ID	% Size fraction	% Organic	Amt (g)	Vol (ml)	Cr mg/kg	Cd mg/kg	Si mg/kg	Ti mg/kg	Fe mg/kg	Ba mg/k	Mn mg/kg
Sieve 12	1	1.67	2.4	100	19.2	0.0	223.3	320.8	12500	12.5	120.8
Sieve 25	18.8	0.4	7.45	100	13.4	0.0	84.0	174.5	7517	8.5	63.1
Sieve 40	44.8	0.38	7.95	100	9.9	0.0	54.8	101.9	6415	5.7	44.0
Sieve 60	25	0.514	7.78	100	12.3	0.1	71.5	93.8	7326	6.0	45.0
Sieve 80	5.6	0.718	8.35	100	14.4	0.4	115.7	143.7	6347	5.7	47.9
Sieve 100	2	0.83	2.42	100	49.6	1.2	287.6	376.0	14050	17.8	124.0
Sieve 270	2.4	2.19	4.56	100	39.5	1.1	214.0	208.3	8114	12.7	76.8
Bott.Pan	0.4	13	0.77	100	80.5	5.2	994.8	298.7	16883	29.9	207.8
Composite	---	0.6	9.96	100	10.0	0.0	74.9	97.4	4920	4.3	33.1
					0.2	0.0	2.2	3.2	125	0.1	1.2
					2.5	0.0	15.8	32.8	1413	1.6	11.9
					4.5	0.0	24.6	45.6	2874	2.5	19.7
					3.1	0.0	17.9	23.5	1832	1.5	11.2
					0.8	0.0	6.5	8.0	355	0.3	2.7
					1.0	0.0	5.8	7.5	281	0.4	2.5
					0.9	0.0	5.1	5.0	195	0.3	1.8
					0.3	0.0	4.0	1.2	68	0.1	0.8
Check Composite					13.3 Sum	0.1 Sum	81.8 Sum	126.9 Sum	7142 Sum	6.9 Sum	51.9 Sum

Table III.G-6: Metal Concentration versus Particle Size for a River Bottom Sediment Sample Collected on the East Bank of the Channel at Route 128, January 31, 1992

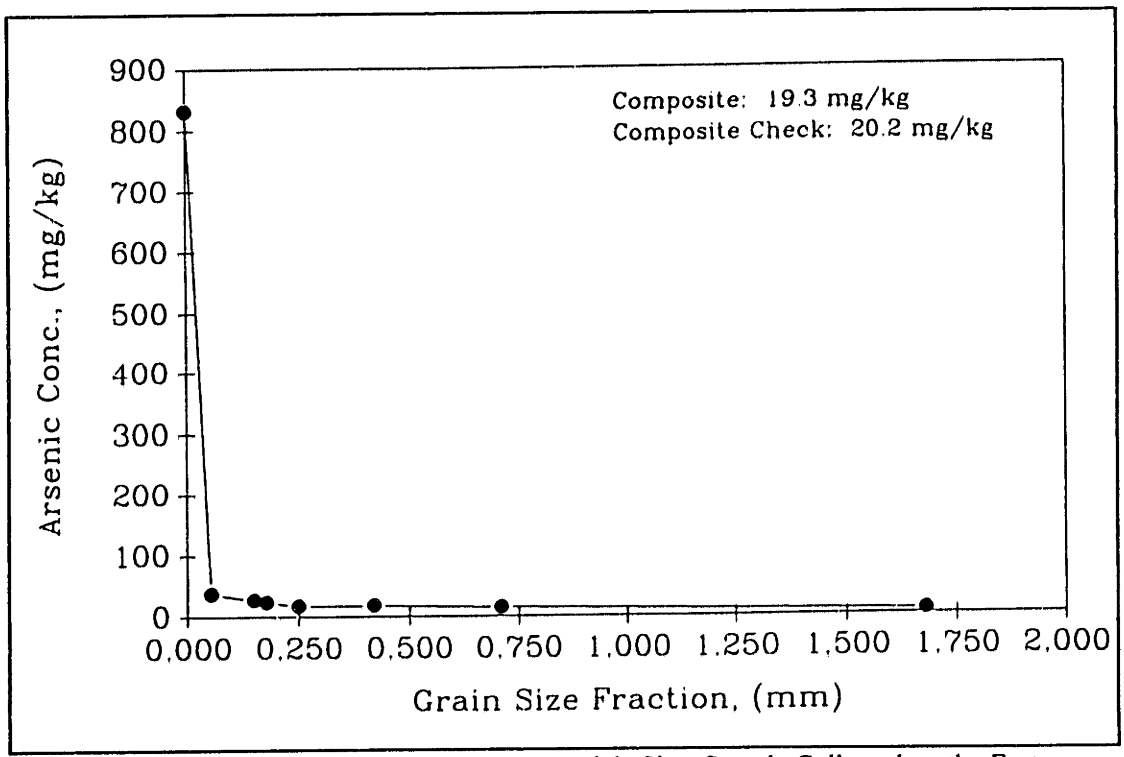

Figure III.G-6: Arsenic Concentration versus Particle Size, Sample Collected on the East Bank of Channel at Route 128, January 31, 1992

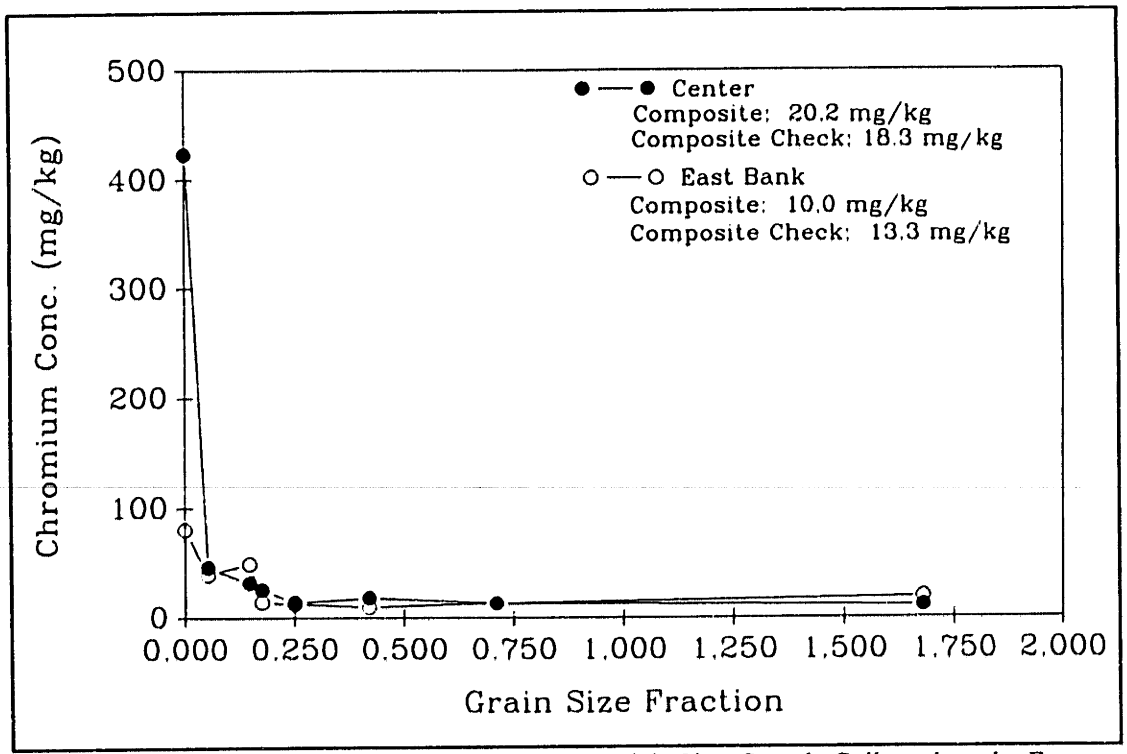

Figure III.G-7: Chromium Concentration versus Particle Size, Sample Collected on the East Bank of Channel at Route 128, January 31, 1992

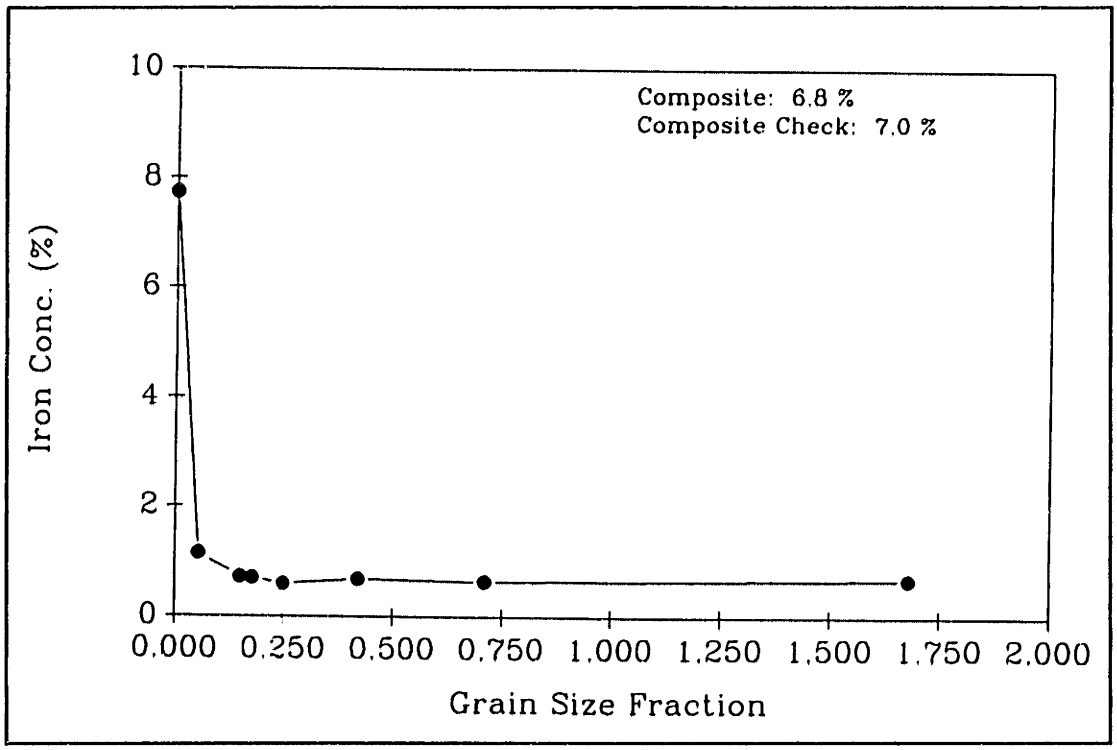

Figure III.G-8: Iron Concentration versus Particle Size, Sample Collected on the East Bank of Channel at Route 128, January 31, 1992

SEQUENTIAL EXTRACTIONS: Sequential extraction techniques are used to partition the solid-associated metals into several chemical phases. The technique involves the application of various chemical extractants to sediment samples, where each successive treatment is more drastic in chemical action or of a different nature than the previous one. (Chao, 1984) Investigations verifying these techniques report reasonable selectivity of the extractants for the fraction of interest. (Tessier, et. al 1979; Robbins, et. al, 1984; Chao, 1984) However, also reported is: a) lack of complete solubilization of a given fraction using its corresponding extractant, and b) some solubilizaton of a different fraction which was not intended to be released by the given extractant. Due to these issues, it is emphasized that the fractions below are "operationally defined" (Tessier et. al., 1979) and are dependent upon the procedure used. The objective of the sequential extraction procedure was to determine the environmental conditions under which the solid bound metals would likely be released into solution. The fractions considered included:

1) *Water Soluble Fraction*: Usually this portion is negligible, especially for samples collected from a river bed which is in constant contact with water. The primary purpose of this step was to determine the effect of de-ionized water application during the wet-sieving procedure.

2) *Exchangeable Fraction*: Metals associated with this phase are held through electrostatic attraction on exchange sites on the surface of the solid matrix. Changes in water ionic composition (e.g. in areas of changing salinity) can affect the distribution of exchangeable metals.

3) *Carbonate Fraction*: This fraction includes metals which have either inorganically or biogenetically co-precipitated with carbonates. The release of metals from this fraction is associated with changes in pH.

4) *Bound to Iron and Manganese Oxides*: In general Fe and Mn oxides have large absorption capacities for trace metals. Since the dissolution and precipitation of Fe and Mn oxides is Eh sensitive, the release of metals from this phase is dependent upon the oxidation conditions of the system. Under oxic conditions metals in this phase will be bound to the solid oxide whereas under reducing conditions trace metals will be released to solution.

5) *Organic Fraction*: Organic matter in sediments is usually of biological origin. Trace metals become associated with organic matter through biological uptake or through

absorption. Under oxidizing conditions in natural waters organic matter can be degraded leading to the release of trace metals to solution.

6) *Residual Fraction*: Metals in the residual fraction are probably incorporated into the crystalline structure of the mineral fraction of the sediment. These metals are not expected to be released in solution under conditions normally encounted in nature.

The methodology used for the extraction procedure included the following: (Please note the order of extractions proceed from step 3 to step 10)

1) *Sample Preparation*: 1 to 2 g of each sediment sample were dried in an oven at 105 °C.

2) *Separation of Extractant from Sediments*: Separations were performed after each successive extraction. The method follows Tessier et. al., 1979 with minor modifications.
   - Samples were centrifuged at 10,000 rpm for 30 minutes using 50 ml polypropylene centrifuge tubes.
   - Supernatant was decanted and was later diluted to a 50 ml volume. This solution was then stored for later metals analysis.
   - To remove residual extractant, 8 ml of de-ionized water was added to the sediment residue and shaken. The sediment-deionized water mixture was centrifuged again for 30 minutes at 10,000 rpm. The second supernatant was then discarded.
   - To assure residual removal, the step above was repeated a second time.

3) *Water Soluble Fraction*: (after Gatehouse, 1977)
   - A known mass of sediment (between 0.5 to 2 grams) was added to a 50 ml polypropylene centrifuge tube.
   - 10 ml of de-ionized water were added to the sediment.
   - The mixture was allowed to soak for 1 hour.
   - The mixture was then shaken vigorously for 20 minutes on a mechanical shaker.
   - The mixture was then centrifuged and the supernatant was separated from the sediment. (See step 2) Prior to bringing the supernatant up to volume, 1 ml of 1:4 HNO_3 was added to the supernatant after it was removed from the sediment.

4) *Absorbed Fraction*: (after Tessier et. al., 1979)
   - 16 ml of 1 M $MgCl_2$ was added to the sediment.
   - The mixture was then shaken at room temperature for 1 hour.
   - The mixture was then centrifuged and the supernatant was removed.

5) *Carbonate Fraction*: (after Chao, 1984)

- 10 ml of 1 M NaOAc (adjusted to a pH = 5 with acetic acid, HOAc) was added to the sediment residue in each centrifuge tube.
- The mixture was then shaken for 20 minutes.
- The mixture was then centrifuged and the supernatant was separated.
- The prior three steps were repeated two more times. The supernatant from all three NaOAc additions was stored in one container.

6) *Bound to Fe and Mn Oxides*: (after Chester & Hughes, 1967)

- 20 ml of 1 M Hydroxylamine hydrochloride in 25% acetic acid were added to the sediment residue in each centrifuge tube.
- The mixture was shaken for 4 hours at room temperature.
- The mixture was then centrifuged and the supernatant was separated.

7) *Organic Fraction*: (after Tessier, et. al., 1979; Arnseth & Turner, 1988)

- 6 ml of 0.02 M HNO_3 and 10 ml of 30% H_2O_2 were added to the sediment residue.
- The mixture was heated to 95 °C for 2 hours with occasional agitation.
- An additional 3 ml of 0.02 m HNO_3 and 3 ml of 30% H_2O_2 were added and the solution was re-heated for 3 hour at 95 °C with intermittant agitation. The solution was allowed to cool and 5 ml of 3.2 M NH_4Ac in 20% HNO_3 were added. The mixture was allowed to soak for 30 minutes with intermittant agitation.
- The mixture was then centrifuged and the supernatant was separated.

8) *Residual*: This step corresponded to the HNO_3 - H_2O_2 - HCl digestion procedure described in section III.4.

For the present study, a bottom sediment sample (collected at Route 128, east bank, January 31, 1992) was partitioned into size fractions (refer to grain size distribution section in this appendix). For the sequential extraction procedure, 2 size fractions were analyzed: 1) size fraction finer than 53 μm, (passed the 270 sieve), and 2) 53 to 149 μm size fraction (retained between the 270 and 100 sieves) Additionally, a blank sample (i.e. no sediment) was carried through the procedure. All extractants were analyzed using ICP-AES.

RESULTS

Sediment samples were split, where one set was analyzed using the sequential extraction procedure while the other set was put through a full digestion (as given in the residual extraction step). Quality control analysis consisted of comparing the sum of the metal concentrations in the various extracts to the bulk concentration from the full digestions. Results of this analysis indicate poor analytical quality where

the sum of the extractants for the finer than 53 μm size range was consistently 50% lower than the full digestion for most metals analyzed. The sample corresponding to the 53 to 140 μm size range was also significantly off, where the sum of the extractants was consistently 50% greater than the full sample digestion for most metals analyzed. This error is attributed to analytical and sample preparation errors. To help avoid sample preparation errors, homogenation of the sediment samples is recommended prior to splitting the samples. Homogenation would include crushing the sediment to a powder using an agate mortar.

Despite the poor quality of the data, the results of the analysis are presented in table III.G-7 and III.G-8 for reference. Although values are given to the various fractions, these results should be considered purely qualitative and not quantitative. From the data, one may speculate that most of the Fe, Cr and Si, for both size fractions is bound as an iron oxide coating on particles, in the organic phase, or in the residual phase. Cd, Ba and Mn, on the other hand, had significant fractions associated with the exchangeable, carbonate, Fe/Mn bound, and residual fractions, with only small amounts associated with the organic fraction. (The only exception is Cd for the 53 to 149 μm size range) Ti was much different than the rest of the metals, with almost the entire metal concentration associated with the residual fraction. Such results indicate that Ti is probably of mineralogical origin and is not readily available for transformation in the environment. Fe and Cr also have mineralogical associations; however, Fe/Mn oxides and organics play an important role in their transport. Under reducing conditions one may expect the dissolution of Fe and Cr from the Fe/Mn oxide particles. The exchangeable and carbonate fractions of Cd, Ba, and Mn are probably the most mobile, where mobilization to solution can be induced through a change in water ionic composition or a change in pH; however, Fe/Mn oxides and mineral composition of the suspended sediment will also have an affect on mobility.

FN: Seqext

	Fe	Cr	Cd	Si	Ti	Ba	Mn
Water Soluble	0%	0%	0%	1%	2%	0%	2%
Exchangable	0%	0%	18%	1%	0%	15%	17%
Carbonate	0%	2%	24%	7%	15%	25%	30%
Bound to Fe Mn	53%	31%	9%	26%	0%	36%	29%
Organic	13%	52%	0%	24%	10%	8%	6%
Residual	34%	16%	48%	41%	73%	16%	16%
Total	100%	100%	100%	100%	100%	100%	100%

Table III.G-7: Qualitative Sequential Extraction Results for Bottom Sediment Sample Collected on the East Bank of the Channel at Route 128, January 31, 1992. Particle size range analyzed corresponded to the fraction finer than 53 μm.

FN: Seqext

	Fe	Cr	Cd	Si	Ti	Ba	Mn
Water Soluble	0%	0%	0%	0%	2%	0%	4%
Exchangable	0%	0%	0%	0%	0%	24%	19%
Carbonate	0%	0%	0%	1%	12%	11%	8%
Bound to Fe Mn	25%	26%	0%	8%	0%	14%	19%
Organic	17%	74%	0%	37%	15%	20%	16%
Residual	58%	0%	100%	53%	71%	30%	34%
Total	100%	100%	100%	100%	100%	100%	100%

Table III.G-8: Qualitative Sequential Extraction Results for Bottom Sediment Sample Collected on the East Bank of the Channel at Route 128, January 31, 1992. Particle size range analyzed corresponded to the fraction within 53 and 149 μm.

APPENDIX IV.A

Streamflow and Precipitation:
Monthly/Yearly Plots and Tables

FN: readmo.wq1

YEAR	JAN	FEB	MAR	APR	MAY	JUN	JUL	AUG	SEP	OCT	NOV	DEC	TOTAL
1899	4.00	3.26	6.48	2.56	1.33	3.36	3.15	1.91	4.67	1.35	2.95	1.50	36.52
1900	5.32	8.69	5.03	2.15	4.60	3.13	1.90	3.17	4.15	3.31	5.05	2.44	48.94
1901	1.33	1.08	5.88	9.59	7.19	1.74	4.65	2.66	3.59	2.67	3.06	8.10	51.54
1902	1.80	6.11	4.69	6.22	1.69	1.98	3.02	3.75	4.01	4.91	0.99	5.60	44.77
1903	3.84	3.16	6.38	4.95	0.48	8.91	3.40	3.42	2.29	3.69	1.33	2.59	44.44
1904	4.42	2.21	2.21	9.90	3.56	2.56	1.88	4.26	5.16	2.02	1.80	2.25	42.23
1905	5.44	1.47	2.92	2.59	1.39	6.11	1.19	3.30	7.87	1.20	2.22	3.72	39.42
1906	2.60	2.53	6.48	2.84	5.14	2.63	5.88	4.18	1.36	2.38	3.31	3.08	42.41
1907	3.97	2.10	2.04	3.21	2.89	3.80	3.58	1.33	7.90	3.36	6.83	3.60	44.61
1908	3.07	4.28	2.72	1.71	4.00	1.58	3.01	4.07	0.86	3.56	1.10	2.66	32.62
1909	4.17	5.33	3.57	3.95	1.97	2.14	3.59	2.75	3.74	1.23	4.06	3.60	40.10
1910	4.54	3.14	1.58	2.32	1.19	4.36	1.98	2.61	2.45	1.48	4.30	1.92	31.87
1911	2.25	2.94	3.31	1.89	0.60	3.90	4.79	3.80	2.94	2.91	4.14	3.57	37.04
1912	2.72	2.42	5.04	4.05	5.73	0.29	6.44	2.02	3.02	1.45	3.10	4.80	41.08
1913	2.48	2.64	4.51	3.76	3.45	0.93	1.68	3.47	3.66	7.56	2.13	3.23	39.50
1914	3.34	3.65	4.09	6.32	2.76	1.44	2.34	2.78	0.23	1.51	2.92	3.69	35.07
1915	5.52	3.54	0.00	2.72	1.68	1.70	11.66	6.66	0.70	2.80	2.93	5.47	45.38
1916	1.22	5.37	3.37	5.14	4.59	5.86	3.13	2.30	3.11	1.01	1.94	2.91	39.95
1917	2.92	2.41	4.18	2.90	4.00	4.78	1.19	3.40	1.46	5.76	1.39	2.66	37.05
1918	2.92	3.02	2.02	4.10	0.85	3.04	2.99	2.81	8.37	1.02	2.24	2.06	35.44
1919	3.68	3.61	4.01	2.46	5.44	0.88	3.22	3.83	5.65	2.63	6.20	1.53	43.14
1920	2.75	6.46	4.18	5.75	3.27	5.27	1.94	2.02	4.27	1.16	5.30	4.77	47.14
1921	2.09	3.43	2.16	5.48	1.86	3.97	9.79	1.96	1.74	1.53	6.43	2.28	42.72
1922	1.77	2.72	4.27	1.37	5.08	11.27	4.88	3.29	3.68	2.73	1.06	3.13	45.25
1923	6.95	1.67	2.60	5.09	1.56	2.89	1.97	3.17	0.82	3.73	4.13	4.83	39.41
1924	3.77	2.55	1.71	5.25	3.10	2.53	2.70	4.80	7.95	0.05	2.56	1.52	38.49
1925	4.29	2.14	7.66	2.95	2.05	5.62	3.13	2.37	2.16	4.66	3.94	5.53	46.50
1926	2.53	4.41	2.83	2.26	2.19	1.80	2.08	3.30	1.32	3.95	3.89	3.09	33.65
1927	2.32	3.39	1.30	1.43	2.19	2.27	3.04	5.28	2.68	4.10	4.18	4.65	36.83
1928	2.10	3.37	1.45	5.13	2.77	6.63	3.65	3.84	4.18	2.96	2.28	2.57	40.93
1929	3.14	3.76	3.49	6.81	3.50	1.28	1.19	4.53	2.41	2.49	2.88	3.63	39.11
1930	2.48	2.05	3.29	1.90	3.38	2.19	4.07	2.77	0.79	4.45	3.69	2.20	33.26
1931	3.27	2.72	4.94	3.07	3.53	6.70	3.76	4.11	1.97	2.43	1.26	3.67	41.43
1932	2.92	1.90	4.83	2.01	1.17	1.81	2.04	5.09	7.24	7.26	5.25	1.29	42.81
1933	2.27	3.46	7.22	6.51	2.70	1.27	1.47	4.41	9.97	3.50	0.96	3.47	47.21
1934	3.17	3.29	5.13	3.09	2.52	4.00	1.25	1.73	6.43	3.89	2.03	2.70	39.23
1935	6.13	3.23	1.06	4.72	1.44	6.21	2.67	1.98	4.03	0.58	4.36	0.90	37.31
1936	6.60	3.09	7.23	3.01	2.05	2.73	1.75	4.49	4.15	1.59	1.37	8.24	46.30
1937	4.50	1.80	3.21	4.61	3.13	3.45	0.97	3.91	3.04	4.48	5.18	4.89	43.17
1938	4.08	2.07	2.11	3.12	3.51	7.18	11.42	2.19	8.33	2.93	1.86	2.85	51.65
1939	2.08	3.48	4.00	4.47	2.02	2.77	0.73	3.13	2.45	4.66	0.77	2.92	33.48
1940	2.22	4.34	3.68	4.65	3.52	2.41	2.58	0.80	4.59	1.05	6.67	2.73	39.24
1941	3.16	1.88	2.51	1.87	2.24	2.09	3.66	3.05	0.58	2.13	2.38	4.08	29.63
1942	4.25	2.98	7.20	2.02	3.34	3.19	5.08	1.82	2.18	2.99	4.72	5.61	45.38
1943	3.09	1.03	3.57	2.60	5.54	2.09	4.79	1.35	0.67	5.84	4.45	1.02	36.04
1944	2.63	2.26	4.22	3.84	0.83	5.32	2.56	2.83	7.22	2.65	6.03	3.18	43.57
1945	2.60	4.40	1.79	2.85	4.28	5.90	3.07	3.07	1.19	2.62	7.77	6.41	45.95
1946	3.91	3.06	1.57	2.74	5.26	3.39	1.90	8.64	2.37	0.37	1.02	4.09	38.32
1947	3.10	1.03	3.69	4.91	3.27	2.58	5.83	1.44	3.33	0.44	6.24	3.09	38.95
1948	4.33	2.11	2.84	2.63	5.38	4.63	4.83	1.08	1.00	3.08	5.41	1.41	38.73
1949	3.47	3.28	1.25	4.25	3.37	0.84	1.78	5.05	4.28	1.93	3.03	1.86	34.39
1950	4.41	3.12	3.67	1.95	1.38	1.38	1.91	4.19	1.56	3.27	6.31	3.53	36.68
1951	3.33	3.79	4.76	1.85	4.74	3.47	4.72	2.11	1.77	5.15	6.84	4.56	47.09
1952	4.64	3.71	3.67	4.45	5.14	1.50	0.93	8.85	1.83	1.32	2.27	4.14	42.45
1953	6.72	2.96	7.57	5.43	4.81	1.09	2.31	0.64	1.46	5.52	5.91	3.81	48.23
1954	2.34	2.53	3.13	3.93	10.97	1.46	2.16	5.88	9.92	1.61	5.27	5.25	54.45

Table IV.A-1: Monthly and Yearly Precipitation, Reading NCDC Station, 1899 to 1993

YEAR	JAN	FEB	MAR	APR	MAY	JUN	JUL	AUG	SEP	OCT	NOV	DEC	TOTAL
1955	0.63	3.69	4.17	3.18	1.86	3.29	1.17	12.45	2.29	8.95	5.88	1.02	48.58
1956	7.80	4.59	6.27	4.13	1.33	1.57	1.93	1.35	3.29	3.06	4.09	4.73	44.14
1957	3.25	1.35	2.32	3.20	2.65	1.02	1.94	1.60	0.57	2.34	5.69	4.46	30.39
1958	10.19	3.83	3.46	6.01	3.66	2.17	4.71	4.56	5.97	3.45	3.20	1.58	52.79
1959	2.78	2.94	5.32	3.33	0.93	6.56	6.02	2.52	1.62	4.95	4.23	4.77	45.97
1960	3.18	4.77	3.28	3.40	3.39	2.39	4.56	2.00	7.37	2.72	3.22	3.61	43.89
1961	2.30	3.10	4.38	5.89	3.78	1.95	3.00	4.88	8.45	2.60	4.50	4.52	49.35
1962	3.24	4.85	2.44	5.04	2.25	2.79	1.92	4.24	4.58	12.85	4.24	5.18	53.62
1963	3.51	3.18	4.38	1.53	3.27	1.56	2.63	2.60	3.84	2.00	9.24	2.51	40.25
1964	4.88	4.76	3.87	4.15	0.85	1.80	2.78	1.60	1.78	2.99	2.45	4.99	36.90
1965	2.12	3.99	2.23	2.23	1.87	3.48	0.47	1.88	2.49	2.00	2.25	2.04	27.05
1966	5.62	3.47	1.87	1.50	3.29	2.54	2.02	1.62	4.72	3.09	4.57	2.32	36.63
1967	2.25	3.84	3.95	4.69	7.39	2.77	3.00	4.28	3.60	1.14	4.00	6.66	47.57
1968	3.62	1.13	7.63	2.39	3.80	7.06	1.40	2.53	1.75	2.04	7.36	6.73	47.44
1969	2.35	7.14	2.90	3.99	1.66	1.29	3.80	2.57	5.26	1.73	9.08	10.55	52.32
1970	0.92	5.29	4.53	3.66	3.99	4.22	2.05	4.76	2.96	2.93	3.41	5.67	44.39
1971	1.75	4.65	2.75	3.12	4.24	2.66	3.89	2.34	2.00	2.63	6.56	2.72	39.31
1972	1.74	6.44	6.87	3.62	5.78	9.35	3.66	1.17	3.74	3.47	8.38	7.12	61.34
1973	3.54	2.13	2.75	7.30	4.42	5.27	2.96	5.29	2.19	3.72	1.97	8.25	49.79
1974	3.32	3.01	4.22	3.16	5.14	2.44	1.46	1.96	7.78	2.67	2.45	4.88	42.49
1975	5.76	3.44	3.34	2.74	2.16	2.65	2.13	6.43	6.58	5.64	6.19	6.69	53.75
1976	4.82	2.35	3.30	2.73	2.80	0.36	5.34	6.16	2.08	4.42	0.81	3.61	38.78
1977	5.93	2.70	6.91	4.65	4.25	4.77	2.43	3.90	4.82	5.52	5.51	7.25	58.64
1978	8.54	2.67	2.79	2.54	4.78	1.88	2.55	3.28	0.64	3.36	2.54	4.41	39.98
1979	13.00	3.57	3.02	3.93	4.02	2.95	2.26	5.57	3.11	4.07	3.92	1.22	50.64
1980	0.60	1.01	5.62	4.93	2.55	3.49	3.72	1.50	1.62	5.64	3.68	1.21	35.57
1981	0.93	7.22	0.82	3.65	1.80	3.36	5.30	0.91	4.18	4.62	4.88	6.61	44.28
1982	5.50	3.25	2.48	3.10	4.53	11.77	3.88	2.75	2.50	3.99	3.67	1.13	48.55
1983	5.88	5.54	10.80	7.33	3.93	1.61	1.51	4.76	1.38	3.56	11.02	6.15	63.47
1984	2.60	7.68	7.60	4.73	9.70	4.08	4.16	1.04	1.25	3.59	2.69	4.10	53.22
1985	1.25	2.07	3.23	1.91	3.75	3.91	5.65	5.34	3.73	3.27	7.81	1.45	43.37
1986	4.29	3.25	4.02	2.29	1.36	6.30	4.67	3.10	1.57	2.53	6.42	8.81	48.61
1987	7.39	0.33	4.35	10.09	1.44	1.72	1.00	3.72	7.81	2.74	3.38	2.79	46.76
1988	2.72	4.21	3.75	2.71	4.31	1.61	8.80	1.40	1.49	3.13	7.56	1.14	42.83
1989	0.80	3.13	3.25	4.66	3.55	4.41	3.31	5.46	3.97	7.02	4.03	1.38	44.97
1990	4.29	4.10	2.00	5.68	6.63	0.77	4.80	8.13	1.64	9.69	2.29	4.11	54.13
1991	3.93	1.97	3.92	4.34	1.87	3.12	2.36	6.10	7.01	3.10	4.06	3.64	45.42
1992	3.19	2.32	3.87	2.67	2.08	5.56	3.69	4.59	3.06	2.65	4.71	6.78	45.17
1993	2.23	4.36	7.72	4.64	1.25	1.53	2.28	1.75	4.16				
AVE	3.67	3.36	3.88	3.87	3.33	3.39	3.30	3.49	3.57	3.31	4.08	3.85	43.09
STD D	2.00	1.51	1.85	1.78	1.84	2.23	2.04	1.94	2.36	2.02	2.12	2.00	6.80
MAX	13.00	8.69	10.80	10.09	10.97	11.77	11.66	12.45	9.97	12.85	11.02	10.55	63.47
MIN	0.60	0.33	0.00	1.37	0.48	0.29	0.47	0.64	0.23	0.05	0.77	0.90	27.05

Table IV.A-1: con'd

FN:winchrai

YEAR	JAN	FEB	MAR	APR	MAY	JUN	JUL	AUG	SEP	OCT	NOV	DEC	TOTAL
1875	3.24	3.62	5.76	4.46	3.89	7.73	3.84	3.50	3.32	5.06	5.62	0.97	51.01
1876	1.63	3.67	8.72	4.37	2.83	1.09	8.67	0.87	4.49	1.90	6.64	2.12	47.00
1877	3.07	0.76	6.72	3.44	3.17	1.69	2.30	5.94	0.39	7.61	7.11	0.89	43.09
1878	5.67	5.72	3.86	5.09	0.69	2.69	3.66	7.57	3.12	4.76	5.61	4.65	53.09
1879	1.82	2.73	3.52	4.65	1.86	3.98	2.39	5.48	1.00	0.77	3.74	3.74	35.68
1880	2.62	4.23	2.49	2.18	2.02	1.49	7.23	3.64	1.42	1.70	1.90	2.50	33.42
1881	6.32	3.05	4.49	1.54	2.59	5.65	2.92	0.57	2.03	1.18	3.15	3.38	36.87
1882	3.93	6.39	2.66	2.13	4.58	2.06	2.77	1.05	8.45	1.45	1.76	2.26	39.49
1883	2.29	3.16	2.17	2.42	3.60	1.62	2.54	0.85	1.44	4.20	1.98	3.36	29.63
1884	5.04	4.97	4.30	3.12	3.00	2.05	3.41	5.07	1.28	2.51	1.98	4.69	41.42
1885	2.29	3.51	1.14	3.33	3.90	2.01	1.80	5.15	1.32	5.60	6.38	2.01	38.44
1886	6.40	7.20	3.72	1.91	2.78	1.56	2.26	6.72	7.79	4.73	6.30	4.94	56.31
1887	4.27	4.81	5.41	4.90	1.66	2.71	6.74	4.76	1.46	3.02	3.16	3.43	46.33
1888	3.80	3.25	4.53	2.82	4.96	2.21	3.70	3.48	3.04	2.78	4.06	4.99	43.62
1889	4.60	3.74	4.00	2.88	4.85	2.11	2.11	5.97	8.20	4.87	6.68	5.12	55.13
1890	2.60	3.39	6.21	2.49	6.41	3.42	2.27	3.56	3.50	8.39	1.41	4.32	47.97
1891	6.32	4.51	5.93	2.73	2.17	4.33	3.02	3.30	2.37	4.53	2.43	3.20	44.84
1892	4.49	3.03	3.76	0.74	4.88	4.26	1.54	4.49	1.61	0.91	4.10	1.10	34.91
1893	2.26	3.36	1.92	3.09	5.18	1.81	1.94	5.91	2.07	3.96	1.85	4.31	37.56
1894	3.23	2.73	0.96	2.60	4.24	0.31	3.14	1.24	1.97	4.93	3.58	4.18	33.11
1895	3.26	0.44	2.58	3.91	3.59	3.89	4.13	5.56	2.56	9.70	6.02	2.64	48.28
1896	1.98	3.81	7.14	1.56	1.89	2.18	2.00	2.32	7.99	3.01	2.51	2.18	38.57
1897	3.95	2.37	3.26	3.20	4.84	5.53	3.34	3.53	2.67	0.34	6.06	3.92	43.01
1898	4.51	3.38	2.17	5.76	4.55	1.64	4.39	8.23	2.30	7.62	6.06	3.89	54.50
1899	3.23	4.00	5.34	1.31	0.93	2.77	2.67	2.23	5.45	1.08	3.27	1.30	33.58
1900	4.61	8.08	4.68	2.00	4.49	2.16	1.87	2.23	2.53	3.00	4.64	2.11	42.40
1901	2.55	1.44	4.83	7.78	6.10	0.95	4.46	3.48	3.60	2.45	2.71	6.53	46.88
1902	2.14	5.28	6.18	4.07	0.58	1.32	2.37	3.43	2.45	3.95	1.19	5.91	38.87
1903	3.31	3.70	5.68	4.14	0.41	9.90	2.25	3.02	1.63	3.65	1.38	2.25	41.32
1904	4.59	2.60	1.74	8.47	3.18	3.04	1.51	3.19	5.10	1.69	1.58	2.22	38.91
1905	5.26	1.70	2.59	2.73	1.26	6.14	1.10	3.65	7.72	1.28	2.51	3.69	39.63
1906	2.88	2.76	9.27	2.55	5.15	2.95	5.22	2.57	2.02	2.69	2.83	5.90	46.79
1907	2.90	2.19	2.43	3.31	3.06	3.71	1.91	1.33	8.88	2.98	6.76	3.88	43.34
1908	3.48	4.27	3.26	2.41	3.81	0.78	2.40	3.97	0.62	3.66	1.04	2.65	32.35
1909	4.04	5.31	3.80	4.23	1.96	4.27	2.27	3.53	5.12	1.28	4.31	3.95	44.07
1910	4.80	4.84	1.02	2.68	1.32	4.59	1.47	1.19	2.38	1.13	3.71	2.28	31.41
1911	2.78	3.18	3.47	2.45	1.01	3.69	6.30	4.32	3.34	2.93	4.02	3.72	41.21
1912	3.13	2.50	4.98	3.71	5.10	0.35	5.27	2.13	2.58	1.69	2.94	4.89	39.27
1913	3.49	2.59	4.80	4.31	3.83	1.55	3.83	3.39	2.96	6.83	2.45	3.10	43.13
1914	3.58	2.80	4.61	6.19	2.68	2.15	2.56	3.44	0.06	1.39	2.79	3.03	35.28
1915	6.42	3.49	0.04	3.33	1.54	5.24	8.48	8.29	0.84	3.08	2.46	5.30	48.51
1916	1.55	5.71	4.41	5.26	3.92	5.59	3.28	2.32	1.80	1.38	1.84	3.19	40.25
1917	2.96	1.48	2.42	3.25	4.27	3.65	1.26	7.48	1.49	6.03	1.00	2.40	37.69
1918	3.56	3.51	2.46	4.31	1.37	2.67	3.63	2.18	9.42	1.13	2.05	4.07	40.36
1919	3.50	2.99	2.57	1.08	3.16	1.62	2.19	4.04	5.41	1.12	8.26	1.58	37.52
1920	3.18	7.70	4.16	5.74	4.98	7.15	1.88	1.37	3.50	1.12	5.53	4.70	51.01
1921	2.45	3.94	2.91	5.34	2.13	4.10	9.11	1.25	2.68	1.13	6.80	4.73	46.57
1922	1.60	3.30	5.50	1.61	5.40	11.47	3.75	3.90	3.25	2.80	1.25	4.20	48.03
1923	8.43	2.71	3.83	5.31	1.17	2.33	2.53	2.82	0.66	3.64	3.61	5.48	42.52
1924	3.98	2.36	2.47	4.55	3.52	2.81	1.99	6.71	9.87	0.09	2.29	1.47	42.11
1925	3.64	2.10	6.08	2.76	2.40	5.10	4.20	1.16	3.02	4.31	3.42	4.68	42.87
1926	2.35	4.35	2.50	2.21	3.16	1.68	3.67	3.08	1.46	4.52	3.97	2.84	35.79
1927	2.30	4.40	1.51	1.82	2.82	2.07	4.51	6.61	2.21	4.58	4.50	5.39	42.72
1928	2.54	3.59	2.21	4.93	3.10	7.15	4.46	4.02	4.39	3.57	2.29	2.41	44.66
1929	3.32	3.46	2.81	7.94	3.21	2.63	1.49	4.07	1.45	2.34	2.78	3.95	39.45
1930	2.33	2.12	3.35	1.85	2.93	2.12	4.78	2.22	0.63	4.86	4.36	1.93	33.48

Table IV.A-2: Monthly and Yearly Precipitation, Winchester Station, 1875 to 1993

YEAR	JAN	FEB	MAR	APR	MAY	JUN	JUL	AUG	SEP	OCT	NOV	DEC	TOTAL
1931	3.61	2.68	4.44	2.81	3.70	8.04	1.99	5.17	1.26	2.63	1.08	3.60	41.01
1932	4.10	1.93	5.19	1.38	1.55	3.06	2.55	6.96	6.83	7.86	5.72	1.75	48.88
1933	2.30	3.92	7.54	7.38	2.29	1.23	2.23	3.15	10.33	3.43	1.01	3.54	48.35
1934	3.54	3.30	5.10	3.16	2.14	4.36	1.34	1.95	7.83	3.30	3.35	2.71	42.08
1935	5.97	3.11	1.71	4.78	1.27	5.80	1.58	1.37	3.97	0.55	4.74	0.92	35.77
1936	7.26	3.22	7.27	3.35	1.93	2.33	1.21	5.82	5.64	1.46	1.55	8.70	49.74
1937	4.60	1.86	3.30	4.19	3.10	3.49	1.47	7.02	3.71	4.45	6.18	4.88	48.25
1938	3.75	2.12	2.42	3.18	4.25	6.08	12.08	1.98	7.57	2.69	3.29	2.97	52.38
1939	2.09	3.64	4.68	4.89	2.67	2.95	0.47	2.78	2.09	4.36	1.05	2.76	34.43
1940	2.35	3.85	3.75	5.10	3.72	2.00	4.40	1.38	4.12	1.19	6.21	2.52	40.59
1941	3.59	1.82	2.33	1.83	2.39	2.56	2.85	3.26	0.62	1.86	2.77	4.00	29.88
1942	4.16	3.12	7.20	1.98	2.48	3.41	3.24	2.74	2.24	3.14	4.65	5.31	43.67
1943	2.94	1.13	4.19	3.35	5.22	1.85	3.78	1.67	1.53	6.29	3.94	0.91	36.80
1944	2.71	2.15	3.94	3.84	0.70	4.96	1.72	2.33	6.63	2.99	6.02	2.96	40.95
1945	2.76	3.68	2.08	2.88	4.64	6.26	2.55	3.74	1.14	2.75	8.15	6.90	47.53
1946	3.70	3.10	1.28	2.72	5.09	2.93	3.60	10.37	2.10	0.32	1.32	4.36	40.89
1947	3.15	1.11	3.34	4.53	4.80	2.97	4.39	3.54	2.46	0.63	7.31	3.92	42.15
1948	4.53	2.04	2.87	2.61	4.87	5.43	4.81	1.49	1.20	3.05	4.79	1.34	39.03
1949	4.34	3.39	1.13	4.20	3.49	0.71	1.87	4.47	4.21	1.77	2.83	2.18	34.59
1950	4.25	3.39	3.74	2.12	1.32	1.25	1.23	4.22	1.67	2.77	6.01	2.83	34.80
1951	3.99	3.06	4.23	3.38	4.92	3.89	3.53	3.33	1.90	5.22	6.84	4.42	48.71
1952	4.29	4.50	3.76	3.98	5.10	2.18	0.67	5.66	2.15	1.32	2.36	3.78	39.75
1953	5.79	3.68	8.11	5.97	3.76	0.90	2.43	1.85	2.19	5.19	6.15	4.63	50.65
1954	2.88	2.53	3.14	4.86	10.44	1.95	2.75	6.10	9.06	2.61	5.50	4.77	56.59
1955	0.43	3.52	3.87	3.20	2.13	3.95	3.60	14.82	1.98	9.45	5.54	0.88	53.37
1956	6.78	4.76	6.13	3.76	2.05	1.40	2.09	1.61	4.10	3.87	3.31	5.36	45.22
1957	2.60	1.64	2.74	3.15	3.38	1.60	2.29	1.20	0.87	2.96	5.40	4.98	32.81
1958	9.23	4.44	4.21	6.13	3.34	2.17	4.44	3.56	5.62	3.44	3.06	1.62	51.26
1959	2.52	3.40	5.30	3.67	0.79	8.65	8.19	2.83	1.52	4.42	4.13	4.38	49.80
1960	3.08	4.34	3.60	3.18	3.46	1.86	4.69	1.91	6.64	2.49	2.99	3.66	41.90
1961	2.88	3.42	4.82	5.72	4.14	1.80	3.25	4.55	7.36	2.07	4.11	3.91	48.03
1962	3.18	4.96	2.52	2.74	2.72	2.68	2.31	3.34	4.19	13.13	3.36	5.53	50.66
1963	3.43	3.15	4.33	1.17	2.77	1.60	2.73	1.80	3.84	1.91	10.49	2.35	39.57
1964	4.31	4.73	3.20	4.08	0.85	2.23	3.56	1.29	2.37	3.28	2.16	4.54	36.60
1965	2.15	3.56	3.60	2.47	1.47	3.32	0.56	1.74	2.65	2.23	2.26	1.96	27.97
1966	4.61	3.95	1.19	1.28	2.68	2.65	2.57	1.99	4.32	2.76	4.92	2.61	35.53
1967	2.33	3.36	3.60	4.41	7.83	3.29	3.50	4.05	3.65	1.21	3.17	6.13	46.53
1968	3.09	1.21	6.46	2.16	3.63	6.28	1.07	2.46	1.51	1.64	7.01	6.24	42.76
1969	1.59	4.34	1.83	3.94	2.08	1.63	3.65	2.07	5.04	1.89	8.14	9.55	45.75
1970	0.73	4.82	3.65	3.37	3.22	4.22	1.65	4.50	2.53	2.31	3.55	4.86	39.41
1971	1.49	4.49	3.03	2.74	3.55	2.17	3.28	2.36	1.43	2.85	6.68	2.42	36.49
1972	1.67	7.51	5.98	3.36	6.78	7.19	2.51	1.49	3.86	3.28	8.64	5.53	57.80
1973	2.58	2.48	2.15	6.79	4.04	5.21	4.42	3.34	1.84	3.23	1.71	8.09	45.88
1974	2.65	4.12	3.88	3.79	3.87	1.96	1.66	2.41	6.27	2.52	1.81	5.29	40.23
1975	4.84	2.92	2.61	2.19	1.30	2.49	1.90	5.13	6.56	6.05	5.54	5.71	47.24
1976	4.44	2.08	2.67	2.30	2.37	1.19	5.08	6.52	1.70	3.46	0.57	3.54	35.92
1977	4.08	2.39	5.72	4.14	4.09	2.91	2.43	3.04	6.04	4.68	5.65	5.73	50.90
1978	8.12	1.49	2.58	2.17	4.05	2.30	1.95	3.79	0.84	2.91	2.30	4.49	36.99
1979	12.81	3.40	2.60	3.33	3.98	1.70	2.42	4.99	3.36	3.65	3.08	1.12	46.44
1980	0.56	0.95	5.39	4.28	1.79	2.88	2.43	0.91	1.43	4.04	3.29	0.82	28.77
1981	0.68	6.61	0.82	2.98	1.36	1.45	4.54	1.55	2.91	4.10	3.83	4.91	35.74
1982	5.86	1.63	2.41	2.08	3.30	11.60	3.47	2.55	1.06	2.93	3.18	1.02	41.09
1983	4.55	4.36	8.98	7.20	4.97	1.46	0.77	4.51	1.30	3.83	10.54	6.98	59.45
1984	2.68	8.30	6.08	4.44	9.79	4.96	4.22	0.81	1.44	3.58	2.48	2.44	51.22
1985	0.49	1.43	2.94	1.46	3.16	3.93	7.06	6.61	3.09	2.54	7.90	1.12	41.73

Table IV.A-2: con'd

YEAR	JAN	FEB	MAR	APR	MAY	JUN	JUL	AUG	SEP	OCT	NOV	DEC	TOTAL
1986	3.93	3.12	3.10	1.67	1.20	6.41	4.44	2.04	0.82	2.45	5.31	8.48	42.97
1987	5.08	0.71	4.73	9.23	2.03	1.86	1.10	3.68	7.72	2.62	3.14	2.02	43.92
1988	2.26	2.05	3.90	2.20	5.48	2.50	6.54	1.73	1.70	2.00	7.56	1.15	39.07
1989	0.74	2.68	3.66	4.79	3.62	4.52	3.58	5.70	4.43	7.07	3.65	0.93	45.37
1990	2.95	1.43	1.55	5.61	7.27	1.13	5.59	5.66	1.63	8.99	2.32	3.93	48.06
1991	3.50	1.83	3.89	3.55	3.24	2.85	2.09	6.45	7.35	2.54	4.50	1.68	43.47
1992	4.40	1.90	3.58	3.81	1.38	5.49	3.68	5.40	3.79	2.78	4.45	5.51	46.17
1993	1.20	3.34	2.57	4.67	0.82	1.78	2.73	1.65	4.69				
AVE	3.66	3.37	3.83	3.55	3.28	3.30	3.24	3.64	3.47	3.31	4.01	3.69	42.36
STD D	1.81	1.45	1.82	1.59	1.67	2.19	1.89	2.20	2.44	2.19	2.14	1.80	6.52
MAX	12.81	8.30	9.27	9.23	10.44	11.60	12.08	14.82	10.33	13.13	10.54	9.55	59.45
MIN	0.43	0.44	0.04	0.74	0.41	0.31	0.47	0.57	0.06	0.09	0.57	0.82	27.97

Table IV.A-2: con'd

fn: return

Return Frequency	Rain Depth* (inches)
2 year	3.1
5 year	4.0
10 year	4.5
25 year	5.4
50 year	5.9
100 year	6.5

*(Soil Conservation Service, 1975)
Interpolated Values

Table IV.A-3: 24 Hour Precipitation Return Periods

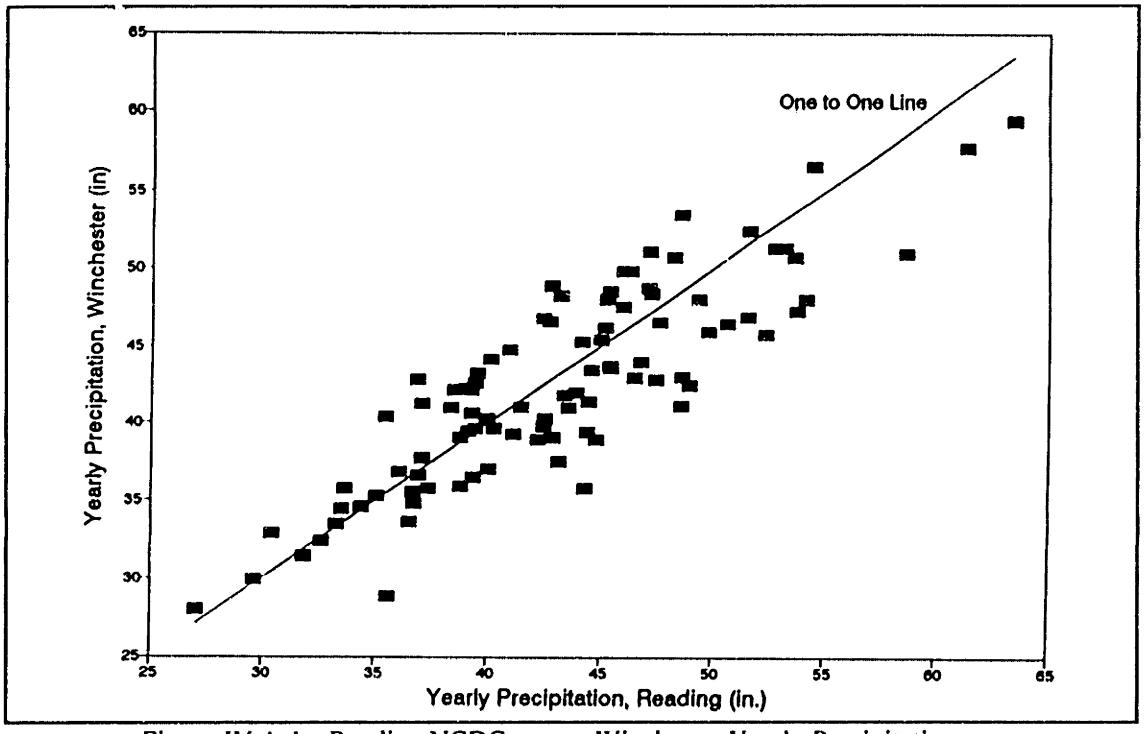

Figure IV.A-1: Reading NCDC versus Winchester Yearly Precipitation 1899 to 1992

FN: comprai

DATE (Jun '90)	Precipitation Gaging Station		
	Reading (in)	Burlington (in)	Winchester (in)
1	0.17	0.20	0.03
2	0.01	0.00	0.20
3	0.00	0.20	0.00
4	0.00	0.00	0.00
5	0.03	0.00	0.00
6	0.00	0.00	0.00
7	0.00	0.00	0.00
8	0.00	0.00	0.00
9	0.02	0.00	0.00
10	0.00	0.00	0.00
11	0.01	0.00	0.00
12	0.27	0.28	0.00
13	0.06	0.10	0.50
14	0.00	0.00	0.00
15	0.00	0.00	0.00
16	0.00	0.00	0.00
17	0.00	0.00	0.00
18	0.00	0.00	0.00
19	0.00	0.00	0.00
20	0.38	0.00	0.00
21	0.00	0.28	0.35
22	0.06	0.00	0.00
23	0.00	0.00	0.05
24	0.12	0.10	0.11
25	3.72	4.70	1.95
26	0.00	0.00	2.40
27	0.00	0.00	0.00
28	0.00	0.00	0.00
29	0.01	0.00	0.00
30	0.00	0.00	0.00
31	0.00	0.00	0.00
Sum	4.86	5.86	5.59

Table IV.A-4; Daily Precipitation at Reading, Burlington, and Winchester Stations, June 1990

FN: comprai

DATE	TIME	Precip Gaging Station	
		Reading (in)	Burlington (in)
July 24	14:00	0.01	0.01
	15:00	0.02	0.02
	16:00	0.00	0.01
	17:00	0.00	0.00
	18:00	0.00	0.00
	19:00	0.00	0.00
	20:00	0.00	0.04
	21:00	0.07	0.04
	22:00	0.00	0.00
	23:00	0.00	0.00
July 25	0:00	0.00	0.00
	1:00	0.07	0.06
	2:00	0.11	0.20
	3:00	0.92	0.28
	4:00	0.04	0.16
	5:00	0.02	0.03
	6:00	0.06	0.03
	7:00	0.06	0.09
	8:00	0.18	0.18
	9:00	0.39	0.44
	10:00	0.50	0.77
	11:00	0.17	0.51
	12:00	0.34	0.47
	13:00	0.59	0.90
	14:00	0.24	0.55
	15:00	0.02	0.05
	16:00	0.01	0.00
Sum		3.82	4.84

Table IV.A-5: Hourly Precipitation at Reading and Burlington, July 24 to 25, 1990

fn: gsum

Month	Flow		Elevation	
	Ave Flow (cfs)	% Time Data Available	Ave Water Elevation (ft NGVD)	% Time Data Available
Jan '91	8.5	99.8	15.8	99.8
Feb '91	9.2	98.1	15.9	99.1
Mar '91	11.5	100.0	16.1	100.0
Apr '91	11.8	99.7	16.2	99.7
May '91	8.4	99.7	16.2	99.7
Jun '91	1.9	100.0	15.9	100.0
Jul '91	1.6	100.0	15.9	10.0
Aug '91	3.0	88.6	16.0	88.6
Sep '91	5.5	100.0	16.1	100.0
Oct '91	5.6	100.0	16.0	100.0
Nov '91	12.6	70.0	16.2	70.0
Dec '91	12.1	66.4	16.2	66.4
Jan '92	12.4	47.1	16.2	47.1
Feb '92	11.6	62.3	16.1	62.3
Mar '92	13.4	56.5	16.1	56.5
Apr '92	10.0	91.1	16.1	91.1
May '92	6.4	99.7	16.1	99.9
Jun '92	5.0	100.0	16.2	100.0
Jul '92	1.8	99.7	16.1	99.7
Aug '92	4.4	100.0	16.1	100.0
Sep '92	1.8	100.0	16.1	100.0
Oct '92	2.3	96.9	16.2	96.9
Nov '92	7.8	97.1	16.2	97.1
Dec '92	15.0	90.0	16.2	90.0
Jan '93	11.1	67.6	15.9	67.6
Feb '93	----	----	----	----
Overall Ave	7.3	89.2	16.1	89.2
Inst. Max	38.9	----	17.7	----
Inst. Min	1.5 (or 0)	----	14.6	----

Table IV.A-6: Monthly Flow and Water Surface Elevations, Wedge Pond, Gage #1 (P.O.R. Jan 15, 1991 to Jan 24, 1993)

fn: gsum

Month	Flow		Elevation	
	Ave Flow (cfs)	% Time Data Available	Ave Water Elevation (ft NGVD)	% Time Data Available
Jan '91	14.5	60.4	46.6	60.4
Feb '91	12.8	77.8	46.5	77.8
Mar '91	14.0	91.5	46.6	91.5
Apr '91	12.3	99.9	46.4	99.9
May '91	14.0	40.6	46.5	40.6
Jun '91	3.1	62.3	45.8	62.3
Jul '91	2.5	100.0	45.7	100.0
Aug '91	4.3	94.3	45.8	94.3
Sep '91	8.7	100.0	46.1	100.0
Oct '91	6.4	100.0	46.1	100.0
Nov '91	10.9	100.0	46.3	100.0
Dec '91	10.6	91.0	46.4	91.0
Jan '92	13.3	66.8	46.5	66.8
Feb '92	9.2	57.6	46.2	57.6
Mar '92	11.5	55.7	46.4	55.7
Apr '92	10.7	41.2	46.4	41.2
May '92	5.0	36.7	46.0	36.7
Jun '92	9.4	84.3	46.2	84.3
Jul '92	4.2	100.0	45.9	100.0
Aug '92	6.1	100.0	46.0	100.0
Sep '92	3.7	100.0	45.8	100.0
Oct '92	3.7	77.8	45.8	77.8
Nov '92	6.8	100.0	46.0	100.0
Dec '92	15.4	83.7	46.6	83.7
Jan '93	12.4	43.6	46.5	43.6
Feb '93	19.3	37.8	46.7	37.8
Overall Ave	8.8	77.5	46.2	77.5
Inst. Max	75.1	----	49.0	----
Inst. Min	1.1	----	45.5	----

Table IV.A-7: Monthly Flow and Water Surface Elevations, Route 128, Gage #2 (P.O.R. Jan 10, 1991 to Feb 26, 1993)

fn: gsum

Month	Flow		Elevation	
	Ave Flow (cfs)	% Time Data Available	Ave Water Elevation (ft NGVD)	% Time Data Available
Jan '91	----	----	----	----
Feb '91	----	----	----	----
Mar '91	18.7	100.0	33.4	100.0
Apr '91	14.2	26.8	33.2	26.8
May '91	12.9	100.0	33.2	100.0
Jun '91	3.9	22.1	32.7	22.1
Jul '91	7.6	69.3	33.0	69.3
Aug '91	16.9	93.8	33.1	93.8
Sep '91	30.5	96.4	33.4	96.4
Oct '91	14.8	100.0	33.3	100.0
Nov '91	27.8	100.0	33.6	100.0
Dec '91	26.9	93.9	33.6	93.9
Jan '92	33.7	46.4	33.7	46.4
Feb '92	15.3	46.0	33.3	46.0
Mar '92	16.0	95.4	33.3	95.4
Apr '92	15.4	100.0	33.3	100.0
May '92	13.7	100.0	33.2	100.0
Jun '92	22.2	99.9	33.4	99.9
Jul '92	7.1	98.7	32.9	98.7
Aug '92	13.7	100.0	33.1	100.0
Sep '92	9.0	81.9	33.0	81.9
Oct '92	12.0	80.9	33.1	80.9
Nov '92	25.6	99.3	33.5	99.3
Dec '92	38.2	65.8	33.8	65.8
Jan '93	35.8	48.4	33.8	48.4
Feb '93	----	----	----	----
Overall Ave	18.6	81.5	33.3	81.5
Inst. Max	307.4	----	35.9	----
Inst. Min	3.2	----	32.7	----

Table IV.A-8: Monthly Flow and Water Surface Elevations, Montvale, Gage #3 (P.O.R. Mar 3, 1991 to Jan 24, 1993)

fn: gsum

Month	Flow		Elevation	
	Ave Flow (cfs)	% Time Data Available	Ave Water Elevation (ft NGVD)	% Time Data Available
Jan '91	13.1	46.4	41.9	46.4
Feb '91	14.1	100.0	42.0	100.0
Mar '91	15.2	92.7	42.0	92.7
Apr '91	----	----	----	----
May '91	10.4	83.1	42.3	83.1
Jun '91	4.8	37.0	42.1	37.0
Jul '91	1.3	52.5	41.3	52.6
Aug '91	4.9	57.5	41.6	57.5
Sep '91	6.5	69.7	41.8	69.7
Oct '91	4.3	79.5	41.9	79.5
Nov '91	1.1	64.9	41.5	64.9
Dec '91	----	----	----	----
Jan '92	24.3	100.0	41.7	100.0
Feb '92	12.8	72.5	41.7	72.5
Mar '92	15.2	87.9	41.9	87.9
Apr '92	15.7	99.7	42.4	99.7
May '92	10.1	99.3	42.3	99.3
Jun '92	9.7	99.6	42.6	99.6
Jul '92	5.3	72.7	42.4	72.7
Aug '92	8.7	100.0	42.5	100.0
Sep '92	4.3	100.0	42.4	100.0
Oct '92	1.9	100.0	42.5	100.0
Nov '92	6.8	95.5	42.0	95.5
Dec '92	20.8	71.7	42.3	74.6
Jan '93	15.1	86.0	41.8	86.0
Feb '93	18.1	37.3	41.9	37.3
Overall Ave	9.7	78.7	42.1	78.9
Inst. Max	131.5	----	44.1	----
Inst. Min	0.0	----	41.2	----

Table IV.A-9: Monthly Flow and Water Surface Elevations, Horn Pond, Gage #4
(P.O.R. May 24, 1991 to Nov 22, 1991 and Jan 31, 1992 to Feb 26, 1993)

fn: gsum

Month	Gage 1 (cfs)	Gage 2 (cfs)	Gage 3 (cfs)	Gage 4 (cfs)	Gage 5 (cfs)
Jan	10.1	13.5	34.8	18.7	37.8
Feb	10.2	13.0	15.3	14.3	33.9
Mar	12.2	13.0	17.4	15.2	39.5
Apr	10.9	11.9	15.2	15.7	36.7
May	7.4	9.7	13.3	10.3	25.9
Jun	3.4	6.7	18.9	8.4	21.5
Jul	1.7	3.3	7.3	3.6	13
Aug	3.8	5.2	15.3	7.3	21.9
Sep	3.7	6.2	20.6	5.2	22.9
Oct	4.0	5.2	13.5	3.0	16.5
Nov	9.8	8.9	26.7	4.5	32.1
Dec	13.8	12.9	31.5	20.8	48.1

Table IV.A-10: Mean Monthly Flow, All Stations
January 1991 to January 1993

FN:usgsmo.wq1

YEAR	JAN	FEB	MAR	APR	MAY	JUN	JUL	AUG	SEP	OCT	NOV	DEC	AVE
1939					28.9	11.4	1.74	1.2	1.28	1.37	1.35	1.59	
1940	10.1	13	81.8	99.3	42.1	21.7	9.13	1.31	2.99	0.87	13.6	23.6	26.6
1941	27	47.1	36.4	26.7	15.5	4.41	0.88	0.68	0.74	0.48	0.59	0.63	13.4
1942	8.47	33.2	88.7	44.8	19.8	8.07	4.67	1.45	0.88	0.81	4.72	36.9	21.0
1943	28.1	46.3	64.2	32.9	50.9	16.1	2.93	1.51	0.64	3.29	11.8	6.64	22.1
1944	14.4	25.4	42.7	49.3	18.8	10.8	2.6	0.75	5.52	3.75	14.7	48.8	19.8
1945	33.2	30.2	95.3	33.6	45.3	29.7	10.2	5.18	1.38	1.97	15.5	80.5	31.8
1946	69.3	50.7	81	26.6	28.5	27.5	2.45	24.9	7.14	6.17	2.86	11.9	28.3
1947	28.4	23.8	58.5	34.8	46	14.6	4.7	3.33	4.49	0.63	17.9	9.45	20.6
1948	10	38.9	125	53.1	31.9	47.7	22.8	2.49	0.85	0.7	10.2	9.72	29.4
1949	18.1	42.7	42.9	46.4	22.7	3.88	0.86	0.7	1.86	0.79	3.2	6.02	15.8
1950	19.2	26.9	63	38.7	13.2	3.39	0.69	1.01	0.56	0.5	8.6	21.4	16.4
1951	33.9	77.6	71.2	66	26	25.7	9.86	5.37	2.97	10.5	67.4	49.5	37.2
1952	71.8	59.5	100	47.9	47.3	24.4	2.71	7.87	2.29	1.06	1.02	7.29	31.1
1953	31.8	57.3	88.9	114	58.3	6.4	1.56	0.95	0.71	1.56	18.8	54.2	36.2
1954	30.8	39.5	45.2	49.3	134	25.2	6.28	7.48	78.2	18.9	39.1	58.9	44.4
1955	38.4	37.4	66.8	33.3	21.9	14.4	7.04	79.4	21.4	74	102	21.2	43.1
1956	78.3	70.6	70.1	117	34.3	12	2.52	1.22	1.34	2.63	7.13	17.8	34.6
1957	34.5	33	38.2	44.5	15	3.02	1.01	0.62	0.49	0.54	1.66	13.1	15.5
1958	90.9	55.6	103	85.6	48.9	12.8	8.1	6.09	7.38	18.9	21.5	21.1	40.0
1959	23.5	32.4	65.3	42.2	15.6	26	40.4	12.6	7.32	8.45	15.3	34.6	27.0
1960	36.6	69.6	43.6	60.3	22.5	16.1	6.22	3.53	13.4	7.39	18.5	16.1	26.2
1961	24.8	33.7	71.3	84.8	38.4	14.3	6.1	7.26	34.6	24	28.8	25.9	32.8
1962	55	21.5	81.3	55.3	23.9	10.9	3.64	4.07	5.01	104	59.5	56	40.0
1963	40.5	26	89.6	32.7	20.7	8.04	3.76	2.44	2.88	4.02	31.6	41	25.3
1964	48.5	54.4	70.9	61.7	15.7	5.85	4.81	2.13	2.3	3.2	3.32	12.9	23.8
1965	8.3	33.2	30.5	23	11.3	8.67	1.89	1.81	1.74	1.96	1.86	2.38	10.6
1966	2.34	16.9	33.6	12.4	13	7.15	2.27	1.77	3.65	2.67	9.76	3.95	9.1
1967	16.5	23.2	48.8	64.6	72.5	27.1	12.9	8.59	11.7	7.25	10.4	21	27.0
1968	21.2	37.6	102	27.6	20.6	30.7	11.5	5.31	2.99	2.54	18.9	33.3	26.2
1969	31.3	21.4	81.2	76.2	24.1	7.75	6.6	7.78	9.92	5.71	51	95.7	34.9
1970	40.9	76.4	45.6	71.6	32.9	22.3	6.98	9.2	4.68	7.05	13.2	14.2	28.8
1971	9.55	37.1	74.2	32.3	33.8	13.9	5.97	4.87	2.59	3.55	15.9	14.8	20.7
1972	15.9	32.2	124	48.1	58.8	91.6	21.7	8.57	11.2	9.9	51.2	68.6	45.1
1973	48.7	55.5	32	72.9	36.1	22.2	28.1	22.3	9.9	8.36	10.1	58.8	33.7
1974	43.4	45	45.7	46	35.7	17	7.81	2.75	13	10.9	8.16	34	25.8
1975	57.9	41.3	41.5	40.8	14.8	9.48	2.94	8.71	17.6	29	56	46.2	30.5
1976	74.5	63.4	41.2	26.4	18.6	3.69	9.95	23.6	8.83	11.9	5.63	7.11	24.6
1977	10.4	23.6	97.3	55.2	47.8	16.1	7.82	11.4	10.3	22.4	45.1	75.1	35.2
1978	87.4	28.6	73	50.3	35.1	12.8	5.16	7.19	1.59	4.47	3.22	15.6	27.0
1979	169	40.5	59.5	40.2	33.5	17.7	9.8	15.7	13.3	21.6	29.4	12.5	38.6
1980	7.74	4.39	32.7	50.5	22.5	9.85	11.7	4.04	3.41	14.1	11.8	7.11	15.0
1981	3.42	51.4	33.5	24.4	14	10.4	14	5.3	7.2	13.1	28.4	45.6	20.9
1982	73.3	65.4	36.4	31.9	23.5	159	32.5	18.2	11.5	15.4	20.3	14.2	41.8
1983	27.4	67.6	167	104	43.2	20	6.51	10.8	7.45	10.3	65.5	89.5	51.6
1984	30.1	104	96.2	95.4	68.3	104	26.2	7.56	5.64	10.6	11.8	21.2	48.4
1985	12.1	20.2	26.4	20.2	16.3	14.2	16.8	23.2	25.4	17.2	56.7	32.2	23.4
1986	35.2	39.4	63.2	25	13.8	40.9	23.5	10.5	5.33	7.02	26.4	93.7	32.0
1987	52.4	25.7	55.1	175	37.6	12.1	5.82	9.3	28.1	15.2	12.7	23.3	37.7
1988	18.5	44.3	45.8	30.1	37.4	17	30.5	12.5	9.81	9.58	36.2	17.5	25.8
1989	7.96	13.8	19.2	54.8	40.5	25.8	12.6	18.8	13.7	25	40.9	12.2	23.8
1990	32.3	54	33.3	58.5	55.2	19.7	21.4	53.6	10.6	63.2	34.1	31.6	39.0
1991	32.4	41.2	43.5	40	28.2	13.6	6.68	20.1	33	20.4	38.2	37.3	29.5
1992	40.2	26.6	35.4	33.3	23.6	29.3	14	23.6	12.8	12.6	26	58.9	28.0
1993	40.7	44.6	82.3	117	23	10.7	7.07	6.13	11.2				
AVE	36.2	41.2	64.5	54.2	33.1	21.8	9.8	10.0	9.4	12.7	23.3	31.0	29.0
STD D	28.4	18.8	29.2	30.4	20.1	25.8	9.0	13.2	12.3	18.5	21.0	24.8	9.5
MAX	169.0	104.0	167.0	175.0	134.0	159.0	40.4	79.4	78.2	104.0	102.0	95.7	51.6
MIN	2.34	4.39	19.20	12.40	11.30	3.02	0.69	0.62	0.49	0.48	0.59	0.63	9.12

Table IV.A-11: Monthly Streamflow, Gage 5, USGS Station, 1939 to 1993

APPENDIX IV.B

Streamflow and Precipitation:
Hourly Plots, Jan 1991 to Sep 1993

STREAMFLOW & PRECIPITATION: HOURLY PLOTS, JAN '91 to SEP '93

Hourly streamflow and precipitation plots are provided for the January 1991 to September 1993 period of record. Streamflow is provided for each of the 5 gaging stations. Precipitation corresponds to the Reading Station. Each page corresponds to a one-half month time period. The time between successive symbols on these plots (circles for the USGS flow data, x's for the precipitation data) is one hour. To accomodate different flow conditions, the vertical scale has been adjusted periodically throughout the record.

Vertical lines towards zero flows mark the beginning and the end of time periods with no streamflow data. During times when no streamflow data was available, streamflow was assigned a value -100. Therefore, at the point where the gap in the streamflow record begins, the streamflow values go from a positive streamflow value to a value of -100. When the streamflow measurements were again available, the plotted streamflows go from a -100 value to a positive value. The net result are vertical lines periodically observed in the data. Because these vertical lines are due to the manner in which gaps in the streamflow record were handled and should therefore be ignored.

ANOMALOUS FLUCTUATIONS IN THE STREAMFLOW DATA

A description of anomalous fluctuations is included in this appendix to supplement section IV.2 which discusses the more consistent behavior of the streamflow system. Although the anomalous fluctuations are of interest from a hydrologic point of view, the phenomena discussed in this section were not included within the model formulation. The omission does not strongly affect model performance.

The anomalous fluctuations described in this section have been attributed to: 1) a flow reversal between the Aberjona and Wedge Pond, 2) freezing and thawing effects, 3) Atlantic Gelatin withdrawal and other channel losses, 4) sensitivity of the streamflow monitoring system, and 5) other causes. Specific examples of these anomalies are described below.

Flow Reversal Between the Aberjona River and Wedge Pond

The anomalous fluctuation which occurred August 22, 1991 at the USGS station was due to the reversal of streamflow from the Aberjona to Wedge Pond. The streamflow direction at the Wedge Pond station was typically from west to east. However, on one occasion during a field sampling trip the flow was observed in the opposite direction. The observed flow reversal occurred at 9:30 am August 22, 1991, three days after Hurricane Bob. The cause of the flow reversal was associated with backwater from the Aberjona River. Prior to Hurricane Bob, the preceding months were very dry and the Horn Pond and Wedge Pond reservoirs were low. During the hurricane, the reservoirs were permitted to fill, restricting the flow of water through the downstream end of the Horn Pond Creek tributary. Flow along the Aberjona River, on the other hand, remained high. As a result, the water elevation of the Aberjona River at the junction with Horn Pond Creek was higher than the water elevation of Wedge Pond. Therefore, during this time river flow direction was reversed causing a backflow from the Aberjona into the Wedge Pond reservoir. Such a flow reversal (or backwater effect) is predicted by F.E.M.A. 1979, for events with return period greater than 10 years.

The fact that the water had come from the Aberjona was verified in three ways. First, at the river junction, a portion of the Aberjona River flow was visually observed to be diverted toward Wedge Pond. The remaining Aberjona River flow continued downstream toward the USGS gage. Secondly, a large dip in the USGS streamflow hydrograph (August 22, 1992, appendix IV.B) was observed during the time the reversal was observed. One interpretation of this dip is that water was suddenly diverted somewhere upstream from the USGS station. The third indication that the water came from the Aberjona, is associated with the quality of a sample collected during the flow reversal. Typically, the concentrations of metals of the samples collected at the Wedge Pond station were much lower than the concentrations of samples collected from the Aberjona River. The sample collected during the flow reversal had metal concentrations similar to those found in the Aberjona River, which is consistent with the notion that the water originates from the Aberjona. Therefore, during a flow reversal, not only is the flow of water to the Wedge Pond reservoir increased, but also, the supply of contaminants to the reservoir is enhanced. Due to the quiescent conditions of Wedge Pond, a large fraction of the particulate metals coming from the Aberjona during reverse flow conditions could possibly settle within the pond and remain in the bottom sediments.

The amount of water associated with the flow reversal was quantified in two ways. The first was through a direct measurement. Upon arriving at the Wedge Pond station and noting the flow reversal, the velocity probe was oriented in the opposite direction such that velocities could be measured during the flow reversal. (Note that velocities can only be measured in one direction using the available field equipment) The probe was left in this direction until after the flow returned to its normal direction.

The volume of water computed by measuring flow in the opposite direction, is considered to be a conservative estimate since measurements began after the reversal had initiated. The volume of the water determined in this way was 275,000 ft^3 which represents approximately 3% of the volume of Wedge Pond. The second method of quantification was by drawing a smooth curve between 6:00 am and 6:00 pm during August 22, 1991 on the USGS hydrograph. The volume of water between this curve and the measured flow at the USGS station is assumed to be the volume of water associated with the flow reversal. The volume of water computed in this manner was 854,000 ft^3 or 9% the volume of Wedge Pond. Using 854,000 ft^3, and the metal concentrations corresponding to the flow reversal sample, the excess mass of particulate metal[16] supplied to the Wedge Pond during this event was approximately 23 g of Cr, 20 g of Cu, and 125 kg of Fe. Because of these small quantities and because flow reversals are not assumed to be frequent, the extra water and metals supplied to the pond during flow reversals over the course of a year is probably insignificant. However, during the short time periods when flow reversals occur, there is a possibility for a short-term disruption of the ecologic, chemical, and hydraulic status of the pond.

The August 22 flow pattern at the USGS station is very similar to the fluctuations observed October 1, 4, and 18, 1991. The similarities include that: 1) both August and October fluctuations followed large storm events, 2) each dip was characterized by a quick drop (within about 2 hours) to near zero values, and 3) each rise was characterized by a quick initial increase followed by a more gradual increase. Due to these similarities one may speculate that the October fluctuations were also associated with a flow reversal.

Additionally, on October 3, 1991 a significant peak occurred in the USGS hydrograph although there was no precipitation and no snowmelt. One possible explanation is that this peak was due to a discharge from the Horn Pond reservoir. However, such a sharp peak would not be expected from a Horn Pond discharge because of the attenuating affects of the Wedge Pond reservoir upstream of the gaging station. This peak is especially conspicuous since dips in the streamflow hydrograph were observed shortly before and after the peak. Furthermore, it appears as though the pattern of this peak followed a "mirror image" of the dips - a quick initial increase (versus a decline) in flow followed by a quick drop (vs increase) in flow and a more gradual decline (vs increase) after the initial decline. From this pattern, one may postulate that this peak had some relationship to the dips in the data.

One possible scenario is that flow was actually sloshing back and forth between the Aberjona and Wedge Pond. One can analogously compare this behavior with a surge tank and controlled reservoir system,

---

[16] (Particulate Conc during a Flow Reversal - Mean Particulate Conc) * SS Flux

where Wedge Pond serves as the "surge tank" and the Aberjona River serves as the "reservoir". For such a system, if the release of water from a reservoir is suddenly halted (i.e. a diversion of flow from the Aberjona to Wedge Pond), the excess momentum of the system is diverted to a surge tank which fills up with water. Because of the momentum excess, the elevation of the water in the surge tank can be higher than the elevation of water in the reservoir. For this situation, water will then flow from the surge tank back to the reservoir. After the water surges back to the reservoir, if the elevation of the reservoir is greater than the elevation in the tank, then water will again proceed to re-fill the surge tank. This surging of water back and forth between the tank and the reservoir would continue until frictional resistance dissipated the excess momentum of the water.

In other words, one may speculate that streamflow did reverse back from the Aberjona to Wedge Pond on October 1. This water from the Aberjona surged into Wedge Pond causing an elevation increase in the pond. Because of the momentum associated with this reversal, the elevation of the pond at the end of the flow reversal cycle was higher than the elevation in the Aberjona. Due to the high Wedge Pond water elevation, the flow reversed again toward the Aberjona causing the peak flow observed on October 3. However, the momentum of this release may have also over-compensated the removal of water from the pond resulting in a net elevation deficit. This deficit then again caused a flow reversal from the Aberjona back to Wedge Pond as evidenced by the dip in the USGS hydrograph on October 4.

Another similar "mirror image" in the flow pattern was observed February 3 to 4, 1992. The behavior during these times may also perhaps be attributable to a sloshing of water between the Aberjona River and Wedge Pond.

Freezing and Thawing Effects

Other anomalous fluctuations in the data were characterized by sharp decreases and increases in streamflows as observed at the USGS station. These fluctuations are typified by the March 18, 1993 to May 2, 1993 hydrograph record. These types of fluctuations may have been associated with snowmelt, which dominated the streamflow hydrographs during these time periods. Comparison of the flow record with the temperature record (figure IV.B-1) indicates that several of these fluctuations occurred as the temperature fell to near or below freezing. (especially note March 26, March 28 and March 31) One interpretation of this trend is that these fluctuations were caused by the freezing and thawing of the snowmelt supply to the river. During a freezing cycle, the snowmelt refreezes and no longer contributes to the river's flow. The result is a sharp decrease in streamflow. During the thawing cycle, the frozen meltwater re-melts and contributes to the streamflow of the river, resulting in a sharp increase in streamflow. In an attempt to quantify these affects, a snowmelt model was written where the routing of snowmelt was halted during below freezing temperatures. This attempt was capable of capturing some of these fluctuations;however, the timing of other fluctuations did not coincide in time. The inconsistent trends could have been due to the temperature data, which was collected at the northern end of the watershed, and which therefore may not have been representative of the temperature at the southern end of the watershed. For example, in the northern end of the watershed, the ground elevations are higher than elevations on the southern end. This elevation difference may result in temperatures that are lower on the north end than on the south end.

Nevertheless, snowmelt contribution and temperature fluctuations is one possible explanation for these fluctuations simply because they were most prevalent when: 1) snowmelt was a contributing component to streamflow, and 2) during times when temperatures oscillated above and below freezing.

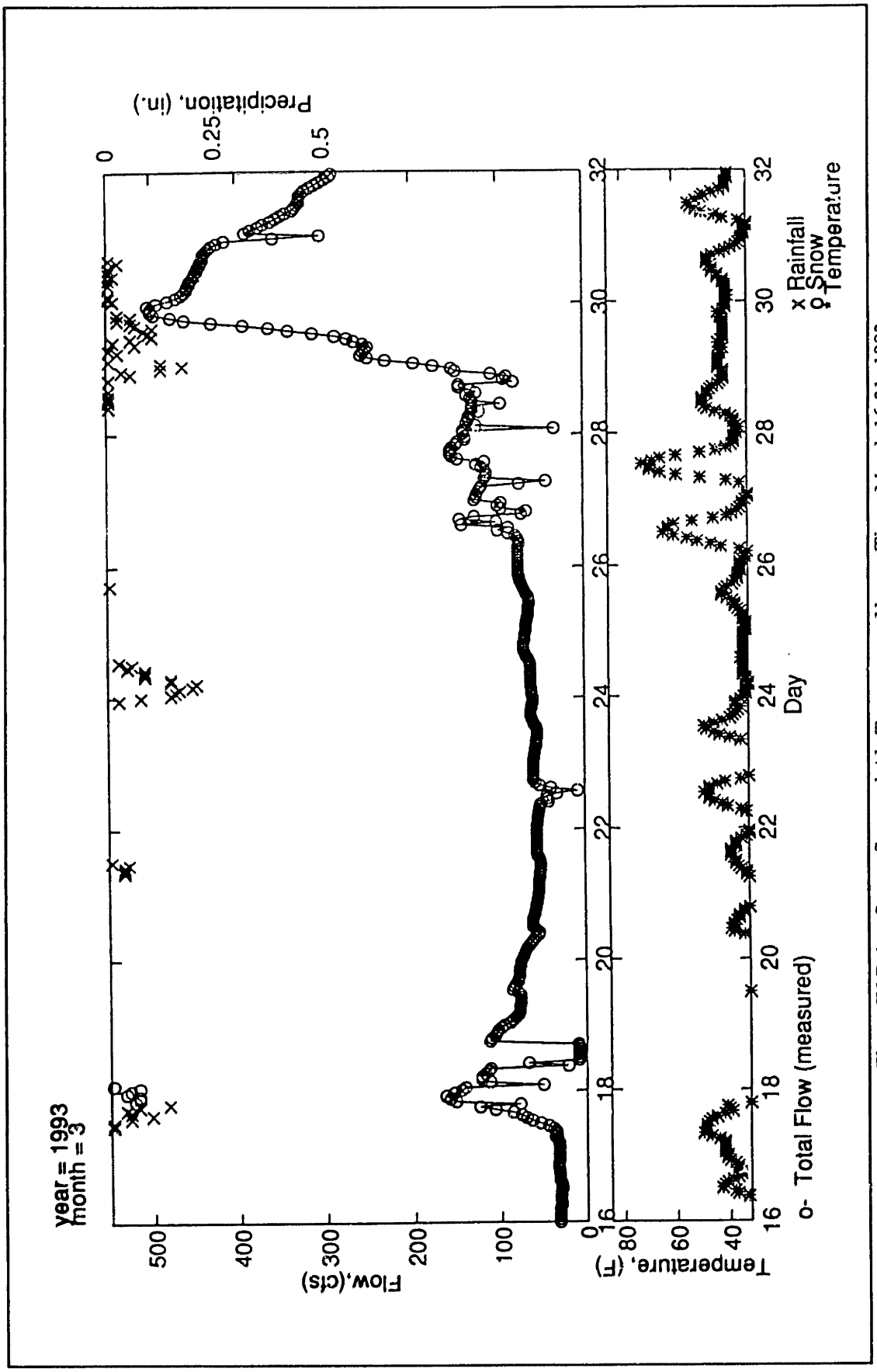

Figure IV.B-1: Streamflow and Air Temperature Versus Time, March 16-31, 1993

Atlantic Gelatin Withdrawal and Other Channel Losses

On occasion during extremely low flow conditions, streamflow at Montvale was slightly larger than streamflow at the USGS. (July 18-26, 1991; August 1-10, 1991; September 9-14, 1991; September 16-19, 1992; October 28-31, 1992) This occurrence may have been due to a combination of: 1) very low baseflow contributions from each of the sub-basins, 2) groundwater withdrawals at the Atlantic Gelatin site (just downstream of Montvale), 3) evaporation/exfiltration of water from the channel and/or, 4) a loss of water from the Aberjona River to Wedge Pond. For example, during July 22, 1991, the contribution from Wedge Pond station was negligible, the flow at Montvale was approximately 4.5 cfs and the flow at the USGS station was approximately 2 cfs. If one ignores the area draining the Wedge Pond gage, the drainage area at Montvale and USGS gages would be 8.2 mi^2 and 14.5 mi^2, respectively. Assuming that all the flow at Montvale was baseflow, then one would expect an additional contribution of baseflow from the drainage area between Montvale and the USGS station of 3.5 cfs (=4.5*(14.5-8.2)/8.2). The expected flow at the USGS station would therefore be 8 cfs (= 3.5+4.5). The difference between the expected and the observed flow is 6 cfs (8-2). This difference, or "lost" water, is in part due to the Atlantic Gelatin withdrawal which removes an average of 2.8 cfs. The rest of the lost water, 3.2 cfs (6-2.8) may have been due to some other loss. Other losses may include channel evaporation, exfiltration of water into the groundwater system between Montvale and the USGS, and possibly a flow reversal of water from the Aberjona River into Wedge Pond.

Sensitivity of the Streamflow Monitoring System

Low flows at the Wedge Pond station were characterizedby an oscillation between 1.5 and 9.1 cfs. This oscillation was due to: 1) the fluctuation of the gage point velocity, v_p, near the resolution limit, and 2) the calibration relationship for Wedge Pond which is given in section III.3 as:

$$Q = 2.88D^{2.032}v_p^{0.225} + 1.529$$

For Wedge Pond the water depth, D, was relatively constant near a value of 2.3 feet. During low flows the gage point velocity, v_p, tends to vary between 0 ft/s and, because of instrument resolution, 0.04 ft/s. For v_p equal to 0 ft/s and 0.04 ft/s, Q equals 1.5 cfs and 9.1 cfs, respectively.

Other Causes

Other possible causes of anomalous fluctuations in the USGS data may be associated with the control structures along the river. For example, adjustments to a set of gates which are located under Winchester Falls could have possibly affected streamflow. The maximum total estimated capacity of these gates is 100 cfs. Other factors may include; 1) changes in the industrial discharge or uptake rates of water, or 2) errors in the streamflow measurements.

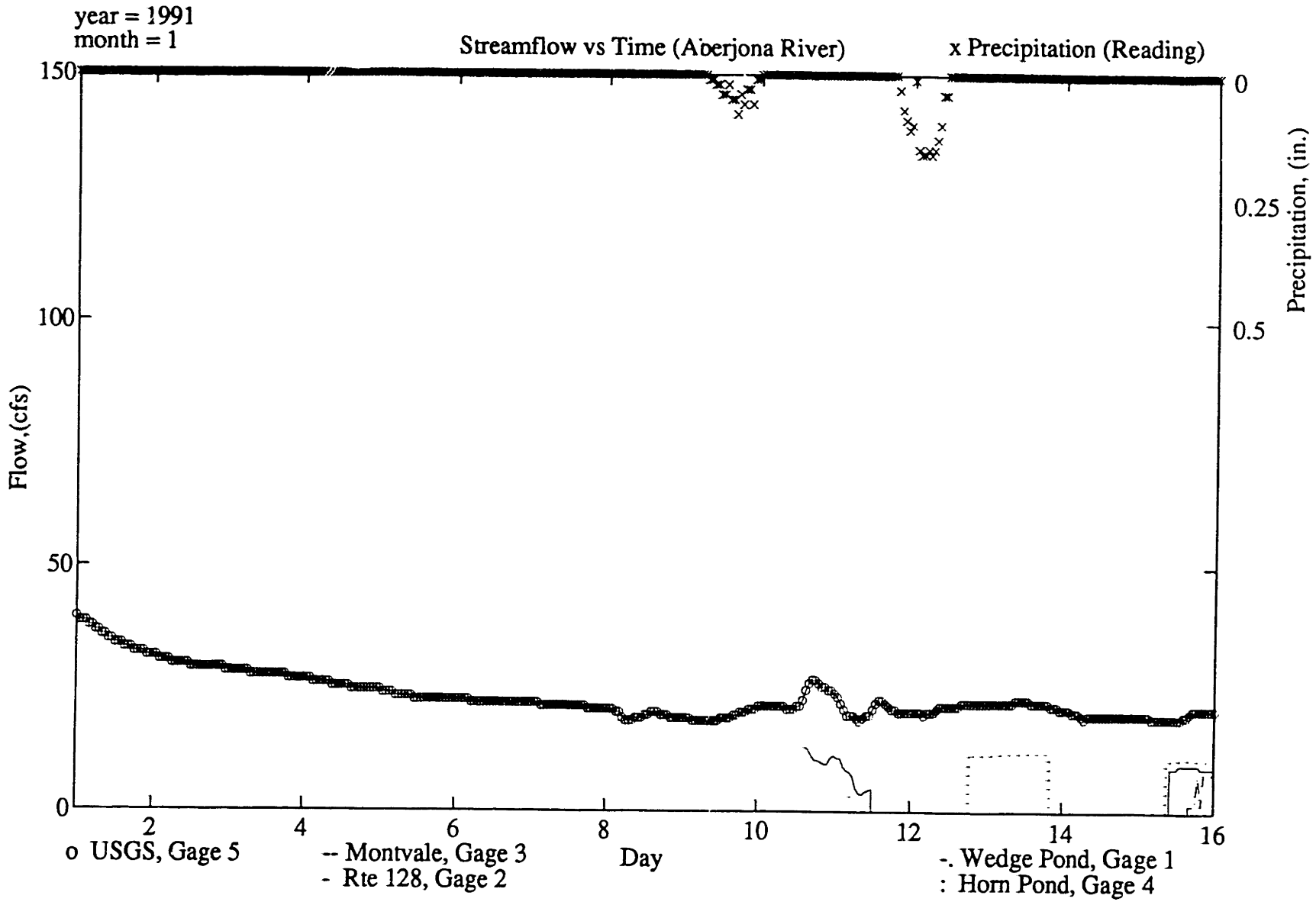
year = 1991
month = 1
Streamflow vs Time (Aberjona River)
x Precipitation (Reading)
150
100
50
0
Flow,(cfs)
0
0.25
0.5
Precipitation, (in.)
2
4
6
8
10
12
14
16
Day
o USGS, Gage 5
-- Montvale, Gage 3
- Rte 128, Gage 2
-. Wedge Pond, Gage 1
: Horn Pond, Gage 4

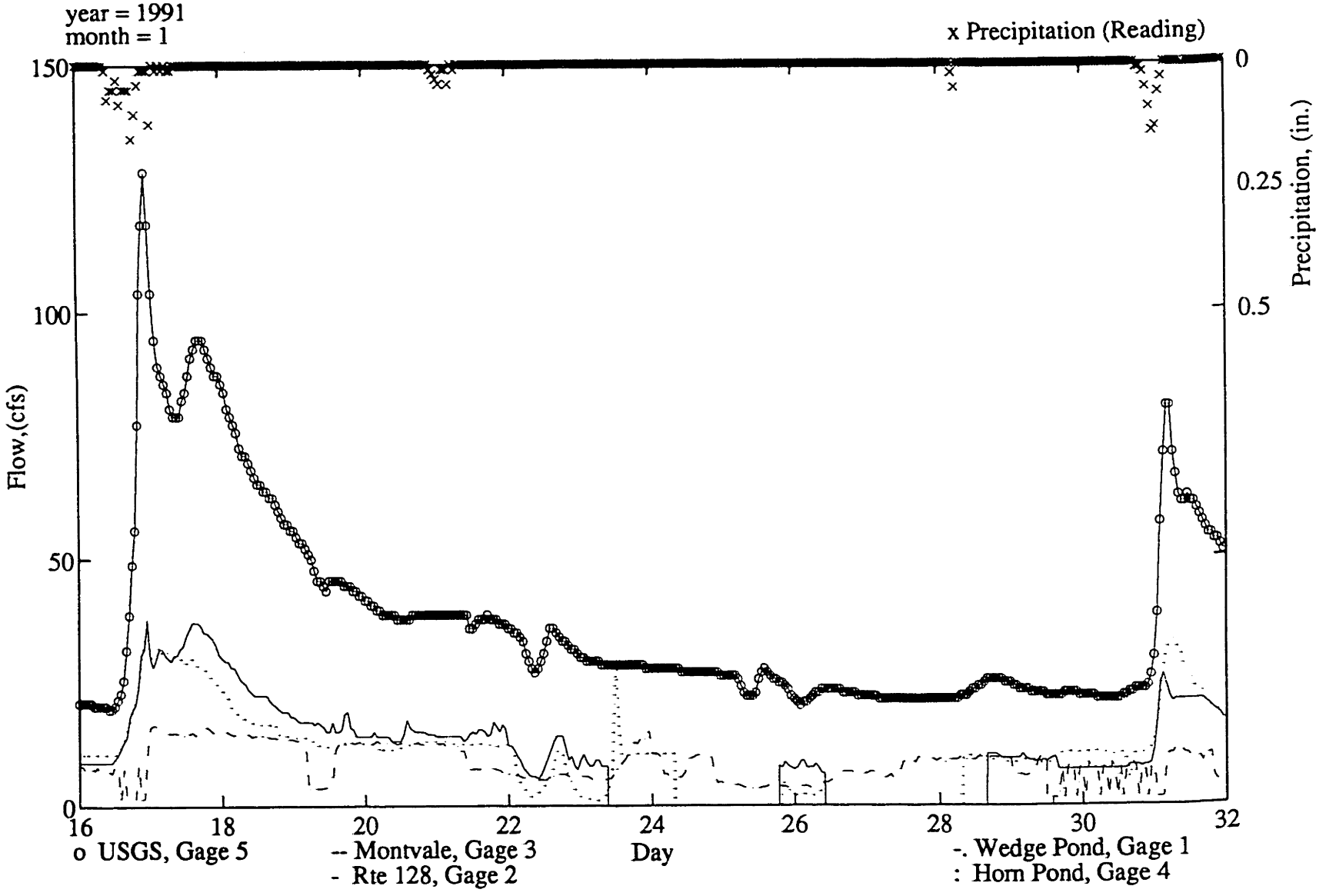
year = 1991
month = 1
x Precipitation (Reading)
150
100
50
0
0
0.25
0.5
Precipitation, (in.)
Flow,(cfs)
16
18
20
22
24
26
28
30
32
Day
o USGS, Gage 5
-- Montvale, Gage 3
- Rte 128, Gage 2
-. Wedge Pond, Gage 1
: Horn Pond, Gage 4

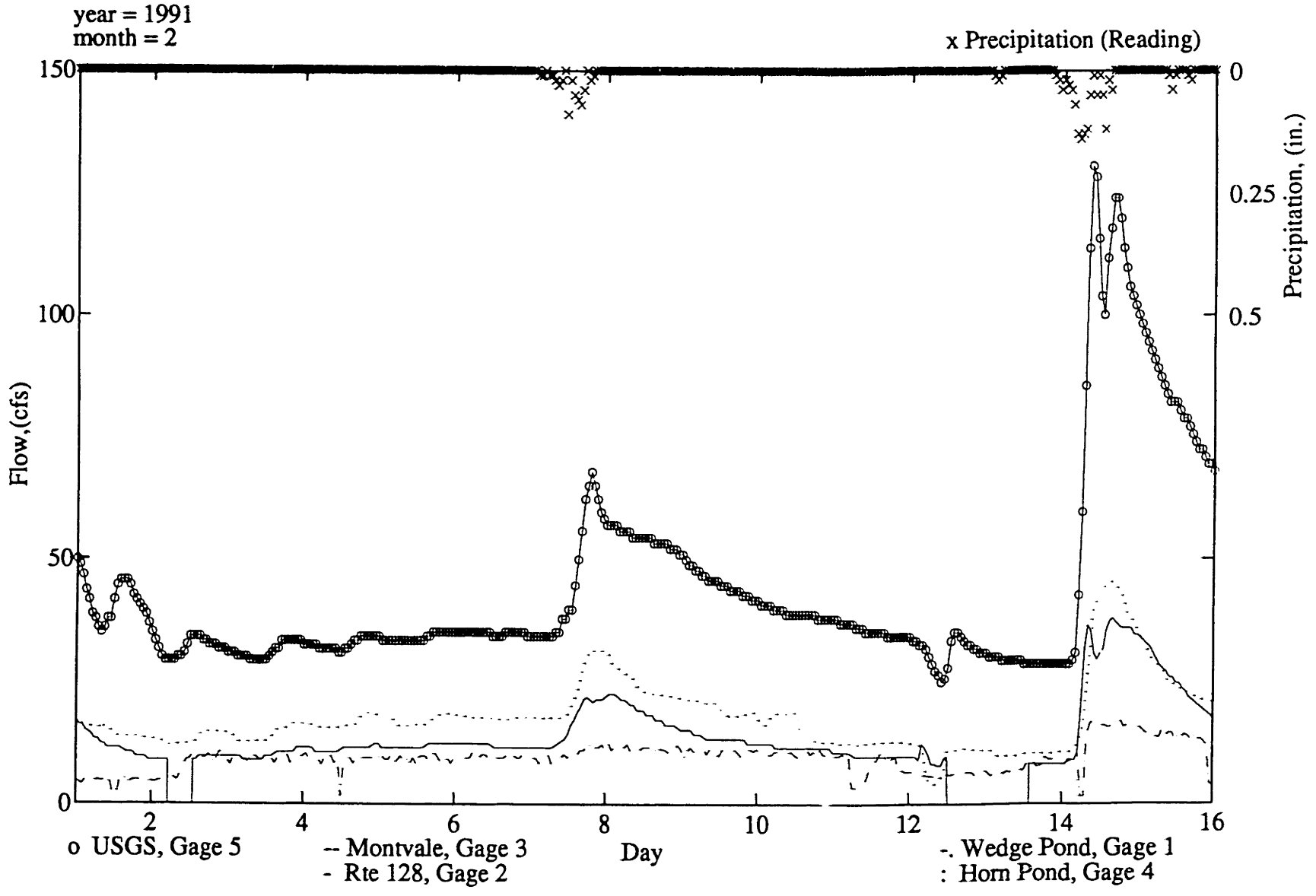
year = 1991
month = 2
x Precipitation (Reading)
150
100
50
0
0
0.25
0.5
Precipitation, (in.)
Flow,(cfs)
2
4
6
8
10
12
14
16
Day
o USGS, Gage 5
-- Montvale, Gage 3
- Rte 128, Gage 2
-. Wedge Pond, Gage 1
: Horn Pond, Gage 4

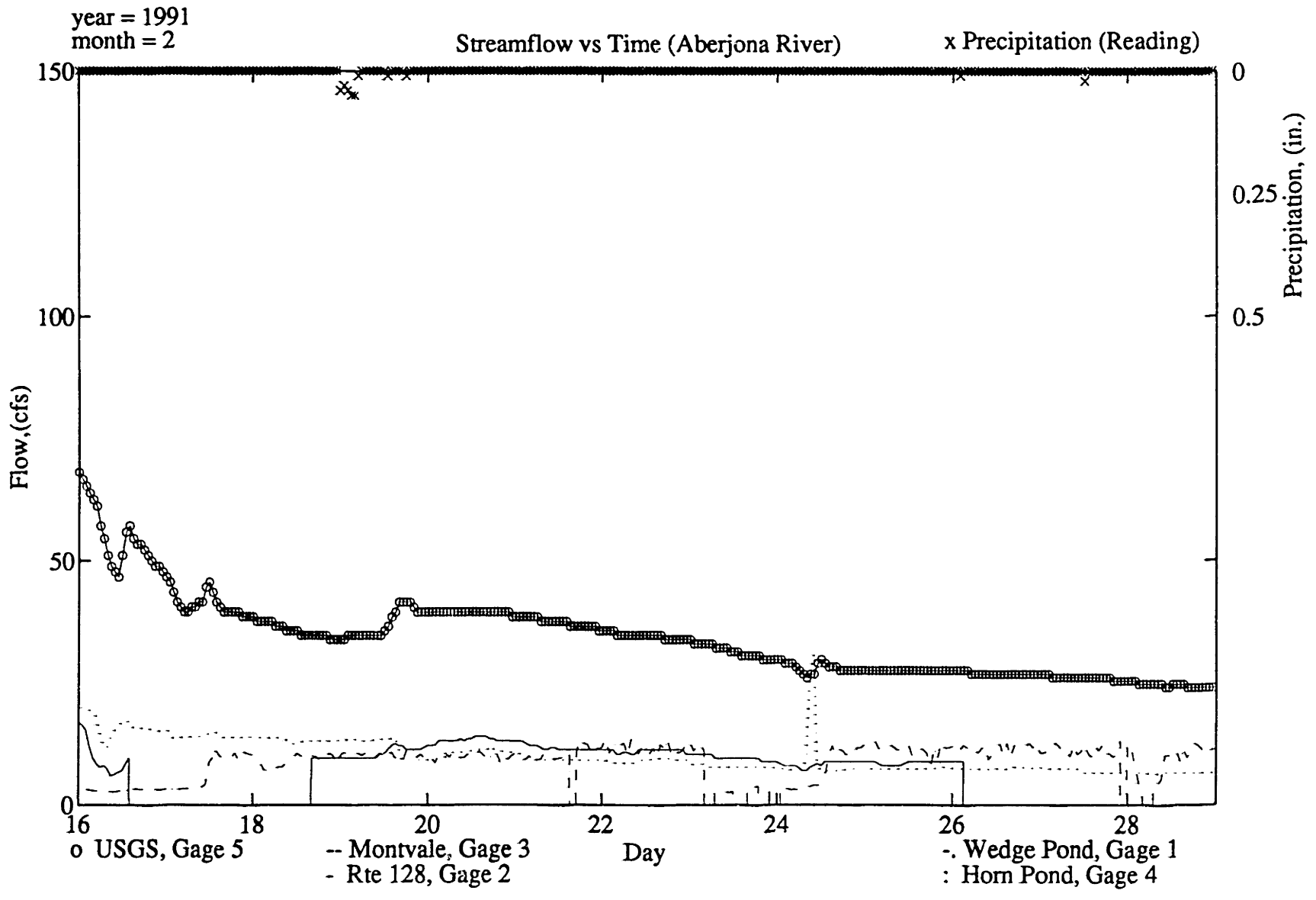
year = 1991
month = 2
Streamflow vs Time (Aberjona River)
x Precipitation (Reading)
150
100
50
0
0
0.25
0.5
Precipitation, (in.)
Flow,(cfs)
16
18
20
22
24
26
28
Day
o USGS, Gage 5
-- Montvale, Gage 3
- Rte 128, Gage 2
-. Wedge Pond, Gage 1
: Horn Pond, Gage 4

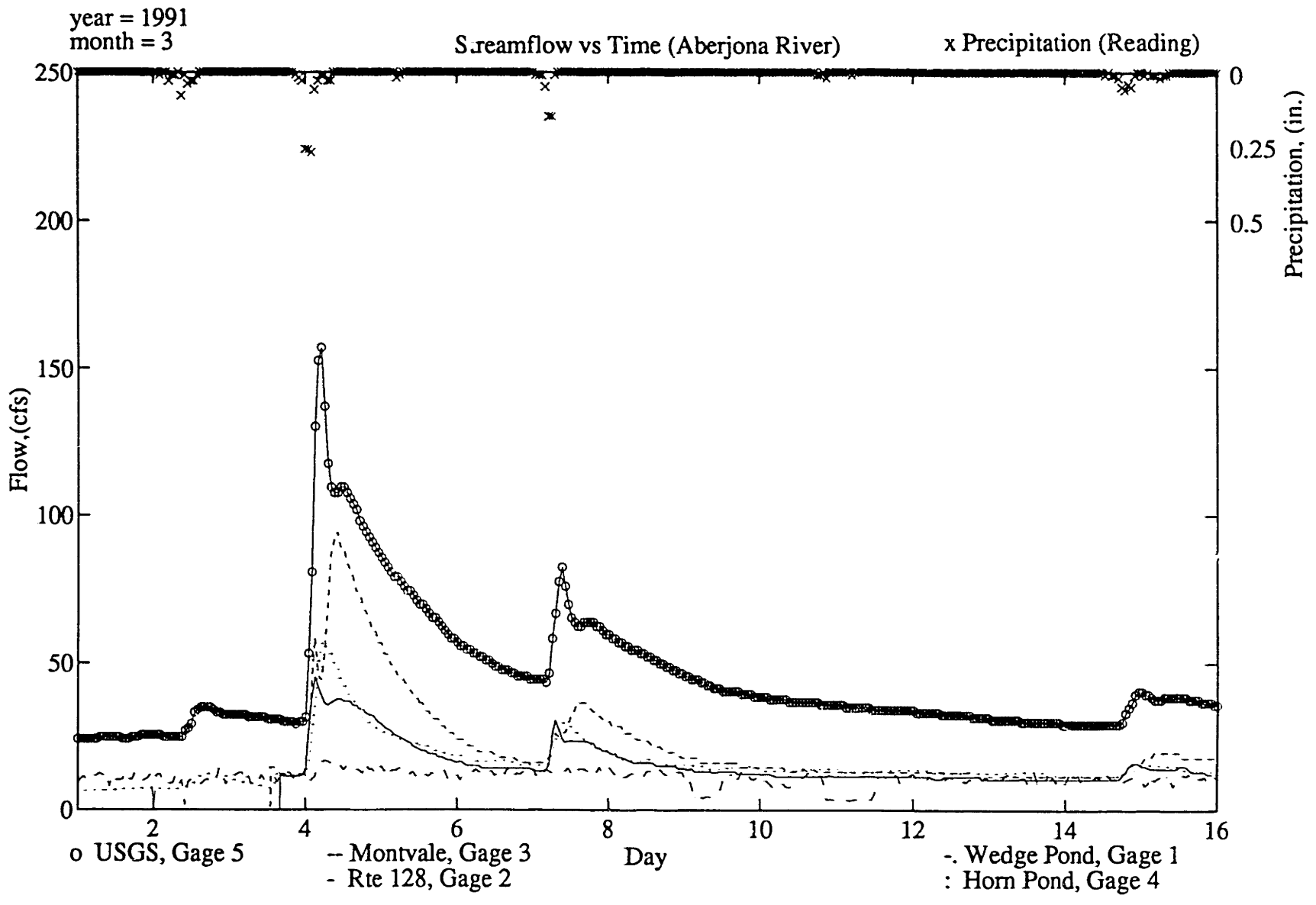
year = 1991
month = 3
Streamflow vs Time (Aberjona River)
x Precipitation (Reading)
250
200
150
100
50
0
Flow,(cfs)
0
0.25
0.5
Precipitation, (in.)
2
4
6
8
10
12
14
16
Day
o USGS, Gage 5
-- Montvale, Gage 3
- Rte 128, Gage 2
-. Wedge Pond, Gage 1
: Horn Pond, Gage 4

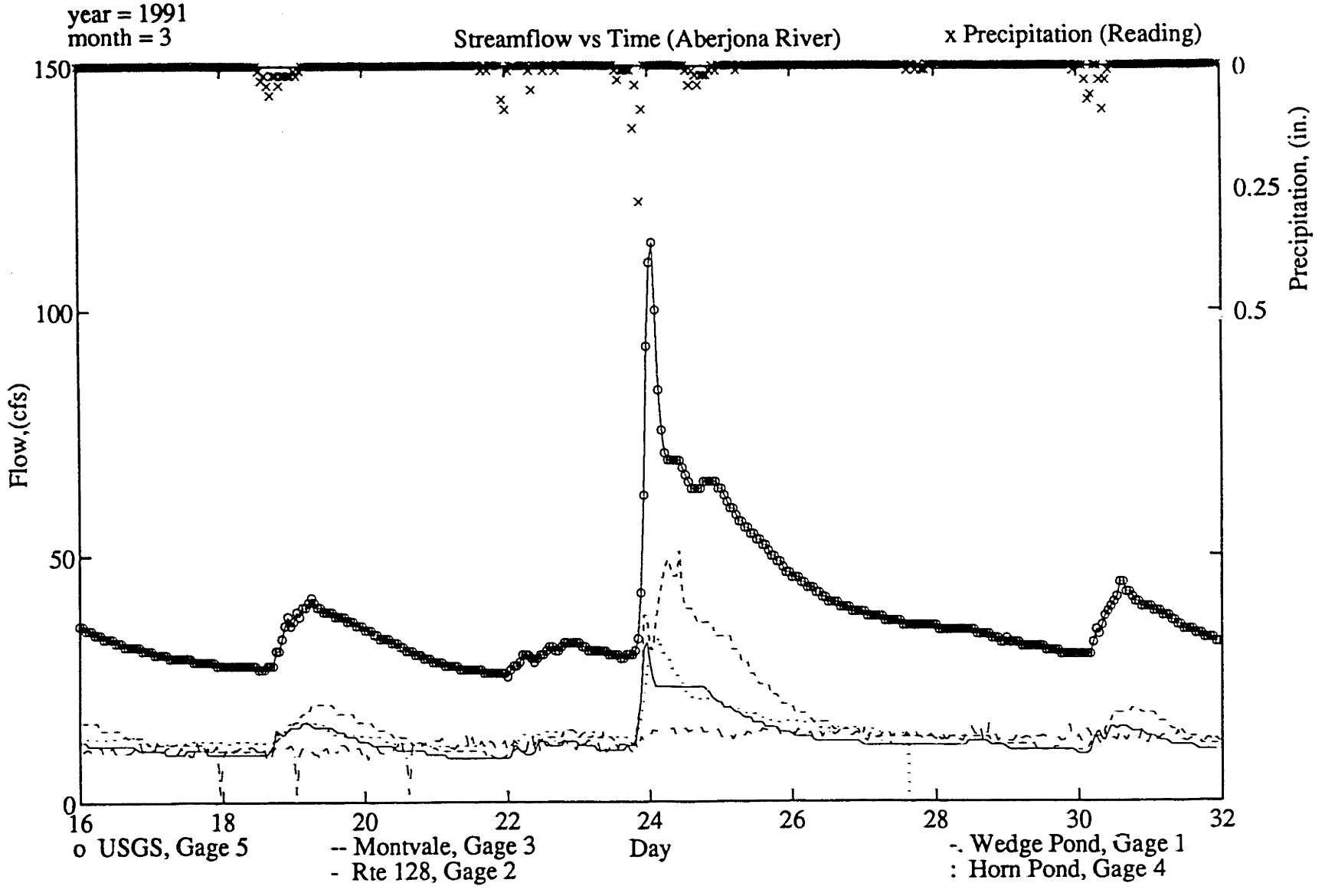
year = 1991
month = 3
Streamflow vs Time (Aberjona River)
x Precipitation (Reading)
150
100
50
0
0
0.25
0.5
Precipitation, (in.)
Flow,(cfs)
16
18
20
22
24
26
28
30
32
Day
o USGS, Gage 5
-- Montvale, Gage 3
- Rte 128, Gage 2
-. Wedge Pond, Gage 1
: Horn Pond, Gage 4

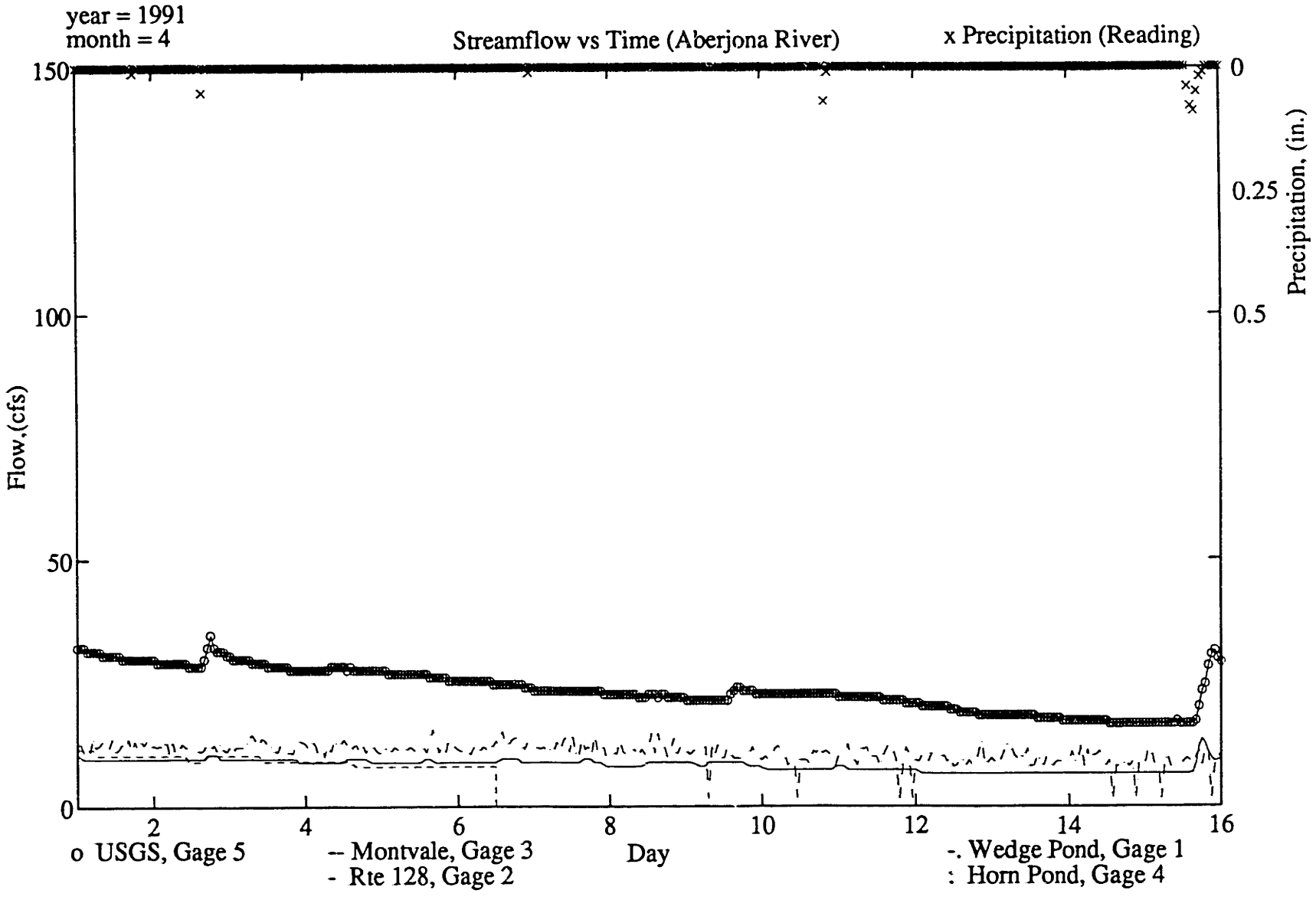
year = 1991
month = 4
Streamflow vs Time (Aberjona River)
x Precipitation (Reading)
150
100
50
0
0
0.25
0.5
Precipitation, (in.)
Flow,(cfs)
2
4
6
8
10
12
14
16
Day
o USGS, Gage 5
-- Montvale, Gage 3
- Rte 128, Gage 2
-. Wedge Pond, Gage 1
: Horn Pond, Gage 4

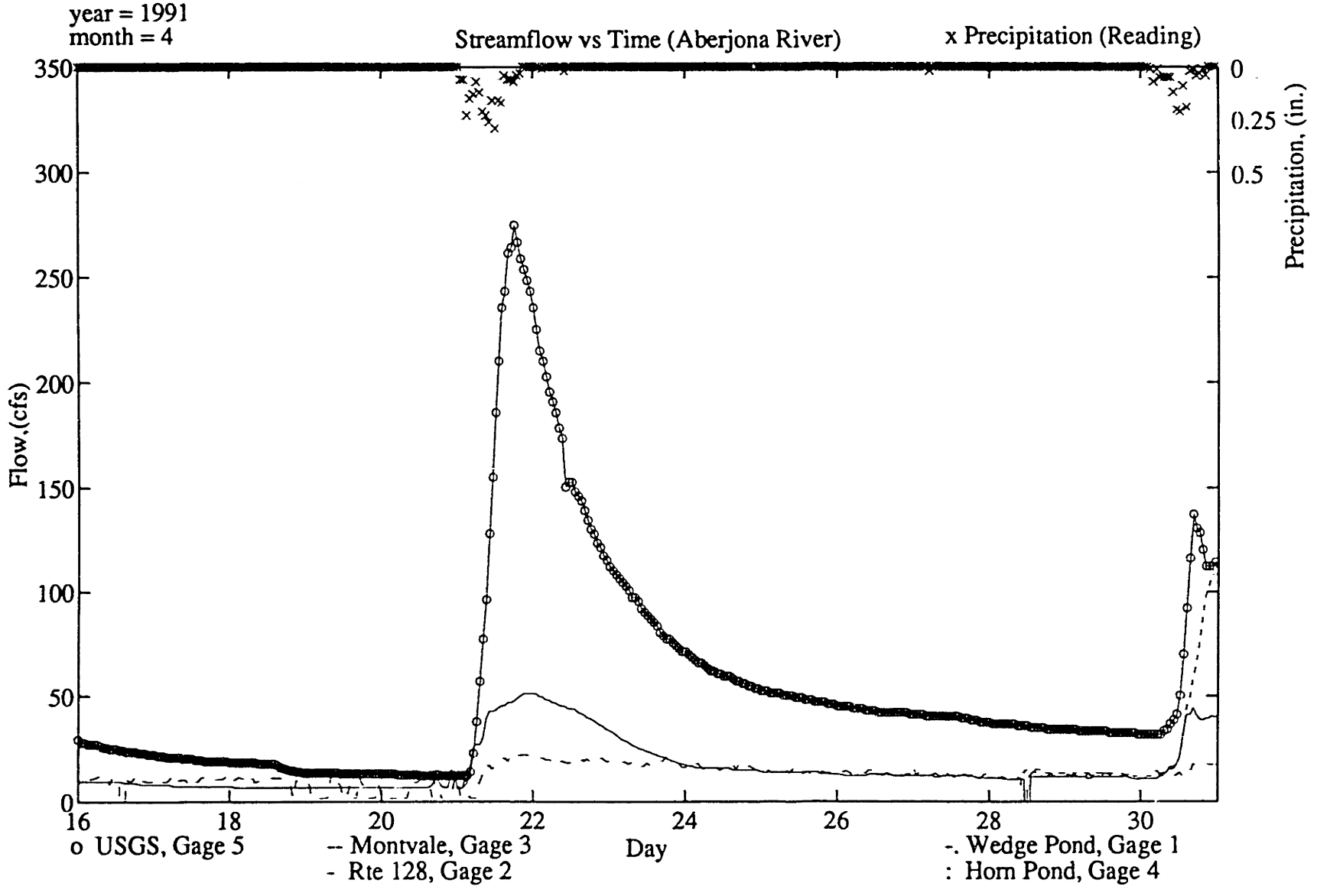
year = 1991
month = 4
Streamflow vs Time (Aberjona River)
x Precipitation (Reading)
Flow,(cfs)
Precipitation, (in.)
Day
o USGS, Gage 5
-- Montvale, Gage 3
- Rte 128, Gage 2
-. Wedge Pond, Gage 1
: Horn Pond, Gage 4

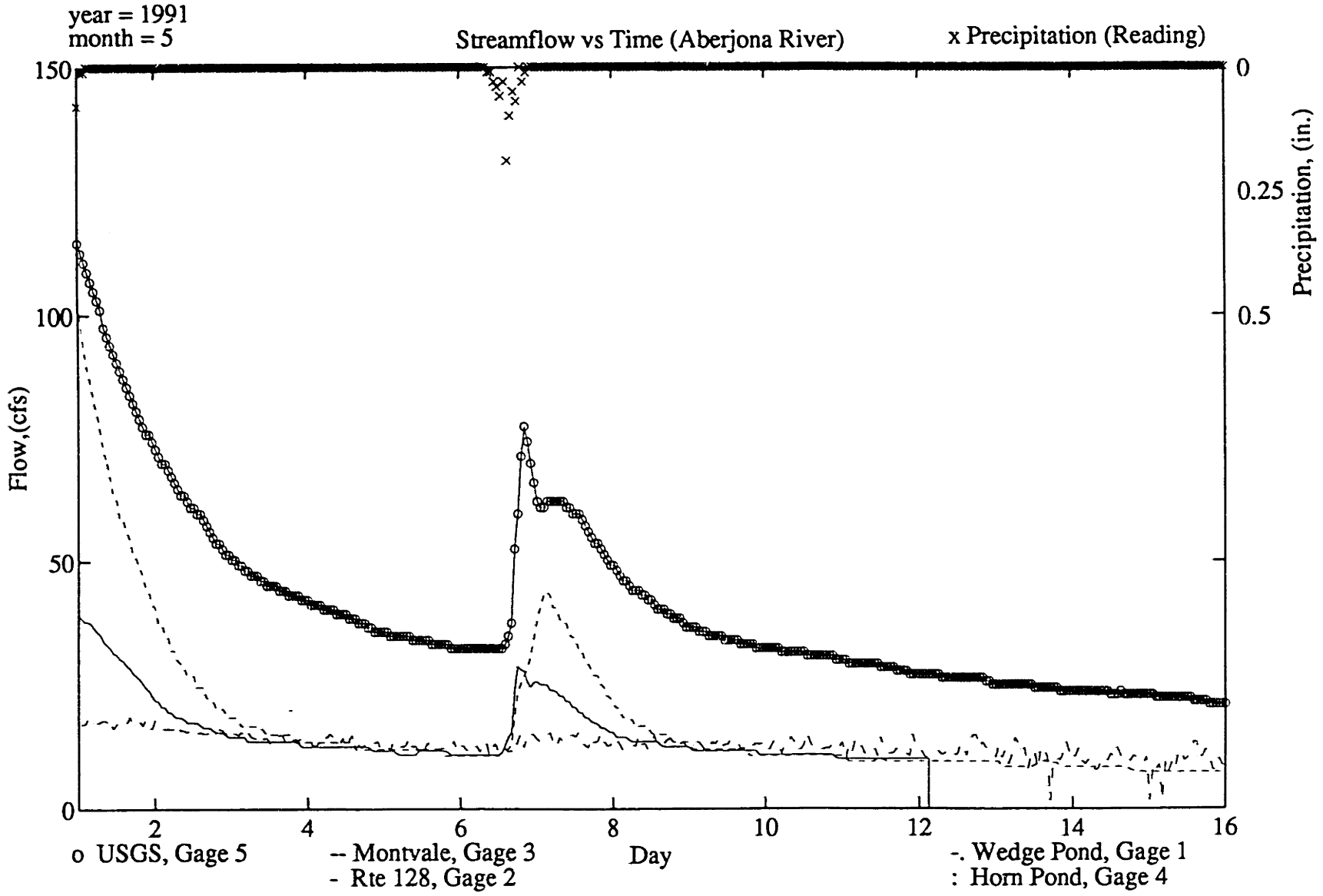
year = 1991
month = 5
Streamflow vs Time (Aberjona River)
x Precipitation (Reading)
150
100
50
0
0
0.25
0.5
Precipitation, (in.)
Flow,(cfs)
2
4
6
8
10
12
14
16
Day
o USGS, Gage 5
-- Montvale, Gage 3
- Rte 128, Gage 2
-. Wedge Pond, Gage 1
: Horn Pond, Gage 4

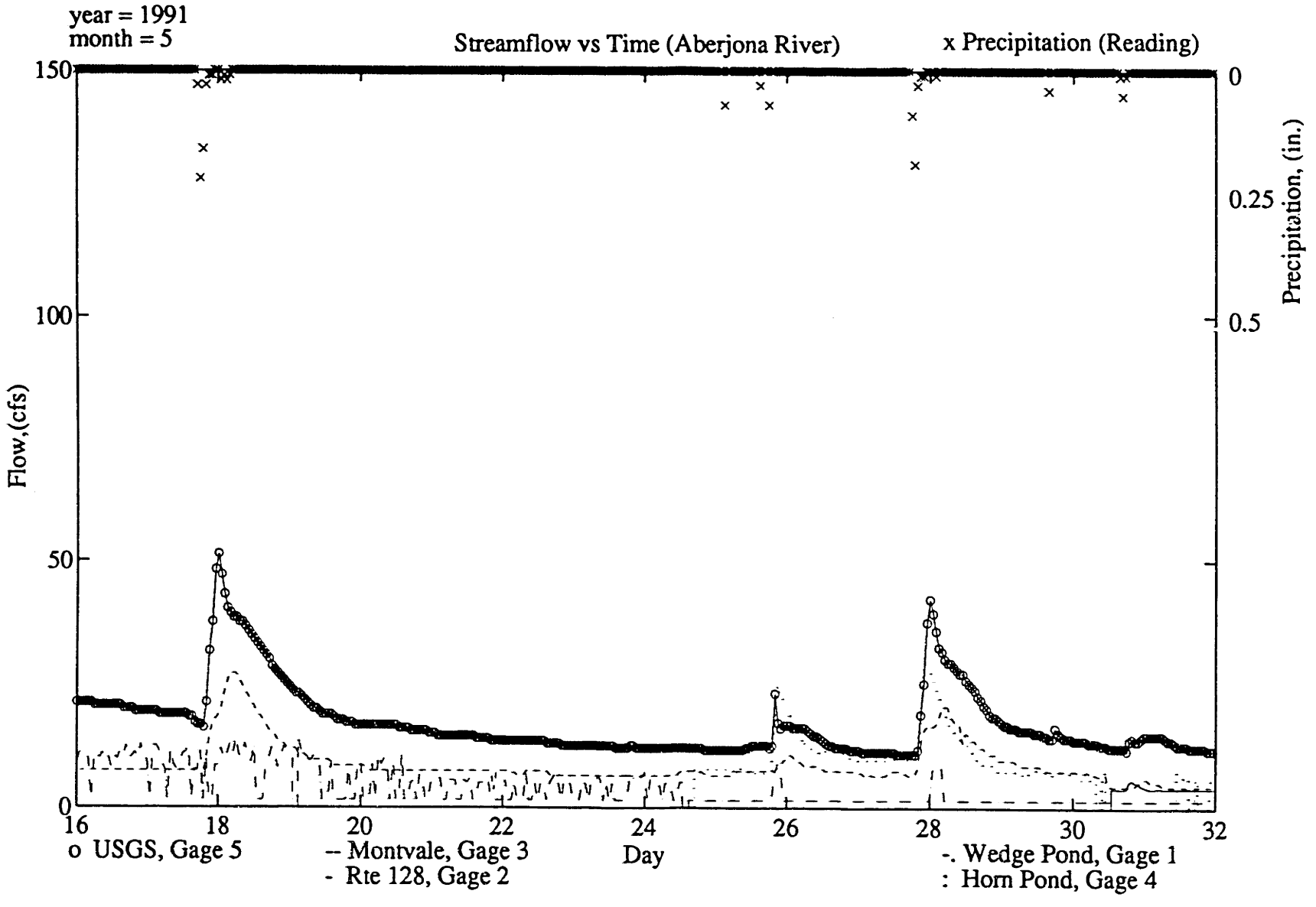
year = 1991
month = 5
Streamflow vs Time (Aberjona River)
x Precipitation (Reading)
150
100
50
0
Flow,(cfs)
0
0.25
0.5
Precipitation, (in.)
16
18
20
22
24
26
28
30
32
Day
o USGS, Gage 5
-- Montvale, Gage 3
- Rte 128, Gage 2
-. Wedge Pond, Gage 1
: Horn Pond, Gage 4

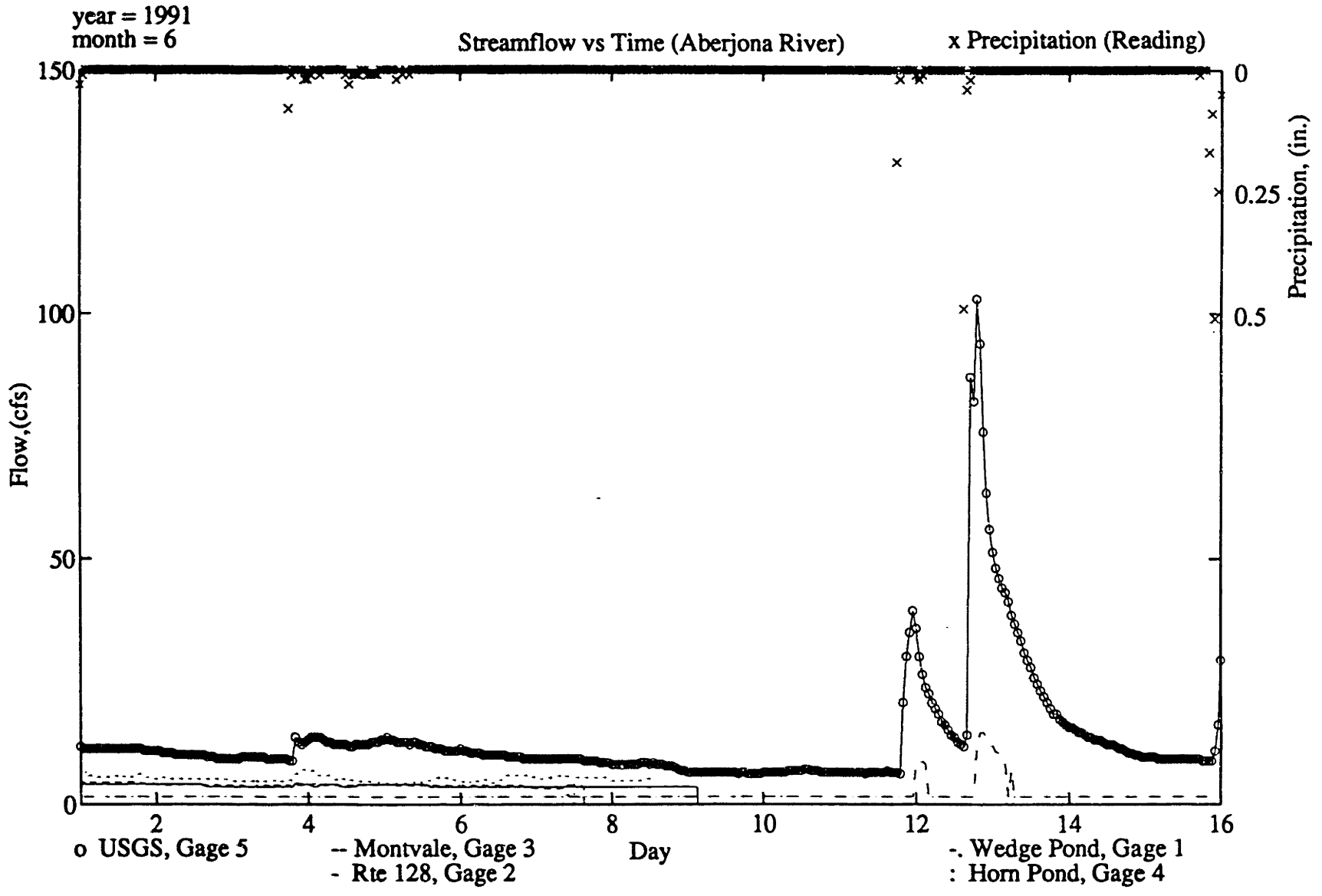
year = 1991
month = 6
Streamflow vs Time (Aberjona River)
x Precipitation (Reading)
150
100
50
0
0
0.25
0.5
Precipitation, (in.)
Flow,(cfs)
2
4
6
8
10
12
14
16
Day
o USGS, Gage 5
-- Montvale, Gage 3
- Rte 128, Gage 2
-. Wedge Pond, Gage 1
: Horn Pond, Gage 4

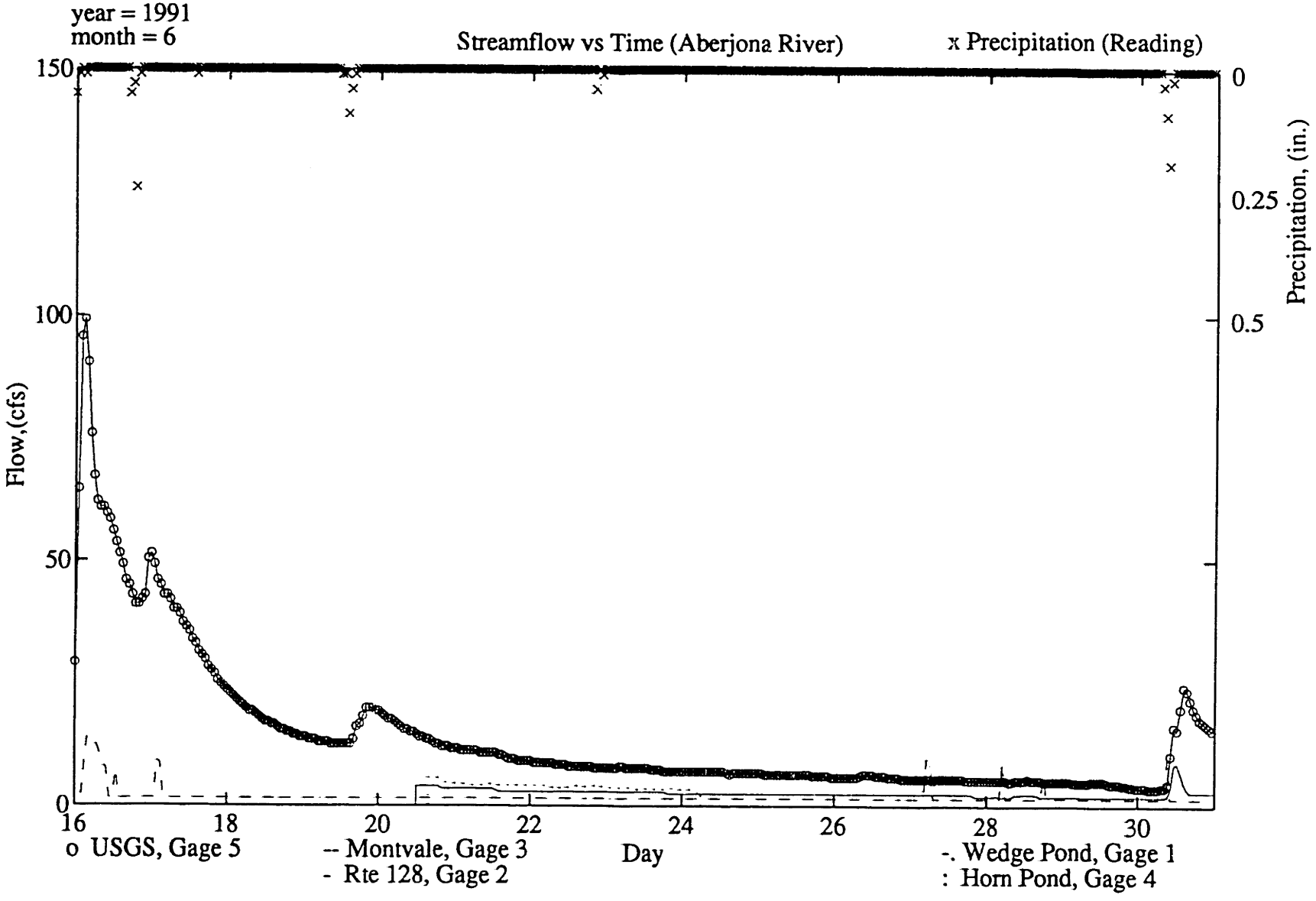
year = 1991
month = 6
Streamflow vs Time (Aberjona River)
x Precipitation (Reading)
150
100
50
0
Flow,(cfs)
0
0.25
0.5
Precipitation, (in.)
16
18
20
22
24
26
28
30
Day
o USGS, Gage 5
-- Montvale, Gage 3
- Rte 128, Gage 2
-. Wedge Pond, Gage 1
: Horn Pond, Gage 4

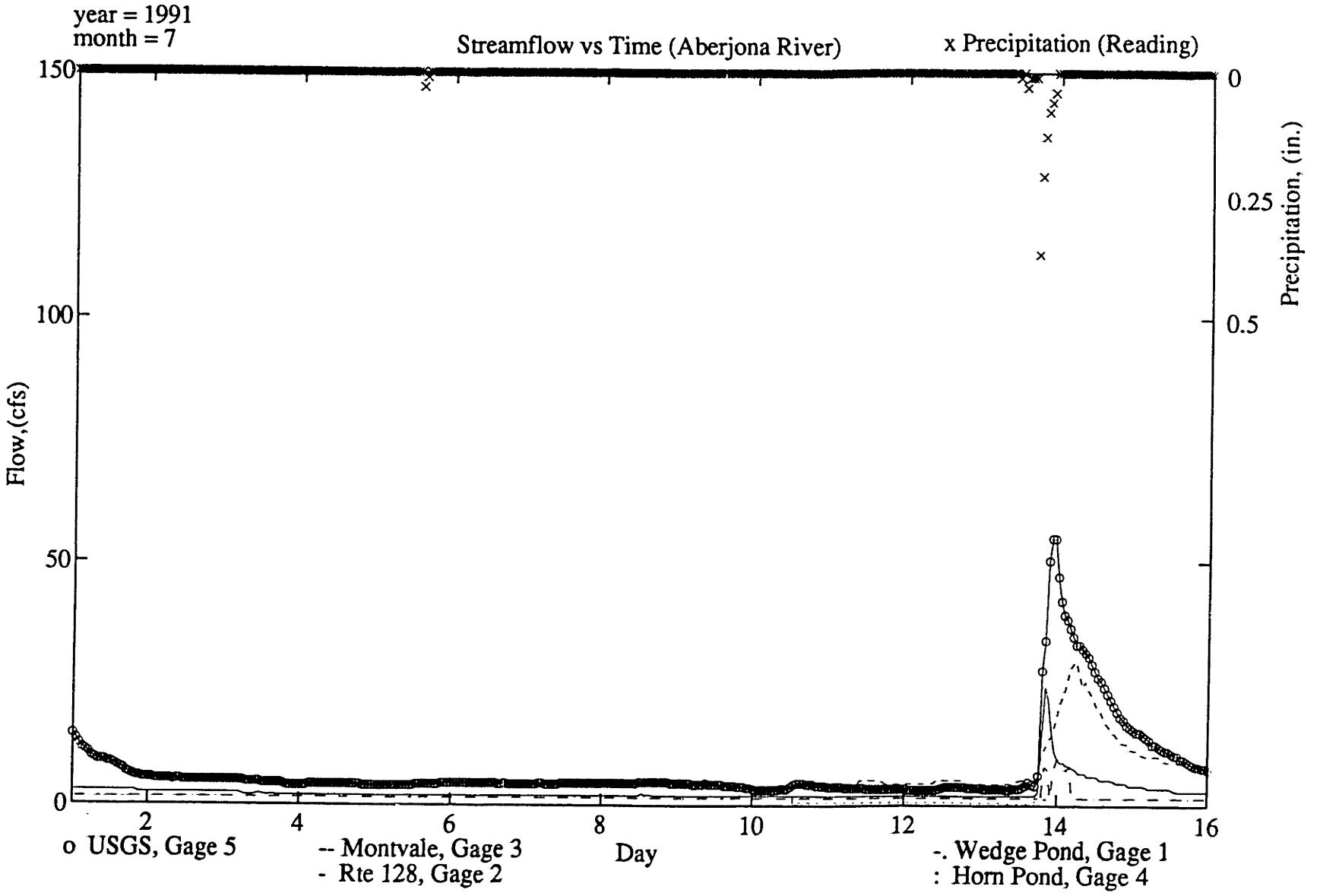
year = 1991
month = 7
Streamflow vs Time (Aberjona River)
x Precipitation (Reading)
150
100
50
0
0
0.25
0.5
Flow,(cfs)
Precipitation, (in.)
2
4
6
8
10
12
14
16
Day
o USGS, Gage 5
-- Montvale, Gage 3
- Rte 128, Gage 2
-. Wedge Pond, Gage 1
: Horn Pond, Gage 4

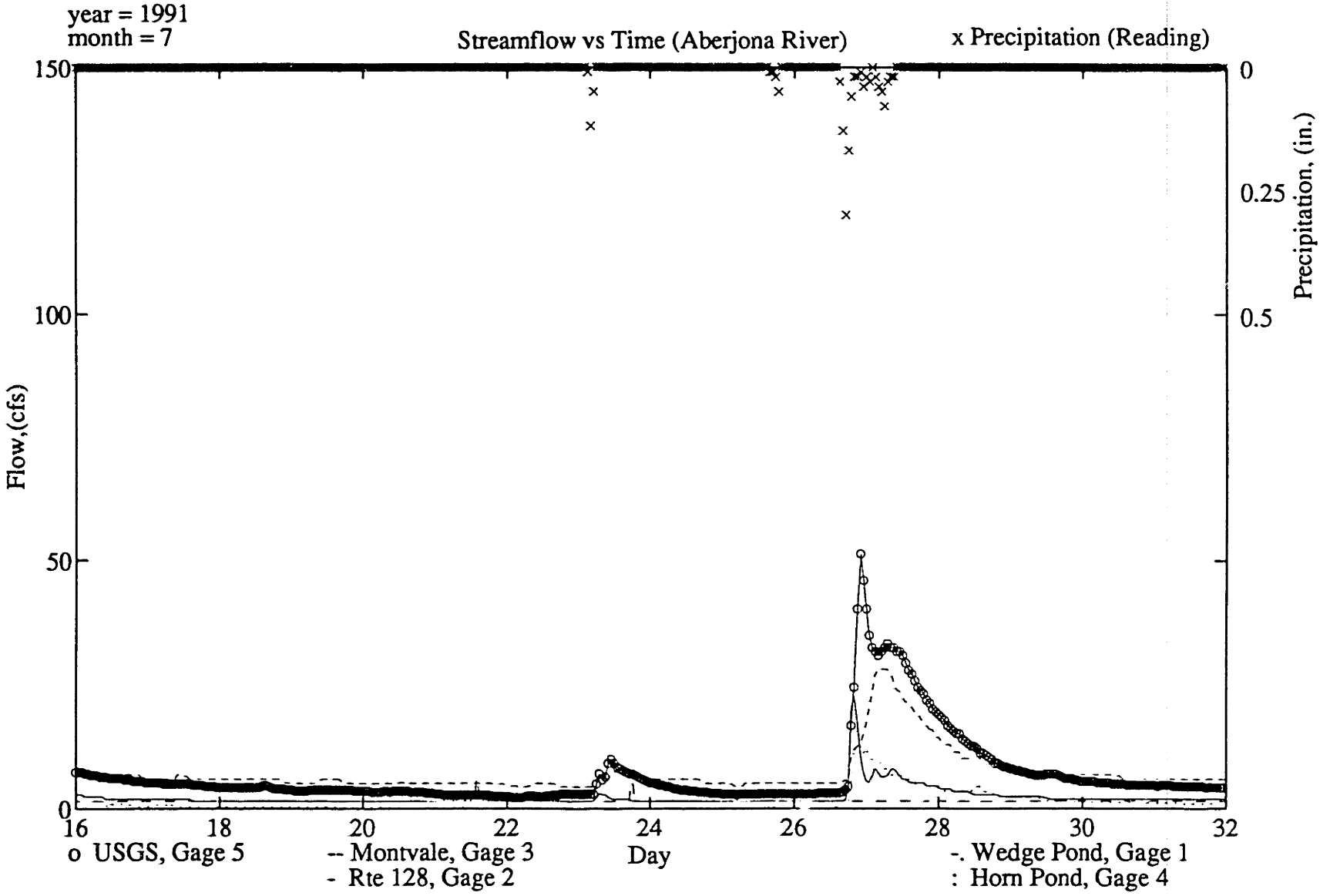
year = 1991
month = 7
Streamflow vs Time (Aberjona River)
x Precipitation (Reading)
150
100
50
0
Flow,(cfs)
0
0.25
0.5
Precipitation, (in.)
16
18
20
22
24
26
28
30
32
Day
o USGS, Gage 5
-- Montvale, Gage 3
- Rte 128, Gage 2
-. Wedge Pond, Gage 1
: Horn Pond, Gage 4

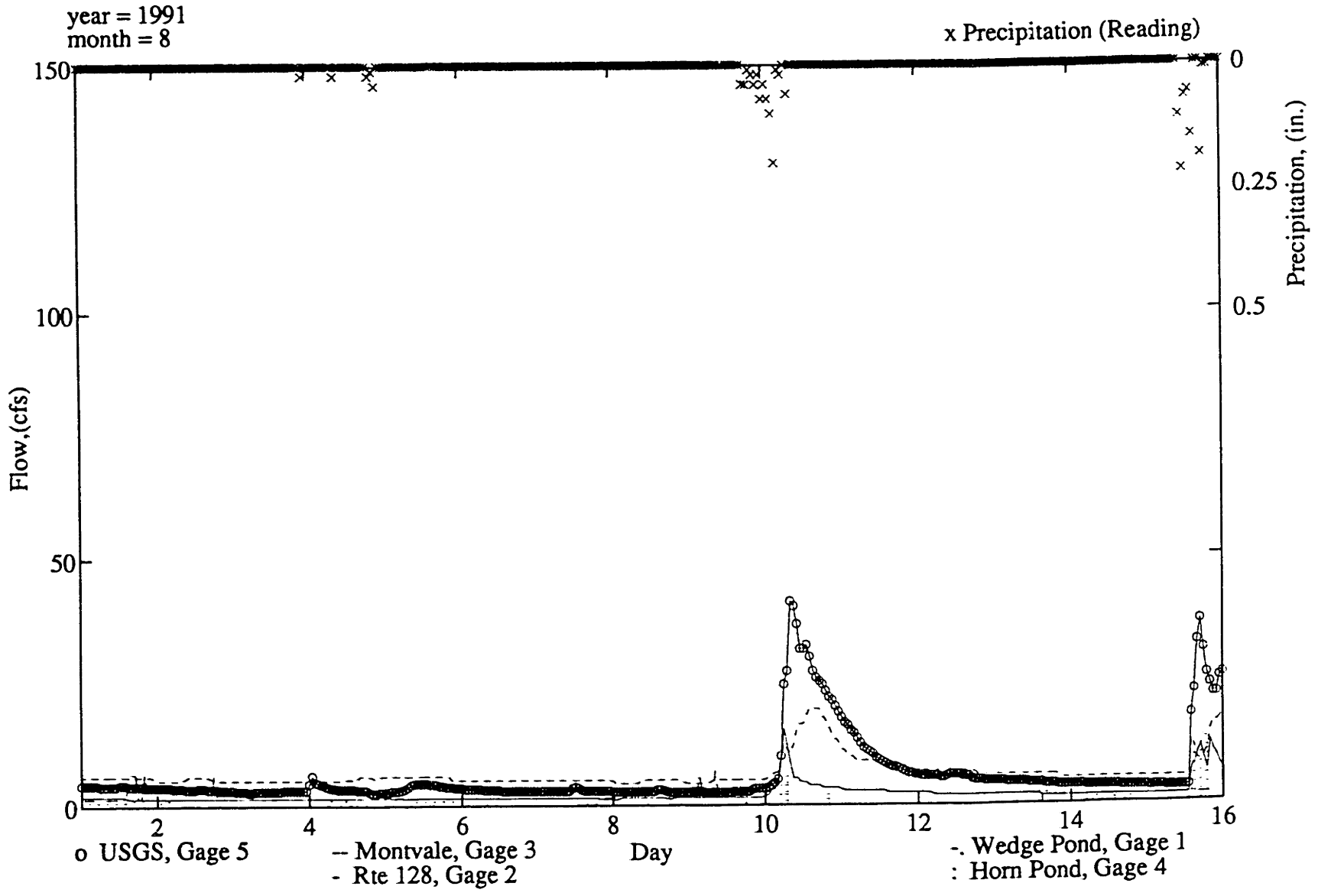
year = 1991
month = 8
x Precipitation (Reading)
150
100
50
0
0
0.25
0.5
Precipitation, (in.)
Flow,(cfs)
2
4
6
8
10
12
14
16
Day
o USGS, Gage 5
-- Montvale, Gage 3
- Rte 128, Gage 2
-. Wedge Pond, Gage 1
: Horn Pond, Gage 4

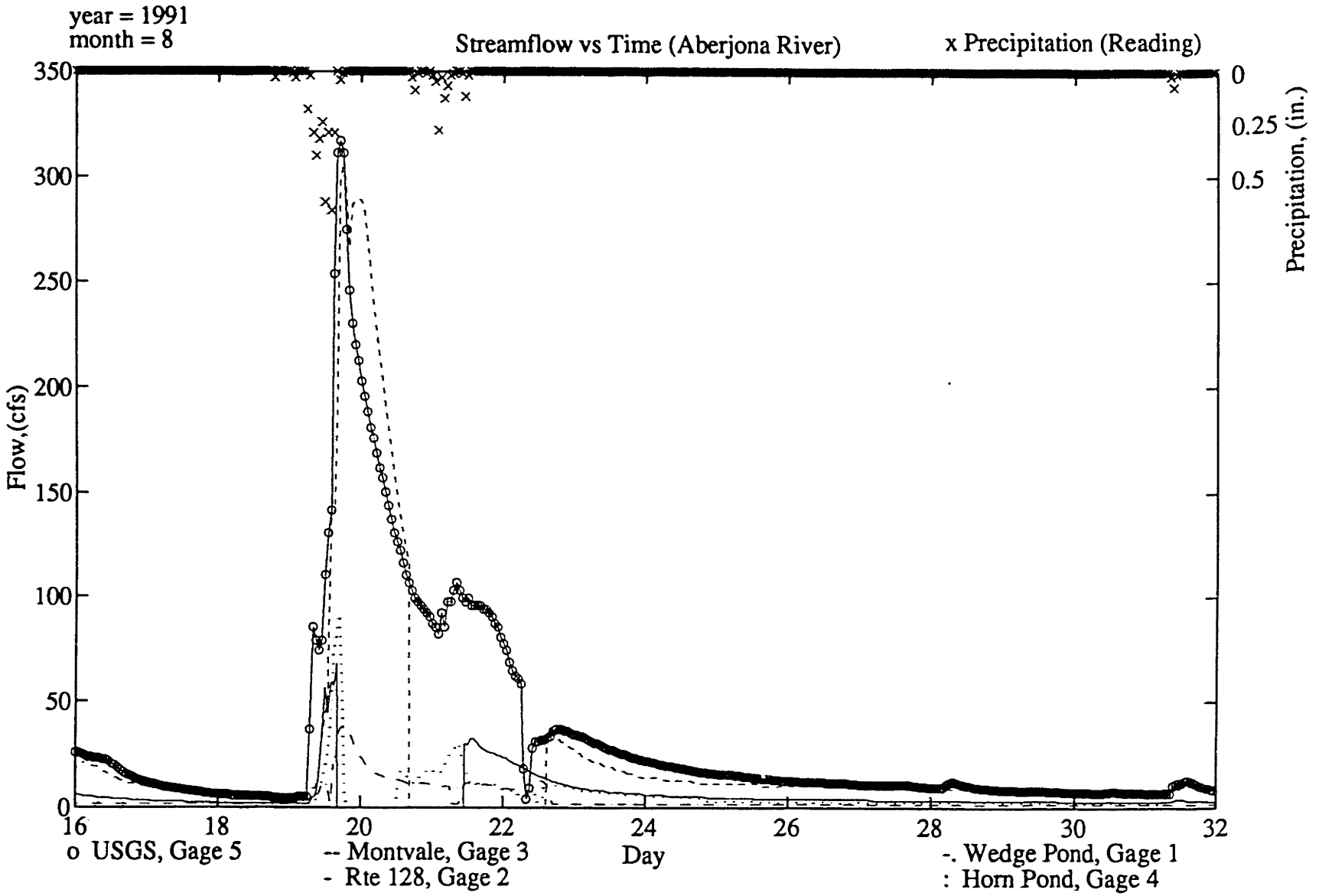
year = 1991
month = 8
Streamflow vs Time (Aberjona River)
x Precipitation (Reading)
Flow,(cfs)
Precipitation, (in.)
Day
o USGS, Gage 5
-- Montvale, Gage 3
- Rte 128, Gage 2
-. Wedge Pond, Gage 1
: Horn Pond, Gage 4

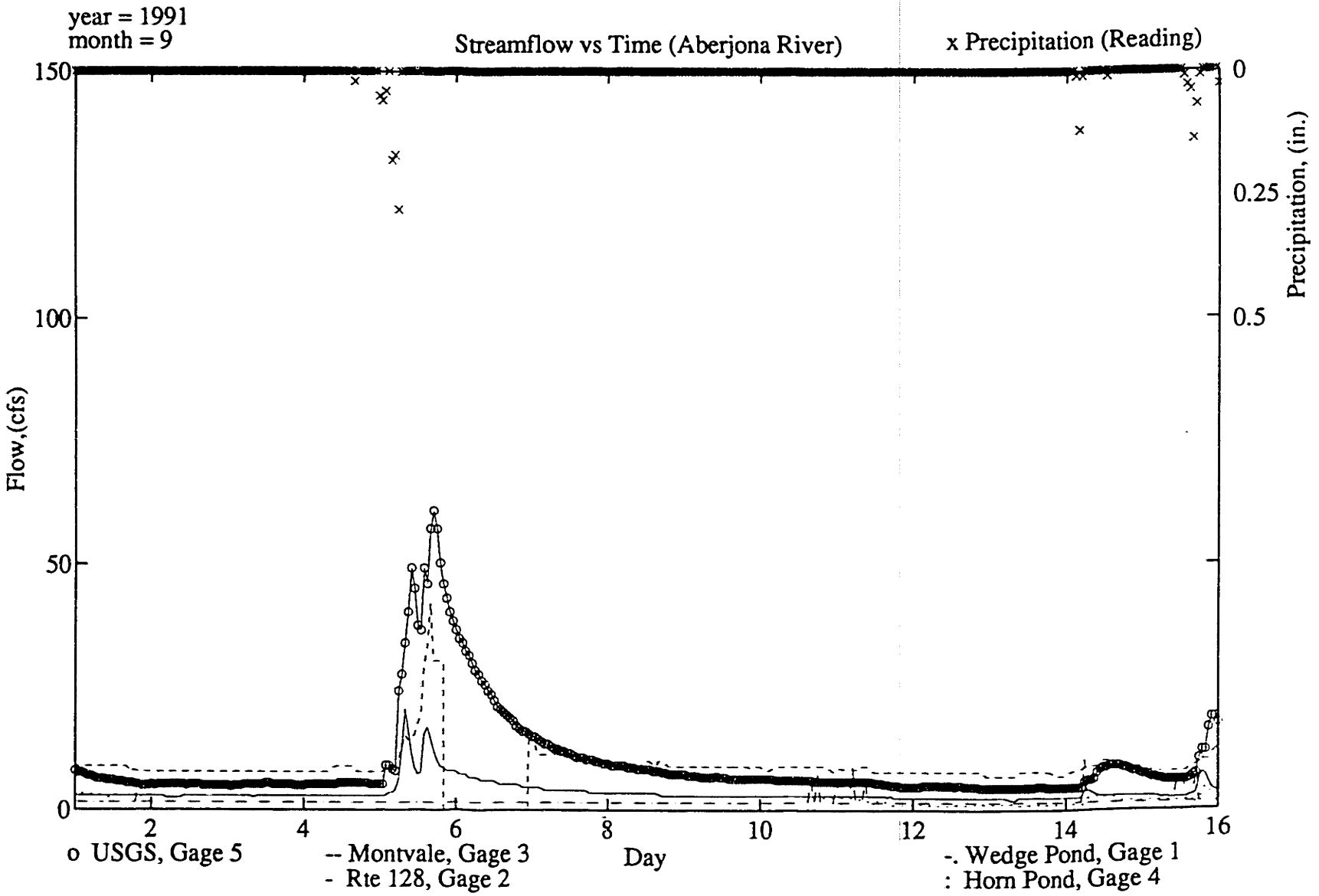
year = 1991
month = 9
Streamflow vs Time (Aberjona River)
x Precipitation (Reading)
150
100
50
0
0
0.25
0.5
Precipitation, (in.)
Flow,(cfs)
2
4
6
8
10
12
14
16
Day
o USGS, Gage 5
-- Montvale, Gage 3
- Rte 128, Gage 2
-. Wedge Pond, Gage 1
: Horn Pond, Gage 4

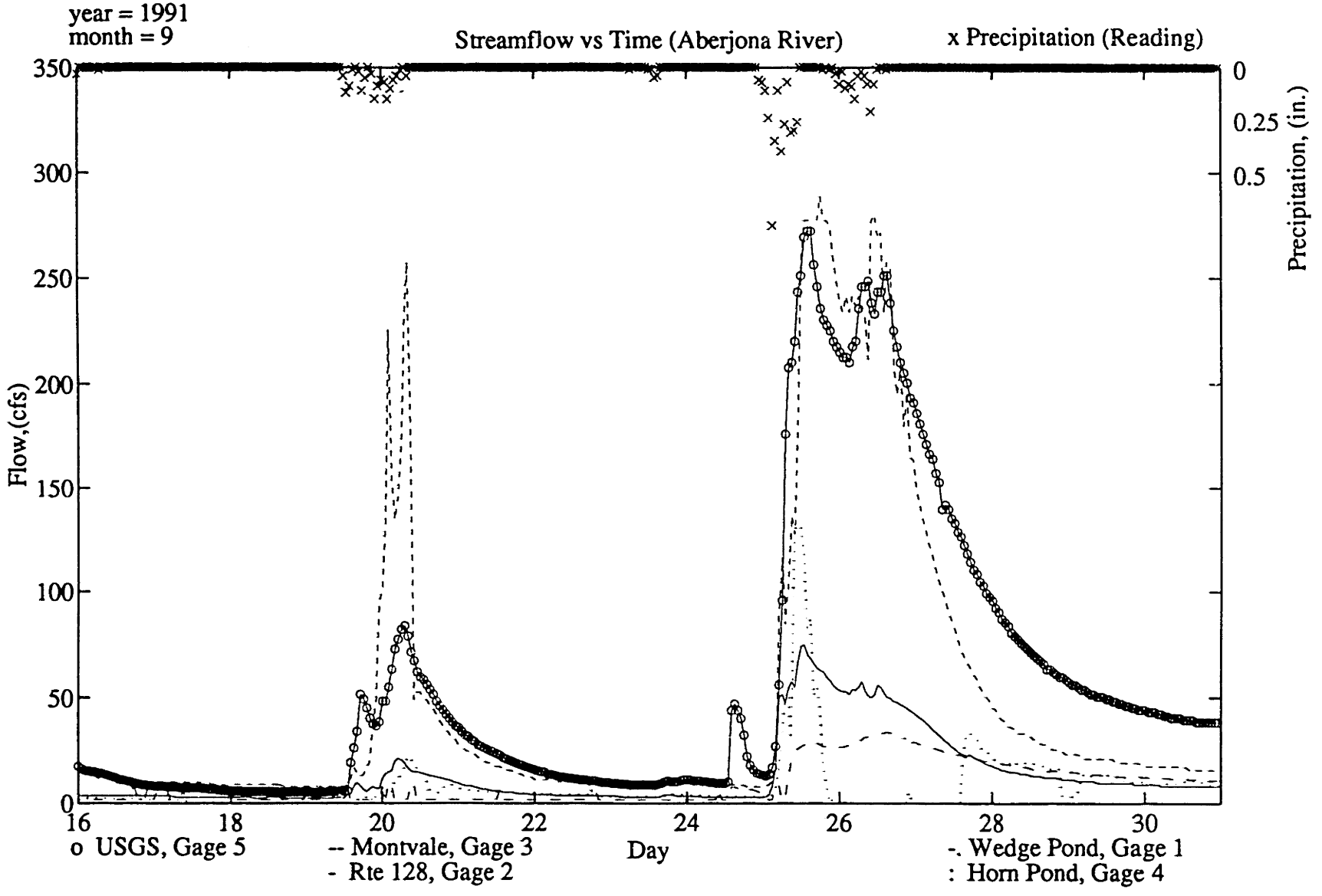
year = 1991
month = 9
Streamflow vs Time (Aberjona River)
x Precipitation (Reading)
Flow,(cfs)
Precipitation, (in.)
Day
o USGS, Gage 5
-- Montvale, Gage 3
- Rte 128, Gage 2
-. Wedge Pond, Gage 1
: Horn Pond, Gage 4

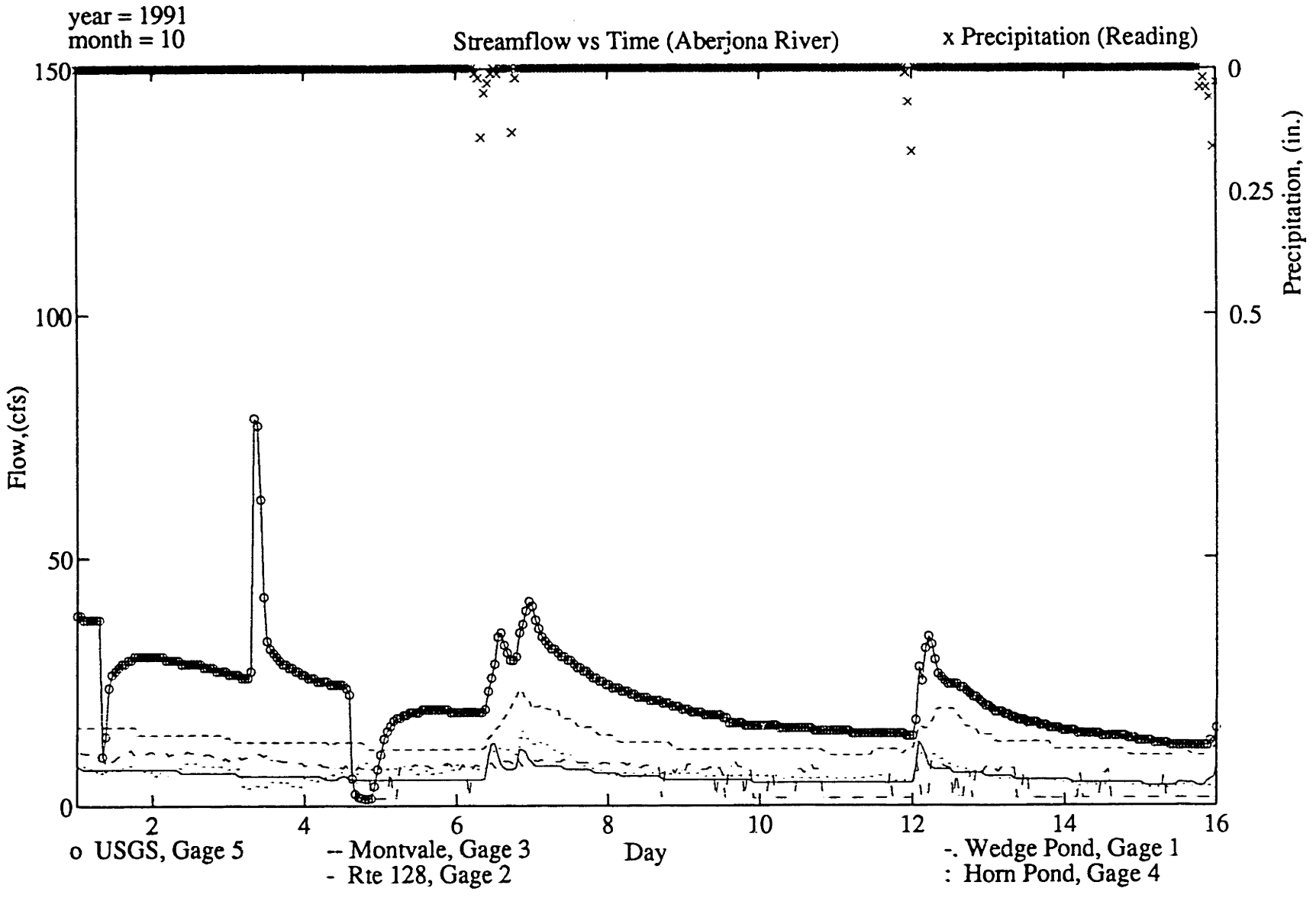
year = 1991
month = 10
Streamflow vs Time (Aberjona River)
x Precipitation (Reading)
150
100
50
0
0
0.25
0.5
Precipitation, (in.)
Flow,(cfs)
2
4
6
8
10
12
14
16
Day
o USGS, Gage 5
-- Montvale, Gage 3
- Rte 128, Gage 2
-. Wedge Pond, Gage 1
: Horn Pond, Gage 4

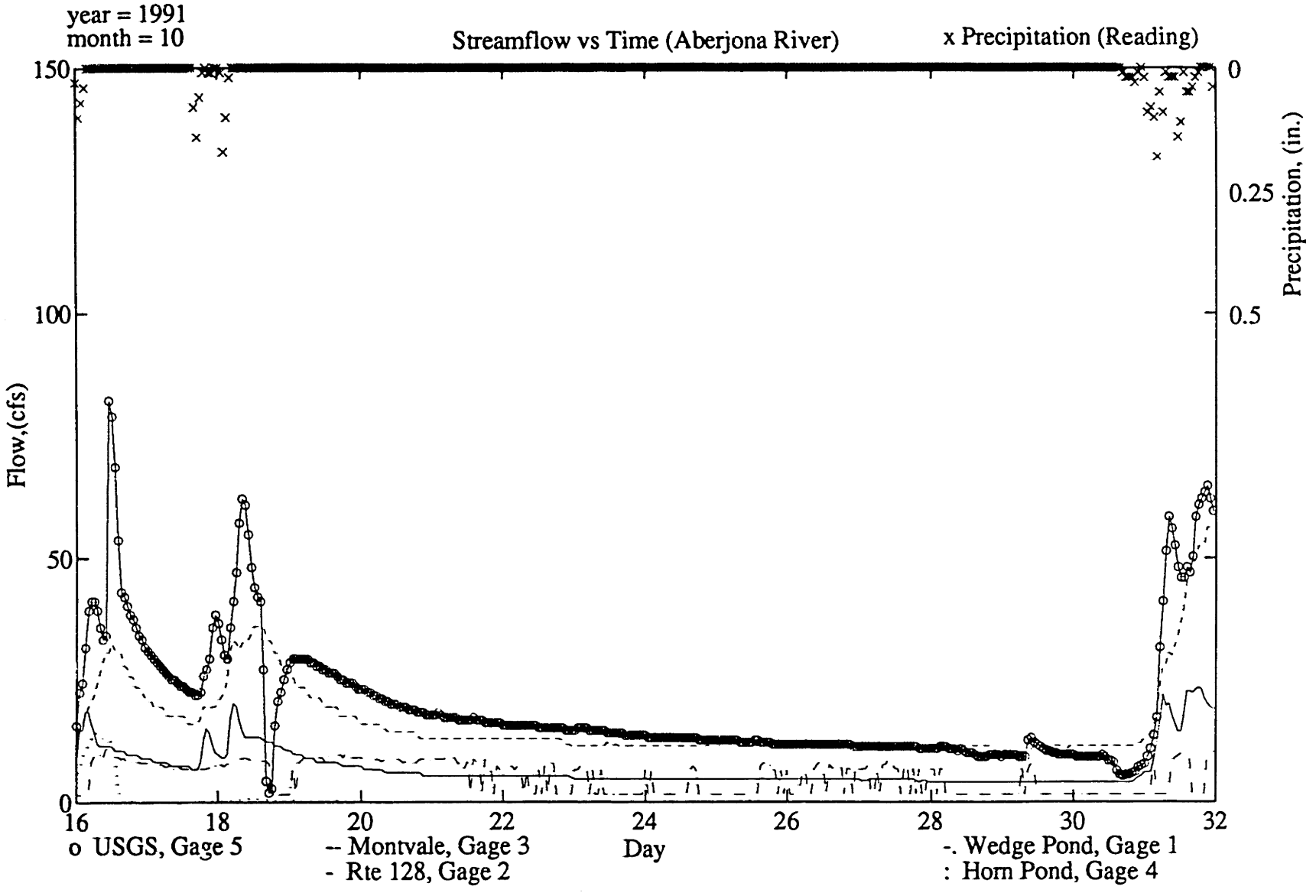
year = 1991
month = 10
Streamflow vs Time (Aberjona River)
x Precipitation (Reading)
150
100
50
0
0
0.25
0.5
Precipitation, (in.)
Flow,(cfs)
16
18
20
22
24
26
28
30
32
Day
o USGS, Gage 5
-- Montvale, Gage 3
- Rte 128, Gage 2
-. Wedge Pond, Gage 1
: Horn Pond, Gage 4

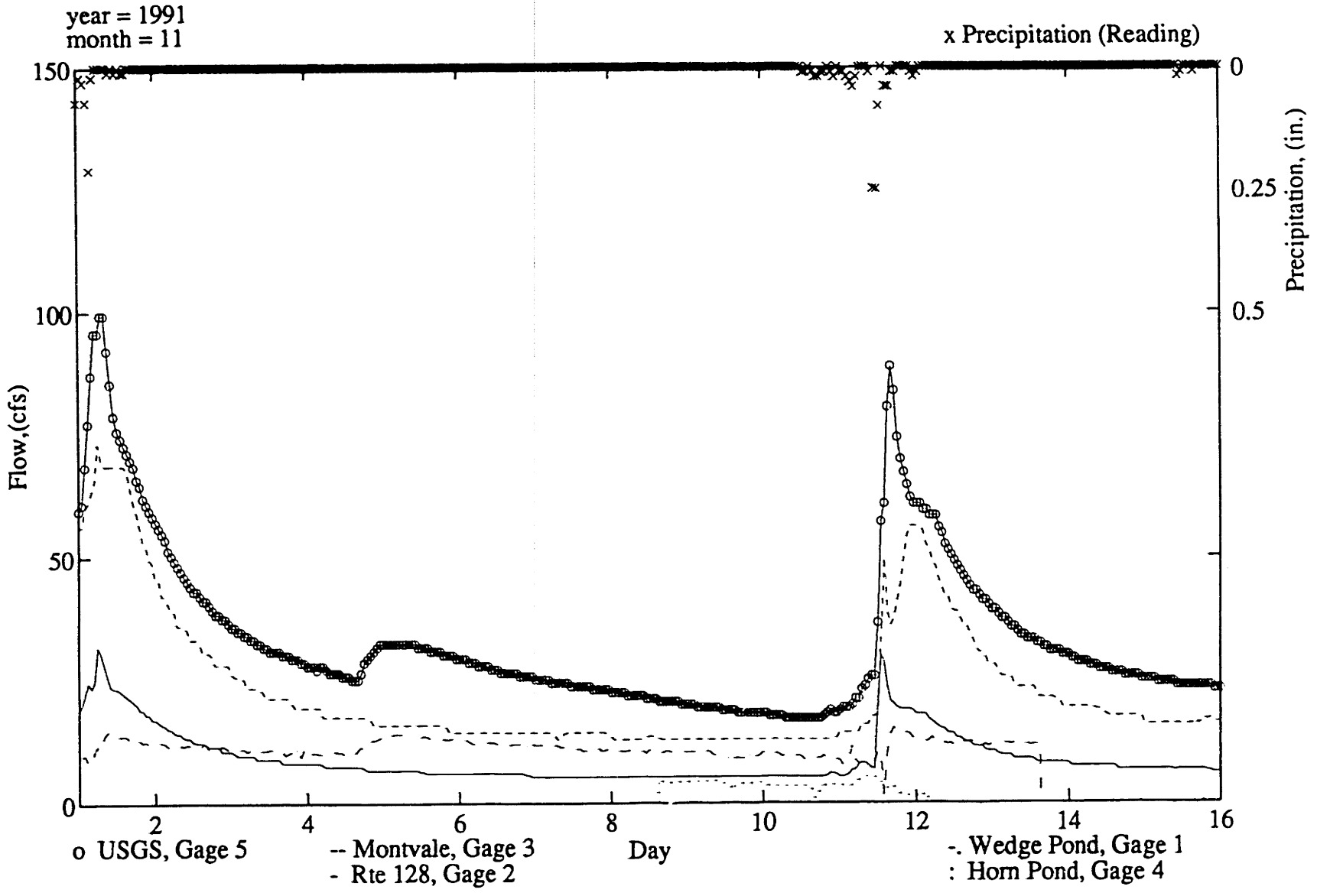
year = 1991
month = 11
x Precipitation (Reading)
150
100
50
0
0
0.25
0.5
Precipitation, (in.)
Flow,(cfs)
2
4
6
8
10
12
14
16
Day
o USGS, Gage 5
-- Montvale, Gage 3
- Rte 128, Gage 2
-. Wedge Pond, Gage 1
: Horn Pond, Gage 4

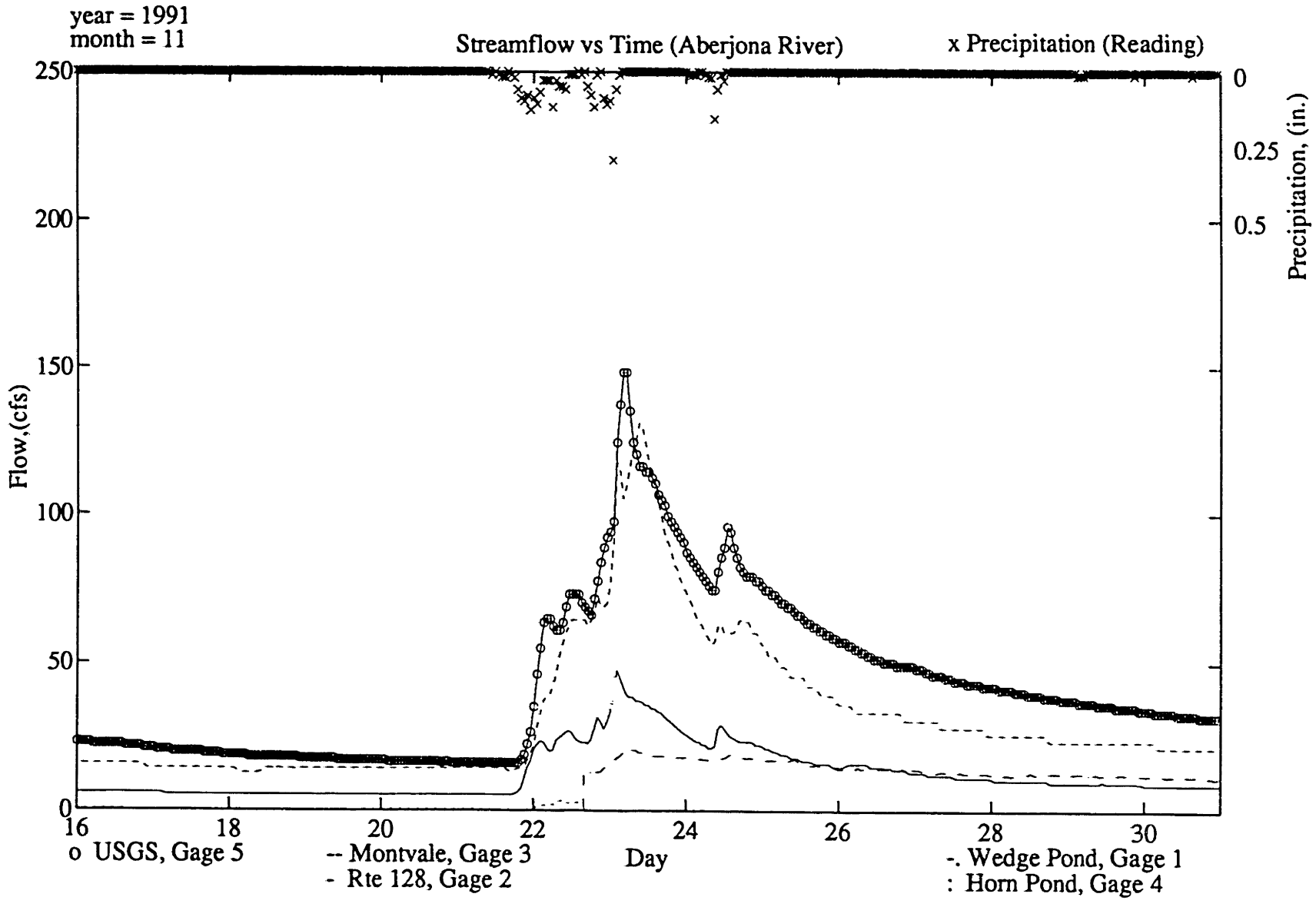
year = 1991
month = 11
Streamflow vs Time (Aberjona River)
x Precipitation (Reading)
Flow,(cfs)
Precipitation, (in.)
250
200
150
100
50
0
0
0.25
0.5
16
18
20
22
24
26
28
30
Day
o USGS, Gage 5
-- Montvale, Gage 3
- Rte 128, Gage 2
-. Wedge Pond, Gage 1
: Horn Pond, Gage 4

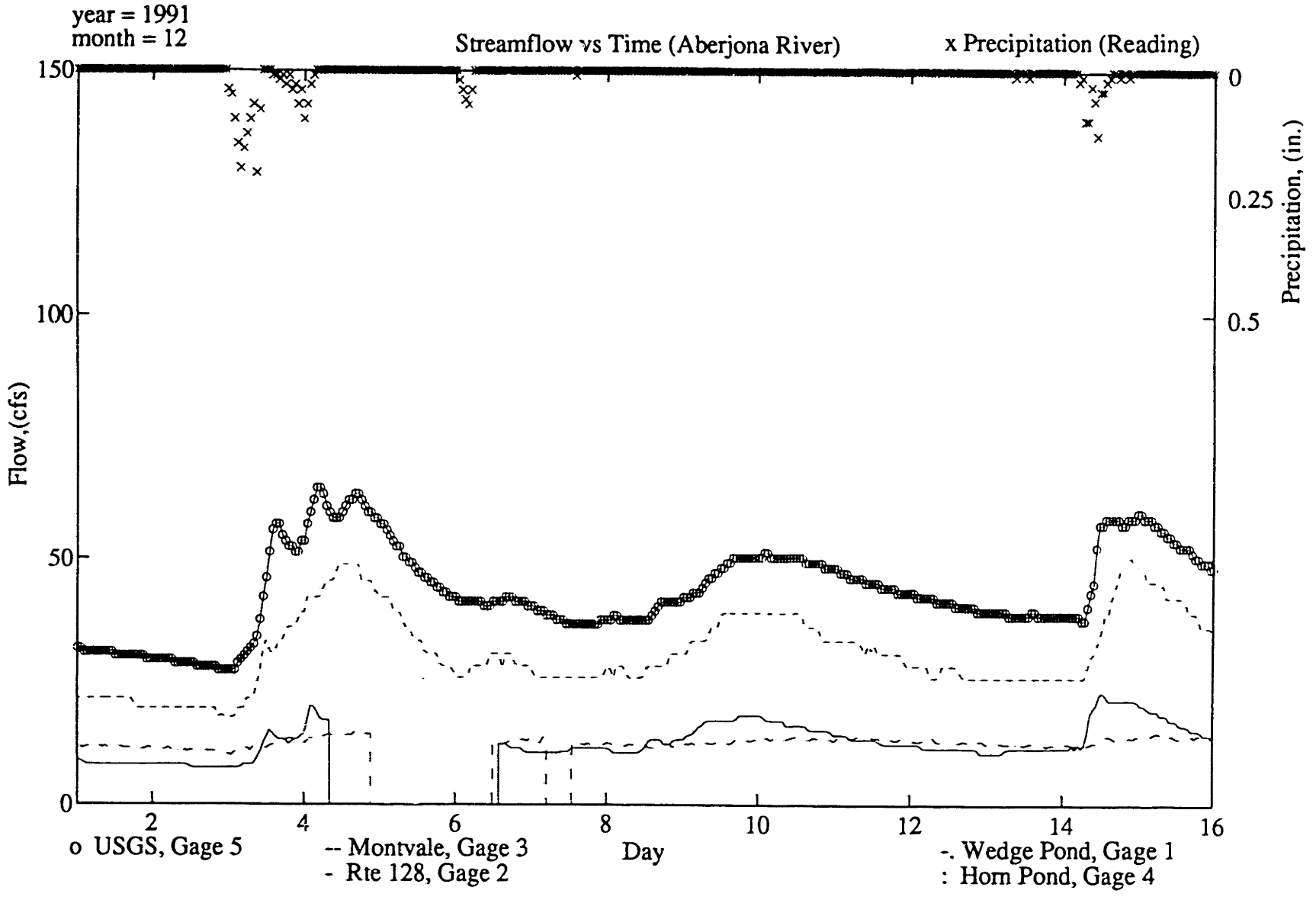
year = 1991
month = 12
Streamflow vs Time (Aberjona River)
x Precipitation (Reading)
150
100
50
0
Flow,(cfs)
0
0.25
0.5
Precipitation, (in.)
2
4
6
8
10
12
14
16
Day
o USGS, Gage 5
-- Montvale, Gage 3
- Rte 128, Gage 2
-. Wedge Pond, Gage 1
: Horn Pond, Gage 4

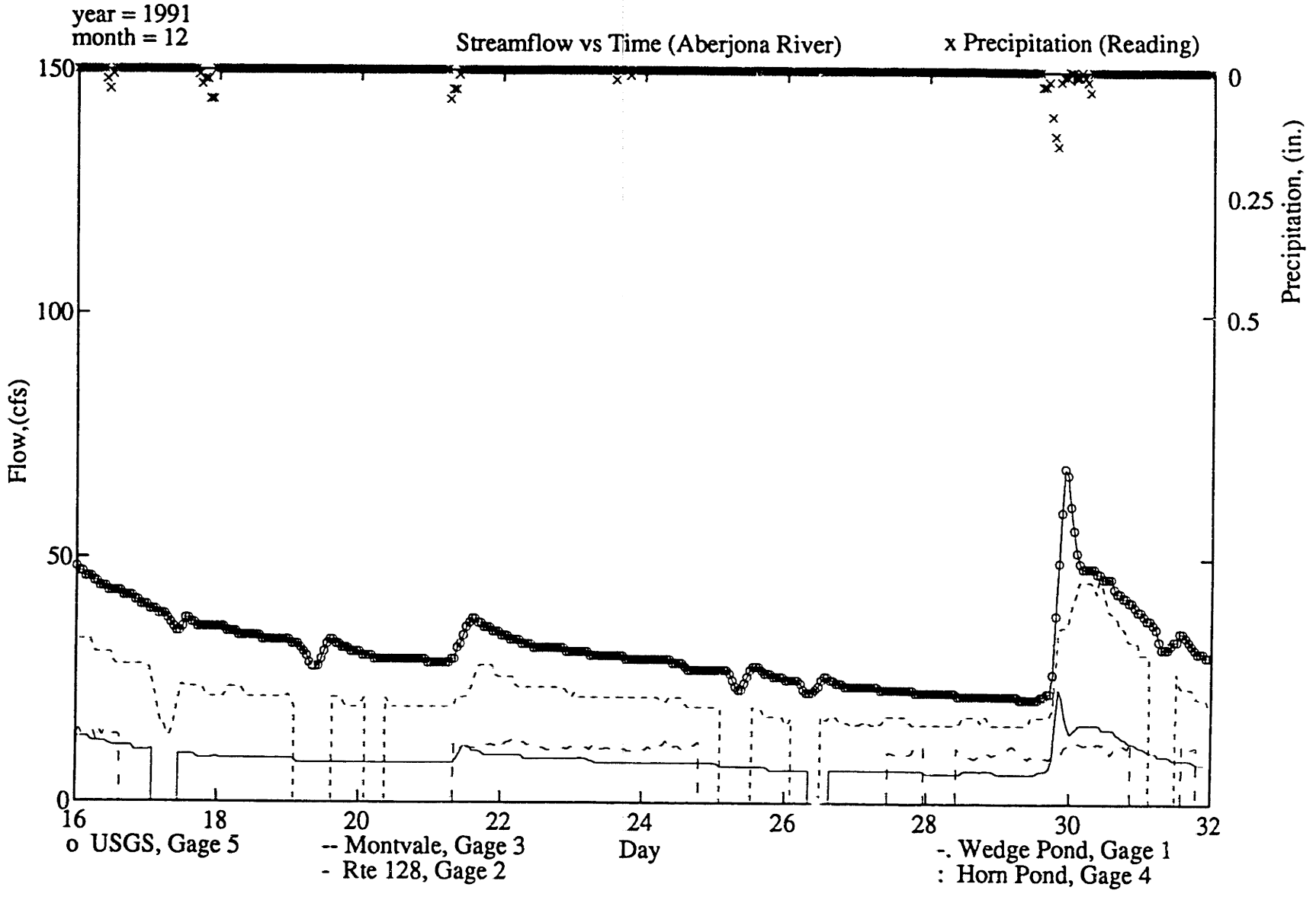
year = 1991
month = 12
Streamflow vs Time (Aberjona River)
x Precipitation (Reading)
150
100
50
0
Flow,(cfs)
0
0.25
0.5
Precipitation, (in.)
16
18
20
22
24
26
28
30
32
Day
o USGS, Gage 5
-- Montvale, Gage 3
- Rte 128, Gage 2
-. Wedge Pond, Gage 1
: Horn Pond, Gage 4

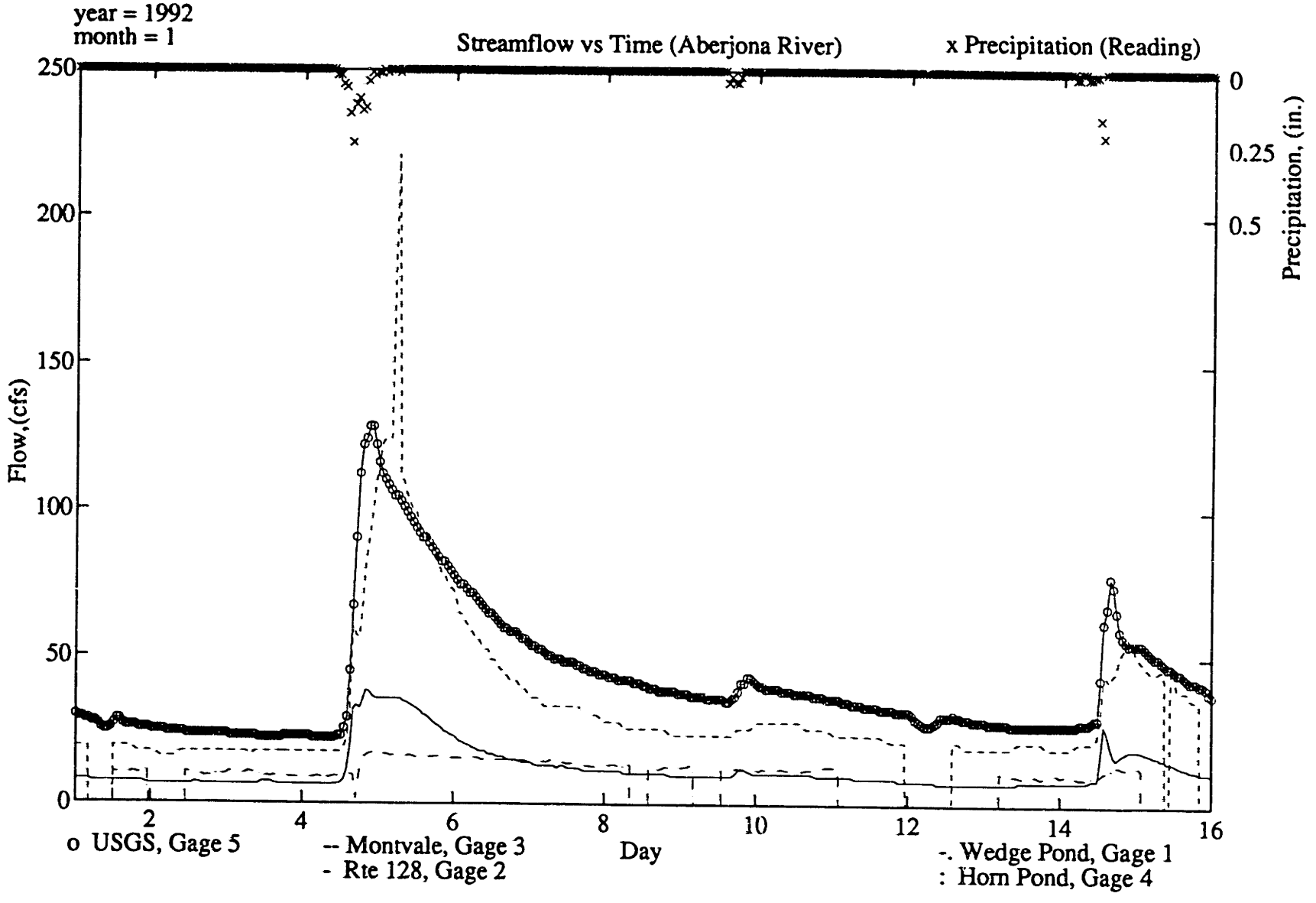
year = 1992
month = 1
Streamflow vs Time (Aberjona River)
x Precipitation (Reading)
Flow,(cfs)
Precipitation, (in.)
250
200
150
100
50
0
0
0.25
0.5
2
4
6
8
10
12
14
16
Day
o USGS, Gage 5
-- Montvale, Gage 3
- Rte 128, Gage 2
-. Wedge Pond, Gage 1
: Horn Pond, Gage 4

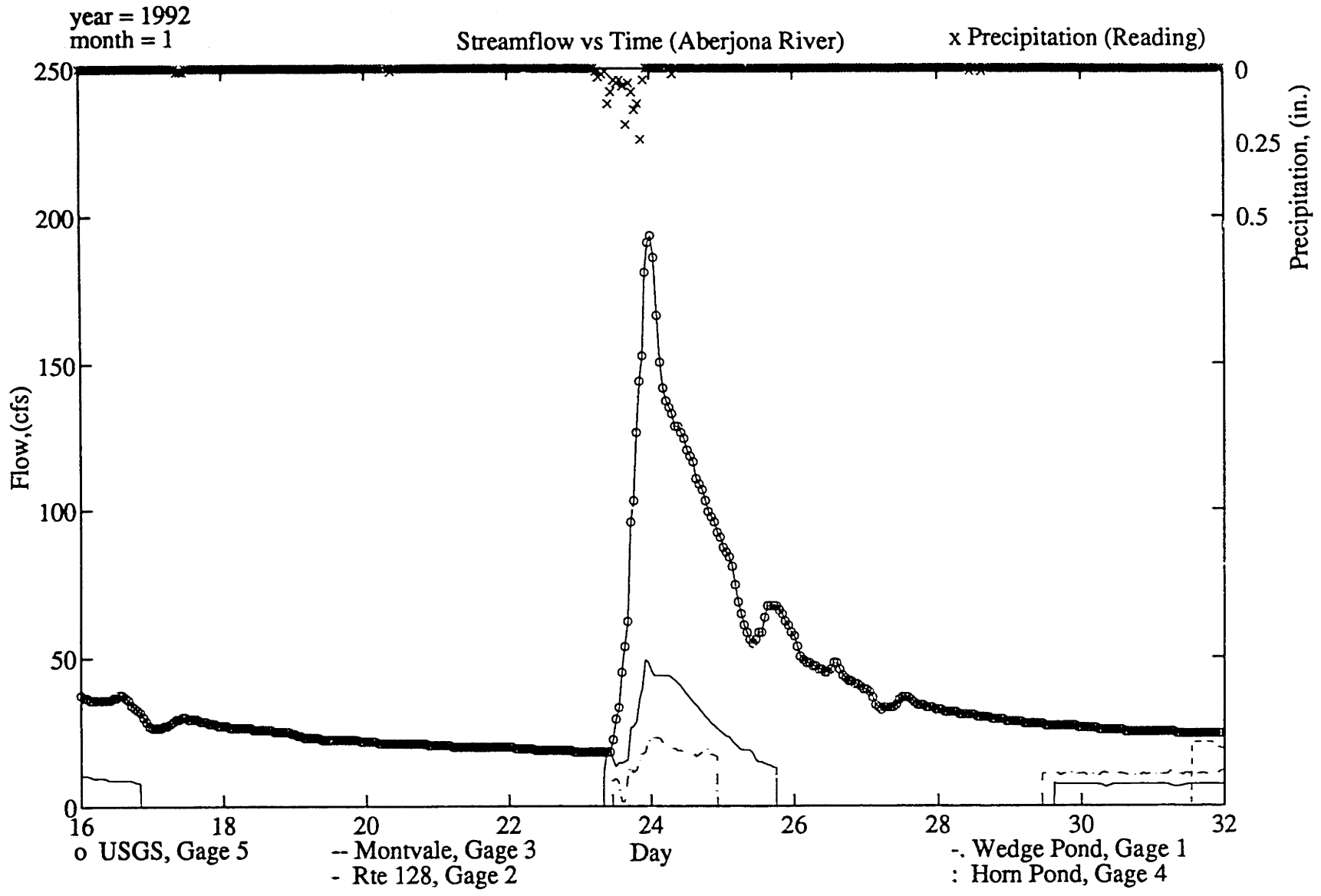
year = 1992
month = 1
Streamflow vs Time (Aberjona River)
x Precipitation (Reading)
250
200
150
100
50
0
Flow,(cfs)
0
0.25
0.5
Precipitation, (in.)
16
18
20
22
24
26
28
30
32
Day
o USGS, Gage 5
-- Montvale, Gage 3
- Rte 128, Gage 2
-. Wedge Pond, Gage 1
: Horn Pond, Gage 4

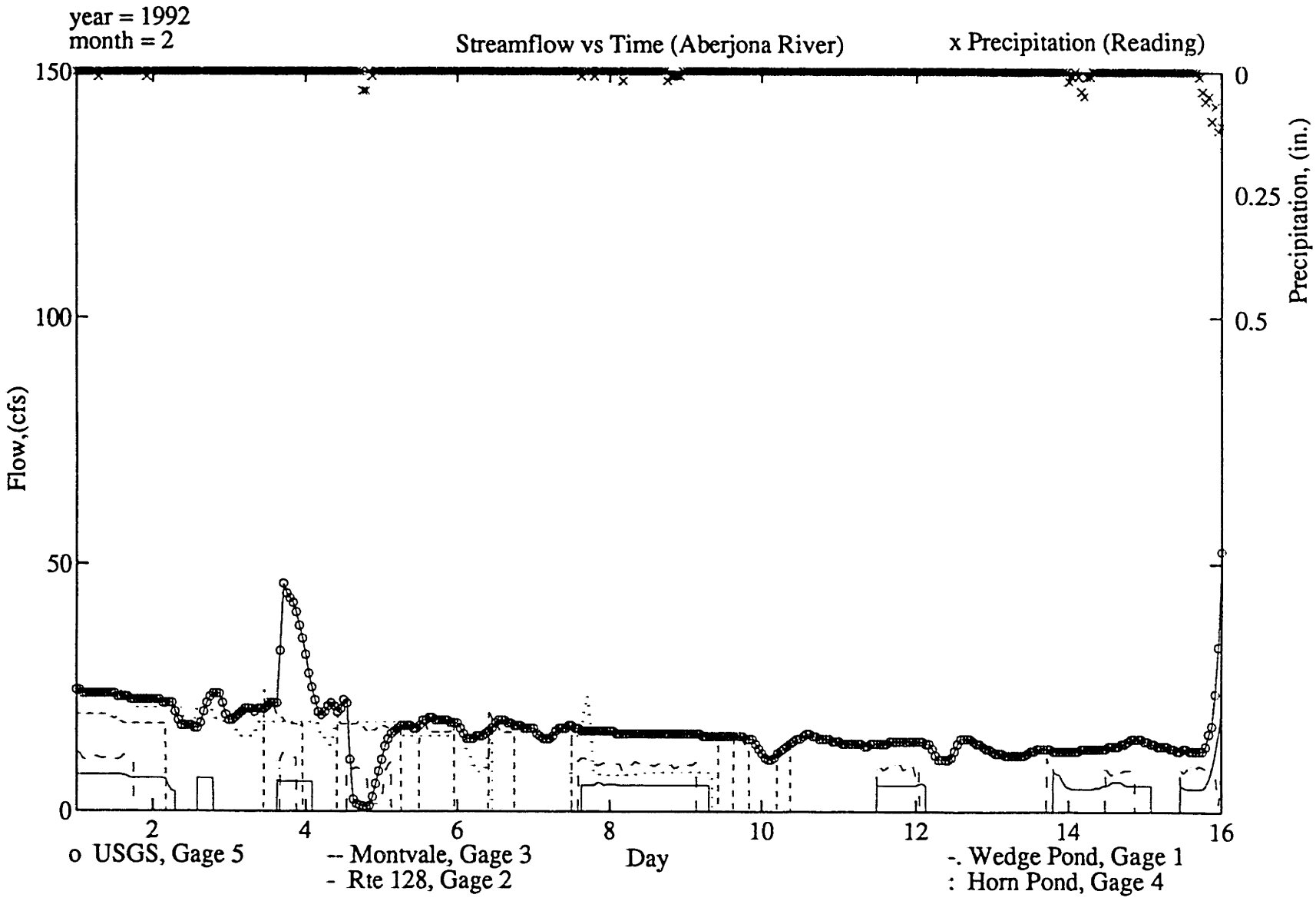
year = 1992
month = 2
Streamflow vs Time (Aberjona River)
x Precipitation (Reading)
150
100
50
0
Flow,(cfs)
0
0.25
0.5
Precipitation, (in.)
2
4
6
8
10
12
14
16
Day
o USGS, Gage 5
-- Montvale, Gage 3
- Rte 128, Gage 2
-. Wedge Pond, Gage 1
: Horn Pond, Gage 4

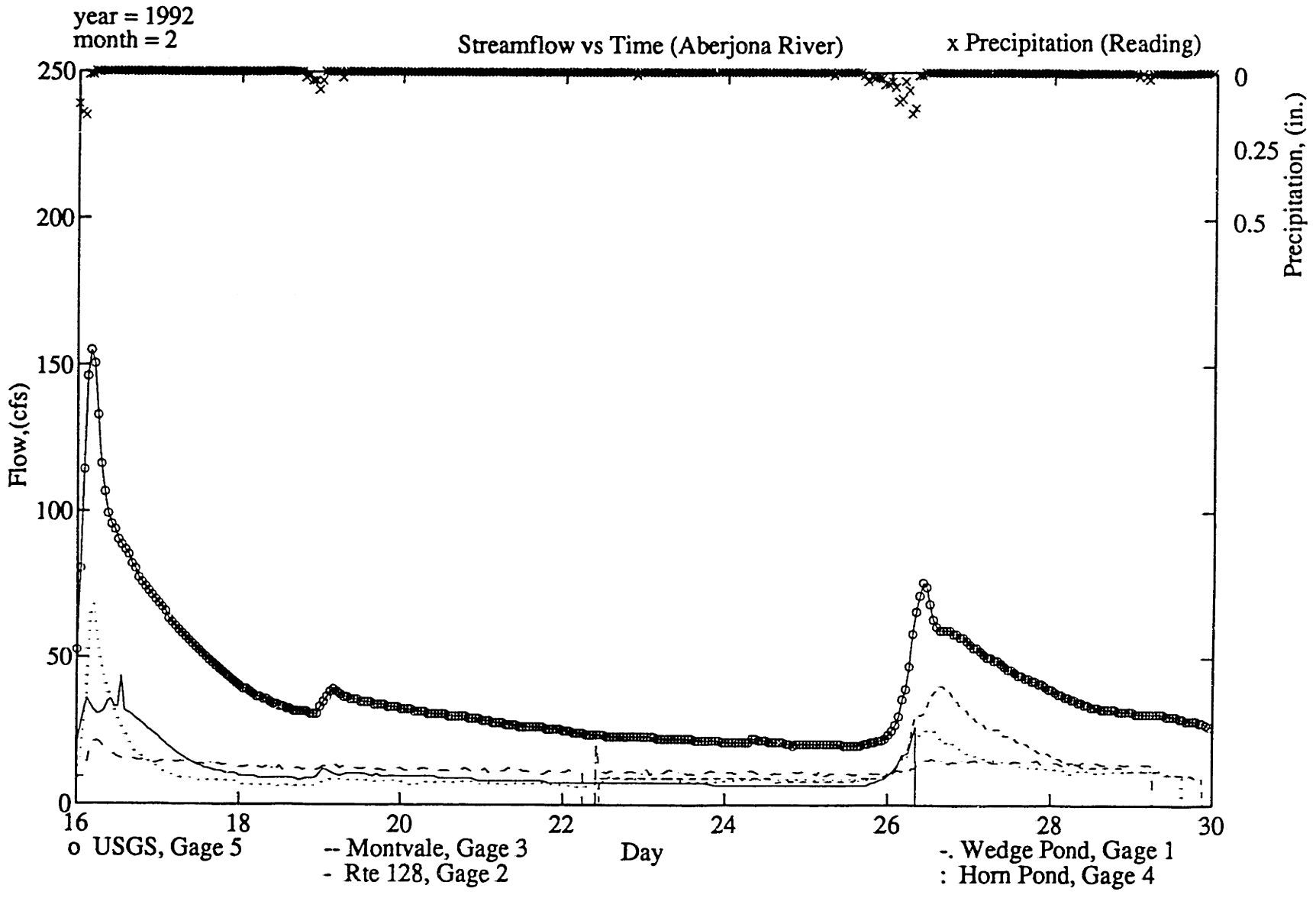
year = 1992
month = 2
Streamflow vs Time (Aberjona River)
x Precipitation (Reading)
250
200
150
100
50
0
Flow,(cfs)
0
0.25
0.5
Precipitation, (in.)
16
18
20
22
24
26
28
30
Day
o USGS, Gage 5
-- Montvale, Gage 3
- Rte 128, Gage 2
-. Wedge Pond, Gage 1
: Horn Pond, Gage 4

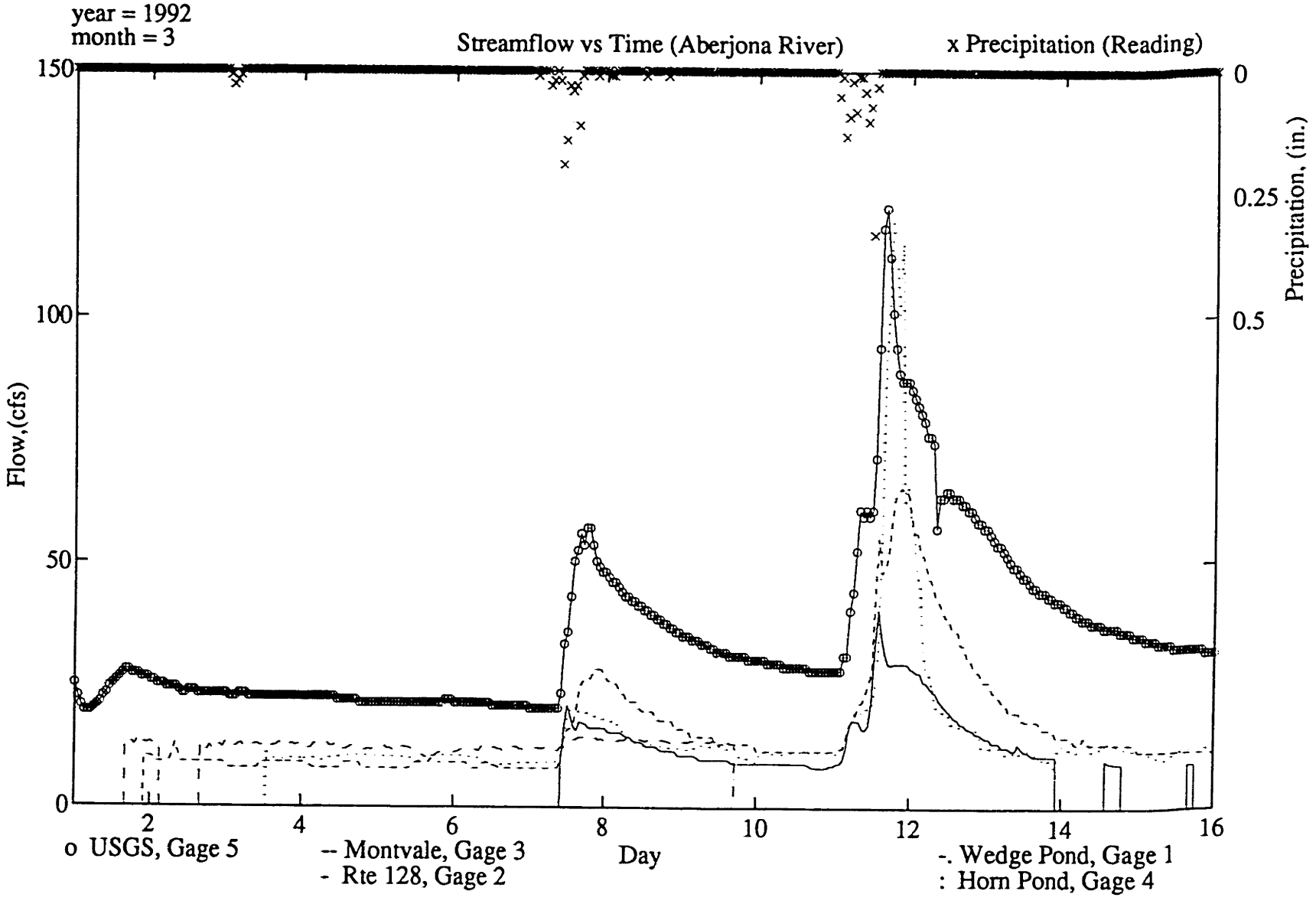
year = 1992
month = 3
Streamflow vs Time (Aberjona River)
x Precipitation (Reading)
150
100
50
0
0
0.25
0.5
Precipitation, (in.)
Flow,(cfs)
2
4
6
8
10
12
14
16
Day
o USGS, Gage 5
-- Montvale, Gage 3
- Rte 128, Gage 2
-. Wedge Pond, Gage 1
: Horn Pond, Gage 4

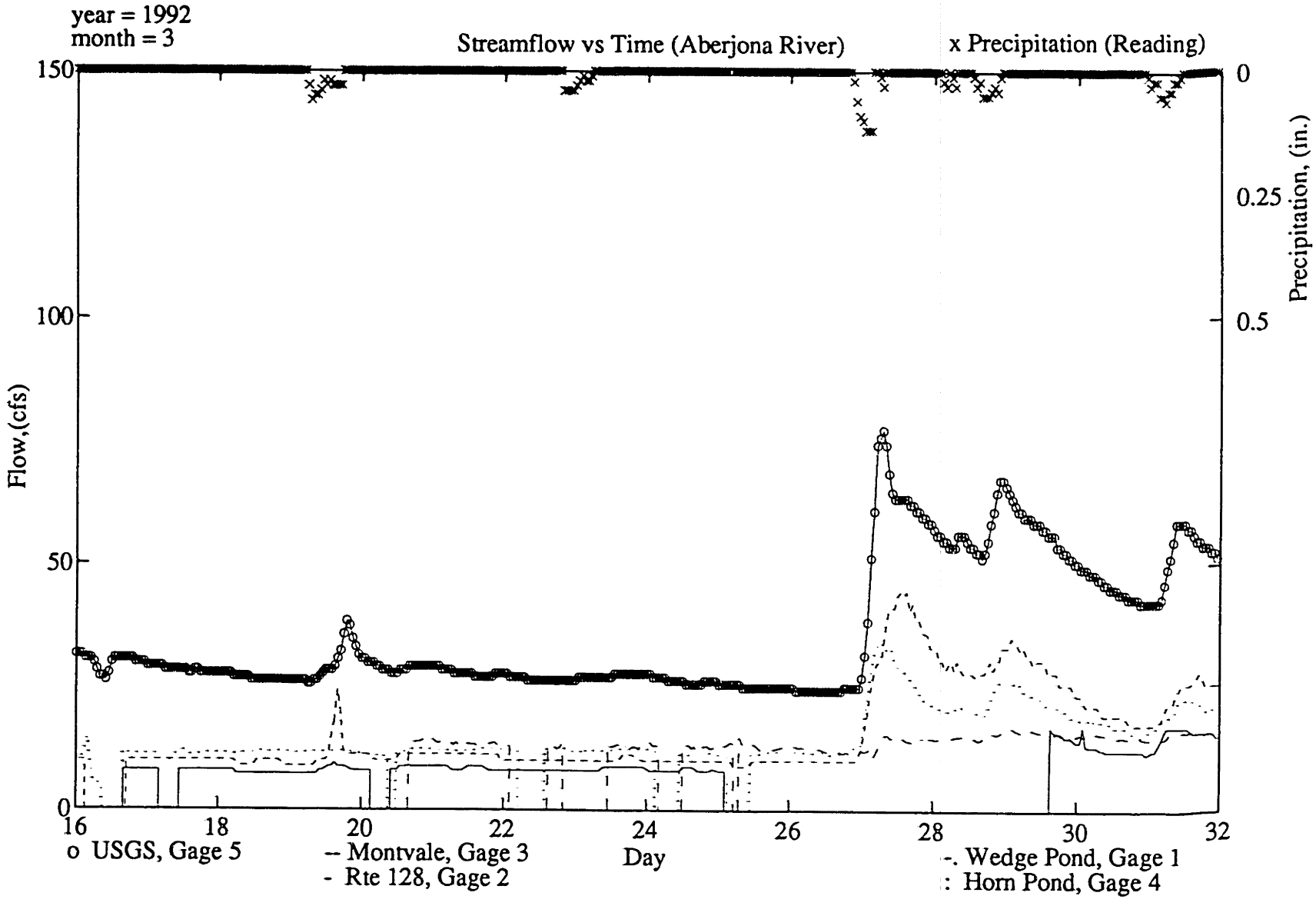
year = 1992
month = 3
Streamflow vs Time (Aberjona River)
x Precipitation (Reading)
150
100
50
0
0
0.25
0.5
Precipitation, (in.)
Flow,(cfs)
16
18
20
22
24
26
28
30
32
Day
o USGS, Gage 5
-- Montvale, Gage 3
- Rte 128, Gage 2
-. Wedge Pond, Gage 1
: Horn Pond, Gage 4

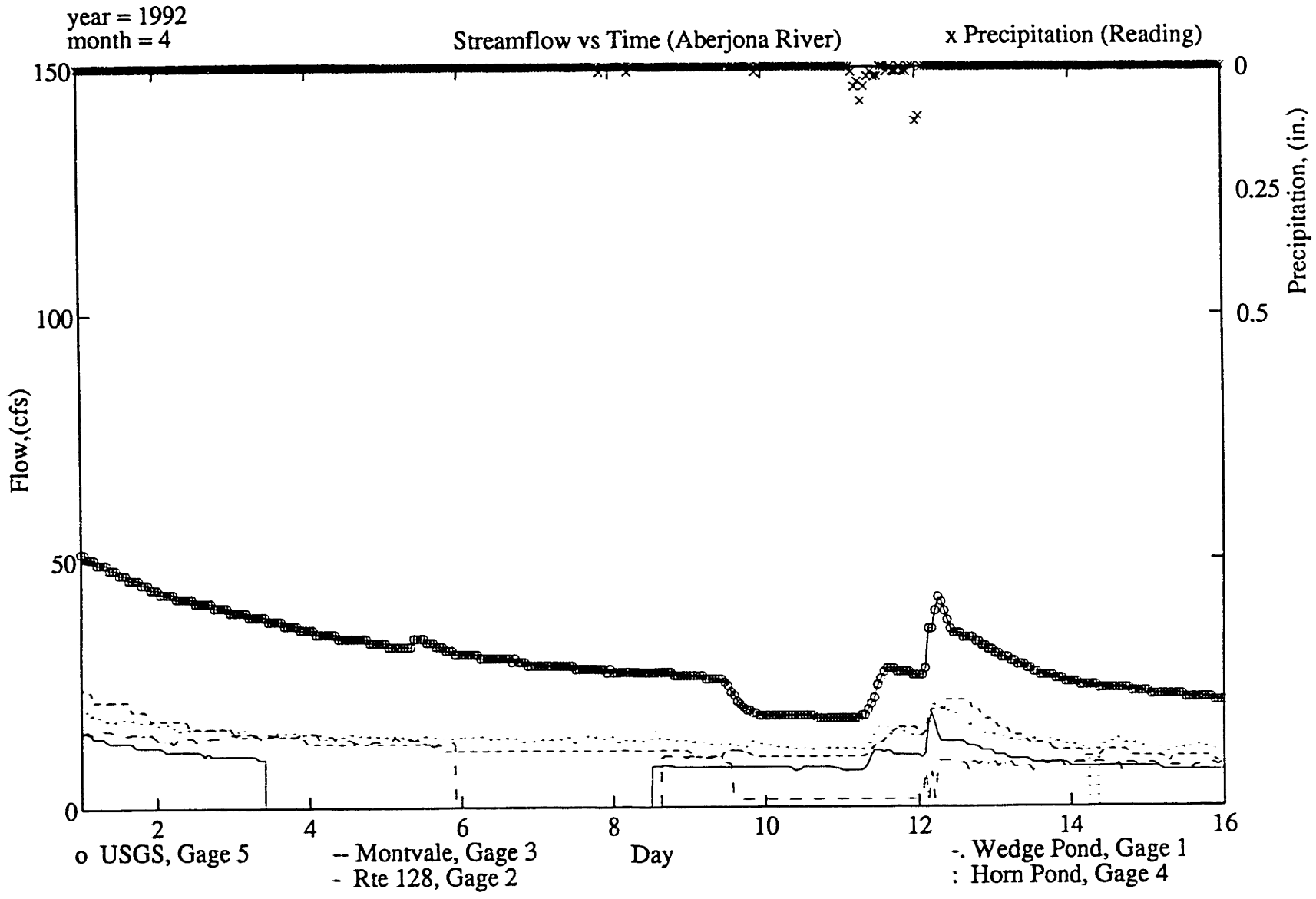
year = 1992
month = 4
Streamflow vs Time (Aberjona River)
x Precipitation (Reading)
150
100
50
0
Flow,(cfs)
0
0.25
0.5
Precipitation, (in.)
2
4
6
8
10
12
14
16
Day
o USGS, Gage 5
-- Montvale, Gage 3
- Rte 128, Gage 2
-. Wedge Pond, Gage 1
: Horn Pond, Gage 4

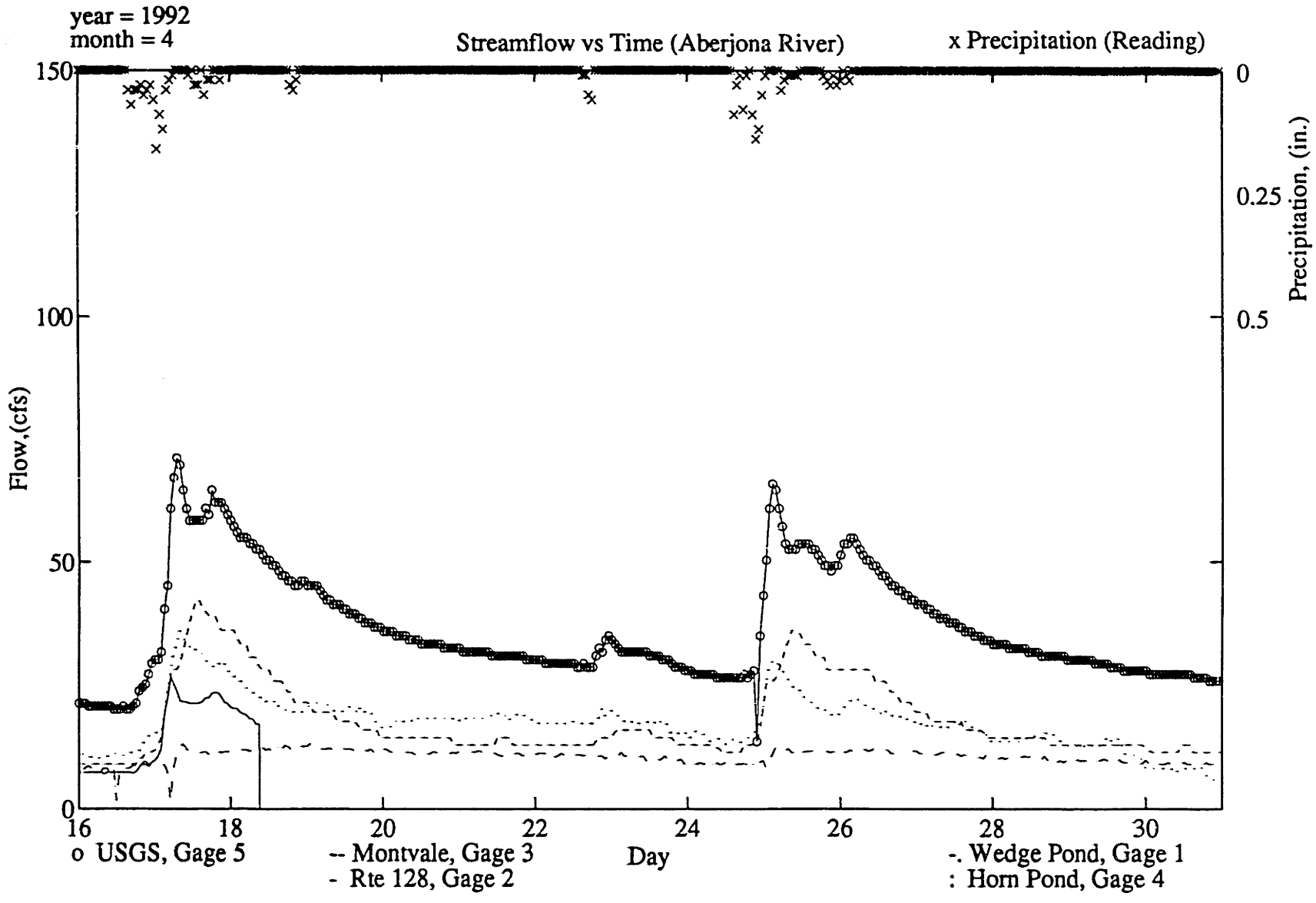
year = 1992
month = 4
Streamflow vs Time (Aberjona River)
x Precipitation (Reading)
150
100
50
0
0
0.25
0.5
Precipitation, (in.)
Flow,(cfs)
16
18
20
22
24
26
28
30
Day
o USGS, Gage 5
-- Montvale, Gage 3
- Rte 128, Gage 2
-. Wedge Pond, Gage 1
: Horn Pond, Gage 4

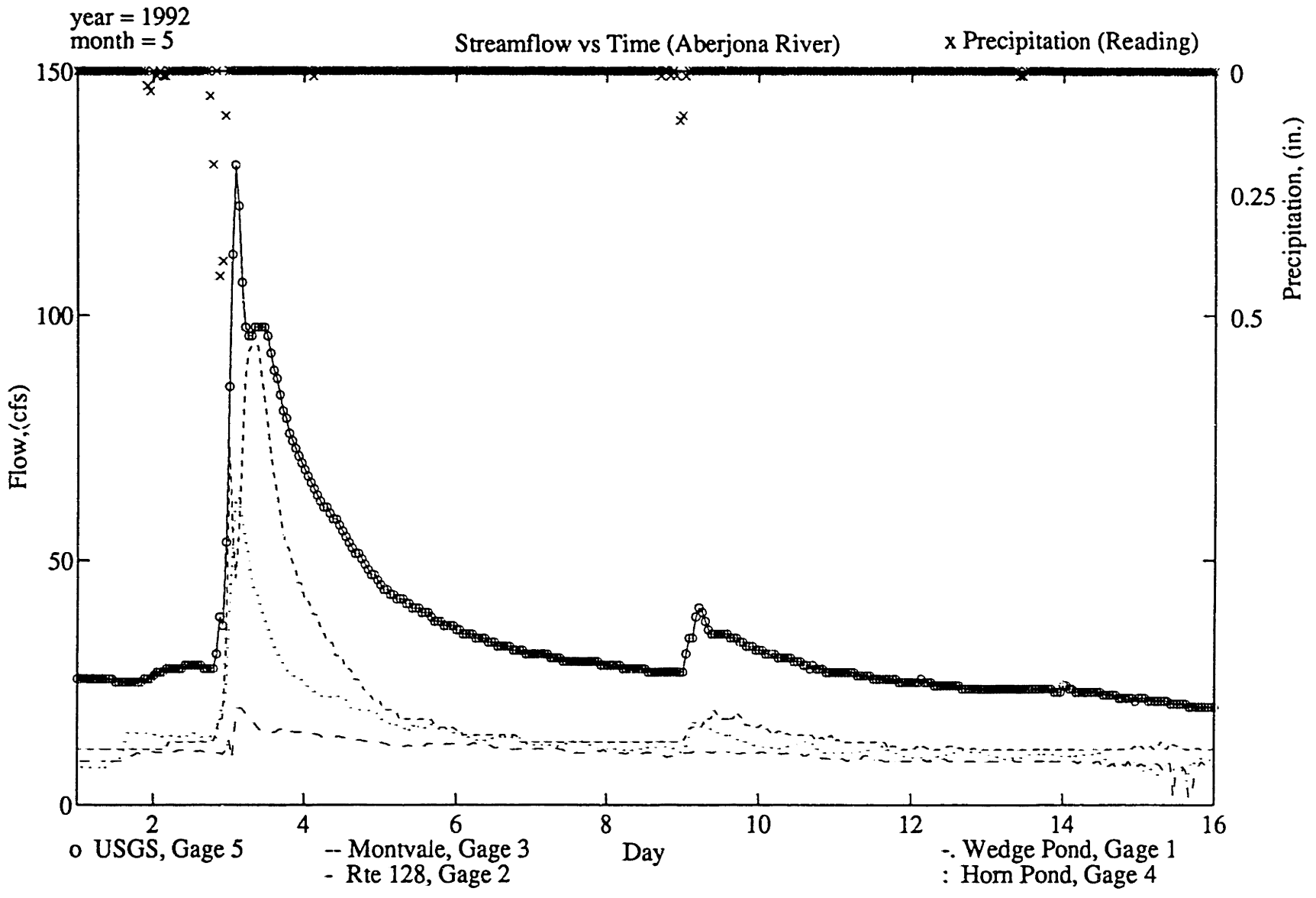
year = 1992
month = 5
Streamflow vs Time (Aberjona River)
x Precipitation (Reading)
150
100
50
0
0
0.25
0.5
Precipitation, (in.)
Flow,(cfs)
2
4
6
8
10
12
14
16
Day
o USGS, Gage 5
-- Montvale, Gage 3
- Rte 128, Gage 2
-. Wedge Pond, Gage 1
: Horn Pond, Gage 4

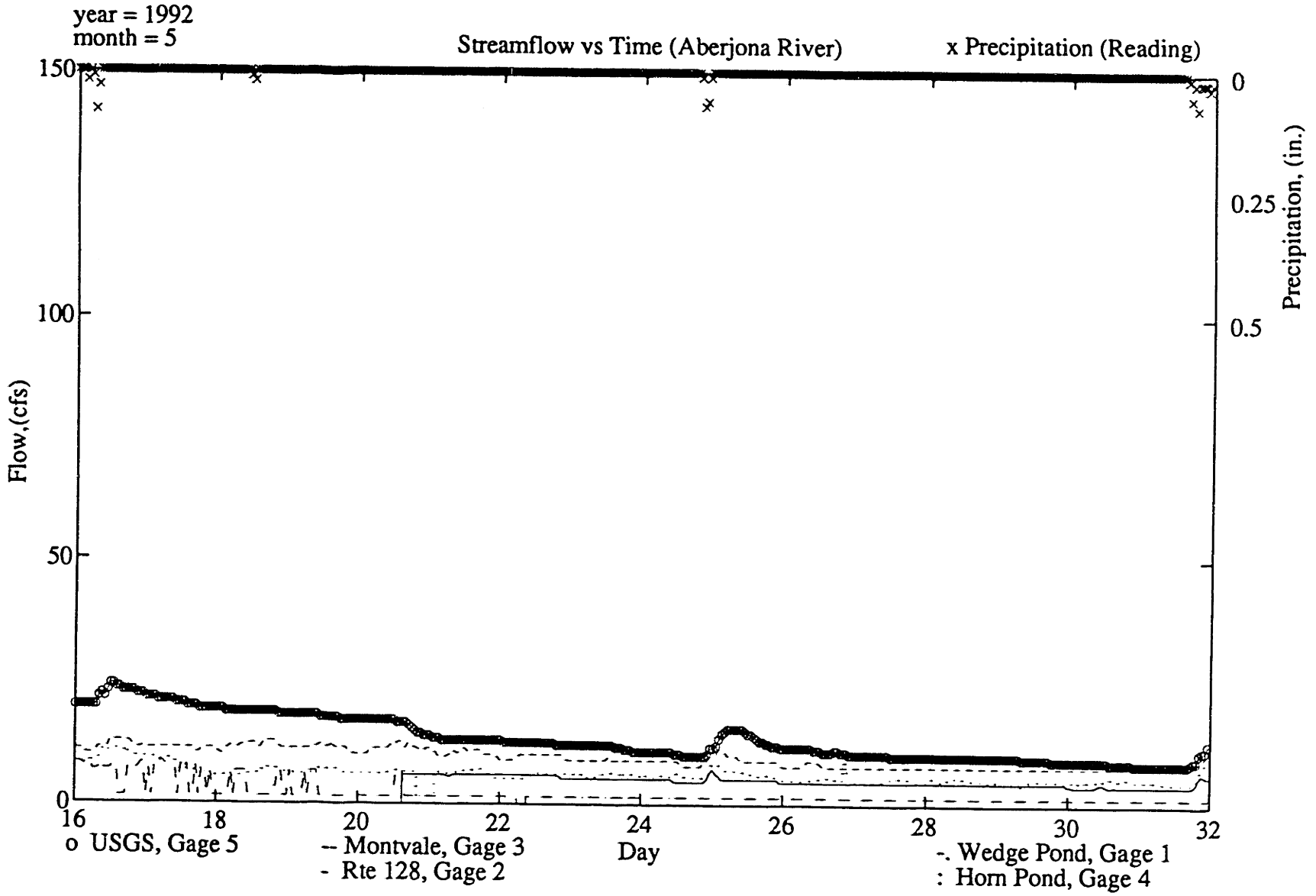
year = 1992
month = 5
Streamflow vs Time (Aberjona River)
x Precipitation (Reading)
150
100
50
0
Flow,(cfs)
0
0.25
0.5
Precipitation, (in.)
16
18
20
22
24
26
28
30
32
Day
o USGS, Gage 5
-- Montvale, Gage 3
- Rte 128, Gage 2
-. Wedge Pond, Gage 1
: Horn Pond, Gage 4

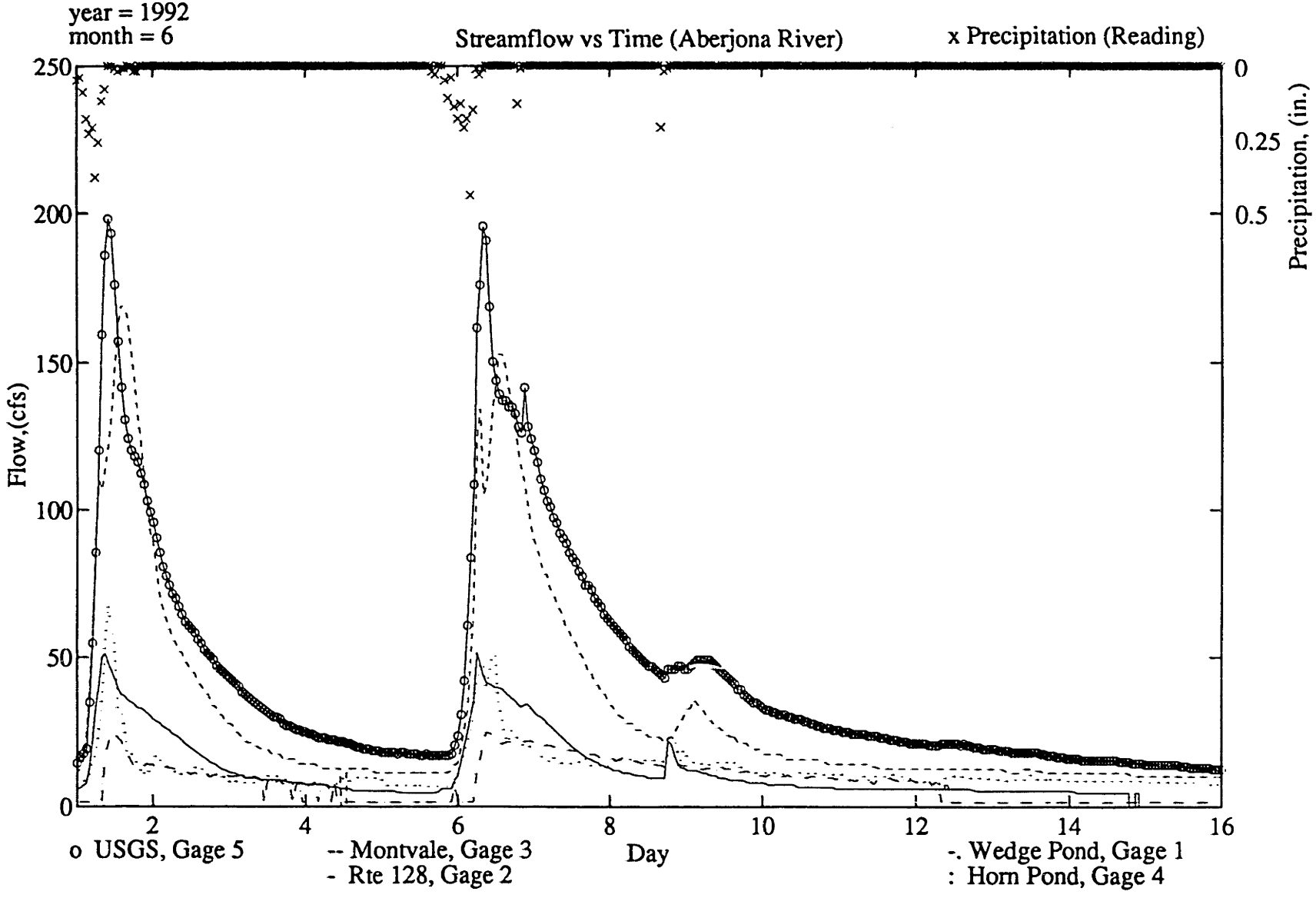
year = 1992
month = 6
Streamflow vs Time (Aberjona River)
x Precipitation (Reading)
Flow,(cfs)
Precipitation, (in.)
250
200
150
100
50
0
0
0.25
0.5
2
4
6
8
10
12
14
16
Day
o USGS, Gage 5
-- Montvale, Gage 3
- Rte 128, Gage 2
-. Wedge Pond, Gage 1
: Horn Pond, Gage 4

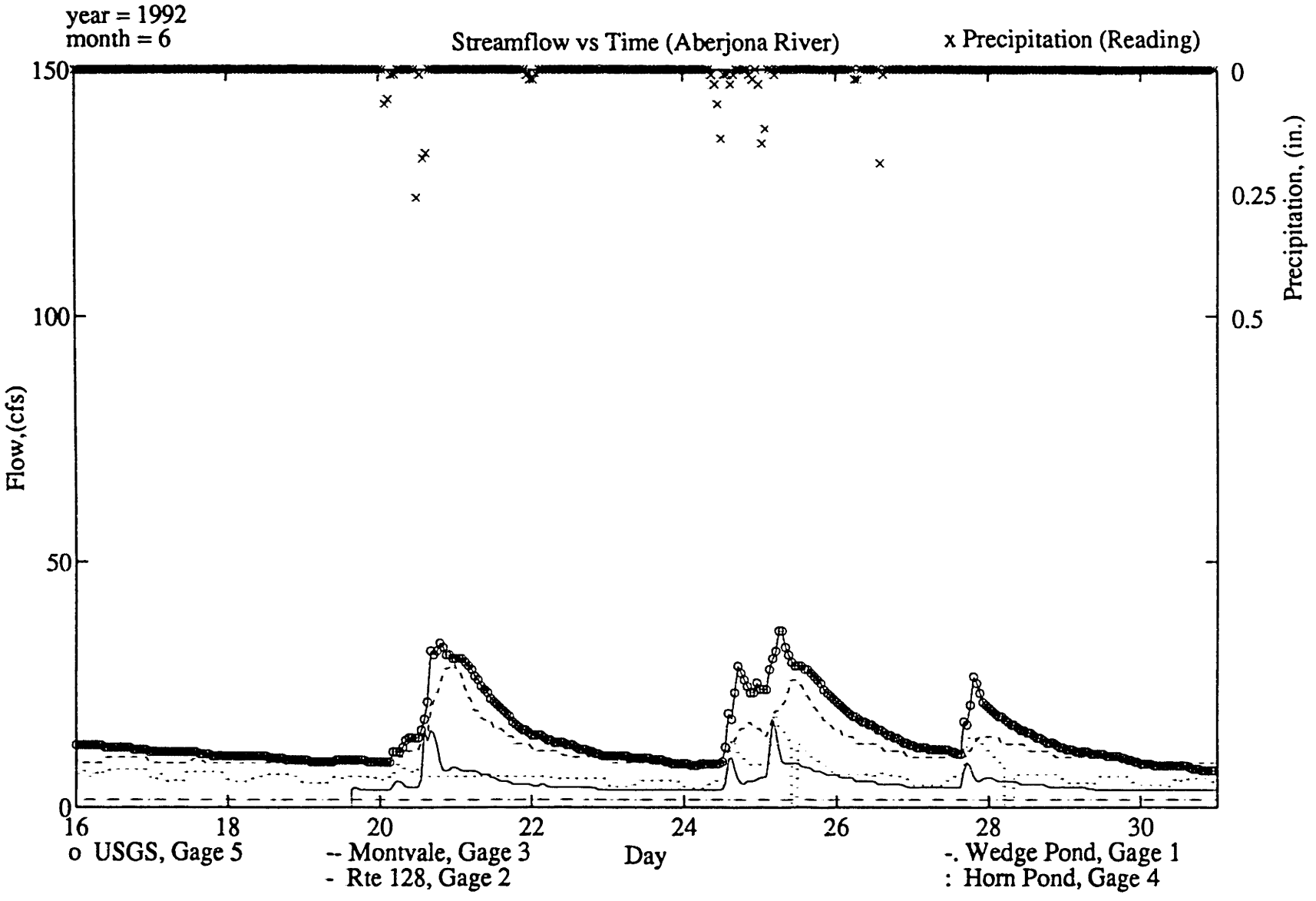
year = 1992
month = 6
Streamflow vs Time (Aberjona River)
x Precipitation (Reading)
150
100
50
0
0
0.25
0.5
Precipitation, (in.)
Flow,(cfs)
16
18
20
22
24
26
28
30
Day
o USGS, Gage 5
-- Montvale, Gage 3
- Rte 128, Gage 2
-. Wedge Pond, Gage 1
: Horn Pond, Gage 4

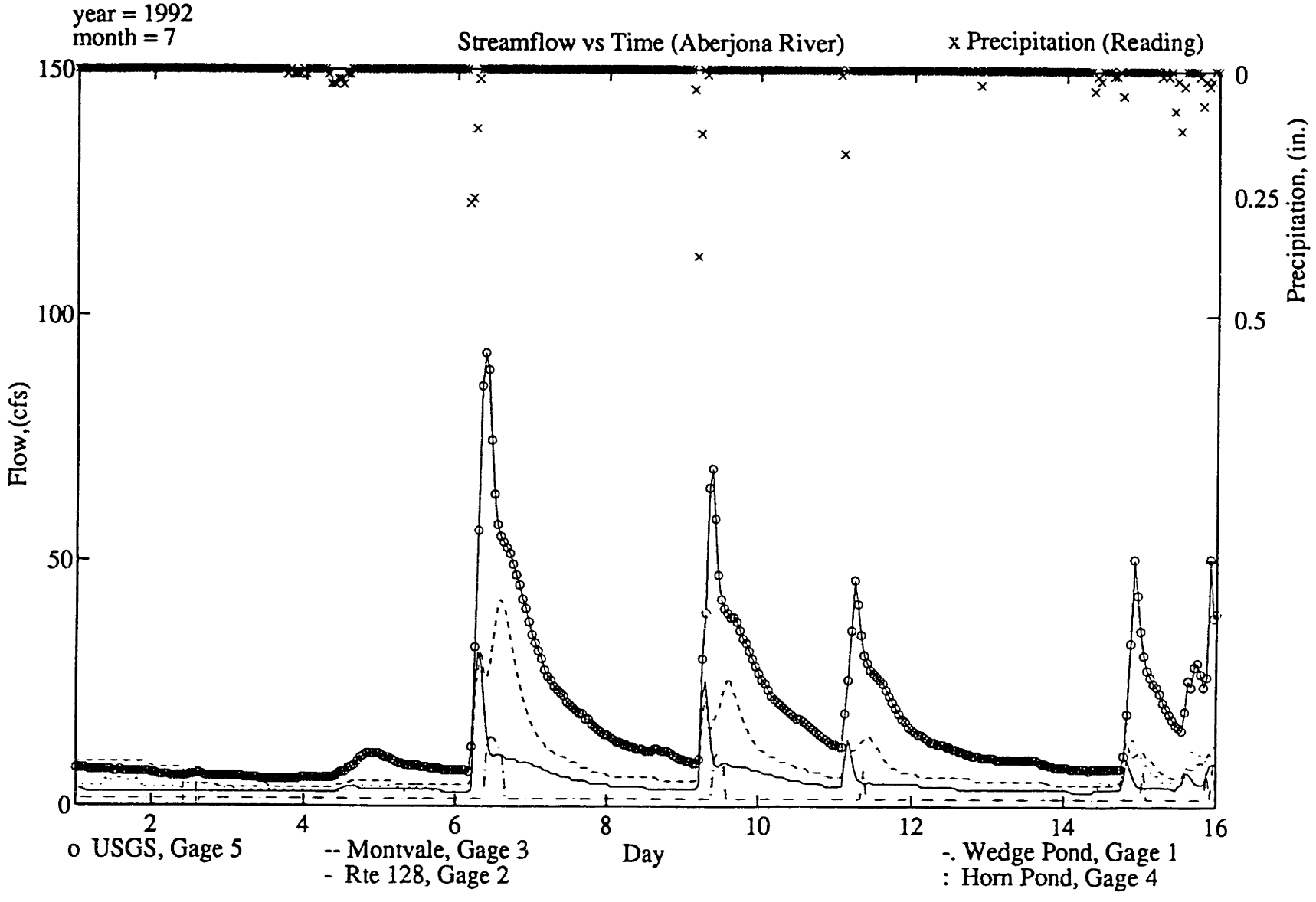
year = 1992
month = 7
Streamflow vs Time (Aberjona River)
x Precipitation (Reading)
150
100
50
0
0
0.25
0.5
Precipitation, (in.)
Flow,(cfs)
2
4
6
8
10
12
14
16
Day
o USGS, Gage 5
-- Montvale, Gage 3
- Rte 128, Gage 2
-. Wedge Pond, Gage 1
: Horn Pond, Gage 4

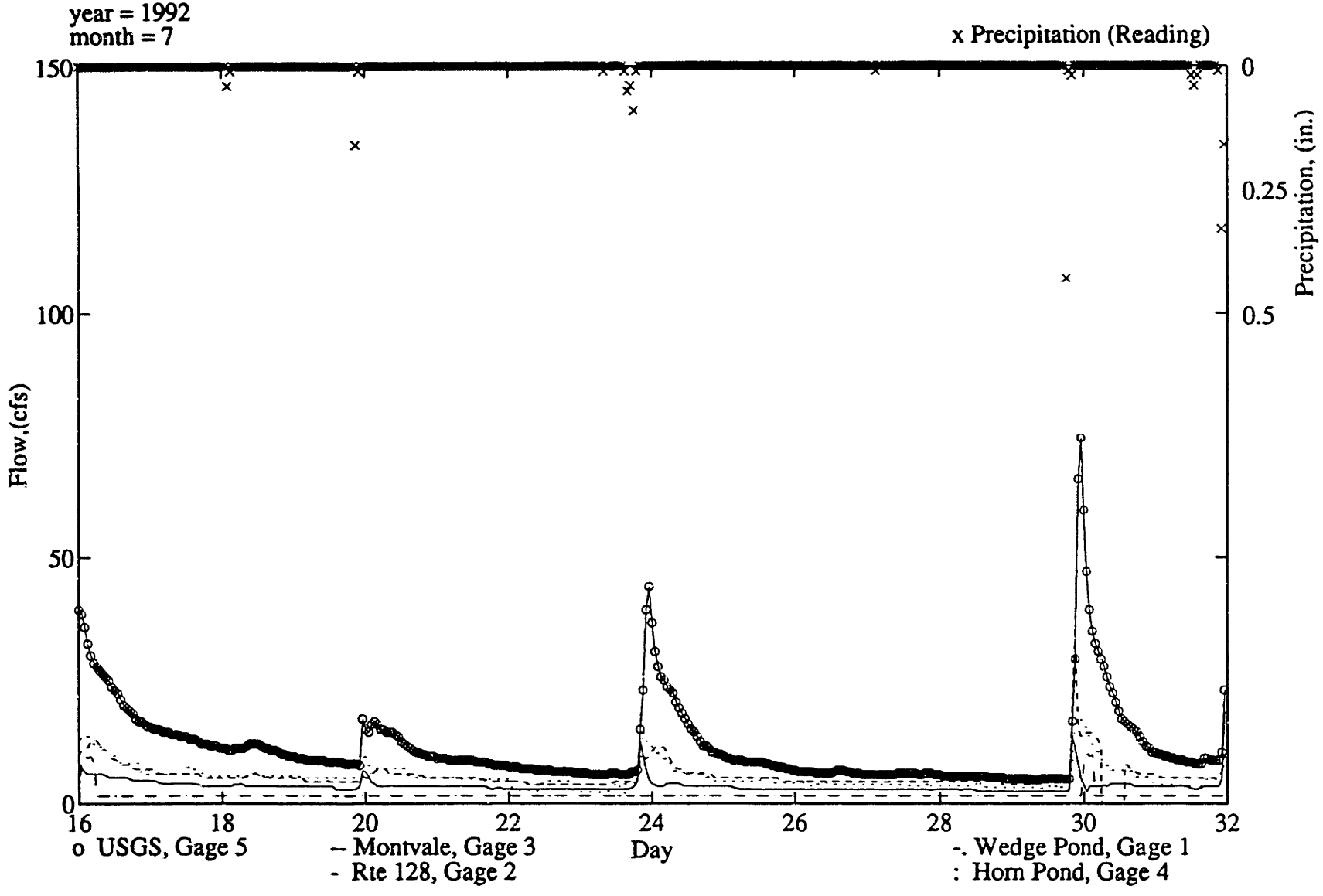
year = 1992
month = 7
x Precipitation (Reading)
150
100
50
0
0
0.25
0.5
Precipitation, (in.)
Flow,(cfs)
16
18
20
22
24
26
28
30
32
Day
o USGS, Gage 5
-- Montvale, Gage 3
- Rte 128, Gage 2
-. Wedge Pond, Gage 1
: Horn Pond, Gage 4

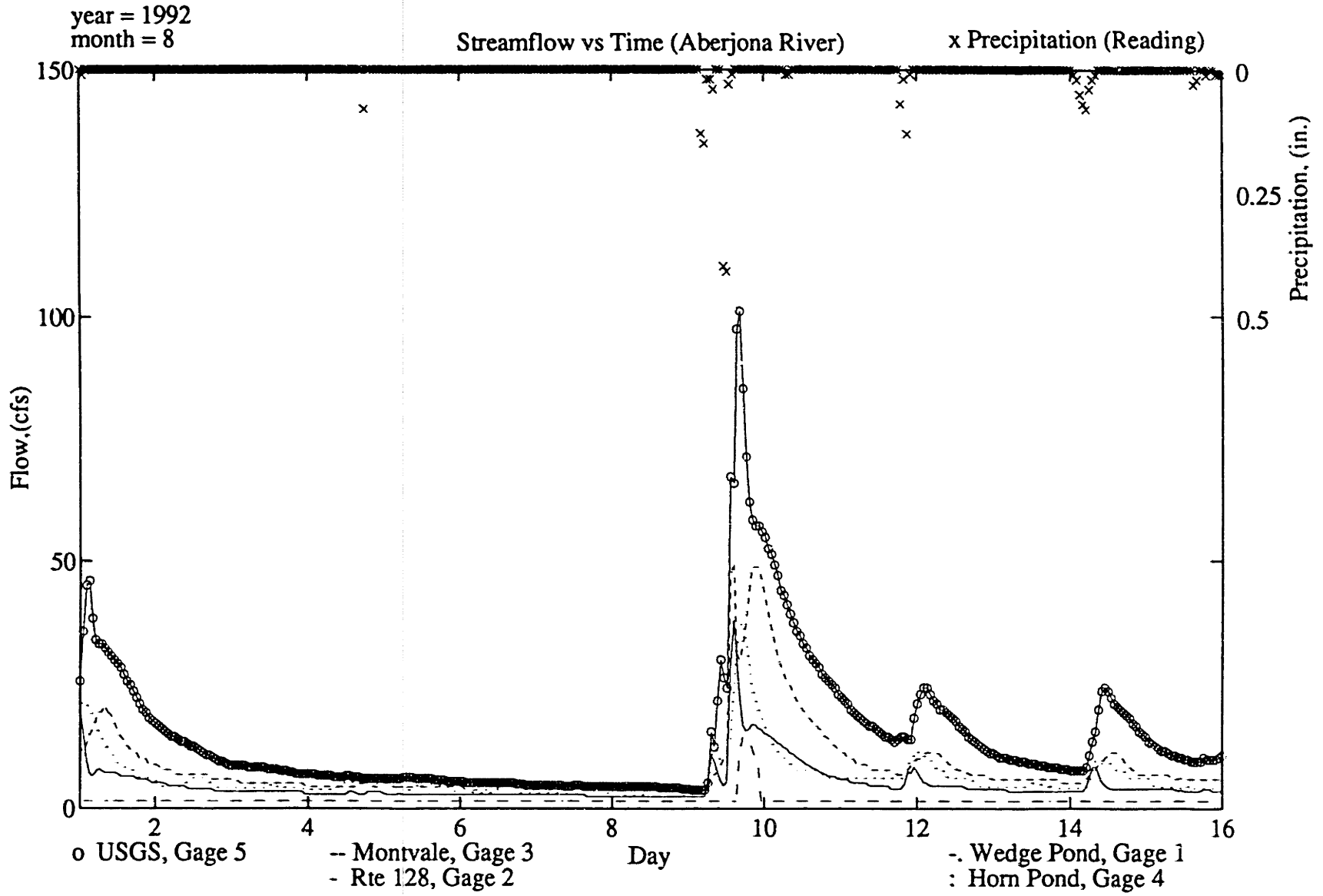
year = 1992
month = 8
Streamflow vs Time (Aberjona River)
x Precipitation (Reading)
150
100
50
0
0
0.25
0.5
Precipitation, (in.)
Flow,(cfs)
2
4
6
8
10
12
14
16
Day
o USGS, Gage 5
-- Montvale, Gage 3
- Rte 128, Gage 2
-. Wedge Pond, Gage 1
: Horn Pond, Gage 4

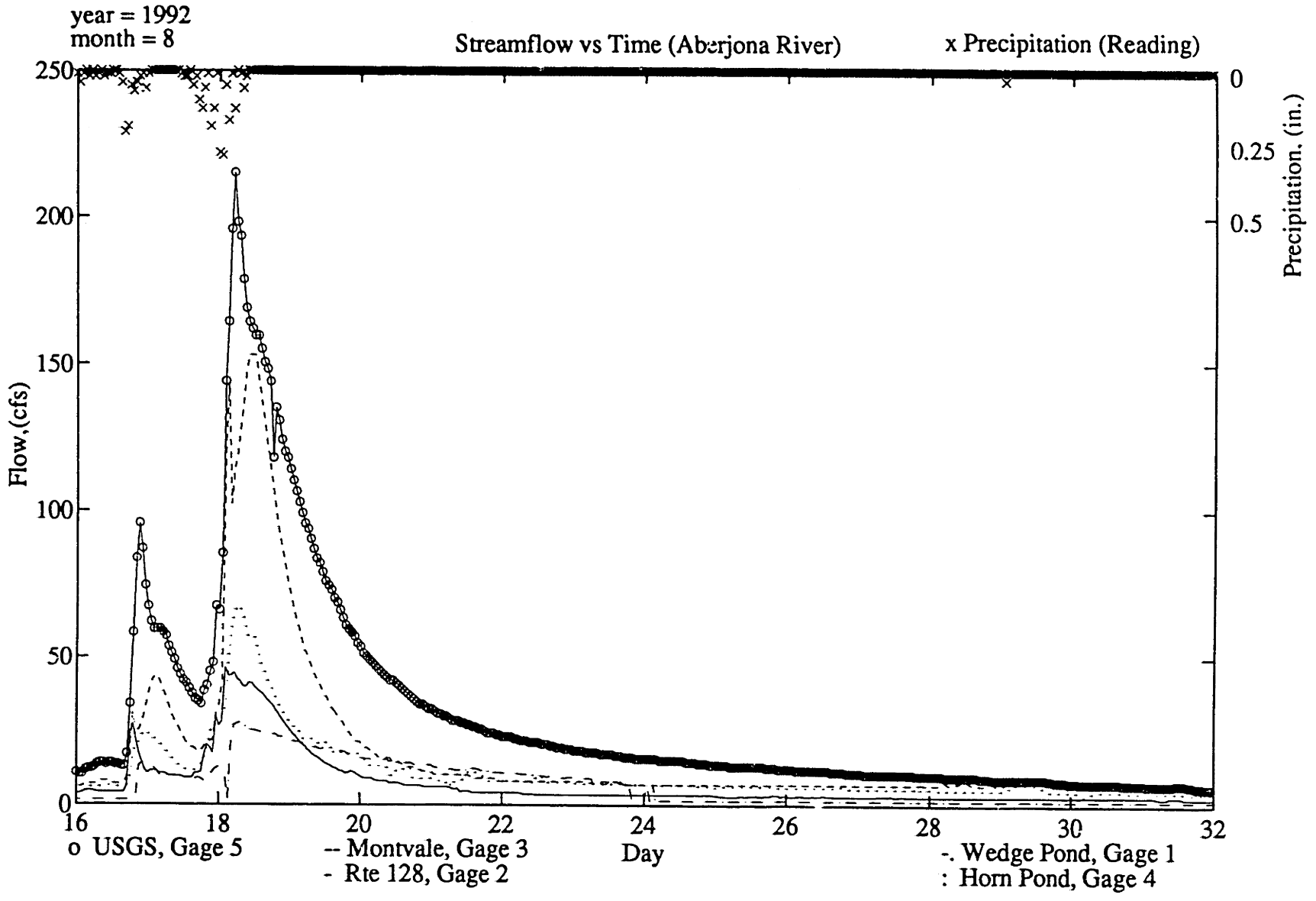
year = 1992
month = 8
Streamflow vs Time (Aberjona River)
x Precipitation (Reading)
Flow,(cfs)
Precipitation, (in.)
250
200
150
100
50
0
0
0.25
0.5
16
18
20
22
24
26
28
30
32
Day
o USGS, Gage 5
-- Montvale, Gage 3
- Rte 128, Gage 2
-. Wedge Pond, Gage 1
: Horn Pond, Gage 4

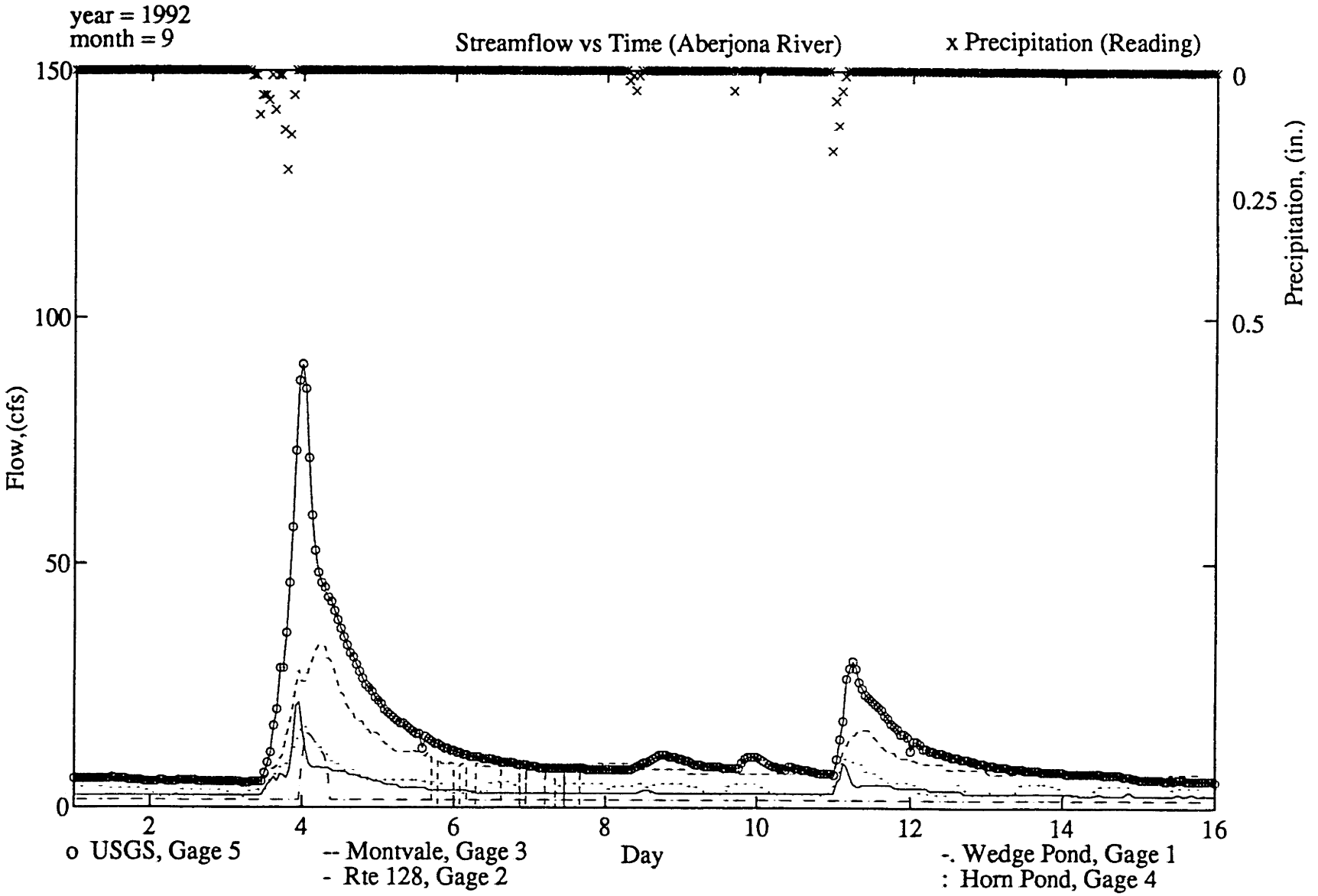
year = 1992
month = 9
Streamflow vs Time (Aberjona River)
x Precipitation (Reading)
150
100
50
0
Flow,(cfs)
0
0.25
0.5
Precipitation, (in.)
2
4
6
8
10
12
14
16
Day
o USGS, Gage 5
-- Montvale, Gage 3
- Rte 128, Gage 2
-. Wedge Pond, Gage 1
: Horn Pond, Gage 4

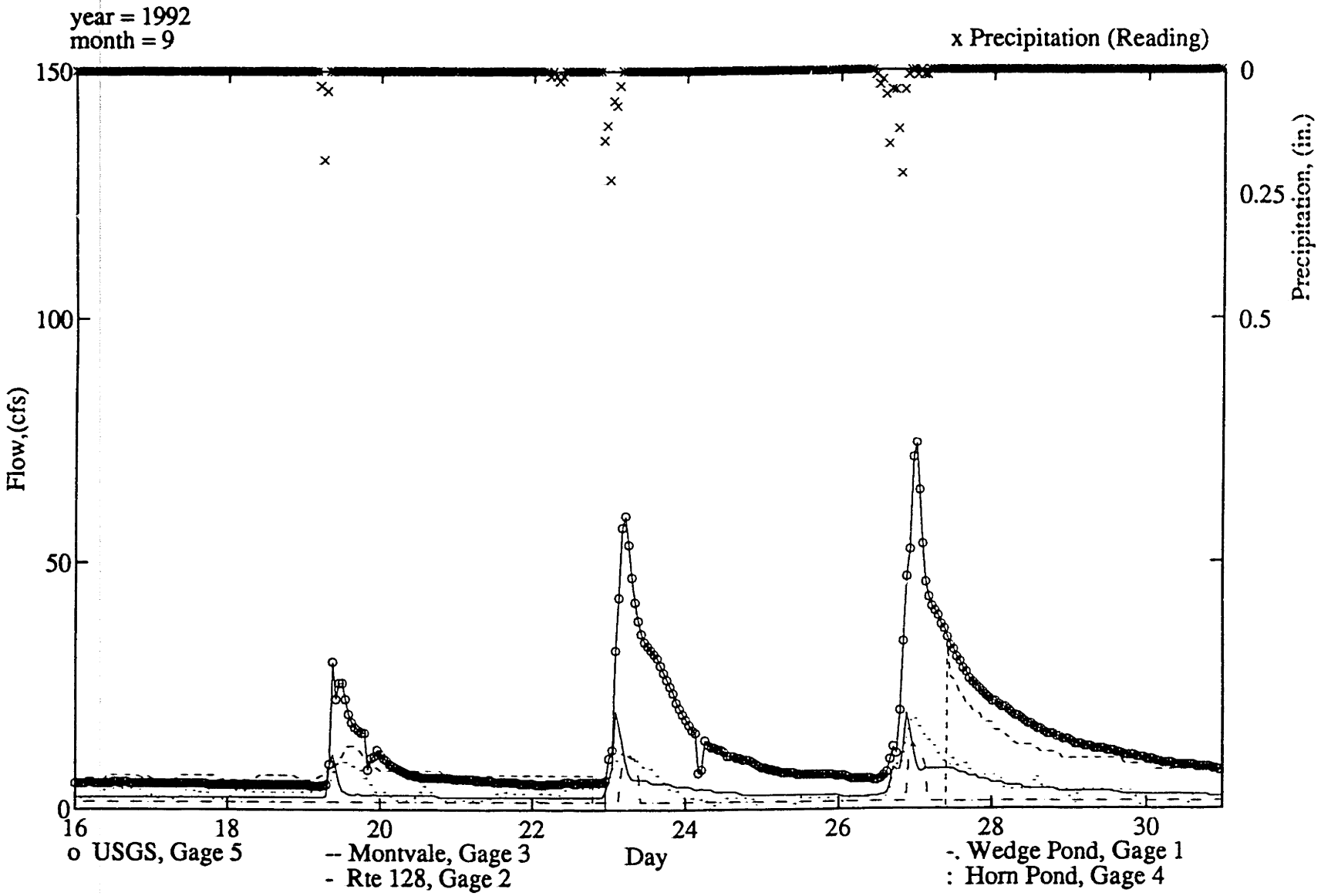
year = 1992
month = 9
x Precipitation (Reading)
150
100
50
0
Flow,(cfs)
0
0.25
0.5
Precipitation, (in.)
16
18
20
22
24
26
28
30
Day
o USGS, Gage 5
-- Montvale, Gage 3
- Rte 128, Gage 2
-. Wedge Pond, Gage 1
: Horn Pond, Gage 4

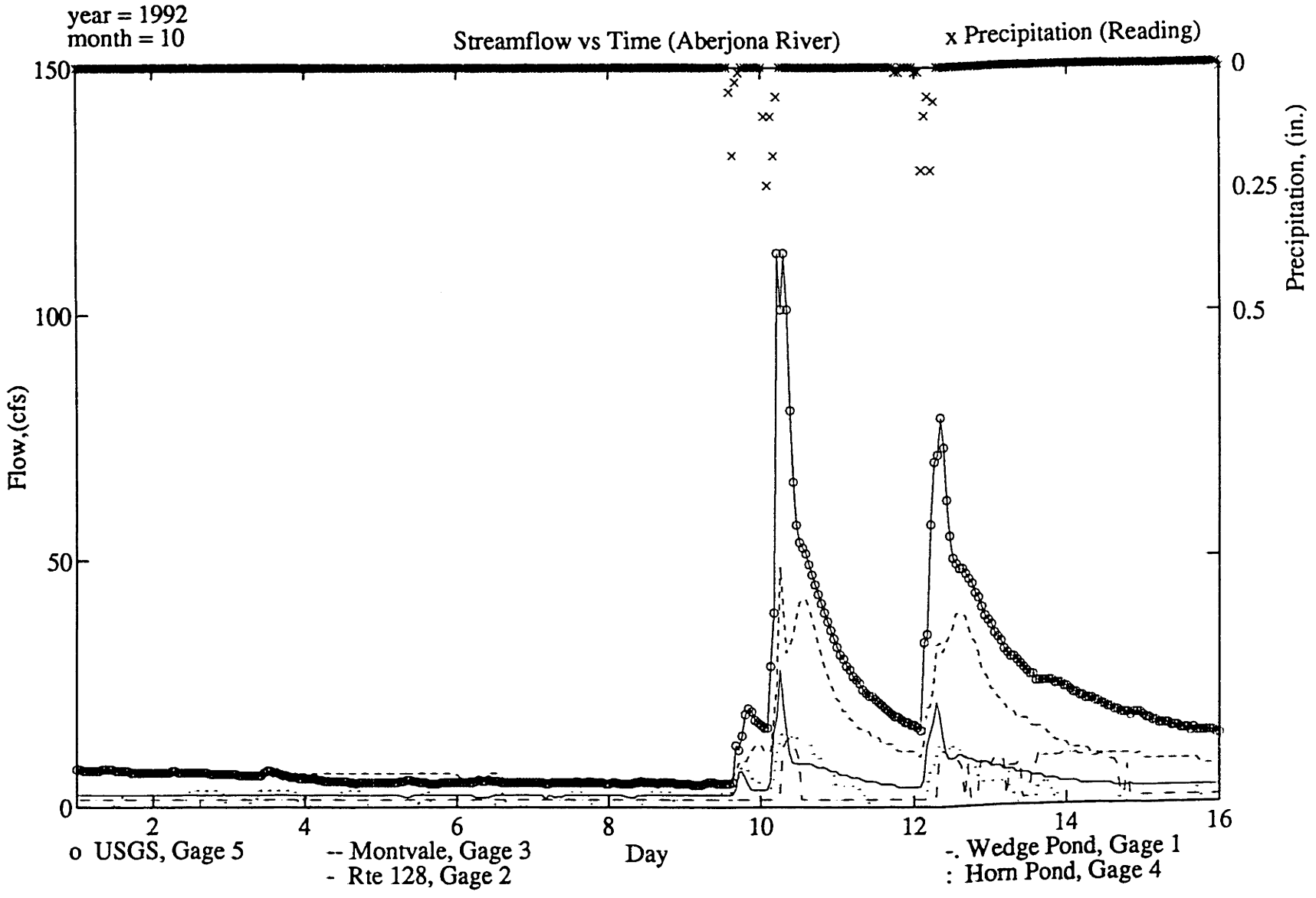
year = 1992
month = 10
Streamflow vs Time (Aberjona River)
x Precipitation (Reading)
150
100
50
0
Flow,(cfs)
0
0.25
0.5
Precipitation, (in.)
2
4
6
8
10
12
14
16
Day
o USGS, Gage 5
-- Montvale, Gage 3
- Rte 128, Gage 2
-. Wedge Pond, Gage 1
: Horn Pond, Gage 4

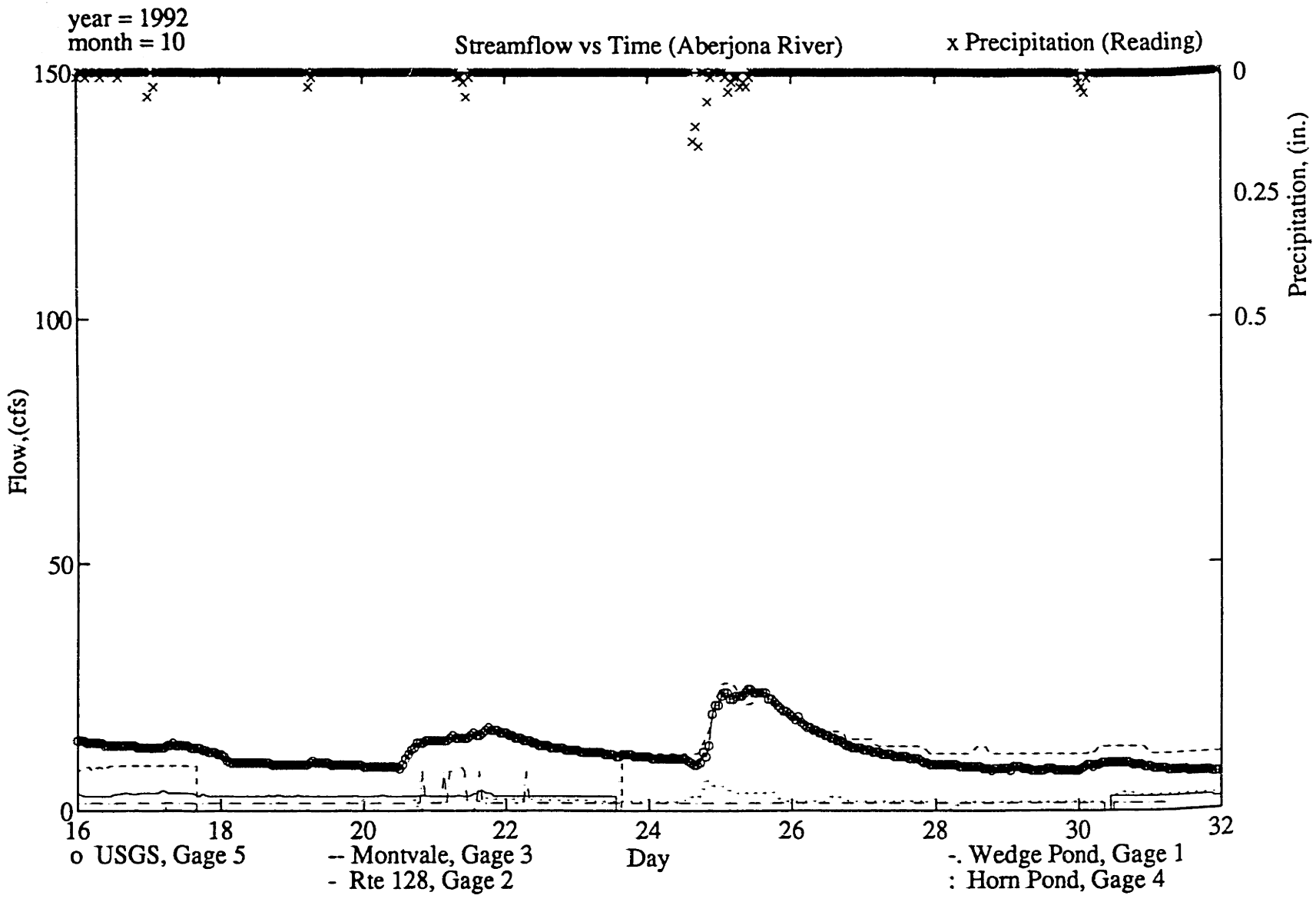
year = 1992
month = 10
Streamflow vs Time (Aberjona River)
x Precipitation (Reading)
150
100
50
0
Flow,(cfs)
0
0.25
0.5
Precipitation, (in.)
16
18
20
22
24
26
28
30
32
Day
o USGS, Gage 5
-- Montvale, Gage 3
- Rte 128, Gage 2
-. Wedge Pond, Gage 1
: Horn Pond, Gage 4

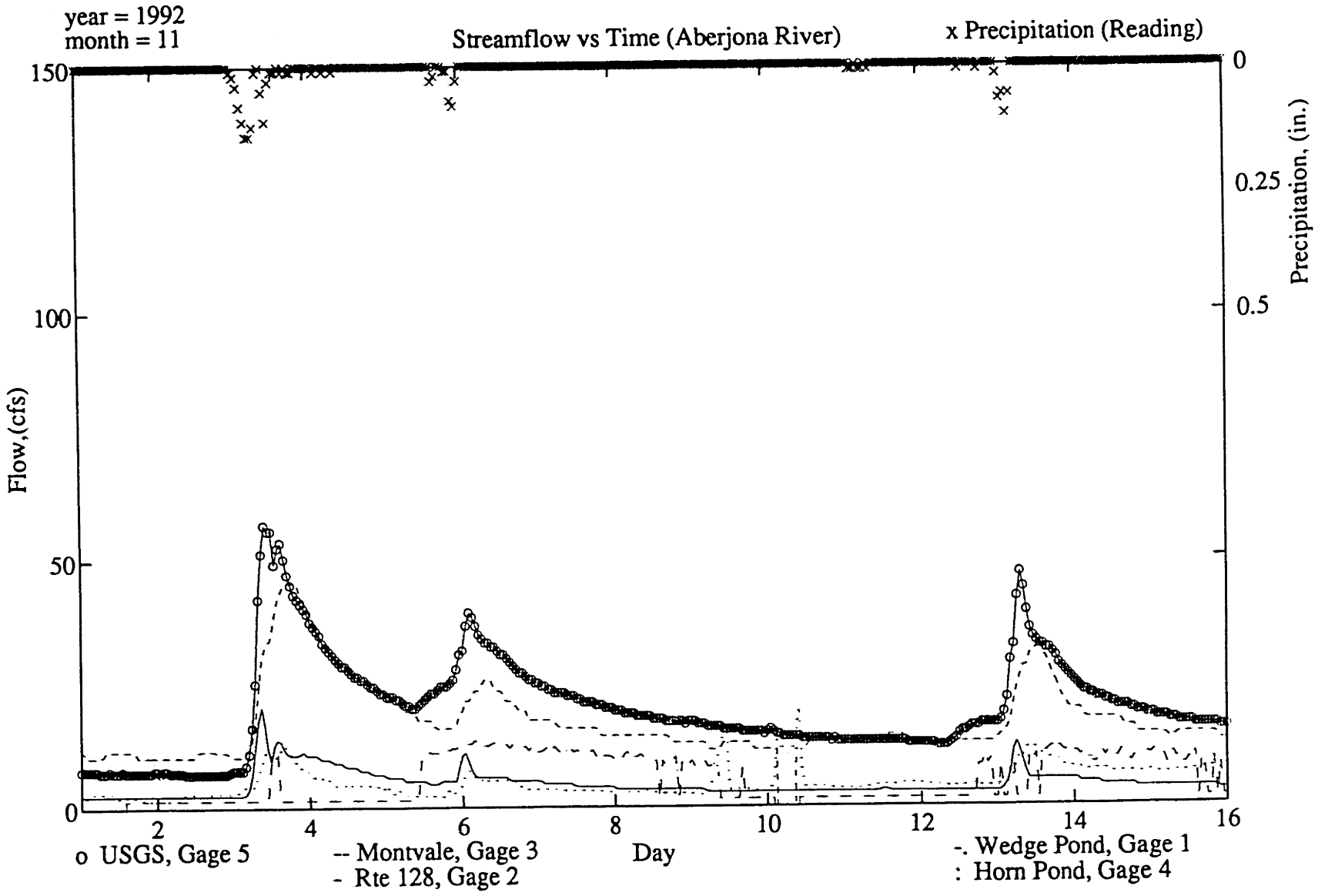
year = 1992
month = 11
Streamflow vs Time (Aberjona River)
x Precipitation (Reading)
150
100
50
0
Flow,(cfs)
0
0.25
0.5
Precipitation, (in.)
2
4
6
8
10
12
14
16
Day
o USGS, Gage 5
-- Montvale, Gage 3
- Rte 128, Gage 2
-. Wedge Pond, Gage 1
: Horn Pond, Gage 4

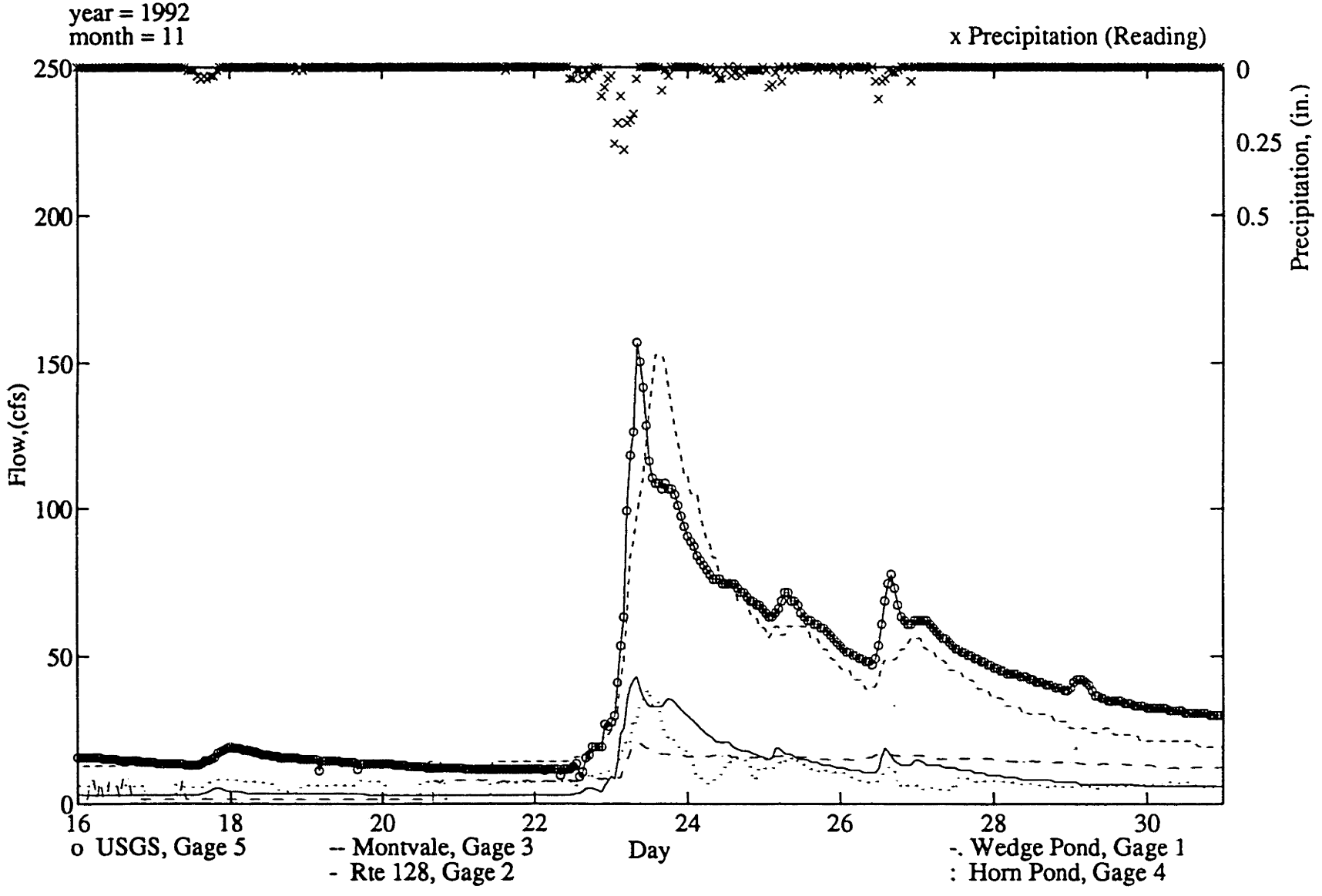
year = 1992
month = 11
x Precipitation (Reading)
250
200
150
100
50
0
Flow,(cfs)
0
0.25
0.5
Precipitation, (in.)
16
18
20
22
24
26
28
30
Day
o USGS, Gage 5
-- Montvale, Gage 3
- Rte 128, Gage 2
-. Wedge Pond, Gage 1
: Horn Pond, Gage 4

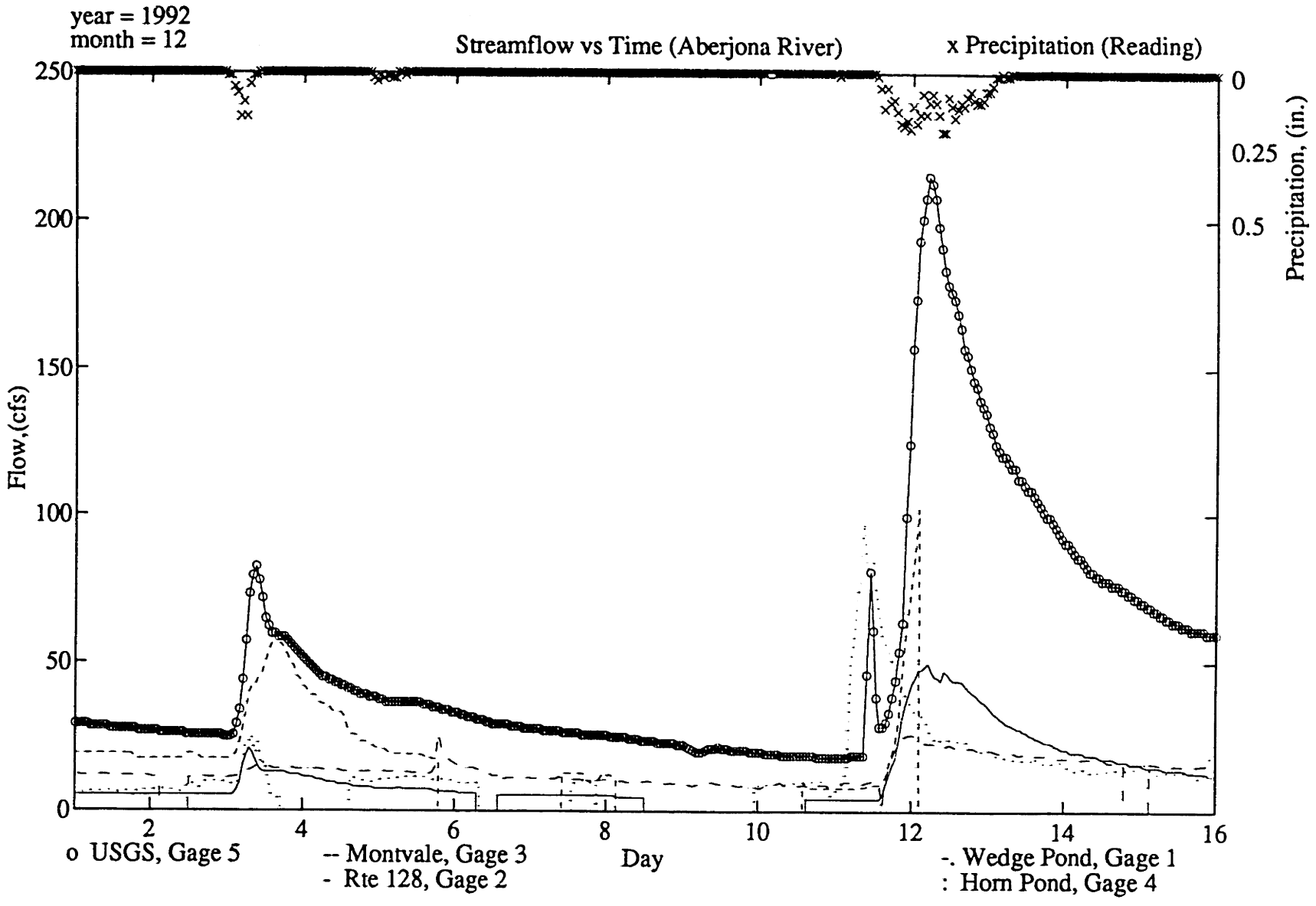
year = 1992
month = 12
Streamflow vs Time (Aberjona River)
x Precipitation (Reading)
Flow,(cfs)
Precipitation, (in.)
250
200
150
100
50
0
0
0.25
0.5
2
4
6
8
10
12
14
16
Day
o USGS, Gage 5
-- Montvale, Gage 3
- Rte 128, Gage 2
-. Wedge Pond, Gage 1
: Horn Pond, Gage 4

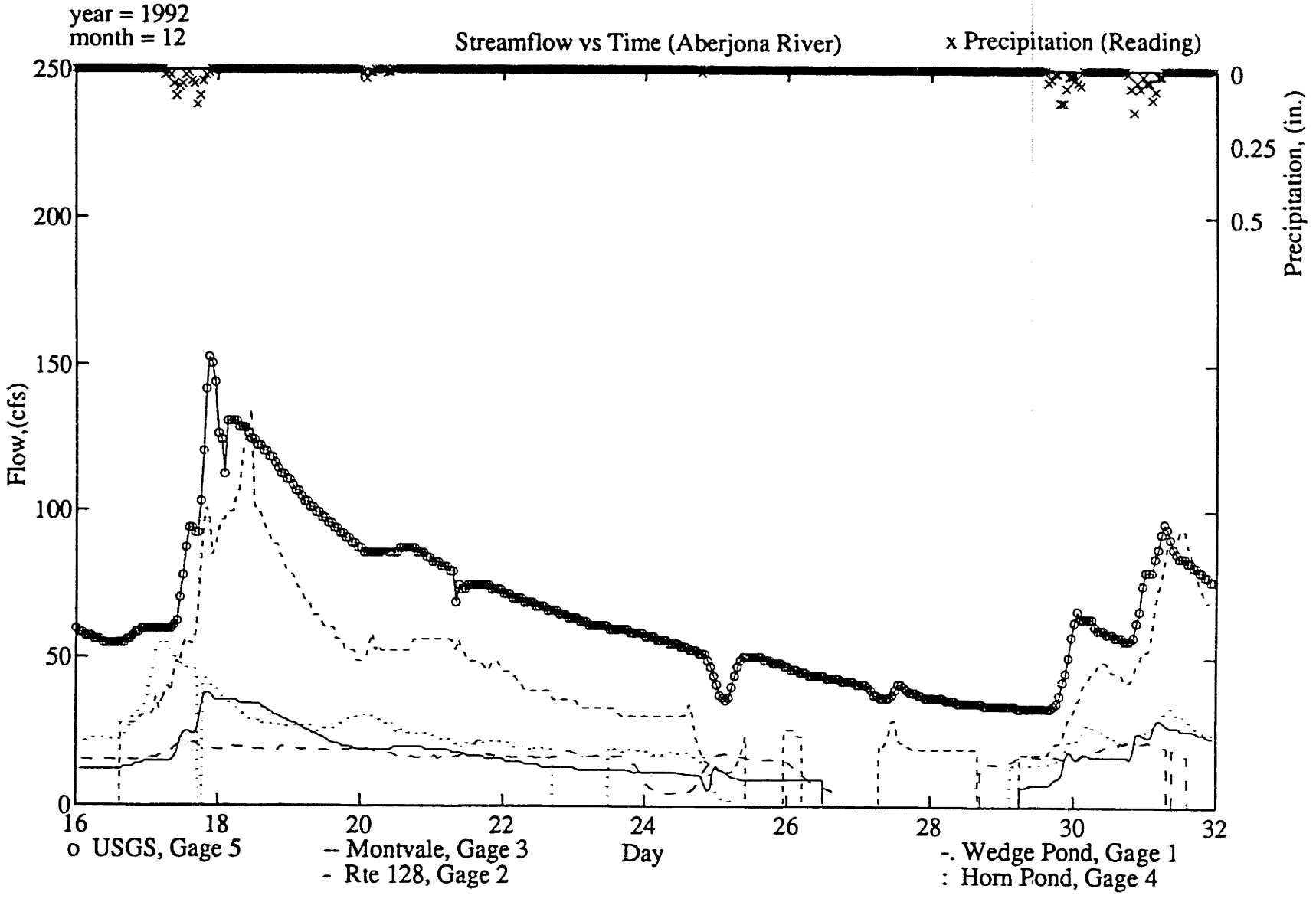
year = 1992
month = 12
Streamflow vs Time (Aberjona River)
x Precipitation (Reading)
250
200
150
100
50
0
Flow,(cfs)
0
0.25
0.5
Precipitation, (in.)
16
18
20
22
24
26
28
30
32
Day
o USGS, Gage 5
-- Montvale, Gage 3
- Rte 128, Gage 2
-. Wedge Pond, Gage 1
: Horn Pond, Gage 4

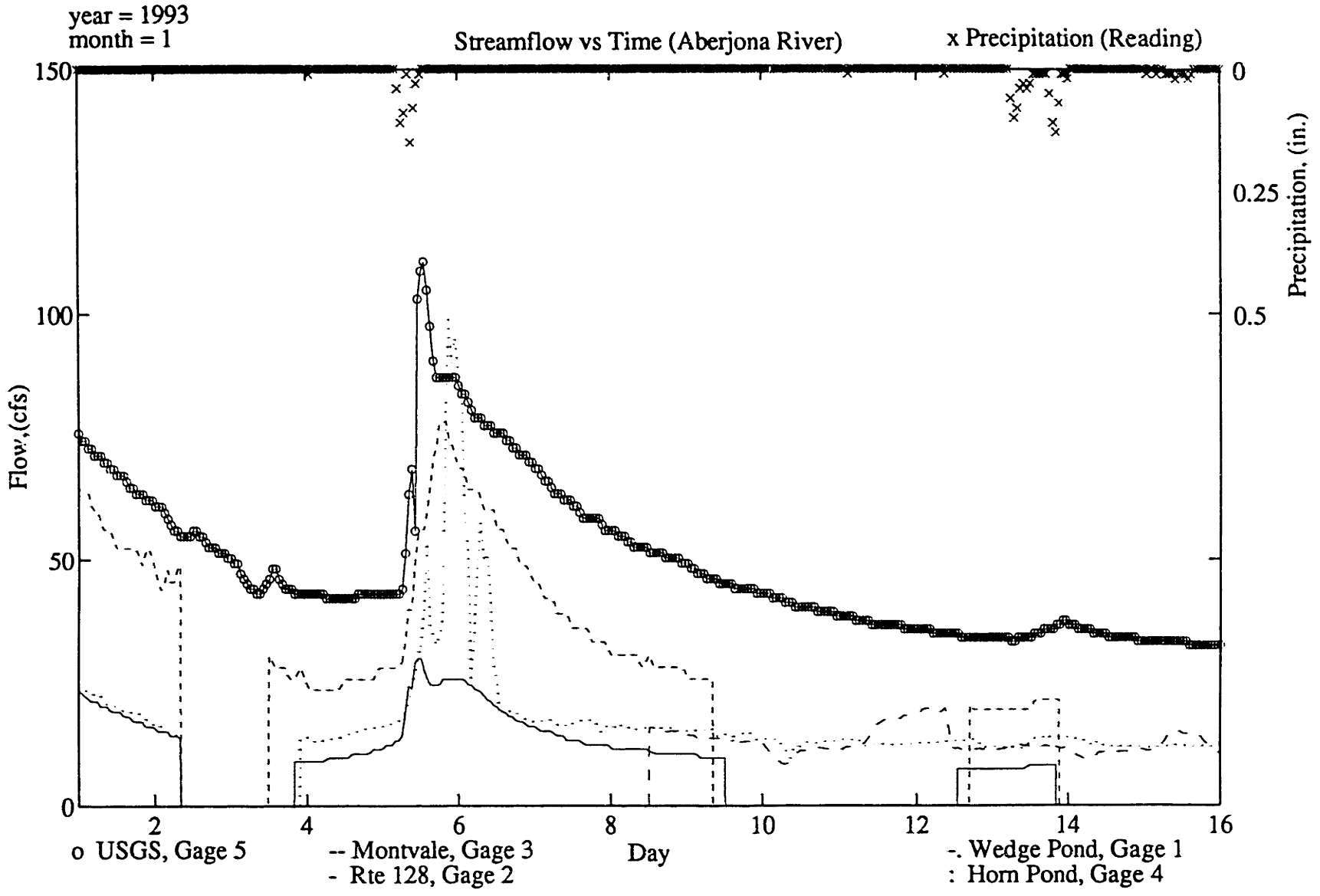
year = 1993
month = 1
Streamflow vs Time (Aberjona River)
x Precipitation (Reading)
150
100
50
0
0
0.25
0.5
Flow, (cfs)
Precipitation, (in.)
2
4
6
8
10
12
14
16
Day
o USGS, Gage 5
-- Montvale, Gage 3
- Rte 128, Gage 2
-. Wedge Pond, Gage 1
: Horn Pond, Gage 4

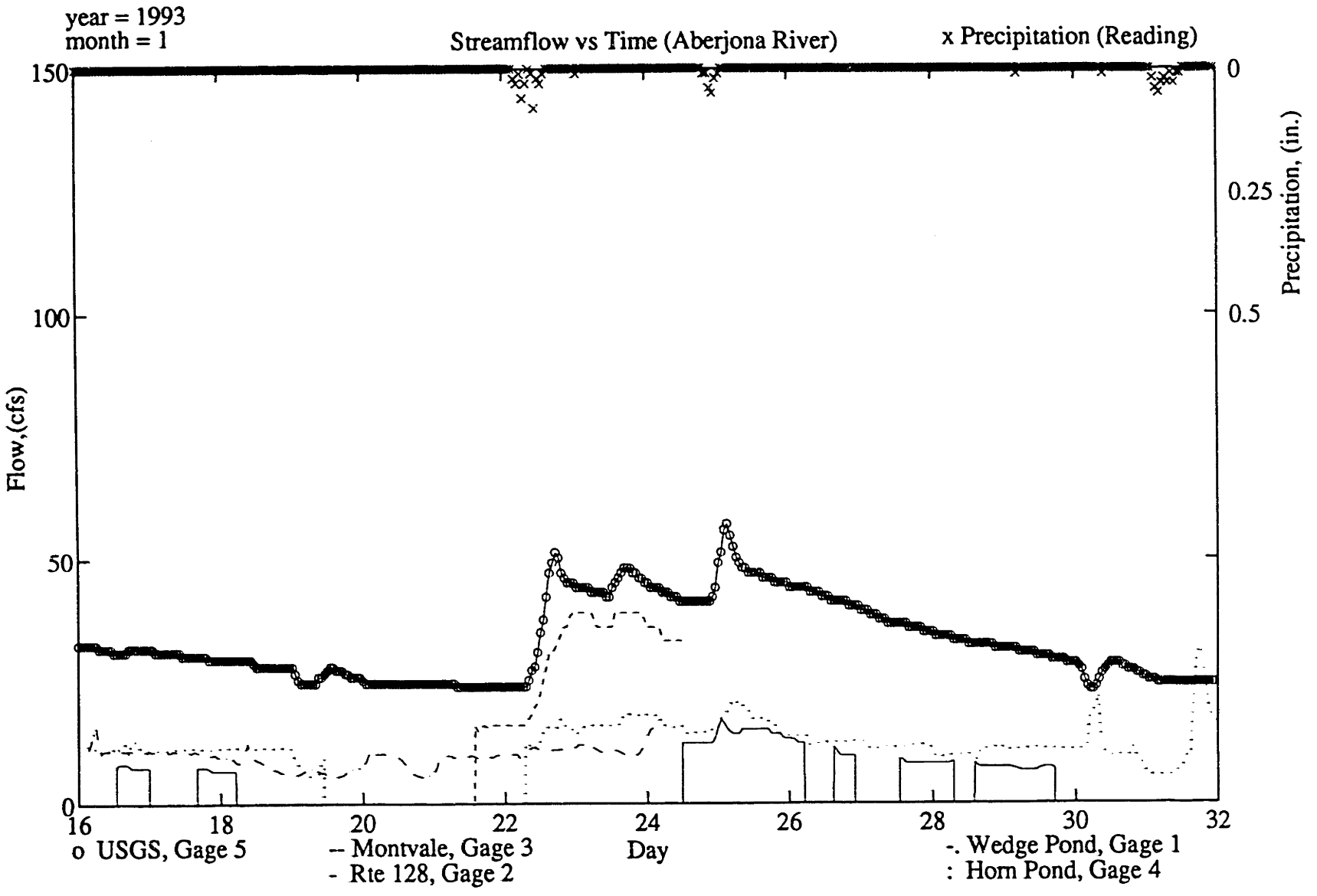
year = 1993
month = 1
Streamflow vs Time (Aberjona River)
x Precipitation (Reading)
150
100
50
0
Flow,(cfs)
0
0.25
0.5
Precipitation, (in.)
16
18
20
22
24
26
28
30
32
Day
o USGS, Gage 5
-- Montvale, Gage 3
- Rte 128, Gage 2
-. Wedge Pond, Gage 1
: Horn Pond, Gage 4

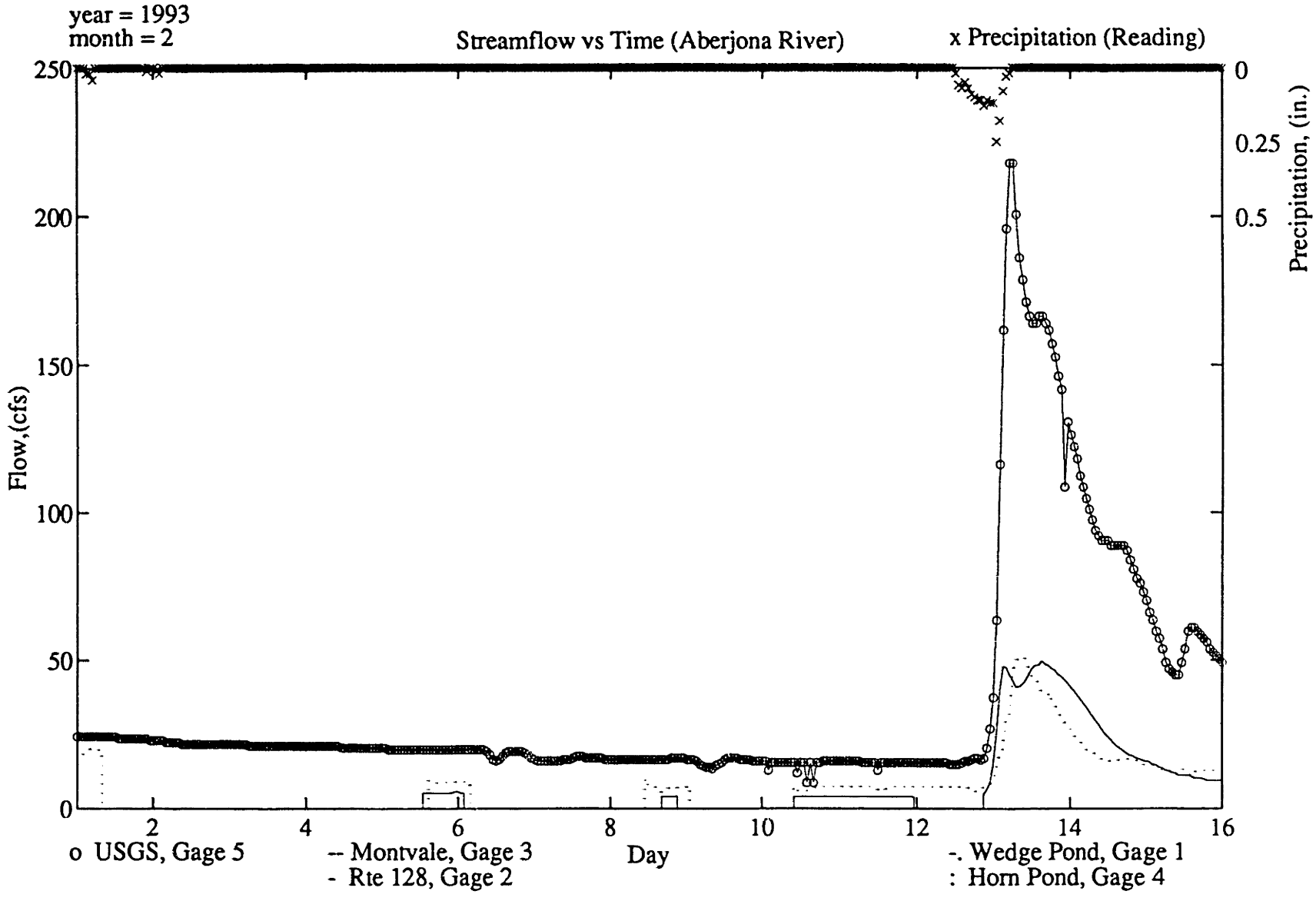
year = 1993
month = 2
Streamflow vs Time (Aberjona River)
x Precipitation (Reading)
Flow,(cfs)
Precipitation, (in.)
250
200
150
100
50
0
0
0.25
0.5
2
4
6
8
10
12
14
16
Day
o USGS, Gage 5
-- Montvale, Gage 3
- Rte 128, Gage 2
-. Wedge Pond, Gage 1
: Horn Pond, Gage 4

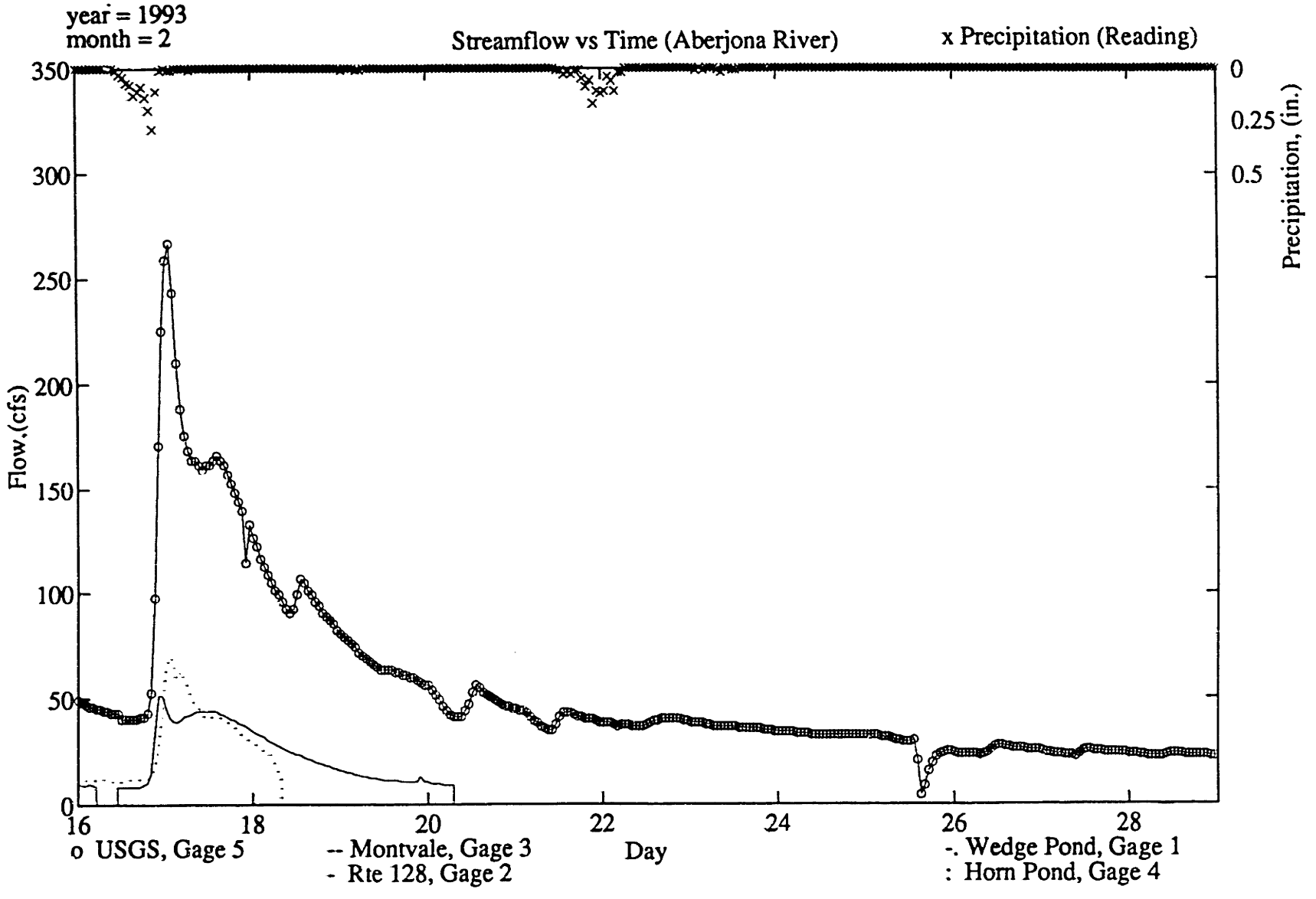
year = 1993
month = 2
Streamflow vs Time (Aberjona River)
x Precipitation (Reading)
Flow,(cfs)
Precipitation, (in.)
350
300
250
200
150
100
50
0
0
0.25
0.5
16
18
20
22
24
26
28
Day
o USGS, Gage 5
-- Montvale, Gage 3
- Rte 128, Gage 2
-. Wedge Pond, Gage 1
: Horn Pond, Gage 4

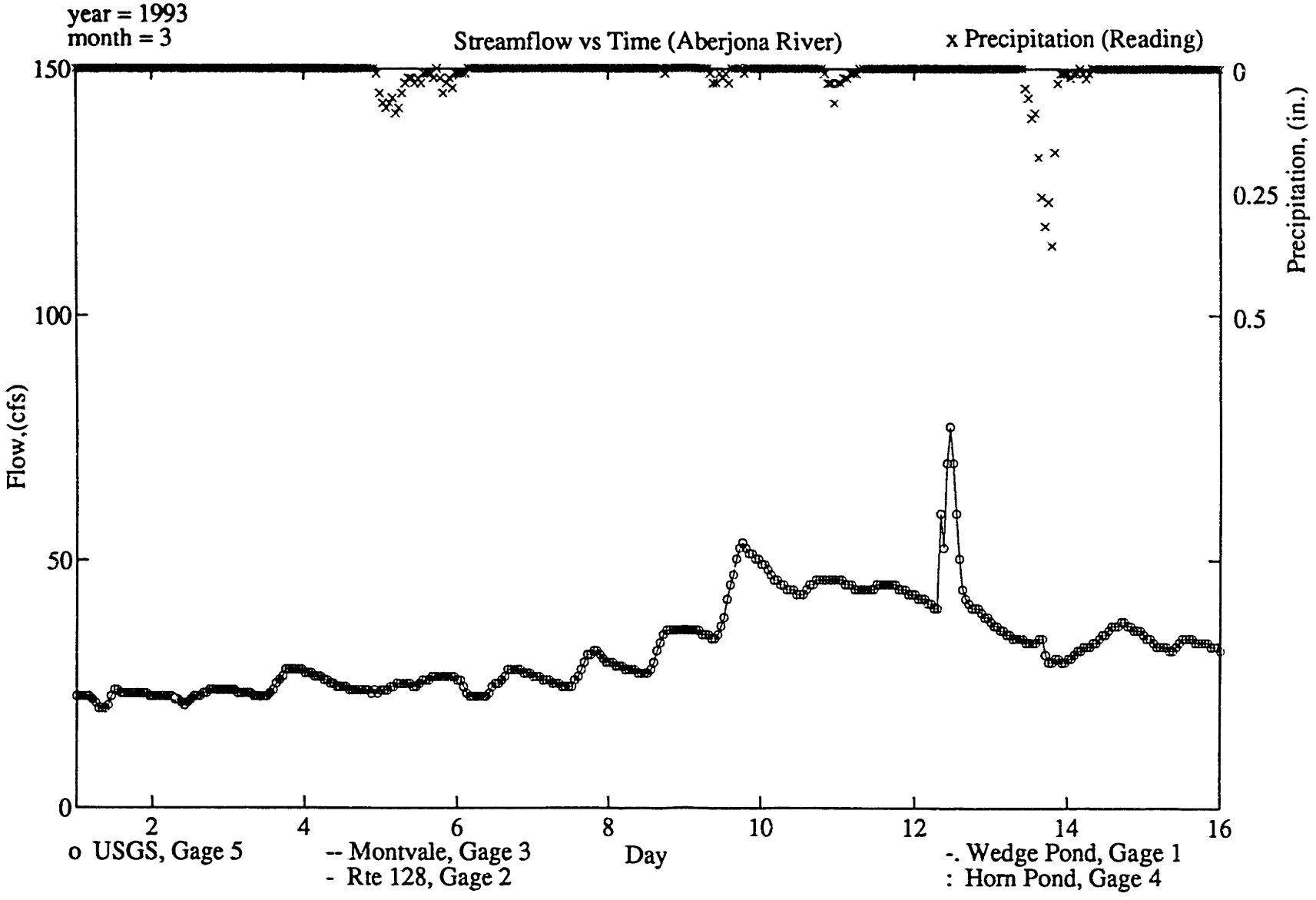
year = 1993
month = 3
Streamflow vs Time (Aberjona River)
x Precipitation (Reading)
150
100
50
0
0
0.25
0.5
Precipitation, (in.)
Flow,(cfs)
2
4
6
8
10
12
14
16
Day
o USGS, Gage 5
-- Montvale, Gage 3
- Rte 128, Gage 2
-. Wedge Pond, Gage 1
: Horn Pond, Gage 4

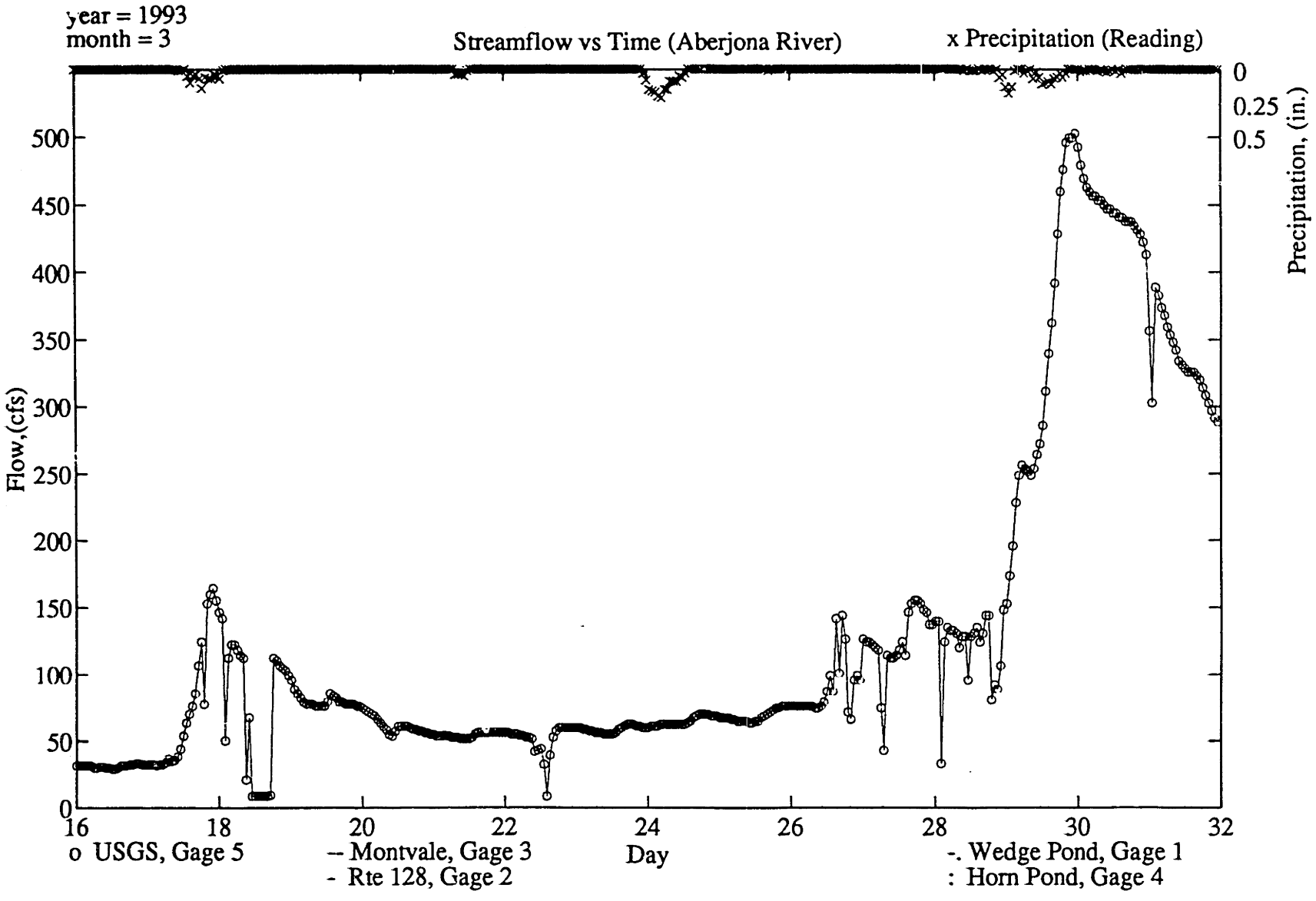
year = 1993
month = 3
Streamflow vs Time (Aberjona River)
x Precipitation (Reading)
Flow,(cfs)
Precipitation, (in.)
0
0.25
0.5
500
450
400
350
300
250
200
150
100
50
0
16
18
20
22
24
26
28
30
32
Day
o USGS, Gage 5
-- Montvale, Gage 3
- Rte 128, Gage 2
-. Wedge Pond, Gage 1
: Horn Pond, Gage 4

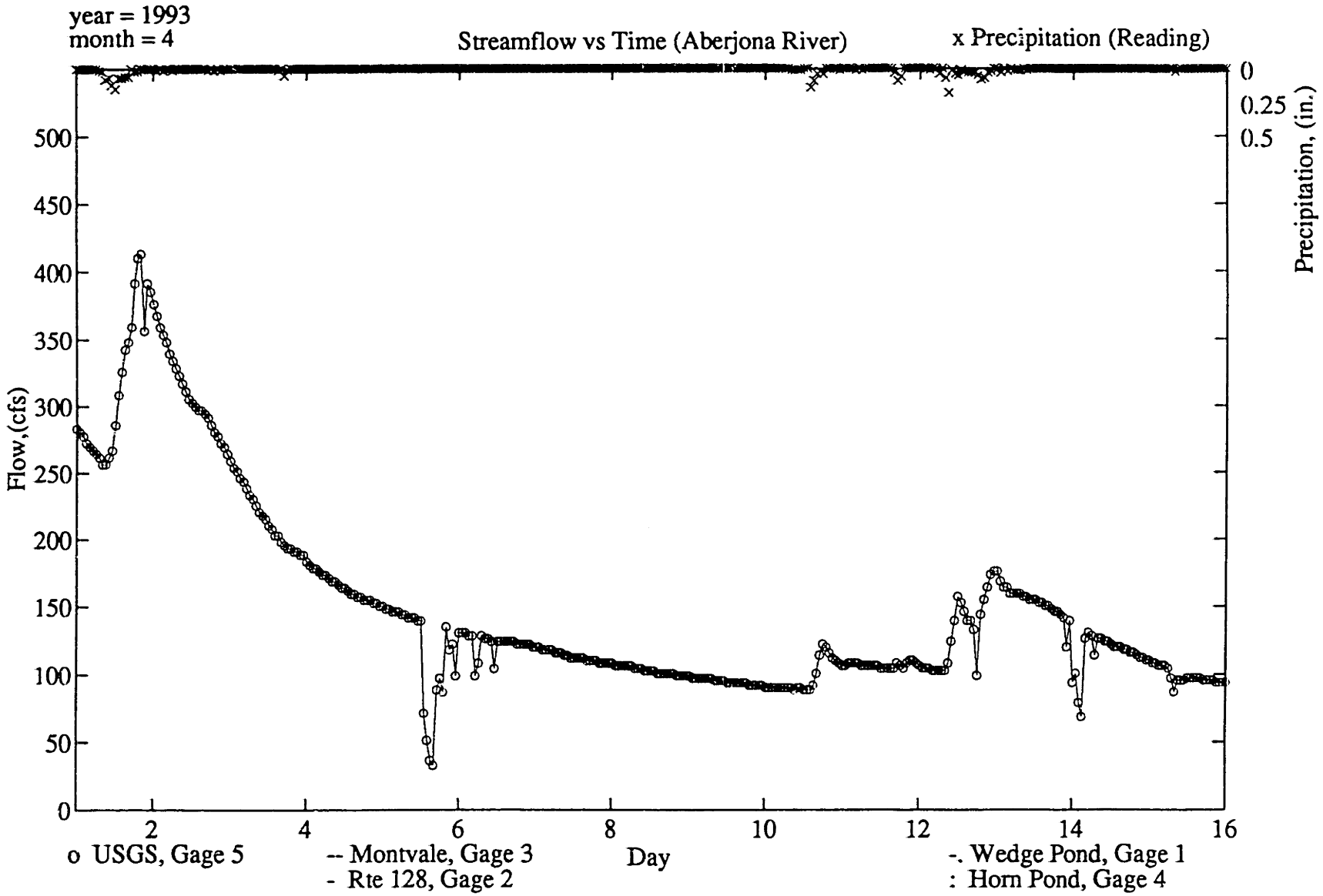
year = 1993
month = 4
Streamflow vs Time (Aberjona River)
x Precipitation (Reading)
Flow,(cfs)
Precipitation, (in.)
0
0.25
0.5
500
450
400
350
300
250
200
150
100
50
0
2
4
6
8
10
12
14
16
Day
o USGS, Gage 5
-- Montvale, Gage 3
- Rte 128, Gage 2
-. Wedge Pond, Gage 1
: Horn Pond, Gage 4

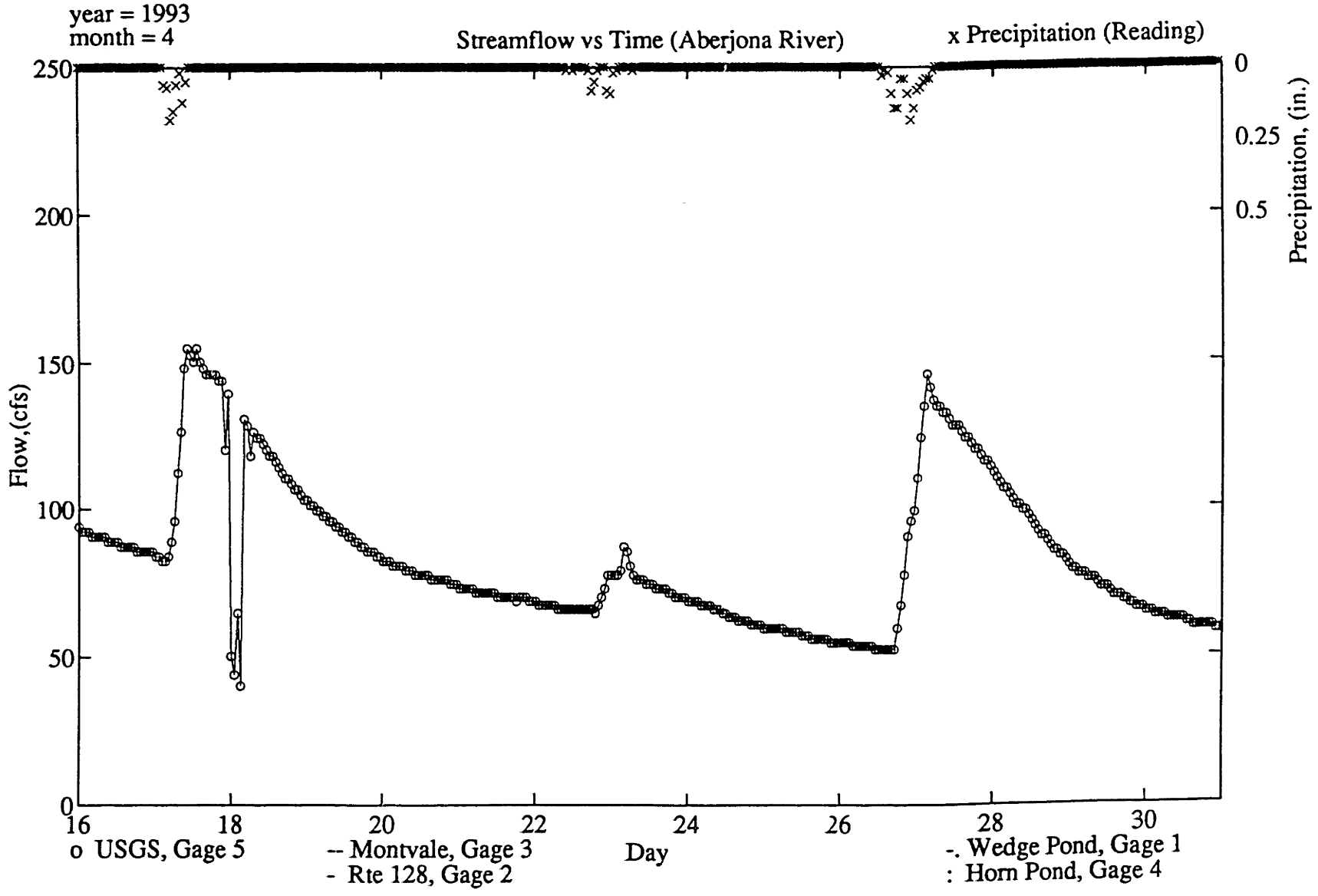
year = 1993
month = 4
Streamflow vs Time (Aberjona River)
x Precipitation (Reading)
250
200
150
100
50
0
Flow,(cfs)
0
0.25
0.5
Precipitation, (in.)
16
18
20
22
24
26
28
30
Day
o USGS, Gage 5
-- Montvale, Gage 3
- Rte 128, Gage 2
-. Wedge Pond, Gage 1
: Horn Pond, Gage 4

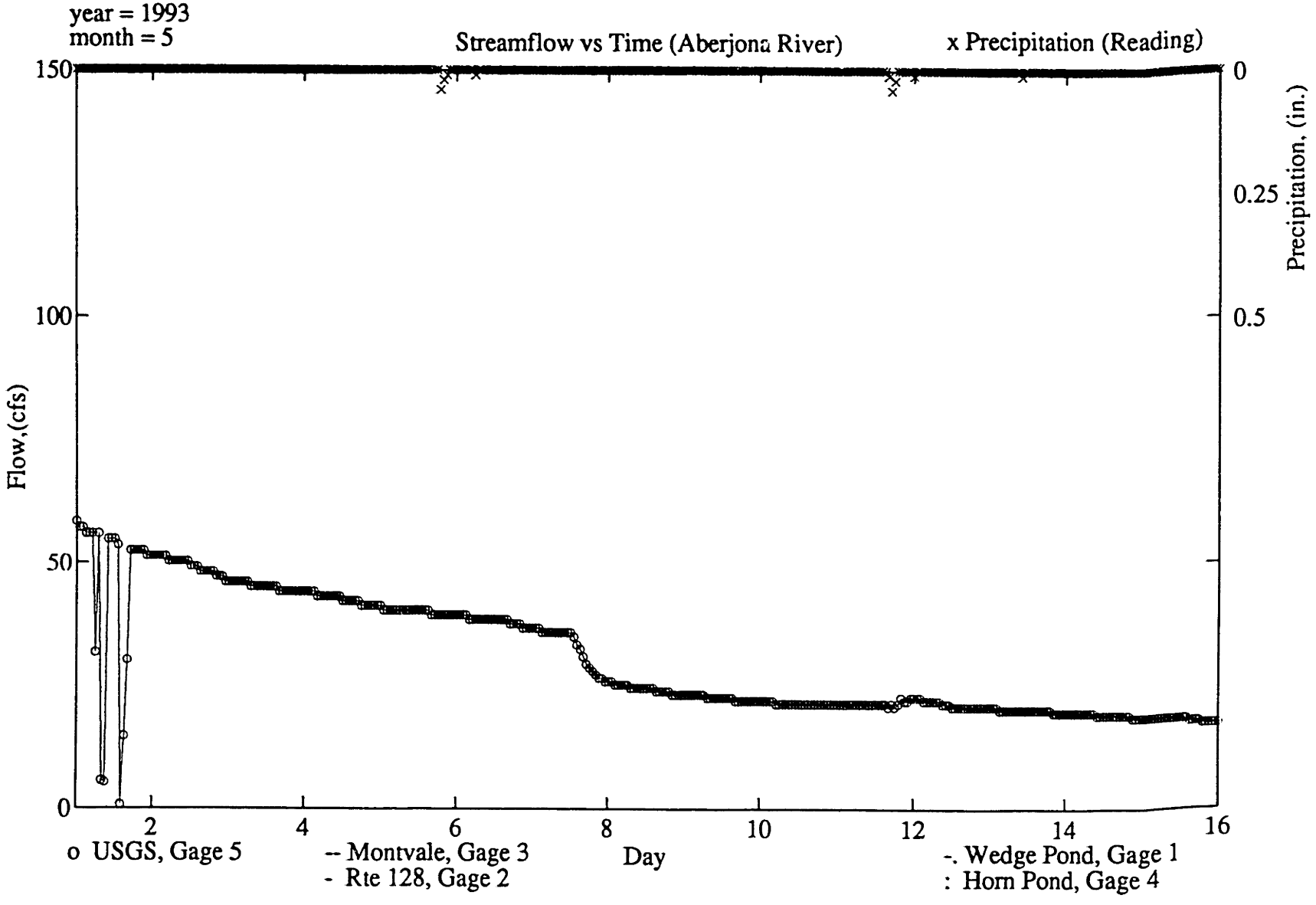
year = 1993
month = 5
Streamflow vs Time (Aberjona River)
x Precipitation (Reading)
150
100
50
0
Flow,(cfs)
0
0.25
0.5
Precipitation, (in.)
2
4
6
8
10
12
14
16
Day
o USGS, Gage 5
-- Montvale, Gage 3
- Rte 128, Gage 2
-. Wedge Pond, Gage 1
: Horn Pond, Gage 4

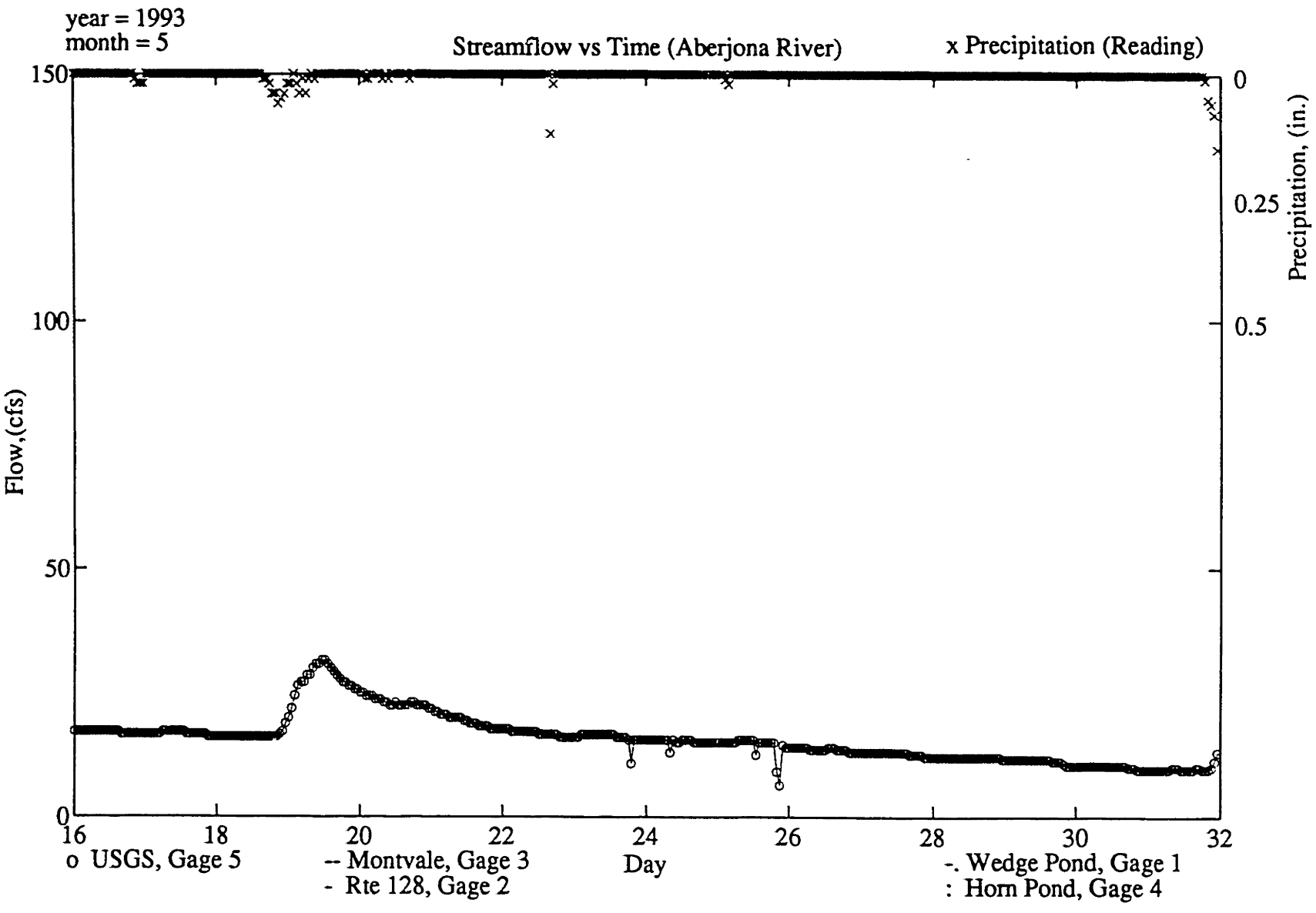
year = 1993
month = 5
Streamflow vs Time (Aberjona River)
x Precipitation (Reading)
150
100
50
0
Flow,(cfs)
0
0.25
0.5
Precipitation, (in.)
16
18
20
22
24
26
28
30
32
Day
o USGS, Gage 5
-- Montvale, Gage 3
- Rte 128, Gage 2
-. Wedge Pond, Gage 1
: Horn Pond, Gage 4

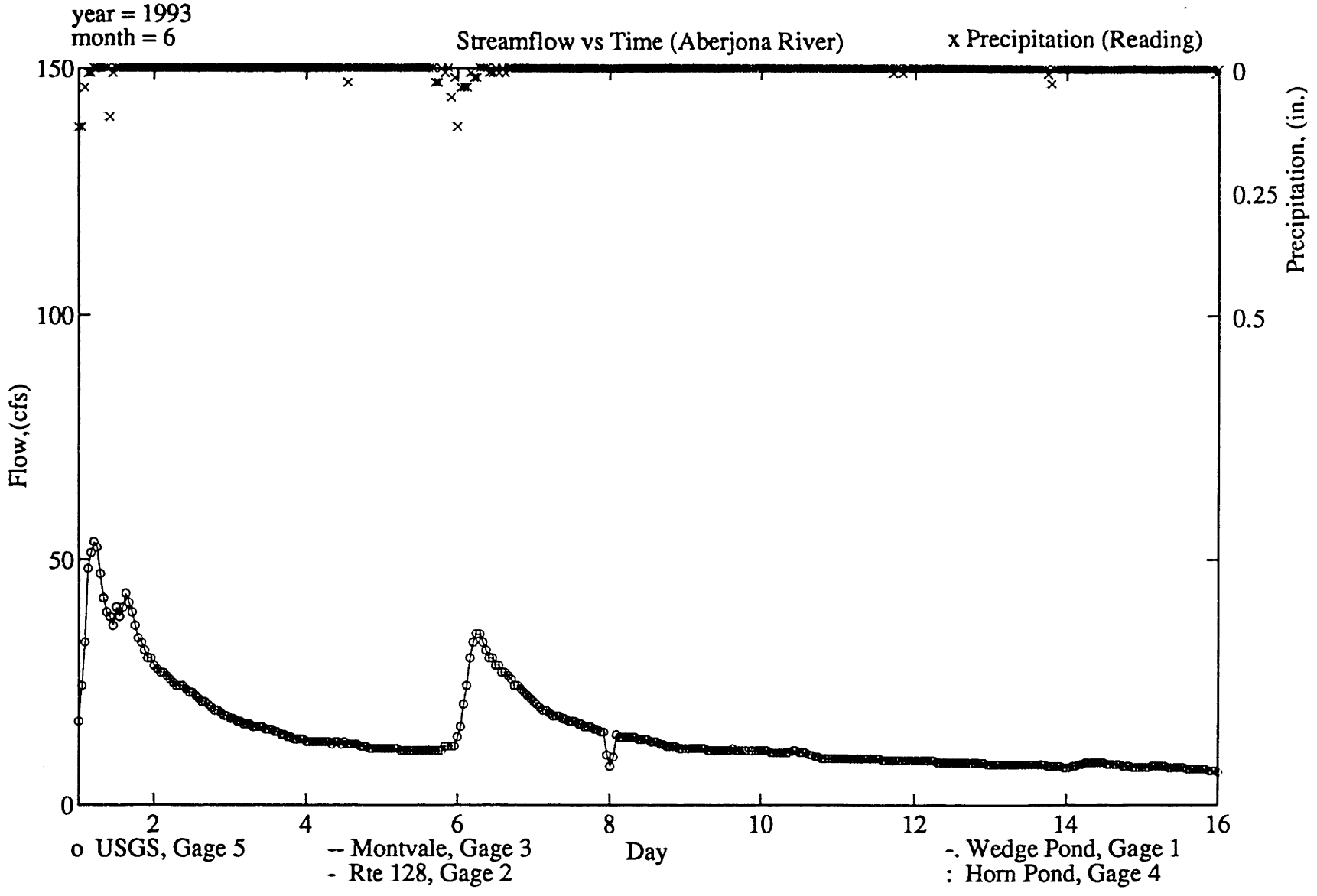
year = 1993
month = 6
Streamflow vs Time (Aberjona River)
x Precipitation (Reading)
150
100
50
0
0
0.25
0.5
Precipitation, (in.)
Flow,(cfs)
2
4
6
8
10
12
14
16
Day
o USGS, Gage 5
-- Montvale, Gage 3
- Rte 128, Gage 2
-. Wedge Pond, Gage 1
: Horn Pond, Gage 4

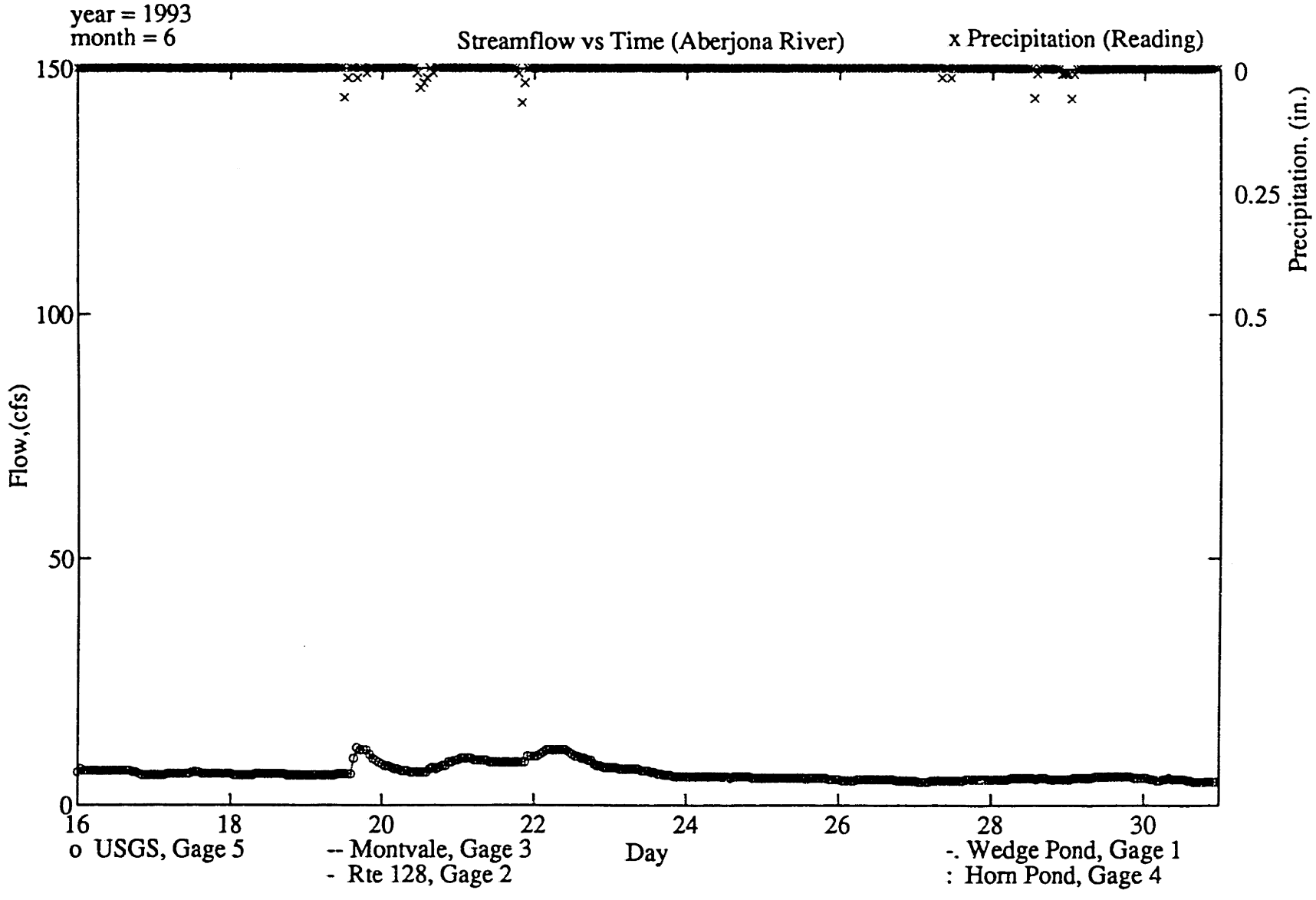
year = 1993
month = 6
Streamflow vs Time (Aberjona River)
x Precipitation (Reading)
150
100
50
0
Flow,(cfs)
0
0.25
0.5
Precipitation, (in.)
16
18
20
22
24
26
28
30
Day
o USGS, Gage 5
-- Montvale, Gage 3
- Rte 128, Gage 2
-. Wedge Pond, Gage 1
: Horn Pond, Gage 4

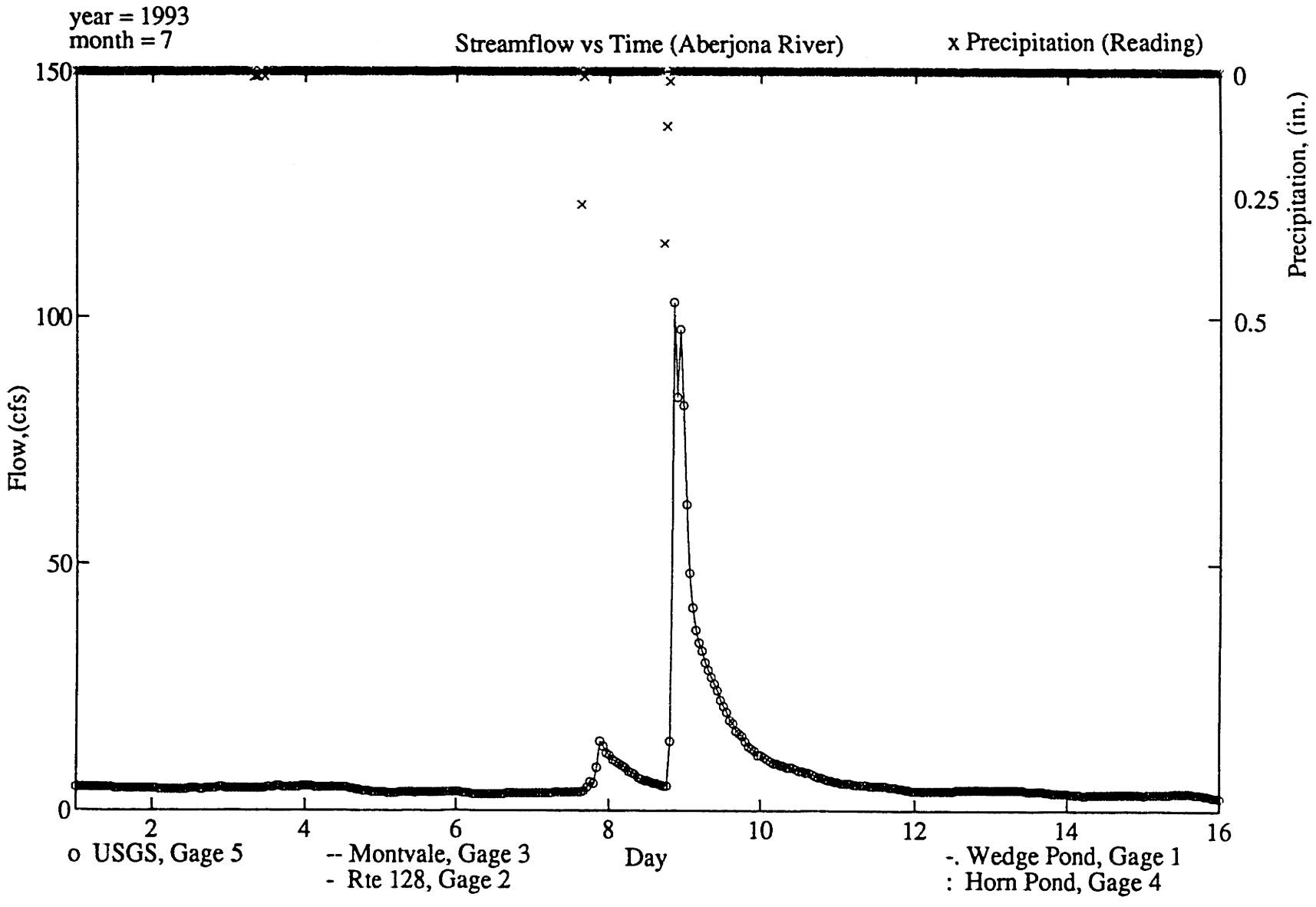
year = 1993
month = 7
Streamflow vs Time (Aberjona River)
x Precipitation (Reading)
150
100
50
0
0
0.25
0.5
Precipitation, (in.)
Flow,(cfs)
2
4
6
8
10
12
14
16
Day
o USGS, Gage 5
-- Montvale, Gage 3
- Rte 128, Gage 2
-. Wedge Pond, Gage 1
: Horn Pond, Gage 4

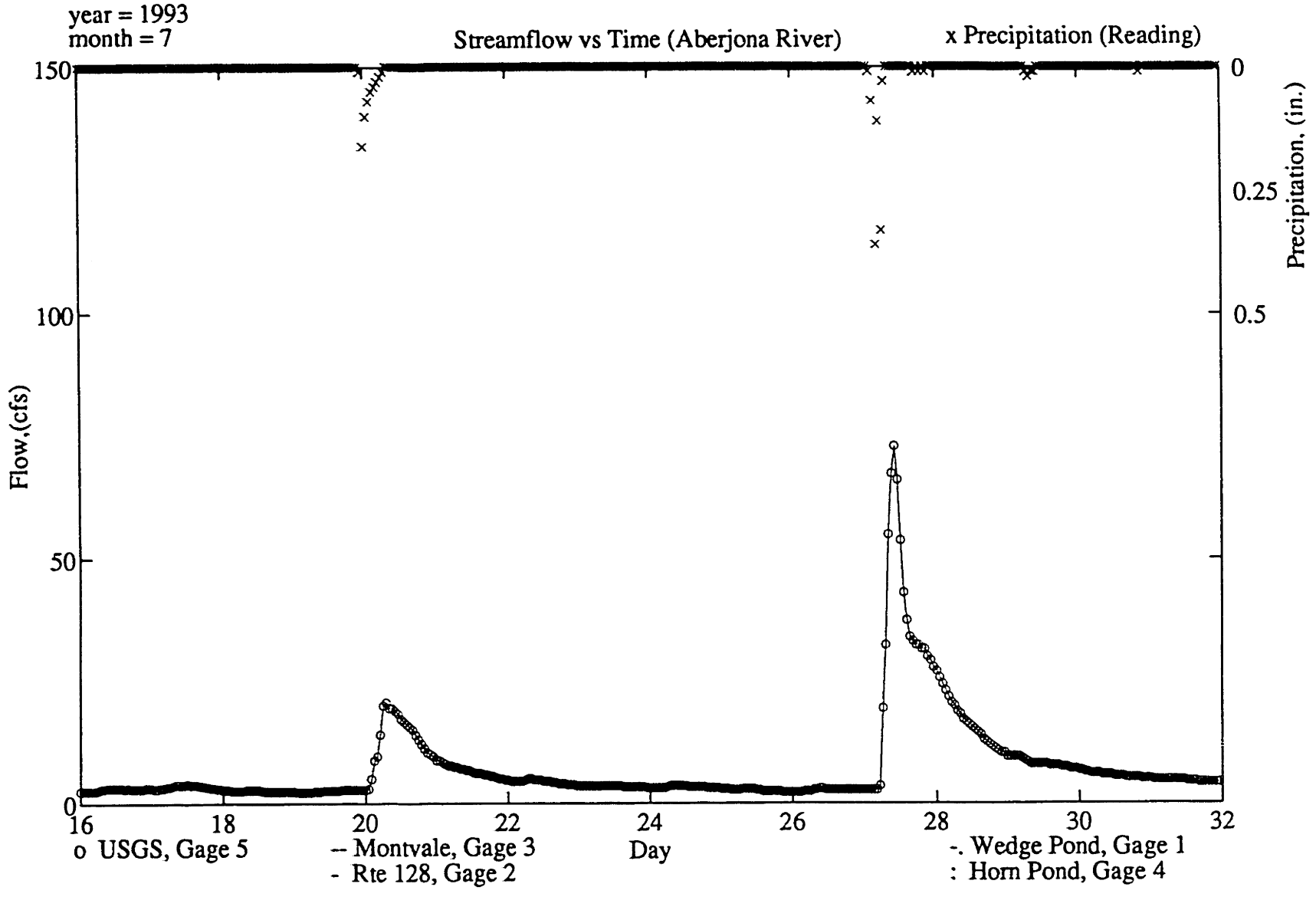
year = 1993
month = 7
Streamflow vs Time (Aberjona River)
x Precipitation (Reading)
150
100
50
0
Flow,(cfs)
0
0.25
0.5
Precipitation, (in.)
16
18
20
22
24
26
28
30
32
Day
o USGS, Gage 5
-- Montvale, Gage 3
- Rte 128, Gage 2
-. Wedge Pond, Gage 1
: Horn Pond, Gage 4

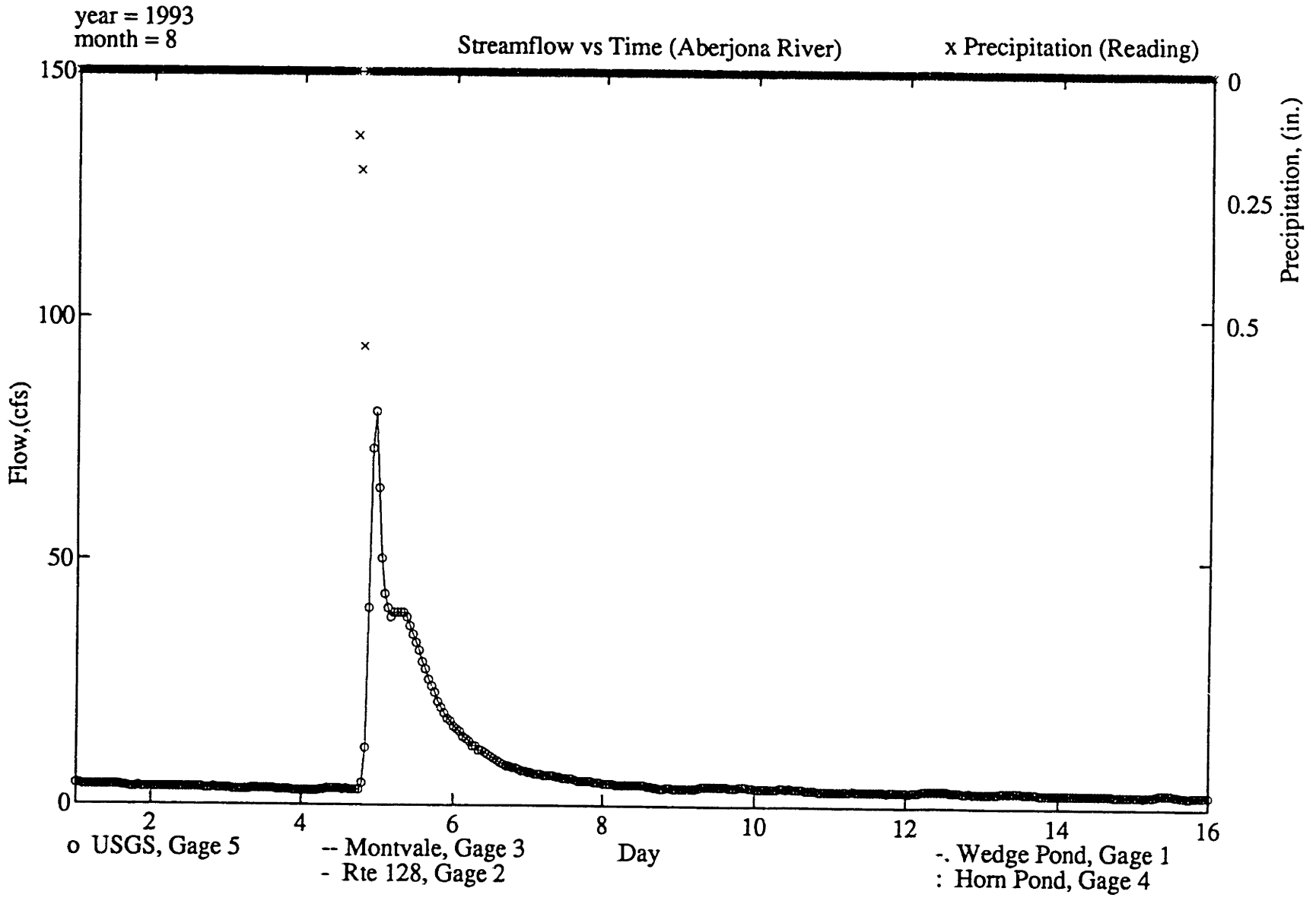
year = 1993
month = 8
Streamflow vs Time (Aberjona River)
x Precipitation (Reading)
150
100
50
0
Flow,(cfs)
0
0.25
0.5
Precipitation, (in.)
2
4
6
8
10
12
14
16
Day
o USGS, Gage 5
-- Montvale, Gage 3
- Rte 128, Gage 2
-. Wedge Pond, Gage 1
: Horn Pond, Gage 4

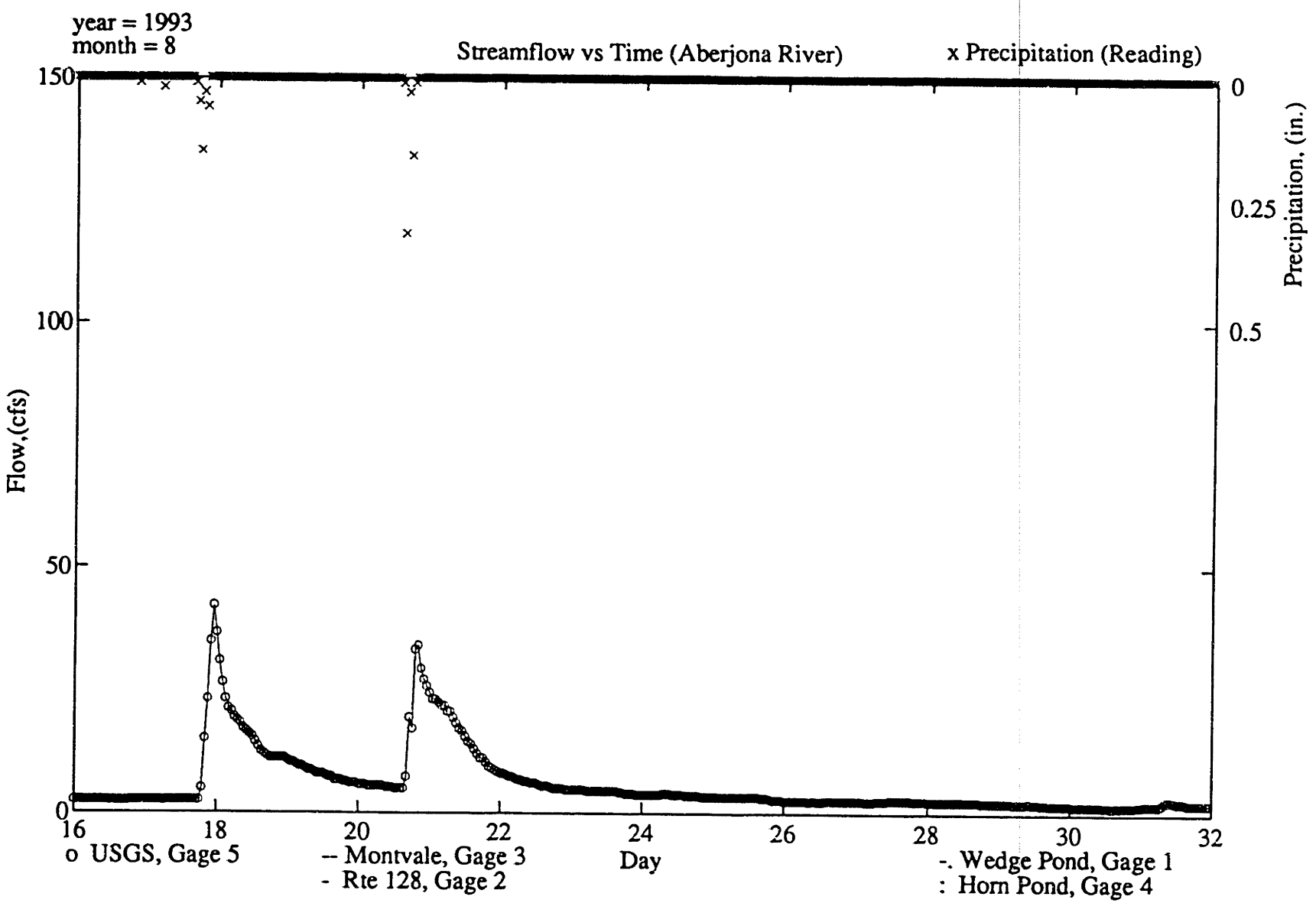
year = 1993
month = 8
Streamflow vs Time (Aberjona River)
x Precipitation (Reading)
150
100
50
0
Flow,(cfs)
0
0.25
0.5
Precipitation, (in.)
16
18
20
22
24
26
28
30
32
Day
o USGS, Gage 5
-- Montvale, Gage 3
- Rte 128, Gage 2
-. Wedge Pond, Gage 1
: Horn Pond, Gage 4

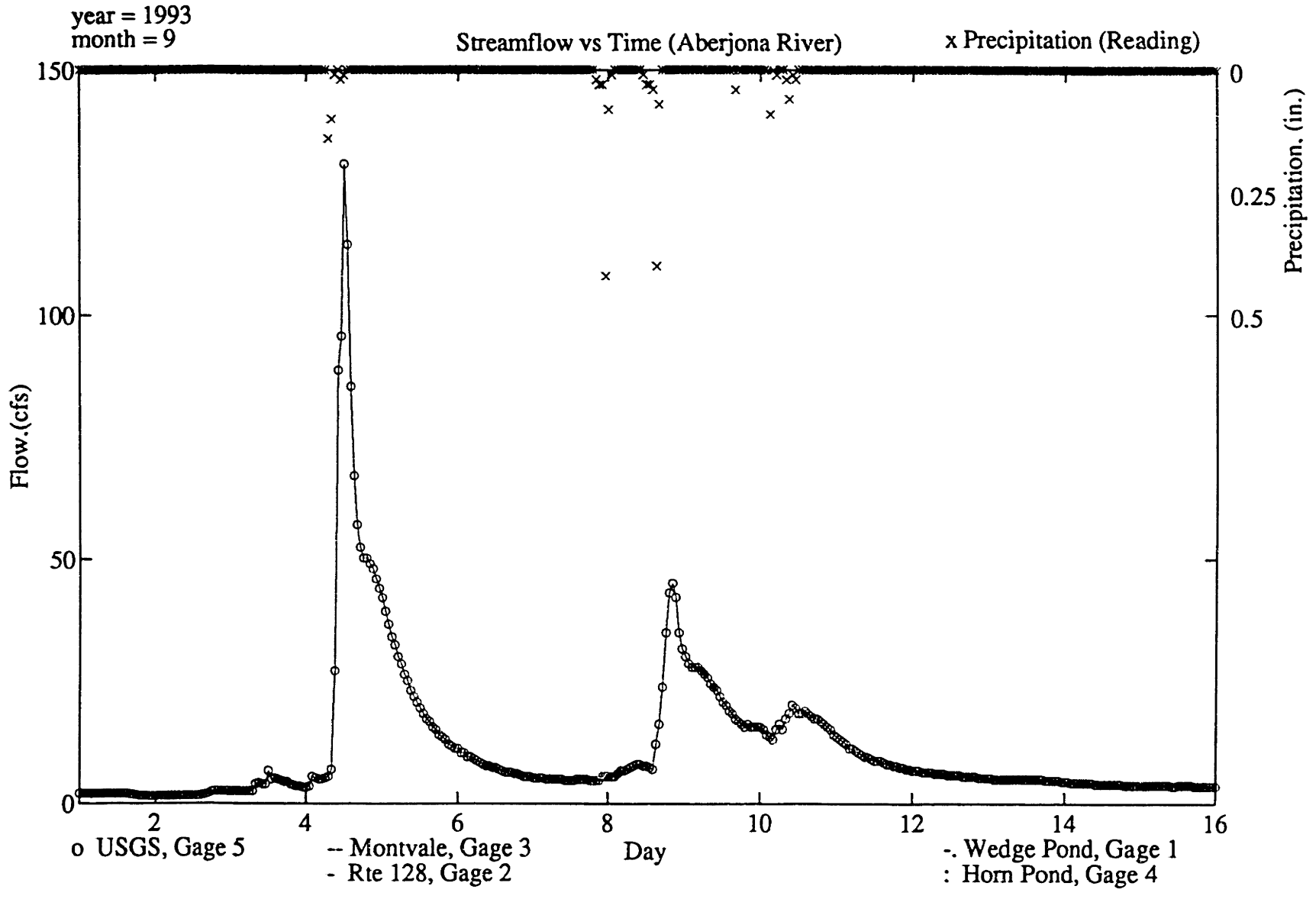
year = 1993
month = 9
Streamflow vs Time (Aberjona River)
x Precipitation (Reading)
150
100
50
0
0
0.25
0.5
Precipitation, (in.)
Flow,(cfs)
2
4
6
8
10
12
14
16
Day
o USGS, Gage 5
-- Montvale, Gage 3
- Rte 128, Gage 2
-. Wedge Pond, Gage 1
: Horn Pond, Gage 4

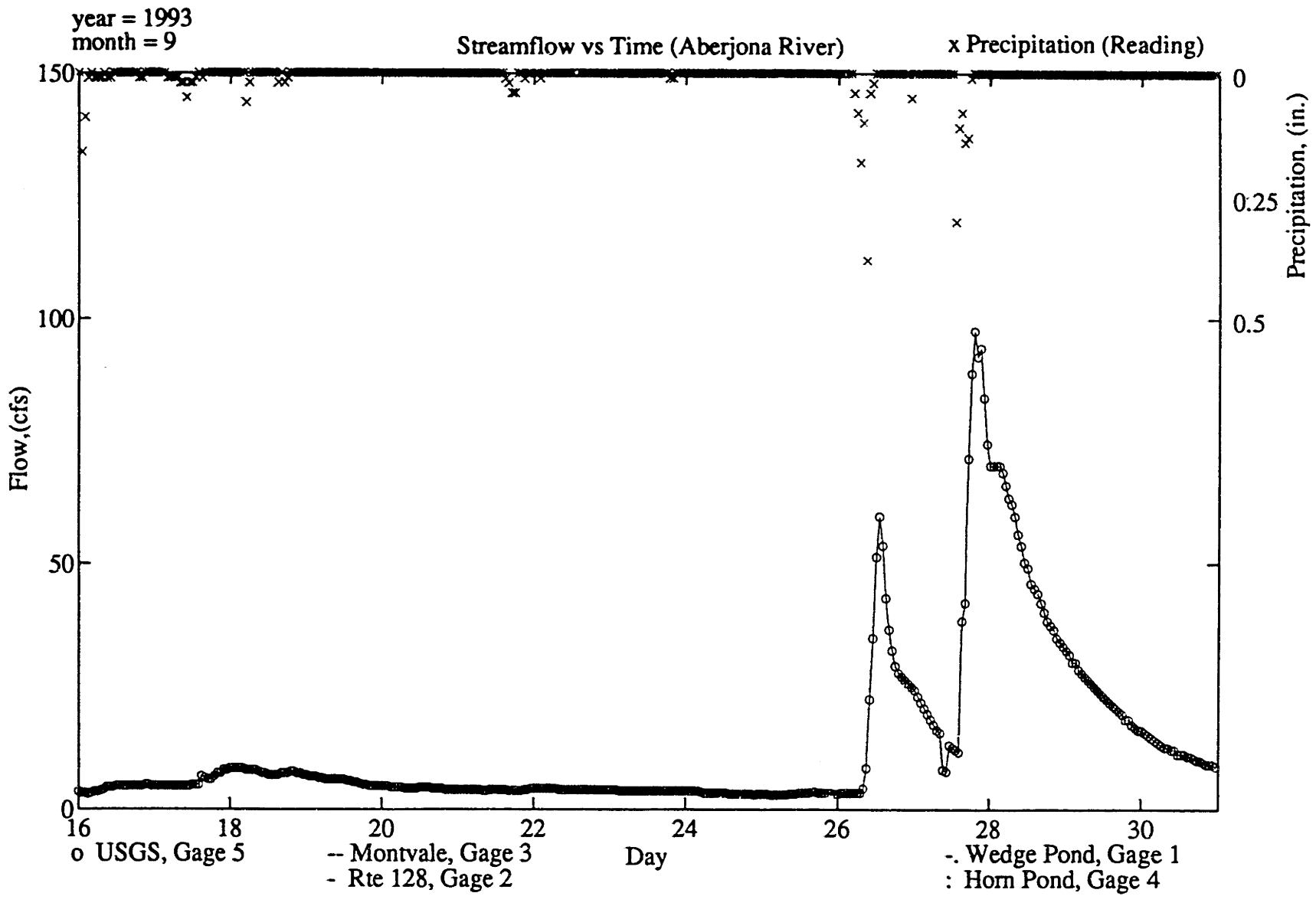
year = 1993
month = 9
Streamflow vs Time (Aberjona River)
x Precipitation (Reading)
150
100
50
0
0
0.25
0.5
Precipitation, (in.)
Flow,(cfs)
16
18
20
22
24
26
28
30
Day
o USGS, Gage 5
-- Montvale, Gage 3
- Rte 128, Gage 2
-. Wedge Pond, Gage 1
: Horn Pond, Gage 4

APPENDIX IV.C

Streamflow and Precipitation:
ASCII Format

AVAILABLE STREAMFLOW DATA

U.S.G.S. Station, Gage 5

Streamflow has been monitored at gage 5 by the United States Geological Survey (U.S.G.S) since 1939. Within this appendix, the following data are included: 1) daily and monthly streamflow for the entire period of record (upto Sept. 30, 1993), and 2) hourly data from January 1, 1987 to September 30, 1993. Paper copies of hourly stage data from 1980 to the present are available from the USGS. Data in digital form are also available for the prior two years of the request date. For hourly data prior to 1980, the record must be re-read manually from the original charts which are stored in the USGS archives.

M.I.T. Stations, Gages 1,2,3 & 4

Raw and processed streamflow data collected through the current study (January 1991 to January 1993) are included within this appendix. Data collected prior to this study (1987 to 1991) is available through Durant, 1991.

TIME CHANGE AND DATA REPORTING

In the vicinity of time changes (standard to daylight savings and vice versa) there may be at most a one hour discrepancy between the MIT gages and the USGS gage. Since the USGS station reports data on local time, they are forced to adjust their measurements by one hour after each time change. The USGS method for incorporating time changes is to prorate the 4 extra or missing 15 minute readings over a 6 week period after the time change. Every 1.5 weeks during the proration period one value is either added or deleted, such that each day has only 96 values or 24 hours worth of data.

The MIT data is also reported, for the most part, in local time. On a given day after the time change (within about a week) all the clocks in the field equipment were reset to local times. To assure that each day has 24 hours of data, either one hour of data was deleted or one hour of data was inserted (the inserted data was given as a negative value to indicate that it is missing) at the time when the clocks were reset.

ORGANIZATION OF STREAMFLOW DATA ON TAPE

Streamflow files (raw and processed data files) are included in ASCII format within the following sub-directory: /raw/gage. The amount of disk space needed to download all of this data is 18.4 Megabytes.

A description of each of the files is included in table IV.C-1. The time period covered by each file is indicated in the second line of the description column. For each set of 6 numbers, the first two numbers correspond to the year, the second two correspond to the month, and the last two correspond to the day. The data-format notation in the table corresponds to Fortran77.

Raw Streamflow Data

Within all the raw data files (?.da? files, where ? is a number) negative data values have been inserted for times when data is either missing or erroneous. The value of the negative number corresponds to a particular error code. (table IV.C-2) The determination of the error codes relied heavily on field notes and on the following assumptions:

1) Increases in flows are generally characterized by increases in depth and velocity. For example, a large increase in depth accompanied by a stable near zero velocity measurement, during freezing conditions, is indicative of water freezing in the air bubbler line and resulting in erroneously high depth readings. Similarly, an increase in depth accompanied by a decrease in velocity may be indicative of the probe being buried by river sediment, especially if on the following field trip a buried probe was noted.

2) Large fluctuations in readings which have no increasing or decreasing trend should be looked at with suspicion. A sudden drop in gage depth and velocity measurements followed by a sudden increase may be interpreted as a fluctuating power source. Additionally, a sudden drop in gage depth accompanied by a sudden zero velocity is indicative of probe dislodgement, especially if a dislodged probe is noted on the next maintenance trip. When a probe is dislodged, it tends to float toward the surface and its orientation is such that a zero velocity is recorded.

3) Simultaneous depth and velocity readings are never truly zero. Zero for both readings may

be indicative of a low battery voltage. Zero readings due to low battery voltage is especially evident when the frequency of zero depth/velocity readings increases in time until a charged battery is installed.

One should keep in mind that interpretation of erroneous data is somewhat subjective. As a result, there is the possibility that good data may have been identified as erroneous, while erroneous data may have not been identified as such.

Processed Streamflow Data

Hourly averaged data are provided within the ?.hour files. Negative data values in these files also correspond to missing or erroneous values. The value of the negative value within these files, however, has no special meaning.

ABBREVIATIONS

For the ?.hour data files
aved = average gage depth for the hourly time step (ft)
avev = average gage velocity for the hourly time step (ft/s)
elev = water surface elevation (ft. NGVD)
area = average cross-sectional area of flow (ft^2)
flow = streamflow (cfs)
counta = number of times gage attempted a reading within given hour
countd = number of times gage recorded a successful depth reading within a given hour
countv = number of times gage recorded a successful velocity reading within a given hour

File Name	Description	Format
1.da1	Raw Data for Gage 1 910115 to 910828	month,day,year,hour,minutes,gage depth(ft),gage velocity(ft/s) 5(1x,i2.2),3x,f8.3,7x,f8.3
1.da2	Raw Data for Gage 1 910828 to 920501	Same as above
1.da3	Raw Data for Gage 1 920501 to 930124	Same as above
2.da1	Raw Data for Gage 2 910101 to 911025	Same as above
2.da2	Raw Data for Gage 2 911025 to 920320	Same as above
2.da3	Raw Data for Gage 2 920320 to 930226	Same as above
3.da1	Raw Data for Gage 3 910303 to 920115	Same as above
3.da2	Raw Data for Gage 3 920115 to 920505	Same as above
3.da3	Raw Data for Gage 3 920505 to 930124	Same as above
4.da0	Raw Data for Gage 4 901116 to 910329	Same as above
4.da1	Raw Data for Gage 4 910524 to 911122	Same as above
4.da2	Raw Data for Gage 4 920131 to 921202	Samve as above
4.da3	Raw Data for Gage 4 921202 to 930226	Same as above
4.da8	Raw Data for Gage 4 901116 to 901231	Same as above
1.hour	Processed Data for Gage 1 910115 to 930124	year,month,day,hour,aved,avev,elev,area,flow, counta,countd,countv 4i2.2,2(3x,f7.3),3x,f13.3,2(3x,f9.3),6x,2(i2,1x),i2
2.hour	Processed Data for Gage 2 910110 to 930226	Same as above
3.hour	Processed Data for Gage 3 910303 to 930124	Same as above
4.hour	Processed Data for Gage 4 910101 to 930226	Same as above

Table IV.C-1: Raw and Processed Streamflow Data, File Descriptions

File Name	Description	Format
5.hour	Hourly Streamflow Data, Gage 5 871001 to 930930	year,month,day,hour,elev,flow 4i2.2,3x,f6.2,3x,f8.2
USGS.day	Daily Streamflow Data, Gage 5 390416 to 930930	year,month,day, daily average streamflow(cfs) 3i2.2,1x,f7.2
USGSMO. dat	Monthly Average Streamflow, Gage 5 May'39 to Sep'93	year,monthly average for Jan ,.. Dec (cfs) i4,12(4x,f4)

Table IV.C-1: con'd

Error Code	Description
-2.000	not correct
-3.000	not correct, sedimentation suspected
-4.000	not correct, freezing suspected
-5.000	dead battery
-6.000	battery faultering
-7.000	maintenance
-8.000	no data
-9.000	reverse flow
-10.000	plugged probe line
-11.000	gage flooded
-12.000	probe dislodged
-13.000	gage malfunctioning
-14.000	no data (during gage repair)
-15.000	not correct, probe blocked by debris
-16.000	power supply faultering
-17.000	depth reading unreasonably low, power supply malfunction
-18.000	incorrect data due to vandalism

Table IV.C-2: Error Codes Used in Streamflow Raw Data Files

AVAILABLE PRECIPITATION DATA

All precipitation data included within this appendix corresponds to the Reading stations[17]. Daily data is available in the Reading Town Records from 1899 to the present. Monthly values since 1899 are included in table IV.A-1 in appendix IV.A. Within this appendix the following records are included; 1) monthly and daily precipitation from 1957 to 1993, and 2) hourly precipitation from February 1981 to September 1993. The values reported in this appendix are a digital form (ASCII format) of the hand-recorded values as provided by Mr. Lautzenheiser of the N.C.D.C. However, within the original record minor discrepancies between daily and the sum of the hourly values have been noted but not corrected in the attached digital record. Furthermore, the July, August, and September 1982 hourly precipitation values were missing from the original record and are therefore omitted in the attached digital record.

ORGANIZATION OF PRECIPITATION DATA ON TAPE

All precipitation data are included in the following sub-directory; /raw/rain. The amount of disk space needed to download this data is 0.8 Megabytes. A description of each of the files is included in table IV.C-3. An explanation of the "description" and "format" columns is included in the previous section.

File Name	Description	Format
reading.dat	Hourly Precipitation at the Reading Station 810201 to 930930	year,month,day,hourly rainfall@ 1:00 ... 24:00 (inches) i4,1x,i2,1x,i2,24(1x,f4.2)
rain.day	Daily Precipitation at the Reading Station 570101 to 930930	year,month,day,daily precipitation (inches) 3i2.2,2x,f4.2
rain.monthly	Monthly Precipitation at the Reading Station Jan'57 to Sep'93	year,month,monthly rainfall (inches) i2.0,3x,i2.0,2x,f6.2

Table IV.C-3: Raw Precipitation Data, File Description

[17]The record at the Reading stations corresponds to two different station locations. For details, refer to sections III.2 and IV.1 in the main text.

APPENDIX IV.D

Suspended Sediment:
Detailed Data & Transport Capacity Computations

DETAILED SUSPENDED SEDIMENT DATA

This section includes: 1) a set of tables (tables IV.D-1 to IV.D-5) which summarize all the numerical values of the suspended sediment determinations, 2) additional plots of the USGS suspended sediment data (figures IV.D-1 to IV.D-3), 3) a discussion of suspended sediment components, and 4) a set of additional turbidity plots (figures IV.D-14 to IV.D-17).

TABLES SUMMARIZING VALUES OF SUSPENDED SEDIMENT ANALYSES

For the analyses, both 0.5 and 1.5 μm pore size filters were used. The pore size corresponding to the data is indicated in parenthesis within each column. Total and volatile suspended sediment concentrations were measured directly. Non-volatile concentrations were obtained by difference. Analytical methods are described in sections III.4 and appendix III.E.

fn:met1

Date/Time YR-MO-DA-HR	Flow (cfs)	SS Con (mg/L) (0.5um)	SS Conc (mg/L) (1.5um)	SS Flux (kg/hr) (0.5um)	SS Flux (kg/hr) (1.5um)	Volatile Conc (mg/l) (1.5um)	Volatile Conc (%) (1.5um)	Non-Volatile SS (mg/l) (1.5um)
Wedge Pond								
91041516	5.0							
91052015	1.3							
91052413	0.0		15.9		0.00			
91052814	2.7		1.5		0.41			
91060713	0.9		15.1		1.35	6.8	45	8.3
91071613	1.3	12.8	5.5	1.73	0.75	4.1	75	1.4
91082011	12.0	10.8	10.7	13.17	13.03	5.3	50	5.4
91082210*	10.2	5.1	3.3	5.25	3.42	1.7	52	1.6
91092110	1.6	8.9	10.7	1.40	1.69	10.6	99	0.1
91110210	10.2	8.3	7.9	8.61	8.24	6.8	86	1.1
91122111	6.6	5.9	5.3	3.95	3.54	2.9	55	2.4
92011512	11.2		4.4			1.8	41	2.6
92022214	8.9	3.2	3.5	2.92	3.18	2.1	60	1.4
92032915	17.4	6.5	6.2	11.60	11.01	2.6	42	3.6
92041814	14.0	8.4	8.1	11.95	11.58	3.3	41	4.8
92052209	1.4	7.6	2.8	1.04	0.39	1.4	50	1.4
92061115	7.0	3.5	3.4	2.51	2.42	2.1	62	1.3
92072316	1.2	7.3	6.0	0.85	0.70	4.8	80	1.2
92081314	0.9	11.4	6.0	1.01	0.53	5.0	83	1.0
92092714	5.2	7.1	7.1	3.77	3.76	5.8	82	1.3
92101213	13.3	6.2	7.3	8.44	9.88	5.1	70	2.2
92110114	1.2	4.7	4.6	0.57	0.55	3.1	68	1.5
92121715	17.9	4.0	4.4	7.37	8.03	3.1	71	1.3
93012511	12.7	3.1	3.2	4.00	4.13	1.8	57	1.4

* Reverse Flow Direction
BQ: Below Limit of Quantification

Table IV.D-1: Suspended Sediment Data for Wedge Pond Station, Gage #1

fn:met2

Date/Time YR-MO-DA-HR	Flow (cfs)	SS Conc (mg/L) (0.5um)	SS Conc (mg/L) (1.5um)	SS Flux (kg/hr) (0.5um)	SS Flux (kg/hr) (1.5um)	Volatile Conc (mg/l) (1.5um)	Volatile Conc (%) (1.5um)	Non-Volatile SS (mg/l) (1.5um)
Rte 128								
91032911	9.3							
91041512	4.9							
91053013	5.0		2.8		1.4			
91060710	4.0		5.3		2.2	2.1	40	3.2
91062010	6.3	5.7	4.4	3.7	2.8	2.3	52	2.1
91071610	3.1	6.3	5.7	2.0	1.8	2.9	50	2.8
91072610	0.8	6.3	4.4	0.5	0.4	1.9	42	2.5
91081310	2.2	7.3	6.5	1.6	1.5	3.0	46	3.5
91082110	31.0	7.9	7.3	24.9	23.1	3.5	48	3.8
91092114	8.2	9.1	7.1	7.6	5.9	4.7	66	2.4
91110213	12.7	7.7	4.5	10.0	5.8	3.1	70	1.4
91121711	8.0		3.5		2.9	2.4	69	1.1
92011509	13.0		4.8		6.3	1.8	38	3.0
92022209	7.2	6.7	4.7	4.9	3.5	1.5	32	3.2
92032915	17.6	5.2	3.9	9.3	7.0	1.9	47	2.1
92041809	13.8	3.6	3.6	5.0	5.1	1.8	49	1.8
92052215	4.4	6.5	5.7	2.9	2.6	2.4	43	3.3
92061110	7.1	9.0	7.8	6.5	5.7	3.2	42	4.6
92072309	2.0	11.2	11.0	2.2	2.2	4.5	40	6.6
92081309	2.6	7.6	7.4	2.0	1.9	3.1	42	4.3
92092709	10.4	8.5	6.7	9.0	7.1	3.3	50	3.4
92101209	16.4	6.7	6.4	11.2	10.7	3.0	47	3.4
92110109	2.4	4.8	5.4	1.2	1.3	2.7	49	2.7
92121710	18.3	12.6	13.7	23.5	25.5	4.7	34	9.0
93012509	14.6	4.8	1.3	7.1	1.9	1.9	(100)	(0)
93052509	5.3	6.2		3.3				

Table IV.D-2: Suspended Sediment Data for Route 128 Station, Gage #2

fn:met3

Date/Time YR-MO-DA-HR	Flow (cfs)	SS Conc (mg/L) (0.5um)	SS Conc (mg/L) (1.5um)	SS Flux (kg/hr) (0.5um)	SS Flux (kg/hr) (1.5um)	Volatile Conc (mg/l) (1.5um)	Volatile Conc (%) (1.5um)	Non-Volatile SS (mg/l) (1.5um)
Montvale								
91032914	16.1							
91041510	8.9							
91052011	9.8		3.30		3.30			
91052410	10.0		3.00		3.07			
91052811	17.8		5.60		10.16			
91053010	7.2		2.80		2.06			
91060715	5.4		2.00		1.10	1.15	58	0.85
91071616	4.2	2.40	1.90	1.03	0.81	1.29	68	0.61
91072616	2.2	1.70	1.20	0.38	0.27	0.80	69	0.40
91081316	3.1	2.70	1.70	0.86	0.54	1.11	65	0.59
91082016	88.0	7.94	6.40	71.19	57.38	2.97	46	3.43
91082016	88.0	8.23		73.79				
91082016	88.0	8.53		76.48				
91082215	26.1	3.87	2.40	10.30	6.39	1.48	62	0.92
91092113	16.6	4.81	4.60	8.12	7.77	3.93	85	0.67
91110212	26.3	3.20	1.90	8.56	5.08	1.90	100	0.00
91121713	16.5	8.08	8.00	13.61	13.47	3.77	47	4.23
92011510	31.1		5.70		18.05	2.34	41	3.36
92022211	8.7	6.85	5.90	6.06	5.22	2.56	43	3.34
92032909	34.8	3.71	2.50	13.13	8.85	1.85	74	0.65
92041810	31.0	3.51	3.00	11.09	9.47	1.45	48	1.55
92052214	8.6	5.75	4.80	5.06	4.23	2.20	46	2.60
92061112	12.3	8.15	5.50	10.17	6.86	2.44	44	3.06
92072311	3.9	4.22	3.20	1.68	1.27	1.55	48	1.65
92081310	6.9	4.29	2.80	3.03	1.98	1.39	50	1.41
92092711	20.9	6.91	5.60	14.73	11.94	2.80	50	2.80
92101210	26.7	12.98	12.60	35.33	34.30	5.68	45	6.92
92110110	4.5	3.23	2.10	1.49	0.97	1.23	59	0.87
92121711	30.9	18.71	8.00		25.18	3.30	41	4.70
93012510	11.9	3.70	3.20		3.88	1.45	45	1.75

Table IV.D-3: Suspended Sediment Data for Montvale Station, Gage #3

fn:met4

Date/Time YR-MO-DA-HR	Flow (cfs)	SS Conc (mg/L) (0.5um)	SS Conc (mg/L) (1.5um)	SS Flux (kg/hr) (0.5um)	SS Flux (kg/hr) (1.5um)	Volatile Conc (mg/l) (1.5um)	Volatile Conc (%) (1.5um)	Non-Volatile SS (mg/l) (1.5um)
Horn Pond								
91052416	5.7		1.40		0.81			
91052814	10.5		5.40		5.79			
91060712	4.7		11.10		5.34	6.73	61	4.37
91071611	2.0	4.50	4.80	0.92	0.98	2.48	52	2.33
91072613	1.2	1.20	1.20	0.15	0.15	0.87	73	0.33
91081313	1.6	3.70	2.60	0.58	0.41	2.08	80	0.52
91082013	21.6	20.60	19.60	45.33	43.13	7.93	40	11.67
91082211	9.6	4.57	3.90	4.46	3.81	2.90	74	1.00
91092111	4.5	5.95	6.70	2.70	3.04	5.61	84	1.09
92022213	7.5	2.24	1.50	1.72	1.15	0.77	51	0.73
92032914	16.4	4.70	4.70	7.85	7.85	2.16	46	2.54
92041812	15.0	2.05	1.90	3.12	2.89	1.02	54	0.88
92052211	5.1	5.11	3.70	2.67	1.93	1.71	46	1.99
92061114	6.1	3.54	3.60	2.19	2.23	2.22	62	1.39
92072313	2.6	3.10	2.70	0.81	0.70	1.91	71	0.79
92081312	3.2	2.39	2.40	0.78	0.78	1.74	73	0.66
92092712	9.1	12.25	11.50	11.29	10.60	3.95	34	7.55
92101212	17.9	10.14	9.60	18.49	17.51	3.83	40	5.77
92110112	3.3	0.77	0.60	0.26	0.20	0.77	(100)	(0)
92121712	44.1	2.41	2.10	10.83	9.44	1.16	55	0.94
93012511	20.1	2.80	2.60	5.73	5.32	1.23	47	1.37

BQ: Below Limit of Quantification

Table IV.D-4: Suspended Sediment Data for Horn Pond Station, Gage #4

fn:met5

Date/Time YR-MO-DA-HR	Flow (cfs)	SS Conc (mg/L) (0.5um)	SS Conc (mg/L) (1.5um)	SS Flux (kg/hr) (0.5um)	SS Flux (kg/hr) (1.5um)	Volatile Conc (mg/l) (1.5um)	Volatile Conc (%) (1.5um)	Non-Volatile SS (mg/l) (1.5um)
USGS								
91052415	12.1		3.40		4.2			
91052812	18.8		5.40		10.3			
91060714	26.7		1.80		4.9	0.95	53	0.85
91062012	13.5	4.80	4.40	6.6	6.1	2.58	59	1.82
91071615	6.1	2.50	2.20	1.6	1.4	1.64	75	0.56
91072615	3.1	1.30	0.80	0.4	0.3	0.55	69	0.25
91081314	4.3	2.00	1.80	0.9	0.8	1.42	79	0.38
91082009	139.5	9.95	8.55	141.4	121.5	3.57	42	4.98
91082114	95.7	7.42	6.90	72.4	67.3	3.16	46	3.74
91082209	9.2	7.77	4.50	7.3	4.2	2.35	52	2.15
91082209	12.6	8.10		10.4				
91082209	14.4	9.20		13.5				
91092109	26.2	3.72	2.90	9.9	7.7	3.10	(100)	(0)
91110209	45.5	4.34	3.90	20.1	18.1	2.96	76	0.94
91122109	32.4	4.95	4.40	16.3	14.5	2.47	56	1.93
92011513	45.0		4.40		20.2	1.46	33	2.94
92022215	23.0	3.45	3.00	8.1	7.0	1.22	41	1.78
92032912	57.2	4.28	3.60	24.9	21.0	1.63	45	1.97
92041815	49.0	4.55	4.30	22.7	21.5	1.90	44	2.40
92052208	12.6	4.23	3.80	5.4	4.9	1.89	50	1.91
92061117	22.4	4.48	4.00	10.2	9.1	1.96	49	2.04
92072315	5.8	1.75	1.50	1.0	0.9	1.05	70	0.45
92072922	74.4	34.3		3.5				
92081008	35.6	5.6		20.3				
92081010	34.9	5.0		17.8				
92081012	32.4	4.6		15.2				
92081014	30.8	4.4		13.8				
92081016	28.5	4.4		12.8				
92081018	27.1	4.9		13.5				
92081020	25.0	4.6		11.7				
92081022	23.7	5.1		12.3				
92081100	22.4	4.6		10.5				
92081102	20.6	5.5		11.5				
92081104	19.4	4.9		9.7				
92081315	8.8	2.14	2.10	1.9	1.9	1.43	68	0.67

BQ: Below Limit of Quantification

Table IV.D-5: Suspended Sediment Data for USGS Station, Gage #5

Date/Time YR-MO-DA-HR	Flow (cfs)	SS Conc (mg/L) (0.5um)	SS Conc (mg/L) (1.5um)	SS Flux (kg/hr) (0.5um)	SS Flux (kg/hr) (1.5um)	Volatile Conc (mg/l) (1.5um)	Volatile Conc (%) (1.5um)	Non-Volatile SS (mg/l) (1.5um)
92081801	75.9	17.1		132.4				
92081802	144.0	60.3		885.2				
92081803	159.5	50.4		819.5				
92081804	196.7	61.3		1229.0				
92081805	222.7	69.4		1575.7				
92081806	202.9	42.0		868.5				
92081807	196.7	32.2		645.6				
92081808	178.5	25.5		463.9				
92081809	168.9	22.4		385.7				
92081810	164.1	20.5		343.0				
92081811	161.8	23.0		379.4				
92081812	166.4	21.5		364.7				
92081813	159.5	20.3		330.1				
92081814	157.2	19.2		307.7				
92081815	152.7	17.7		275.6				
92081816	148.0	17.4		262.5				
92081817	144.0	14.9		218.7				
92081818	139.5	14.2		201.9				
92081819	135.1	12.6		173.5				
92081820	130.8	13.0		173.3				
92081821	126.5	11.9		153.5				
92081822	122.4	10.9		136.0				
92081823	118.3	10.4		125.5				
92081900	114.4	10.4		121.3				
92092715	28.5	4.14	3.60	12.0	10.5	2.03	56	1.57
92101215	48.1	6.43	6.30	31.5	30.9	3.43	54	2.87
92110115	7.4	2.86	2.00	2.2	1.5	1.36	68	0.64
92112305	99.3	42.7		432.3				
92112307	139.5	42.8		608.6				
92112308	159.5	48.0		780.5				
92112407	77.4	17.9		141.3				
92121119	42.1	32.4		139.0				
92121120	52.5	36.4		195.0				
92121121	60.9	31.8		197.3				
92121122	99.3	45.2		457.6				
92121123	135.1	46.2		636.2				
92121200	157.2	50.5		809.4				
92121201	171.2	51.4		897.0				
92121202	196.7	47.3		948.4				
92121203	200.5	45.2		923.6				
92121204	207.7	41.8		885.1				
92121205	215.1	40.4		886.0				
92121206	212.7	35.5		769.6				
92121207	210.2	30.1		644.9				
92121208	200.5	26.1		533.3				
92121209	191.0	19.6		381.6				
92121210	188.5	16.1		309.3				
92121216	159.5	8.8		143.1				
92121217	152.7	7.8		121.4				
92121218	150.5	7.2		110.5				

BQ: Below Limit of Quantification

Table IV.D-5: con'd

fn:met5

Date/Time YR-MO-DA-HR	Flow (cfs)	SS Conc (mg/L) (0.5um)	SS Conc (mg/L) (1.5um)	SS Flux (kg/hr) (0.5um)	SS Flux (kg/hr) (1.5um)	Volatile Conc (mg/l) (1.5um)	Volatile Conc (%) (1.5um)	Non-Volatile SS (mg/l) (1.5um)
92121713	82.2	15.30	14.20	128.1	118.9	5.99	42	8.21
93012513	47.1	7.40	7.10	35.5	34.0	2.53	36	4.57
93032614	87.1	23.3		206.9				
93032615	141.7	19.2		277.3				
93032616	101.1	21.8		224.7				
93032617	144.0	21.3		312.7				
93032618	126.5	22.6		291.4				
93032619	71.5	20.2		147.2				
93032620	66.0	15.8		106.3				
93032910	264.2	35.5		956.1				
93032911	272.2	21.1		585.5				
93032912	285.8	25.4		740.0				
93032913	311.3	34.9		1107.5				
93032914	339.5	59.1		2045.4				
93032915	362.2	55.9		2064.0				
93032916	391.7	70.7		2823.1				
93032917	428.3	82.0		3580.2				
93032918	459.8	81.5		3820.1				
93032919	476.0	86.4		4192.5				
93032920	495.7	76.9		3885.9				
93032921	499.1	73.8		3754.8				
93032922	499.1	62.2		3164.6				
93032923	502.4	61.4		3144.6				
93033000	492.4	51.3		2575.0				
93033001	479.2	42.1		2056.6				
93033002	469.5	26.4		1263.5				
93033008	453.4	18.9		873.6				
93033119	308.4	9.9		311.2				
93040116	348.0	39.9		1415.5				
93040117	359.4	19.5		714.4				
93040118	391.7	29.0		1158.0				
93040119	410.0	39.0		1630.0				
93040120	413.0	30.8		1296.7				
93040121	356.5	18.1		657.8				
93040122	391.7	15.4		614.9				
93040123	385.7	10.5		412.8				
93040200	376.8	13.9						
93040217	291.4	5.7		169.3				
93052509	15.6	5.20		8.2				

BQ: Below Limit of Quantification

Table IV.D-5: con'd

ADDITIONAL PLOTS OF SUSPENDED SEDIMENT DATA COLLECTED AT THE USGS

This section also includes additional plots for the suspended sediment data collected at the USGS station (figures IV.D-1 to IV.D-3). These plots provide a more detailed identification of the data points presented in figure IV.3-11.

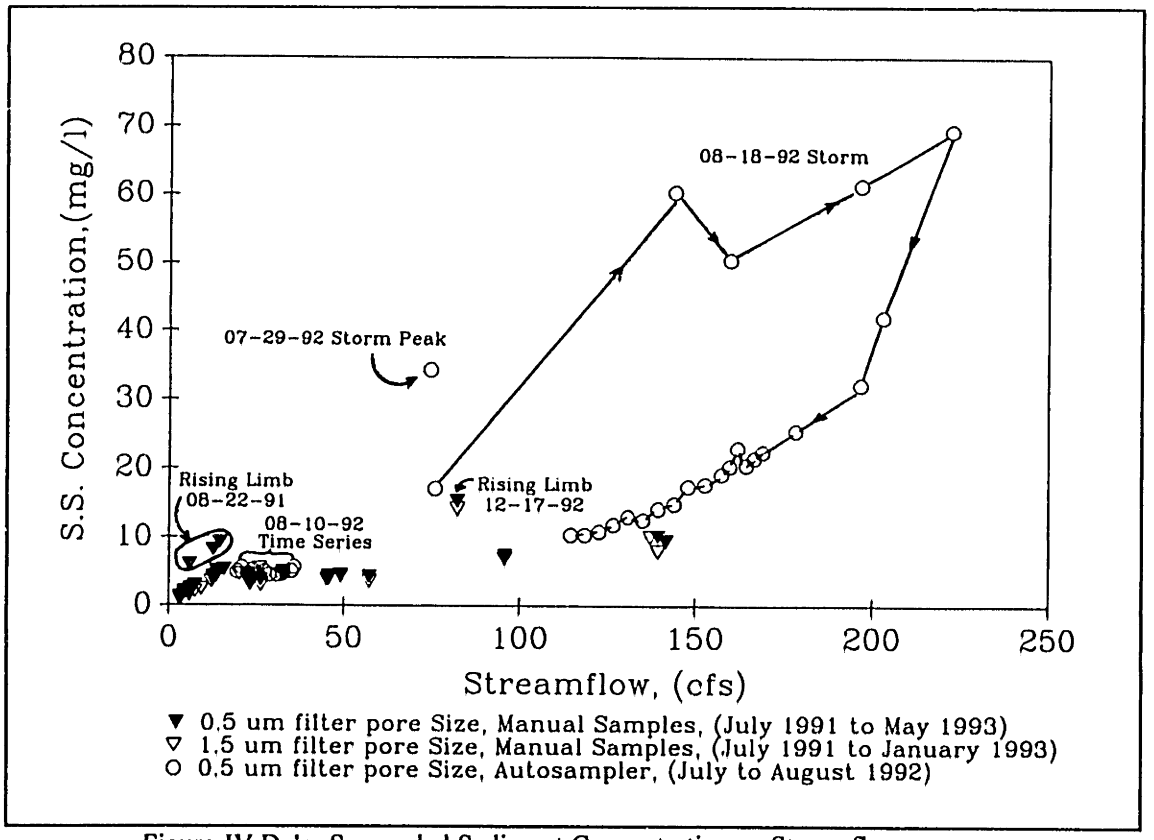

Figure IV.D-1: Suspended Sediment Concentration vs Streamflow
USGS Station, Gage #5, August Storm

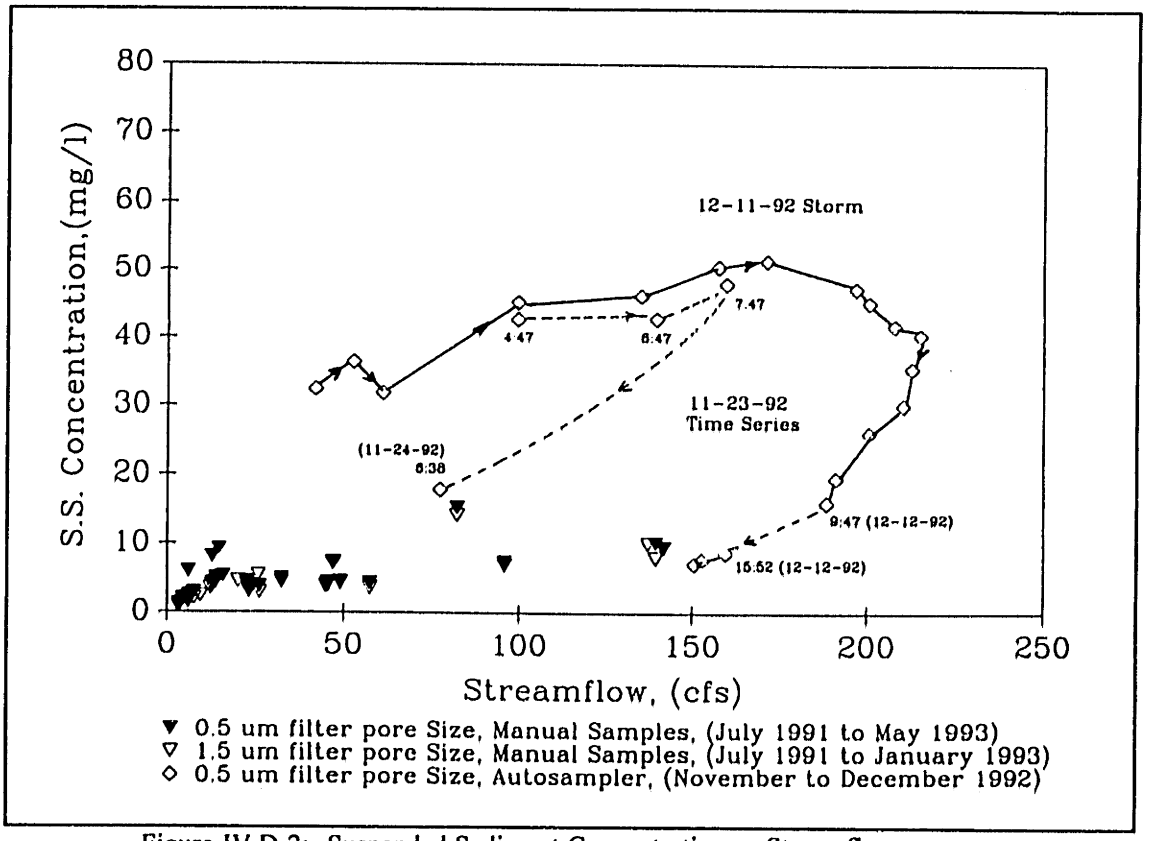

Figure IV.D-2: Suspended Sediment Concentration vs Streamflow
USGS Station, Gage #5, December Storm

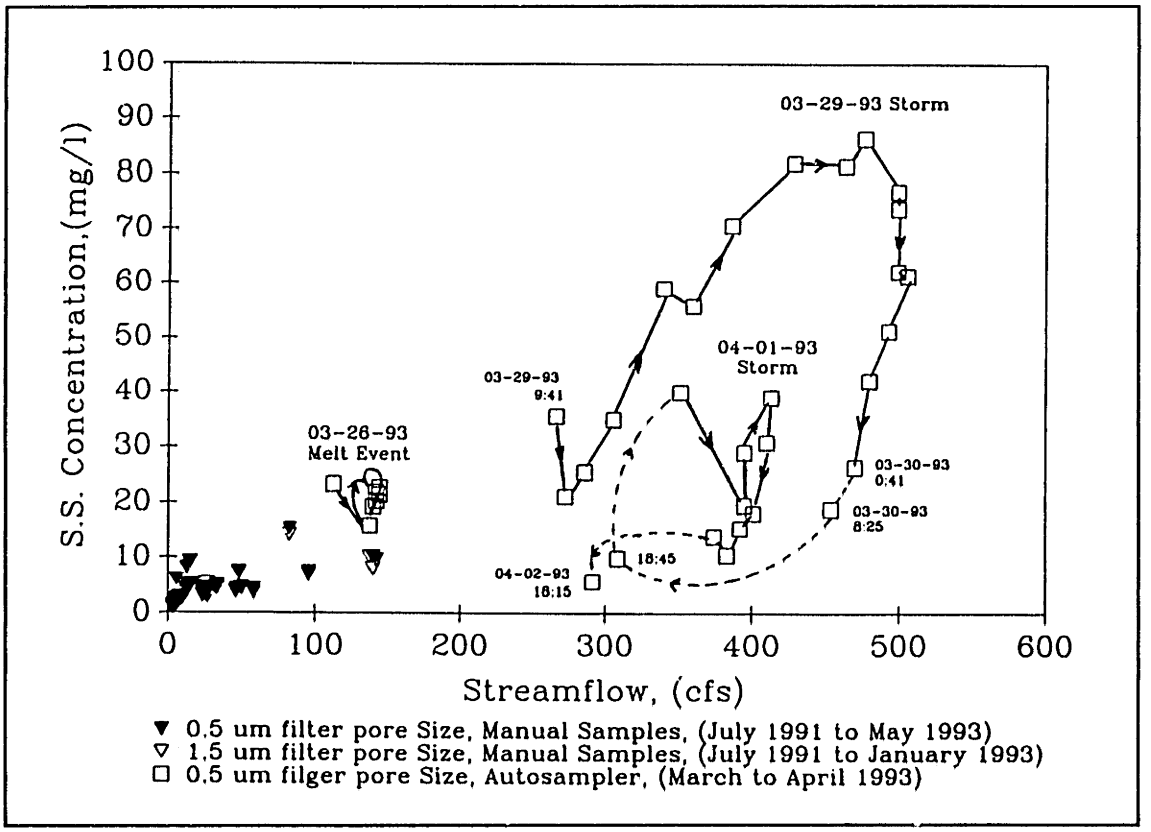

Figure IV.D-3: Suspended Sediment Concentration vs Streamflow
USGS Station, Gage #5, March Storm

SUSPENDED SEDIMENT COMPONENTS: EFFECTS OF STREAMFLOW AND TOTAL SUSPENDED SEDIMENTS

Results of component analysis for the suspended sediments are given in figures IV.D-4 through IV.D-13. Total suspended sediments were assumed to be composed of the following components:

$$\text{Total SS Conc} = \text{Volatile} + \text{Non-Volatile}$$
$$= \text{Organic} + \text{Fe oxide} + \text{Other}$$

Volatile solids were assumed to be composed primarily of organic material. Non-Volatile solids were assumed to be equal to the difference between the total and volatile suspended sediment concentrations. Non-volatile concentrations were subdivided into iron oxide and "other" suspended material. Iron oxide concentrations were obtained by analyzing each sample for total Fe. Iron concentrations were then converted to an equivalent iron oxide concentration by assuming that iron was primarily in the form of $Fe(OH)_3$. Given that the total suspended sediment concentration was known, the concentration of "other" was obtained by difference. "Other" suspended sediments may have been composed of materials of mineralogical origin and urban debris which were not classified. All concentrations corresponded to a 1.5 µm pore size filter.

Please note that some samples were analyzed only for their volatile solids concentration. For these samples, the iron oxide and "other" concentrations were not available and do not appear on the plots.

Wedge Pond

Results in figure IV.D-4 indicate that the organic component of suspended sediment was significantly variable and was not strongly correlated with values of streamflow. This lack of correlation may have been due to factors such as water temperature which affected the organic concentration more strongly. On the other hand, Fe oxide concentrations appeared to remain relatively constant with streamflow, which indicates that the flux of Fe oxide to this station was proportional to the streamflow. "Other" suspended material appeared to increase slightly with instantaneous values of flow, indicating that streamflow may be an important factor to consider in modeling this component.

Comparisons of each component with total suspended sediment concentration is provided in figure IV.D-5. Results indicate that organic suspended sediment concentrations increased strongly with increasing

total suspended sediment concentrations. In most cases the organic sediment represented the bulk of the suspended material. Therefore, modeling this trend will be required to capture the bulk of the variability of suspended sediment concentrations. Similarly, the general trend for "other" suspended sediments was for an increase with increasing totals. However, one outlier implies that this may not have been always be the case. Results also indicate that iron oxide concentrations remained relatively constant regardless of the total suspended sediment concentration. Due to their different behavior, iron oxides and organic sediments were likely associated with different sediment sources. If the iron oxide and organic sediments had come from the same source, the ratio of iron oxide to organics should have remained constant regardless of the total sediment concentration. Additionally with such trends, the concentration of iron on a per particle basis (mass suspended iron/mass of ss) decreased with increasing total suspended sediment concentration. In other words, the particulate iron concentrations (per particle basis) were diluted by organic sediments as the total suspended sediment concentrations increased.

Route 128

As observed for other stations, figure IV.D-6 indicates that the organic component of suspended sediment was variable and not correlated with streamflow. The interpretation of this trend is that organic sediment concentrations were affected more strongly by other factors, perhaps water temperature. Similar results were observed for the "other" component. The iron oxide component, on the other hand, appeared to decrease with increasing flows, indicating that during lower flow conditions a given volume of streamflow (at the iron source) was capable of "picking-up" more suspended iron. One interpretation of this result is that a primary source of iron was from the groundwater system, where iron was solubilized from the aquifer material. The longer the residence time of the water within the ground the more time available for solubilization. Once these groundwaters reached the river, the soluble reduced iron can then be oxidized and precipitated out of solution forming suspended material. In a simplified model, where the source of river water is from groundwater, lower streamflows may be associated with waters that have longer groundwater residence times. The reasoning for this statement is as follows. Assume that the groundwater system during low flows is at steady state with a relatively constant aquifer volume. Additionally assume that the primary water removal mechanism is through exfiltration into the river (i.e. river streamflow). Such a situation may occur when evapotranspiration is negligible and when groundwater exfiltration is balanced by aquifer recharge. For this case one may then define:

$$t_R = V/Q$$

where: t_R = Hydraulic Residence Time

V = Volume of the Groundwater Aquiter

Q = Streamflow

With such a model, smaller streamflows will result in longer groundwater residence times and therefore more time for these groundwaters to solubilize iron from the soil. As a result, higher iron concentrations can be expected during lower streamflows.

For the Route 128 station, all the components of suspended sediments generally increased with increasing total suspended sediment concentrations (figure IV.D-7). One interpretation of this result is that all the components shared the same sediment source. In other words, one can imagine a sediment source where all the components were present in a constant ratio. As more sediment was removed from its source, more of each individual component was also removed.

Montvale

For flows less than 20 cfs, all components increased with increasing streamflow (figure IV.D-8). However, the data were inconsistent with this trend for flows greater than 20 cfs. Considering all the data no clear trend is observed between suspended sediment components and streamflow. The data in figure IV.D-9 indicate that all suspended sediment components increased with increasing total suspended sediment concentration. This observation is consistent with the observation at Route 128 and is indicative that at these low flows, all the sediment components shared the same sediment source.

Horn Pond

Organic and "other" suspended sediment components were variable and uncorrelated with streamflow (figure IV.D-10). This lack of correlation may indicate that some other factor was responsible for the variability. The iron oxide component, on the other hand, was relatively constant regardless of the streamflow. As for the Wedge Pond data, organic and "other" suspended sediment concentrations generally increased with increasing total concentrations whereas the iron oxide component tended to remain relatively constant. As for the Wedge Pond data, this trend is interpreted as separate organic and iron sources.

USGS

With one exception, the data plotted in figure IV.D-12 correspond to the falling limb of the streamflow hydrograph. The exception is the December 1992 sample which was collected on the rising limb. For all the data, both the organic and "other" suspended sediment components generally increased with increasing streamflow. The organic concentration associated with the December point was greater than for other samples collected at similar flows on the falling limb. This indicates that increased organic

concentrations enter the river in association with quick flow which typically dominates the rising limb of the streamflow hydrograph. The Fe oxide component however remained relatively constant with changes in streamflow. Such a trend indicates that the Fe oxide concentration on a per particle basis (mass of Fe oxide per mass of suspended sediment) decreased as flows increased, due to dilution by other components of suspended sediments.

Both organic and "other" suspended sediment concentrations increased with increasing suspended sediment concentration (figure IV.D-13). The same trend was observed for upstream sediments at Wedge Pond and Montvale stations. The Fe oxide concentration appears to have increased slightly with increasing total concentrations. This trend is intermediate between the observed trend at Wedge Pond (Fe oxide constant) and Montvale (Fe oxide increased with increasing total concentration). Such a result is consistent with these findings, since the USGS station receives waters from each of these upstream stations.

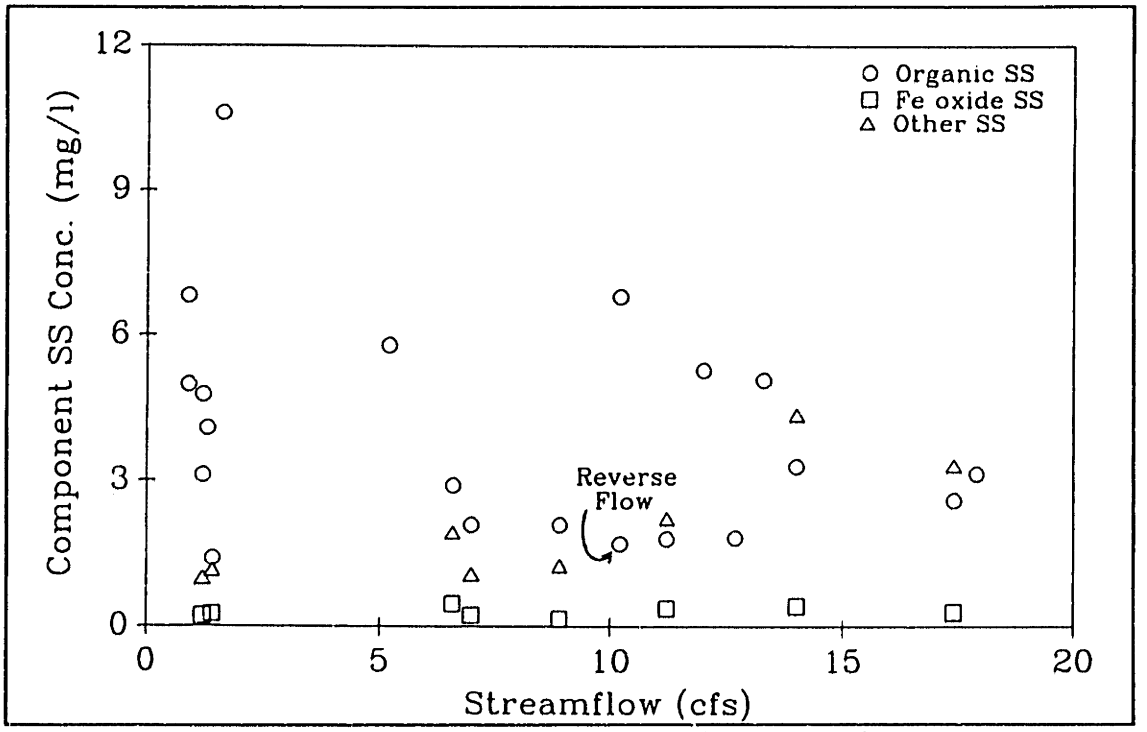

Figure IV.D-4: Component SS Concentration vs Streamflow
Wedge Pond Station, Gage #1

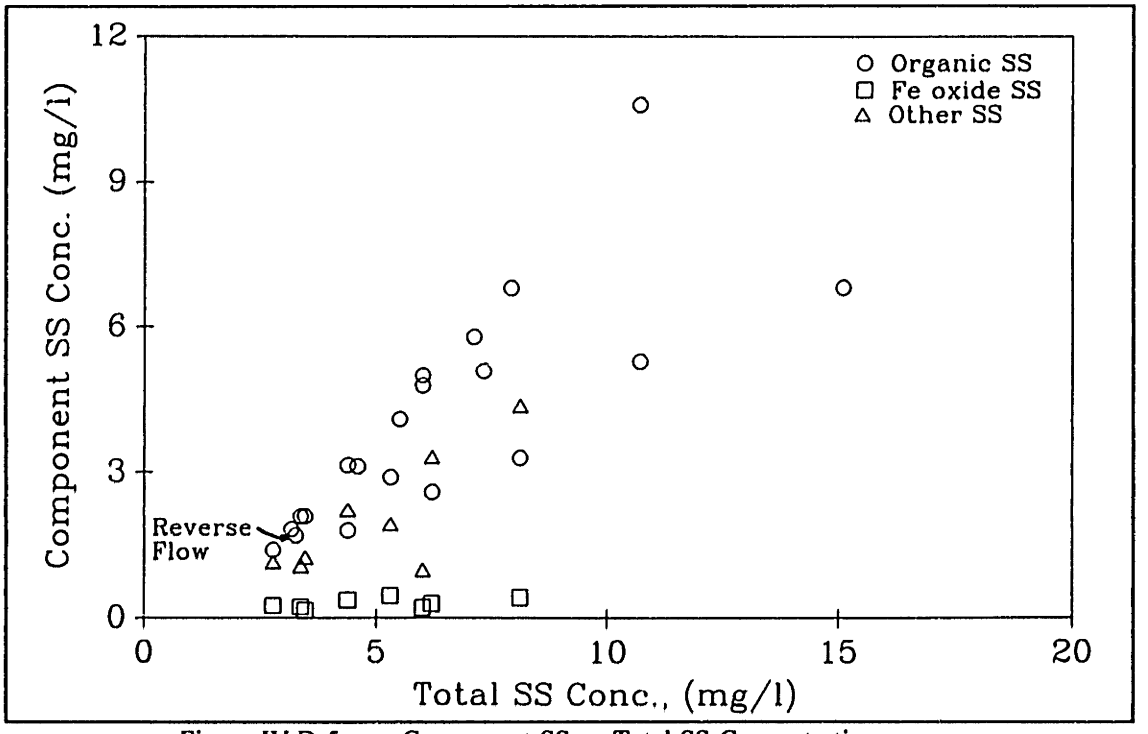

Figure IV.D-5: Component SS vs Total SS Concentration
Wedge Pond Station, Gage #1

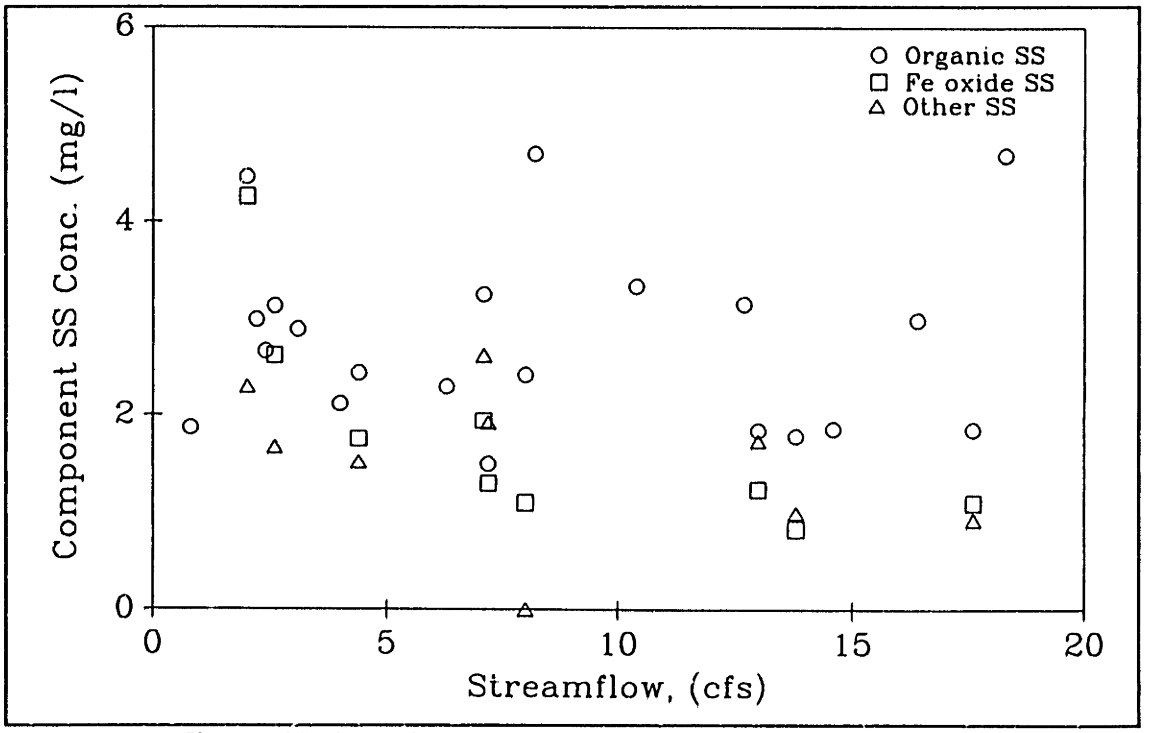

Figure IV.D-6: Component SS Concentration vs Streamflow
Route 128 Station, Gage #2

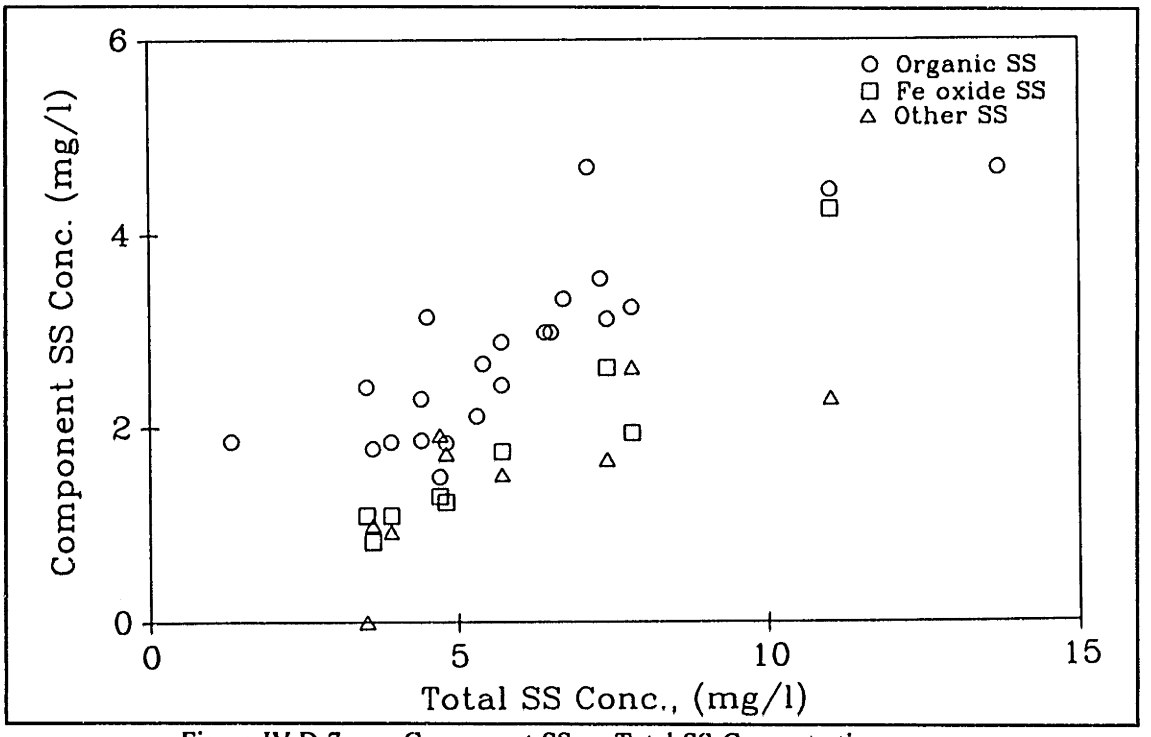

Figure IV.D-7: Component SS vs Total SS Concentration
Route 128 Station, Gage #2

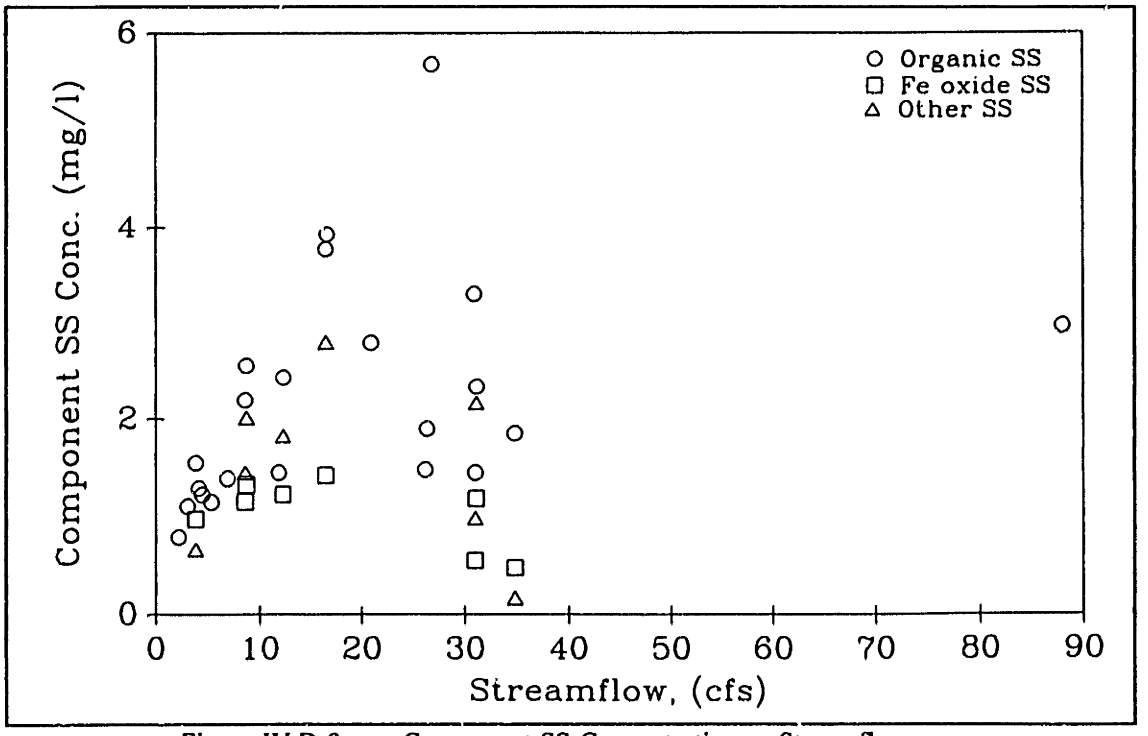

Figure IV.D-8: Component SS Concentration vs Streamflow
Montvale Station, Gage #3

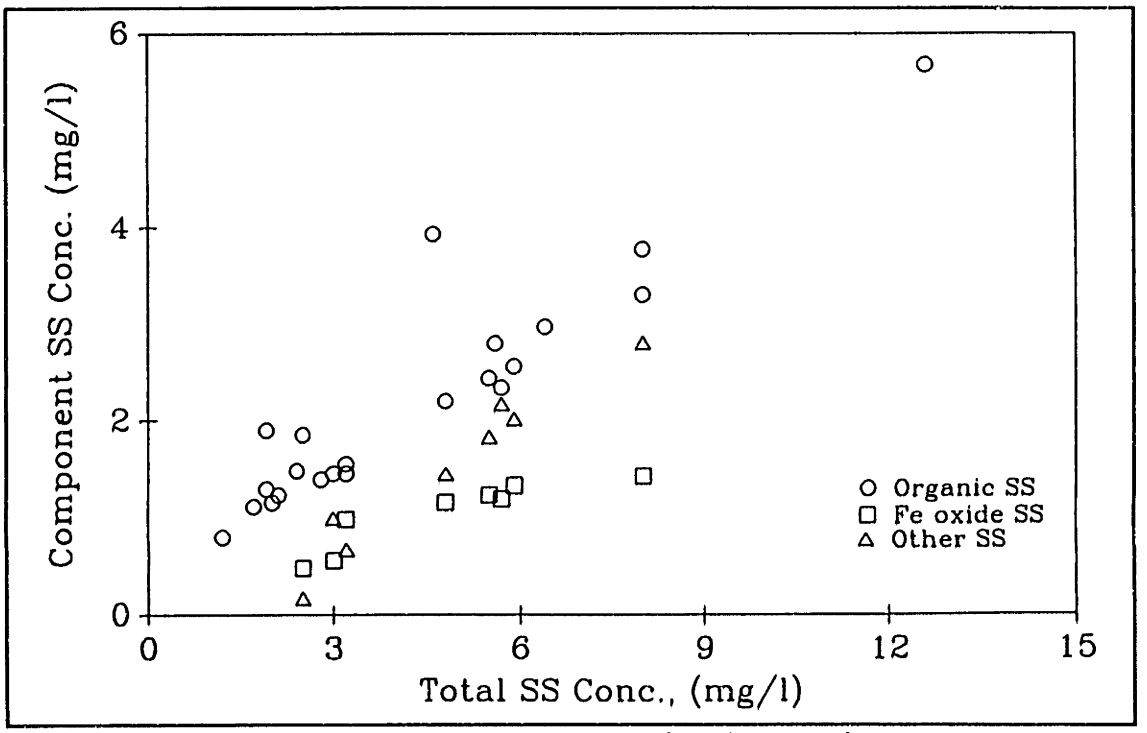

Figure IV.D-9: Component SS vs Total SS Concentration
Montvale Station, Gage #3

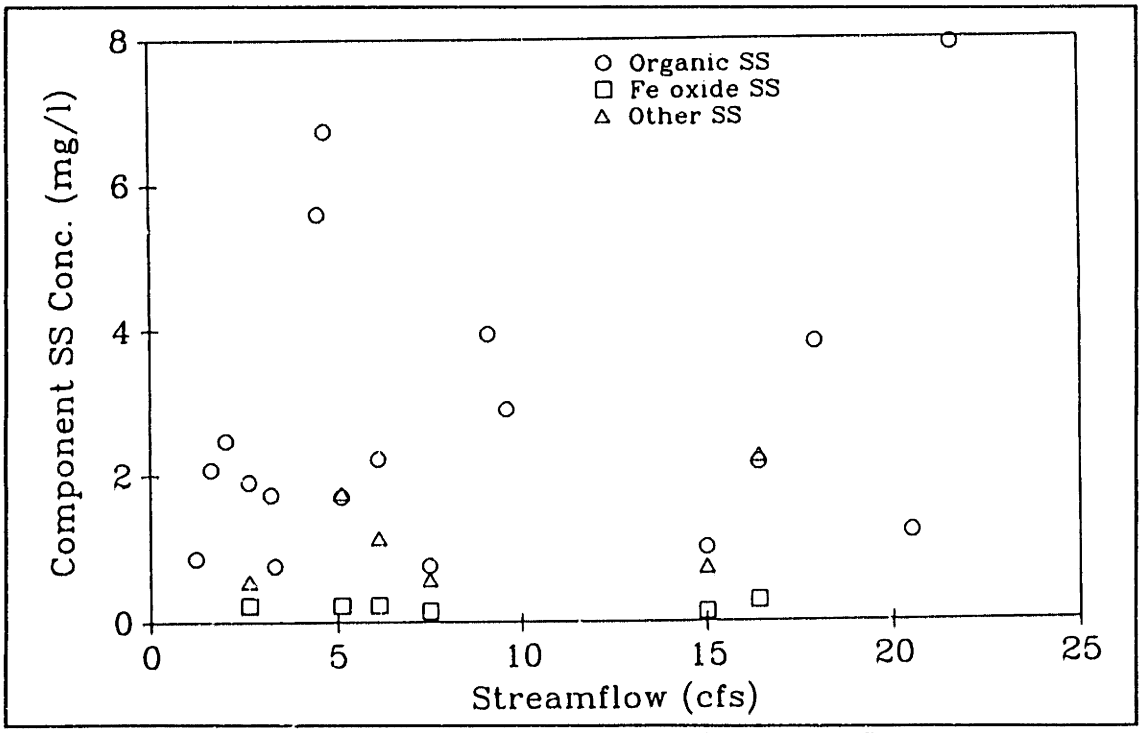

Figure IV.D-10: Component SS Concentration vs Streamflow
Horn Pond Station, Gage #4

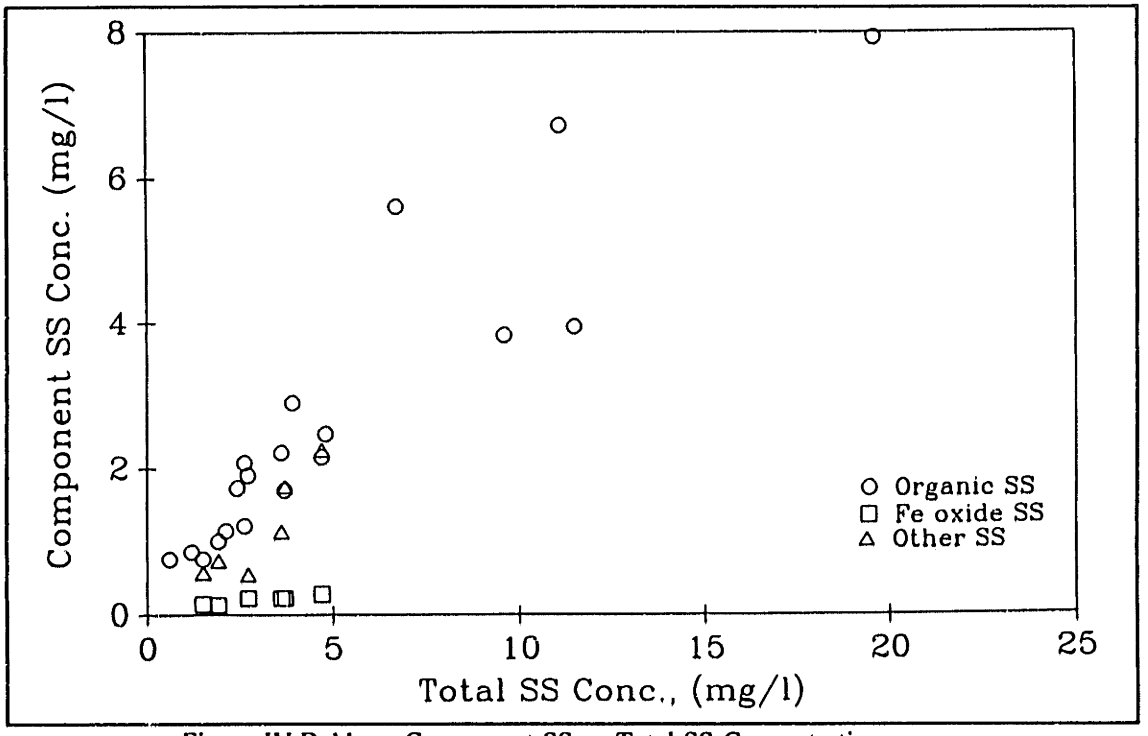

Figure IV.D-11: Component SS vs Total SS Concentration
Horn Pond Station, Gage #4

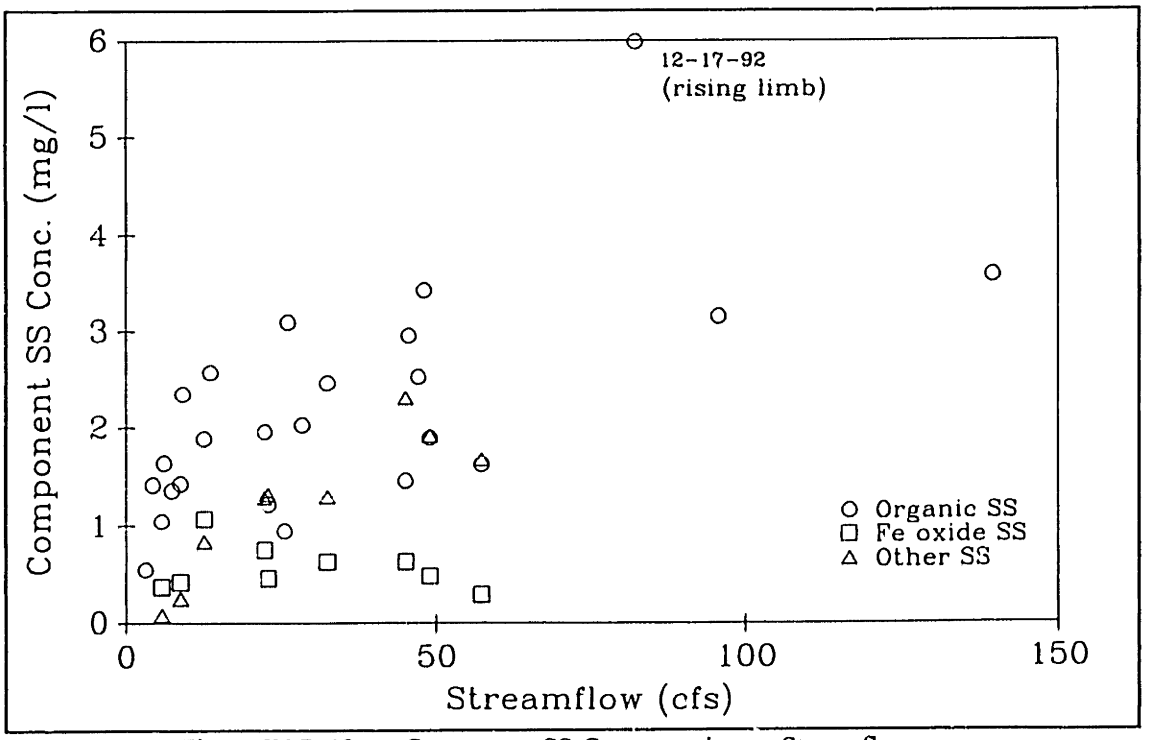

Figure IV.D-12: Component SS Concentration vs Streamflow
USGS Station, Gage #5

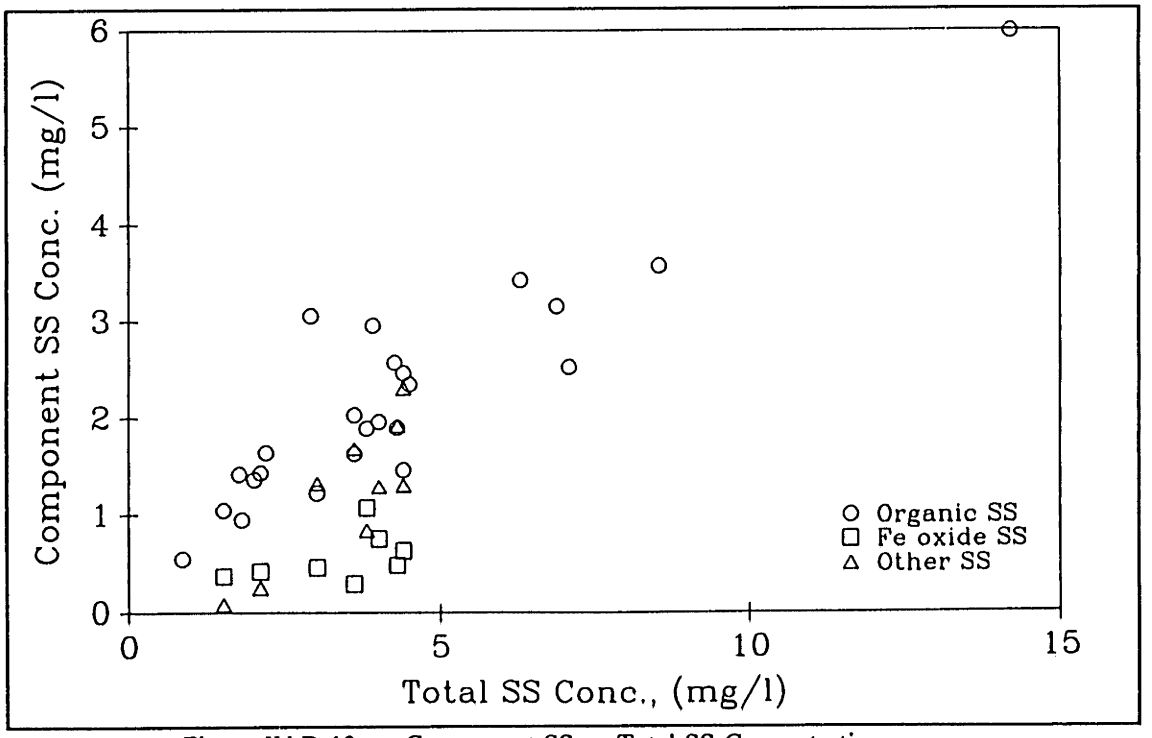

Figure IV.D-13: Component SS vs Total SS Concentration
USGS Station, Gage #5

ADDITIONAL TURBIDITY PLOTS

A set of turbidity plots is included in figures IV.D-14 to IV.D-17. These plots are considered to be a supplement to the turbidity data presented in section IV.3.7.2.

On these figures the nephelometric turbidity units (NTUs) were multiplied by 10 for proper vertical scaling. Streamflow for all five gaging stations and precipitation at the Reading station are included on the plots for reference. Symbols for turbidity, streamflow, and precipitation are spaced at one hour time intervals. Please note changes in the scale of the vertical axis from one plot to another.

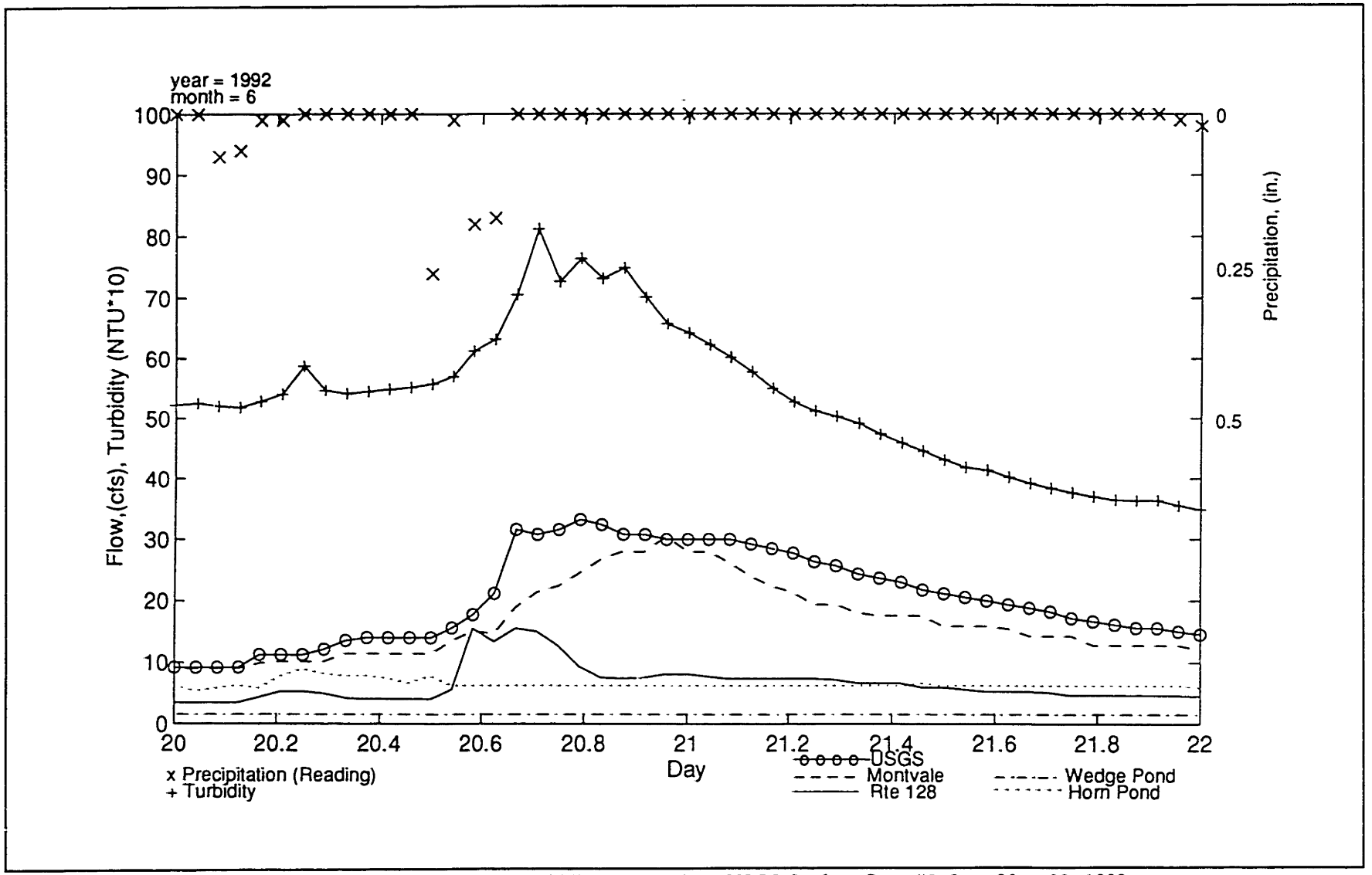

Figure IV.D-14: Streamflow & Turbidity versus Time, USGS Station, Gage #5, June 20 to 22, 1992

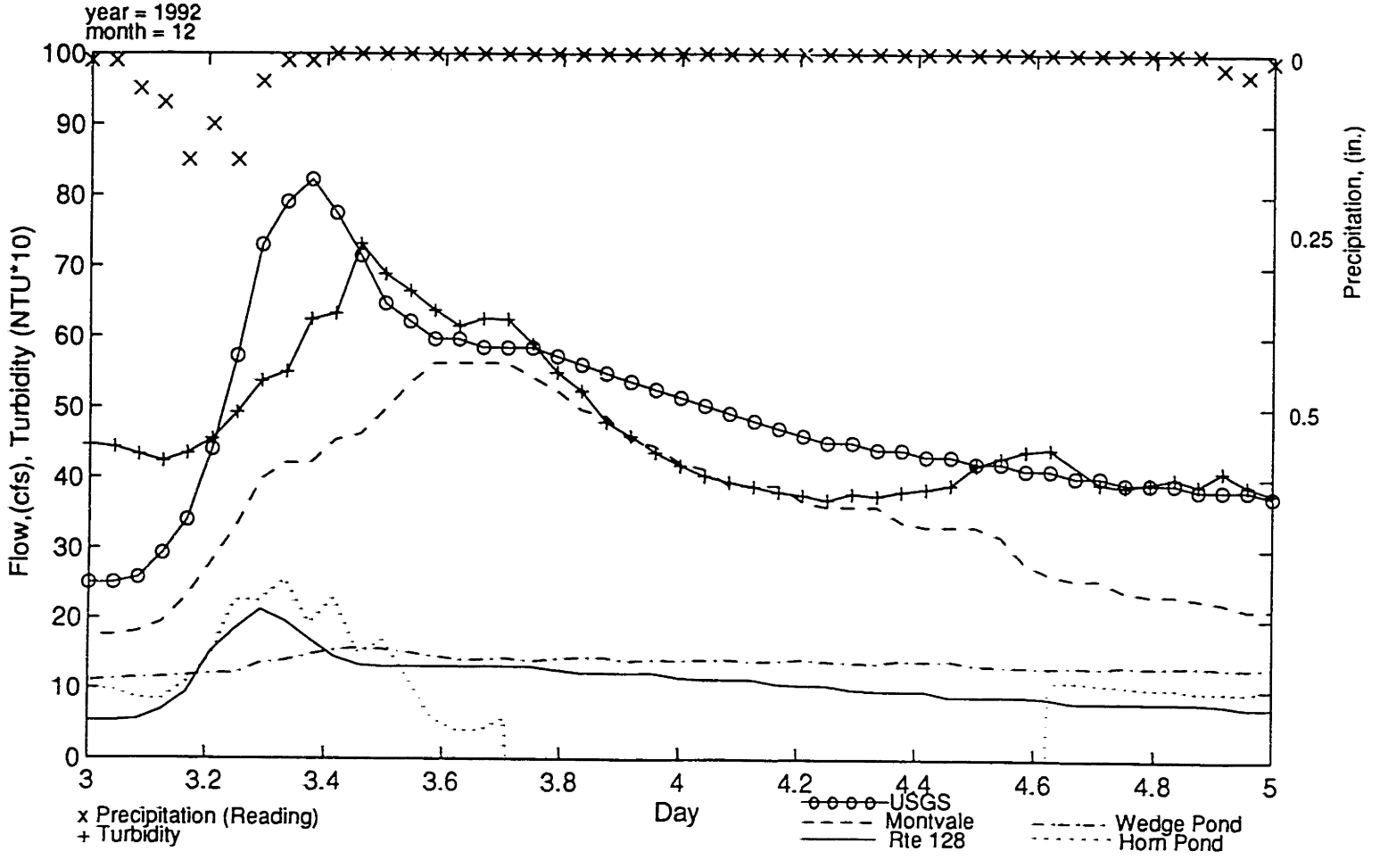

Figure IV.D-15: Streamflow & Turbidity versus Time, USGS Station, Gage #5, December 3 to 5, 1992

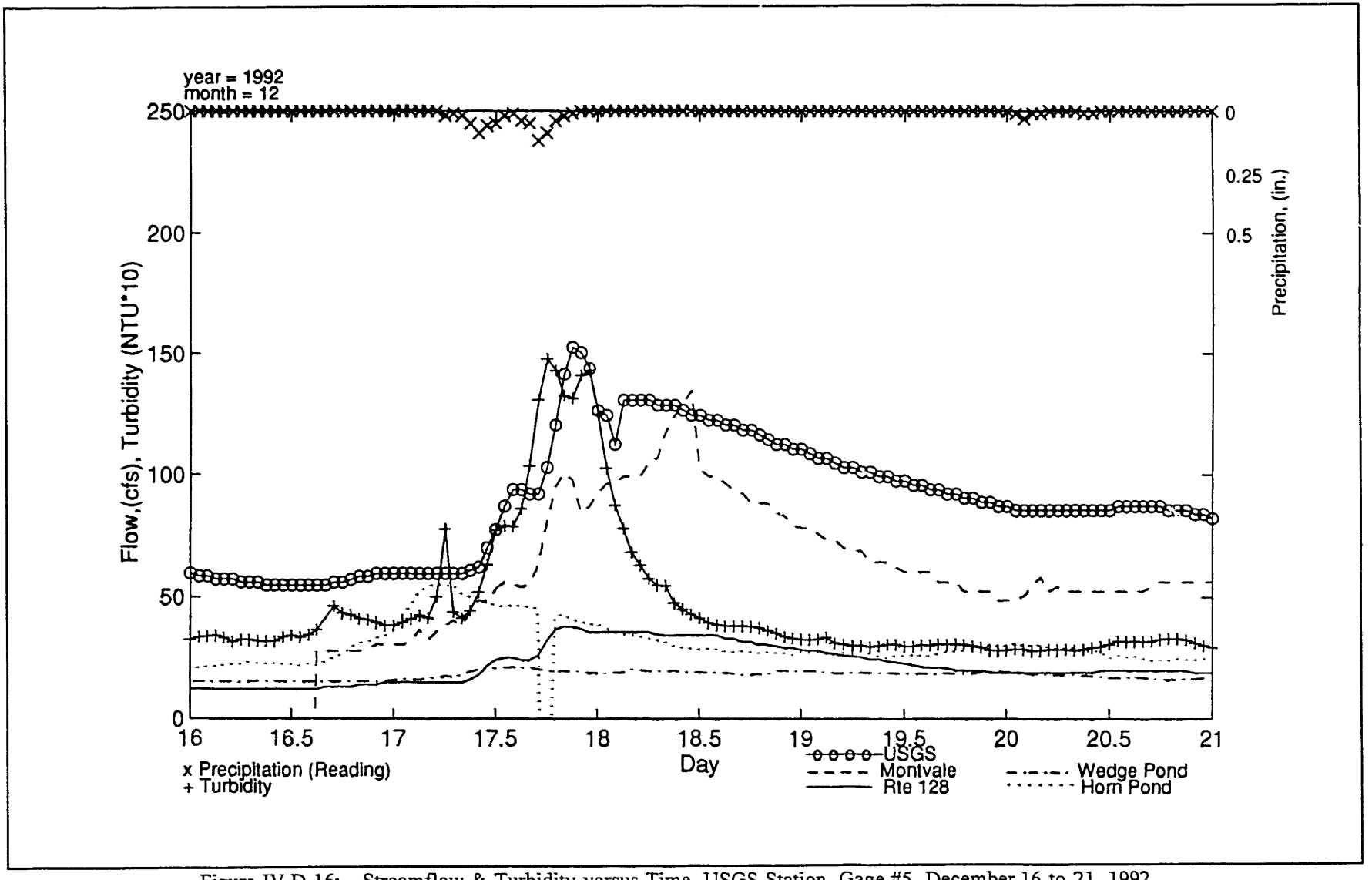

Figure IV.D-16: Streamflow & Turbidity versus Time, USGS Station, Gage #5, December 16 to 21, 1992

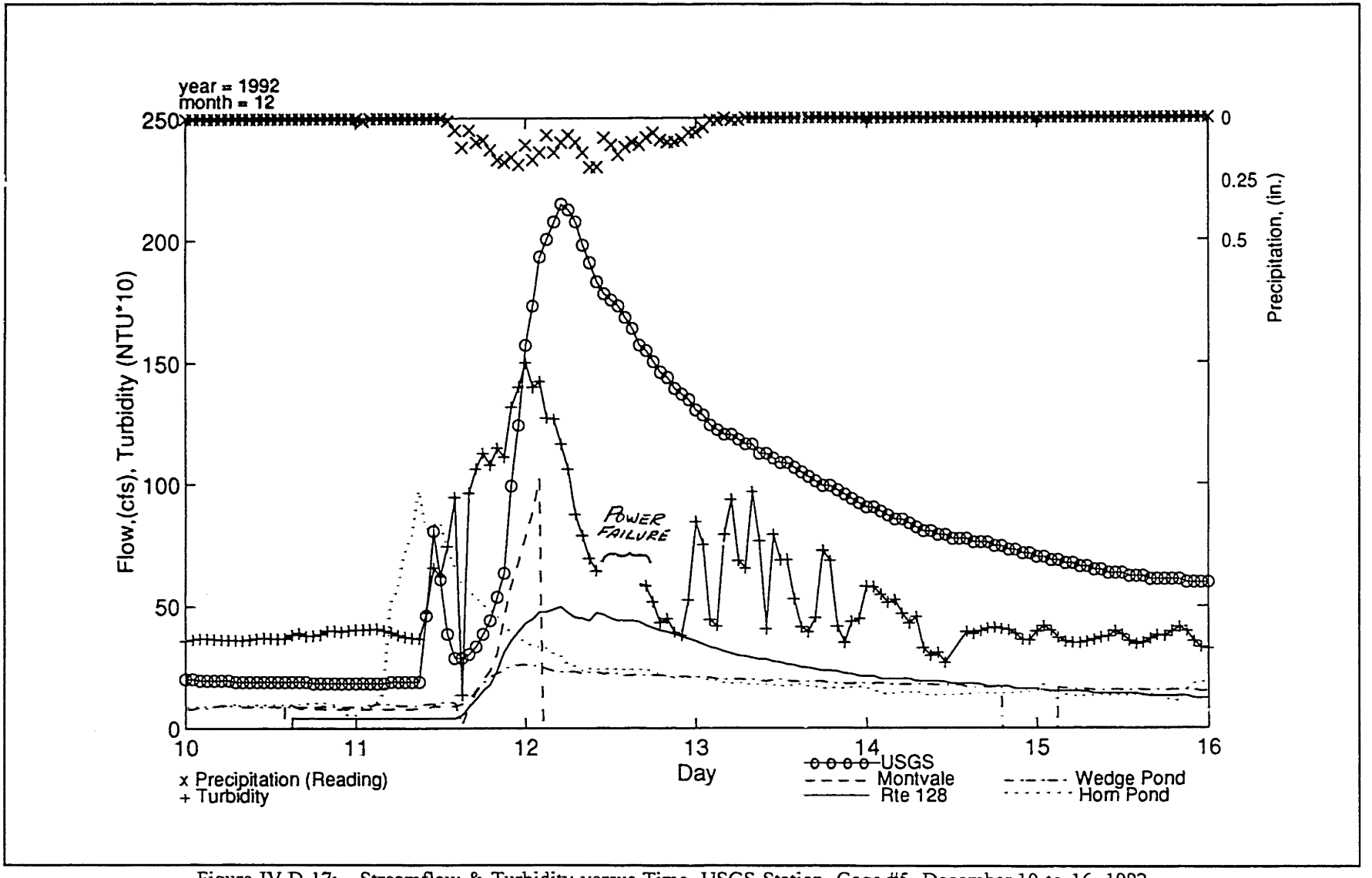

Figure IV.D-17: Streamflow & Turbidity versus Time, USGS Station, Gage #5, December 10 to 16, 1992

TRANSPORT CAPACITY COMPUTATIONS

The computations below represent one of several methods by which transport capacities can be estimated. Depending upon the method used, the computed capacity can vary significantly. For this reason, the "theorectical" capacity computed in the following pages should be considered to represent an order-of-magnitude estimate.

Computations are summarized in tables IV.D-6 and IV.D-7 and figures IV.D-18 and IV.D-19. Each step of the computation is outlined below.

Grain Size Distribution

Two grain size distributions were used to calculate the sediment transport capacity of the river. The first assumption was that the river bed is composed entirely of 10 μm sediments. This sediment size corresponds to the average size of suspended material measured at the USGS station. (See appendix III.E) The second size distribution used for calculation purposes corresponds to the distribution of a sample collected in the center of the channel at Route 128 on January 31, 1992. The distribution from the 26.5 μm to 2000 μm size range was measured directly through sieve analysis. The distribution was extended below 26.5 μm by assuming that the logarithm of the fraction of sediment in a given size range decreased proportionally with the logarithm of the mean particle diameter. The rate of decrease corresponded to the rate of decrease between the 101 and 26.5 μm sizes. The primary assumption is that this distribution is representative of the river sediment size distribution at the USGS station and that none of the sediments of a given size range are flushed out during a given flow condition. This size distribution is given table IV.D-7.

Of the two distributions, the capacities obtained from the measured distribution (Route 128, January 31, 1992) will be assumed to be the correct one. Transport capacities for a uniform 10μm bottom sediment distribution are included for comparative purposes only.

Mean Particle Diameter (μm)	Fraction of Sediment in Given Size Range (%)
1.8	0.0095
7.0	0.062
26.5	0.43
101	2.6
163	2.4
214	7.9
335	23.5
565	23.2
1195	24.1
2000	15.9

Table IV.D-6: Grain Size Distribution Corresponding to the Route 128 Sample

Calculation of S_*

S_* is the parameter used in the modified Shields Diagram (Madsen, 1975) to determine the critical Shields parameter given fluid and sediment properties.

$$S_* = \frac{d}{4\upsilon}((s-1)\cdot g\cdot d)^{1/2}$$

where: d = Particle Diameter

s = Specific Gravity of the Sediment (= 2.65)

g = Gravitational Acceleration

υ = Kinematic Viscosity of Water (= 10^{-6} at 20 °C)

Determination of Critical Shields Parameter, ψ_c

The Critical Shields Parameter, ψ_c, is a parameter used to estimate the shear stress needed to initiate particle motion. For S_* greater than 0.7, a modified Shields Diagram (a plot of S_* vs ψ_c) was used to determine values of Shields Parameter, ψ_c. For S_* less than 0.7, the following relationship was used (Madsen, 1991):

$$\psi_c = \left[\frac{4.03 \times 10^{-6}}{S_*}\right]^{1/4.25}$$

Inherent in the use of Shield's curve is that all particles are assumed to be cohesionless.

Determination of Critical Shear Stress, τ_c

By definition:

$$\tau_c = \psi_c(s-1)\rho g d$$

where: ρ = density of water ($\approx$ 1000 kg/m^3 at 20 °C)

Calculation of the Settling Velocity, w_s

Stoke's Law for discrete particle settling (for small Reynold's numbers):

$$w_s = \frac{g}{18\mu}(\rho_s - \rho)d^2$$

where: μ = Dynamic Viscosity (= 10^{-3} at 20 °C)

ρ_s = Density of the sediment = $s\cdot\rho$

Determination of Water Surface Elevation, E, Flow, Q, and Water Depth, h

Elevation versus flow was obtained from USGS rating table number 26. The channel bottom elevation at the station is 8.9 ft NGVD (F.E.M.A., 1979). The water depth, h in feet, is then calculated using the following expression.

$$h = E - 8.9$$

Computation of the Shear Velocity, u_* (Assume uniform steady flow in a rectangular wide channel)

$$u_* = (RSg)^{1/2} \qquad \text{eqn. IV.D-1}$$

where: R = Hydraulic Radius $\approx$ h
S = Bottom Slope

Assuming that Manning's equation (in English units) is valid:

$$S = \left[\frac{Qn}{1.49W(h)^{5/3}} \right]^2 \qquad \text{eqn. IV.D-2}$$

where: Q = Streamflow, cfs
W = Width of Channel $\approx$ 44 ft
n = Manning's Roughness Coefficient, (assume = 0.027)

Combining equation IV.D-1 and IV.D-2:

$$u_* = \frac{Q}{427.9} h^{.7/6}$$

Computation of Bottom Shear Stress, τ_b

$$\tau_b = \rho(u_*)^2$$

Computation of Bedload Flux per Unit Channel Width, q_{sb}

Applying Meyer-Peter Muller (Madsen, 1975) expression to each size class:

$$q_{sb} = 8 \left[\frac{\tau_b - \tau_c}{\rho} \right]^{3/2} \frac{f}{(s-1)g}$$

where: τ_c = Critical Shear Stress
f = fraction of sediment in a given size class

Computation of Bedload Concentration, C_{sb}

Then by definition of q_{sb}, C_{sb} is equal to:

$$C_{sb} = q_{sb} W \rho_s / Q$$

For C_{sb} in mg/L, q_{sb} in m^2/s, and Q in cfs:

$$C_{sb} = 1.255 * 10^9 \ q_{sb}/Q$$

Computation of Suspended Sediment Concentration, C_{ss}

Applying Einstein's equations (Einstein, 1950):

$$C_{ss} = C_{sb} \left[\ln \frac{30xh}{k_s'} I_1 - I_2 \right]$$

$$= C_{sb} \left[\ln(23100)\, I_1 - I_2 \right]$$

where: x = Factor for smooth vs rough turbulent flow
(= 1 for rough turbulent flow)

k_s' = Equivalent (skin friction) sand roughness of the boundary
(Assume $\approx d_{65} \approx 400$ μm)

I_1, I_2 = Einstein integral numbers 1 and 2
Functions of $a_* = 2d/h$ and $z = w_s/(Ku_*)$
Solved using Einstein integral tables (Einstein, 1950)
K = Von Karman Coefficient (= 0.4)

Results

The suspended sediment capacities obtained from the measured grain size distribution (Route 128, 01-31-92 sample) are provided in figures IV.D-18 and IV.D-19. For modeling purposes, the curve was approximated by a straight line. Points used in the approximation corresponded to the suspended sediment concentrations less than 200 mg/L. These points were used since suspended sediment concentrations modeled rarely exceeded the 200 mg/L value.

Mean Diameter (um)	Fraction (%)	S*	Shield's Paramet	tau(c) N/m^2	w(s) (m/s)
1.8	0.009	0.0024	0.222	0.0065	3E-06
7	0.062	0.019	0.137	0.0156	4E-05
26.5	0.4%	0.14	0.086	0.0368	6E-04
101	2.6%	1.02	0.085	0.1390	9E-03
163	2.4%	2.09	0.054	0.1425	2E-02
213.5	7.9%	3.14	0.047	0.1624	4E-02
335	23.5%	6.17	0.035	0.1898	1E-01
565	25.2%	13.51	0.031	0.2835	3E-01
1195	24.1%	41.55	0.038	0.7350	1E+00
2000	15.9%	89.96	0.044	1.4244	4E+00

fn:ss2

Elev (ft) NGVD	Flow (cfs)	h (ft)	u* (ft/s)	tau(b) N/m^2	Bedload Concentration Corresponding to a given Size Class									
					1.8um (mg/l)	7um (mg/L	26.5um (mg/L)	101um (mg/L)	163um (mg/L)	213um (mg/L	335um (mg/L)	565um (mg/L)	1195u (mg/L	2000um (mg/L)
10.30	1.0	1.40	0.0016	0.000										
10.38	2.0	1.47	0.0030	0.001										
10.44	3.0	1.54	0.0043	0.002										
10.48	4.0	1.58	0.0055	0.003										
10.52	5.0	1.62	0.0067	0.004										
10.56	6.0	1.66	0.0078	0.006										
10.59	7.0	1.69	0.0089	0.007	6.6E-06									
10.62	8.0	1.72	0.0099	0.009	3.3E-05									
10.65	9.0	1.74	0.0110	0.011	6.8E-05									
10.67	10.0	1.77	0.0120	0.013	1.1E-04									
10.78	15.0	1.88	0.0168	0.026	3.4E-04	9E-04								
10.87	20.0	1.97	0.0212	0.042	6.2E-04	3E-03	1.5E-03							
10.95	25.0	2.05	0.0253	0.059	9.1E-04	4E-03	0.01							
11.02	30.0	2.12	0.0292	0.079	1.2E-03	0.01	0.02							
11.09	35.0	2.19	0.0329	0.100	1.5E-03	0.01	0.04							
11.14	40.0	2.24	0.0365	0.124	1.9E-03	0.01	0.05							
11.19	45.0	2.29	0.0400	0.149	2.2E-03	0.01	0.07	0.01	0.01					
11.24	50.0	2.34	0.0433	0.175	2.6E-03	0.02	0.09	0.07	0.05	0.04				
11.33	60.0	2.43	0.0498	0.230	3.3E-03	0.02	0.12	0.23	0.20	0.46	0.62			
11.40	70.0	2.50	0.0562	0.293	4.1E-03	0.03	0.16	0.44	0.39	1.05	2.19	0.06		
11.47	80.0	2.57	0.0622	0.359	4.9E-03	0.03	0.19	0.66	0.59	1.69	4.01	1.18		
11.53	90.0	2.63	0.0681	0.431	0.01	0.04	0.23	0.89	0.81	2.39	6.05	2.85		
11.59	100.0	2.69	0.0737	0.504	0.01	0.04	0.27	1.13	1.03	3.10	8.13	4.72		
11.64	110.0	2.74	0.0793	0.585	0.01	0.05	0.31	1.38	1.26	3.86	10.40	6.84		
11.69	120.0	2.79	0.0847	0.667	0.01	0.05	0.35	1.63	1.49	4.63	12.66	9.01		
11.74	130.0	2.84	0.0899	0.751	0.01	0.06	0.39	1.88	1.72	5.38	14.91	11.19	0.07	
11.78	140.0	2.88	0.0953	0.843	0.01	0.07	0.44	2.15	1.97	6.22	17.39	13.61	1.20	
11.83	150.0	2.93	0.1000	0.930	0.01	0.07	0.47	2.39	2.19	6.94	19.56	15.76	2.71	
11.87	160.0	2.97	0.1050	1.025	0.01	0.08	0.52	2.66	2.44	7.76	21.99	18.16	4.61	
11.96	180.0	3.06	0.1141	1.210	0.01	0.09	0.60	3.14	2.88	9.23	26.38	22.54	8.59	
12.04	200.0	3.14	0.1230	1.406	0.02	0.10	0.68	3.64	3.34	10.75	30.93	27.07	13.00	

Table IV.D-7: Computation Table for Suspended Sediment Transport Capacity
Grain Size Distribution from Route 128 Sample, 01-31-92

fn:se2

ELEV (ft,NGVD)	FLOW (cfs)	h (ft)	u* (ft/s)	tau(b) N/m^2	Suspended Sediment Parameters for d=1.8um z	a*	I(1)	I(2)	Cse (mg/l)
10.30	1.0	1.40	0.0016	0.000	0.02	8.4E-06	23289	24765	
10.38	2.0	1.47	0.0030	0.001	0.01	8.0E-06	24507	26092	
10.44	3.0	1.54	0.0043	0.002	0.01	7.7E-06	25480	27153	
10.48	4.0	1.58	0.0055	0.003	0.00	7.5E-06	26210	27949	
10.52	5.0	1.62	0.0067	0.004	0.00	7.3E-06	26858	28657	
10.56	6.0	1.66	0.0078	0.006	0.00	7.1E-06	27506	29364	
10.59	7.0	1.69	0.0089	0.007	0.00	7.0E-06	27991	29895	1.75
10.62	8.0	1.72	0.0099	0.009	0.00	6.9E-06	28476	30426	8.87
10.65	9.0	1.74	0.0110	0.011	0.00	6.8E-06	28881	30868	18.67
10.67	10.0	1.77	0.0120	0.013	0.00	6.7E-06	29285	31310	30.04
10.78	15.0	1.88	0.0168	0.026	0.00	6.3E-06	31062	33256	102.55
10.87	20.0	1.97	0.0212	0.042	0.00	6.0E-06	32514	34848	193.51
10.95	25.0	2.05	0.0253	0.059	0.00	5.8E-06	33803	36263	297.33
11.02	30.0	2.12	0.0292	0.079	0.00	5.6E-06	34931	37501	412.84
11.09	35.0	2.19	0.0329	0.100	0.00	5.4E-06	35977	38651	537.09
11.14	40.0	2.24	0.0365	0.124	0.00	5.3E-06	36861	39624	673.41
11.19	45.0	2.29	0.0400	0.149	0.00	5.2E-06	37665	40509	819.15
11.24	50.0	2.34	0.0433	0.175	0.00	5.0E-06	38468	41393	969.43
11.33	60.0	2.43	0.0498	0.230	0.00	4.9E-06	39913	42985	1291.76
11.40	70.0	2.50	0.0562	0.293	0.00	4.7E-06	41036	44223	1656.58
11.47	80.0	2.57	0.0622	0.359	0.00	4.6E-06	42158	45462	2036.16
11.53	90.0	2.63	0.0681	0.431	0.00	4.5E-06	43119	46523	2447.93
11.59	100.0	2.69	0.0737	0.504	0.00	4.4E-06	44080	47584	2870.86
11.64	110.0	2.74	0.0793	0.585	0.00	4.3E-06	44880	48469	3330.92
11.69	120.0	2.79	0.0847	0.667	0.00	4.2E-06	45680	49353	3801.86
11.74	130.0	2.84	0.0899	0.751	0.00	4.2E-06	46480	50238	4280.81
11.78	140.0	2.88	0.0953	0.843	0.00	4.1E-06	47120	50945	4805.97
11.83	150.0	2.93	0.1000	0.930	0.00	4.0E-06	47919	51830	5297.20
11.87	160.0	2.97	0.1050	1.025	0.00	4.0E-06	48558	52537	5837.73
11.96	180.0	3.06	0.1141	1.210	0.00	3.9E-06	49995	54129	6882.28
12.04	200.0	3.14	0.1230	1.406	0.00	3.8E-06	51271	55545	7989.98

Table IV.D-7: con'd

fn:ss2

ELEV (ft,NGVD)	FLOW (cfs)	h (ft)	u* (ft/s)	tau(b) N/m^2	Suspended Sediment Parameters for d=7um z	a*	I(1)	I(2)	C(i)
10.30	1.0	1.40	0.0016	0.000	0.23	3.3E-05	6178	6368	
10.38	2.0	1.47	0.0030	0.001	0.12	3.1E-05	6502	6709	
10.44	3.0	1.54	0.0043	0.002	0.08	3.0E-05	6760	6982	
10.48	4.0	1.58	0.0055	0.003	0.07	2.9E-05	6954	7187	
10.52	5.0	1.62	0.0067	0.004	0.05	2.8E-05	7125	7369	
10.56	6.0	1.66	0.0078	0.006	0.05	2.8E-05	7297	7551	
10.59	7.0	1.69	0.0089	0.007	0.04	2.7E-05	7426	7687	
10.62	8.0	1.72	0.0099	0.009	0.04	2.7E-05	7555	7824	
10.65	9.0	1.74	0.0110	0.011	0.03	2.6E-05	7662	7937	
10.67	10.0	1.77	0.0120	0.013	0.03	2.6E-05	7769	8051	
10.78	15.0	1.88	0.0168	0.026	0.02	2.4E-05	8241	8552	70.52
10.87	20.0	1.97	0.0212	0.042	0.02	2.3E-05	8626	8961	215.15
10.95	25.0	2.05	0.0253	0.059	0.01	2.2E-05	8968	9325	389.78
11.02	30.0	2.12	0.0292	0.079	0.01	2.2E-05	9267	9643	587.47
11.09	35.0	2.19	0.0329	0.100	0.01	2.1E-05	9545	9939	801.70
11.14	40.0	2.24	0.0365	0.124	0.01	2.1E-05	9779	10189	1037.53
11.19	45.0	2.29	0.0400	0.149	0.01	2.0E-05	9993	10417	1290.15
11.24	50.0	2.34	0.0433	0.175	0.01	2.0E-05	10206	10644	1550.96
11.33	60.0	2.43	0.0498	0.230	0.01	1.9E-05	10589	11053	2110.87
11.40	70.0	2.50	0.0562	0.293	0.01	1.8E-05	10887	11372	2744.93
11.47	80.0	2.57	0.0622	0.359	0.01	1.8E-05	11185	11690	3404.88
11.53	90.0	2.63	0.0681	0.431	0.01	1.7E-05	11440	11963	4120.89
11.59	100.0	2.69	0.0737	0.504	0.00	1.7E-05	11695	12236	4856.39
11.64	110.0	2.74	0.0793	0.585	0.00	1.7E-05	11907	12463	5656.44
11.69	120.0	2.79	0.0847	0.667	0.00	1.6E-05	12119	12691	6475.46
11.74	130.0	2.84	0.0899	0.751	0.00	1.6E-05	12331	12918	7308.43
11.78	140.0	2.88	0.0953	0.843	0.00	1.6E-05	12501	13100	8221.74
11.83	150.0	2.93	0.1000	0.930	0.00	1.6E-05	12713	13328	9076.10
11.87	160.0	2.97	0.1050	1.025	0.00	1.5E-05	12882	13510	10016.14
11.96	180.0	3.06	0.1141	1.210	0.00	1.5E-05	13264	13919	11832.79
12.04	200.0	3.14	0.1230	1.406	0.00	1.5E-05	13602	14283	13759.22

Table IV.D-7: con'd

fn:ss2

ELEV (ft,NGVD)	FLOW (cfs)	h (ft)	u* (ft/s)	tau(b) N/m^2	Suspended Sediment Parameters for d=26.5um z	a*	I(1)	I(2)	C(i)
10.30	1.0	1.40	0.0016	0.000	3.28	1.24E-04	450	630	
10.38	2.0	1.47	0.0030	0.001	1.74	1.18E-04	520	700	
10.44	3.0	1.54	0.0043	0.002	1.22	1.13E-04	630	800	
10.48	4.0	1.58	0.0055	0.003	0.94	1.10E-04	800	1000	
10.52	5.0	1.62	0.0067	0.004	0.78	1.07E-04	1000	1020	
10.56	6.0	1.66	0.0078	0.006	0.67	1.05E-04	1010	1040	
10.59	7.0	1.69	0.0089	0.007	0.58	1.03E-04	1010	1040	
10.62	8.0	1.72	0.0099	0.009	0.52	1.01E-04	1010	1040	
10.65	9.0	1.74	0.0110	0.011	0.47	9.96E-05	1010	1040	
10.67	10.0	1.77	0.0120	0.013	0.43	9.82E-05	1010	1040	
10.78	15.0	1.88	0.0168	0.026	0.31	9.25E-05	1000	1020	
10.87	20.0	1.97	0.0212	0.042	0.24	8.83E-05	1000	1020	5.64
10.95	25.0	2.05	0.0253	0.059	0.20	8.48E-05	1000	1020	44.96
11.02	30.0	2.12	0.0292	0.079	0.18	8.20E-05	1000	1020	96.73
11.09	35.0	2.19	0.0329	0.100	0.16	7.96E-05	1000	1020	153.81
11.14	40.0	2.24	0.0365	0.124	0.14	7.76E-05	1000	1020	216.50
11.19	45.0	2.29	0.0400	0.149	0.13	7.59E-05	1000	1020	282.76
11.24	50.0	2.34	0.0433	0.175	0.12	7.43E-05	1000	1020	349.49
11.33	60.0	2.43	0.0498	0.230	0.10	7.16E-05	1000	1020	488.91
11.40	70.0	2.50	0.0562	0.293	0.09	6.96E-05	1000	1020	644.32
11.47	80.0	2.57	0.0622	0.359	0.08	6.77E-05	1000	1020	799.74
11.53	90.0	2.63	0.0681	0.431	0.08	6.61E-05	1000	1020	965.70
11.59	100.0	2.69	0.0737	0.504	0.07	6.46E-05	980	1010	1105.06
11.64	110.0	2.74	0.0793	0.585	0.07	6.35E-05	980	1010	1279.66
11.69	120.0	2.79	0.0847	0.667	0.06	6.23E-05	980	1010	1453.58
11.74	130.0	2.84	0.0899	0.751	0.06	6.12E-05	980	1010	1625.68
11.78	140.0	2.88	0.0953	0.843	0.05	6.04E-05	980	1010	1816.50
11.83	150.0	2.93	0.1000	0.930	0.05	5.93E-05	980	1010	1983.92
11.87	160.0	2.97	0.1050	1.025	0.05	5.85E-05	980	1010	2171.90
11.96	180.0	3.06	0.1141	1.210	0.05	5.68E-05	980	1010	2514.74
12.04	200.0	3.14	0.1230	1.406	0.04	5.54E-05	980	1010	2872.29

Table IV.D-7: con'd

fn:ss2

ELEV (ft,NGVD)	FLOW (cfs)	h (ft)	u* (ft/s)	tau(b) N/m^2	Suspended Sediment Parameters for d=101um				
					z	a*	I(1)	I(2)	C(i)
10.30	1.0	1.40	0.0016	0.000	47.67	4.73E-04	0.15	0.9	
10.38	2.0	1.47	0.0030	0.001	25.33	4.49E-04	0.17	1.05	
10.44	3.0	1.54	0.0043	0.002	17.69	4.32E-04	0.19	1.07	
10.48	4.0	1.58	0.0055	0.003	13.72	4.19E-04	0.35	2	
10.52	5.0	1.62	0.0067	0.004	11.30	4.09E-04	0.48	3.5	
10.56	6.0	1.66	0.0078	0.006	9.69	3.99E-04	0.7	3.8	
10.59	7.0	1.69	0.0089	0.007	8.48	3.92E-04	0.8	3.8	
10.62	8.0	1.72	0.0099	0.009	7.58	3.85E-04	0.82	3.8	
10.65	9.0	1.74	0.0110	0.011	6.85	3.80E-04	0.8	3.8	
10.67	10.0	1.77	0.0120	0.013	6.27	3.74E-04	0.52	3	
10.78	15.0	1.88	0.0168	0.026	4.48	3.53E-04	0.52	3	
10.87	20.0	1.97	0.0212	0.042	3.55	3.36E-04	0.52	3	
10.95	25.0	2.05	0.0253	0.059	2.98	3.23E-04	0.52	3	
11.02	30.0	2.12	0.0292	0.079	2.58	3.13E-04	0.52	3	
11.09	35.0	2.19	0.0329	0.100	2.29	3.03E-04	0.52	3	
11.14	40.0	2.24	0.0365	0.124	2.06	2.96E-04	0.52	3	
11.19	45.0	2.29	0.0400	0.149	1.88	2.89E-04	0.48	2.5	0.00
11.24	50.0	2.34	0.0433	0.175	1.74	2.83E-04	0.48	2.5	0.00
11.33	60.0	2.43	0.0498	0.230	1.51	2.73E-04	0.48	2.5	0.00
11.40	70.0	2.50	0.0562	0.293	1.34	2.65E-04	0.48	2.5	0.00
11.47	80.0	2.57	0.0622	0.359	1.21	2.58E-04	0.4	2.5	0.00
11.53	90.0	2.63	0.0681	0.431	1.11	2.52E-04	0.4	2.5	0.00
11.59	100.0	2.69	0.0737	0.504	1.02	2.46E-04	0.39	2.5	0.00
11.64	110.0	2.74	0.0793	0.585	0.95	2.42E-04	0.39	2.5	0.00
11.69	120.0	2.79	0.0847	0.667	0.89	2.38E-04	0.37	2.5	0.00
11.74	130.0	2.84	0.0899	0.751	0.84	2.33E-04	0.37	2.1	0.00
11.78	140.0	2.88	0.0953	0.843	0.79	2.30E-04	0.3	2.1	0.00
11.83	150.0	2.93	0.1000	0.930	0.75	2.26E-04	0.3	2.1	0.00
11.87	160.0	2.97	0.1050	1.025	0.72	2.23E-04	0.3	2.1	0.00
11.96	180.0	3.06	0.1141	1.210	0.66	2.17E-04	0.3	2.1	0.00
12.04	200.0	3.14	0.1230	1.406	0.61	2.11E-04	0.3	2.1	0.00

Table IV.D-7: con'd

fn:ss2

Elev (ft) NGVD	Flow (cfs)	h (ft)	u* (ft/s)	tau(b) N/m^2	SS from All Size Fractions (mg/L)
10.30	1.0	1.40	0.0016	0.000	0.00
10.38	2.0	1.47	0.0030	0.001	0.00
10.44	3.0	1.54	0.0043	0.002	0.00
10.48	4.0	1.58	0.0055	0.003	0.00
10.52	5.0	1.62	0.0067	0.004	0.00
10.56	6.0	1.66	0.0078	0.006	0.00
10.59	7.0	1.69	0.0089	0.007	1.75
10.62	8.0	1.72	0.0099	0.009	8.87
10.65	9.0	1.74	0.0110	0.011	18.67
10.67	10.0	1.77	0.0120	0.013	30.04
10.78	15.0	1.88	0.0168	0.026	173.1
10.87	20.0	1.97	0.0212	0.042	414.3
10.95	25.0	2.05	0.0253	0.059	732.1
11.02	30.0	2.12	0.0292	0.079	1097
11.09	35.0	2.19	0.0329	0.100	1493
11.14	40.0	2.24	0.0365	0.124	1927
11.19	45.0	2.29	0.0400	0.149	2392
11.24	50.0	2.34	0.0433	0.175	2870
11.33	60.0	2.43	0.0498	0.230	3892
11.40	70.0	2.50	0.0562	0.293	5046
11.47	80.0	2.57	0.0622	0.359	6241
11.53	90.0	2.63	0.0681	0.431	7535
11.59	100.0	2.69	0.0737	0.504	8832
11.64	110.0	2.74	0.0793	0.585	10267
11.69	120.0	2.79	0.0847	0.667	11731
11.74	130.0	2.84	0.0899	0.751	13215
11.78	140.0	2.88	0.0953	0.843	14844
11.83	150.0	2.93	0.1000	0.930	16357
11.87	160.0	2.97	0.1050	1.025	18026
11.96	180.0	3.06	0.1141	1.210	21230
12.04	200.0	3.14	0.1230	1.406	24621

Table IV.D-7: con'd

Mean Diameter (um)	Fraction (%)	S*	Shield's Paramet	tau(c) N/m^2	w(s) (m/s)
10	100	0.0318	0.121	0.0196	9E-05

fn:ss3

Elev (ft) NGVD	Flow (cfs)	h (ft)	u* (ft/s)	tau(b) N/m^2	Bedload 10um (mg/l)	Suspended Sediment Parameters for d=10 z	a*	I(1)	I(2)	Css (mg/l)
10.30	1.0	1.40	0.0016	0.000		0.47	4.7E-05	4361	4458	
10.38	2.0	1.47	0.0030	0.001		0.25	4.4E-05	4589	4697	
10.44	3.0	1.54	0.0043	0.002		0.17	4.3E-05	4771	4888	
10.48	4.0	1.58	0.0055	0.003		0.13	4.2E-05	4908	5031	
10.52	5.0	1.62	0.0067	0.004		0.11	4.1E-05	5029	5158	
10.56	6.0	1.66	0.0078	0.006		0.10	4.0E-05	5150	5286	
10.59	7.0	1.69	0.0089	0.007		0.08	3.9E-05	5241	5381	
10.62	8.0	1.72	0.0099	0.009		0.07	3.8E-05	5332	5477	
10.65	9.0	1.74	0.0110	0.011		0.07	3.8E-05	5408	5556	
10.67	10.0	1.77	0.0120	0.013		0.06	3.7E-05	5483	5636	
10.78	15.0	1.88	0.0168	0.026	69.9	0.04	3.5E-05	5816	5986	4E+06
10.87	20.0	1.97	0.0212	0.042	323.0	0.03	3.3E-05	6088	6273	2E+07
10.95	25.0	2.05	0.0253	0.059	623.6	0.03	3.2E-05	6329	6527	4E+07
11.02	30.0	2.12	0.0292	0.079	949.5	0.03	3.1E-05	6540	6750	6E+07
11.09	35.0	2.19	0.0329	0.100	1286.4	0.02	3.0E-05	6736	6957	8E+07
11.14	40.0	2.24	0.0365	0.124	1647.2	0.02	2.9E-05	6902	7132	1E+08
11.19	45.0	2.29	0.0400	0.149	2022.0	0.02	2.9E-05	7052	7292	1E+08
11.24	50.0	2.34	0.0433	0.175	2393.1	0.02	2.8E-05	7203	7451	2E+08
11.33	60.0	2.43	0.0498	0.230	3159.2	0.01	2.7E-05	7473	7737	2E+08
11.40	70.0	2.50	0.0562	0.293	4010.6	0.01	2.6E-05	7684	7960	3E+08
11.47	80.0	2.57	0.0622	0.359	4849.8	0.01	2.6E-05	7894	8183	4E+08
11.53	90.0	2.63	0.0681	0.431	5743.5	0.01	2.5E-05	8074	8374	5E+08
11.59	100.0	2.69	0.0737	0.504	6621.1	0.01	2.4E-05	8254	8565	5E+08
11.64	110.0	2.74	0.0793	0.585	7574.1	0.01	2.4E-05	8403	8724	6E+08
11.69	120.0	2.79	0.0847	0.667	8515.5	0.01	2.4E-05	8553	8884	7E+08
11.74	130.0	2.84	0.0899	0.751	9439.3	0.01	2.3E-05	8703	9043	8E+08
11.78	140.0	2.88	0.0953	0.843	10470	0.01	2.3E-05	8823	9170	9E+08
11.83	150.0	2.93	0.1000	0.930	11354	0.01	2.2E-05	8972	9329	1E+09
11.87	160.0	2.97	0.1050	1.025	12357	0.01	2.2E-05	9092	9457	1E+09
11.96	180.0	3.06	0.1141	1.210	14151	0.01	2.1E-05	9361	9743	1E+09
12.04	200.0	3.14	0.1230	1.406	16017	0.01	2.1E-05	9600	9998	2E+09

Table IV.D-8: Computation Table for Suspended Sediment Transport Capacity Uniform, 10 μm Particle Diameter Assumption

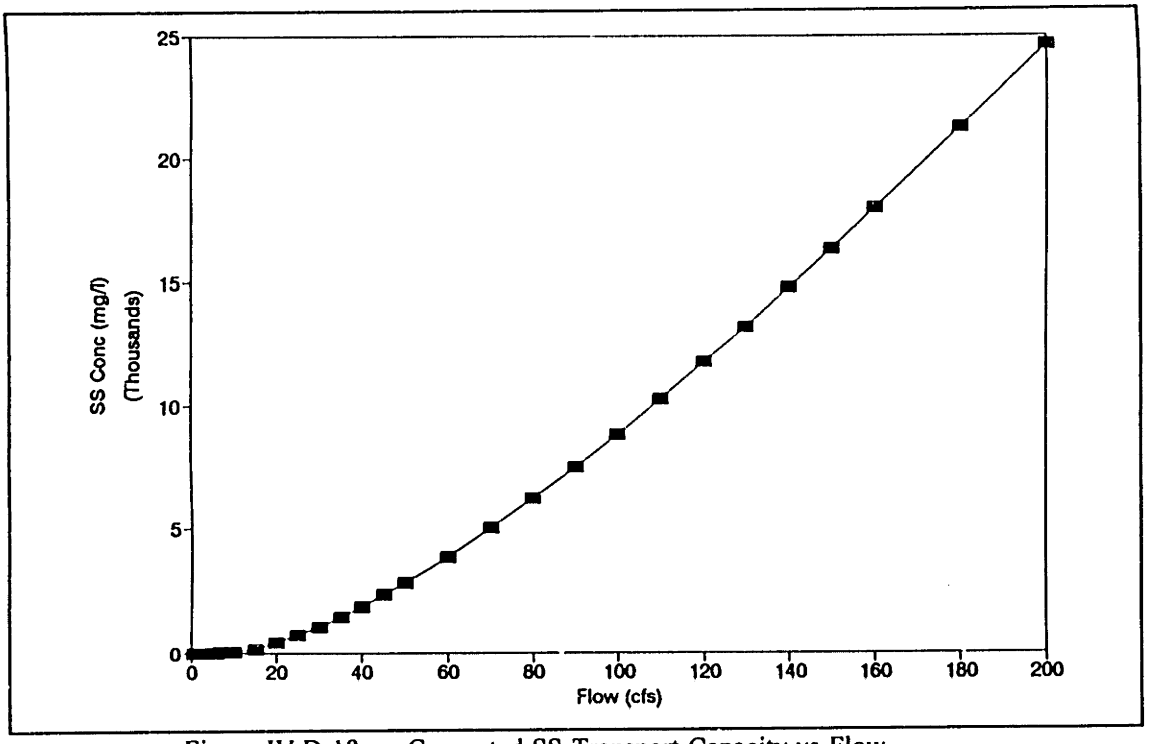

Figure IV.D-18: Computed SS Transport Capacity vs Flow
USGS Station, Gage #5

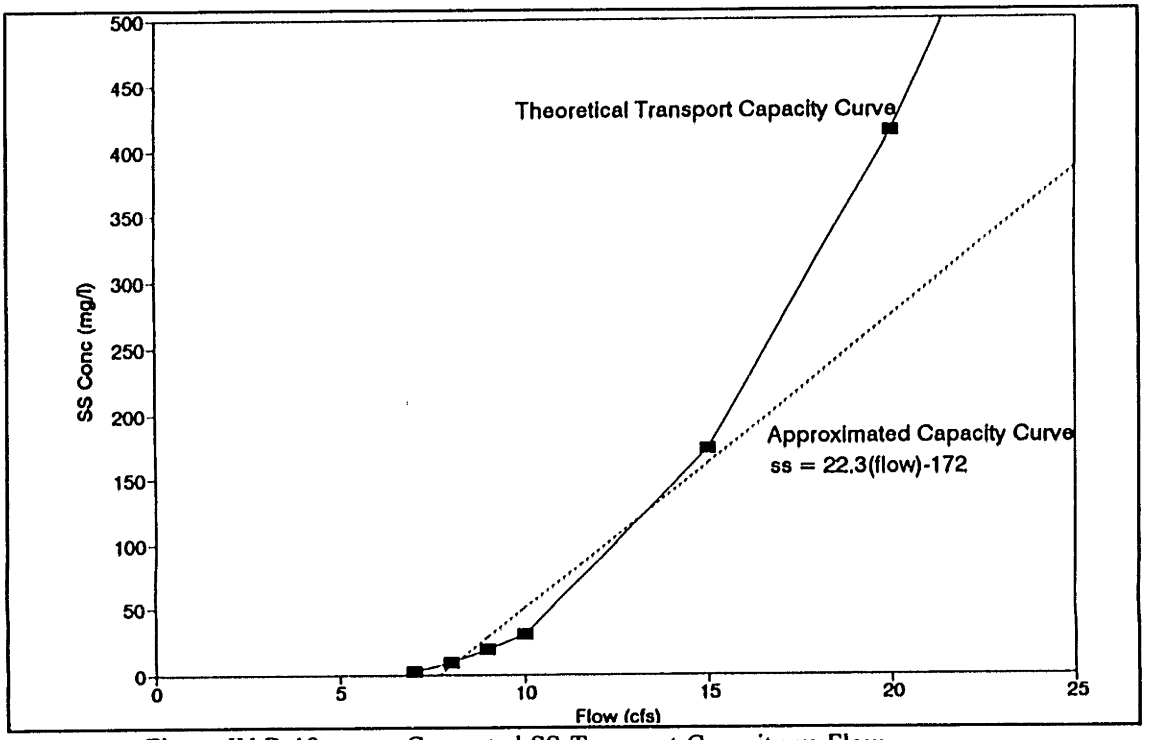

Figure IV.D-19: Computed SS Transport Capacity vs Flow
USGS Station, Gage #5, (Flows < 25 cfs)

APPENDIX IV.E

As, Fe, Cr, and Cu:
Detailed Data Tables,
Evaluation of Individual Storms,
and Supplemental Figures for Section IV.4.2

DETAILED DATA TABLES

Metal concentrations and fluxes of each sample are provided in tables IV.E-1 to IV.E-20 in appendix IV.E. For reference each table also provides values of streamflow and suspended sediment concentrations corresponding to each sample. The filter pore size used to separate the samples into dissolved and particulate phases is provided at the top of each column. All data plots, however, correspond to samples filtered through 0.5 μm pore size filters.

fn: met1

Date/Time YR-MO-DA-H	Flow (cfs)	SS Conc (mg/L) (0.5um)	SS Conc (mg/L) (1.5um)	Particulate SS As Conc (mg/kg) (0.5um)	Particulate SS As Conc (ug/l) (0.5um)	Particulate SS As Flux (g/hr) (0.5um)	Dissolved DS As Conc (ug/l) (0.5um)	Dissolved DS As Flux (g/hr) (0.5um)
Wedge Pond								
91041516	5.0							
91052015	1.3							
91052413	0.0		15.9					
91052814	2.7		1.5					
91060713	0.9		15.1					
91071613	1.3	12.8	5.5					
91082011	12.0	10.8	10.7					
91082210*	10.2	5.1	3.3					
91092110	1.6	8.9	10.7					
91110210	10.2	8.3	7.9					
91122111	6.6	5.9	5.3					
92011512	11.2		4.4					
92022214	8.9	3.2	3.5	16	0.05	0.05	0.50	0.45
92032915	17.4	6.5	6.2	17	0.11	0.20	0.50	0.89
92041814	14.0	8.4	8.1	20	0.17	0.24	0.47	0.67
92052209	1.4	7.6	2.8	14	0.11	0.01	0.70	0.10
92061115	7.0	3.5	3.4	20	0.07	0.05	0.47	0.33
92072316	1.2	7.3	6.0	26	0.19	0.02	2.10	0.25
92081314	0.9	11.4	6.0	33	0.38	0.03	2.29	0.20
92092714	5.2	7.1	7.1	24	0.17	0.09	1.23	0.65
92101213	13.3	6.2	7.3	24	0.15	0.20	1.33	1.80
92110114	1.2	4.7	4.6	43	0.20	0.02	2.16	0.26
92121715	17.9	4.0	4.4	7	0.03	0.05	1.46	2.67
93012511	12.7	3.1	3.2	17	0.05	0.07	1.30	1.68

* Reverse Flow Direction
BQ: Below Limit of Quantification

Table IV.E-1: Arsenic Measurements at Gage #1, Wedge Pond

fn: met2

Date/Time YR-MO-DA-HR	Flow (cfs)	SS Conc (mg/L) (0.5um)	SS Conc (mg/L) (1.5um)	Particulate SS As Conc (mg/kg) (0.5um)	Particulate SS As Conc (ug/l) (0.5um)	Particulate SS As Flux (g/hr) (0.5um)	Dissolved DS As Conc (ug/l) (0.5um)	Dissolved DS As Flux (g/hr) (0.5um)
Rte 128								
91032911	9.3							
91041512	4.9							
91053013	5.0		2.8					
91060710	4.0		5.3					
91062010	6.3	5.7	4.4					
91071610	3.1	6.3	5.7					
91072610	0.8	6.3	4.4					
91081310	2.2	7.3	6.5					
91082110	31.0	7.9	7.3					
91092114	8.2	9.1	7.1					
91110213	12.7	7.7	4.5					
91121711	8.0		3.5					
92011509	13.0		4.8					
92022209	7.2	6.7	4.7	739	4.93	3.63	6.62	4.88
92032915	17.6	5.2	3.9	625	3.24	5.82	3.18	5.71
92041809	13.8	3.6	3.6	705	2.52	3.55	6.28	8.85
92052215	4.4	6.5	5.7	1287	8.37	3.79	7.82	3.54
92061110	7.1	9.0	7.8	905	8.11	5.89	9.99	7.26
92072309	2.0	11.2	11.0	1368	15.31	3.07	8.75	1.76
92081309	2.6	7.6	7.4	1058	8.05	2.12	7.03	1.85
92092709	10.4	8.5	6.7	805	6.82	7.24	6.70	7.11
92101209	16.4	6.7	6.4	781	5.26	8.77	2.50	4.17
92110109	2.4	4.8	5.4	1116	5.35	1.30	9.03	2.19
92121710	18.3	12.6	13.7	181	2.29	4.26	6.25	11.63
93012509	14.6	4.8	1.3	658	3.16	4.70	10.57	15.72
93052509	5.3	6.2					0.90	0.48

Table IV.E-2: Arsenic Measurements at Gage #2, Route 128

fn: met3

Date/Time YR-MO-DA-HR	Flow (cfs)	SS Conc (mg/L) (0.5um)	SS Conc (mg/L) (1.5um)	Particulate SS As Conc (mg/kg) (0.5um)	SS As Conc (ug/l) (0.5um	SS As Flux (g/hr) (0.5um	Dissolved DS As Conc (ug/l) (0.5um)	DS As Flux (g/hr) (0.5um
Montvale								
91032914	16.1							
91041510	8.9							
91052011	9.8		3.30					
91052410	10.0		3.00					
91052811	17.8		5.60					
91053010	7.2		2.80					
91060715	5.4		2.00					
91071616	4.2	2.40	1.90					
91072616	2.2	1.70	1.20					
91081316	3.1	2.70	1.70					
91082016	88.0	7.94	6.40					
91082016	88.0	8.23						
91082016	88.0	8.53						
91082215	26.1	3.87	2.40					
91092113	16.6	4.81	4.60					
91110212	26.3	3.20	1.90					
91122113	16.5	8.08	8.00					
92011510	31.1		5.70					
92022211	8.7	6.85	5.90	994	6.81	6.03	4.10	3.63
92032909	34.8	3.71	2.50	557	2.07	7.32	3.70	13.11
92041810	31.0	3.51	3.00	491	1.72	5.45	2.39	7.55
92052214	8.6	5.75	4.80	885	5.09	4.48	5.37	4.73
92061112	12.3	8.15	5.50	782	6.37	7.96	7.26	9.07
92072311	3.9	4.22	3.20	1151	4.86	1.93	4.19	1.67
92081310	6.9	4.29	2.80	1244	5.34	3.78	3.94	2.79
92092711	20.9	6.91	5.60	768	5.31	11.32	2.69	5.74
92101210	26.7	12.98	12.60	745	9.67	26.34	3.21	8.74
92110110	4.5	3.23	2.10	1195	3.86	1.79	5.39	2.49
92121711	30.9	18.71	8.00	309	5.78	18.21	4.09	12.88
93012510	11.9	3.70	3.20	492	1.82	2.21	4.17	5.06

Table IV.E-3: Arsenic Measurements at Gage #3, Montvale

fn: met4

Date/Time YR-MO-DA-HR	Flow (cfs)	SS Conc (mg/L) (0.5um)	SS Conc (mg/L) (1.5um)	Particulate SS As Conc (mg/kg) (0.5um)	Particulate SS As Conc (ug/l) (0.5um)	Particulate SS As Flux (g/hr) (0.5um)	Dissolved DS As Conc (ug/l) (0.5um)	Dissolved DS As Flux (g/hr) (0.5um)
Horn Pond								
91052416	5.7		1.40					
91052814	10.5		5.40					
91060712	4.7		11.10					
91071611	2.0	4.50	4.80					
91072613	1.2	1.20	1.20					
91081313	1.6	3.70	2.60					
91082013	21.6	20.60	19.60					
91082211	9.6	4.57	3.90					
91092111	4.5	5.95	6.70					
92022213	7.5	2.24	1.50	8.0	0.018	0.014	0.50	0.38
92032914	16.4	4.70	4.70	6.0	0.028	0.047	0.50	0.84
92041812	15.0	2.05	1.90	4.0	0.008	0.012	0.27	0.41
92052211	5.1	5.11	3.70	9.0	0.046	0.024	0.16	0.08
92061114	6.1	3.54	3.60	1.0	0.004	0.002	0.43	0.27
92072313	2.6	3.10	2.70	15.0	0.047	0.012	0.34	0.09
92081312	3.2	2.39	2.40	BQ	BQ	BQ	0.36	0.12
92092712	9.1	12.25	11.50	52.0	0.637	0.588	0.47	0.43
92101212	17.9	10.14	9.60	14.0	0.142	0.259	0.12	0.22
92110112	3.3	0.77	0.60	21.0	0.016	0.005	0.18	0.06
92121712	44.1	2.41	2.10	16.0	0.039	0.173	0.15	0.67
93012511	20.1	2.80	2.60	15.0	0.042	0.086	0.15	0.31

BQ: Below Limit of Quantification

Table IV.E-4: Arsenic Measurements at Gage #4, Horn Pond

fn: met5

Date/Time YR-MO-DA-HR	Flow (cfs)	SS Conc (mg/L) (0.5um)	SS Conc (mg/L) (1.5um)	Particulate SS As Conc (mg/kg) (0.5um)	Particulate SS As Conc (ug/l) (0.5um)	Particulate SS As Flux (g/hr) (0.5um)	Dissolved DS As Conc (ug/l) (0.5um)	Dissolved DS As Flux (g/hr) (0.5um)
USGS								
91052415	12.1		3.40					
91052812	18.8		5.40					
91060714	26.7		1.80					
91062012	13.5	4.80	4.40					
91071615	6.1	2.50	2.20					
91072615	3.1	1.30	0.80					
91081314	4.3	2.00	1.80					
91082009	139.5	9.95	8.55					
91082114	95.7	7.42	6.90					
91082209	9.2	7.77	4.50					
91082209	12.6	8.10						
91082209	14.4	9.20						
91092109	26.2	3.72	2.90					
91110209	45.5	4.34	3.90					
91122109	32.4	4.95	4.40					
92011513	45.0		4.40					
92022215	23.0	3.45	3.00	332	1.15	2.69	3.13	7.35
92032912	57.2	4.28	3.60	204	0.87	5.09	1.95	11.37
92041815	49.0	4.55	4.30	238	1.08	5.41	1.40	6.99
92052208	12.6	4.23	3.80	489	2.07	2.65	2.67	3.42
92061117	22.4	4.48	4.00	375	1.68	3.83	5.08	11.59
92072315	5.8	1.75	1.50	720	1.26	0.74	3.35	1.98
92072922	74.4	34.3		206	7.05	53.49	1.61	12.22
92081008	35.6	5.6		363	2.03	7.37	3.52	12.77
92081010	34.9	5.0		424	2.12	7.54	3.12	11.09
92081012	32.4	4.6		446	2.05	6.77	3.06	10.11
92081014	30.8	4.4		463	2.04	6.39	3.29	10.33
92081016	28.5	4.4		449	1.97	5.74	2.14	6.22
92081018	27.1	4.9		497	2.43	6.71	3.33	9.19
92081020	25.0	4.6		503	2.31	5.89	2.10	5.35
92081022	23.7	5.1		495	2.53	6.09	2.05	4.95
92081100	22.4	4.6		532	2.45	5.59	1.94	4.43
92081102	20.6	5.5		501	2.76	5.77	2.00	4.19
92081104	19.4	4.9		512	2.51	4.96	1.84	3.63
92081315	8.8	2.14	2.10	694	1.49	1.33	3.69	3.31

BQ: Below Limit of Quantification

Table IV.E-5: Arsenic Measurements at Gage #5, USGS

Date/Time YR-MO-DA-HR	Flow (cfs)	SS Conc (mg/L) (0.5um)	SS Conc (mg/L) (1.5um)	Particulate SS As Conc (mg/kg) (0.5um)	Particulate SS As Conc (ug/l) (0.5um)	Particulate SS As Flux (g/hr) (0.5um)	Dissolved DS As Conc (ug/l) (0.5um)	Dissolved DS As Flux (g/hr) (0.5um)
92081801	75.9	17.1		197	3.37	26.12	2.22	17.19
92081802	144.0	60.3		68	4.08	59.83	2.41	35.38
92081803	159.5	50.4		94	4.73	76.95	1.81	29.43
92081804	196.7	61.3		99	6.06	121.42	1.95	39.10
92081805	227.7	69.4					1.89	42.91
92081806	202.9	42.0		110	4.62	95.57	1.91	39.50
92081807	196.7	32.2		150	4.83	96.74	1.65	33.08
92081808	178.5	25.5		122	3.12	56.81	1.94	35.30
92081809	168.9	22.4		153	3.43	59.02	2.23	38.40
92081810	164.1	20.5		151	3.10	51.93	1.98	33.13
92081811	161.8	23.0		180	4.13	68.12	1.95	32.16
92081812	166.4	21.5		170	3.66	62.16	1.90	32.23
92081813	159.5	20.3		155	3.14	51.10	3.12	50.65
92081814	157.2	19.2		183	3.51	56.20	1.99	31.90
92081815	152.7	17.7		168	2.97	46.25	2.11	32.85
92081816	148.0	17.4		192	3.33	50.30	2.28	34.40
92081817	144.0	14.9		146	2.18	31.96	2.00	29.36
92081818	139.5	14.2		219	3.11	44.16	2.06	29.29
92081819	135.1	12.6		185	2.33	32.04	2.19	30.16
92081820	130.8	13.0		237	3.08	40.99	2.28	30.39
92081821	126.5	11.9		235	2.79	35.99	2.04	26.31
92081822	122.4	10.9		177	1.92	24.00	2.24	27.95
92081823	118.3	10.4		212	2.21	26.62	2.15	25.94
92081900	114.4	10.4		273	2.84	33.09	2.29	26.70
92092715	28.5	4.14	3.60	295	1.22	3.55	2.06	5.98
92101215	48.1	6.43	6.30	194	1.25	6.12	2.23	10.94
92110115	7.4	2.86	2.00	426	1.22	0.92	2.87	2.17
92112305	99.3	42.7		105	4.48	45.30	2.40	24.30
92112307	139.5	42.8		112	4.78	68.00	2.11	30.00
92112308	159.5	48.0		112	5.36	87.10	2.15	35.00
92112407	77.4	17.9		202	3.62	28.50	3.32	26.20
92121119	42.1	32.4		137	4.44	19.06	1.97	8.45
92121120	52.5	36.4		150	5.45	29.18	2.33	12.48
92121121	60.9	31.8		153	4.88	30.29	2.39	14.83
92121122	99.3	45.2		123	5.56	56.34	2.49	25.21
92121123	135.1	46.2		108	4.98	68.63	2.14	29.47
92121200	157.2	50.5		118	5.94	95.24	1.90	30.45
92121201	171.2	51.4		115	5.89	102.73	1.48	25.83
92121202	196.7	47.3		105	4.99	100.02	1.40	28.07
92121203	200.5	45.2		120	5.41	110.55	1.79	36.58
92121204	207.7	41.8		109	4.54	96.11	1.26	26.68
92121205	215.1	40.4		118	4.75	104.21	1.22	26.76
92121206	212.7	35.5		114	4.05	87.71	1.27	27.53
92121207	210.2	30.1		129	3.90	83.46	1.24	26.57
92121208	200.5	26.1		165	4.30	87.87	1.28	26.16
92121209	191.0	19.6		183	3.58	69.74	1.47	28.62
92121210	188.5	16.1		137	2.21	42.41	1.43	27.47
92121216	159.5	8.8		162	1.42	23.12	1.93	31.38
92121217	152.7	7.8		165	1.28	20.00	2.27	35.34
92121218	150.5	7.2		158	1.14	17.46	2.40	36.83

BQ: Below Limit of Quantification

Table IV.E-5; (con'd)

fn: met5

Date/Time YR-MO-DA-HR	Flow (cfs)	SS Conc (mg/L) (0.5um)	SS Conc (mg/L) (1.5um)	Particulate SS As Conc (mg/kg) (0.5um)	Particulate SS As Conc (ug/l) (0.5um)	Particulate SS As Flux (g/hr) (0.5um)	Dissolved DS As Conc (ug/l) (0.5um)	Dissolved DS As Flux (g/hr) (0.5um)
92121713	82.2	15.30	14.20	92	1.41	11.80	4.09	34.28
93012513	47.1	7.40	7.10	139	1.03	4.93	3.05	14.63
93032614	87.1	23.3		95	2.22	19.73	1.30	11.55
93032615	141.7	19.2		53	1.02	14.79	1.71	24.70
93032616	101.1	21.8		41	0.89	9.19	1.39	14.33
93032617	144.0	21.3		70	1.49	21.82	1.53	22.46
93032618	126.5	22.6		41	0.92	11.84	1.25	16.12
93032619	71.5	20.2		47	0.96	6.98	1.24	9.03
93032620	66.0	15.8		20	0.32	2.15	1.59	10.70
93032910	264.2	35.5		144	5.12	137.89	0.95	25.59
93032911	272.2	21.1		145	3.06	84.86	1.29	35.80
93032912	285.8	25.4		212	5.40	157.23	1.22	35.54
93032913	311.3	34.9		163	5.67	180.04	1.26	39.98
93032914	339.5	59.1		134	7.90	273.28	1.25	43.26
93032915	362.2	55.9		117	6.55	241.72	1.95	72.00
93032916	391.7	70.7		97	6.88	274.86	1.48	59.10
93032917	428.3	82.0		86	7.06	308.32	2.08	90.82
93032918	459.8	81.5		94	7.63	357.45	1.53	71.71
93032919	476.0	86.4		90	7.78	377.37	1.80	87.34
93032920	495.7	76.9		92	7.07	35? .4	1.74	87.93
93032921	499.1	73.8		83	6.14	312.23	1.69	85.98
93032922	499.1	62.2		87	5.39	274.08	2.01	102.27
93032923	502.4	61.4		88	5.40	276.61	1.78	91.16
93033000	492.4	51.3		85	4.36	218.65	1.93	96.88
93033001	479.2	42.1		87	3.68	179.57	1.90	92.81
93033002	469.5	26.4		86	2.28	109.04	1.87	89.50
93033008	453.4	18.9		83	1.58	72.90	1.98	91.52
93033119	308.4	9.9						
93040116	348.0	39.9						
93040117	359.4	19.5						
93040118	391.7	29.0						
93040119	410.0	39.0						
93040120	413.0	30.8						
93040121	356.5	18.1						
93040122	391.7	15.4						
93040123	385.7	10.5						
93040200	376.8	13.9						
93040217	291.4	5.7						
93052509	15.6	5.20					1.17	1.86

BQ: Below Limit of Quantification

Table IV.E-5: (con'd)

fn: met1

Date/Time YR-MO-DA-HR	Flow (cfs)	SS Con (mg/L) (0.5um)	SS Conc (mg/L) (1.5um)	Particulate SS Fe Conc (%) 0.5um	Particulate SS Fe Conc (mg/l) 0.5um	Particulate SS Fe Flux (g/hr) 0.5um	Dissolved DS Fe Conc (mg/l) 0.5um	Dissolved DS Fe Flux (g/hr) 0.5um	Particulate SS Fe Conc (%) 1.5um	Particulate SS Fe Conc (mg/l) 1.5um	Particulate SS Fe Flux (g/hr) 1.5um	Dissolved DS Fe Conc (mg/l) 1.5um	Dissolved DS Fe Flux (g/hr) 1.5um
Wedge Pond													
91041516	5.0												
91052015	1.3												
91052413	0.0		15.9										
91052814	2.7		1.5										
91060713	0.9		15.1										
91071613	1.3	12.8	5.5										
91082011	12.0	10.8	10.7	3.2	0.35	424							
91082210*	10.2	5.1	3.3	7.8	0.40	410							
91092110	1.6	8.9	10.7	1.1	0.09	15							
91110210	10.2	8.3	7.9	1.9	0.16	165							
91122111	6.6	5.9	5.3	4.0	0.24	160			4.5	0.24	161		
92011512	11.2		4.4						4.3	0.19	213		
92022214	8.9	3.2	3.5	2.8	0.09	82	0.24	218	2.3	0.08	74		
92032915	17.4	6.5	6.2	2.3	0.15	264	0.32	569	2.4	0.15	260		
92041814	14.0	8.4	8.1	2.4	0.20	286	0.15	215	2.7	0.22	312		
92052209	1.4	7.6	2.8	4.0	0.30	41	0.26	36	4.8	0.13	19		
92061115	7.0	3.5	3.4	2.8	0.10	70	0.12	85	3.5	0.12	85		
92072316	1.2	7.3	6.0	2.0	0.15	17	0.08	9	1.8	0.11	12	0.08	9
92081314	0.9	11.4	6.0	1.4	0.16	14	0.12	11	1.5	0.09	8	0.12	11
92092714	5.2	7.1	7.1	1.6	0.11	61	0.06	32				0.04	21
92101213	13.3	6.2	7.3	2.5	0.16	210	0.11	149				0.08	108
92110114	1.2	4.7	4.6	3.3	0.16	19	0.13	16				0.11	13
92121715	17.9	4.0	4.4	2.7	0.11	199	0.18	329				0.20	365
93012511	12.7	3.1	3.2	3.7	0.12	149	0.24	310				0.23	297

* Reverse Flow Direction
BQ: Below Limit of Quantification

Table IV.E-6: Iron Measurements at Gage #1, Wedge Pond

fn: met2

Date/Time YR-MO-DA-HR	Flow (cfs)	SS Conc (mg/L) (0.5um)	SS Conc (mg/L) (1.5um)	Particulate SS Fe Conc (%) 0.5um	Particulate SS Fe Conc (mg/l) 0.5um	Particulate SS Fe Flux (g/hr) 0.5um	Dissolved DS Fe Conc (mg/l) 0.5um	Dissolved DS Fe Flux (g/hr) 0.5um	Particulate SS Fe Conc (%) 1.5um	Particulate SS Fe Conc (mg/l) 1.5um	Particulate SS Fe Flux (g/hr) 1.5um	Dissolved DS Fe Conc (mg/l) 1.5um	Dissolved DS Fe Flux (g/hr) 1.5um
Rte 128													
91032911	9.3												
91041512	4.9												
91053013	5.0		2.8										
91060710	4.0		5.3										
91062010	6.3	5.7	4.4										
91071610	3.1	6.3	5.7										
91072610	0.8	6.3	4.4										
91081310	2.2	7.3	6.5										
91082110	31.0	7.9	7.3	20.5	1.62	5110							
91092114	8.2	9.1	7.1	16.0	1.46	1213							
91110213	12.7	7.7	4.5	9.3	0.72	932							
91121711	8.0		3.5						16.3	0.57	465		
92011509	13.0		4.8						13.3	0.64	842		
92022209	7.2	6.7	4.7	12.3	0.82	607	0.86	634	14.2	0.67	492		
92032915	17.6	5.2	3.9	11.7	0.61	1090	0.66	1185	14.5	0.57	1015		
92041809	13.8	3.6	3.6	11.9	0.43	600	0.61	859	11.8	0.43	599		
92052215	4.4	6.5	5.7	15.2	0.99	447	1.00	453	15.9	0.91	410		
92061110	7.1	9.0	7.8	12.1	1.09	789	1.50	1090	13.0	1.01	737		
92072309	2.0	11.2	11.0	16.0	1.79	360	0.88	177	20.1	2.21	443	0.44	88
92081309	2.6	7.6	7.4	16.1	1.22	322	0.86	226	18.3	1.36	357	1.10	289
92092709	10.4	8.5	6.7	12.7	1.08	1141	0.48	509				0.50	531
92101209	16.4	6.7	6.4	10.6	0.71	1192	0.29	484				0.30	501
92110109	2.4	4.8	5.4	18.5	0.88	215	0.84	204				0.42	102
92121710	18.3	12.6	13.7	5.3	0.68	1257	0.84	1564				0.80	1489
93012509	14.6	4.8	1.3	11.4	0.55	815	0.47	699				0.62	922
93052509	5.3	6.2											

Table IV.E-7: Iron Measurements at Gage #2, Route 128

fn: met3

Date/Time YR-MO-DA-HR	Flow (cfs)	SS Conc (mg/L) (0.5um)	SS Conc (mg/L) (1.5um)	Particulate SS Fe Conc (%) 0.5um	Particulate SS Fe Conc (mg/l) 0.5um	Particulate SS Fe Flux (g/hr) 0.5um	Dissolved DS Fe Conc (mg/l) 0.5um	Dissolved DS Fe Flux (g/hr) 0.5um	Particulate SS Fe Conc (%) 1.5um	Particulate SS Fe Conc (mg/l) 1.5um	Particulate SS Fe Flux (g/hr) 1.5um	Dissolved DS Fe Conc (mg/l) 1.5um	Dissolved DS Fe Flux (g/hr) 1.5um
Montvale													
91032914	16.1												
91041510	8.9												
91052011	9.8		3.30										
91052410	10.0		3.00										
91052811	17.8		5.60										
91053010	7.2		2.80										
91060715	5.4		2.00										
91071616	4.2	2.40	1.90										
91072616	2.2	1.70	1.20										
91081316	3.1	2.70	1.70										
91082016	88.0	7.94	6.40	23.1	1.84	16479							
91082016	88.0	8.23		20.7	1.70	15287							
91082016	88.0	8.53		19.2	1.63	14654							
91082215	26.1	3.87	2.40	10.6	0.41	1091							
91092113	16.6	4.81	4.60	14.4	0.69	1167							
91110212	26.3	3.20	1.90	11.8	0.38	1012							
91122113	16.5	8.08	8.00	10.5	0.84	1423			9.29	0.74	1252		
92011510	31.1		5.70						10.94	0.62	1976		
92022211	8.7	6.85	5.90	11.2	0.77	683	0.61	540	11.64	0.69	608		
92032909	34.8	3.71	2.50	8.9	0.33	1166	0.39	1382	9.78	0.24	867		
92041810	31.0	3.51	3.00	9.1	0.32	1004	0.35	1106	9.61	0.29	911		
92052214	8.6	5.75	4.80	12.0	0.69	610	0.74	652	12.47	0.60	527		
92061112	12.3	8.15	5.50	9.7	0.79	984	1.10	1374	11.67	0.64	802		
92072311	3.9	4.22	3.20	14.8	0.63	249	0.52	207	15.90	0.51	202	0.84	334
92081310	6.9	4.29	2.80	13.8	0.59	418	0.50	354				0.88	623
92092711	20.9	6.91	5.60	9.6	0.66	1414	0.30	640				0.33	704
92101210	26.7	12.98	12.60	9.2	1.19	3243	0.36	981				0.31	844
92110110	4.5	3.23	2.10	15.5	0.50	232	0.38	176				0.43	199
92121711	30.9	18.71	8.00	6.4	1.19	3743	0.73	2299				0.53	1669
93012510	11.9	3.70	3.20	12.2	0.45	548	0.32	388				0.40	485

Table IV.E-8: Iron Measurements at Gage #3, Montvale

fn: met4

Date/Time YR-MO-DA-HR	Flow (cfs)	SS Conc (mg/L) (0.5um)	SS Conc (mg/L) (1.5um)	Particulate SS Fe Conc (%) 0.5um	Particulate SS Fe Conc (mg/l) 0.5um	Particulate SS Fe Flux (g/hr) 0.5um	Dissolved DS Fe Conc (mg/l) 0.5um	Dissolved DS Fe Flux (g/hr) 0.5um	Particulate SS Fe Conc (%) 1.5um	Particulate SS Fe Conc (mg/l) 1.5um	Particulate SS Fe Flux (g/hr) 1.5um	Dissolved DS Fe Conc (mg/l) 1.5um	Dissolved DS Fe Flux (g/hr) 1.5um
Horn Pond													
91052416	5.7		1.40										
91052814	10.5		5.40										
91060712	4.7		11.10										
91071611	2.0	4.50	4.80										
91072613	1.2	1.20	1.20										
91081313	1.6	3.70	2.60										
91082013	21.6	20.60	19.60	2.80	0.58	1270							
91082211	9.6	4.57	3.90	3.36	0.15	150							
91092111	4.5	5.95	6.70	3.75	0.22	101							
92022213	7.5	2.24	1.50	5.12	0.11	88	0.20	154	5.65	0.08	65		
92032914	16.4	4.70	4.70	3.16	0.15	248	0.23	385	3.09	0.15	243		
92041812	15.0	2.05	1.90	3.84	0.08	120	0.18	274	3.78	0.07	109		
92052211	5.1	5.11	3.70	3.10	0.16	83	0.12	63	3.31	0.12	64		
92061114	6.1	3.54	3.60	3.79	0.13	83	0.30	186	3.30	0.12	74		
92072313	2.6	3.10	2.70	4.50	0.14	36	0.24	63	4.45	0.12	31	0.28	73
92081312	3.2	2.39	2.40	4.12	0.10	32	0.21	69				0.26	85
92092712	9.1	12.25	11.50	3.47	0.43	392	0.25	226				0.23	212
92101212	17.9	10.14	9.60	3.99	0.40	738	0.21	383				0.17	310
92110112	3.3	0.77	0.60	6.64	0.05	17	0.14	47				0.14	47
92121712	44.1	2.41	2.10	4.30	0.10	466	0.22	989				0.21	945
93012511	20.1	2.80	2.60	5.91	0.17	339	0.26	532				0.22	451

BQ: Below Limit of Quantification

Table IV.E-9: Iron Measurements at Gage #4, Horn Pond

fn: met5

Date/Time YR-MO-DA-HR	Flow (cfs)	SS Conc (mg/L) (0.5um)	SS Conc (mg/L) (1.5um)	Particulate SS Fe Conc (%) 0.5um	Particulate SS Fe Conc (mg/l) 0.5um	Particulate SS Fe Flux (g/hr) 0.5um	Dissolved DS Fe Conc (mg/l) 0.5um	Dissolved DS Fe Flux (g/hr) 0.5um	Particulate SS Fe Conc (%) 1.5um	Particulate SS Fe Conc (mg/l) 1.5um	Particulate SS Fe Flux (g/hr) 1.5um	Dissolved DS Fe Conc (mg/l) 1.5um	Dissolved DS Fe Flux (g/hr) 1.5um
USGS													
91052415	12.1		3.40										
91052812	18.8		5.40										
91060714	26.7		1.80										
91062012	13.5	4.80	4.40										
91071615	6.1	2.50	2.20										
91072615	3.1	1.30	0.80										
91081314	4.3	2.00	1.80										
91082009	139.5	9.95	8.55	10.5									
91082114	95.7	7.42	6.90	7.0									
91082209	9.2	7.77	4.50										
91082209	12.6	8.10		5.8									
91082209	14.4	9.20		5.1									
91092109	26.2	3.72	2.90	8.0									
91110209	45.5	4.34	3.90	6.1									
91122109	32.4	4.95	4.40	8.2	0.41	1341			7.4	0.33	1075		
92011513	45.0		4.40						7.4	0.33	1503		
92022215	23.0	3.45	3.00	7.4	0.26	599	0.39	915	7.9	0.24	555		
92032912	57.2	4.28	3.60	5.5	0.24	1375	0.31	1808	4.1	0.15	865		
92041815	49.0	4.55	4.30	5.4	0.25	1233	0.29	1449	5.8	0.25	1247		
92052208	12.6	4.23	3.80	12.7	0.54	689	0.47	601	14.6	0.56	711		
92061117	22.4	4.48	4.00	9.3	0.42	952	0.86	1963	9.7	0.39	887		
92072315	5.8	1.75	1.50	14.6	0.26	151	0.39	231	12.9	0.19	115	0.50	296
92072922	74.4	34.3		5.4	1.84	13992	0.24	1821					
92081008	35.6	5.6		6.4	0.36	1307	0.17	617					
92081010	34.9	5.0		7.2	0.36	1285	0.16	569					
92081012	32.4	4.6		9.3	0.43	1408	0.21	694					
92081014	30.8	4.4		10.0	0.44	1380	0.25	785					
92081016	28.5	4.4		10.9	0.48	1398	0.33	959					
92081018	27.1	4.9		11.3	0.56	1532	0.35	965					
92081020	25.0	4.6		11.9	0.55	1396	0.31	790					
92081022	23.7	5.1		10.9	0.56	1343	0.26	627					
92081100	22.4	4.6		12.7	0.59	1338	0.31	708					
92081102	20.6	5.5		12.7	0.70	1468	0.31	649					
92081104	19.4	4.9		13.4	0.65	1292	0.34	671					
92081315	8.8	2.14	2.10	10.5	0.23	202	0.46	413	10.7	0.22	202	0.50	449

BQ: Below Limit of Quantification

Table IV.E-10: Iron Measurements at Gage #5, USGS

Date/Time YR-MO-DA-HR	Flow (cfs)	SS Conc (mg/L) (0.5um)	SS Conc (mg/L) (1.5um)	Particulate SS Fe Conc (%) 0.5um	Particulate SS Fe Conc (mg/l) 0.5um	Particulate SS Fe Flux (g/hr) 0.5um	Dissolved DS Fe Conc (mg/l) 0.5um	Dissolved DS Fe Flux (g/hr) 0.5um	Particulate SS Fe Conc (%) 1.5um	Particulate SS Fe Conc (mg/l) 1.5um	Particulate SS Fe Flux (g/hr) 1.5um	Dissolved DS Fe Conc (mg/l) 1.5um	Dissolved DS Fe Flux (g/hr) 1.5um
92081801	75.9	17.1		4.4	0.74	5756	0.22	1703					
92081802	144.0	60.3		3.5	2.13	31257	0.21	3083					
92081803	159.5	50.4		4.1	2.08	33745	0.19	3090					
92081804	196.7	61.3		4.5	2.76	55416	0.20	4010					
92081805	222.7	69.4					0.16	3633					
92081806	202.9	42.0		4.4	1.85	38346	0.14	2895					
92081807	196.7	32.2		4.4	1.40	28118	0.15	3007					
92081808	178.5	25.5		4.4	1.11	20244	0.18	3275					
92081809	168.9	22.4		4.3	0.97	16343	0.18	3099					
92081810	164.1	20.5		4.3	0.89	14831	0.18	3011					
92081811	161.8	23.0		4.8	1.11	18283	0.17	2804					
92081812	166.4	21.5		5.1	1.10	18703	0.19	3223					
92081813	159.5	20.3		4.8	0.97	15712	0.24	3903					
92081814	157.2	19.2		4.7	0.90	14379	0.18	2885					
92081815	152.7	17.7		4.8	0.85	13240	0.19	2958					
92081816	148.0	17.4		4.7	0.82	12389	0.19	2867					
92081817	144.0	14.9		5.0	0.75	10967	0.21	3083					
92081818	139.5	14.2		5.3	0.75	10653	0.22	3128					
92081819	135.1	12.6		5.2	0.66	9073	0.24	3305					
92081820	130.8	13.0		5.2	0.67	8937	0.26	3466					
92081821	126.5	11.9		5.5	0.65	8375	0.28	3612					
92081822	122.4	10.9		5.6	0.61	7643	0.29	3618					
92081823	118.3	10.4		5.9	0.61	7387	0.25	3016					
92081900	114.4	10.4		6.5	0.67	7822	0.31	3614					
92092715	28.5	4.14	3.60	6.2	0.26	742	0.23	668				0.22	639
92101215	48.1	6.43	6.30	5.2	0.34	1654	0.22	1079				0.20	981
92110115	7.4	2.86	2.00	10.5	0.30	226	0.32	241				0.37	279
92112305	99.3	42.7		4.1	1.74	17645	0.48	4860					
92112307	139.5	42.8		4.0	1.70	24152	0.32	4550					
92112308	159.5	48.0		3.6	1.72	27998	0.28	4553					
92112407	77.4	17.9		4.8	0.86	6819	0.64	5051					
92121119	42.1	32.4		4.6	1.49	6390	0.49	2102					
92121120	52.5	36.4		4.7	1.70	9081	0.49	2624					
92121121	60.9	31.8		4.6	1.47	9150	0.52	3227					
92121122	99.3	45.2		4.6	2.08	21106	0.44	4455					
92121123	135.1	46.2		4.4	2.03	27928	0.34	4682					
92121200	157.2	50.5		4.6	2.33	37332	0.26	4167					
92121201	171.2	51.4		4.4	2.28	39715	0.20	3490					
92121202	196.7	47.3		4.7	2.22	44430	0.22	4411					
92121203	200.5	45.2		4.5	2.03	41461	0.20	4087					
92121204	207.7	41.8		4.7	1.95	41324	0.13	2753					
92121205	215.1	40.4		4.4	1.78	39101	0.15	3290					
92121206	212.7	35.5		4.5	1.60	34600	0.14	3035					
92121207	210.2	30.1		4.7	1.43	30599	0.15	3214					
92121208	200.5	26.1		4.8	1.26	25759	0.15	3065					
92121209	191.0	19.6		5.0	0.99	19188	0.18	3407					
92121210	188.5	16.1		5.0	0.81	15588	0.16	3074					
92121216	159.5	8.8		5.2	0.46	7423	0.26	4228					
92121217	152.7	7.8		5.6	0.43	6766	0.30	4671					
92121218	150.5	7.2		5.5	0.39	6018	0.29	4450					

BQ: Below Limit of Quantification

Table IV.E-10: (con'd)

fn: met5

Date/Time YR-MO-DA-HR	Flow (cfs)	SS Conc (mg/L) (0.5um)	SS Conc (mg/L) (1.5um)	Particulate SS Fe Conc (%) 0.5um	Particulate SS Fe Conc (mg/l) 0.5um	Particulate SS Fe Flux (g/hr) 0.5um	Dissolved DS Fe Conc (mg/l) 0.5um	Dissolved DS Fe Flux (g/hr) 0.5um	Particulate SS Fe Conc (%) 1.5um	Particulate SS Fe Conc (mg/l) 1.5um	Particulate SS Fe Flux (g/hr) 1.5um	Dissolved DS Fe Conc (mg/l) 1.5um	Dissolved DS Fe Flux (g/hr) 1.5um
92121713	82.2	15.30	14.20	4.3	0.66	5503	0.40	3352				0.40	3352
93012513	47.1	7.40	7.10	7.0	0.52	2476	0.23	1103				0.40	1919
93032614	87.1	23.3		3.8	0.88	7838	0.27	2398					
93032615	141.7	19.2		4.0	0.77	11099	0.27	3900					
93032616	101.1	21.8		4.3	0.94	9704	0.24	2473					
93032617	144.0	21.3		4.4	0.94	13871	0.27	3963					
93032618	126.5	22.6		4.7	1.06	13647	0.22	2837					
93032619	71.5	20.2		4.4	0.89	6449	0.22	1603					
93032620	66.0	15.8		4.6	0.72	4853	0.33	2220					
93032910	264.2	35.5		3.8	1.34	36072	0.24	6464					
93032911	272.2	21.1		4.3	0.91	25124	0.26	7215					
93032912	285.8	25.4		4.2	1.07	31136	0.27	7866					
93032913	311.3	34.9		4.3	1.49	47242	0.25	7934					
93032914	339.5	59.1		3.8	2.23	77236	0.25	8652					
93032915	362.2	55.9		3.9	2.19	80900	0.24	8861					
93032916	391.7	70.7		3.8	2.66	106055	0.23	9184					
93032917	428.3	82.0		3.9	3.23	141076	0.23	10042					
93032918	459.8	81.5		3.8	3.10	145325	0.23	10781					
93032919	476.0	86.4		3.9	3.39	164365	0.27	13101					
93032920	495.7	76.9		3.9	2.96	149552	0.28	14149					
93032921	499.1	73.8		3.6	2.66	135329	0.25	12720					
93032922	499.1	62.2		3.8	2.37	120384	0.29	14755					
93032923	502.4	61.4		3.8	2.34	119992	0.31	15877					
93033000	492.4	51.3		3.8	1.94	97517	0.31	15561					
93033001	479.2	42.1		3.7	1.56	76122	0.33	16120					
93033002	469.5	26.4		5.3	1.39	66555	0.36	17230					
93033008	453.4	18.9		5.5	1.04	47928	0.35	16177					
93033119	308.4	9.9					0.20	6288					
93040116	348.0	39.9					0.19	6740					
93040117	359.4	19.5											
93040118	391.7	29.0					0.20	7986					
93040119	410.0	39.0											
93040120	413.0	30.8					0.21	8841					
93040121	356.5	18.1											
93040122	391.7	15.4											
93040123	385.7	10.5					0.21	8257					
93040200	376.8	13.9											
93040217	291.4	5.7					0.23	6832					
93052509	15.6	5.20											

BQ: Below Limit of Quantification

Table IV.E-10: (con'd)

fn: met1

Date/Time YR-MO-DA-H	Flow (cfs)	SS Conc (mg/L) (0.5um)	SS Conc (mg/L) (1.5um)	Particulate SS Cr Conc (mg/kg) (0.5um)	Particulate SS Cr Conc (ug/l) (0.5um)	Particulate SS Cr Flux (g/hr) (0.5um)	Dissolved DS Cr Conc (ug/l) (0.5um)	Dissolved DS Cr Flux (g/hr) (0.5um)	Particulate SS Cr Conc (mg/kg) (1.5um)	Particulate SS Cr Conc (ug/l) (1.5um)	Particulate SS Cr Flux (g/hr) (1.5um)
Wedge Pond											
91041516	5.0										
91052015	1.3										
91052413	0.0		15.9								
91052814	2.7		1.5								
91060713	0.9		15.1								
91071613	1.3	12.8	5.5								
91082011	12.0	10.8	10.7	BQ	BQ	BQ					
91082210*	10.2	5.1	3.3	238	1.21	1.25					
91092110	1.6	8.9	10.7	BQ	BQ	BQ					
91110210	10.2	8.3	7.9	BQ	BQ	BQ					
91122111	6.6	5.9	5.3	310	1.83	1.23					
92011512	11.2		4.4						81	0.36	0.41
92022214	8.9	3.2	3.5	BQ	BQ	BQ	BQ	BQ	67	0.23	0.21
92032915	17.4	6.5	6.2	54	0.35	0.62	BQ	BQ			
92041814	14.0	8.4	8.1	BQ	BQ	BQ	BQ	BQ			
92052209	1.4	7.6	2.8	58	0.44	0.06	BQ	BQ	58	0.16	0.02
92061115	7.0	3.5	3.4	83	0.29	0.21	BQ	BQ	58	0.20	0.14
92072316	1.2	7.3	6.0	BQ	BQ	BQ	BQ	BQ	BQ	BQ	BQ
92081314	0.9	11.4	6.0	BQ	BQ	BQ	BQ	BQ	BQ	BQ	BQ
92092714	5.2	7.1	7.1	BQ	BQ	BQ	BQ	BQ			
92101213	13.3	6.2	7.3	BQ	BQ	BQ	BQ	BQ			
92110114	1.2	4.7	4.6	BQ	BQ	BQ	BQ	BQ			
92121715	17.9	4.0	4.4	BQ	BQ	BQ	BQ	BQ			
93012511	12.7	3.1	3.2	54	0.17	0.22	BQ	BQ			

* Reverse Flow Direction
BQ: Below Limit of Quantification

Table IV.E-11: Chromium Measurements at Gage #1, Wedge Pond

fn: met2

Date/Time YR-MO-DA-HR	Flow (cfs)	SS Conc (mg/L) (0.5um)	SS Conc (mg/L) (1.5um)	Particulate SS Cr Conc (mg/kg) (0.5um)	Particulate SS Cr Conc (ug/l) (0.5um)	Particulate SS Cr Flux (g/hr) (0.5um)	Dissolved DS Cr Conc (ug/l) (0.5um)	Dissolved DS Cr Flux (g/hr) (0.5um)	Particulate SS Cr Conc (mg/kg) (1.5um)	Particulate SS Cr Conc (ug/l) (1.5um)	Particulate SS Cr Flux (g/hr) (1.5um)
Rte 128											
91032911	9.3										
91041512	4.9										
91053013	5.0		2.8								
91060710	4.0		5.3								
91062010	6.3	5.7	4.4								
91071610	3.1	6.3	5.7								
91072610	0.8	6.3	4.4	349	2.20	0.18					
91081310	2.2	7.3	6.5								
91082110	31.0	7.9	7.3	393	3.10	9.81					
91092114	8.2	9.1	7.1	220	2.00	1.66					
91110213	12.7	7.7	4.5	259	2.00	2.60					
91121711	8.0		3.5						640	2.24	1.83
92011509	13.0		4.8						713	3.42	4.52
92022209	7.2	6.7	4.7	428	2.85	2.10	1.60	1.18	354	1.66	1.23
92032915	17.6	5.2	3.9	528	2.74	4.92	1.75	3.14	636	2.48	4.45
92041809	13.8	3.6	3.6	673	2.40	3.38	1.42	2.00	645	2.32	3.27
92052215	4.4	6.5	5.7	375	2.44	1.10	1.52	0.69	312	1.78	0.80
92061110	7.1	9.0	7.8	498	4.46	3.24	2.24	1.63	357	2.78	2.02
92072309	2.0	11.2	11.0	451	5.05	1.01	1.22	0.25	457	5.03	1.01
92081309	2.6	7.6	7.4	326	2.48	0.65	1.28	0.34			
92092709	10.4	8.5	6.7	245	2.08	2.20	0.89	0.94			
92101209	16.4	6.7	6.4	316	2.13	3.55	0.59	0.98			
92110109	2.4	4.8	5.4	239	1.14	0.28	1.38	0.33			
92121710	18.3	12.6	13.7	228	2.88	5.36	1.86	3.46			
93012509	14.6	4.8	1.3	288	1.38	2.06	0.98	1.46			
93052509	5.3	6.2									

Table IV.E-12: Chromium Measurements at Gage #2, Route 128

fn: met3

Date/Time YR-MO-DA-HR	Flow (cfs)	SS Conc (mg/L) (0.5um)	SS Conc (mg/L) (1.5um)	Particulate SS Cr Conc (mg/kg) (0.5um)	Particulate SS Cr Conc (ug/l) (0.5um	Particulate SS Cr Flux (g/hr) (0.5um	Dissolved DS Cr Conc (ug/l) (0.5um)	Dissolved DS Cr Flux (g/hr) (0.5um	Particulate SS Cr Conc (mg/kg) (1.5um)	Particulate SS Cr Conc (ug/l) (1.5u	Particulate SS Cr Flux (g/hr) (1.5u
Montvale											
91032914	16.1										
91041510	8.9										
91052011	9.8		3.30								
91052410	10.0		3.00								
91052811	17.8		5.60								
91053010	7.2		2.80								
91060715	5.4		2.00								
91071616	4.2	2.40	1.90								
91072616	2.2	1.70	1.20	304	0.52	0.1					
91081316	3.1	2.70	1.70								
91082016	88.0	7.94	6.40	298	2.37	21.2					
91082016	88.0	8.23		340	2.80	25.1					
91082016	88.0	8.53		180	1.54	13.8					
91082215	26.1	3.87	2.40	351	1.36	3.6					
91092113	16.6	4.81	4.60	391	1.88	3.2					
91110212	26.3	3.20	1.90	482	1.54	4.1					
91122113	16.5	8.08	8.00	735	5.94	10.0			235	1.88	3.17
92011510	31.1		5.70						1034	5.89	18.68
92022211	8.7	6.85	5.90	677	4.64	4.1	1.58	1.4	680	4.01	3.55
92032909	34.8	3.71	2.50	568	2.11	7.5	1.82	6.4	538	1.35	4.76
92041810	31.0	3.51	3.00	558	1.96	6.2	1.40	4.4	586	1.76	5.56
92052214	8.6	5.75	4.80	480	2.76	2.4	1.99	1.8	404	1.94	1.71
92061112	12.3	8.15	5.50	587	4.78	6.0	2.24	2.8	706	3.88	4.85
92072311	3.9	4.22	3.20	579	2.44	1.0	1.40	0.6	429	1.37	0.55
92081310	6.9	4.29	2.80	401	1.72	1.2	1.60	1.1			
92092711	20.9	6.91	5.60	630	4.35	9.3	1.30	2.8			
92101210	26.7	12.98	12.60	873	11.33	30.9	1.22	3.3			
92110110	4.5	3.23	2.10	304	0.98	0.5	1.33	0.6			
92121711	30.9	18.71	8.00	537	10.05	31.6	1.99	6.3			
93012510	11.9	3.70	3.20	444	1.64	2.0	1.17	1.4			

Table IV.E-13: Chromium Measurements at Gage #3, Montvale

fn: met4

Date/Time YR-MO-DA-HR	Flow (cfs)	SS Conc (mg/L) (0.5um)	SS Conc (mg/L) (1.5um)	Particulate SS Cr Conc (mg/kg) (0.5um)	Particulate SS Cr Conc (ug/l) (0.5um)	Particulate SS Cr Flux (g/hr) (0.5um)	Dissolved DS Cr Conc (ug/l) (0.5um)	Dissolved DS Cr Flux (g/hr) (0.5um)	Particulate SS Cr Conc (mg/kg) (1.5um)	Particulate SS Cr Conc (ug/l) (1.5um)	Particulate SS Cr Flux (g/hr) (1.5um)
Horn Pond											
91052416	5.7		1.40								
91052814	10.5		5.40								
91060712	4.7		11.10								
91071611	2.0	4.50	4.80								
91072613	1.2	1.20	1.20								
91081313	1.6	3.70	2.60								
91082013	21.6	20.60	19.60	55	1.13	2.49					
91082211	9.6	4.57	3.90	BQ	BQ	BQ					
91092111	4.5	5.95	6.70	BQ	BQ	BQ					
92022213	7.5	2.24	1.50	66	0.15	0.11	BQ	BQ			
92032914	16.4	4.70	4.70	69	0.32	0.54	BQ	BQ			
92041812	15.0	2.05	1.90	BQ	BQ	BQ	BQ	BQ			
92052211	5.1	5.11	3.70	50	0.26	0.13	BQ	BQ	44	0.16	0.09
92061114	6.1	3.54	3.60	BQ	BQ	BQ	BQ	BQ	49	0.18	0.11
92072313	2.6	3.10	2.70	BQ	BQ	BQ	BQ	BQ	65	0.18	0.05
92081312	3.2	2.39	2.40	BQ	BQ	BQ	BQ	BQ			
92092712	9.1	12.25	11.50	65	0.80	0.73	BQ	BQ			
92101212	17.9	10.14	9.60	75	0.76	1.39	BQ	BQ			
92110112	3.3	0.77	0.60	62	0.05	0.02	BQ	BQ			
92121712	44.1	2.41	2.10	BQ	BQ	BQ	BQ	BQ			
93012511	20.1	2.80	2.60	57	0.16	0.33	BQ	BQ			

BQ: Below Limit of Quantification

Table IV.E-14: Chromium Measurements at Gage #4, Horn Pond

fn: met5

Date/Time YR-MO-DA-HR	Flow (cfs)	SS Conc (mg/L) (0.5um)	SS Conc (mg/L) (1.5um)	Particulate SS Cr Conc (mg/kg) (0.5um)	Particulate SS Cr Conc (ug/l) (0.5um)	Particulate SS Cr Flux (g/hr) (0.5um)	Dissolved DS Cr Conc (ug/l) (0.5um)	Dissolved DS Cr Flux (g/hr) (0.5um)	Particulate SS Cr Conc (mg/kg) (1.5um)	Particulate SS Cr Conc (ug/l) (1.5um)	Particulate SS Cr Flux (g/hr) (1.5um)
USGS											
91052415	12.1		3.40								
91052812	18.8		5.40								
91060714	26.7		1.80								
91062012	13.5	4.80	4.40								
91071615	6.1	2.50	2.20								
91072615	3.1	1.30	0.80								
91081314	4.3	2.00	1.80								
91082009	139.5	9.95	8.55	256	2.55	36.2					
91082114	95.7	7.42	6.90	250	1.86	18.1					
91082209	9.2	7.77	4.50								
91082209	12.6	8.10		222	1.80	2.3					
91082209	14.4	9.20		219	2.01	3.0					
91092109	26.2	3.72	2.90	259	0.96	2.6					
91110209	45.5	4.34	3.90	237	1.03	4.8					
91122109	32.4	4.95	4.40	460	2.28	7.5			135	0.59	1.96
92011513	45.0		4.40	BQ	BQ	BQ			91	0.40	1.84
92022215	23.0	3.45	3.00	299	1.03	2.4	0.22	0.52			
92032912	57.2	4.28	3.60	220	0.94	5.5	0.44	2.57			
92041815	49.0	4.55	4.30	227	1.03	5.2	0.46	2.30	215	0.92	4.62
92052208	12.6	4.23	3.80	333	1.41	1.8	0.36	0.46	43	0.16	0.21
92061117	22.4	4.48	4.00	363	1.63	3.7	0.88	2.01	43	0.17	0.39
92072315	5.8	1.75	1.50	198	0.35	0.2	0.30	0.18	117	0.18	0.10
92072922	74.4	34.3		BQ	BQ	BQ	0.37	2.81			
92081008	35.6	5.6		127	0.71	2.6	0.85	3.08			
92081010	34.9	5.0		95	0.48	1.7	0.80	2.84			
92081012	32.4	4.6		155	0.71	2.4	0.84	2.77			
92081014	30.8	4.4		103	0.45	1.4	0.85	2.67			
92081016	28.5	4.4		84	0.37	1.1	0.92	2.67			
92081018	27.1	4.9		77	0.38	1.0	0.92	2.54			
92081020	25.0	4.6		101	0.46	1.2	0.92	2.34			
92081022	23.7	5.1		BQ	BQ	BQ	0.88	2.12			
92081100	22.4	4.6		102	0.47	1.1	0.91	2.08			
92081102	20.6	5.5		BQ	BQ	BQ	0.96	2.01			
92081104	19.4	4.9		96	0.47	0.9	0.95	1.88			
92081315	8.8	2.14	2.10	132	0.28	0.3	0.54	0.48	BQ	BQ	BQ

BQ: Below Limit of Quantification

Table IV.E-15: Chromium Measurements at Gage #5, USGS

Date/Time YR-MO-DA-HR	Flow (cfs)	SS Conc (mg/L) (0.5um)	SS Conc (mg/L) (1.5um)	Particulate SS Cr Conc (mg/kg) (0.5um)	Particulate SS Cr Conc (ug/l) (0.5um)	Particulate SS Cr Flux (g/hr) (0.5um)	Dissolved DS Cr Conc (ug/l) (0.5um)	Dissolved DS Cr Flux (g/hr) (0.5um)	Particulate SS Cr Conc (mg/kg) (1.5um)	Particulate SS Cr Conc (ug/l) (1.5um)	Particulate SS Cr Flux (g/hr) (1.5um)
92081801	75.9	17.1		130	2.23	17.3	0.85	6.58			
92081802	144.0	60.3		134	8.08	118.6	0.66	9.69			
92081803	159.5	50.4		221	11.12	180.8	0.76	12.36			
92081804	196.7	61.3		300	18.42	369.2	0.73	14.64			
92081805	222.7	69.4					0.47	10.67			
92081806	202.9	42.0		318	13.35	276.1	0.34	7.03			
92081807	196.7	32.2		298	9.60	192.4	0.36	7.22			
92081808	178.5	25.5		320	8.16	148.5	0.37	6.73			
92081809	168.9	22.4		266	5.95	102.4	0.76	13.09			
92081810	164.1	20.5		252	5.17	86.5	0.47	7.86			
92081811	161.8	23.0		289	6.65	109.7	0.51	8.41			
92081812	166.4	21.5		342	7.35	124.7	0.62	10.52			
92081813	159.5	20.3		327	6.64	108.0	1.54	25.04			
92081814	157.2	19.2		348	6.68	107.0	0.81	12.98			
92081815	152.7	17.7		332	5.87	91.4	0.75	11.68			
92081816	148.0	17.4		383	6.66	100.5	0.70	10.56			
92081817	144.0	14.9		298	4.44	65.2	0.78	11.45			
92081818	139.5	14.2		366	5.20	73.9	0.82	11.66			
92081819	135.1	12.6		294	3.71	51.0	0.76	10.47			
92081820	130.8	13.0		340	4.43	59.0	0.79	10.53			
92081821	126.5	11.9		377	4.48	57.8	0.68	8.77			
92081822	122.4	10.9		475	5.17	64.5	0.57	7.11			
92081823	118.3	10.4		211	2.19	26.4	0.65	7.84			
92081900	114.4	10.4		294	3.05	35.6	0.70	8.16			
92092715	28.5	4.14	3.60	331	1.37	4.0	0.35	1.02			
92101215	48.1	6.43	6.30	268	1.72	8.5	BQ	BQ			
92110115	7.4	2.86	2.00	228	0.65	0.5	0.37	0.28			
92112305	99.3	42.7		140	5.97	60.5	1.63	16.50			
92112307	139.5	42.8		171	7.30	103.8	0.83	11.80			
92112308	159.5	48.0		149	7.13	116.0	0.96	15.60			
92112407	77.4	17.9		124	2.22	17.5	1.05	8.30			
92121119	42.1	32.4		384	12.45	53.4	0.62	2.66			
92121120	52.5	36.4		366	13.34	71.4	0.69	3.70			
92121121	60.9	31.8		490	15.58	96.7	0.99	6.14			
92121122	99.3	45.2		406	18.34	185.7	0.68	6.88			
92121123	135.1	46.2		361	16.67	229.5	0.71	9.78			
92121200	157.2	50.5		378	19.08	305.8	1.02	16.35			
92121201	171.2	51.4		350	17.98	313.7	0.85	14.83			
92121202	196.7	47.3		368	17.39	348.6	1.01	20.25			
92121203	200.5	45.2		357	16.12	329.3	1.02	20.84			
92121204	207.7	41.8		379	15.83	335.2	0.61	12.92			
92121205	215.1	40.4		278	11.25	246.7	0.50	10.97			
92121206	212.7	35.5		298	10.57	229.1	0.51	11.06			
92121207	210.2	30.1		314	9.45	202.4	0.47	10.07			
92121208	200.5	26.1		340	8.89	181.6	0.45	9.20			
92121209	191.0	19.6		344	6.75	131.4	0.49	9.54			
92121210	188.5	16.1		240	3.86	74.2	0.49	9.41			
92121216	159.5	8.8		125	1.10	17.9	0.50	8.13			
92121217	152.7	7.8		214	1.67	26.0	0.45	7.01			
92121218	150.5	7.2		79	0.57	8.7	0.43	6.60			

BQ: Below Limit of Quantification

Table IV.E-15: (con'd)

fn: met5

Date/Time YR-MO-DA-HR	Flow (cfs)	SS Conc (mg/L) (0.5um)	SS Conc (mg/L) (1.5um)	Particulate SS Cr Conc (mg/kg) (0.5um)	Particulate SS Cr Conc (ug/l) (0.5um)	Particulate SS Cr Flux (g/hr) (0.5um)	Dissolved DS Cr Conc (ug/l) (0.5um)	Dissolved DS Cr Flux (g/hr) (0.5um)	Particulate SS Cr Conc (mg/kg) (1.5um)	Particulate SS Cr Conc (ug/l) (1.5um)	Particulate SS Cr Flux (g/hr) (1.5um)
92121713	82.2	15.30	14.20	261	3.99	33.5	0.46	3.86			
93012513	47.1	7.40	7.10	222	1.64	7.9	0.10	0.48			
93032614	87.1	23.3		198	4.60	40.9	0.65	5.77			
93032615	141.7	19.2		180	3.46	49.9	0.64	9.24			
93032616	101.1	21.8		132	2.88	29.7	0.63	6.49			
93032617	144.0	21.3		136	2.89	42.4	0.75	11.01			
93032618	126.5	22.6		128	2.89	37.2	0.60	7.74			
93032619	71.5	20.2		86	1.73	12.6	0.56	4.08			
93032620	66.0	15.8		152	2.39	16.1	1.16	7.80			
93032910	264.2	35.5		236	8.36	225.3	0.94	25.32			
93032911	272.2	21.1		241	5.09	141.1	1.08	29.97			
93032912	285.8	25.4		262	6.67	194.2	0.96	27.97			
93032913	311.3	34.9		279	9.73	308.7	0.91	28.88			
93032914	339.5	59.1		213	12.58	435.5	0.92	31.84			
93032915	362.2	55.9		258	14.41	532.0	0.95	35.08			
93032916	391.7	70.7		253	17.89	714.4	0.55	21.96			
93032917	428.3	82.0		253	20.76	906.6	0.58	25.32			
93032918	459.8	81.5		268	21.81	1022.3	0.62	29.06			
93032919	476.0	86.4		305	26.34	1278.2	0.64	31.06			
93032920	495.7	76.9		289	22.19	1121.2	0.77	38.91			
93032921	499.1	73.8		258	19.05	969.0	0.58	29.51			
93032922	499.1	62.2		288	17.88	909.8	0.83	42.23			
93032923	502.4	61.4		307	18.85	965.3	0.93	47.63			
93033000	492.4	51.3		267	13.71	688.0	0.81	40.66			
93033001	479.2	42.1		274	11.53	563.5	0.89	43.48			
93033002	469.5	26.4		337	8.89	425.6	1.04	49.78			
93033008	453.4	18.9		346	6.54	302.4	0.86	39.75			
93033119	308.4	9.9					0.90	28.29			
93040116	348.0	39.9					0.70	24.83			
93040117	359.4	19.5									
93040118	391.7	29.0					0.73	29.15			
93040119	410.0	39.0									
93040120	413.0	30.8					0.94	39.58			
93040121	356.5	18.1									
93040122	391.7	15.4									
93040123	385.7	10.5					0.73	28.70			
93040200	376.8	13.9									
93040217	291.4	5.7					0.72	21.39			
93052509	15.6	5.20									

BQ: Below Limit of Quantification

Table IV.E-15: (con'd)

fn:met1

Date/Time YR-MO-DA-H	Flow (cfs)	SS Conc (mg/L) (0.5um)	SS Conc (mg/L) (1.5um)	Particulate SS Cu Conc (mg/kg) (0.5um)	Particulate SS Cu Conc (ug/l) (0.5um)	Particulate SS Cu Flux (g/hr) (0.5um)	Dissolved DS Cu Conc (ug/l) (0.5um)	Dissolved DS Cu Flux (g/hr) (0.5um)	Particulate SS Cu Conc (mg/kg) (1.5um)	Particulate SS Cu Conc (ug/l) (1.5um)	Particulate SS Cu Flux (g/hr) (1.5um)
Wedge Pond											
91041516	5.0										
91052015	1.3										
91052413	0.0		15.9								
91052814	2.7		1.5								
91060713	0.9		15.1								
91071613	1.3	12.8	5.5								
91082011	12.0	10.8	10.7	68	0.95	1.16					
91082210*	10.2	5.1	3.3	283	1.43	1.49					
91092110	1.6	8.9	10.7	43	0.38	0.06					
91110210	10.2	8.3	7.9	37	0.31	0.32					
91122111	6.6	5.9	5.3	258	1.52	1.02			243	1.29	0.86
92011512	11.2		4.4						81	0.36	0.41
92022214	8.9	3.2	3.5	66	0.21	0.19	1.94	1.76	67	0.23	0.21
92032915	17.4	6.5	6.2	54	0.35	0.62	2.66	4.73	84	0.52	0.93
92041814	14.0	8.4	8.1	78	0.65	0.93	2.76	3.95	72	0.58	0.83
92052209	1.4	7.6	2.8	96	0.73	0.10	3.64	0.50	117	0.33	0.05
92061115	7.0	3.5	3.4	99	0.35	0.25	2.22	1.58	117	0.40	0.28
92072316	1.2	7.3	6.0	225	1.64	0.19	2.76	0.32	96	0.58	0.07
92081314	0.9	11.4	6.0	53	0.60	0.05	1.67	0.15			
92092714	5.2	7.1	7.1	51	0.36	0.19	0.53	0.28			
92101213	13.3	6.2	7.3	93	0.58	0.78	3.50	4.74			
92110114	1.2	4.7	4.6	50	0.24	0.03	1.90	0.23			
92121715	17.9	4.0	4.4	65	0.26	0.48	3.99	7.28			
93012511	12.7	3.1	3.2	108	0.33	0.43	4.31	5.57			

* Reverse Flow Direction
BQ: Below Limit of Quantification

Table IV.E-16: Copper Measurements at Gage #1, Wedge Pond

fn:met2

Date/Time YR-MO-DA-HR	Flow (cfs)	SS Conc (mg/L) (0.5um)	SS Conc (mg/L) (1.5um)	Particulate SS Cu Conc (mg/kg) (0.5um)	Particulate SS Cu Conc (ug/l) (0.5um)	Particulate SS Cu Flux (g/hr) (0.5um)	Dissolved DS Cu Conc (ug/l) (0.5um)	Dissolved DS Cu Flux (g/hr) (0.5um)	Particulate SS Cu Conc (mg/kg) (1.5um)	Particulate SS Cu Conc (ug/l) (1.5um)	Particulate SS Cu Flux (g/hr) (1.5um)
Rte 128											
91032911	9.3										
91041512	4.9										
91053013	5.0		2.8								
91060710	4.0		5.3								
91062010	6.3	5.7	4.4								
91071610	3.1	6.3	5.7								
91072610	0.8	6.3	4.4	698	4.40	0.36					
91081310	2.2	7.3	6.5								
91082110	31.0	7.9	7.3	397	3.13	9.91					
91092114	8.2	9.1	7.1	389	3.53	2.94					
91110213	12.7	7.7	4.5	274	2.12	2.75					
91121711	8.0		3.5						320	1.12	0.91
92011509	13.0		4.8						713	3.42	4.52
92022209	7.2	6.7	4.7	461	3.07	2.27	9.78	7.21			
92032915	17.6	5.2	3.9	317	1.65	2.95	9.49	17.04	381	1.49	2.67
92041809	13.8	3.6	3.6	350	1.25	1.76	9.38	13.21	258	0.93	1.31
92052215	4.4	6.5	5.7	414	2.69	1.22	10.42	4.72	312	1.78	0.80
92061110	7.1	9.0	7.8	455	4.08	2.96	7.94	5.77	513	4.00	2.91
92072309	2.0	11.2	11.0	486	5.44	1.09	6.28	1.26	518	5.70	1.14
92081309	2.6	7.6	7.4	413	3.14	0.83	5.07	1.33			
92092709	10.4	8.5	6.7	367	3.11	3.30	6.37	6.76			
92101209	16.4	6.7	6.4	547	3.68	6.14	6.98	11.65			
92110109	2.4	4.8	5.4	532	2.55	0.62	7.33	1.78			
92121710	18.3	12.6	13.7	318	4.02	7.48	14.22	26.47			
93012509	14.6	4.8	1.3	431	2.07	3.08	11.02	16.39			
93052509	5.3	6.2									

Table IV.E-17: Copper Measurements at Gage #2, Route 128

fn:met3

Date/Time YR-MO-DA-HR	Flow (cfs)	SS Conc (mg/L) (0.5um)	SS Conc (mg/L) (1.5um)	Particulate SS Cu Conc (mg/kg) (0.5um)	Particulate SS Cu Conc (ug/l) (0.5um	Particulate SS Cu Flux (g/hr) (0.5um	Dissolved DS Cu Conc (ug/l) (0.5um)	Dissolved DS Cu Flux (g/hr) (0.5um	Particulate SS Cu Conc (mg/kg) (1.5um)	Particulate SS Cu Conc (ug/l) (1.5u	Particulate SS Cu Flux (g/hr) (1.5u
Montvale											
91032914	16.1										
91041510	8.9										
91052011	9.8		3.30								
91052410	10.0		3.00								
91052811	17.8		5.60								
91053010	7.2		2.80								
91060715	5.4		2.00								
91071616	4.2	2.40	1.90								
91072616	2.2	1.70	1.20	357	0.61	0.1					
91081316	3.1	2.70	1.70								
91082016	88.0	7.94	6.40	238	1.89	17.0					
91082016	88.0	8.23		231	1.90	17.1					
91082016	88.0	8.53		250	2.13	19.1					
91082215	26.1	3.87	2.40	336	1.30	3.5					
91092113	16.6	4.81	4.60	344	1.65	2.8					
91110212	26.3	3.20	1.90	362	1.16	3.1					
91122113	16.5	8.08	8.00	435	3.51	5.9			340	2.72	4.6
92011510	31.1		5.70						517	2.95	9.3
92022211	8.7	6.85	5.90	461	3.16	2.8	6.39	5.7	480	2.83	2.5
92032909	34.8	3.71	2.50	308	1.14	4.0	8.54	30.3	323	0.81	2.9
92041810	31.0	3.51	3.00	324	1.14	3.6	9.18	29.0	273	0.82	2.6
92052214	8.6	5.75	4.80	303	1.74	1.5	22.31	19.6	337	1.62	1.4
92061112	12.3	8.15	5.50	397	3.24	4.0	7.22	9.0	482	2.65	3.3
92072311	3.9	4.22	3.20	320	1.35	0.5	8.34	3.3	393	1.26	0.5
92081310	6.9	4.29	2.80	279	1.20	0.8	5.45	3.9			
92092711	20.9	6.91	5.60	390	2.69	5.7	4.58	9.8			
92101210	26.7	12.98	12.60	484	6.28	17.1	6.43	17.5			
92110110	4.5	3.23	2.10	283	0.91	0.4	5.91	2.7			
92121711	30.9	18.71	8.00	366	6.85	21.6	12.86	40.5			
93012510	11.9	3.70	3.20	402	1.49	1.8	10.79	13.1			

Table IV.E-18: Copper Measurements at Gage #3, Montvale

fn:met4

Date/Time YR-MO-DA-HR	Flow (cfs)	SS Conc (mg/L) (0.5um)	SS Conc (mg/L) (1.5um)	Particulate SS Cu Conc (mg/kg) (0.5um)	Particulate SS Cu Conc (ug/l) (0.5um)	Particulate SS Cu Flux (g/hr) (0.5um)	Dissolved DS Cu Conc (ug/l) (0.5um)	Dissolved DS Cu Flux (g/hr) (0.5um)	Particulate SS Cu Conc (mg/kg) (1.5um)	Particulate SS Cu Conc (ug/l) (1.5um)	Particulate SS Cu Flux (g/hr) (1.5um)
Horn Pond											
91052416	5.7		1.40								
91052814	10.5		5.40								
91060712	4.7		11.10								
91071611	2.0	4.50	4.80								
91072613	1.2	1.20	1.20	354	0.42	0.05					
91081313	1.6	3.70	2.60								
91082013	21.6	20.60	19.60	83	1.71	3.76					
91082211	9.6	4.57	3.90	53	0.24	0.24					
91092111	4.5	5.95	6.70	52	0.31	0.14					
92022213	7.5	2.24	1.50	66	0.15	0.11	1.46	1.12			
92032914	16.4	4.70	4.70	57	0.27	0.45	2.65	4.43	55	0.26	0.43
92041812	15.0	2.05	1.90	72	0.15	0.22	2.63	4.01			
92052211	5.1	5.11	3.70	50	0.26	0.13	1.96	1.02	44	0.16	0.09
92061114	6.1	3.54	3.60	76	0.27	0.17	0.85	0.53	49	0.18	0.11
92072313	2.6	3.10	2.70	35	0.11	0.03	4.29	1.12	65	0.18	0.05
92081312	3.2	2.39	2.40	43	0.10	0.03	1.65	0.54	BQ	BQ	BQ
92092712	9.1	12.25	11.50	BQ	BQ	BQ	1.44	1.33			
92101212	17.9	10.14	9.60	96	0.97	1.78	3.04	5.55			
92110112	3.3	0.77	0.60	62	0.05	0.02	2.14	0.71			
92121712	44.1	2.41	2.10	114	0.27	1.24	5.63	25.32			
93012511	20.1	2.80	2.60	114	0.32	0.65	4.70	9.63			

BQ: Below Limit of Quantification

Table IV.E-19: Copper Measurements at Gage #4, Horn Pond

fn:met5

Date/Time YR-MO-DA-HR	Flow (cfs)	SS Conc (mg/L) (0.5um)	SS Conc (mg/L) (1.5um)	Particulate SS Cu Conc (mg/kg) (0.5um)	Particulate SS Cu Conc (ug/l) (0.5um)	Particulate SS Cu Flux (g/hr) (0.5um)	Dissolved DS Cu Conc (ug/l) (0.5um)	Dissolved DS Cu Flux (g/hr) (0.5um)	Particulate SS Cu Conc (mg/kg) (1.5um)	Particulate SS Cu Conc (ug/l) (1.5um)	Particulate SS Cu Flux (g/hr) (1.5um)
USGS											
91052415	12.1		3.40								
91052812	18.8		5.40								
91060714	26.7		1.80								
91062012	13.5	4.80	4.40								
91071615	6.1	2.50	2.20								
91072615	3.1	1.30	0.80	442	0.57	0.2					
91081314	4.3	2.00	1.80								
91082009	139.5	9.95	8.55	309	3.07	43.7					
91082114	95.7	7.42	6.90	316	2.34	22.9					
91082209	9.2	7.77	4.50								
91082209	12.6	8.10		222	1.80	2.3					
91082209	14.4	9.20		186	1.71	2.5					
91092109	26.2	3.72	2.90	353	1.31	3.5					
91110209	45.5	4.34	3.90	270	1.17	5.4					
91122109	32.4	4.95	4.40	350	1.73	5.7			315	1.39	4.58
92011513	45.0		4.40						273	1.20	5.51
92022215	23.0	3.45	3.00	219	0.76	1.8	3.99	9.4	234	0.70	1.65
92032912	57.2	4.28	3.60	186	0.80	4.6	6.05	35.3	76	0.27	1.60
92041815	49.0	4.55	4.30	213	0.97	4.8	6.81	34.0	188	0.81	4.04
92052208	12.6	4.23	3.80	222	0.94	1.2	6.17	7.9	258	0.98	1.25
92061117	22.4	4.48	4.00	259	1.16	2.6	4.65	10.6	348	1.39	3.18
92072315	5.8	1.75	1.50	154	0.27	0.2	6.46	3.8			
92072922	74.4	34.3		215	7.38	56.0	4.84	36.7			
92081008	35.6	5.6		212	1.19	4.3	5.79	21.0			
92081010	34.9	5.0		171	0.86	3.1	4.57	16.3			
92081012	32.4	4.6		186	0.85	2.8	5.94	19.6			
92081014	30.8	4.4		186	0.82	2.6	5.33	16.7			
92081016	28.5	4.4		189	0.83	2.4	4.66	13.5			
92081018	27.1	4.9		173	0.85	2.3	5.35	14.8			
92081020	25.0	4.6		182	0.84	2.1	5.05	12.9			
92081022	23.7	5.1		167	0.85	2.1	6.21	15.0			
92081100	22.4	4.6		184	0.84	1.9	6.25	14.3			
92081102	20.6	5.5		150	0.83	1.7	6.58	13.8			
92081104	19.4	4.9		173	0.85	1.7	6.70	13.2			
92081315	8.8	2.14	2.10	198	0.42	0.4	3.91	3.5	233	0.49	0.44

BQ: Below Limit of Quantification

Table IV.E-20: Copper Measurements at Gage #5, USGS

Date/Time YR-MO-DA-HR	Flow (cfs)	SS Conc (mg/L) (0.5um)	SS Conc (mg/L) (1.5um)	Particulate SS Cu Conc (mg/kg) (0.5um)	Particulate SS Cu Conc (ug/l) (0.5um)	Particulate SS Cu Flux (g/hr) (0.5um)	Dissolved DS Cu Conc (ug/l) (0.5um)	Dissolved DS Cu Flux (g/hr) (0.5um)	Particulate SS Cu Conc (mg/kg) (1.5um)	Particulate SS Cu Conc (ug/l) (1.5um)	Particulate SS Cu Flux (g/hr) (1.5um)
92081801	75.9	17.1		217	3.72	28.8	8.15	63.1			
92081802	144.0	60.3		219	13.22	194.0	6.32	92.8			
92081803	159.5	50.4		235	11.86	192.8	5.12	83.3			
92081804	196.7	61.3		313	19.19	384.7	5.65	101.3			
92081805	222.7	69.4					4.23	96.0			
92081806	202.9	42.0		300	12.61	260.8	4.48	92.6			
92081807	196.7	32.2		275	8.86	177.6	4.86	97.4			
92081808	178.5	25.5		320	8.16	148.5	4.91	89.3			
92081809	168.9	22.4		299	6.69	115.2	5.01	86.3			
92081810	164.1	20.5		324	6.65	111.2	3.83	64.1			
92081811	161.8	23.0		289	6.65	109.7	3.74	61.7			
92081812	166.4	21.5		308	6.62	112.2	3.88	65.8			
92081813	159.5	20.3		291	5.91	96.0	6.16	100.2			
92081814	157.2	19.2		309	5.94	95.1	4.46	71.5			
92081815	152.7	17.7		332	5.87	91.4	4.96	77.2			
92081816	143.0	17.4		298	5.16	78.2	3.87	58.4			
92081817	144.0	14.9		348	5.18	76.1	4.98	73.1			
92081818	139.5	14.2		366	5.20	73.9	6.93	98.5			
92081819	135.1	12.6		353	4.45	61.2	4.39	60.5			
92081820	130.8	13.0		340	4.43	59.0	4.37	58.3			
92081821	126.5	11.9		314	3.74	48.2	4.45	57.4			
92081822	122.4	10.9		339	3.69	46.1	8.77	109.4			
92081823	118.3	10.4		351	3.65	44.0	4.48	54.0			
92081900	114.4	10.4		367	3.82	44.5	4.54	52.9			
92092715	28.5	4.14	3.60	253	1.05	3.0	3.25	9.4			
92101215	48.1	6.43	6.30	306	1.97	9.7	6.15	30.2			
92110115	7.4	2.86	2.00	280	0.80	0.6	5.92	4.5			
92112305	99.3	42.7		267	11.41	115.5	11.95	121.0			
92112307	139.5	42.8		303	12.98	184.5	10.64	151.3			
92112308	159.5	48.0		327	15.68	254.9	10.36	168.5			
92112407	77.4	17.9		277	4.96	39.2	9.05	71.4			
92121119	42.1	32.4		401	13.00	55.8	9.51	40.8			
92121120	52.5	36.4		428	15.56	83.3	8.97	48.0			
92121121	60.9	31.8		402	12.79	79.4	8.85	54.9			
92121122	99.3	45.2		357	16.12	163.2	7.47	75.6			
92121123	135.1	46.2		337	15.55	214.2	9.38	129.2			
92121200	157.2	50.5		344	17.39	278.8	9.89	158.5			
92121201	171.2	51.4		339	17.41	303.9	8.27	144.3			
92121202	196.7	47.3		332	15.70	314.9	7.87	157.8			
92121203	200.5	45.2		320	14.45	295.3	6.99	142.8			
92121204	207.7	41.8		325	13.59	287.7	6.14	130.0			
92121205	215.1	40.4		334	13.50	296.0	6.82	149.6			
92121206	212.7	35.5		329	11.68	253.2	6.56	142.2			
92121207	210.2	30.1		332	10.00	214.3	6.67	142.9			
92121208	200.5	26.1		340	8.89	181.6	6.46	132.0			
92121209	191.0	19.6		341	6.69	130.3	6.79	132.2			
92121210	188.5	16.1		309	4.97	95.4	7.08	136.0			
92121216	159.5	8.8		313	2.75	44.7	7.08	115.1			
92121217	152.7	7.8		286	2.23	34.7	7.10	110.6			
92121218	150.5	7.2		316	2.27	34.9	7.13	109.4			

BQ: Below Limit of Quantification

Table IV.E-20; (con'd)

fn:met5

Date/Time YR-MO-DA-HR	Flow (cfs)	SS Conc (mg/L) (0.5um)	SS Conc (mg/L) (1.5um)	Particulate SS Cu Conc (mg/kg) (0.5um)	Particulate SS Cu Conc (ug/l) (0.5um)	Particulate SS Cu Flux (g/hr) (0.5um)	Dissolved DS Cu Conc (ug/l) (0.5um)	Dissolved DS Cu Flux (g/hr) (0.5um)	Particulate SS Cu Conc (mg/kg) (1.5um)	Particulate SS Cu Conc (ug/l) (1.5um)	Particulate SS Cu Flux (g/hr) (1.5um)
92121713	82.2	15.30	14.20	300	4.59	38.5	9.62	80.6			
93012513	47.1	7.40	7.10	267	1.98	9.5	9.37	44.9			
93032614	87.1	23.3		198	4.60	40.9	9.87	87.7			
93032615	141.7	19.2		210	4.03	58.2	9.88	142.7			
93032616	101.1	21.8		212	4.61	47.5	9.96	102.6			
93032617	144.0	21.3		190	4.05	59.4	10.42	153.0			
93032618	126.5	22.6		179	4.04	52.1	9.39	121.1			
93032619	71.5	20.2		171	3.46	25.2	9.16	66.7			
93032620	66.0	15.8		149	2.36	15.8	10.13	68.1			
93032910	264.2	35.5		283	10.04	270.3	8.90	239.7			
93032911	272.2	21.1		295	6.22	172.5	7.95	220.6			
93032912	285.8	25.4		327	8.31	242.0	7.60	221.4			
93032913	311.3	34.9		295	10.30	326.8	7.60	241.2			
93032914	339.5	59.1		252	14.87	514.6	7.04	243.6			
93032915	362.2	55.9		289	16.14	595.8	6.90	254.8			
93032916	391.7	70.7		278	19.62	783.5	6.73	268.7			
93032917	428.3	82.0		281	23.07	1007.3	6.16	269.0			
93032918	459.8	81.5		282	22.96	1076.1	5.95	278.9			
93032919	476.0	86.4		304	26.27	1274.9	6.42	311.5			
93032920	495.7	76.9		311	23.89	1207.5	7.31	369.4			
93032921	499.1	73.8		272	20.09	1022.3	6.76	343.9			
93032922	499.1	62.2		306	19.03	968.5	7.27	369.9			
93032923	502.4	61.4		307	18.85	965.3	7.06	361.6			
93033000	492.4	51.3		312	15.99	802.6	7.03	352.9			
93033001	479.2	42.1		301	12.69	619.8	6.86	335.1			
93033002	469.5	26.4		421	11.12	532.0	7.07	338.4			
93033008	453.4	18.9		404	7.63	352.8	7.33	338.8			
93033119	308.4	9.9					7.71	242.4			
93040116	348.0	39.9					9.75	345.9			
93040117	359.4	19.5									
93040118	391.7	29.0					7.73	308.7			
93040119	410.0	39.0									
93040120	413.0	30.8					7.87	331.3			
93040121	356.5	18.1									
93040122	391.7	15.4									
93040123	385.7	10.5					8.02	315.3			
93040200	376.8	13.9									
93040217	291.4	5.7					8.15	242.1			
93052509	15.6	5.20									

BQ: Below Limit of Quantification

Table IV.E-20; (con'd)

EVALUATION OF INDIVIDUAL STORMS

The streamflow and suspended sediment responses of three storm events are included below for reference. These events correspond to the August 18, 1992, December 11, 1992, and the March/April 1993 events which were sampled extensively for metal determinations. The characteristics of metal transport during these events are discussed extensively in section IV.4.2.

August 18, 1992 Storm

Streamflows and suspended sediment concentrations during the August 18, 1992 storm are given in figures IV.E-1, IV.E-2, and IV.E-3. The high streamflows were due to a 1.77 inch rainfall event as measured at the Reading station. The peak streamflow for this storm was 223 cfs. From figure IV.E-1, the maximum rainfall intensity occurred at 2:00 on August 18, 1992 and the streamflow peak occurred at 5:00. Therefore, the lag time between precipitation and streamflow response at gage 5 was 3 hours.

Throughout this event, streamflow appeared to respond directly to precipitation. For each hourly precipitation depth, larger depths appeared to cause a larger increases in streamflow. For example, a small amount of rainfall occurred at 0:00 August 18 and was followed by a large amount of rainfall at 1:00. The streamflow response at 3:00 (0:00 + 3 hours) corresponding to the small rainfall depth was preceded by a slower rate of increase. During the following hour, which corresponded to the larger rainfall depth, the flow was characterized by a quicker rate of increase. The same pattern was observed on the falling limb of the streamflow hydrograph, where smaller rainfall depths corresponded to a quicker declines in the streamflows and larger rainfall depths corresponded to slower declines.

Figure IV.E-1 also illustrates an approximate separation of the stormflow into quick, slow, and longterm baseflow components. Given this separation, the volume of quick water for this event was 0.04 inches while the volume of slow water was 0.20 inches. Therefore the quick and slow responses for this event accounted for approximately 2.3% and 11.3% of the incident precipitation, respectively.

The peak suspended sediment concentration was 69 mg/l which coincided with the timing of the streamflow peak. Additionally, the time when the suspended sediment concentration was larger than 20 mg/l corresponded to the time when quick flow was active. As discussed in section IV.3 the large increases in suspended sediments can be associated with areas physically separated from the river which are flushed of sediments by quick flow.

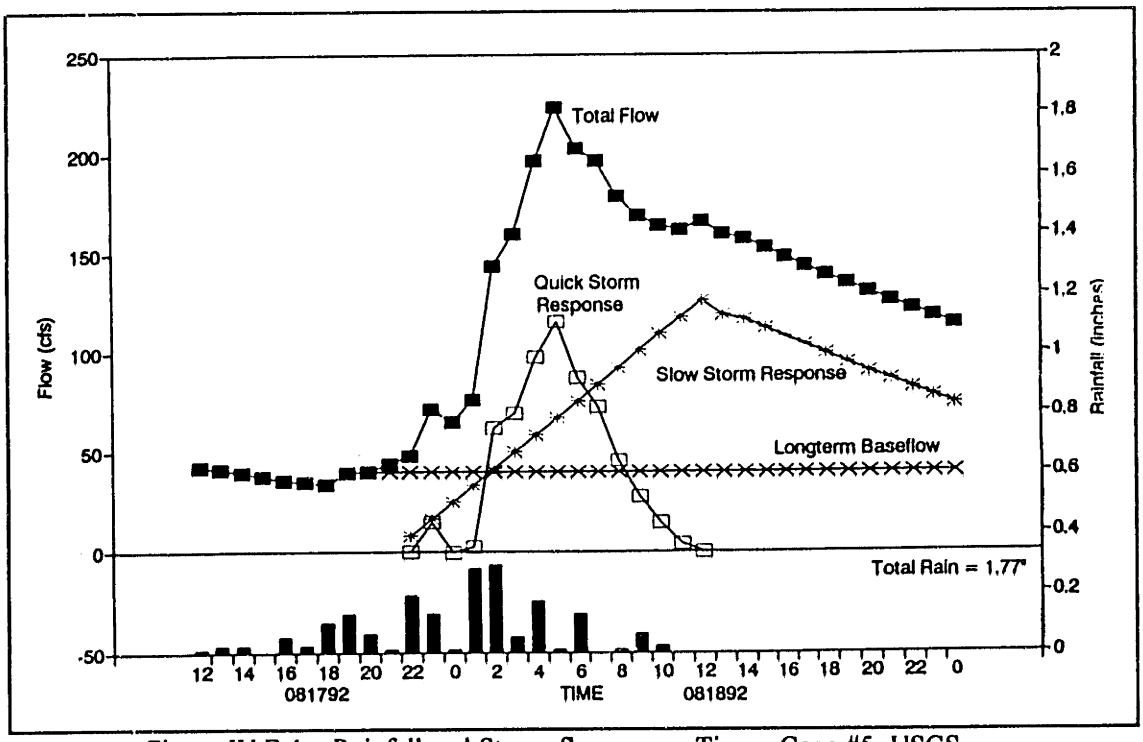

Figure IV.E-1: Rainfall and Streamflow versus Time, Gage #5, USGS
August 18, 1992 Storm

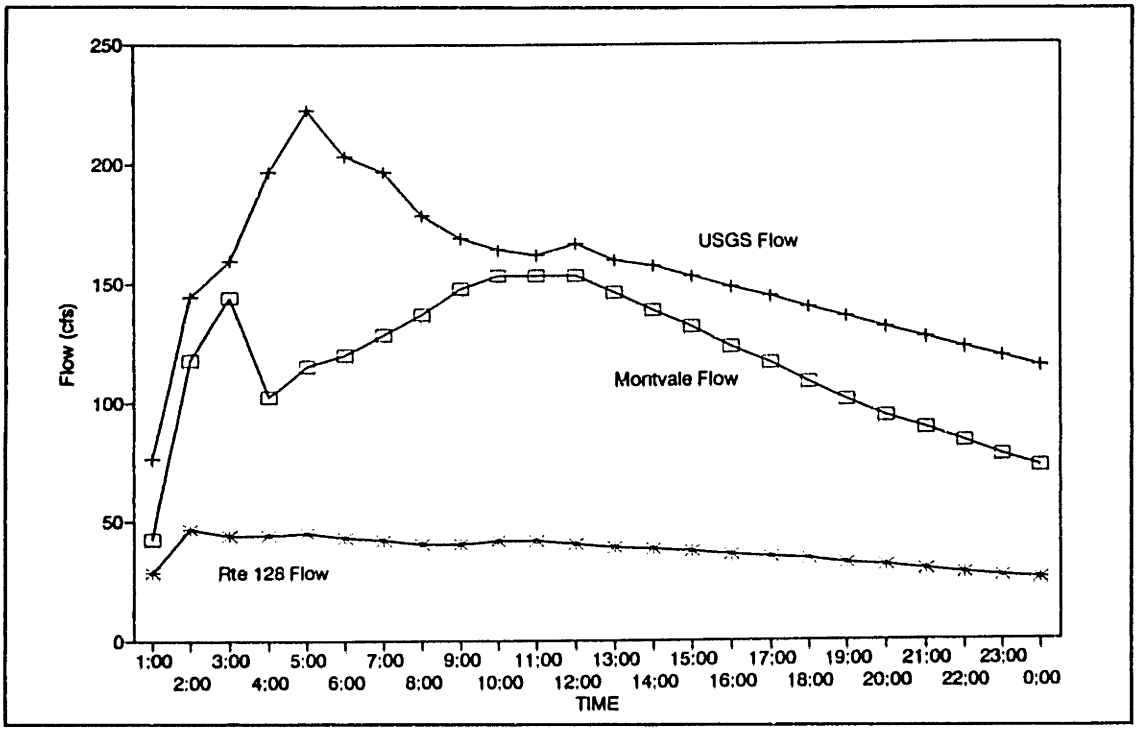

Figure IV.E-2: Streamflow versus Time, Gages 2,3, & 5
August 18, 1992 Storm

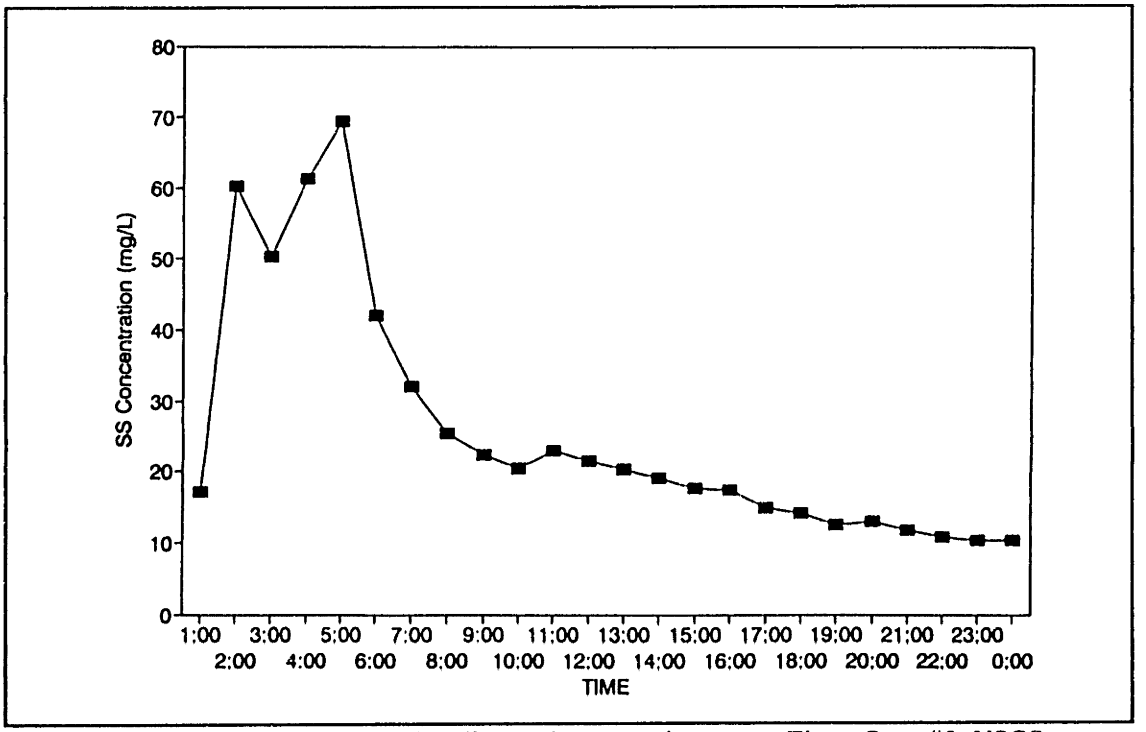

Figure IV.E-3: Suspended Sediment Concentration versus Time, Gage #5, USGS
August 18, 1992 Storm

December 11, 1992 Storm

The December 11, 1992 storm occurred in response to a 1.74 inch rainfall event. (figure IV.E-4) After the first 15 hours of the storm, precipitation continued as snowfall. As for the August storm, the streamflow appeared to respond directly to the rainfall. The peak streamflow for this event was 215 cfs.

Figure IV.E-5 illustrates the separation of the stormflow into quick, slow, and longterm baseflow components. Given this separation, the volume of quick water for this event was 0.05 inches while the volume of slow water was 0.36 inches. Therefore the quick and slow responses accounted for approximately 2.7% and 21% of the incident precipitation, respectively.

The peak suspended sediment concentration for this event was 51.4 mg/l. (figure IV.E-7) The peak suspended sediment concentration occurred 4 hours before the peak streamflow. The time when suspended sediment concentrations were greater than 40 mg/l corresponded to the time when quick flow was active.

The August and December storms exhibited generally similar behavior. Both storms had similar rainfall depths and similar peak streamflows. The fraction of rainfall converted to quick flow was also similar for both events. Such results indicate that quick streamflow responds in a reproducible fashion to similar size events. However, a smaller fraction of rainfall was converted to slow storm water for the August event. This difference may have been due to differences in antecedent conditions.

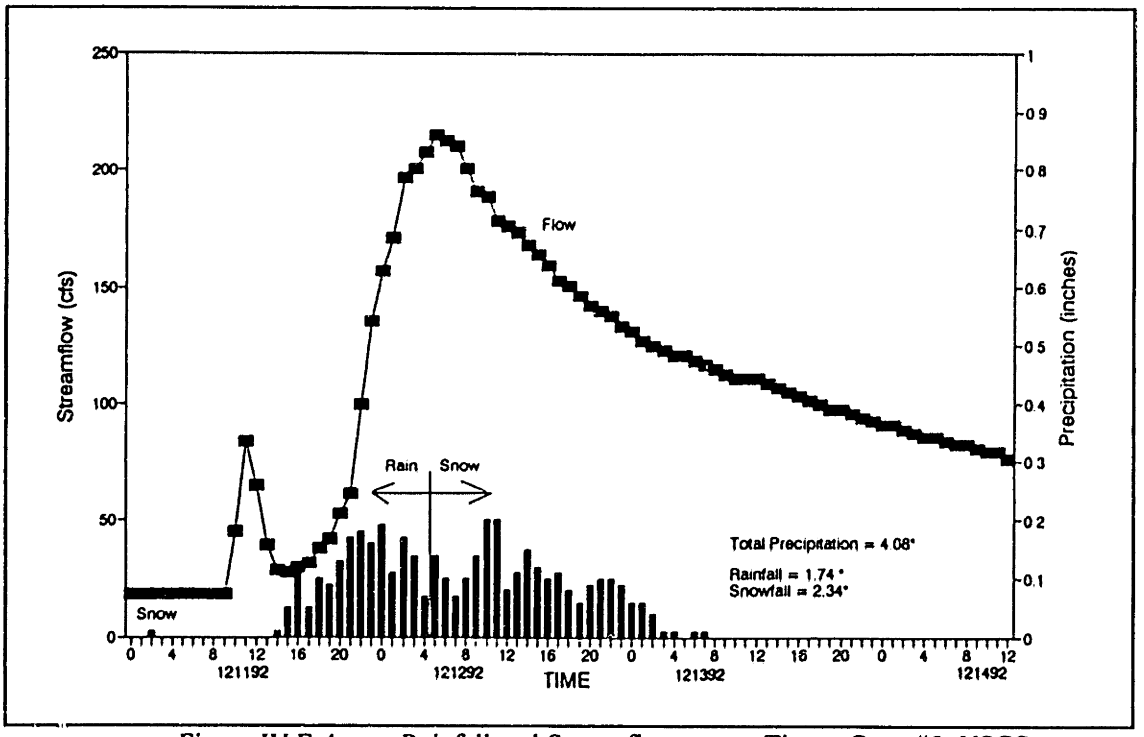

Figure IV.E-4: Rainfall and Streamflow versus Time, Gage #5, USGS December 11, 1992 Storm

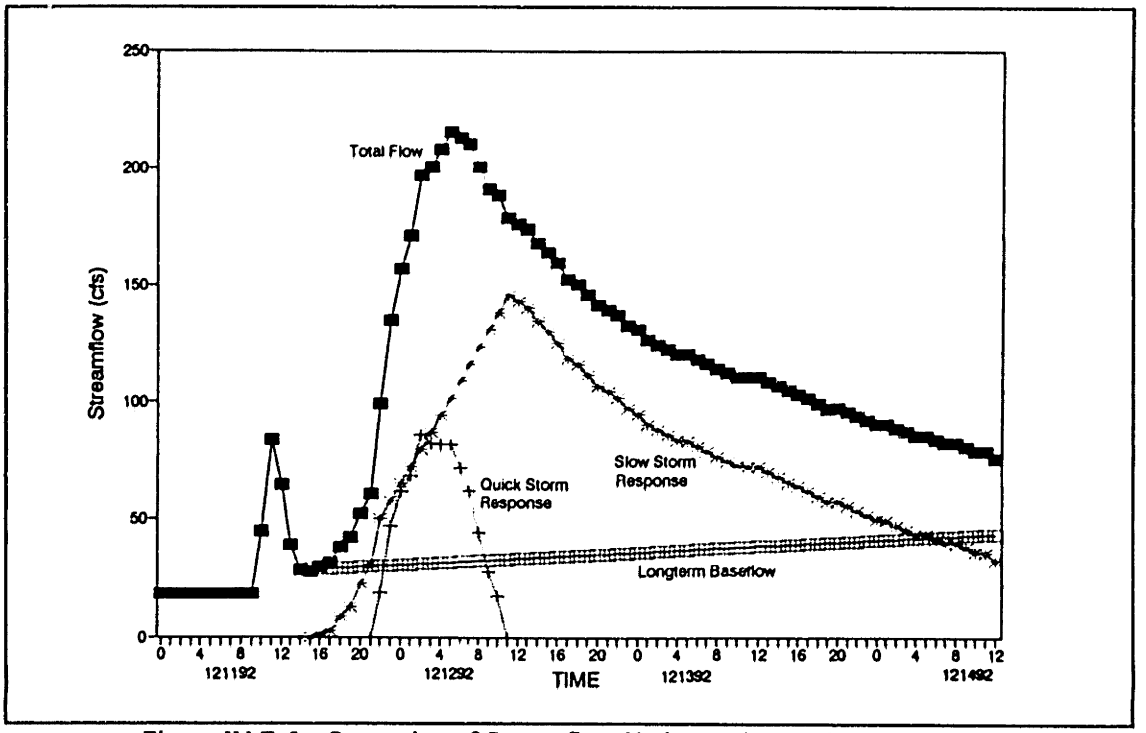

Figure IV.E-5: Separation of Streamflow Hydrograph Into Components Gage #5, USGS, December 11, 1992 Storm

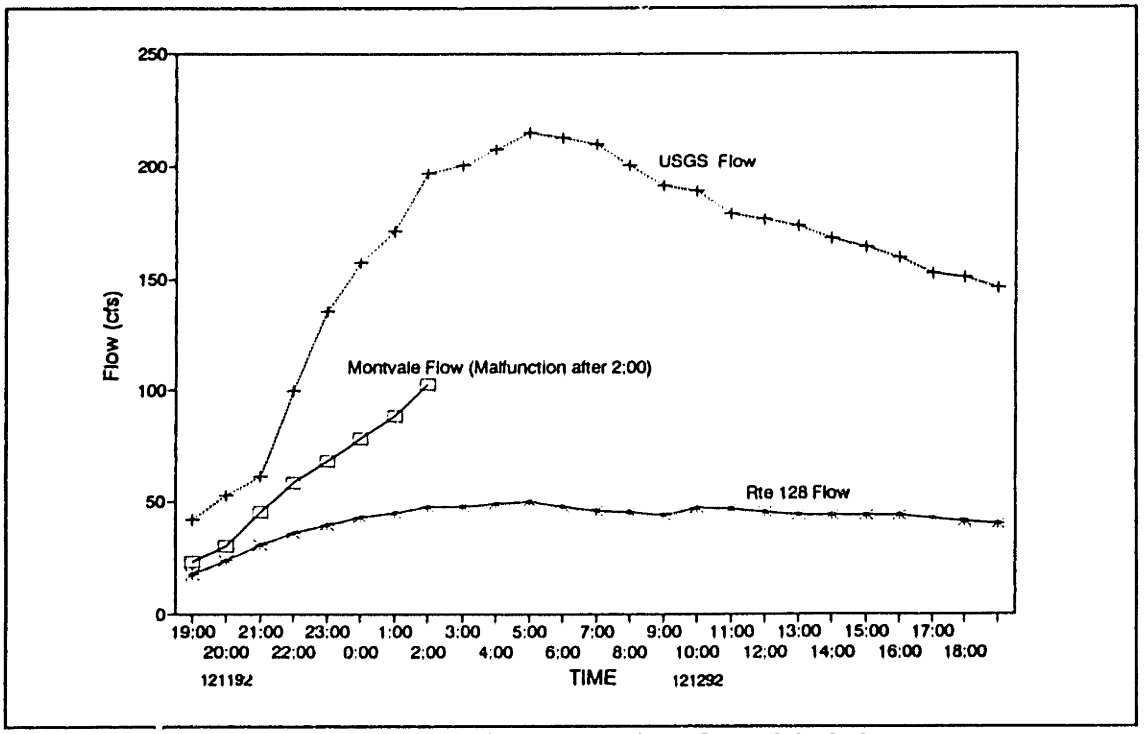

Figure IV.E-6: Streamflow versus Time, Gages 2,3, & 5
December 11, 1992 Storm

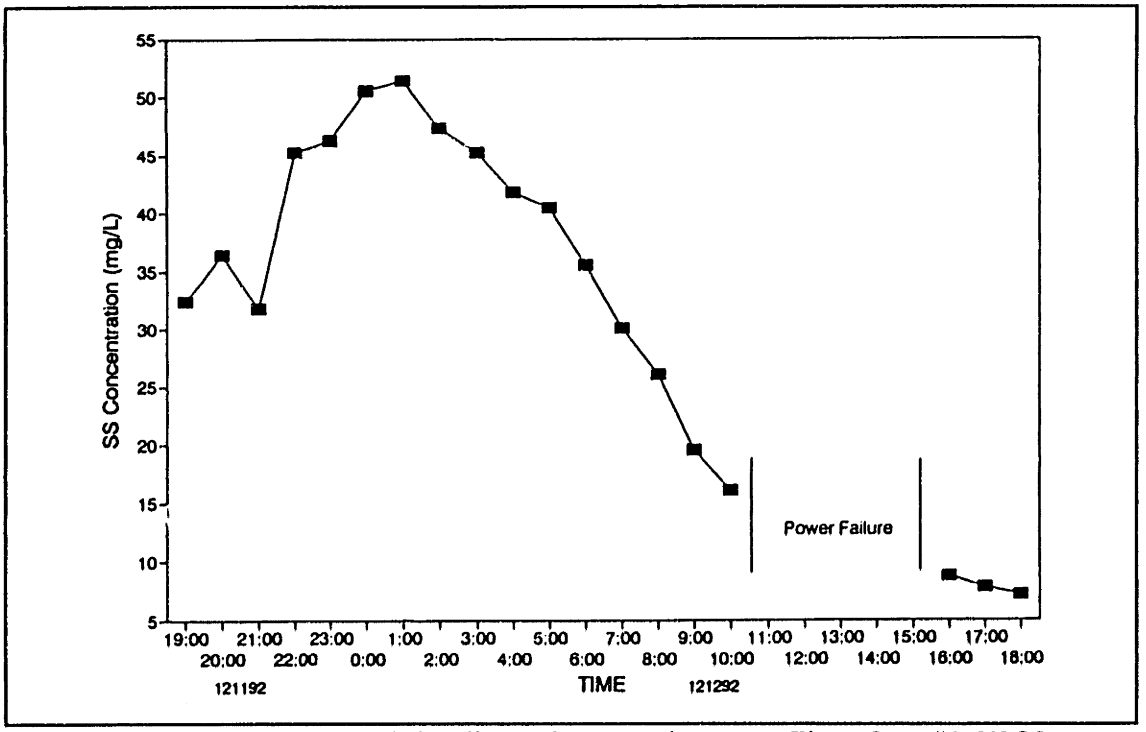

Figure IV.E-7: Suspended Sediment Concentration versus Time, Gage #5, USGS
December 11, 1992 Storm

March/April Events

Streamflows for the March/April sampling events were strongly affected by snowmelt. During March 26, 1993, a peak streamflow of 144 cfs occurred. This peak was not preceded by a precipitation event and was therefore due to snowmelt only. (figure IV.E-8) During and preceding this peak, a significant amount of snow was present within the basin. On this day, the temperature increased from 32 °C at 5:00 to 64 °C at 12:00, causing the snow to melt. (figure IV.E-9) The peak streamflow occurred at 17:00 just a few hours after the peak temperature.

The second event, which occurred March 29, 1993, was affected by both snowmelt and by rainfall. (figure IV.E-8) The amount of rainfall associated with this event was 1.6 inches. The peak streamflow was 502 cfs. It is estimated that approximately 300 cfs of the peak was associated with snowmelt.

Intermittent samples were collected until the third and final event. This event occurred April 1, 1993 and was also affected by both snowmelt and rainfall. (figures IV.E-8 and IV.E-9) The amount of rainfall associated with this event was 0.78 inches. The peak streamflow was 413 cfs. This large peak (given the small precipitation) was due to a combination of: 1) snowmelt, and 2) the receding limb of the March 29th storm. Approximately 300 cfs of the April 1 peak may be associated with the combined effects of snowmelt and the prior storm's receding flows.

Figure IV.E-10 illustrates the separation of the stormflow into quick (part due to rainfall only), slow + snowmelt, and longterm baseflow components. The volume of quick water (associated with the rainfall) for this event was 0.06 inches. Therefore the quick response accounted for approximately 3.5% of the incident rainfall.

Suspended sediment concentrations during the March 26 snowmelt were approximately 20 mg/l (figure IV.E-12). These concentrations were somewhat higher than would be expected during longterm baseflow or slow storm flows, and indicates that melt waters were capable of supplying waters with suspended sediment concentrations higher than slow or longterm baseflow waters.

Suspended sediment concentrations during the March 29 event were higher than concentrations observed during other storm events. (figure IV.E-12) The peak concentration for this event was 86 mg/l. Comparing the suspended sediment concentration plot with the various streamflow components one will note that the time when suspended sediments were greater than 40 mg/l corresponded to the time when quick flow was greater than 20 cfs. This observation supports the notion that quick flows supply bursts of sediments to the river.

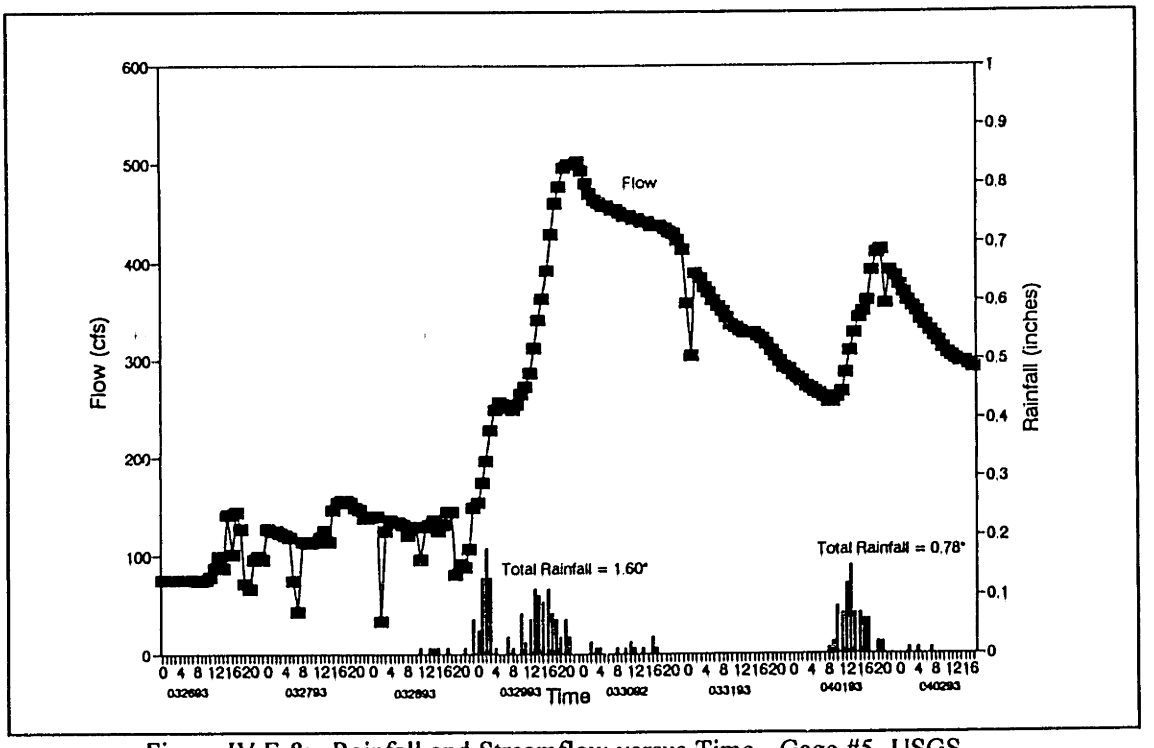

Figure IV.E-8: Rainfall and Streamflow versus Time, Gage #5, USGS March/April 1993 Event

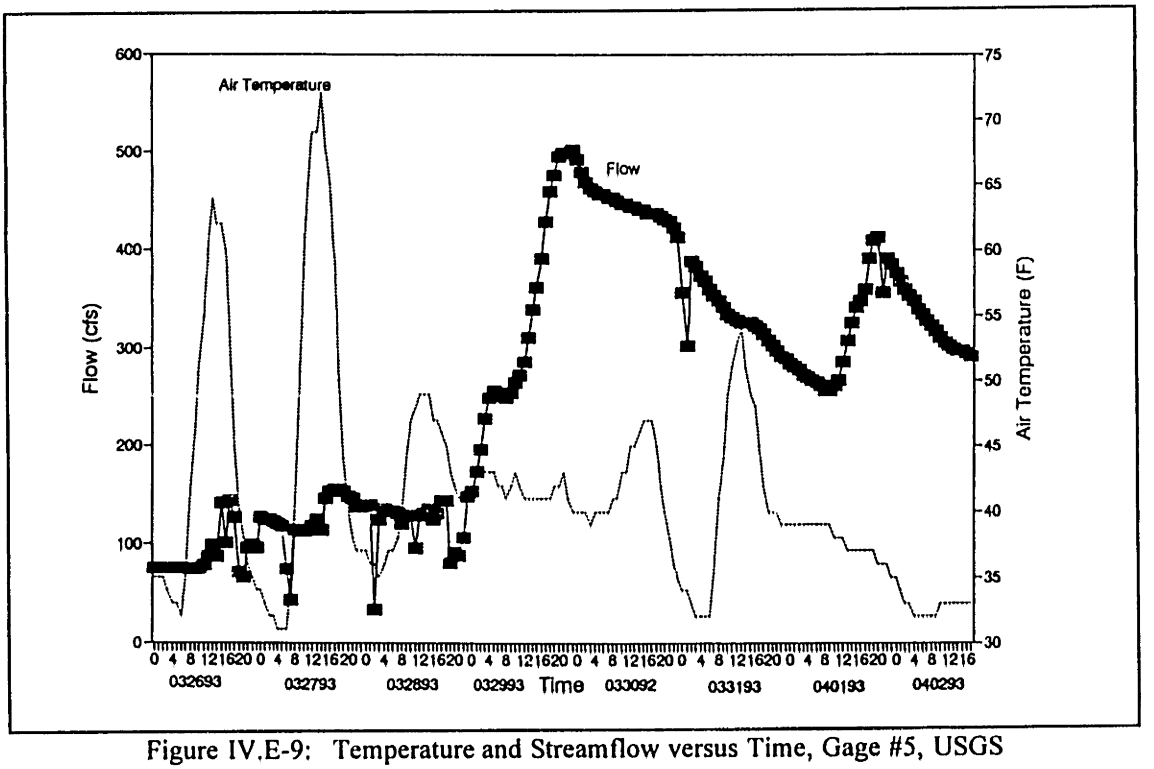

Figure IV.E-9: Temperature and Streamflow versus Time, Gage #5, USGS March/April 1993 Event

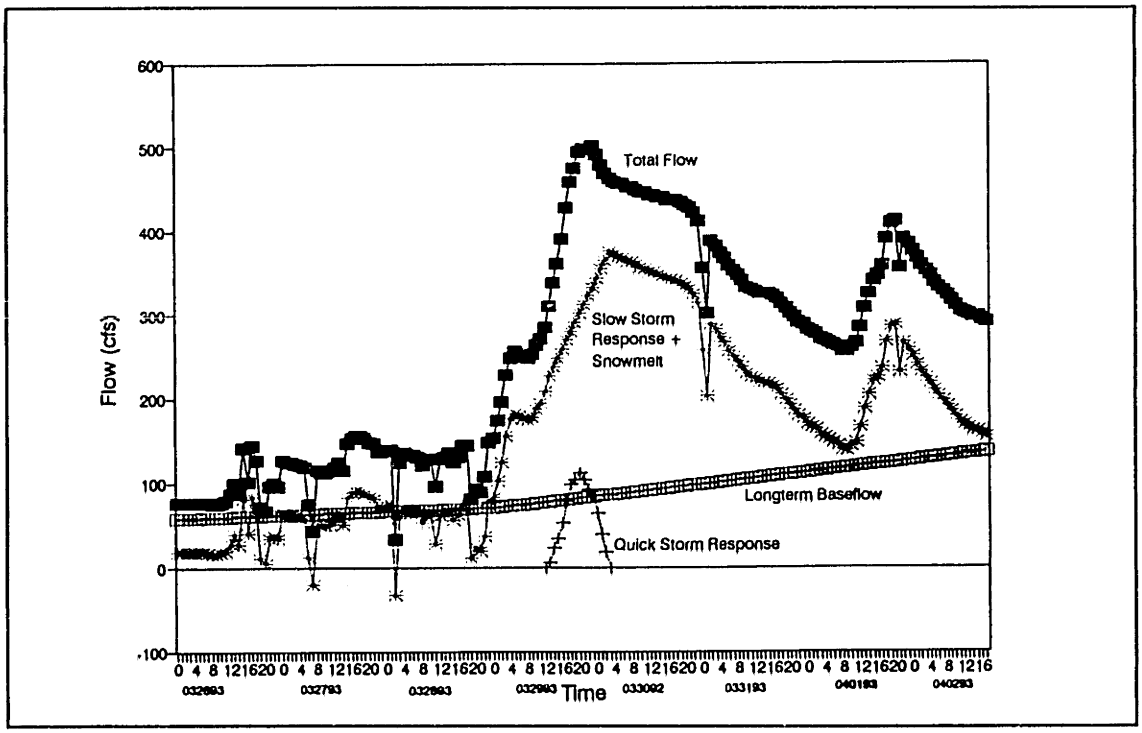

Figure IV.E-10: Separation of Streamflow Hydrograph Into Components
Gage #5, USGS, March/April 1993 Event

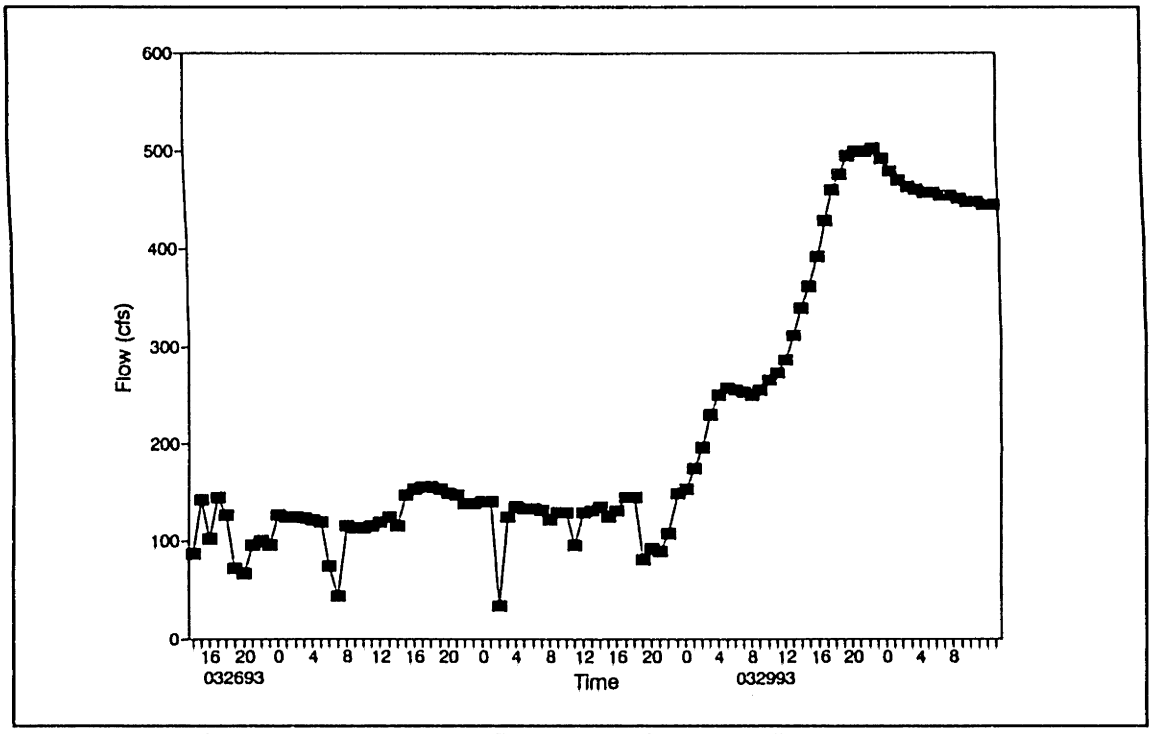

Figure IV.E-11: Streamflow versus Time, Gage #5, USGS March 1993 Event

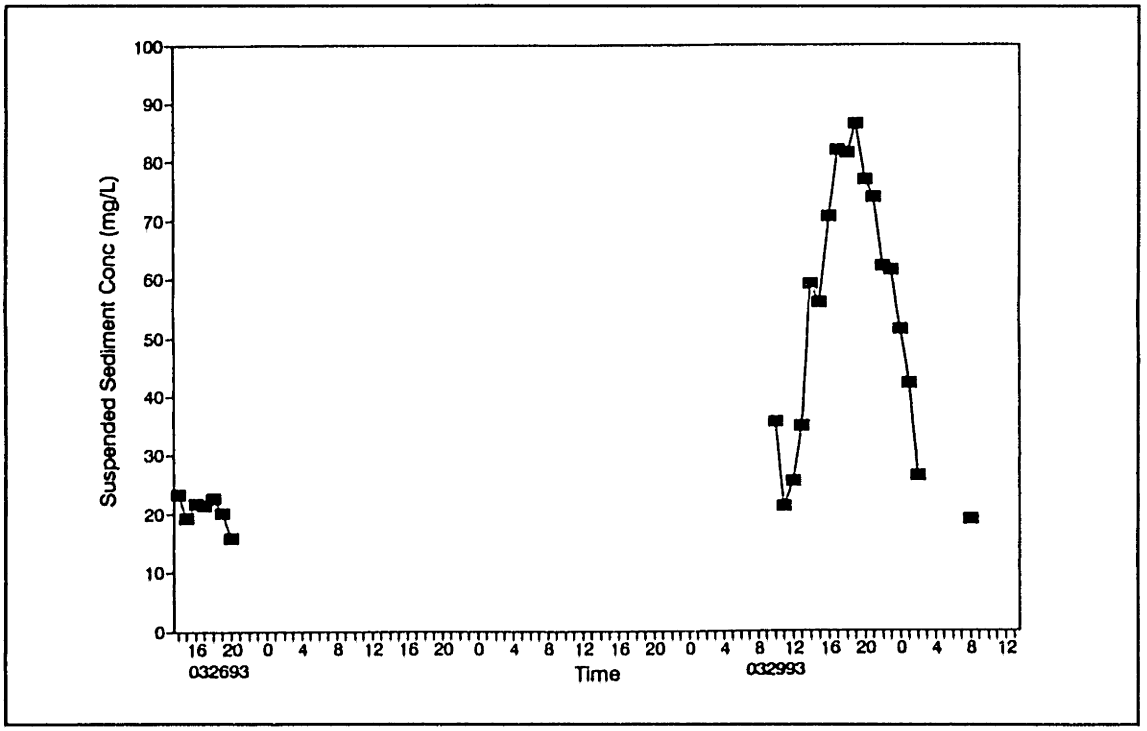

Figure IV.E-12: Suspended Sediment Concentration versus Time, Gage #5, USGS March 1993 Event

SUPPLEMENTAL FIGURES FOR SECTION IV.4.2

Metals data for the December and March/April events are plotted in figures IV.E-13 through IV.E-58. These figures are a supplement to the August storm event figures included in the main body of the text; figures IV.E-13 through IV.E-21 and figures IV.E-36 through IV.E-44 correspond to the discussion presented in section IV.4.2.3; figures IV.E-22 through IV.E-30 and figures IV.E-45 through IV.E-54 correspond to the discussion presented in section IV.4.2.4; and, figures IV.E-31 through IV.E-34 and figures IV.E-55 through IV.E-58 correspond to the discussion presented in section IV.4.2.5.

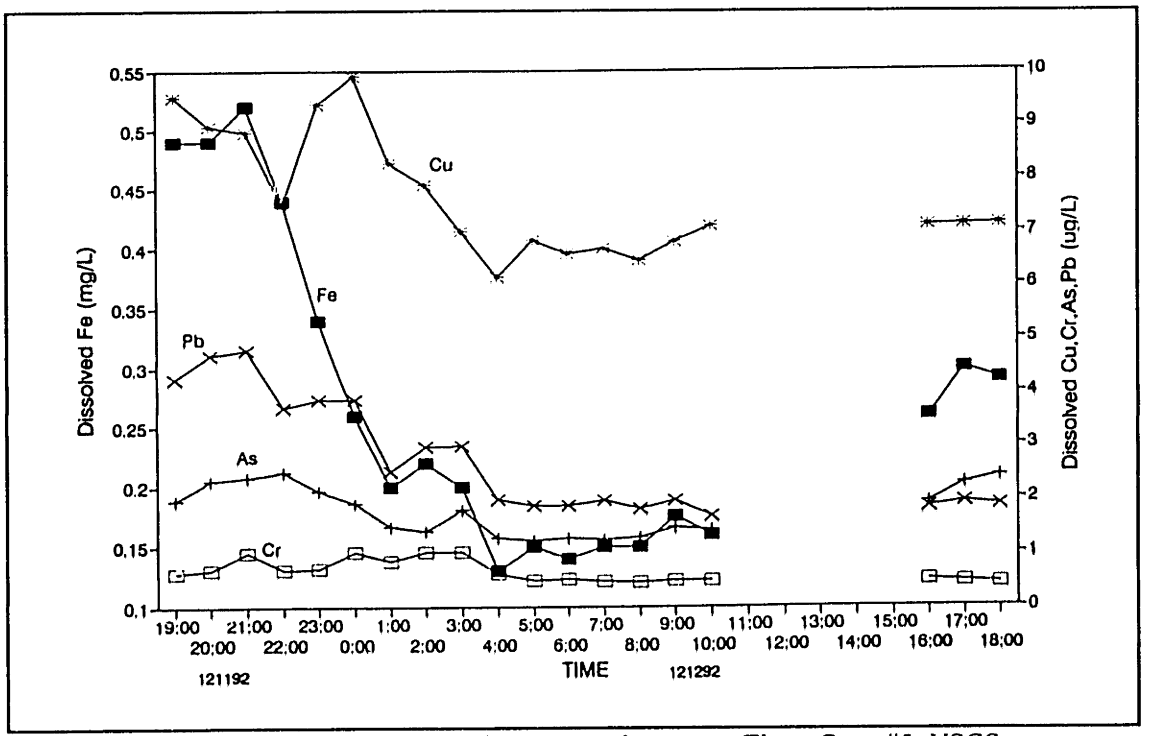

Figure IV.E-13: Dissolved Metal Concentration versus Time, Gage #5, USGS December 11, 1992 Storm

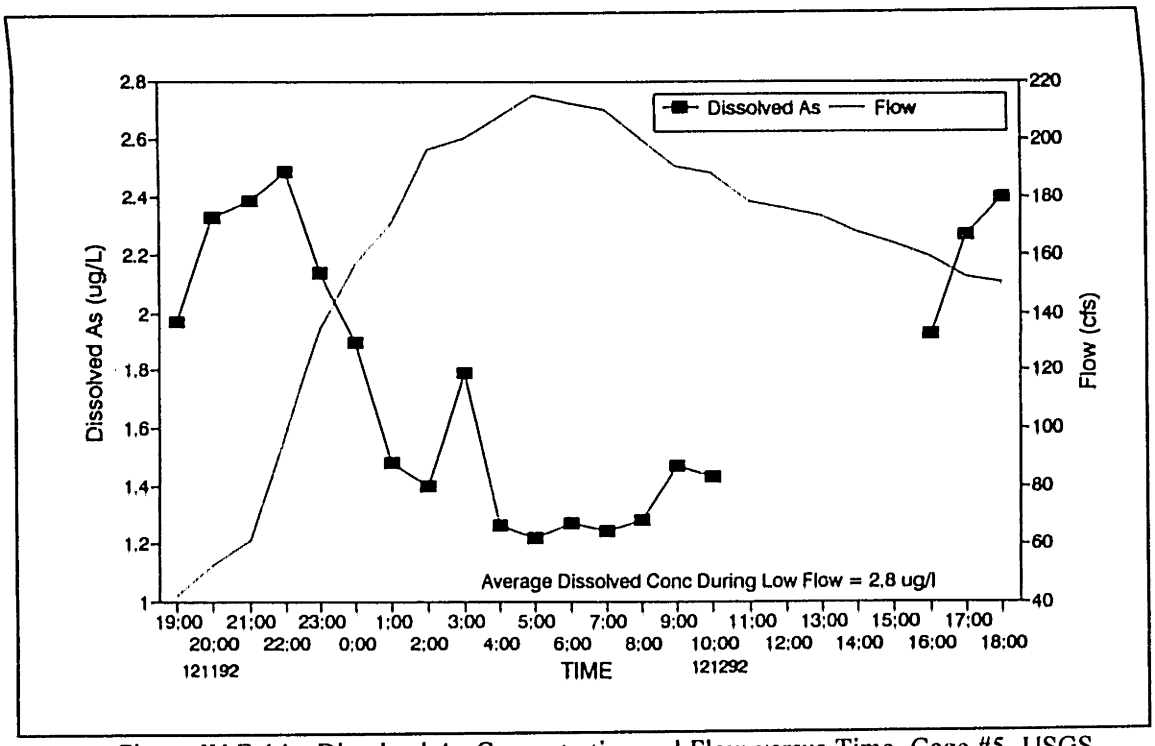

Figure IV.E-14: Dissolved As Concentration and Flow versus Time, Gage #5, USGS December 11, 1992 Storm

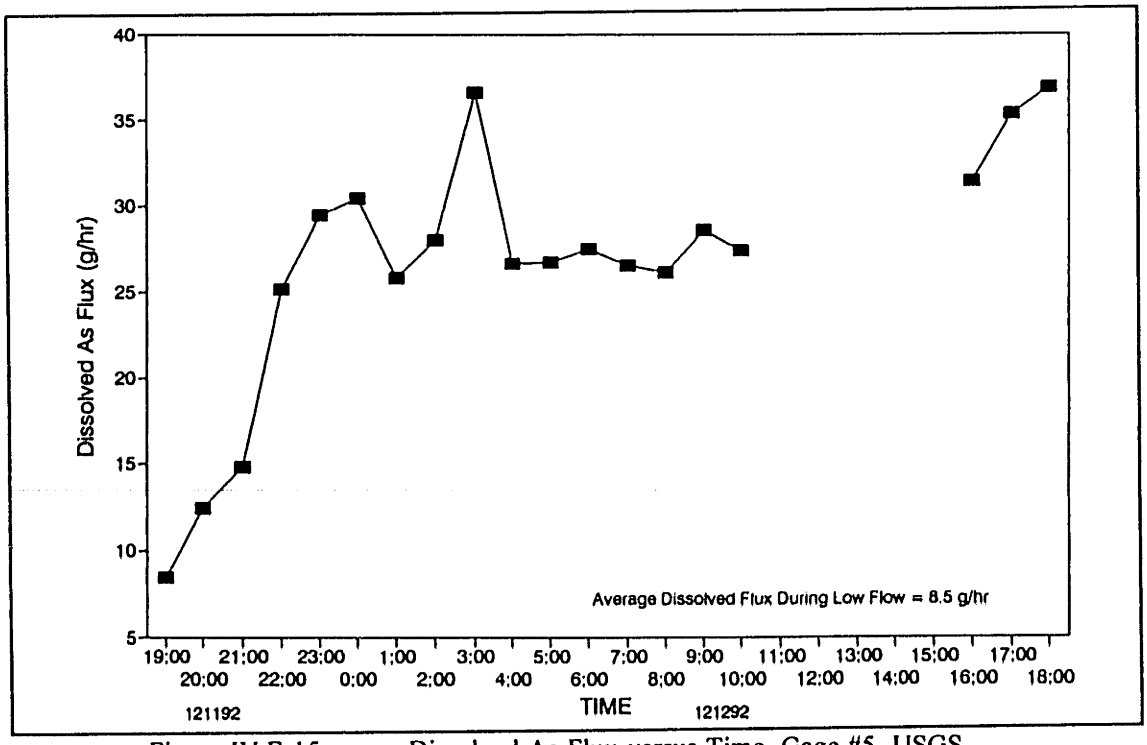

Figure IV.E-15: Dissolved As Flux versus Time, Gage #5, USGS December 11, 1992 Storm

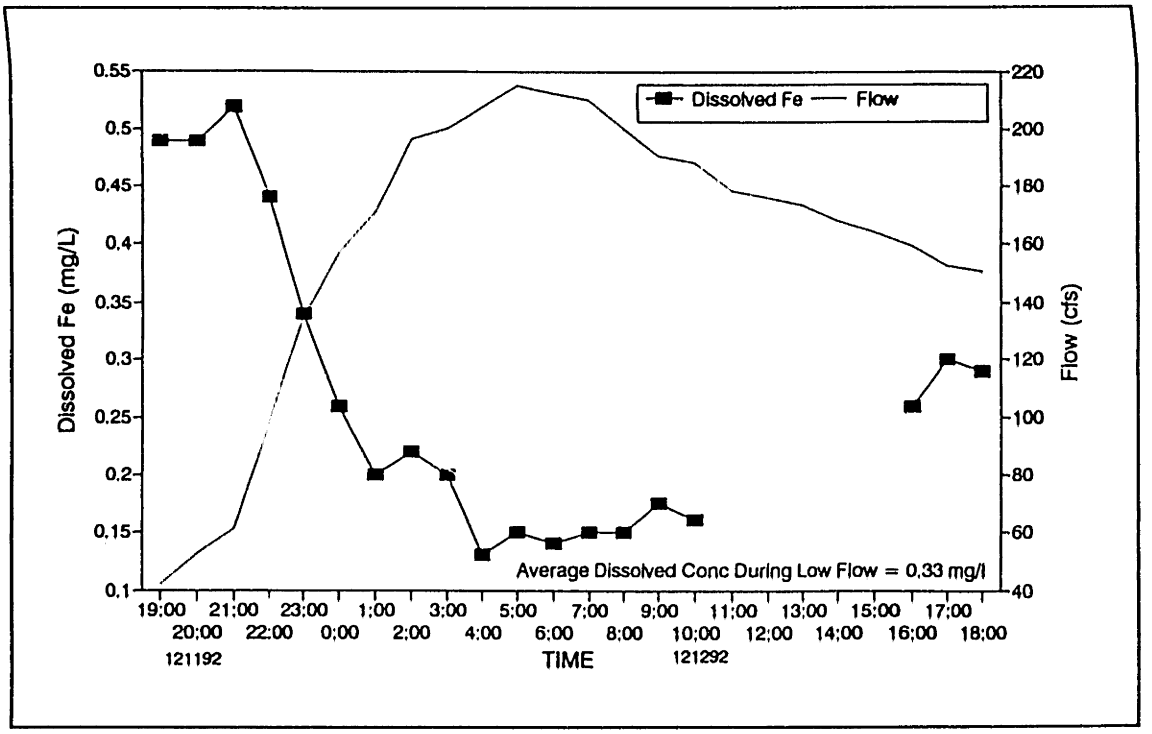

Figure IV.E-16: Dissolved Fe Concentration and Flow versus Time, Gage #5, USGS December 11, 1992 Storm

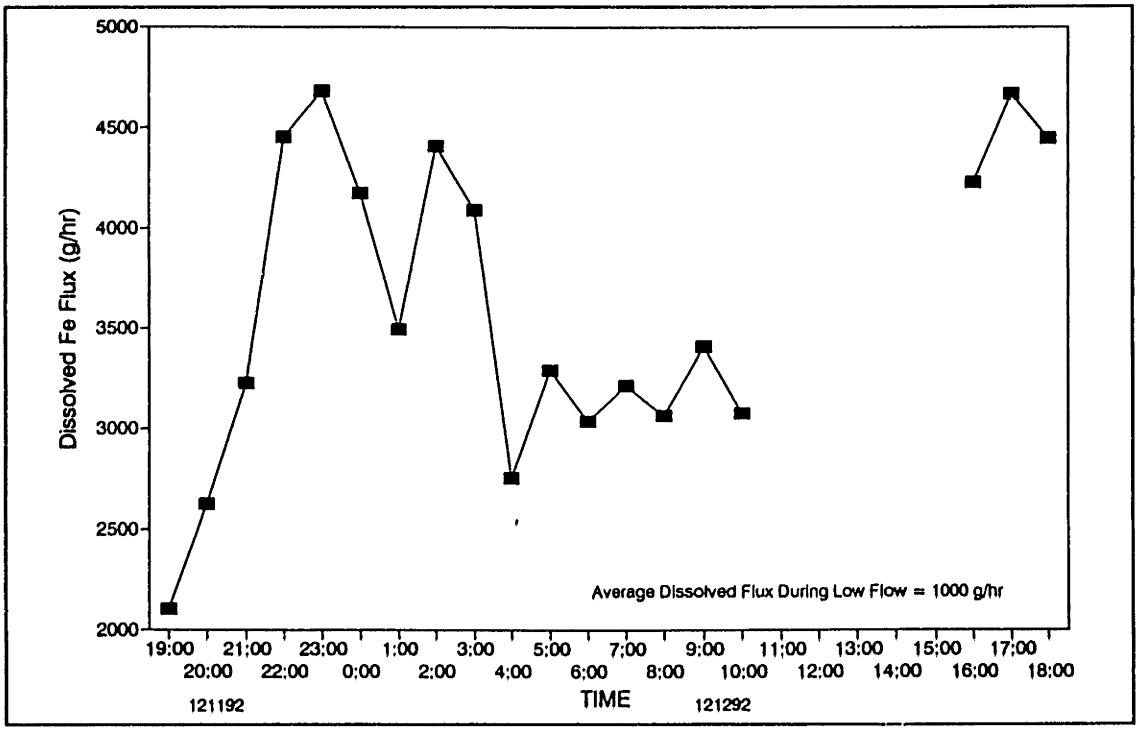

Figure IV.E-17: Dissolved Fe Flux versus Time, Gage #5, USGS December 11, 1992 Storm

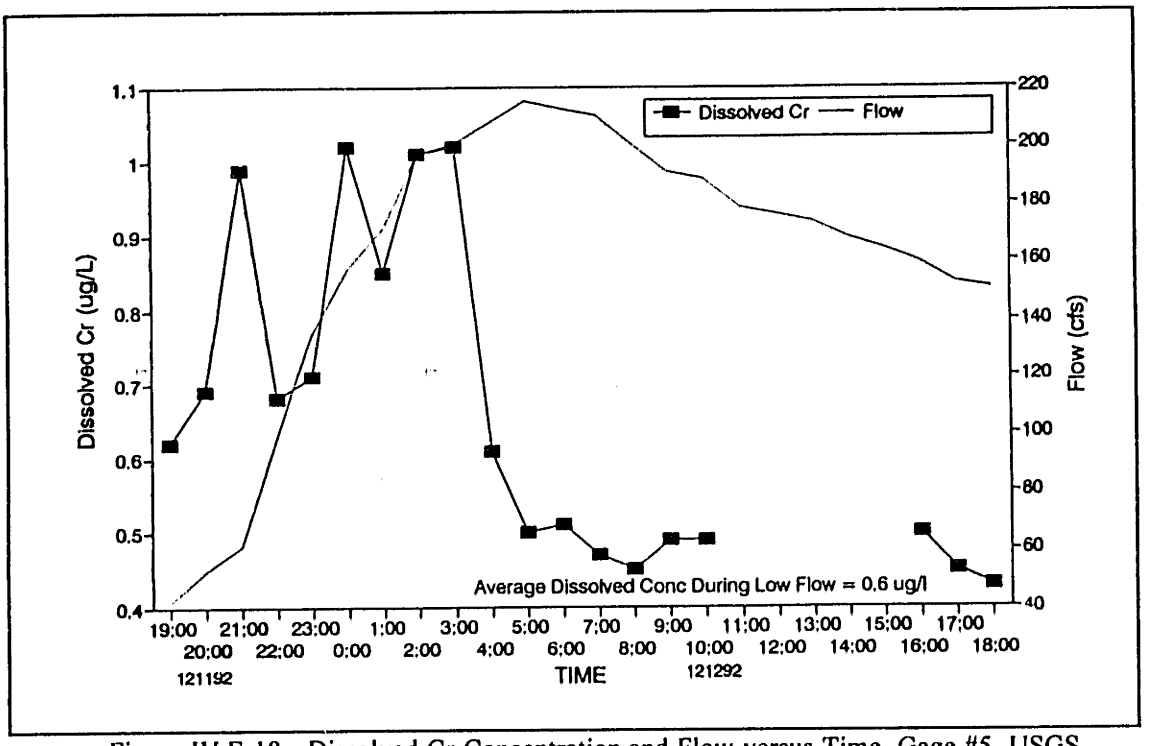

Figure IV.E-18: Dissolved Cr Concentration and Flow versus Time, Gage #5, USGS December 11, 1992 Storm

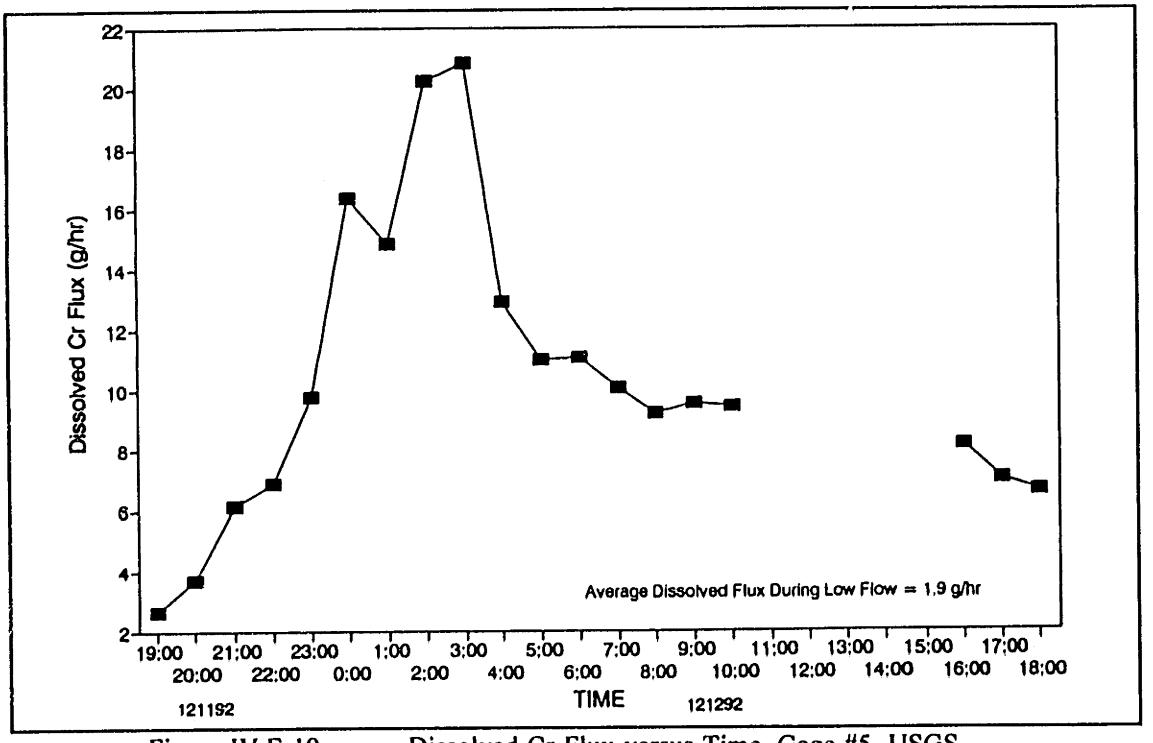

Figure IV.E-19: Dissolved Cr Flux versus Time, Gage #5, USGS December 11, 1992 Storm

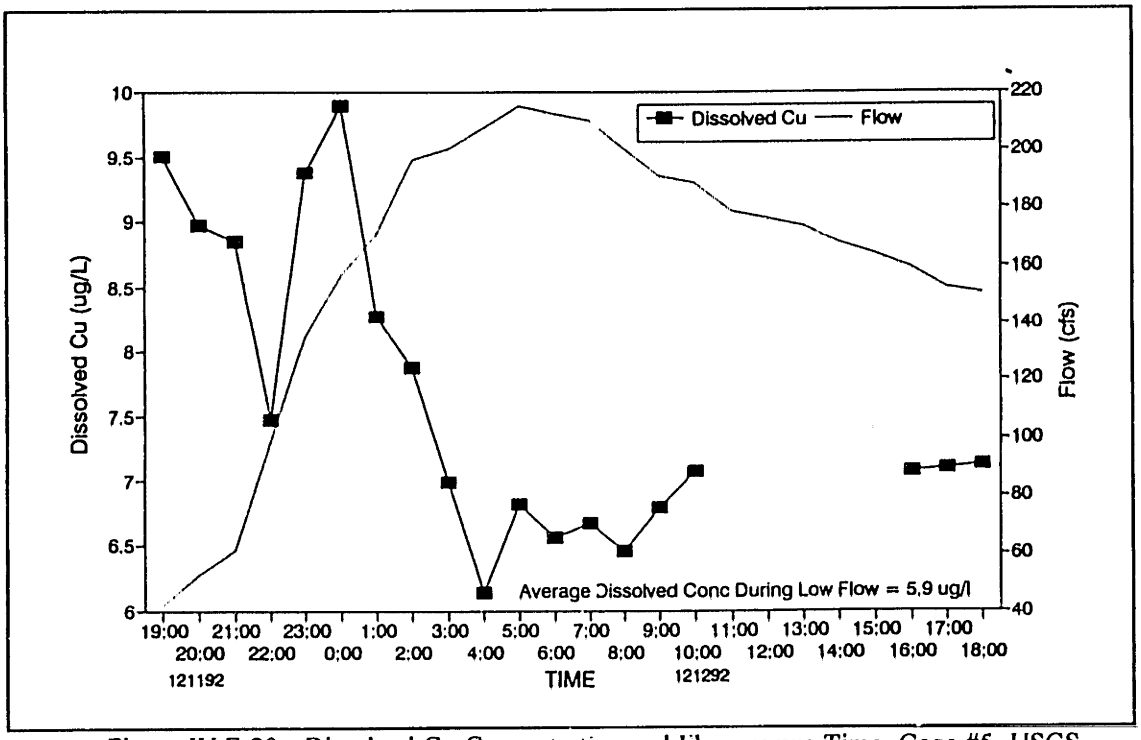

Figure IV.E-20: Dissolved Cu Concentration and Flow versus Time, Gage #5, USGS December 11, 1992 Storm

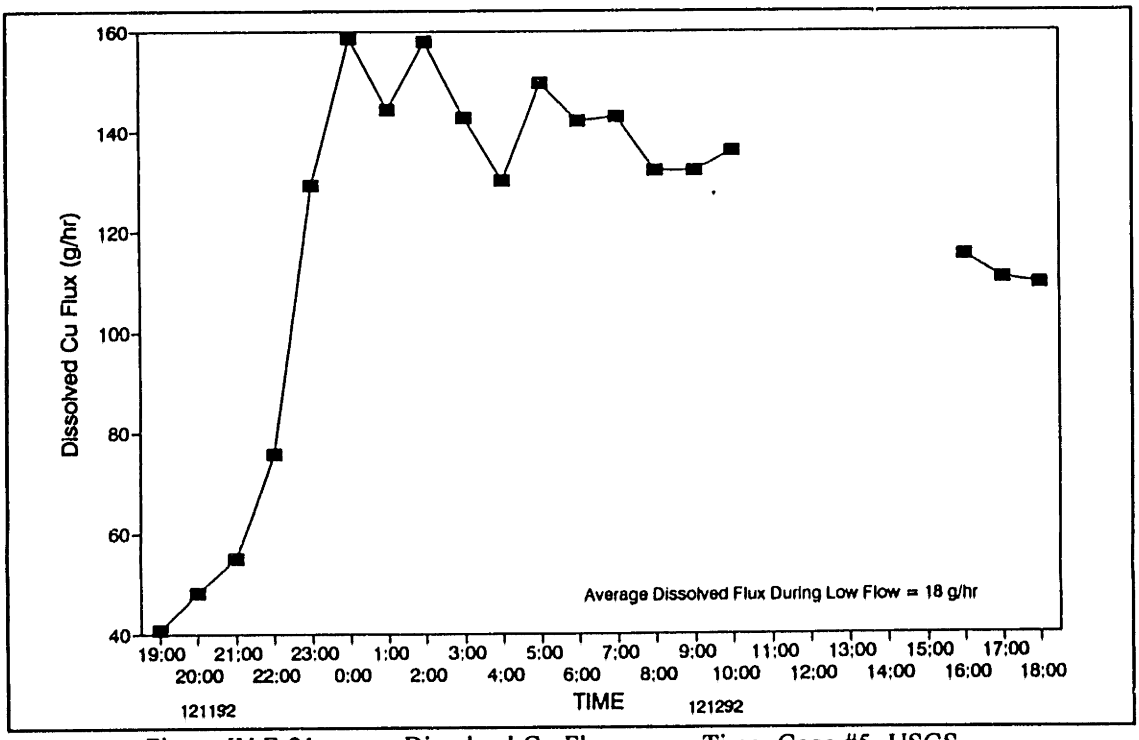

Figure IV.E-21: Dissolved Cu Flux versus Time, Gage #5, USGS December 11, 1992 Storm

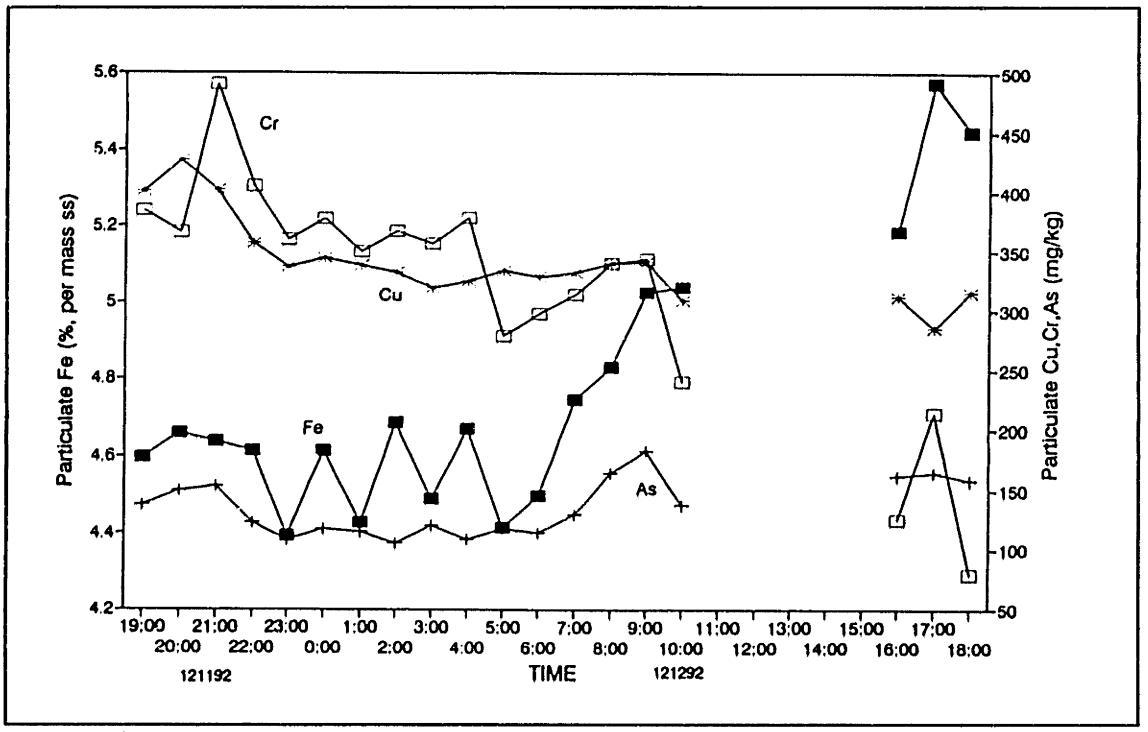

Figure IV.E-22: Particulate Metal Concentration versus Time, Gage #5,USGS December 11, 1992 Storm

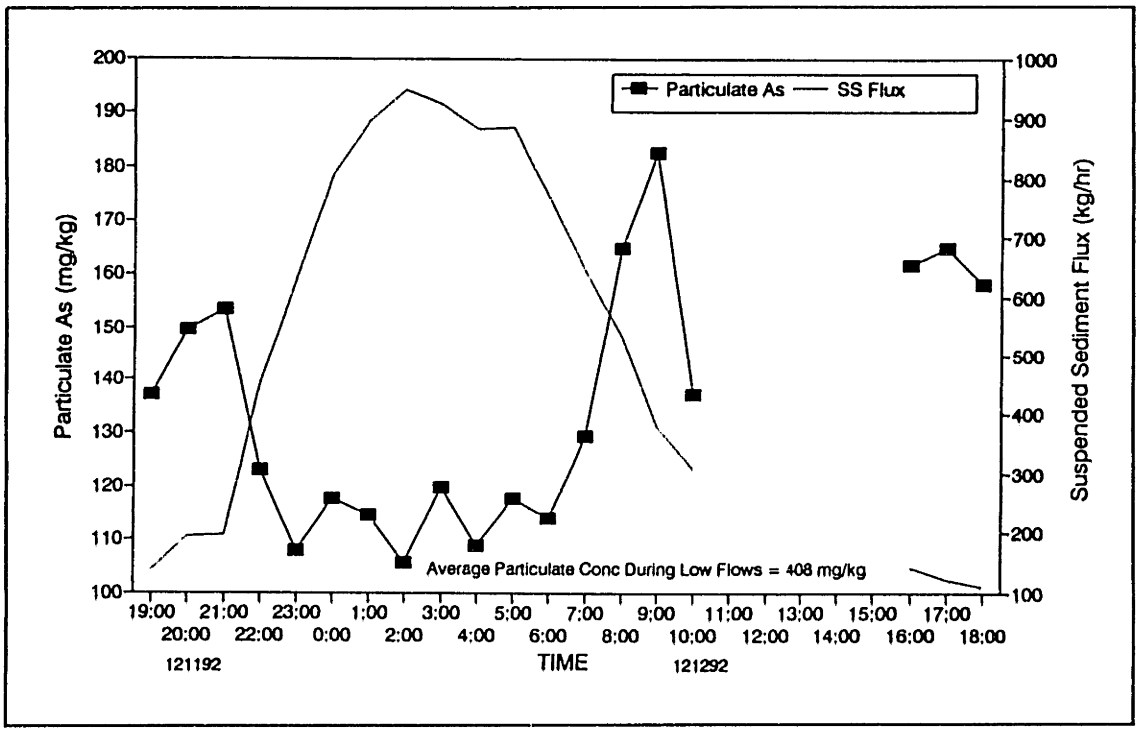

Figure IV.E-23: Particulate As Concentration and Flow versus Time, Gage #5, USGS December 11, 1992 Storm

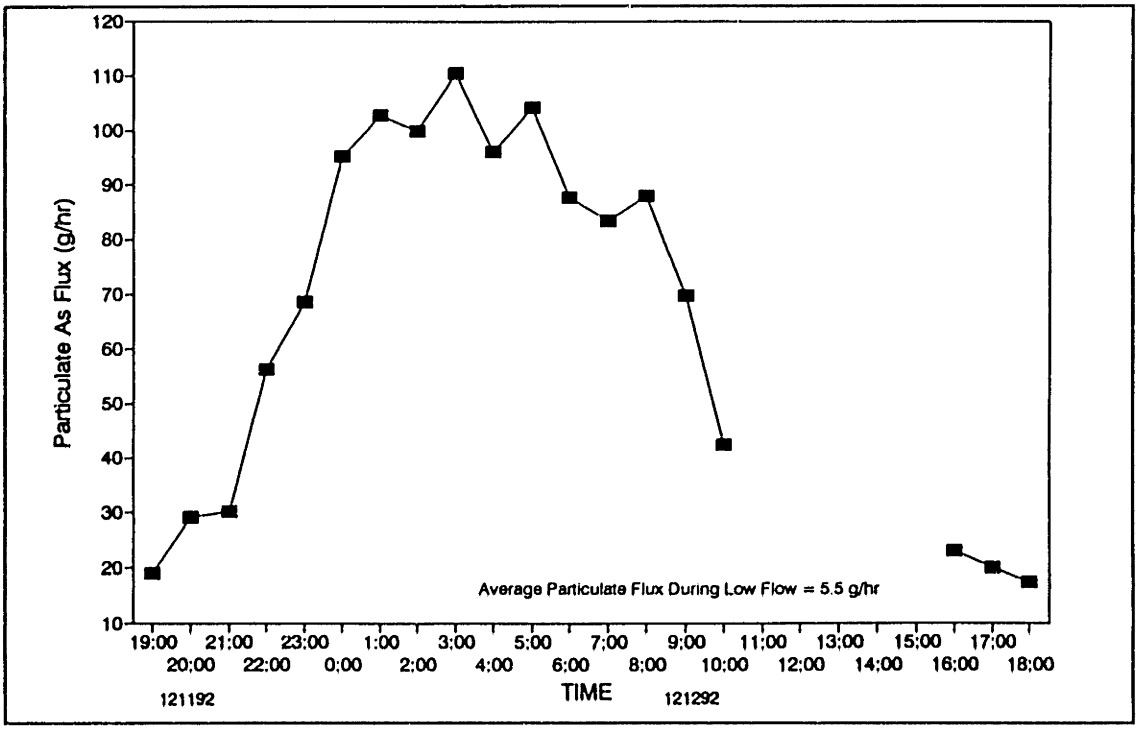

Figure IV.E-24: Particulate As Flux versus Time, Gage #5, USGS December 11, 1992 Storm

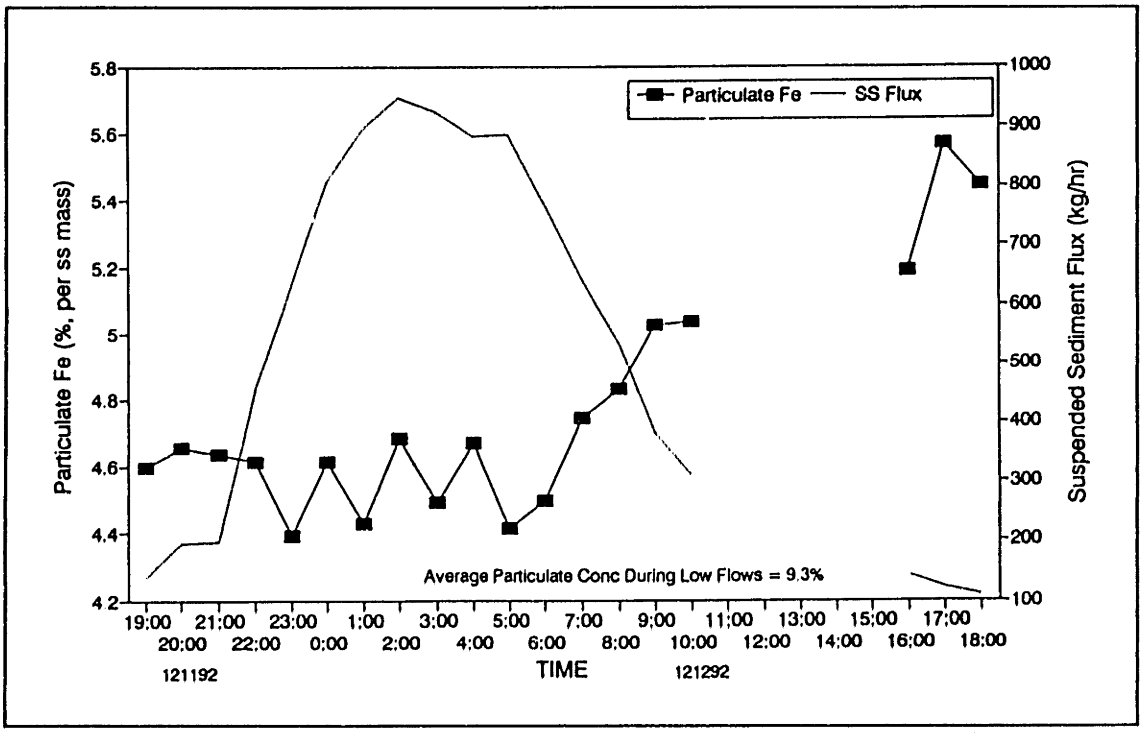

Figure IV.E-25: Particulate Fe Concentration and Flow versus Time, Gage #5, USGS December 11, 1992 Storm

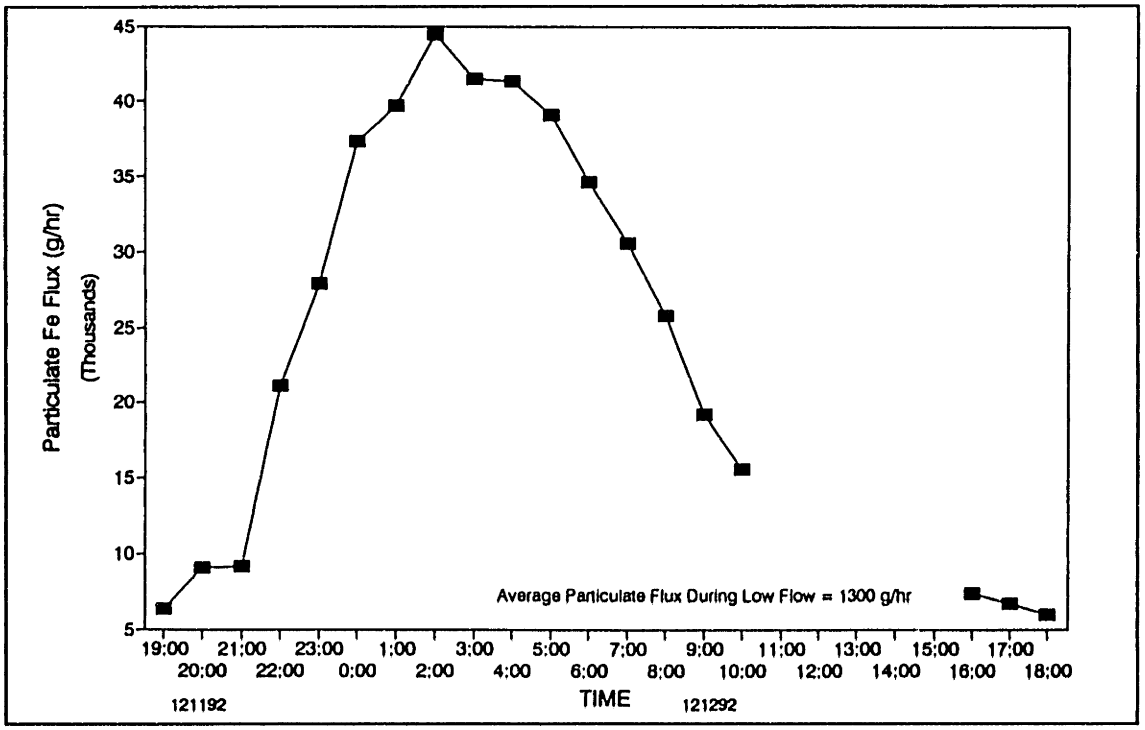

Figure IV.E-26: Particulate Fe Flux versus Time, Gage #5, USGS December 11, 1992 Storm

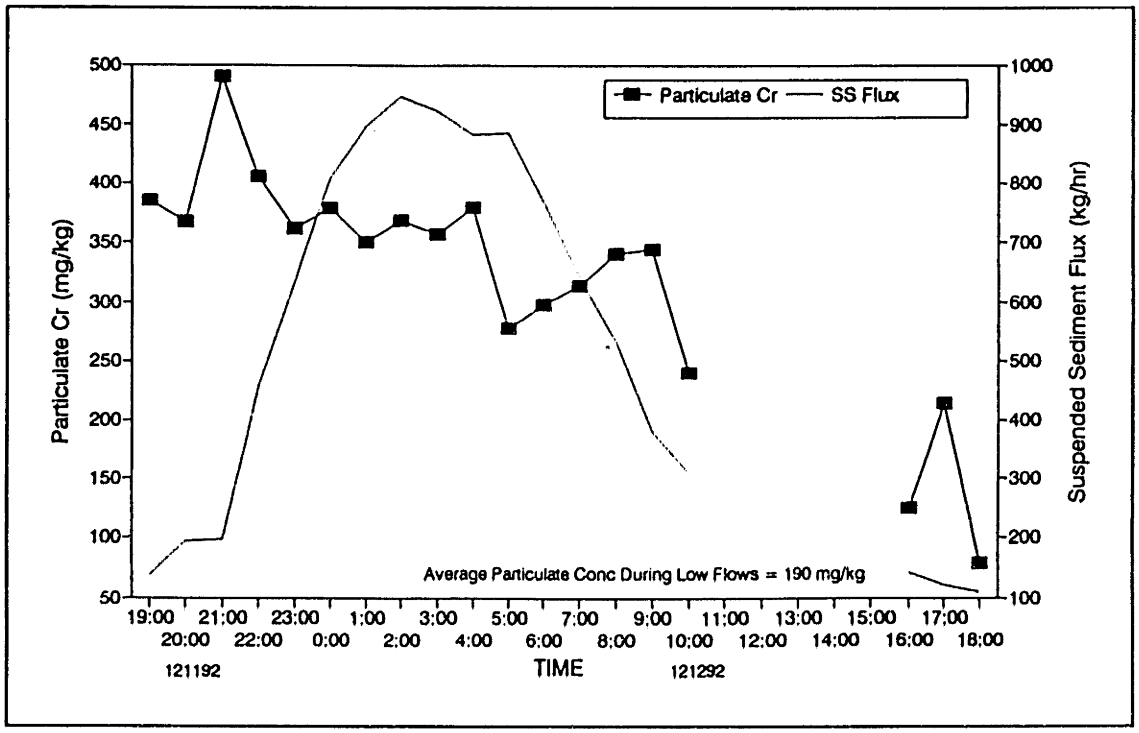

Figure IV.E-27: Particulate Cr Concentration and Flow versus Time, Gage #5, USGS December 11, 1992 Storm

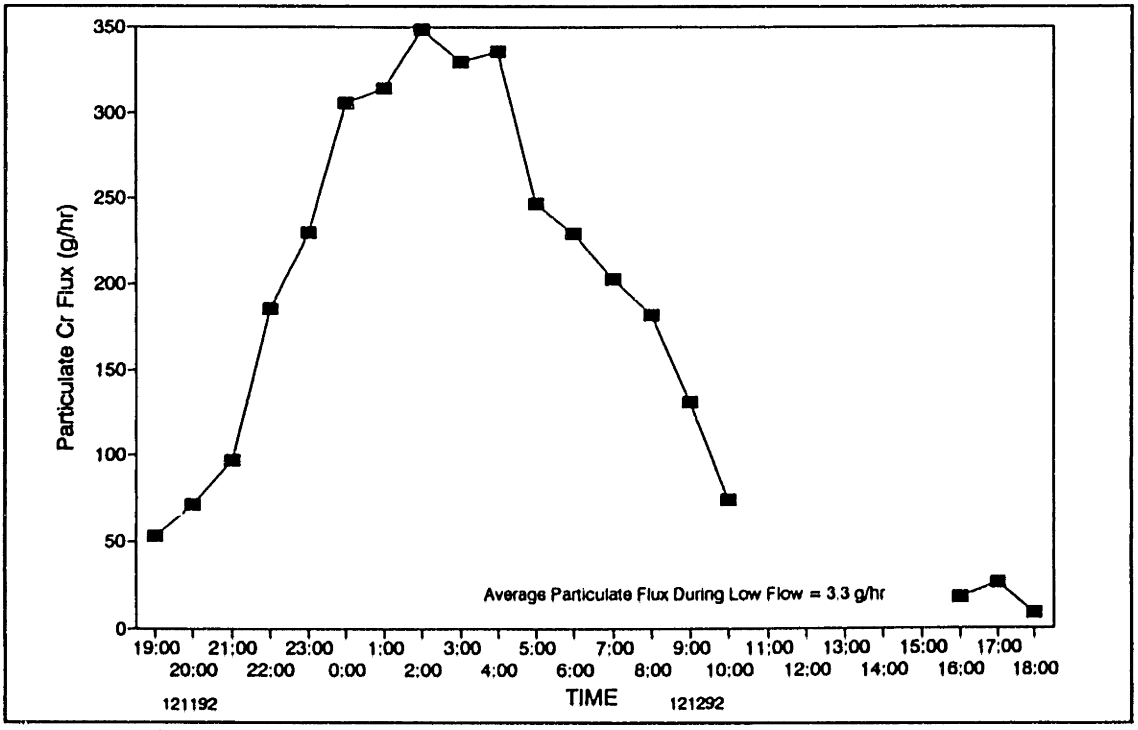

Figure IV.E-28: Particulate Cr Flux versus Time, Gage #5, USGS December 11, 1992 Storm

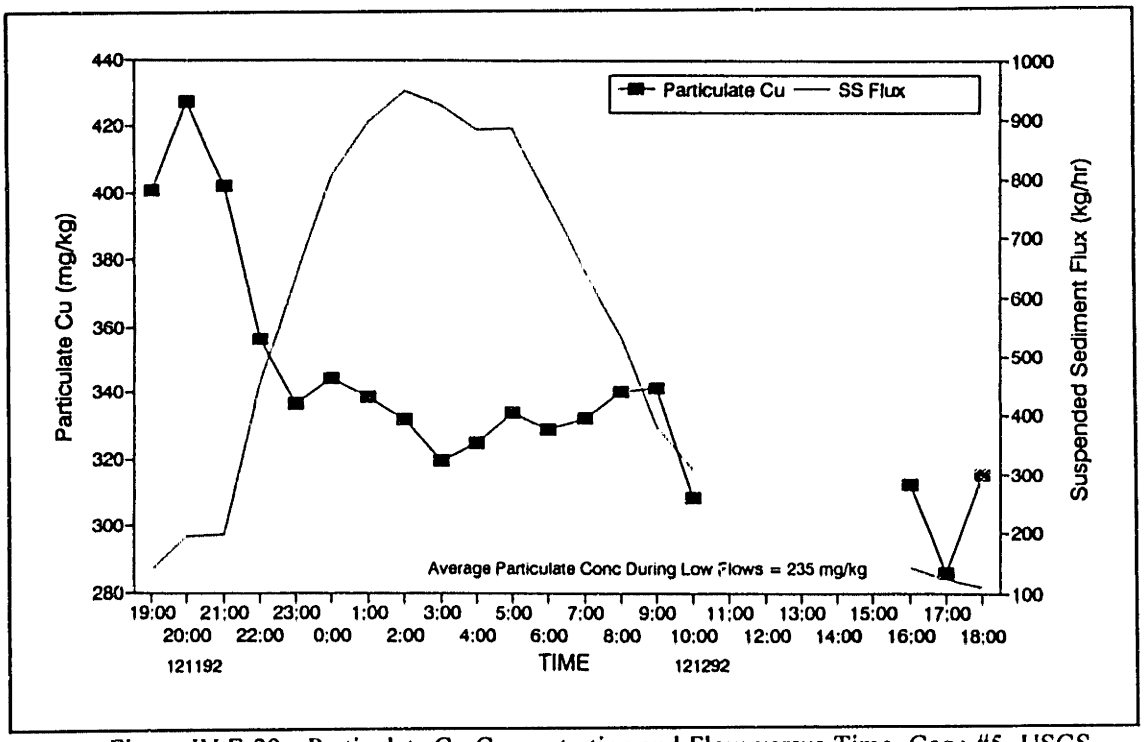

Figure IV.E-29: Particulate Cu Concentration and Flow versus Time, Gage #5, USGS December 11, 1992 Storm

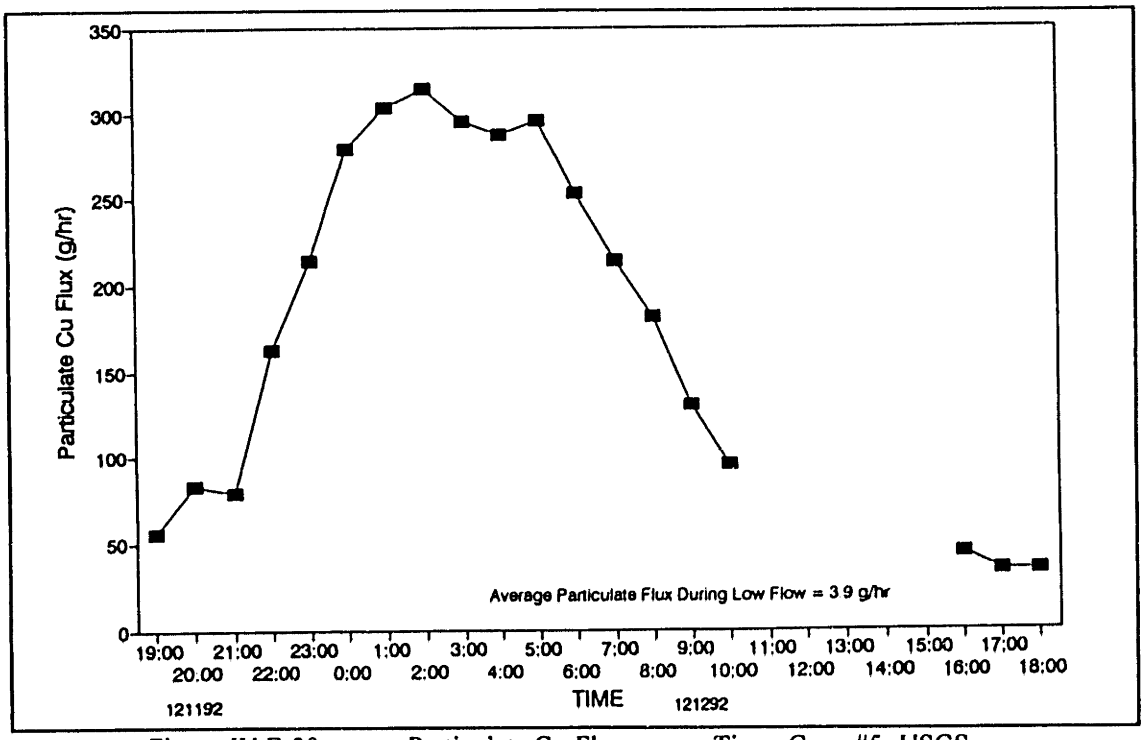

Figure IV.E-30: Particulate Cu Flux versus Time, Gage #5, USGS December 11, 1992 Storm

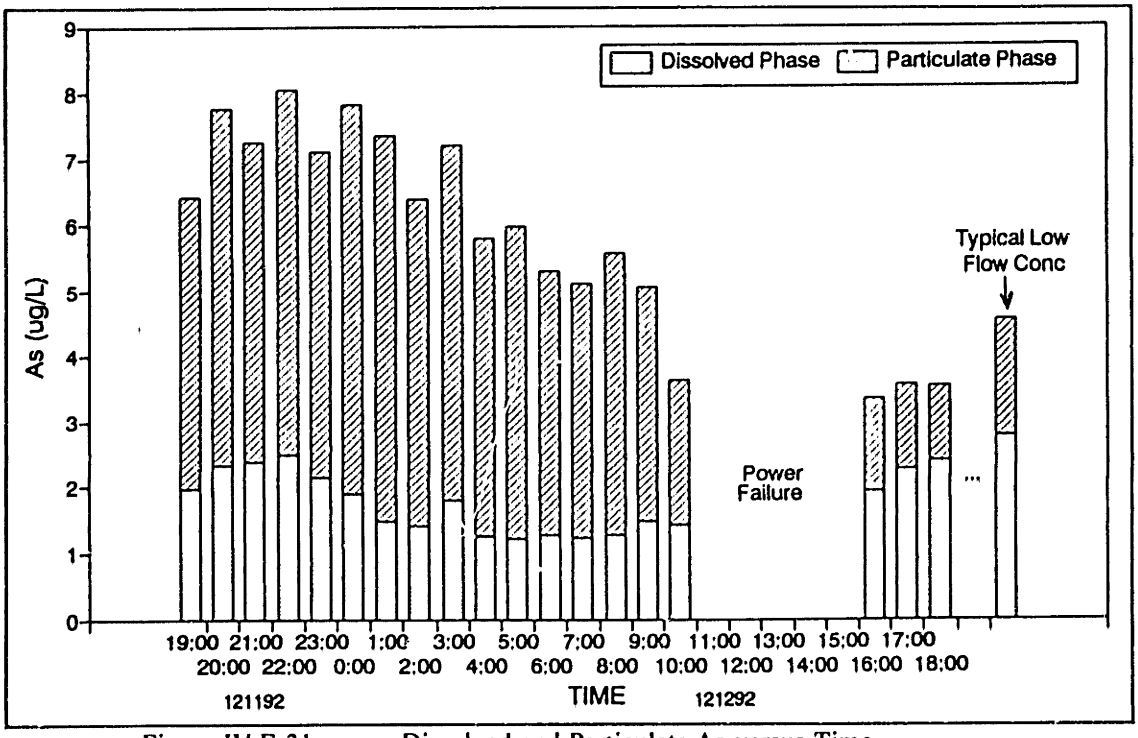

Figure IV.E-31: Dissolved and Particulate As versus Time
Gage #5, USGS, December 11, 1992 Storm

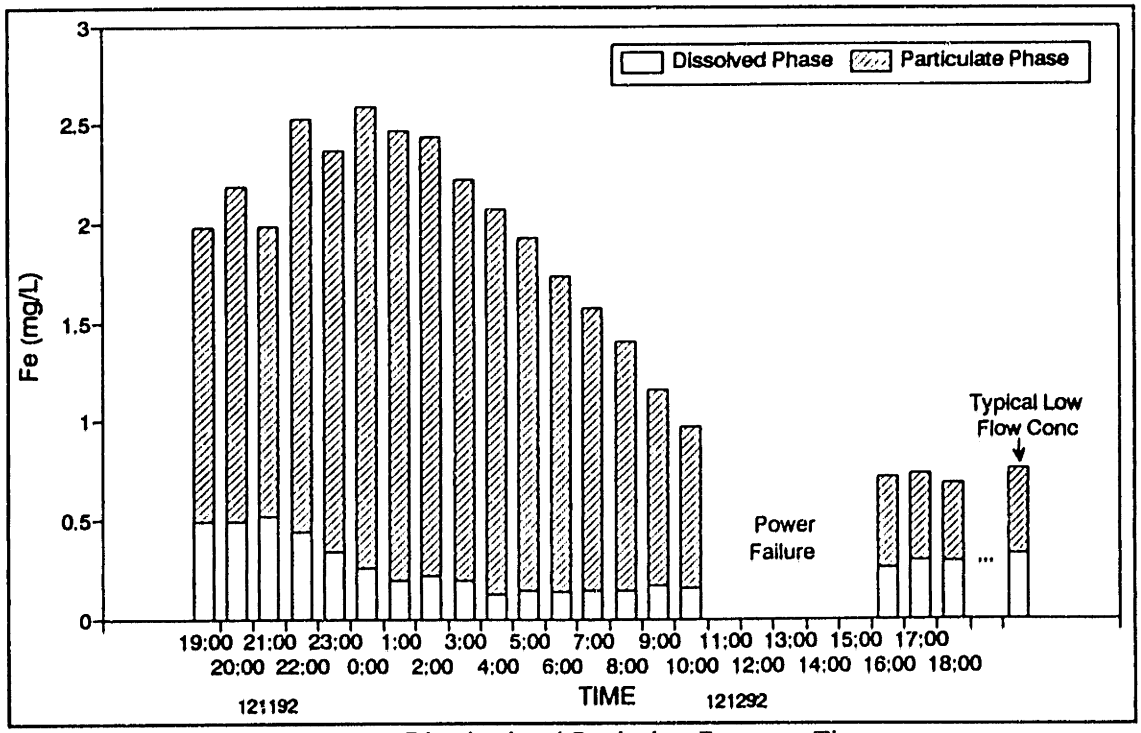

Figure IV.E-32: Dissolved and Particulate Fe versus Time
Gage #5, USGS, December 11, 1992 Storm

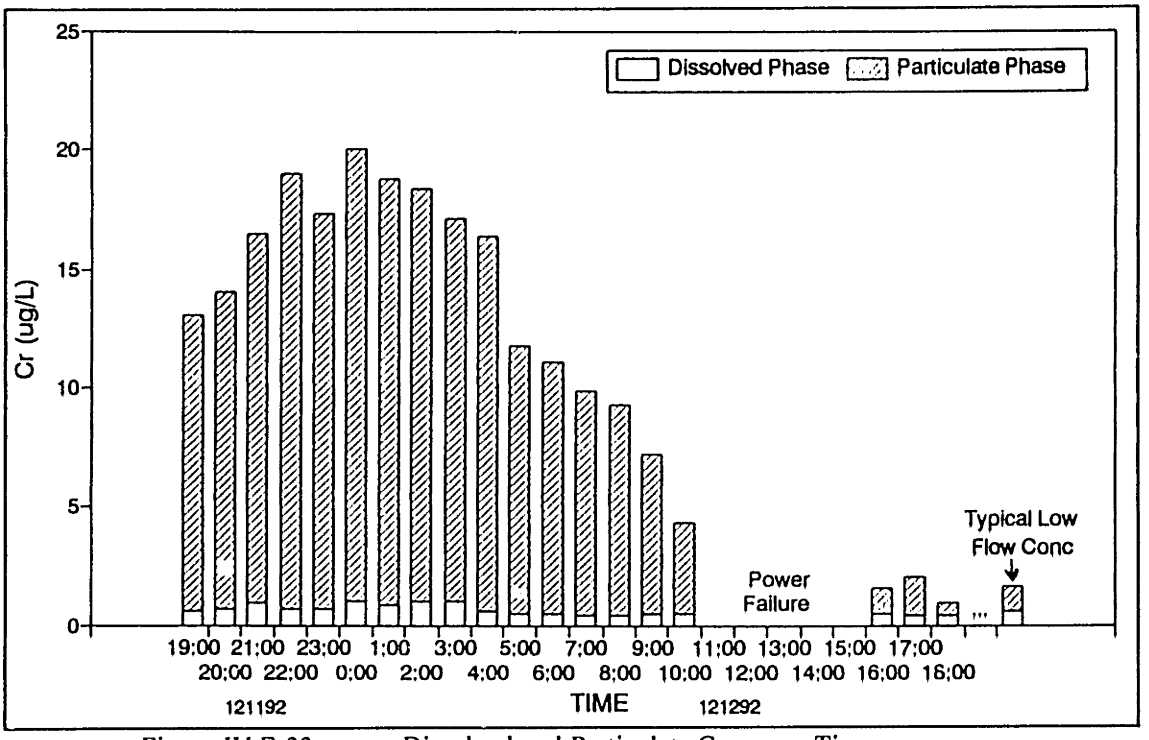

Figure IV.E-33: Dissolved and Particulate Cr versus Time
Gage #5, USGS, December 11, 1992 Storm

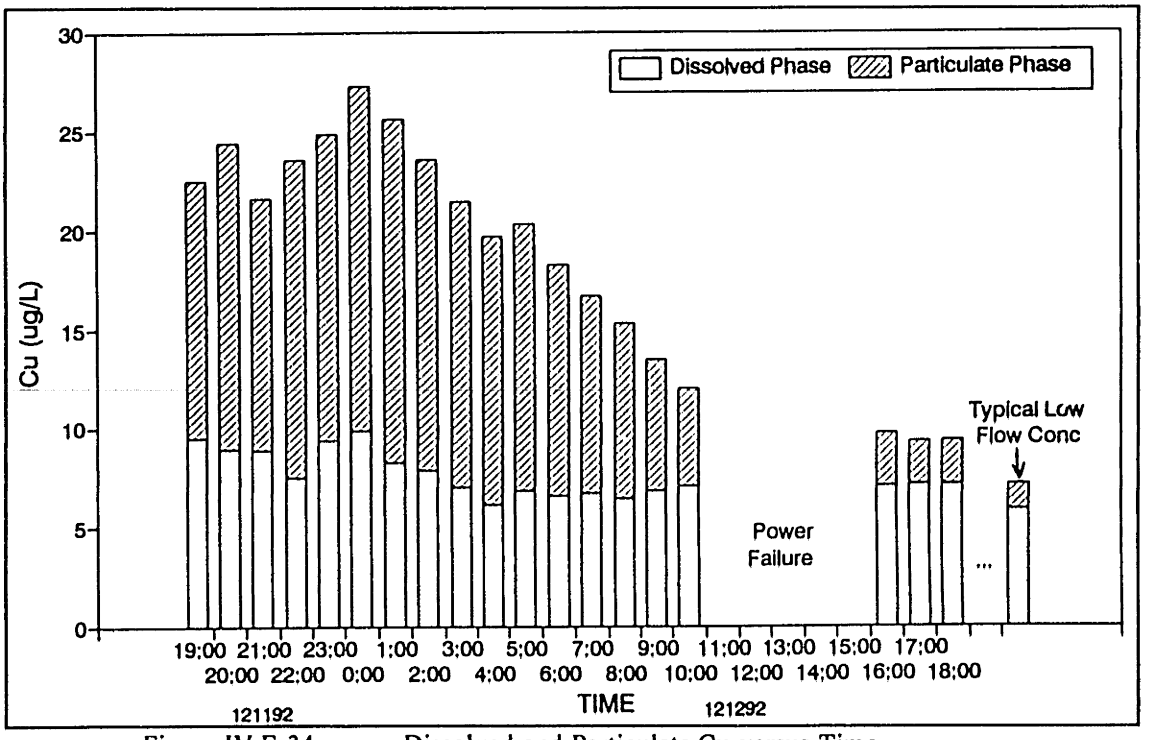

Figure IV.E-34: Dissolved and Particulate Cu versus Time
Gage #5, USGS, December 11, 1992 Storm

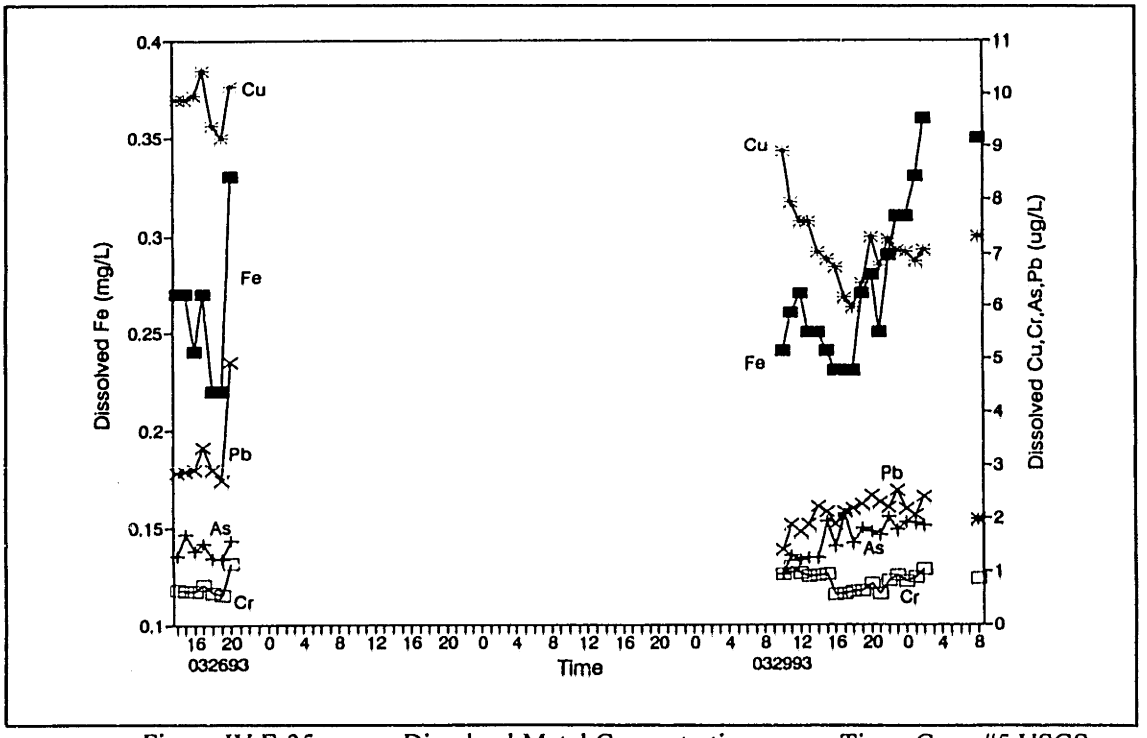

Figure IV.E-35: Dissolved Metal Concentration versus Time, Gage #5,USGS March 26 to 30, 1993

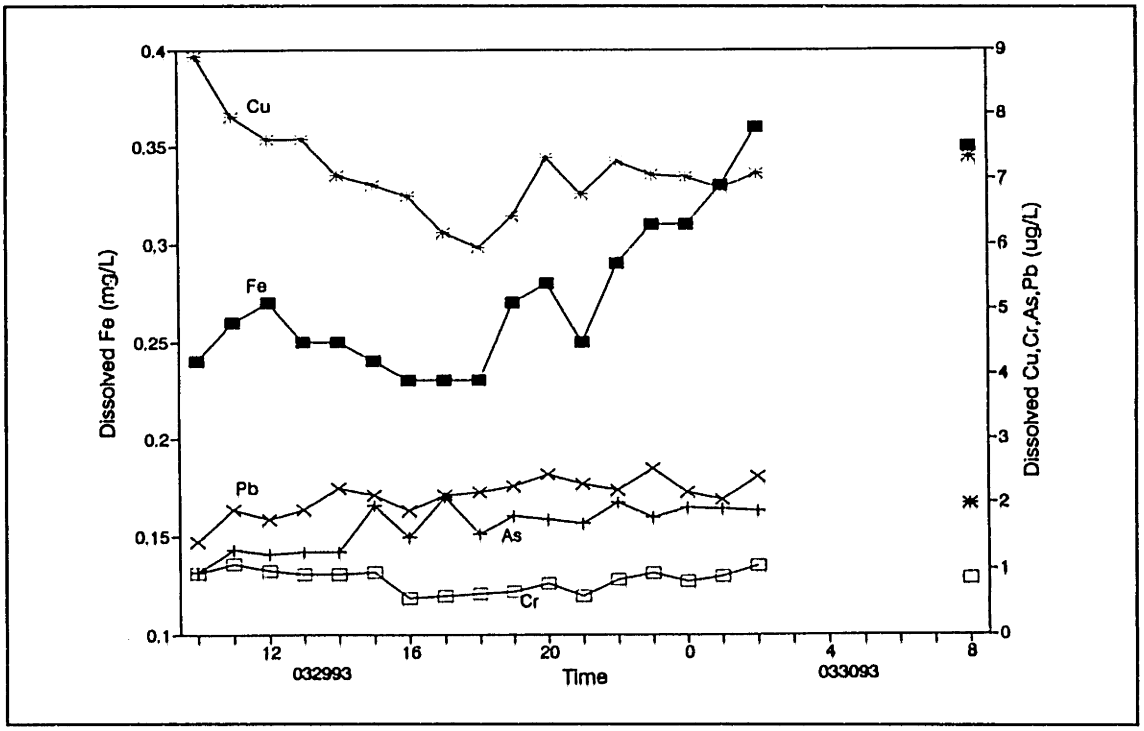

Figure IV.E-36: Dissolved Metal Concentration versus Time, Gage #5,USGS March 29 to 30, 1993

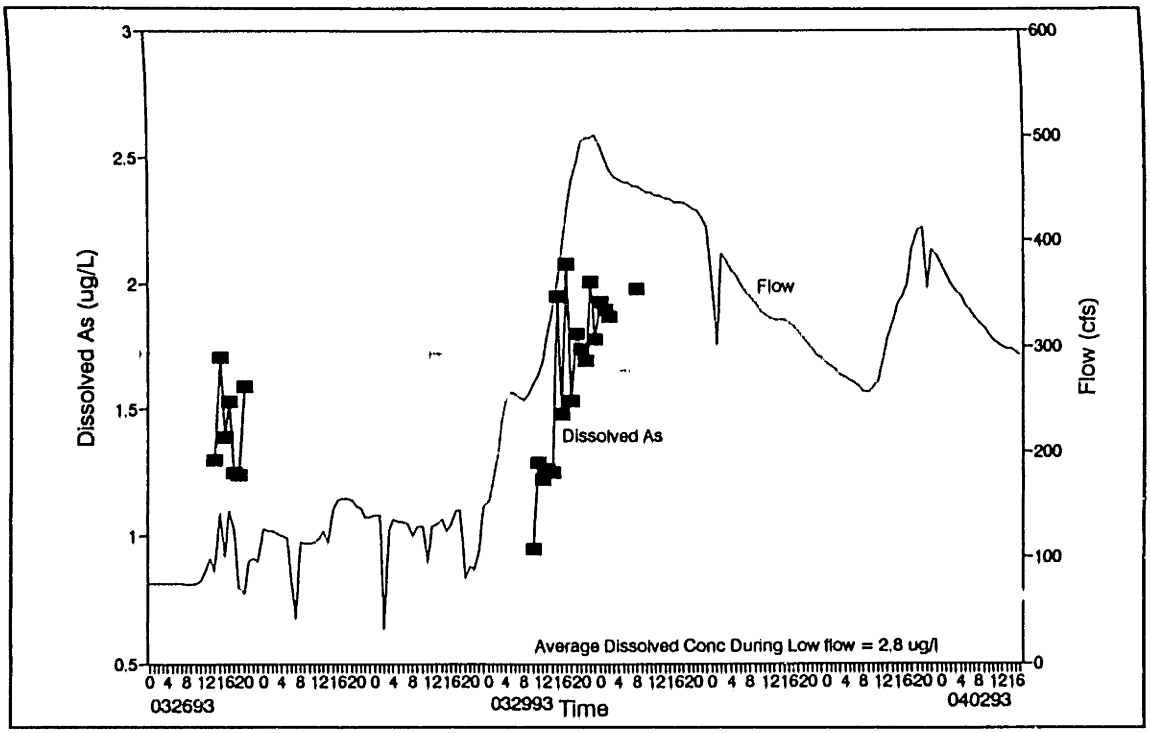

Figure IV.E-37: Dissolved As Concentration and Flow versus Time, Gage #5, USGS March 36 to April 2, 1993

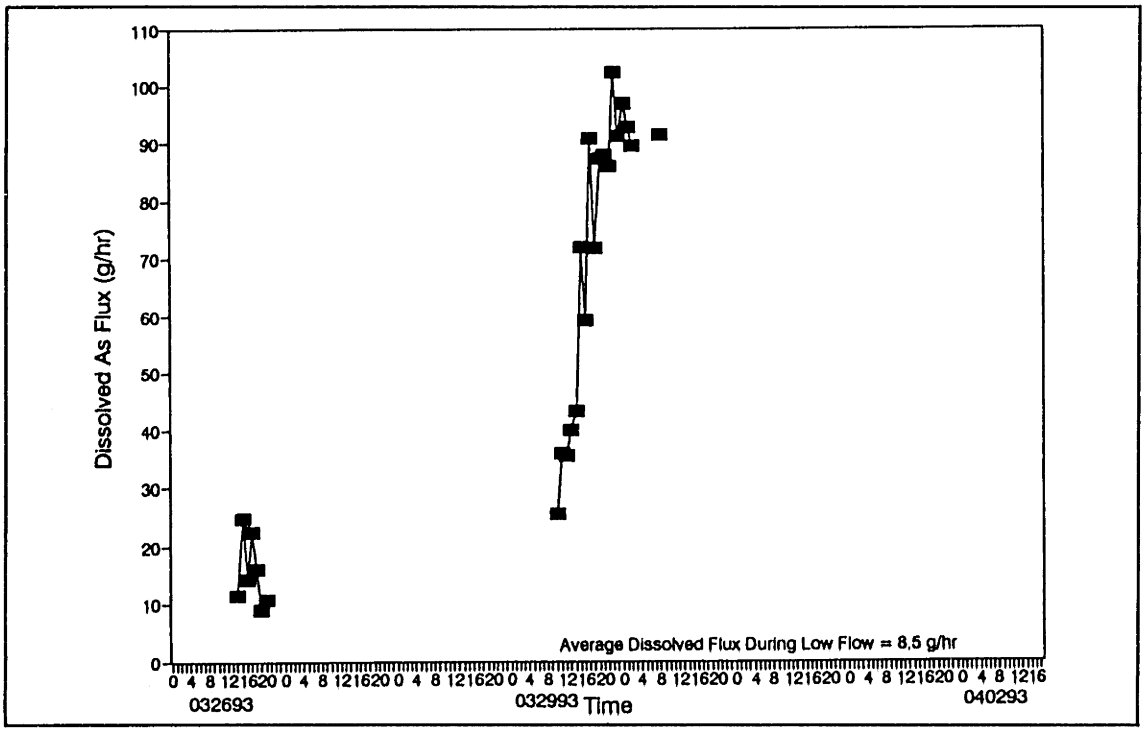

Figure IV.E-38: Dissolved As Flux versus Time, Gage #5, USGS March 36 to April 2, 1993

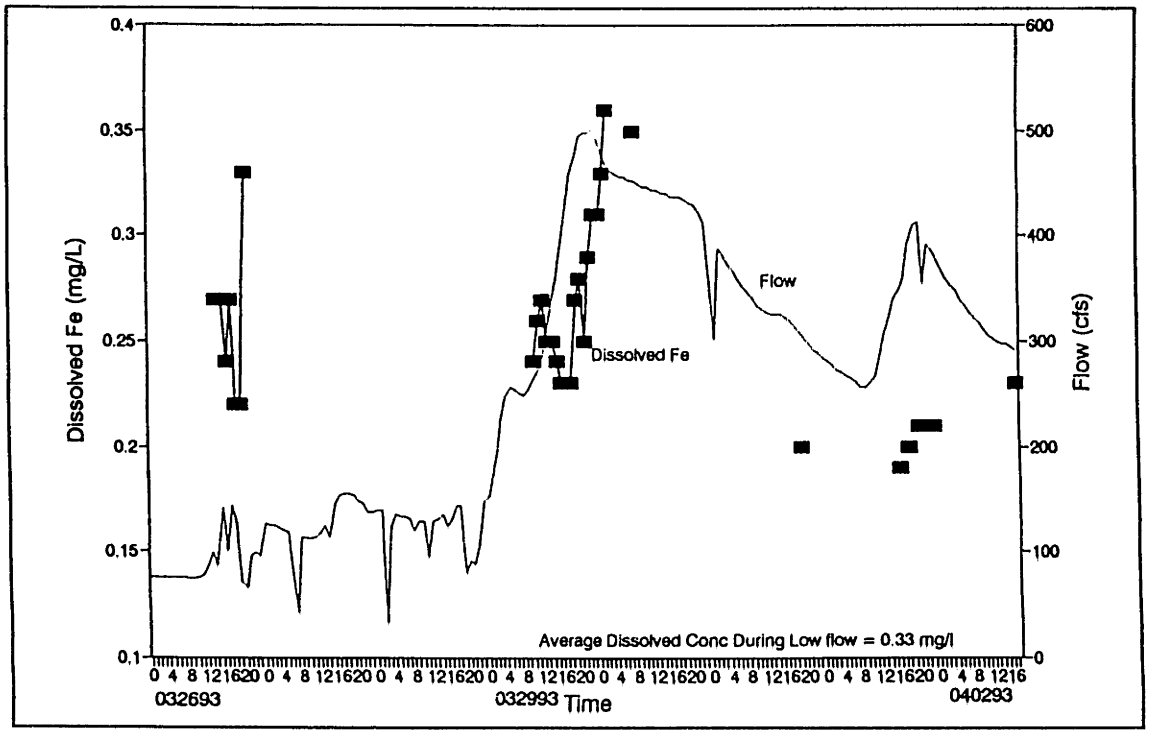

Figure IV.E-39: Dissolved Fe Concentration and Flow versus Time, Gage #5, USGS March 26 to April 2, 1993

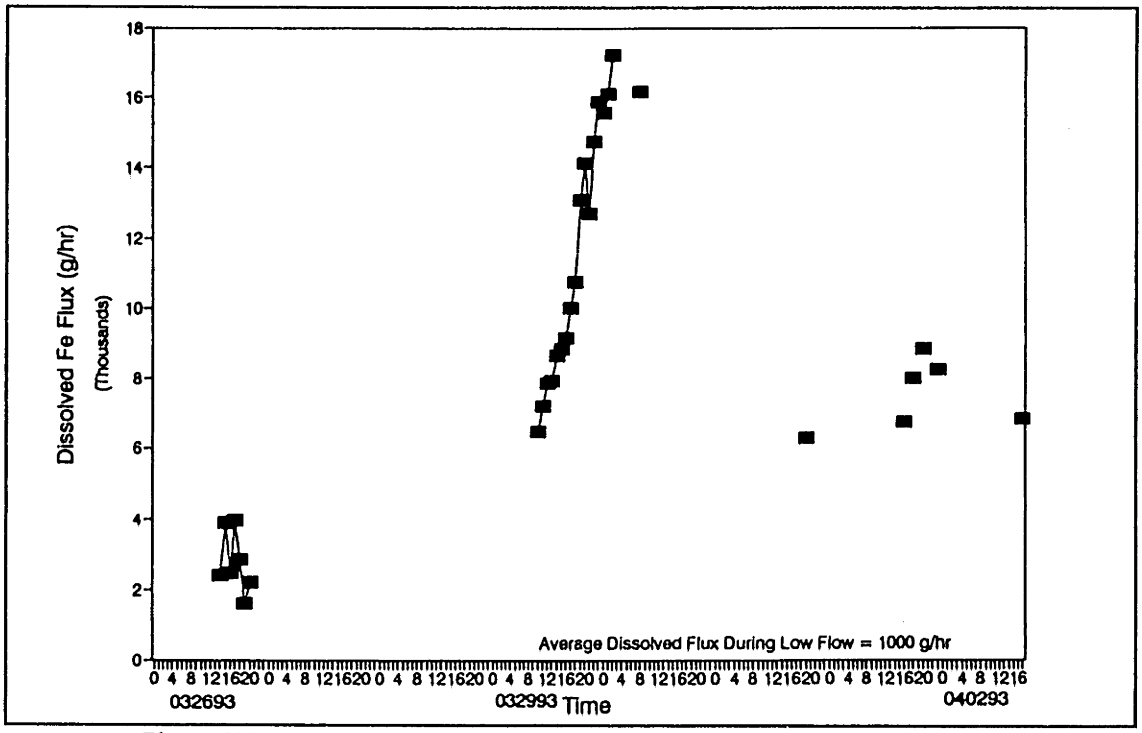

Figure IV.E-40: Dissolved Fe Flux versus Time, Gage #5, USGS March 26 to April 2, 1993

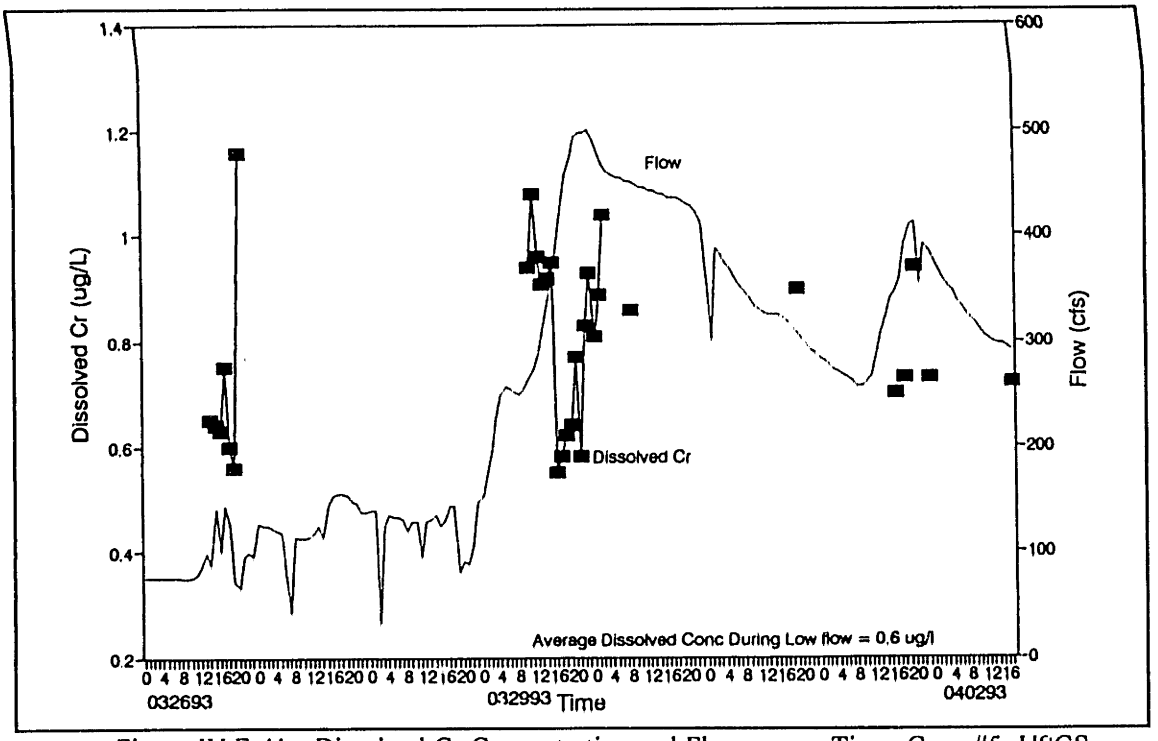

Figure IV.E-41: Dissolved Cr Concentration and Flow versus Time, Gage #5, USGS March 26 to April 2, 1993

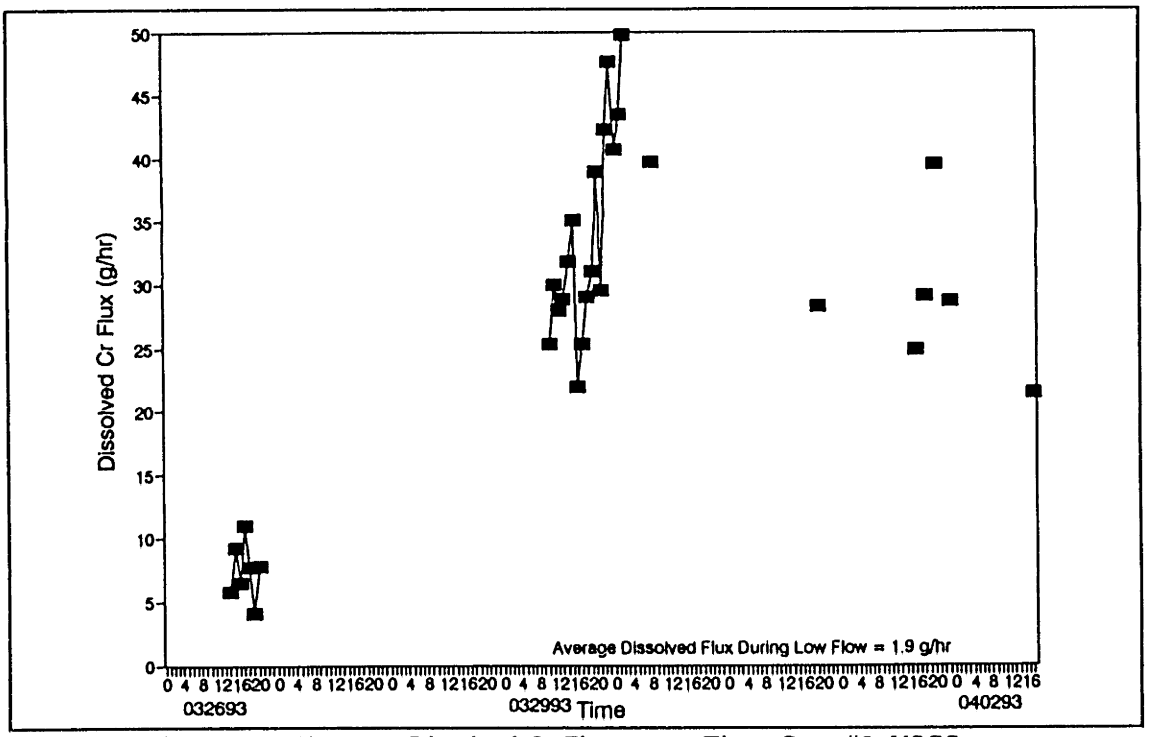

Figure IV.E-42: Dissolved Cr Flux versus Time, Gage #5, USGS March 26 to April 2, 1993

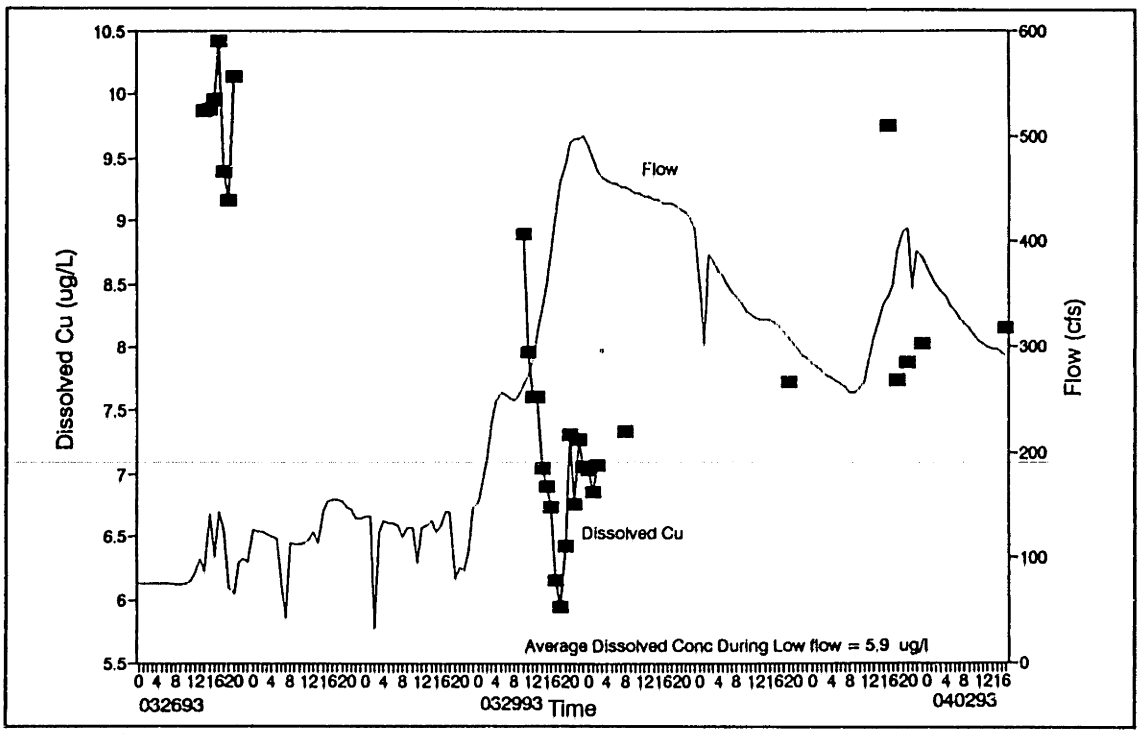

Figure IV.E-43: Dissolved Cu Concentration and Flow versus Time, Gage #5, USGS March 26 to April 2, 1993

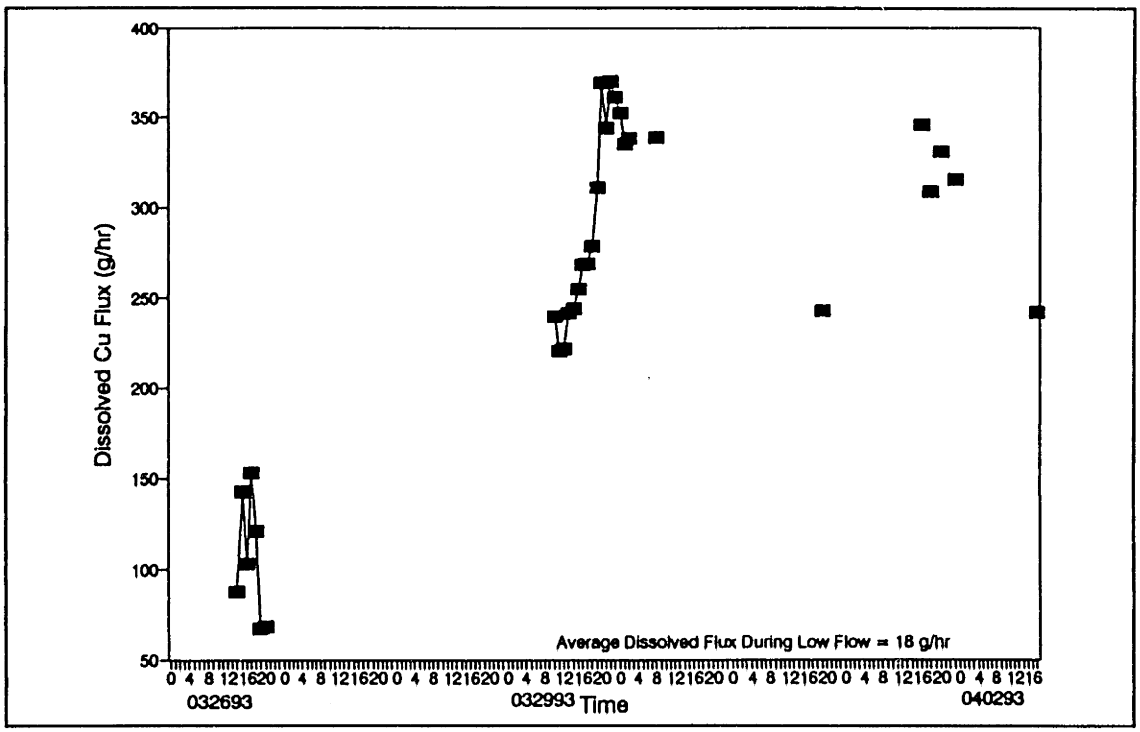

Figure IV.E-44: Dissolved Cu Flux versus Time, Gage #5, USGS March 25 to April 2, 1993

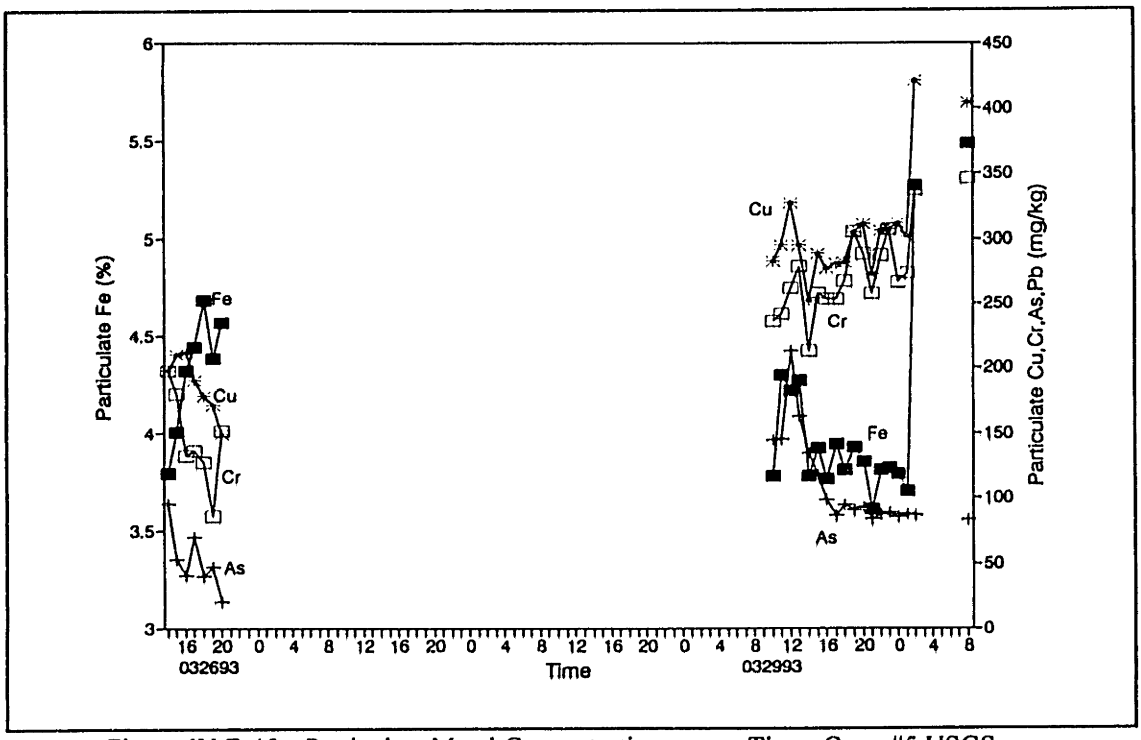

Figure IV.E-45: Particulate Metal Concentration versus Time, Gage #5,USGS
March 26 to 29, 1993

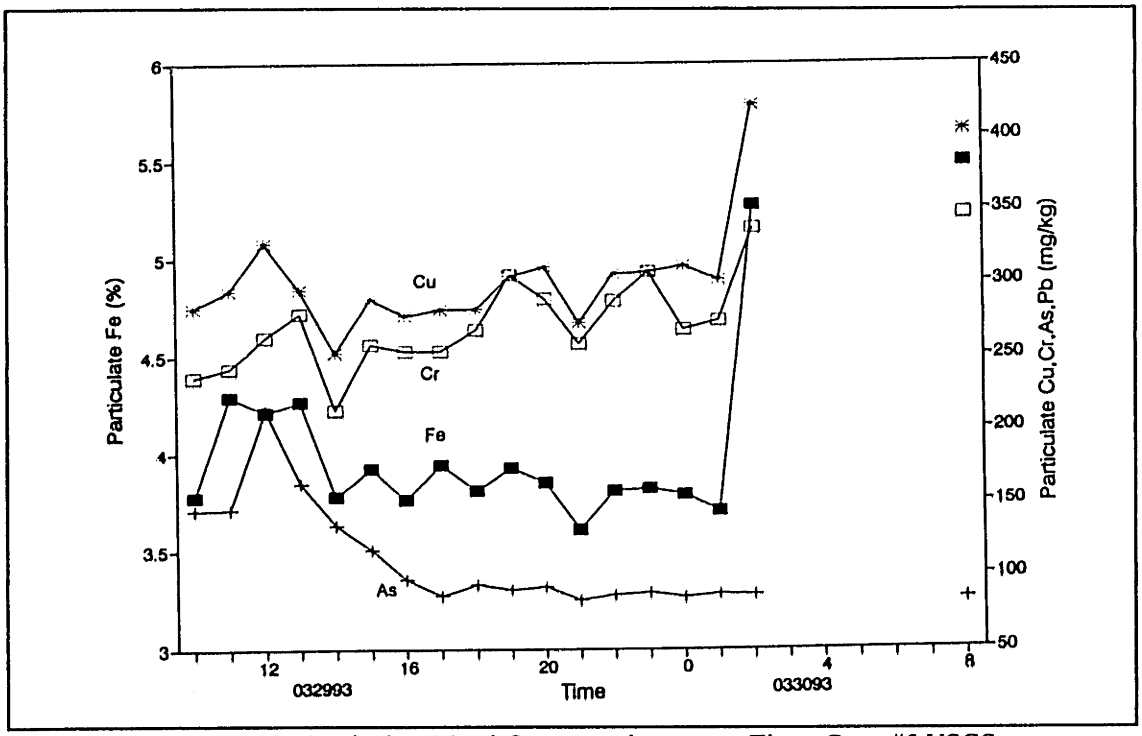

Figure IV.E-46: Particulate Metal Concentration versus Time, Gage #5,USGS
March 39 to 30, 1993

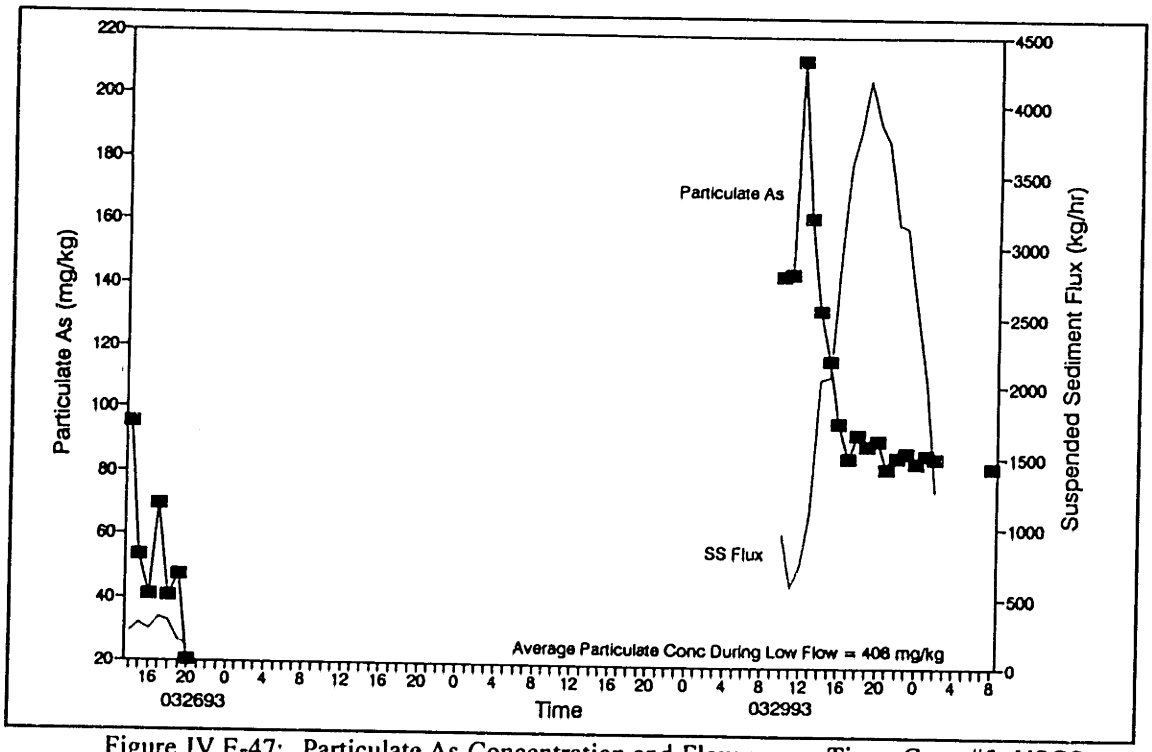

Figure IV.E-47: Particulate As Concentration and Flow versus Time, Gage #5, USGS March 26 to 30, 1993

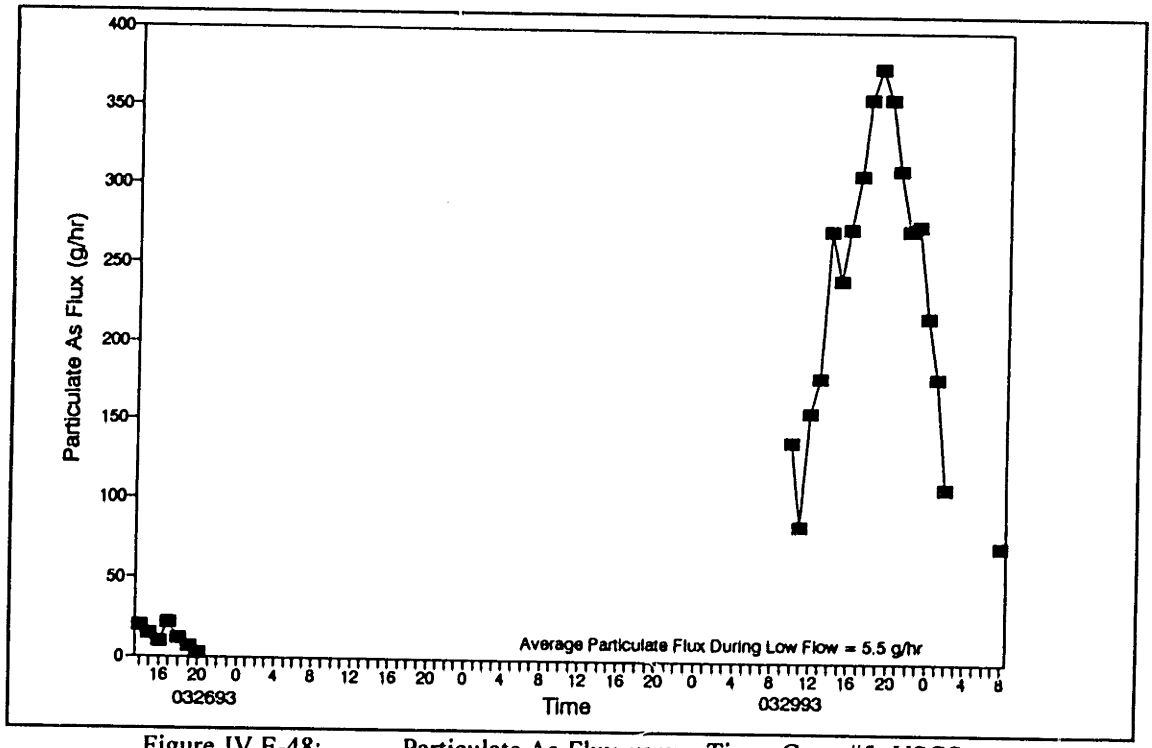

Figure IV.E-48: Particulate As Flux versus Time, Gage #5, USGS March 26 to 30, 1993

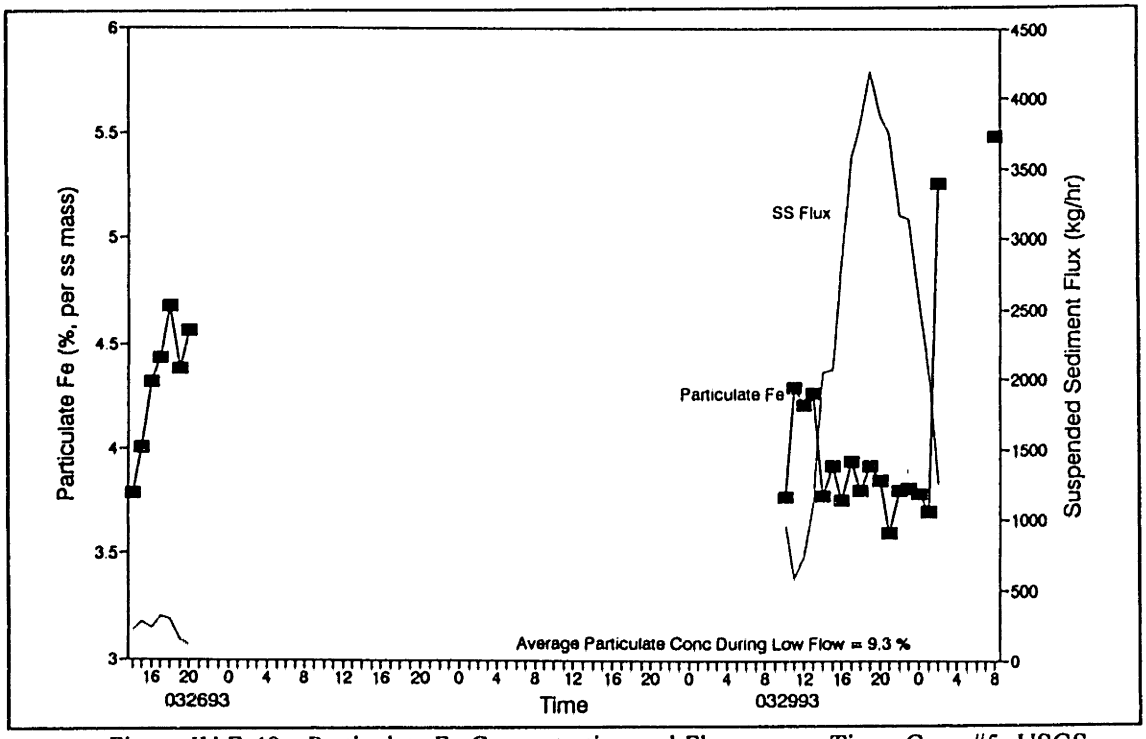

Figure IV.E-49: Particulate Fe Concentration and Flow versus Time, Gage #5, USGS March 26 to 30, 1993

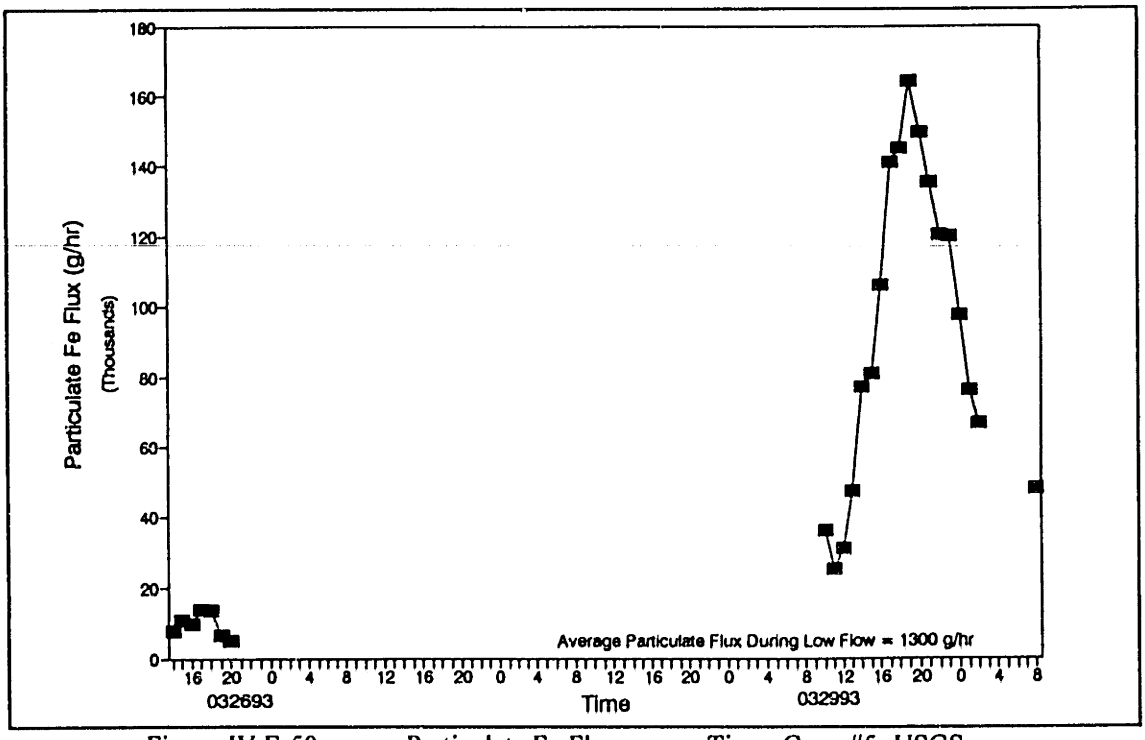

Figure IV.E-50: Particulate Fe Flux versus Time, Gage #5, USGS March 26 to 30, 1993

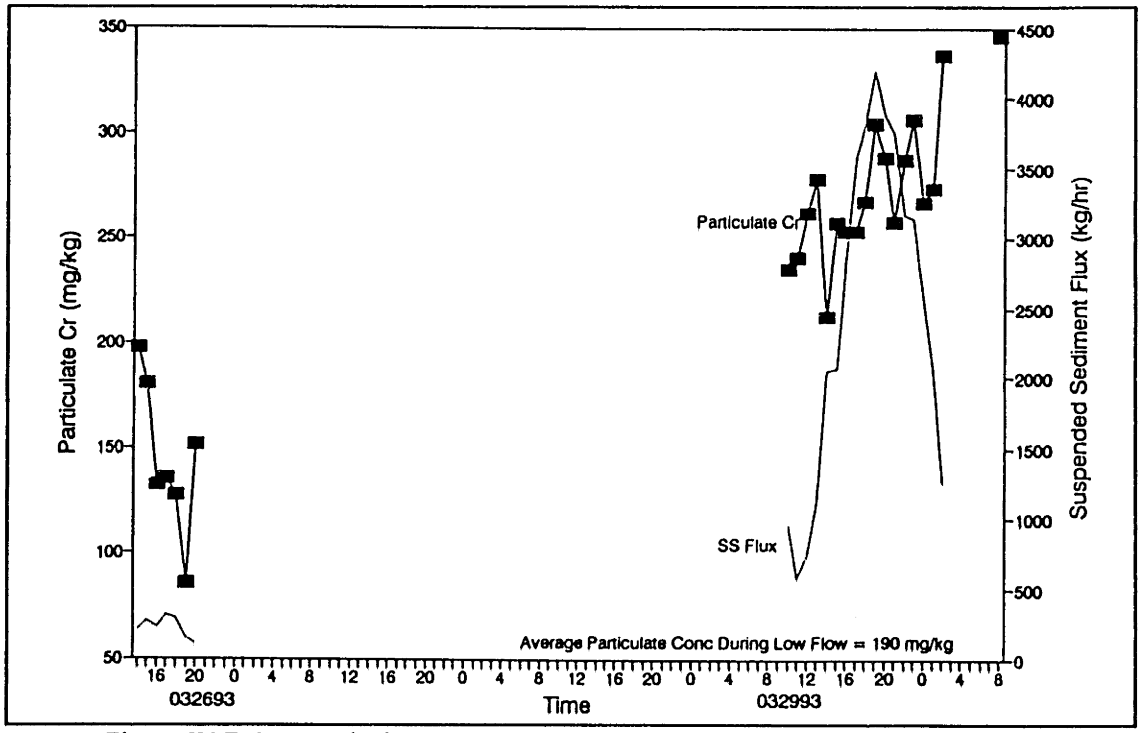

Figure IV.E-51: Particulate Cr Concentration and Flow versus Time, Gage #5, USGS March 26 to 30, 1993

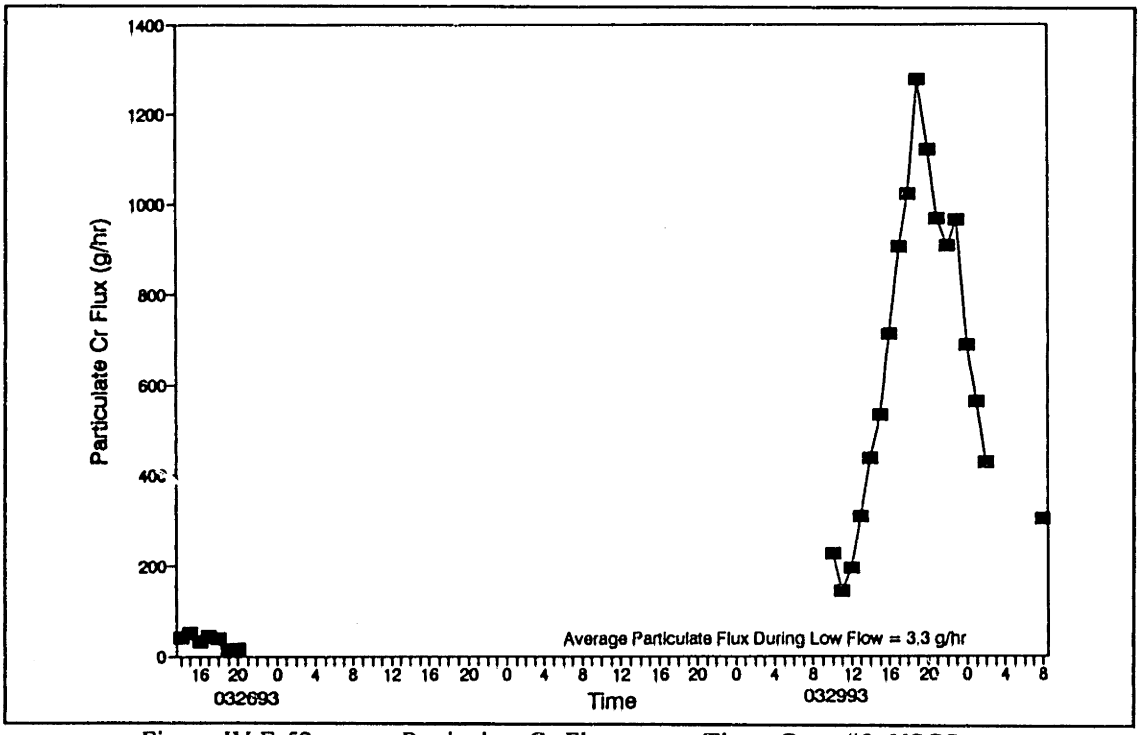

Figure IV.E-52: Particulate Cr Flux versus Time, Gage #5, USGS March 26 to 30, 1993

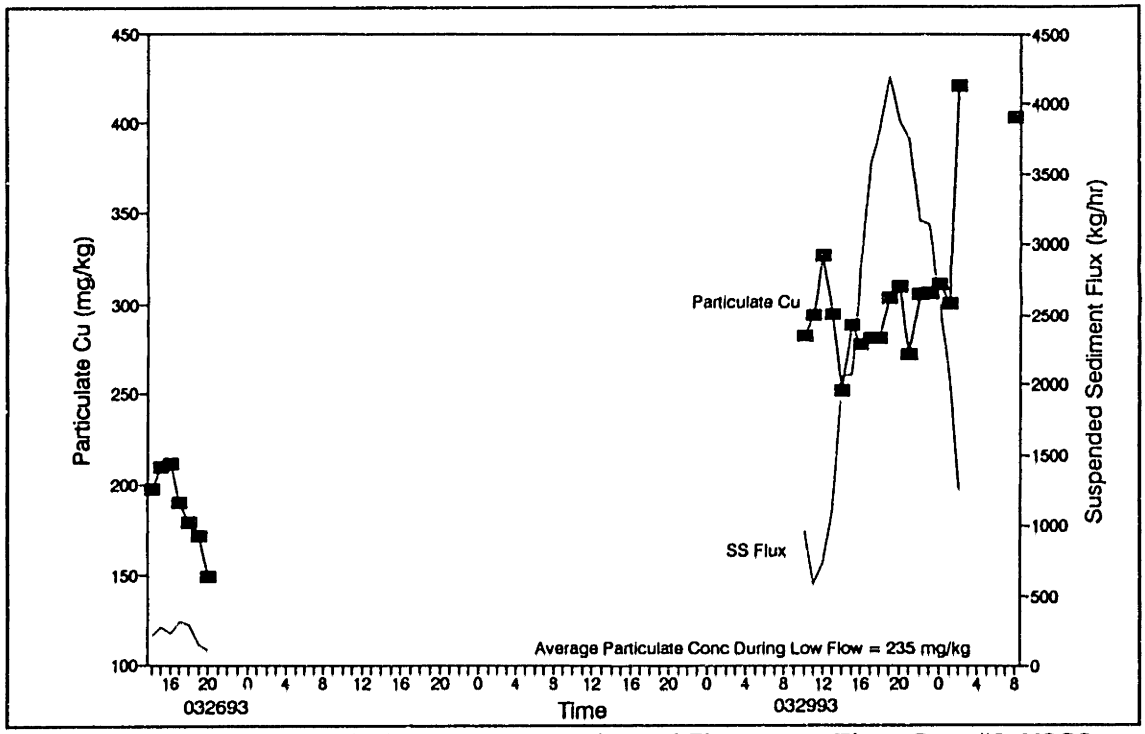

Figure IV.E-53: Particulate Cu Concentration and Flow versus Time, Gage #5, USGS March 26 to 30 1993

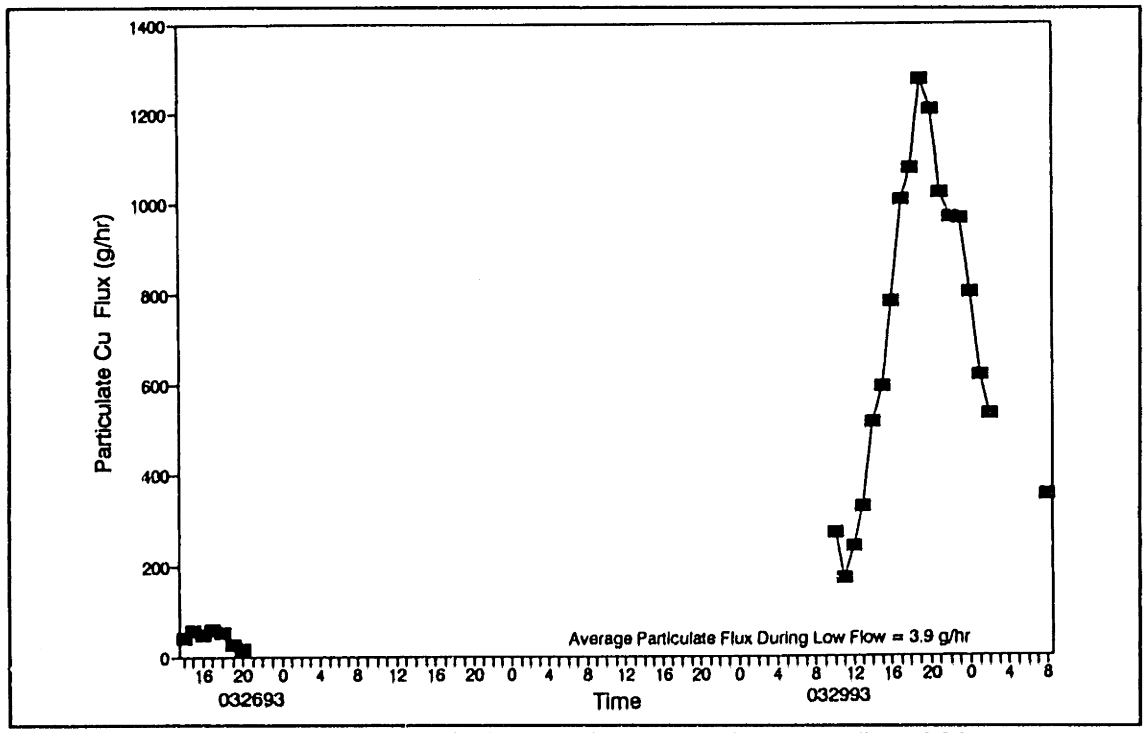

Figure IV.E-54: Particulate Cu Flux versus Time, Gage #5, USGS March 26 to 30, 1993

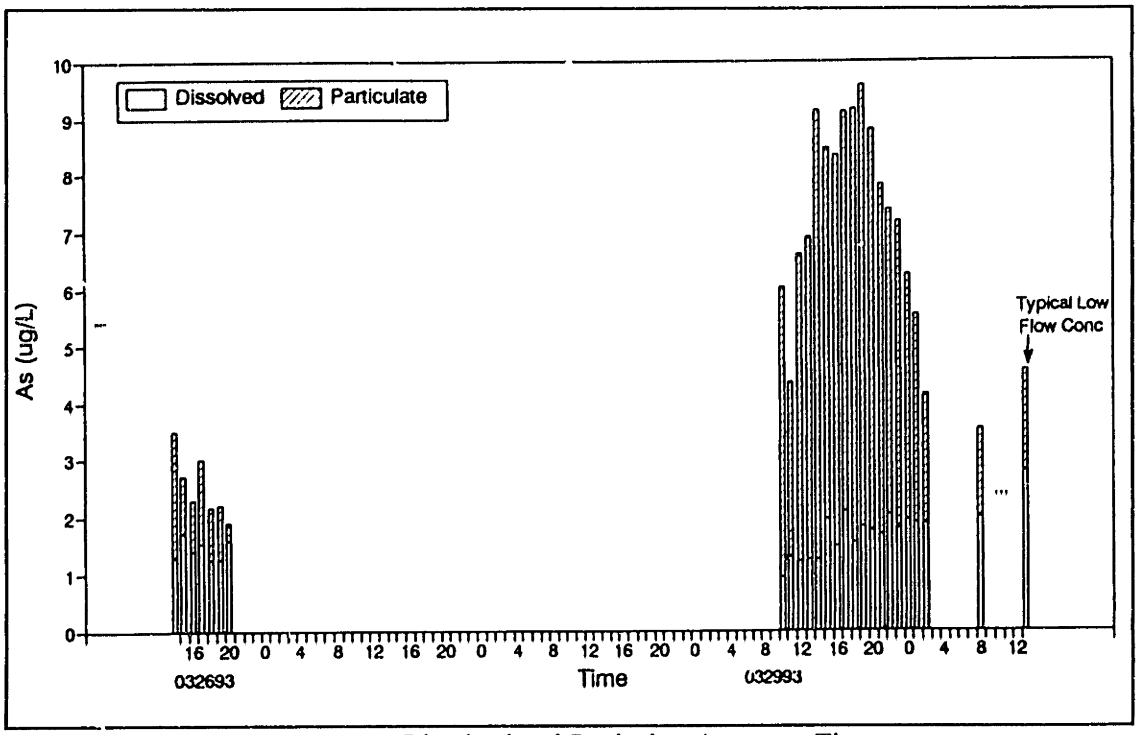

Figure IV.E-55: Dissolved and Particulate As versus Time
Gage #5, USGS, March 26 to 30, 1993

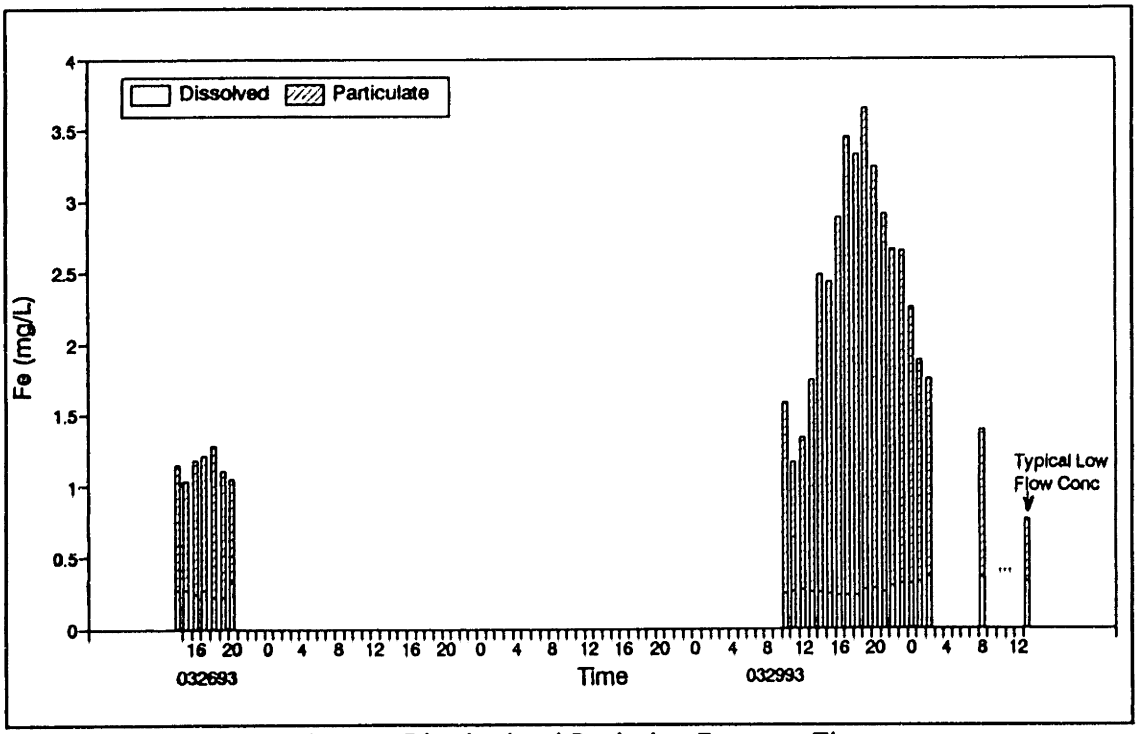

Figure IV.E-56: Dissolved and Particulate Fe versus Time
Gage #5, USGS, March 26 to 30, 1993

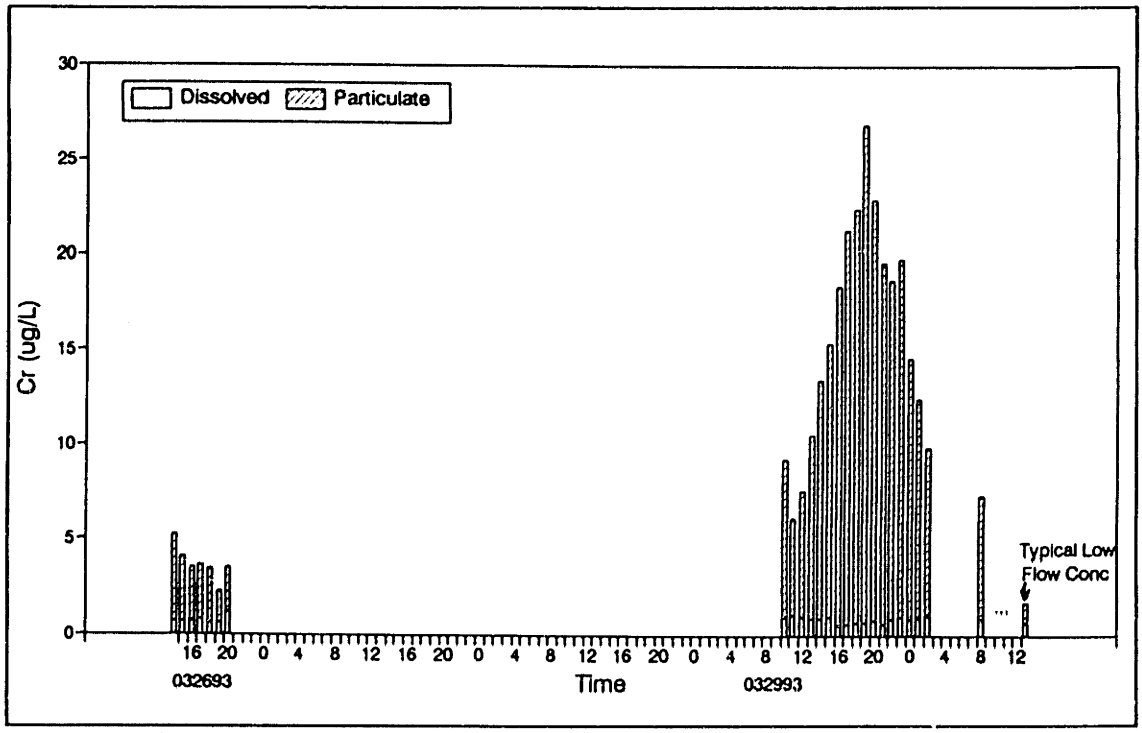

Figure IV.E-57: Dissolved and Particulate Cr versus Time
Gage #5, USGS, March 26 to 30, 1993

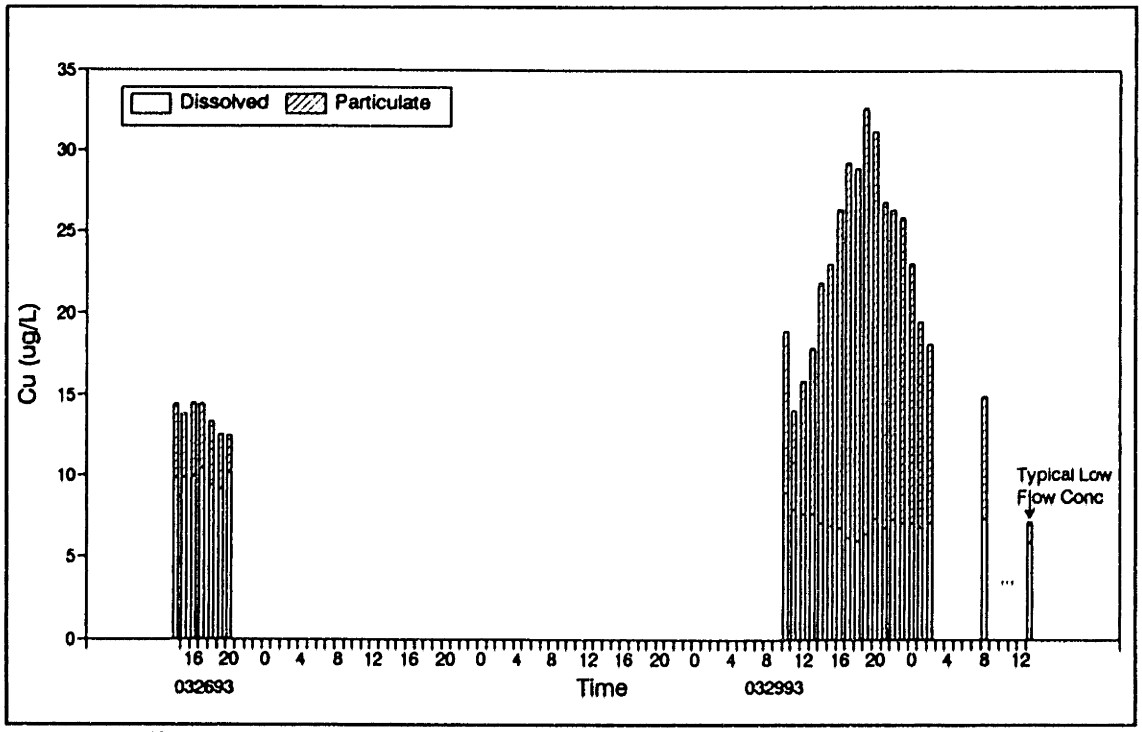

Figure IV.E-58: Dissolved and Particulate Cu versus Time
Gage #5, USGS, March 26 to 30, 1993

APPENDIX V.A

Computer Model Source Code and Selected Input Files: Printouts

SUMMARY OF MODEL INPUT AND OUTPUT FILES

A summary of the input and output files are given in tables V.A-1 and V.A-2 below. Some of these files, along with the computer model source code (written in Fortran 77), are also printed-out within this appendix.

File Name	Description
rain.1991 rain.1992 rain.1993	Hourly rainfall data (inches) for 1991, 1992, and 1993 model runs. (Reading station)
temp.1991 temp.1992 temp.1993	Hourly temperature data (°F) for 1991, 1992, and 1993 model runs. (Reading station) -1 corresponds to temperatures less than 32 °F
flow2.1991 flow2.1992 flow2.1993	Hourly streamflow data measured at gage 2, (cfs) for 1991, 1992, and 1993. -100 corresponds to times with no data.
flow3.1991 flow3.1992 flow3.1993	Hourly streamflow data measured at gage 3, (cfs) for 1991, 1992, and 1993. -100 corresponds to times with no data.
flow1.1991 flow2.1991 flow3.1993	Hourly streamflow data measured at gage 1, (cfs) for 1991, 1992, and 1993. -100 corresponds to times with no data.
flow5.1991 flow5.1992 flow5.1993	Hourly streamflow data measured at gage 5, (cfs) for 1991, 1992, and 1993. -100 corresponds to times with no data.
ui.wn	Parameter file for modeling streamflow from the Woburn North sub-basin.
ui.wc	Parameter file for modeling streamflow from the Woburn Central sub-basin.
ui.wi	Parameter file for modeling streamflow from the Winchester sub-basin.
ss.para	Parameter file for modeling suspended sediments.
metals.wn	Parameter file for modeling metals from the Woburn North sub-basin.
metals.wc	Parameter file for modeling metals from the Woburn Central sub-basin.
metals.ww	Parameter file for modeling metals from the Woburn West sub-basin.
metals.wi	Parameter file for modeling metals from the Winchester sub-basin.

Table V.A-1: Summary of Computer Program Input Files

File Name	Description
balance	Mass balance summary for the run period.
storms	Summary of quick and slow storms for the run period.
f.wn	Quick, slow, and longterm baseflows from the Woburn North sub-basin.
f.wc	Quick, slow, and longterm baseflows from the Woburn Central sub-basin.
f.wi	Quick, slow, and longterm baseflows from the Winchester sub-basin.
f.ww	Streamflow from the Woburn West sub-basin.
f.ag	Streamflow after the Atlantic Gelatin Withdrawal.
f1.c1	Routed streamflow at the end of channel 1.
f2.c2	Routed streamflow at the end of channel 2.
out.check	Rainfall, Snowfall, Air Temperature, and Modeled and Measured Flows at Each Gaging Station.
ss.wn	Quick, slow, and longterm baseflow suspended sediments from the Woburn North sub-basin.
ss.wc	Quick, slow, and longterm baseflow suspended sediments from the Woburn Central sub-basin.
ss.wi	Quick, slow, and longterm baseflow suspended sediment from the Winchester sub-basin.
ss.ww	Organic and Inorganic suspended sediment from the Woburn West sub-basin.
ssa.ag	Suspended Sediments At the Atlantic Gelatin Site.
ss1.c1	Routed suspended sediment flux at the end of channel 1.
ss2.c2	Routed suspended sediment flux at the end of channel 2.

Table V.A-2: Summary of Computer Program Output Files

File Name	Description
temp.rmea	19 day antecedent precipitation for each time step.
test.melt	Meltwater, Effective Rainfall, and Temperature for each time step.
melt.check	Rain, Snow, Accumulated Snow, Temperature, and Meltwater for each time step.
Fep.wn	Particulate iron output from the Woburn North sub-basin.
Fed.wn	Dissolved iron output from the Woburn North sub-basin.
Asp.wn	Particulate arsenic output from the Woburn North sub-basin.
Asd.wn	Dissolved arsenic output from the Woburn North sub-basin.
Crp.wn	Particulate chromium output from the Woburn North sub-basin.
Crd.wn	Dissolved chromium output from the Woburn North sub-basin.
Cup.wn	Particulate copper output from the Woburn North sub-basin.
Cud.wn	Dissolved cooper output from the Woburn North sub-basin.
*.wc	As above except that the output corresponds to the Woburn Central sub-basin.
*.wi	As above except that the output corresponds to the Winchester sub-basin.
*a.ag	As above except that the output corresponds to the Atlantic Gelatin site.
*.ww	As above except that the output corresponds to the Woburn West sub-basin.
*1.c1	As above except that the output corresponds to the downstream end of channel 1.
*2.c2	As above except that the output corresponds to the downstream end of channel 2.

Table V.A-2: con'd

COMPUTER MODEL SOURCE CODE: PRINT-OUT

```
c ***********************************************************************
c *  fn: uim.f
c ***********************************************************************
c * This program reads as input rainfall & air temperature data and:
c *
c *    1) Determines Sub-basin Flow Response using Unit Hydrographs,
c *    2) Routes Flow & Pollutants Using a Linear Muskingumm Method,
c *    3) Computes the SS associated with Quick, Slow, & LTBF flows,
c *    4) Computes Dissolved and Particulate Metal Parameters for
c *       As, Fe, Cu, & Cr associated with each flow & sediment
c *       component.
c *
c ***********************************************************************

c ********************
c  Initialize Program
c ********************
c  To change year of run:
c             change n parameter
c             change the begin date
c             change rain.199? and flow?.199? open statements
c             1991, n=8409, db=91011515
c             1992, n=8784, db=92010100
c             1993, n=6552, db=93010100
c             set snow accumulation, snaccum, at beginning of
c                model run


c       n = number of hours to be modeled
        parameter(n=8409)

        integer dayb,year(n),month(n),day(n),hour(n),filen,meas,NU
        integer fils,film,filf,filr,idr(n),i,idt(n)
        integer filFep,filAsp,filCrp,filCup
        integer filFed,filAsd,filCrd,filCud
        integer filt,melp(n)
        integer cntmi,cntmo,cntwe,cntwi,id(n),id2(n)
        real snow(n),melt(n),temp(n),flowm(n),um(n),melte(n)
        real flowr(n)
        real rain(n),ieff(n),q(n),s(n),flq(n),fls(n),flmi(n)
        real o1q(0:n),o1s(0:n),o1l(0:n)
        real inf(0:n),K,KR,X,flqc(n),flsc(n),flmo(n)
        real flqw(n),flsw(n),flwe(n),flqwi(n),flswi(n)
        real fltwi(n),flwi(n),flmoc(n),flmic(n)
        real flwec(n),flwic(n)
        real bfwn(n),bfwc(n),bfww(n),bfwi(n)
        real wnqmg(n),wnsmg(n),wcqmg(n),wcsmg(n),bfwnmg(n),bfwcmg(n)
        real wnqo2(0:n),wnso2(0:n),wcqo2(0:n),wcso2(0:n)
        real bfwno2(0:n),bfwco2(0:n)
        real accum2(0:n),smbf2(n),smss2(n),smqs2(n),accumq2(0:n),smch2(n)
        real sstot2(n),smtot2(n)
        real accum3(0:n),smbf3(n),smss3(n),smqs3(n),accumq3(0:n),smch3(n)
        real sstot3(n),smtot3(n)
        real accum5(0:n),smbf5(n),smss5(n),smqs5(n),accumq5(0:n),smch5(n)
        real sstot5(n),smtot5(n)
        real smto1(0:n),smto1a(n),smto2a(n)
        real conv,conv1,ssto1(n),ssmoc(n),smchg(n)
        real smto3c(n),smto2(0:n),smto5c(n),ssto5c(n),smag3(n),smto3a(n)
        real area,agwith,cuma,accum(0:n)
        real flmir(n),flm(n),ssagc(n),flw(n),ssagr(n)
        real sum1i,sum2i,sum3i,sum4i,sum5i,sum6i
        real sum1o,sum2o,sum3o,sum4o,sum5o,sum6o,net,frs(0:n),frq(0:n)
        real summic,summoc,sumwec,sumwic
        real summim,summom,sumwem,sumwim
        real summi,summo,sumwe,sumwi,sumbf
        real sums5,sumFp5,sumFd5,sumAp5,sumAd5
        real sumRp5,sumRd5,sumUp5,sumUd5
```

```
real Fdqm2(n),Fdsm2(n),Fdbm2(n),Fpqm2(n),Fpsm2(n),Fpbm2(n)
real Adqm2(n),Adsm2(n),Adbm2(n),Apqm2(n),Apsm2(n),Apbm2(n)
real Rdqm2(n),Rdsm2(n),Rdbm2(n),Rpqm2(n),Rpsm2(n),Rpbm2(n)
real Udqm2(n),Udsm2(n),Udbm2(n),Upqm2(n),Upsm2(n),Upbm2(n)
real Fdqm3(n),Fdsm3(n),Fdbm3(n),Fpqm3(n),Fpsm3(n),Fpbm3(n)
real Adqm3(n),Adsm3(n),Adbm3(n),Apqm3(n),Apsm3(n),Apbm3(n)
real Rdqm3(n),Rdsm3(n),Rdbm3(n),Rpqm3(n),Rpsm3(n),Rpbm3(n)
real Udqm3(n),Udsm3(n),Udbm3(n),Upqm3(n),Upsm3(n),Upbm3(n)
real Fdqm5(n),Fdsm5(n),Fdbm5(n),Fpqm5(n),Fpsm5(n),Fpbm5(n)
real Adqm5(n),Adsm5(n),Adbm5(n),Apqm5(n),Apsm5(n),Apbm5(n)
real Rdqm5(n),Rdsm5(n),Rdbm5(n),Rpqm5(n),Rpsm5(n),Rpbm5(n)
real Udqm5(n),Udsm5(n),Udbm5(n),Upqm5(n),Upsm5(n),Upbm5(n)

real Fpcm2(n),Apcm2(n),Rpcm2(n),Upcm2(n)
real Fpcm3(n),Apcm3(n),Rpcm3(n),Upcm3(n)
real Fpcm5(n),Apcm5(n),Rpcm5(n),Upcm5(n)

real Fptm2(n),Fdtm2(n),Aptm2(n),Adtm2(n)
real Rptm2(n),Rdtm2(n),Uptm2(n),Udtm2(n)
real Fptm3(n),Fdtm3(n),Aptm3(n),Adtm3(n)
real Rptm3(n),Rdtm3(n),Uptm3(n),Udtm3(n)
real Fptm1(n),Fdtm1(n),Aptm1(n),Adtm1(n)
real Rptm1(n),Rdtm1(n),Uptm1(n),Udtm1(n)
real Fptm5(n),Fdtm5(n),Aptm5(n),Adtm5(n)
real Rptm5(n),Rdtm5(n),Uptm5(n),Udtm5(n)

real Fpto1(0:n),Fdto1(0:n),Apto1(0:n),Adto1(0:n)
real Rpto1(0:n),Rdto1(0:n),Upto1(0:n),Udto1(0:n)
real Fpto1a(n),Apto1a(n)
real Rpto1a(n),Upto1a(n)
real Fpto2a(n),Apto2a(n)
real Rpto2a(n),Upto2a(n)

real Fmtp3c(n),Fmtd3c(n),Amtp3c(n),Amtd3c(n)
real Rmtp3c(n),Rmtd3c(n),Umtp3c(n),Umtd3c(n)

real Fmtp3a(n),Fmtd3a(n),Amtp3a(n),Amtd3a(n)
real Rmtp3a(n),Rmtd3a(n),Umtp3a(n),Umtd3a(n)

real Fmtp5c(n),Fmtd5c(n),Amtp5c(n),Amtd5c(n)
real Rmtp5c(n),Rmtd5c(n),Umtp5c(n),Umtd5c(n)

real Fstp3c(n),Fstd3c(n),Astp3c(n),Astd3c(n)
real Rstp3c(n),Rstd3c(n),Ustp3c(n),Ustd3c(n)

real Fstp5c(n),Fstd5c(n),Astp5c(n),Astd5c(n)
real Rstp5c(n),Rstd5c(n),Ustp5c(n),Ustd5c(n)

real Fpto1c(n),Fdto1c(n),Apto1c(n),Adto1c(n)
real Rpto1c(n),Rdto1c(n),Upto1c(n),Udto1c(n)
real Fpto1s(n),Apto1s(n),Rpto1s(n),Upto1s(n)

real Fpto2c(n),Fdto2c(n),Apto2c(n),Adto2c(n)
real Rpto2c(n),Rdto2c(n),Upto2c(n),Udto2c(n)
real Fpto2s(n),Apto2s(n),Rpto2s(n),Upto2s(n)

real Fmpo2(0:n),Fmdo2(0:n),Ampo2(0:n),Amdo2(0:n)
real Rmpo2(0:n),Rmdo2(0:n),Umpo2(0:n),Umdo2(0:n)

real accumF(0:n),accumA(0:n),accumR(0:n),accumU(0:n)

real smchgF(n),smchgA(n),smchgR(n),smchgU(n)
real smch(n),smchF(n),smchA(n),smchR(n),smchU(n)

real mass(0:n),smwe(n),Ct(n),T(n),C(n)

real bfm(200),bfmax(200),bfmin(200)
```

```
      real rm(12),rmax(12),rmin(12),rmea(n)

      real eff(n)


c ********************
c SET Begin DATE/TIME
c ********************
c       dayb=begin date/time
        dayb=91011515

c ********************
c    Open Data Files
c ********************

         open(3,file='rain.1991',status='old')
         open(4,file='temp.1991',status='old')
         open(32,file='flow2.1991',status='old')
         open(33,file='flow3.1991',status='old')
         open(31,file='flow1.1991',status='old')
         open(35,file='flow5.1991',status='old')

c ************************
c   Open Parameter Files
c ************************

c Woburn North Basin Response Parameters
         open(12,file='ui.wn',status='old')

c Woburn Central Basin Response Parameters
         open(13,file='ui.wc',status='old')

c Winchester Basin Response Parameters
         open(15,file='ui.wi',status='old')

c WN, WC, & WI SS Parameters
         open(2,file='ss.para',status='old')


c Metals Info for each Basin
         open(42,file='metals.wn',status='old')
         open(43,file='metals.wc',status='old')
c         open(41,file='metals.ww',status='old')
         open(45,file='metals.wi',status='old')

c *************************
c   Open Output Files
c *************************

c  Mass Balance Info entire run period
         open(60,file='balance',status='unknown')
         rewind 60

c  Mass Balance Info, on a storm by storm basis
         open(16,file='storms',status='unknown')
         rewind 16

c  Woburn North Flow Data
          open(102,file='f.wn',status='unknown')
c  Woburn Central Flow Data
          open(103,file='f.wc',status='unknown')
c  Atlantic Gelatin Flow Data
c          open(104,file='f.ag',status='unknown')
c  Woburn West Flow Data
c          open(101,file='f.ww',status='unknown')
c  Winchester Flow Data
          open(105,file='f.wi',status='unknown')
```

```
c  Channel 1 Outlet Flow Data
c          open(106,file='f1.c1',status='unknown')
c  Channel 2 Outlet Flow Data
c          open(107,file='f2.c2',status='unknown')

c  Woburn North SS Data
       open(22,file='ss.wn',status='unknown')
c  Woburn Central SS Data
       open(23,file='ss.wc',status='unknown')
c  Atlantic Gelatin SS Effect
c          open(24,file='ssa.ag',status='unknown')
c  Woburn West SS Data
c          open(21,file='ss.ww',status='unknown')
c  Winchester SS Data
       open(25,file='ss.wi',status='unknown')
c  Channel 1 Outlet
c          open(26,file='ss.c1',status='unknown')
c  Channel 2 Outlet
c          open(27,file='ss.c2',status='unknown')


c  Woburn North Metals Data
       open(52,file='Fep.wn',status='unknown')
       open(152,file='Fed.wn',status='unknown')

       open(72,file='Asp.wn',status='unknown')
       open(172,file='Asd.wn',status='unknown')

       open(82,file='Crp.wn',status='unknown')
       open(182,file='Crd.wn',status='unknown')

       open(92,file='Cup.wn',status='unknown')
       open(192,file='Cud.wn',status='unknown')

c  Woburn Central Metals Data
       open(53,file='Fep.wc',status='unknown')
       open(153,file='Fed.wc',status='unknown')

       open(73,file='Asp.wc',status='unknown')
       open(173,file='Asd.wc',status='unknown')

       open(83,file='Crp.wc',status='unknown')
       open(183,file='Crd.wc',status='unknown')

       open(93,file='Cup.wc',status='unknown')
       open(193,file='Cud.wc',status='unknown')

c  Atlantic Gelatin Metals Data
c          open(54,file='Fep.ag',status='unknown')
c          open(154,file='Fed.ag',status='unknown')

c          open(74,file='Asp.ag',status='unknown')
c          open(174,file='Asd.ag',status='unknown')

c          open(84,file='Crp.ag',status='unknown')
c          open(184,file='Crd.ag',status='unknown')

c          open(94,file='Cup.ag',status='unknown')
c          open(194,file='Cud.ag',status='unknown')


c  Winchester Metals Data
       open(55,file='Fep.wi',status='unknown')
       open(155,file='Fed.wi',status='unknown')

       open(75,file='Asp.wi',status='unknown')
       open(175,file='Asd.wi',status='unknown')
```

```
          open(85,file='Crp.wi',status='unknown')
          open(185,file='Crd.wi',status='unknown')

          open(95,file='Cup.wi',status='unknown')
          open(195,file='Cud.wi',status='unknown')

c  Channel 1 Outlet Metal Data
c          open(56,file='Fep1.c1',status='unknown')
c          open(156,file='Fed1.c1',status='unknown')

c          open(76,file='Asp1.c1',status='unknown')
c          open(176,file='Asd1.c1',status='unknown')

c          open(86,file='Crp1.c1',status='unknown')
c          open(186,file='Crd1.c1',status='unknown')

c          open(96,file='Cup1.c1',status='unknown')
c          open(196,file='Cud1.c1',status='unknown')

c  Channel 2 Outlet Metal Data
c          open(57,file='Fep2.c2',status='unknown')
c          open(157,file='Fed2.c2',status='unknown')

c          open(77,file='Asp2.c2',status='unknown')
c          open(177,file='Asd2.c2',status='unknown')

c          open(87,file='Crp2.c2',status='unknown')
c          open(187,file='Crd2.c2',status='unknown')

c          open(97,file='Cup2.c2',status='unknown')
c          open(197,file='Cud2.c2',status='unknown')


c ************************************
c * READ RAINFALL AND TEMPERATURE DATA
c ************************************
          filr=3
          filt=4
          call rdrain(n,dayb,day,month,year,hour,rain,filr,
     $               temp,snow,filt)

c  ************************************
c  * Set ATLANTIC GELATIN WITHDRAWAL RATE
c  ************************************
         agwith=2.8

c  ************************************
c  * Read Baseflow Parameters
c  ************************************
          call readbf(bfm,bfmax,bfmin,rm,rmax,rmin)

c  ****************************************
c  * Compute Woburn West Flow
c  ****************************************
         filen=11
         filf=101
         call ww(n,year,month,day,hour,bfww,sumbf,filf,filen)

c ********************************************************
c  Begin WOBURN-NORTH Computations
c ********************************************************

c  Compute  Flow from Woburn-North Sub-basin
c  ************************************
          filen=12
          filf=102
          cuma=0
```

```
      print*,'Beginning WOBURN-NORTH Computations'
      call wn(dayb,rain,n,q,s,flq,fls,filen,bfwn,area,
     $        agwith,idr,ieff,year,month,day,hour,bfww,
     $        filf,snow,temp,melt,flowm,um,idt,melte,
     $        flowr,melp,
     $        bfm,bfmax,bfmin,
     $        rm,rmax,rmin,rmea,eff)



c  Data to be compared with Gage #2 Flow
c  ************************************
      meas=32

      call fndata(dayb,n,flmi,meas)
      summic=0.0
      summim=0.0
      summi=0.0
      cntmi=0
      do 870 i=1,n
           flmic(i)=flq(i)+fls(i)+bfwn(i)
           summi=summi+flmic(i)
      if(flmi(i).ge.0)then
           cntmi=cntmi+1
           summic=summic+flmic(i)
           summim=summim+flmi(i)
      endif
 870  continue


c  Compute SS from Woburn-North Sub-basin
c  **************************************
      fils=22
c     Identify falling versus rising limb of hydrograph
c     (Needed to compute transport capacity)
      call fid(n,flmic,id,id2)

      call ss(dayb,rain,n,flq,fls,flmic,bfwn,accum2,smbf2,smss2,smqs2,
     $        accumq2,smch2,sstot2,smtot2,area,fils,cuma,frs,frq,
     $        year,month,day,hour,id2)



c  Compute Metals from Woburn-North Sub-basin
c  ******************************************
      film=42
      filFep=52
      filAsp=72
      filCrp=82
      filCup=92
      filFed=152
      filAsd=172
      filCrd=182
      filCud=192

      call met(film,n,flq,fls,bfwn,smqs2,smss2,smbf2,
     $       smch2,filFep,filAsp,filCrp,filCup,
     $       filFed,filAsd,filCrd,filCud,
     $       Fdqm2,Fdsm2,Fdbm2,Fpqm2,Fpsm2,Fpbm2,Fptm2,Fdtm2,
     $       Adqm2,Adsm2,Adbm2,Apqm2,Apsm2,Apbm2,Aptm2,Adtm2,
     $       Rdqm2,Rdsm2,Rdbm2,Rpqm2,Rpsm2,Rpbm2,Rptm2,Rdtm2,
     $       Udqm2,Udsm2,Udbm2,Upqm2,Upsm2,Upbm2,Uptm2,Udtm2,
     $       Fpcm2,Apcm2,Rpcm2,Upcm2,frs,frq)


c  Route Flow,SS,& Metals from Wob-North through Channel 1
```

```
c  ********************************************************

c  Muskingham Parameters for Channel 1 (Rte 128 to Montvale)
c  Number of Subreaches
        NU = 1
c  K = Travel time of flood wave through the entire channel,hrs
        K = 7
c  KR = Travel Time through a Reach
        KR= K/NU
c  X = Wedge Storage Parameter,  0 =< X  =< 0.5
c  X = 0, No Wedge Storage, No backwater, Reservoir Routing
c  X = 0.5, Full Wedge Storage
        X = 0.0

        write(60,*)'WOBURN-NORTH ROUTING'
        write(60,*)'Water Routing, sum cfs'
        write(60,*)'Quick Water'
        call rt1(n,flq,o1q,inf,NU,KR,X)
        write(60,*)'Slow Water'
        call rt1(n,fls,o1s,inf,NU,KR,X)
        write(60,*)'LTBF Water'
        call rt1(n,bfwn,o11,inf,NU,KR,X)
        print*,'Finished Water Routing through CHANNEL 1'

        write(60,*)'Sediment Routing, sum grams'
        call rt1(n,smtot2,smto1,inf,NU,KR,X)
        print*,'Finished Sediment Routing through Channel 1'

        write(60,*)'Metal Routing, sum grams'
        write(60,*)'Iron'
        write(60,*)'particulate'
        call rt1(n,Fptm2,Fpto1,inf,NU,KR,X)
        write(60,*)'dissolved'
        call rt1(n,Fdtm2,Fdto1,inf,NU,KR,X)
        write(60,*)'Arsenic'
        write(60,*)'particulate'
        call rt1(n,Aptm2,Apto1,inf,NU,KR,X)
        write(60,*)'dissolved'
        call rt1(n,Adtm2,Adto1,inf,NU,KR,X)
        write(60,*)'Chromium'
        write(60,*)'particulate'
        call rt1(n,Rptm2,Rpto1,inf,NU,KR,X)
        write(60,*)'dissolved'
        call rt1(n,Rdtm2,Rdto1,inf,NU,KR,X)
        write(60,*)'Copper'
        write(60,*)'particulate'
        call rt1(n,Uptm2,Upto1,inf,NU,KR,X)
        write(60,*)'dissolved'
        call rt1(n,Udtm2,Udto1,inf,NU,KR,X)
        print*,'Finished Metal Routing through Channel 1'


c Sum-up Routed Flow,SS, & Metals from Woburn-North
c ************************************************
        conv=(0.3048**3)*3600.
        conv1=conv/1000.

        filf=106
        fils=26
        filFep=56
        filAsp=76
        filCrp=86
        filCup=96
        filFed=156
        filAsd=176
        filCrd=186
        filCud=196
```

```
      open(filf,file='f1.c1',status='unknown')
      rewind filf
      open(filFed,file='Fed1.c1',status='unknown')
      rewind filFed
      open(filAsd,file='Asd1.c1',status='unknown')
      rewind filAsd
      open(filCrd,file='Crd1.c1',status='unknown')
      rewind filCrd
      open(filCud,file='Cud1.c1',status='unknown')
      rewind filCud

c      write(filf,*)'    flmir  '
c      write(filFed,*)'    Fdto1','    Fdto1c'
c      write(filAsd,*)'    Adto1','    Adto1c'
c      write(filCrd,*)'    Rdto1','    Rdto1c'
c      write(filCud,*)'    Udto1','    Udto1c'

      do 732 i=1,n
         flmir(i)=o1q(i)+o1s(i)+o1l(i)
         if(flmir(i).eq.0.0)then
            ssto1(i)=-100
            Fpto1c(i)=-100
            Fdto1c(i)=-100
            Apto1c(i)=-100
            Adto1c(i)=-100
            Rpto1c(i)=-100
            Rdto1c(i)=-100
            Upto1c(i)=-100
            Udto1c(i)=-100
         else
            ssto1(i)=smto1(i)/(flmir(i)*conv)
            Fpto1c(i)=Fpto1(i)/(flmir(i)*conv)
            Fdto1c(i)=Fdto1(i)/(flmir(i)*conv)
            Apto1c(i)=Apto1(i)/(flmir(i)*conv1)
            Adto1c(i)=Adto1(i)/(flmir(i)*conv1)
            Rpto1c(i)=Rpto1(i)/(flmir(i)*conv1)
            Rdto1c(i)=Rdto1(i)/(flmir(i)*conv1)
            Upto1c(i)=Upto1(i)/(flmir(i)*conv1)
            Udto1c(i)=Udto1(i)/(flmir(i)*conv1)
         endif

         if(smto1(i).le.0)then
            Fpto1s(i)=-100
            Apto1s(i)=-100
            Rpto1s(i)=-100
            Upto1s(i)=-100
         else
            Fpto1s(i)=Fpto1(i)*100/(smto1(i))
            Apto1s(i)=Apto1(i)*1e6/(smto1(i))
            Rpto1s(i)=Rpto1(i)*1e6/(smto1(i))
            Upto1s(i)=Upto1(i)*1e6/(smto1(i))
         endif



      write(filf,356)flmir(i)
      write(filFed,356)Fdto1(i),Fdto1c(i)
      write(filAsd,356)Adto1(i),Adto1c(i)
      write(filCrd,356)Rdto1(i),Rdto1c(i)
      write(filCud,356)Udto1(i),Udto1c(i)
 356  format(3f10.2)
 732  continue

      print*,'Finished Writing Diss.Data at Channel 1 Outlet'
      print*
      close(filf)
      close(filFed)
```

```
      close(filAsd)
      close(filCrd)
      close(filCud)


c Check for Deposition/Erosion of Particles in Channel
c *****************************************************
      open(fils,file='ss1.c1',status='unknown')
      rewind fils
      open(filFep,file='Fep1.c1',status='unknown')
      rewind filFep
      open(filAsp,file='Asp1.c1',status='unknown')
      rewind filAsp
      open(filCrp,file='Crp1.c1',status='unknown')
      rewind filCrp
      open(filCup,file='Cup1.c1',status='unknown')
      rewind filCup

c     Identify falling versus rising limb of hydrograph
c     (Needed to compute transport capacity)
      call fid(n,flmir,id,id2)
      call ssdc(cuma,n,flmir,smto1,ssto1,smto1a,fils,
     $              accum,smch,
     $              Fpto1,Apto1,
     $              Rpto1,Upto1,
     $              Fpto1a,Apto1a,
     $              Rpto1a,Upto1a,
     $              accumF,accumA,accumR,accumU,
     $              smchF,smchA,smchR,smchU,
     $              filFep,filAsp,filCrp,filCup,
     $              Fpto1s,Fpto1c,Apto1s,Apto1c,
     $              Rpto1s,Rpto1c,Upto1s,Upto1c,
     $              film,id2)


      close(fils)
      close(filFep)
      close(filAsp)
      close(filCrp)
      close(filCup)


c ***********************************************************
c  Begin WOBURN-CENTRAL Computations
c ***********************************************************

c  Compute Flow from Woburn-Central Sub-basin
c  ******************************************
      filen=13
      filf=103
      print*,'Beginning WOBURN-CENTRAL Computations'
      call wn(dayb,rain,n,q,s,flqc,flsc,filen,bfwc,area,
     $         agwith,idr,ieff,year,month,day,hour,bfww,
     $         filf,snow,temp,melt,flowm,um,idt,melte,
     $         flowr,melp,
     $        bfm,bfmax,bfmin,
     $        rm,rmax,rmin,rmea,eff)


c  Compute Flows to be Compared with Gage#3
c  ****************************************
      meas=33

      call fndata(dayb,n,flmo,meas)
      summoc=0.0
```

```
        summom=0.0
        summo=0.0
        cntmo=0
        do 584 i=1,n
             flmoc(i)=flqc(i)+flsc(i)+bfwc(i)+flmir(i)
             summo=summo+flmoc(i)
        if(flmo(i).ge.0)then
             cntmo=cntmo+1
             summoc=summoc+flmoc(i)
             summom=summom+flmo(i)
        endif
 584    continue


c  Compute SS from Woburn-Central Sub-basin
c  ****************************************
       fils=23
c       Identify falling versus rising limb of hydrograph
c       (Needed to compute transport capacity)
       call fid(n,flmoc,id,id2)

       call ss(dayb,rain,n,flqc,flsc,flmoc,bfwc,accum3,smbf3,smss3,
     $          smqs3,accumq3,smch3,sstot3,smtot3,area,fils,cuma,
     $          frs,frq,year,month,day,hour,id2)

c  Compute Metals from Woburn-Central Sub-basin
c  ********************************************
        film=43
        filFep=53
        filAsp=73
        filCrp=83
        filCup=93
        filFed=153
        filAsd=173
        filCrd=183
        filCud=193
        call met(film,n,flqc,flsc,bfwc,smqs3,smss3,smbf3,
     $         smch3,filFep,filAsp,filCrp,filCup,
     $         filFed,filAsd,filCrd,filCud,
     $         Fdqm3,Fdsm3,Fdbm3,Fpqm3,Fpsm3,Fpbm3,Fptm3,Fdtm3,
     $         Adqm3,Adsm3,Adbm3,Apqm3,Apsm3,Apbm3,Aptm3,Adtm3,
     $         Rdqm3,Rdsm3,Rdbm3,Rpqm3,Rpsm3,Rpbm3,Rptm3,Rdtm3,
     $         Udqm3,Udsm3,Udbm3,Upqm3,Upsm3,Upbm3,Uptm3,Udtm3,
     $         Fpcm3,Apcm3,Rpcm3,Upcm3,frs,frq)

c  Sum up Sediment & Metals Contributions from Wob-N & Wob-C at Gage #3
c  ********************************************************************
        do 585 i=1,n

             smto3c(i)=smtot3(i)+smto1(i)
             ssmoc(i)=(smto3c(i))/(flmoc(i)*conv)

             Fmtp3c(i)=Fptm3(i)+Fpto1a(i)
             Fmtd3c(i)=Fdtm3(i)+Fdto1(i)
             Amtp3c(i)=Aptm3(i)+Apto1a(i)
             Amtd3c(i)=Adtm3(i)+Adto1(i)
             Rmtp3c(i)=Rptm3(i)+Rpto1a(i)
             Rmtd3c(i)=Rdtm3(i)+Rdto1(i)
             Umtp3c(i)=Uptm3(i)+Upto1a(i)
             Umtd3c(i)=Udtm3(i)+Udto1(i)

             Fstp3c(i)=Fmtp3c(i)/(flmoc(i)*conv)
             Fstd3c(i)=Fmtd3c(i)/(flmoc(i)*conv)
             Astp3c(i)=Amtp3c(i)/(flmoc(i)*conv1)
             Astd3c(i)=Amtd3c(i)/(flmoc(i)*conv1)
             Rstp3c(i)=Rmtp3c(i)/(flmoc(i)*conv1)
             Rstd3c(i)=Rmtd3c(i)/(flmoc(i)*conv1)
```

```
            Ustp3c(i)=Umtp3c(i)/(flmoc(i)*conv1)
            Ustd3c(i)=Umtd3c(i)/(flmoc(i)*conv1)

 585    continue

c ***********************************************************
c  Begin ATLANTIC GELATIN AREA Computations
c ***********************************************************
       print*,'Beginning ATL GELATIN Computations'
       filf=104
       open(filf,file='f.ag',status='unknown')
       rewind filf
c       write(filf,*)'Flow after Atl Gelatin, cfs'
       sum1i=0.0
       sum2i=0.0
       sum3i=0.0
       sum4i=0.0
       sum5i=0.0
       sum6i=0.0
       sum1o=0.0
       sum2o=0.0
       sum3o=0.0
       sum4o=0.0
       sum5o=0.0
       sum6o=0.0
       do 859 i=1,n

          sum1i=sum1i+o1q(i)
          sum2i=sum2i+o1s(i)
          sum5i=sum5i+o11(i)
          sum3i=sum3i+flqc(i)
          sum4i=sum4i+flsc(i)
          sum6i=sum6i+bfwc(i)

          if(flmoc(i).le.agwith)then

            wnqmg(i)=0.0
            wnsmg(i)=0.0
            wcqmg(i)=0.0
            wcsmg(i)=0.0
            bfwnmg(i)=0.0
            bfwcmg(i)=0.0

          else

            wnqmg(i)=o1q(i)-(agwith*(o1q(i)/flmoc(i)))
            wnsmg(i)=o1s(i)-(agwith*(o1s(i)/flmoc(i)))
            bfwnmg(i)=o11(i)-(agwith*(o11(i)/flmoc(i)))
            wcqmg(i)=flqc(i)-(agwith*(flqc(i)/flmoc(i)))
            wcsmg(i)=flsc(i)-(agwith*(flsc(i)/flmoc(i)))
            bfwcmg(i)=bfwc(i)-(agwith*(bfwc(i)/flmoc(i)))

          endif

          sum1o=sum1o+wnqmg(i)
          sum2o=sum2o+wnsmg(i)
          sum5o=sum5o+bfwnmg(i)
          sum3o=sum3o+wcqmg(i)
          sum4o=sum4o+wcsmg(i)
          sum6o=sum6o+bfwcmg(i)

          flm(i)=wnqmg(i)+wnsmg(i)+wcqmg(i)+wcsmg(i)
     $             +bfwnmg(i)+bfwcmg(i)

          write(filf,872)flm(i)
 872      format(f8.2)
```

```
 859    continue

        close(filf)
        net=(sum1i+sum2i+sum3i+sum4i+sum5i+sum6i-sum1o-sum2o
     $       -sum3o-sum4o-sum5o-sum6o)/n

        write(60,*)
        write(60,*)'WATER BALANCE FOR ATLANTIC GELATIN AREA'
        write(60,*)'Water Removal Rate',agwith,'cfs'
        write(60,*)
        write(60,*)'wnqmg Input =',sum1i,'Output =',sum1o
        write(60,*)'wnsmg Input =',sum2i,'Output =',sum2o
        write(60,*)'bfwnmg Input=',sum5i,'Output =',sum5o
        write(60,*)'wcqmg Input =',sum3i,'Output =',sum3o
        write(60,*)'wcsmg Input =',sum4i,'Output =',sum4o
        write(60,*)'bfwcmg Input=',sum6i,'Output =',sum6o
        write(60,*)
        write(60,*)'Net Input Minus Output =',net,'cfs'

        print*,'Removed Water Due to Atlantic Gelatin Pumping'

c  Adjust Sediment & Metals Flux from upstream due to well pumping
c  ***************************************************************
        fils=24
        filFep=54
        filAsp=74
        filCrp=84
        filCup=94
        filFed=154
        filAsd=174
        filCrd=184
        filCud=194

c       Identify falling versus rising limb of hydrograph
c       (Needed to compute transport capacity)
        call fid(n,flm,id,id2)
        call ssag(cuma,agwith,n,flmoc,smto3c,smto3a,fils,smag3,
     $       accum,smchg,
     $    Fmtp3c,Fmtd3c,Amtp3c,Amtd3c,Rmtp3c,Rmtd3c,Umtp3c,Umtd3c,
     $    Fmtp3a,Fmtd3a,Amtp3a,Amtd3a,
     $    Rmtp3a,Rmtd3a,Umtp3a,Umtd3a,
     $    accumF,accumA,accumR,accumU,smchgF,smchgA,smchgR,smchgU,
     $    filFep,filAsp,filCrp,filCup,filFed,filAsd,filCrd,filCud,
     $    film,id2)

c  Route Flow, Sediment, & Metals Through Channel 2
c  ************************************************
        NU = 1
        K = 8
        KR= K/NU
        X = 0.0
        write(60,*)'ROUTING THROUGH CHANNEL 2'
        write(60,*)'Water Routing, sum cfs'
        write(60,*)'wnqmg'
        call rt1(n,wnqmg,wnqo2,inf,NU,KR,X)
        write(60,*)'wnsmg'
        call rt1(n,wnsmg,wnso2,inf,NU,KR,X)
        write(60,*)'wcqmg'
        call rt1(n,wcqmg,wcqo2,inf,NU,KR,X)
        write(60,*)'wcsmg'
        call rt1(n,wcsmg,wcso2,inf,NU,KR,X)
        write(60,*)'bfwnmg'
        call rt1(n,bfwnmg,bfwno2,inf,NU,KR,X)
        write(60,*)'bfwcmg'
        call rt1(n,bfwcmg,bfwco2,inf,NU,KR,X)
        print*,'Finished Water Routing Through CHANNEL 2'
        write(60,*)
```

```
      write(60,*)'Sediment Routing, Total Mass,g'
      call rt1(n,smto3a,smto2,inf,NU,KR,X)
      print*,'Finished Sediment Routing Through Channel 2'
      write(60,*)
      write(60,*)'Metals Routing, Total Mass, g'
      write(60,*)'Iron'
      write(60,*)'Particulate'
      call rt1(n,Fmtp3a,Fmpo2,inf,NU,KR,X)
      write(60,*)'Dissolved'
      call rt1(n,Fmtd3a,Fmdo2,inf,NU,KR,X)
      write(60,*)'Arsenic'
      write(60,*)'Particulate'
      call rt1(n,Amtp3a,Ampo2,inf,NU,KR,X)
      write(60,*)'Dissolved'
      call rt1(n,Amtd3a,Amdo2,inf,NU,KR,X)
      write(60,*)'Chromium'
      write(60,*)'Particulate'
      call rt1(n,Rmtp3a,Rmpo2,inf,NU,KR,X)
      write(60,*)'Dissolved'
      call rt1(n,Rmtd3a,Rmdo2,inf,NU,KR,X)
      write(60,*)'Copper'
      write(60,*)'Particulate'
      call rt1(n,Umtp3a,Umpo2,inf,NU,KR,X)
      write(60,*)'Dissolved'
      call rt1(n,Umtd3a,Umdo2,inf,NU,KR,X)
      print*,'Finished Metal Routing Through Channel 2'

c Sum-up Routed Flow,SS, & Metals at Gage #3
c ******************************************
      conv=(0.3048**3)*3600.
      filf=107
      fils=27
      filFep=57
      filAsp=77
      filCrp=87
      filCup=97
      filFed=157
      filAsd=177
      filCrd=187
      filCud=197

      open(filf,file='f2.c2',status='unknown')
      rewind filf
      open(filFed,file='Fed2.c2',status='unknown')
      rewind filFed
      open(filAsd,file='Asd2.c2',status='unknown')
      rewind filAsd
      open(filCrd,file='Crd2.c2',status='unknown')
      rewind filCrd
      open(filCud,file='Cud2.c2',status='unknown')
      rewind filCud

c      write(filf,*)'      flw'
c      write(filFed,*)'    Fmdo2','    Fdto2c'
c      write(filAsd,*)'    Amdo2','    Adto2c'
c      write(filCrd,*)'    Rmdo2','    Rdto2c'
c      write(filCud,*)'    Umdo2','    Udto2c'

      do 737 i=1,n
         flw(i)=wnqo2(i)+wnso2(i)+wcqo2(i)+wcso2(i)+bfwno2(i)
     $             +bfwco2(i)
         if(flw(i).lt.0.01)then
            flw(i)=0.0
            ssagr(i)=-100
            Fpto2c(i)=-100
            Fdto2c(i)=-100
            Apto2c(i)=-100
```

```
              Adto2c(i)=-100
              Rpto2c(i)=-100
              Rdto2c(i)=-100
              Upto2c(i)=-100
              Udto2c(i)=-100
            else
              ssagr(i)=smto2(i)/(flw(i)*conv)
              Fpto2c(i)=Fmpo2(i)/(flw(i)*conv)
              Fdto2c(i)=Fmdo2(i)/(flw(i)*conv)
              Apto2c(i)=Ampo2(i)/(flw(i)*conv1)
              Adto2c(i)=Amdo2(i)/(flw(i)*conv1)
              Rpto2c(i)=Rmpo2(i)/(flw(i)*conv1)
              Rdto2c(i)=Rmdo2(i)/(flw(i)*conv1)
              Upto2c(i)=Umpo2(i)/(flw(i)*conv1)
              Udto2c(i)=Umdo2(i)/(flw(i)*conv1)
            endif



            if(smto2(i).le.0)then
              Fpto2s(i)=-100
              Apto2s(i)=-100
              Rpto2s(i)=-100
              Upto2s(i)=-100
            else
              Fpto2s(i)=Fmpo2(i)*100/(smto2(i))
              Apto2s(i)=Ampo2(i)*1e6/(smto2(i))
              Rpto2s(i)=Rmpo2(i)*1e6/(smto2(i))
              Upto2s(i)=Umpo2(i)*1e6/(smto2(i))
            endif



          write(filf,357)flw(i)
          write(filFed,357)Fmdo2(i),Fdto2c(i)
          write(filAsd,357)Amdo2(i),Adto2c(i)
          write(filCrd,357)Rmdo2(i),Rdto2c(i)
          write(filCud,357)Umdo2(i),Udto2c(i)
 357      format(3f10.2)

 737       continue

          print*,'Finished Computing Parameters at Channel 2 Outlet'
          print*
          close(filf)
          close(filFed)
          close(filAsd)
          close(filCrd)
          close(filCud)

c Check for Deposition/Erosion of Particles in Channel
c ***************************************************
          open(fils,file='ss2.c2',status='unknown')
          rewind fils
          open(filFep,file='Fep2.c2',status='unknown')
          rewind filFep
          open(filAsp,file='Asp2.c2',status='unknown')
          rewind filAsp
          open(filCrp,file='Crp2.c2',status='unknown')
          rewind filCrp
          open(filCup,file='Cup2.c2',status='unknown')
          rewind filCup

c         Identify falling versus rising limb of hydrograph
c         (Needed to compute transport capacity)
          call fid(n,flw,id,id2)
          call ssdc(cuma,n,flw,smto2,ssagr,smto2a,fils,
```

```
     $               accum,smch,
     $               Fmpo2,Ampo2,
     $               Rmpo2,Umpo2,
     $               Fpto2a,Apto2a,
     $               Rpto2a,Upto2a,
     $               accumF,accumA,accumR,accumU,
     $               smchF,smchA,smchR,smchU,
     $               filFep,filAsp,filCrp,filCup,
     $               Fpto2s,Fpto2c,Apto2s,Apto2c,
     $               Rpto2s,Rpto2c,Upto2s,Upto2c,
     $               film,id2)


        close(fils)
        close(filFep)
        close(filAsp)
        close(filCrp)
        close(filCup)

c ***********************************************************
c  Begin WOBURN-WEST Computations
c ***********************************************************

c  Flow From Woburn-West Sub-basin (See beginning of Program)
c  ***********************************************************


c  Comparison of Computed Flow with Gage#1 Flow, flwe
c  ************************************************
        meas=31

        call fndata(dayb,n,flwe,meas)
        sumwec=0.0
        sumwem=0.0
        sumwe=0.0
        cntwe=0
        do 777 i=1,n
           flwec(i)=bfww(i)
           sumwe=sumwe+flwec(i)
        if(flwe(i).ge.0)then
           cntwe=cntwe+1
           sumwec=sumwec+flwec(i)
           sumwem=sumwem+flwe(i)
        endif
 777    continue
        print*,'Finished Cage#1 Comparison'


c  Compute SS & Metals from Woburn-West Sub-basin
c  *********************************************
        fils=21
        film=41
        filFep=51
        filAsp=71
        filCrp=81
        filCup=91
        filFed=151
        filAsd=171
        filCrd=181
        filCud=191

        call wess(n,fils,film,
     $            filFep,filAsp,filCrp,filCup,
     $            filFed,filAsd,filCrd,filCud,
     $            bfww,day,month,year,hour,mass,
     $            smwe,Ct,T,C,
     $            Fdtm1,Adtm1,Rdtm1,Udtm1,
```

```
     $            Fptm1,Aptm1,Rptm1,Uptm1)

c ***********************************************************
c  Begin WINCHESTER Computations
c ***********************************************************

c  Compute Flow From Winchester Sub-basin
c  *************************************
        print*,'Beginning WINCHESTER Computations'
        filen=15
        filf=105
        call wn(dayb,rain,n,q,s,flqwi,flswi,filen,bfwi,area,
     $          agwith,idr,ieff,year,month,day,hour,bfww,
     $          filf,snow,temp,melt,flowm,um,idt,melte,
     $          flowr,melp,
     $         bfm,bfmax,bfmin,
     $         rm,rmax,rmin,rmea,eff)



c  Comparison with Computed Flow with Gage #5 Flow
c  **********************************************
        meas=35
        call fndata(dayb,n,flwi,meas)
        sumwic=0.0
        sumwim=0.0
        sumwi=0.0
        cntwi=0
        do 864 i=1,n
           fltwi(i)=flqwi(i)+flswi(i)+bfwi(i)
           flwic(i)=fltwi(i)+flwec(i)+flw(i)
           sumwi=sumwi+flwic(i)
        if(flwi(i).ge.0)then
           cntwi=cntwi+1
           sumwic=sumwic+flwic(i)
           sumwim=sumwim+flwi(i)
        endif
 864    continue

c  Compute SS from Winchester Sub-basin
c  ************************************
        fils=25
c       Identify falling versus rising limb of hydrograph
c       (Needed to compute transport capacity)
        call fid(n,flwic,id,id2)
        call ss(dayb,rain,n,flqwi,flswi,flwic,bfwi,accum5,smbf5,smss5,
     $          smqs5,accumq5,smch5,sstot5,smtot5,area,fils,cuma,
     $          frs,frq,year,month,day,hour,id2)

c  Compute Metals from Winchester Sub-basin
c  ****************************************
        film=45
        filFep=55
        filAsp=75
        filCrp=85
        filCup=95
        filFed=155
        filAsd=175
        filCrd=185
        filCud=195
       call met(film,n,flqwi,flswi,bfwi,smqs5,smss5,smbf5,
     $         smch5,filFep,filAsp,filCrp,filCup,
     $         filFed,filAsd,filCrd,filCud,
     $         Fdqm5,Fdsm5,Fdbm5,Fpqm5,Fpsm5,Fpbm5,Fptm5,Fdtm5,
     $         Adqm5,Adsm5,Adbm5,Apqm5,Apsm5,Apbm5,Aptm5,Adtm5,
     $         Rdqm5,Rdsm5,Rdbm5,Rpqm5,Rpsm5,Rpbm5,Rptm5,Rdtm5,
```

```
     $         Udqm5,Udsm5,Udbm5,Upqm5,Upsm5,Upbm5,Uptm5,Udtm5,
     $         Fpcm5,Apcm5,Rpcm5,Upcm5,frs,frq)

c  Sum up Sediment & Metals Contributions at Gage #5
c  ************************************************
        sums5=0.0
        sumFp5=0.0
        sumAp5=0.0
        sumRp5=0.0
        sumUp5=0.0
        sumFd5=0.0
        sumAd5=0.0
        sumRd5=0.0
        sumUd5=0.0
        do 865 i=1,n

           smto5c(i)=smto2a(i)+smtot5(i)+smwe(i)
           ssto5c(i)=smto5c(i)/(flwic(i)*conv)

           Fmtp5c(i)=Fpto2a(i)+Fptm5(i)+Fptm1(i)
           Fmtd5c(i)=Fmdo2(i)+Fdtm5(i)+Fdtm1(i)
           Amtp5c(i)=Apto2a(i)+Aptm5(i)+Aptm1(i)
           Amtd5c(i)=Amdo2(i)+Adtm5(i)+Adtm1(i)
           Rmtp5c(i)=Rpto2a(i)+Rptm5(i)+Rptm1(i)
           Rmtd5c(i)=Rmdo2(i)+Rdtm5(i)+Rdtm1(i)
           Umtp5c(i)=Upto2a(i)+Uptm5(i)+Uptm1(i)
           Umtd5c(i)=Umdo2(i)+Udtm5(i)+Udtm1(i)

           sums5=sums5+smto5c(i)
           sumFp5=sumFp5+Fmtp5c(i)
           sumAp5=sumAp5+Amtp5c(i)
           sumRp5=sumRp5+Rmtp5c(i)
           sumUp5=sumUp5+Umtp5c(i)
           sumFd5=sumFd5+Fmtd5c(i)
           sumAd5=sumAd5+Amtd5c(i)
           sumRd5=sumRd5+Rmtd5c(i)
           sumUd5=sumUd5+Umtd5c(i)

           Fstp5c(i)=Fmtp5c(i)/(flwic(i)*conv)
           Fstd5c(i)=Fmtd5c(i)/(flwic(i)*conv)
           Astp5c(i)=Amtp5c(i)/(flwic(i)*conv1)
           Astd5c(i)=Amtd5c(i)/(flwic(i)*conv1)
           Rstp5c(i)=Rmtp5c(i)/(flwic(i)*conv1)
           Rstd5c(i)=Rmtd5c(i)/(flwic(i)*conv1)
           Ustp5c(i)=Umtp5c(i)/(flwic(i)*conv1)
           Ustd5c(i)=Umtd5c(i)/(flwic(i)*conv1)
 865    continue

        write(60,*)'SEDIMENT BALANCE AT GAGE 5'
        write(60,*)'Sum Mass Flux,g=',sums5
        write(60,*)
        write(60,*)'METAL BALANCE AT GAGE 5'
        write(60,*)'Dissolved:      Fe            As         ',
     $             ' Cr          Cu'
        write(60,*)'Sum Mass,g=',sumFd5,sumAd5,sumRd5,sumUd5
        write(60,*)
        write(60,*)'Particulate:     Fe            As         ',
     $             ' Cr          Cu'
        write(60,*)'Sum Mass,g=',sumFp5,sumAp5,sumRp5,sumUp5
        write(60,*)

c  ************************************************************
c  WRITE FLOW DATA TO OUTPUT FILE
c  ************************************************************

c    Open Output File, to Compare Computed vs Modeled Flows
       open(5,file='out.check',status='unknown')
```

```
      rewind 5
      call wr(n,year,day,month,hour,rain,
     $          flmic,flmi,flmo,flmoc,flwec,flwe,
     $          flwic,flwi,
     $          summic,summoc,sumwec,sumwic,
     $          summim,summom,sumwem,sumwim,
     $          summi,summo,sumwe,sumwi,
     $          cntmi,cntmo,cntwe,cntwi,temp,snow)

c  ************************************************************
c  Write SS Summary DATA to File
c  ************************************************************

      open(65,file='ssf.flux',status='unknown')
      rewind 65
c      write(65,*)'    Gage 2     Gage 3     Gage 1     Gage 5'
c      write(65,*)'    SSflux     SSflux     SSflux     SSflux'
      open(70,file='ssc.conc',status='unknown')
      rewind 70
c      write(70,*)'    Gage 2     Gage 3     Gage 1     Gage 5'
c      write(70,*)'    SSconc     SSconc     SSconc     SSconc'

      do 745 i=1,n
      write(65,941)smtot2(i),smto3c(i),smwe(i),smto5c(i)
      write(70,941)sstot2(i),ssmoc(i),Ct(i),ssto5c(i)
 941  format(3(1x,f10.1),1x,f12.1)

 745  continue
      print*,'Finished Writing ssf.flux & ssc.conc'
      close(65)
      close(70)

c  ************************************************************
c  Write Fe Summary Data to File
c  ************************************************************
      open(66,file='tempFf.flux',
     $               status='unknown')
      rewind 66
c      write(66,255)'        Gage 2      ',
c     $             '        Gage 3      ',
c     $             '        Gage 1      ',
c     $             '        Gage 5      '
c      write(66,255)'    Feflux:Dis & Prt',
c     $             '    Feflux:Dis & Prt',
c     $             '    Feflux:Dis & Prt',
c     $             '    Feflux:Dis & Prt'
 255  format(4(a20,1x))
 455  format(4(a32,1x))
      do 457 i=1,n
      write(66,256)Fdtm2(i),Fptm2(i),Fmtd3c(i),Fmtp3c(i),
     $             Fdtm1(i),Fptm1(i),Fmtd5c(i),Fmtp5c(i)
 256  format(4(2f10.2,1x))
 456  format(3f10.2,3x,3f10.2,3x,3f10.2,3x,3f10.2)
 457  continue
      close(66)
      print*,'Finished Writing tempFf.flux file'


      open(67,file='tempFc.conc',
     $               status='unknown')
      rewind 67
c      write(67,455)'                Gage 2           ',
c     $             '                Gage 3           ',
c     $             '                Gage 1           ',
c     $             '                Gage 5           '
c      write(67,455)'     Dis,mg/l  Part,%  Part,mg/l',
c     $             '     Dis,mg/l  Part,%  Part,mg/l',
```

```
c     $               '     Dis,mg/l  Part,%  Part,mg/l',
c     $               '     Dis,mg/l  Part,%  Part,mg/l'
        do 458 i=1,n
        write(67,456) Fdtm2(i)/(flmic(i)*conv),
     $    Fptm2(i)*100./smtot2(i),Fptm2(i)/(flmic(i)*conv),
     $    Fstd3c(i),Fmtp3c(i)*100./smto3c(i),Fstp3c(i),
     $    Fdtm1(i)/(flwec(i)*conv),Fptm1(i)*100./smwe(i),
     $    Fptm1(i)/(flwec(i)*conv),
     $    Fstd5c(i),Fmtp5c(i)*100./smto5c(i),Fstp5c(i)
 458    continue
        close(67)
        print*,'Finished Writing tempFc.conc file'

c  ***************************************************************
c  Write As Summary Data to File
c  ***************************************************************
        open(68,file='tempAf.flux',
     $               status='unknown')
        rewind 68
c        write(68,255)'        Gage 2      ',
c     $               '        Gage 3      ',
c     $               '        Gage 1      ',
c     $               '        Gage 5      '
c        write(68,255)'    Asflux:Dis & Prt',
c     $               '    Asflux:Dis & Prt',
c     $               '    Asflux:Dis & Prt',
c     $               '    Asflux:Dis & Prt'
        do 558 i=1,n
        write(68,256)Adtm2(i),Aptm2(i),Amtd3c(i),Amtp3c(i),
     $               Adtm1(i),Aptm1(i),Amtd5c(i),Amtp5c(i)
 558    continue
        close(68)
        print*,'Finished Writing tempAf.flux file'


        open(69,file='tempAc.conc',
     $               status='unknown')
        rewind 69
c        write(69,455)'              Gage 2           ',
c     $               '              Gage 3           ',
c     $               '              Gage 1           ',
c     $               '              Gage 5           '
c        write(69,455)'     Dis,ug/l  mg/kg   Part,ug/l',
c     $               '     Dis,ug/l  mg/kg   Part,ug/l',
c     $               '     Dis,ug/l  mg/kg   Part,ug/l',
c     $               '     Dis,ug/l  mg/kg   Part,ug/l'

        do 559 i=1,n
        write(69,456)Adtm2(i)/(flmic(i)*conv1),
     $    Aptm2(i)*1e6/smtot2(i),Aptm2(i)/(flmic(i)*conv1),
     $    Astd3c(i),Amtp3c(i)*1e6/smto3c(i),Astp3c(i),
     $    Adtm1(i)/(flwec(i)*conv1),Aptm1(i)*1e6/smwe(i),
     $    Aptm1(i)/(flwec(i)*conv1),
     $    Astd5c(i),Amtp5c(i)*1e6/smto5c(i),Astp5c(i)

 559    continue
        close(69)
        print*,'Finished Writing tempAc.conc file'

c  ***************************************************************
c  Write Cr Summary Data to File
c  ***************************************************************
        open(61,file='tempRf.flux',
     $               status='unknown')
        rewind 61
c        write(61,255)'        Gage 2      ',
c     $               '        Gage 3      ',
```

```
c     $                '         Gage 1       ',
c     $                '         Gage 5       '
c        write(61,255)'     Crflux:Dis & Prt',
c     $                '     Crflux:Dis & Prt',
c     $                '     Crflux:Dis & Prt',
c     $                '     Crflux:Dis & Prt'
         do 562 i=1,n
         write(61,256)Rdtm2(i),Rptm2(i),Rmtd3c(i),Rmtp3c(i),
     $               Rdtm1(i),Rptm1(i),Rmtd5c(i),Rmtp5c(i)

 562     continue
         close(61)
         print*,'Finished Writing tempRf.flux File'

         open(62,file='tempRc.conc',
     $               status='unknown')
         rewind 62
c        write(62,455)'               Gage 2             ',
c     $               '               Gage 3             ',
c     $               '               Gage 1             ',
c     $               '               Gage 5             '
c        write(62,455)'      Dis,ug/l  mg/kg   Part,ug/l',
c     $               '      Dis,ug/l  mg/kg   Part,ug/l',
c     $               '      Dis,ug/l  mg/kg   Part,ug/l',
c     $               '      Dis,ug/l  mg/kg   Part,ug/l'

         do 560 i=1,n
         write(62,456)Rdtm2(i)/(flmic(i)*conv1),
     $     Rptm2(i)*1e6/smtot2(i),Rptm2(i)/(flmic(i)*conv1),
     $     Rstd3c(i),Rmtp3c(i)*1e6/smto3c(i),Rstp3c(i),
     $     Rdtm1(i)/(flwec(i)*conv1),Rptm1(i)*1e6/smwe(i),
     $     Rptm1(i)/(flwec(i)*conv1),
     $     Rstd5c(i),Rmtp5c(i)*1e6/smto5c(i),Rstp5c(i)
 560     continue
         close(62)
         print*,'Finished Writing tempRc.conc File'

c  ************************************************************
c  Write Cu Summary Data to File
c  ************************************************************
         open(63,file='tempUf.flux',
     $               status='unknown')
         rewind 63
c        write(63,255)'         Gage 2       ',
c     $               '         Gage 3       ',
c     $               '         Gage 1       ',
c     $               '         Gage 5       '
c        write(63,255)'     Cuflux:Dis & Prt',
c     $               '     Cuflux:Dis & Prt',
c     $               '     Cuflux:Dis & Prt',
cc    $               '     Cuflux:Dis & Prt'
         do 563 i=1,n
         write(63,256)Udtm2(i),Uptm2(i),Umtd3c(i),Umtp3c(i),
     $               Udtm1(i),Uptm1(i),Umtd5c(i),Umtp5c(i)

 563     continue
         close(63)
         print*,'Finished Writing tempUf.flux File'

         open(64,file='tempUc.conc',
     $              status='unknown')
         rewind 64
c        write(64,455)'               Gage 2             ',
c     $               '               Gage 3             ',
c     $               '               Gage 1             ',
c     $               '               Gage 5             '
c        write(64,455)'      Dis,ug/l  mg/kg   Part,ug/l',
```

```
c     $                '     Dis,ug/l  mg/kg   Part,ug/l',
c     $                '     Dis,ug/l  mg/kg   Part,ug/l',
c     $                '     Dis,ug/l  mg/kg   Part,ug/l'

        do 564 i=1,n
        write(64,456)Udtm2(i)/(flmic(i)*conv1),
     $    Uptm2(i)*1e6/smtot2(i),Uptm2(i)/(flmic(i)*conv1),
     $    Ustd3c(i),Umtp3c(i)*1e6/smto3c(i),Ustp3c(i),
     $    Udtm1(i)/(flwec(i)*conv1),Uptm1(i)*1e6/smwe(i),
     $    Uptm1(i)/(flwec(i)*conv1),
     $    Ustd5c(i),Umtp5c(i)*1e6/smto5c(i),Ustp5c(i)

 564    continue
        close(64)
        print*,'Finished Writing tempUc.conc File'


      close(60)
      close(15)

      stop
      end


c 1*****************************************************************
        subroutine priorr(n1,rm,rmea,melt,rai,yea,mont,da,hou)

c   This subroutine computes the sum of the prior rainfall and
c   meltwater for x hours prior to time i
c ****************************************************************

        integer i,x,n1,j,u,yea(n1),mont(n1),da(n1),hou(n1)
        real rm(12),rmea(n1),sum,melt(n1),rai(n1)

        open(1005,file='temp.rmea',status='unknown')
        rewind 1005

        x=24*19

        do 1 i=1,n1
         if(i.le.x)then
            rmea(i)=rm(mont(i))
            goto 8
         endif

         sum=0
         u=x-1
         do 2 j=0,u
           sum=sum+rai(i-j)+melt(i-j)
 2       continue
         rmea(i)=sum*30./(real(x)/24)

 8       write(1005,19)yea(i),mont(i),da(i),hou(i),rmea(i)
 19      format(4i2.2,3x,f8.3)
 1       continue

        return
        end

c  1*****************************************************************
        subroutine readbf(bfm,bfmax,bfmin,rm,rmax,rmin)

c  This subroutine reads the parameters required for the baseflow
c  Computation
c  ****************************************************************
        integer i
        real bfm(200),bfmax(200),bfmin(200)
```

```
      real rm(12),rmax(12),rmin(12)

      open(1002, file='bf.ave',status='old')
      rewind 1002

      read(1002,*)
      read(1002,*)
      do 1 i=1,12
        read(1002,11)bfm(i),bfm(i+100)
 11     format(15x,2x,f8.4,2x,f8.4)
c        print*,bfm(i),bfm(i+100)
 1    continue

      read(1002,*)
      read(1002,*)
      read(1002,*)
      read(1002,*)
      do 2 i=1,12
        read(1002,11)bfmax(i),bfmax(i+100)
c        print*,bfmax(i),bfmax(i+100)
 2    continue

      read(1002,*)
      read(1002,*)
      read(1002,*)
      read(1002,*)
      do 3 i=1,12
        read(1002,11)bfmin(i),bfmin(i+100)
c        print*,bfmin(i),bfmin(i+100)
 3    continue

      read(1002,*)
      read(1002,*)
      read(1002,*)
      do 4 i=1,12
        read(1002,12)rm(i)
 12     format(17x,2x,f8.4)
c        print*,rm(i)
 4    continue

      read(1002,*)
      read(1002,*)
      read(1002,*)
      do 5 i=1,12
        read(1002,12)rmax(i)
c        print*,rmax(i)
 5    continue

      read(1002,*)
      read(1002,*)
      read(1002,*)
      do 6 i=1,12
        read(1002,12)rmin(i)
c        print*,rmin(i)
 6    continue

      return
      end


c 1*****************************************************************

      subroutine fid(n1,tflow,id,id2)

c  This subroutine determines rising versus falling limbs of the
c  streamflow hydrograph
```

```
c ****************************************************************

        integer n1,i,j,k,id(n1),id2(n1)
        integer i1,i2,count,count2
        real tflow(n1),lflow,slope,fch,lflowm1


c    Read Data, and identify rising, falling, and baseflows
c ****************************************************************


      do 1 k = 1,n1

c       Compute log of the flows and the slope between
c       two successive flows
c       log is natural logarithm
        if((tflow(k).le.0.0001).or.(k.eq.1))then
              lflow=0
              slope=0
              id(k)=3
              goto 1
        endif
        lflowm1=lflow
        lflow=log(tflow(k))
        slope=lflow-lflowm1

c       Identifier for falling versus rising limbs
c       if id(k)=1, rising limb
c       if id(k)=2, falling limb
c       if id(k)=3, baseflow

        id(k)=0
        if(slope.gt.0.001)id(k)=1
        if(id(k).eq.0,id(k)=2
        if((slope.gt.-.06).and.(slope.lt.0.001))id(k)=3


1     continue


c       ****************************************************************
c       * Determine Times corresponding to Initiation and Cessation
c       * of Direct Runoff
c       ****************************************************************

        do 18 k=1,n1

        id2(k)=3

c       If for 4 or more hours, a rising limb (id(k)=1)
c       steep falling limb (id(k)=2)

c       Skip first three data points

        if(k.eq.1)goto 18
        if(k.eq.2)goto 18
        if(k.eq.3)goto 18


        if((((id(k).lt.3).and.(id(k-1).lt.3)).and.(id(k-2).lt.3))
     $     .and.(id(k-3).lt.3))then

c           Search for begin dro (id2=4) and end dro (id2=-4)
c           Note: id2=-7 corresponds to bf that was used to determine
c                         the end of the previous storm, this data is
cannot
c                       be used to determine the beginning of the next
```

```
c                       storm.
c                  At least 2 hours must separate two different storms


c              Determine length of time dro active (=count)
               count=0
               do 20 j=k,n1
                  count=count+1
                  if((((id(j-3).lt.3).and.(id(j-2).eq.3)).and.
     $              (id(j-1).eq.3)).and.(id(j).eq.3))then
                        goto 189
                  endif
 20            continue


c               ************************************
c               *    Separate rising & falling limb
c               ************************************


c              Set i1 to one hour before beginning of storm
 189           i1=k-3-1
               if(i1.lt.2)i1=2

               i2=i1+count+1
               if(i2.gt.n1-1)i2=n1-1

               if(count.lt.4)goto 18


               count2=-1

               do 23 j=i1,i2
                  count2=count2+1
 23            continue
               id2(i2)=-4
               id2(i1)=4

               id2(i2+1)=-7

c             Reset id2 to distinguish dro rising (=+9),and
c             dro falling (=-9)

              do 47 j=i1,i2
                  if(tflow(j).gt.0.0001)then
                        if(tflow(j).gt.tflow(j-1))id2(j)=+9
                        if(tflow(j).le.tflow(j-1))id2(j)=-9
                  endif
 47           continue


c             Set k to one hour after the storm
c             at the do loop, one will be added to k
c            Next storm search will begin two hours after the previous storm
              k=k+count-4+1
              if(k.gt.n1)k=n1
              endif

 18           continue

              print*,'Finished identifying Rising vs Falling Hydrograph'
              return
              end



c 1*************************************************************
```

```
      subroutine ssdc(cuma,n1,flowt,smto3c,ssto,smto3a,fils,
     $              accum,smch,
     $              Fmtp3c,Amtp3c,
     $              Rmtp3c,Umtp3c,
     $              Fmtp3a,Amtp3a,
     $              Rmtp3a,Umtp3a,
     $              accumF,accumA,accumR,accumU,
     $              smchF,smchA,smchR,smchU,
     $              filFep,filAsp,filCrp,filCup,
     $              Fptos,Fptoc,Aptos,Aptoc,
     $              Rptos,Rptoc,Uptos,Uptoc,
     $              film,id2)

c   This subroutine checks for sediment & metal deposition/erosion
c   at the end of each channel

c ****************************************************************

      integer fils,n1,i,film,id2(n1)
      integer filFep,filAsp,filCrp,filCup
      real cuma,flowt(n1),smto3c(0:n1),smto3a(n1),smch(n1)
      real smmax,ssbf,maxf,bfpot,accum(0:n1)
      real conv,flmag,depos,sumi,sumt,sum1,sum2,sumn
      real sums,conv1,eros,Cs,f
      real sstot,Fpc,Apc,Rpc,Upc,Fdc,Adc,Rdc,Udc
      real Fpcc,Apcc,Rpcc,Upcc
      real deposF,deposA,deposR,deposU
      real erosF,erosA,erosR,erosU
      real Fmtp3c(0:n1),Amtp3c(0:n1),Rmtp3c(0:n1),Umtp3c(0:n1)
      real Fmtp3a(n1),Amtp3a(n1)
      real Rmtp3a(n1),Umtp3a(n1)
      real thres
      real accumF(0:n1),accumA(0:n1),accumR(0:n1),accumU(0:n1)
      real smchF(n1),smchA(n1),smchR(n1),smchU(n1)
      real sumiFp,sumtFp,sum1Fp
      real sum2Fp,sumnFd,sumnFp,sumsFp
      real sumiAp,sumtAp,sum1Ap
      real sum2Ap,sumnAd,sumnAp,sumsAp
      real sumiRp,sumtRp,sum1Rp
      real sum2Rp,sumnRd,sumnRp,sumsRp
      real sumiUp,sumtUp,sum1Up
      real sum2Up,sumnUd,sumnUp,sumsUp
      real Fptos(n1),Fptoc(n1),Aptos(n1),Aptoc(n1)
      real Rptos(n1),Rptoc(n1),Uptos(n1),Uptoc(n1)
      real ssto(n1),sscap,fch
      real Fedq,Feds,Fedb,Fepq,Feps,Fepb
      real Asdq,Asds,Asdb,Aspq,Asps,Aspb
      real Crdq,Crds,Crdb,Crpq,Crps,Crpb
      real Cudq,Cuds,Cudb,Cupq,Cups,Cupb

c     Read in SS Parameters
      rewind 2
       read(2,1093)f,bfpot,Cswn,Cswc,Cswi,Csch1,Csch2,Csag
 1093  format(/f7.3/f7.3,6(/f9.7))

       if(fils.eq.26)Cs=Csch1
       if(fils.eq.27)Cs=Csch2

c       print*,'f=',f,' bfpot=',bfpot,' Cs=',Cs
c       print*,'Cswn=',Cswn,'Cswc=',Cswc,'Cswi=',Cswi
c       print*,'Csch1=',Csch1,'Csch2=',Csch2,'Csag=',Csag

      rewind film
      read(film,1094)Fedq,Feds,Fedb,Fepq,Feps,Fepb,
     $              Asdq,Asds,Asdb,Aspq,Asps,Aspb,
     $              Crdq,Crds,Crdb,Crpq,Crps,Crpb,
     $              Cudq,Cuds,Cudb,Cupq,Cups,Cupb
```

```
 1094   format(4(//3(f7.2/)/3(f7.2/)))

c        print*,'Fe'
c        print*,'Quick Dissolved=',Fedq
c        print*,'Slow Dissolved =',Feds
c        print*,'LTBF Dissolved =',Fedb
c        print*,'Quick Particulate =',Fepq
c        print*,'Slow Particulate  =',Feps
c        print*,'LTBF Particulate  =',Fepb
c        print*,'As'
c        print*,'Quick Dissolved=',Asdq
c        print*,'Slow Dissolved =',Asds
c        print*,'LTBF Dissolved =',Asdb
c        print*,'Quick Particulate =',Aspq
c        print*,'Slow Particulate  =',Asps
c        print*,'LTBF Particulate  =',Aspb
c        print*,'Cr'
c        print*,'Quick Dissolved=',Crdq
c        print*,'Slow Dissolved =',Crds
c        print*,'LTBF Dissolved =',Crdb
c        print*,'Quick Particulate =',Crpq
c        print*,'Slow Particulate  =',Crps
c        print*,'LTBF Particulate  =',Crpb
c        print*,'Cu'
c        print*,'Quick Dissolved=',Cudq
c        print*,'Slow Dissolved =',Cuds
c        print*,'LTBF Dissolved =',Cudb
c        print*,'Quick Particulate =',Cupq
c        print*,'Slow Particulate  =',Cups
c        print*,'LTBF Particulate  =',Cupb

         accum(0)=200000*cuma
         accumF(0)=(((f*Feps+((1-f)*Fepb)))/100.)*accum(0)
         accumA(0)=(((f*Asps+((1-f)*Aspb)))/1e6)*accum(0)
         accumR(0)=(((f*Crps+((1-f)*Crpb)))/1e6)*accum(0)
         accumU(0)=(((f*Cups+((1-f)*Cupb)))/1e6)*accum(0)

c        Conversion factor to mg/l,=101.94
         conv=(0.3048**3)*3600.
c        Conversion factor to ug/l
         conv1=conv/1000.

         maxf=((bfpot-0.286)/0.316)*(cuma/(2.5+6.2+5.8))

         sumi=0.0
         sumt=0.0
         sums=0.0
         sumn=0.0
         sumiFp=0.0
         sumtFp=0.0
         sumsFp=0.0
         sumnFp=0.0
         sumiAp=0.0
         sumtAp=0.0
         sumsAp=0.0
         sumnAp=0.0
         sumiRp=0.0
         sumtRp=0.0
         sumsRp=0.0
         sumnRp=0.0
         sumiUp=0.0
         sumtUp=0.0
         sumsUp=0.0
         sumnUp=0.0

c           write(fils,*)'  in smto  ','in ssto','  out smto',
```

```
c     $ '         accum     ','      smch  ','   depos1      ','sstot   '
c           write(filFep,637)'     Fmtp3a','  Fpcc','    Fpc',
c     $                      '     Fmtp3a','  Fpcc','    Fpc',
c     $                      '   accumF','  smchF ','depF1   '
c           write(filFep,637)'     in    g','     % ','  mg/L',
c     $                      '    out   g','     % ','  mg/L',
c     $                      '     g    ','    g   ','    g   '


c           write(filAsp,637)'     Amtp3a','  Apcc','    Apc',
c     $                      '     Amtp3a','  Apcc','    Apc',
c     $                      '   accumA','  smchA ','depA1   '
c           write(filCrp,637)'     Rmtp3a','  Rpcc','    Rpc',
c     $                      '     Rmtp3a','  Rpcc','    Rpc',
c     $                      '   accumR','  smchR ','depR1   '
c           write(filCup,637)'     Umtp3a','  Upcc','    Upc',
c     $                      '     Umtp3a','  Upcc','    Upc',
c     $                      '   accumU','  smchU ','depU1   '


c           write(filAsp,637)'        g ',' mg/kg','  ug/L',
c     $                      '        g  ',' mg/kg','  ug/L',
c     $                      '     g    ','    g   ','    g   '
c           write(filCrp,637)'        g  ',' mg/kg','  ug/L',
c     $                      '        g  ',' mg/kg','  ug/L',
c     $                      '     g    ','    g   ','    g   '
c           write(filCup,637)'        g  ',' mg/kg','  ug/L',
c     $                      '        g  ',' mg/kg','  ug/L',
c     $                      '     g    ','    g   ','    g   '

 637        format(2(3x,a10,2x,a6,2x,a6),7x,a8,5x,a7,3x,a7)
            print*,'cuma=',cuma

          do 1 i=1,n1
            eros=0.0
            depos=0.0
            deposF=0.0
            deposA=0.0
            deposR=0.0
            deposU=0.0
            smch(i)=0.0
            smchF(i)=0.0
            smchA(i)=0.0
            smchR(i)=0.0
            smchU(i)=0.0

            sumi=sumi+smto3c(i)
            sumiFp=Fmtp3c(i)+sumiFp
            sumiAp=Amtp3c(i)+sumiAp
            sumiRp=Rmtp3c(i)+sumiRp
            sumiUp=Umtp3c(i)+sumiUp


            smto3a(i)=smto3c(i)
            Fmtp3a(i)=Fmtp3c(i)
            Amtp3a(i)=Amtp3c(i)
            Rmtp3a(i)=Rmtp3c(i)
            Umtp3a(i)=Umtp3c(i)

            accum(i)=accum(i-1)
            accumF(i)=accumF(i-1)
            accumA(i)=accumA(i-1)
            accumR(i)=accumR(i-1)
            accumU(i)=accumU(i-1)
```

```
c Determine erodible amount

              if(accum(i).le.0)then
                smch(i)=0.0
                smchF(i)=0.0
                smchA(i)=0.0
                smchR(i)=0.0
                smchU(i)=0.0

                accum(i)=0.0
                accumF(i)=0.0
                accumA(i)=0.0
                accumR(i)=0.0
                accumU(i)=0.0

              endif

              if(accum(i).gt.0)then
                thres=maxf
                eros=Cs*(((flowt(i)-thres)/cuma)**4)*(accum(i))
                if(eros.lt.0.0)eros=0.0
                erosF=eros*(accumF(i)/accum(i))
                erosA=eros*(accumA(i)/accum(i))
                erosR=eros*(accumR(i)/accum(i))
                erosU=eros*(accumU(i)/accum(i))

                accum(i)=accum(i)-eros
                accumF(i)=accumF(i)-erosF
                accumA(i)=accumA(i)-erosA
                accumR(i)=accumR(i)-erosR
                accumU(i)=accumU(i)-erosU

                smch(i)=eros
                smchF(i)=erosF
                smchA(i)=erosA
                smchR(i)=erosR
                smchU(i)=erosU

                   if(accum(i).lt.0)then
                      smch(i)=smch(i)+accum(i)
                      smchF(i)=smchF(i)+accumF(i)
                      smchA(i)=smchA(i)+accumA(i)
                      smchR(i)=smchR(i)+accumR(i)
                      smchU(i)=smchU(i)+accumU(i)

                      accum(i)=0.0
                      accumF(i)=0.0
                      accumA(i)=0.0
                      accumR(i)=0.0
                      accumU(i)=0.0
                   endif
                endif


c  Check for Deposition of Sediment & Particulate Metals

c  Calculate SS Capacity


           if(id2(i).ge.4)then
              fch=7.848*(cuma/(6.2+2.5+5.8))
              if(flowt(i).ge.fch)then
                 sscap=(22.284*flowt(i)*14.5/cuma)-172.117
              endif
              if(flowt(i).lt.fch)then
                 sscap=(0.316*flowt(i)*14.5/cuma)+0.286
              endif
```

```
endif
if(id2(i).lt.4)then
   sscap=(0.316*flowt(i)*14.5/cuma)+0.286
endif
smmax=flowt(i)*sscap*conv


    if(smto3a(i).gt.smmax)then

       depos=smto3a(i)-smmax
       deposF=Fmtp3a(i)*(depos/smto3a(i))
       deposA=Amtp3a(i)*(depos/smto3a(i))
       deposR=Rmtp3a(i)*(depos/smto3a(i))
       deposU=Umtp3a(i)*(depos/smto3a(i))

       accum(i)=accum(i)+depos
       accumF(i)=accumF(i)+deposF
       accumA(i)=accumA(i)+deposA
       accumR(i)=accumR(i)+deposR
       accumU(i)=accumU(i)+deposU

       smto3a(i)=smto3a(i)-depos
       Fmtp3a(i)=Fmtp3a(i)-deposF
       Amtp3a(i)=Amtp3a(i)-deposA
       Rmtp3a(i)=Rmtp3a(i)-deposR
       Umtp3a(i)=Umtp3a(i)-deposU

    endif

    smto3a(i)=smto3a(i)+smch(i)
    Fmtp3a(i)=Fmtp3a(i)+smchF(i)
    Amtp3a(i)=Amtp3a(i)+smchA(i)
    Rmtp3a(i)=Rmtp3a(i)+smchR(i)
    Umtp3a(i)=Umtp3a(i)+smchU(i)

    sumt=sumt+smch(i)
    sumtFp=sumtFp+smchF(i)
    sumtAp=sumtAp+smchA(i)
    sumtRp=sumtRp+smchR(i)
    sumtUp=sumtUp+smchU(i)

    sums=sums+depos
    sumsFp=sumsFp+deposF
    sumsAp=sumsAp+deposA
    sumsRp=sumsRp+deposR
    sumsUp=sumsUp+deposU

    sumn=sumn+smto3a(i)-smch(i)
    sumnFp=sumnFp+Fmtp3a(i)-smchF(i)
    sumnAp=sumnAp+Amtp3a(i)-smchA(i)
    sumnRp=sumnRp+Rmtp3a(i)-smchR(i)
    sumnUp=sumnUp+Umtp3a(i)-smchU(i)

 if(smto3a(i).gt.0.0)then
     Fpcc=Fmtp3a(i)*100./(smto3a(i))
     Apcc=Amtp3a(i)*(1e6)/(smto3a(i))
     Rpcc=Rmtp3a(i)*(1e6)/(smto3a(i))
     Upcc=Umtp3a(i)*(1e6)/(smto3a(i))
 else
     Fpcc=-1.0
     Apcc=-1.0
     Rpcc=-1.0
     Upcc=-1.0
 endif

 if(flowt(i).gt.0)then
     sstot=smto3a(i)/(flowt(i)*conv)
```

```
                Fpc=Fmtp3a(i)/(flowt(i)*conv)
                Apc=Amtp3a(i)/(flowt(i)*conv1)
                Rpc=Rmtp3a(i)/(flowt(i)*conv1)
                Upc=Umtp3a(i)/(flowt(i)*conv1)
            else
                sstot=-1.0
                Fpc=-1.0
                Apc=-1.0
                Rpc=-1.0
                Upc=-1.0
                Fdc=-1.0
                Adc=-1.0
                Rdc=-1.0
                Udc=-1.0
            endif

            write(fils,12)smto3c(i),ssto(i),smto3a(i),accum(i),
     $              smch(i),depos,sstot
12          format(f10.2,1x,f8.2,1x,f10.2,1x,f14.1,1x,f10.2,1x,
     $              f10.2,1x,f8.2)
            write(filFep,63)Fmtp3c(i),Fptos(i),Fptoc(i),
     $              Fmtp3a(i),Fpcc,Fpc,
     $              accumF(i),smchF(i),deposF

            write(filAsp,63)Amtp3c(i),Aptos(i),Aptoc(i),
     $              Amtp3a(i),Apcc,Apc,
     $              accumA(i),smchA(i),deposA

            write(filCrp,63)Rmtp3c(i),Rptos(i),Rptoc(i),
     $              Rmtp3a(i),Rpcc,Rpc,
     $              accumR(i),smchR(i),deposR

            write(filCup,63)Umtp3c(i),Uptos(i),Uptoc(i),
     $              Umtp3a(i),Upcc,Upc,
     $              accumU(i),smchU(i),deposU


63          format(2(3x,f10.2,2f8.2),1x,f14.2,2f10.2)

1           continue

            sum1=sumi+accum(0)
            sum2=sumt+sumn+accum(n1)
            sum1Fp=sumiFp+accumF(0)
            sum1Ap=sumiAp+accumA(0)
            sum1Rp=sumiRp+accumR(0)
            sum1Up=sumiUp+accumU(0)
            sum2Fp=sumtFp+sumnFp+accumF(n1)
            sum2Ap=sumtAp+sumnAp+accumA(n1)
            sum2Rp=sumtRp+sumnRp+accumR(n1)
            sum2Up=sumtUp+sumnUp+accumU(n1)

            write(60,*)
            write(60,*)
            write(60,*)'SEDIMENT DEPOSITION CHECK'
            write(60,*)'Channel Storage, Time Zero=',accum(0)
            write(60,*)'Total Mass Input          =',sumi
            write(60,*)'Total Mass Input+Storage(0)',sum1
            write(60,*)
            write(60,*)'Channel Storage, Time(n)    =',accum(n1)
            write(60,*)'Total Transport of Deposited=',sumt
            write(60,*)'Total Transport Not-Deposited',sumn
            write(60,*)'Total Transport+Storage(n)  =',sum2
            write(60,*)
            write(60,*)'Total amount deposited      =',sums
            write(60,*)
            write(60,*)
```

```
            write(60,*)'METAL BALANCE FOR CHANNEL AREA'
            write(60,*)'Particulates'
            write(60,*)'                                        ',
     $           'Fe          As          Cr          Cu'
            write(60,*)'Storage at time zero  =',
     $           accumF(0),accumA(0),accumR(0),accumU(0)
            write(60,*)'Total Mass Input      =',
     $           sumiFp,sumiAp,sumiRp,sumiUp
            write(60,*)'Tot Mass In+Storage(0)=',
     $           sum1Fp,sum1Ap,sum1Rp,sum1Up
            write(60,*)
            write(60,*)'AtlGel Storage,Time(n) =',
     $           accumF(n1),accumA(n1),accumR(n1),accumU(n1)
            write(60,*)'Tot Transp of Deposited=',
     $           sumtFp,sumtAp,sumtRp,sumtUp
            write(60,*)'Tot Transport Not-Deposited',
     $           sumnFp,sumnAp,sumnRp,sumnUp
            write(60,*)'Tot Transp+Storage(n) =',
     $           sum2Fp,sum2Ap,sum2Rp,sum2Up
            write(60,*)
            write(60,*)'Total amount deposited=',
     $           sumsFp,sumsAp,sumsRp,sumsUp
            write(60,*)
            write(60,*)

            print*
            print*,'Finished adjusting sediment & metal flux'
            print*

            close(fils)
            close(filFep)
            close(filAsp)
            close(filCrp)
            close(filCup)
            return
            end

c ***************************************************************
      subroutine ww(n1,year,month,day,hour,bf,sumbf,filf,fil)
c This subroutine inputs the Flow for the Woburn West
c Sub-basin.  The hourly flows are interpolated from the
c monthly means.
c ***************************************************************

      integer filf,month(n1),day(n1),year(n1),hour(n1)
      integer i,tday,fil,n1
      real bf(n1),t
      real early,late,te,tl,dint,dint2,sumbf

      open(filf,file='f.ww',status='unknown')
      rewind filf

c      print*,'I am in the ww subroutine'
c      write(filf,*)' Date     Flow(cfs)'

      sumbf=0
      do 1 i=1,n1

      tday=lday(year,month)
      t=month(i)+(real(day(i))/real(tday))

c     Interpolation of p

         dint=0.5

         if(t.gt.12+dint)then
               early=13.78
```

```
      late=10.67
      te=12.+dint
      tl=13.+dint
endif
if(t.le.1+dint)then
      early=13.78
      late=10.67
      te=dint
      tl=1.+dint
endif
if((t.gt.1+dint).and.(t.le.2+dint))then
      early=10.67
      late=10.15
      te=1.+dint
      tl=2.+dint
endif
if((t.gt.2+dint).and.(t.le.3+dint))then
      early=10.15
      late=12.21
      te=2.+dint
      tl=3.+dint
endif
if((t.gt.3+dint).and.(t.le.4+dint))then
      early=12.21
      late=10.93
      te=3.+dint
      tl=4.+dint
endif
if((t.gt.4+dint).and.(t.le.5+dint))then
      early=10.93
      late=7.39
      te=4.+dint
      tl=5.+dint
endif
if((t.gt.5+dint).and.(t.le.6+dint))then
      early=7.39
      late=3.45
      te=5.+dint
      tl=6.+dint
endif
if((t.gt.6+dint).and.(t.le.7+dint))then
      early=3.45
      late=1.70
      te=6.+dint
      tl=7.+dint
endif
if((t.gt.7+dint).and.(t.le.8+dint))then
      early=1.70
      late=3.75
      te=7.+dint
      tl=8.+dint
endif
if((t.gt.8+dint).and.(t.le.9+dint))then
      early=3.75
      late=3.67
      te=8.+dint
      tl=9.+dint
endif
if((t.gt.9+dint).and.(t.le.10+dint))then
      early=3.67
      late=3.97
      te=9.+dint
      tl=10.+dint
endif
if((t.gt.10+dint).and.(t.le.11+dint))then
      early=3.97
      late=3.82
```

```
                te=10.+dint
                tl=11.+dint
            endif
            if((t.gt.11+dint).and.(t.le.12+dint))then
                early=3.82
                late=13.78
                te=11.+dint
                tl=12.+dint
            endif

          if(te.eq.tl)bf(i)=late
          if(te.ne.tl)bf(i)=early-(((te-t)/(te-tl))*(early-late))

       write(filf,8)year(i),month(i),day(i),hour(i),bf(i)
 8         format(4i2.2,3x,f8.2)

          sumbf=sumbf+bf(i)
1         continue

         sumbf=sumbf*(3600./1e6)
         write(60,*)
         write(60,*)
         write(60,*)'WATER RESPONSE FROM WOBURN - WEST'
         write(60,*)'Flow Volume =',sumbf,'million ft3'
         write(60,*)

         print*,'Completed WOBURN WEST Flow Computation'
         print*
          return
          end



c 1*************************************************************
        subroutine wess(n1,fils,film,
     $              filFep,filAsp,filCrp,filCup,
     $              filFed,filAsd,filCrd,filCud,
     $              bfww,day,month,year,hour,mass,
     $              smwe,Ct,T,C,
     $              Fedtm,Asdtm,Crdtm,Cudtm,
     $              Feptm,Asptm,Crptm,Cuptm)

c  This subroutine computes SS and Metal Fluxes at Wedge Pond.
c  Two components of SS, an organic and inorganic, are assumed.
c  The organic portion is modeled by modeling
c  Wedge Pond as a large Continuous Flow Stirred Tank Reactor
c  for "Growth of Organic SS." (Constant Reactor Volume)
c  A constant concentration of each metal is assumed for
c  Streamflow and Suspended Sediment.
c ***************************************************************

          real bfww(n1)
        real flowt,T(n1),monfr,pi,C(n1),Co,V,K20,mass(0:n1)
        real conv,conv1,conv2,conv3,conv4,smwe(n1),Ci,Ct(n1)
          real Fed,Fep,Asd,Asp,Crd,Crp,Cud,Cup
          real Fedtm(n1),Asdtm(n1),Crdtm(n1),Cudtm(n1)
          real Feptm(n1),Asptm(n1),Crptm(n1),Cuptm(n1)
          real Fedts,Asdts,Crdts,Cudts
          real Fepts,Aspts,Crpts,Cupts
          real sumFed,sumFep,sumAsd,sumAsp
          real sumCrd,sumCrp,sumCud,sumCup
          real sumo,sumi,of,if
          integer i,year(n1),month(n1),hour(n1),day(n1),tday
          integer film,fils,filFep,filAsp,filCrp,filCup,n1
          integer filFed,filAsd,filCrd,filCud
          integer k,count
          real vres, qmean,restim
```

```
        data pi/3.1415926536/

c     Read Data
c        Water Volume for Wedge Pond,ft**3
         V=9900000.
c        Input Organic Conc mg/L
         Co=1.8
c        Mass of Organic Sediment in Wedge Pond, mg
         mass(0)=(Co*V*(0.3048**3)*1000.)
c        Per second
         K20=1.05e-7
         conv=(0.3048**3)*1000.
         conv1=(0.3048**3)*3600.
         conv2=conv1/1000.
         conv3=(1.0/1e6)
         conv4=(1.0/100)

         open(film,file='metals.ww',status='old')
         rewind film

c  Woburn West Metals Data
          open(filFep,file='Fep.ww',status='unknown')
          rewind filFep
          open'filFed,file='Fed.ww',status='unknown')
          rewind filFed

          open(filAsp,file='Asp.ww',status='unknown')
          rewind filAsp
          open(filAsd,file='Asd.ww',status='unknown')
          rewind filAsd

          open(filCrp,file='Crp.ww',status='unknown')
          rewind filCrp
          open(filCrd,file='Crd.ww',status='unknown')
          rewind filCrd

          open(filCup,file='Cup.ww',status='unknown')
          rewind filCup
          open(filCud,file='Cud.ww',status='unknown')
          rewind filCud

          open(fils,file='ss.ww',status='unknown')
          rewind fils

c         write(fils,231)'Date','Temperature','Flow',
c      $   'Mass WP,kg','OrgConc','smwe,g','Outlet Conc,mg/l'
 231     format(4x,a4,1x,a11,2x,a4,3x,
     $          a10,1x,a7,1x,a6,1x,a16)

c        Read Metals Info
c           print*,'film=',film
           read(film,34)Fed,Fep,Asd,Asp,Crd,Crp,Cud,Cup
 34        format(4(//f7.2//f7.2/))

c         print*,'Fe'
c         print*,'Dissolved=',Fed
c         print*,'Particulate =',Fep
c         print*,'As'
c         print*,'Dissolved=',Asd
c         print*,'Particulate =',Asp
c         print*,'Cr'
c         print*,'Dissolved=',Crd
c         print*,'Particulate =',Crp
c         print*,'Cu'
c         print*,'Dissolved=',Cud
c         print*,'Particulate =',Cup
```

```
c        write(filFep,*)'Particulate'
c        write(filFed,*)'Dissolved'
c        write(filFep,*)' Mass,g','      % ',' mg/l'
c        write(filFed,*)'Mass,g','   mg/l  '

c        write(filAsp,*)'Particulate'
c        write(filAsd,*)'Dissolved'
c        write(filAsp,*)' MASSmg',' mg/kg',' ug/l'
c        write(filAsd,*)'  MASSmg',' ug/l  '

c        write(filCrp,*)'Particulate'
c        write(filCrd,*)'Dissolved'
c        write(filCrp,*)' MASSmg',' mg/kg',' ug/l'
c        write(filCrd,*)'  MASSmg',' ug/l  '

c        write(filCup,*)'Particulate'
c        write(filCud,*)'Dissolved'
c        write(filCup,*)' MASSmg',' mg/kg',' ug/l'
c        write(filCud,*)'  MASSmg',' ug/l  '

          sumFed=0.0
          sumFep=0.0
          sumAsd=0.0
          sumAsp=0.0
          sumCrd=0.0
          sumCrp=0.0
          sumCud=0.0
          sumCup=0.0
          sumo=0.0
          sumi=0.0
        do 1 i=1,n1

c       Input Inorganic Conc mg/L
c       Ci=2.0
c       Ci=(4.0e6)*(bfww(i)/V)
        count=0
        vres=0.0
        do 199 k=i,999999
           if(i-count.le.0)goto 201
           vres=(bfww(i-count)*3600)+vres
           count=count+1
           if(vres.gt.V)goto 201
 199    continue
 201    qmean=vres/real(count)
        restim=V/(qmean)
        Ci=((3.6e6)/3600)*(1/restim)


c       if((month(i).eq.3).and.(day(i).eq.29))print*,'Ci=',Ci

        flowt=bfww(i)
c        print*,'flowt=',flowt
c        print*,'year,month,day=',year(i),month(i),day(i)
        tday=lday(year,month)
c        print*,'tday=',tday
        monfr=real(month(i))+(real(day(i))/real(tday))
c       Sin function in terms of Radians
        T(i)=(12.0*sin((pi*monfr/6)-(4.7*pi/6)))+14

c        print*,'Date=',monfr,'T(i)=',T(i)

        C(i)=((Co*flowt*conv*3600.)+mass(i-1))/
     $  ((V+(flowt*3600.)-(K20*(1.30**(T(i)-20))*V*3600.))*conv)

c        print*,'C(',i,')=',C(i)

        mass(i)=C(i)*V*conv
```

```
c       Total Sediment mass Flux, g/hr
c       (Organic + Inorganic Fraction)
        of=(C(i)*flowt*conv1)
        if=(Ci*flowt*conv1)
        smwe(i)=of+if
        sumo=sumo+of
        sumi=sumi+if
        Ct(i)=C(i)+Ci
c        print*,'smwe=',smwe(i)

c       Compute Metal Fluxes
c          Dissolved
           Fedtm(i)=flowt*Fed*conv1
           Asdtm(i)=flowt*Asd*conv2
           Crdtm(i)=flowt*Crd*conv2
           Cudtm(i)=flowt*Cud*conv2

          sumFed=sumFed+Fedtm(i)
          sumAsd=sumAsd+Asdtm(i)
          sumCrd=sumCrd+Crdtm(i)
          sumCud=sumCud+Cudtm(i)

           Fedts=(Fedtm(i)/flowt)/conv1
           Asdts=(Asdtm(i)/flowt)/conv2
           Crdts=(Crdtm(i)/flowt)/conv2
           Cudts=(Cudtm(i)/flowt)/conv2

c           print*,'Fedts=',Fedts

c          Particulate
           Feptm(i)=smwe(i)*Fep*conv4
           Asptm(i)=smwe(i)*Asp*conv3
           Crptm(i)=smwe(i)*Crp*conv3
           Cuptm(i)=smwe(i)*Cup*conv3

          sumFep=sumFep+Feptm(i)
          sumAsp=sumAsp+Asptm(i)
          sumCrp=sumCrp+Crptm(i)
          sumCup=sumCup+Cuptm(i)

           Fepts=(Feptm(i)/smwe(i))/conv4
           Aspts=(Asptm(i)/smwe(i))/conv3
           Crpts=(Crptm(i)/smwe(i))/conv3
           Cupts=(Cuptm(i)/smwe(i))/conv3

c           print*,'Fepts=',Fepts

        write(fils,86)year(i),month(i),day(i),hour(i),T(i),flowt,
     $              mass(i)/1e6,C(i),smwe(i),Ct(i)
 86     format(1x,4i2.2,2x,2f8.2,f10.2,f8.2,f10.2,f8.2)

        write(filFep,89)Feptm(i),Fepts,Ct(i)*Fepts*conv4
        write(filFed,35)Fedtm(i),Fedts

        write(filAsp,89)Asptm(i),Aspts,Ct(i)*Aspts/1000.
        write(filAsd,35)Asdtm(i),Asdts

        write(filCrp,89)Crptm(i),Crpts,Ct(i)*Crpts/1000.
        write(filCrd,35)Crdtm(i),Crdts

        write(filCup,89)Cuptm(i),Cupts,Ct(i)*Cupts/1000.
        write(filCud,35)Cudtm(i),Cudts

 89     format(3f8.2)
 35     format(2f8.2)

1      continue
```

```
      write(60,*)
      write(60,*)'SUB-BASIN SEDIMENT BALANCE,grams'
      write(60,*)'Organic Sediment  =',sumo
      write(60,*)'Inorganic Sediment=',sumi
      write(60,*)'Total Sediment    =',sumo+sumi

      write(60,*)
      write(60,*)'METALS OUTPUT FROM SUB-BASIN, grams'
      write(60,*)'Fe  Dissolved=',sumFed,'Particulate=',sumFep
      write(60,*)'As  Dissolved=',sumAsd,'Particulate=',sumAsp
      write(60,*)'Cr  Dissolved=',sumCrd,'Particulate=',sumCrp
      write(60,*)'Cu  Dissolved=',sumCud,'Particulate=',sumCup
      write(60,*)

      print*,'Finished wess subroutine'
      print*
      close(fils)
      close(film)
      close(filFep)
      close(filAsp)
      close(filCrp)
      close(filCup)
      close(filFed)
      close(filAsd)
      close(filCrd)
      close(filCud)

    return
    end

c 1*************************************************************
      subroutine met(film,n1,flowq,flows,bf,smqs,smss,smbf,
     $     smch,filFep,filAsp,filCrp,filCup,
     $     filFed,filAsd,filCrd,filCud,
     $     Fedqm,Fedsm,Fedbm,Fepqm,Fepsm,Fepbm,Feptm,Fedtm,
     $     Asdqm,Asdsm,Asdbm,Aspqm,Aspsm,Aspbm,Asptm,Asdtm,
     $     Crdqm,Crdsm,Crdbm,Crpqm,Crpsm,Crpbm,Crptm,Crdtm,
     $     Cudqm,Cudsm,Cudbm,Cupqm,Cupsm,Cupbm,Cuptm,Cudtm,
     $     Fepcm,Aspcm,Crpcm,Cupcm,frs,frq)

c This subroutine computes the metal fluxes associated
c with each Flow and Sediment Component.
c Used to model Metals from Woburn-North,Woburn-Central,&
c Winchester Sub-basins
c *************************************************************
      integer film,n1,i
      integer filFep,filAsp,filCrp,filCup
      integer filFed,filAsd,filCrd,filCud
      real flowq(n1),flows(n1),bf(n1),frs(0:n1),frq(0:n1)
      real smqs(n1),smss(n1),smbf(n1),smch(n1)
      real Fedq,Feds,Fedb,Fepq,Feps,Fepb
      real Asdq,Asds,Asdb,Aspq,Asps,Aspb
      real Crdq,Crds,Crdb,Crpq,Crps,Crpb
      real Cudq,Cuds,Cudb,Cupq,Cups,Cupb
      real Fedqm(n1),Fedsm(n1),Fedbm(n1),Fedtm(n1)
      real Fepqm(n1),Fepsm(n1),Fepbm(n1),Feptm(n1)
      real Asdqm(n1),Asdsm(n1),Asdbm(n1),Asdtm(n1)
      real Aspqm(n1),Aspsm(n1),Aspbm(n1),Asptm(n1)
      real Crdqm(n1),Crdsm(n1),Crdbm(n1),Crdtm(n1)
      real Crpqm(n1),Crpsm(n1),Crpbm(n1),Crptm(n1)
      real Cudqm(n1),Cudsm(n1),Cudbm(n1),Cudtm(n1)
      real Cupqm(n1),Cupsm(n1),Cupbm(n1),Cuptm(n1)
      real Fepcm(n1),Aspcm(n1),Crpcm(n1),Cupcm(n1)
      real conv1,conv2,conv3,conv4
      real Fedts,Fepts,Asdts,Aspts,Crdts,Crpts
      real Cudts,Cupts
      real sumFed,sumFep,sumAsd,sumAsp
```

```
      real sumCrd,sumCrp,sumCud,sumCup,flowt
      real sumFedq,sumFeds,sumFedb
      real sumFepq,sumFeps,sumFepb,sumFepc
      real sumAsdq,sumAsds,sumAsdb
      real sumAspq,sumAsps,sumAspb,sumAspc
      real sumCrdq,sumCrds,sumCrdb
      real sumCrpq,sumCrps,sumCrpb,sumCrpc
      real sumCudq,sumCuds,sumCudb
      real sumCupq,sumCups,sumCupb,sumCupc


      rewind film
      rewind filFep
      rewind filAsp
      rewind filCrp
      rewind filCup
      rewind filFed
      rewind filAsd
      rewind filCrd
      rewind filCud

      read(film,1)Fedq,Feds,Fedb,Fepq,Feps,Fepb,
     $             Asdq,Asds,Asdb,Aspq,Asps,Aspb,
     $             Crdq,Crds,Crdb,Crpq,Crps,Crpb,
     $             Cudq,Cuds,Cudb,Cupq,Cups,Cupb
 1    format(4(//3(f7.2/)/3(f7.2/)))

c      print*,'Fe'
c      print*,'Quick Dissolved=',Fedq
c      print*,'Slow Dissolved =',Feds
c      print*,'LTBF Dissolved =',Fedb
c      print*,'Quick Particulate =',Fepq
c      print*,'Slow Particulate  =',Feps
c      print*,'LTBF Particulate  =',Fepb
c      print*,'As'
c      print*,'Quick Dissolved=',Asdq
c      print*,'Slow Dissolved =',Asds
c      print*,'LTBF Dissolved =',Asdb
c      print*,'Quick Particulate =',Aspq
c      print*,'Slow Particulate  =',Asps
c      print*,'LTBF Particulate  =',Aspb
c      print*,'Cr'
c      print*,'Quick Dissolved=',Crdq
c      print*,'Slow Dissolved =',Crds
c      print*,'LTBF Dissolved =',Crdb
c      print*,'Quick Particulate =',Crpq
c      print*,'Slow Particulate  =',Crps
c      print*,'LTBF Particulate  =',Crpb
c      print*,'Cu'
c      print*,'Quick Dissolved=',Cudq
c      print*,'Slow Dissolved =',Cuds
c      print*,'LTBF Dissolved =',Cudb
c      print*,'Quick Particulate =',Cupq
c      print*,'Slow Particulate  =',Cups
c      print*,'LTBF Particulate  =',Cupb

c      convert (cfs*(mg/l) to grams per hour)
       conv1=(0.3048**3)*(3600.)
c       print*,'conv1=',conv1
c      convert (cfs*(ug/l)to grams per hour)
       conv2=conv1/1000.
c       print*,'conv2=',conv2
c      convert (g/hour)*(mg/kg) to grams per hour
       conv3=(1.0/(1000.*1000.))
c       print*,'conv3=',conv3
c      convert (g/hour*%) to grams per hour
       conv4=(1.0/100)
```

```
c          print*,'conv4=',conv4

c          write(filFep,*)' Particulate'
c          write(filAsp,*)' Particulate'
c          write(filCrp,*)' Particulate'
c          write(filCup,*)' Particulate'
c          write(filFed,*)' Dissolved'
c          write(filAsd,*)' Dissolved'
c          write(filCrd,*)' Dissolved'
c          write(filCud,*)' Dissolved'

c          write(filFep,37)'Quick,g','Slow,g','LTBF','Channel','Total',
c     $                    '  %  ','mg/L'
c          write(filFed,36)'Quick,g','Slow,g','LTBF','Total','mg/l'

c          write(filAsp,37)'Quick,g','Slow,g','LTBF','Channel','Total',
c     $                    'mg/kg','ug/L'
c          write(filAsd,36)'Quick,g','Slow,g','LTBF','Total','ug/L'

c          write(filCrp,37)'Quick,g','Slow,g','LTBF','Channel','Total',
c     $                    'mg/kg','ug/L'
c          write(filCrd,36)'Quick,g','Slow,g','LTBF','Total','ug/L'

c          write(filCup,37)'Quick,g','Slow,g','LTBF','Channel','Total',
c     $                    'mg/kg','ug/L'
c          write(filCud,36)'Quick,g','Slow,g','LTBF','Total','ug/L'

 37       format(2x,a7,3x,a6,4x,a4,1x,2x,a7,1x,2x,a5,2x,
     $           2x,a5,2x,1x,a4,1x)
 36       format(2x,a7,3x,a6,4x,a4,1x,4x,a5,1x,1x,a4,1x)

          sumFed=0.0
          sumFep=0.0
          sumAsd=0.0
          sumAsp=0.0
          sumCrd=0.0
          sumCrp=0.0
          sumCud=0.0
          sumCup=0.0
          sumFedq=0.0
          sumFeds=0.0
          sumFedb=0.0
          sumFepq=0.0
          sumFeps=0.0
          sumFepb=0.0
          sumFepc=0.0
          sumAsdq=0.0
          sumAsds=0.0
          sumAsdb=0.0
          sumAspq=0.0
          sumAsps=0.0
          sumAspb=0.0
          sumAspc=0.0
          sumCrdq=0.0
          sumCrds=0.0
          sumCrdb=0.0
          sumCrpq=0.0
          sumCrps=0.0
          sumCrpb=0.0
          sumCrpc=0.0
          sumCudq=0.0
          sumCuds=0.0
          sumCudb=0.0
          sumCupq=0.0
          sumCups=0.0
          sumCupb=0.0
          sumCupc=0.0
```

```
      do 10 i=1,n1
        flowt=flowq(i)+flows(i)+bf(i)
c        print*,'i=',i,'flowt=',flowt

c       Dissolved Calculation

        Fedqm(i)=flowq(i)*Fedq*conv1
        Fedsm(i)=flows(i)*Feds*conv1
        Fedbm(i)=bf(i)*Fedb*conv1

        Fedtm(i)=Fedqm(i)+Fedsm(i)+Fedbm(i)
        sumFed=sumFed+Fedtm(i)
        sumFedq=sumFedq+Fedqm(i)
        sumFeds=sumFeds+Fedsm(i)
        sumFedb=sumFedb+Fedbm(i)

        Asdqm(i)=flowq(i)*Asdq*conv2
        Asdsm(i)=flows(i)*Asds*conv2
        Asdbm(i)=bf(i)*Asdb*conv2

        Asdtm(i)=Asdqm(i)+Asdsm(i)+Asdbm(i)
        sumAsd=sumAsd+Asdtm(i)
        sumAsdq=sumAsdq+Asdqm(i)
        sumAsds=sumAsds+Asdsm(i)
        sumAsdb=sumAsdb+Asdbm(i)

        Crdqm(i)=flowq(i)*Crdq*conv2
        Crdsm(i)=flows(i)*Crds*conv2
        Crdbm(i)=bf(i)*Crdb*conv2

        Crdtm(i)=Crdqm(i)+Crdsm(i)+Crdbm(i)
        sumCrd=sumCrd+Crdtm(i)
        sumCrdq=sumCrdq+Crdqm(i)
        sumCrds=sumCrds+Crdsm(i)
        sumCrdb=sumCrdb+Crdbm(i)

        Cudqm(i)=flowq(i)*Cudq*conv2
        Cudsm(i)=flows(i)*Cuds*conv2
        Cudbm(i)=bf(i)*Cudb*conv2

        Cudtm(i)=Cudqm(i)+Cudsm(i)+Cudbm(i)
        sumCud=sumCud+Cudtm(i)
        sumCudq=sumCudq+Cudqm(i)
        sumCuds=sumCuds+Cudsm(i)
        sumCudb=sumCudb+Cudbm(i)

        if(flowt.gt.0)then
          Fedts=(Fedtm(i)/flowt)/conv1
          Asdts=(Asdtm(i)/flowt)/conv2
          Crdts=(Crdtm(i)/flowt)/conv2
          Cudts=(Cudtm(i)/flowt)/conv2
        else
          Fedts=-1
          Asdts=-1
          Crdts=-1
          Cudts=-1
        endif


c       Particulate Calculation

        Fepqm(i)=smqs(i)*Fepq*conv4
        Fepsm(i)=smss(i)*Feps*conv4
        Fepbm(i)=smbf(i)*Fepb*conv4
        Fepcm(i)=smch(i)*(((1-frs(i)-frq(i))*Fepb)+
     $              (frs(i)*Feps)+(frq(i)*Fepq))*conv4
```

```
c          print*,'sumsed=',smqs(i)+smss(i)+smbf(i)+smch(i)

           Feptm(i)=Fepqm(i)+Fepsm(i)+Fepbm(i)+Fepcm(i)
           sumFep=sumFep+Feptm(i)
           sumFepq=sumFepq+Fepqm(i)
           sumFeps=sumFeps+Fepsm(i)
           sumFepb=sumFepb+Fepbm(i)
           sumFepc=sumFepc+Fepcm(i)

           Aspqm(i)=smqs(i)*Aspq*conv3
           Aspsm(i)=smss(i)*Asps*conv3
           Aspbm(i)=smbf(i)*Aspb*conv3
           Aspcm(i)=smch(i)*(((1-frs(i)-frq(i))*Aspb)+
     $               (frs(i)*Asps)+(frq(i)*Aspq))*conv3

           Asptm(i)=Aspqm(i)+Aspsm(i)+Aspbm(i)+Aspcm(i)
           sumAsp=sumAsp+Asptm(i)
           sumAspq=sumAspq+Aspqm(i)
           sumAsps=sumAsps+Aspsm(i)
           sumAspb=sumAspb+Aspbm(i)
           sumAspc=sumAspc+Aspcm(i)

           Crpqm(i)=smqs(i)*Crpq*conv3
           Crpsm(i)=smss(i)*Crps*conv3
           Crpbm(i)=smbf(i)*Crpb*conv3
           Crpcm(i)=smch(i)*(((1-frs(i)-frq(i))*Crpb)+
     $               (frs(i)*Crps)+(frq(i)*Crpq))*conv3

           Crptm(i)=Crpqm(i)+Crpsm(i)+Crpbm(i)+Crpcm(i)
           sumCrp=sumCrp+Crptm(i)
           sumCrpq=sumCrpq+Crpqm(i)
           sumCrps=sumCrps+Crpsm(i)
           sumCrpb=sumCrpb+Crpbm(i)
           sumCrpc=sumCrpc+Crpcm(i)

           Cupqm(i)=smqs(i)*Cupq*conv3
           Cupsm(i)=smss(i)*Cups*conv3
           Cupbm(i)=smbf(i)*Cupb*conv3
           Cupcm(i)=smch(i)*(((1-frs(i)-frq(i))*Cupb)+
     $               (frs(i)*Cups)+(frq(i)*Cupq))*conv3

           Cuptm(i)=Cupqm(i)+Cupsm(i)+Cupbm(i)+Cupcm(i)
           sumCup=sumCup+Cuptm(i)
           sumCupq=sumCupq+Cupqm(i)
           sumCups=sumCups+Cupsm(i)
           sumCupb=sumCupb+Cupbm(i)
           sumCupc=sumCupc+Cupcm(i)

           if(smqs(i)+smss(i)+smbf(i)+smch(i).gt.0)then
            Fepts=(Feptm(i)/(smqs(i)+smss(i)+smbf(i)+smch(i)))/conv4
            Aspts=(Asptm(i)/(smqs(i)+smss(i)+smbf(i)+smch(i)))/conv3
            Crpts=(Crptm(i)/(smqs(i)+smss(i)+smbf(i)+smch(i)))/conv3
            Cupts=(Cuptm(i)/(smqs(i)+smss(i)+smbf(i)+smch(i)))/conv3
           else
            Fepts=-1
            Aspts=-1
            Crpts=-1
            Cupts=-1
           endif

         write(filFep,89)Fepqm(i),Fepsm(i),Fepbm(i),Fepcm(i),Feptm(i),
     $          Fepts,Feptm(i)/(flowt*conv1)
         write(filFed,35)Fedqm(i),Fedsm(i),Fedbm(i),Fedtm(i),Fedts

         write(filAsp,89)Aspqm(i),Aspsm(i),Aspbm(i),Aspcm(i),Asptm(i),
     $          Aspts,Asptm(i)/(flowt*conv2)
         write(filAsd,35)Asdqm(i),Asdsm(i),Asdbm(i),Asdtm(i),Asdts
```

```
      write(filCrp,89)Crpqm(i),Crpsm(i),Crpbm(i),Crpcm(i),Crptm(i),
     $          Crpts,Crptm(i)/(flowt*conv2)
      write(filCrd,35)Crdqm(i),Crdsm(i),Crdbm(i),Crdtm(i),Crdts

      write(filCup,89)Cupqm(i),Cupsm(i),Cupbm(i),Cupcm(i),Cuptm(i),
     $          Cupts,Cuptm(i)/(flowt*conv2)
      write(filCud,35)Cudqm(i),Cudsm(i),Cudbm(i),Cudtm(i),Cudts

89    format(5(1x,f9.1),1x,f8.2,1x,f6.2)
35    format(4(2x,f7.2),1x,f5.2)

10    continue

      write(60,*)'METALS OUTPUT FROM SUB-BASIN,grams'
      write(60,*)'Fe  Dissolved=',sumFed,'Particulate=',sumFep
      write(60,*)'As  Dissolved=',sumAsd,'Particulate=',sumAsp
      write(60,*)'Cr  Dissolved=',sumCrd,'Particulate=',sumCrp
      write(60,*)'Cu  Dissolved=',sumCud,'Particulate=',sumCup
      write(60,*)'frs(0)=',frs(0),'frs(n)=',frs(n1)
      write(60,*)'frq(0)=',frq(0),'frq(n)=',frq(n1)
      write(60,*)
      write(60,*)'Fe Transported'
      write(60,*)'Quick Dissolved=',sumFedq
      write(60,*)'Slow Dissolved=',sumFeds
      write(60,*)'LTBF Dissolved=',sumFedb
      write(60,*)'Quick Particulate=',sumFepq
      write(60,*)'Slow Particulate=',sumFeps
      write(60,*)'LTBF Particulate=',sumFepb
      write(60,*)'Channel Particulate=',sumFepc
      write(60,*)
      write(60,*)'As Transported'
      write(60,*)'Quick Dissolved=',sumAsdq
      write(60,*)'Slow Dissolved=',sumAsds
      write(60,*)'LTBF Dissolved=',sumAsdb
      write(60,*)'Quick Particulate=',sumAspq
      write(60,*)'Slow Particulate=',sumAsps
      write(60,*)'LTBF Particulate=',sumAspb
      write(60,*)'Channel Particulate=',sumAspc
      write(60,*)
      write(60,*)'Cr Transported'
      write(60,*)'Quick Dissolved=',sumCrdq
      write(60,*)'Slow Dissolved=',sumCrds
      write(60,*)'LTBF Dissolved=',sumCrdb
      write(60,*)'Quick Particulate=',sumCrpq
      write(60,*)'Slow Particulate=',sumCrps
      write(60,*)'LTBF Particulate=',sumCrpb
      write(60,*)'Channel Particulate=',sumCrpc
      write(60,*)
      write(60,*)'Cu Transported'
      write(60,*)'Quick Dissolved=',sumCudq
      write(60,*)'Slow Dissolved=',sumCuds
      write(60,*)'LTBF Dissolved=',sumCudb
      write(60,*)'Quick Particulate=',sumCupq
      write(60,*)'Slow Particulate=',sumCups
      write(60,*)'LTBF Particulate=',sumCupb
      write(60,*)'Channel Particulate=',sumCupc
      write(60,*)
      write(60,*)

      print*,'Finished metals subroutine'
      print*
      close(filFep)
      close(filAsp)
      close(filCrp)
      close(filCup)
      close(filFed)
      close(filAsd)
```

```
      close(filCrd)
      close(filCud)
      return
      end

c 1*****************************************************
      subroutine wr(n1,yea,da,mont,hou,rai,
     $          flmic,flmi,flmo,flmoc,flwec,flwe,
     $          flwic,flwi,
     $          summic,summoc,sumwec,sumwic,
     $          summim,summom,sumwem,sumwim,
     $          summi,summo,sumwe,sumwi,
     $          cntmi,cntmo,cntwe,cntwi,temp,snow)

c     This subroutine writes the Computed vs Modeled Flow
c     Data to a file called out.check
c *****************************************************
      integer i,n1,da(n1),mont(n1),yea(n1),hou(n1)
      integer cntmi,cntmo,cntwe,cntwi
      real flmic(n1),flmi(n1),flmo(n1),flmoc(n1)
      real flwec(n1),flwe(n1),flwic(n1),flwi(n1)
      real rai(n1),snow(n1),temp(n1)
      real summic,summoc,sumwec,sumwic
      real summim,summom,sumwem,sumwim
      real summi,summo,sumwe,sumwi
      real rr2n,rr3n,rr5n,rr1n,rr2d,rr3d,rr5d,rr1d

      summic=summic/(real(cntmi))
      summoc=summoc/(real(cntmo))
      sumwec=sumwec/(real(cntwe))
      sumwic=sumwic/(real(cntwi))

      summi=summi*3600./1e6
      summo=summo*3600./1e6
      sumwe=sumwe*3600./1e6
      sumwi=sumwi*3600./1e6

      summim=summim/(real(cntmi))
      summom=summom/(real(cntmo))
      sumwem=sumwem/(real(cntwe))
      sumwim=sumwim/(real(cntwi))

c Write Data to File
c      write(5,24)'Gage#2','Gage#3',
c     $           'Gage#1','Gage#5'

 24   format(31x,a6,14x,a6,14x,a6,14x,a6)
c      write(5,23)'Date/Time','Rain',
c     $           'Computed','Measured',
c     $           'Computed','Measured',
c     $           'Computed','Measured',
c     $           'Computed','Measured'
 23   format(a9,1x,a4,12x,
     $          4(a8,1x,a8,3x))


      rr2n=0.0
      rr2d=0.0
      rr3n=0.0
      rr3d=0.0
      rr5n=0.0
      rr5d=0.0
      rr4n=0.0
      rr4d=0.0

      do 16 i=1,n1
       write(5,19)yea(i),mont(i),da(i),hou(i),rai(i),i,
```

```
     $              snow(i),temp(i),
     $              flmic(i),flmi(i),
     $              flmoc(i),flmo(i),
     $              flwec(i),flwe(i),
     $              flwic(i),flwi(i)
 19      format(4i2.2,2x,f4.2,1x,i5,1x,f4.2,1x,f3.0,1x,
     $           4(f8.2,1x,f8.2,3x))

         if(flmi(i).ge.0)then
           rr2n=rr2n+((flmic(i)-flmi(i))**2)
           rr2d=rr2d+((flmi(i)-summim)**2)
         endif
         if(flmo(i).ge.0)then
           rr3n=rr3n+((flmoc(i)-flmo(i))**2)
           rr3d=rr3d+((flmo(i)-summom)**2)
         endif
         if(flwe(i).ge.0)then
           rr1n=rr1n+((flwec(i)-flwe(i))**2)
           rr1d=rr1d+((flwe(i)-sumwem)**2)
         endif
         if(flwi(i).ge.0)then
           rr5n=rr5n+((flwic(i)-flwi(i))**2)
           rr5d=rr5d+((flwi(i)-sumwim)**2)
         endif

 16      continue

         write(5,*)
c         write(5,17)'Total Modeled',summi,summo,sumwe,sumwi
 17      format(a13,8x,4(f8.2,12x))
c         write(5,22)'10^6 ft^3'
 22      format(a9)
         write(5,*)
c         write(5,124)'Comparison of Acceptable Measured Flows'
 124     format(a39)
c         write(5,123)'Ave (cfs)     ',summic,summim,
c     $              summoc,summom,sumwec,sumwem,sumwic,sumwim
 123     format(a13,8x,4(f8.2,1x,f8.2,3x))

         write(60,*)
         write(60,*)'Tot Modeled Flow (Gage2)=',summi,'10^6 ft^3'
         write(60,*)'Tot Modeled Flow (Gage3)=',summo,'10^6 ft^3'
         write(60,*)'Tot Modeled Flow (Gage1)=',sumwe,'10^6 ft^3'
         write(60,*)'Tot Modeled Flow (Gage5)=',sumwi,'10^6 ft^3'
         write(60,*)
         write(60,124)'Comparison of Acceptable Measured Flows'
         write(60,125)'Gage 2(cfs) Meas Ave=',summim,
     $                '  Modeled Ave=',summic
         write(60,125)'Gage 3(cfs) Meas Ave=',summom,
     $                '  Modeled Ave=',summoc
         write(60,125)'Gage 1(cfs) Meas Ave=',sumwem,
     $                '  Modeled Ave=',sumwec
         write(60,125)'Gage 5(cfs) Meas Ave=',sumwim,
     $                '  Modeled Ave=',sumwic
 125     format(a23,f8.2,a14,f8.2)

         write(60,*)
         write(60,*)' Gage 2, R2=',1-(rr2n/rr2d)
         write(60,*)' Gage 3, R2=',1-(rr3n/rr3d)
         write(60,*)' Gage 1, R2=',1-(rr1n/rr1d)
         write(60,*)' Gage 5, R2=',1-(rr5n/rr5d)

         close(5)
         print*
         print*,'Completed Writing out.check file'
         return
         end
```

```
c 1*************************************************************
           subroutine rdrain(n1,db,da,mont,yea,hou,rai,filr,
     $                           temp,snow,filt)
c This subroutine reads the precipitation and temperature data
c  and distinguishes between rain and snow
c *************************************************************
       integer check,j,k,db,n1,filr,filt
       integer yea(n1),mont(n1),da(n1),hou(n1)
       real rai(n1),sumr,vol
       real temp(n1),snow(n1),sumsn,vos

       rewind filt
       rewind filr

      sumr=0.0
      sumsn=0.0
      do 1 k=1,99999

        read(filr,101)yea(k),mont(k),da(k),hou(k)
 101    format(4i2.2)
        check=int((yea(k)*1e6))+int((mont(k)*1e4))+
     $        int((da(k)*100))+(hou(k))


        if(((((mont(k).eq.11).or.(mont(k).eq.12)).or.
     $        (mont(k).eq.1)).or.(mont(k).eq.2)).or.
     $        (mont(k).eq.3)).or.(mont(k).eq.4))
     $        read(filt,*)


        if(check.ne.db)then
            goto 1
        else
            backspace filr
            backspace filt
            do 3 j=1,n1


             read(filr,102)yea(j),mont(j),da(j),hou(j),rai(j)
 102         format(4i2.2,5x,f5.2)

             if(((((mont(j).eq.11).or.(mont(j).eq.12)).or.
     $           (mont(j).eq.1)).or.(mont(j).eq.2)).or.
     $           (mont(j).eq.3)).or.(mont(j).eq.4))then

                read(filt,103)temp(j)
 103            format(8x,5x,f5.0)

                if(temp(j).lt.32)then
                  snow(j)=rai(j)
                  rai(j)=0.0
                else
                  snow(j)=0.0
                endif
             else
                temp(j)=-2.
                snow(j)=0.0
             endif
c Note: snow(j) is snow volume for time j in 'equivalent rain depth'
c       units


             sumr=sumr+rai(j)
             sumsn=sumsn+snow(j)

 3           continue
```

```
            goto 2
          endif
 1        continue

 2        print*,'Completed reading RAINFALL data'
          print*

          vol=sumr*25.*(5280.**2)/(12.*1e6)
          vos=sumsn*25.*(5280.**2)/(12.*1e6)

          write(60,*)'Start Date =',db
          write(60,*)'Hours Modeled =',n1
          write(60,12)'TOTAL RAIN =',sumr,'inches    =',vol,'million ft3'
          write(60,12)'TOTAL SNOW =',sumsn,'in(eq.rai)',vos,
     $                  'million ft3'
          write(60,12)'TOTAL PREC =',sumr+sumsn,'inches  =',vos+vol,
     $                  'million ft3'

 12       format(//2x,a12,1x,f6.2,1x,a10,1x,f8.2,1x,a11)

          close(3)
          return
          end


c 1*************************************************************
         subroutine wn(db,rai,n1,uq,us,flowq,flows,
     $                 fil,bf,area,agwitn,idr,ieff,
     $                 yea,mont,da,hou,bfww,filf,snow,temp,
     $                 melt,flowm,um,idt,melte,flowr,melp,
     $                 bfm,bfmax,bfmin,
     $                 rm,rmax,rmin,rmea,eff)

c This subroutine produces a flow hydrograph for a
c Sub-basin using a Unit Hydrograph Technique.
c Used to model flow from Woburn-North,Woburn-Central, & Winchester
c Sub-basins.
c *************************************************************
         integer uiqn,uisn,i,n1,idr(n1),filf,uimn,idt(n1)
         integer db,fil,yea(n1),mont(n1),da(n1),hou(n1),melp(n1)
         integer TQ,TS,TM
         real area,areaft,KQ,KS,uq(n1),us(n1),rai(n1),flowq(n1)
         real flows(n1),bf(n1),sumq,sums,sumbf,agwith,IAQ,IAS
         real ieff(n1),sumi,sumuq,sumus,bfww(n1)
         real snow(n1),temp(n1),melt(n1),snowf,flowm(n1)
         real IAM,KM,um(n1),sumum,melte(n1),st
         real flowr(n1)
         real  bfm(200),bfmax(200),bfmin(200)
         real  rm(12),rmax(12),rmin(12),rmea(n1)
         real  eff(n1)

c  Start Quick & Slow Response Calculations

        rewind fil
        rewind filf

        read(fil,11)area
 11     format(//f4.1)
c        print*,area
        areaft=area*(5280**2)

        read(fil,12)IAQ
        read(fil,15)IAS
        read(fil,15)IAM
c        print*,'IAQ,IAS,IAM=',IAQ,IAS,IAM

        read(fil,12)KQ
```

```
        read(fil,15)KS
        read(fil,15)KM
c        print*,'KQ,KS,KM=',KQ,KS,KM
 12     format(////f5.2)
 15     format(f5.2)

        read(fil,112)TQ
        read(fil,115)TS
        read(fil,115)TM
c        print*,'TQ,TS,TM=',TQ,TS,TM

 112     format(////i3)
 115     format(i3)

        read(fil,196)snowf
 196    format(//f8.6)
c        print*,'snowf=',snowf


        write(60,*)
        write(60,*)
        write(16,*)
        write(16,*)
        if(fil.eq.12)then
           write(60,*)'WATER RESPONSE FROM WOBURN - NORTH'
           write(16,*)'STORM SUMMARY FOR WOBURN - NORTH'
        endif
        if(fil.eq.13)then
           write(60,*)'WATER RESPONSE FROM WOBURN - CENTRAL'
           write(16,*)'STORM SUMMARY FOR WOBURN - CENTRAL'
        endif
        if(fil.eq.15)then
           write(60,*)'WATER RESPONSE FROM WINCHESTER'
           write(16,*)'STORM SUMMARY FOR WINCHESTER'
        endif
        write(60,*)'Area =',area

c Initialize u?(i), & flow?(i)
        do 8 i=1,n1
          uq(i)=0.0
          us(i)=0.0
          um(i)=0.0
          flowq(i)=0.0
          flows(i)=0.0
          flowm(i)=0.0
 8      continue

c Read Quick Flow Parameters
        read(fil,13)uiqn
c        print*,'uiqn=',uiqn
 13     format(//i3)

        read(fil,*)
        read(fil,*)
        sumuq=0.0
        do 1 i=1,uiqn
           read(fil,14)uq(i)
c           print*,uq(i)
 14        format(f8.1)
           sumuq=sumuq+uq(i)
 1      continue
           sumuq=sumuq*3600.*12./((5280**2)*area)
c           print*,'sumuq=',sumuq,'inches'

        do 183 i=1,uiqn
            uq(i)=uq(i)/sumuq
 183    continue
```

```
c Read Slow Flow parameters
       read(fil,13)uisn
c       print*,'uisn=',uisn

       read(fil,*)
       read(fil,*)
       sumus=0.0
       do 2 i=1,uisn
           read(fil,14)us(i)
c          print*,us(i)
          sumus=sumus+us(i)
 2     continue
          sumus=sumus*3600.*12./((5280**2)*area)
c          print*,'sumus=',sumus,'inches'

        do 184 i=1,uisn
           us(i)=us(i)/sumus
 184    continue


c Read Meltwater Parameters
       read(fil,13)uimn
c       print*,'uimn=',uimn

       read(fil,*)
       read(fil,*)
       sumum=0.0
       do 162 i=1,uimn
           read(fil,14)um(i)
c           print*,um(i)
          sumum=sumum+um(i)
 162     continue
          sumum=sumum*3600.*12./((5280**2)*area)
c          print*,'sumum=',sumum,'inches'

          st=0.0
          do 185 i=1,uimn
              um(i)=um(i)/sumum
              st=st+um(i)
 185      continue
          st=st*3600.*12./((5280**2)*area)
c          print*,'st=',st


c Compute Flow from Unit Hydrograph
c Quick
        write(16,*)
        write(16,*)'QUICK STORMS'
        call stormid(n1,rai,idr,TQ,KQ,IAQ,ieff,
     $           yea,mont,da,hou,sumi)
        call flowui(n1,idr,uiqn,uq,ieff,sumq,flowq,
     $              eff,flowr)

       write(60,*)'Quick Water Vol =',sumq,'million ft3'
       write(60,*)'Effective Rain=',sumi,'in.',
     $              sumi*area*(5280.**2)/(12.*1e6),'10^6 ft^3'
       write(60,*)
       print*,'Completed Computation of Quick Response'


c Slow
        write(16,*)
        write(16,*)'SLOW STORMS'
        call stormid(n1,rai,idr,TS,KS,IAS,ieff,
     $           yea,mont,da,hou,sumi)
        call flowui(n1,idr,uisn,us,ieff,sums,flows,
```

```
     $              eff,flowr)

        write(60,*)'Slow Rain  Water Vol =',sums,'million ft3'
        write(60,*)'Effective Rain=',sumi,'in.',
     $              sumi*area*(5280.**2)/(12.*1e6),'10^6 ft^3'
        write(60,*)
        print*,'Completed Computation of Slow Response'


c Meltwater

        call meltwater(n1,snow,melt,yea,mont,da,hou,
     $          temp,snowf,rai,melp)
        call meltid(n1,melt,idr,TM,ieff,yea,mont,da,hou,sumi,
     $              KM,IAM,temp,idt)

        call meltflow(n1,uimn,um,ieff,sums,flowm,idt,idr,melte,
     $                    flowr,melp)
        write(60,*)'Effective Snowmelt Vol=',sumi,'in.',
     $              sumi*area*(5280.**2)/(12.*1e6),'10^6 ft^3'
        write(60,*)'Snowmelt Water Vol,Slow =',sums,'million ft3'
        write(60,*)
       print*,'Completed Computation of Meltwater Response'

c Add fraction Routed meltwater to the quick storm response
c Add the remaining Routed meltwater to the slow storm response
        do 136 i=1,n1
            flows(i)=flows(i)+(0.4*flowm(i))
            flowq(i)=flowq(i)+(0.6*flowm(i))
 136    continue



c  Long-term Baseflow
       call priorr(n1,rm,rmea,melt,rai,yea,mont,da,hou)
       call ltbf(n1,fil,yea,mont,da,hou,bf,agwith,
     $           area,sumbf,flows,bfww,
     $           bfm,bfmax,bfmin,
     $           rm,rmax,rmin,rmea,flowq)


c       write(filf,77)'     flowq',' flows','ltbf','  flt'
 77    format(7x,a10,3x,a6,5x,a4,4x,a5)
       do 832 i=1,n1
       write(filf,833)yea(i),mont(i),da(i),hou(i),
     $                 flowq(i),flows(i),bf(i),
     $                 flowq(i)+flows(i)+bf(i),flowm(i)
 833   format(4i2.2,5(1x,f8.2))
 832   continue

       write(60,*)'Baseflow Volume =',sumbf,'million ft3'
       write(60,*)
       write(60,*)

        close(fil)
        close(filf)
        return
        end


c ***************************************************************
        subroutine meltid(n1,melt,idr,uin,ieff,
     $          yea,mont,da,hou,sumi,F,IA,temp,idt)

c This subroutine identifies individual snowmelt events and
c computes the effective snowmelt.
c ***************************************************************
```

```
      integer i,j,k,idr(n1),tresp,uin,u,ir1,ir2,it1,it2,x
      integer yea(n1),mont(n1),da(n1),hou(n1),n1,idt(n1)
      integer count
      real melt(n1),sumch,ieff(n1),sumieff,sumi,summelt
      real F,IA,temp(n1),melts2

c      print*,'F in melt subroutine=',F
c      print*,'IA in melt subroutine=',IA
c      print*,'n1=',n1
      write(16,*)'MELTWATER EVENTS'

c Identify Individual Melt Events, idr=0:no storm, idr>0:storm
      open(99,file='test.melt',status='unknown')
      rewind 99

c      Initialize storm
      do 400 i=1,n1
          ieff(i)=0.0
          idt(i)=0
          idr(i)=0
400   continue


      do 801 i=1,n1

       if(temp(i).le.32)goto 801
c      Beginning of Melt Route Event = it1
       it1=i
c      Find end of melt route event
       count=0
       do 319 j=it1,n1
          if(temp(j).le.32)goto 320
          count=count+1
319    continue
320    it2=it1+count-1
       if(it2.gt.n1)it2=n1
       do 321 j=it1,it2
           idt(j)=count
321    continue
       i=it2
c     One is added to i at the continue statement
801   continue

      sumi=0.0
      do 312 i=uin,n1
         if(melt(i).le.0.00)goto 312
c        Beginning of Storm = ir1
         ir1=i
c        Find end of event (time after which uin hours without melt)
         count=0

         do 36 j=ir1,n1
            sumch=0.0
            u=uin-1
            do 32 k=0,u
            sumch=melt(j-k)+sumch
32          continue
            if(sumch.le.0.000)goto 87
            if(j.eq.n1)goto 87
            count=count+1
36       continue
87       ir2=ir1+count-uin
         if(j.eq.n1)ir2=n1

         summelt=0.0
         sumieff=0.0
         do 354 j=ir1,ir2
```

```
                idr(j)=count-uin+1
                if(ir2.eq.n1)idr(j)=count+1
                summelt=summelt+melt(j)

                if(summelt.le.IA)ieff(j)=0.0
                if(summelt.gt.IA)then
                       if(summelt-IA.ge.melt(j))then
                         ieff(j)=melt(j)*F
                       else
                         ieff(j)=(summelt-IA)*F
                       endif
                 sumieff=sumieff+ieff(j)
                 sumi=sumi+ieff(j)
                endif
 354          continue

c              print*,'Finished idr in meltid'

              write(16,*)'Storm Date:',yea(ir1),mont(ir1),da(ir1),
     $                    hou(ir1)
              write(16,*)'Snowmelt =',summelt,'in.',
     $                   'Snowmeltef =',sumieff,'in.'
              write(16,*)
c             reset storm search to uin hours after last storm (1 is added
to i
c             at the continue statement
              i=ir2+uin

 312      continue

         do 777 i=1,n1
          write(99,77)yea(i),mont(i),da(i),hou(i),melt(i),idr(i),ieff(i),
     $                temp(i),idt(i)
 77       format(4i2.2,f10.4,2x,i4,2x,f10.4,1x,f4.0,1x,i5)
 777      continue

          print*,'Finished Melt Event Identification'

          return
          end


c ****************************************************************
         subroutine meltwater(n1,snow,melt,yea,mont,da,hou,
     $                    temp,snowf,rain,melp)

c This subroutine computes snowmelt depth using a degree-hour
c method.  Melt(i) and snow(i) are in 'equivalent rain inches.'
c ****************************************************************
         integer n1,yea(n1),mont(n1),da(n1),hou(n1),i,melp(n1)
         integer flag
         real snow(n1),melt(n1),temp(n1),rain(n1)
         real snaccum,fact,snowf,meltp,max,lagdh,lagdr
         real dh1,dh2,dh3,dh4,dh5,dh6,dh0,snsum,meltsum

         snsum=0.0
         meltsum=0.0

c  Initial snaccum on Jan 1, 1991 & Jan 1 1992
          snaccum=0.0
c  Initial snaccum on Jan 1, 1993 0:00  = 1.006
c         snaccum=1.006
         max=0.0
         open(135,file='melt.check',status='unknown')
         rewind 135

         do 1 i=1,n1
```

```
      if(((((mont(i).eq.11).or.(mont(i).eq.12)).or.
     $    (mont(i).eq.1)).or.(mont(i).eq.2)).or.
     $    (mont(i).eq.3)).or.(mont(i).eq.4))then

         snsum=snsum+snow(i)
         snaccum=snaccum+snow(i)
         if(snaccum.gt.max)max=snaccum

         if(temp(i).gt.32)then

                 if(i.le.6)then
                     melt(i)=0.0
                     melp(i)=0
                     goto 987
                 endif

                 dh0=temp(i)-32
                 dh1=temp(i-1)-32
                 dh2=temp(i-2)-32
                 dh3=temp(i-3)-32
                 dh4=temp(i-4)-32
                 dh5=temp(i-5)-32
                 dh6=temp(i-6)-32
                 if(temp(i-1).lt.32)dh1=0.0
                 if(temp(i-2).lt.32)dh2=0.0
                 if(temp(i-3).lt.32)dh3=0.0
                 if(temp(i-4).lt.32)dh4=0.0
                 if(temp(i-5).lt.32)dh5=0.0
                 if(temp(i-6).lt.32)dh6=0.0
                 lagdh=dh0+dh1+dh2+dh3+dh4+dh5+dh6
                 lagdr=dh0+dh1+dh2+dh3+dh4+dh5+dh6


c If melp = 1,2 or 3 Then Snowmelt Is Initiated

 823             if(snaccum.le.0.0)then
                melt(i)=0.0
                if(lagdh.le.80)then
                   melp(i)=0
                   if((rain(i).gt.0.00).and.
     $                  (lagdr.gt.18))melp(i)=2
                else
                   melp(i)=1
                   if((rain(i).gt.0.00).and.
     $                  (lagdr.gt.18))melp(i)=3
                endif

           else

                if(lagdh.gt.80)then
                  meltp=snowf*((temp(i)-32)**1.5)
                  melp(i)=1
                  if((rain(i).gt.0.00).and.
     $                (lagdr.gt.18))melp(i)=3
                else
                  meltp=0.0
                  melp(i)=0.0
                  if((rain(i).gt.0.00).and.
     $                (lagdr.gt.18))melp(i)=2
                endif
            if((rain(i).gt.0.00).and.(lagdr.gt.18))
     $     meltp=0.36*snowf*((temp(i)-32)**1.5)*((rain(i)*100)**1.5)
                if(meltp.lt.snaccum)then
                     melt(i)=meltp
                     snaccum=snaccum-meltp
                else
                     melt(i)=snaccum
```

```
                    snaccum=0.0
                endif
            endif

c Adjust melp(i) such that the falling limb of temp graph routing
c will occur

        if(i.gt.1)then

          if(((melp(i).eq.0).and.(melp(i-1).gt.0)).and.
     $       (temp(i).ge.32))melp(i)=4
        endif

        else
            melt(i)=0.0
            melp(i)=0
            if(((melp(i).eq.0).and.(melp(i-1).gt.0)).and.
     $          (temp(i).ge.32))melp(i)=4

        endif

        if((melp(i).eq.4).and.(snaccum.gt.0))then
              lagdh=99999
              lagdr=99999
              goto 823
        endif

 987    write(135,11)yea(i),mont(i),da(i),hou(i),rain(i),snow(i),
     $               snaccum,temp(i),melt(i),melp(i)
 11     format(4i2.2,5(1x,f10.3),1x,i2)

        meltsum=meltsum+melt(i)

       if(i.eq.n1)then
       write(60,*)'Snow Accumulation @ End of Melt Season=',snaccum
       endif

       else
       melt(i)=0.0
       melp(i)=0
       endif
 1     continue


c       print*,'snsum= in meltwater subroutine',snsum
c       print*,'meltsum=                      ',meltsum

       write(60,*)
       write(60,*)'MAXIMUM SNOW ACCUMULATION=',max

        return
        end


c ************************************************************
        subroutine ltbf(n1,fil,year,month,day,hour,bf,agwith,
     $              area,sumbf,flows,bfww,
     $              bfm,bfmax,bfmin,
     $              rm,rmax,rmin,rmea,flowq)

c This subroutine computes the long-term baseflow for a given
c Sub-basin
c ************************************************************

      integer fil,month(n1),day(n1),year(n1),hour(n1)
       integer i,tday,n1
       real agwith,area,t,p,agflow
```

```
      real early,late,te,tl,dint,dint2,sumbf,rec
      real flows(n1),flowq(n1),bf(n1),bfww(n1)

      real bfm(200),bfmax(200),bfmin(200)
      real rm(12),rmax(12),rmin(12),rmea(n1)

      sumbf=0
      do 1 i=1,n1

      tday=lday(year,month)
      t=month(i)+(real(day(i))/real(tday))



c      if(fil.eq.11)bf(i)=1.53

c     Interpolation of p
      if(((fil.eq.15).or.(fil.eq.13)).or.(fil.eq.12))then

         dint=(((real(tday)-15.)/2.)+15.)/real(tday)
         dint2=(7.)/real(tday)

         if(t.gt.12+dint)then
              if(rmea(i).ge.rm(12))then
               early=(((rmea(i)-rm(12))/(rmax(12)-rm(12)))*
     $              (bfmax(12+100)-bfm(12+100)))+bfm(12+100)
               late=(((rmea(i)-rm(12))/(rmax(12)-rm(12)))*
     $              (bfmax(1)-bfm(1)))+bfm(1)
             endif
              if(rmea(i).lt.rm(12))then
               early=(((rmea(i)-rm(12))/(rmin(12)-rm(12)))*
     $              (bfmin(12+100)-bfm(12+100)))+bfm(12+100)
               late=(((rmea(i)-rm(12))/(rmin(12)-rm(12)))*
     $              (bfmin(1)-bfm(1)))+bfm(1)
             endif
               te=12.+dint
               tl=13.+dint2
         endif

         if(t.le.1+dint2)then
              if(rmea(i).ge.rm(1))then
               early=(((rmea(i)-rm(1))/(rmax(1)-rm(1)))*
     $              (bfmax(12+100)-bfm(12+100)))+bfm(12+100)
               late=(((rmea(i)-rm(1))/(rmax(1)-rm(1)))*
     $              (bfmax(1)-bfm(1)))+bfm(1)
             endif
              if(rmea(i).lt.rm(1))then
               early=(((rmea(i)-rm(1))/(rmin(1)-rm(1)))*
     $              (bfmin(12+100)-bfm(12+100)))+bfm(12+100)
               late=(((rmea(i)-rm(1))/(rmin(1)-rm(1)))*
     $              (bfmin(1)-bfm(1)))+bfm(1)
             endif
               te=dint
               tl=1.+dint2
         endif

         if((t.le.12+dint).and.(t.gt.1+dint2))then

         if((t.gt.real(month(i))+dint2).and.
     $          (t.le.real(month(i))+dint))then

              if(rmea(i).ge.rm(month(i)))then
               early=(((rmea(i)-rm(month(i)))/
     $              (rmax(month(i))-rm(month(i))))*
     $              (bfmax(month(i))-bfm(month(i))))+bfm(month(i))
               late=(((rmea(i)-rm(month(i)))/
```

```
$                    (rmax(month(i))-rm(month(i))))*
$                    (bfmax(month(i)+100)-bfm(month(i)+100)))
$                    +bfm(month(i)+100)
          endif

           if(rmea(i).lt.rm(month(i)))then
            early=(((rmea(i)-rm(month(i)))/
$                    (rmin(month(i))-rm(month(i))))*
$                    (bfmin(month(i))-bfm(month(i))))+bfm(month(i))
            late=(((rmea(i)-rm(month(i)))/
$                    (rmin(month(i))-rm(month(i))))*
$                    (bfmin(month(i)+100)-bfm(month(i)+100)))
$                    +bfm(month(i)+100)

          endif

            te=real(month(i))+dint2
            tl=real(month(i))+dint
       endif

       if(t.gt.real(month(i))+dint)then

           if(rmea(i).ge.rm(month(i)))then
            early=(((rmea(i)-rm(month(i)))/
$                    (rmax(month(i))-rm(month(i))))*
$                    (bfmax(month(i)+100)-bfm(month(i)+100)))
$                    +bfm(month(i)+100)
            late=(((rmea(i)-rm(month(i)))/
$                    (rmax(month(i))-rm(month(i))))*
$                    (bfmax(month(i)+1)-bfm(month(i)+1)))
$                    +bfm(month(i)+1)
          endif

           if(rmea(i).lt.rm(month(i)))then
            early=(((rmea(i)-rm(month(i)))/
$                    (rmin(month(i))-rm(month(i))))*
$                    (bfmin(month(i)+100)-bfm(month(i)+100)))
$                    +bfm(month(i)+100)
            late=(((rmea(i)-rm(month(i)))/
$                    (rmin(month(i))-rm(month(i))))*
$                    (bfmin(month(i)+1)-bfm(month(i)+1)))
$                    +bfm(month(i)+1)

            endif
            te=real(month(i))+dint
            tl=real(month(i))+1+dint2
       endif

       if(t.le.real(month(i))+dint2)then

           if(rmea(i).ge.rm(month(i)))then
            early=(((rmea(i)-rm(month(i)))/
$                    (rmax(month(i))-rm(month(i))))*
$                    (bfmax(month(i)+100-1)-bfm(month(i)+100-1)))
$                    +bfm(month(i)+100-1)
            late=(((rmea(i)-rm(month(i)))/
$                    (rmax(month(i))-rm(month(i))))*
$                    (bfmax(month(i))-bfm(month(i))))
$                    +bfm(month(i))
          endif

           if(rmea(i).lt.rm(month(i)))then
            early=(((rmea(i)-rm(month(i)))/
$                    (rmin(month(i))-rm(month(i))))*
$                    (bfmin(month(i)+100-1)-bfm(month(i)+100-1)))
$                    +bfm(month(i)+100-1)
            late=(((rmea(i)-rm(month(i)))/
```

```
     $                  (rmin(month(i))-rm(month(i))))*
     $                  (bfmin(month(i))-bfm(month(i))))
     $                  +bfm(month(i))

                  endif
                  te=real(month(i))-1+dint
                  tl=real(month(i))+dint2
            endif
            endif

          if(te.eq.tl)p=late
          if(te.ne.tl)p=early-(((te-t)/(te-tl))*(early-late))
c           print*,'te=',te,'tl=',tl,'i=',i
c           print*,'p=',p
c           bf(i)=(p+agwith-bfww(i))*(area/(6.2+2.5+5.8))
            bf(i)=1.2*(p+agwith-1.53)*(area/(6.2+2.5+5.8))
           if(bf(i).lt.0)bf(i)=0.0
c            print*,'I am here'
            if(i.eq.1)goto 832

            if(flows(i).lt.0.05)then
             if(bf(i-1).gt.0.0)then
              rec=exp(alog(bf(i-1))-0.0023)
              if(rec.lt.0)rec=0.0
              if(bf(i).gt.rec)bf(i)=rec
             endif
            endif

c            if((flows(i).gt.0.05).or.(flowq(i).gt.0.05))then
               if(bf(i).gt.bf(i-1)+0.25)then
                  bf(i)=bf(i-1)+0.25
               endif
             endif

 832     sumbf=sumbf+bf(i)
1        continue

        sumbf=sumbf*(3600./1e6)
        print*,'Completed Baseflow Computation'

         close(fil)
         return
         end



c ***************************************************************
         subroutine flowui(n1,idr,uin,u,ieff,sumf,flow,
     $                     eff,flowr)
c This subroutine computes flow using the unit hydrograph method
c ***************************************************************
         integer i,j,k,idr(n1),uin,c,n1
         real sum,u(n1),ieff(n1),sumf,flow(n1)
         real eff(n1),flowr(n1)

         do 888 i=1,n1
           flow(i)=0.0
           eff(i)=0.0
 888     continue


         do 823 k=1,n1
            if(idr(k).eq.0)goto 823

            do 456 i=1,n1
               flowr(i)=0.0
 456        continue
```

```
            c=idr(k)+uin+k
            if(c.gt.n1)c=n1
             it1=k
             it2=k+idr(k)-1
             if(it2.gt.n1)it2=n1
             do 87 z=it1,it2
               eff(z)=ieff(z)
 87          continue
          do 5 i=k,c
          sum=0
           do 4 j=k,i
            if(j.gt.n1)goto 823
            sum=(eff(j)*u(i-j+1))+sum
 4        continue

          flowr(i)=sum

 5        continue


           do 834 x=1,n1
           flow(x)=flow(x)+flowr(x)
 834       continue


          k=k+idr(k)-1
          if(k.ge.n1-1)k=n1

 823      continue


         sumf=0.0

         do 2 k=1,n1
          sumf=sumf+flow(k)
 2       continue
         sumf=sumf*(3600./1e6)

         return
         end

c ****************************************************************
         subroutine meltflow(n1,uin,u,ieff,sumf,flow,idt,idr,
     $                       melte,flo,flowr,melp)
c This subroutine computes flow using the unit hydrograph method
c ****************************************************************
         integer i,j,k,uin,c,n1,idt(n1),count,idr(n1),x,z
         integer it1,it2,y,flag,w,netr,mx,count2,melp(n1)
         real sum,u(n1),ieff(n1),sumf,melte(n1),flow(n1)
         real flowr(n1),fl

         do 901 i=1,n1
           flow(i)=0.0
           melte(i)=0.0
 901     continue



         do 823 k=1,n1
            if(idr(k).eq.0)goto 823
            if(idt(k).eq.0)goto 823

            do 456 i=1,n1
               flowr(i)=0.0
 456        continue

            c=idt(k)+uin+k
```

```
            if(c.gt.n1)c=n1
             it1=k
             it2=k+idt(k)-1
             if(it2.gt.n1)it2=n1
             do 87 z=it1,it2
               melte(z)=ieff(z)
 87          continue
        do 5 i=k,c
        sum=0
         do 4 j=k,i
          if(j.gt.n1)goto 823
          sum=(melte(j)*u(i-j+1))+sum
 4      continue

        flowr(i)=sum

 5      continue


        do 834 x=1,n1
         flow(x)=flow(x)+flowr(x)
 834     continue


        k=k+idt(k)-1
        if(k.ge.n1-1)k=n1

 823    continue


       sumf=0.0

       do 2 k=1,n1
        sumf=sumf+flow(k)
 2     continue
       sumf=sumf*(3600./1e6)


       return
       end



c ***************************************************************
       subroutine stormid(n1,rai,idr,uin,F,IA,ieff,
     $          yea,mont,da,hou,sumi)

c This subroutine identifies individual storms and computes the
c effective rainfall.
c ***************************************************************
        integer i,j,k,idr(n1),tresp,uin,u,ir1,ir2
        integer yea(n1),mont(n1),da(n1),hou(n1),n1
        real rai(n1),F,IA,sumch,ieff(n1),sumieff,sumi


c Identify Individual Storms, idr=0:no storm, idr>0:storm
c       open(99,file='test.rain',status='unknown')
c       rewind 99
c        write(99,*)'uin=',uin

c       Initialize storm
        do 400 i=1,n1
            idr(i)=0
            ieff(i)=0.0
 400    continue

        tresp=uin
```

```
          sumi=0.0
          do 312 i=uin,n1
             if(rai(i).lt.0.005)goto 312
c            Beginning of Storm = ir1
             ir1=i
c            Find end of storm (time after which uin hours without rain)
             count=0
             do 36 j=ir1,n1
                sumch=0.0
                u=uin-1
                do 32 k=0,u
                sumch=rai(j-k)+sumch
 32             continue
                if(sumch.le.0.005)goto 87
                if(j.eq.n1)goto 87
                count=count+1
 36          continue

 87          ir2=ir1+count-uin
             sumrain=0.0
             sumieff=0.0
             do 354 j=ir1,ir2
                idr(j)=count-uin+1
                sumrain=sumrain+rai(j)
                if(sumrain.le.IA)ieff(j)=0.0
                if(sumrain.gt.IA)then
                       if(sumrain-IA.gt.rai(j))then
                         ieff(j)=rai(j)*F
                       else
                         ieff(j)=(sumrain-IA)*F
                       endif
                 sumieff=sumieff+ieff(j)
                 sumi=sumi+ieff(j)
                endif

 354         continue

             write(16,*)'Storm Date:',yea(ir1),mont(ir1),da(ir1),
     $                  hou(ir1)
             write(16,*)'Storm Rain=',sumrain,'in.',
     $                  '  Eff Rain=',sumieff,'in.'
             write(16,*)
c            reset storm search to uin hours after last storm (1 is added
to i
c            at the continue statement
             i=ir2+uin

 312     continue

c        do 777 i=1,n1
c         write(99,77)yea(i),mont(i),da(i),hou(i),rai(i),idr(i),ieff(i)
c 77      format(4i2.2,f7.2,2x,i4,2x,f10.4)
c 777     continue

c         print*,'Finished Storm Identification'

          return
          end


c  1*****************************************************************
          subroutine ss(db,rai,n1,flowq,flows,flowt,bf,accum,smbf,
     $                  smss,smqs,accumq,smch,sstot,smtot,area,
     $                  fils,cuma,frs,frq,
     $                  year,month,day,hour,id2)

c  This subroutine computes suspended sediment mass & concentration
```

```
c  ***************************************************************
        integer db,n1,i,count,fils,id2(n1)
        integer year(n1),month(n1),day(n1),hour(n1)
        real rai(n1),flowq(n1),flows(n1),bf(n1),accum(0:n1)
        real bfpot,maxf,maxlq,k,flowt(n1),flt,frs(0:n1),frq(0:n1)
        real ssbf,conv,smch(n1),ssss,eros,area,f
        real smbf(n1),smss(n1),accumq(0:n1),smqs(n1)
        real sstot(n1),smtot(n1),cuma,smbft,smsst,smbfi,smssi
        real smcht,smqst,depos,smqsi,sscap,fch
        real sum1,sum2,sum3,sum4,thres,thresq
        real erosr,Cs,Cq,Cr,thresr,accumr,smrs,frac
        real Cr2,Cr3,Cr5
        real Cswn,Cswc,Cswi,Csch1,Csch2,Csag
        real b,sbs,sbq,sbc

c        Read in SS Parameters
         rewind 2
         read(2,1093)f,bfpot,Cswn,Cswc,Cswi,Csch1,Csch2,Csag,
     $                thresq,maxlq,k,Cq,
     $                thresr,frac,Cr2,Cr3,Cr5
 1093    format(/f7.3/f7.3,6(/f9.7)//f7.3/f9.2/f7.3/f11.9//f7.3/
     $           f7.3/f9.7/f9.7/f9.7)
          if(fils.eq.22)then
               Cr=Cr2
               Cs=Cswn
          endif
          if(fils.eq.23)then
                Cr=Cr3
                Cs=Cswc
          endif
          if(fils.eq.25)then
                Cr=Cr5
                Cs=Cswi
          endif


c          print*,'f=',f,' bfpot=',bfpot,' Cs=',Cs
c         print*,'thresq=',thresq,' maxlq=',maxlq,' k=',k,' Cq=',Cq
c         print*,'thresr=',thresr,' frac=',frac,' Cr=',Cr
c          print*,'Cr2=',Cr2,'Cr3=',Cr3,'Cr5=',Cr5
c          print*,'Cswn=',Cswn,'Cswc=',Cswc,'Cswi=',Cswi
c          print*,'Csch1=',Csch1,'Csch2=',Csch2,'Csag=',Csag

        accum(0)=200000*area
        accumq(0)=(maxlq/k)*area
        frs(0)=f
        frq(0)=0.0

        conv=(0.3048**3)*3600.0
c       conv=101.9
        cuma=cuma+area
c        print*,'cuma=',cuma
c 200    print*,'area=',area

        maxf=((bfpot-0.286)/0.316)*(cuma/(6.2+2.5+5.8))

        smbft=0.0
        smsst=0.0
        smcht=0.0
        smqst=0.0
        smbfi=0.0
        smssi=0.0
        smqsi=0.0
        count=0

           rewind fils
c           write(fils,77)'    accum','      accumq',
```

```
c     $            '   smbf','   smss','  smqs','   smch',
c     $            '   smtot','  sstot'
 77         format(12x,a10,3x,a12,8x,a7,7x,a7,6x,a7,5x,a7,
     $             6x,a8,2x,a7)

        do 1 i=1,n1

c   Compute ss associated with baseflow & slow storm inputs
            smbfi=smbfi+(bfpot*bf(i)*conv)
            smssi=smssi+(bfpot*flows(i)*conv)


            if(flowt(i).lt.maxf)then

              ssbf=0.316*(flowt(i)*(6.2+2.5+5.8)/cuma)+0.286
              ssss=ssbf
              accum(i)=accum(i-1)+((bfpot-ssbf)*(bf(i)+flows(i))*conv)
c             print*,'I am in frs,frq if, i=',i,'  accum=',accum(i)
              frs(i)=((frs(i-1)*accum(i-1))
     $                 +(bfpot-ssbf)*flows(i)*conv)/accum(i)
              frq(i)=(frq(i-1)*accum(i-1))/accum(i)
            else

               ssbf=bfpot
               ssss=ssbf
               accum(i)=accum(i-1)
               frs(i)=frs(i-1)
               frq(i)=frq(i-1)
            endif


            smbf(i)=ssbf*bf(i)*conv
            smss(i)=ssss*flows(i)*conv
            smbft=smbft+smbf(i)
            smsst=smsst+smss(i)

c  Compute ss associated with quick storm response (from flowq&rain)
          depos=(maxlq*area)-(k*accumq(i-1))
          accumq(i)=accumq(i-1)+depos
          eros=Cq*(accumq(i))*(((flowq(i)-thresq)/area)**4)
          if(eros.lt.0.0)eros=0.0
          accumq(i)=accumq(i)-eros

             if(flowq(i).le.0)then
                smqs(i)=0.0
             else
c               smqs(i)=(1*flowq(i)*conv)+eros
                smqs(i)=eros
               if(accumq(i).lt.0)then
                       smqs(i)=smqs(i)+accumq(i)
                       accumq(i)=0
               endif
             endif

             if(rai(i).gt.0.001)then
                 accumr=accumq(i)*frac
                 accumq(i)=accumq(i)-accumr
                 erosr=Cr*accumr*((rai(i)-thresr)**4)
                 if(erosr.lt.0.0)erosr=0.0
                 accumr=accumr-eros
                 smrs=erosr
                 if(accumr.lt.0.0)then
                    smrs=smrs+accumr
                    accumr=0.0
                 endif
                 smqs(i)=smrs+smqs(i)
                 accumq(i)=accumq(i)+accumr
```

```
            endif

            smqst=smqst+smqs(i)
            smqsi=smqsi+depos

c   Compute ss from channel
            thres=maxf
            eros=Cs*(((flowt(i)-thres)/cuma)**4)*(accum(i))
            if(eros.lt.0)eros=0.0
            accum(i)=accum(i)-eros
            smch(i)=eros
                   if(accum(i).lt.0)then
                        smch(i)=smch(i)+accum(i)
                        accum(i)=0
                   endif
            smcht=smcht+smch(i)

c   Sum up all contributions to ss transport from the sub-basin
            smtot(i)=smbf(i)+smss(i)+smqs(i)+smch(i)
            flt=bf(i)+flowq(i)+flows(i)
            if(flt.gt.0)then
              sstot(i)=smtot(i)/(flt*conv)
            else
              sstot(i)=-1.0
            endif

c   Check SS Transport Capacity

c   Calculate SS Capacity  (id2(i)>4 rising)
c                          (id2(i)<4 falling)

          if(id2(i).ge.4)then
             fch=7.848*(cuma/(6.2+2.5+5.8))
             if(flowt(i).ge.fch)then

                sscap=(22.284*flowt(i)*14.5/cuma)-172.117
             endif
             if(flowt(i).lt.fch)then
                sscap=(0.316*flowt(i)*14.5/cuma)+0.286
             endif
          endif
          if(id2(i).lt.4)then
             sscap=(0.316*flowt(i)*14.5/cuma)+0.286
          endif
          smmax=flowt(i)*sscap*conv

          if(smtot(i).gt.smmax)then
             b=accum(i)
             accum(i)=accum(i)+smtot(i)-smmax
             sbs=smss(i)
             sbq=smqs(i)
             sbc=smch(i)
             smbf(i)=(smmax/smtot(i))*smbf(i)
             smss(i)=(smmax/smtot(i))*smss(i)
             smqs(i)=(smmax/smtot(i))*smqs(i)
             smch(i)=(smmax/smtot(i))*smch(i)
             smtot(i)=(smmax/smtot(i))*smtot(i)

c             print*,'accum(',i,')=',accum(i),'b=',b
c             print*,'smtot=',smtot(i),'smmax=',smmax

             frs(i)=((frs(i)*b)+(sbs-smss(i))+
     $                ((sbc-smch(i))*frs(i)))/accum(i)
             frq(i)=((frq(i)*b)+(sbq-smqs(i))+
     $                ((sbc-smch(i))*frq(i)))/accum(i)
```

```
          endif
        if(flt.gt.0)then
          sstot(i)=smtot(i)/(flt*conv)
        else
          sstot(i)=-1.0
        endif

          write(fils,89)year(i),month(i),day(i),hour(i),
     $          accum(i),accumq(i),
     $          smbf(i),smss(i),smqs(i),smch(i),
     $          smtot(i),sstot(i)
 89       format(4i2.2,1x,2f15.2,1x,5f13.2,3x,f7.2)

 1        continue

          sum1=accum(0)+smssi+smbfi
          sum2=accum(n1)+smsst+smbft+smcht
          sum3=accumq(0)+smqsi
          sum4=accumq(n1)+smqst

          write(60,*)
          write(60,*)'SUB-BASIN SEDIMENT BALANCE, grams'
          write(60,*)'Channel Storage,Time Zero =',accum(0),'grams'
          write(60,*)'Total Slow Sediment Input =',smssi,'grams'
          write(60,*)'Total Baseflow Sed  Input =',smbfi,'grams'
          write(60,*)'Total Mass Input +Storage(0) =',sum1
          write(60,*)
          write(60,*)'Total Slow Transported    =',smsst
          write(60,*)'Total BF   Transported    =',smbft
          write(60,*)'Transported From Channel  =',smcht
          write(60,*)'Amount Remaining in Channel Storage=',accum(n1)
          write(60,*)'Total Mass Transport+Storage(n) =',sum2
          write(60,*)
          write(60,*)'Quick Area Storage,Time Zero =',accumq(0),'grams'
          write(60,*)'Total Quick Sediment Input=',smqsi,'grams'
          write(60,*)'Total Mass Input +Storage(0) =',sum3
          write(60,*)
          write(60,*)'Amount Remaining in Quick Storage  =',accumq(n1)
          write(60,*)'Total Quick Transported   =',smqst
          write(60,*)'Total Mass Transport+Storage(n) =',sum4
          write(60,*)
          print*,'Finished ss subroutine'

          return
          end

c  1*************************************************************
          subroutine ssag(cuma,agwith,n1,flowt,smto3c,smto3a,fils,
     $               smag3,accumg,smchg,
     $               Fmtp3c,Fmtd3c,Amtp3c,Amtd3c,
     $               Rmtp3c,Rmtd3c,Umtp3c,Umtd3c,
     $               Fmtp3a,Fmtd3a,Amtp3a,Amtd3a,
     $               Rmtp3a,Rmtd3a,Umtp3a,Umtd3a,
     $               accumF,accumA,accumR,accumU,
     $               smchgF,smchgA,smchgR,smchgU,
     $               filFep,filAsp,filCrp,filCup,
     $               filFed,filAsd,filCrd,filCud,
     $               film,id2)

c    This subroutine adjusts the sediment flux through gage 3 due
c    to the well pumping at atlantic gelatin
c  *************************************************************
          integer fils,n1,i,film,id2(n1)
          integer filFep,filAsp,filCrp,filCup
          integer filFed,filAsd,filCrd,filCud
          real agwith,cuma,flowt(n1),smto3c(n1),smto3a(n1),smchg(n1)
          real smmax,ssbf,smag3(n1),maxf,bfpot,accumg(0:n1)
```

```
      real conv,flmag,depos,depos2,sumi,sumt,sum1,sum2,sumn
      real sums,conv1,eros,Cs,f
      real sstot,Fpc,Apc,Rpc,Upc,Fdc,Adc,Rdc,Udc
      real Fpcc,Apcc,Rpcc,Upcc
      real deposF,deposA,deposR,deposU
      real depos2F,depos2A,depos2R,depos2U
      real erosF,erosA,erosR,erosU
      real Fmtd3c(n1),Amtd3c(n1),Rmtd3c(n1),Umtd3c(n1)
      real Fmtp3c(n1),Amtp3c(n1),Rmtp3c(n1),Umtp3c(n1)
      real Fmtp3a(n1),Fmtd3a(n1),Amtp3a(n1),Amtd3a(n1)
      real Rmtp3a(n1),Rmtd3a(n1),Umtp3a(n1),Umtd3a(n1)
      real thres,fch,sscap
      real accumF(0:n1),accumA(0:n1),accumR(0:n1),accumU(0:n1)
      real smchgF(n1),smchgA(n1),smchgR(n1),smchgU(n1)
      real sumiFd,sumiFp,sumtFp,sum1Fp
      real sum2Fp,sumnFd,sumnFp,sumsFp
      real sumiAd,sumiAp,sumtAp,sum1Ap
      real sum2Ap,sumnAd,sumnAp,sumsAp
      real sumiRd,sumiRp,sumtRp,sum1Rp
      real sum2Rp,sumnRd,sumnRp,sumsRp
      real sumiUd,sumiUp,sumtUp,sum1Up
      real sum2Up,sumnUd,sumnUp,sumsUp
      real Fedq,Feds,Fedb,Fepq,Feps,Fepb
      real Asdq,Asds,Asdb,Aspq,Asps,Aspb
      real Crdq,Crds,Crdb,Crpq,Crps,Crpb
      real Cudq,Cuds,Cudb,Cupq,Cups,Cupb


c     Read in SS Parameters
      rewind 2
      read(2,1093)f,bfpot,Cswn,Cswc,Cswi,Csch1,Csch2,Csag
 1093 format(/f7.3/f7.3,6(/f9.7))

      Cs=Csag

c       print*,'f=',f,' bfpot=',bfpot,' Cs=',Cs
c       print*,'Cswn=',Cswn,'Cswc=',Cswc,'Cswi=',Cswi
c       print*,'Csch1=',Csch1,'Csch2=',Csch2,'Csag=',Csag

      rewind film
      read(film,1094)Fedq,Feds,Fedb,Fepq,Feps,Fepb,
     $               Asdq,Asds,Asdb,Aspq,Asps,Aspb,
     $               Crdq,Crds,Crdb,Crpq,Crps,Crpb,
     $               Cudq,Cuds,Cudb,Cupq,Cups,Cupb
 1094 format(4(//3(f7.2/)/3(f7.2/)))

c     print*,'Fe'
c     print*,'Quick Dissolved=',Fedq
c     print*,'Slow Dissolved =',Feds
c     print*,'LTBF Dissolved =',Fedb
c     print*,'Quick Particulate =',Fepq
c     print*,'Slow Particulate  =',Feps
c     print*,'LTBF Particulate  =',Fepb
c     print*,'As'
c     print*,'Quick Dissolved=',Asdq
c     print*,'Slow Dissolved =',Asds
c     print*,'LTBF Dissolved =',Asdb
c     print*,'Quick Particulate =',Aspq
c     print*,'Slow Particulate  =',Asps
c     print*,'LTBF Particulate  =',Aspb
c     print*,'Cr'
c     print*,'Quick Dissolved=',Crdq
c     print*,'Slow Dissolved =',Crds
c     print*,'LTBF Dissolved =',Crdb
c     print*,'Quick Particulate =',Crpq
c     print*,'Slow Particulate  =',Crps
c     print*,'LTBF Particulate  =',Crpb
```

```
c         print*,'Cu'
c         print*,'Quick Dissolved=',Cudq
c         print*,'Slow Dissolved =',Cuds
c         print*,'LTBF Dissolved =',Cudb
c         print*,'Quick Particulate =',Cupq
c         print*,'Slow Particulate  =',Cups
c         print*,'LTBF Particulate  =',Cupb

          accumg(0)=200000*cuma
          accumF(0)=(((f*Feps+((1-f)*Fepb)))/100.)*accumg(0)
          accumA(0)=(((f*Asps+((1-f)*Aspb)))/1e6)*accumg(0)
          accumR(0)=(((f*Crps+((1-f)*Crpb)))/1e6)*accumg(0)
          accumU(0)=(((f*Cups+((1-f)*Cupb)))/1e6)*accumg(0)

c         Conversion factor to mg/l,=101.94
          conv=(0.3048**3)*3600.
c         Conversion factor to ug/l
          conv1=conv/1000.

          maxf=((bfpot-0.286)/0.316)*(cuma/(2.5+6.2+5.8))

          sumi=0.0
          sumt=0.0
          sums=0.0
          sumn=0.0
          sumiFd=0.0
          sumnFd=0.0
          sumiFp=0.0
          sumtFp=0.0
          sumsFp=0.0
          sumnFp=0.0
          sumiAd=0.0
          sumnAd=0.0
          sumiAp=0.0
          sumtAp=0.0
          sumsAp=0.0
          sumnAp=0.0
          sumiRd=0.0
          sumnRd=0.0
          sumiRp=0.0
          sumtRp=0.0
          sumsRp=0.0
          sumnRp=0.0
          sumiUd=0.0
          sumnUd=0.0
          sumiUp=0.0
          sumtUp=0.0
          sumsUp=0.0
          sumnUp=0.0

          open(fils,file='ssa.ag',status='unknown')
          rewind fils
          open(filFep,file='Fepa.ag',status='unknown')
          rewind filFep
          open(filAsp,file='Aspa.ag',status='unknown')
          rewind filAsp
          open(filCrp,file='Crpa.ag',status='unknown')
          rewind filCrp
          open(filCup,file='Cupa.ag',status='unknown')
          rewind filCup
          open(filFed,file='Feda.ag',status='unknown')
          rewind filFed
          open(filAsd,file='Asda.ag',status='unknown')
          rewind(filAsd)
          open(filCrd,file='Crda.ag',status='unknown')
          rewind filCrd
          open(filCud,file='Cuda.ag',status='unknown')
```

```
      rewind filCud

c           write(fils,*)'   smto3a',
c     $      '     accumg','        smchg','  depos1+2','    sstot'

c           write(filFep,637)'    Fmtp3a','  Fpcc','   Fpc',
c     $                    ' accumF ',' smchgF','depF1+2'
c           write(filFed,638)'   Fmtd3a','  Fdc'
c           write(filFep,637)'       g  ','    % ','  mg/L',
c     $                    '   g    ','   g   ','   g   '
c           write(filFed,638)'    g   ','  mg/L'


c           write(filAsp,637)'    Amtp3a','  Apcc','   Apc',
c     $                    ' accumA ',' smchgA','depA1+2'
c           write(filAsd,638)'  Amtd3a','   Adc'

c           write(filCrp,637)'    Rmtp3a','  Rpcc','   Rpc',
c     $                    ' accumR ','  smchgR','depR1+2'
c           write(filCrd,638)'  Rmtd3a','   Rdc'

c           write(filCup,637)'    Umtp3a','  Upcc','   Upc',
c     $                    ' accumU ',' smchgU','depU1+2'
c           write(filCud,638)'  Umtd3a','    Udc'


c           write(filAsp,637)'       g  ',' mg/kg','  ug/L',
c     $                    '   g    ','   g   ','   g   '
c           write(filAsd,638)'    g   ','  ug/L'

c           write(filCrp,637)'       g  ',' mg/kg','  ug/L',
c     $                    '   g    ','   g   ','   g   '
c           write(filCrd,638)'    g   ','  ug/L'

c           write(filCup,637)'       g  ',' mg/kg','  ug/L',
c     $                    '   g    ','   g   ','   g   '
c           write(filCud,638)'    g   ','  ug/L'

 637       format(3x,a10,2x,a6,2x,a6,1x,a8,4x,a7,3x,a7)
 638       format(3x,a9,2x,a6)

c           print*,'cuma=',cuma

      do 1 i=1,n1
         eros=0.0
         depos2=0.0
         depos=0.0
         depos2F=0.0
         deposF=0.0
         depos2A=0.0
         deposA=0.0
         depos2R=0.0
         deposR=0.0
         depos2U=0.0
         deposU=0.0
         smchg(i)=0.0
         smchgF(i)=0.0
         smchgA(i)=0.0
         smchgR(i)=0.0
         smchgU(i)=0.0

         sumi=sumi+smto3c(i)
         sumiFp=Fmtp3c(i)+sumiFp
         sumiAp=Amtp3c(i)+sumiAp
         sumiRp=Rmtp3c(i)+sumiRp
         sumiUp=Umtp3c(i)+sumiUp
```

```
            sumiFd=Fmtd3c(i)+sumiFd
            sumiAd=Amtd3c(i)+sumiAd
            sumiRd=Rmtd3c(i)+sumiRd
            sumiUd=Umtd3c(i)+sumiUd

            smto3a(i)=smto3c(i)
            Fmtp3a(i)=Fmtp3c(i)
            Fmtd3a(i)=Fmtd3c(i)
            Amtp3a(i)=Amtp3c(i)
            Amtd3a(i)=Amtd3c(i)
            Rmtp3a(i)=Rmtp3c(i)
            Rmtd3a(i)=Rmtd3c(i)
            Umtp3a(i)=Umtp3c(i)
            Umtd3a(i)=Umtd3c(i)

c   Removal of Water,Sediment & Part/Diss Metals Assoc.
c   with Water Pumped-Out
            flmag=flowt(i)-agwith
            if(flmag.gt.0.0)then

            Fmtd3a(i)=Fmtd3a(i)*(flowt(i)-agwith)/flowt(i)
            Amtd3a(i)=Amtd3a(i)*(flowt(i)-agwith)/flowt(i)
            Rmtd3a(i)=Rmtd3a(i)*(flowt(i)-agwith)/flowt(i)
            Umtd3a(i)=Umtd3a(i)*(flowt(i)-agwith)/flowt(i)
               depos=(agwith/flowt(i))*smto3a(i)
               deposF=(agwith/flowt(i))*Fmtp3a(i)
               deposA=(agwith/flowt(i))*Amtp3a(i)
               deposR=(agwith/flowt(i))*Rmtp3a(i)
               deposU=(agwith/flowt(i))*Umtp3a(i)
            else
               flmag=0.0
               Fmtd3a(i)=0.0
               Amtd3a(i)=0.0
               Rmtd3a(i)=0.0
               Umtd3a(i)=0.0
               depos=smto3a(i)
               deposF=Fmtp3a(i)
               deposA=Amtp3a(i)
               deposR=Rmtp3a(i)
               deposU=Umtp3a(i)
            endif

            smto3a(i)=smto3a(i)-depos
            Fmtp3a(i)=Fmtp3a(i)-deposF
            Amtp3a(i)=Amtp3a(i)-deposA
            Rmtp3a(i)=Rmtp3a(i)-deposR
            Umtp3a(i)=Umtp3a(i)-deposU

            accumg(i)=accumg(i-1)+depos
            accumF(i)=accumF(i-1)+deposF
            accumA(i)=accumA(i-1)+deposA
            accumR(i)=accumR(i-1)+deposR
            accumU(i)=accumU(i-1)+deposU


c Compute the Erodible Sediment

             if(accumg(i).le.0)then
               smchg(i)=0.0
               smchgF(i)=0.0
               smchgA(I)=0.0
               smchgR(i)=0.0
               smchgU(i)=0.0

               accumg(i)=0.0
               accumF(i)=0.0
               accumA(i)=0.0
```

```
                accumR(i)=0.0
                accumU(i)=0.0

              endif

              if(accumg(i).gt.0)then
                thres=maxf
                eros=Cs*(((flmag-thres)/cuma)**4)*(accumg(i))
                if(eros.lt.0.0)eros=0.0
                erosF=eros*(accumF(i)/accumg(i))
                erosA=eros*(accumA(i)/accumg(i))
                erosR=eros*(accumR(i)/accumg(i))
                erosU=eros*(accumU(i)/accumg(i))

                accumg(i)=accumg(i)-eros
                accumF(i)=accumF(i)-erosF
                accumA(i)=accumA(i)-erosA
                accumR(i)=accumR(i)-erosR
                accumU(i)=accumU(i)-erosU

                smchg(i)=eros
                smchgF(i)=erosF
                smchgA(i)=erosA
                smchgR(i)=erosR
                smchgU(i)=erosU

                   if(accumg(i).lt.0)then
                      smchg(i)=smchg(i)+accumg(i)
                      smchgF(i)=smchgF(i)+accumF(i)
                      smchgA(i)=smchgA(i)+accumA(i)
                      smchgR(i)=smchgR(i)+accumR(i)
                      smchgU(i)=smchgU(i)+accumU(i)

                      accumg(i)=0.0
                      accumF(i)=0.0
                      accumA(i)=0.0
                      accumR(i)=0.0
                      accumU(i)=0.0
                   endif
                endif

c  Check for Deposition of Sediment & Particulate Metals
c  Calculate SS Capacity

c  Rising limb of hydrograph
            if(id2(i).ge.4)then
               fch=7.848*(cuma/(6.2+2.5+5.8))
               if(flowt(i).ge.fch)then
                  sscap=(22.284*flowt(i)*14.5/cuma)-172.117
               endif
               if(flowt(i).lt.fch)then
                  sscap=(0.316*flowt(i)*14.5/cuma)+0.286
               endif
            endif

c  Falling limb of hydrograph
            if(id2(i).lt.4)then
               sscap=(0.316*flowt(i)*14.5/cuma)+0.286
            endif
            smmax=flowt(i)*sscap*conv

                if(smto3a(i).gt.smmax)then

                   depos2=smto3a(i)-smmax
                   depos2F=Fmtp3a(i)*(depos2/smto3a(i))
                   depos2A=Amtp3a(i)*(depos2/smto3a(i))
                   depos2R=Rmtp3a(i)*(depos2/smto3a(i))
```

```
        depos2U=Umtp3a(i)*(depos2/smto3a(i))

        accumg(i)=accumg(i)+depos2
        accumF(i)=accumF(i)+depos2F
        accumA(i)=accumA(i)+depos2A
        accumR(i)=accumR(i)+depos2R
        accumU(i)=accumU(i)+depos2U

        smto3a(i)=smto3a(i)-depos2
        Fmtp3a(i)=Fmtp3a(i)-depos2F
        Amtp3a(i)=Amtp3a(i)-depos2A
        Rmtp3a(i)=Rmtp3a(i)-depos2R
        Umtp3a(i)=Umtp3a(i)-depos2U

      endif

      smto3a(i)=smto3a(i)+smchg(i)
      Fmtp3a(i)=Fmtp3a(i)+smchgF(i)
      Amtp3a(i)=Amtp3a(i)+smchgA(i)
      Rmtp3a(i)=Rmtp3a(i)+smchgR(i)
      Umtp3a(i)=Umtp3a(i)+smchgU(i)

      sumt=sumt+smchg(i)
      sumtFp=sumtFp+smchgF(i)
      sumtAp=sumtAp+smchgA(i)
      sumtRp=sumtRp+smchgR(i)
      sumtUp=sumtUp+smchgU(i)

      sums=sums+depos+depos2
      sumsFp=sumsFp+deposF+depos2F
      sumsAp=sumsAp+deposA+depos2A
      sumsRp=sumsRp+deposR+depos2R
      sumsUp=sumsUp+deposU+depos2U

      sumn=sumn+smto3a(i)-smchg(i)
      sumnFp=sumnFp+Fmtp3a(i)-smchgF(i)
      sumnAp=sumnAp+Amtp3a(i)-smchgA(i)
      sumnRp=sumnRp+Rmtp3a(i)-smchgR(i)
      sumnUp=sumnUp+Umtp3a(i)-smchgU(i)

      sumnFd=sumnFd+Fmtd3a(i)
      sumnAd=sumnAd+Amtd3a(i)
      sumnRd=sumnRd+Rmtd3a(i)
      sumnUd=sumnUd+Umtd3a(i)

    if(smto3a(i).gt.0.0)then
        Fpcc=Fmtp3a(i)*100./(smto3a(i))
        Apcc=Amtp3a(i)*(1e6)/(smto3a(i))
        Rpcc=Rmtp3a(i)*(1e6)/(smto3a(i))
        Upcc=Umtp3a(i)*(1e6)/(smto3a(i))
    else
        Fpcc=-1.0
        Apcc=-1.0
        Rpcc=-1.0
        Upcc=-1.0
    endif

    if(flmag.gt.0)then
        sstot=smto3a(i)/(flmag*conv)
        Fpc=Fmtp3a(i)/(flmag*conv)
        Apc=Amtp3a(i)/(flmag*conv1)
        Rpc=Rmtp3a(i)/(flmag*conv1)
        Upc=Umtp3a(i)/(flmag*conv1)

        Fdc=Fmtd3a(i)/(flmag*conv)
        Adc=Amtd3a(i)/(flmag*conv1)
        Rdc=Rmtd3a(i)/(flmag*conv1)
```

```
            Udc=Umtd3a(i)/(flmag*conv1)

          else
              sstot=-1.0
              Fpc=-1.0
              Apc=-1.0
              Rpc=-1.0
              Upc=-1.0
              Fdc=-1.0
              Adc=-1.0
              Rdc=-1.0
              Udc=-1.0
          endif

          write(fils,12)smto3a(i),accumg(i),
     $                smchg(i),depos,depos2,sstot
12        format(f10.2,2(1x,f14.1),2(1x,f10.2),1x,f8.2)

          write(filFep,63)Fmtp3a(i),Fpcc,Fpc,
     $          accumF(i),smchgF(i),deposF+depos2F
          write(filFed,66)Fmtd3a(i),Fdc

          write(filAsp,63)Amtp3a(i),Apcc,Apc,
     $          accumA(i),smchgA(i),deposA+depos2A
          write(filAsd,66)Amtd3a(i),Adc

          write(filCrp,63)Rmtp3a(i),Rpcc,Rpc,
     $          accumR(i),smchgR(i),deposR+depos2R
          write(filCrd,66)Rmtd3a(i),Rdc

          write(filCup,63)Umtp3a(i),Upcc,Upc,
     $          accumU(i),smchgU(i),deposU+depos2U
          write(filCud,66)Umtd3a(i),Udc

63        format(3x,f10.2,2f8.2,1x,f8.2,3f10.2)
66        format(1x,f10.2,1x,f8.2)

1         continue

          sum1=sumi+accumg(0)
          sum2=sumt+sumn+accumg(n1)
          sum1Fp=sumiFp+accumF(0)
          sum1Ap=sumiAp+accumA(0)
          sum1Rp=sumiRp+accumR(0)
          sum1Up=sumiUp+accumU(0)
          sum2Fp=sumtFp+sumnFp+accumF(n1)
          sum2Ap=sumtAp+sumnAp+accumA(n1)
          sum2Rp=sumtRp+sumnRp+accumR(n1)
          sum2Up=sumtUp+sumnUp+accumU(n1)

          write(60,*)
          write(60,*)
          write(60,*)'SEDIMENT BALANCE FOR ATL GELATIN AREA'
          write(60,*)'Atl Gel Storage, Time Zero=',accumg(0)
          write(60,*)'Total Mass Input          =',sumi
          write(60,*)'Total Mass Input+Storage(0)',sum1
          write(60,*)
          write(60,*)'Atl Gel Storage, Time(n)    =',accumg(n1)
          write(60,*)'Total Transport of Deposited=',sumt
          write(60,*)'Total Transport Not-Deposited',sumn
          write(60,*)'Total Transport+Storage(n)  =',sum2
          write(60,*)
          write(60,*)'Total amount deposited      =',sums
          write(60,*)
          write(60,*)
          write(60,*)'METAL BALANCE FOR ATL GELATIN AREA'
          write(60,*)'Particulates'
```

```
            write(60,*)'                                        ',
     $           'Fe          As          Cr          Cu'
            write(60,*)'Storage at time zero  =',
     $           accumF(0),accumA(0),accumR(0),accumU(0)
            write(60,*)'Total Mass Input      =',
     $           sumiFp,sumiAp,sumiRp,sumiUp
            write(60,*)'Tot Mass In+Storage(0)=',
     $           sum1Fp,sum1Ap,sum1Rp,sum1Up
            write(60,*)
            write(60,*)'AtlGel Storage,Time(n) =',
     $           accumF(n1),accumA(n1),accumR(n1),accumU(n1)
            write(60,*)'Tot Transp of Deposited=',
     $           sumtFp,sumtAp,sumtRp,sumtUp
            write(60,*)'Tot Transport Not-Deposited',
     $           sumnFp,sumnAp,sumnRp,sumnUp
            write(60,*)'Tot Transp+Storage(n) =',
     $           sum2Fp,sum2Ap,sum2Rp,sum2Up
            write(60,*)
            write(60,*)'Total amount deposited=',
     $           sumsFp,sumsAp,sumsRp,sumsUp
            write(60,*)
            write(60,*)'Dissolved'
            write(60,*)'Fe Input=',sumiFd,'Fe Output=',sumnFd,
     $           'Net Input=',sumiFd-sumnFd
            write(60,*)'As Input=',sumiAd,'As Output=',sumnAd,
     $           'Net Input=',sumiAd-sumnAd
            write(60,*)'Cr Input=',sumiRd,'Cr Output=',sumnRd,
     $           'Net Input=',sumiRd-sumnRd
            write(60,*)'Cu Input=',sumiUd,'Cu Output=',sumnUd,
     $           'Net Input=',sumiUd-sumnUd
            write(60,*)
            write(60,*)

            print*,'Finished adjusting sediment & metal flux'
            print*

            close(fils)
            close(filFep)
            close(filAsp)
            close(filCrp)
            close(filCup)
            close(filFed)
            close(filAsd)
            close(filCrd)
            close(filCud)
            return
            end

c  1*************************************************************
        subroutine fndata(db,n1,flog,mea)
c  This subroutine reads the measured flow data corresponding to
c  each gaging station.
c  *************************************************************
        integer j,k,n1
        integer check,db,mea
        real flog(n1)

        rewind mea
c        print*,'mea=',mea,'db=',db,'n1=',n1

c Find the Measured Flow
      do 111 k=1,99999
        read(mea,191)check
 191    format(i8)
c        print*,'check=',check
        if(check.ne.db)then
            goto 111
```

```
        else
            backspace mea
            do 113 j=1,n1
                      read(mea,*,end=112)check,flog(j)
c                     print*,'flog(',j,')=',flog(j)
 113         continue
             goto 112
           endif
 111   continue
 112      if(mea.eq.32)print*,'Completed reading Gage#2 data'
          if(mea.eq.33)print*,'Completed reading Gage#3 data'
          if(mea.eq.31)print*,'Completed reading Gage#1 data'
          if(mea.eq.35)print*,'Completed reading Gage#5 data'

         close(mea)
         return
         end

c 1*************************************************************
         subroutine rt1(n1,flowt,out,inflow,N,KR,X)

c  This subroutine routes streamflow, sediment, and metal
c  fluxes using the Muskingham Routing Method
c ************************************************************
         integer n1,N,i,j,z,u
         real flowt(n1),X,C1,C2,C3,out(0:n1),KR,inflow(0:n1)
         real sumi,sumo

         C1 = (1-(2*KR*X))/((2*KR*(1-X))+1)
         C2 = (1+(2*KR*X))/((2*KR*(1-X))+1)
         C3 = (2*KR*(1-X)-1)/((2*KR*(1-X))+1)

c         print*,'C1=',C1
c         print*,'C2=',C2
c         print*,'C3=',C3

c Compute Outflow
         sumi=0.0
         do 3 i=1,n1
              inflow(i)=flowt(i)
              sumi=sumi+inflow(i)
c             print*,'inflow(',i,')=',inflow(i)
 3       continue

c         out(0)=inflow(1)
c         inflow(0)=inflow(1)
          out(0)=0
          inflow(0)=0

         u=n1-1
         sumo=0.0
         do 2 j=1,N
         do 1 i=0,u
              out(i+1)=(C1*inflow(i+1))+(C2*inflow(i))+(C3*out(i))
 1       continue
              do 4 z=1,n1
                   inflow(z)=out(z)
              if(j.eq.N)then
                   sumo=sumo+out(z)
              endif
 4            continue
 2       continue

c         do 8 i=1,90
c              print*,'out(',i,')=',out(i)
c 8       continue
```

```
      write(60,*)'Total Input to Channel   ',sumi
      write(60,*)'Total Output From Channel',sumo

      return
      end


c *******************************************************
      integer function lday(yr,mo)
c This function computes the last day of the month given
c the month and year.
c *******************************************************
      integer yr,mo
      if(mo.eq.1)lday=31
      if((mo.eq.2).and.
     $  (real(nint(yr/4.0)).eq.real(yr/4.0)))then
         lday=29
      endif
      if((mo.eq.2).and.
     $  (real(nint(yr/4.0)).ne.real(yr/4.0)))then
         lday=28
      endif
      if(mo.eq.3)lday=31
      if(mo.eq.4)lday=30
      if(mo.eq.5)lday=31
      if(mo.eq.6)lday=30
      if(mo.eq.7)lday=31
      if(mo.eq.8)lday=31
      if(mo.eq.9)lday=30
      if(mo.eq.10)lday=31
      if(mo.eq.11)lday=30
      if(mo.eq.12)lday=31
      return
      end
```

SELECTED INPUT FILES: PRINT-OUT

Woburn-North Sub-basin
Area, (miles^2)
6.2

Initial Abstraction (inches)
IAQ, for Quick Response IAS, For Slow Response IAM, For Meltwater
00.06 IAQ
00.30 IAS
00.20 IAM

Fraction of total rain that is considered effective rainfall
KQ, For Quick Response KS, For Slow Response KM, For Meltwater
00.03 KQ
00.10 KS
00.75 KM

Time Constant for Separation of Individual Events
TQ, For Quick Response TS, For Slow Response TM, For Meltwater
8 TQ
24 TS
24 TM

Snowmelt Coefficient (inches per Fahrenheit-day)
0.000380

Number of Ordinates in Unit Hydrograph, Quick Response
8

Unit Hydrograph Ordinates, Quick Response
0.0 1
400.0 2
800.0 3
1200.0 4
2400.0 5
1200.0 6
800.0 7
400.0 8

Number of Ordinates in Unit Hydrograph, Slow Response
73

Unit Hydrograph Ordinates, Slow Response
100.0 1
140.0 2
160.0 3
180.0 4
187.0 5
194.0 6
201.0 7
206.0 8
211.0 9
216.0 10
220.0 11
224.0 12
225.0 13
225.0 14
220.0 15
215.0 16
210.0 17
205.0 18
200.0 19
195.0 20
185.0 21

File: ui.wn

```
 170.0        22
 160.0        23
 150.0        24
 140.0        25
 130.0        26
 120.0        27
 110.0        28
 100.0        29
  95.0        30
  90.0        31
  85.0        32
  80.0        33
  75.0        34
  70.0        35
  65.0        36
  60.0        37
  55.0        38
  50.0        39
  48.0        40
  46.0        41
  44.0        42
  42.0        43
  40.0        44
  38.0        45
  36.0        46
  34.0        47
  32.0        48
  30.0        49
  28.0        50
  26.0        51
  24.0        52
  22.0        53
  20.0        54
  19.0        55
  18.0        56
  17.0        57
  16.0        58
  15.0        59
  14.0        60
  13.0        61
  12.0        62
  11.0        63
  10.0        64
   9.0        65
   8.0        66
   7.0        67
   6.0        68
   5.0        69
   4.0        70
   3.0        71
   2.0        72
   1.0        73

Number of Ordinates in Unit Hydrograph, Meltwater Response
244

Unit Hydrograph Ordinates, Meltwater Response
 660.0         1
 640.0         2
 620.0         3
 600.0         4
 580.0         5
 560.0         6
 540.0         7
 520.0         8
```

File: ui.wn (con'd)

500.0	9
480.0	10
460.0	11
440.0	12
420.0	13
400.0	14
380.0	15
360.0	16
340.0	17
320.0	18
300.0	19
280.0	20
250.0	21
245.0	22
240.0	23
235.0	24
230.0	25
225.0	26
220.0	27
215.0	28
210.0	29
205.0	30
200.0	31
195.0	32
190.0	33
185.0	34
180.0	35
175.0	36
170.0	37
165.0	38
160.0	39
155.0	40
150.0	41
145.0	42
140.0	43
135.0	44
130.0	45
125.0	46
120.0	47
115.0	48
110.0	49
105.0	50
100.0	51
98.0	52
96.0	53
94.0	54
92.0	55
90.0	56
88.0	57
86.0	58
84.0	59
82.0	60
80.0	61
78.0	62
76.0	63
74.0	64
72.0	65
70.0	66
68.0	67
66.0	68
64.0	69
62.0	70
60.0	71
58.0	72
56.0	73
54.0	74

File: ui.wn (con'd)

52.0	75
50.0	76
49.0	77
48.0	78
47.0	79
46.0	80
45.0	81
44.0	82
43.0	83
42.0	84
41.0	85
40.0	86
39.0	87
38.0	88
37.0	89
36.0	90
35.0	91
34.0	92
33.0	93
32.0	94
31.0	95
30.0	96
29.0	97
28.0	98
27.0	99
26.0	100
25.0	101
25.0	102
24.0	103
23.0	104
22.0	105
21.0	106
20.0	107
19.5	108
19.0	109
18.5	110
18.0	111
17.5	112
17.0	113
16.5	114
16.0	115
15.5	116
15.0	117
14.8	118
14.6	119
14.4	120
14.2	121
14.0	122
13.8	123
13.6	124
13.4	125
13.2	126
13.0	127
12.8	128
12.6	129
12.4	130
12.2	131
12.0	132
11.8	133
11.6	134
11.4	135
11.2	136
11.0	137
10.8	138
10.6	139
10.4	140

File: ui.wn (con'd)

```
10.2        141
10.0        142
 9.9        143
 9.8        144
 9.7        145
 9.6        146
 9.5        147
 9.4        148
 9.3        149
 9.2        150
 9.1        151
 9.0        152
 8.9        153
 8.8        154
 8.7        155
 8.6        156
 8.5        157
 8.4        158
 8.3        159
 8.2        160
 8.1        161
 8.0        162
 7.9        163
 7.8        164
 7.7        165
 7.6        166
 7.5        167
 7.4        168
 7.3        169
 7.2        170
 7.1        171
 7.0        172
 6.9        173
 6.8        174
 6.7        175
 6.6        176
 6.5        177
 6.4        178
 6.3        179
 6.2        180
 6.1        181
 6.0        182
 5.9        183
 5.8        184
 5.7        185
 5.6        186
 5.5        187
 5.4        188
 5.3        189
 5.2        190
 5.1        191
 5.0        192
 4.9        193
 4.8        194
 4.7        195
 4.6        196
 4.5        197
 4.4        198
 4.3        199
 4.2        200
 4.1        201
 4.0        202
 3.9        203
 3.8        204
 3.7        205
 3.6        206
```

File: ui.wn (con'd)

```
3.5         207
3.4         208
3.3         209
3.2         210
3.1         211
3.0         212
2.9         213
2.8         214
2.7         215
2.6         216
2.5         217
2.4         218
2.3         219
2.2         220
2.1         221
2.0         222
1.9         223
1.8         224
1.7         225
1.6         226
1.5         227
1.4         228
1.3         229
1.2         230
1.1         231
1.0         232
0.9         233
0.8         234
0.7         235
0.6         236
0.5         237
0.6         238
0.5         239
0.4         240
0.3         241
0.2         242
0.1         243
0.0         244
```

File: ui.wn (con'd)

```
Woburn-Central Sub-basin
Area, (miles^2)
2.5


Initial Abstraction (inches)
IAQ, for Quick Response   IAS, For Slow Response
00.06     IAQ
00.20     IAS
00.20     IAM


Fraction of total rain that is considered effective rainfall
KQ, For Quick Response    KS, For Slow Response
00.08      KQ
00.75      KS
00.75      KM


Time Constant for Separation of Individual Events
TQ, For Quick Response    TS, For Slow Response  TM, For Meltwater
  8         TQ
 24         TS
 24         TM

Snowmelt Coefficient (inches per Fahrenheit-day)
0.000380

Number of Ordinates in Unit Hydrograph, Quick Response
8

Unit Hydrograph Ordinates, Quick Response
   0.0        1
 400.0        2
 800.0        3
1200.0        4
2400.0        5
1200.0        6
 800.0        7
 400.0        8

Number of Ordinates in Unit Hydrograph, Slow Response
73

Unit Hydrograph Ordinates, Slow Response
 100.0         1
 140.0         2
 160.0         3
 180.0         4
 187.0         5
 194.0         6
 201.0         7
 206.0         8
 211.0         9
 216.0        10
 220.0        11
 224.0        12
 225.0        13
 225.0        14
 220.0        15
 215.0        16
 210.0        17
 205.0        18
 200.0        19
 195.0        20
 185.0        21
```

File: ui.wc (con'd)

```
 170.0        22
 160.0        23
 150.0        24
 140.0        25
 130.0        26
 120.0        27
 110.0        28
 100.0        29
  95.0        30
  90.0        31
  85.0        32
  80.0        33
  75.0        34
  70.0        35
  65.0        36
  60.0        37
  55.0        38
  50.0        39
  48.0        40
  46.0        41
  44.0        42
  42.0        43
  40.0        44
  38.0        45
  36.0        46
  34.0        47
  32.0        48
  30.0        49
  28.0        50
  26.0        51
  24.0        52
  22.0        53
  20.0        54
  19.0        55
  18.0        56
  17.0        57
  16.0        58
  15.0        59
  14.0        60
  13.0        61
  12.0        62
  11.0        63
  10.0        64
   9.0        65
   8.0        66
   7.0        67
   6.0        68
   5.0        69
   4.0        70
   3.0        71
   2.0        72
   1.0        73

Number of Ordinates in Unit Hydrograph, Meltwater Response
244

Unit Hydrograph Ordinates, Meltwater Response
 660.0         1
 640.0         2
 620.0         3
 600.0         4
 580.0         5
 560.0         6
 540.0         7
 520.0         8
 500.0         9
```

File: ui.wc (con'd)

```
480.0          10
460.0          11
440.0          12
420.0          13
400.0          14
380.0          15
360.0          16
340.0          17
320.0          18
300.0          19
280.0          20
250.0          21
245.0          22
240.0          23
235.0          24
230.0          25
225.0          26
220.0          27
215.0          28
210.0          29
205.0          30
200.0          31
195.0          32
190.0          33
185.0          34
180.0          35
175.0          36
170.0          37
165.0          38
160.0          39
155.0          40
150.0          41
145.0          42
140.0          43
135.0          44
130.0          45
125.0          46
120.0          47
115.0          48
110.0          49
105.0          50
100.0          51
 98.0          52
 96.0          53
 94.0          54
 92.0          55
 90.0          56
 88.0          57
 86.0          58
 84.0          59
 82.0          60
 80.0          61
 78.0          62
 76.0          63
 74.0          64
 72.0          65
 70.0          66
 68.0          67
 66.0          68
 64.0          69
 62.0          70
 60.0          71
 58.0          72
 56.0          73
 54.0          74
 52.0          75
```

File: ui.wc (con'd)

```
50.0        76
49.0        77
48.0        78
47.0        79
46.0        80
45.0        81
44.0        82
43.0        83
42.0        84
41.0        85
40.0        86
39.0        87
38.0        88
37.0        89
36.0        90
35.0        91
34.0        92
33.0        93
32.0        94
31.0        95
30.0        96
29.0        97
28.0        98
27.0        99
26.0       100
25.0       101
25.0       102
24.0       103
23.0       104
22.0       105
21.0       106
20.0       107
19.5       108
19.0       109
18.5       110
18.0       111
17.5       112
17.0       113
16.5       114
16.0       115
15.5       116
15.0       117
14.8       118
14.6       119
14.4       120
14.2       121
14.0       122
13.8       123
13.6       124
13.4       125
13.2       126
13.0       127
12.8       128
12.6       129
12.4       130
12.2       131
12.0       132
11.8       133
11.6       134
11.4       135
11.2       136
11.0       137
10.8       138
10.6       139
10.4       140
10.2       141
```

File: ui.wc (con'd)

10.0	142
9.9	143
9.8	144
9.7	145
9.6	146
9.5	147
9.4	148
9.3	149
9.2	150
9.1	151
9.0	152
8.9	153
8.8	154
8.7	155
8.6	156
8.5	157
8.4	158
8.3	159
8.2	160
8.1	161
8.0	162
7.9	163
7.8	164
7.7	165
7.6	166
7.5	167
7.4	168
7.3	169
7.2	170
7.1	171
7.0	172
6.9	173
6.8	174
6.7	175
6.6	176
6.5	177
6.4	178
6.3	179
6.2	180
6.1	181
6.0	182
5.9	183
5.8	184
5.7	185
5.6	186
5.5	187
5.4	188
5.3	189
5.2	190
5.1	191
5.0	192
4.9	193
4.8	194
4.7	195
4.6	196
4.5	197
4.4	198
4.3	199
4.2	200
4.1	201
4.0	202
3.9	203
3.8	204
3.7	205
3.6	206
3.5	207

File: ui.wc (con'd)

```
3.4         208
3.3         209
3.2         210
3.1         211
3.0         212
2.9         213
2.8         214
2.7         215
2.6         216
2.5         217
2.4         218
2.3         219
2.2         220
2.1         221
2.0         222
1.9         223
1.8         224
1.7         225
1.6         226
1.5         227
1.4         228
1.3         229
1.2         230
1.1         231
1.0         232
0.9         233
0.8         234
0.7         235
0.6         236
0.5         237
0.6         238
0.5         239
0.4         240
0.3         241
0.2         242
0.1         243
0.0         244
```

File: ui.wc (con'd)

```
Winchester Sub-basin
Area, (miles^2)
5.8


Initial Abstaction (inches)
IAQ, for Quick Response   IAS, for Slow Response
00.15     IAQ
00.25     IAS
00.20     IAM


Fraction of total rain that is considered effective rainfall
KQ, For Quick Response    KS, For Slow Response
00.14      KQ
00.20      KS
00.85      KM


Time Constant for Separation of Individual Events
TQ, For Quick Response    TS, For Slow Response  TM, For Meltwater
  8         TQ
 24         TS
 24         TM

Snowmelt Coefficient (inches per Fahrenheit-day)
0.000380

Number of Ordinates in Unit Hydrograph, Quick Response
8

Unit Hydrograph Ordinates, Quick Response
   0.0        1
 400.0        2
 800.0        3
1200.0        4
2400.0        5
1200.0        6
 800.0        7
 400.0        8

Number of Ordinates in Unit Hydrograph, Slow Response
73

Unit Hydrograph Ordinates, Slow Response
 100.0         1
 140.0         2
 160.0         3
 180.0         4
 187.0         5
 194.0         6
 201.0         7
 206.0         8
 211.0         9
 216.0        10
 220.0        11
 224.0        12
 225.0        13
 225.0        14
 220.0        15
 215.0        16
 210.0        17
 205.0        18
 200.0        19
 195.0        20
 185.0        21
```

```
 170.0        22
 160.0        23
 150.0        24
 140.0        25
 130.0        26
 120.0        27
 110.0        28
 100.0        29
  95.0        30
  90.0        31
  85.0        32
  80.0        33
  75.0        34
  70.0        35
  65.0        36
  60.0        37
  55.0        38
  50.0        39
  48.0        40
  46.0        41
  44.0        42
  42.0        43
  40.0        44
  38.0        45
  36.0        46
  34.0        47
  32.0        48
  30.0        49
  28.0        50
  26.0        51
  24.0        52
  22.0        53
  20.0        54
  19.0        55
  18.0        56
  17.0        57
  16.0        58
  15.0        59
  14.0        60
  13.0        61
  12.0        62
  11.0        63
  10.0        64
   9.0        65
   8.0        66
   7.0        67
   6.0        68
   5.0        69
   4.0        70
   3.0        71
   2.0        72
   1.0        73

Number of Ordinates in Unit Hydrograph, Meltwater Response
244

Unit Hydrograph Ordinates, Meltwater Response
 660.0         1
 640.0         2
 620.0         3
 600.0         4
 580.0         5
 560.0         6
 540.0         7
 520.0         8
 500.0         9
```

File: ui.wi (con'd)

```
480.0        10
460.0        11
440.0        12
420.0        13
400.0        14
380.0        15
360.0        16
340.0        17
320.0        18
300.0        19
280.0        20
250.0        21
245.0        22
240.0        23
235.0        24
230.0        25
225.0        26
220.0        27
215.0        28
210.0        29
205.0        30
200.0        31
195.0        32
190.0        33
185.0        34
180.0        35
175.0        36
170.0        37
165.0        38
160.0        39
155.0        40
150.0        41
145.0        42
140.0        43
135.0        44
130.0        45
125.0        46
120.0        47
115.0        48
110.0        49
105.0        50
100.0        51
 98.0        52
 96.0        53
 94.0        54
 92.0        55
 90.0        56
 88.0        57
 86.0        58
 84.0        59
 82.0        60
 80.0        61
 78.0        62
 76.0        63
 74.0        64
 72.0        65
 70.0        66
 68.0        67
 66.0        68
 64.0        69
 62.0        70
 60.0        71
 58.0        72
 56.0        73
 54.0        74
 52.0        75
```

File: ui.wi (con'd)

50.0	76
49.0	77
48.0	78
47.0	79
46.0	80
45.0	81
44.0	82
43.0	83
42.0	84
41.0	85
40.0	86
39.0	87
38.0	88
37.0	89
36.0	90
35.0	91
34.0	92
33.0	93
32.0	94
31.0	95
30.0	96
29.0	97
28.0	98
27.0	99
26.0	100
25.0	101
25.0	102
24.0	103
23.0	104
22.0	105
21.0	106
20.0	107
19.5	108
19.0	109
18.5	110
18.0	111
17.5	112
17.0	113
16.5	114
16.0	115
15.5	116
15.0	117
14.8	118
14.6	119
14.4	120
14.2	121
14.0	122
13.8	123
13.6	124
13.4	125
13.2	126
13.0	127
12.8	128
12.6	129
12.4	130
12.2	131
12.0	132
11.8	133
11.6	134
11.4	135
11.2	136
11.0	137
10.8	138
10.6	139
10.4	140
10.2	141

File: ui.wi (con'd)

```
10.0        142
 9.9        143
 9.8        144
 9.7        145
 9.6        146
 9.5        147
 9.4        148
 9.3        149
 9.2        150
 9.1        151
 9.0        152
 8.9        153
 8.8        154
 8.7        155
 8.6        156
 8.5        157
 8.4        158
 8.3        159
 8.2        160
 8.1        161
 8.0        162
 7.9        163
 7.8        164
 7.7        165
 7.6        166
 7.5        167
 7.4        168
 7.3        169
 7.2        170
 7.1        171
 7.0        172
 6.9        173
 6.8        174
 6.7        175
 6.6        176
 6.5        177
 6.4        178
 6.3        179
 6.2        180
 6.1        181
 6.0        182
 5.9        183
 5.8        184
 5.7        185
 5.6        186
 5.5        187
 5.4        188
 5.3        189
 5.2        190
 5.1        191
 5.0        192
 4.9        193
 4.8        194
 4.7        195
 4.6        196
 4.5        197
 4.4        198
 4.3        199
 4.2        200
 4.1        201
 4.0        202
 3.9        203
 3.8        204
 3.7        205
 3.6        206
 3.5        207
```

File: ui.wi (con'd)

```
3.4         208
3.3         209
3.2         210
3.1         211
3.0         212
2.9         213
2.8         214
2.7         215
2.6         216
2.5         217
2.4         218
2.3         219
2.2         220
2.1         221
2.0         222
1.9         223
1.8         224
1.7         225
1.6         226
1.5         227
1.4         228
1.3         229
1.2         230
1.1         231
1.0         232
0.9         233
0.8         234
0.7         235
0.6         236
0.5         237
0.6         238
0.5         239
0.4         240
0.3         241
0.2         242
0.1         243
0.0         244
```

File: ui.wi (con'd)

```
SS Deposition/Erosion Parameters
  0.010      f (Fraction of Channel Sediment from flows at time=0)
  5.000      bfpot (Potential SS Conc Assoc. with flows & ltbf)
0.0000800    Cswn (Proportionality factor for erosion from channel)
0.0000800    Cswc
0.0000800    Cswi
0.0000800    Csch1
0.0000800    Csch2
0.0000800    Csag

  0.000      thresq (Flowq Threshold for Erosion)
200000.00    maxlq (Input Deposition Rate, grams per hour per mi**2)
  0.010      k (Input Loss Rate Coefficient, per hour)
0.000000130     Cq (Proportionality factor for flowq erosion from quick
areas)

  0.000      thresr (Rain Threshold for Erosion)
  0.200      frac (Fraction of Quick Area Accessible by Rainfall)
  3.000       Gage 2  Cr (Proportionality factor for Rain Assoc eros from
quick areas)
  3.000      Gage 3
  3.000      Gage 5
```

File: ss.para

Woburn North Sub-basin, Metal Parameters

IRON

0.06	Quick Dissolved Fe,mg/l
0.30	Slow Dissolved Fe,mg/l
0.95	Long term Baseflow Dissolved Fe,mg/l
2.50	Quick Particulate Fe,%
3.50	Slow Particulate Fe,%
20.00	Long term Baseflow Particulate Fe,%

ARSENIC

0.90	Quick Dissolved As, ug/l
2.50	Slow Dissolved As, ug/l
8.50	Long term Baseflow Dissolved As, ug/l
40.00	Quick Particulate As, mg/kg
20.00	Slow Particulate As, mg/kg
1100.00	Long term Baseflow Particulate As, mg/kg

CHROMIUM

0.20	Quick Dissolved Cr, ug/l
1.00	Slow Dissolved Cr, ug/l
1.50	Long term Baseflow Dissolved Cr, ug/l
120.00	Quick Particulate Cr, mg/kg
120.00	Slow Particulate Cr, mg/kg
600.00	Long term Baseflow Cr, mg/kg

COPPER

6.10	Quick Dissolved Cu, ug/l
7.00	Slow Dissolved Cu, ug/l
7.90	Long term Baseflow Dissolved Cu, ug/l
400.00	Quick Particulate Cu, mg/kg
150.00	Slow Particulate Cu, mg/kg
450.00	Long term Baseflow Cu, mg/kg

File: metals.wn

Woburn Central Sub-basin, Metal Parameters

IRON

0.20	Quick Dissolved Fe,mg/l
0.20	Slow Dissolved Fe,mg/l
0.35	Long term Baseflow Dissolved Fe,mg/l
2.00	Quick Particulate Fe,%
2.00	Slow Particulate Fe,%
12.00	Long term Baseflow Particulate Fe,%

ARSENIC

1.50	Quick Dissolved As, ug/l
1.70	Slow Dissolved As, ug/l
0.50	Long term Baseflow Dissolved As, ug/l
40.00	Quick Particulate As, mg/kg
20.00	Slow Particulate As, mg/kg
600.00	Long term Baseflow Particulate As, mg/kg

CHROMIUM

0.50	Quick Dissolved Cr, ug/l
0.70	Slow Dissolved Cr, ug/l
4.10	Long term Baseflow Dissolved Cr, ug/l
450.00	Quick Particulate Cr, mg/kg
120.00	Slow Particulate Cr, mg/kg
950.00	Long term Baseflow Cr, mg/kg

COPPER

3.10	Quick Dissolved Cu, ug/l
2.80	Slow Dissolved Cu, ug/l
14.00	Long term Baseflow Dissolved Cu, ug/l
300.00	Quick Particulate Cu, mg/kg
20.00	Slow Particulate Cu, mg/kg
400.00	Long term Baseflow Cu, mg/kg

File: metals.wc

Winchester Sub-basin, Metal Parameters

IRON

0.05	Quick Dissolved Fe,mg/l
0.20	Slow Dissolved Fe,mg/l
0.80	Long term Baseflow Dissolved Fe,mg/l
5.00	Quick Particulate Fe,%
1.00	Slow Particulate Fe,%
15.00	Long term Baseflow Particulate Fe,%

ARSENIC

1.50	Quick Dissolved As, ug/l
1.50	Slow Dissolved As, ug/l
3.00	Long term Baseflow Dissolved As, ug/l
100.00	Quick Particulate As, mg/kg
20.00	Slow Particulate As, mg/kg
500.00	Long term Baseflow Particulate As, mg/kg

CHROMIUM

0.90	Quick Dissolved Cr, ug/l
0.00	Slow Dissolved Cr, ug/l
0.50	Long term Baseflow Dissolved Cr, ug/l
350.00	Quick Particulate Cr, mg/kg
20.00	Slow Particulate Cr, mg/kg
300.00	Long term Baseflow Cr, mg/kg

COPPER

11.00	Quick Dissolved Cu, ug/l
1.40	Slow Dissolved Cu, ug/l
8.00	Long term Baseflow Dissolved Cu, ug/l
350.00	Quick Particulate Cu, mg/kg
00.00	Slow Particulate Cu, mg/kg
200.00	Long term Baseflow Cu, mg/kg

File: metals.wi

Woburn West Sub-basin, Metal Parameters

IRON

0.16	Dissolved Fe,mg/l
2.50	Particulate Fe,%

ARSENIC

1.20	Dissolved As, ug/l
22.00	Particulate As, mg/kg

CHROMIUM

0.10	Dissolved Cr, ug/l
30.00	Particulate Cr, mg/kg

COPPER

2.50	Dissolved Cu, ug/l
80.00	Particulate Cu, mg/kg

File: metals.ww

APPENDIX V.B

Computer Model Source Code, Input Files, & Output Files: ASCII Format

INPUT & SOURCE CODE

The model source code, executable, and input files are included in ASCII format within the following sub-directory: /model/input. The source code was written in Fortran 77. The amount of disk space needed to download all the files from this sub-directory is 4.9 Megabytes. The source code on the tape corresponds to the 1991 run period. Three executable files are included: one for the 1991 run period, one for the 1992 run period, and one for the 1993 run period.

A description of each of the files is included in table V.B-1. The question mark, "?", in the file name and description corresponds to a particular model year or to a particular sub-basin. For example, for the files with file extension "199?", substituting "?" with "2" implies that the file corresponds to the 1992 run period. For files with file extention "w?", substituting "?" with:

"n" implies the Woburn North sub-basin
"c" implies the Woburn Central sub-basin
"i" implies the Winchester sub-basin
"w" implies the Woburn West sub-basin

Within the flow?.199? files, a value of -100.00 implies that no data was available for the given time step. Within the temp.199? files, a value of -1 implies that temperature for the given time step was less than 32 °F.

File Name	Description	Format
flow1.199?	Measured Hourly Streamflow at Gage 1 for the 199? run period	year,month,day,hour,measured hourly streamflow(cfs) 4i2.2,3x,f9.3
flow2.199?	Measured Hourly Streamflow at Gage 2 for the 199? run period	Same as above
flow3.199?	Measured Hourly Streamflow at Gage 3 for the 199? run period	Same as above
flow5.199?	Measured Hourly Streamflow at Gage 5 for the 199? run period	Same as above
rain.199?	Measured Hourly Precipitation at the Reading Station for the 199? run period	year,month,day,hour,precipitation(inches) 4i2.2,5x,f5.2
temp.199?	Hourly Temperature for Nov through Apr for the 199? run period	year,month,day,hour,temperature(°F) 4i2.2,6x,f4.0
metals.w?	Metal Input Parameters for a Particular Sub-basin	As labeled in the file
ui.w?	Streamflow Model Input Parameters for a Particular Sub-basin	As labeled in the file
ss.para	Suspended Sediment Input Parameters	As labeled in the file
bf.ave	Ave, max, & min longterm baseflow at USGS (bi-monthly,cfs) and precipitation at Reading (monthly,in.)	As labeled in the file
uim.f	Model Source Code (As written it will perform computations for the 1991 run period)	
uim9?.o	Executable file for the 199? run period	

Table V.B-1: Mode. Input Data, File Descriptions

OUTPUT

The output data files are included in ASCII format for the 1991, 1992, and 1993 run periods. Output for each run period are stored in the following sub-directories, where each sub-directory corresponds to a separate run period: (The amount of disk space needed to download the data from each sub-directory is indicated after the sub-directory name.)

/model/1991	40.0 Meg
/model/1992	41.8 Meg
/model/1993	31.4 Meg

A description of each of the files is included in table V.B-2. The data-format notation in table V.B-2 corresponds to Fortran 77. The question mark, "?", in the file name corresponds to a particular sub-basin or main channel component, where 1) files with file extension "w?" correspond to sub-basin files (The nomenclature is the same as mentioned above) and, 2) files with file extension "c?" correspond to main channel components. For the channel-component files, substituting a "1" for the "?" implies channel 1 whereas substituting a "2" for the "?" implies channel 2.

The symbol, "**" corresponds to a specific metal where "**" set to:

"As" implies arsenic
"Cr" implies chromium
"Cu" implies copper
"Fe" implies iron

Specific metals are also identified by "*", where "*" set to:

"A" implies arsenic
"R" implies chromium
"U" implies copper
"F" implies iron

For example, **d.w? where "As" is substituted for "**" and "c" is substituted for "?" implies that the file corresponds to arsenic within the Woburn Central sub-basin.

ABBREVIATIONS

*For **d?.w? and **p?.w?*

**pqm = Quick Particulate Metal Mass Transported in a Given Time Step (g)
**psm = Slow Particulate Metal Mass Transported (g)
**pbm = Longterm-baseflow Particulate Metal Mass Transported (g)
**pcm = Channel Particulate Metal Mass Transported (g)
**ptm = Total Particulate Metal Mass Transported (g)
**pts = Particulate Metal Concentration of Sediment Transported
(% for Fe, mg/kg for As, Cr, & Cu)
**ptc = Particulate Metal Concentration of the River Water
(mg/l for Fe, µg/l for As, Cr, & Cu)
**dqm = Quick Dissolved-Metal Mass Transported in a Given Time Step (g)
**dsm = Slow Dissolved-Metal Mass Transported (g)
**dbm = Longterm-baseflow Dissolved-Metal Mass Transported (g)
**dcm = Channel Dissolved-Metal Mass Transported (g)
**dtm = Total Dissolved-Metal Mass Transported (g)
**dts = Dissolved-Metal Concentration of the River Water
(mg/l for Fe, µg/l for As, Cr, & Cu)

*For **d?.c? and **p?.c?*

**dto? = Routed Dissolved-Metal Flux at the End of A Channel
**dto?c = Dissolved-Metal Concentration at the End of a Channel
**mtp3c = Particulate-Metal Mass at End of Channel Before deposition/erosion check (g)
**ptos = Particulate-Metal Concentration at End of Channel Before deposition/erosion check
(% for Fe, mg/kg for As, Cr, & Cu)
**ptoc = Particulate-Metal Concentration at End of Channel Before deposition/erosion check
(mg/l for Fe, µg/l for As, Cr, & Cu)
**mtp3a = Particulate-Metal Mass at End of Channel After deposition/erosion check (g)
**pcc = Particulate-Metal Concentration at End of Channel After deposition/erosion check
(% for Fe, mg/kg for As, Cr, & Cu)
**pc = Particulate-Metal Concentration at End of Channel Before deposition/erosion check
(mg/l for Fe, µg/l for As, Cr, & Cu)
accum** = Mass of Sediment Accumulated at End of Channel (g)
smch** = Potential Mass of Channel Particulate Metal that can be Eroded (g)
depos** = Mass of Channel Particulate Metal that is Deposited (g)

*For **da.ag and **pa.ag*

**td3a = Dissolved-Metal Mass After the Atlantic Gelatin Withdrawal
**dc = Dissolved-Metal Concentration After the Atlantic Gelatin Withdrawal
**mtp3a = Particulate-Metal Mass after Atlantic Gelatin Withdrawal (g)
**pcc = Particulate-Metal Concentration after Atlantic Gelatin Withdrawal
(% for Fe, mg/kg for As, Cr, & Cu)
**pc = Particulate-Metal Concentration after the Atlantic Gelatin Withdrawal
(mg/l for Fe, µg/l for As, Cr, & Cu)
accum** = Mass of Sediment Accumulated at the Atlantic Gelatin Site (g)
smch** = Potential Mass of Channel Particulate Metal that can be Eroded (g)
depos** = Mass of Channel Particulate Metal that is Deposited (g)

for f.w?
flowq = Quick Streamflow (cfs) (includes flowm contribution)
flows = Slow Streamflow (cfs) (includes flowm contribution)
bf = Longterm Baseflow (cfs)
tot = Total Streamflow (cfs)
flowm = Melt Flow (cfs)

For ss.w?
accum = Mass of Sediment Accumulated in the Sub-basin Channel (g)
accumq = Mass of Sediment Accumulated in Quick Area (g)
smbf = Mass of Longterm-Baseflow Sediment Transported (g)
smss = Mass of Slow Sediment Transported (g)
smqs = Mass of Quick Sediment Transported (g)
smch = Mass of Channel Sediment Transported (g)
smtot = Total Mass of Sediment Transported from Sub-basin (g)
sstot = Total Suspended Sediment Concentration of Water Transported from Sub-basin (mg/l)
T = Water Temperature (°F)
flowt = Total Flow from Woburn West Sub-basin (cfs)
mass = Total Mass of Organic Suspended Sediments in Wedge Pond (kg)
C = Organic Suspended Sediment Concentration (mg/l)
smwe = Total Mass of Sediment Transported from the Woburn West Sub-basin (g)
Ct = Total Suspended Sediment Concentration (mg/l)

For ss?.c?
smto3c = Suspended Sediment Mass at End of Channel Before Deposition/Erosion Check (g)
ssto = Suspended Sediment Conc at End of Channel Before Deposition/Erosion Check (mg/l)
smto3a = Suspended Sediment Mass at End of Channel After Depostiion/Erosion Check (g)
accum = Mass of Sediment Accumulated in the Sub-basin Channel (g)
smch = Potential Mass of Channel Sediment that Can be Transported (g)
depos = Mass of Sediment that is Deposited (g)
sstot = Suspended Sediment Conc at End of Channel After Deposition/Erosion Check (mg/l)

For ssa.ag
smto3a = Suspended Sediment Mass After the Atlantic Gelatin Site (g)
accumg = Mass of Sediment Accumulated at the Atlantic Gelatin Site (g)
smchg = Potential Mass of Sediment that Can be Eroded (g)
depos = Mass of Sediment that is Deposited Due to Water Withdrawal (g)
depos2 = Mass of Sediment that is Deposited because of Transport Capacity Considerations (g)
sstot = Suspended Sediment Concentration After the Atlantic Gelatin Site (mg/l)

For ssc.conc
sstot2 = Suspended Sediment Concentration at Gage 2 (mg/l)
ssmoc = Suspended Sediment Concentration at Gage 3 (mg/l)
Ct = Suspended Sediment Concentration at Gage 1 (mg/l)
ssto5c = Suspended Sediment Concentration at Gage 5 (mg/l)

For ssf.flux
smtot2 = Suspended Sediment Flux at Gage 2 (g/hr)
smto3c = Suspended Sediment Flux at Gage 3 (g/hr)
smwe = Suspended Sediment Flux at Gage 1 (g/hr)
smto5c = Suspended Sediment Flux at Gage 5 (g/hr)

*For temp*c.flux*
*dtm2 = Dissolved-Metal Concentration at Gage 2
(mg/l for Fe, µg/l for As, Cr, & Cu)
*ptm2 = Particulate-Metal Concentration at Gage 2
(% for Fe, mg/kg for As, Cr, & Cu)
*ptm2c = Particulate-Metal Concentration at Gage 2
(mg/l for Fe, µg/l for As, Cr, & Cu)
*std3c = Dissolved-Metal Concentration at Gage 3
(mg/l for Fe, µg/l for As, Cr, & Cu)
*mtp3c = Particulate-Metal Concentration at Gage 3
(% for Fe, mg/kg for As, Cr, & Cu)
*stp3c = Particulate-Metal Concentration at Gage 3
(mg/l for Fe, µg/l for As, Cr, & Cu)
*dtm1 = Dissolved-Metal Concentration at Gage 1
(mg/l for Fe, µg/l for As, Cr, & Cu)
*ptm1 = Particulate-Metal Concentration at Gage 1
(% for Fe, mg/kg for As, Cr, & Cu)
*ptm1c = Particulate-Metal Concentration at Gage 1
(mg/l for Fe, µg/l for As, Cr, & Cu)
*std5c = Dissolved-Metal Concentration at Gage 5
(mg/l for Fe, µg/l for As, Cr, & Cu)
*mtp5c = Particulate-Metal Concentration at Gage 5
(mg/l for Fe, µg/l for As, Cr, & Cu)
*stp5c = Particulate-Metal Concentration at Gage 5
(mg/l for Fe, µg/l for As, Cr, & Cu)

*For temp*f.flux*
*dtm2 = Dissolved-Metal Flux at Gage 2 (g/hr)
*ptm2 = Particulate-Metal Flux at Gage 2 (g/hr)
*mtd3c = Dissolved-Metal Flux at Gage 3 (g/hr)
*mtp3c = Particulate-Metal Flux at Gage 3 (g/hr)
*dtm1 = Dissolved-Metal Flux at Gage 1 (g/hr)
*ptm1 = Particulate-Metal Flux at Gage 1 (g/hr)
*mtd5c = Dissolved-Metal Flux at Gage 5 (g/hr)
*mtp5c = Particulate-Metal Flux at Gage 5 (g/hr)

For out.check
rai = rainfall (inch)
i = time step
snow = snowfall (inch)
temp = air temperature (°F)
flmic = Modeled Streamflow at Gage 2 (cfs)
flmi = Measured Streamflow at Gage 2 (cfs)
flmoc = Modeled Streamlfow at Gage 3 (cfs)
flmo = Measured Streamflow at Gage 3 (cfs)
flwec = Modeled Streamflow at Gage 1 (cfs)

flwe = Measured Streamflow at Gage 1 (cfs)
flwic = Modeled Streamflow at Gage 5 (cfs)
flwi = Measured Streamflow at Gage 5 (cfs)

For melt.check
rain = rainfall depth (inches)
snow = snowfall depth (inches)
snaccum = depth of accumulated snow (inches)
temp = air temperature (°F)
melt = snowmelt depth (inches)
melp = identifies times when snowmelt is initiated

For temp.rmea
rmea = Sum of rainfall and snowmelt during the prior 19 days

For test.melt
melt = snowmelt depth (inches)
idr = number of hours for the given snowmelt event
ieff = effective snowmelt depth (inches)
temp = air temperature (°F)
idt = total number of hours temperature is above 32 °F for current melt event

File Name	Description	Format
**d.w?	dissolved metal transported from a sub-basin	For wn, wc, & wi **dqm,**dsm,**dbm,**dtm,**dts 4(2x,f7.2),1x,f5.2 For ww **dtm,**dts 2f8.2
**d?.c?	dissolved metal results after routing through a main channel component	**dto?,**dto?c 2f10.2
**da.ag	dissolved metal results for the Atl. Gelatin site	**td3a,**dc 1x,f10.2,1x,f8.2
**p.w?	particulate metal transported from a sub-basin	For wn, wc, & wi **pqm,**psm,**pbm,**pcm,**ptm,**pts,**ptc 5(1x,f9.1),1x,f8.2,1x,f6.2 For ww **ptm,**pts,**ptc 3f8.2
**p?.c?	particulate metal results after routing through a main channel component	**mtp3c,**ptos,**ptoc,**mtp3a,**pcc,**pc, accum**,smch**,depos** 2(3x,f10.2,2f8.2),1x,f14.2,2f10.2
**pa.ag	particulate metal results for the Atl. Gelatin site	**mtp3a,**pcc,**pc,accum**,smch**,depos** 3x,f10.2,2f8.2,1x,f8.2,3f10.2
f.w?	streamflow from a sub-basin	For wn, wc, & wi year,month,day,hour,flowq,flows,bf,tot,flowm 4i2.2,5(1x,f8.2) For ww year,month,day,hour,flow(cfs) 4i2.2,3x,f8.2
f?.c?	streamflow at downstream end of main channel component	streamflow(cfs) f10.2
f.ag	streamflow immediately after the Atlantic Gelatin site	streamflow(cfs) f8.2
ss.w?	suspended sediments from a sub-basin	For wn, wc,& wi year,month,day,hour,accum,accumq,smbf,smss, smqs,smch,smtot,sstot 4i2.2,1x,2f15.2,1x,5f13.2,3x,f7.2 For ww year,month,day,hour,T,flowt,mass,C,smwe,Ct 1x,4i2.2,2c,2f8.2,f10.2,f8.2,f10.2,f8.2
ss?.c?	suspended sediments at downstream end of main channel component	smto3c,ssto,smto3a,accum,smch,depos,sstot f10.2,1x,f8.2,1x,f10.2,1x,f14.1,1x,2(f10.2,1x),f8.2
ssa.ag	suspended sediments after the Atlantic Gelatin site	smto3a,accumg,smchg,depos,depos2,sstot f10.2,2(1x,f14.1),2(1x,f10.2),1x,f8.2

Table V.B-2: Model Output, File Descriptions

File Name	Description	Format
ssc.conc	suspended sediment concentrations for gages 2,3,1, & 5	sstot2,ssmoc,Ct,ssto5c 3(1x,f10.1),1x,f12.1
ssf.flux	suspended sediment fluxes for gages 2,3,1, & 5	smtot2,smto3c,smwe,smto5c 3(1x,f10.1),1x,f12.1
temp*c.conc	metal concentrations for gages 2,3,1, & 5	*dtm2,*ptm2,*ptm2c,*std3c,*mtp3c,*stp3c,*dtm1,*ptm1,*ptm1c,*std5c,*mtp5c,*stp5c 3f10.2,3x,3f10.2,3x,3f10.2,3x,3f10.2
temp*f.flux	metal fluxes for gages 2,3,1, & 5	*dtm2,*ptm2,*mtd3c,*mtp3c,*dtm1,*ptm1,*mtd5c,*mtp5c 4(2f10.2,1x)
out.check	rainfall, snowfall, and modeled and measured streamflows	year,month,day,hour,rai,i,snow,temp,flmic,flmi,flmoc,flmo,flwec,flwe,flwic,flwi 4i2.2,2x,f4.2,1x,i5,1x,f4.2,1x,f3.0,1x,4(f8.2,1x,f8.2,3x)
melt.check	rainfall, snowfall, temperature, and snowmelt	year,month,day,hour,rain,snow,snaccum,temp,melt,melp 4i2.2,5(1x,f10.3),1x,i2
temp.rmea	sum of rainfall and snowmelt in prior 19 days	year,month,day,hour,rmea 4i2.2,3x,f8.3
test.melt	total snowmelt and effective snowmelt for the Winchester sub-basin	year,month,day,hour,melt,idr,ieff,temp,idt 4i2.2,f10.4,2x,i4,2x,f10.4,1x,f4.0,1x,i5
storms	Summary of individual storm depths (total and effective) for quick, slow, and melt systems	As labeled in file
balance	Summary of water, sediment, and metal contribution from each component	As labeled in file

Table V.B-2: con'd

APPENDIX V.C

Model Performance: Supplemental Discussion and Plots

This appendix may be considered to be a supplement to the discussion of model performance presented in section V.3 in the main body of the text. The additional information includes: 1) a discussion of some of the papers summarized in table V.3-1, 2) modeled versus measured plots for streamflow at each of the five gaging stations, 3) supplemental discussion of the streamflow model by presenting additional streamflow time series plots, and 4) details of model performance for chromium, iron, and copper.

DISCUSSION OF SOME PAPERS SUMMARIZED IN TABLE V.3-1

The good performance described in the Thomas, 1990 study was due, in part, to selectively choosing the storm events for which the model was calibrated and verified. For this study 230 events were measured. Of these events, 142 were rejected by the authors due to "inconsistencies" between precipitation and streamflow measurements. Since "inconsistent" input data can only be rejected after measuring the output, the reported R^2 value is higher than would be expected in a true application of the model where output measurements are not available.

The authors in the Tucci and Clarke, 1980 study claimed that a large portion of their model errors were due to errors in the input measurements. To further support the authors' claims, one may note that the watershed investigated by Franchini & Pacciani, 1991 is of a very similar size but 4 rain gages were accessible in this study whereas only 1 rain gage was available in the Tucci & Clarke, 1980 study. The R^2 values from each study were significantly different, with the poorer R^2 associated with the study with fewer rain gages. The difference in the number of rain gages supports the authors' claims that input errors were a primary cause of the poorer R^2 values obtained in the Tucci & Clarke, 1980 study.

The extremely poor results of the Loague and Freeze, 1985 model application were most likely due to the failure of the models to capture the overall mechanisms of streamflow generation. In other words, a large reason for the poor performance may have been due to an inadequate formulation of the model for the watersheds investigated.

MODELED V. MEASURED STREAMFLOW PLOTS

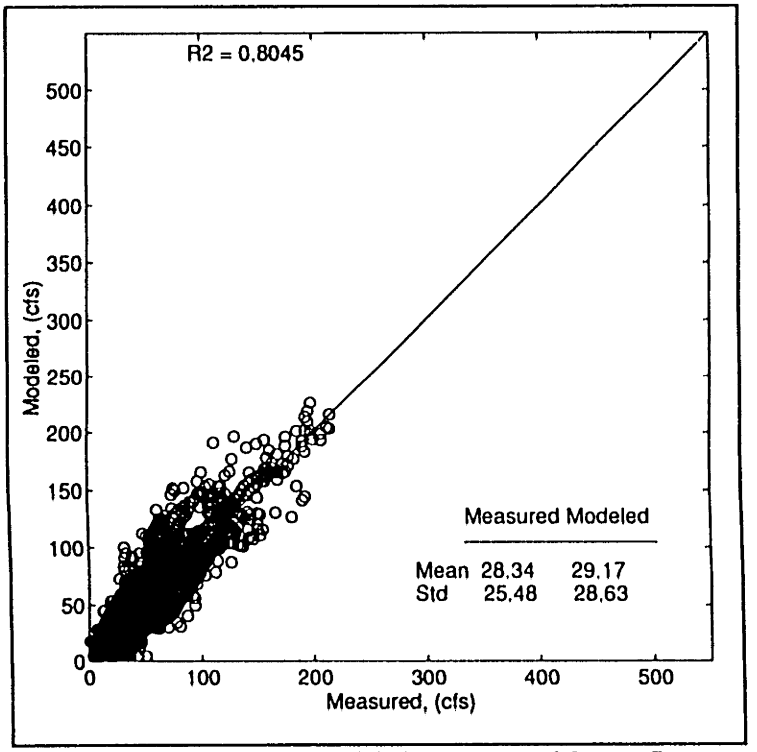

Figure V.C-1: Modeled vs Measured Streamflow
Gage 5, 1992 (Calibration)

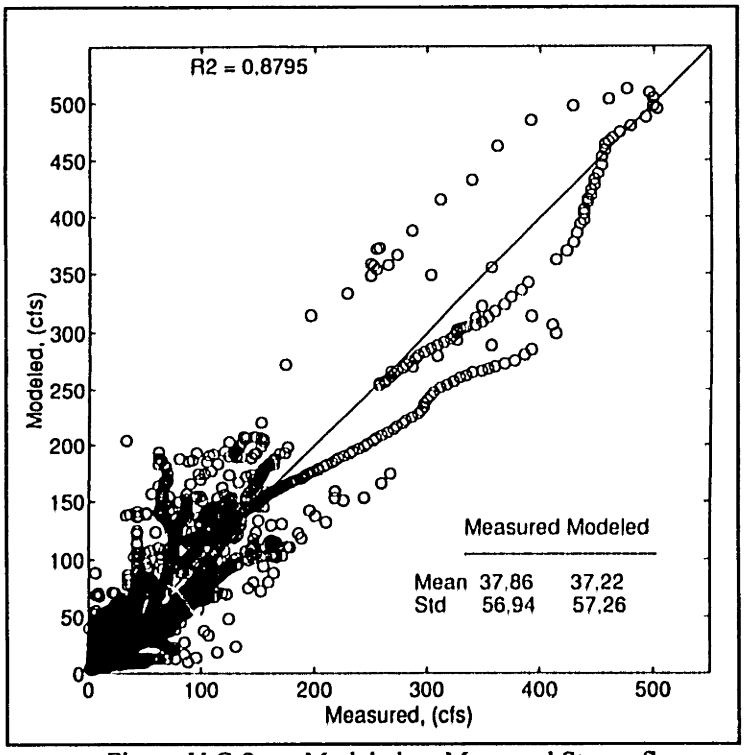

Figure V.C-2: Modeled vs Measured Streamflow
Gage 5, 1993 (Calibration)

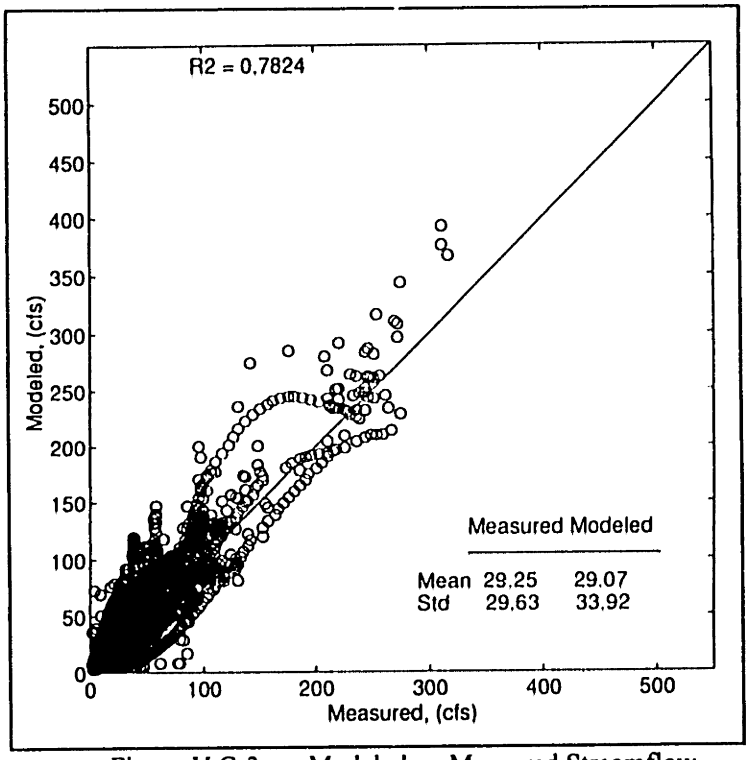

Figure V.C-3: Modeled vs Measured Streamflow Gage 5, 1991 (Verification)

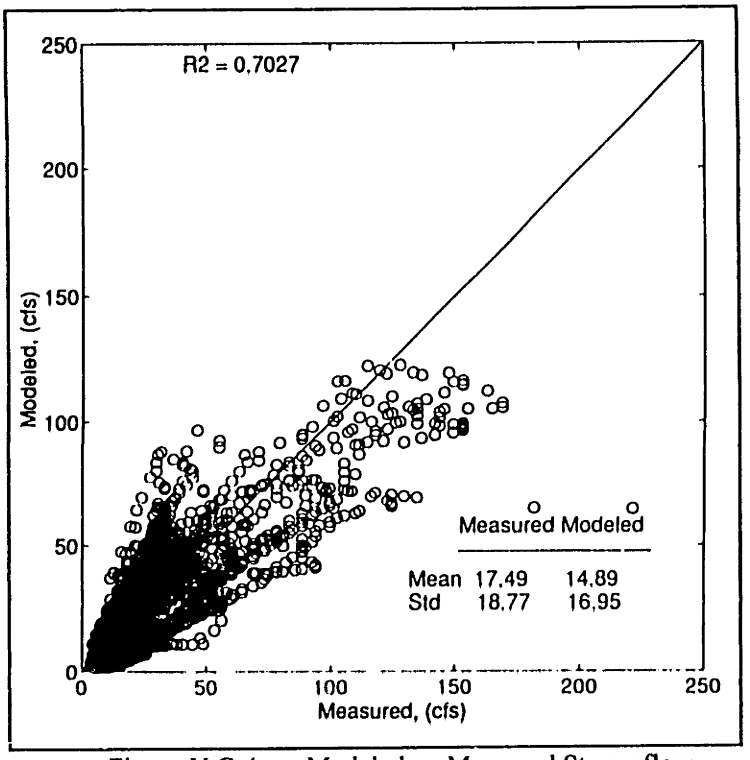

Figure V.C-4: Modeled vs Measured Streamflow Gage 3, 1992 (Calibration)

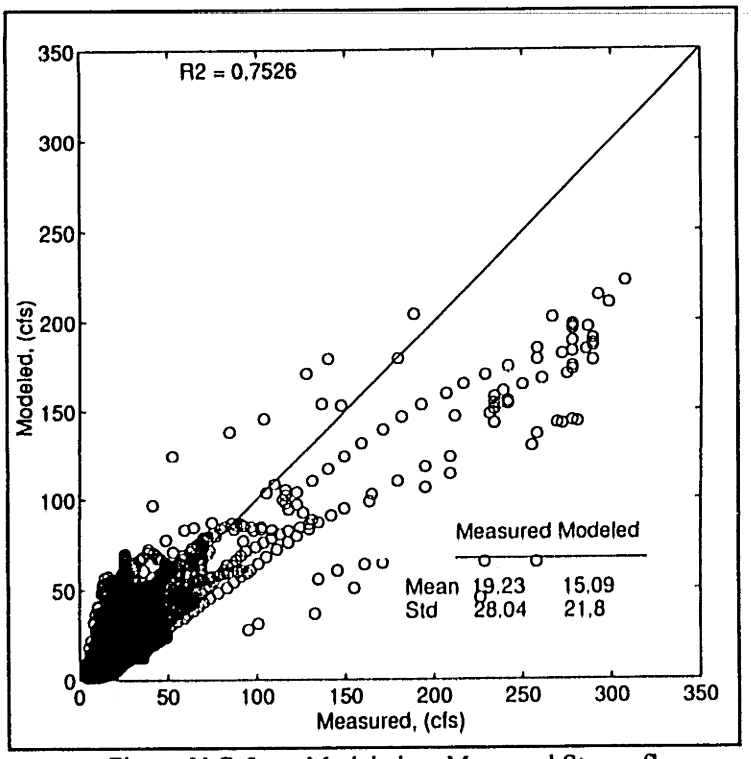

Figure V.C-5: Modeled vs Measured Streamflow Gage 3, 1991 (Verification)

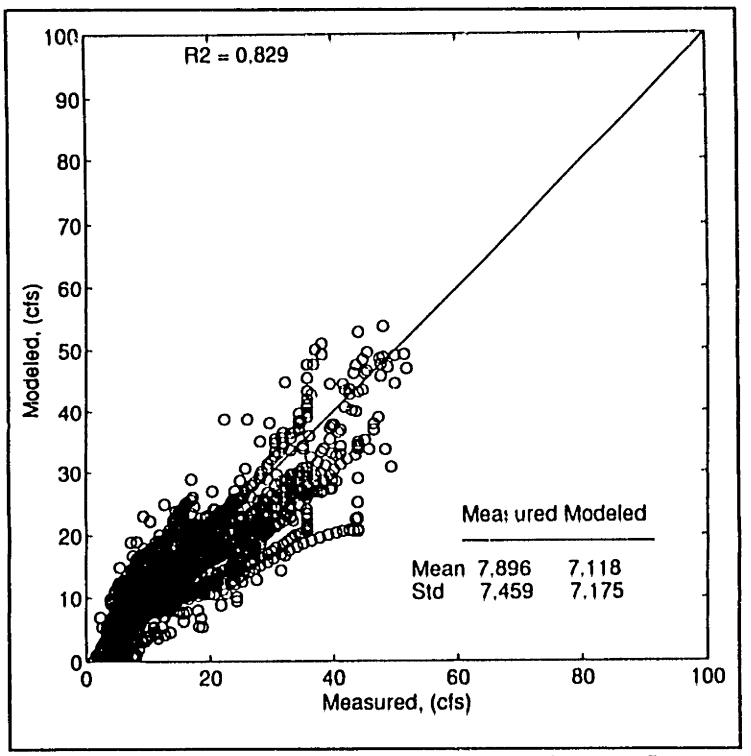

Figure V.C-6: Modeled vs Measured Streamflow
Gage 2, 1992 (Calibration)

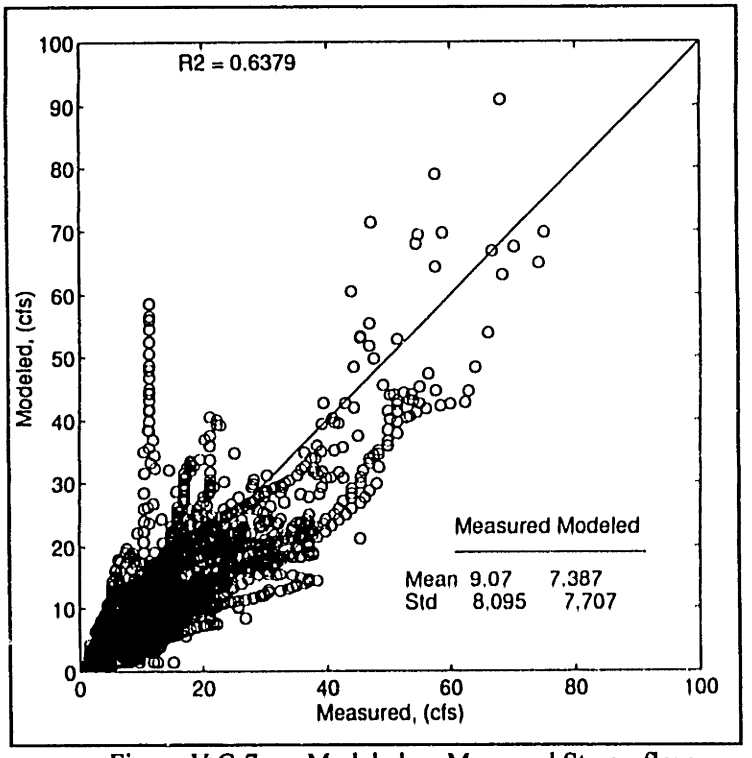

Figure V.C-7: Modeled vs Measured Streamflow
Gage 2, 1991 (Verification)

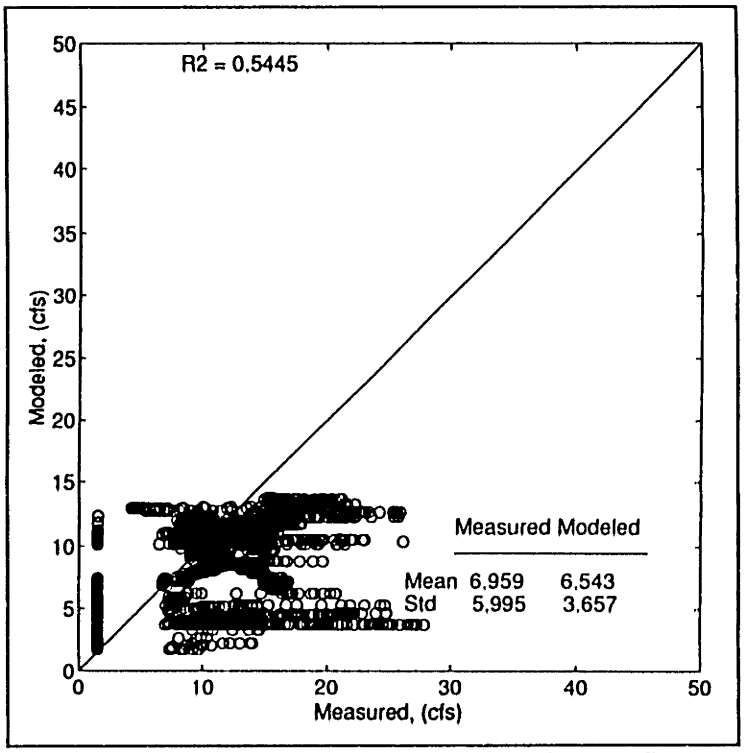

Figure V.C-8: Modeled vs Measured Streamflow
Gage 1, 1992

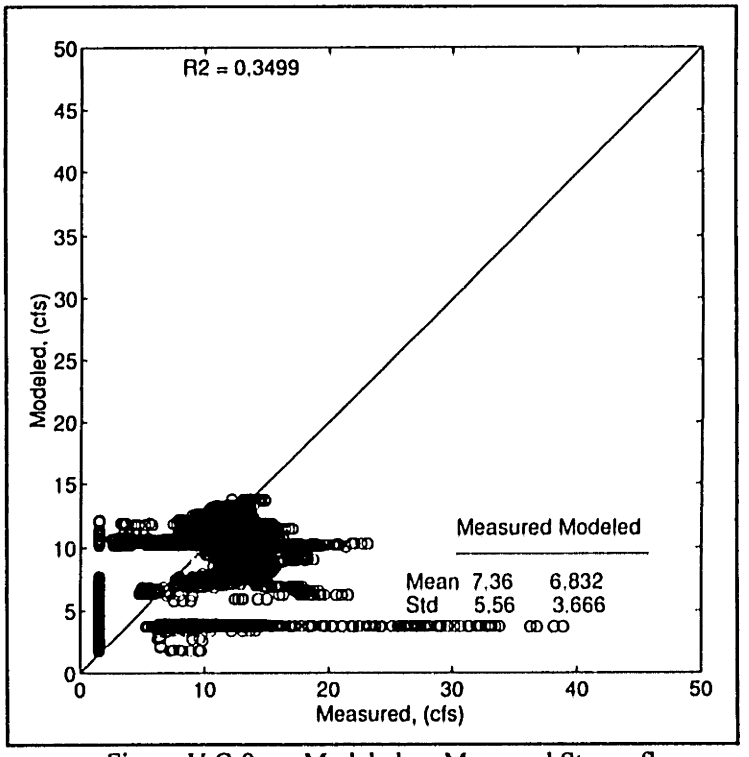

Figure V.C-9: Modeled vs Measured Streamflow
Gage 1, 1991

SUPPLEMENTAL ANALYSIS: DISCUSSION OF STREAMFLOW TIME SERIES PLOTS

Selected time series plots are included in figures V.C-10 to V.C-33. These plots were chosen to emphasize both the positive and negative aspects of model performance. (For further analysis, all the hourly results for the 1992, and 1993 calibration years and the 1991 verification year are included in ASCII format in Appendix V.B)

On each of the time series plots, snow and rainfall are plotted on the inverted scales. Modeled flow corresponds to the solid line and the measured flow corresponds to the dotted line. Times before and after the sharp increase and decrease of the dotted lines to zero, correspond to times when no measured streamflow data were available. Other lines correspond to modeled components which were added together to obtain the total modeled flow. The "+" signs on these plots correspond to times when samples were taken. Additionally, for model runs during the months of November through April the air temperature (> 32°F) is plotted on the lower axis.

Streamflow Model at Gage 2,3, & 5

For May 1992, the model at gage 5 was capable of reproducing the receding flows during low flow conditions (figure V.C-10). Both the quick and slow response were slightly overestimated for the event occurring on May 2. At gages 2 and 3, however, the receding limb was slightly under-estimated during later parts of the month (figures V.C-11 and V.C-12). This result indicates that the time constant, R, for the sub-basins draining gage 2 and 3 may be slightly different than the value estimated for the watershed as a whole. Additionally, at gage 3, the quick flow was slightly over-estimated whereas the peak of the slow response was under-estimated.

For August 1992, (figures V.C-13 to V.C-15) the model was capable of reproducing the peak streamflows and a large portion of the receding flows for both gages 2 and 5. For the event sampled at gage 5 on August 18th (times of sample collection are provided by the "+" symbols), the streamflow model performed very well. For the event sampled at gage 5 on August 10th, the model slightly over-estimated the measured streamflow during the times that samples were collected. At gage 3, the larger storm events were not modeled as well. The August 10 quick and slow responses at gage 3 were over-estimated by the model while the August 18 quick and slow responses were slightly under-estimated.

For November 1992 (figures V.C-16 to V.C-18), the model generally under-estimated the low flow from November 5 to November 23 at all three gaging stations. These results indicate that streamflows during this time were uncharacteristically low, when compared to the 1957 to 1993 streamflow record at gage

5. Four samples were collected during the November 24 storm event at gage 5. The model slightly over-estimated the streamflows for these samples. At gage 2 the streamflows were well estimated, whereas at gage 3 the streamflow for the event were slightly under-estimated.

For December 1992, the later parts of the modeled receding limbs of the December 10th and December 17th events were observed to recede too quickly at gage 5. (figure V.C-19) For the December 10th through 11th sample collection times, however, the model performed very well. The rising limb and the peak flow of this event were well estimated. The streamflow for the sample collected on the rising limb of the December 17th event, however, was not very accurately modeled at either of the 3 monitoring stations. (figures V.C-19 to V.C-21) This error is due to the combination of: 1) slight time shift between the modeled and measured streamflows and, 2) the under-estimation of the baseflow prior to the storm. Also one may note a small peak at gage 5 during the December 10th storm which occurred prior to the larger peak. Strangely, this smaller peak occurred before any precipitation was recorded at the Reading station. The only explanation for this observation is that a small amount of localized precipitation had occurred over the southern part of the watershed, prior to the larger event which was recorded at the Reading station.

Figures V.C-22 and V.C-23 correspond to streamflows which were strongly affected by snowmelt. For March 1993, the flows from March 7 to March 24 were slightly under-estimated. On the 24th, the model predicted a streamflow response to a precipitation event, while the measured data showed no evidence of a streamflow response. This observation indicates that either: 1) precipitation during March 24 actually occurred as snow, or 2) the precipitation measured at Reading over-represented the precipitation on the entire watershed. The following two peaks, on March 26 and March 27, were snowmelt responses due to temperature spikes. The model, also predicted a snowmelt response; however, the rate of the increase and decrease in streamflow were not precisely modeled. Furthermore, the measured data show abrupt and somewhat random fluctuations in streamflow which the model was not able to capture. These abrupt fluctuations are believed to be associated with short-term freezing and thawing of the water entering the river. (See appendix IV.B for discussion) Since the model does not halt the routing of snowmelt once the temperatures fall below freezing, the model is unable to capture abrupt changes in streamflow. During the March 29 event, the model was capable of properly estimating the peak flow. However, flows on the rising limb were slightly over-estimated by the model, whereas flows on the falling limb were slightly under-estimated. The April 2 event, was a precipitation event which was super-imposed on the receding limb of the March 29 event. For this particular event, the model under-estimated the peak flow. For the most part, the remaining events in April were reasonably well estimated. The differences between modeled and measured flow for this later period were associated with small errors in the estimation of baseflows.

Examples of model performance during the 1991 verification year are given for the months of May and August in figures V.C-24 to V.C-29. The May plots (figures V.C-24 to V.C-26) illustrate the model performance during a series of relatively small storms. For all stations, the timing of the streamflow response and the magnitudes of the peak flows were reasonably modeled. Relatively small errors occurred in the estimation of the slow response immediately after the peak.

The August plots (figures V.C-27 to V.C-29) are examples of model performance during a large storm event. For each of the three stations the peak flows during the August 19th storm were slightly off. The largest errors occurred at gage 3, where both the quick and slow peaks were under-estimated by the model. Additionally, a dip in the measured streamflow data is observed at gage 5 on August 23. This dip was attributed to a reverse flow of water from the Aberjona River to Wedge Pond. (See appendix IV.B for discussion) The model was not formulated to capture these reverse flows. However, the error due to the model's inability to capture the reverse flows is negligible.

Streamflow Model at Gage 1

Streamflow for the Woburn West sub-basin is an input into the model. The data is input by linearly interpolating average monthly values of streamflow as observed during the 1991 and 1992 period of record at gage 1.

To illustrate the adequacy of this method of streamflow input, selected time series plots are presented in figures V.C-30 to V.C-33. From these figures, the overall average flow is modeled considerably well. However, one may also note that this method of streamflow input is unable to capture the short-term fluctuations in streamflow associated with storm events. These short term fluctuations (figures V.C-30 and V.C-31), however, are small relative to the volume of water being transported along the Aberjona River, especially for the smaller storm events. To quantify an extreme case of the error, the August 16 through 24th event (a large storm) is considered. During this time period, the volume of streamflow from the Wedge Pond station was under-estimated by 6.0×10^6 ft^3 which represented approximately 17% of the streamflow at the USGS station. The 17% error therefore represents an upper bound on the effect of the Woburn West streamflow input on the modeling of streamflow at gage 5.

The 17% error (extreme case) is relatively small if one also considers: 1) the errors in modeling the streamflows along the Aberjona River, and 2) that the concentration of metals tends to be much lower for the Woburn West sub-basin than for areas draining into the Aberjona River; thus the overall error in the flux of metals would be even smaller than the error in the streamflow estimate.

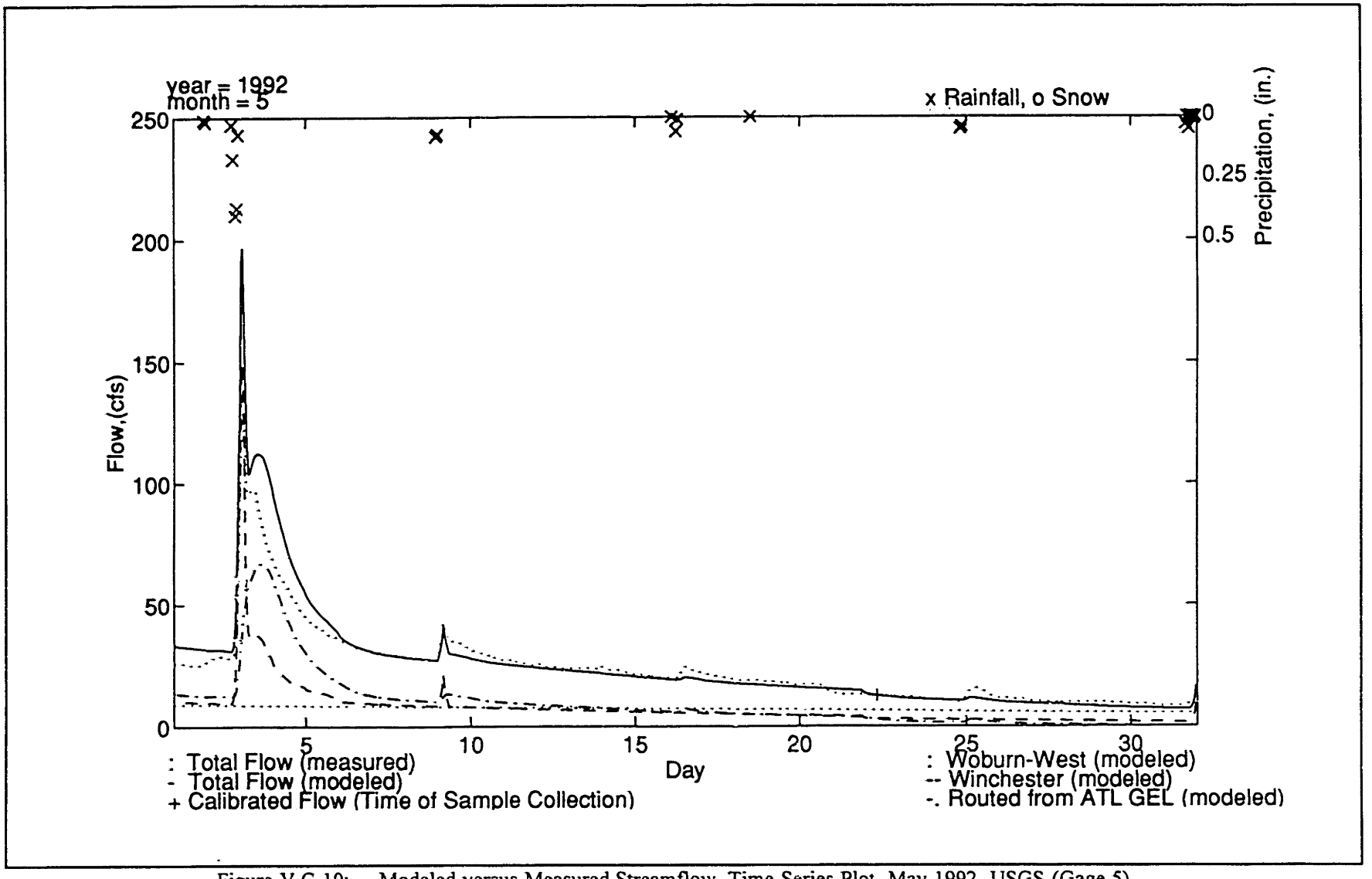

Figure V.C-10: Modeled versus Measured Streamflow, Time Series Plot, May 1992, USGS (Gage 5)

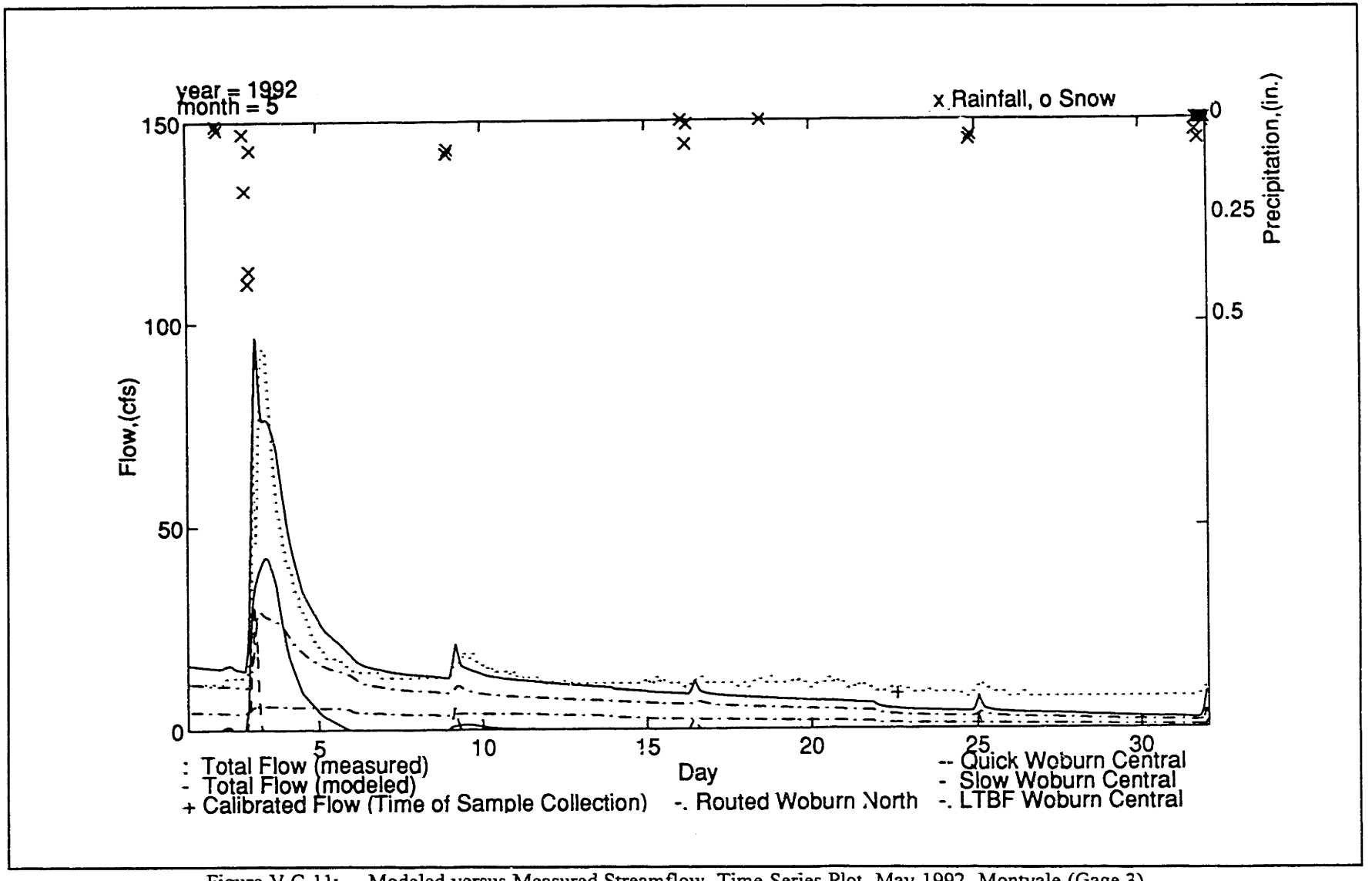

Figure V.C-11: Modeled versus Measured Streamflow, Time Series Plot, May 1992, Montvale (Gage 3)

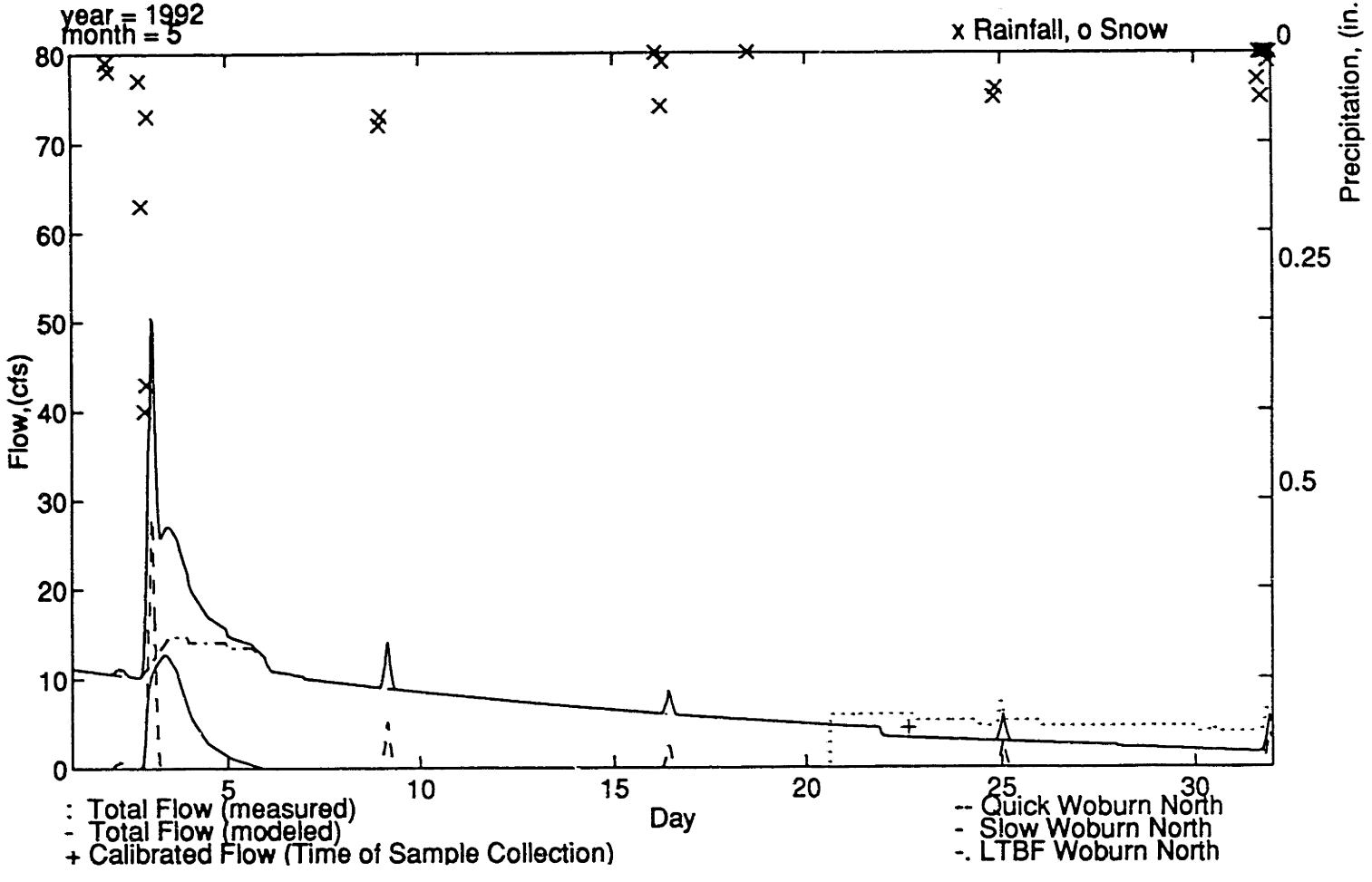

Figure V.C-12: Modeled versus Measured Streamflow, Time Series Plot, May 1992, Rte 128 (Gage 2)

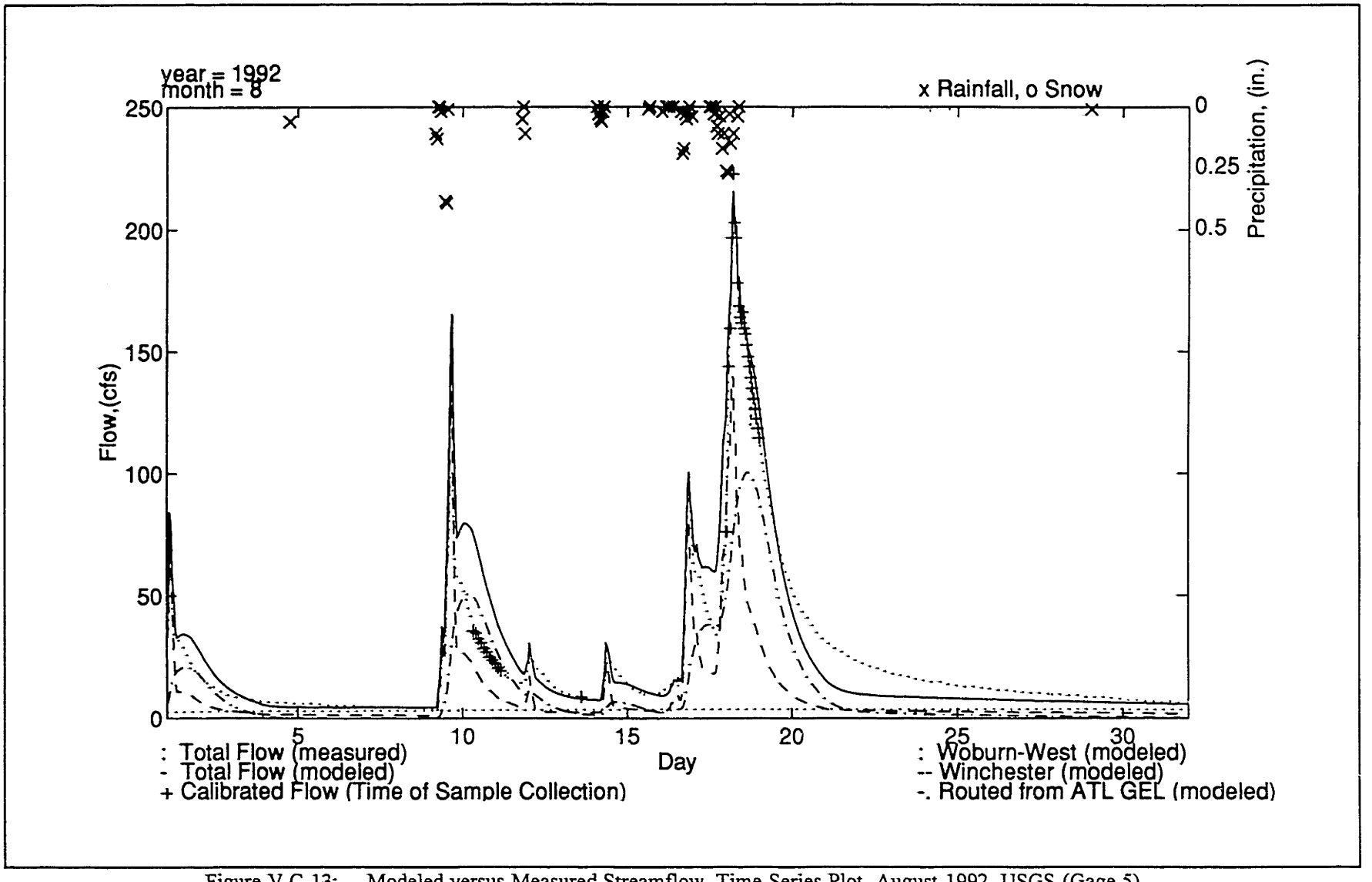

Figure V.C-13: Modeled versus Measured Streamflow, Time Series Plot, August 1992, USGS (Gage 5)

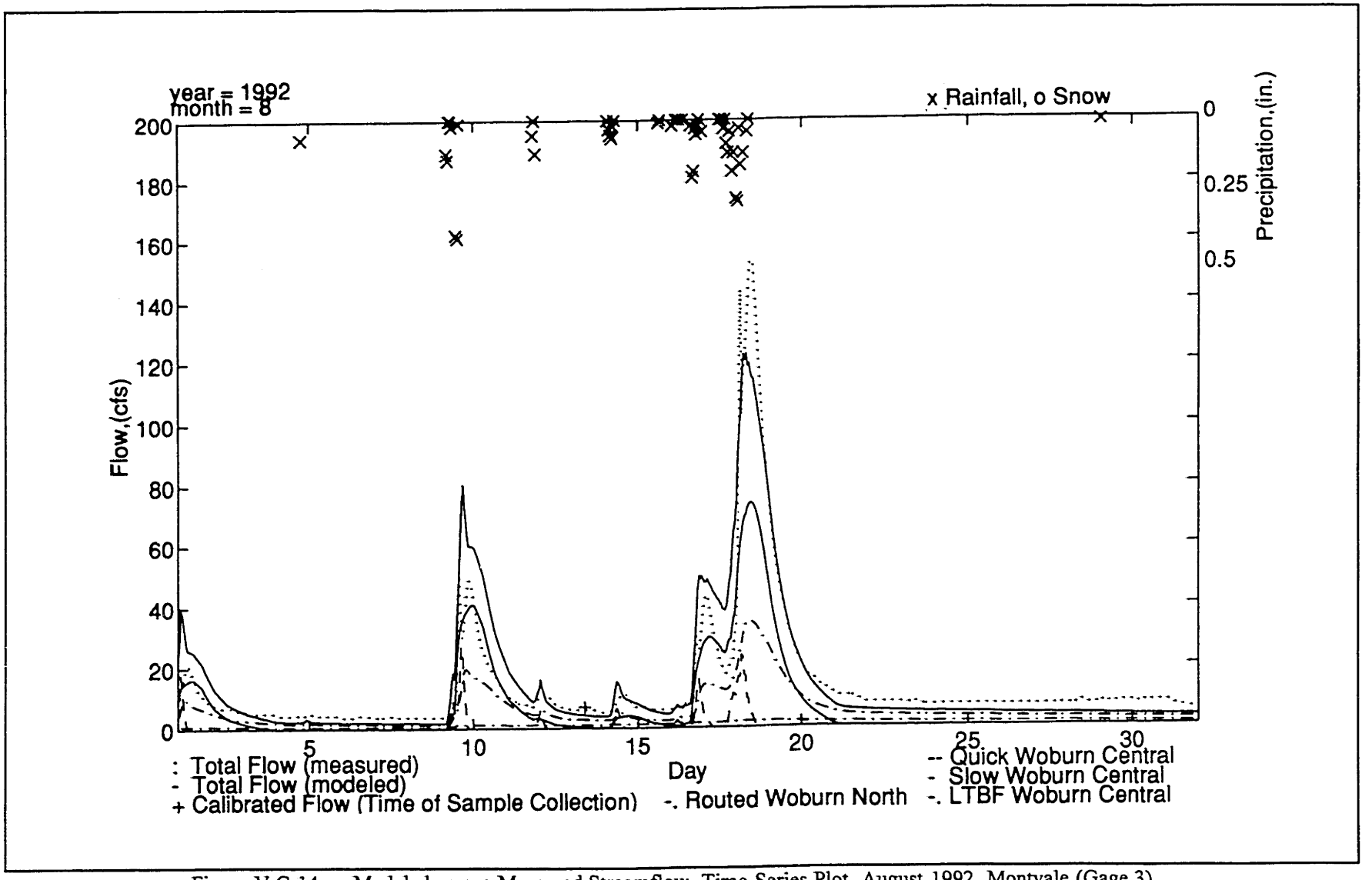

Figure V.C-14: Modeled versus Measured Streamflow, Time Series Plot, August 1992, Montvale (Gage 3)

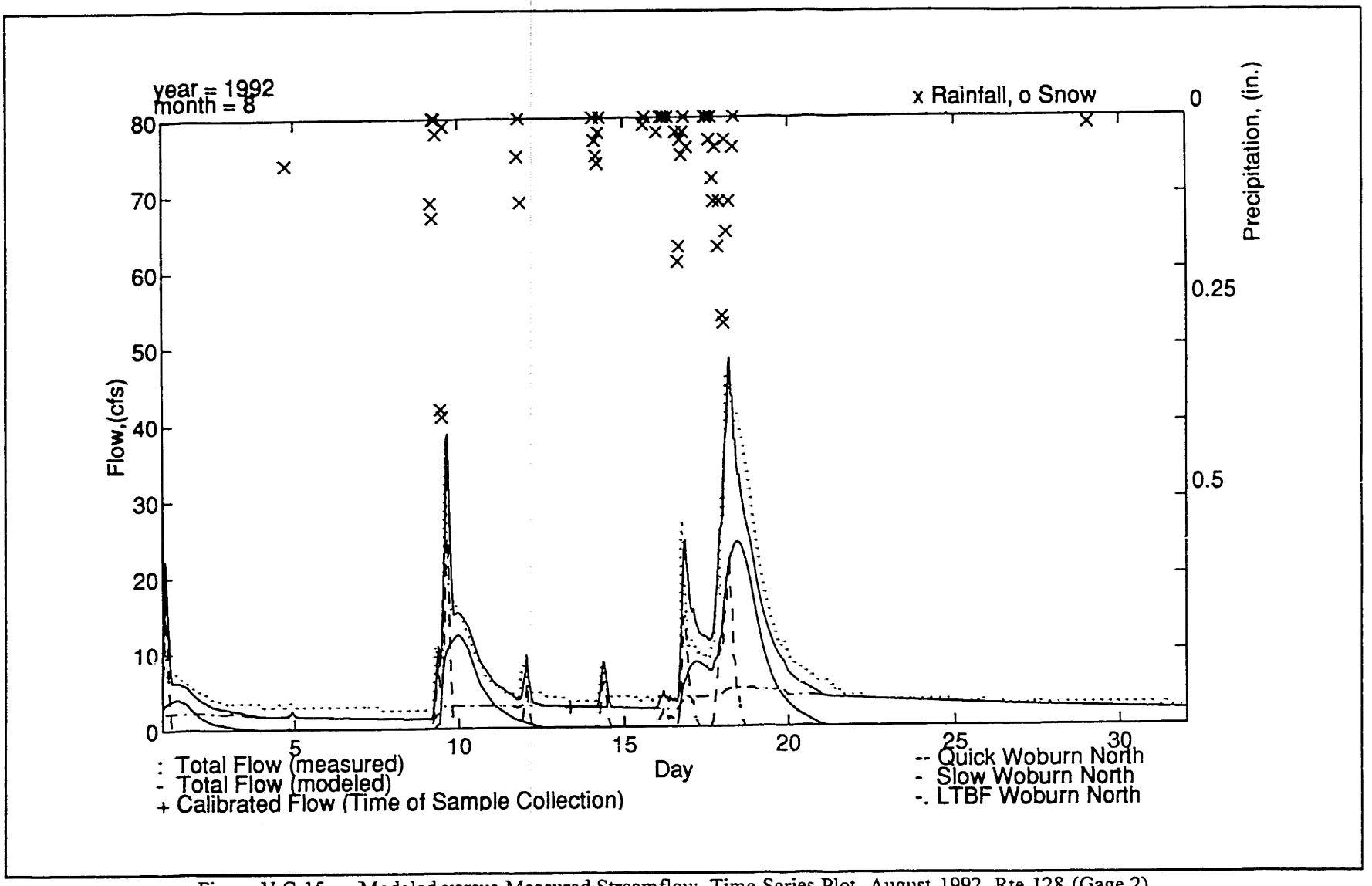

Figure V.C-15: Modeled versus Measured Streamflow, Time Series Plot, August 1992, Rte 128 (Gage 2)

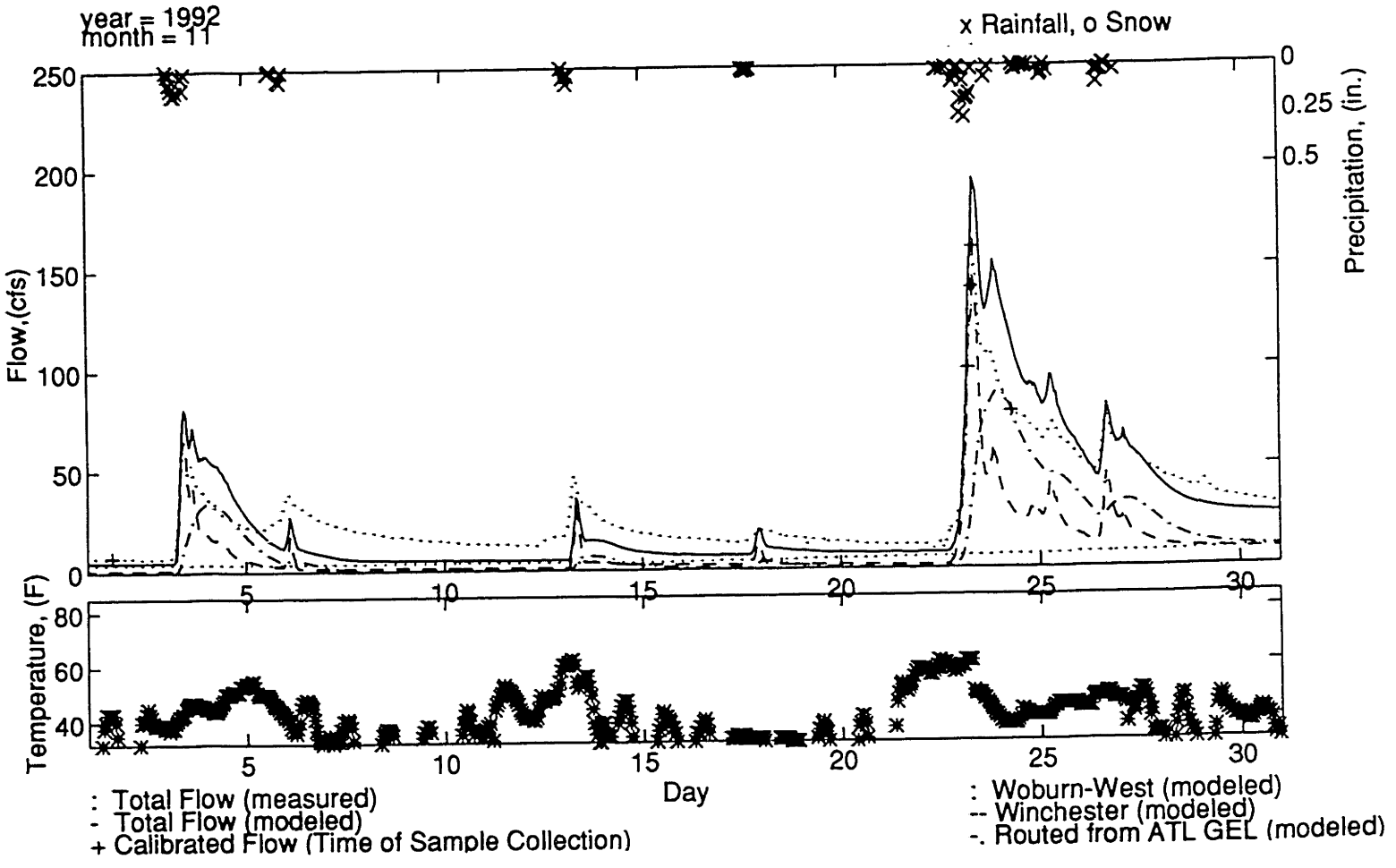

Figure V.C-16: Modeled versus Measured Streamflow, Time Series Plot, November 1992, USGS (Gage 5)

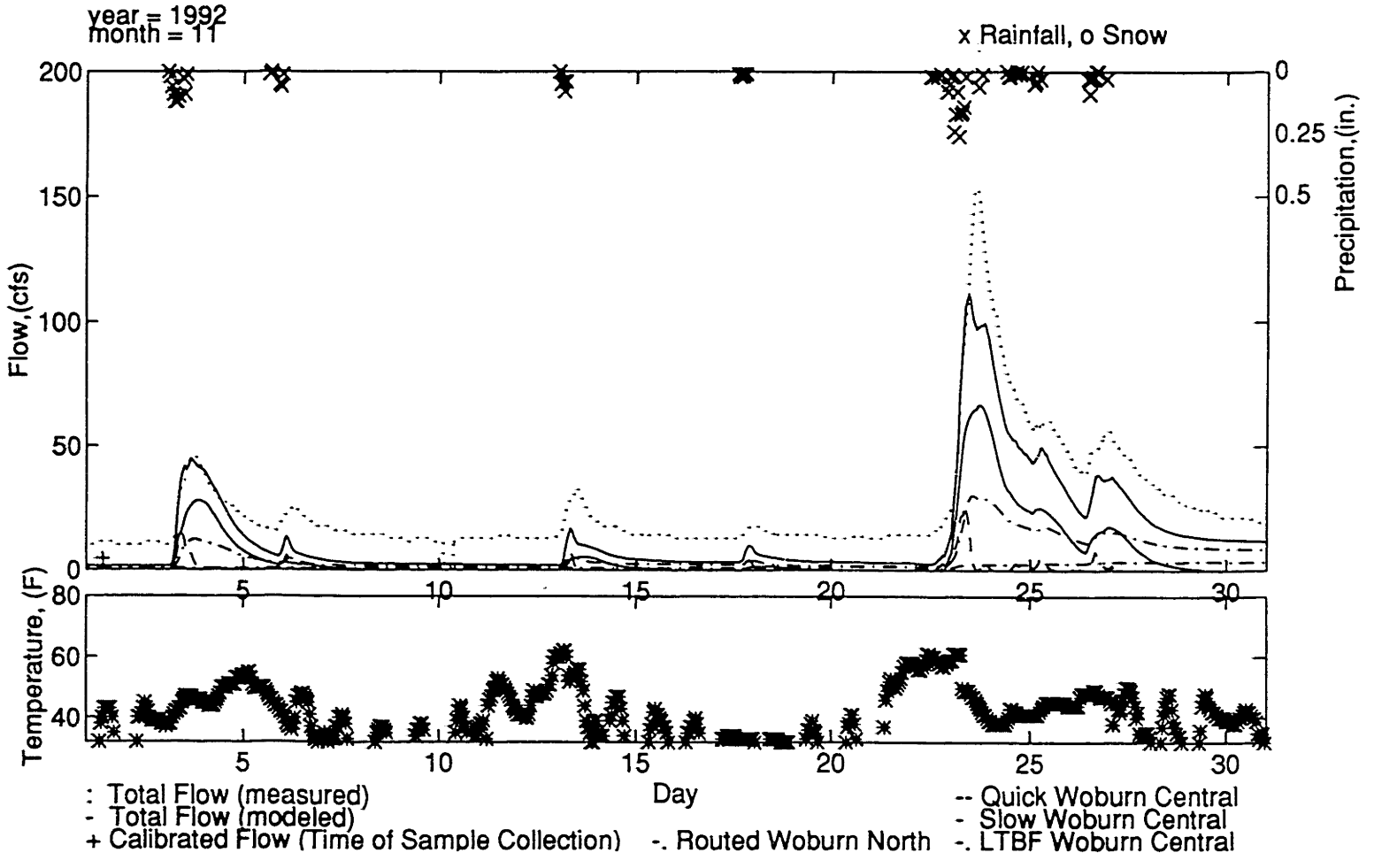

Figure V.C-17: Modeled versus Measured Streamflow, Time Series Plot, November 1992, Montvale (Gage 3)

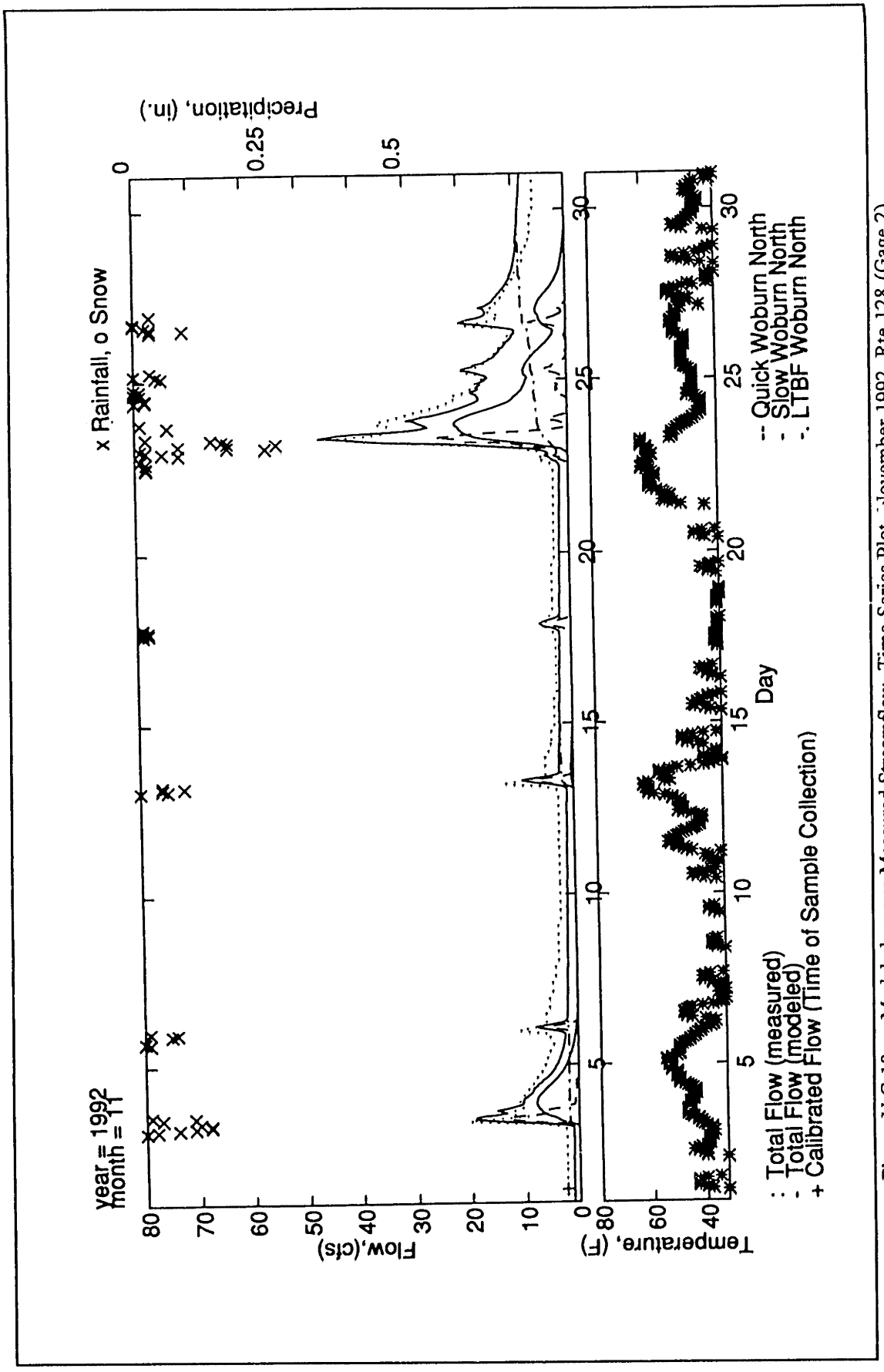

Figure V.C-18: Modeled versus Measured Streamflow, Time Series Plot, November 1992, Rte 128 (Gage 2)

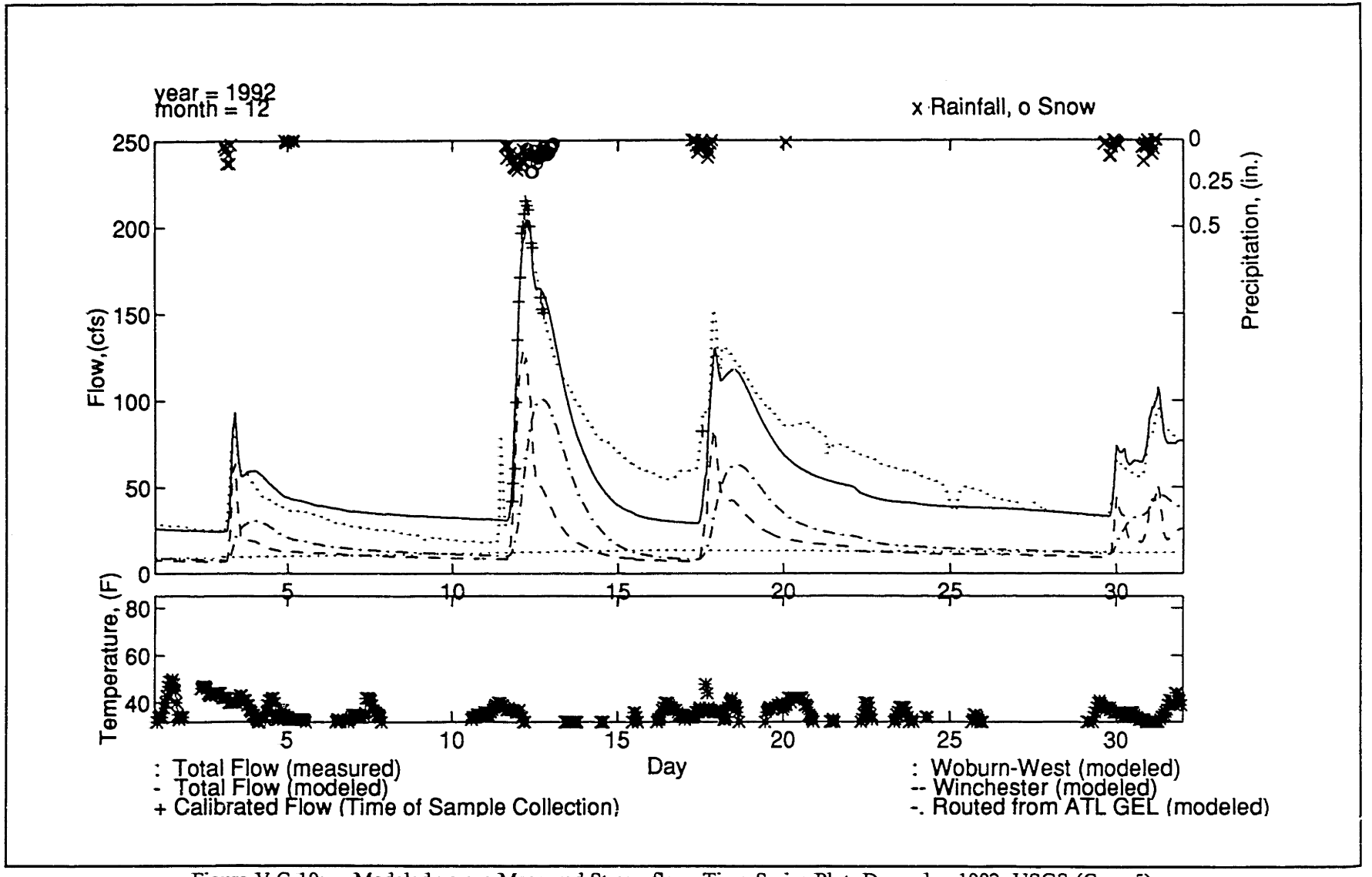

Figure V.C-19: Modeled versus Measured Streamflow, Time Series Plot, December 1992, USGS (Gage 5)

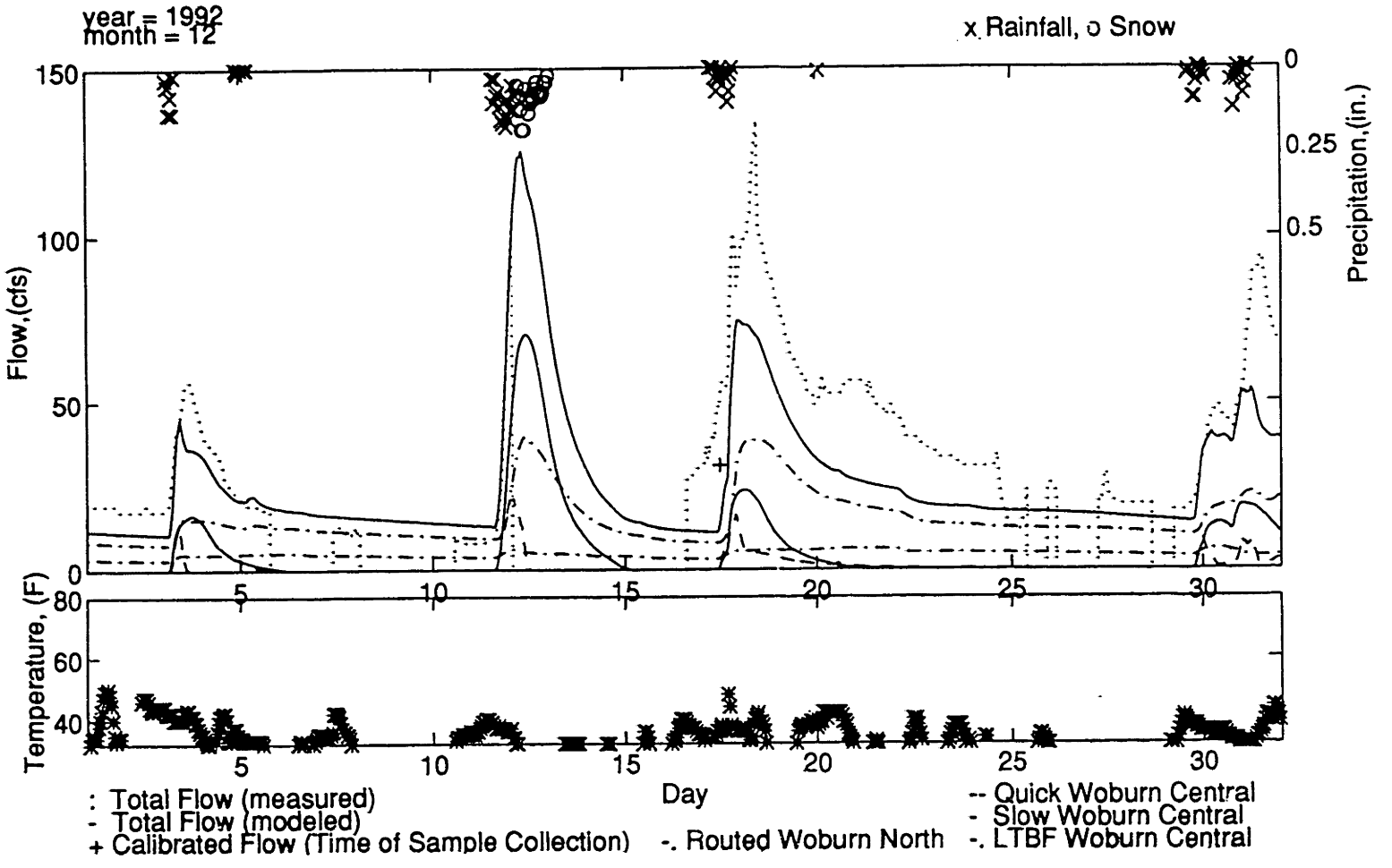

Figure V.C-20: Modeled versus Measured Streamflow, Time Series Plot, December 1992, Montvale (Gage 3)

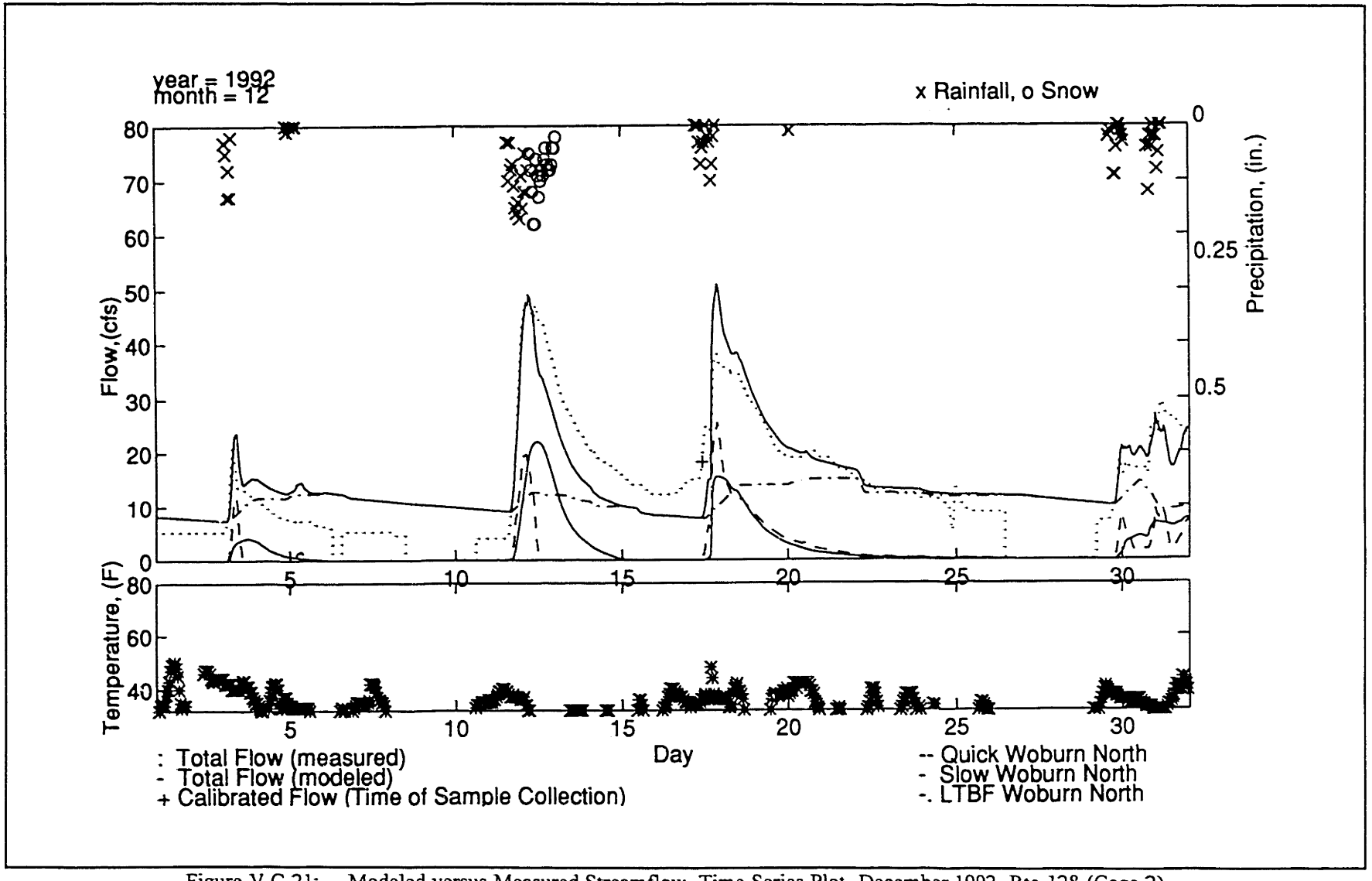

Figure V.C-21: Modeled versus Measured Streamflow, Time Series Plot, December 1992, Rte 128 (Gage 2)

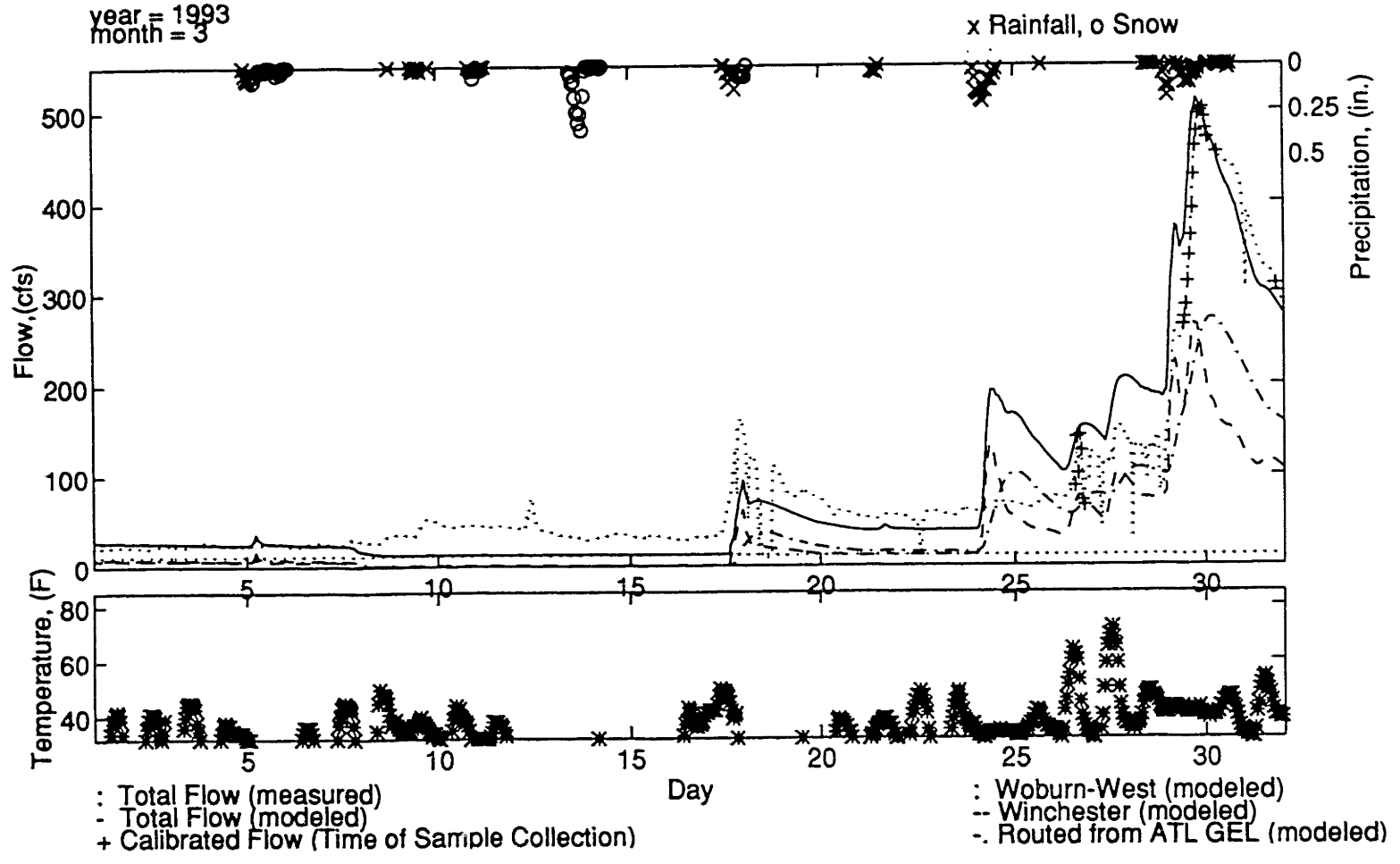

Figure V.C-22: Modeled versus Measured Streamflow, Time Series Plot, March 1993, USGS (Gage 5)

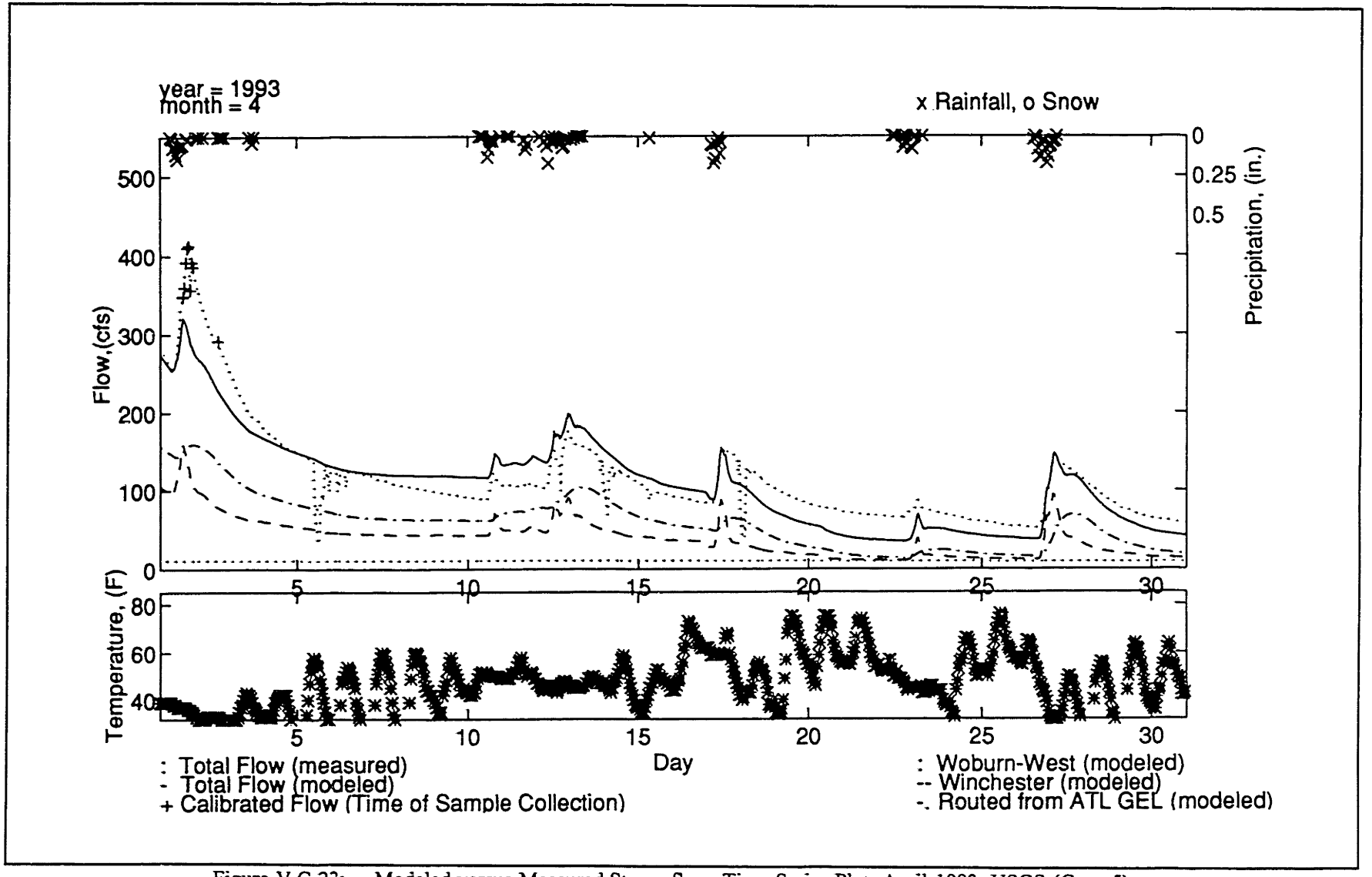

Figure V.C-23: Modeled versus Measured Streamflow, Time Series Plot, April 1993, USGS (Gage 5)

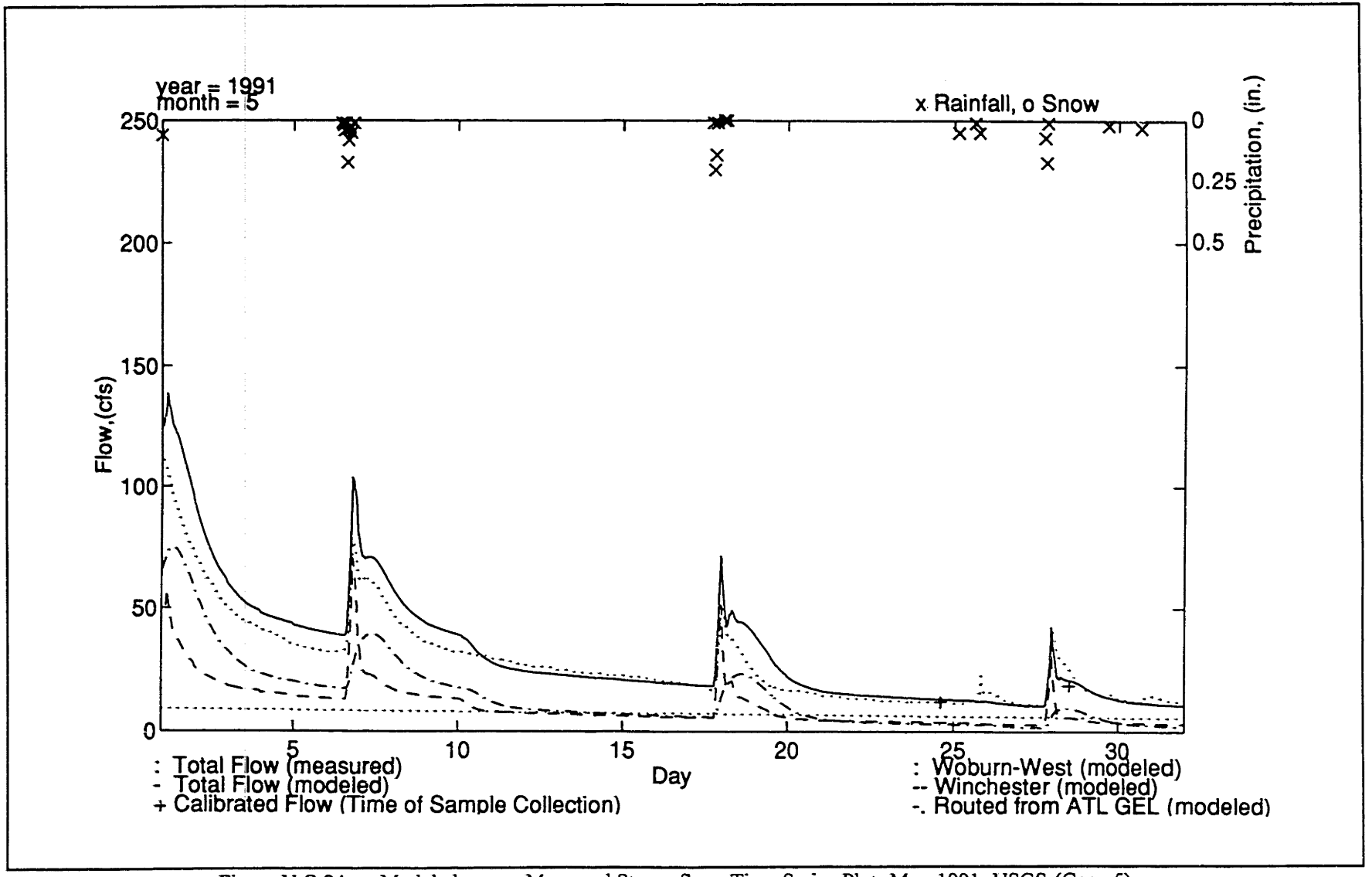

Figure V.C-24: Modeled versus Measured Streamflow, Time Series Plot, May 1991, USGS (Gage 5)

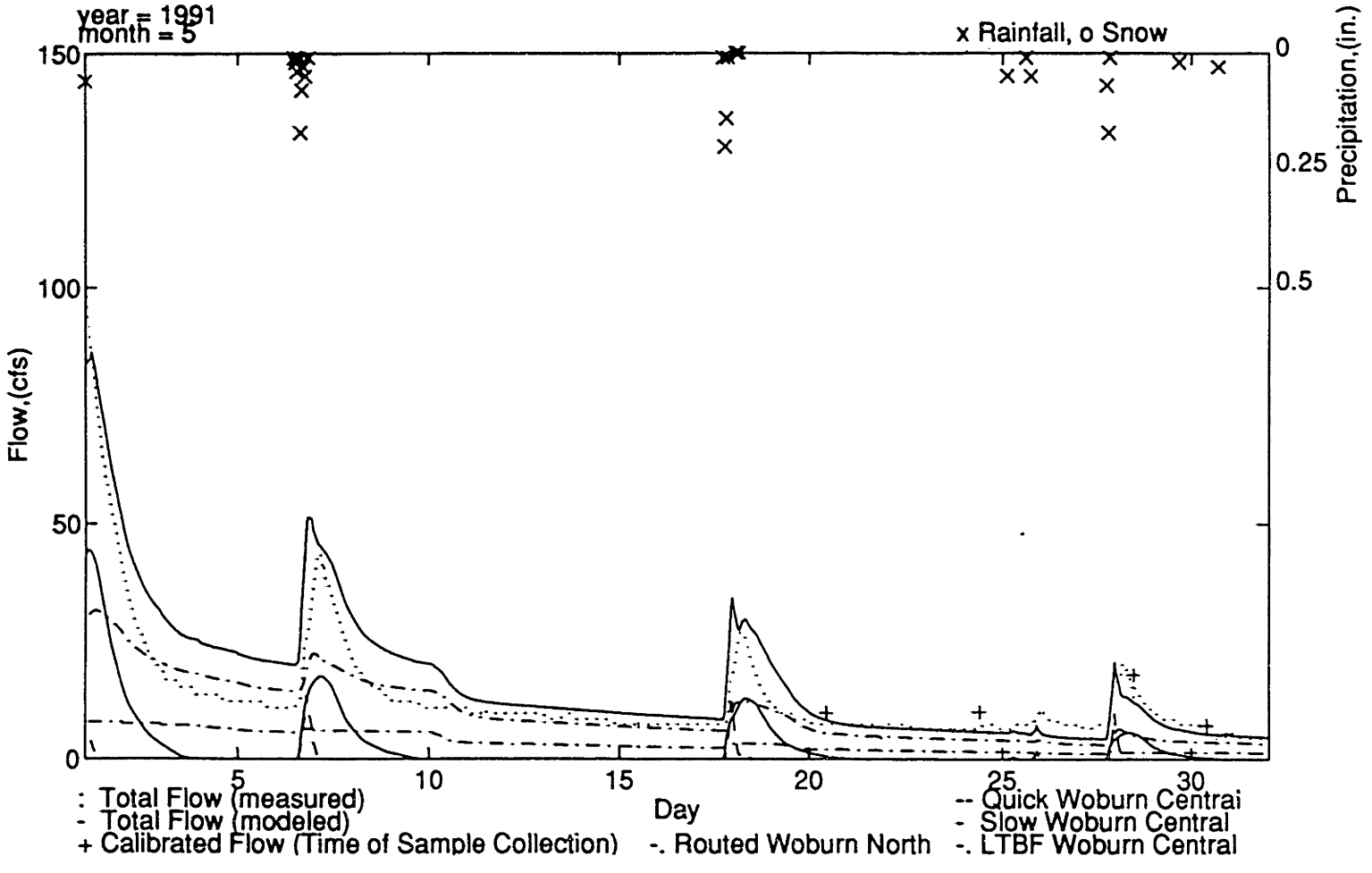

Figure V.C-25: Modeled versus Measured Streamflow, Time Series Plot, May 1991, Montvale (Gage 3)

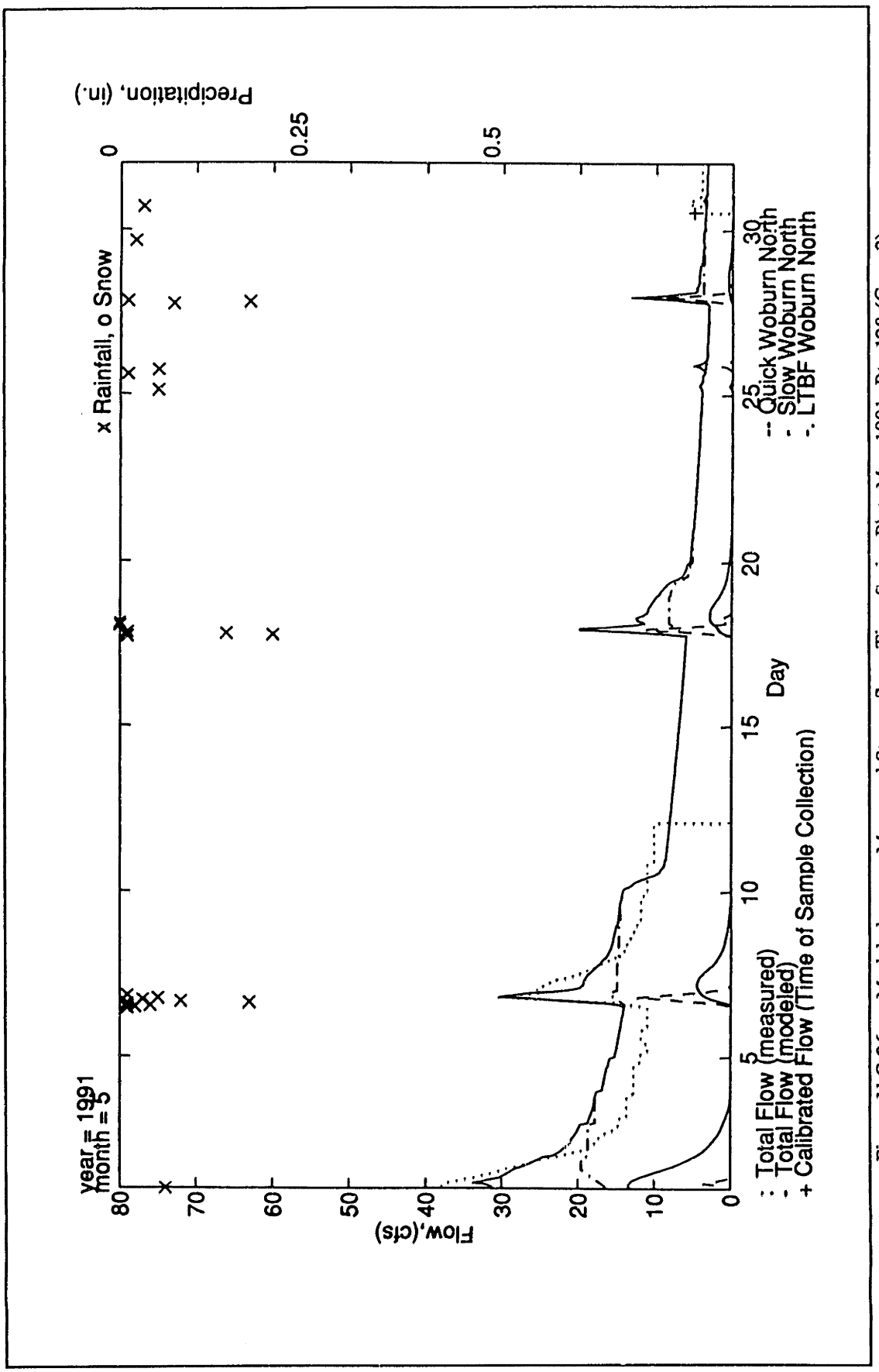

Figure V.C-26: Modeled versus Measured Streamflow, Time Series Plot, May 1991, Rte 128 (Gage 2)

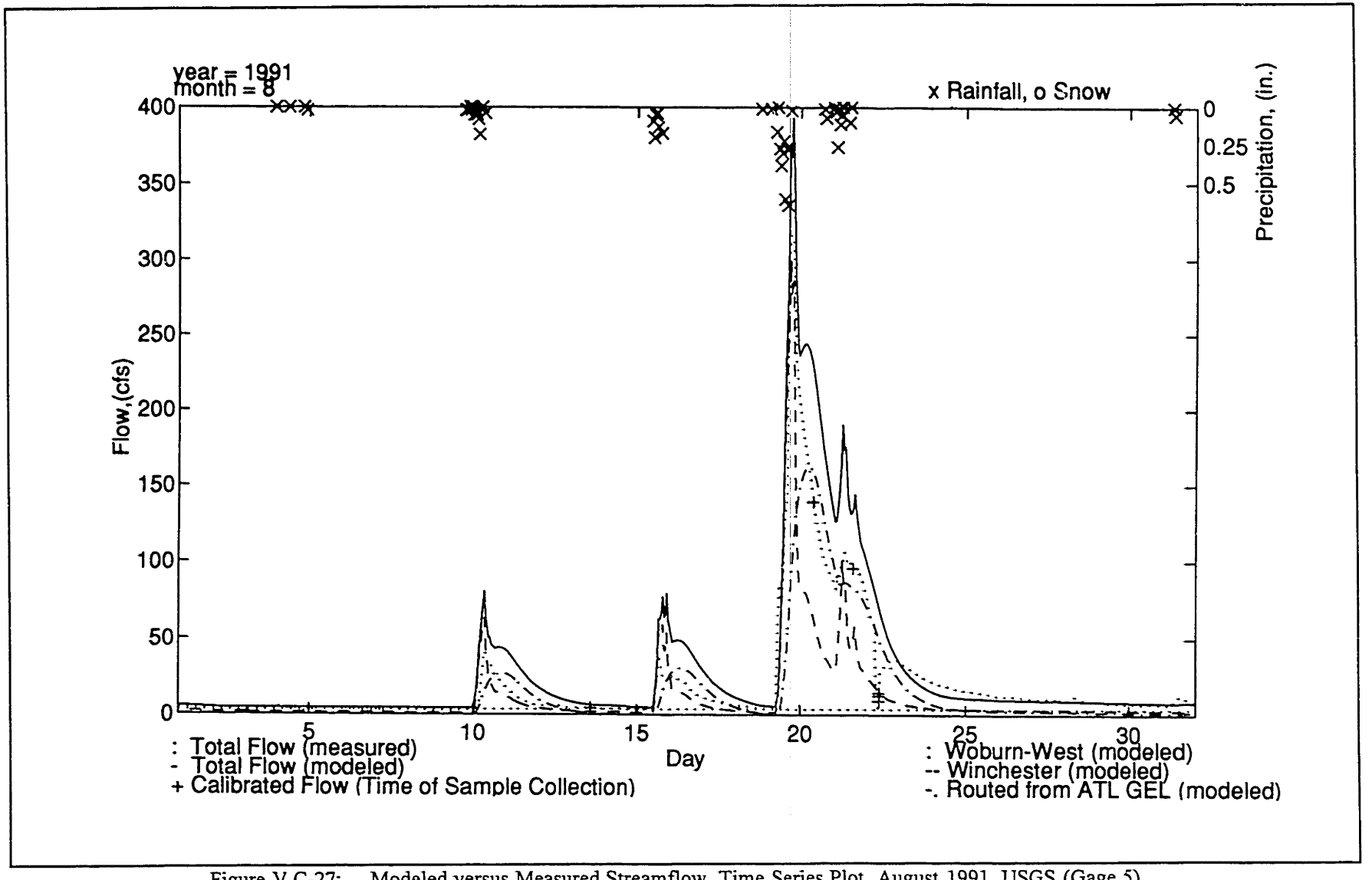

Figure V.C-27: Modeled versus Measured Streamflow, Time Series Plot, August 1991, USGS (Gage 5)

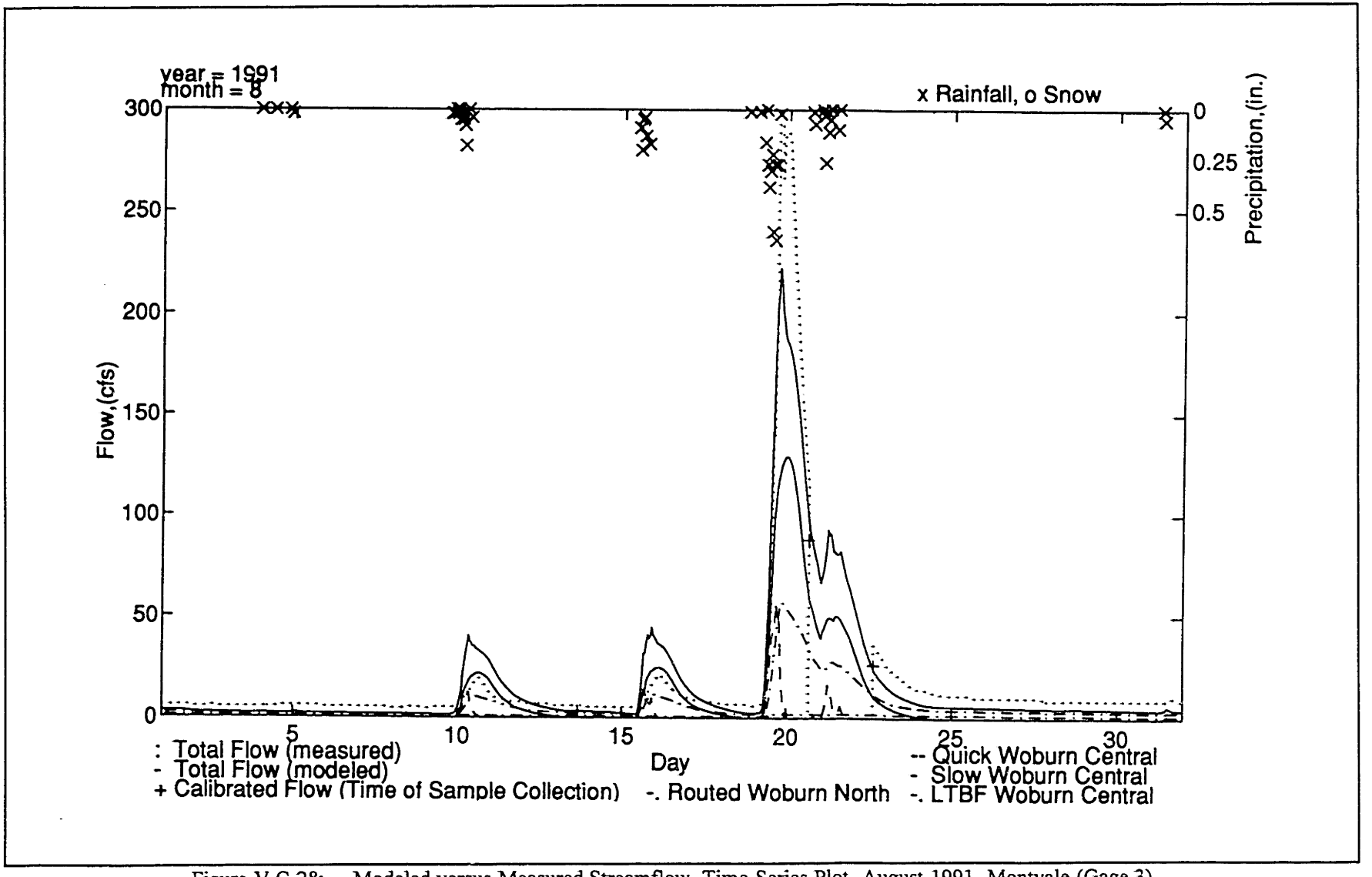

Figure V.C-28: Modeled versus Measured Streamflow, Time Series Plot, August 1991, Montvale (Gage 3)

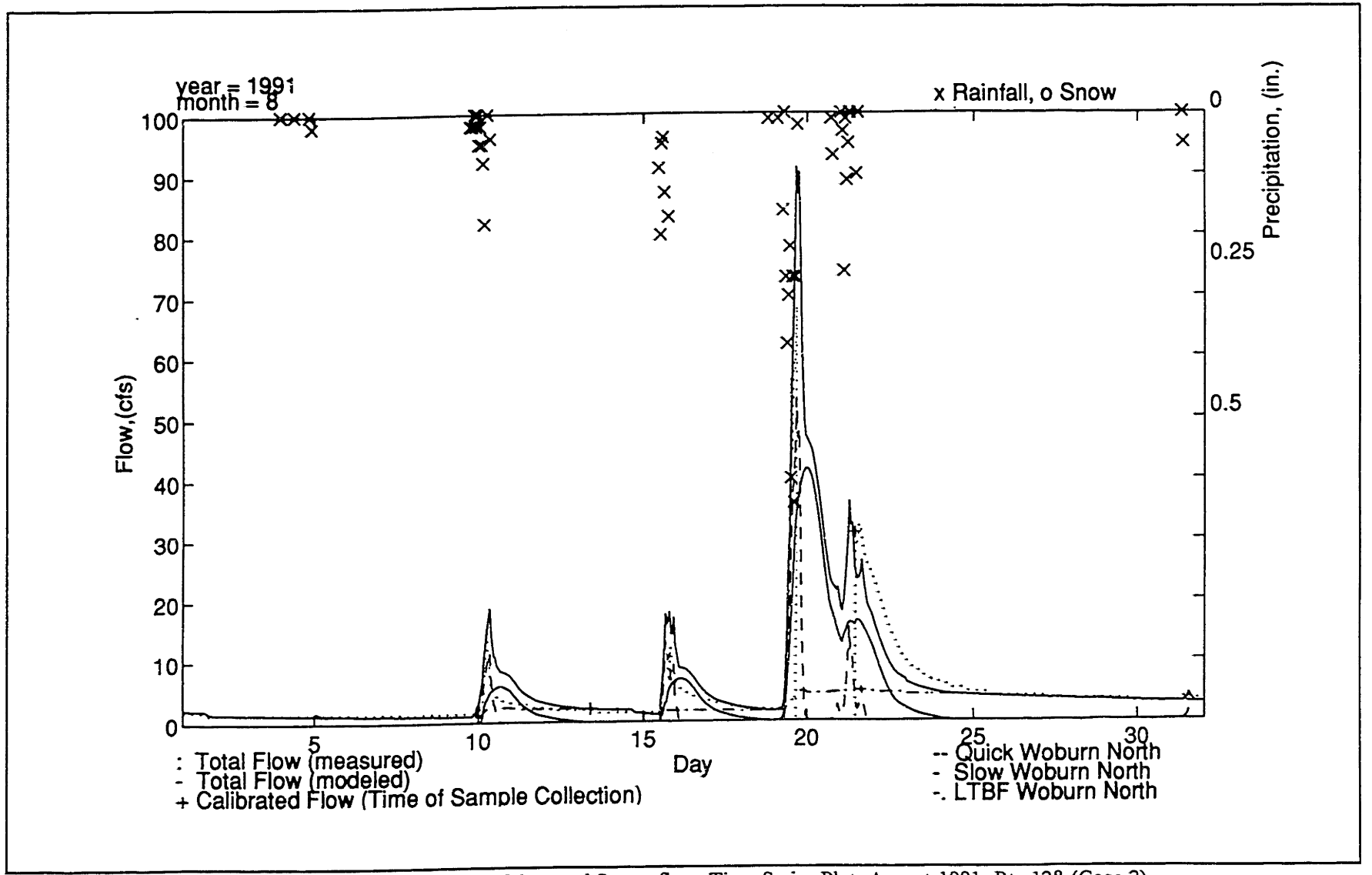

Figure V.C-29: Modeled versus Measured Streamflow, Time Series Plot, August 1991, Rte 128 (Gage 2)

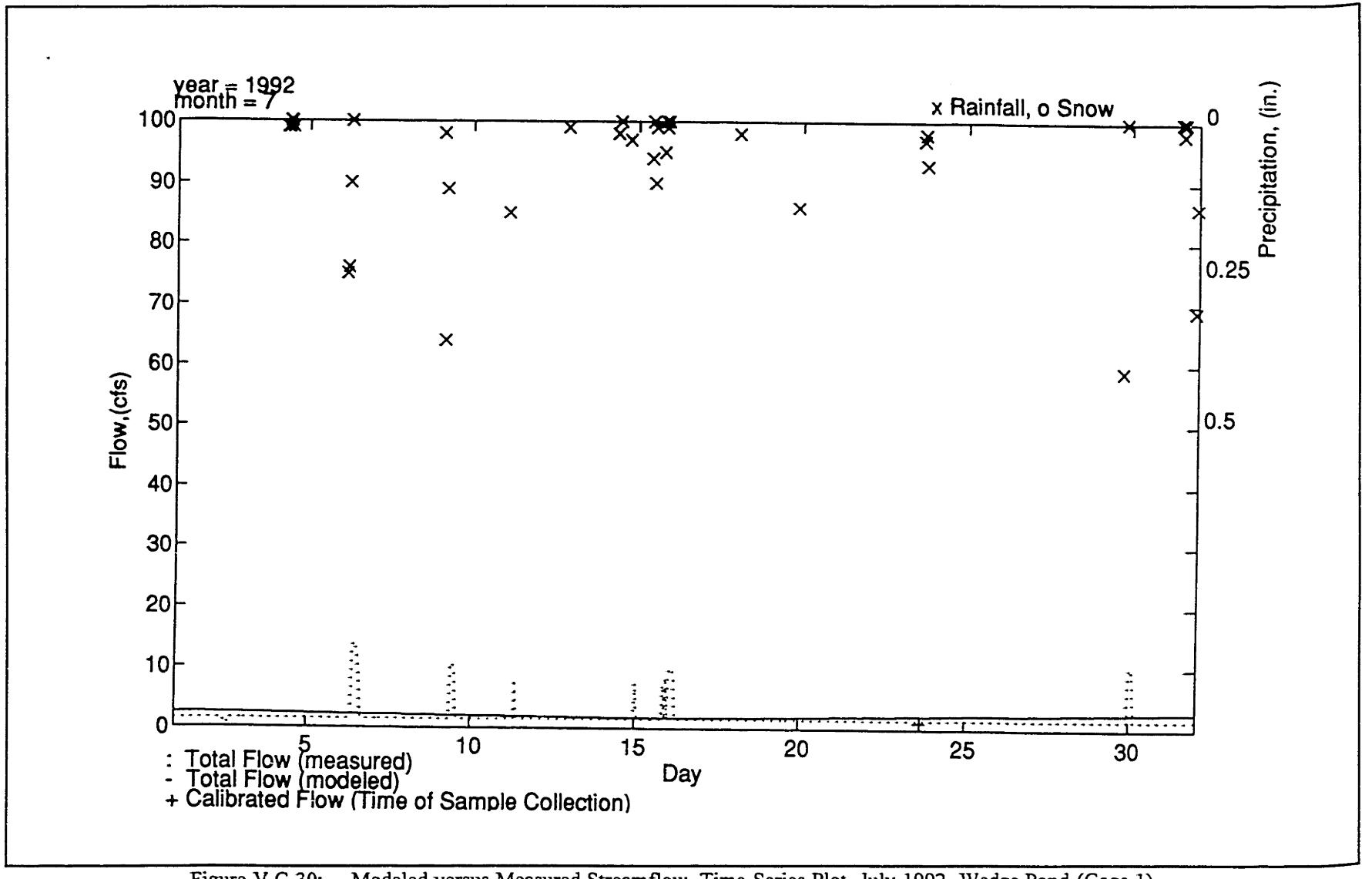

Figure V.C-30: Modeled versus Measured Streamflow, Time Series Plot, July 1992, Wedge Pond (Gage 1)

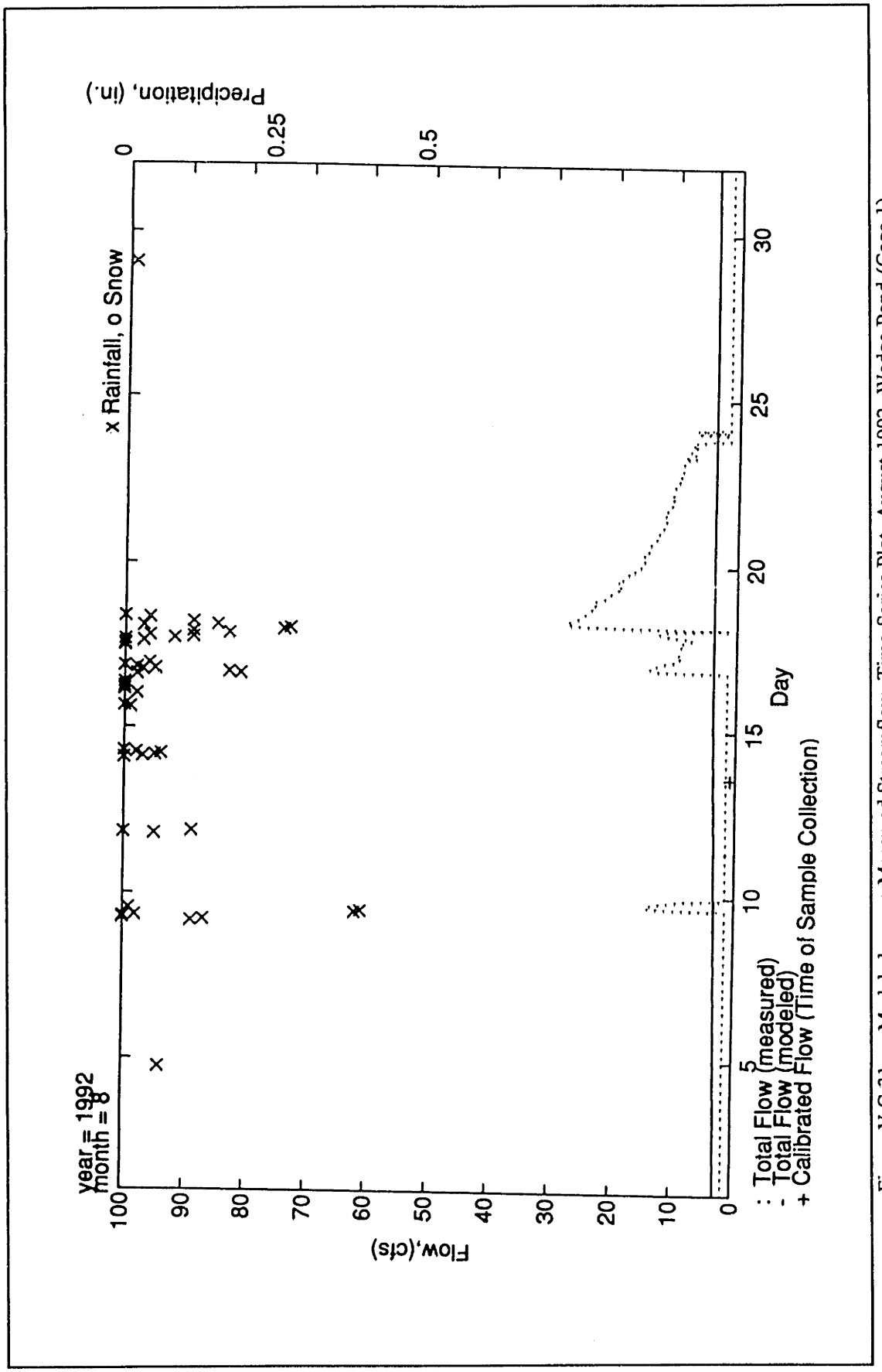

Figure V.C-31: Modeled versus Measured Streamflow, Time Series Plot, August 1992, Wedge Pond (Gage 1)

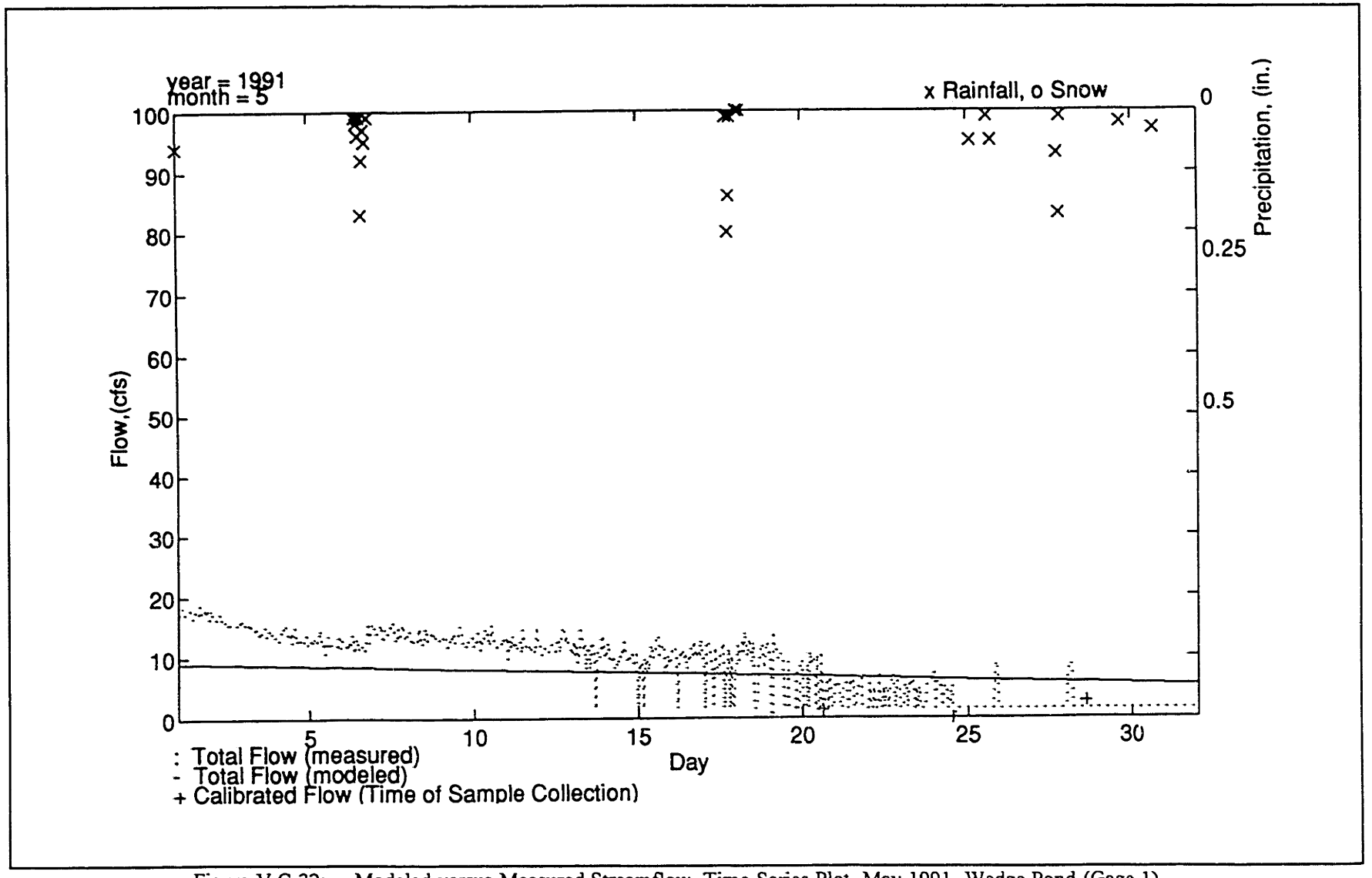

Figure V.C-32: Modeled versus Measured Streamflow, Time Series Plot, May 1991, Wedge Pond (Gage 1)

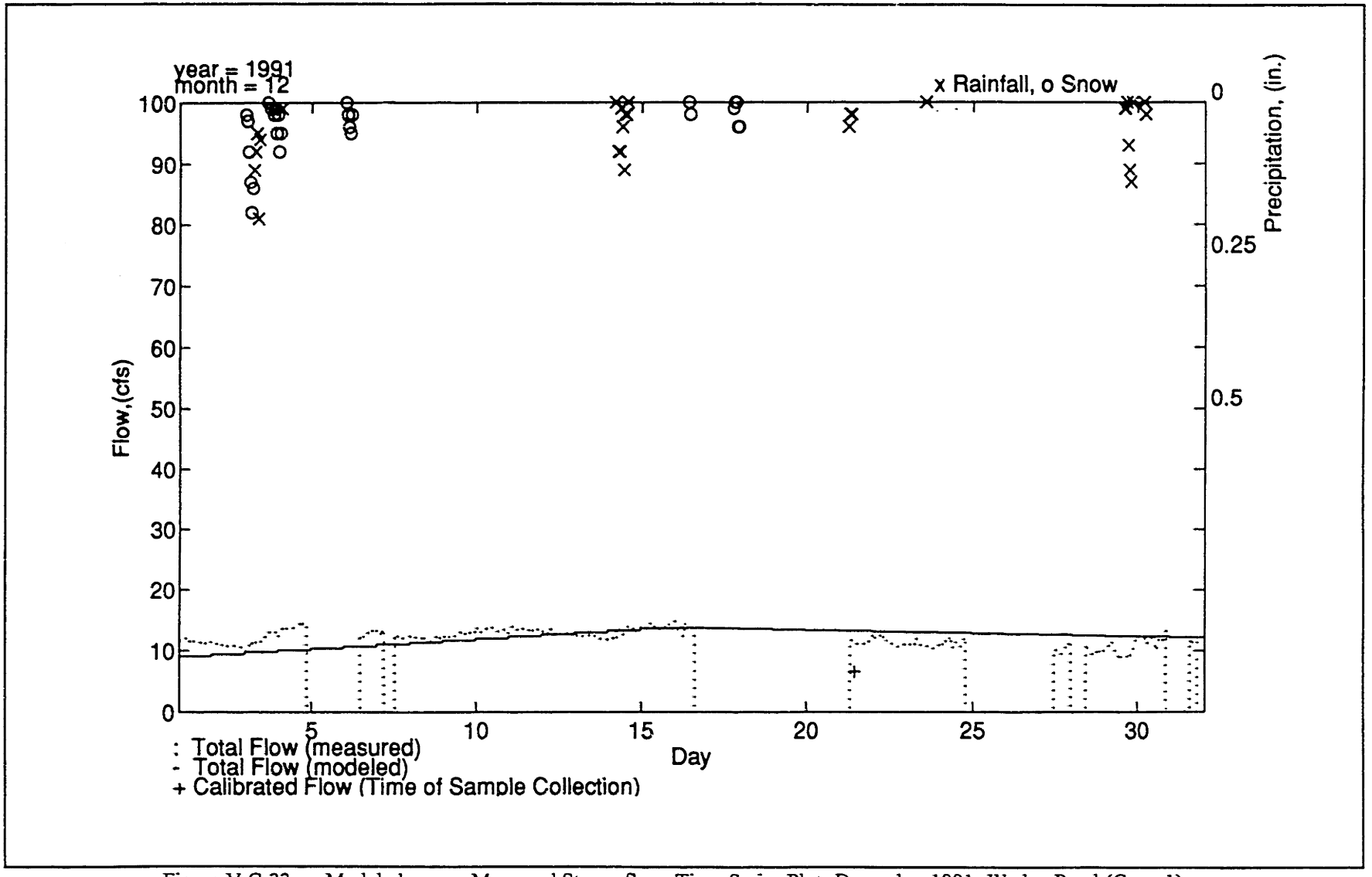

Figure V.C-33: Modeled versus Measured Streamflow, Time Series Plot, December 1991, Wedge Pond (Gage 1)

DETAILS OF MODEL PERFORMANCE: DISSOLVED METALS

The computer model results for dissolved iron, chromium, and copper are discussed in the following pages. Dissolved arsenic results are included in section V.3.2 in the main body of the text.

Iron

The dissolved iron R^2 values were equal to 0.44 and 0.62 for the 1992 and 1993 model years. The 1992 modeled versus measured flux plot (figure V.C-34) is characterized by an general scatter above and below the one to one line. This scatter is due to the model's incapability of capturing short term fluctuations in dissolved iron concentrations (figure V.C-35 and figure V.C-36) and is also associated with errors in the streamflow measurements (December 17 sample, figure V.C-19).

For 1993, the measured dissolved iron fluxes were modeled within a factor of 2 (figure V.C-37). During the March 29 event (figure V.C-38), the measured flux had a much steeper rate of increase than the modeled value. This incompatibility was due to the combination of: 1) an over-estimation of the streamflow at the beginning of the storm (figure V.C-22), and 2) an under-estimation of the dissolved iron concentration during later parts of the storm (figure V.C-38).

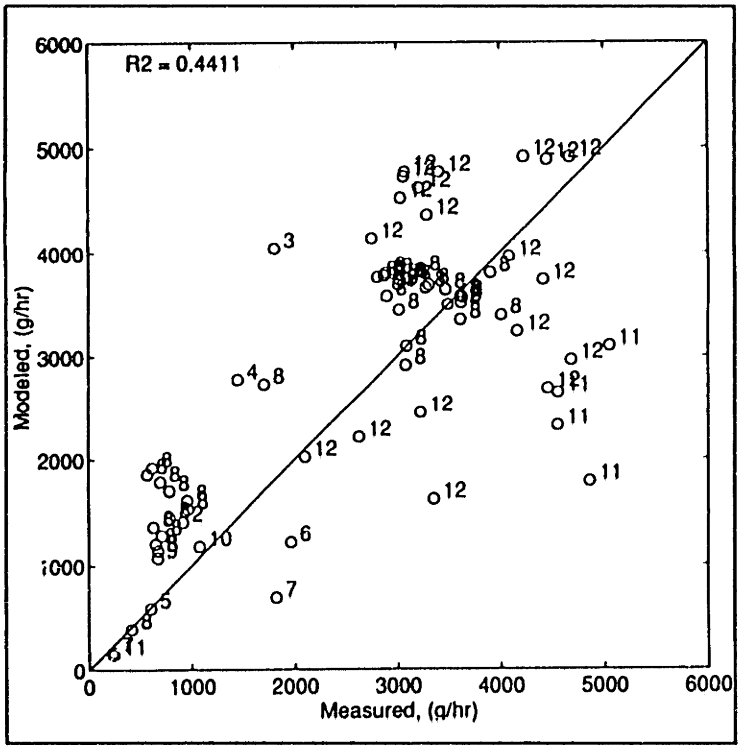

Figure V.C-34: Modeled vs Measured Dissolved Iron Flux
Gage 5, 1992 (Calibration)

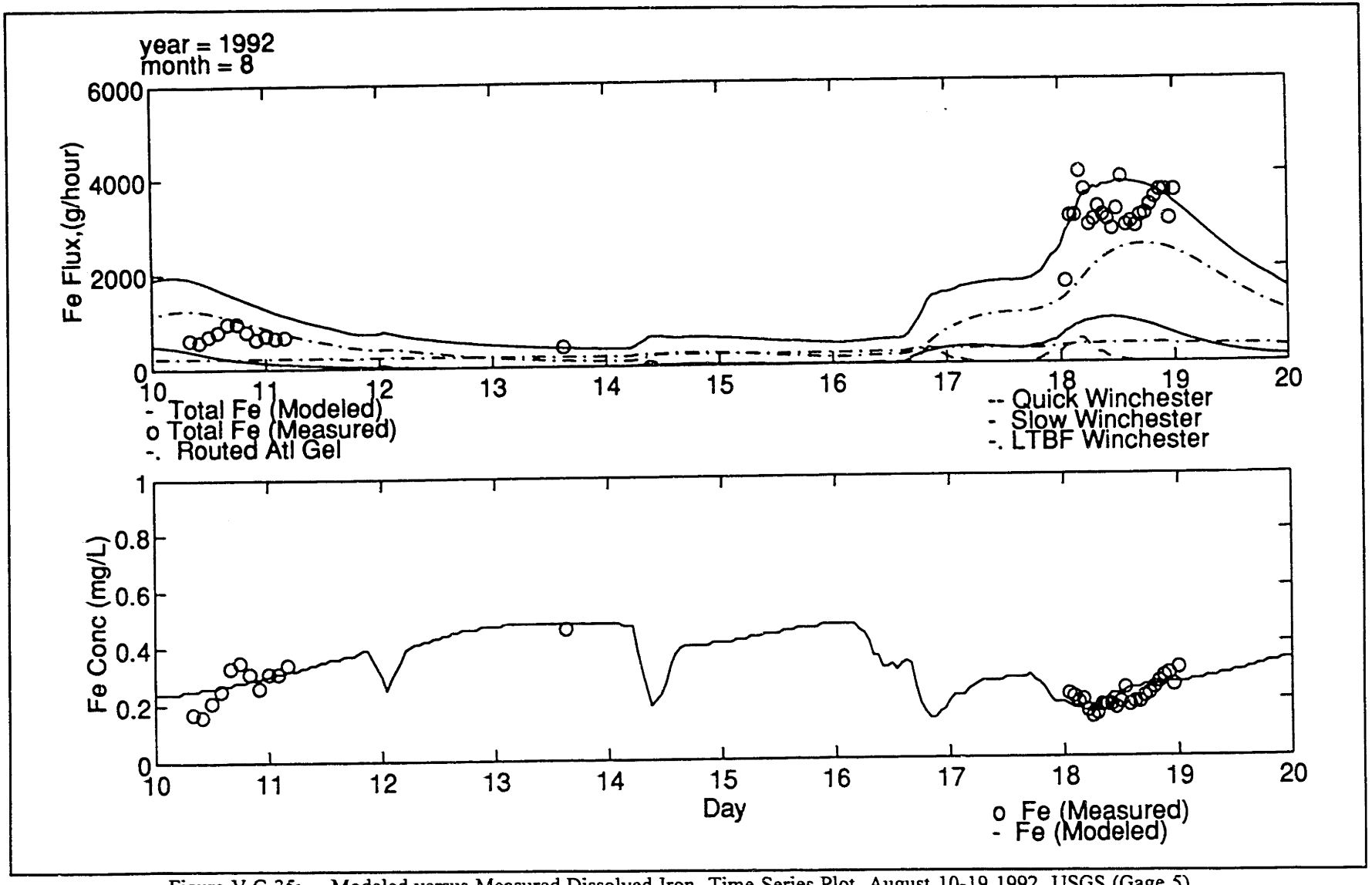

Figure V.C-35: Modeled versus Measured Dissolved Iron, Time Series Plot, August 10-19 1992, USGS (Gage 5)

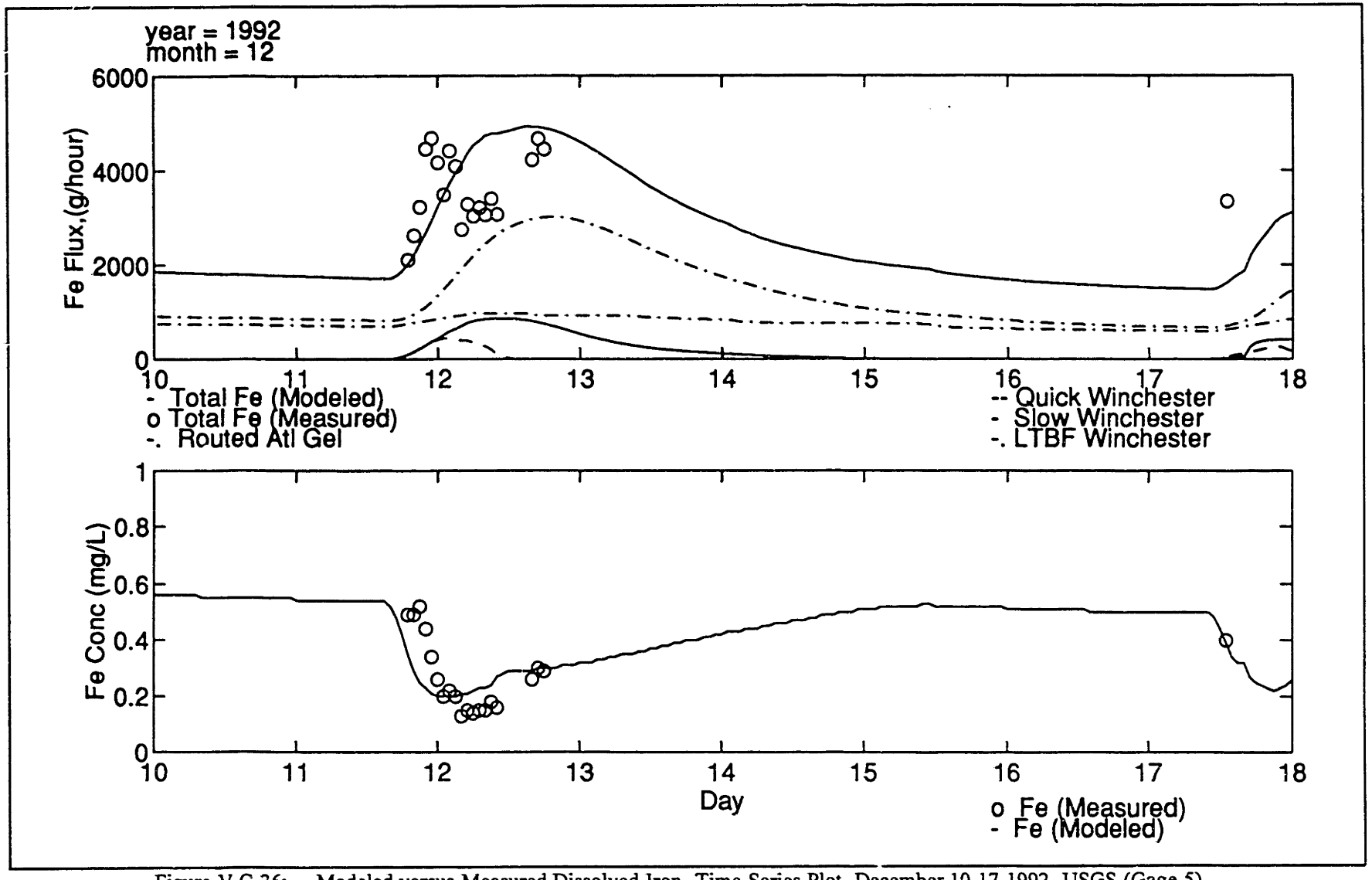

Figure V.C-36: Modeled versus Measured Dissolved Iron, Time Series Plot, December 10-17 1992, USGS (Gage 5)

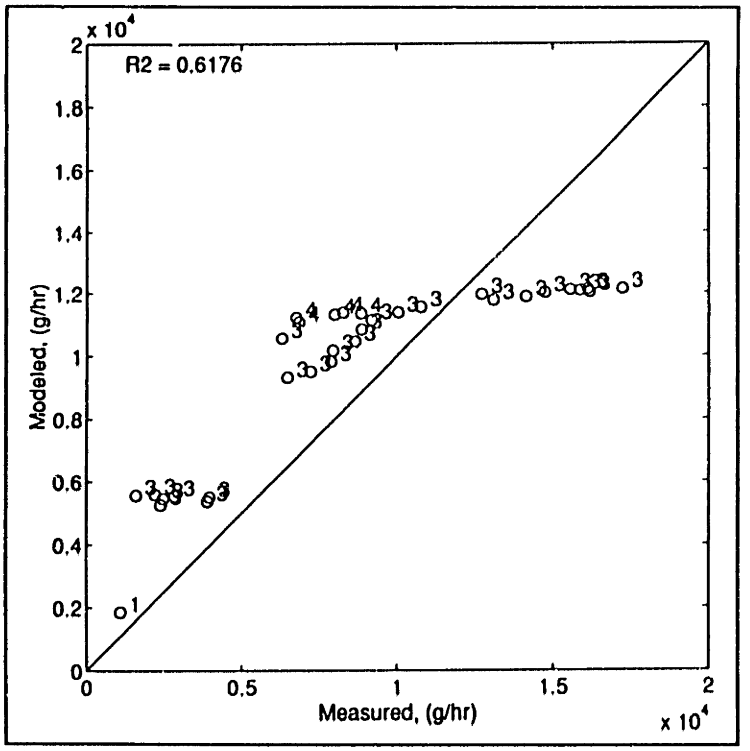

Figure V.C-37: Modeled vs Measured Dissolved Iron Flux Gage 5, 1993 (Verification)

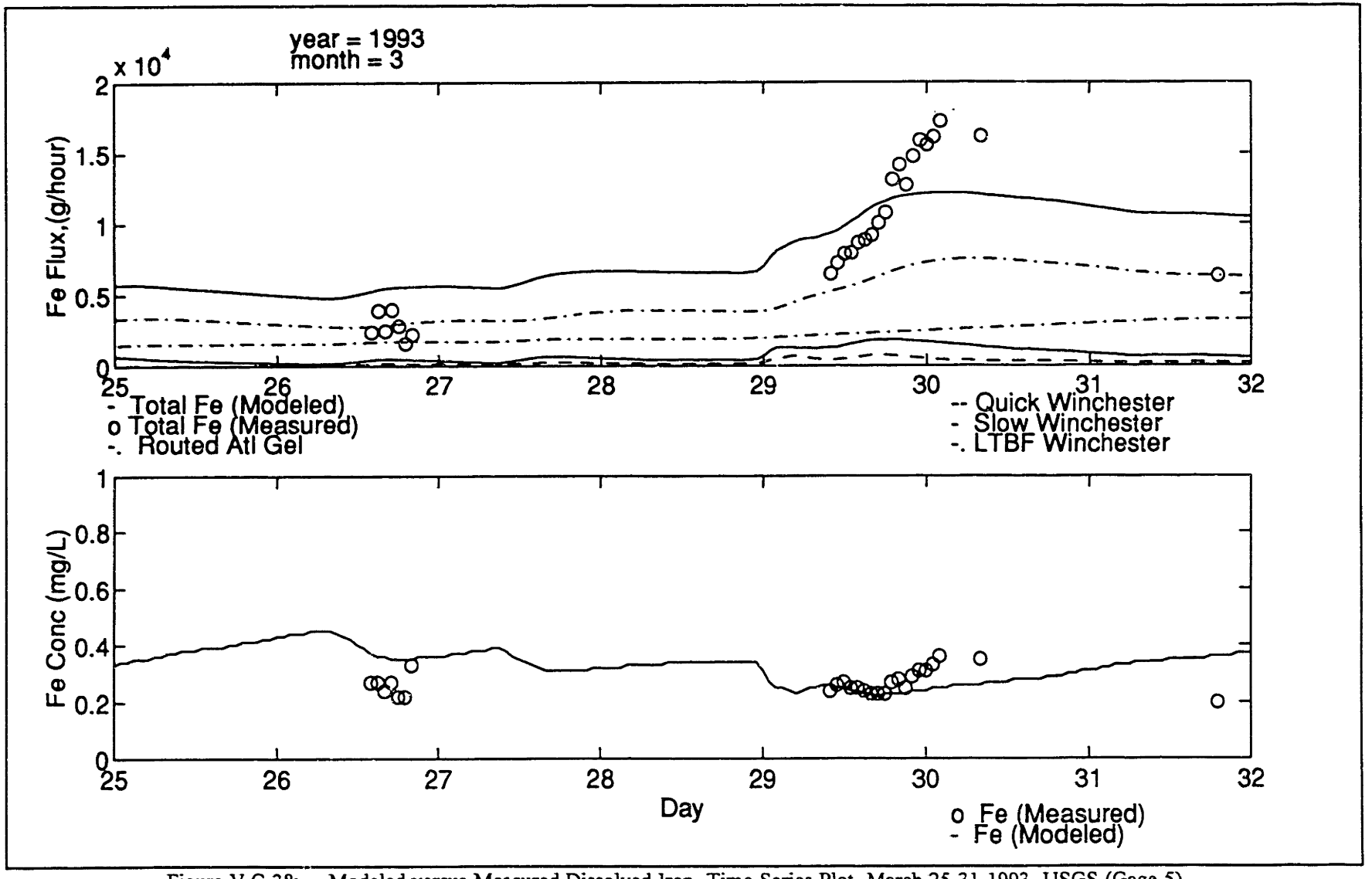

Figure V.C-38: Modeled versus Measured Dissolved Iron, Time Series Plot, March 25-31 1993, USGS (Gage 5)

Chromium

R^2 values for dissolved chromium were 0.60 and 0.73 for the 1992 and 1993 model runs. Measured chromium fluxes for the 1992 model year were, for the most part, well modeled. (figure V.C-39) The most notable outlier, however, is the August 18 13:00 sample which corresponded to the concentration blip in the August 18th storm data. (figure V.C-40) Because of the way the model is formulated, the model was not capable of capturing abrupt changes in metal concentrations.

For 1993, the dissolved chromium fluxes were modeled within a factor of 2. (figure V.C-42) During the March 29 event (figure V.C-43), the measured flux was characterized by larger fluctuations than the model predicted. The lack of fluctuations in the model was due to the inability of the model to reproduce abrupt changes in dissolved metal concentrations.

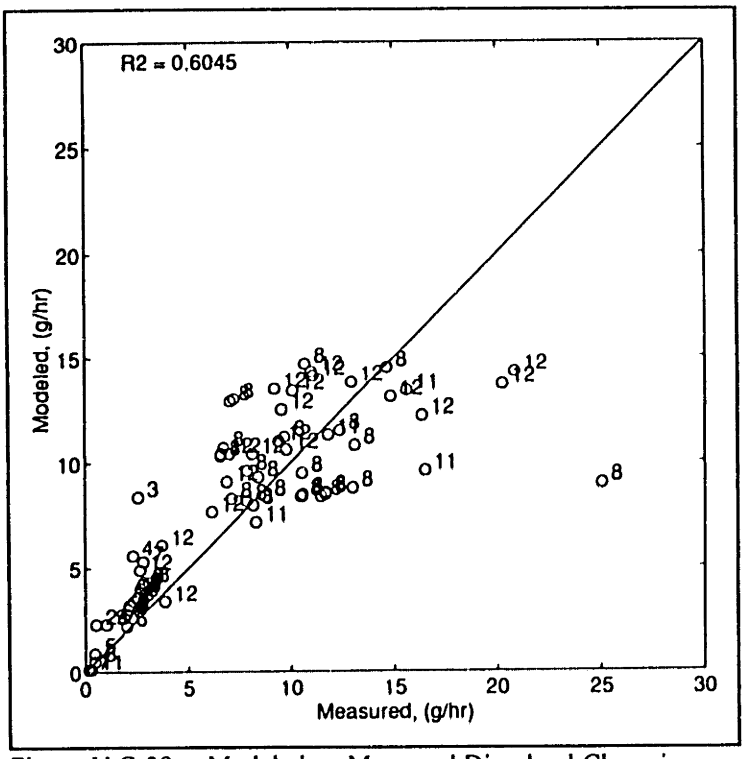

Figure V.C-39: Modeled vs Measured Dissolved Chromium Flux, Gage 5, 1992 (Calibration)

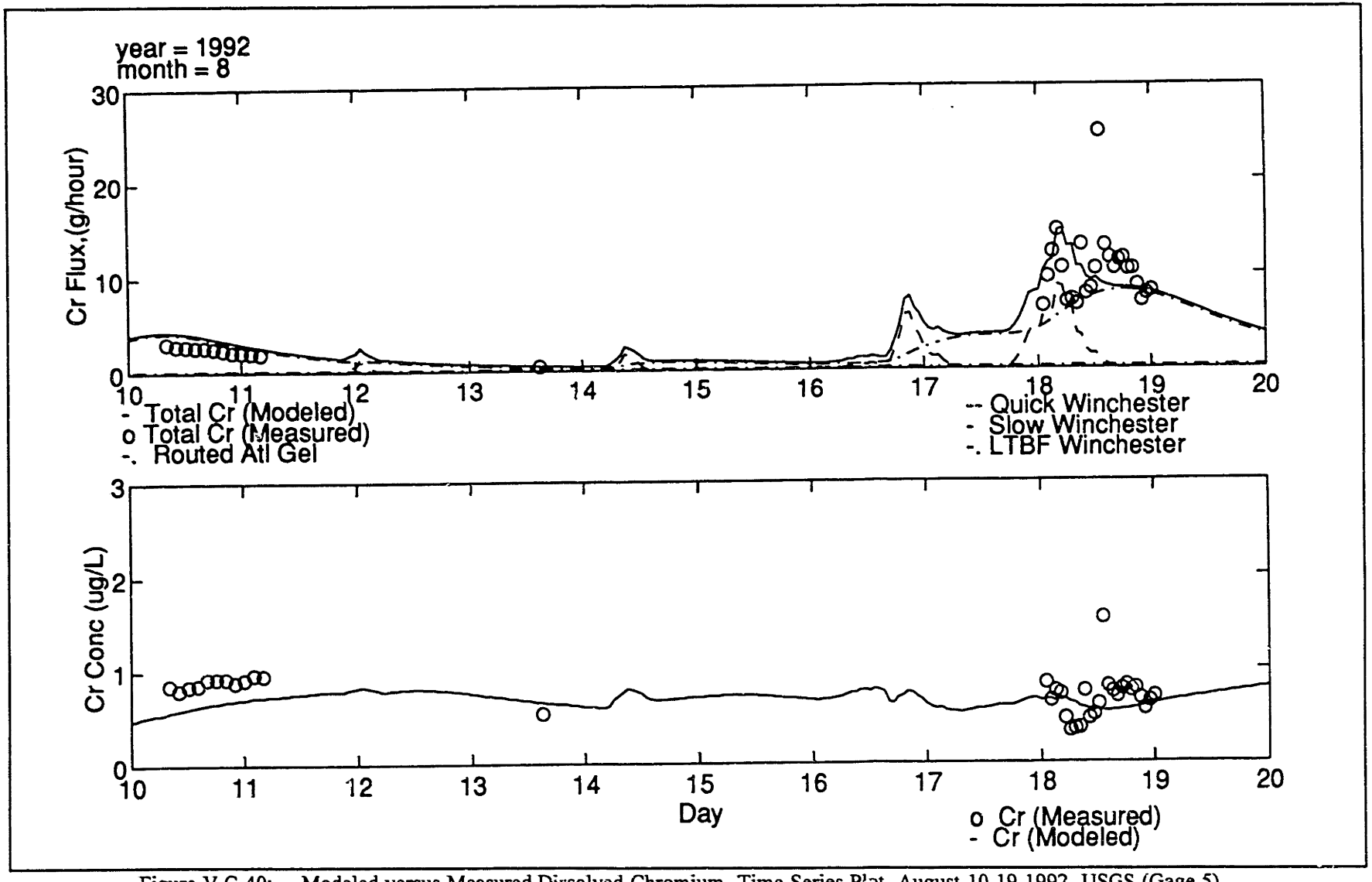

Figure V.C-40: Modeled versus Measured Dissolved Chromium, Time Series Plot, August 10-19 1992, USGS (Gage 5)

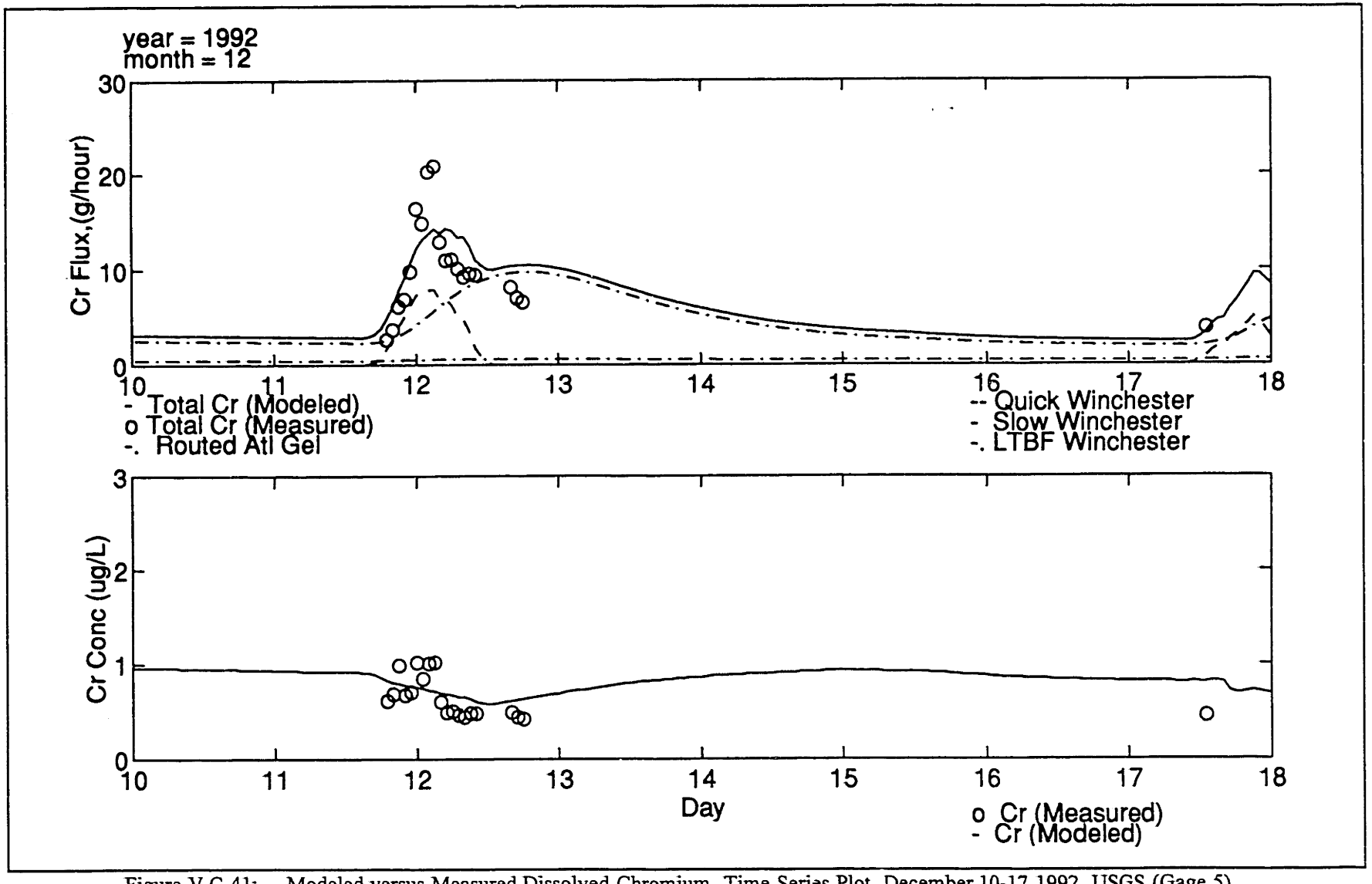

Figure V.C-41: Modeled versus Measured Dissolved Chromium, Time Series Plot, December 10-17 1992, USGS (Gage 5)

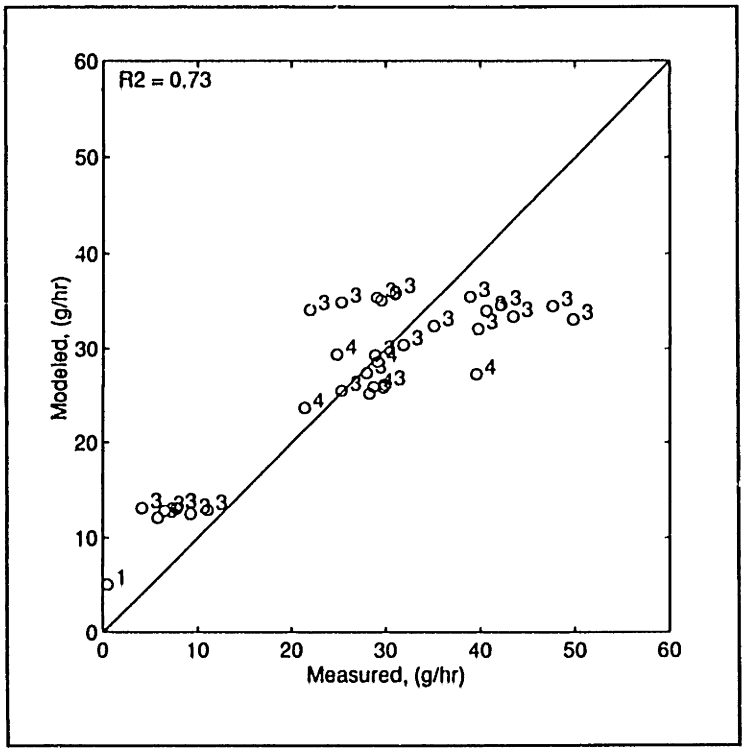

Figure V.C-42: Modeled vs Measured Dissolved Chromium Flux, Gage 5, 1993 (Verification)

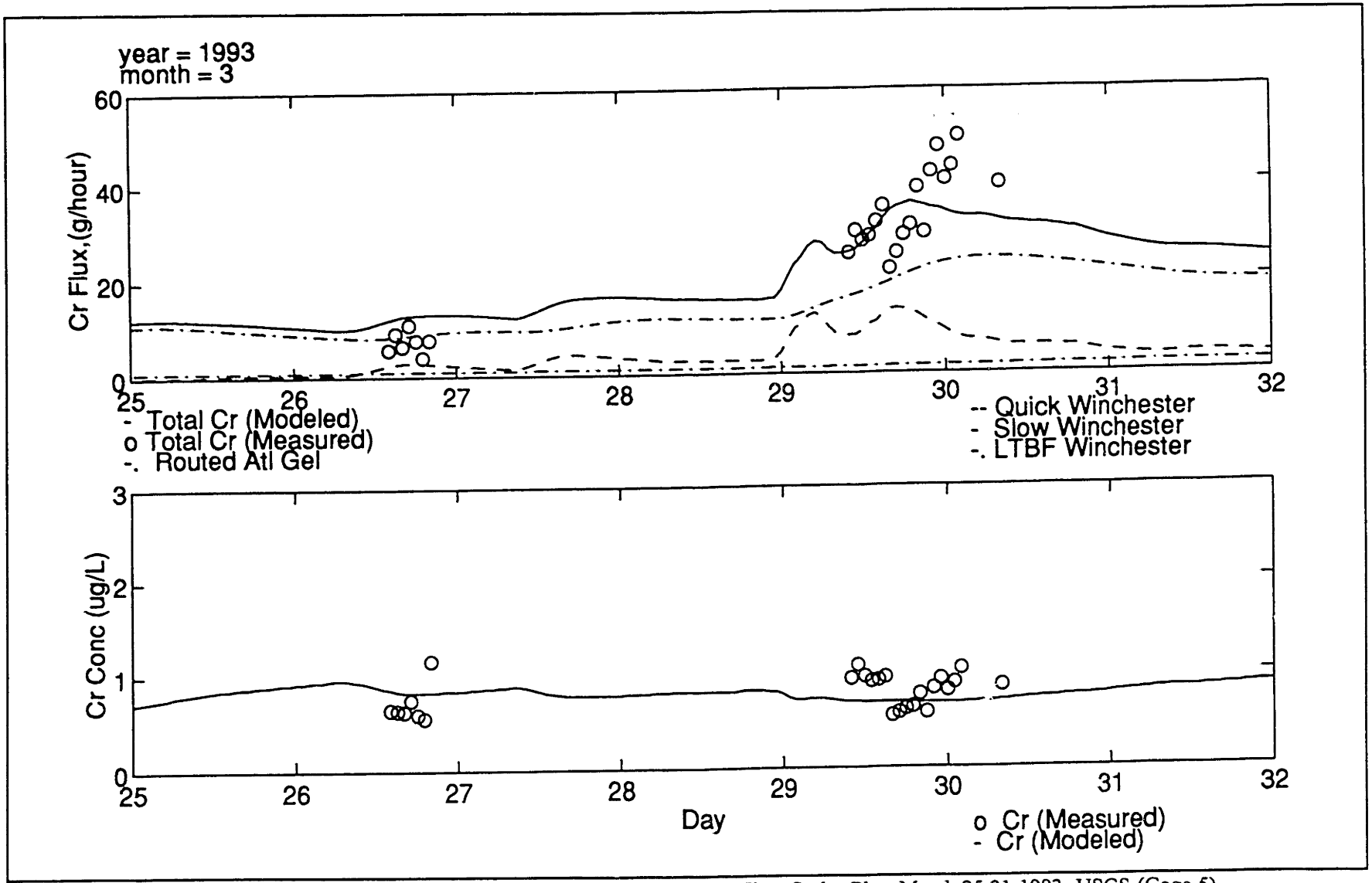

Figure V.C-43: Modeled versus Measured Dissolved Chromium, Time Series Plot, March 25-31 1993, USGS (Gage 5)

Copper

Dissolved copper had the best results with respect to the R^2 values. The R^2 values obtained for the 1992 and 1993 model runs were 0.77 and 0.69 respectively. For 1992, the primary source of error for the copper runs was the model's inability to reproduce short term changes in the measured dissolved copper concentrations. (figures V.C-45 and V.C-46)

The 1993 model run was characterized by a relatively good fit of the data. (figure V.C-47) Part of the reason for this good fit was due to the fact that dissolved copper concentrations were under-estimated during early part of the March 29 storm (figure V.C-48) when streamflow was over-estimated. The net effect was a balance of errors, resulting in a good fit of the data.

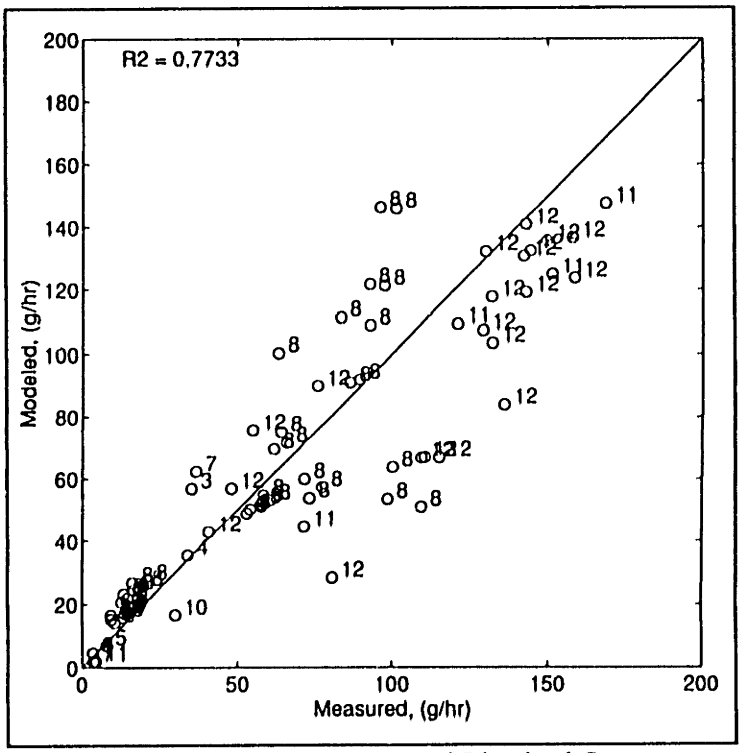

Figure V.C-44: Modeled vs Measured Dissolved Copper Flux, Gage 5, 1992 (Calibration)

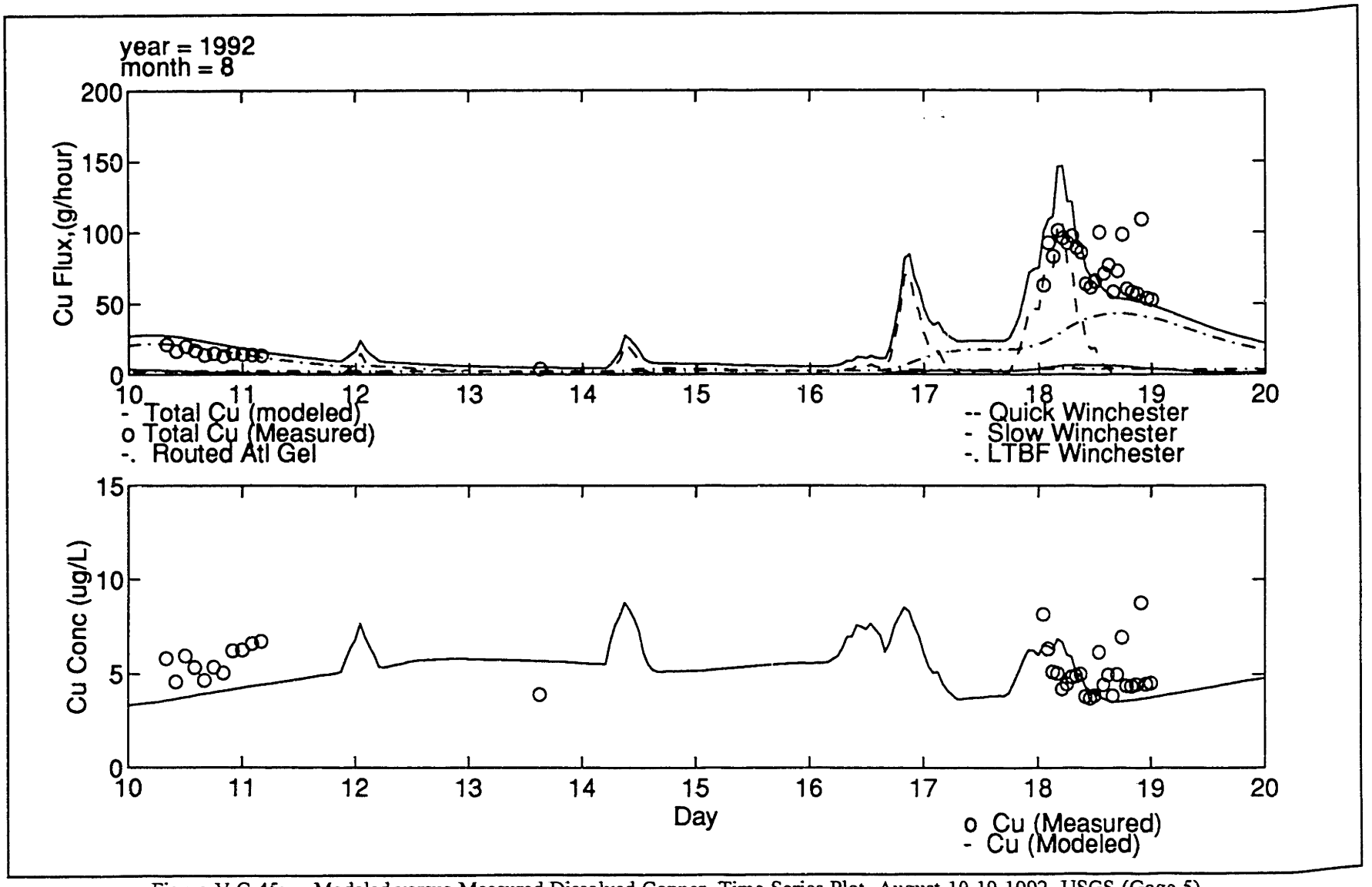

Figure V.C-45: Modeled versus Measured Dissolved Copper, Time Series Plot, August 10-19 1992, USGS (Gage 5)

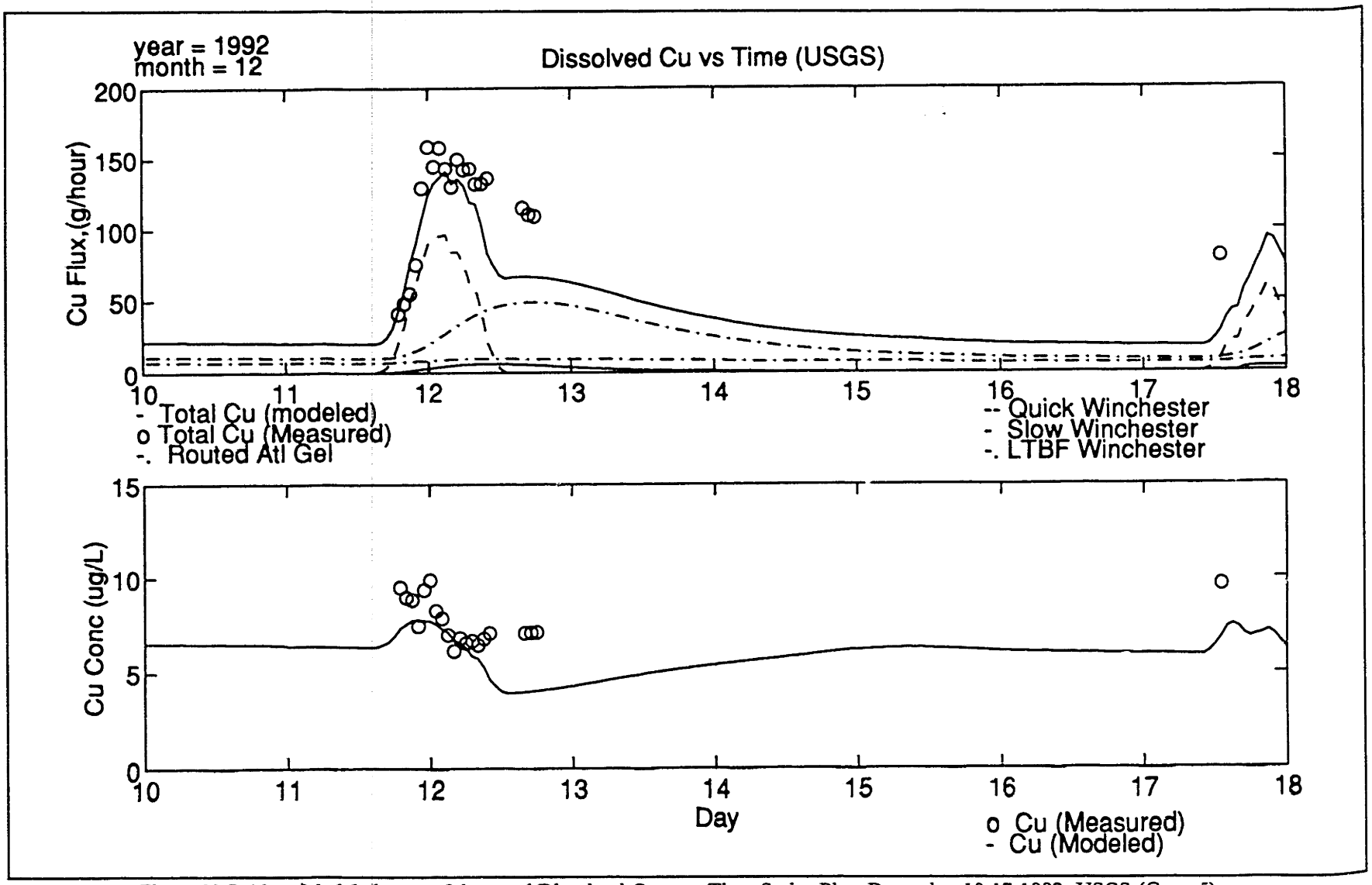

Figure V.C-46: Modeled versus Measured Dissolved Copper, Time Series Plot, December 10-17 1992, USGS (Gage 5)

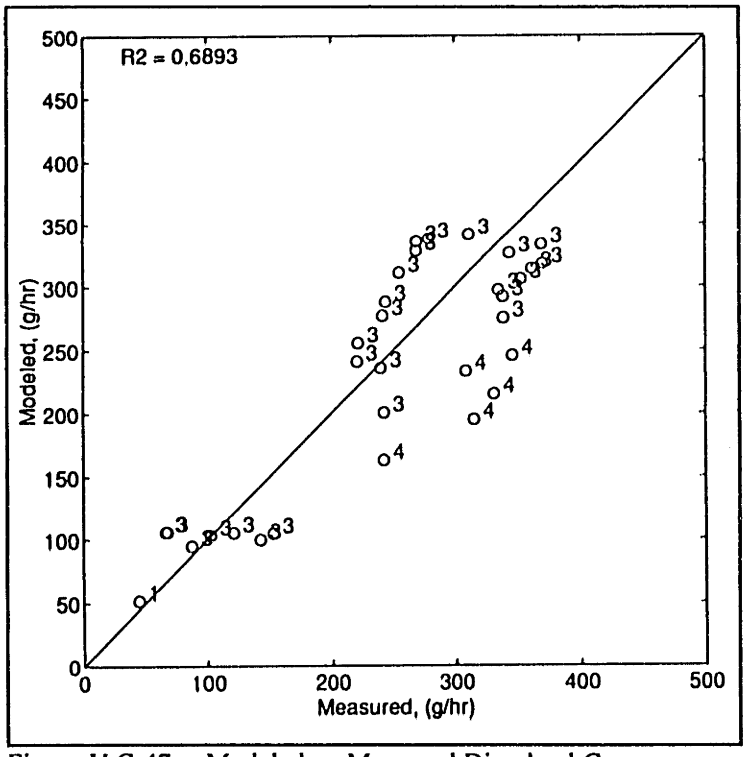

Figure V.C-47: Modeled vs Measured Dissolved Copper Flux, Gage 5, 1993 (Verification)

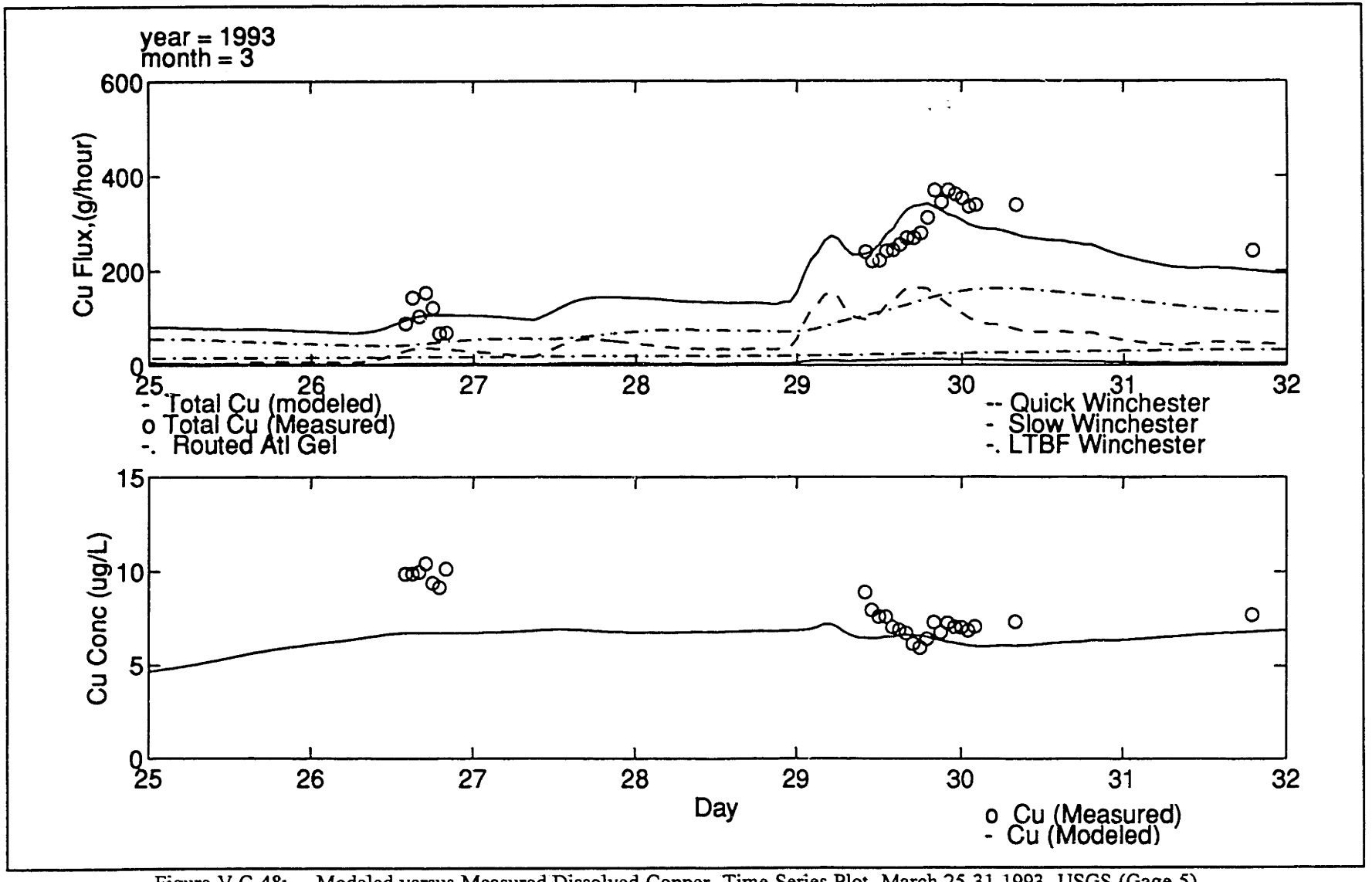

Figure V.C-48: Modeled versus Measured Dissolved Copper, Time Series Plot, March 25-31 1993, USGS (Gage 5)

DETAILS OF MODEL PERFORMANCE: PARTICULATE METALS

Discussion of model performance for particulate iron, chromium, and copper are included in the following pages. Particulate arsenic results are included in section V.3.5 in the main body of the text.

Iron

The R^2 value for particulate iron fluxes during the 1992 calibration year was 0.04. For this data set, the model estimated most of the measured fluxes reasonably well. The primary error was associated with the November samples. Without the November samples, the R^2 value computed was 0.80.

Time series plots for iron were very similar to the plots for arsenic. During the August 18th sampling period (figure V.C-50), the model was capable of capturing the initial burst of particulate iron flux at the beginning of the storm event and the slower decline in the flux which followed immediately after the initial burst. For this sampling period, the model reproduced the iron concentration very well at the beginning of the sampling period and slightly under-estimated the concentration toward the end of the sampling period. The over-estimation of the iron flux for the first sample can be associated with a timing error in the suspended sediment concentrations modeled (figure V.3-12). The model, as evidenced by the August 13th sample, was also capable of capturing the extremely low iron fluxes which occurred during very low flow. The August 10th sampling period was also reasonably well modeled. However, for these data, the errors in modeling the streamflow, suspended sediment concentration, and particulate arsenic concentrations partially canceled out.

For the November samples (figure V.C-51) the model over-estimated the particulate iron flux in the vicinity of the peak. This error was primarily due to the over-estimation of the suspended sediment flux for this event (figure V.3-13).

For the December samples (figure V.C-52), the model performed very well. The model was capable of capturing, on a point by point basis,: 1) the overall rate of increase and decrease in the iron flux and, 2) the magnitude of the peak iron flux. Only, the last three samples in the set were somewhat over-estimated. This over-estimation was due to the combined over-estimation (but slight) of the streamflow, suspended sediment concentration, and iron concentration.

The R^2 value for the 1993 pseudo-verification year was 0.47. For the March 29th event (figure V.C-54), the model was again capable of reproducing the rate of increase and decrease in the particulate iron flux.

However, the lack of one to one correspondence between the modeled and measured data was primarily due to a time shift error between the modeled and the measured data.

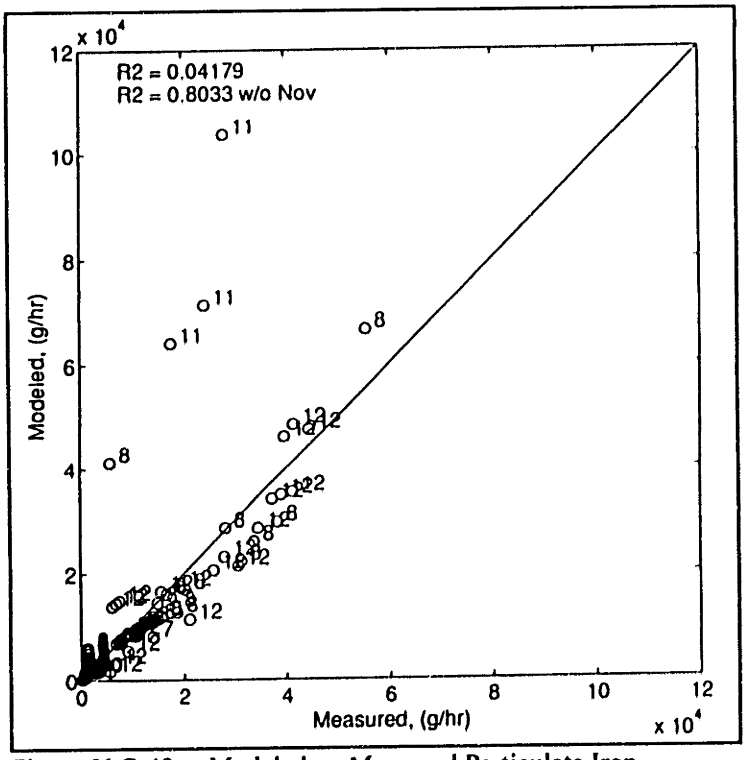

Figure V.C-49: Modeled vs Measured Particulate Iron Flux, Gage 5, 1992 (Calibration)

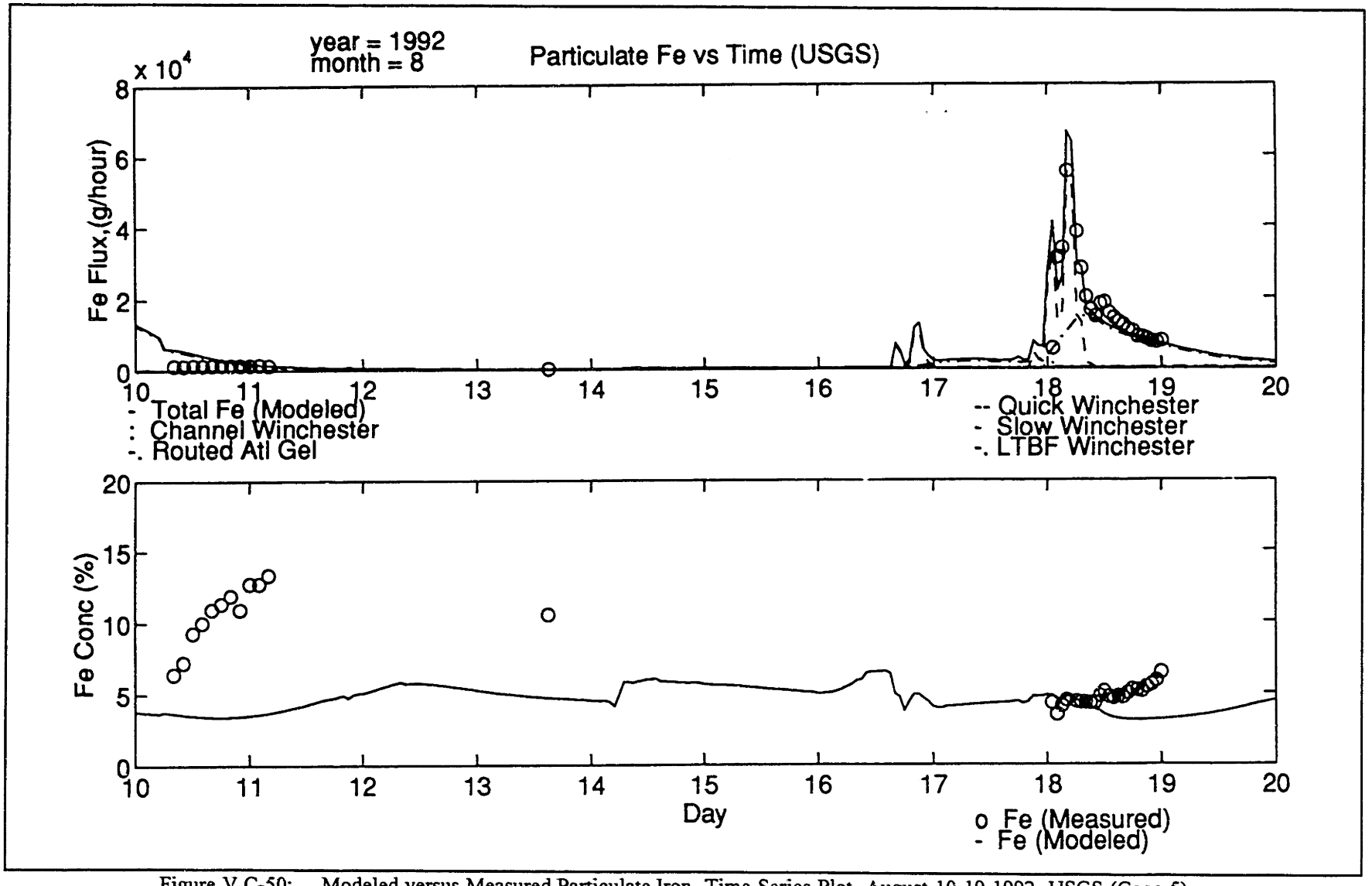

Figure V.C-50: Modeled versus Measured Particulate Iron, Time Series Plot, August 10-19 1992, USGS (Gage 5)

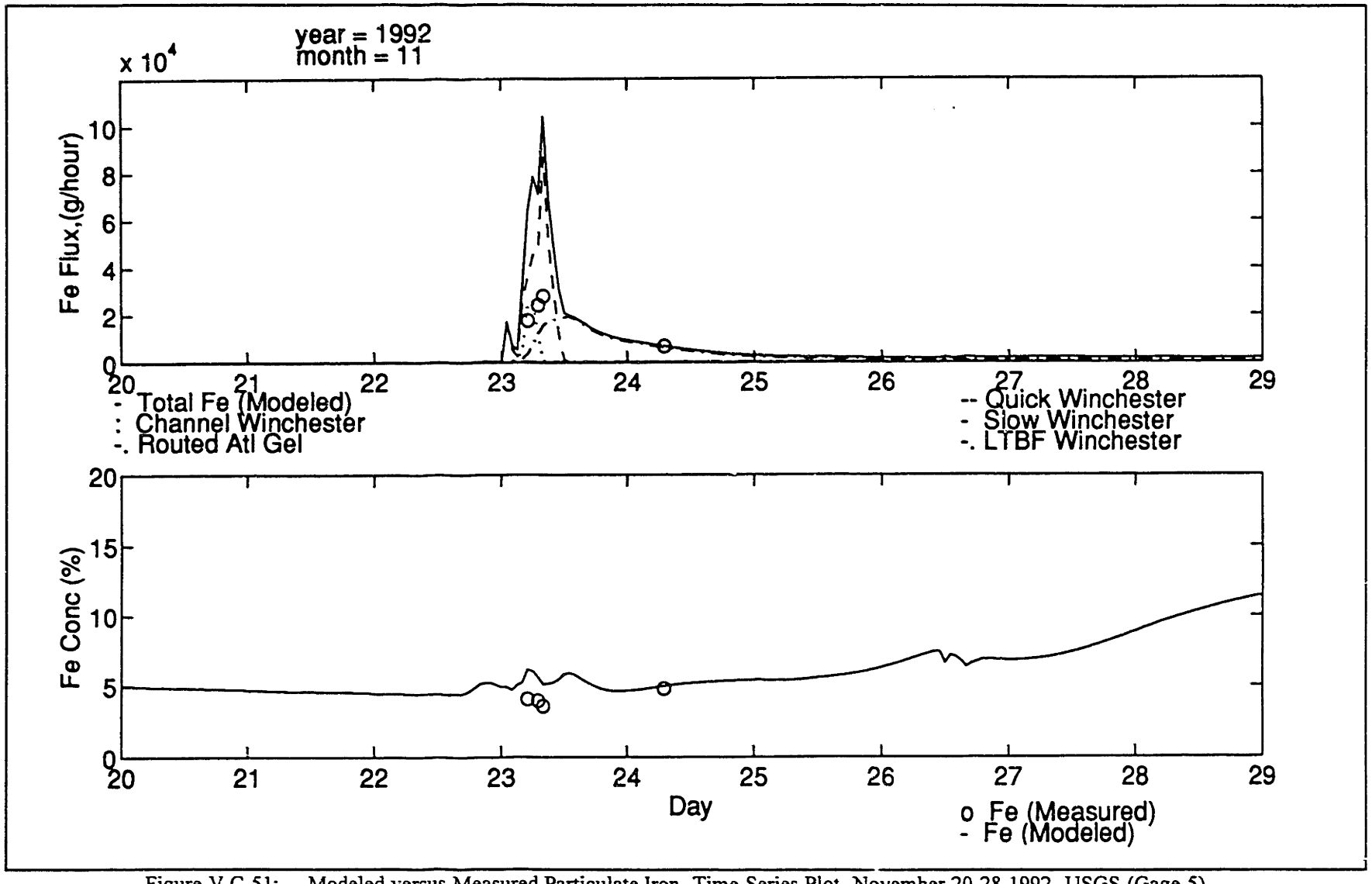

Figure V.C-51: Modeled versus Measured Particulate Iron, Time Series Plot, November 20-28 1992, USGS (Gage 5)

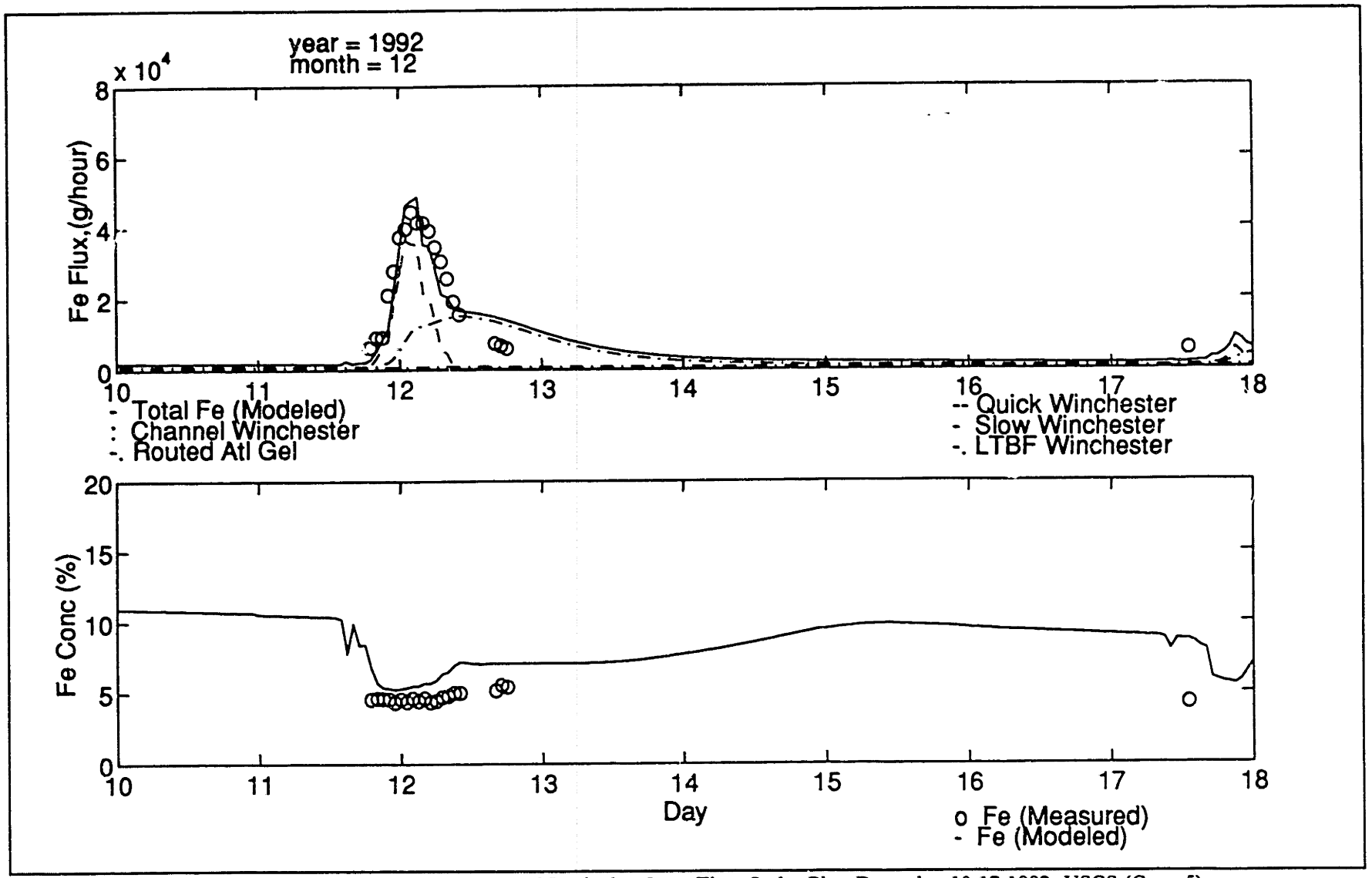

Figure V.C-52: Modeled versus Measured Particulate Iron, Time Series Plot, December 10-17 1992, USGS (Gage 5)

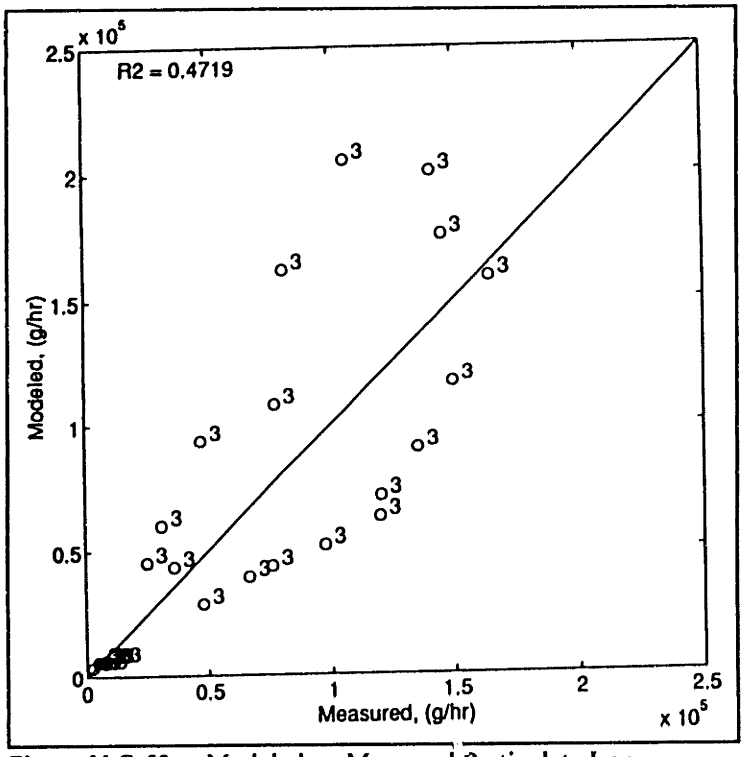

Figure V.C-53: Modeled vs Measured Particulate Iron Flux, Gage 5, 1993 (Pseudo-verification)

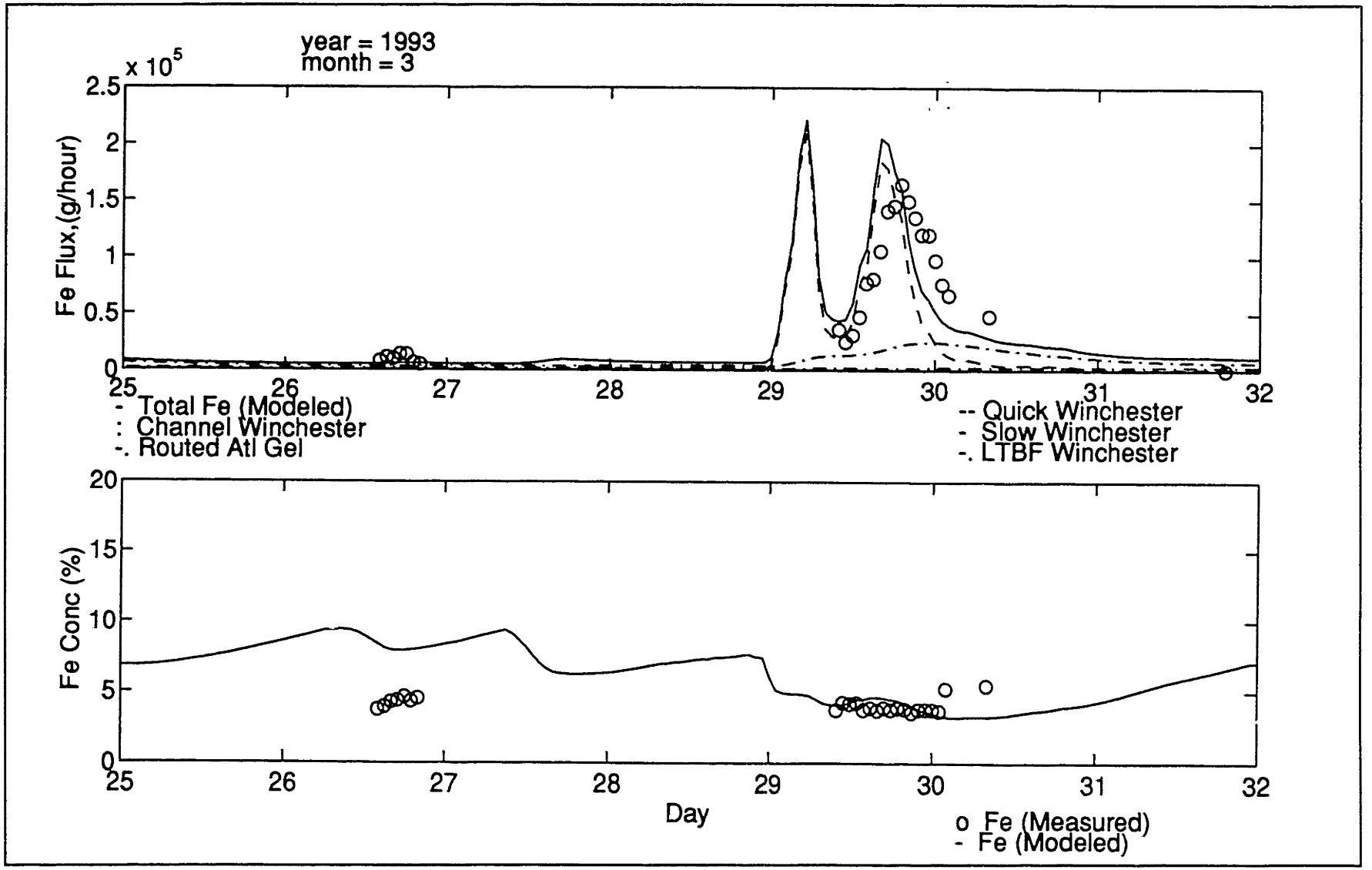

Figure V.C-54: Modeled versus Measured Particulate Iron, Time Series Plot, March 25-31 1993, USGS (Gage 5)

Chromium

The R^2 value for particulate chromium fluxes at gage 5 for the 1992 calibration data was -.06. The poor R^2 value was due to the poor fit of three samples which were collected during November. Without these samples the R^2 value was 0.71.

The time series plots for chromium are very similar to the plots for the other metals. During the August 18th event (figure V.C-56), the model was capable of capturing the initial burst of particulate chromium that was transported by the river at the very beginning of the storm followed by the slower rate of decrease that occurred immediately following the initial burst. The good fit of the modeled and measured chromium flux for the August 18th event was primarily associated with the good fit of the suspended sediment fluxes. Additionally, as indicated by the August 13th sample, the model was also capable of capturing the very small particulate fluxes that occurred during very low flow conditions. The model slightly over-estimated the chromium flux for the samples collected during the August 10th sampling period. This over-estimation was associated with the over-estimation of the particulate chromium and suspended sediment concentrations.

The over-estimation of the chromium flux for the November 1992 data (figure V.C-57) was primarily due to the over-estimation of the suspended sediment flux and secondarily to the over-estimation of the particulate chromium concentrations.

The December 1992 fluxes (figure V.C-58) were reasonably well modeled. As for the other metals during this sample set, there was a one to one correspondence between measured and modeled fluxes. The rate of increase and decrease in the particulate flux was well estimated and the timing and magnitude of the peak were also very closely approximated.

The R^2 value for the 1993 pseudo-verification year was 0.44. During the March 29th event (figure V.C-60), the model again was capable of capturing the rate of increase and decrease in the particulate chromium flux. The magnitude of the peak was also closely approximated. The primary error, however, is associated with a time shift between the modeled and measured fluxes.

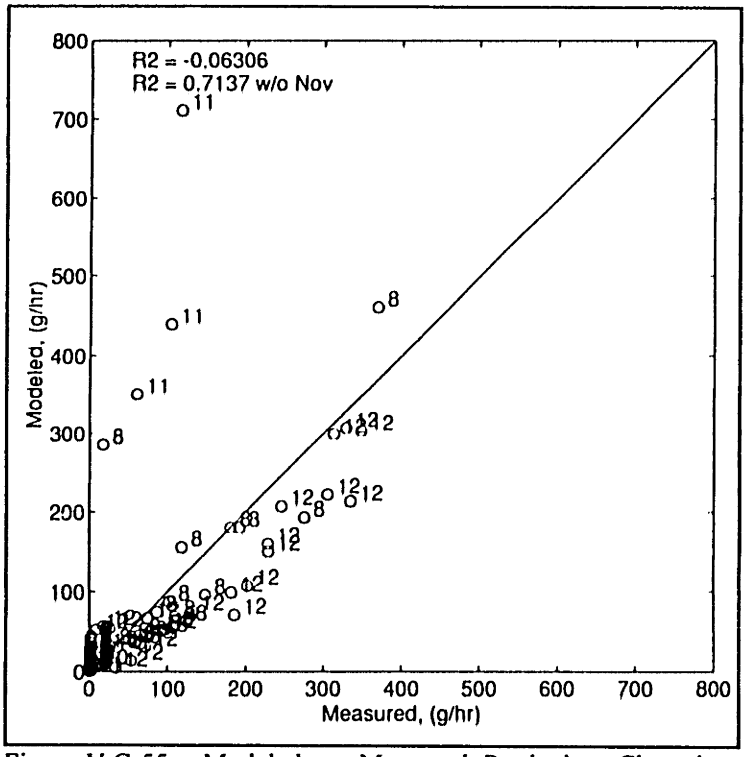

Figure V.C-55: Modeled vs Measured Particulate Chromium Flux, Gage 5, 1992 (Calibration)

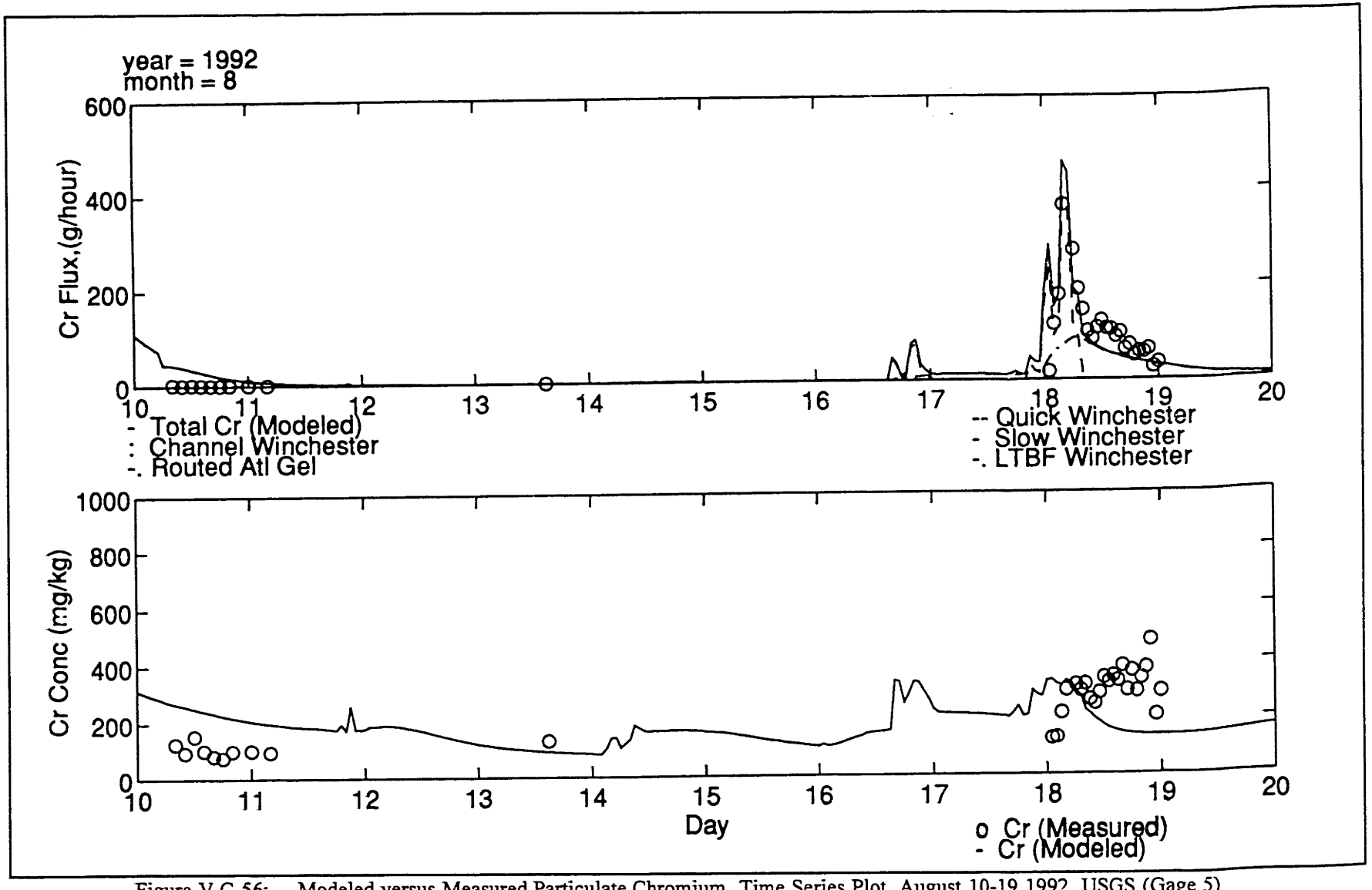

Figure V.C-56: Modeled versus Measured Particulate Chromium, Time Series Plot, August 10-19 1992, USGS (Gage 5)

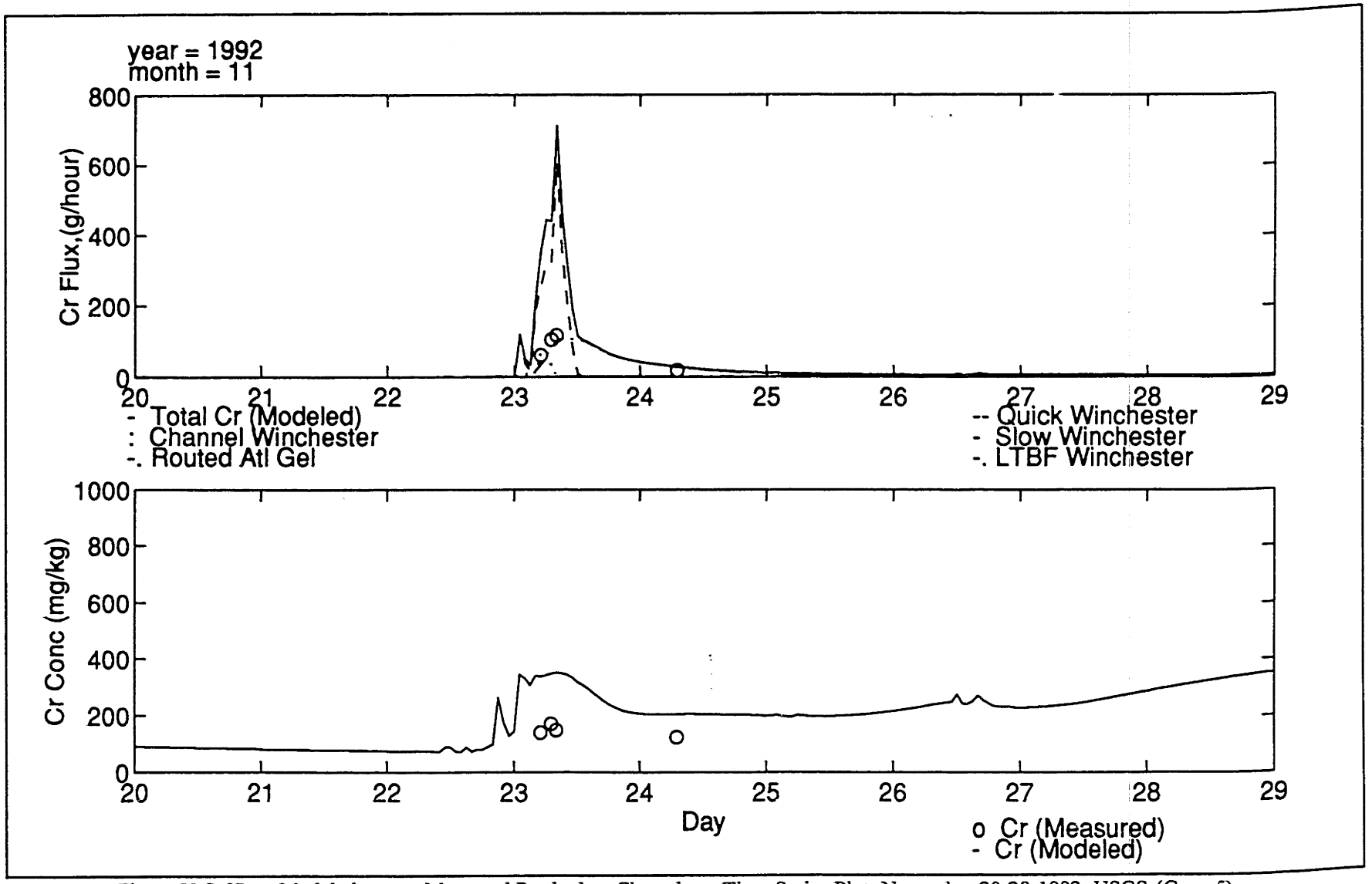

Figure V.C-57: Modeled versus Measured Particulate Chromium, Time Series Plot, November 20-28 1992, USGS (Gage 5)

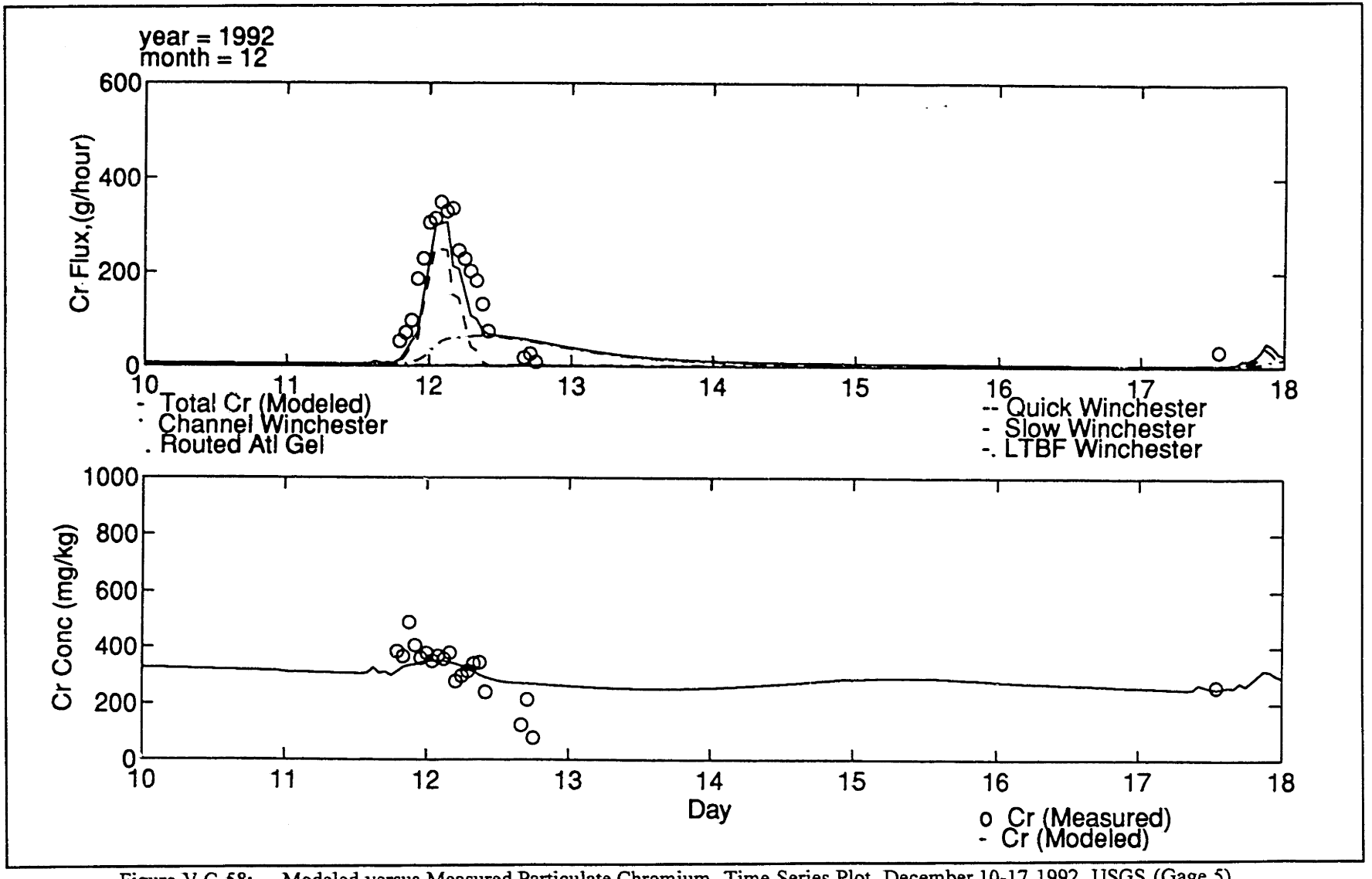

Figure V.C-58: Modeled versus Measured Particulate Chromium, Time Series Plot, December 10-17 1992, USGS (Gage 5)

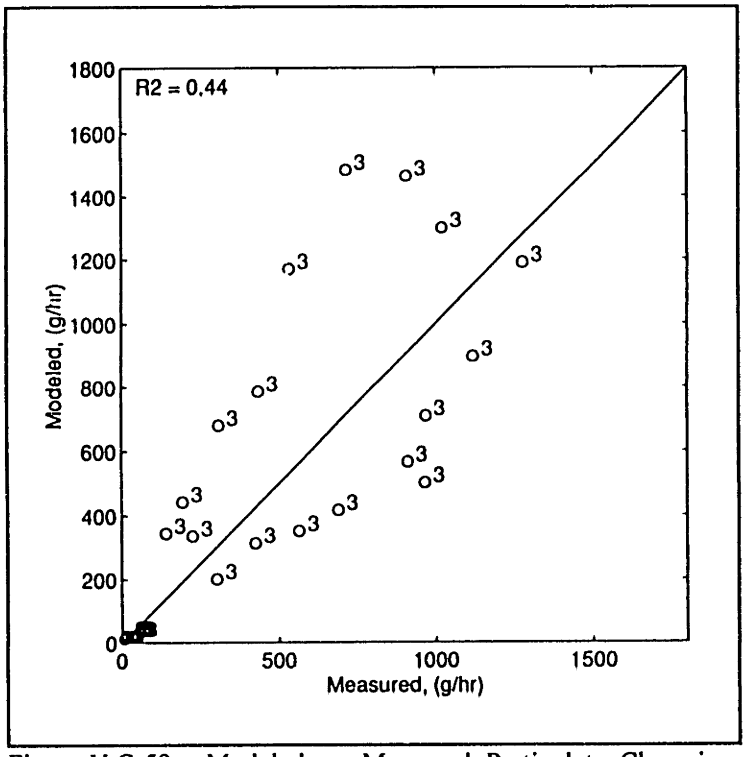

Figure V.C-59: Modeled vs Measured Particulate Chromium Flux, Gage 5, 1993 (Pseudo-verification)

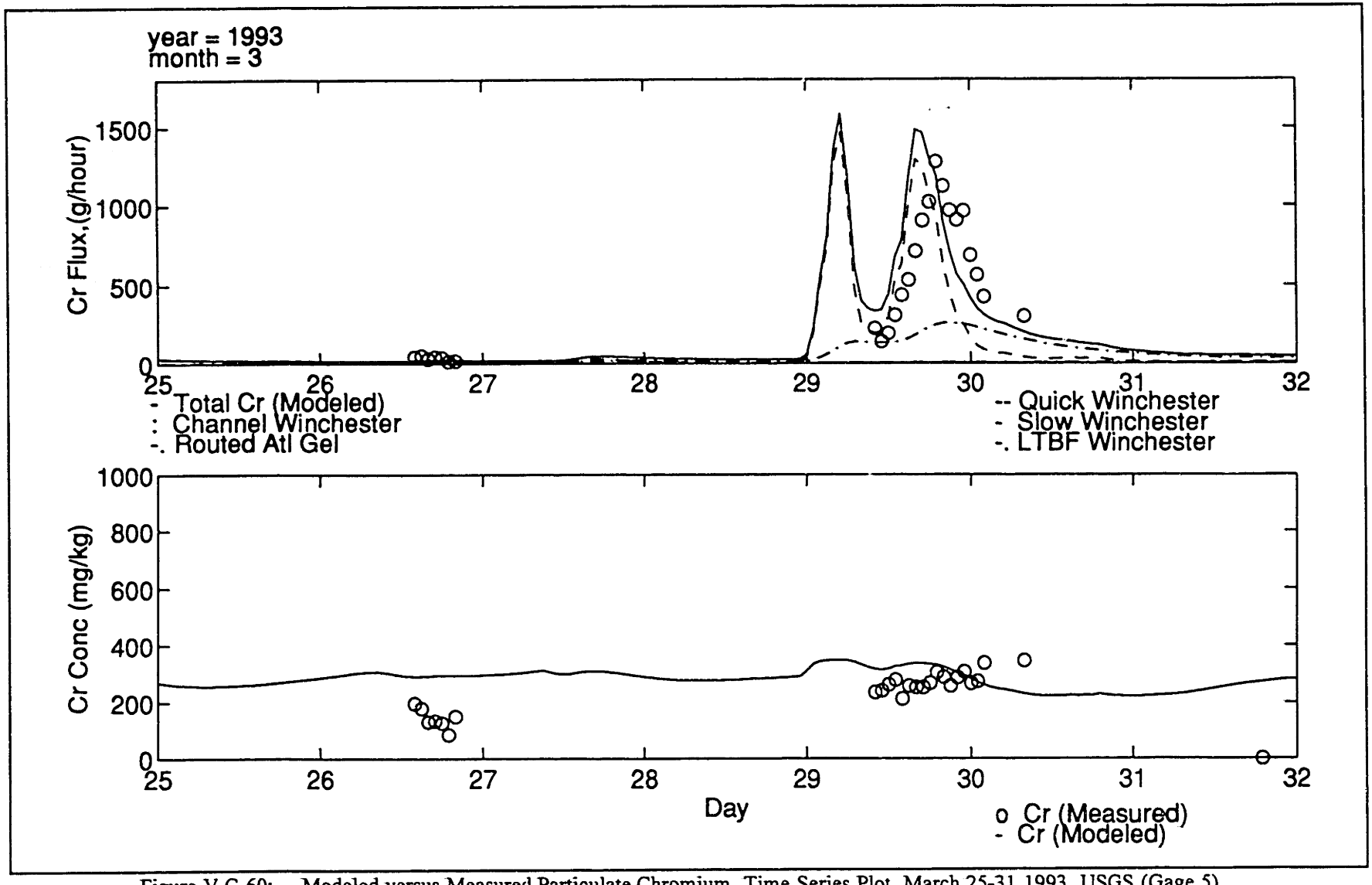

Figure V.C-60: Modeled versus Measured Particulate Chromium, Time Series Plot, March 25-31 1993, USGS (Gage 5)

Copper

The R^2 value for particulate copper fluxes for the 1992 samples was 0.37. The low R^2 was primarily due to the November outliers. Without the November samples, the R^2 a higher value of 0.77 was computed.

Again, the time series plots for copper were very similar to the time series plots for other metals. For the August samples (figure V.C-62), the modeling of the copper flux was highly dependent upon the proper modeling of the suspended sediment flux. From the time series plot, it is evident that the model was capable of capturing the initial burst of particulate copper which was observed at the beginning of the sampled event and was also capable of capturing the slower rate of decline which was observed immediately after the initial burst. Additionally, the model was capable of capturing the extremely low flux which was observed during very low flow conditions.

For the November samples (figure V.C-63), the model again over-estimated the particulate metal flux. This over-estimation was primarily due to the over-estimation of the suspended sediment flux for this sampling sequence.

For the December event (figure V.C-64), the model performed well. The model was capable of capturing the rate of increase and decrease in the copper flux. Additionally, the magnitude and timing of the copper peak were also closely approximated.

The R^2 value for the 1993 pseudo-verification samples was 0.54. As for the other metals (figure V.C-66), the model was capable of capturing the rate of increase and decrease in the particulate copper flux. Also the magnitude of the peak was also reasonably approximated. The primary error was associated with the timing between the measured and modeled values.

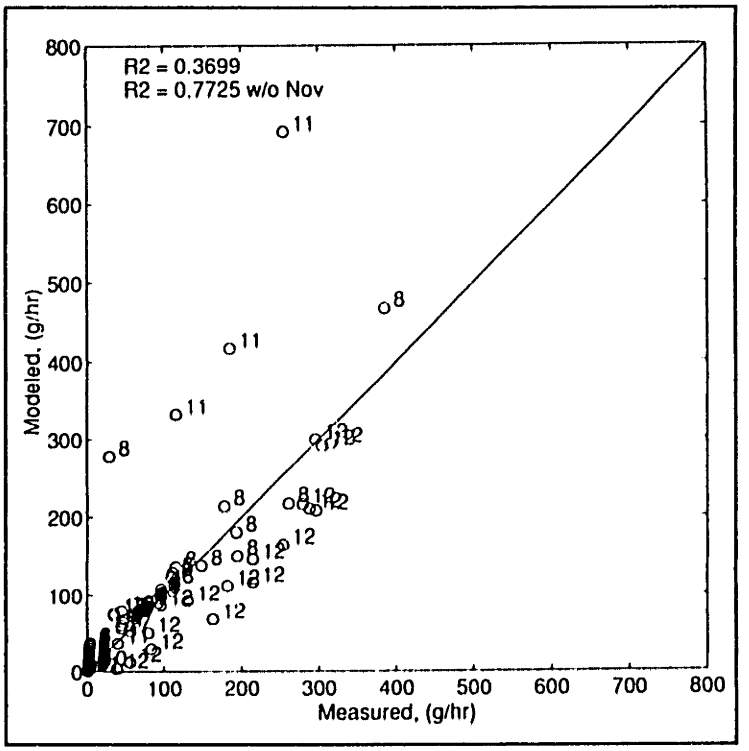

Figure V.C-61: Modeled vs Measured Particulate Copper Flux, Gage 5, 1992 (Calibration)

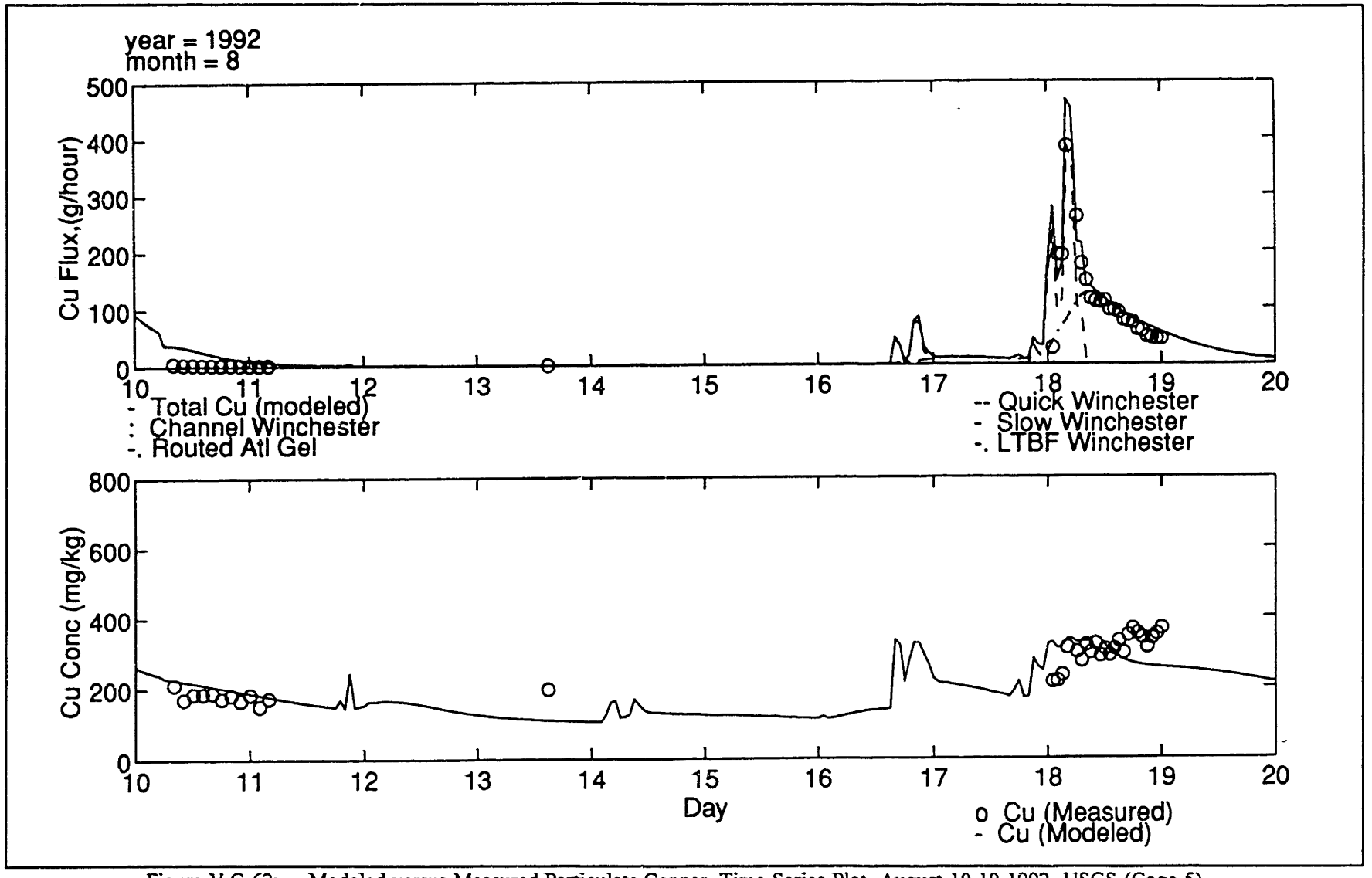

Figure V.C-62: Modeled versus Measured Particulate Copper, Time Series Plot, August 10-19 1992, USGS (Gage 5)

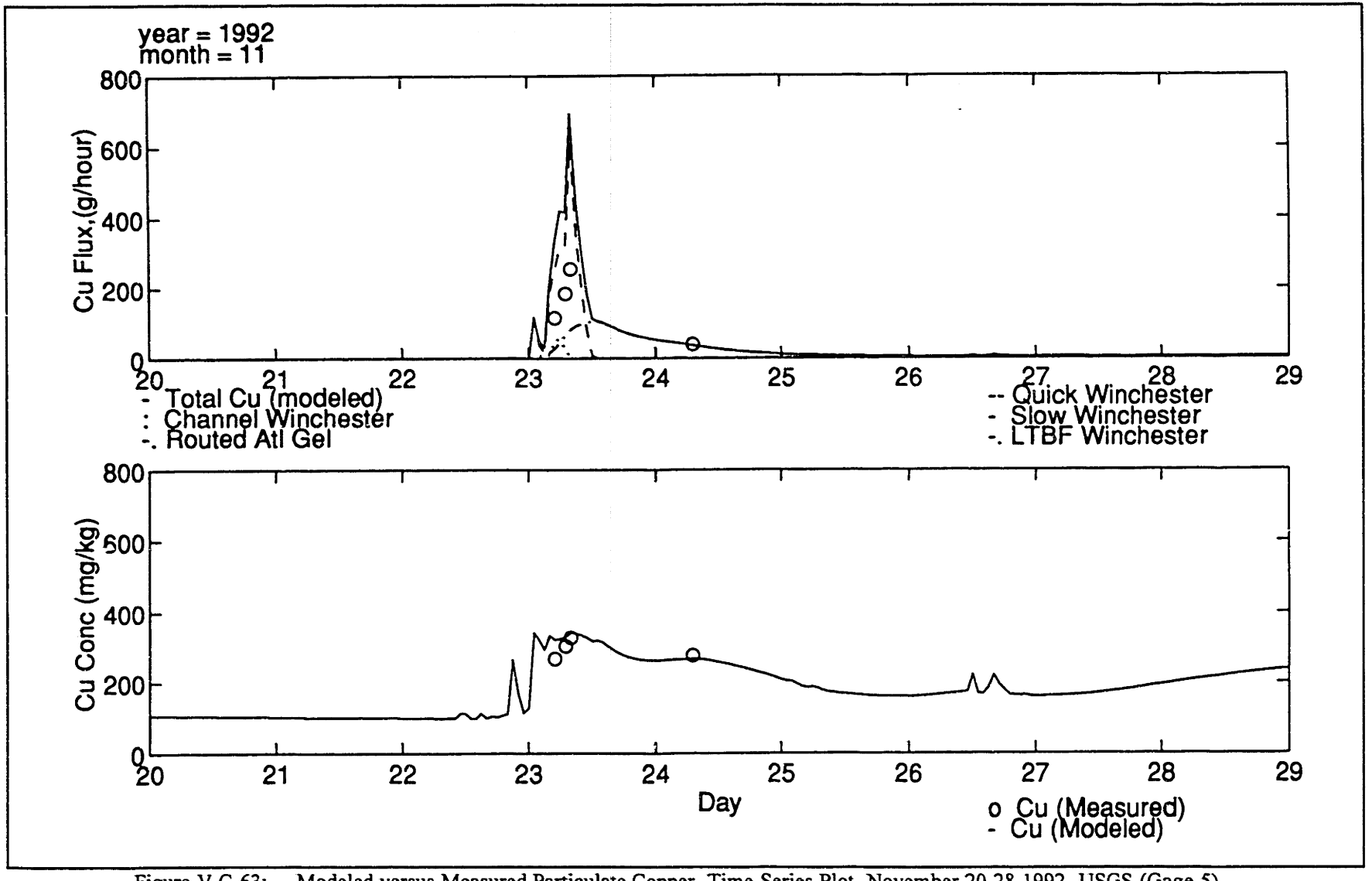

Figure V.C-63: Modeled versus Measured Particulate Copper, Time Series Plot, November 20-28 1992, USGS (Gage 5)

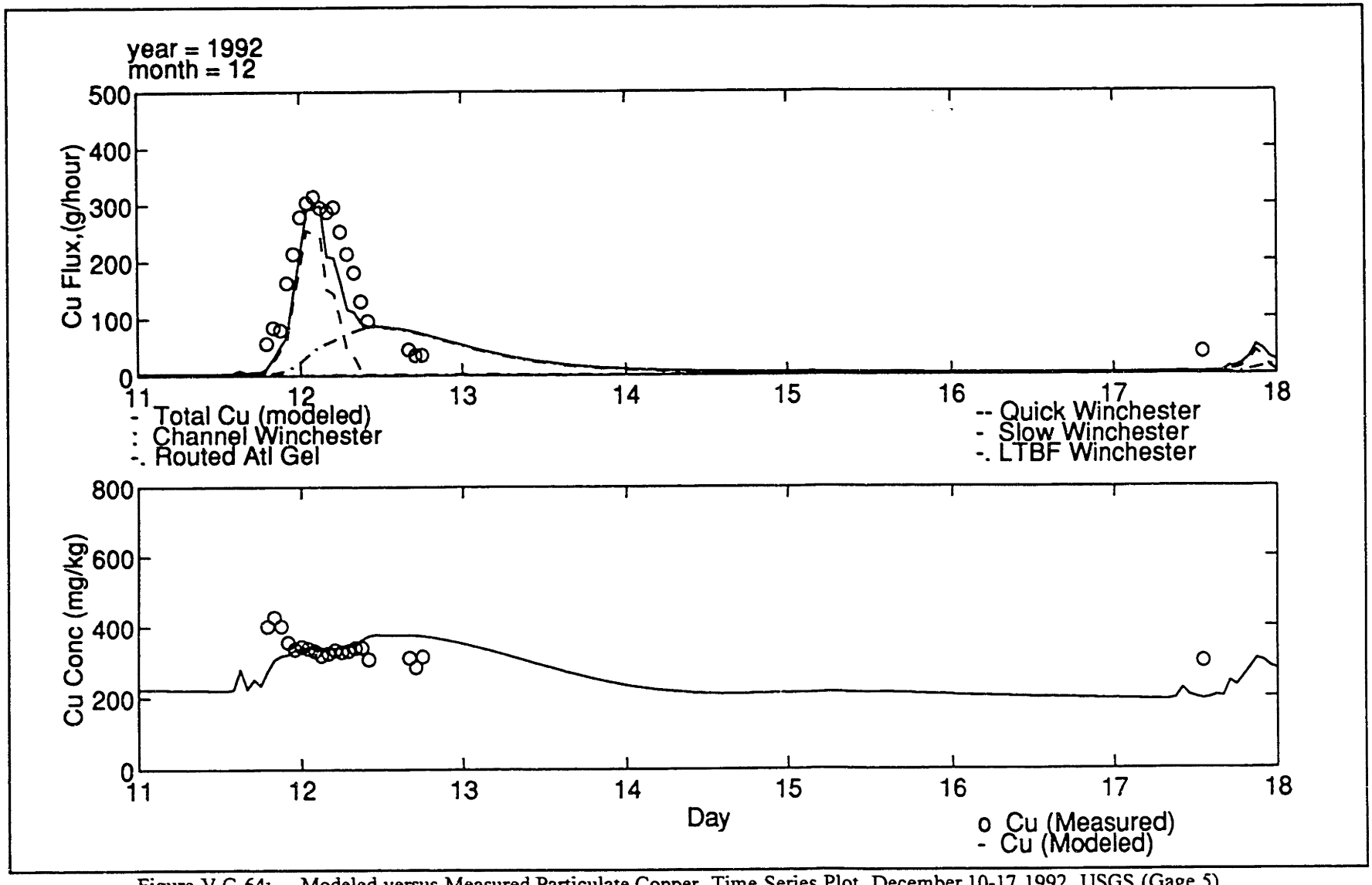

Figure V.C-64: Modeled versus Measured Particulate Copper, Time Series Plot, December 10-17 1992, USGS (Gage 5)

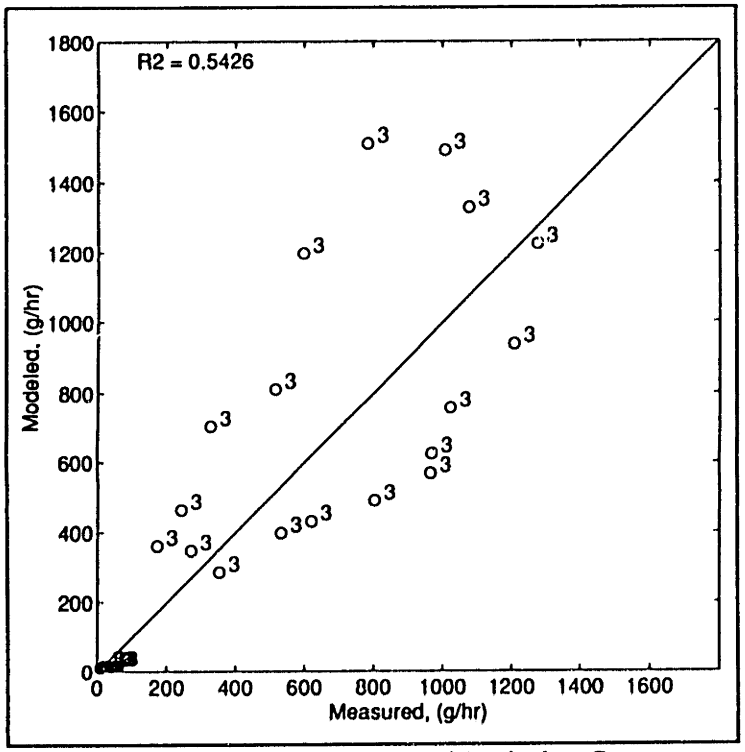

Figure V.C-65: Modeled vs Measured Particulate Copper Flux, Gage 5, 1993 (Pseudo-verification)

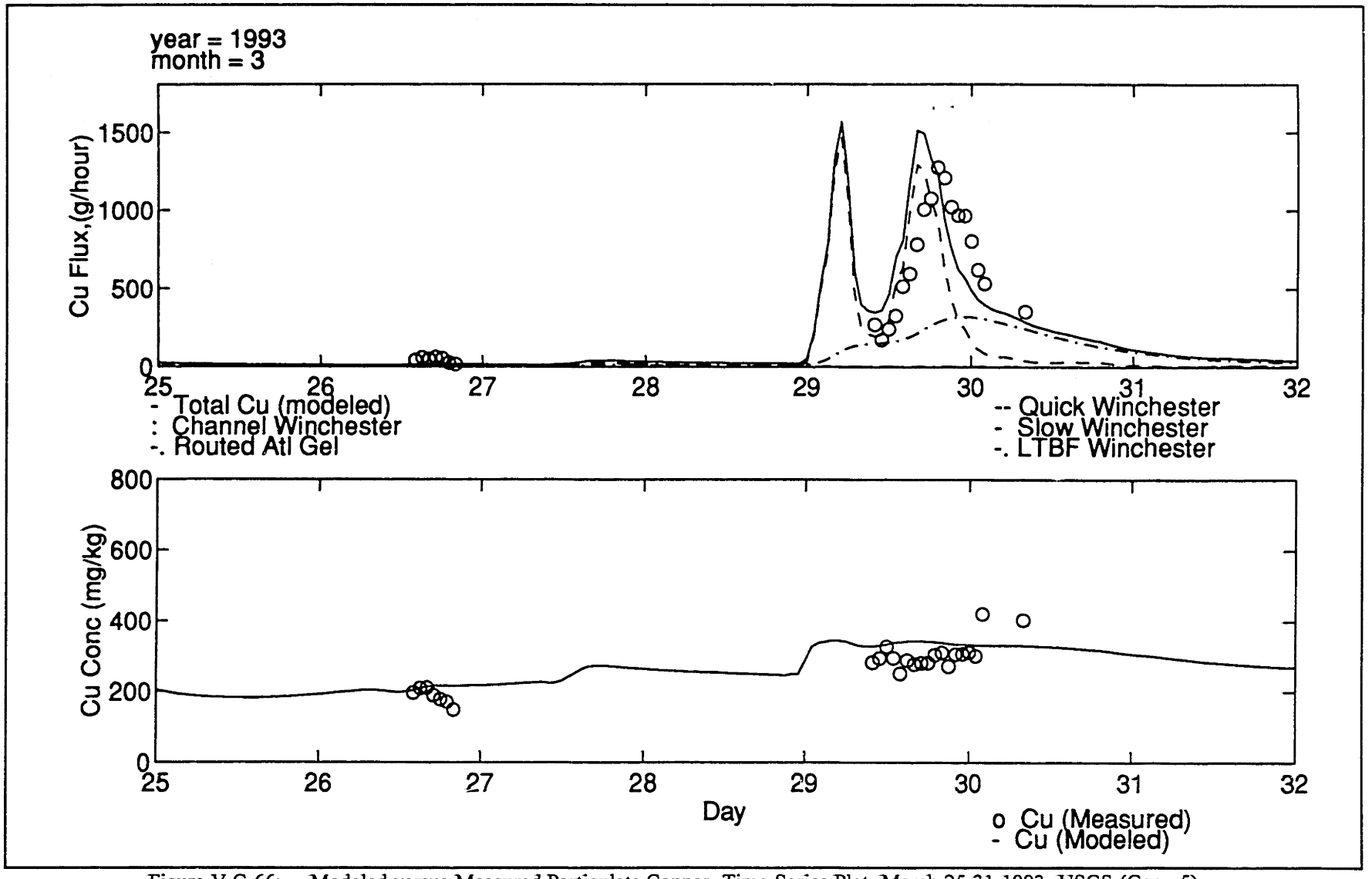

Figure V.C-66: Modeled versus Measured Particulate Copper, Time Series Plot, March 25-31 1993, USGS (Gage 5)

APPENDIX VI.A

A Method for Disaggregating Daily Rainfall Values

A methodology for obtaining realizations of hourly rainfall from daily data is developed. Specifically, statistics of available hourly raw data are used to generate statistically equivalent hourly realizations for time periods for which only daily rainfall records are available. The work includes;

1) Obtaining statistics from raw data. This step requires; 1) the computation of overall hourly and daily statistics, and 2) computation of hourly statistics conditional on the corresponding daily rainfall values.
2) Simulation of a large number of hourly precipitation values using an appropriate model. The hourly values simulated should be statistically equivalent to the raw hourly data. The purpose of this step is to obtain extreme values and other statistically equivalent hourly rainfall sequences which are not included in the original hourly raw data set. The model used for simulation is the Modified Bartlett-Lewis Rectangular Pulses model.
3) Obtaining realizations of hourly precipitation from daily data. This step includes categorization of the simulated hourly data into daily rainfall classes. Given a daily rainfall value, corresponding "disaggregated" hourly values are obtained by randomly sampling from the appropriate class of simulated hourly sequences.
4) Comparison of statistics for the raw, simulated, and disaggregated data. This section includes a brief comparison of overall statistics at hourly and daily levels of aggregation and a comparison of conditional hourly statistics given a daily precipitation value. Additionally, histograms of raw, simulated and disaggregated data for various daily precipitation categories are also included.

1. STATISTICS FROM THE RAW DATA

The precipitation data used for analysis is the Reading station (NCDC) data. (See section III.2.1 in main thesis for station description)

Hourly Statistics

Hourly precipitation values for the Reading station were available for the 1981 to 1991 period of record. The corresponding hourly statistics are summarized for each month in Table VI.A-1.

Daily Statistics

For the 1981 to 1991 period of record, the daily statistics for each month are given in Table VI.A-2.

Month	Mean (mm)	Variance (mm^2)	Corr (1)	Corr (2)	Corr (3)	P(0)	P(<.5)	P(<1)
Jan	0.132	0.347	0.852	0.711	0.598	0.899	0.929	0.954
Feb	0.133	0.361	0.795	0.624	0.490	0.887	0.952	0.954
Mar	0.156	0.449	0.785	0.651	0.553	0.878	0.918	0.945
Apr	0.165	0.533	0.804	0.651	0.545	0.883	0.924	0.948
May	0.140	0.477	0.549	0.361	0.287	0.892	0.931	0.955
Jun	0.139	0.564	0.569	0.396	0.289	0.897	0.934	0.957
Jul	0.138	0.925	0.384	0.235	0.186	0.933	0.953	0.969
Aug	0.148	1.007	0.545	0.364	0.300	0.925	0.949	0.967
Sep	0.101	0.529	0.521	0.326	0.235	0.937	0.961	0.974
Oct	0.150	0.938	0.566	0.371	0.256	0.914	0.941	0.960
Nov	0.192	0.775	0.775	0.608	0.474	0.887	0.918	0.942
Dec	0.115	0.377	0.771	0.631	0.544	0.916	0.946	0.966

Note: Correlation Level of Significance > |0.02|
Corr(1) = Lag 1 Correlation
P(0) = Probability of 0 inches of rain

Table VI.A-1: Hourly Statistics for Various Months (1981-1991 Period of Record)

Month	Mean (mm)	Variance (mm^2)	Corr (1)	Corr (2)	Corr (3)	P(0)	P(<.5)	P(<1)
Jan	3.167	58.26	0.088	-.106	0.054	0.665	0.684	0.719
Feb	3.186	65.48	0.049	-.021	-.070	0.646	0.681	0.724
Mar	3.746	77.33	0.152	0.019	-.060	0.587	0.619	0.661
Apr	3.964	102.4	0.153	-.012	-.043	0.570	0.630	0.687
May	3.365	62.24	0.086	0.054	0.180	0.555	0.603	0.658
Jun	3.327	68.36	0.267	0.062	0.213	0.587	0.613	0.647
Jul	3.301	91.24	-.015	-.017	0.017	0.649	0.681	0.720
Aug	3.555	110.0	0.068	0.066	-.014	0.649	0.685	0.728
Sep	2.417	47.86	0.047	0.043	0.040	0.721	0.758	0.796
Oct	3.598	89.31	0.169	-.059	-.070	0.699	0.720	0.749
Nov	4.597	128.9	0.049	-.063	0.083	0.626	0.648	0.700
Dec	2.760	59.51	0.164	-.047	-.051	0.673	0.702	0.742

Note: Correlation Level of Significance > |0.12|
Corr(1) = Lag 1 Correlation
P(0) = Probability of 0 inches of rain

Table VI.A-2: Daily Statistics for Various Months (1981-1991 Period of Record)

Since both hourly and daily statistics vary from month to month, modeling and disaggregation should be performed on a monthly basis. For exemplification purposes, the **month of July** has been choosen. This month was choosen since: 1) modeling of the type of storms typical of summer months is well suited for the simulation model used, (Entekhabi, personal conversation), and 2) no snowfall occurs in this month.

Hourly data is available from 1983 to 1991 for the month of July. The 1981 and 1982 July hourly precipitation values were missing from the record. Daily precipitation values are available from 1957 to 1991. The time period of 1957 to 1980, which corresponds to the time period when only daily rainfall data is available, will be the time period for which disaggregation of daily data will be performed.

For July, the mean daily precipitation for the entire period of record (1957-1991) is 2.73 mm. During the 1983-1991 time period, the average mean daily precipitation is 3.3 mm while the mean daily precipitation for the 1957-1980 time period is significantly lower at 2.4 mm. (Table VI.A-3) Additionally, the variance of the daily precipitation for the 1983-1991 period is almost twice the daily variance observed for the 1957-1980 period, while the proportion of dry days for the 1957-1980 period (0.69) is slightly higher than the proportion of dry days (0.65) for the 1983-1991. Extreme values for each time period also vary. The maximum daily rainfall for the 1983-1991 period is 94.5 mm (3.72") which is larger than the maximum daily rainfall (62.5 mm = 2.5") observed in the 1957-1980 period.

In order to work with the statistical differences in the daily data between the two time periods, the use of conditional statistics will be incorporated. Basically, use of conditional statistics implies that the conditional statistics for the July 1983-1991 record (statistics of hourly rainfall given a daily value) will be used to describe the conditional statistics of the rainfall for the July 1957-1980 time period.

The computation of conditional statistics for the July 1983-1991 time period incorporates the use of daily classes where daily classes are defined in 5.08 mm (0.2") increments. These statistics were computed to compare results from the simulation and from the disaggregation with values of the raw data (i.e. July 1983-1991 values).

Time Period	Mean (mm)	Variance (mm^2)	Corr (1)	Corr (2)	Corr (3)	P(0)	P(<.5)	P(<1)
1983-1991	3.30	91.2	-.015	-.017	.018	0.649	0.681	0.720
1957-1980	2.40	47.7	-.004	-.055	-.043	0.687	0.721	0.761

Note: Corr Level of Significance: > |0.12| for 1983-1991 period; > |0.07| for 1957-1980 period

Table VI.A-3: Comparison of Daily Statistics from 1983-1991 with the Statistics from 1957-1991

2. SIMULATION OF HOURLY RAINFALL

Simulation Model

The model choosen for simulation is the Modified Bartlett-Lewis Rectangular Pulses (MBLRP) Model. The application of the original model, the Bartlett-Lewis Rectangular Pulses (BLRP) model for modeling rainfall, was introduced by Rodriguez-Iturbe, Cox, and Isham, 1987. The model is a cluster-based model which implies that a cluster of rain cells is associated with each storm. Cluster-based models, in general, have the flexibility of representing more than one time scale and are capable of providing considerable physical realism of the rainfall process. (Rodriguez-Iturbe, Febres de Power, & Valdes, 1987) These properties are distinct characteristics of cluster models which make them well suited for disaggregation purposes. Statistical analysis of rainfall using these types of models have been capable of describing cumulative rainfall characteristics over a range of time scales from 1 to 24 hours without changing the model parameters. (Rodriguez-Iturbe, Febres de Power, & Valdes, 1987) Additionally, these models perform well at describing the extreme values of rainfall at various levels of aggregation. (Rodriguez-Iturbe, Febres de Power, & Valdes, 1987)

For the BLRP model, storm origins are Poisson distributed with average arrival rate, λ. For any given storm, the time of cell origination is exponentially distributed with parameter γ. This approach implies that the storm length is the time of cell origination plus the time during which cells are active after cell origination ceases. The number of cells corresponding to a given storm, C, is random and geometrically distributed with mean μ_c, while the inter-arrival time between cells is poisson distributed with parameter, β. For the BLRP model, rain cells are modeled as rectangular pulses of random duration and random but constant intensity. Thus the total rain intensity at any given time is the sum of all cell intensities which are active at that time. For the BLRP model, cell duration is exponentially distributed with parameter, η, and cell depth is exponentially distributed with mean, μ_x. (See Table VI.A-4) The MBLRP differs from the BLRP through the cell duration parameter, η, which is permitted to vary randomly between storms in the MBLRP model. (Rodriguez-Iturbe, Cox, and Isham, 1988)

MODELED VARIABLE	DISTRIBUTION	PARAMETER
Storm Inter-arrival time	Poisson	λ $1/\lambda$ = mean
Inter-arrival time of cells (Once Storm Begins)	Poisson	β $1/\beta$ = mean
Time of new cell origins for each storm	Exponential	γ $1/\gamma$ = mean
Cell Duration	Exponential	η $1/\eta$ = mean
Cell Depth	Exponential	$1/\mu_x$ μ_x = mean
Mean number cells per storm	Geometric	μ_c (= $1+\kappa/\phi$) μ_c = mean
Derived Parameters		$\kappa = \beta/\eta$ $\phi = \gamma/\eta$

Table VI.A-4: Summary of MBLRP Model Parameters
(After Rodriguez-Iturbe, Cox, & Isham, 1987)

Model Implementation

Overall Statistics at the 1 hour and 24 hour aggregation levels were used to obtain the optimal model parameters for the MBLRP simulation model. The model parameters were obtained through use of an optimization program (Entekhabi and Hawk, 1992) which incorporates a Davidon-Fletcher-Powell non-linear minimization technique for obtaining the best fit model parameters using six user specified statistical values. The statistical values specified for the optimization procedure include the 1 hour mean, variance, P(0), and lag one correlation and the 24 hour variance and P(0).

For the July data statistics, the model parameters computed were: (Note: $\alpha = E[\eta]^2/Var[\eta]$ and $\upsilon = E[\eta]/Var[\eta]$)

λ = 0.01323 /hr
υ = 0.3276
α = 2.9926
μ_x = 7.4728 mm/hr
ϕ = 0.0270
κ = 0.2054

These parameters were then input into the MBLRP simulation program (Entekhabi and Hawk, 1992) and was run for a simulation time of 100,000 hours or 134 months of July data. The overall hourly statistics of the simulation correspond well with the hourly statistics of the raw data, (Table VI.A-5) whereas the 24 hour statistics, except for the correlations, agree. These results are as expected since the 1 hour mean, variance, lag 1 correlation, and P(0) and the 24 hour variance and P(0) were used to compute the MBLRP model parameters, whereas the 24 hour lag 1 correlation was not included in the parameter optimization process.

Level & Data Set	Mean (mm)	Variance (mm^2)	Corr (1)	Corr (2)	Corr (3)	P(0)
1 hour Raw Data CSL=.02	0.138	0.925	0.384	0.235	0.186	0.933
1 hour Simulated CSL=.006	0.140	0.945	0.394	0.217	0.169	0.916
1 hour Disaggreg CSL=.015	0.100	0.730	0.255	0.226	0.107	0.951
24 hour Raw Data CSL=.13	3.30	94.24	-.015	-.017	0.017	0.649
24 hour Simulated CSL=.03	3.36	87.23	0.222	0.064	0.032	0.673
24 hour Disaggreg CSL=.07	2.40	47.69	-.004	-.055	-.043	0.687

Note: CSL = Correlation Significance Level

Table VI.A-5: Comparison of 1 hr and 24 hr Statistics for the Raw, Simulated, and Disaggregated data.

3. REALIZATIONS OF HOURLY RAINFALL CONDITIONAL ON THE DAILY SUM

Realizations of hourly rainfall, h, for a given daily class, d, were obtained by:

1) Categorization of the hourly simulated data based upon the daily sum.
2) Given a daily rainfall value, corresponding "disaggregated" hourly values are obtained by randomly sampling from the appropriate class of simulated hourly sequences.

Categorization

The hourly simulated data was categorized into daily classes, where classes are defined in 5.08 mm (0.2") increments. The 24 hour sequences defining a day are assumed independent, implying that each hourly value in a series is associated with only one daily class. In order to incorporate the extreme values of the simulated data (202 mm = 7.9"), 41 daily classes were defined (Table VI.A-6). These classes include a class 0 which corresponds to a day with no rain.

These increments were chosen for convenience only. These increments are wide enough such that at least a few simulated values fall within them for the lower 20 classes. The maximum value of the data to be disaggregated falls in class 13. In order to make the increments more efficient, use of increments of varying widths is recommended, where smaller widths are used for lower classes and wider widths are used for higher classes. Use of the varying widths will tend to distribute the number of days within each class more uniformly such that number of simulation values can be minimized. It is recognized that the number of simulation values falling in each class may not be sufficient for disaggregation purposes. For future runs, consideration should be given to increasing the number of simulation values and varying the width increments.

From table VI.A-6, the necessity for simulation step is evident. Note that although the raw data has larger extreme values, the number of days which fall in the lower classes is smaller for the raw data than for the data to be disaggregated. If sampling directly from the raw data was attempted, one would have to use an hourly distribution (given the daily class) multiple times. Although this method would give proper statistics, it is not physically realistic since exact hourly precipitation distributions rarely repeat themselves in nature. The simulation allows the sampling of hourly distributions from a set which has not necessarily occured. The simulation, if properly parameterized, will tend to preserve overall daily trends if any exist, and with exact replicates of prior distributions being highly unlikely. The value of the simulation step is also noted by observing that the data to be disaggregated has precipitation values in classes 12 and 13 where the raw data does not. The simulation, on the other hand, does provide values within these categories, from which hourly sequences can be randomly sampled.

Random Sampling

Once daily categorization of the hourly sequence of the simulated data has been completed, the daily class of the daily rainfall value to be disaggregated is determined. Once determined, a random number between 1 and no | d is choosen, using a random number generator. (Press, et. al., 1989) (no | d = the number of simulated days falling within the daily class) The random number generator is "re-seeded" after each determination to ensure that the sequence of random numbers is not repeated. Once a random number (random number = i) is obtained, the "i th" hourly sequence in the list of simulated values corresponding to the proper daily class is retrieved. This hourly sequence is then rescaled by the ratio of: (24 hour data value to be disaggregated/the sum of the sampled 24, 1 hour simulated values). The difference between the 24 hour data value and the sampled 24 hour simulated value is no more than the 5.08mm (0.2"), which is the width increment associated with each class. For clarification purposes a diagram illustrating the random sampling procedure is given in figure VI.A-1.

	Frequency Count (# days in ea. class)		
	# raw	# simul	# disag
class 0 0<ppt=<0	181	2898	507
class 1 0<ppt=<0.2	56	622	140
class 2 0.2<ppt=<0.4	16	232	40
class 3 0.4<ppt=<0.6	6	127	18
class 4 0.6<ppt=<0.8	6	93	10
class 5 0.8<ppt=<1	5	51	13
class 6 1<ppt=<1.2	4	33	8
class 7 1.2<ppt=<1.4	0	23	3
class 8 1.4<ppt=<1.6	0	27	1
class 9 1.6<ppt=<1.8	0	11	0
class 10 1.8<ppt=<2	2	8	0
class 11 2<ppt=<2.2	1	2	0
class 12 2.2<ppt=<2.4	1	3	2
class 13 2.4<ppt=<2.6	0	4	2
class 14 2.6<ppt=<2.8	0	2	0
class 15 2.8<ppt=<3	0	3	0
class 16 3<ppt=<3.2	0	4	0
class 17 3.2<ppt=<3.4	0	0	0
class 18 3.4<ppt=<3.6	0	1	0
class 19 3.6<ppt=<3.8	1	2	0
class 20 3.8<ppt=<4	0	3	0
class 21 4<ppt=<4.2	0	0	0
class 22 4.2<ppt=<4.4	0	0	0
class 23 4.4<ppt=<4.6	0	2	0
class 24 4.6<ppt=<4.8	0	0	0
class 25 4.8<ppt=<5	0	0	0
class 26 5<ppt=<5.2	0	0	0
class 27 5.2<ppt=<5.4	0	1	0
class 28 5.4<ppt=<5.6	0	0	0
class 29 5.6<ppt=<5.8	0	0	0
class 30 5.8<ppt=<6	0	0	0
class 31 6<ppt=<6.2	0	0	0
class 32 6.2<ppt=<6.4	0	0	0
class 33 6.4<ppt=<6.6	0	0	0
class 34 6.6<ppt=<6.8	0	1	0
class 35 6.8<ppt=<7	0	0	0
class 36 7<ppt=<7.2	0	0	0
class 37 7.2<ppt=<7.4	0	0	0
class 38 7.4<ppt=<7.6	0	0	0
class 39 7.6<ppt=<7.8	0	0	0
class 40 7.8<ppt=<8	0	1	0

Table VI.A-6: Daily Class Summary (ppt = precipitation in inches)

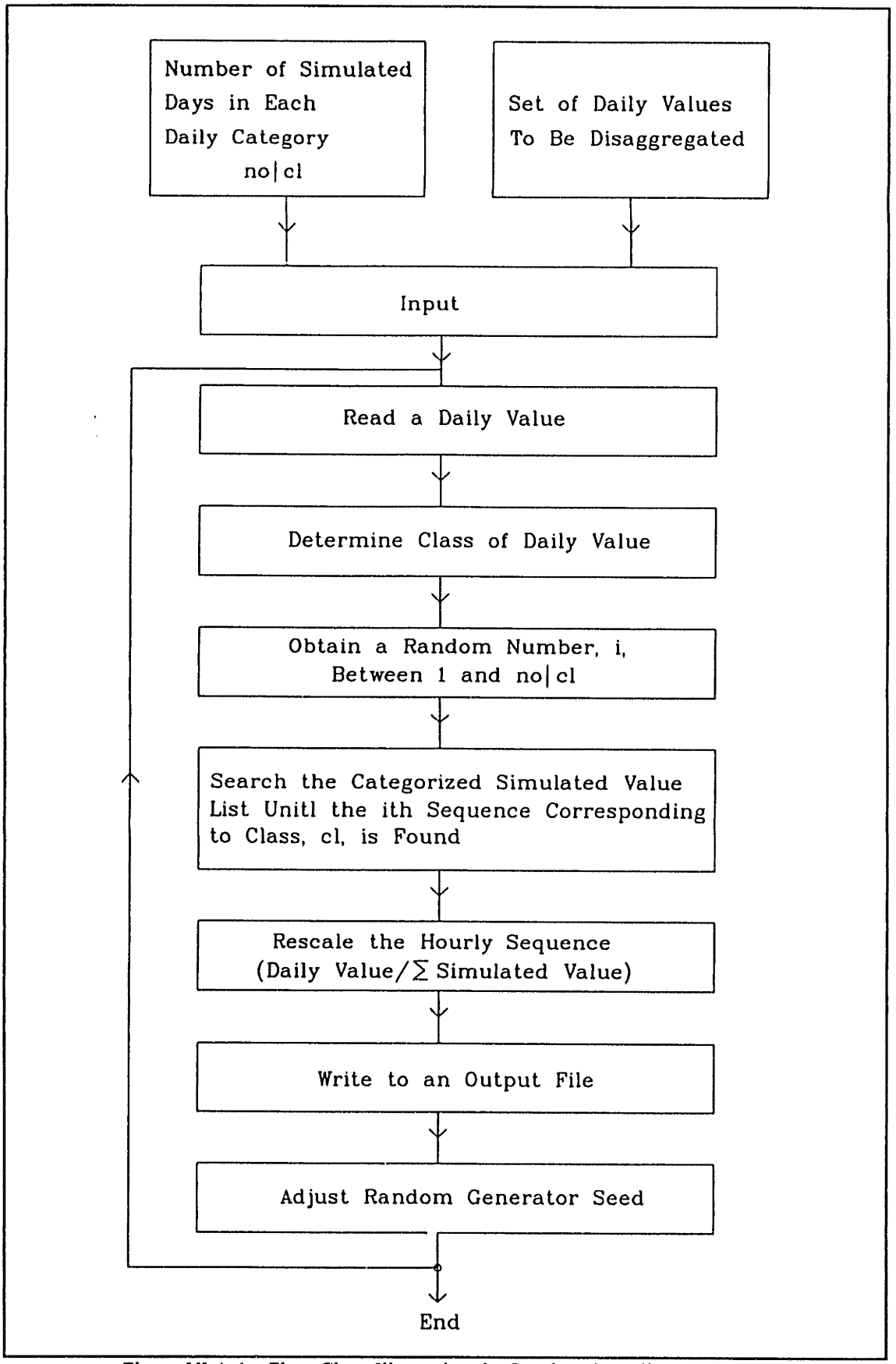

Figure VI.A-1: Flow Chart Illustrating the Random Sampling Procedure

4. STATISTICAL COMPARISON OF RAW, SIMULATED, AND DISAGGREGATED DATA

Comparison of the conditional statistics is given in figures VI.A-2 to VI.A-4. The horizontal axis of these figures represents the midpoint of the daily class, whereas the vertical axis corresponds to the statistic of the hourly values given the daily class.

Good aggreement is obtained between the conditional means, E[h | d], (figure VI.A-2) of the raw, simulated, and disaggregated data. Note that the linear relationship extends beyond the raw data values. Also the points plotted on the horizontal axis correspond to data sets which had no data within a given class.

The conditional variance, Var[h | d] (figure VI.A-3) tends to perform well for the lower classes (classes corresponding to 25 mm (1") or less), whereas significant scatter is associated with the higher classes. Considering that approximately 98% of the disaggregated data falls in the lower classes (25 mm = 1" or less), one may conclude that overall the variance is conserved reasonably well.

The probability of zero rain, P[0 | d], (figure VI.A-4) as expected tends to decrease with increasing class. From the figure, good agreement between the raw and disaggregated data is obtained for classes corresponding to a daily rainfall less that 1". Above the 1" daily rainfall category, the scatter increases significantly. The scatter is due in part to the few number of data points used in computing the P[0 | d] for the larger classes (Refer to Table VI.A-6).

For comparative purposes, probability plots of hourly rainfall distributions for various daily categories are given in figures VI.A-5 to VI.A-8. For these figures, note that: 1) the dash-dot line represents the raw data (1983-1991 July Data), 2) the dotted line represents the simulated data, and 3) the dashed line represents the disaggregated data (1957-1980 July Data). Since the P[0 | d] for each data set tends to over-whelm the frequency distribution of the non-zero hourly values, they are not plotted. However, the value of P[0 | d] is printed on the graphs for informative purposes. Also in order to smooth the bar plot, the hourly values were lumped together in bins of equal width. The width was set conveniently at 0.508 mm (0.02").

From the figures note that for the lower classes, figure VI.A-5 (class 1) and figure VI.A-6 (class 2), the probaility distributions of hourly rainfall given a daily class tend to agree reasonably well. Note that the P[0 | d] for each data set are very close to one another. Without good agreement of the P[0 | d] between the data sets, the non-zero probability plots would be inadequate. For the higher classes, figure VI.A-7 (class 6) and figure VI.A-8 (class 8), the fit between the non-zero hourly probability plots is not

as good. Also note for these figures that the P[0 | d] for the data sets do not correspond well with one another. The P[0 | d=6] for the raw data in figure VI.A-7 is equal to 0.54 whereas the P[0 | d=6] for the disaggregated data is 0.65. Because of the the higher probability of the non-zero values (1-.54 = 0.46) in the raw data plot, most of the raw data hourly probabilities are higher than the corresponding disaggregated values, especially for the smaller values of hourly rainfall. Additionally, once the number of days within a given daily class becomes very small (figure VI.A-8) the probability histograms become increasingly poorer. For figure VI.A-8, the raw data had no days within the given daily class. Thus the best estimate of the hourly probability distribution is given by the simulated data set. Since the simulated data set had many (27) days within this class, its shape is the typical exponential shape curve observed for the lower daily classes. However, since the disaggregated data had only one day within the category, its bar graph is discontinuous and represents the fact that only one hourly value represents each bar plotted in the graph. Thus, the probability plot for the disaggregated data is unrepresentative. In order to obtain a more representative plot, the disaggregation should be performed several times. The results of several disaggregations will increase the number of days for the disaggregation plot and a more appropriate comparison may be made.

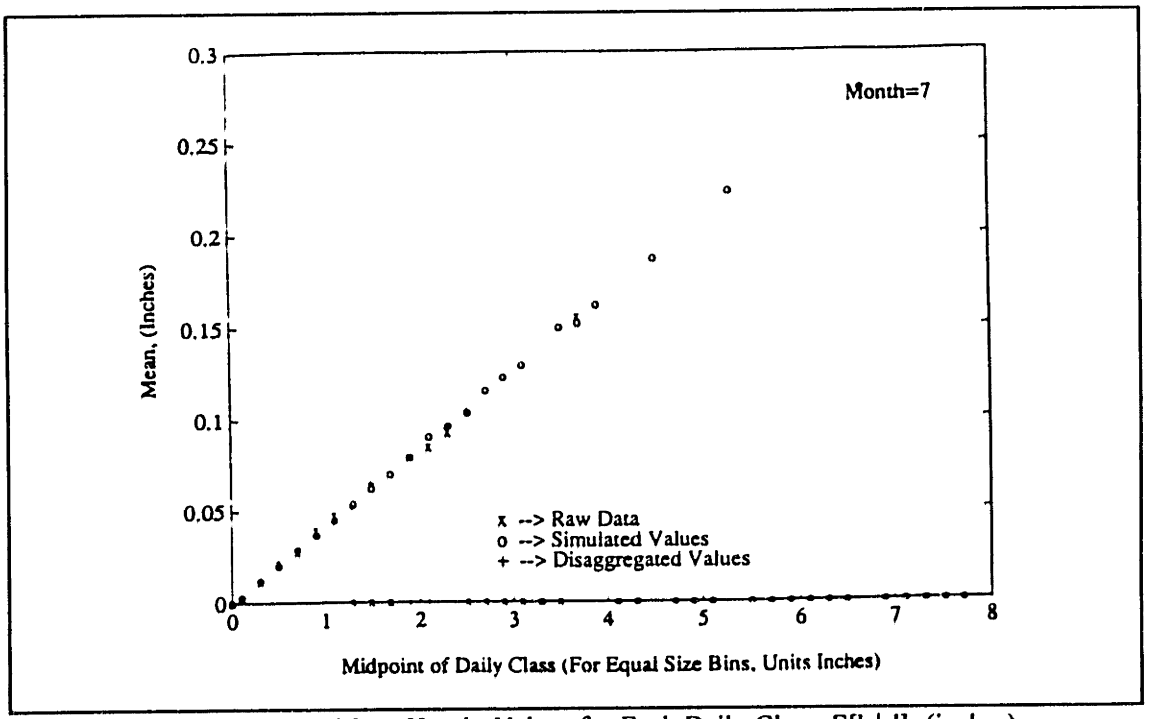

Figure VI.A-2: Mean Hourly Values for Each Daily Class, E[h|d], (inches)

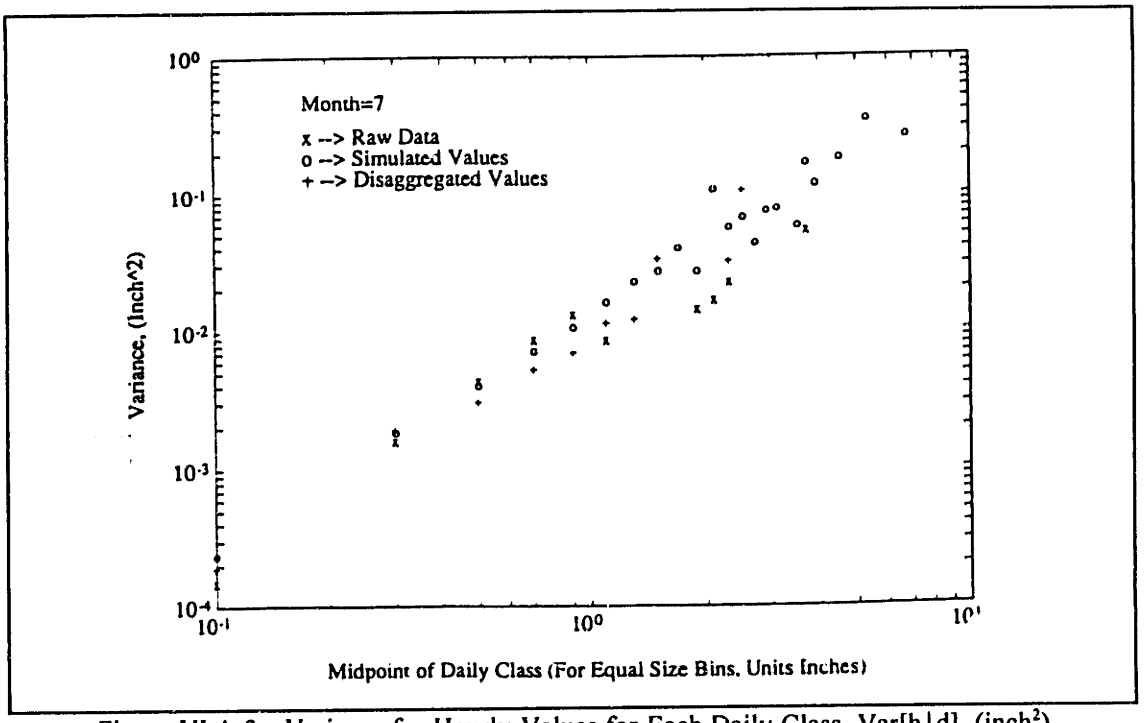

Figure VI.A-3: Variance for Hourly Values for Each Daily Class, Var[h|d], (inch^2)

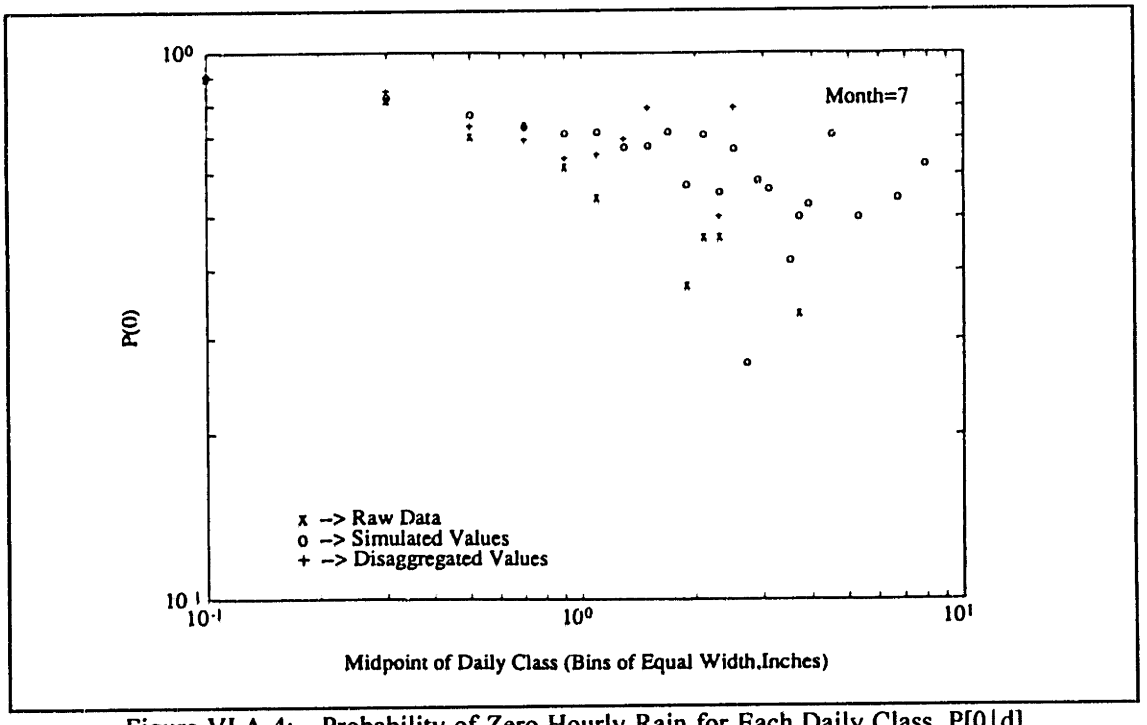

Figure VI.A-4: Probability of Zero Hourly Rain for Each Daily Class, P[0|d]

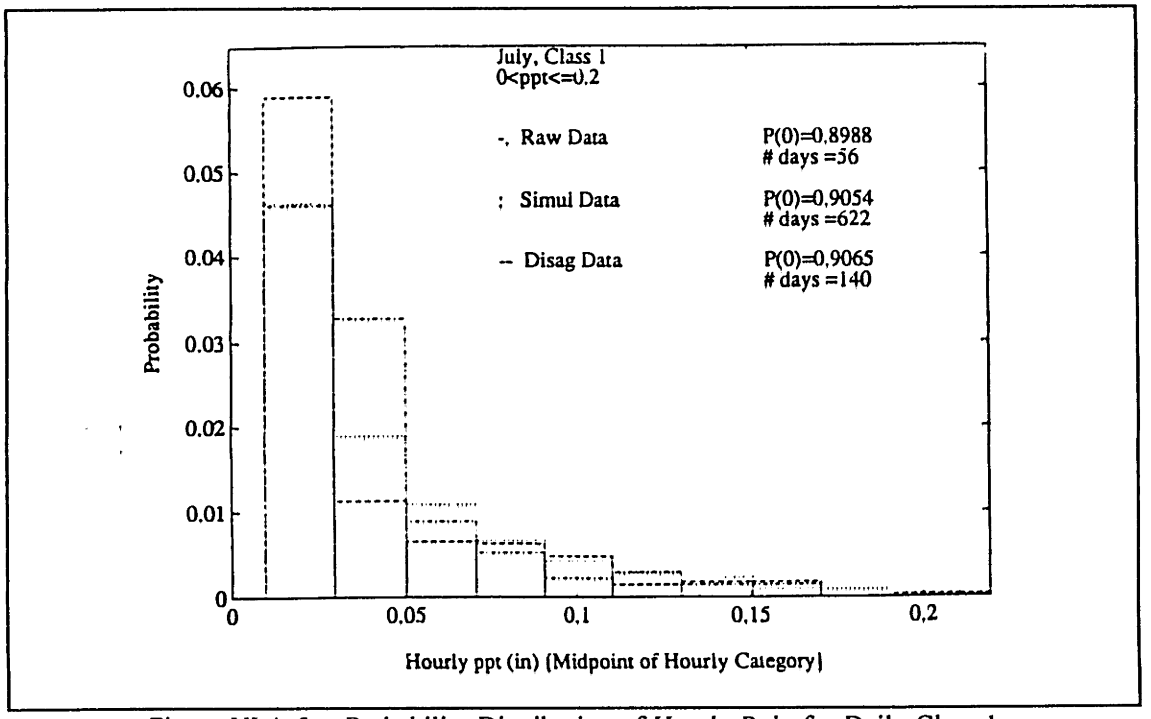

Figure VI.A-5: Probability Distribution of Hourly Rain for Daily Class 1

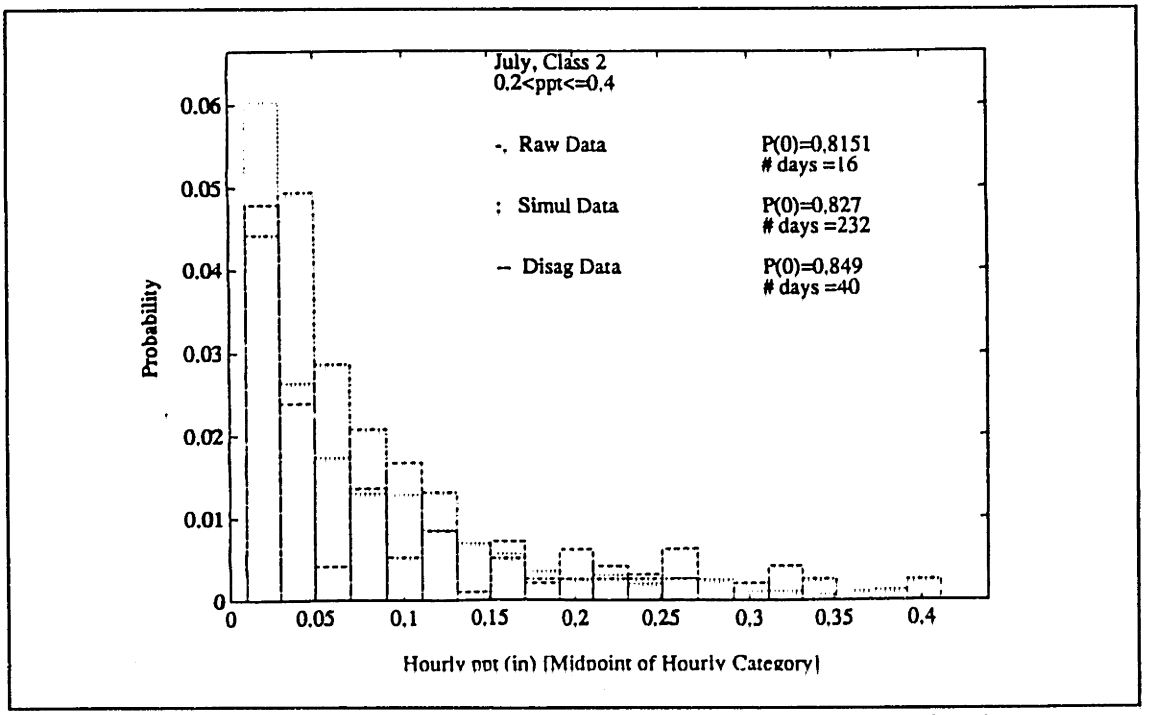

Figure VI.A-6: Probability Distribution of Hourly Rain for Daily Class 2

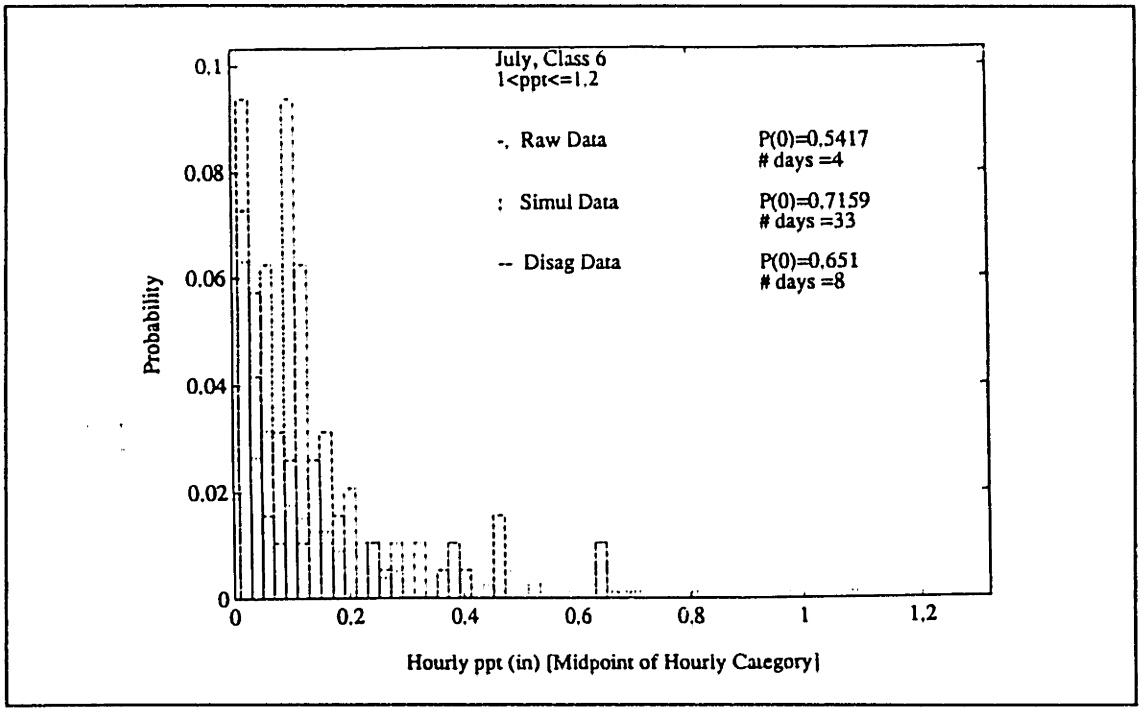

Figure VI.A-7: Probability Distribution of Hourly Rain for Daily Class 6

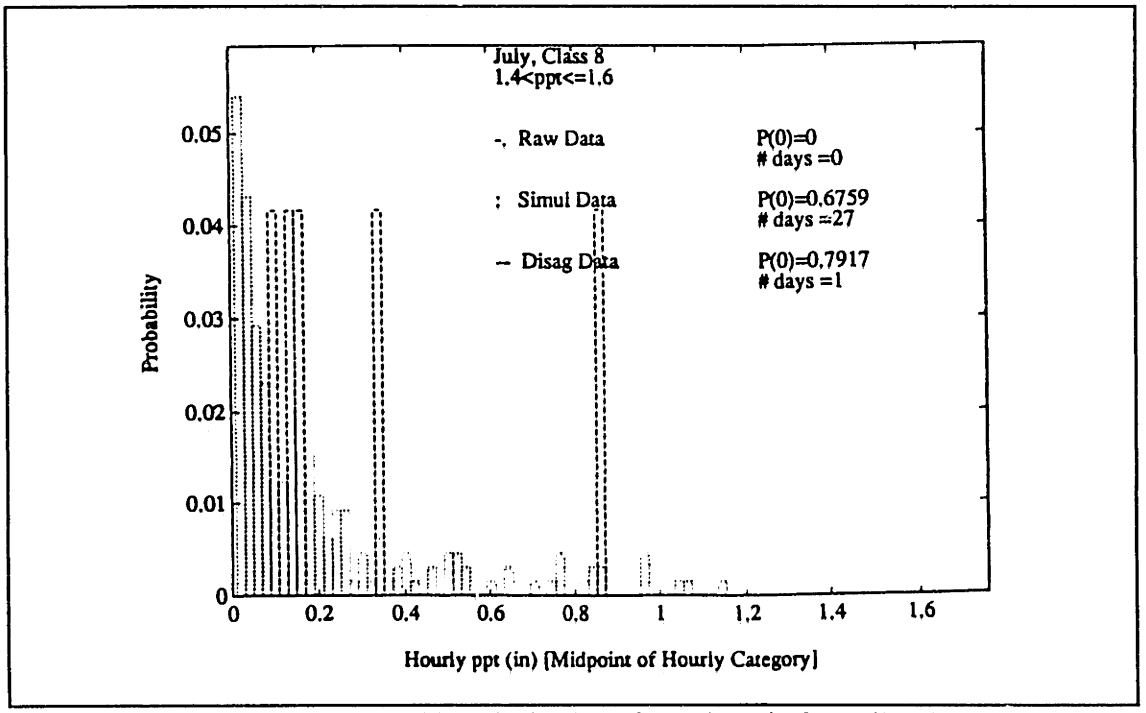

Figure VI.A-8: Probability Distribution of Hourly Rain for Daily Class 8

CONCLUSIONS

The procedure presented in this appendix provides a method for obtaining realizations of hourly rainfall from daily data. The procedure described can be applied only when a record of hourly rainfall is available, and is specifically useful for generating statistically equivalent hourly realizations for time periods in which only daily rainfall records are available.

From the preliminary analysis presented, the methodology is apparently capable of reproducing conditional statistics for the lower (< 25 mm (1")) daily precipitaion values.

Acknowledgements: I thank both Professor Dara Entekhabi and Kelly Hawk for their suggestions concerning problem approach and their help with the various computer programs. I also thank Professor Ignacio Rodriguez-Iturbe for his suggestions concerning this topic.